

Total Synthesis of Pseudo-Dimeric Cyclobutane Natural Products via Brønsted Acid-Catalyzed
Asymmetric [2+2] Photocycloadditions

By

Matthew James Genzink

A dissertation submitted in partial fulfillment of
the requirements for the degree of

Doctor of Philosophy

(Chemistry)

at the

UNIVERSITY OF WISCONSIN–MADISON

2023

Date of final oral examination: June 1, 2023

The dissertation is approved by the following members of the final oral committee:

Tehshik P. Yoon, Professor, Organic Chemistry

Zachary K. Wickens, Assistant Professor, Organic Chemistry

Andrew J. Boydston, Yamamoto Family Professor, Materials Chemistry

Shannon S. Stahl, Steenbock Professor of Chemical Sciences, Inorganic Chemistry

Total Synthesis of Pseudo-Dimeric Cyclobutane Natural Products via Brønsted Acid-Catalyzed
Asymmetric [2+2] Photocycloadditions

Matthew James Genzink

Under the supervision of Tehshik P. Yoon
at the University of Wisconsin–Madison

Abstract

Pseudo-dimeric cyclobutanes constitute a large class of natural products. Though a [2+2] cycloaddition would be the most direct way to access these molecules, its use in total synthesis has been limited due to selectivity challenges in the cycloaddition. The work in this dissertation details the development of a new platform for enantioselective [2+2] photocycloadditions based on chiral Brønsted acid catalysis and its application to the total synthesis of (pseudo)-dimeric cyclobutane natural products. Initial mechanistic investigations revealed that the reaction proceeds via a chromophore activation mechanism in which coordination of the catalyst to the substrate engenders a red-shifted substrate absorption. This insight enabled the development of (hetero)dimerization reactions, the products of which could be transformed into enantioenriched natural products.

Acknowledgements

I am indebted to many individuals for their help and support throughout my PhD studies, none more so than to my advisor, Tehshik Yoon. Tehshik, you have demonstrated what it means to be a scientist and have cultivated an environment where the students in your lab grow into independent thinkers. Since I joined the lab, you have prioritized my personal growth over how many papers I publish. You have acted more as an advisor than a boss, allowing me the freedom to follow my intellectual curiosity, develop my own interests, and learn skillful failure. You have shown me that there is beauty in science, both in the way it is conducted, and in the way it is communicated. I am extraordinarily grateful for your mentorship.

I would also like to acknowledge the other members of my thesis committee: Zach Wickens, AJ Boydston, and Shannon Stahl. Zach and AJ, thank you for the time you have invested in me and for the encouragement and advice you have generously given during our meetings. My development as a scientist has been profoundly shaped through our interactions. Shannon, thank you for agreeing to join my committee this year and for showing me the importance of developing a “chemical intuition”.

My PhD studies would not have been possible without the individuals who maintain the facilities in the department including Heike Hofstetter, Charlie Fry, Cathy Clewett, Ilia Guzei, and Martha Vestling. Thank you for your patience in training me to run NMR experiments and understand X-ray and mass spectrometry data. You have enabled my own research and that of the whole department.

I would also like to thank all the Yoon group members. I have had the privilege of working alongside many incredible scientists during my time at UW. These individuals are a constant source of inspiration and joy, and a big reason I have so enjoyed my time in graduate school.

Evan: Thank you for showing me the ropes and teaching me the basics of synthesis.

Grace: Thank you for the encouragement and support you have consistently provided. I learn from you every day, particularly in how to solve difficult problems and communicate effectively.

Wes: You have taught me to be interested and invested in the science of my peers and have pushed me to be a better scientist. Apart from Tehshik, I owe most of my growth to you.

Sam G.: Thank you for encouraging me to pursue what I love.

Andrew, Caitlin, and Francesca: This is the post-doc dream team. I aspire to become the excellent mentor that you all are.

Ellie and Cade: Thank you for creating a wonderful office environment. You are the reason I have enjoyed these last two years of my PhD more than any other. Ellie, I am inspired by (and often fail to emulate) your determination and tenacity. I'm lucky I won our total synthesis bet because I don't think I'd win many others. Cade, you have a thoughtfulness and mature approach to problem solving that is more characteristic of a fifth-year student than a second-year student. Sorry for beating you in so many sports.

Tahoe: Your enthusiasm and charisma are infectious. Sorry I don't know what you're saying most of the time.

Guy and Rodrigo: You are the most curious scientists I know. Thank you for all you have taught me.

Last, I'd like to thank my family and friends for their constant support. Mom, Dad, Abby, and Stu, thank you for encouraging me to pursue my passions and for showing interest in my chemistry even when I explain it poorly. Dima, Yuliya, Lev, Sonya, and Esenya, thank you for your friendship and loving home. D-Dog, Jibby, TBC, Sammer, Danny, and Connor thank you for

all the Tuesday night conversations and trips to Florida, the Faroes, Rome, CDMX, *the Badlands*, and chill weekends in Chicago. I love you all.

Table of Contents

Chapter 1	Chiral Organic Photocatalysts in Asymmetric Photochemical Synthesis	1
1.1	Previous Publication of this Work	2
1.2	Introduction	2
1.3	Arenes.....	7
1.4	Ketones.....	25
1.4.1	Ketones without Hydrogen-Bonding Domains.....	25
1.4.2	Chiral Ketones with Hydrogen-Bonding Domains.....	26
1.4.3	Enamine and Iminium Chromophores	40
1.4.4	Chiral Counterions	50
1.5	Conclusion.....	57
1.6	References	60
Chapter 2	Chiral Brønsted Acid-Controlled Asymmetric [2+2] Photocycloadditions.....	76
2.1	Previous Publication of this Work	77
2.2	Introduction	77
2.3	Results and Discussion.....	79
2.3.1	Reaction Optimization	79
2.3.2	Substrate Scope.....	81
2.3.3	Mechanistic Studies	84
2.4	Conclusion.....	88
2.5	Contributions.....	88
2.6	Supporting Information	88
2.6.1	General Information.....	88
2.6.2	Catalyst Synthesis	90
2.6.3	Substrate Synthesis	96

2.6.4	Asymmetric [2+2] Photocycloaddition Reactions	107
2.6.5	Racemic [2+2] Photocycloaddition Reaction	130
2.6.6	Cleavage Reactions of Complex Cycloadduct.....	143
2.6.7	Mechanistic Experiments.....	144
2.6.8	Assignment of Diastereomers by 1D-NOE.....	147
2.6.9	X-Ray Crystallographic Data.....	148
2.6.10	Computational Data	191
2.6.11	NMR Data.....	202
2.6.12	HPLC Data.....	241
2.7	References	278
Chapter 3 Total Synthesis of Truxinate Natural Products Enabled by Enantioselective [2+2] Photocycloadditions		285
3.1	Introduction	286
3.2	Results and Discussion.....	288
3.2.1	Dimerization Optimization and Substrate Scope	289
3.2.2	Total Synthesis of Dimeric Truxinates	291
3.2.3	Heterodimerization Optimization and Substrate Scope	294
3.2.4	Total Synthesis of Piperarborenine D.....	296
3.2.5	Mechanistic Studies	297
3.3	Conclusion.....	299
3.4	Contributions.....	300
3.5	Supporting Information	300
3.5.1	General Information.....	300
3.5.2	Catalyst Synthesis	301
3.5.3	Substrate Synthesis	306
3.5.4	Asymmetric [2+2] Dimerization Photocycloaddition Reactions.....	319

3.5.5	Racemic [2+2] Dimerization Photocycloaddition Reaction	328
3.5.6	Asymmetric [2+2] Heterodimerization Photocycloaddition Reactions	334
3.5.7	Racemic [2+2] Heterodimerization Photocycloaddition Reactions.....	346
3.5.8	Synthetic Derivatization of Cycloadducts	352
3.5.9	Natural Product Synthesis.....	355
3.5.10	Incompatible Substrates	368
3.5.11	Monomethylation gives Unsymmetrical Products.....	368
3.5.12	UV-Vis Absorption Experiments.....	369
3.5.13	Non-Linear Effect Experiments	371
3.5.14	X-Ray Crystallographic Data.....	372
3.5.15	NMR Data.....	401
3.5.16	Comparison of Natural and Synthetic Natural Product NMR Spectra	458
3.5.17	HPLC Data.....	465
3.6	References	504
Chapter 4	Progress Towards the Asymmetric Total Synthesis of Sceptrin	509
4.1	Introduction	510
4.2	Results and Discussion.....	512
4.3	Conclusion.....	515
4.4	Contributions.....	515
4.5	Supporting Information	515
4.5.1	Previous Sceptrin Syntheses	515
4.5.2	General Information.....	518
4.5.3	Compound Synthesis	519
4.5.4	UV-Vis Absorption Experiments.....	522
4.5.5	NMR Data.....	523

4.6 References 527

Table of Figures

Figure 1.1 Selected Examples of Chiral Benzenecarboxylate Sensitizers	10
Figure 1.2 Chiral Thioxanthone-Derived Sensitizers	38
Figure 1.3 Photocatalysts with Chiral Counteranions.....	51
Figure 2.1 Mechanistic Studies. a, Ultraviolet-visible spectra of 2.1 and 2.4 in CH ₂ Cl ₂ . b, X-ray crystal structure of acid-bound substrate. c, Binding depiction of acid-bound substrate. d, HOMO(π) and LUMO(π^*) of 2.1 and 2.1-H⁺-2.41 . Note: AC-3=2.4 and 1=2.1	85
Figure 2.2 Comparative absorption spectra of the Brønsted acid catalyst (AC-3=2.4), substrate (1=2.1), and 20 and 100 mol% loading of acid catalyst in substrate dissolved in CH ₂ Cl ₂ . The spectra were all recorded in quartz tubes under ambient conditions.	145
Figure 1.3 Stacked NMR spectra of titration of 0 to 11 equiv. of 2.4 into 2.1 . Note: AC-3=2.4 and 1=2.1	Error! Bookmark not defined.
Figure 2.4 Preliminary binding isotherm, measured vs. calculated. Note: AC-3=2.4	147
Figure 2.5 Observed nOe Enhancements.....	148
Figure 2.6 A molecular drawing of yoon61 shown with 50% probability ellipsoids	151
Figure 2.7 A molecular drawing of the hydrogen bonding interactions between the cation and anion in yoon62a shown with 50% probability ellipsoids. Selected H atoms are shown. Minor disorder components and solvent molecules are omitted.	163
Figure 2.8 A molecular drawing of the hydrogen bonding interactions between the cation and anion in yoon62a shown with 50% probability ellipsoids. Selected H atoms are shown. Minor disorder components and solvent molecules are omitted.	164
Figure 2.9 A molecular drawing of the anion in yoon62a shown with 50% probability ellipsoids. All disorder components at C7 are shown whereas all H atoms are omitted.	165
Figure 2.10 A molecular drawing of yoon62a shown with 50% probability ellipsoids. The two diethyl ether solvent molecules are shown with their disorder components. All H atoms are omitted.	166
Figure 2.11 PMO diagram for 2.1 and 2.1-H⁺-2.41 . Each molecule was fragmented into the cinnamoyl part and the remaining portion of the molecule.	192
Figure 2.12 Natural transition orbital (NTO) pairs of 2 nd singlet excitation (S ₀ → S ₂) for (a) 2.1 and (b) 2.1-H⁺-2.41 . Each pair contributes more than 96% to the related excited state.	194
Figure 3.1 Incompatible dimerization and heterodimerization substrates. Note: < 10% yield was observed if no yield is given above.....	368

Figure 3.2 Absorption spectra of 3.19 and 3.19 with 3.2 and emission spectra of Tuna Blue and 456 nm Kessil lamps.....	370
Figure 3.3 Absorption spectra of 3.24 and 3.24 with 3.2 and emission spectra of Tuna Blue and 456 nm Kessil lamps.....	371
Figure 3.4 Non-linear effect experiment for dimerization of 3.1 with 3.2	372
Figure 3.5 A molecular drawing of Yoon59a shown with 50% probability ellipsoids. All H atoms are omitted.	375
Figure 3.6 A molecular drawing of Yoon70a shown with 50% probability ellipsoids; all minor disorder components are omitted.....	388
Figure 3.7 A molecular drawing of Yoon70a displaying the disordered H-atoms bound to C9 with selected atom labels. All atoms are shown with 50% probability ellipsoids; all H-atoms that are not bound to C9 or to chiral carbons are omitted.....	389
Figure 4.1 Absorption spectra of 4.3 and 4.3 with 3.2	522

Table of Schemes

Scheme 1.1 General Mechanisms of Enantiocontrol by Chiral Chromophores in Asymmetric Photocatalysis	5
Scheme 1.2 Primary Versus Secondary Photoreactions.....	7
Scheme 1.3 Exciplex Formation and Deactivation Pathways	8
Scheme 1.4 Cyclopropane Isomerization Catalyzed by a Naphthylamide Sensitizer.....	8
Scheme 1.5 Sulfoxide Deracemization Catalyzed by a Naphthylamide Sensitizer	9
Scheme 1.6 Allene Deracemization Catalyzed by a Steroid Sensitizer	10
Scheme 1.7 Mechanism of Cyclooctene Isomerization Catalyzed by Benzenecarboxylate Sensitizers	12
Scheme 1.8 Effect of Temperature on Photosensitized Cyclooctene Isomerization.....	13
Scheme 1.9 Effect of Solvent on Photosensitized Cyclooctene Isomerization	16
Scheme 1.10 Cyclooctene Isomerization Catalyzed by a Cyclophane Sensitizer.....	17
Scheme 1.11 Cycloheptane Isomerization and Cycloaddition Catalyzed by Benzenecarboxylate Sensitizers	18
Scheme 1.12 Cyclohexane Isomerization and Cycloaddition Catalyzed by Benzenecarboxylate Sensitizers	19
Scheme 1.13 Polar Photoaddition of Alcohols to Alkenes Catalyzed by Naphthalenecarboxylate Sensitizers	21
Scheme 1.14 Diels–Alder Cycloaddition Catalyzed by a Cyanoarene Sensitizer.....	22
Scheme 1.15 Cyclopropane Isomerization Catalyzed by a Cyanoarene Sensitizer	22
Scheme 1.16 Excited-State Protonation Catalyzed by a VANOL-Derived Sensitizer	23
Scheme 1.17 Polar Photoaddition Catalyzed by an Acridinium Sensitizer.....	24
Scheme 1.18 Intramolecular [2+2] Cycloaddition Catalyzed by an Atropisomeric Thiourea Sensitizer.....	25
Scheme 1.19 Cyclopropane Isomerization Catalyzed by an Aryl Ketone Sensitizer.....	25
Scheme 1.20 Oxa-di- π -methane Rearrangement Catalyzed by an Aryl Ketone Sensitizer	26

Scheme 1.21 Intramolecular [2+2] Cycloaddition Catalyzed by a Hydrogen-Bonding Ketone Sensitizer.....	27
Scheme 1.22 Intramolecular [2+2] Cycloaddition via a Hydrogen-Bonding Amide Template...	28
Scheme 1.23 Intramolecular Cyclization Catalyzed by a Hydrogen-Bonding Benzophenone Sensitizer.....	30
Scheme 1.24 Intramolecular [2+2] Cycloaddition Catalyzed by a Xanthone Sensitizer	31
Scheme 1.25 Intermolecular [2+2] Cycloaddition Catalyzed by a Xanthone Sensitizer	32
Scheme 1.26 Intermolecular [2+2] Cycloaddition Catalyzed by a Thioxanthone Sensitizer.....	33
Scheme 1.27 Aza-Paternò-Büchi Reaction Catalyzed by a Thioxanthone Sensitizer	33
Scheme 1.28 Allene Deracemization Catalyzed by a Thioxanthone Sensitizer.....	35
Scheme 1.29 Primary Allene Amide Deracemization Catalyzed by a Thioxanthone Sensitizer .	35
Scheme 1.30 Sulfoxide Deracemization Catalyzed by a Xanthone Sensitizer	36
Scheme 1.31 Di- π -Methane Rearrangement–Cyclopropane Deracemization Cascade Catalyzed by a Thioxanthone Sensitizer.....	36
Scheme 1.32 Cyclopropane Deracemization Catalyzed by a Thioxanthone Sensitizer	37
Scheme 1.33 Intermolecular [2+2] Cycloadditions Catalyzed by a BINOL-Derived Thioxanthone Sensitizer.....	38
Scheme 1.34 Intermolecular [2+2] Cycloaddition of Iminium Ions Catalyzed by a BINOL-Derived Thioxanthone Sensitizer.....	39
Scheme 1.35 1,2-Diamine Synthesis Catalyzed by a BINOL-Derived Thioxanthone Sensitizer	40
Scheme 1.36 Electron Donor–Acceptor Complex Formation and Excitation	41
Scheme 1.37 Aldehyde α -Alkylation via EDA Complex Excitation	42
Scheme 1.38 Photoinduced Enamine Catalysis Mechanisms	42
Scheme 1.39 Ketone α -Alkylation via EDA Complex Excitation	43
Scheme 1.40 Aldehyde α -Alkylation via Direct Enamine Excitation.....	44
Scheme 1.41 Aldehyde α -Alkylation Promoted by a Bifunctional Photoaminocatalyst.....	44
Scheme 1.42 Enal β -Alkylation via Direct Iminium Ion Excitation	45

Scheme 1.43 Enal β -Alkylation Mechanism	46
Scheme 1.44 Cyclopentanol Synthesis via Iminium Ion Catalysis	47
Scheme 1.45 Cascade Reaction via Iminium Ion Catalysis	48
Scheme 1.46 C–H Functionalization of Toluene Derivatives via Iminium Ion Catalysis	48
Scheme 1.47 EDA Complex Formation with Iminium Electron Acceptors	49
Scheme 1.48 Intermolecular [2+2] Cycloaddition via a Chiral Iminium Chromophore.....	50
Scheme 1.49 Hydroetherification via Chiral Ion-Pairing Catalysis	52
Scheme 1.50 [3+2] Cycloaddition via Chiral Ion-Pairing Catalysis	52
Scheme 1.51 Diels–Alder Cycloaddition Catalyzed by an Oxopyrylium Sensitizer	53
Scheme 1.52 Dicarbofunctionalization of Enamides via Ion-Pairing Catalysis.....	54
Scheme 1.53 Toluene Functionalization via Excitation of Benzopyrylium Intermediates	55
Scheme 1.54 Perfluoroalkylation of Enolates via Ion-Pairing Catalysis.....	56
Scheme 1.55 Aerobic Oxidation of β -Ketoesters via Ion-Pairing Catalysis	57
Scheme 2.1 Asymmetric acid-catalyzed photoreactions. a, Intramolecular [2+2] photocycloadditions via Lewis acid-catalyzed chromophore activation; LA = Lewis acid. b, Intermolecular [2+2] photocycloadditions via Lewis acid-catalyzed triplet activation. c, Intermolecular [2+2] photocycloadditions via Bronsted acid-catalyzed chromophore activation; HA = Brønsted acid.	78
Scheme 2.2 Optimization Studies. ^a Yields and diastereomer ratios determined by ¹ H NMR spectroscopy. ^b Enantiomeric excess of the major diastereomer determined by chiral HPLC. ^c Ratio of trans-cis isomer to trans-trans isomer. ^d Conducted at room temperature. ^e Conducted in the dark.	80
Scheme 2.3 Scope Studies. Reactions conducted using 1 equiv 2-acyl imidazole, 10 equiv alkene, 20 mol% 2.4 in toluene, irradiating for 14 h with a Kessil H150 LED unless otherwise noted. Yields represent the isolated yield of both diastereomers. Enantiomeric excess of the major diastereomer determined by chiral HPLC. ^a Conducted for 24 h.	82
Scheme 2.4 Scope Studies. Reactions conducted using 1 equiv 2-acyl imidazole, 10 equiv alkene, 20 mol% 2.4 in toluene, irradiating for 14 h with a Kessil H150 LED unless otherwise noted. Yields represent the isolated yield of both diastereomers. Enantiomeric excess of the major diastereomer determined by chiral HPLC. ^a Conducted for 24 h. ^b Conducted with 40 mol% acid catalyst 2.4 . ^c Conducted in CH ₂ Cl ₂	83

Scheme 2.5 Auxiliary Cleavage. The imidazolyl group of the cycloadduct is readily cleaved in good yield with retention of enantioselectivity.....	84
Scheme 2.6 Effect of structurally diverse Brønsted acids on the cycloaddition. Yields and diastereomer ratios determined by ¹ H NMR spectroscopy.....	86
Scheme 3.1 (A) Chemical structures of dimeric cyclobutane natural products. (B) Chemical structures of pseudo-dimeric cyclobutane natural products. (C) Synthetic strategies towards truxinate and truxillate natural products. (D) Selectivity challenges in asymmetric heterodimerization reactions. (E) Synthesis of pseudo-dimeric cyclobutane natural products via enantioselective photocycloadditions.	287
Scheme 3.2 Optimization, substrate scope, and cleavage for the enantioselective dimerization reaction. ^a 5mol% catalyst.	291
Scheme 3.3 Total syntheses of dimeric truxinate natural products.	293
Scheme 3.4 Heterodimerization scope and synthesis of piperarborenine D. ^a Reaction conducted at -78 °C.	296
Scheme 3.5 Mechanistic studies. Competition experiment between homo- and heterodimerization as a function of acid loading (top). Approaches of ground-state coupling partner leading to both diastereomers for the heterodimerization (bottom left). Approaches of ground-state coupling partner leading to both diastereomers for the homodimerization (bottom right).....	298
Scheme 3.6 Monomethylation of 3.4 in toluene.....	369
Scheme 3.7 Monomethylation approach gives access to enantiopure, unsymmetrically substituted cyclobutanes from dimerization.....	369
Scheme 4.1 Biosynthetic proposal for sceptrin.	510
Scheme 4.2 Key all-trans cyclobutane intermediates in previous sceptrin syntheses.....	511
Scheme 4.3 Proposed synthetic route to sceptrin.	513
Scheme 4.4 Aldol condensation to form substrate for cycloaddition.....	513
Scheme 4.5 Optimization of photochemical [2+2] cycloaddition.....	514
Scheme 4.6 Attempts at benzyl deprotection	515
Scheme 4.7 Asymmetric sceptrin synthesis by Baran.....	516
Scheme 4.8 Asymmetric sceptrin synthesis by Chen.....	517
Scheme 4.9 Racemic synthesis of sceptrin by Jamison.....	518

Table of Tables

Table 2.1 Crystal data and structure refinement for yoon61	151
Table 2.2 Fractional Atomic Coordinates ($\times 10^4$) and Equivalent Isotropic Displacement Parameters ($\text{\AA}^2 \times 10^3$) for yoon61. U_{eq} is defined as 1/3 of the trace of the orthogonalised U_{IJ} tensor.	153
Table 2.3 Anisotropic Displacement Parameters ($\text{\AA}^2 \times 10^3$) for yoon61. The Anisotropic displacement factor exponent takes the form: $-2\pi^2[h^2a^{*2}U_{11}+2hka^*b^*U_{12}+\dots]$	154
Table 2.4 Bond Lengths for yoon61.....	155
Table 2.5 Bond Angles for yoon61	156
Table 2.6 Torsion Angles for yoon61	157
Table 2.7 Hydrogen Atom Coordinates ($\text{\AA} \times 10^4$) and Isotropic Displacement Parameters ($\text{\AA}^2 \times 10^3$) for yoon61	159
Table 2.8 Crystal data and structure refinement for yoon62a.....	166
Table 2.9 Fractional Atomic Coordinates ($\times 10^4$) and Equivalent Isotropic Displacement Parameters ($\text{\AA}^2 \times 10^3$) for yoon62a. U_{eq} is defined as 1/3 of of the trace of the orthogonalised U_{IJ} tensor.....	168
Table 2.10 Anisotropic Displacement Parameters ($\text{\AA}^2 \times 10^3$) for yoon62a. The Anisotropic displacement factor exponent takes the form: $-2\pi^2[h^2a^{*2}U_{11}+2hka^*b^*U_{12}+\dots]$	172
Table 2.11 Bond Lengths for yoon62a.....	176
Table 2.12 Bond Angles for yoon62a	179
Table 2.13 Hydrogen Bonds for yoon62a	182
Table 2.14 Torsion Angles for yoon62a.....	182
Table 2.15 Hydrogen Atom Coordinates ($\text{\AA} \times 10^4$) and Isotropic Displacement Parameters ($\text{\AA}^2 \times 10^3$) for yoon62a.....	186
Table 2.16 Atomic Occupancy for yoon62a	190
Table 2.17 TDDFT calculated singlet excited states for 2.1 . Only orbital contributions > 10% are shown.	193
Table 2.18 TDDFT calculated singlet excited states for 2.1–H⁺–2.41 . Only orbital contributions > 10% are shown.....	194
Table 3.1 Crystal data and structure refinement for yoon59a.....	376

Table 3.2 Fractional Atomic Coordinates ($\times 10^4$) and Equivalent Isotropic Displacement Parameters ($\text{\AA}^2 \times 10^3$) for yoon59a. U_{eq} is defined as 1/3 of the trace of the orthogonalised U_{ij} tensor.....	377
Table 3.3 Anisotropic Displacement Parameters ($\text{\AA}^2 \times 10^3$) for yoon59a. The Anisotropic displacement factor exponent takes the form: $-2\pi^2[h^2a^{*2}U_{11}+2hka^*b^*U_{12}+\dots]$	379
Table 3.4 Bond Lengths for yoon59a.....	380
Table 3.5 Bond Angles for yoon59a.....	381
Table 3.6 Torsion Angles for yoon59a.....	382
Table 3.7 Hydrogen Atom Coordinates ($\text{\AA} \times 10^4$) and Isotropic Displacement Parameters ($\text{\AA}^2 \times 10^3$) for yoon59a.....	384
Table 3.8 Crystal data and structure refinement for Yoon70a.....	390
Table 3.9 Fractional Atomic Coordinates ($\times 10^4$) and Equivalent Isotropic Displacement Parameters ($\text{\AA}^2 \times 10^3$) for Yoon70a. U_{eq} is defined as 1/3 of the trace of the orthogonalised U_{ij} tensor.....	391
Table 3.10 Anisotropic Displacement Parameters ($\text{\AA}^2 \times 10^3$) for Yoon70a. The Anisotropic displacement factor exponent takes the form: $-2\pi^2[h^2a^{*2}U_{11}+2hka^*b^*U_{12}+\dots]$	393
Table 3.11 Bond Lengths for Yoon70a.....	394
Table 3.12 Bond Angles for Yoon70a.....	395
Table 3.13 Torsion Angles for Yoon70a.....	396
Table 3.14 Hydrogen Atom Coordinates ($\text{\AA} \times 10^4$) and Isotropic Displacement Parameters ($\text{\AA}^2 \times 10^3$) for Yoon70a.....	398
Table 3.15 Atomic Occupancy for Yoon70a.....	400
Table 3.16 ^1H NMR Comparison between Synthetic and Natural Isatisycloneolignan A.....	458
Table 3.17 ^{13}C NMR Comparison between Synthetic and Natural Isatisycloneolignan A.....	459
Table 3.18 ^1H NMR Comparison between Synthetic and Natural Nigramide R.....	459
Table 3.19 ^{13}C NMR Comparison between Synthetic and Natural Nigramide R.....	460
Table 3.20 ^1H NMR Comparison between Synthetic and Natural Barbarumamide C.....	461
Table 3.21 ^{13}C NMR Comparison between Synthetic and Natural Barbarumamide C.....	461
Table 3.22 ^1H NMR Comparison between Synthetic and Natural Piperarborenine D.....	462

Table 3.23 ^{13}C NMR Comparison between Synthetic and Natural Piperarborenine D	463
--	-----

Chapter 1 Chiral Organic Photocatalysts in Asymmetric Photochemical Synthesis

1.1 Previous Publication of this Work

Portions of this work have been published previously:

Genzink, M. J.; Kidd, J. B.; Swords, W. B.; Yoon, T. P. Chiral Photocatalyst Structures in Asymmetric Photochemical Synthesis. *Chem. Rev.* **2022**, *122*, 1654–1716.

1.2 Introduction

The chirality of a molecule can have a profound influence on its biological and physical properties. Methods that produce enantiomerically enriched products from achiral starting materials are therefore of particular importance for the synthesis of a variety of materials, including drug molecules, agrochemicals, and polymers. The 2001 Nobel Prize for Chemistry, awarded for the development of the field of asymmetric catalysis, underscores the centrality of this problem in contemporary synthetic chemistry.^{1–3} Several decades of sustained interest in enantioselective reaction method development has resulted in the elucidation of a large number of structurally diverse chiral catalyst architectures that effectively control stereochemical outcomes in almost every class of synthetically important transformation.

Photochemical reactions offer a conspicuous exception to this general trend. The emergence of general strategies for enantioselective catalytic photoreactions is a relatively recent development, and the variety of organic photoreactions that can be conducted in a highly enantioselective manner remains comparatively limited. This is despite the long fascination chemists have had with light-promoted reactions, both because of the distinctive reactive intermediates that are most readily available by photochemical activation, and because photochemical reactions often result in topologically complex molecular architectures that can be synthesized in no other way.^{4–6} It stands to reason, therefore, that there exist complications specific to enantioselective catalytic photochemical reactions in comparison to better-established

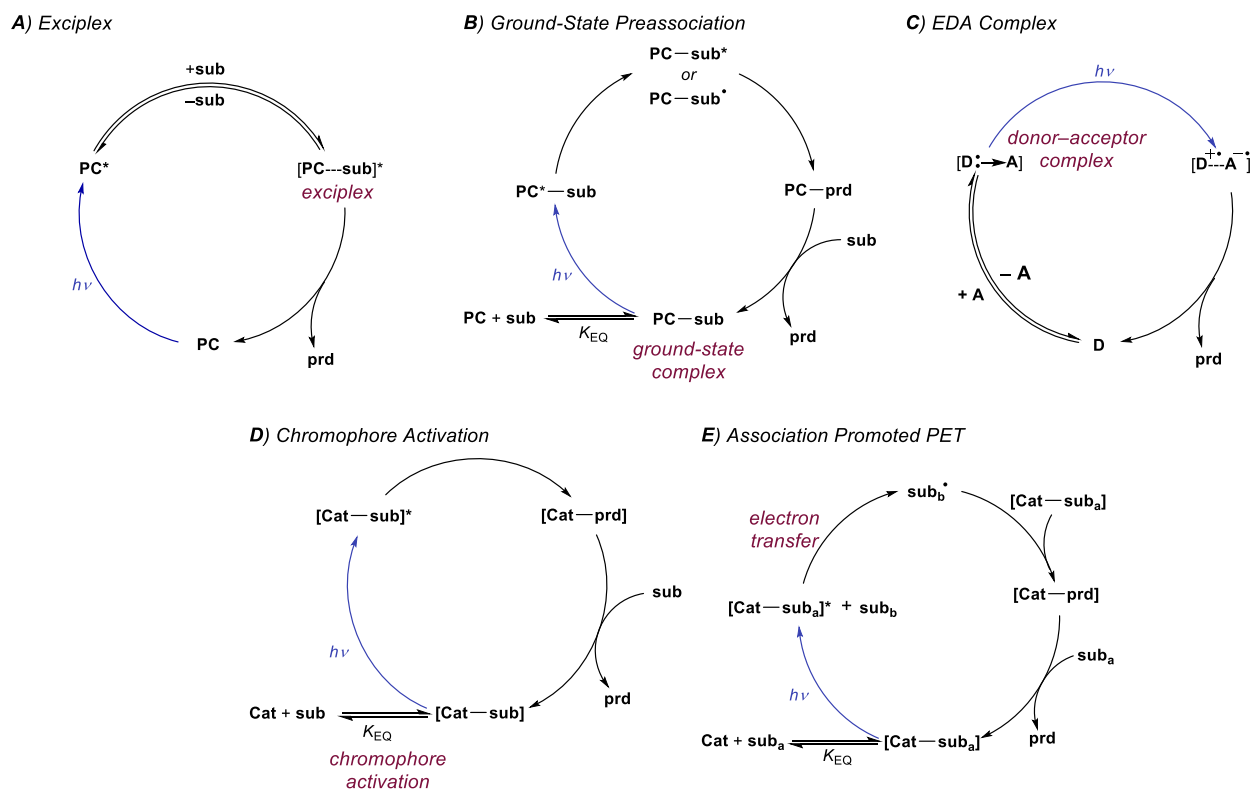
asymmetric ground-state reactions. Correspondingly, the chiral catalyst structures that have proven to be most effective in asymmetric photochemistry have often been structurally unique.

One central challenge common to all areas of asymmetric catalysis is the problematic participation of racemic background processes. Product-forming reaction pathways that occur outside of the stereodifferentiating environment of a chiral catalyst necessarily result in racemic products. Thus, no matter how enantioselective a catalytic process might be, the enantioselectivity of the overall reaction is diminished if background processes are competitive. There are two features specific to photochemical activation that are uniquely challenging in this regard. The first is the possibility of competitive direct photoexcitation. If an achiral substrate molecule directly absorbs light under the conditions of a catalytic photoreaction, the resulting photoexcited species can react to give racemic product prior to interacting with the chiral catalyst. Second, many of the most widely exploited photocatalytic systems operate via collisional activation mechanisms. When a photocatalyst activates an organic substrate by a diffusional electron- or energy-transfer event, the encounter complex is typically short-lived. If dissociation of the deactivated photocatalyst and activated substrate is faster than the rate of subsequent bond formation, any chiral information associated with the photocatalyst cannot influence the stereochemical outcome of the reaction.

Thus, early investigations of catalytic asymmetric photochemistry that introduced chiral elements into well-studied organic sensitizers met with limited success.^{7,8} Examples that resulted in measurable stereinduction generally involved the formation of an exciplex, where a donor–acceptor interaction between the substrate and excited-state photocatalyst results in the formation of a longer-lived excited-state complex. Because the exciplex extends the lifetime of the encounter complex, product-formation can occur within the chiral environment of the photocatalyst. These studies provided a valuable proof-of-principle for the possibility of

photocatalytic stereinduction but suffered from low enantiomeric excess (ee) due to ill-defined substrate–catalyst interactions and relatively short exciplex lifetimes.

Highly enantioselective catalytic photoreactions have become increasingly common over the past two decades. A guiding strategy that underlies many of the most successful methods in asymmetric photocatalysis is the preassociation principle originally articulated for macromolecular photoactive hosts by Inoue⁹ and expanded for small molecule asymmetric photocatalysis by Krische.¹⁰ This principle argues that the participation of background product-forming pathways will be minimized when a chiral photocatalyst is capable of binding the substrate in the ground state. If the substrate in the complex is excited — either by direct excitation or sensitization — more readily than the free substrate, and if the rate of the photoreaction is faster than the rate of disassociation of the complex, then product formation will predominantly occur within the chiral environment of the photocatalyst with minimal competition from racemic background processes. Although Krische’s seminal example utilized hydrogen-bonding interactions as a strategy to enforce preassociation, many other strategies have subsequently been reported. These include the formation of electron donor–acceptor (EDA) complexes, where the formation of a ground-state association is driven by charge transfer between the catalyst and substrate; chromophore activation, where coordination of a chiral catalyst to a substrate results in a new compound with altered light-absorbing properties; and association-induced photoinduced electron transfer (PET), where photon absorption is followed by a redox cascade generating reactive radicals that react with a ground-state activated substrate. (**Scheme 1.1**). The research area of asymmetric photochemistry has been the subject of several previous reviews.^{11–20}



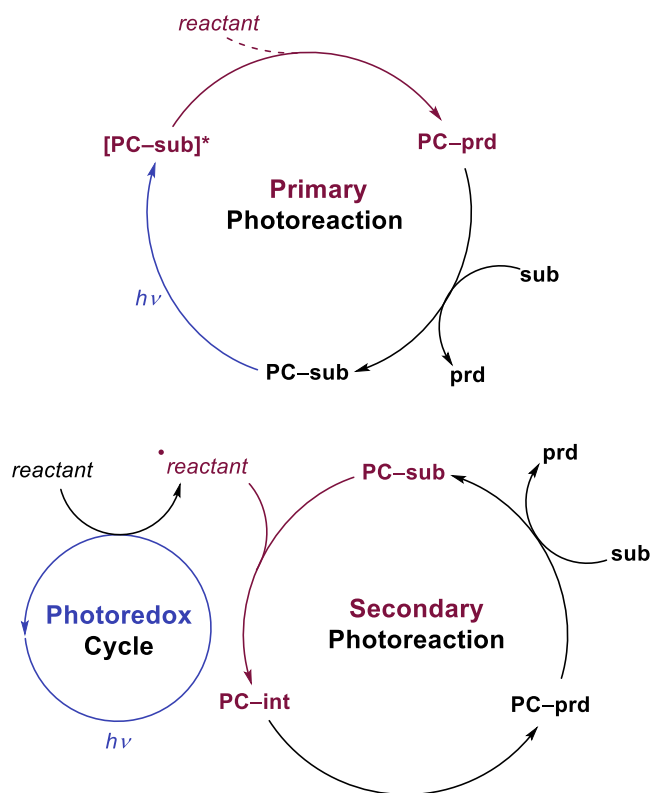
Scheme 1.1 General Mechanisms of Enantiocontrol by Chiral Chromophores in Asymmetric Photocatalysis

While some privileged catalyst structures have proven to be equally applicable to both ground-state and excited-state asymmetric reactions, the challenges specific to photochemical activation have required the invention of novel catalyst structures. This chapter seeks to provide an examination of the field of catalytic enantioselective photochemistry through the lens of the structures that have proven to be useful as chiral photocatalysts.

The term “photocatalysis” has been used in a somewhat ambiguous fashion throughout the literature of synthetic photochemistry. In this chapter, a broad definition of photocatalysis is adopted and any enantioselective catalytic reaction where the stereoinducing chiral catalyst forms part of the light-absorbing complex is covered, regardless of the photophysical properties of the species in isolation. Dual-catalytic reactions where the chromophore and the chiral stereoinducing co-catalyst are separate molecular entities are excluded; this topic has been reviewed previously.²¹

The scope of this chapter is also limited to solution-phase photoreactions catalyzed by small-molecule organic photocatalysts; stereoselective photochemistry in the solid state is a broad topic and merits separate treatment.^{22–24}

There are also important distinctions that can be made among the mechanisms of photocatalytic reactions involving the nature of the reactive intermediates participating in the key bond-forming events. Primary photoreactions are those that involve bond-forming processes of organic compounds in their electronically excited states. These are distinct from secondary photoreactions, in which the key bond-forming processes are those of photochemically generated reactive intermediates such as radicals or radical ions in their electronic ground states (**Scheme 1.2**). While the reactivity patterns available from primary and secondary photoreactions differ significantly, it can sometimes be challenging to unambiguously determine which is operative in a given photoreaction. This chapter thus covers both classes of photocatalytic reactions, and the organization of the topics centers on the structure of the chiral catalyst rather than on mechanistic considerations.

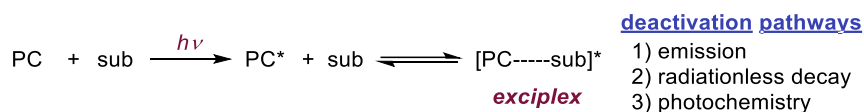


Scheme 1.2 Primary Versus Secondary Photoreactions

1.3 Arenes

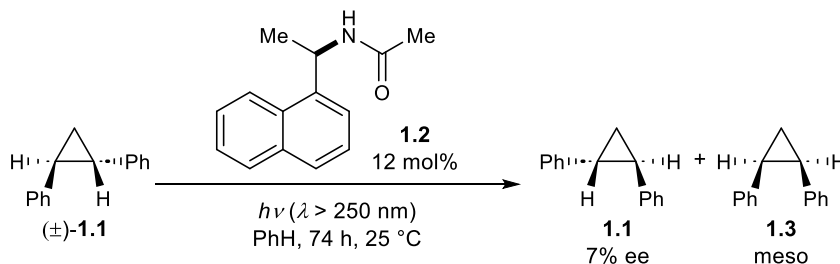
Much of the early work in asymmetric photochemistry involved the use of chiral arene sensitizers capable of forming exciplexes. An exciplex is an electronically excited molecular complex formed between two species that are not associated in the ground state but are held together by charge-transfer interactions in the excited state (**Scheme 1.3**).²⁵ Exciplexes have unique photophysical properties relative to their individual components. They have the potential to fluoresce (singlet exciplex) and phosphoresce (triplet exciplex), undergo radiationless decay, or chemically react to form a new species.²⁶ Hence, the best spectroscopic evidence for the formation of an exciplex is the observation of quenching of the sensitizer fluorescence and the appearance of a new emission band that does not correspond to the emission of either component of the exciplex

in isolation. Notably, substrate activation via exciplex formation is mechanistically distinct from energy transfer. In an exciplex, the exciton is shared between the sensitizer and the substrate, while during energy transfer, the exciton is transferred from the sensitizer to the substrate, resulting in a ground-state sensitizer.



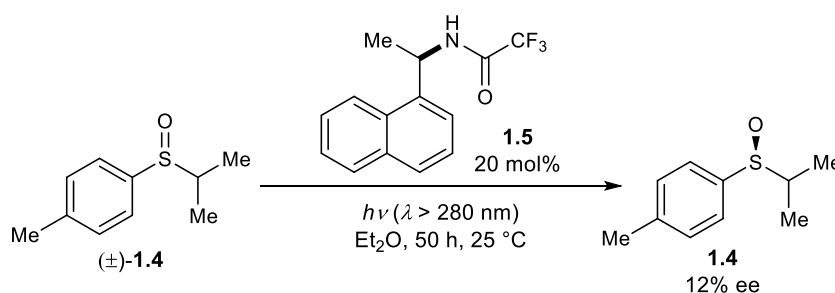
Scheme 1.3 Exciplex Formation and Deactivation Pathways

Hammond reported one of the first examples of an enantioselective photoreaction in 1965 (Scheme 1.4).²⁷ An optically active naphthylamide sensitizer (**1.2**) effects the isomerization of cyclopropane **1.1** to a mixture of *cis*- and optically enriched *trans*-1,2-diphenylcyclopropanes upon irradiation with UV light. Notably, only a 12 mol% loading of **1.2** gives **1.1** in 7% ee.^{28,29} Naphthylamides bound to silica were also tested as isomerization catalysts, but the enantioselectivity was reduced to 1% ee.³⁰ Hammond initially proposed a triplet sensitization mechanism where different energy-transfer rate constants from the chiral sensitizer to (*R*)- and (*S*)-**1.1** lead to enantioenrichment.³¹⁻³³ However, it was later shown that the reaction proceeds through a singlet exciplex.³⁴ Interconversion of (*R*)- and (*S*)-**1.1** likely occurs via cleavage of the excited cyclopropane to a 1,3-diradical followed by ring-closure.



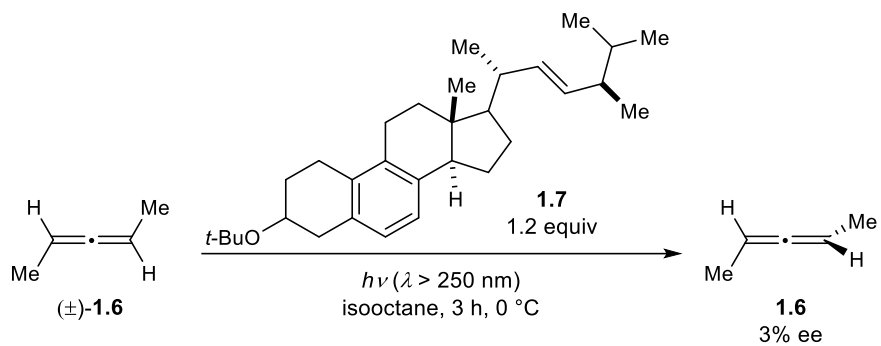
Scheme 1.4 Cyclopropane Isomerization Catalyzed by a Naphthylamide Sensitizer

Naphthylamide sensitizers were also studied by Kagan for their ability to deracemize sulfoxides (**Scheme 1.5**). When racemic sulfoxide **1.4** is irradiated in the presence of **1.5**, the optical purity of the recovered substrate is modestly enriched (12% ee).^{35,36} Mechanistic studies on sulfoxide racemization performed by Hammond suggest that this deracemization proceeds through a singlet exciplex.³⁷⁻³⁹ The excited-state configurational lability of the sulfoxide could arise either from direct inversion via a planar electronically excited sulfoxide or from α -cleavage and subsequent radical–radical recombination.^{40,41}



Scheme 1.5 Sulfoxide Deracemization Catalyzed by a Naphthylamide Sensitizer

Several chiral naphthylamide sensitizers were also examined in the 1,5-aryl shift, di- π -methane cascade rearrangement of racemic oxepinones. The ratio of sensitization rate constants ($k_R/k_S = 1.04$) suggests an enantioselective transformation, but the ee of the product was not measured.⁴² Weiss reported the deracemization of 2,3-pentadiene (**1.6**) catalyzed by chiral aromatic steroid **1.7** (**Scheme 1.6**).⁴³ Allenes are axially chiral and configurationally stable in the ground state but can undergo stereochemical inversion via a planar, achiral excited state. The authors did not fully elucidate the mechanism but did note that singlet and triplet sensitization from the chiral sensitizer is thermodynamically endergonic.



Scheme 1.6 Allene Deracemization Catalyzed by a Steroid Sensitizer

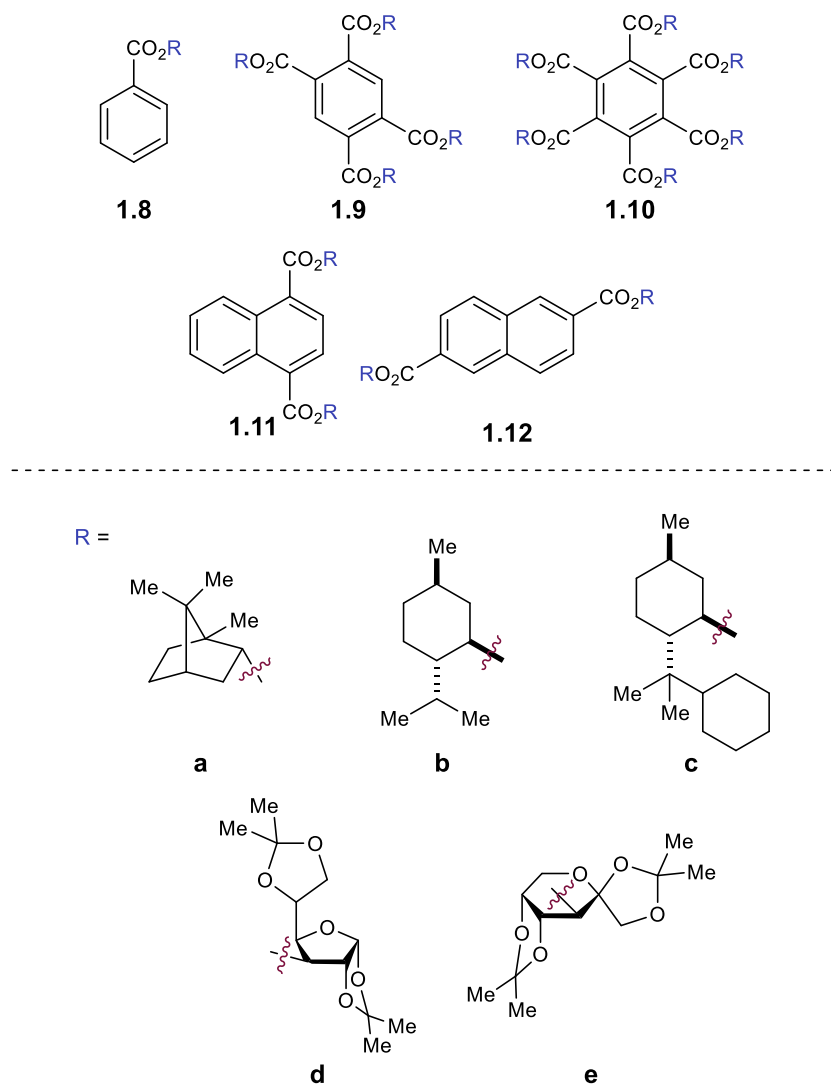
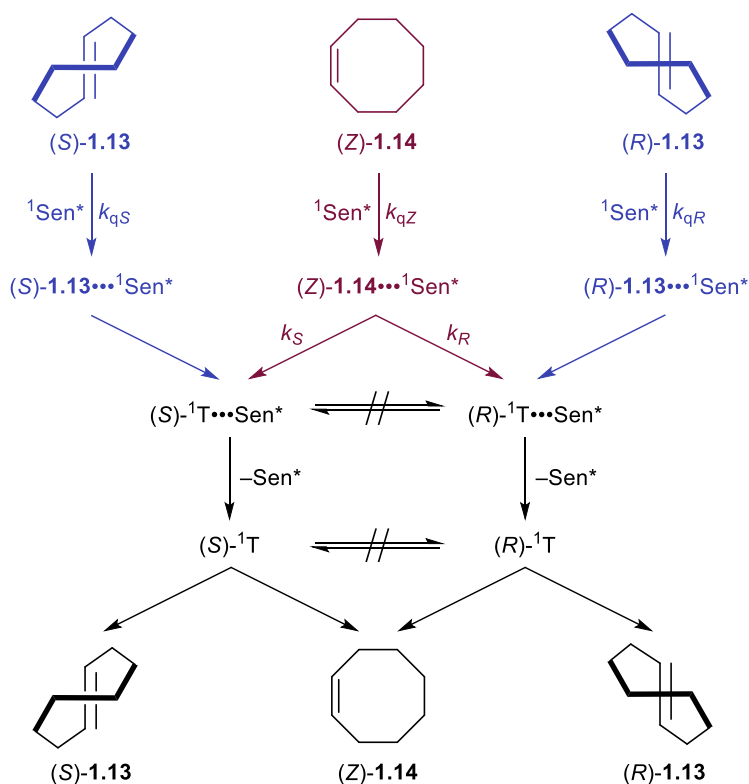


Figure 1.1 Selected Examples of Chiral Benzenecarboxylate Sensitizers

Inoue studied the photochemical isomerization of achiral (*Z*)-cyclooctene (**1.14**) to chiral (*E*)-cyclooctene (**1.13**) using benzenecarboxylates as singlet exciplex sensitizers (**Figure 1.1**).^{44,45} Initial reports described the production of (*E*)-cyclooctene in low ee (4% ee), but this process provided the opportunity to study the mechanism of stereinduction in detail.^{46,47} The isomerization proceeds through a singlet exciplex consisting of the excited photocatalyst and cyclooctene (**Scheme 1.7**). Rotational relaxation within the initial exciplex produces one of two diastereomeric exciplexes featuring a chiral twisted excited cyclooctene ((*S*) or (*R*)-¹T). While the exciplex-bound (*Z*)-cyclooctene may decay to either twisted diastereomeric complex, exciplex-bound (*S*)- or (*R*)-cyclooctene decay to the respective (*S*)- or (*R*)-¹T. After sensitizer dissociation, the excited twisted cyclooctene decays to either (*Z*)- or (*E*)-cyclooctene. An enantioselective transformation is achieved as there exists no route for the direct interconversion between the diastereomeric (*R*)- and (*S*)-twisted-cyclooctene exciplexes without first reforming (*Z*)-cyclooctene. Thus, the enantiodetermining step of this process could be either (1) sensitizer quenching by (*E*)-cyclooctene to form diastereomeric exciplexes (k_{qS} vs. k_{qR}) or (2) stereoselective rotational relaxation from (*Z*)-cyclooctene to the diastereomeric twisted exciplex intermediates (k_S vs. k_R). A kinetic resolution of (*E*)-cyclooctene produced in situ from (*Z*)-cyclooctene was attempted to distinguish these possibilities. If different sensitizer quenching rates by (*E*)-cyclooctene dictate enantioselectivity, then an increase in ee over the course of the reaction is expected. On the other hand, if the ee is invariant with time the enantioselectivity is the result of different rates of rotational relaxation from the (*Z*)-cyclooctene exciplex to the twisted-cyclooctene exciplexes. No change in the ee was observed over the course of the reaction, implying that rotational relaxation of the (*Z*)-exciplex is the enantiodetermining step.

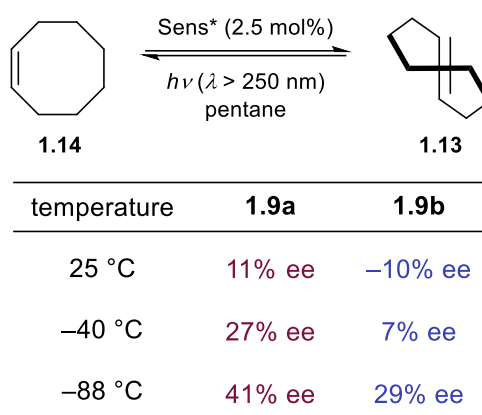


Scheme 1.7 Mechanism of Cyclooctene Isomerization Catalyzed by Benzenecarboxylate Sensitizers

The importance of the singlet exciplex for obtaining high levels of enantioselectivity was investigated using benzyl ether sensitizers, which form singlet exciplexes with (*Z*)-cyclooctene at high substrate concentrations but undergo collisional triplet energy transfer at low substrate concentrations. The ee obtained with the benzyl ethers decreases with decreasing substrate concentration, suggesting that the singlet process is more selective than the triplet. While the catalyst–substrate interaction is long-lived in the singlet exciplex due to the charge-transfer exciplex interaction, the triplet sensitized process likely only involves a fleeting interaction between the catalyst and alkene. Thus, the triplet alkene isomerizes after dissociation from the catalyst, leading to negligible asymmetric induction.⁴⁸

Extensive screening of benzenepolycarboxylate, aromatic amide, and phosphoryl ester sensitizers gave improved enantioselectivity and revealed a surprising relationship between ee and

reaction temperature (**Scheme 1.8**).⁴⁹⁻⁵² For bornyl sensitizer **1.9a**, the ee of (*E*)-cyclooctene increases with decreasing temperature, affording **1.13** in 41% ee at $-88\text{ }^{\circ}\text{C}$. For menthyl sensitizer **1.9b**, the opposite enantiomer of **1.13** is favored at $25\text{ }^{\circ}\text{C}$, but the enantioselectivity decreases with decreasing temperatures, and at $-19\text{ }^{\circ}\text{C}$ **1.13** is formed as a racemate. Below this equipodal temperature, the product chirality inverts, and the ee of the antipodal enantiomer increases with decreasing temperature. This runs contrary to the common assumption that enantioselectivity and temperature should be inversely related, which is an oversimplification of the factors controlling enantioselectivity.



Scheme 1.8 Effect of Temperature on Photosensitized Cyclooctene Isomerization

The differential Eyring equation (eq **1.1**) provides a more complete explanation of the temperature-dependent enantioselectivity.⁵³ The differential activation entropy ($\Delta\Delta S_{S-R}^{\ddagger}$) and enthalpy ($\Delta\Delta H_{S-R}^{\ddagger}$) for a given reaction are determined by plotting $\ln(k_S/k_R)$ vs. T^{-1} .⁵⁴ Here, (k_S/k_R) is the ratio of rate constants leading to the enantiomeric products and can be calculated from the enantiomeric ratio (e.r.). When the entropy and enthalpy terms have opposite signs, they favor formation of the same enantiomer; if their signs are the same, the terms favor opposite enantiomers. Notably, if the differential activation entropy is large and the entropy and enthalpy terms favor

opposite enantiomers, which is the case with **1.9b**, the favored enantiomer will switch with a change in temperature.

$$\Delta\Delta G_{S-R}^{\ddagger} = \ln\left(\frac{k_S}{k_R}\right) = \ln(\text{e. r.}) = -\Delta\Delta H_{S-R}^{\ddagger}/RT + \Delta\Delta S_{S-R}^{\ddagger}/R \quad \text{eq. 1.1}$$

For cyclooctene photoisomerization catalyzed by **1.9b**, the differential thermodynamic terms are $\Delta\Delta H_{S-R}^{\ddagger} = -0.77 \text{ kcal mol}^{-1}$ and $\Delta\Delta S_{S-R}^{\ddagger} = -1.30 \text{ cal mol}^{-1} \text{ K}^{-1}$. Therefore, at low temperatures, the enthalpy term dominates, favoring (*S*)-cyclooctene, while at higher temperatures the entropy term dominates, favoring (*R*)-cyclooctene. Further studies showed that the temperature-switching phenomenon is characteristic of *ortho*-benzenecarboxylates, and an extensive screening of these sensitizers showed **1.9c** to be optimal, giving 64% ee at $-89 \text{ }^{\circ}\text{C}$.^{55,56}

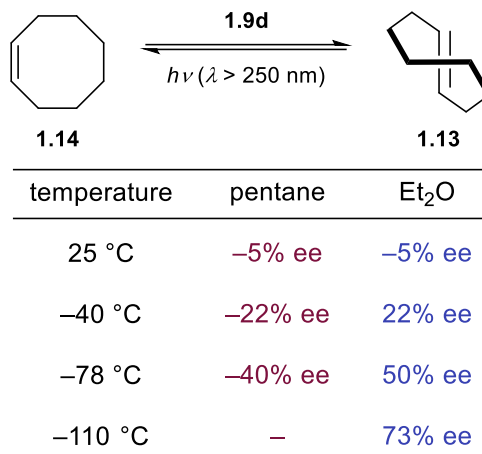
Pressure can also be used as an entropy-related tool to control enantioselectivity.^{57,58} The pressure dependence of a reaction at constant temperature is given by **eq. 1.2**:

$$\ln\left(\frac{k_S}{k_R}\right)_T = -(\Delta\Delta V_{S-R}^{\ddagger}/RT)P + C \quad \text{eq. 1.2}$$

where $\Delta\Delta V_{S-R}^{\ddagger}$ is the difference in activation volume between the diastereomeric transition states. Using **eq. 1.2**, Inoue determined $\Delta\Delta V_{S-R}^{\ddagger}$ for a variety of sensitizers.^{59,60} In general, *ortho*-benzenecarboxylates show the greatest pressure dependence on enantioselectivity, and several instances where the product chirality switches as a function of pressure were reported. With **9b**, (*R*)-cyclooctene was obtained in 11% ee at atmospheric pressure, while (*S*)-cyclooctene was obtained in 18% ee at 400 MPa. For most of the sensitizers examined, the pressure effect becomes discontinuous above 200–400 MPa, suggesting a change in mechanism of the isomerization.⁶¹ There is no observed correlation between $\Delta\Delta S_{S-R}^{\ddagger}$ and $\Delta\Delta V_{S-R}^{\ddagger}$, implying that both temperature and pressure can be optimized independently for high enantioselectivity. The optimal conditions were predicted by mathematically modeling $\ln(k_S/k_R)$ as a function of P and T⁻¹. In

theory, the maximum of the fitted three-dimensional plot corresponds to the pressure and temperature that should provide the highest ee.⁵⁹

The enantioselectivity of the reaction is relatively insensitive to solvent for most sensitizers; however, an unusual relationship was observed using saccharide sensitizer **1.9d** (**Scheme 1.9**).⁶² The isomerization was conducted in pentane and diethyl ether at several temperatures between -110 °C and 25 °C. At 25 °C, (*R*)-cyclooctene is formed in approximately 5% ee in both solvents. In pentane, the ee increases with decreasing temperatures, reaching 40% at -78 °C. On the other hand, the chirality inverts in diethyl ether with an equipodal point at -19 °C, ultimately reaching 73% ee for (*S*)-cyclooctene at -110 °C. These results can be rationalized by the signs of the differential activation entropy and enthalpy, which for pentane are both positive, while for diethyl ether are both negative. The switching of product chirality as a function of solvent was attributed to the solvation of the ether groups of the saccharide esters. Given the solvent effect on enantioselectivity, the reaction was also conducted in supercritical carbon dioxide because the solvent properties can be dramatically tuned within a relatively narrow range of pressure and temperature near the critical density. The differential activation volume was determined from **eq. 1.2**; however, the relationship between $\ln(k_S/k_R)$ and pressure is not linear over the measured pressure range, suggesting that different $\Delta\Delta V_{S-R}^\ddagger$ values exist in the near-critical and high-pressure regions.⁶³ Together, these results demonstrate how mechanistic understanding can be used to tune catalyst structure in combination with reaction conditions to optimize the enantioselectivity of a photocatalytic reaction.

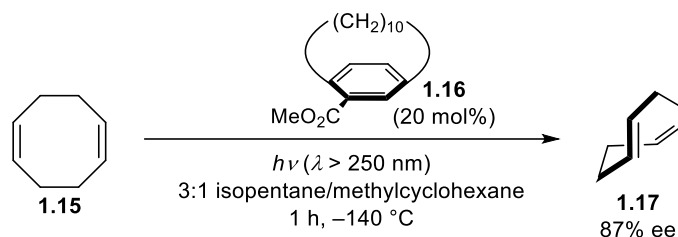


Scheme 1.9 Effect of Solvent on Photosensitized Cyclooctene Isomerization

Using the same class of benzenepolycarboxylate sensitizers, several other cyclic alkenes were subjected to the photoisomerization conditions. In the case of (*Z*)-1-methylcyclooctene, the ee does not exceed 7%.^{64,65} Compared to (*Z*)-cyclooctene, the *E/Z* ratio at the photostationary state (PSS) is low, which was attributed to greater steric destabilization in the exciplex. The *E/Z* ratios could be improved by tethering the sensitizers to the substrate in a diastereodifferentiating isomerization.^{66–68} (*Z,Z*)-1,3-Cyclooctadiene undergoes photoinduced isomerization to the *E,Z*-isomer in 18% ee using **1.10b**;⁶⁹ however, the photoisomerization of 1,5-cyclooctadiene provides only 5% ee.⁷⁰ The latter reaction is pressure-dependent, favoring (–)-(*E,Z*)-1,5-cyclooctadiene in 4% ee at atmospheric pressure and (+)-(*E,Z*)-1,5-cyclooctadiene in 4% ee at 300 MPa.⁶¹

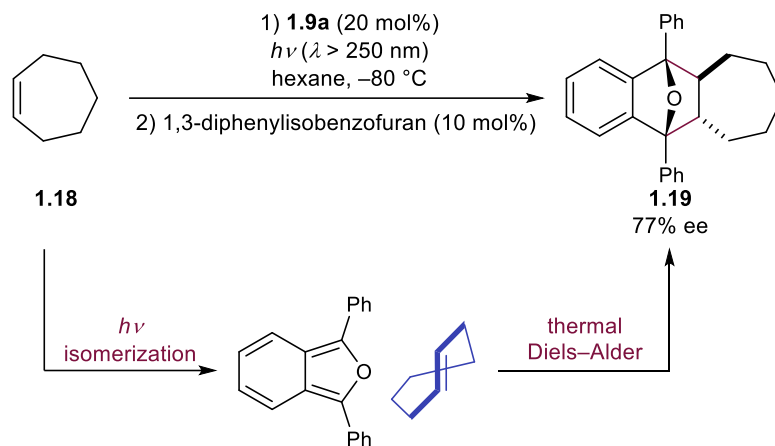
Inoue also examined planar–chiral paracyclophanes as exciplex-forming sensitizers in the photoisomerization of cyclooctenes (**Scheme 1.10**).⁷¹ Using sensitizer **1.16**, the isomerization proceeded to give photostationary *E/Z* ratios of approximately 0.01, which is smaller than observed with simpler arenecarboxylate sensitizers (0.1–0.4). The authors hypothesized that steric hindrance in the exciplex of (*E,Z*)-**1.17** compared to (*Z,Z*)-**1.15** with the bulkier paracyclophane accounts for the lower *E/Z* ratios. Spectroscopic experiments showed that

(*Z,Z*)-**1.15** efficiently quenched sensitizer **1.16** with exciplex formation confirmed by the appearance of a new emission feature. The enantioselectivity increased with decreasing temperatures, affording (*E,Z*)-**1.17** in 87% ee at $-140\text{ }^{\circ}\text{C}$.



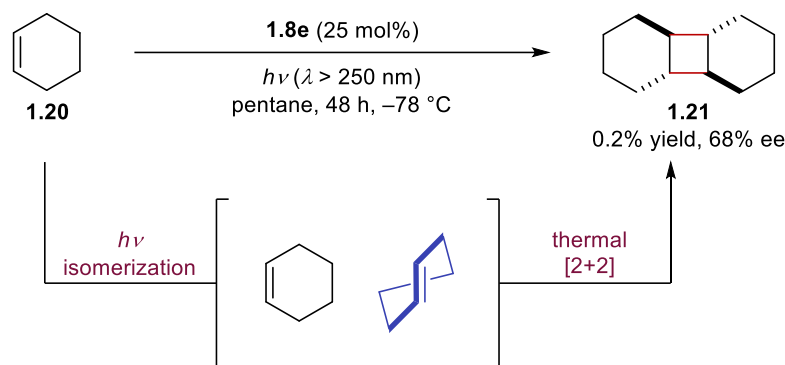
Scheme 1.10 Cyclooctene Isomerization Catalyzed by a Cyclophane Sensitizer

Cycloheptene (**1.18**) can also be photochemically isomerized using chiral arene sensitizers; however, due to the thermal instability of (*E*)-cycloheptene, the enantioselectivity was assessed by trapping with 1,3-diphenylisobenzofuran in a stereospecific Diels–Alder cycloaddition (**Scheme 1.11**).⁷² The best enantioselectivity (77% ee) was obtained with **1.9a** in hexane at $-80\text{ }^{\circ}\text{C}$. With most sensitizers, the ee was greater for (*E*)-cycloheptene than (*E*)-cyclooctene. This trend was reflected in the calculated $\Delta\Delta H_{S-R}^{\ddagger}$ and $\Delta\Delta S_{S-R}^{\ddagger}$ values, which are typically greater by a factor of 2–3 for cycloheptene than for cyclooctene. The authors concluded that the approach of cycloheptene to the photocatalyst is less hindered, enabling a more intimate interaction in the exciplex and consequently greater stereocontrol.



Scheme 1.11 Cycloheptane Isomerization and Cycloaddition Catalyzed by Benzenecarboxylate Sensitizers

Under similar photoisomerization conditions, (*Z*)-cyclohexene (**1.20**) forms a mixture of [2+2]-cycloaddimer diastereomers via initial photochemical isomerization to the (*E*)-isomer followed by thermal cycloaddition (**Scheme 1.12**).⁷³ The cycloaddition may occur by two mechanisms: a concerted, stereospecific dimerization, or a stepwise stereoablative radical dimerization. The plot of $\ln(k_S/k_R)$ vs. T^{-1} is not linear at high temperatures, which was attributed to the contribution of the stepwise mechanism. At low temperatures, however, the relationship is linear. At -78 °C, the *trans-anti-trans* isomer (**1.21**) is obtained in 68% ee using sensitizer **1.8e**. Photochemically produced (*E*)-cyclohexene also reacts with 1,3-cyclohexadiene in a thermal [4+2] cycloaddition. Complex mixtures of dimeric products are formed, and only the *exo*-[4+2] product is obtained in appreciable ee (8%).⁷⁴

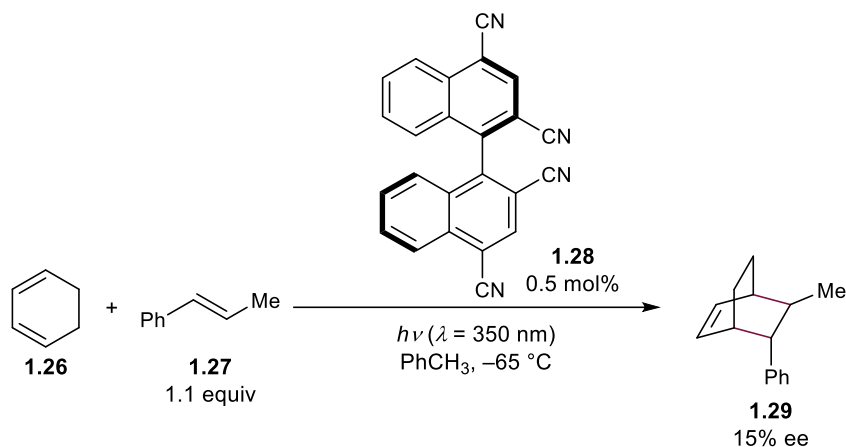


Scheme 1.12 Cyclohexane Isomerization and Cycloaddition Catalyzed by Benzenecarboxylate Sensitizers

With the insights gained from the studies of cyclic alkene isomerization discussed above, Inoue revisited the asymmetric isomerization of 1,2-diarylcyclopropanes originally reported by Hammond.²⁷ Several arenecarboxylate sensitizers were tested, but the highest reported ee for *trans*-**1.1** was 10%.^{75–77}

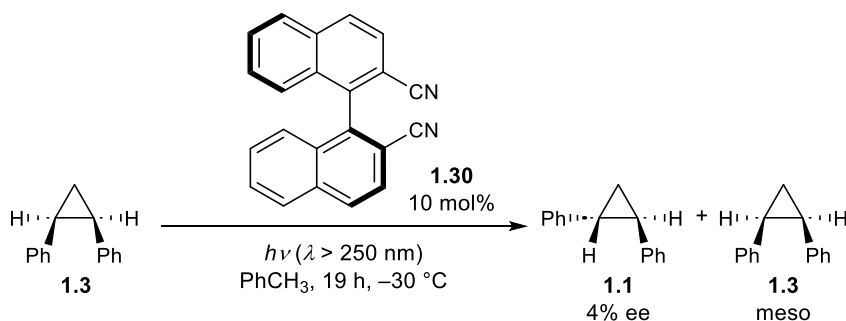
Bimolecular photoreactions are particularly difficult to control through an exciplex mechanism because the enantiodetermining step must occur in a ternary complex comprising the sensitizer and both substrates. This requirement can be satisfied by the attack of a reactant on a substrate–catalyst exciplex. Because the exciplex possesses a significant degree of charge transfer, it is often essential to conduct the reaction in nonpolar solvents to avoid dissociation into a solvent-separated radical-ion pair from which any subsequent reaction is likely to be racemic. This is problematic for electron-transfer reactions, which are slow under these conditions. Hence, it can be challenging to obtain both good yield and high ee simultaneously. This was the case in a [2+2] cycloaddition of electron-rich styrenes reported by Inoue.⁷⁸ While the reaction catalyzed by **1.9b** proceeded to high yield in CH_3CN , the negligible enantioselectivity observed was likely due to racemic reactivity from the free styrene radical cation. In pentane and ether, which both favor exciplex formation, no product was observed.

A similar effect was observed in the anti-Markovnikov photoaddition of methanol to 1,1-diphenylpropene (**1.22**). Here, nonpolar solvents give the ether product in low yield (< 10%) and high ee (up to 27%), while polar solvents afford the product in high yield (up to 60%) and low ee (< 1%).⁷⁹ As a potential solution to this problem, saccharide esters of naphthalenecarboxylic acids (**1.11d**, **1.11e**, and **1.12e**) were used as sensitizers.⁸⁰ The authors proposed that these sensitizers provide microenvironmental polarity control where the saccharide moiety creates a high-polarity region in the direct vicinity of the sensitizer, allowing for electron transfer, within a low-polarity bulk solution, ensuring that the sensitizer and substrate do not dissociate. Using these sensitizers, high enantioselectivity is maintained, while the yield is improved to 20–40%. Less hindered alcohols generally give higher yields but lower enantioselectivity (**Scheme 1.13**). The best ee (58%) was achieved with sensitizer **1.12e** using *i*-PrOH as the nucleophile, but the yield was only 1%.⁸¹ Based on computational and fluorescence quenching studies, the authors proposed that the difference in free energy between the diastereomeric sensitizer–substrate exciplexes is the primary determinant for enantioselectivity. The temperature and pressure effects on the reaction were evaluated, and similar effects were observed as with the cyclooctene isomerization.^{82–86} When the reaction is conducted in supercritical carbon dioxide, there is a sudden increase in the product ee when transitioning from the near-critical to supercritical state, indicating a substantial difference in solvent environment in this pressure region. At the critical state, there is significant solvent clustering, where the local density of CO₂ is greater around the exciplex than in the bulk solution. Further, the solvent environments for the diastereomeric exciplexes can be significantly different due to this clustering, increasing the difference in free energy. In a related intramolecular photoaddition of a tethered alcohol, this clustering behavior was manipulated by adding cosolvents



Scheme 1.14 Diels–Alder Cycloaddition Catalyzed by a Cyanoarene Sensitizer

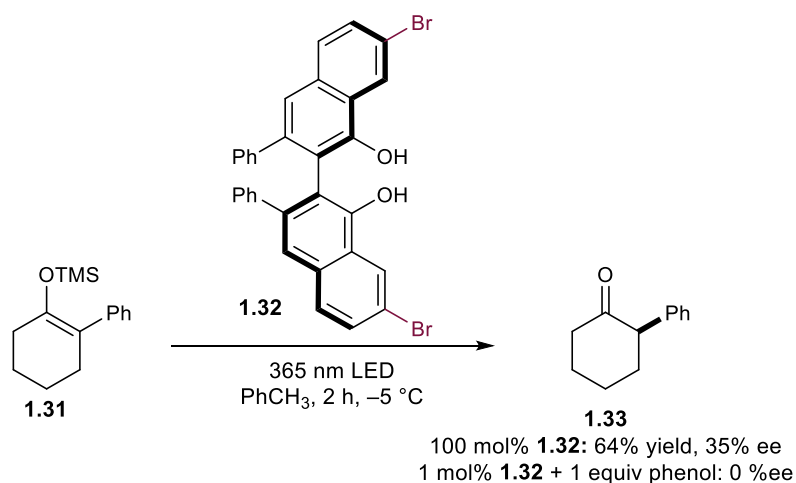
Mattay showed that a similar electron-deficient sensitizer (**1.30**) also catalyzes the enantioselective *cis-trans* isomerization of cyclopropanes (**Scheme 1.15**).^{95,96} Mechanistic experiments performed with radical cation quencher 1,2,4-trimethoxybenzene showed solvent-dependent reactivity analogous to that observed by Schuster. In toluene, in which an exciplex is formed, enantioenriched *trans*-**1.1** is obtained in 4% ee. Racemic product is obtained in MeCN, suggesting the existence of an electron-transfer mechanism that produces solvent-separated radical-ion pairs.



Scheme 1.15 Cyclopropane Isomerization Catalyzed by a Cyanoarene Sensitizer

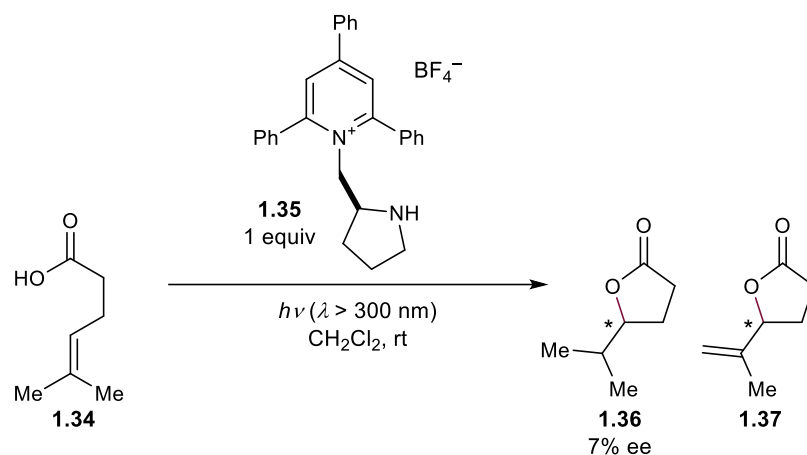
Hanson studied axially chiral VANOL-derived catalysts as excited-state proton-transfer reagents for the stereoselective protonation of silyl enol ethers (**Scheme 1.16**).⁹⁷ The shift of electron density upon excitation of the chromophore increases the acidity of the hydroxyl protons,

enabling a protonation event that would be thermodynamically unfavorable in the ground state.⁹⁸ Stoichiometric loadings of **1.32** afford ketone **1.33** in 64% yield and 35% ee. The presence of a bromine substituent on the arene backbone is necessary for productive reactivity, which was attributed to its ability to facilitate intersystem crossing. When only 1 mol% of **1.32** is used with one equiv of phenol as a sacrificial proton source, racemic product is formed. The authors hypothesized that the loss of enantioselectivity is due to excited-state proton transfer from **1.32** to phenol to create PhOH_2^+ , which then protonates the substrate.



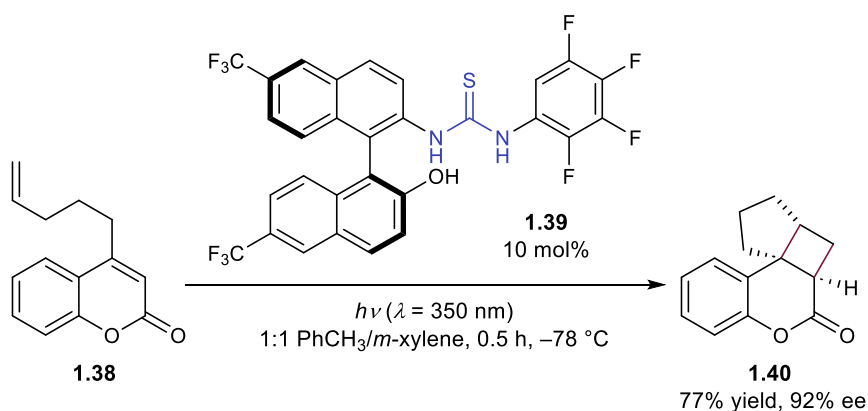
Scheme 1.16 *Excited-State Protonation Catalyzed by a VANOL-Derived Sensitizer*

Sabater studied chiral pyridinium photoredox catalysts for the cyclization of **1.34** to afford a mixture of saturated lactone **1.36** and unsaturated lactone **1.37** (Scheme 1.17). Optimal results were achieved with sensitizer **1.35**, which gave 7% ee for **1.36**.⁹⁹ The reaction proceeds through photoinduced electron transfer (PET) oxidation of the alkene to the radical cation, followed by enantiodetermining nucleophilic attack of the pendant alcohol.



Scheme 1.17 Polar Photoaddition Catalyzed by an Acridinium Sensitizer

Sivaguru, Sibi, and coworkers developed an intramolecular [2+2] photocycloaddition of 4-alkenyl coumarins (**1.38**) catalyzed by chiral thiourea **1.39** (Scheme 1.18).^{100–102} The photoadducts are produced with 77–96% ee using only 10 mol% chiral catalyst. Hydrogen bonding between the thiourea and carbonyl moieties on the catalyst and substrate organize the substrate within the chiral environment of the catalyst. Both the substrate and sensitizer efficiently absorb light, but the reaction without catalyst is slow, accounting for the lack of a significant racemic background reaction. Stern–Volmer quenching studies revealed that both static and dynamic quenching of the catalyst by the substrate is operative, and the authors proposed that both pathways lead to enantioenriched product. In the static quenching mechanism, the ground-state substrate-catalyst complex absorbs light, and the substrate undergoes cyclization. In the dynamic quenching mechanism, unbound catalyst is excited and forms a triplet exciplex with the substrate, which can undergo the cycloaddition. Sivaguru also reported the enantioselective 6π -cyclization of acrylanilides catalyzed by chiral thioureas, but the highest enantioselectivity obtained was 13% ee.¹⁰³

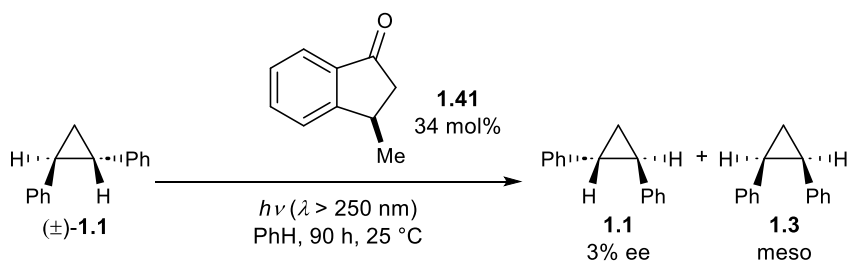


Scheme 1.18 Intramolecular [2+2] Cycloaddition Catalyzed by an Atropisomeric Thiourea Sensitizer

1.4 Ketones

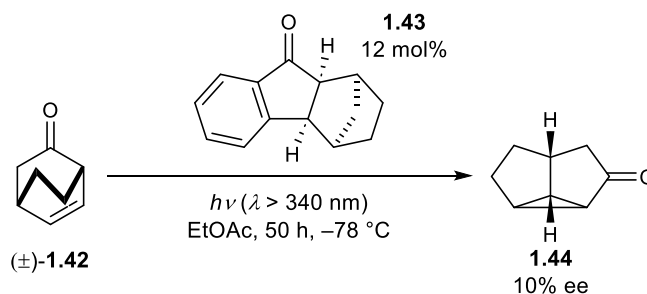
1.4.1 Ketones without Hydrogen-Bonding Domains

Aromatic ketones have fast rates of intersystem crossing and are often employed as triplet sensitizers.²⁵ Despite the high efficiency with which they sensitize a variety of organic transformations, chiral aromatic ketones without hydrogen-bonding domains have not promoted highly enantioselective reactions. This is likely because the sensitizer quickly dissociates from the excited substrate after sensitization, leading to poor stereocontrol.^{104,105} For instance, Ouannès and coworkers reported the asymmetric isomerization of **1.1** using chiral indanone triplet sensitizer **1.41** (Scheme 1.19). After 70 hours of UV irradiation, the product distribution reached a photostationary state consisting of a 3:1 ratio of *cis*:*trans* isomers and 3% ee for **1.1**.¹⁰⁶



Scheme 1.19 Cyclopropane Isomerization Catalyzed by an Aryl Ketone Sensitizer

Chiral indanone sensitizer **1.43** catalyzed the kinetic resolution of ketone **1.42** via an oxa-di- π -methane rearrangement (**Scheme 1.20**). At low temperature and low levels of conversion, the rearranged product (**1.44**) was formed in 10% ee.¹⁰⁷

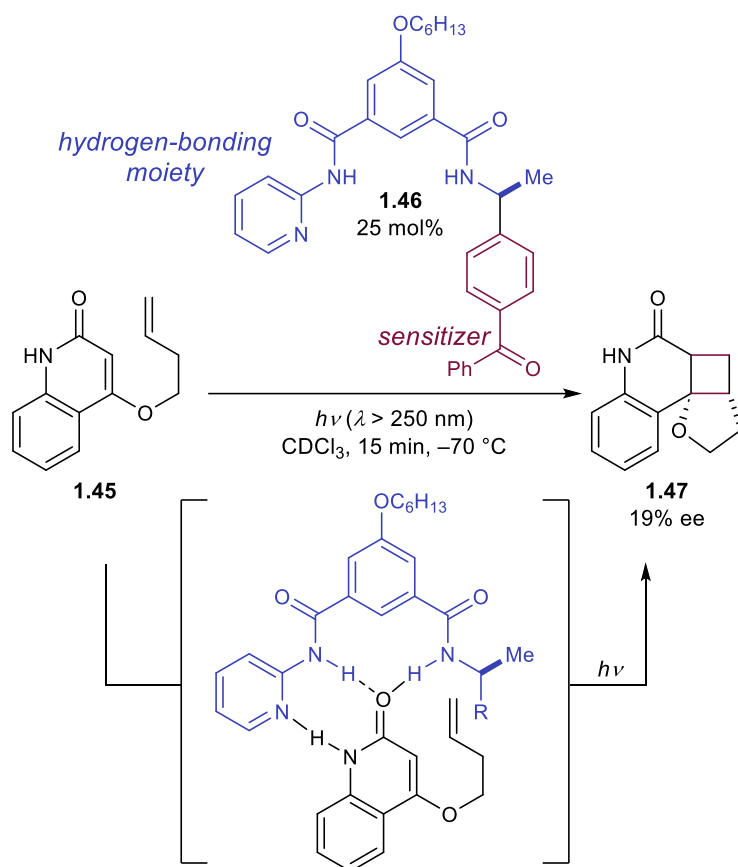


Scheme 1.20 Oxa-di- π -methane Rearrangement Catalyzed by an Aryl Ketone Sensitizer

1.4.2 Chiral Ketones with Hydrogen-Bonding Domains

Prior to 2000, most enantioselective photoreactions involved simple chiral sensitizers where the transfer of chiral information occurs within a transient excited-state interaction with limited organization. Consequently, the enantioselectivities obtained were often low, consistent with the lack of a well-defined substrate–catalyst interaction during the enantiodetermining step. In 2003, Krische proposed that two key criteria would be essential for a highly enantioselective photocatalytic reaction: (1) the substrate must exist in a well-defined chiral environment upon binding to the catalyst, and (2) the catalyst–substrate interaction must confer a kinetic advantage to the photoreaction.¹⁰ As a potential solution to the first challenge, Krische proposed that chiral hydrogen-bonding catalysts could bind a substrate in the ground state prior to excitation ensuring a well-defined chiral environment after substrate excitation. Krische hypothesized that the second criterion could also be satisfied by introducing a benzophenone triplet sensitizer within the structure of the catalyst, creating a binding-induced rate enhancement due to the distance dependence of energy transfer. With 2 equiv of catalyst **1.46**, quinolone **1.45** cyclizes to cyclobutane **1.47** in 21% ee via a [2+2] intramolecular photocycloaddition (**Scheme 1.21**).

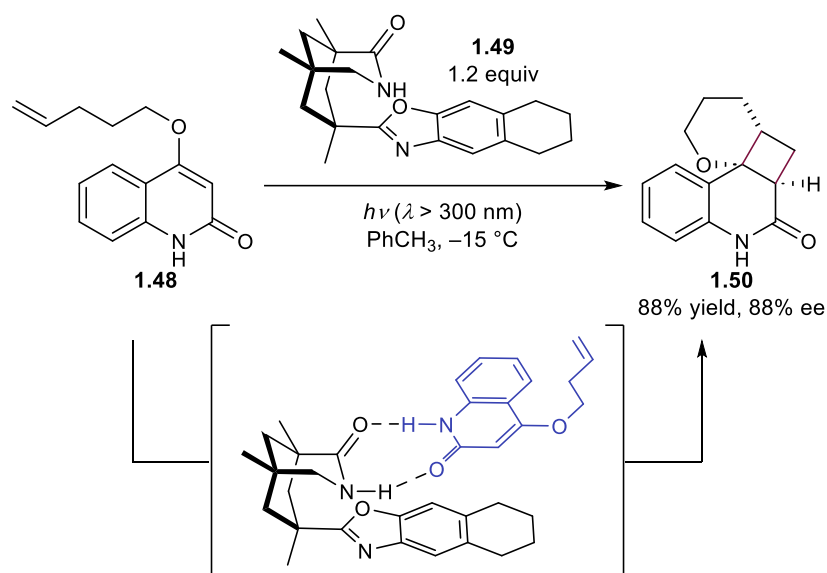
Notably, the catalyst loading could be lowered to 25 mol% with only a slight loss in enantioselectivity (19% ee). A Job plot and NMR binding studies confirmed complete catalyst-substrate association under the reaction conditions. These results indicate that the catalyst confers a kinetic advantage to the reaction, and that the modest enantioselectivity is the result of poor enantiofacial bias within the hydrogen-bonding complex rather than a contribution from uncatalyzed background reaction.



Scheme 1.21 Intramolecular [2+2] Cycloaddition Catalyzed by a Hydrogen-Bonding Ketone Sensitizer

Thus, Krische's hydrogen-bonding catalyst addressed the second challenge, but did not solve the first. The Bach group, on the other hand, initially solved the first challenge, but not the second. Bach prepared chiral templates derived from Kemp's triacid that form 1:1 ground-state complexes with amide-containing substrates through hydrogen-bonding interactions.¹⁰⁸ In this

precomplexation strategy, a superstoichiometric loading of the chiral template ensures that the substrate is always bound within a chiral environment after absorbing light. Bach initially disclosed a diastereoselective Paternò–Büchi reaction using the template strategy.^{109,110} Chiral template **1.49** is optimal for a related intramolecular enantioselective [2+2] photocycloaddition of 2-quinolone **1.48** (Scheme 1.22).^{111,112} It contains both a rigid cyclohexyl backbone, restricting the conformational flexibility, and a sterically demanding benzoxazole moiety, producing effective facial differentiation in a prochiral substrate. The best enantioselectivity is achieved at low temperatures and in nonpolar solvents, both of which maximize hydrogen-bonding interactions.

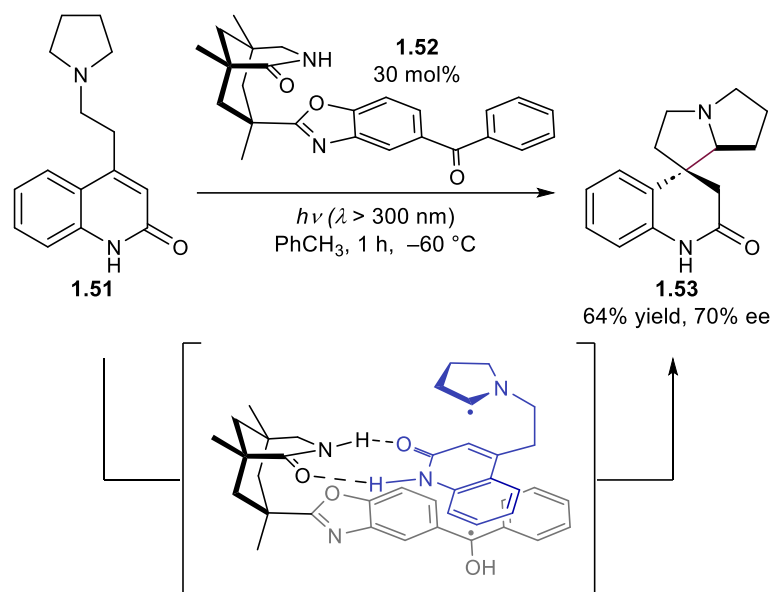


Scheme 1.22 Intramolecular [2+2] Cycloaddition via a Hydrogen-Bonding Amide Template

Chiral hosts related to **1.49** were examined in several mechanistically diverse photoreactions including intramolecular [2+2]^{113–115}, intermolecular [2+2]^{116–120}, [4+2]^{121,122}, and [4+4]^{123,124} cycloadditions, as well as Norrish–Yang cyclizations^{125,126} and electrocyclizations¹²⁷. In several cases ee's greater than 90% were reported; however, in every case superstoichiometric loadings of the template are required because the rate of photoreaction is similar for bound and

unbound substrate. In order to ensure high enantioselectivity, nearly all of the substrate must be bound to the template to prevent unbound substrate reacting through a racemic pathway.

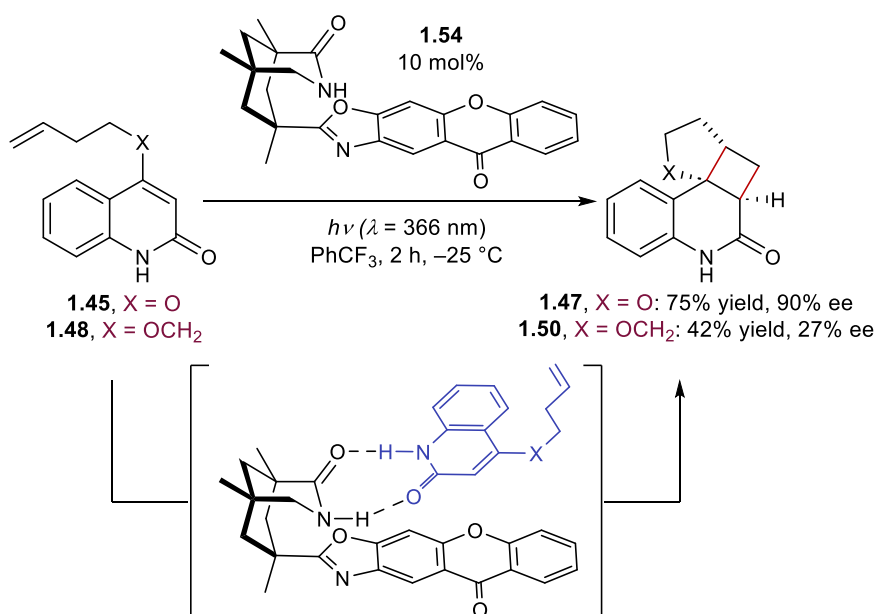
In 2005, Bach made a significant contribution to the field of asymmetric photocatalysis by incorporating a sensitizer into the chiral template.^{128,129} Adding an aromatic ketone sensitizer to the existing chiral Kemp's acid motif retained the desired hydrogen-bonding functionality of the original template while introducing the ability to catalyze the photochemical reaction of the bound substrate. Only 30 mol% of **1.52** was required in the cyclization of pyrrolidine **1.51** to spirocycle **1.53** in 70% ee (**Scheme 1.23**). The proposed mechanism invokes a ground-state hydrogen-bonding complex between the catalyst and substrate, situating the substrate within the chiral environment of the photocatalyst. Excitation of the ketone catalyst is followed by PET, oxidizing the bound substrate. After intramolecular proton transfer, the resulting α -amino radical cyclizes, setting the stereochemistry and producing **1.53** after back electron transfer and protonation. Notably, only a catalytic loading of **1.52** is required in the reaction because cyclization does not occur in the absence of **1.52**.



Scheme 1.23 Intramolecular Cyclization Catalyzed by a Hydrogen-Bonding Benzophenone Sensitizer

Extension of ketone catalyst **1.52** to energy-transfer reactions required further modification of the catalyst structure. In an intramolecular [2+2] cycloaddition of quinolone **1.45**, benzophenone **1.52** afforded the cyclobutane in 39% ee, while xanthone **1.54** afforded the cycloadduct in 90% ee (**Scheme 1.24**).¹³⁰ For both **1.52** and **1.54**, the catalyst is completely bound to the substrate at the start of the reaction, thus the ground-state association does not account for the selectivity change.¹³¹ Instead, the increase in selectivity was rationalized based on the efficiency of sensitization and the rate of the subsequent reaction.¹³² Notably, substrate **1.45** absorbs at the irradiation wavelength. However, the xanthone photocatalyst **1.54** has a much larger extinction coefficient than the substrate and absorbs nearly all the photons under the reaction conditions. Thus, the racemic background reaction is attenuated and high enantioselectivity achieved. Conversely, benzophenone **1.52**, which has a much lower extinction coefficient at 366 nm, does not effectively attenuate the competitive racemic background reaction, rationalizing the lowered selectivity.¹³³ Finally, to ensure high levels of stereoinduction, the rate of the enantiodetermining step must outcompete the rate of substrate dissociation. After excitation, dissociation prior to

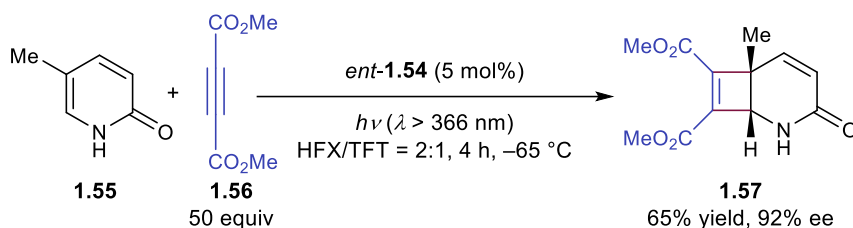
cyclization leads to racemic product. Unlike xanthone, photoexcited benzophenone is not planar, which may facilitate faster substrate dissociation.¹³⁴ This dissociation hypothesis is bolstered by the lower ee (27%) obtained when substrate **1.48** is sensitized by the xanthone photocatalyst. Laser flash photolysis experiments revealed that the rate of intramolecular photoreaction for **1.45** is approximately three times greater than for **1.48**. Hence, while **1.45** reacts prior to dissociation, Bach proposed that the rates of cyclization and dissociation are similar for **1.48** and result in the lower enantioselectivity.



Scheme 1.24 Intramolecular [2+2] Cycloaddition Catalyzed by a Xanthone Sensitizer

Given the competition between dissociation and cyclization, intermolecular photoreactions are considerably more difficult to design than intramolecular variants. Despite this challenge, Bach developed an intermolecular [2+2] photocycloaddition between pyridone **1.55** and acetylenedicarboxylates that is catalyzed by *ent*-**1.54** (Scheme 1.25).¹³⁵ Because the pyridone does not absorb the wavelengths of light used in the reaction conditions, there is not a significant correlation between catalyst loading and ee, however, there is a correlation between alkyne loading and ee. It was proposed that a higher concentration of coupling partner leads to a faster bimolecular

reaction and less possibility of substrate dissociation. The photochemical rearrangement of spirooxindole epoxides was also examined using xanthone **1.54**, yielding product in up to 33% ee.¹³⁶ Bach similarly attributed the poor selectivity to a slow rate of rearrangement relative to substrate dissociation from the catalyst.

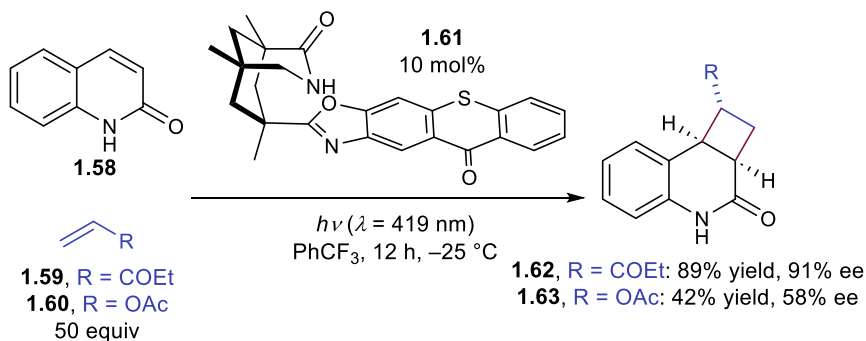


Scheme 1.25 Intermolecular [2+2] Cycloaddition Catalyzed by a Xanthone Sensitizer

Although **1.54** was successful in promoting highly enantioselective reactions, there are several problems inherent with the xanthone chromophore that limited reaction development. First, photoexcited **1.54** is very active towards hydrogen atom abstraction. In toluene, the sensitizer decomposes in less than 10 min under 366 nm irradiation, limiting the choice of reaction solvents.¹³⁷ The sensitizer also does not have a significant absorption in the visible region, necessitating irradiation at UV wavelengths that have a greater possibility of exciting free substrate. Thioxanthone **1.61** solves both problems: it is more stable under irradiation in toluene and possesses a significant absorption in the visible region. While the triplet energy of thioxanthone **1.61** (63 kcal/mol) is lower than xanthone **1.54** (76 kcal/mol), it is high enough to sensitize a variety of substrate molecules. The new sensitizer was evaluated in the canonical quinolone intramolecular [2+2] photoreaction producing cycloadducts in up to 96% ee under visible light irradiation.¹³⁷ Under similar conditions, 3-alkylquinolones with tethered alkenes and allenes were also amenable to the intramolecular cycloaddition.¹³⁸

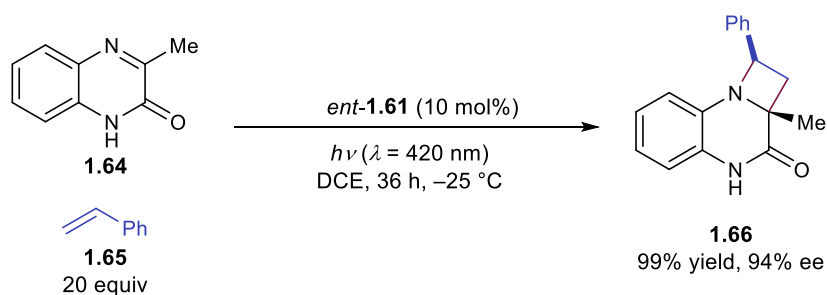
An intermolecular [2+2] photocycloaddition between quinolone **1.58** and a variety of alkene coupling partners was also catalyzed by **1.61**; however, 50 equiv of the coupling partner

were needed to ensure cyclization occurs prior to dissociation from the catalyst (**Scheme 1.26**).¹³⁹ It follows from this analysis that alkenes that react at slower rates should be expected to give lower enantioselectivities. Vinyl acetate (**1.60**) reacts more than an order of magnitude slower than ethyl vinyl ketone (**1.59**) when sensitized by an achiral thioxanthone, and consequently gave cycloadducts in significantly lower ee (91% ee vs. 58% ee).



Scheme 1.26 Intermolecular [2+2] Cycloaddition Catalyzed by a Thioxanthone Sensitizer

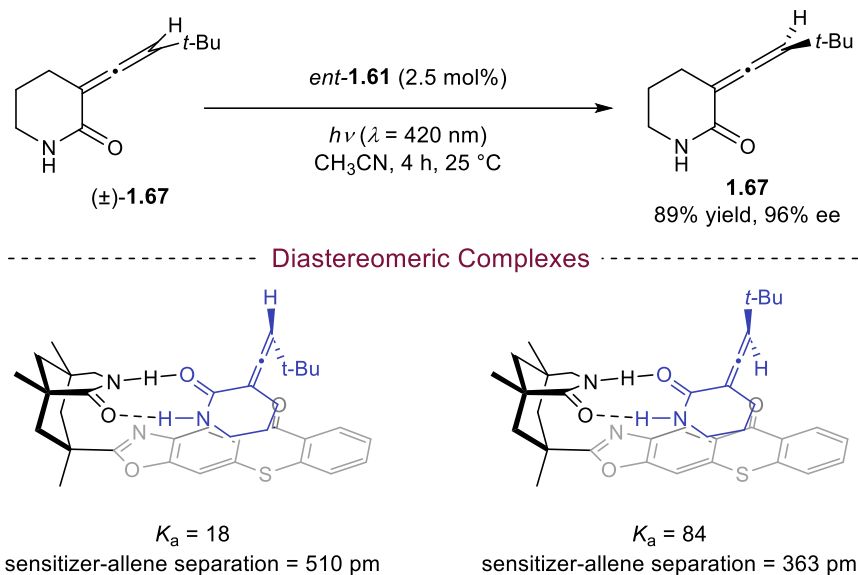
Thioxanthone *ent*-**1.61** is also an effective photocatalyst for enantioselective aza-Paternò–Büchi reactions that produce chiral azetidines.¹⁴⁰ Cyclic imine **1.64** was tested in the [2+2] reaction shown in **Scheme 1.27**, because *N*-substituted quinoxalinones were previously shown to undergo [2+2] cycloadditions with arylalkenes.¹⁴¹ A variety of styrenes were accommodated as coupling partners in the reaction affording azetidines in high yields and up to 98% ee.



Scheme 1.27 Aza-Paternò–Büchi Reaction Catalyzed by a Thioxanthone Sensitizer

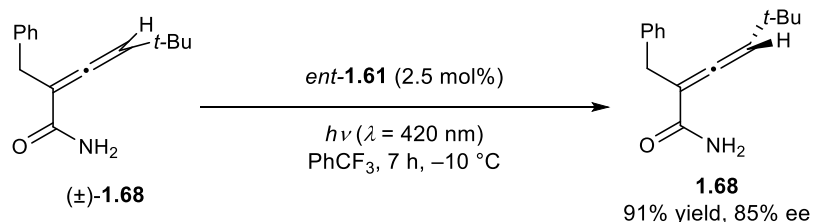
In addition to cycloadditions, thioxanthone **1.61** has proven to be applicable to photocatalytic deracemization. Under optimized reaction conditions Bach found that allene **1.67**

could be deracemized in up to 97% ee (**Scheme 1.28**).^{142,143} Mechanistically, triplet energy transfer to chiral allene **1.67** from thioxanthone **1.61** produces the achiral triplet-state allene.¹⁴⁴ A measured quantum yield of racemization of $\Phi = 0.52$ suggests that the excited achiral triplet allene decays with equal probability to **1.67** or *ent*-**1.67**. Deracemization is therefore achieved during the sensitization step of the reaction. Because both the allene and sensitizer are chiral, two distinct diastereomeric ground-state sensitizer–allene complexes can form. NMR titrations provided association constants of $K_a = 84$ and 18 for the respective diastereomeric complexes. The stronger-binding enantiomer is preferentially sensitized and thus selectively depleted over the course of the reaction, enriching the population of the weaker-binding antipode. Notably, the strategy relies on the fact that after sensitization the excited triplet allene dissociates from the catalyst and decays unselectively to the ground state leading to racemization of the stronger binding enantiomer. If, on the other hand, the allene always remained bound to the sensitizer during decay back to the ground state, retention of configuration would likely be expected. Thus, in contrast to cycloaddition reactions where dissociation of excited-state substrate is typically a hurdle in reaction development, dissociation is necessary to achieve high enantioselectivity in deracemization reactions. Computational studies also suggested that the separation between allene and thioxanthone was smaller for the stronger-binding complex, leading to more efficient energy transfer than the other diastereomeric complex. Thus, both the difference in ground-state association constants and the excited-state sensitization efficiencies for the two diastereomeric complexes are responsible for the high selectivity for deracemization.



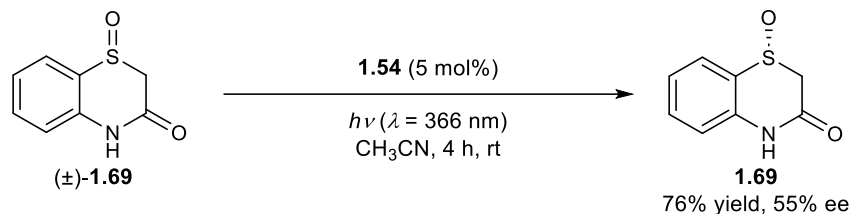
Scheme 1.28 Allene Deracemization Catalyzed by a Thioxanthone Sensitizer

Thioxanthone **1.61** also catalyzed the deracemization of primary amides in up to 93% ee (**Scheme 1.29**).¹⁴⁵ A combination of experimental and computational studies again confirmed that both ground-state association constants and excited-state sensitization efficiencies contribute to the enantioselectivity.



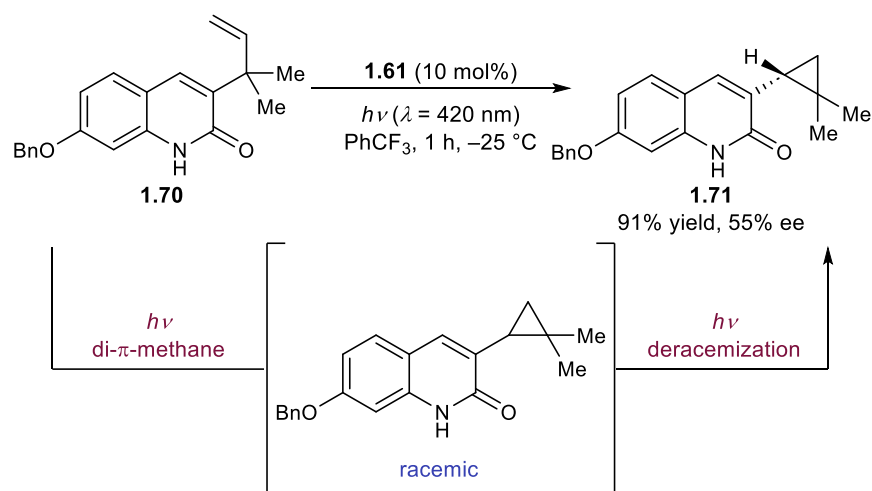
Scheme 1.29 Primary Allene Amide Deracemization Catalyzed by a Thioxanthone Sensitizer

Xanthone **1.54** catalyzes the deracemization of cyclic sulfoxides in up to 55% ee (Scheme 30).¹⁴⁶ An analogous mechanism was proposed in which one enantiomer of **1.69** binds more strongly to **1.54** than *ent*-**1.69**, leading to more efficient sensitization for the former. Once excited, the substrate dissociates from the chiral catalyst and can undergo stereochemical inversion prior to relaxation to the ground state. Over time, the enantiomer that binds the catalyst more strongly is preferentially depleted via unselective racemization.



Scheme 1.30 Sulfoxide Deracemization Catalyzed by a Xanthone Sensitizer

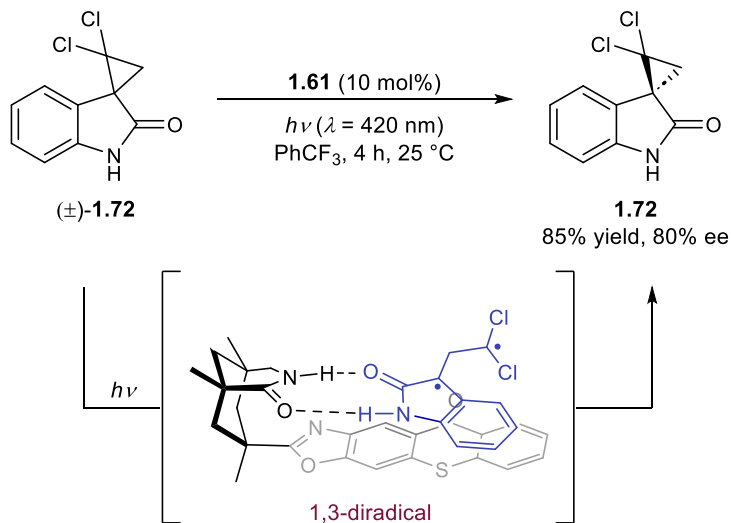
In theory, any substrates that racemize in the excited state could be amenable to photoderacemization. Bach and coworkers discovered the photoderacemization of 3-cyclopropylquinolones by **1.61** serendipitously when attempting to develop an enantioselective di- π -methane rearrangement (**Scheme 1.31**).¹⁴⁷ They observed that the enantioselectivity of the cyclopropane product increased from nearly 0% ee to 55% ee within the first hour of irradiation.



Scheme 1.31 Di- π -Methane Rearrangement–Cyclopropane Deracemization Cascade Catalyzed by a Thioxanthone Sensitizer

Detailed mechanistic studies were undertaken for the related deracemization of spirocyclopropyl oxindoles (**Scheme 1.32**).¹⁴⁸ Transient absorption studies suggested a triplet energy transfer from the sensitizer to cyclopropyl substrate **1.72**. The spectral position and shape of the transient signal of the triplet substrate also matched that calculated for the expected ring-opened 1,3-diradical. As with allene deracemization, both the ground-state association constants and excited-state sensitization kinetics of the diastereomeric substrate–catalyst complexes were

invoked to account for the enantioenrichment of the product. The triplet lifetime of the 1,3-diradical is 22 μ s while the lifetime of the substrate–sensitizer complex is below 1 μ s, implying that the 1,3-diradical dissociates from the catalyst prior to cyclization. This kinetic regime is desirable since cyclization within the chiral domain of the catalyst would favor retention of configuration.



Scheme 1.32 Cyclopropane Deracemization Catalyzed by a Thioxanthone Sensitizer

Despite the wide range of photochemical reactions that can be catalyzed by xanthone **1.54** and thioxanthone **1.61**, the reactions are limited to lactam-containing substrates.¹⁴⁹ In an attempt to expand the range of available binding motifs, Bach and coworkers have recently prepared new catalysts that incorporate a thioxanthone sensitizer into an alternate chiral hydrogen-bonding scaffold (**Figure 1.2**). While thiourea-linked thioxanthone **1.74** does not induce high levels of enantioselectivity in a sensitized 6π -electrocyclization (12% ee),¹⁵⁰ BINOL-derived phosphoric acid **1.73** catalyzes an intermolecular [2+2] cycloaddition between carboxylic acid **1.75** and cyclopentene (**1.76**) in 86% ee (**Scheme 1.33**).¹⁵¹ NMR studies demonstrated that the carboxylic acid substrate binds the BINOL catalyst under the reaction conditions. Computational studies support a 1:1 complex but suggest that several binding modes are similar in energy, which may

account for the moderate enantioselectivity. Takagi has studied a simpler BINOL-derived phosphoric acid lacking a thioxanthone substituent in asymmetric intramolecular [2+2] photocycloadditions of quinolones. However, in this reaction a stoichiometric loading of the acid template was necessary, presumably because both bound and unbound substrate react at similar rates.¹⁵²

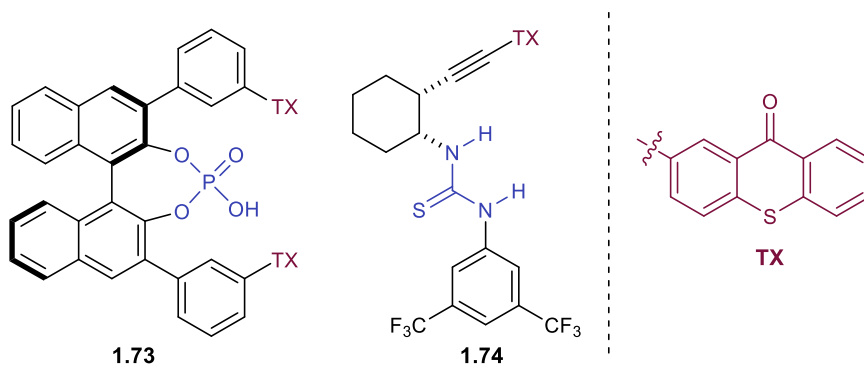
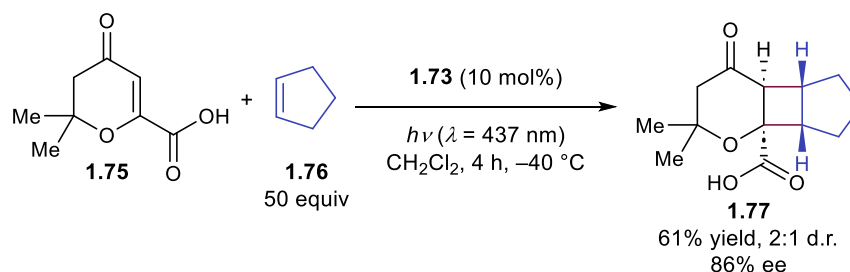


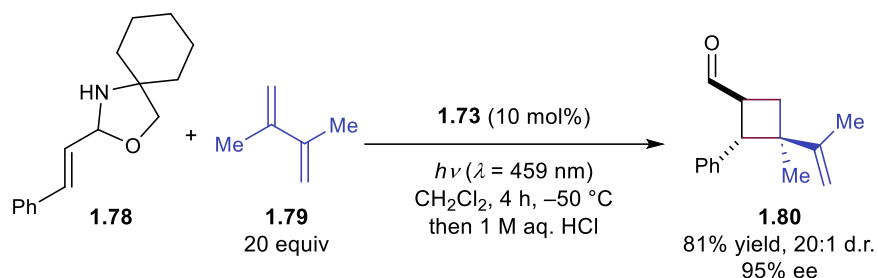
Figure 1.2 Chiral Thioxanthone-Derived Sensitizers



Scheme 1.33 Intermolecular [2+2] Cycloadditions Catalyzed by a BINOL-Derived Thioxanthone Sensitizer

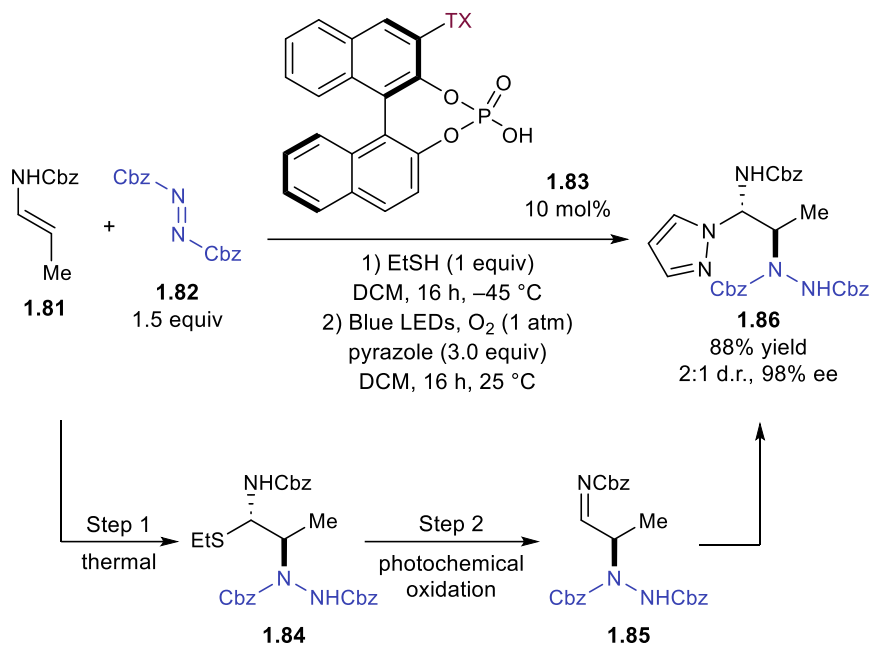
Thioxanthone **1.73** catalyzes the enantioselective photocycloaddition of *N,O*-acetal **1.78** and alkene **1.79** in 95% ee (**Scheme 1.34**). NMR studies revealed that **1.78** exists as a mixture of the cyclic *N,O*-acetal and the ring-opened imine. UV-Vis absorption studies showed that a bathochromic shift occurs upon protonation of the imine, while emission studies providing the triplet energies of the iminium ion and thioxanthone catalyst (51 kcal/mol and 56 kcal/mol, respectively) showed that energy transfer to the iminium was exothermic. Conversely, both the

N,O-acetal and unprotonated imine are unable to be sensitized by the photoexcited thioxanthone catalyst.



Scheme 1.34 Intermolecular [2+2] Cycloaddition of Iminium Ions Catalyzed by a BINOL-Derived Thioxanthone Sensitizer

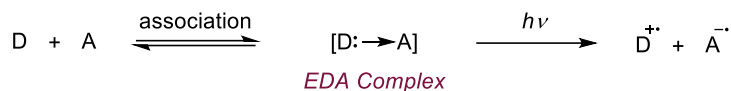
Masson developed a non- C_2 -symmetric BINOL-derived catalyst with a tethered thioxanthone chromophore for the enantioselective synthesis of 1,2-diamines (**Scheme 1.35**).¹⁵³ This reaction occurs in two steps. In the first, the nucleophilic enecarbamate reacts with the electrophilic azodicarboxylate in an enantioselective thermal reaction. The resulting imine is unstable under the reaction conditions; thus ethanethiol is added to generate α -carbamoylsulfide **1.84**. In the second step, pyrazole is added and the reaction is irradiated with blue light. The authors propose that α -carbamoylsulfide **1.84** is photochemically oxidized to the sulfur radical cation, triggering mesolytic cleavage of thiyl radical and ultimately generating imine **1.85**, which is intercepted by pyrazole in a thermal, diastereodetermining reaction. Notably, both stereodetermining steps in this reaction are thermal, while the only photochemical step regenerates the reactive imine intermediate.



Scheme 1.35 1,2-Diamine Synthesis Catalyzed by a BINOL-Derived Thioxanthone Sensitizer

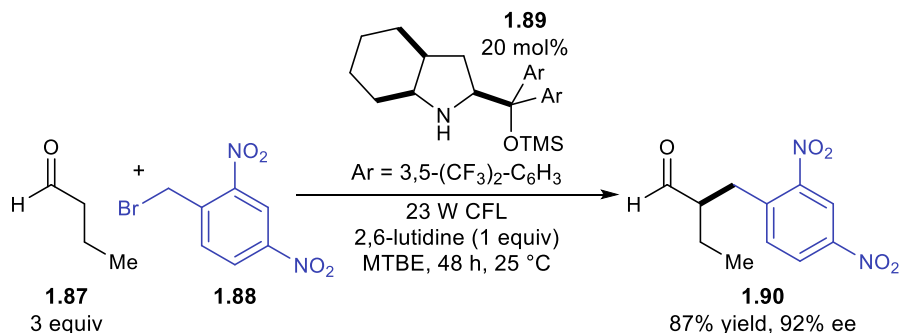
1.4.3 Enamine and Iminium Chromophores

Melchiorre introduced a new strategy in asymmetric photocatalysis in which the light-absorbing species is an electron donor–acceptor (EDA) complex.^{154,155} In this strategy, an electron-rich donor molecule and an electron-poor acceptor molecule associate in the ground state, comprising an EDA complex (**Scheme 1.36**).¹⁵⁶ The photophysical properties of the complex are distinct from the donor or acceptor in isolation. This association leads to the formation of a new charge-transfer absorption band, which at the simplest level can be understood as an intracomplex electron transfer from the donor HOMO to the acceptor LUMO. In most cases, orbital mixing between the donor and acceptor changes the relative position of the frontier molecular orbitals, stabilizing the formation of the EDA complex. The appearance of color when mixing two colorless compounds is a hallmark of EDA complexes and was the original observation that led Mulliken to formulate the charge transfer theory.¹⁵⁷

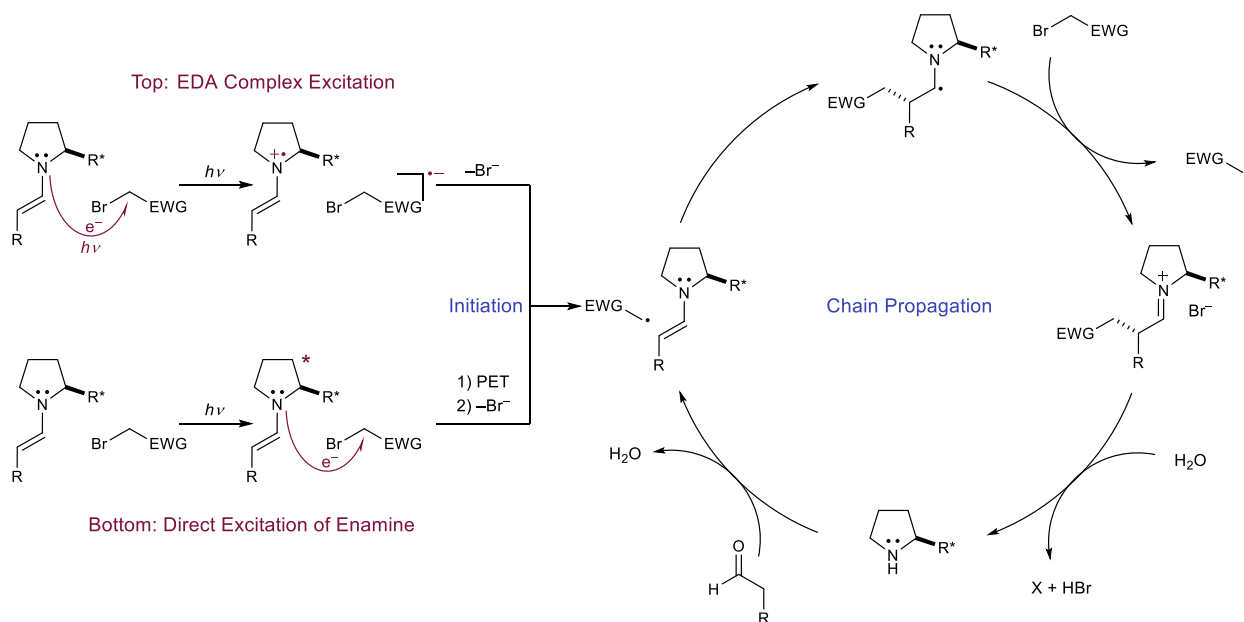


Scheme 1.36 *Electron Donor–Acceptor Complex Formation and Excitation*

In 2013, Melchiorre exploited this strategy to promote the enantioselective α -alkylation of aldehydes with alkyl halides (**Scheme 1.37**).¹⁵⁸ This reaction was based on organocatalyzed photoredox reactions developed by MacMillan.¹⁵⁹ In both designs, a chiral secondary amine organocatalyst condenses with an aldehyde to form an enamine intermediate. However, unlike the previous organocatalyzed reactions, an exogenous photocatalyst was not needed. Although neither enamine nor alkyl bromide absorb visible light individually, the mixture exhibited a broad absorption feature in the visible region, characteristic of the formation of an EDA complex. Spectrophotometric analyses confirmed the 1:1 ground-state association with an association constant of $K_{\text{EDA}} = 11.6$ determined from Benesi–Hildebrand analysis.¹⁶⁰ Upon excitation of the ground-state complex, an electron is promoted from the enamine donor to the alkyl bromide acceptor, forming a radical ion pair (**Scheme 1.38**, top). The short-lived radical anion undergoes bromide cleavage to produce an iminium ion and an alkyl radical. The authors first proposed a closed catalytic cycle in which radical-radical recombination forms an iminium intermediate which is then hydrolyzed to afford the α -alkylated product, but further investigations revealed that the quantum yield (Φ) of the reaction with both benzyl and phenacyl bromides is $\Phi > 20$, consistent with a radical chain mechanism.¹⁶⁰ Notably, the chiral catalyst is involved in both the photochemical initiation and the ground-state enantiodetermining radical addition into the enamine.

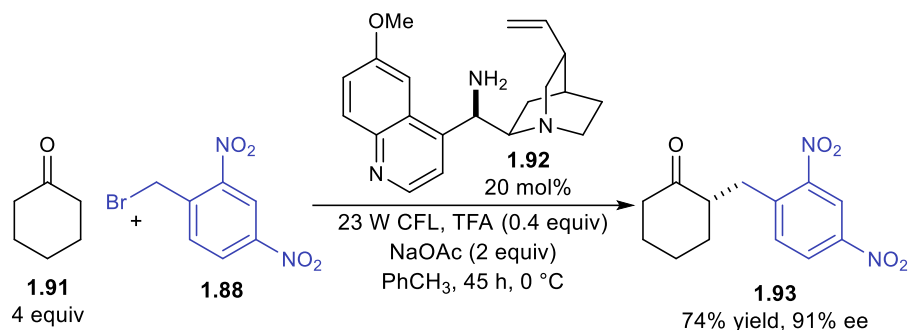


Scheme 1.37 Aldehyde α -Alkylation via EDA Complex Excitation



Scheme 1.38 Photoinduced Enamine Catalysis Mechanisms

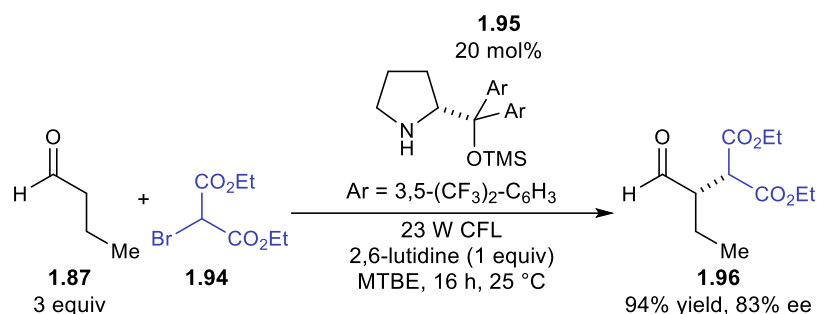
A similar photo-organocatalytic strategy proved applicable to ketone substrates when coupled with cinchona-based primary amine catalyst **1.92** (**Scheme 1.39**).¹⁶¹ Both electron poor benzyl bromides (**1.88**) and phenacyl bromides were competent electron acceptors, but the reaction was limited to cyclic ketones as precursors to the chiral enamine electron donors.



Scheme 1.39 Ketone α -Alkylation via EDA Complex Excitation

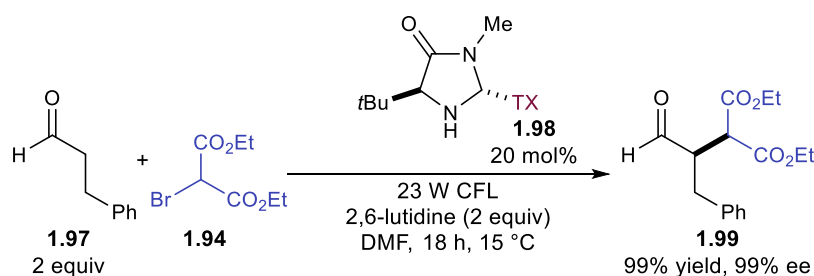
Melchiorre and coworkers also showed that bromomalonates (**1.94**) are competent electron acceptors in the α -alkylation of aldehydes (**1.87**) and enals using amine organocatalysts (**Scheme 1.40**).¹⁶² Alkylated products were obtained in up to 94% ee, and complete γ -selectivity was observed in radical addition to enals. The authors initially assumed the intermediacy of an EDA complex between the enamine and bromomalonate; however, no charge transfer band was observed in the UV-Vis absorption spectrum of the mixture. Instead, the enamine was the only reaction component that significantly absorbed light under the optimized conditions. A series of Stern–Volmer quenching studies showed that the bromomalonate quenched the excited-state emission of the enamine. From this study, the authors proposed that PET reduction of the bromomalonate by the excited enamine followed by loss of bromide resulted in the formation of an electrophilic malonyl radical that would subsequently react with another equivalent of ground-state enamine (**Scheme 1.38**, bottom). The chain propagation step is likely different than in the EDA reaction because the α -aminoradical is incapable of reducing the bromomalonate. Instead, the α -aminoradical abstracts bromine from another equivalent of bromomalonate. Collapse of the bromoamine intermediate expels bromide, forming an iminium intermediate, which is hydrolyzed to the product. Notably, the photochemical step in both the EDA and PET reactions serves only to initiate the radical chain. Other classes of electron acceptors including (phenylsulfonyl)alkyl

iodides were also amenable to the PET reaction.¹⁶³ After desulfonylation, α -methylation and α -benzylation products could be obtained in high yield and enantioselectivity.



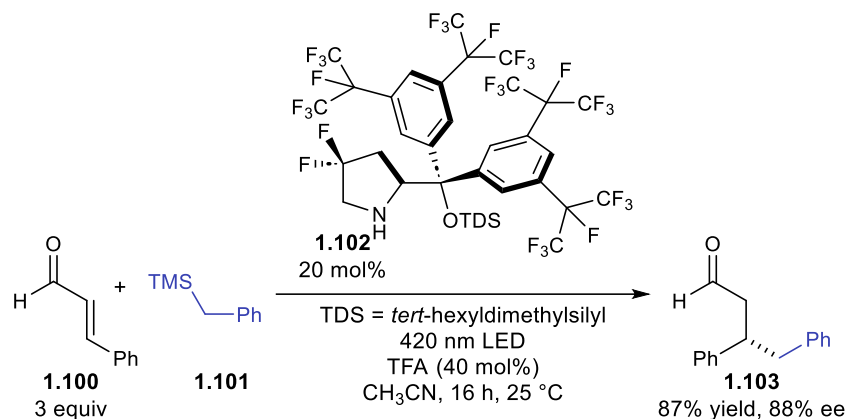
Scheme 1.40 Aldehyde α -Alkylation via Direct Enamine Excitation

A similar reaction was reported by Alemán with a thioxanthone-substituted organocatalyst (**1.98**) yielding alkylated aldehydes in high yields and enantioselectivities (**Scheme 1.41**). In this case, the bromomalonate is reduced by the thioxanthone catalyst instead of the enamine, initiating the radical chain.¹⁶⁴



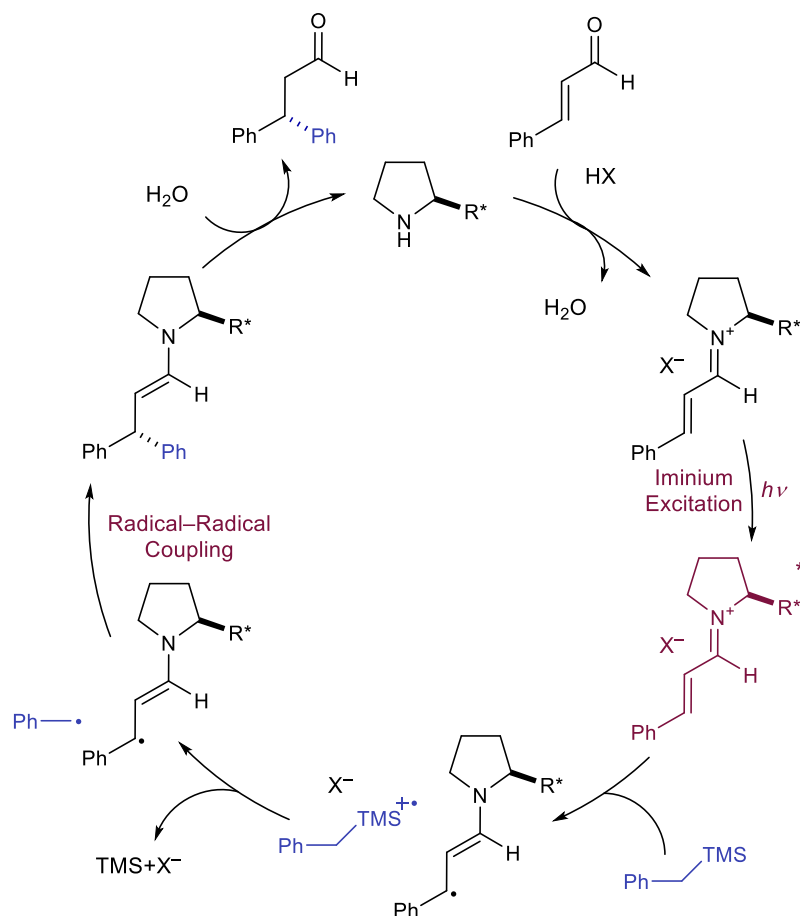
Scheme 1.41 Aldehyde α -Alkylation Promoted by a Bifunctional Photoaminocatalyst

In 2017, Melchiorre and coworkers showed that chiral iminium ions generated in situ by condensation of α,β -unsaturated aldehydes (**1.100**) with chiral amine catalysts (**1.102**) could promote the asymmetric β -alkylation of enals (**Scheme 1.42**).¹⁶⁵ Enamine and iminium photocatalysis are similar yet complementary strategies. Electron-rich enamines are nucleophilic in the ground state and become potent single-electron reductants after photoexcitation. In contrast, iminium ions act as electrophiles in the ground state and are strong oxidants after photoexcitation, allowing the use of complementary radical precursors.



Scheme 1.42 Enal β -Alkylation via Direct Iminium Ion Excitation

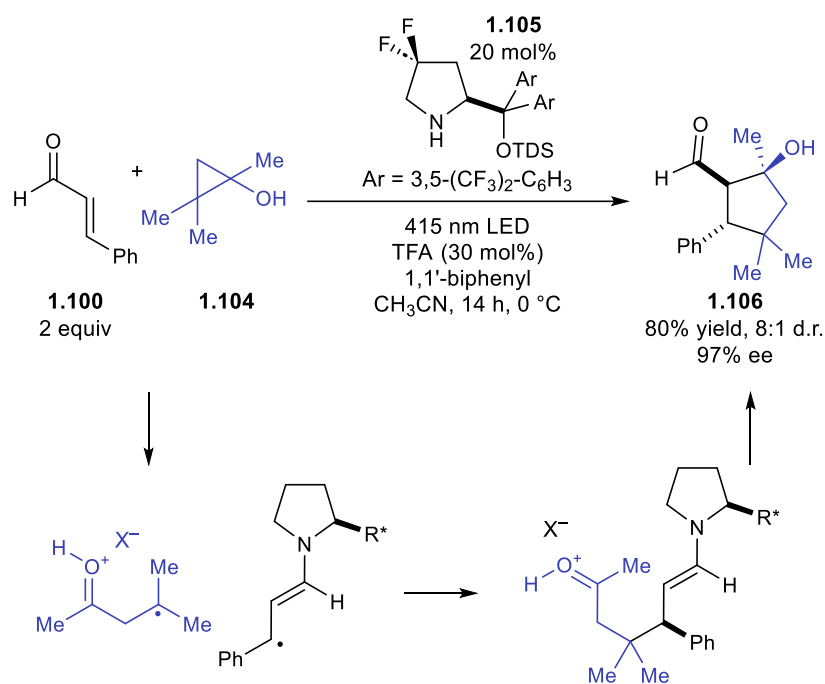
Melchiorre proposed a mechanism in which a chiral iminium ion directly absorbs visible light and functions as a single-electron oxidant to an electron-rich alkyl trimethylsilane (**1.101**) (Scheme 1.43). The silyl radical cation undergoes mesolytic fragmentation to afford a stabilized alkyl radical and trimethylsilyl cation. Coupling of the β -enaminy radical intermediate with the alkyl radical affords an enamine, which after hydrolysis yields the β -alkylated aldehyde. This radical–radical coupling mechanism was proposed instead of a radical chain mechanism because the putative propagation step, single electron transfer (SET) between the silane and α -iminyl radical cation, would be endergonic. Although this method is limited to benzyl radicals or radicals stabilized by an adjacent heteroatom, unstabilized alkyl radicals could be accommodated when using a dihydropyridine radical precursor.¹⁶⁶ This approach gave selective 1,4-addition and offers an advance over thermal iminium catalysis with organometallic nucleophiles, which often produces a mixture of 1,2- and 1,4-addition adducts.



Scheme 1.43 Enal β -Alkylation Mechanism

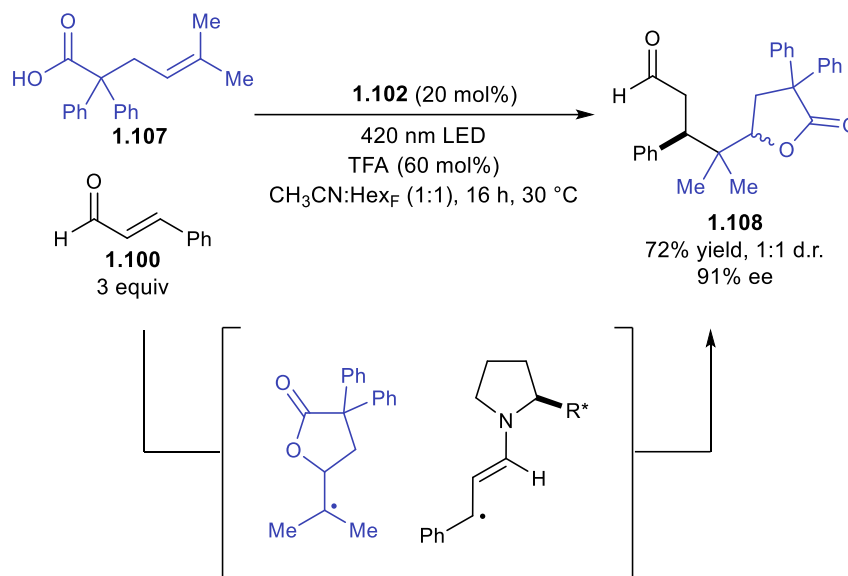
The initial product of a radical–radical coupling under iminium photocatalysis is an enamine, which can further react with an electrophilic moiety if one is present. Melchiorre and coworkers leveraged this insight to design a photochemical cascade reaction in which the excited-state and ground-state reactivity of organocatalytic intermediates were exploited to form cyclopentanols (**1.106**) in excellent diastereo- and enantioselectivity (**Scheme 1.44**).¹⁶⁷ Cyclopropanols (**1.104**) were used as electron donors, reducing the photoexcited iminium, to generate β -keto radical cation intermediates after ring-opening. In analogy to previous work, stereocontrolled radical–radical coupling affords an enamine intermediate. The ground-state enamine nucleophile cyclizes with the electrophilic ketone in a second stereocontrolled step. A redox mediator, 1,1'-biphenyl, was added to the reaction to increase efficiency. Mechanistic

experiments revealed that the excellent enantioselectivity of the reaction arises from a kinetic resolution in the thermal cyclization. The major enantiomer formed in the radical–radical coupling cyclizes quickly, leading to stereochemical amplification over the two steps, while the minor enantiomer does not cyclize.



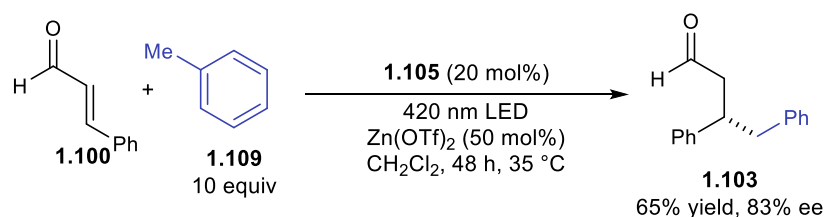
Scheme 1.44 Cyclopentanol Synthesis via Iminium Ion Catalysis

Another example of the cascade strategy enabled the stereoselective construction of complex butyrolactones (**1.108**).¹⁶⁸ Photoexcitation of an iminium derived from an enal substrate results in oxidation of alkene **1.107**, the appended carboxylic acid moiety of which can cyclize (**Scheme 1.45**). Enantioselective radical–radical coupling produces cascade product **1.108** in high enantioselectivity. Because the first cyclization occurs in the absence of the chiral catalyst, no diastereoselectivity was observed. A similar cascade was subsequently developed with allene-appended carboxylic acids, ultimately yielding bicyclic lactones with moderate enantioselectivity.¹⁶⁹



Scheme 1.45 Cascade Reaction via Iminium Ion Catalysis

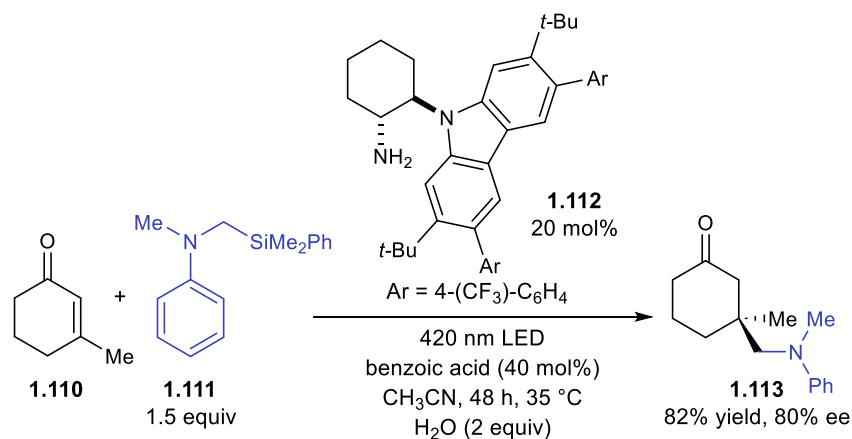
Toluene derivatives also reductively quench the iminium excited state leading to β -benzylated aldehydes from the corresponding enals (**Scheme 1.46**).¹⁷⁰ Following oxidation of toluene, the benzylic C–H bond is significantly acidified; the pK_a is estimated to be -13 in CH₃CN.¹⁷¹ Deprotonation results in a benzyl radical that undergoes radical–radical coupling with the β -enaminy radical intermediate. Zn(OTf)₂ was a necessary additive in this process; the Zn²⁺ cation was proposed to serve as an acid to promote iminium formation, while the triflate counteranion was proposed to deprotonate the photogenerated toluene radical cation.



Scheme 1.46 C–H Functionalization of Toluene Derivatives via Iminium Ion Catalysis

Melchiorre also demonstrated that chiral iminium ions can act as electron acceptors in photocatalytically active EDA complexes (**Scheme 1.47**).¹⁷² Aliphatic eniminium ions typically absorb in the UV regime (< 400 nm). The iminium produced from condensation of

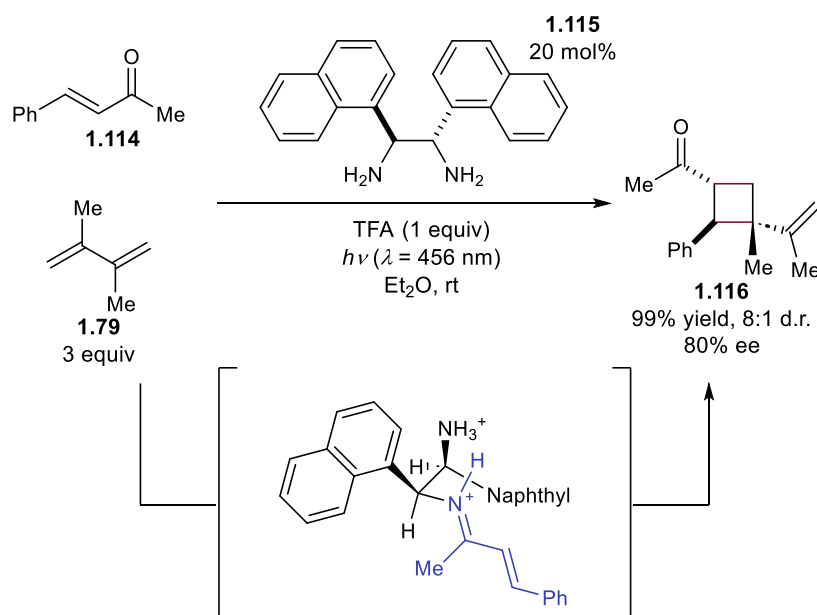
carbazole-functionalized amine **1.112** and cyclohexanones, however, absorbs strongly in the visible region. This absorption band was assigned as an intramolecular charge transfer between the electron-rich carbazole and electron-poor iminium. Excitation of the intramolecular EDA complex furnishes a carbazole radical cation which oxidizes an α -silyl amine (**1.111**). The resulting radical is stereoselectively intercepted by a ground state iminium ion. The overall reaction, which proceeds through a chain mechanism, results in the β -alkylation of enones.



Scheme 1.47 EDA Complex Formation with Iminium Electron Acceptors

Iminium ion catalysis has also been applied to [2+2] photocycloadditions. The absorption profile of enones features an (n,π^*) transition that is red-shifted in comparison to the (π,π^*) transition characteristic of analogous iminium species.¹⁷³ Hence, it can be difficult to minimize the participation of racemic background cycloadditions through direct excitation because the iminium ion cannot be selectively excited. However, the lowest triplet excited state is typically lower in energy for iminium ions than for enones, which could allow for their selective photosensitization. Bach developed an enantioselective [2+2] photoreaction using chiral iminium ions and a Ru triplet sensitizer, but catalysis was inefficient, likely due to competing unproductive electron-transfer quenching of the photocatalyst.¹⁷⁴ In 2020 Alemán developed a catalytic enantioselective [2+2] cycloaddition that circumvented the racemic reactivity problem by employing amine catalysis with

stereogenic naphthyl substituents (**Scheme 1.48**).¹⁷⁵ These served as electron donors in an intramolecular EDA complex with the electron-accepting imine. The intramolecular charge-transfer band was sufficiently red-shifted compared to the free enone to allow for its selective excitation. With 20 mol% catalyst **1.115**, cycloadduct **1.116** was produced in 99% yield and 80% ee. Computational analysis confirmed that the lowest energy transition was the expected charge transfer, while the reactive (π,π^*) imine excited state lies slightly higher in energy. The authors proposed that thermal population of the (π,π^*) state from the charge-transfer excited state produces an equilibrium population able to undergo the [2+2] cycloaddition. This method was also applied to an intramolecular [2+2] cycloaddition, enabling the synthesis of tricyclic products in high enantioselectivity.¹⁷⁶



Scheme 1.48 Intermolecular [2+2] Cycloaddition via a Chiral Iminium Chromophore

1.4.4 Chiral Counterions

Recently, several groups have attempted to apply chiral anion catalysis to asymmetric photochemistry.^{177,178} Chiral anions are intriguing for applications in photoredox chemistry

because they can associate with any cationic intermediate through electrostatic interactions, circumventing the need for specific substrate binding moieties such as carbonyls. Further, many of the most common organic and inorganic photoredox catalysts are cationic, offering a conceptually straightforward means to incorporate a chiral counteranion structure into an asymmetric photoredox reaction (**Figure 1.3**).

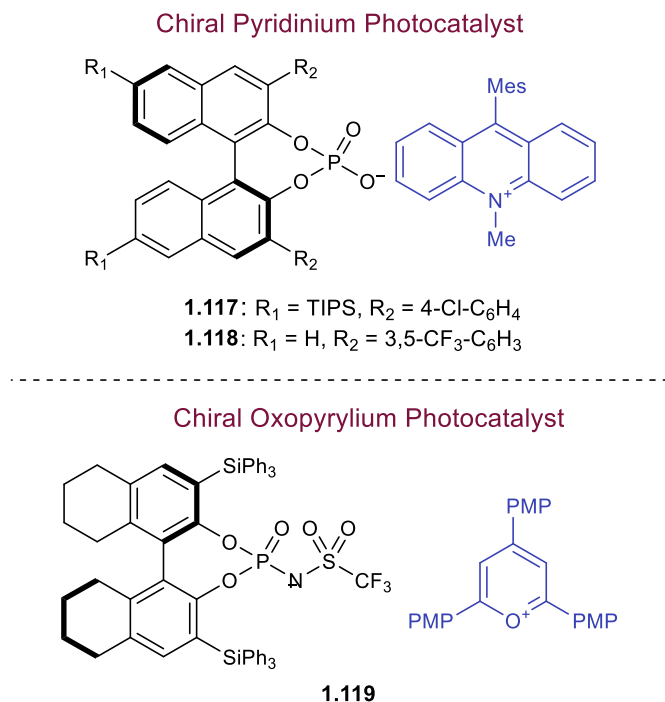
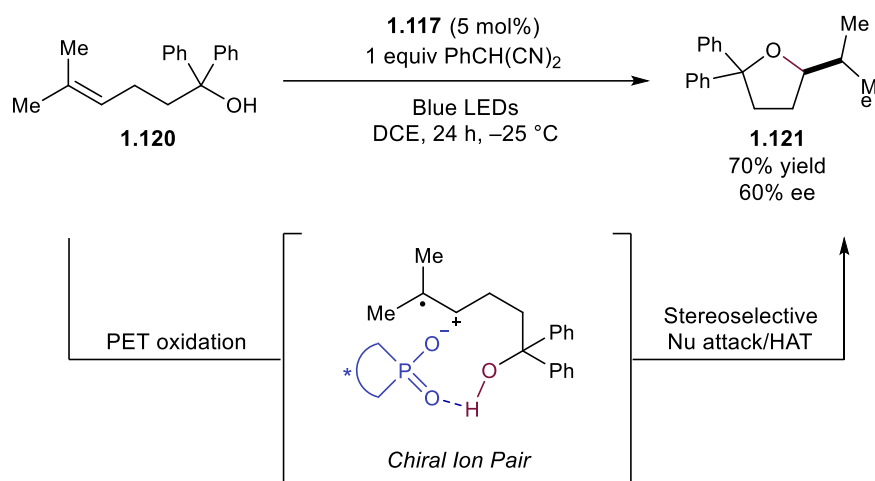


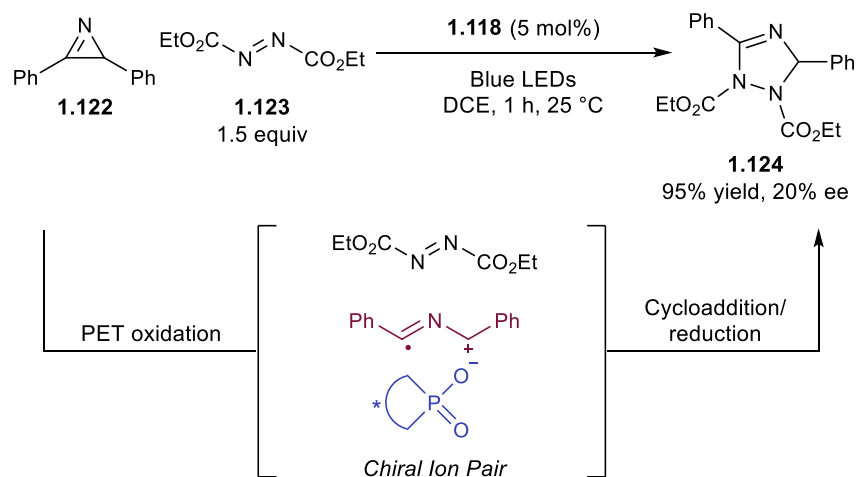
Figure 1.3 Photocatalysts with Chiral Counteranions

Luo demonstrated the feasibility of this approach by developing an asymmetric version of the anti-Markovnikov hydroetherification originally reported by Nicewicz.^{179,180} Under the optimized conditions an acridinium photocatalyst with a BINOL-derived phosphate counteranion (**1.117**) afforded cyclic ether **1.121** in 60% ee (**Scheme 1.49**). The reaction proceeds through initial oxidation of alkene **1.120** to the radical cation, which pairs with the chiral anion, followed by enantiodetermining nucleophilic attack of the pendant alcohol. Hydrogen atom transfer from 2-phenylmalononitrile to the resulting carbon-centered radical yields the cyclic ether product.



Scheme 1.49 Hydroetherification via Chiral Ion-Pairing Catalysis

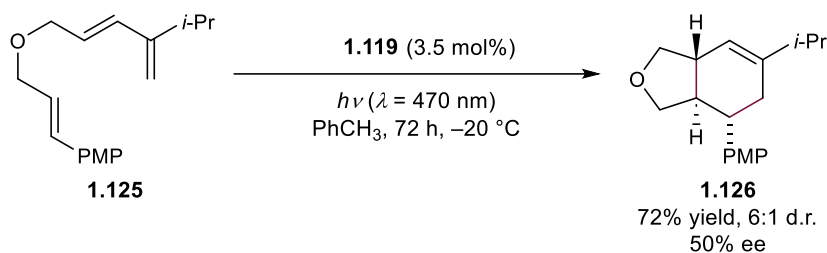
Other stereoselective radical cation photoreactions have utilized chiral phosphonate counteranions. Tang examined chiral acridinium catalyst **1.118** in a [3+2] cycloaddition between 2*H*-azirine **1.122** and azodicarboxylate **1.123**; however, the 1,2,4-triazoline product (**1.124**) was only formed in 20% ee (**Scheme 1.50**).¹⁸¹



Scheme 1.50 [3+2] Cycloaddition via Chiral Ion-Pairing Catalysis

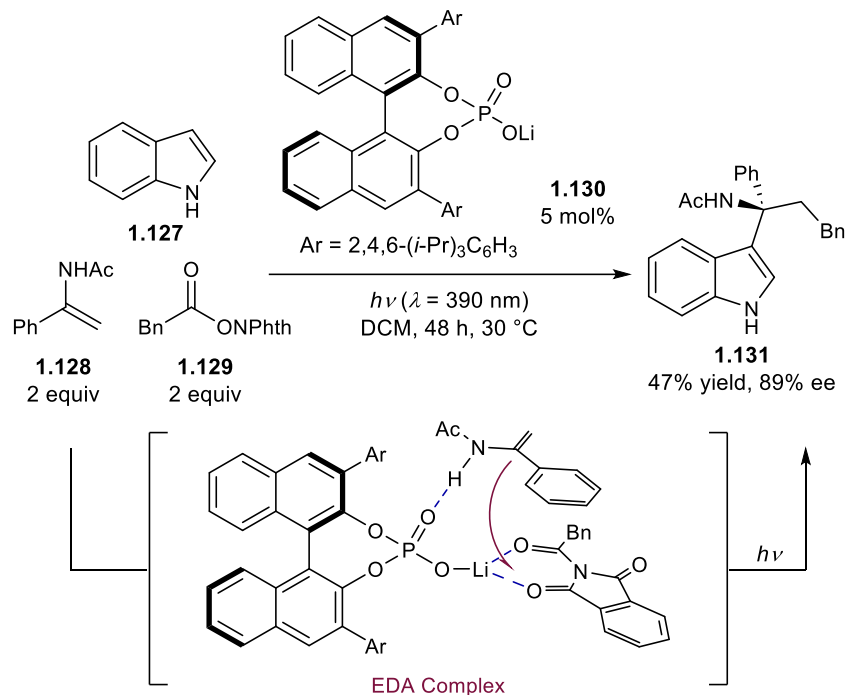
Nicewicz examined a range of BINOL-derived chiral anions with an oxopyrylium photocatalyst in a radical-cation Diels–Alder reaction, with a maximum selectivity of 50% ee with catalyst **1.119** (**Scheme 1.51**).¹⁸² When screening solvents, the authors observed an inverse

relationship between enantioselectivity and solvent dielectric constant, consistent with the hypothesis that an intimately interacting ion pair is critical for asymmetric induction. The generally modest enantioselectivities reported to date using this strategy reflect its early stage of development.



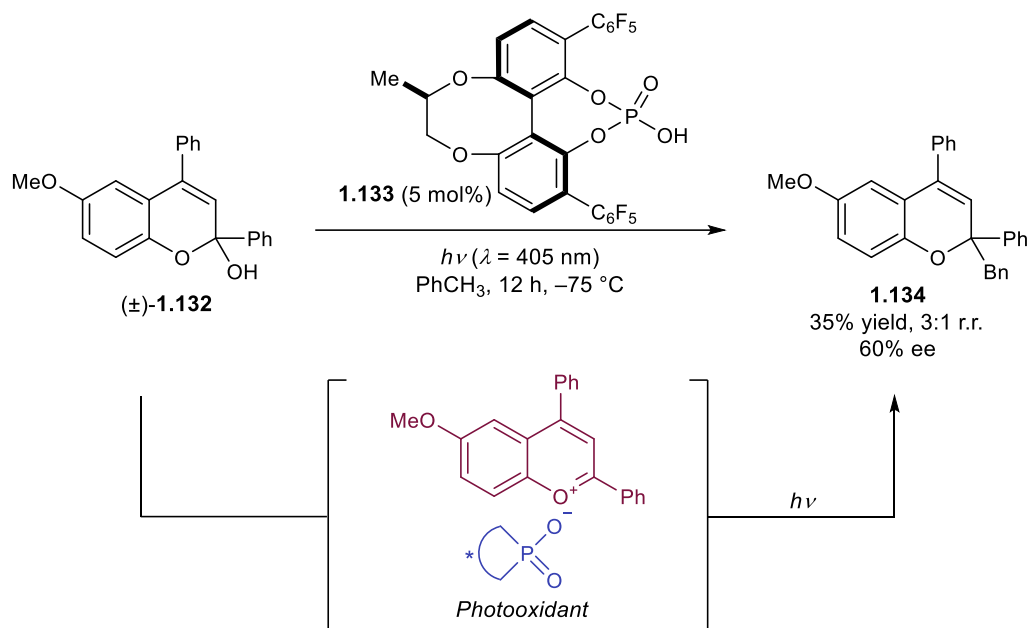
Scheme 1.51 Diels–Alder Cycloaddition Catalyzed by an Oxopyrylium Sensitizer

Wang developed an asymmetric dicarbofunctionalization of enamides that proceeded in both the presence and absence of a ruthenium photosensitizer (**Scheme 1.52**).¹⁸³ In the absence of a photosensitizer, indole **1.127**, enamide **1.128**, and redox-active ester **1.129** were coupled in the presence of a chiral phosphate base to form **1.131** in 47% yield and 89% ee. A Job plot analysis indicated a ground-state preorganization of the phosphate base, enamide **1.128** and ester **1.129** into an EDA complex. Photoexcitation of this EDA complex led to reduction of the redox-active ester followed by rapid decarboxylation. The formed benzyl radical and enamide-derived radical combine to form an iminium intermediate. In the presence of the phosphate catalyst, indole **1.127** then attacks the electrophilic iminium cation via a Friedel–Crafts reaction to provide enantioenriched indole **1.131**.



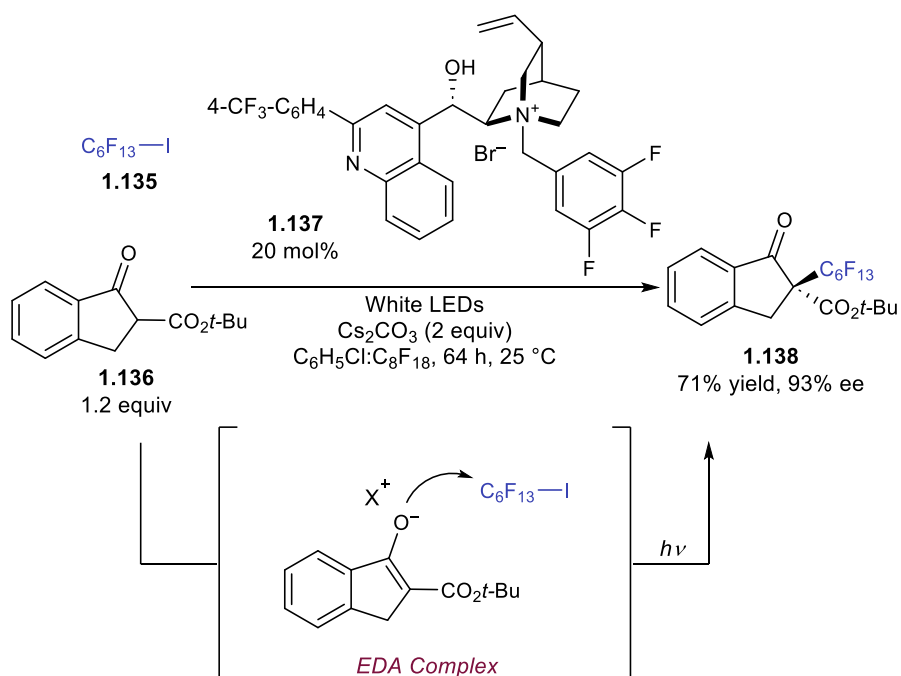
Scheme 1.52 Dicarbofunctionalization of Enamides via Ion-Pairing Catalysis

Terada reported the radical addition of toluene-derived radicals to benzopyrylium intermediates to generate chromene derivatives (**Scheme 1.53**).¹⁸⁴ Protonation of chromenol **1.132** by phosphoric acid **1.133** produces a photoactive benzopyrylium intermediate that can photooxidize toluene. Upon deprotonation, the resulting toluyl radical undergoes addition to another equivalent of benzopyrylium. Reduction of the radical adduct by the reduced benzopyrylium affords the product and regenerates the photooxidant. Because the radical addition occurs in the presence of the conjugate base of the acid, the authors tested chiral phosphoric acid **1.133** in an enantioselective reaction, obtaining **1.134** in 60% ee.



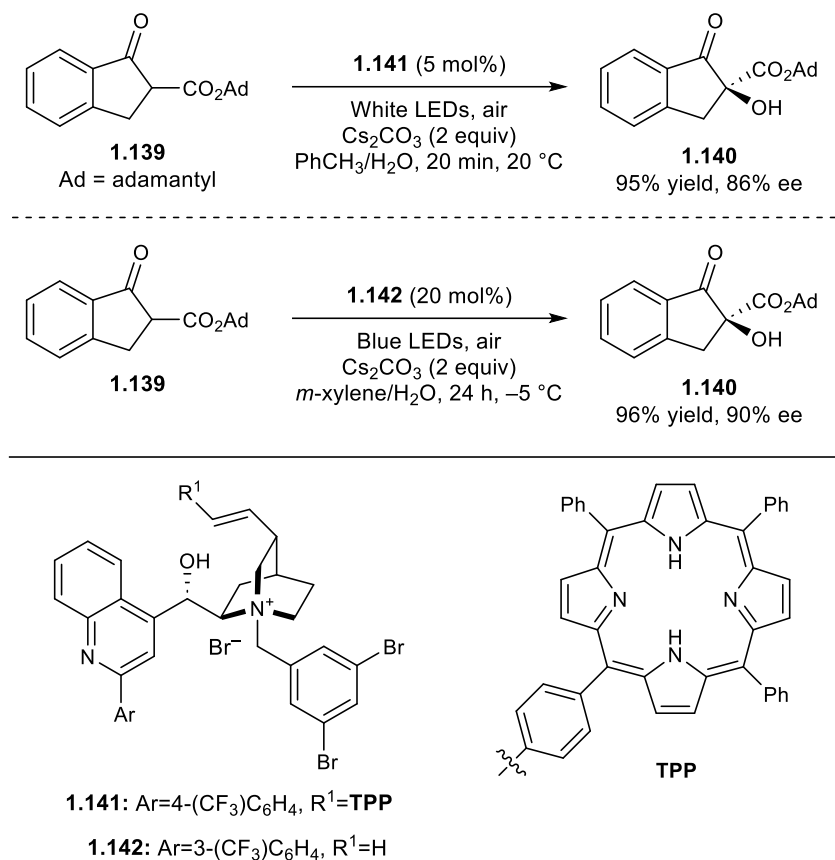
Scheme 1.53 Toluene Functionalization via Excitation of Benzopyrylium Intermediates

Finally, Melchiorre developed an asymmetric perfluoroalkylation of β -ketoesters exploiting an EDA complex activation strategy (**Scheme 1.54**).¹⁸⁵ In the presence of base and cinchona-derived phase transfer catalyst **1.137**, β -ketoester **1.136** is converted to the corresponding enolate with a chiral counteranion. The electron-rich enolate forms a ground-state association with an electron-poor perfluoroalkyl iodide (**1.135**) constituting an EDA complex. After excitation of the EDA complex and cleavage of the alkyl iodide, the perfluoroalkyl radical is proposed to be trapped by another equivalent of the enolate in the enantiodetermining step. The resulting ketyl radical abstracts an iodide from a perfluoroalkyl iodide, regenerating the alkyl radical and propagating a radical chain. Finally, the iodide adduct collapses to form the product. Subsequent computational studies suggested that multiple hydrogen-bonding interaction between the enolate and catalyst account for the high enantioselectivity.¹⁸⁶ This work is notably distinct from previous photo-organocatalyzed reports. In prior work the chiral catalyst was covalently bonded to the substrate in the enamine intermediate, while in this study the catalyst is ion paired to the enolate electron donor.



Scheme 1.54 Perfluoroalkylation of Enolates via Ion-Pairing Catalysis

In 2018, Meng showed that a cinchona-derived catalyst (**1.141**) tethered to a photocatalyst promotes β -ketoester oxidation via sensitization of oxygen in up to 86% ee (**Scheme 1.55**).¹⁸⁷ In 2019 the same group discovered that the reaction also proceeds with a similar catalyst lacking the photosensitizing unit (**1.142**).¹⁸⁸ As in the Melchiorre precedent above, an EDA complex was proposed between the deprotonated substrate enolate and the catalyst. The authors proposed that the excited EDA complex sensitizes oxygen, which then reacts with the enolate, eventually affording the hydroxylated product. The reaction was also performed in a flow photomicroreactor where the product was obtained in similar yield and enantioselectivity in under 1 h.



Scheme 1.55 Aerobic Oxidation of β -Ketoesters via Ion-Pairing Catalysis

1.5 Conclusion

After several decades of relatively slow development, there has been a recent, rapid increase in the pace of discovery of photocatalytic reactions that deliver enantioselectivities on par with those obtained in modern ground-state asymmetric catalytic reactions. In many cases, chiral photocatalyst structures have been developed by adapting catalyst classes originally designed for use in ground-state transformations. Several of these show promise to become privileged scaffolds within asymmetric photochemistry as well, including the secondary-amine catalysts studied by Melchiorre and oxazaborolidine catalysts investigated by Bach. Various photocatalyst structures unique to excited-state reactions have also been created to address the specific challenges relevant in asymmetric photochemistry. Many of these, including the chiral (thio)xanthone catalysts

pioneered by Bach, incorporate a chiral moiety into the structure of a known photosensitizing moiety.

While the structures of these photocatalysts are diverse, and the mechanisms by which they operate varied, a common design principle across multiple catalyst classes is the requirement for ground-state association of the substrate to the photocatalyst prior to excitation. This preassociation is one way to ensure that the catalyst meets the criteria described above. Preassociation sets the substrate within the chiral environment of the catalyst, and in most cases increases the rate of the enantioselective transformation over any competitive racemic background reactivity. However, as a consequence, the structures of these chiral catalysts and the resulting catalyst–substrate interactions have often been rigid and well-defined. This idea is similar to many of the early strategies for asymmetric catalysis in conventional, ground-state reactions; however, there has been a growing recognition that catalyst flexibility can be an important design strategy for thermally activated reactions.¹⁸⁹ As the field of asymmetric photocatalysis continues to develop, it stands to reason that the breadth of potential catalyst structures for enantioselective photocatalysis might be similarly broad.

The field of asymmetric photochemistry is poised for significant development over the next few decades. At this early stage in the development of the field, most examples of highly asymmetric photocatalytic reactions have been proof-of-principle academic investigations, and these insights have yet to be translated to commercial applications. As the pharmaceutical industry in particular becomes more interested in the scaleup of photocatalytic processes,^{190,191} issues concerning maximization of quantum yield and light flux¹⁹² may become more important than they have been to date. Despite the impressive advances that have emerged in the field of asymmetric photocatalysis in recent years, many challenges remain unsolved, perhaps the most important of

which is the need for generality. Some photocatalyst structures show promise to develop into privileged structures for enantioselective photochemical synthesis, catalyzing several highly enantioselective organic photoreactions with selectivities over 90% ee. These structures, however, are exceptional, and continued investigations are required to both establish their generality and to identify other classes of privileged asymmetric photocatalysts. While asymmetric photoreactions have the potential to greatly expedite the synthesis of complex products in unexplored areas of chemical diversity space, the continued development of more general methods is required before these reactions are used routinely by non-photochemists. We expect that the insights gained in research in this field to date will provide a solid foundation for continued transformative innovation.

1.6 References

- ¹ Sharpless, K. B. Searching for New Reactivity (Nobel Lecture). *Angew. Chem. Int. Ed.* **2002**, *41*, 2024–2032.
- ² Noyori, R. Asymmetric Catalysis: Science and Opportunities (Nobel Lecture 2001). *Adv. Synth. Catal.* **2003**, *345*, 15–32.
- ³ Knowles, W. S. Asymmetric Hydrogenations (Nobel Lecture 2001). *Adv. Synth. Catal.* **2003**, *345*, 3–13.
- ⁴ Ciamician, G. The Photochemistry of the Future. *Science* **1912**, *36*, 385–394.
- ⁵ Roth, H. D. The Beginnings of Organic Photochemistry. *Angew. Chem. Int. Ed.* **1989**, *28*, 1193–1207.
- ⁶ Inoue, Y.; Ramamurthy, V. *Molecular and Supramolecular Photochemistry, Volume 11: Chiral Photochemistry*; Marcel Dekker, **2004**.
- ⁷ Inoue, Y. Asymmetric Photochemical Reactions in Solution. *Chem. Rev.* **1992**, *92*, 741–770.
- ⁸ Sherbrook, E. M.; Yoon, T. P. Asymmetric Catalysis of Triplet-State Photoreactions. In *Specialist Periodical Reports: Photochemistry*; Albini, A., Protti, S., Eds.; Royal Society of Chemistry: Croydon, UK, 2019; Vol. *46*, pp 432–448.
- ⁹ Inoue, Y.; Dong, F.; Yamamoto, K.; Tong, L. H.; Tsuneishi, H.; Hakushi, T.; Tai, A. Inclusion-Enhanced Optical Yield and *E/Z* Ratio in Enantiodifferentiating Photoisomerization of Cyclooctene Included and Sensitized by β -Cyclodextrin Monobenzoate. *J. Am. Chem. Soc.* **1995**, *117*, 11033–11034.
- ¹⁰ Cauble, D. F.; Lynch, V.; Krische, M. J. Studies on the Enantioselective Catalysis of Photochemically Promoted Transformations: “Sensitizing Receptors” as Chiral Catalysts. *J. Org. Chem.* **2003**, *68*, 15–21.
- ¹¹ Griesbeck, A. G.; Meierhenrich, U. J. Asymmetric Photochemistry and Photochirogenesis. *Angew. Chem. Int. Ed.* **2002**, *41*, 3147–3154.
- ¹² Yang, C.; Inoue, Y. Supramolecular Photochirogenesis. *Chem. Soc. Rev.* **2014**, *43*, 4123–4143.
- ¹³ Brimiouille, R.; Lenhart, D.; Maturi, M. M.; Bach, T. Enantioselective Catalysis of Photochemical Reactions. *Angew. Chem. Int. Ed.* **2015**, *54*, 3872–3890.

-
- ¹⁴ Garrido-Castro, A. F. Asymmetric Induction in Photocatalysis – Discovering a New Side to Light-Driven Chemistry. *Tetrahedron Lett.* **2018**, *59*, 1286–1294.
- ¹⁵ Rao, M.; Wu, W.; Yang, C. Recent Progress on the Enantioselective Excited-State Photoreactions by Pre-Arrangement of Photosubstrate(s). *Green Synth. Catal.* **2021**, *2*, 131–144.
- ¹⁶ Rigotti, T.; Alemán, J. Visible Light Photocatalysis – From Racemic to Asymmetric Activation Strategies. *Chem. Commun.* **2020**, *56*, 11169–11190.
- ¹⁷ Nijland, A.; Harutyunyan, S. R. Light on the Horizon? Catalytic Enantioselective Photoreactions. *Catal. Sci. Technol.* **2013**, *3*, 1180–1189.
- ¹⁸ Zhao, J.-J.; Zhang, H.-H.; Yu, S. Enantioselective Radical Functionalization of Imines and Iminium Intermediates via Visible-Light Photoredox Catalysis. *Synthesis* **2021**, *53*, 1706–1718.
- ¹⁹ Prentice, C.; Morrisson, J.; Smith, A. D.; Zysman-Coleman, E. Recent Developments in Enantioselective Photocatalysis. **2020**, *16*, 2363–2441.
- ²⁰ Hong, B.-C. Enantioselective Synthesis Enabled by Visible Light Photocatalysis. *Org. Biomol. Chem.* **2020**, *18*, 4298–4353.
- ²¹ Skubi, K. L.; Blum, T. R.; Yoon, T. P. Dual Catalysis Strategies in Photochemical Synthesis. *Chem. Rev.* **2016**, *116*, 10035–10074.
- ²² Ramamurthy, V.; Sivaguru, J. Supramolecular Photochemistry as a Potential Synthetic Tool: Photocycloaddition. *Chem. Rev.* **2016**, *116*, 9914–9993.
- ²³ Ramamurthy, V.; Mondal, B. Supramolecular Photochemistry Concepts Highlighted with Select Examples. *J. Photochem. Photobiol. C* **2015**, *23*, 68–102.
- ²⁴ Ramamurthy, V.; Venkatesan, K. Photochemical Reactions of Organic Crystals. *Chem. Rev.* **1987**, *87*, 433–481.
- ²⁵ Turro, N. J. *Modern Molecular Photochemistry*; The Benjamin/Cummings Publishing Company, Inc., **1978**.
- ²⁶ Förster, T. Excimers. *Angew. Chem. Int. Ed.* **1969**, *8*, 333–343.
- ²⁷ Hammond, G. S.; Cole, R. S. Asymmetric Induction During Energy Transfer. *J. Am. Chem. Soc.* **1965**, *87*, 3256–3257.
- ²⁸ Aratani, T.; Nakanisi, Y.; Nozaki, H. The Absolute Configuration of *cis*-2-Phenylcyclopropanecarboxylic Acid. *Tetrahedron Lett.* **1969**, *10*, 1809–1810.

-
- ²⁹ Aratani, T.; Nakanisi, H.; Nozaki, H. The Absolute Configuration of *cis*-2-Phenylcyclopropanecarboxylic Acid and Related Compounds. *Tetrahedron*, **1970**, *26*, 1675–1684.
- ³⁰ Horner, L.; Klaus, J. Photochemisch Induzierte Reaktionen mi Grenzflächengebundenen Sensibilisatoren. *J. Liebigs Ann. Chem.* **1981**, 792–810.
- ³¹ Hammond, G. S.; Saltiel, J. Mechanisms of Photoreactions in Solution. XVIII. Energy Transfer with Nonvertical Transitions. *J. Am. Chem. Soc.* **1963**, *85*, 2516–2517.
- ³² Hammond, G. S.; Wyatt, P.; DeBoer, C. D.; Turro, N. J. Photosensitized Isomerization Involving Saturated Centers. *J. Am. Chem. Soc.* **1964**, *86*, 2532–2533.
- ³³ Hammond, G. S.; Saltiel, J.; Lamola, A. A.; Turro, N. J.; Bradshaw, J. S.; Cowan, D. O.; Counsell, R. C. Vogt, V.; Dalton, C. Mechanisms of Photochemical Reactions in Solution. XXII. Photochemical *cis*–*trans* Isomerization. *J. Am. Chem. Soc.* **1964**, *86*, 3197–3217.
- ³⁴ Murov, S. L.; Cole, R. S.; Hammond, G. S. Mechanisms of Photochemical Reactons in Solution. LIV. A New Mechanism for Photosensitization. *J. Am. Chem. Soc.* **1968**, *90*, 2957–2958.
- ³⁵ Balavoine, G.; Jugé, S.; Kagan, H. B. Photoactivation Optique du Methyl *p*-Tolyl Sulfoxide Racémique par Emploi d'un Sensibilisateur Chiral. *Tetrahedron Lett.* **1973**, *14*, 4159–4162.
- ³⁶ Kagan, H. B.; Fiaud, J. C. New Approaches in Asymmetric Synthesis. *Top. Stereochem.* **1978**, *10*, 175–285.
- ³⁷ Mislow, K.; Axelrod, M.; Rayner, D. R.; Gotthardt, H.; Coyne, L. M.; Hammond, G. S. Light-Induced Pyramidal Inversion of Sulfoxides. *J. Am. Chem. Soc.* **1965**, *87*, 4958–4959.
- ³⁸ Cooke, R. S.; Hammond, G. S. Mechanisms of Photochemical Reaction in Solution. LV. Naphthalene-Sensitized Photoracemization of Sulfoxides. *J. Am. Chem. Soc.* **1968**, *90*, 2958–2959.
- ³⁹ Cooke, R. S.; Hammond, G. S. Mechanisms of Photochemical Reactions in Solution. LXII. Naphthalene-Sensitized Photoracemization of Sulfoxides. *J. Am. Chem. Soc.* **1970**, *92*, 2739–2745.
- ⁴⁰ Kropp, P. J.; Fryxell, G. E.; Tubergen, M. W.; Hager, M. W.; Harris Jr., G. D.; McDermott Jr., T. P.; Tornero-Velez, R. Photochemistry of Phenyl Thioethers and Phenyl Selenoethers. Radical vs. Ionic Behavior. *J. Am. Chem. Soc.* **1991**, *113*, 7300–7310.
- ⁴¹ Vos, B. W.; Jenks, W. S. Evidence for a Nonradical Pathway in the Photoracemization of Aryl Sulfoxides. *J. Am. Chem. Soc.* **2002**, *124*, 2544–2547.

-
- ⁴² Hoshi, N.; Furukawa, Y.; Hagiwara, H.; Uda, H.; Sato, K. Enantiomer Differentiation in the Photoinduced 1,5-Phenyl Shift of 3-Methyl-3-Phenyl-2(3*H*)-Oxepinone Utilizing Chiral Sensitizers. *Chem. Lett.* **1980**, *9*, 47–50.
- ⁴³ Drucker, C. S.; Toscano, V. G.; Weiss, R. G. A General Method for the Determination of Steric Effects during Collisional Energy Transfer. Partial Photoresolution of Penta-2,3-Diene. *J. Am. Chem. Soc.* **1973**, *95*, 6482–6484.
- ⁴⁴ Swenton, J. S. Photoisomerization of *cis*-Cyclooctene to *trans*-Cyclooctene. *J. Org. Chem.* **1969**, *34*, 3217–3218.
- ⁴⁵ Cope, A. C.; Ganellin, C. R.; Johnson, H. W.; Van Auken, T. V.; Winkler, H. J. S. Molecular Asymmetry of Olefins. I. Resolution of *trans*-Cyclooctene. *J. Am. Chem. Soc.* **1963**, *85*, 3276–3279.
- ⁴⁶ Inoue, Y.; Kunitomi, Y.; Takamuku, S.; Sakurai, H. Asymmetric *cis*–*trans* Photoisomerization of Cyclo-octene Sensitized by Chiral Aromatic Esters. *J. Chem. Soc., Chem. Commun.* **1978**, 1024–1025.
- ⁴⁷ Inoue, Y.; Takamuku, S.; Kunitomi, Y.; Sakurai, H. Singlet Photosensitization of Simple Alkenes. Part 1. *cis*–*trans*-Photoisomerization of Cyclo-octene Sensitized by Aromatic Esters. *J. Chem. Soc., Perkin Trans. 2* **1980**, 1672–1678.
- ⁴⁸ Tsuneishi, H.; Hakushi, T.; Inoue, Y. Singlet- versus Triplet-Sensitized Enantiodifferentiating Photoisomerization of Cyclooctene: Remarkable Effects of Spin Multiplicity upon Optical Yield. *J. Chem. Soc., Perkin Trans. 2* **1996**, 1601–1605.
- ⁴⁹ Inoue, Y.; Yokoyama, T.; Yamasaki, N.; Tai, A. An Optical Yield that Increases with Temperature in a Photochemically Induced Enantiomeric Isomerization. *Nature*, **1989**, *341*, 225–226.
- ⁵⁰ Inoue, Y.; Yokoyama, T.; Yamasaki, N.; Tai, A. Temperature Switching of Product Chirality upon Photosensitized Enantiodifferentiating *Cis*–*Trans* Isomerization of Cyclooctene. *J. Am. Chem. Soc.* **1989**, *111*, 6480–6482.
- ⁵¹ Shi, M.; Inoue, Y. Enantiodifferentiating Photoisomerization of (*Z*)-Cyclooctene and (*Z,Z*)-Cycloocta-1,3-diene Sensitized by Chiral Aromatic Amides. *J. Chem. Soc., Perkin Trans. 2* **1998**, 1725–1729.
- ⁵² Shi, M.; Inoue, Y. Geometrical Photoisomerization of (*Z*)-Cyclooctene Sensitized by Aromatic Phosphate, Phosphonate, Phosphinate, Phosphine Oxide and Chiral Phosphoryl Esters. *J. Chem. Soc., Perkin Trans. 2* **1998**, 2421–2427.

-
- ⁵³ Mori, T.; Relevance of the Entropy Factor in Stereoselectivity Control of Asymmetric Photoreactions. *Synlett* **2020**, *31*, 1259–1267.
- ⁵⁴ Inoue, Y.; Wada, T.; Asaoka, S.; Sato, H.; Pete, J.-P. Photochirogenesis: Multidimensional Control of Asymmetric Photochemistry. *Chem. Commun.* **2000**, 251–259.
- ⁵⁵ Inoue, Y.; Yamasaki, N.; Yokoyama, T.; Tai, A. Enantiodifferentiating *Z–E* Photoisomerization of Cyclooctene Sensitized by Chiral Polyalkyl Benzenepolycarboxylates. *J. Org. Chem.* **1992**, *57*, 1332–1345.
- ⁵⁶ Inoue, Y.; Yamasaki, N.; Yokoyama, T.; Tai, A. Highly Enantiodifferentiating Photoisomerization of Cyclooctene by Congested and/or Triplex-Forming Chiral Sensitizers. *J. Org. Chem.* **1993**, *58*, 1011–1018.
- ⁵⁷ Asano, T.; Le Noble, W. J. Activation and Reaction Volumes in Solution. *Chem. Rev.* **1978**, *78*, 407–489.
- ⁵⁸ Chung, W. S.; Turro, N. J.; Mertes, J.; Mattay, J. Radical Ions and Photochemical Charge-Transfer Phenomena. 22. Pressure-Induced Diastereoselectivity in Photoinduced Diels–Alder Reactions. *J. Org. Chem.* **1989**, *54*, 4881–4887.
- ⁵⁹ Inoue, Y.; Matsushima, E.; Wada, T. Pressure and Temperature Control of Product Chirality in Asymmetric Photochemistry. Enantiodifferentiating Photoisomerization of Cyclooctene Sensitized by Chiral Benzenepolycarboxylates. *J. Am. Chem. Soc.* **1998**, *120*, 10687–10696.
- ⁶⁰ Kaneda, M.; Nakamura, A.; Asaoka, S.; Ikeda, H.; Mori, T.; Wada, T.; Inoue, Y. Pressure Control of Enantiodifferentiating Photoisomerization of Cyclooctenes Sensitized by Chiral Benzenepolycarboxylates. The Origin of Discontinuous Pressure Dependence of the Optical Yield. *Org. Biomol. Chem.* **2003**, *1*, 4435–4440.
- ⁶¹ Kaneda, M.; Asaoka, S.; Ikeda, H.; Mori, T.; Wada, T.; Inoue, Y. Discontinuous Pressure Effect upon Enantiodifferentiating Photosensitized Isomerization of Cyclooctene. *Chem. Commun.* **2002**, 1272–1273.
- ⁶² Inoue, Y.; Ikeda, H.; Kaneda, M.; Sumimura, T.; Everitt, S. R. L.; Wada, T. Entropy-Controlled Asymmetric Photochemistry: Switching of Product Chirality by Solvent. *J. Am. Chem. Soc.* **2000**, *122*, 406–407.
- ⁶³ Saito, R.; Kaneda, M.; Wada, T.; Katoh, A.; Inoue, Y. First Asymmetric Photosensitization in Supercritical Fluid. Exceptionally High Pressure/Density of Optical Yield in Photosensitized Enantiodifferentiating Isomerization of Cyclooctene. *Chem. Lett.* **2002**, *31*, 860–861.

-
- ⁶⁴ Tsuneishi, H.; Hakushi, T.; Tai, A.; Inoue, Y. Enantiodifferentiating Photoisomerization of 1-Methylcyclooct-1-ene Sensitized by Chiral Alkyl Benzenecarboxylates: Steric Effects upon Stereodifferentiation. *J. Chem. Soc., Perkin Trans. 2* **1995**, 2057–2062.
- ⁶⁵ Tsuneishi, H.; Inoue, Y.; Hakushi, T.; Tai, A. Direct and Sensitized Geometrical Photoisomerization of 1-Methylcyclooctene. *J. Chem. Soc., Perkin Trans. 2* **1993**, 457–462.
- ⁶⁶ Sugimura, T.; Shimizu, H.; Umemoto, S.; Tsuneishi, H.; Hakushi, T.; Inoue, Y.; Tai, A. Efficient Diastereodifferentiating *E-Z* Photoisomerization of Cyclooctene Tethered to Intramolecular Sensitizer through Optically Active Pentane-2,4-diyl Unit. *Chem. Lett.* **1998**, 27, 323–324.
- ⁶⁷ Inoue, T.; Matsuyama, K.; Inoue, Y. Diastereodifferentiating *Z-E* Photoisomerization of 3-Benzoyloxycyclooctene: Diastereoselectivity Switching Controlled by Substrate Concentration through Competitive Intra- vs. Intermolecular Photosensitization Processes. *J. Am. Chem. Soc.* **1999**, 121, 9877–9878.
- ⁶⁸ Matsuyama, K.; Inoue, T.; Inoue, Y. Self-Sensitized Diastereodifferentiating *Z-E* Photoisomerization of 3-, 4-, and 5-Benzoyloxycyclooctenes: Intra- versus Intermolecular Photosensitization. *Synthesis* **2001**, 1167–1174.
- ⁶⁹ Inoue, Y.; Tsuneishi, H.; Hakushi, T.; Tai, A. Optically Active (*E,Z*)-1,3-Cyclooctadiene: First Enantioselective Synthesis through Asymmetric Photosensitization and Chiroptical Property. *J. Am. Chem. Soc.* **1997**, 119, 472–478.
- ⁷⁰ Inoue, Y.; Hakushi, T.; Goto, S.; Takamuku, S.; Sakurai, H. Singlet Photosensitization of Simple Alkenes. Part 2. Photochemical Transformation of Cyclo-octa-1,5-dienes Sensitized by Aromatic Ester. *J. Chem. Soc., Perkin Trans. 2* **1980**, 1678–1682.
- ⁷¹ Maeda, R.; Wada, T.; Mori, T.; Kono, S.; Kanomata, N.; Inoue, Y. *Planar-to-Planar* Chirality Transfer in the Excited State. Enantiodifferentiating Photoisomerization of Cyclooctenes Sensitized by Planar-Chiral Paracyclophane. *J. Am. Chem. Soc.* **2011**, 133, 10379–10381.
- ⁷² Hoffmann, R.; Inoue, Y. Trapped Optically Active (*E*)-Cycloheptene Generated by Enantiodifferentiating *Z-E* Photoisomerization of Cycloheptene Sensitized by Chiral Aromatic Esters. *J. Am. Chem. Soc.* **1999**, 121, 10702–10710.
- ⁷³ Asaoka, S.; Horiguchi, H.; Wada, T.; Inoue, Y. Enantiodifferentiating Photocyclization of Cyclohexene Sensitized by Chiral Benzenecarboxylates. *J. Chem. Soc., Perkin Trans. 2* **2000**, 737–747.
- ⁷⁴ Asaoka, S.; Ooi, M.; Jiang, P.; Wada, T.; Inoue, Y. Enantiodifferentiating Photocyclodimerization of Cyclohexa-1,3-diene Sensitized by Chiral Arenecarboxylates. *J. Chem. Soc., Perkin Trans. 2* **2000**, 77–84.

-
- ⁷⁵ Inoue, Y.; Shimoyama, H.; Yamasaki, N.; Tai, A. Enantiodifferentiating Photoisomerization of 1,2-Diphenylcyclopropane Sensitized by Chiral Aromatic Esters. *Chem. Lett.* **1991**, *20*, 593–596.
- ⁷⁶ Inoue, Y.; Yamasaki, N.; Shimoyama, H.; Tai, A. Enantiodifferentiating Cis–Trans Photoisomerizations of 1,2-Diarylcyclopropanes and 2,3-Diphenyloxirane Sensitized by Chiral Aromatic Esters. *J. Org. Chem.* **1993**, *58*, 1785–1793.
- ⁷⁷ Roth, H. D. Electron-Transfer Photochemistry of *cis*- and *trans*-1,2-Diphenylcyclopropane with Singlet Acceptors: Recombination of Radical Ion Pairs of Singlet and Triplet Multiplicity. *J. Phys. Chem. A* **2003**, *107*, 3432–3437.
- ⁷⁸ Inoue, Y.; Okano, T.; Yamasaki, N.; Tai, A. Enantiodifferentiating Photocyclodimerization of Phenyl Vinyl Ethers and 4-Methoxystyrene Sensitized by Chiral Aromatic Esters. *J. Photochem. Photobiol. A* **1992**, *66*, 61–68.
- ⁷⁹ Inoue, Y.; Okano, T.; Yamasaki, N.; Tai, A. First Photosensitized Enantiodifferentiating Polar Addition: Anti-Markovnikov Methanol Addition to 1,1-Diphenylpropene. *J. Chem. Soc., Chem. Commun.* **1993**, 718–720.
- ⁸⁰ Asaoka, S.; Kitazawa, T.; Wada, T.; Inoue, Y. Enantiodifferentiating Anti-Markovnikov Photoaddition of Alcohols to 1,1-Diphenylalkenes Sensitized by Chiral Naphthalenecarboxylates. *J. Am. Chem. Soc.* **1999**, *121*, 8486–8498.
- ⁸¹ Asaoka, S.; Wada, T.; Inoue, Y. Microenvironmental Polarity Control of Electron-Transfer Photochirogenesis. Enantiodifferentiating Polar Addition of 1,1-Diphenyl-1-alkenes Photosensitized by Saccharide Naphthalenecarboxylates. *J. Am. Chem. Soc.* **2003**, *125*, 3008–3027.
- ⁸² Takehara, Y.; Ohta, N.; Shiraishi, S.; Asaoka, S.; Wada, T.; Inoue, Y. External Electric Field Effects on Exciplex Formation of 1,1-Diphenylpropene with Chiral 1,4-Naphthalenedicarboxylate in PMMA Polymer Films. *J. Photochem. Photobiol. A* **2001**, *145*, 53–60.
- ⁸³ Kaneda, M.; Nishiyama, Y.; Asaoka, S.; Mori, T.; Wada, T.; Inoue, Y. Pressure Control of Enantiodifferentiating Polar Addition of 1,1-Diphenylpropene Sensitized by Chiral Naphthalenecarboxylates. *Org. Biomol. Chem.* **2004**, *2*, 1295–1303.
- ⁸⁴ Nishiyama, Y.; Kaneda, M.; Saito, R.; Mori, T.; Wada, T.; Inoue, Y. Enantiodifferentiating Photoaddition of Alcohols to 1,1-Diphenylpropene in Supercritical Carbon Dioxide: Sudden Jump of Optical Yield at the Critical Density. *J. Am. Chem. Soc.* **2004**, *126*, 6568–6569.
- ⁸⁵ Nishiyama, Y.; Kaneda, M.; Asaoka, S.; Saito, R.; Mori, T.; Wada, T.; Inoue, Y. Mechanistic Studies on the Enantiodifferentiating Anti-Markovnikov Photoaddition of Alcohols to 1,1-Diphenyl-1-alkenes in Near-Critical and Supercritical Carbon Dioxide. *J. Phys. Chem. A* **2007**, *111*, 13432–13440.

-
- ⁸⁶ Yasuhiro, N.; Takehiko, W.; Tadashi, M.; Inoue, Y. Critical Control by Temperature and Pressure of Enantiodifferentiating Anti-Markovnikov Photoaddition of Methanol to Diphenylpropene in Near Critical and Supercritical Carbon Dioxide. *Chem. Lett.* **2007**, *36*, 1488–1489.
- ⁸⁷ Nishiyama, Y.; Wada, T.; Asaoka, S.; Mori, T.; McCarty, T. A.; Kraut, N. D.; Bright, F. V.; Inoue, Y. Entrainer Effect on Photochirogenesis in Near- and Supercritical Carbon Dioxide: Dramatic Enhancement of Enantioselectivity. *J. Am. Chem. Soc.* **2008**, *130*, 7526–7527.
- ⁸⁸ Nishiyama, Y.; Wada, T.; Kakiuchi, K.; Inoue, Y. Entrainer Effects on Enantiodifferentiating Photocyclization of 5-Hydroxy-1,1-diphenylpentane in Near-Critical and Supercritical Carbon Dioxide. *J. Org. Chem.* **2012**, *77*, 5681–5686.
- ⁸⁹ Nishiyama, Y.; Wada, T.; Kakiuchi, K.; Inoue, Y. Microenvironmental Control of Enantiodifferentiating Photocyclization of 5-Hydroxy-1,1-diphenylpentene through Selective Solvation. *Chirality* **2012**, *24*, 400–405.
- ⁹⁰ Kim, J.-I.; Schuster, G. B. Enantioselective Catalysis of the Triplex Diels–Alder Reaction: Addition of *trans*- β -Methylstyrene to 1,3-Cyclohexadiene Photosensitized with (–)-1,1'-Bis(2,4-dicyanonaphthalene). *J. Am. Chem. Soc.* **1990**, *112*, 9635–9637.
- ⁹¹ Calhoun, G. C.; Schuster, G. B. Radical Cation and Triplex Diels–Alder Reaction of 1,3-Cyclohexadiene. *J. Am. Chem. Soc.* **1984**, *106*, 6870–6871.
- ⁹² Calhoun, G. C.; Schuster, G. B. The Triplex Diels–Alder Reaction of Indene and Cyclic Dienes. *J. Am. Chem. Soc.* **1986**, *108*, 8021–8027.
- ⁹³ Akbulut, N.; Hartsough, D.; Kim, J.-I.; Schuster, G. B. The Triplex Diels–Alder Reaction of 1,3-Dienes with Enol, Alkene, and Acetylenic Dienophiles: Scope and Utility. *J. Org. Chem.* **1989**, *54*, 2549–2556.
- ⁹⁴ Kim, J.-I.; Schuster, G. B. Enantioselective Catalysis of the Triplex Diels–Alder Reaction: A Study of Scope and Mechanism. *J. Am. Chem. Soc.* **1992**, *114*, 9309–9317.
- ⁹⁵ Vondenhof, M.; Mattay, J. 1,1'-Binaphthalene-2,2'-Dicarbonitrile in Photochemically Sensitized Enantiodifferentiating Isomerizations. *Chem. Ber.* **1990**, *123*, 2457–2459.
- ⁹⁶ Vondenhof, M.; Mattay, J. Sulfonic Acid Esters Derived from 1,1'-Binaphthalene as New Axially Chiral Photosensitizers. *Tetrahedron Lett.* **1990**, *31*, 985–988.
- ⁹⁷ Das, A.; Ayad, S.; Hanson, K. Enantioselective Protonation of Silyl Enol Ether Using Excited State Proton Transfer Dyes. *Org. Lett.* **2016**, *18*, 5416–5419.

-
- ⁹⁸ Das, A.; Banerjee, T.; Hanson, K. Protonation of Silylenol Ether *via* Excited State Proton Transfer Catalysis. *Chem. Commun.* **2016**, *52*, 1350–1353.
- ⁹⁹ Àlvaro, M.; Formentín, P.; García, H.; Palomares, E.; Sabater, M. J. Chiral N-Alkyl-2,4,6-triphenylpyridiniums as Enantioselective Triplet Photosensitizers. Laser Flash Photolysis and Preparative Studies. *J. Org. Chem.* **2002**, *67*, 5184–5189.
- ¹⁰⁰ Vallavoju, N.; Selvakumar, S.; Jockusch, S.; Sibi, M. P.; Sivaguru, J. Enantioselective Organophotocatalysis Mediated by Atropisomeric Thiourea Derivatives. *Angew. Chem. Int. Ed.* **2014**, *53*, 5604–5608.
- ¹⁰¹ Vallavoju, N.; Selvakumar, S.; Jockusch, S.; Prabhakaran, M. T.; Sibi, M. P.; Sivaguru, J. Evaluating Thiourea Architecture for Intramolecular [2+2] Photocycloaddition of 4-Alkenylcoumarins. *Adv. Synth. Catal.* **2014**, *356*, 2763–2768.
- ¹⁰² Vallavoju, N.; Selvakumar, S.; Pemberton, B. C.; Jockusch, S.; Sibi, M. P.; Sivaguru, J. Organophotocatalysis: Insights into the Mechanistic Aspects of Thiourea-Mediated Intermolecular [2+2] Photocycloadditions. *Angew. Chem. Int. Ed.* **2016**, *55*, 5446–5451.
- ¹⁰³ Raghunathan, R.; Jockusch, S.; Sibi, M. P.; Sivaguru, J. Evaluating Thiourea/Urea Catalyst for Enantioselective 6 π -Photocyclization of Acrylanilides. *J. Photochem. Photobiol. A* **2016**, *331*, 84–88.
- ¹⁰⁴ Rau, H.; Hörmann, M. Kinetic Resolution of Optically Active Molecules and Asymmetric Chemistry: Asymmetrically Sensitized Photolysis of *trans*-3,5-Diphenylpyrazoline. *J. Photochem.* **1981**, *16*, 231–247.
- ¹⁰⁵ Becker, E.; Weiland, R.; Rau, H. Photochemistry of Bichromophoric Molecules with Camphor Structure I: Energy Transfer and Asymmetry Effects. *J. Photochem. Photobiol. A* **1988**, *41*, 311–330.
- ¹⁰⁶ Ouannès, C.; Beugelmans, R.; Roussi, G. Asymmetric Induction during Transfer of Triplet Energy. *J. Am. Chem. Soc.* **1973**, *95*, 8472–8474.
- ¹⁰⁷ Demuth, M.; Raghavan, P. R.; Carter, C.; Nakano, K.; Schaffner, K. Photochemical High-Yield Preparation of Tricyclo[3.3.0.0]Octan-3-ones. Potential Synthons for Polycyclopentanoid Terpenes and Prostacyclin Analogs. *Helv. Chim. Acta* **1980**, *63*, 2434–2439.
- ¹⁰⁸ Kemp, D. S.; Petrakis, K. S. Synthesis and Conformational Analysis of *cis,cis*-1,3,5-Trimethylcyclohexane-1,3,5-tricarboxylic Acid. *J. Org. Chem.* **1981**, *46*, 5140–5143.
- ¹⁰⁹ Bach, T.; Bergmann, H.; Harms, K. High Facial Diastereoselectivity in the Photocycloaddition of a Chiral Aromatic Aldehyde and an Enamide Induced by Intermolecular Hydrogen Bonding. *J. Am. Chem. Soc.* **1999**, *121*, 10650–10651.

-
- ¹¹⁰ Bach, T.; Bergmann, H.; Brummerhop, H.; Lewis, W.; Harms, K. The [2+2]-Photocycloaddition of Aromatic Aldehydes and Ketones to 3,4-Dihydro-2-pyridones: Regioselectivity, Diastereoselectivity, and Reductive Ring Opening of the Product Oxetanes. *Chem. - Eur. J.* **2001**, *7*, 4512–4521.
- ¹¹¹ Bach, T.; Bergmann, H.; Harms, K. Enantioselective Intramolecular [2+2]-Photocycloaddition Reaction in Solution. *Angew. Chem. Int. Ed.* **2000**, *39*, 2302–2304.
- ¹¹² Bach, T.; Bergmann, H.; Grosch, B.; Harms, K.; Herdtweck, E. Synthesis of Enantiomerically Pure 1,5,7-Trimethyl-3-azabicyclo[3.3.1]nonan-2-ones as Chiral Host Compounds for Enantioselective Photochemical Reactions in Solution. *Synthesis* **2001**, 1395–1405.
- ¹¹³ Bach, T.; Bergmann, H.; Grosch, B.; Harms, K. Highly Enantioselective Intra- and Intermolecular [2+2] Photocycloaddition Reactions of 2-Quinolones Mediated by a Chiral Lactam Host: Host–Guest Interactions, Product Configuration, and the Origin of the Stereoselectivity in Solution. *J. Am. Chem. Soc.* **2002**, *124*, 7982–7990.
- ¹¹⁴ Albrecht, D.; Vogt, F.; Bach, T. Diastereo- and Enantioselective Intramolecular [2+2] Photocycloaddition Reactions of 3-(ω' -Alkenyl)- and 3-(ω' -Alkenyloxy)-Substituted 5,6-Dihydro-1*H*-pyridin-2-ones. *Chem. - Eur. J.* **2010**, *16*, 4284–4296.
- ¹¹⁵ Austin, K. A. B.; Herdtweck, E.; Bach, T. Intramolecular [2+2] Photocycloaddition of Substituted Isoquinolones: Enantioselectivity and Kinetic Resolution Induced by a Chiral Template. *Angew. Chem. Int. Ed.* **2011**, *50*, 8416–8419.
- ¹¹⁶ Bach, T.; Bergmann, H. Enantioselective Intermolecular [2+2]-Photocycloaddition Reactions of Alkenes and a 2-Quinolone in Solution. *J. Am. Chem. Soc.* **2000**, *122*, 11525–11526.
- ¹¹⁷ Selig, P.; Bach, T. Photochemistry of 4-(2'-Aminoethyl)quinolones: Enantioselective Synthesis of Tetracyclic Tetrahydro-1*aH*-pyrido[4',3':2,3]-cyclobuta[1,2-*c*] Quinoline-2,11(3*H*,8*H*)-diones by Intra- and Intermolecular [2 + 2]-Photocycloaddition Reactions in Solution. *J. Org. Chem.* **2006**, *71*, 5662–5673.
- ¹¹⁸ Coote, S. C.; Bach, T. Enantioselective Intermolecular [2+2] Photocycloadditions of Isoquinolone Mediated by a Chiral Hydrogen-Bonding Template. *J. Am. Chem. Soc.* **2013**, *135*, 14948–14951.
- ¹¹⁹ Mayr, F.; Wiegand, C.; Bach, T. Enantioselective, Intermolecular [2+2] Photocycloaddition Reactions of 3-Acetoxyquinolone: Total Synthesis of (–)-Pinolinone. *Chem. Commun.* **2014**, *50*, 3353–3355.
- ¹²⁰ Coote, S. C.; Pöthig, A.; Bach, T. Enantioselective Template-Directed [2 + 2] Photocycloadditions of Isoquinolones: Scope, Mechanism and Synthetic Applications. *Chem. - Eur. J.* **2015**, *21*, 6906–6912.

-
- ¹²¹ Grosch, B.; Orlebar, C. N.; Herdtweck, E.; Massa, W.; Bach, T. Highly Enantioselective Diels–Alder Reactions of a Photochemically Generated *o*-Quinodimethane with Olefins. *Angew. Chem. Int. Ed.* **2003**, *42*, 3693–3696.
- ¹²² Grosch, B.; Orlebar, C. N.; Herdtweck, E.; Kaneda, M.; Wada, T.; Inoue, Y.; Bach, T. Enantioselective [4+2]-Cycloaddition Reaction of a Photochemically Generated *o*-Quinodimethane: Mechanistic Details, Association Studies, and Pressure Effects. *Chem. - Eur. J.* **2004**, *10*, 2179–2189.
- ¹²³ Bach, T.; Bergmann, H.; Harms, K. Enantioselective Photochemical Reactions of 2-Pyridones in Solution. *Org. Lett.* **2001**, *3*, 601–603.
- ¹²⁴ Maturi, M. M.; Fukuhara, G.; Tanaka, K.; Kawanami, Y.; Mori, T.; Inoue, Y.; Bach, T. Enantioselective [4+4] Photodimerization of Anthracene-2,6-dicarboxylic Acid Mediated by a C₂-Symmetric Chiral Template. *Chem. Commun.* **2016**, *52*, 1032–1035.
- ¹²⁵ Bach, T.; Aechtner, T.; Neumüller, B. Intermolecular Hydrogen Binding of a Chiral Host and a Prochiral Imidazolidinone: Enantioselective Norrish–Yang Cyclisation in Solution. *Chem. Commun.* **2001**, 607–608.
- ¹²⁶ Bach, T.; Aechtner, T.; Neumüller, B. Enantioselective Norrish–Yang Cyclization Reactions of N-(ω -Oxo- ω -phenylalkyl)-Substituted Imidazolidinones in Solution and in the Solid State. *Chem. - Eur. J.* **2002**, *8*, 2464–2475.
- ¹²⁷ Bach, T.; Grosch, B.; Strassner, T.; Herdtweck, E. Enantioselective [6 π]-Photocyclization Reaction of an Acrylanilide Mediated by a Chiral Host. Interplay between Enantioselective Ring Closure and Enantioselective Protonation. *J. Org. Chem.* **2003**, *68*, 1107–1116.
- ¹²⁸ Bauer, A.; Westkämper, F.; Grimme, S.; Bach, T. Catalytic Enantioselective Reactions Driven by Photoinduced Electron Transfer. *Nature*, **2005**, *436*, 1139–1140.
- ¹²⁹ Inoue, Y. Light on Chirality. *Nature*, **2005**, *436*, 1099–1100.
- ¹³⁰ Müller, C.; Bauer, A.; Bach, T. Light-Driven Enantioselective Organocatalysis. *Angew. Chem. Int. Ed.* **2009**, *48*, 6640–6642.
- ¹³¹ Bakowski, A.; Dressel, M.; Bauer, A.; Bach, T. Enantioselective Radical Cyclisation Reactions of 4-Substituted Quinolones Mediated by a Chiral Template. *Org. Biomol. Chem.* **2011**, *9*, 3516–3529.
- ¹³² Müller, C.; Bauer, A.; Maturi, M. M.; Cuquerella, M. C.; Miranda, M. A.; Bach, T. Enantioselective Intramolecular [2+2]-Photocycloaddition Reactions of 4-Substituted Quinolones Catalyzed by a Chiral Sensitizer with a Hydrogen-Bonding Motif. *J. Am. Chem. Soc.* **2011**, *133*, 16689–16697.

-
- ¹³³ Maturi, M. M.; Wenninger, M.; Alonso, R.; Bauer, A.; Pöthig, A.; Riedle, E.; Bach, T. Intramolecular [2+2] Photocycloaddition of 3- and 4-(But-3-enyl)oxyquinolones: Influence of the Alkene Substitution Pattern, Photophysical Studies, and Enantioselective Catalysis by a Chiral Sensitizer. *Chem. - Eur. J.* **2013**, *19*, 7461–7472.
- ¹³⁴ Hoffmann, Roald.; Swenson, J. R. Ground- and Excited-State Geometries of Benzophenone. *J. Phys. Chem.* **1970**, *74*, 415–420.
- ¹³⁵ Maturi, M. M.; Bach, T. Enantioselective Catalysis of the Intermolecular [2+2] Photocycloaddition between 2-Pyridones and Acetylenedicarboxylates. *Angew. Chem. Int. Ed.* **2014**, *53*, 7661–7664.
- ¹³⁶ Maturi, M. M.; Pöthig, A.; Bach, T. Enantioselective Photochemical Rearrangements of Spirooxindole Epoxides Catalyzed by a Chiral Bifunctional Xanthone. *Aust. J. Chem.* **2015**, *68*, 1682–1692.
- ¹³⁷ Alonso, R.; Bach, T. A Chiral Thioxanthone as an Organocatalyst for Enantioselective [2+2] Photocycloaddition Reactions Induced by Visible Light. *Angew. Chem. Int. Ed.* **2014**, *53*, 4368–4371.
- ¹³⁸ Li, X.; Jandl, C.; Bach, T. Visible-Light-Mediated Enantioselective Photoreactions of 3-Alkylquinolones with 4-*O*-Tethered Alkenes and Allenes. *Org. Lett.* **2020**, *22*, 3618–3622.
- ¹³⁹ Tröster, A.; Alonso, R.; Bauer, A.; Bach, T. Enantioselective Intermolecular [2 + 2] Photocycloaddition Reactions of 2(1*H*)-Quinolones Induced by Visible Light Irradiation. *J. Am. Chem. Soc.* **2016**, *138*, 7808–7811.
- ¹⁴⁰ Li, X.; Großkopf, J.; Jandl, C.; Bach, T. Enantioselective, Visible Light Mediated Aza Paternò-Büchi Reactions of Quinoxalinones. *Angew. Chem. Int. Ed.* **2021**, *60*, 2684–2688.
- ¹⁴¹ Nishio, T.; Omote, Y. Photocycloaddition of Quinoxalin-2-ones and Benzoxazin-2-ones to Aryl Alkenes. *J. Chem. Soc., Perkin Trans. 1* **1987**, 2611–2615.
- ¹⁴² Hölzl-Hobmeier, A.; Bauer, A.; Silva, A. V.; Huber, S. M.; Bannwarth, C.; Bach, T. Catalytic Deracemization of Chiral Allenes by Sensitized Excitation with Visible Light. *Nature*, **2018**, *564*, 240–243.
- ¹⁴³ Plaza, M.; Jandl, C.; Bach, T. Photochemical Deracemization of Allenes and Subsequent Chirality Transfer. *Angew. Chem. Int. Ed.* **2020**, *59*, 12785–12788.
- ¹⁴⁴ Yuan, K.; Wang, P.; Li, H.-X.; Liu, Y.-Z.; Lv, L.-L. Theoretical Survey of the Photochemical Deracemization Mechanism of Chiral Allene 3-(3,3-Dimethyl-1-Buten-1-Ylidene)-2-Piperidinone. *Org. Chem. Front.* **2020**, *7*, 3656–3663.

-
- ¹⁴⁵ Plaza, M.; Großkopf, J.; Breitenlechner, S.; Bannwarth, C.; Bach, T. Photochemical Deracemization of Primary Allene Amides by Triplet Energy Transfer: A Combined Synthetic and Theoretical Study. *J. Am. Chem. Soc.* **2021**, *143*, 11209–11217.
- ¹⁴⁶ Wimberger, L.; Kratz, T.; Bach, T. Photochemical Deracemization of Chiral Sulfoxides Catalyzed by a Hydrogen-Bonding Xanthone Sensitizer. *Synthesis* **2019**, *51*, 4417–4424.
- ¹⁴⁷ Tröster, A.; Bauer, A.; Jandl, C.; Bach, T. Enantioselective Visible-Light-Mediated Formation of 3-Cyclopropylquinolones by Triplet-Sensitized Deracemization. *Angew. Chem. Int. Ed.* **2019**, *58*, 3538–3541.
- ¹⁴⁸ Li, X.; Kutta, R. J.; Jandl, C.; Bauer, A.; Nuernberger, P.; Bach, T. Photochemically Induced Ring Opening of Spirocyclopropyl Oxindoles: Evidence for a Triplet 1,3-Diradical Intermediate and Deracemization by a Chiral Sensitizer. *Angew. Chem. Int. Ed.* **2020**, *59*, 21640–21647.
- ¹⁴⁹ Burg, F.; Bach, T. Lactam Hydrogen Bonds as Control Elements in Enantioselective Transition-Metal-Catalyzed and Photochemical Reactions. *J. Org. Chem.* **2019**, *84*, 8815–8836.
- ¹⁵⁰ Mayr, F.; Mohr, L.-M.; Rodriguez, E.; Bach, T. Synthesis of Chiral Thiourea-Thioxanthone Hybrids. *Synthesis* **2017**, *49*, 5238–5250.
- ¹⁵¹ Pecho, F.; Zou, Y.-Q.; Gramüller, J.; Mori, T.; Huber, S. M.; Bauer, A.; Gschwind, R. M.; Bach, T. A Thioxanthone Sensitizer with a Chiral Phosphoric Acid Binding Site: Properties and Applications in Visible Light-Mediated Cycloadditions. *Chem. - Eur. J.* **2020**, *26*, 5190–5194.
- ¹⁵² Takagi, R.; Tabuchi, C. Enantioselective Intramolecular [2+2] Photocycloaddition using Phosphoric Acid as a Chiral Template. *Org. Biomol. Chem.* **2020**, *18*, 9261–9267.
- ¹⁵³ Lyu, J.; Clarez, A.; Vitale, M. R.; Allain, C.; Masson, G. Preparation of Chiral Photosensitive Organocatalysts and Their Application for the Enantioselective Synthesis of 1,2-Diamines. *J. Org. Chem.* **2020**, *85*, 12843–12855.
- ¹⁵⁴ Crisenza, G. E.; Mazzarella, D.; Melchiorre, P. Synthetic Methods Driven by the Photoactivity of Electron Donor–Acceptor Complexes. *J. Am. Chem. Soc.* **2020**, *142*, 5461–5476.
- ¹⁵⁵ Silvi, M.; Melchiorre, P. Enhancing the Potential of Enantioselective Organocatalysis with Light. *Nature* **2018**, *554*, 41–49.
- ¹⁵⁶ Lima, C. G.; Lima, T.; Duarte, M.; Jurberg, I. D.; Paixão, M. W. Organic Synthesis Enabled by Light-Irradiation of EDA Complexes: Theoretical Background and Synthetic Applications. *ACS Catal.* **2016**, *6*, 1389–1407.
- ¹⁵⁷ Mulliken, R. S. Molecular Compounds and their Spectra. III. The Interaction of Electron Donors and Acceptors. *J. Phys. Chem.* **1952**, *56*, 801–822.

-
- ¹⁵⁸ Arceo, E.; Jurberg, I. D.; Álvarez-Fernández, A.; Melchiorre, P. Photochemical Activity of a Key Donor-Acceptor Complex can Drive Stereoselective Catalytic α -Alkylation of Aldehydes. *Nat. Chem.* **2013**, *5*, 750–756.
- ¹⁵⁹ Nicewicz, D. A.; MacMillan, D. W. C. Merging Photoredox Catalysis with Organocatalysis: The Direct Asymmetric Alkylation of Aldehydes. *Science*, **2008**, *322*, 77–80.
- ¹⁶⁰ Bahamonde, A.; Melchiorre, P. Mechanism of the Stereoselective α -Alkylation of Aldehydes Driven by the Photochemical Activity of Enamines. *J. Am. Chem. Soc.* **2016**, *138*, 8019–8030.
- ¹⁶¹ Arceo, E.; Bahamonde, A.; Bergonzini, G.; Melchiorre, P. Enantioselective Direct α -Alkylation of Cyclic Ketones by Means of Photo-Organocatalysis. *Chem. Sci.* **2014**, *5*, 2438–2442.
- ¹⁶² Silvi, M.; Arceo, E.; Jurberg, I. D.; Cassani, C.; Melchiorre, P. Enantioselective Organocatalytic Alkylation of Aldehydes and Enals Driven by the Direct Photoexcitation of Enamines. *J. Am. Chem. Soc.* **2015**, *137*, 6120–6123.
- ¹⁶³ Filippini, G.; Silvi, M.; Melchiorre, P. Enantioselective Formal α -Methylation and α -Benzoylation of Aldehydes by Means of Photo-Organocatalysis. *Angew. Chem. Int. Ed.* **2017**, *56*, 4447–4451.
- ¹⁶⁴ Rigotti, T.; Casado-Sánchez, A.; Cabrera, S.; Pérez-Ruiz, R.; Liras, M.; O’Shea, V. A.; Alemán, J. A Bifunctional Photoaminocatalyst for the Alkylation of Aldehydes: Design, Analysis, and Mechanistic Studies. *ACS Catal.* **2018**, *8*, 5928–5940.
- ¹⁶⁵ Silvi, M.; Verrier, C.; Rey, Y.; Buzzetti, L.; Melchiorre, P. Visible-Light Excitation of Iminium Ions Enables the Enantioselective Catalytic β -Alkylation of Enals. *Nat. Chem.* **2017**, *9*, 868–873.
- ¹⁶⁶ Verrier, C.; Alandini, N.; Pezzetta, C.; Moliterno, M.; Buzzetti, L.; Hepburn, H. H.; Vega-Peñaloza, A.; Silvi, M.; Melchiorre, P. Direct Stereoselective Installation of Alkyl Fragments at the β -Carbon of Enals via Excited Iminium Ion Catalysis. *ACS Catal.* **2018**, *8*, 1062–1066.
- ¹⁶⁷ Woźniak, Ł.; Magagnano, G.; Melchiorre, P. Enantioselective Photochemical Organocascade Catalysis. *Angew. Chem. Int. Ed.* **2018**, *57*, 1068–1072.
- ¹⁶⁸ Bonilla, P.; Rey, Y. P.; Holden, C. M.; Melchiorre, P. Photo-Organocatalytic Enantioselective Radical Cascade Reactions of Unactivated Olefins. *Angew. Chem. Int. Ed.* **2018**, *57*, 12819–12823.
- ¹⁶⁹ Perego, L. A.; Bonilla, P.; Melchiorre, P. Photo-Organocatalytic Enantioselective Radical Cascade Enabled by Single-Electron Transfer Activation of Allenes. *Adv. Synth. Catal.* **2020**, *362*, 302–307.
- ¹⁷⁰ Mazzarella, D.; Crisenza, G. E. M.; Melchiorre, P. Asymmetric Photocatalytic C–H Functionalization of Toluene and Derivatives. *J. Am. Chem. Soc.* **2018**, *140*, 8439–8443.

-
- ¹⁷¹ Nicholas, A. M.; Arnold, D. R. Thermochemical Parameters for Organic Radicals and Radical Ions. Part 1. The Estimation of the pK_a of Radical Cations based on Thermochemical Calculations. *Can. J. Chem.* **1982**, *60*, 2165–2179.
- ¹⁷² Cao, Z.-Y.; Ghosh, T.; Melchiorre, P. Enantioselective Radical Conjugate Additions Driven by a Photoactive Intramolecular Iminium-Ion-Based EDA Complex. *Nat. Commun.* **2018**, *9*, 3274.
- ¹⁷³ Hörmann, F. M.; Chung, T. S.; Rodriguez, E.; Jakob, M.; Bach, T. Evidence for Triplet Sensitization in the Visible-Light-Induced [2+2] Photocycloaddition of Eniminium Ions. *Angew. Chem. Int. Ed.* **2018**, *57*, 827–831.
- ¹⁷⁴ Hörmann, F. M.; Kerzig, C.; Chung, T. S.; Bauer, A.; Wenger, O. S.; Bach, T. Triplet Energy Transfer from Ruthenium Complexes to Chiral Eniminium Ions: Enantioselective Synthesis of Cyclobutanecarbaldehydes by [2+2] Photocycloaddition. *Angew. Chem. Int. Ed.* **2020**, *59*, 9659–9668.
- ¹⁷⁵ Rigotti, T.; Mas-Ballesté, R.; Alemán, J. Enantioselective Aminocatalytic [2 + 2] Cycloaddition through Visible Light Excitation. *ACS Catal.* **2020**, *10*, 5335–5346.
- ¹⁷⁶ Martínez-Gualda, A. M.; Domingo-Legarda, P.; Rigotti, T.; Díaz-Tendero, S.; Fraile, A.; Alemán, J. Asymmetric [2+2] Photocycloaddition via Charge Transfer Complex for the Synthesis of Tricyclic Chiral Ethers. *Chem. Commun.* **2021**, *57*, 3046–3049.
- ¹⁷⁷ Mahlau, M.; List, B. Asymmetric Counteranion-Directed Catalysis: Concept, Definition, and Applications. *Angew. Chem. Int. Ed.* **2013**, *52*, 518–533.
- ¹⁷⁸ Phipps, R. J.; Hamilton, G. L.; Toste, F. D. The Progression of Chiral Anions from Concepts to Applications in Asymmetric Catalysis. *Nat. Chem.* **2012**, *4*, 603–614.
- ¹⁷⁹ Yang, Z.; Li, H.; Li, S.; Zhang, M.-T.; Luo, S. A Chiral Ion-Pair Photoredox Organocatalyst: Enantioselective Anti-Markovnikov Hydroetherification of Alkenols. *Org. Chem. Front.* **2017**, *4*, 1037–1041.
- ¹⁸⁰ Hamilton, D. S.; Nicewicz, D. A. Direct Catalytic Anti-Markovnikov Hydroetherification of Alkenols. *J. Am. Chem. Soc.* **2012**, *134*, 18577–18580.
- ¹⁸¹ Wang, H.; Ren, Y.; Wang, K.; Man, Y.; Xiang, Y.; Li, N.; Tang, B. Visible Light-Induced Cyclization Reactions for the Synthesis of 1,2,4-Triazolines and 1,2,4-Triazoles. *Chem. Commun.* **2017**, *53*, 9644–9647.
- ¹⁸² Morse, P. D.; Nguyen, T. M.; Cruz, C. L.; Nicewicz, D. A. Enantioselective Counter-Anions in Photoredox Catalysis: The Asymmetric Cation Radical Diels–Alder Reaction. *Tetrahedron*, **2018**, *74*, 3266–3272.

-
- ¹⁸³ Shen, Y.; Shen, M.-L.; Wang, P.-S. Light-Mediated Chiral Phosphate Catalysis for Asymmetric Dicarbofunctionalization of Enamides. *ACS Catal.* **2020**, *10*, 8247–8253.
- ¹⁸⁴ Kikuchi, J.; Kodama, S.; Terada, M. Radical Addition Reaction Between Chromenols and Toluene Derivatives Initiated by Brønsted Acid Catalyst Under Light Irradiation. *Org. Chem. Front.* **2021**, *8*, 4153–4159.
- ¹⁸⁵ Woźniak, Ł.; Murphy, J. J.; Melchiorre, P. Photo-organocatalytic Enantioselective Perfluoroalkylation of β -ketoesters. *J. Am. Chem. Soc.* **2015**, *137*, 5678–5681.
- ¹⁸⁶ Yang, C.; Zhang, W.; Li, Y.-H.; Xue, X.-S.; Li, X.; Cheng, J.-P. Origin of Stereoselectivity of the Photoinduced Asymmetric Phase-Transfer-Catalyzed Perfluoroalkylation of β -Ketoesters. *J. Org. Chem.* **2017**, *82*, 9321–9327.
- ¹⁸⁷ Tang, X.-F.; Feng, S.-H.; Wang, Y.-K.; Yang, F.; Zheng, Z.-H.; Zhao, J.-N.; Wu, Y.-F.; Yin, H.; Liu, G.-Z.; Meng, Q.-W. Bifunctional Metal-Free Photo-Organocatalysts for Enantioselective Aerobic Oxidation of β -Dicarbonyl Compounds. *Tetrahedron*, **2018**, *74*, 3624–3633.
- ¹⁸⁸ Tang, X.-F.; Zhao, J.-N.; Wu, Y.-F.; Feng, S.-H.; Yang, F.; Yu, Z.-Y.; Meng, Q.-W. Visible-Light-Driven Enantioselective Aerobic Oxidation of β -Dicarbonyl Compounds Catalyzed by Cinchona-Derived Phase Transfer Catalysts in Batch and Semi-Flow. *Adv. Syn. Catal.* **2019**, *361*, 5245–5252.
- ¹⁸⁹ Crawford, J.; Sigman, M. Conformational Dynamics in Asymmetric Catalysis: Is Catalyst Flexibility a Design Element? *Synthesis* **2019**, *51*, 1021–1036.
- ¹⁹⁰ Lévesque, F.; Di Maso, M. J.; Narsimhan, K.; Wismer, M. K.; Naber, J. R. Design of a Kilogram Scale, Plug Flow Photoreactor Enabled by High Power LEDs. *Org. Process Res. Dev.* **2020**, *24*, 2935–2940.
- ¹⁹¹ Harper, K.; Grieme, T.; Towne, T.; Mack, D.; Diwan, M.; Ku, Y.-Y.; Griffin, J.; Miller, R.; Zhang, E.-X.; Liu, Z.-W.; Zheng, S.-Y.; Zhang, N.-N.; Grangula, S.; Yuan, J.-L.; Huang, P.-Z.; Gage, J. Commercial-Scale Visible-light Trifluoromethylation of 2-Chlorothiophenol using CF_3I gas. *Org. Process Res. Dev.* **2022**, *26*, 404–412.
- ¹⁹² Cambié, D.; Bottecchia, C.; Straathof, N. J. W.; Hessel, V.; Noël, T. Applications of Continuous-Flow Photochemistry in Organic Synthesis, Material Science, and Water Treatment. *Chem. Rev.* **2016**, *116*, 10276–10341.

Chapter 2 Chiral Brønsted Acid-Controlled Asymmetric [2+2] Photocycloadditions

2.1 Previous Publication of this Work

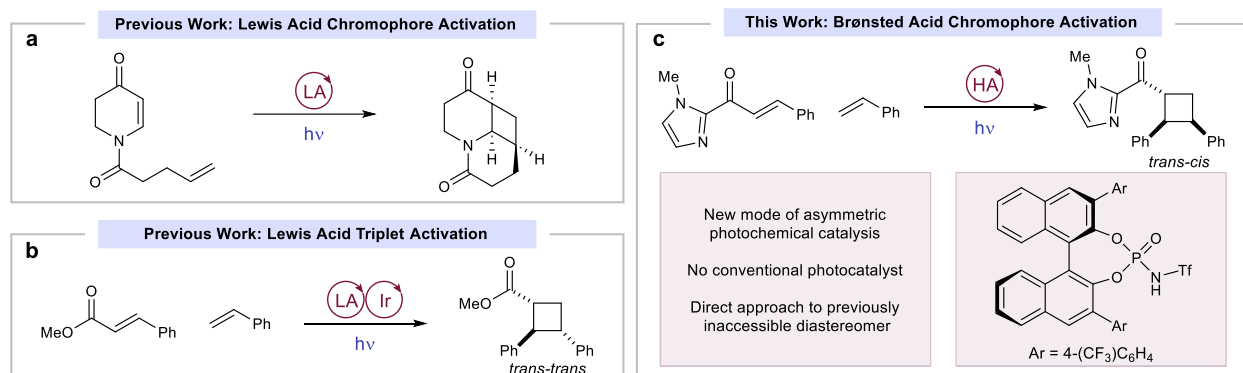
Portions of this work have been published previously:

Sherbrook, E. M.; Genzink, M. J.; Park, B.; Guzei, I. A.; Baik, M.-H.; Yoon, T. P. Chiral Brønsted Acid-Controlled Intermolecular Asymmetric [2+2] Photocycloadditions. *Nat. Commun.* **2021**, *12*, 5735.

2.2 Introduction

A defining characteristic of modern synthetic chemistry is the capacity to conduct complexity-building organic reactions with high levels of stereocontrol. The strategies available to dictate the stereochemical outcome of photochemical reactions, however, remain significantly underdeveloped compared to other classes of organic reactions.¹⁻⁸ The difficulty of conducting asymmetric photochemical reactions has often been attributed to the very short lifetimes and high reactivities associated with electronically excited compounds; these features challenge the ability of catalysts to intercept and modulate the behavior of organic excited states. In the past few years, highly enantioselective photoreactions have increasingly exploited chiral Lewis acids, either as catalysts or as co-catalysts. The insight that the same privileged classes of chiral Lewis acid structures that have been so enabling in ground-state asymmetric synthesis can also be applied to enantioselective photochemistry has increased the pace of discovery in this area. There are two general mechanisms by which chiral Lewis acids can influence the enantioselectivity of excited-state photoreactions. First, Bach pioneered the chromophore activation strategy in which chiral Lewis acids are used to attenuate the singlet excited-state energy of α,β -unsaturated carbonyl compounds (**Scheme 2.1a**).^{9,10} As the absorption of the catalyst-bound substrate occurs more strongly at longer wavelengths than the free substrate, the activated substrate may be selectively excited by judicious choice of irradiation wavelength. Second, our group has developed a mechanistically distinctive strategy that we have termed “triplet activation”. In this approach,

chiral Lewis acid coordination lowers the triplet energy of α,β -unsaturated carbonyls, allowing for their selective activation by a triplet sensitizer over unbound substrate molecules (**Scheme 2.1b**).^{11–13} While fundamentally distinct, both strategies use chiral Lewis acids to modify the excited-state properties of the substrate and preferentially activate the catalyst-bound complex, thereby minimizing racemic background reactivity.



Scheme 2.1 Asymmetric acid-catalyzed photoreactions. *a*, Intramolecular [2+2] photocycloadditions via Lewis acid-catalyzed chromophore activation; LA = Lewis acid. *b*, Intermolecular [2+2] photocycloadditions via Lewis acid-catalyzed triplet activation. *c*, Intermolecular [2+2] photocycloadditions via Brønsted acid-catalyzed chromophore activation; HA = Brønsted acid.

In the first decade of the 21st century, secondary amine and Brønsted acid organocatalysis emerged as an alternative approach to chiral Lewis acid catalysis for a wide range of asymmetric ground-state transformations.^{14–17} Remarkably, these catalysts could control many of the same classes of asymmetric transformations as better-studied chiral Lewis acids, often enabling the use of functionalized substrates that would not be compatible with strongly Lewis acidic catalyst structures. One might reasonably wonder if organocatalysts might prove equally versatile in asymmetric photochemistry. Very recently, Takagi demonstrated that chiral phosphoric acids are effective stoichiometric templates for asymmetric [2+2] photocycloaddition reactions of quinolones, though this interaction had little effect on the photophysical properties of the substrate.¹⁸ Pioneering studies by Melchiorre have demonstrated that secondary amine

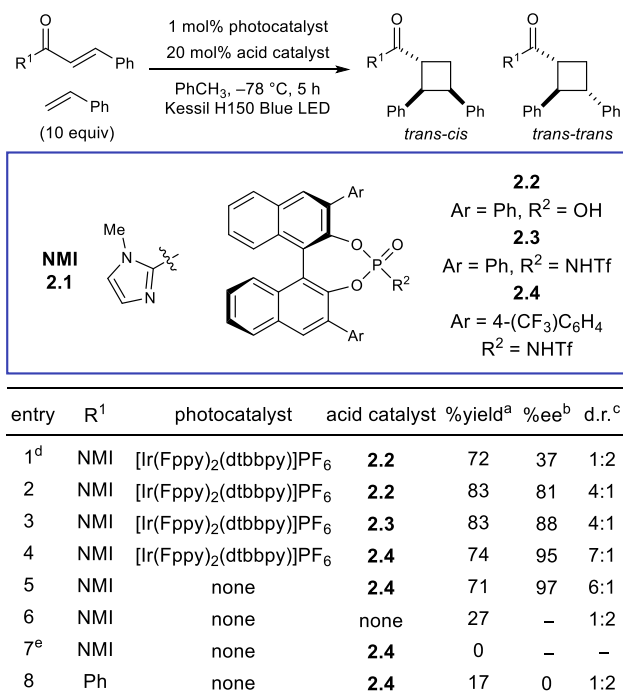
organocatalysts can activate prochiral enals by chromophore activation: the iminium intermediates absorb at longer wavelengths than the free enal substrates, and the excited states have been utilized in a variety of useful organic transformations.^{19,20} Very recently, Bach demonstrated the first example of triplet activation by secondary amine organocatalysis, demonstrating that the vinyl iminium intermediate undergoes energy transfer faster than the free parent enal and can be the key intermediate in an enantioselective [2+2] photocycloaddition.^{21,22} The ability of Brønsted acid catalysts to engage in chromophore and triplet activation mechanisms, however, has been underexplored. While hydrogen-bonding and Brønsted acid catalysts have been studied extensively as chiral sensitizers for asymmetric photoreactions,^{23–25} their ability to alter the photophysical properties of organic substrates has not been significantly exploited. In an isolated example, Sivaguru described an enantioselective intramolecular [2+2] cycloaddition using a chiral thiourea catalyst that could activate a coumarin substrate through both static and dynamic complex formation.^{26,27} Our group also recently reported the first example of triplet activation in a racemic [2+2] photocycloaddition reaction in which the addition of *p*-TsOH co-catalyst was demonstrated to increase the rate of triplet energy transfer from a Ru(II) photocatalyst to 2-acyl imidazole **2.1**, which subsequently underwent a [2+2] photocycloaddition.²⁸

In this work, we report a highly enantio- and diastereoselective excited-state [2+2] cycloaddition catalyzed by a BINOL-derived phosphoramidate Brønsted acid catalyst. A combination of spectroscopic and computational studies indicate that this catalyst operates via the principle of chromophore activation (**Scheme 2.1c**).

2.3 Results and Discussion

2.3.1 Reaction Optimization

The discovery of this chiral organocatalytic photoreaction occurred serendipitously during our studies to further develop the *p*-TsOH/photocatalytic [2+2] cycloaddition method into an asymmetric reaction by use of a chiral Brønsted acid. We began by screening BINOL-derived Brønsted acid co-catalysts, as they constitute a privileged catalyst class in thermal asymmetric transformations (**Scheme 2.2**).²⁹ When **2.1** and styrene were irradiated in the presence of 1 mol% [Ir(Fppy)₂(dtbbpy)]PF₆ and 20 mol% acid catalyst **2.2**, the cycloadduct was obtained in 37% ee in a 1:2 ratio of *trans-cis* to *trans-trans* diastereomers (entry 1). We observed a reversal in the diastereoselectivity at -78 °C and a concomitant increase in enantioselectivity (81% ee, entry 2). The more acidic *N*-triflyl phosphoramidate **2.3** led to a further increase in enantioselectivity (entry 3), consistent with a stronger substrate-catalyst interaction.³⁰ Finally, replacing the phenyl groups on the catalyst with 4-trifluoromethylphenyl groups (**2.4**) led to the optimal catalyst, affording the cycloadduct in 7:1 d.r. and 95% ee (entry 4).



Scheme 2.2 Optimization Studies. ^aYields and diastereomer ratios determined by ¹H NMR spectroscopy. ^bEnantiomeric excess of the major diastereomer determined by chiral HPLC. ^cRatio

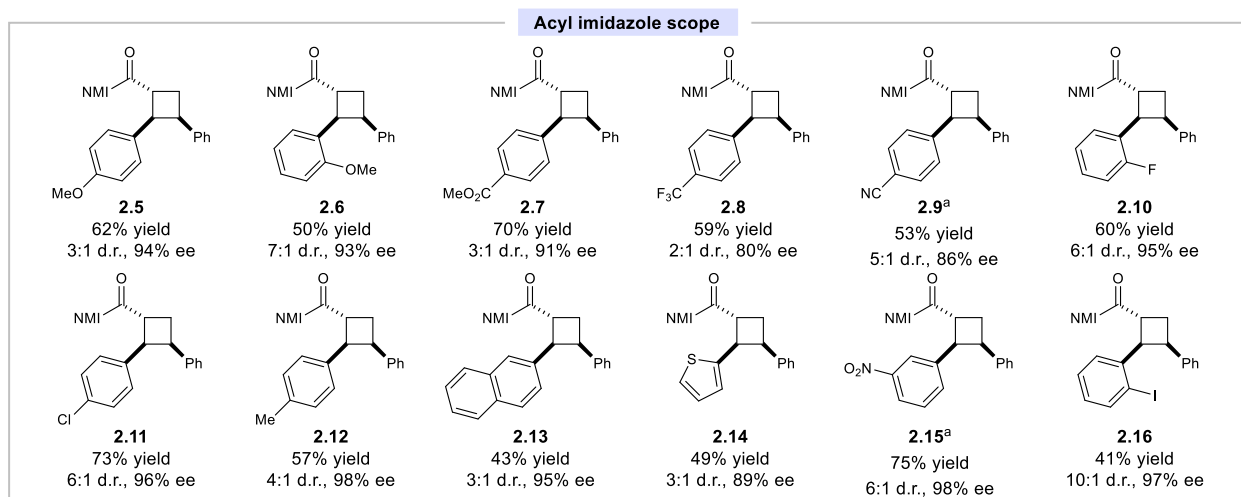
of *trans-cis* isomer to *trans-trans* isomer. ^dConducted at room temperature. ^eConducted in the dark.

To our surprise, control experiments omitting the photocatalyst from the reaction gave nearly identical yield and selectivity (entry 5). This indicates that **2.4** is not only responsible for the selectivity of the reaction but also activates the substrate towards photoexcitation. In the absence of both catalysts, the racemic product was still formed in low yield, indicative of a slow direct photoreaction that is outcompeted by the acid-catalyzed reaction (entry 6). Notably, in this control experiment, the *trans-trans* diastereomer is favored in a 2:1 ratio, indicating that the diastereoselectivity of the acid-catalyzed reaction (entry 5) is a product of catalyst control. Chalcone was also tested as a substrate and gave diminished yields of product with no ee, suggesting that a sufficiently basic functionality capable of interacting with the Brønsted acid catalyst is required (entry 8). The *trans-cis* diastereoselectivity of the major product is notable: direct excitation and triplet sensitized reactions of acyclic enones with alkenes typically favor formation of the *trans-trans* isomer.^{31–34} Indeed, the direct photoreaction conducted in the absence of the chiral Brønsted acid (entry 6) favors the *trans-trans* diastereomer, and thus we conclude that the observed diastereoselectivity is imposed by the acid catalyst. This method constitutes the first enantioselective photocycloaddition that selectively accesses a simple monocyclic diarylcyclobutane with 1,2-*cis* diastereoselectivity.

2.3.2 Substrate Scope

We evaluated the scope of the reaction under optimized reaction conditions (**Scheme 2.3**). A variety of α,β -unsaturated carbonyl compounds with electronically varied β -aryl substituents (**2.5–2.12**) were accommodated, producing the corresponding cycloadducts in high yields and selectivities. Substrates with substituents at the *ortho* position (**2.6**, **2.10**) reacted slower than corresponding substrates with *meta* or *para* substitution but were formed in higher

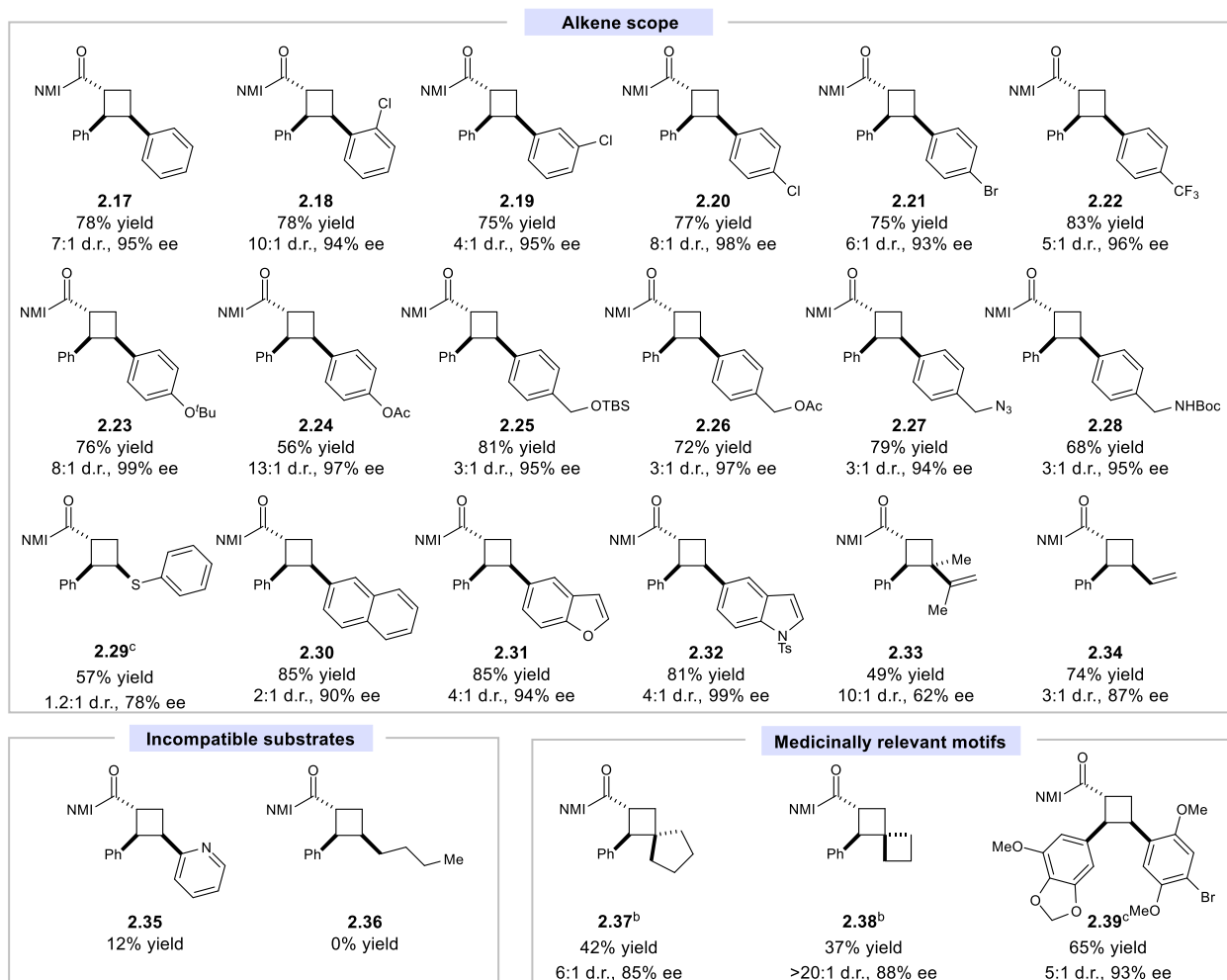
diastereoselectivity. A thienyl substrate (**2.14**) reacted efficiently. Finally, as this reaction does not require a conventional photocatalyst, substrates with oxidation or reduction potentials within the range of common transition metal photocatalysts are tolerated,³⁵ including nitroarenes (**2.15**) and aryl iodides (**2.16**).



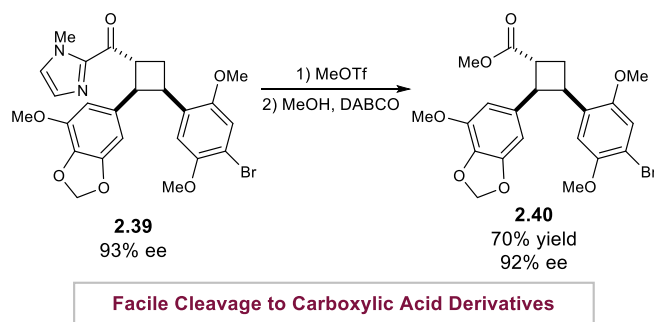
Scheme 2.3 Scope Studies. Reactions conducted using 1 equiv 2-acyl imidazole, 10 equiv alkene, 20 mol% **2.4** in toluene, irradiating for 14 h with a Kessil H150 LED unless otherwise noted. Yields represent the isolated yield of both diastereomers. Enantiomeric excess of the major diastereomer determined by chiral HPLC. ^aConducted for 24 h.

The alkene acceptor scope also includes substitution at each position of the arene acceptor (**2.18–2.20**) and an array of electron-withdrawing (**2.21–2.22**) and -donating (**2.23–2.24**) substituents (**Scheme 2.4**). Notably, a *p*-alkoxy-substituted styrene (**2.23**) was tolerated under these conditions, while the same alkene undergoes rapid polymerization using our previous Lewis acid-catalyzed methods.¹¹ Various functional groups including protected alcohols (**2.22–2.26**), a photolabile azide (**2.27**), and a protected amine (**2.28**) were all tolerated. Heterocycles were also readily transformed including benzofuran- and indole-substituted alkenes (**2.31–2.32**). Substituted and unsubstituted dienes (**2.33–2.34**) were competent substrates. Any substrate that features alternate binding sites for the chiral catalyst, however, generally affords low reactivity (**2.35**). Intriguingly, two aliphatic exocyclic alkenes (**2.37–2.38**) gave moderate yields and good ee to

afford medicinally interesting spirocyclic products.³⁶ Cycloadditions between two densely functionalized reaction partners also provided high enantioselectivity (**2.39**), and cleavage of the imidazolyl group to a methyl ester occurred with no significant loss of stereochemical fidelity (**Scheme 2.5**).



Scheme 2.4 Scope Studies. Reactions conducted using 1 equiv 2-acyl imidazole, 10 equiv alkene, 20 mol% **2.4** in toluene, irradiating for 14 h with a Kessil H150 LED unless otherwise noted. Yields represent the isolated yield of both diastereomers. Enantiomeric excess of the major diastereomer determined by chiral HPLC. ^aConducted for 24 h. ^bConducted with 40 mol% acid catalyst **2.4**. ^cConducted in CH₂Cl₂.



Scheme 2.5 Auxiliary Cleavage. The imidazolyl group of the cycloadduct is readily cleaved in good yield with retention of enantioselectivity.

2.3.3 Mechanistic Studies

An intriguing outcome of our optimization study was the unexpected observation that **2.4** catalyzes this reaction without a separate triplet sensitizer. We therefore elected to investigate its role in greater detail. Neither **2.1** nor **2.4** absorbs appreciably in the visible region (**Figure 2.1a**), and because the emission of the light source does not overlap with the absorption of the acid catalyst, direct excitation of the acid catalyst is not feasible. We therefore conclude that the Brønsted acid is not a conventional triplet photosensitizer in this reaction. The substrate, on the other hand, absorbs weakly at wavelengths >400 nm, accounting for the slow background reaction in the absence of catalyst (**Scheme 2.2**, entry 6). Upon combining colorless solutions of the acid and substrate, the mixture became noticeably yellow, corresponding to a red shift in absorption that increased with added acid catalyst. The emission of the light source overlapped well with bound but poorly with unbound substrate, consistent with relatively minimal contribution from the racemic background reaction.

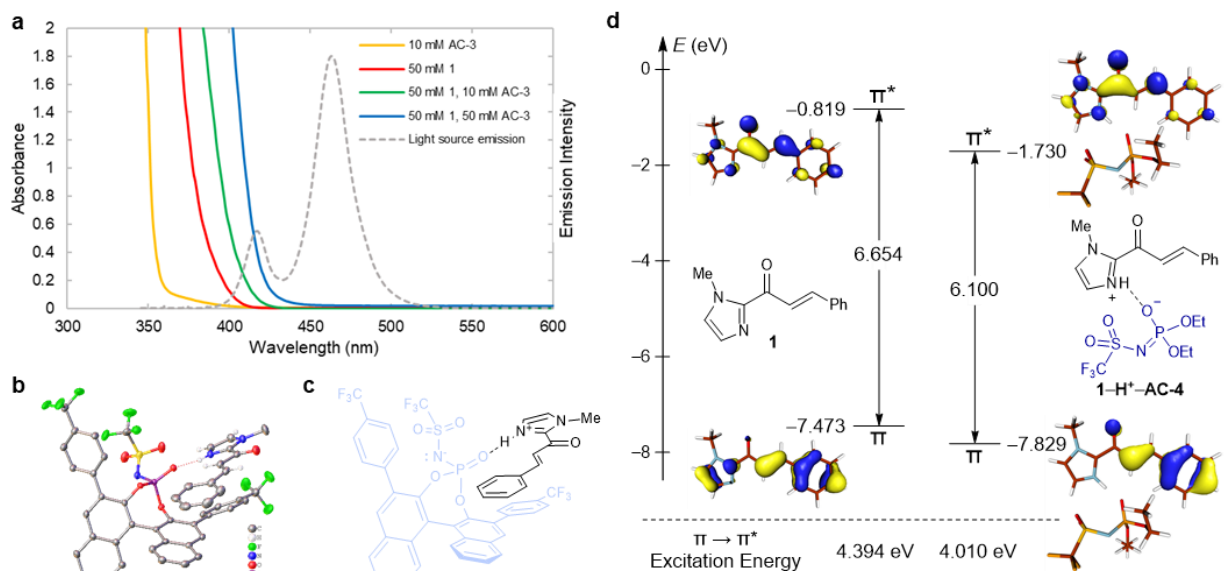
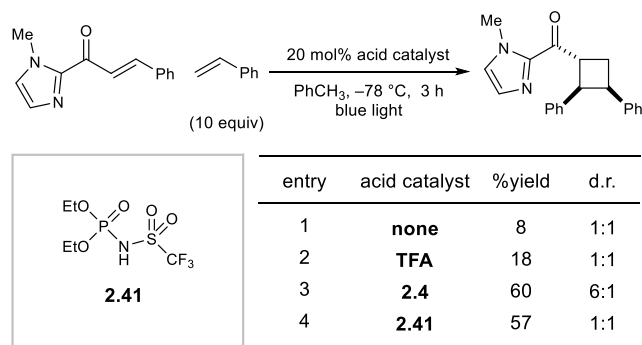


Figure 2.1 Mechanistic Studies. *a*, Ultraviolet-visible spectra of **2.1** and **2.4** in CH_2Cl_2 . *b*, X-ray crystal structure of acid-bound substrate. *c*, Binding depiction of acid-bound substrate. *d*, HOMO (π) and LUMO (π^*) of **2.1** and **2.1-H⁺-2.41**. Note: **AC-3=2.4** and **1=2.1**

We next performed NMR titration experiments with **1** and **2.4** in toluene- d_8 and calculated an association constant of $K_a = 7.5 \times 10^6$ (**Error! Reference source not found.** in Supporting Information). We also isolated the substrate-acid complex from diethyl ether and determined its structure using X-ray crystallography (**Figure 2.1b,c**). Key features of the interaction included an apparent hydrogen bond between the protonated imidazolium on the substrate and the phosphoramidate oxygen on the catalyst. This interaction differs significantly from the typical chelating interactions of acyl imidazoles with chiral Lewis acid catalysts, including the chiral-at-metal Rh catalysts Meggers has utilized in analogous asymmetric [2+2] photocycloaddition reactions.^{37,38} Further, the orientation of the substrate alkene relative to the π surface of the biaryl catalyst renders the top face of the enone more accessible for cycloaddition, which is consistent with the experimentally observed absolute configuration of the cycloadduct. While both the substrate and acid catalyst are white solids, the isolated crystals were yellow, indicating that the

complex absorbs visible light. Together these results are suggestive that the crystal structure could be similar to the catalytically active complex in solution.

Based on these data, we considered two possible modes of substrate activation within the acid-substrate complex. First, we considered a chromophore activation mechanism in which protonation of the substrate lowers the relative energy of its first singlet excited state, thus making direct excitation by visible light achievable. This hypothesis is consistent with the red-shifted absorption of enones in sulfuric acid solution.^{39,40} Second, we considered that the chiral catalyst and enone substrate might form an electron donor–acceptor complex.^{41–45} In this scenario, a new intermolecular transition between the HOMO of the electron-rich phosphoramidate donor and the LUMO of the electron-deficient imidazolium acceptor could be lower in energy than the intramolecular transitions on either individual species. To distinguish between these mechanisms, we examined the influence of various acid catalysts on the yield of the photocycloaddition (**Scheme 2.6**). If the electron donor–acceptor mechanism were operative, acid catalysts lacking the π conjugation of **2.4** would not form photochemically active complexes; however, a variety of acids increased the reaction rate, with similar apparent reaction rates using **2.4** and **2.41**. Therefore, the bathochromic shift in the absorption of the substrate is likely an intrinsic property of the protonated substrate and not the result of a specific donor–acceptor interaction.⁴⁶



Scheme 2.6 Effect of structurally diverse Brønsted acids on the cycloaddition. Yields and diastereomer ratios determined by ¹H NMR spectroscopy.

To understand the origin of this effect, we conducted density functional theory (DFT) and time-dependent density functional theory (TDDFT) calculations (**Figure 2.1d**). Unsurprisingly, the HOMO and LUMO of **2.1** were found to be fully delocalized across the molecule with a HOMO–LUMO gap of 6.65 eV. The π -conjugation in the HOMO can be divided into an imidazolium and a cinnamoyl part. After protonation (**2.1H⁺–2.41**), the HOMO becomes significantly more localized and is dominated by the cinnamoyl part (See Supporting Information for details). This demixing of the two π -components upon protonation weakens the electrostatic impact of the proton on the HOMO energy, resulting in a relatively moderate shift of -0.36 eV. In contrast, the LUMO maintains delocalization across both π -domains and the LUMO energy shifts by -0.91 eV upon protonation. Consequently, the HOMO-LUMO gap is reduced from 6.65 to 6.10 eV, enabling excitation by visible light. TDDFT/Tamm-Dancoff approximation (TDA) calculation and natural transition orbital (NTO) analysis revealed the excitation from HOMO to LUMO ($\pi \rightarrow \pi^*$ transition) in **2.1** and **2.1H⁺–2.41** to be most important, and the excitation energies of 4.40 and 4.01 eV, respectively, were in good agreement with experimental observations.⁴⁷

Given this combination of synthetic, spectroscopic, and computational evidence, we propose that the BINOL-derived acid acts as a dual-purpose catalyst, altering the absorption spectrum of the substrate and providing a stereodifferentiating environment for the cycloaddition. The red-shifted absorption of the bound substrate enables selective excitation of the catalyst-bound complex and minimal competition from direct racemic background photocycloaddition. The resulting excited-state substrate is preorganized relative to the chiral environment defined by the Brønsted acid catalyst, and styrene approaches at the accessible face of the enone, yielding highly enantioenriched product.

2.4 Conclusion

We have developed a highly enantioselective [2+2] photocycloaddition catalyzed by a BINOL phosphoramidate organocatalyst. We believe that these results are significant for a variety of reasons. First, the stereocontrol offered by this reaction is high, and the access it provides to the *trans-cis* diastereomer of diarylcyclobutanes distinguishes it synthetically from previous reports of asymmetric [2+2] photocycloadditions. Thus, while highly enantioselective catalysis of excited-state reactions is a relatively new capability in synthetic chemistry, the level of comprehensive control these methods collectively provide are beginning to approach the sophistication available in more conventional asymmetric reactions. More importantly, this study demonstrates that chiral Brønsted acids can activate enones by altering the absorption properties of the substrate. The extension of the concept of chromophore activation to chiral Brønsted acid-catalyzed photoreactions adds a distinctive approach to the strategic toolbox available for the design of stereocontrolled organic photoreactions.

2.5 Contributions

Evan M. Sherbrook performed the reaction optimization, investigated the scope, and conducted mechanistic experiments. Matthew J. Genzink investigated the scope and conducted mechanistic experiments. Ilia A. Guzei collected and analyzed x-ray crystallographic data. Bohyun Park and Mu-Hyun Baik performed computational experiments. Tehshik P. Yoon provided expertise, resources, and funding.

2.6 Supporting Information

2.6.1 General Information

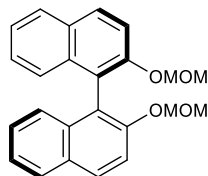
Reagent Preparation: MeCN, THF, CH₂Cl₂, and toluene were purified by elution through alumina as described by Grubbs.⁴⁸ Most styrenes, all dienes, phenyl vinyl sulfide, methylenecyclopentane, and methylenecyclobutane were purchased from SigmaAldrich and distilled prior to use. Catalysts **2.2** and **2.3** were prepared by established methods for the synthesis of BINOL-derived phosphoric acids⁴⁹ and phosphoramidates.⁵⁰ Excluding those prepared below, all other starting materials, catalysts, or solvents were used as received from the supplier. Flash-column chromatography was performed with Silicycle 40-63 Å (230-40 mesh) silica. Photochemical reactions were carried out with an H150-blue Kessil Lamp ($\lambda_{em. (max)} = \sim 450$ nm).

Product Characterization: Diastereomer ratios for reactions were determined by ¹H NMR analysis of unpurified reaction mixtures vs. a phenanthrene internal standard. ¹H and ¹³C NMR data were obtained using a Bruker Avance-500 spectrometer with DCH cryoprobe and are referenced to tetramethylsilane (0.0 ppm) and CDCl₃ (77.0 ppm), respectively. This instrument and supporting facilities are funded by Paul J. Bender, Margaret M. Bender, and the University of Wisconsin. ¹H, ¹⁹F, and ³¹P NMR data were obtained using Bruker Avance-400 spectrometer. This instrument and supporting facilities are funded by the NSF (CHE-1048642) and the University of Wisconsin. NMR data are reported as follows: chemical shift, multiplicity (s = singlet, d = doublet, t = triplet, q = quartet, p = pentet, sext = sextet, sept = septet, m = multiplet), coupling constant(s) in Hz, integration. NMR spectra were obtained at 298 K unless otherwise noted. FT-IR spectra were obtained using a Bruker Tensor 27 spectrometer and are reported in terms of frequency of absorption (cm⁻¹). Melting points (mp) were obtained using a Stanford Research Systems DigiMelt MPA160 melting point apparatus and are uncorrected. Mass spectrometry was performed with a Thermo Q ExactiveTM Plus using ESI-TOF (electrospray ionization-time of flight). This instrument and supporting facilities are funded by the NIH (1S10 OD020022-1) and the University

of Wisconsin. Enantiomeric excesses were determined by chiral HPLC of isolated materials using a Waters e2695 separations module with 2998 PDA detector and Daicel CHIRALPAK® columns and HPLC grade *i*-PrOH and hexanes. Traces were acquired using Empower 3® software. Optical rotations were measured using a Rudolf Research Autopol III polarimeter at room temperature in CH₂Cl₂. UV-Vis absorption spectra were acquired using a Varian Cary® 50 UV-visible spectrophotometer with a spectrophotometer.

2.6.2 Catalyst Synthesis

(R)-(+)-2,2'-Bis(methoxymethoxy)-1,1'-binaphthalene: Reaction performed using a



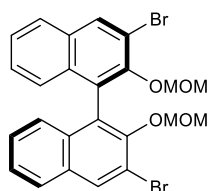
modification of a procedure previously reported by Taylor.⁵¹ A 500 mL round-bottomed flask was charged with 200 mL dry THF, and 3.00 g (75.0 mmol, 2.5 equiv.) of 60% NaH in mineral oil was added. This mixture was cooled to 0 °C

in an ice bath. A solution of 8.59 g (30.0 mmol, 1.0 equiv.) (*R*)-BINOL in 550 mL dry THF was added over approximately 20 min *via* cannula, controlling the resulting gas evolution. Then, 5.70 mL (75.0 mmol, 2.5 equiv.) freshly distilled chloromethyl methyl ether (MOMCl) was added portionwise at 0 °C. The reaction was warmed to room temperature and stirred overnight. The reaction was then slowly quenched with 20 mL sat. aq. NH₄Cl. This mixture was transferred to a separatory funnel with 100 mL CH₂Cl₂. After separating the organic layer, the aqueous layer was extracted with 3 x 100 mL CH₂Cl₂. The combined organics were washed with 20 mL brine, dried over Na₂SO₄, and concentrated. The resulting material was recrystallized from CH₂Cl₂/pentanes to give 9.06 g (24.0 mmol, 80% yield) of a crystalline white solid. Spectral data were consistent with previously reported values.⁵² ¹H NMR (500 MHz, CDCl₃) δ 7.95 (d, *J* = 9.0 Hz, 2H), 7.85 (d, *J* = 8.3 Hz, 2H), 7.57 (d, *J* = 9.0 Hz, 2H), 7.34 (ddd, *J* = 8.0, 6.7, 1.2 Hz, 2H), 7.22 (ddd, *J* =

8.0, 6.7, 1.2 Hz, 2H), 7.15 (d, $J = 8.3$ Hz, 2H), 5.08 (d, $J = 6.9$ Hz, 2H), 4.97 (d, $J = 6.9$ Hz, 2H), 3.14 (s, 6H).

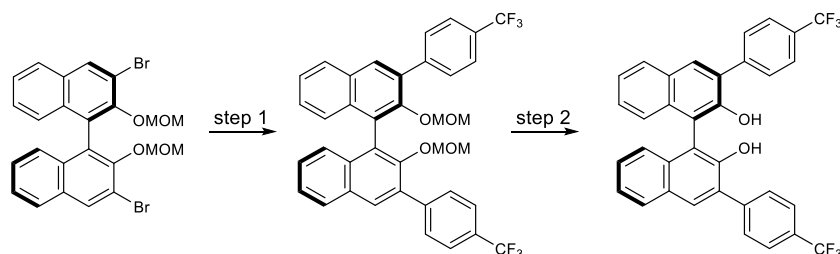
(±)-2,2'-Bis(methoxymethoxy)-1,1'-binaphthalene: Prepared and isolated through the above procedure for (*R*)-(+)-2,2'-Bis(methoxymethoxy)-1,1'-binaphthalene using 1.00 g (25.0 mmol) NaH in 100 mL THF, 2.86 g (10.0 mmol) (±)-BINOL in 25 mL THF, and 1.95 mL (25.0 mmol) MOMCl to give 2.84 g (7.6 mmol, 76% yield) of a white solid. Spectral data were consistent with those reported above.

(*R*)-(+)-3,3'-Dibromo-2,2'-bis(methoxymethoxy)-1,1'-binaphthalene: In a flame-dried 100 mL



round-bottomed flask, 3.74 g (10.0 mmol, 1.0 equiv.) (*R*)-(+)-2,2'-bis(methoxymethoxy)-1,1'-binaphthalene was dissolved in 50 mL dry THF and cooled to -78 °C. Then, 12.5 mL (25.0 mmol, 2.5 equiv.) *n*-BuLi (2.0 M in hexanes) was added portionwise. This mixture was warmed to 0 °C for 1 h before returning to -78 °C and adding a solution of 1.28 mL (25.0 mmol, 2.5 equiv.) Br₂ in 10 mL pentanes. The reaction was then warmed to room temperature and stirred overnight. The remaining Br₂ was quenched by stirring with 30 mL sat. aq. Na₂SO₃ for 30 min. The resulting heterogeneous mixture was transferred to a separatory funnel with 30 mL H₂O. After separating the organic layer, the aqueous layer was extracted with 3 x 100 mL CH₂Cl₂. The combined organics were dried over Na₂SO₄, and concentrated. The resulting residue was dry-loaded onto silica and purified by flash column chromatography with a gradient of 2% → 5% → 10% EtOAc in hexanes to give 2.80 g (5.4 mmol, 54%) of a white solid. Spectroscopic data were consistent with previously reported values. ¹H NMR (500 MHz, CDCl₃) δ 8.27 (s, 2H), 7.80 (d, $J = 8.0$ Hz, 2H), 7.44 (ddd, $J = 8.0$, 6.8, 1.2 Hz, 2H), 7.31 (ddd, $J = 8.3$, 6.8, 1.2 Hz, 2H), 7.18 (d, $J = 8.6$ Hz, 2H), 4.83 (d, $J = 5.9$, 2H), 4.81 (d, $J = 5.9$, 2H), 2.57 (s, 6H).

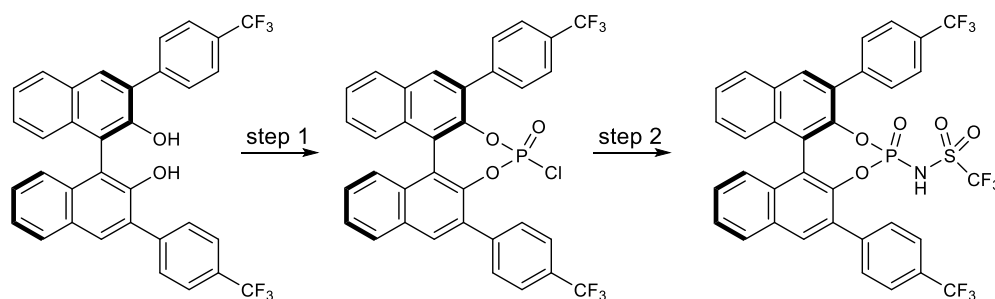
(±)-3,3'-Dibromo-2,2'-bis(methoxymethoxy)-1,1'-binaphthalene: Prepared and isolated through the above procedure for (*R*)-(+)-3,3'-Dibromo-2,2'-bis(methoxymethoxy)-1,1'-binaphthalene using 2.81 g (7.5 mmol) (±)-2,2'-bis(methoxymethoxy)-1,1'-binaphthalene in 50 mL THF, 9.2 mL (18.25 mmol) *n*-BuLi (~2.0 M in hexanes), and 0.93 mL (18.25 mmol) Br₂ in 10 mL pentanes to give 2.08 g (4.0 mmol, 53% yield) of a white solid. Spectral data were consistent with those reported above.



(*R*)-(+)-3,3'-Di-(4-trifluoromethyl)phenyl-[1,1'-binaphthalene]-2,2'-diol: *Step 1:* A 100 mL round-bottomed flask was charged with 2.80 g (5.35 mmol 1.0 equiv.) (*R*)-(+)-3,3'-dibromo-2,2'-bis(methoxymethoxy)-1,1'-binaphthalene, 3.56 g (18.73 mmol, 3.5 equiv.) 4-trifluoromethylphenylboronic acid, 15 mL 2 M aq. Na₂CO₃, and 30 mL 1,2-dimethoxyethane (DME) and fitted with a reflux condenser. The apparatus was purged with N₂ for 15 min before the addition of 340 mg (0.27 mmol, 0.05 equiv.) Pd(PPh₃)₄. The mixture was heated to 95 °C for 16 h. After cooling to room temperature, the mixture was filtered over a pad of Celite, the pad washed with EtOAc, and the resulting solution concentrated. This residue was partitioned between 100 mL EtOAc and 25 mL H₂O. After separating the organic layer, the aqueous layer was extracted with 3 x 20 mL EtOAc. The combined organics were dried over Na₂SO₄ and concentrated. *Step 2:* The resulting yellow solid, primarily composed of MOM-protected cross-coupling product, was

taken up in 30 mL THF, and 0.8 mL conc. HCl was added. The mixture was heated to 65 °C for 3 h. This mixture was concentrated, and the residue partitioned between 100 mL EtOAc and 25 mL H₂O. After separating the organic layer, the aqueous was extracted with 3 x 50 mL EtOAc. The combined organics were dried over Na₂SO₄, then concentrated directly on silica for purification by flash column chromatography with 2 → 5% EtOAc in hexanes to give 2.67 g (4.65 mmol, 87% yield) of a white solid. Spectroscopic data were consistent with previously reported values.⁵³ ¹H NMR (500 MHz, CDCl₃) δ 8.06 (s, 2H), 7.96 (d, *J* = 8.0 Hz, 2H), 7.87 (d, *J* = 8.1 Hz, 4H), 7.74 (d, *J* = 8.2 Hz, 4H), 7.44 (ddd, *J* = 8.0, 6.8, 1.1 Hz, 2H), 7.37 (ddd, *J* = 8.2, 6.8, 1.2 Hz, 2H), 7.23 (d, *J* = 8.2 Hz, 2H), 5.32 (s, 2H).

(±)-3,3'-Di-(4-trifluoromethyl)phenyl-[1,1'-binaphthalene]-2,2'-diol: Prepared and isolated through the above procedure for **(R)-(+)-3,3'-di-(4-trifluoromethyl)phenyl-[1,1'-binaphthalene]-2,2'-diol**. *Step 1:* 2.08 g (4.0 mmol) (±)-3,3'-Dibromo-2,2'-bis(methoxymethoxy)-1,1'-binaphthalene, 2.65 (13.9 mmol) 4-trifluoromethylphenylboronic acid, 260 mg Pd(PPh₃)₄, 15 mL 2 M aq. Na₂CO₃, and 30 mL 1,2-DME were combined to give a yellow solid. *Step 2:* This yellow solid was combined with 20 mL THF and 0.6 mL conc. HCl to give 1.44 g (2.51 mmol, 63% yield) of a white solid. Spectral data were consistent with those reported above.



(R)-4-Trifluoromethylphenyl-BINOL ((trifluoromethyl)sulfonyl)phosphoramidate ((R)-

2.4): Prepared using a modification of a procedure previously reported by Yamamoto. *Step 1:* A 100 mL flame-dried round-bottomed flask was charged with 2.48 g (4.3 mmol, 1.0 equiv.) (R)-(+)-3,3'-di-(4-trifluoromethyl)phenyl-[1,1'-binaphthalene]-2,2'-diol and 25 mL dry CH₂Cl₂, then cooled to 0 °C. To this solution was added 0.84 mL (9.0 mmol, 2.1 equiv.) freshly distilled POCl₃ and 1.90 mL (13.5 mmol, 3.1 equiv.) freshly distilled Et₃N. The reaction was warmed to room temperature and stirred under N₂ for 16 h. The resulting mixture was washed once with 10 mL H₂O. This aqueous layer was extracted with 2 x 10 mL CH₂Cl₂. After drying over Na₂SO₄, the solution was concentrated to give a brown solid, which was passed through a short plug of silica with 5% EtOAc in pentanes to give a quantitative yield of white solid. This organic phosphoryl chloride and carried forward to the next step without additional purification. *Step 2:* A 100 mL flame-dried round-bottomed flask was charged with 2.78 g (4.25 mmol, 1.0 equiv) of the organic phosphoryl chloride synthesized above, 634 mg (4.25 mmol, 1.0 equiv.) trifluoromethanesulfonamide, 1.04 g (8.50 mmol, 2.0 equiv.) dimethylaminopyridine (DMAP), and 50 mL dry CH₂Cl₂. This mixture was stirred under N₂ at room temperature for 24 h. The crude reaction mixture was washed directly with 20 mL 6 M HCl and dried over Na₂SO₄. The resulting solution was concentrated directly onto silica and purified by flash column chromatography with 10% → 50% → 70% EtOAc in pentanes. The resulting solid was dissolved in CH₂Cl₂, washed with 6 M HCl (3 x 50 mL), dried over Na₂SO₄, filtered, and concentrated to give 1.64 g (2.14 mmol, 50% yield) of a white crystalline solid. (dec. pt. = 250+ °C). [α]_D²² -234.0° (c0.970, CH₂Cl₂). ¹H NMR (500 MHz, CDCl₃) δ 8.13 (s, 1H), 8.05 (d, *J* = 8.0 Hz, 1H), 8.04 (s, 1H), 8.02 (d, *J* = 8.0 Hz, 1H), 7.76 (d, *J* = 8.1 Hz, 2H), 7.64–7.60 (m, 7H), 7.56 (ddd, *J* = 8.0, 6.3, 1.4 Hz,

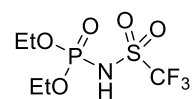
1H), 7.48 (d, $J = 8.3$ Hz, 1H), 7.45–7.35 (m, 3H), 6.35 (br s, 1H). ^{13}C NMR (125 MHz, CDCl_3) δ 142.76, 142.66, 142.41, 142.33, 139.49, 139.20, 132.47, 132.45, 132.19, 132.18, 132.14, 132.02, 132.00, 131.95, 131.91, 131.82, 130.48, 130.22, 130.02, 129.96, 129.70, 128.85, 128.64, 127.49, 127.39, 127.33, 127.10, 127.02, 126.93, 126.85, 125.39, 125.36, 125.33, 125.30, 125.16, 124.96, 124.94, 124.91, 124.88, 124.85, 123.00, 122.78, 122.76, 122.68, 122.33, 121.95, 121.93, 120.84, 120.52, 119.78, 117.22, 114.67. More signals appear in this list than expected from carbons alone due to both C-F and C-P coupling. Due to signal overlap it was not possible to fully deconvolute the splitting patterns that give rise to these individual signals. ^{19}F NMR (377 MHz, CDCl_3) δ –62.92, –63.37, –78.32. ^{31}P NMR (162 MHz, CDCl_3) δ –5.05. HRMS (ESI) calculated for $[\text{C}_{35}\text{H}_{23}\text{F}_9\text{N}_2\text{O}_5\text{PS}]^+$ ($\text{M}+\text{NH}_4^+$) requires m/z 785.0916, found 785.0918.

(±)-4-Trifluoromethylphenyl-BINOL ((trifluoromethyl)sulfonyl)phosphoramidate ((±)-2.4):

Prepared and isolated through the above procedure for **(R)-A1**. *Step 1*: 1.43 g (2.5 mmol) (±)-3,3'-Di-(4-trifluoromethyl)phenyl-[1,1'-binaphthalene]-2,2'-diol, 0.47 mL (5.0 mmol) POCl_3 , and 1.03 mL (7.5 mmol) Et_3N were combined to give a white solid. *Step 2*: This white solid (1.47 g, 2.25 mmol) was combined with 335 mg (2.25 mmol) trifluoromethanesulfonamide, 550 mg (4.50 mmol) DMAP, and 25 mL CH_2Cl_2 to give 0.87 g (1.13 mmol, 50% yield). Spectral data were consistent with those reported above.

Diethyl ((trifluoromethyl)sulfonyl)phosphoramidate (2.41): A flame-dried 250 mL round-

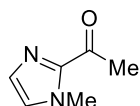
bottomed flask was charged with 0.89 g (6.0 mmol, 1.0 equiv.) trifluoromethylsulfonamide and 1.48 g (12.0 mmol, 2.0 equiv.) 4-dimethylaminopyridine in 50 mL CH_2Cl_2 . To this solution, 0.87 mL (6.0 mmol, 1.0 equiv.) diethyl chlorophosphate was added dropwise at room temperature and the reaction was stirred for 24 h. The reaction mixture was



washed with 6 x 30 mL 6 M HCl then dried over Na₂SO₄, filtered, and concentrated. Spectral data were consistent with previously reported values.⁵⁴ ¹H NMR (500 MHz, CDCl₃) δ 7.30 (s, 1H), 4.28 (m, 4H), 1.41 (t, *J* = 7.1 Hz, 6H).

2.6.3 Substrate Synthesis

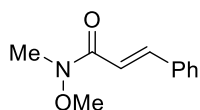
2-Acetyl-1-methylimidazole: A solution of 0.84 mL (10.5 mmol, 1.05 equiv.) 1-methylimidazole



in 25 mL dry THF was prepared in a flame-dried 100 mL round-bottomed flask. After cooling to -78 °C, 5.5 mL (10.5 mmol, 1.05 equiv.) *n*-BuLi (1.91 M in hexanes) was

added portionwise. The reaction was warmed to 0 °C for 30 min before returning to -78 °C. A solution of 1.15 mL (10.0 mmol, 1.0 equiv.) 4-acetylmorpholine in 25 mL THF was prepared in a flame-dried 50 mL pear-shaped flask and added to the solution of deprotonated 1-methylimidazole *via* cannula. The reaction was warmed to room temperature and stirred overnight. The resulting solution was stirred vigorously, then 2 mL glacial acetic acid added dropwise. This solution was transferred to separatory funnel with 100 mL EtOAc, then washed with 30 mL sat. aq. NaHCO₃ and 30 mL sat. aq. NaCl. Each wash solution was back-extracted with 30 mL additional EtOAc. The combined organics were dried over Na₂SO₄ and concentrated. The product was purified by flash column chromatography with 2:3 EtOAc/pentanes to give 700 mg (5.6 mmol, 56% yield) of a colorless oil. Spectral data were consistent with previously reported values.⁵⁵ ¹H NMR (400 MHz, CDCl₃) δ 7.14 (s, 1H), 7.03 (s, 1H), 4.00 (s, 3H), 2.66 (s, 3H).

***N*-Methoxy-*N*-methylcinnamide:** A flame-dried 50 mL round-bottomed flask was charged with

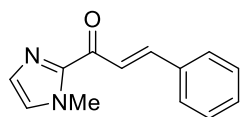


8.64 g (52.0 mmol, 1.0 equiv.) cinnamoyl chloride and 5.34 g (54.7 mmol, 1.05 mmol) *N,O*-dimethylhydroxylamine hydrochloride in 150 mL dry CH₂Cl₂. The

mixture was cooled to 0 °C, and 9.20 mL (114.4, 2.2 equiv.) pyridine was added slowly. The reaction was then warmed to room temperature and stirred overnight. Then 1 M HCl was added,

the organic layer separated, and the aqueous layer extracted with 3 x 25 mL additional EtOAc. The combined organics were washed with 25 mL sat. aq. NaHCO₃ and 25 mL sat. aq. NaCl. The combined organics were dried over Na₂SO₄ and concentrated. The products were purified by flash column chromatography with 1:1 Et₂O/pentanes to give 8.14 g (42.6 mmol, 82% yield) of a viscous oil that solidified after extended drying *in vacuo*. Spectral data were consistent with previously reported values.⁵⁶ ¹H NMR (400 MHz, CDCl₃) δ 7.74 (d, *J* = 15.9 Hz, 1H), 7.59–7.56 (m, 2H), 7.41–7.36 (m, 3H), 7.04 (d, *J* = 15.9 Hz, 1H), 3.77(s, 3H), 3.32 (s, 3H).

2-Cinnamoyl-1-methyl-1*H*-imidazole (2.1): A flame-dried 100 mL round-bottomed flask was



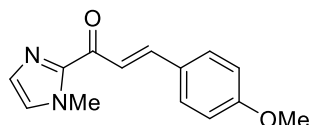
charged with 0.71 mL (8.93 mmol, 1.05 equiv.) *N*-methylimidazole and 30 mL dry THF, then cooled to –78 °C. A volume of 3.6 mL (8.93 mmol, 1.05

equiv.) *n*-BuLi (2.50 M in hexanes) was added portionwise. The reaction was warmed to 0 °C for 30 min, then returned to –78 °C. A solution of 1.62 g (8.50 mmol, 1.0 equiv.) *N*-methoxy-*N*-methylcinnamide in 10 mL THF was prepared in a flame-dried pear-shaped flask and added to the solution of deprotonated 1-methylimidazole *via* cannula. The reaction was warmed to room temperature and stirred overnight. The resulting solution was stirred vigorously, then 2 mL glacial acetic acid was added dropwise. This solution was transferred to separatory funnel with 50 mL EtOAc and shaken with 20 mL water. The organic layer was separated and the aqueous extracted with 3 x 25 mL additional EtOAc. The combined organics were then washed with 30 mL sat. aq. NaHCO₃ and 30 mL sat. aq. NaCl, dried over Na₂SO₄, and concentrated. The products were purified by flash column chromatography with 1:1 Et₂O/pentanes. Yield: 1.32 g (6.2 mmol, 73% yield) of an off-white solid. Spectral data were consistent with previously reported values.⁵⁷ ¹H NMR (400 MHz, CDCl₃) δ 8.08 (d, *J* = 16.0 Hz, 1H), 7.83 (d, *J* = 16.0 Hz, 1H), 7.72–7.68 (m, 2H), 7.43–7.38 (m, 3H), 7.23 (s, 1H), 7.09 (s, 1H), 4.10 (s, 3H).

General Method for the Preparation of Substituted Cinnamoyl Methylimidazole

Derivatives: A round-bottomed flask was charged with 2-acetyl-1-methylimidazole (1.0 equiv.), and a mixture of EtOH and H₂O. This solution was sparged briefly with N₂ (5 min). Aromatic aldehyde (1.0–1.1 equiv., freshly distilled if possible) was then added to the solution, followed by a catalytic quantity of KOH. The reaction was then stirred under N₂ for 12–16 h (overnight). *Work-up 1:* If the resulting solution was heterogeneous, the product was filtered and washed with H₂O and cold EtOH to give the pure desired product. *Work-up 2:* If the resulting solution was homogeneous, the crude reaction mixture was diluted with CH₂Cl₂, transferred to separatory funnel, and shaken with H₂O. The organic layer was separated and the aqueous extracted with three portions of CH₂Cl₂. The combined organics were dried over Na₂SO₄, concentrated, and purified by flash column chromatography.

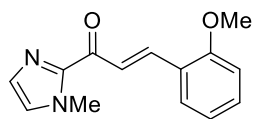
(E)-3-(4-Methoxyphenyl)-1-(1-methyl-1H-imidazol-2-yl)prop-2-en-1-one: Prepared using the



general method above using 372.7 mg (3.0 mmol, 1.0 equiv.) 2-acetyl-1-methylimidazole, 0.26 mL (3.0 mmol, 1.0 equiv.) 4-

methoxybenzaldehyde, ~25 mg (½ pellet) KOH, 6 mL EtOH, and 3 mL H₂O. Work-up 2, then purified by flash column chromatography with 1:1 Et₂O/pentanes to give 382 mg (1.58 mmol, 53% yield) of an off-white solid. Spectral data were consistent with previously reported values.⁵⁸ ¹H NMR (400 MHz, CDCl₃) δ 7.96 (d, *J* = 15.9 Hz, 1H), 7.80 (d, *J* = 15.9 Hz, 1H), 7.66 (d, *J* = 8.7 Hz, 1H), 7.21 (s, 1H), 7.07 (s, 1H), 6.92 (d, *J* = 8.7 Hz, 1H), 4.10 (s, 3H), 3.85 (s, 3H).

(E)-3-(2-Methoxyphenyl)-1-(1-methyl-1H-imidazol-2-yl)prop-2-en-1-one: Prepared using

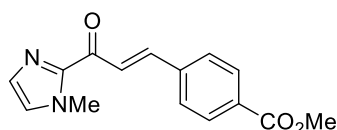


general method above using 499.6 mg (4.0 mmol, 1.0 equiv.) 2-acetyl-1-methylimidazole, 0.41 mL (4.4 mmol, 1.1 equiv.) 2-methoxybenzaldehyde,

~25 mg (½ pellet) KOH, 8 mL EtOH. Work-up 2, then purified by flash column chromatography

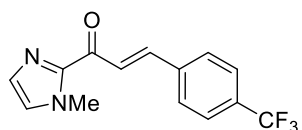
with 1:1 Et₂O/pentanes to give 877 mg (3.6 mmol, 90% yield) of an off-white solid. Spectral data were consistent with previously reported values.⁵⁹ ¹H NMR (400 MHz, CDCl₃) δ 8.24 (d, *J* = 16.2 Hz, 1H), 8.09 (d, *J* = 16.2 Hz, 1H), 7.76 (dd, *J* = 7.6, 1.6 Hz, 1H), 7.37 (ddd, *J* = 8.9, 7.6, 1.6 Hz, 1H), 7.21 (s, 1H), 7.07 (s, 1H), 6.97 (t, *J* = 7.6 Hz, 1H), 6.93 (t, *J* = 8.9 Hz, 1H), 4.10 (s, 3H), 3.91 (s, 3H).

Methyl 4-[(1*E*)-3-(1-methyl-1*H*-imidazol-2-yl)-3-oxoprop-1-en-1-yl]benzoate: Prepared using



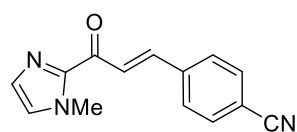
the general method above using 416.0 mg (3.3 mmol, 1.0 equiv.) 2-acetyl-1-methylimidazole, 594 mg (3.6 mmol, 1.1 equiv.) methyl 4-formylbenzoate, ~25 mg (1/2 pellet) KOH, 6 mL MeOH⁶⁰, and 3 mL H₂O. Work-up 1 to give 428 mg (1.58 mmol, 48% yield) of an off-white solid (mp = 138–140 °C). ¹H NMR (400 MHz, CDCl₃) δ 8.15 (d, *J* = 16.0 Hz, 1H), 8.06 (d, *J* = 8.3 Hz, 2H), 7.82 (d, *J* = 16.0 Hz, 1H), 7.75 (d, *J* = 8.3 Hz, 2H), 7.24 (s, 1H), 7.11 (s, 1H), 4.11 (s, 3H), 3.94 (s, 3H). ¹³C NMR (125 MHz, CDCl₃) δ 180.10, 166.54, 143.94, 141.72, 139.19, 131.39, 130.06, 129.56, 128.51, 127.54, 125.02, 52.28, 36.40. HRMS (ESI) calculated for [C₁₅H₁₅N₂O₃]⁺ (M+H⁺) requires *m/z* 271.1077, found 271.1080.

(*E*)-1-(1-Methyl-1*H*-imidazol-2-yl)-3-(4-trifluoromethylphenyl)prop-2-en-1-one: Prepared



using the general method above using 328.0 mg (3.0 mmol, 1.0 equiv.) 2-acetyl-1-methylimidazole, 0.45 mL (3.3 mmol, 1.1 equiv.) 4-trifluoromethylbenzaldehyde, ~25 mg (1/2 pellet) KOH, 12 mL EtOH, and 6 mL H₂O. Work-up 2, then purified by flash column chromatography with 1:1 Et₂O/pentanes to give 442 mg (1.58 mmol, 53% yield) of an off-white solid. Spectral data were consistent with previously reported values.⁵⁹ ¹H NMR (400 MHz, CDCl₃) δ 8.14 (d, *J* = 16.0 Hz, 1H), 7.81 (d, *J* = 16.0 Hz, 1H), 7.79 (d, *J* = 8.3 Hz, 2H), 7.65 (d, *J* = 8.3 Hz, 2H), 7.24 (s, 1H), 7.11 (s, 1H), 4.11 (s, 3H).

(E)-4-(3-(1-Methyl-1H-imidazol-2-yl)-3-oxoprop-1-en-1-yl)benzonitrile: Prepared using the



general method above using 418.0 mg (3.4 mmol, 1.0 equiv.) 2-acetyl-1-

methylimidazole, 476.0 mg (3.6 mmol, 1.1 equiv.) 4-formylbenzonitrile,

~25 mg (1/2 pellet) KOH, 4 mL EtOH, and 2 mL H₂O. Work-up 1 to give 552.0 mg (2.31 mmol,

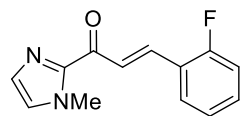
70% yield) of an off-white solid (mp = 228–232 °C). ¹H NMR (500 MHz, CDCl₃) δ 8.15 (d, J = 16.1 Hz, 1H), 7.79-7.76 (m, 3H), 7.69 (d, J = 8.3 Hz, 2H), 7.24 (s, 1H), 7.12 (s, 1H), 4.11 (s, 3H).

¹³C NMR (125 MHz, CDCl₃) δ 179.72, 143.81, 140.53, 139.30, 132.59, 129.71, 128.92, 127.72,

126.14, 118.48, 113.35, 36.38. HRMS (ESI) calculated for [C₁₄H₁₁N₃O]⁺ (M+H⁺) requires *m/z*

238.0975, found 238.097.

(E)-3-(2-Fluorophenyl)-1-(1-methyl-1H-imidazol-2-yl)prop-2-en-1-one: Prepared using the



general method above using 258.0 mg (2.1 mmol, 1.0 equiv.) 2-acetyl-1-

methylimidazole, 0.23 mL (2.2 mmol, 1.1 equiv.) 2-fluorobenzaldehyde, ~25

mg (1/2 pellet) KOH, 8 mL EtOH, and 4 mL H₂O. Work-up 1 to give 270 mg (1.17 mmol, 56%

yield) of a white solid (mp = 136–138 °C). ¹H NMR (400 MHz, CDCl₃) δ 8.13 (d, *J* = 16.2 Hz, 1H), 8.02 (d, *J* = 16.2 Hz, 1H), 7.77 (td, *J* = 7.6, 1.7 Hz, 1H), 7.39-7.35 (m, 1H), 7.23 (d, *J* = 0.9

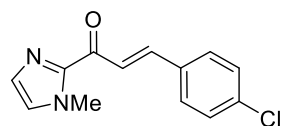
Hz, 1H), 7.17 (t, *J* = 7.6 Hz, 1H), 7.13-7.09 (m, 2H), 4.10 (s, 3H). ¹³C NMR (125 MHz, CDCl₃) δ

180.36, 161.73, 144.02, 135.45, 131.85, 129.46, 128.91, 127.35, 124.84, 124.35, 123.10, 116.14,

36.37. ¹⁹F NMR (377 MHz, CDCl₃) δ -114.39. HRMS (ESI) calculated for [C₁₃H₁₁FN₂O]⁺

(M+H⁺) requires *m/z* 231.0928, found 231.0927.

(E)-3-(4-Chlorophenyl)-1-(1-methyl-1H-imidazol-2-yl)prop-2-en-1-one: Prepared using the



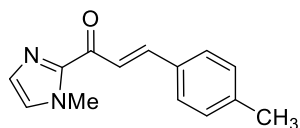
general method above using 248.2 mg (2.0 mmol, 1.0 equiv.) 2-acetyl-1-

methylimidazole, 315.0 mg (2.2 mmol, 1.1 equiv.) 4-chlorobenzaldehyde,

~25 mg (1/2 pellet) KOH, 8 mL EtOH, and 4 mL H₂O. Work-up 1 to give 340.1 mg (1.38 mmol,

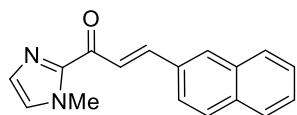
69% yield) of a white solid. Spectral data were consistent with previously reported values.⁵⁸ ¹H NMR (500 MHz, CDCl₃) δ 8.04 (d, *J* = 16.0 Hz, 1H), 7.76 (d, *J* = 16.0 Hz, 1H), 7.62 (d, *J* = 8.5 Hz, 2H), 7.37 (d, *J* = 8.5 Hz, 2H), 7.22 (s, 1H), 7.09 (s, 1H), 4.10 (s, 3H).

(*E*)-1-(1-Methyl-1H-imidazol-2-yl)-3-(*p*-tolyl)prop-2-en-1-one: Prepared using the general



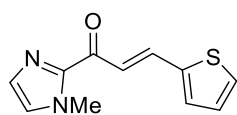
method above using 248.0 mg (2.0 mmol, 1.0 equiv.) 2-acetyl-1-methylimidazole, 0.26 mL (2.2 mmol, 1.1 equiv.) *p*-tolualdehyde, ~25 mg (1/2 pellet) KOH, 8 mL EtOH, and 4 mL H₂O. Work-up 2, then purified by flash column chromatography with 3:7 EtOAc/hexanes to give 323.3 mg (1.43 mmol, 71% yield) of a white solid. Spectral data were consistent with previously reported values.⁵⁸ ¹H NMR (500 MHz, CDCl₃) δ 8.03 (d, *J* = 16.0, 1H), 7.81 (d, *J* = 16.0 Hz, 1H), 7.60 (d, *J* = 8.1 Hz, 2H), 7.22 (m, 2H), 7.20 (s, 1H), 7.07 (s, 1H), 4.10 (s, 3H), 2.38 (s, 3H).

(*E*)-1-(1-Methyl-1H-imidazol-2-yl)-3-(naphthalen-2-yl)prop-2-en-1-one: Prepared using the



general method above using 370 mg (3.0 mmol, 1.0 equiv.) 2-acetyl-1-methylimidazole, 0.52 mg (3.3 mmol, 1.1 equiv.) 2-naphthaldehyde, ~25 mg (1/2 pellet) KOH, 6 mL EtOH, and 3 mL H₂O. Work-up 1 to give 610 mg (2.32 mmol, 78% yield) of an off-white solid (mp = 153–155 °C). ¹H NMR (500 MHz, CDCl₃) δ 8.20 (d, *J* = 15.9 Hz, 1H), 8.09 (s, 1H), 8.00 (d, *J* = 16.0 Hz, 1H), 7.89-7.83 (m, 4H), 7.53-7.51 (m, 2H), 7.25 (s, 1H), 7.10 (s, 1H), 4.13 (s, 3H). ¹³C NMR (125 MHz, CDCl₃) δ 180.47, 144.12, 143.47, 134.40, 133.35, 132.50, 130.58, 129.36, 128.66, 128.58, 127.78, 127.29, 127.27, 126.63, 124.31, 122.97, 36.41. HRMS (ESI) calculated for [C₁₇H₁₄N₂O]⁺ (M+H⁺) requires *m/z* 263.1179, found 263.1177.

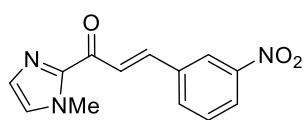
(*E*)-1-(1-Methyl-1H-imidazol-2-yl)-3-(thiophen-2-yl)prop-2-en-1-one: Prepared using the



general method above using 250.0 mg (2.0 mmol, 1.0 equiv.) 2-acetyl-1-methylimidazole, 0.21 mL (2.2 mmol, 1.1 equiv.) 2-

thiophenecarboxaldehyde, ~25 mg (1/2 pellet) KOH, 8 mL EtOH, and 4 mL H₂O. Work-up 2, then purified by flash column chromatography with 4:6 EtOAc/hexanes to give 331.0 mg (1.52 mmol, 75% yield) of an off-white solid. Spectral data were consistent with previously reported values.⁵⁷ ¹H NMR (400 MHz, CDCl₃) δ 7.95 (d, *J* = 15.7 Hz, 1H), 7.84 (d, *J* = 15.7 Hz, 1H), 7.42 (d, *J* = 5.0 Hz, 1H), 7.38 (d, *J* = 3.5 Hz, 1H), 7.22 (s, 1H), 7.08 (s, 1H), 7.08 (dd, *J* = 5.0, 3.5 Hz, 1H), 4.09 (s, 3H).

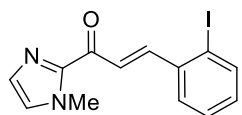
(*E*)-1-(1-Methyl-1H-imidazol-2-yl)-3-(3-nitrophenyl)prop-2-en-1-one: Prepared using the



general method above using 248.7 mg (2.0 mmol, 1.0 equiv.) 2-acetyl-1-methylimidazole, 331.4 mg (2.2 mmol, 1.1 equiv.) 3-

nitrobenzaldehyde, ~25 mg (1/2 pellet) KOH, 8 mL EtOH, and 4 mL H₂O. Work-up 1 to give 420.3 mg (1.63 mmol, 82% yield) of a white solid. (mp = 161–162 °C). ¹H NMR (500 MHz, CDCl₃) δ 8.53 (t, *J* = 2.1 Hz, 1H), 8.25-8.23 (m, 1H), 8.18 (d, *J* = 16.0 Hz, 1H), 7.98 (d, *J* = 7.9 Hz, 1H), 7.83 (d, *J* = 16.0 Hz, 1H), 7.59 (t, *J* = 7.9 Hz, 1H), 7.25 (s, 1H), 7.12 (s, 1H), 4.11 (s, 3H). ¹³C NMR (125 MHz, CDCl₃) δ 179.71, 148.76, 143.78, 140.16, 136.77, 134.10, 129.86, 129.71, 127.72, 125.70, 124.57, 123.01, 36.39. HRMS (ESI) calculated for [C₁₃H₁₁N₃O₃]⁺ (M+H⁺) requires *m/z* 258.0873, found 258.0872.

(*E*)-3-(2-Iodophenyl)-1-(1-methyl-1H-imidazol-2-yl)prop-2-en-1-one: Prepared using the

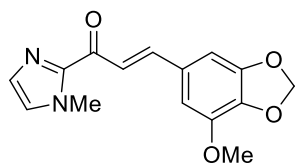


general method above using 247.5 mg (2.0 mmol, 1.0 equiv.) 2-acetyl-1-methylimidazole, 515.0 mg (2.2 mmol, 1.1 equiv.) 2-iodobenzaldehyde, ~25

mg (1/2 pellet) KOH, 8 mL EtOH, and 4 mL H₂O. Work-up 1 to give 508 mg (1.50 mmol, 75% yield) of an off-white solid. Spectral data were consistent with previously reported values.⁶¹ ¹H NMR (500 MHz, CDCl₃) δ 8.05 (d, *J* = 15.8 Hz, 1H), 7.97 (d, *J* = 15.8 Hz, 1H), 7.91 (dd, *J* = 8.0,

1.2 Hz, 1H), 7.82 (dd, $J = 7.9, 1.6$ Hz, 1H), 7.37 (t, $J = 8.0$ Hz, 1H), 7.22 (d, $J = 0.9$ Hz, 1H), 7.10 (s, 1H), 7.06 (td, $J = 7.7, 1.6$ Hz, 1H), 4.11 (s, 3H).

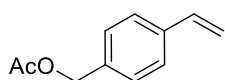
(E)-3-(7-Methoxy-2H-1,3-benzodioxol-5-yl)-1-(1-methyl-1H-imidazol-2-yl)prop-2-en-1-one:



Prepared using the general method above using 250.0 mg (2.0 mmol, 1.0 equiv.) 2-acetyl-1-methylimidazole, 360 mg (2.0 mmol, 1.0 equiv.) 5-methoxypiperonal, ~25 mg (1/2 pellet) KOH, 9 mL EtOH, and 1 mL

H₂O. Work-up 1 to give 480 mg (1.68 mmol, 84% yield) of a yellow solid (mp = 210–212 °C). ¹H NMR (400 MHz, CDCl₃) δ 7.91 (d, $J = 15.8$ Hz, 1H), 7.71 (d, $J = 15.8$ Hz, 1H), 7.21 (d, $J = 0.8$ Hz, 1H), 7.08 (d, $J = 0.8$ Hz, 1H), 6.92 (d, $J = 1.4$ Hz, 1H), 6.88 (d, $J = 1.4$ Hz, 1H), 6.03 (s, 2H), 4.10 (s, 3H), 3.95 (s, 3H). ¹³C NMR (125 MHz, CDCl₃) δ 180.37, 149.29, 144.10, 143.77, 143.41, 137.70, 129.83, 129.25, 127.22, 121.30, 109.31, 102.46, 102.05, 56.67, 36.41. HRMS (ESI) calculated for [C₁₅H₁₅N₂O₄]⁺ (M+H⁺) requires m/z 287.1026, found 287.1027.

1-(Acetoxymethyl)-4-vinylbenzene: To a solution of pyridine (0.5 mL) and acetic anhydride (0.5

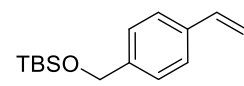


mL) in a flame-dried 50 mL round-bottomed flask was added 1.07 g (8.0 mmol, 1.0 equiv) (4-vinylphenyl)methanol and 98 mg (0.8 mmol, 0.1 equiv.) 4-

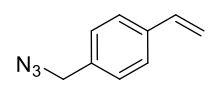
dimethylaminopyridine. The reaction was stirred at room temperature for 20 h, then diluted with water (30 mL) and extracted with EtOAc (3 x 30 mL). The combined organic layers were washed with 1M HCl (30 mL) and sat. aq. NaHCO₃ (30 mL). The organic layers were dried over Na₂SO₄, filtered, and concentrated. The residue was purified by flash column chromatography with a gradient of 0% Et₂O in pentanes → 10% Et₂O in pentanes to give 1.35 g (7.7 mmol, 96%) of a colorless oil. Spectroscopic data were consistent with that previously reported.⁶² ¹H NMR (500

MHz, CDCl₃) δ 7.41 (d, J = 8.3 Hz, 2H), 7.32 (d, J = 8.3 Hz, 2H), 6.72 (dd, J = 17.8, 11.0 Hz, 1H), 5.77 (dd, J = 17.8, 0.8 Hz, 1H), 5.27 (dd, J = 11.0, 0.8 Hz 1H), 5.10 (s, 2H), 2.11 (s, 3H).

***tert*-Butyldimethyl(4-vinylbenzyloxy) silane:** A vial was charged with CH₂Cl₂ (6 mL) and 0.39

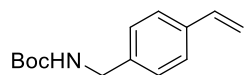
 g (2.87 mmol, 1.0 equiv.) (4-vinylphenyl)methanol followed by 0.25 g (3.73 mmol, 1.3 equiv.) imidazole. The reaction was stirred until everything dissolved then 0.52 g (3.44 mmol, 1.2 equiv.) *tert*-butyldimethylsilyl chloride was added and the reaction was stirred at room temperature for 6 h. The reaction was diluted in sat. aq. NH₄Cl and extracted with CH₂Cl₂ (3 x 10 mL). The organic layers were combined, dried over Na₂SO₄, filtered, and concentrated. The residue was purified with flash column chromatography eluting with a gradient of 0% Et₂O in pentanes \rightarrow 2:1 pentanes:Et₂O. Spectral data were consistent with previously reported values.⁶³ ¹H NMR (500 MHz, CDCl₃) δ 7.38 (AA'BB', J = 8.1 Hz, 2H), 7.28 (AA'BB', J = 8.1 Hz, 2H), 6.71 (dd, J = 17.6, 10.9 Hz, 1H), 5.72 (d, J = 17.6 Hz, 1H), 5.21 (d, J = 10.9 Hz, 1H), 4.73 (s, 2H), 0.94 (s, 9H), 0.10 (s, 6H).

1-(Azidomethyl)-4-vinylbenzene: A flame-dried 250 mL round-bottomed flask was charged with

 0.65 g (10.0 mmol, 2 equiv.) sodium azide and 0.76 g (5.0 mmol, 1.0 equiv.) 4-vinylbenzyl chloride dissolved in 50 mL DMF. The mixture was stirred for 24 h at room temperature. The reaction was diluted with water (100 mL) and extracted with Et₂O (3 x 50 mL). The organic layers were combined and washed with water (2 x 50 mL) and brine (50 mL). The organic layer was dried over Na₂SO₄, filtered, and concentrated. The residue was purified by flash column chromatography eluting from 1:9 EtOAc:hexanes to give 0.75 g (4.7 mmol, 93%) of a light yellow oil. Spectral data were consistent with previously reported values.⁶⁴ ¹H NMR (500

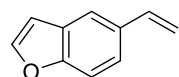
MHz, CDCl₃) δ 7.43 (AA'BB', $J = 8.1$ Hz, 2H), 7.28 (AA'BB', $J = 8.1$ Hz, 2H), 6.72 (dd, $J = 17.7$, 10.9 Hz, 1H), 5.77 (dd, $J = 17.7$, 0.7 Hz, 1H), 5.28 (dd, $J = 10.9$, 0.7 Hz, 1H), 4.33 (s, 2H).

***tert*-Butyl 4-vinylbenzylcarbamate:** A 25 mL round-bottomed flask was charged with 0.78 g (4.9



mmol, 1.0 equiv.) 1-azidomethyl-4-vinyl-benzene, 2.52 g (9.8 mmol, 2.0 equiv.) triphenylphosphine, and 10:1 THF:H₂O (11 mL). The reaction was stirred at room temperature for 24 h, then dissolved in CH₂Cl₂ (20 mL) and extracted with 1 N HCl (2 x 20 mL). The acidic aqueous phases were combined, washed with EtOAc (3 x 20 mL) and adjusted to pH 10 by addition of 3 N NaOH. The alkaline solution was then extracted with CH₂Cl₂ (3 x 50 mL), and the combined organics were dried over Na₂SO₄ and concentrated in vacuo to give the desired amine, which was carried on without further purification. A 250 mL round bottom flask was charged with the crude amine as a solution in CH₂Cl₂ (100 mL), 1.55 g (7.3 mmol, 1.5 equiv.) di-*tert*-butyl dicarbonate, 0.82 mL (5.9 mmol, 1.2 equiv.) NEt₃, and 7 mL MeOH. The resulting solution was then stirred at room temperature overnight under an atmosphere of N₂. The reaction was concentrated, and the residue was purified by flash column chromatography eluting from 20% EtOAc in hexanes to give 0.74 g (3.2 mmol, 65% over two steps) of a colorless oil. Spectral data were consistent with previously reported values.⁶⁵ ¹H NMR (500 MHz, CDCl₃) δ 7.38 (d, $J = 9.0$ Hz, 2 H), 7.26 (d, $J = 9.0$ Hz, 2 H), 6.72 (dd, $J = 10.9$ Hz, 17.6 Hz 1H), 5.75 (dd, $J = 0.9$ Hz, 17.6 Hz, 1 H), 5.25 (dd, $J = 0.9$ Hz, 10.9 Hz, 1 H), 4.31 (d, $J = 5.0$ Hz, 2 H), 1.48 (s, 9 H).

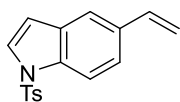
5-Vinyl-1-benzofuran: A flame-dried 25 mL round-bottomed flask was charged with 4.15 g (11.5



mmol, 1.4 equiv.) methyltriphenylphosphonium bromide in 8 mL dry THF and treated with 1.38 g (12.3 mmol, 1.5 equiv.) potassium *tert*-butoxide. The mixture was stirred for

30 min at room temperature before a solution of 1.20 g (8.2 mmol, 1.0 equiv.) 1-benzofuran-5-carbaldehyde in 9 mL THF was added dropwise. The reaction was stirred for 14 h, then diluted with water (50 mL) and extracted with EtOAc (3 x 10 mL). The combined organic layers were dried over Na₂SO₄, filtered, and concentrated. The crude product was purified by flash column chromatography eluting with hexanes to give 0.89 g (6.2 mmol, 75%) of a colorless oil. Spectral data were consistent with previously reported values.⁶⁶ ¹H NMR (500 MHz, CDCl₃) δ 7.62-7.61 (m, 2H), 7.46-7.38 (m, 2H), 6.82 (dd, *J* = 17.6, 10.8 Hz, 1H), 6.75 (dd, *J* = 2.0, 1.2 Hz, 1H), 5.73 (d, *J* = 17.6 Hz, 1H), 5.22 (d, *J* = 10.8 Hz, 1H).

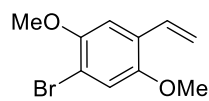
1-Toluenesulfonyl-5-vinyl-1H-indole: A solution of 0.96 g (6.5 mmol, 1.1 equiv.) potassium



vinyltrifluoroborate, 23 mg (0.13 mmol, 0.02 equiv.) PdCl₂, 103 mg (0.39 mmol, 0.06 equiv.) triphenylphosphine, 6.3 g (19.5 mmol, 3.0 equiv.), Cs₂CO₃, and 2.27

g (6.5 mmol, 1.0 equiv.) 5-bromo-1-tosyl-1H-indole in THF/H₂O (9:1) (13 mL) was stirred at 85 °C for 22 h under a N₂ atmosphere in a sealed tube. After cooling to room temperature, the reaction was diluted with H₂O (20 mL) and extracted with CH₂Cl₂ (3 x 50 mL). The combined organic layers were dried over Na₂SO₄, filtered, and concentrated. The crude product was purified by flash column chromatography eluting from 10% EtOAc in hexanes to give 1.17 g (3.9 mmol, 61%) of a colorless oil. Spectral data were consistent with previously reported values.⁶⁷ ¹H NMR (500 MHz, CDCl₃) δ 7.93 (d, *J* = 8.7 Hz, 1H), 7.74 (d, *J* = 8.3 Hz, 1H), 7.54-7.52 (m, 2H), 7.40 (dd, *J* = 8.7, 1.8 Hz, 1H), 7.21 (d, *J* = 8.1 Hz, 1H), 6.76 (dd, *J* = 17.6, 10.9 Hz, 1H), 6.63 (d, *J* = 3.7 Hz, 1H), 5.71 (d, *J* = 17.5 Hz, 1H), 5.21 (d, *J* = 10.9 Hz, 1H), 2.33 (s, 3H).

1-Bromo-2,5-dimethoxy-4-vinylbenzene: A flame-dried 100 mL round-bottomed flask was



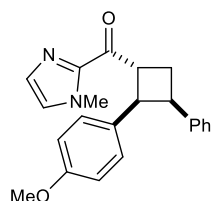
charged with 1.57 g (4.4 mmol, 1.1 equiv.) methyltriphenylphosphonium bromide in 40 mL dry THF. The vessel was cooled to 0 °C, and 500 mg of potassium *tert*-butoxide was added. The mixture was stirred for 30 min before cooling to -78 °C, at which point 0.98 g of 4-bromo-2,5-dimethoxybenzaldehyde in 5 mL THF was added portionwise. The mixture was warmed to room temperature and stirred for 18 h. The reaction mixture was then diluted with 50 mL 1:1 Et₂O/pentanes and filtered over a plug of Celite. The eluent was concentrated directly onto silica, then purified by flash column chromatography with 10% Et₂O in pentanes to give 710 mg (2.90 mmol, 66% yield) of a white solid. Spectral data were consistent with previously reported values.⁶⁸ ¹H NMR (500 MHz, CDCl₃) δ 7.90 (d, *J* = 15.9 Hz, 1H), 7.71 (d, *J* = 15.9 Hz, 1H), 7.26 (s, 1H), 7.08 (s, 1H), 6.92 (d, *J* = 1.3 Hz, 1H), 6.88 (d, *J* = 1.3 Hz, 1H), 6.03 (s, 2H), 4.10 (s, 3H), 3.95 (s, 3H).

2.6.4 Asymmetric [2+2] Photocycloaddition Reactions

General Procedure for Isolation-Scale Asymmetric [2+2] Cycloadditions: An oven-dried Schlenk tube was charged with the 1-methylimidazol enone (0.4 mmol, 1.0 equiv), styrene (4.0 mmol, 10.0 equiv.), (**R**)-**2.4** (0.08 mmol, 0.2 equiv.), and 8 mL toluene. The Schlenk was sealed with a glass stopper and degassed *via* freeze-pump-thaw technique (3 x 5 min). This was then cooled to -78 °C and irradiated with a Kessil Lamp (H150) for 14 h. The reaction mixture was then diluted 2–3x with CH₂Cl₂ before addition of 2 mL sat. aq. NaHCO₃. The mixture was vigorously stirred for 1 min, the organic layer separated, and the aqueous layer extracted with CH₂Cl₂ (2 x 4 mL). The combined organics were dried over Na₂SO₄, concentrated, and analyzed by ¹H NMR vs. internal standard (phenanthrene) to determine conversion and diastereomeric ratio. The crude mixture was then purified *via* flash column chromatography using Et₂O/pentanes as the

eluent, giving an isolated mixture of separable diastereomers. The major diastereomer of each mixture was characterized.

2-(4-Methoxyphenyl)-3-phenylcyclobutyl)(1-methyl-1H-imidazol-2-yl)methanone (2.5):

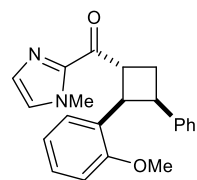


Prepared according to the general procedure for isolation-scale asymmetric experiments using 95.7 mg (0.39 mmol) (*E*)-3-(4-methoxyphenyl)-1-(1-methyl-

1H-imidazol-2-yl)prop-2-en-1-one, 0.44 mL (4.0 mmol) of styrene, 61.3 mg (0.08 mmol) (**R**)-**2.4**, and 8 mL toluene. The resulting material was purified by flash column chromatography eluting with 1:1 Et₂O/pentanes to give 84.8 mg (0.24 mmol, 62% yield) of two diastereomers (3:1 d.r.). Spectroscopic data were consistent with those previously reported.⁵⁹

Major Diastereomer: Viscous semisolid. 94% ee [Daicel CHIRALPAK OD-H, 5% to 50% iPrOH, 18 minutes, 1 mL/min, $t_1=9.87$ min, $t_2=13.37$ min]. $[\alpha]_D^{22} -57.7^\circ$ (c0.45, CH₂Cl₂). ¹H NMR (500 MHz, CDCl₃) δ 7.17 (s, 1H), 7.16–7.13 (m, 2H), 7.09–7.05 (m, 3H), 7.04 (s, 1H), 6.89 (d, $J = 8.5$ Hz, 2H), 6.59 (d, $J = 8.5$ Hz, 2H), 4.98 (q, $J = 8.8$ Hz, 1H), 4.39 (t, $J = 9.2$ Hz, 1H), 4.03 (s, 3H), 3.95 (td, $J = 8.9, 4.8$ Hz, 1H), 3.67 (s, 3H), 2.78–2.69 (m, 2H). HRMS (ESI) calculated for [C₂₂H₂₂N₂O₂]⁺ (M+H⁺) requires m/z 347.1754, found 347.1750.

2-(2-Methoxyphenyl)-3-phenylcyclobutyl)(1-methyl-1H-imidazol-2-yl)methanone (2.6):

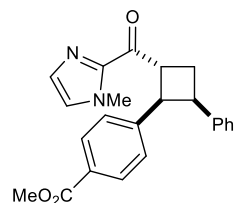


Prepared according to the general procedure for isolation-scale asymmetric experiments using 95.8 mg (0.40 mmol) (*E*)-3-(2-methoxyphenyl)-1-(1-methyl-

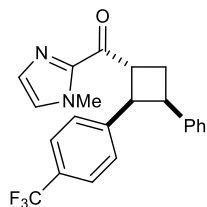
1H-imidazol-2-yl)prop-2-en-1-one, 0.44 mL (4.0 mmol) of styrene, 61.1 mg (0.08 mmol) (**R**)-**2.4**, and 8 mL toluene. The resulting material was purified by flash column chromatography using a gradient of 1:2 Et₂O/pentanes to 1:1 Et₂O/pentanes to give 68.2 mg (0.20

mmol, 50% yield) of two diastereomers (7:1 d.r.). Spectroscopic data were consistent with those previously reported.⁵⁹ Major Diastereomer: Viscous semisolid. 93% ee [Daicel CHIRALPAK OD-H, 5% to 50% iPrOH, 18 minutes, 1 mL/min, $t_1=9.81$ min, $t_2=11.30$ min]. $[\alpha]_D^{22} -115.4^\circ$ (c1.71, CH₂Cl₂). ¹H NMR (500 MHz, CDCl₃) δ 7.20 (s, 1H), 7.17 (d, $J =$ Hz, 1H), 7.12 (d, $J =$ Hz, 2H), 7.08–7.05 (m, 2H), 7.05 (s, 1H), 7.00–6.95 (m, 2H), 6.69 (t, $J = 7.5$ Hz, 1H), 6.54 (d, $J = 8.0$ Hz, 1H), 5.20 (q, $J = 9.4$ Hz, 1H), 4.62 (t, $J = 9.4$ Hz, 1H), 4.01 (s, 3H), 3.99 (td, $J = 9.4, 3.8$ Hz, 1H), 3.65 (s, 3H), 2.81 (dt, 11.7, 9.0 Hz, 1H), 2.62 (ddd, $J = 11.6, 9.5, 3.7$ Hz, 1H). HRMS (ESI) calculated for [C₂₂H₂₂N₂O₂]⁺ (M+H⁺) requires m/z 347.1754, found 347.1751.

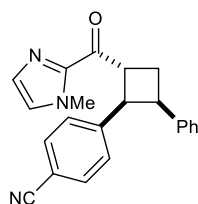
Methyl 4-(2-(1-methyl-1*H*-imidazole-2-carbonyl)-4-phenylcyclobutyl)benzoate (2.7):



Prepared according to the general procedure for isolation-scale asymmetric experiments using 108.2 mg (0.40 mmol) methyl 4-[(1*E*)-3-(1-methyl-1*H*-imidazol-2-yl)-3-oxoprop-1-en-1-yl]benzoate, 0.46 mL (4.0 mmol) of styrene, 61.8 mg (0.08 mmol) (**R**)-**2.4**, and 8 mL toluene. The resulting material was purified by flash column chromatography using a gradient of 1:1 Et₂O/pentanes to 3:1 Et₂O/pentanes to give 90.0 mg (0.24 mmol, 60% yield) of two diastereomers (2:1 d.r.). Major Diastereomer: Viscous semisolid. 91% ee [Daicel CHIRALPAK IC, 5% to 50% iPrOH, 18 minutes, 1 mL/min, $t_1=12.44$ min, $t_2=14.70$ min]. $[\alpha]_D^{22} -97.4^\circ$ (c1.590, CH₂Cl₂). ¹H NMR (500 MHz, CDCl₃) δ 7.72 (d, $J = 8.1$ Hz, 2H), 7.19 (s, 1H), 7.13–7.03 (m, 8H), 5.07 (q, $J = 9.0$ Hz, 1H), 4.50 (t, $J = 9.2$ Hz, 1H), 4.04 (s, 3H), 4.03–4.00 (m, 1H), 3.82 (s, 3H), 2.80–2.76 (m, 2H). ¹³C NMR (125 MHz, CDCl₃) δ 192.59, 167.11, 145.27, 142.40, 140.29, 129.51, 129.03, 128.12, 128.04, 127.91, 127.59, 127.50, 126.11, 51.87, 45.63, 43.65, 42.04, 36.24, 28.64. HRMS (ESI) calculated for [C₂₃H₂₃N₂O₃]⁺ (M+H⁺) requires m/z 375.1703, found 375.1699.

(1-Methyl-1H-imidazol-2-yl)(3-phenyl-2-(4-(trifluoromethyl)phenyl)cyclobutyl)methanone

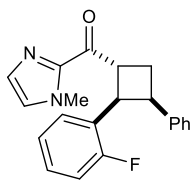
(2.8): Prepared according to the general procedure for isolation-scale asymmetric experiments using 113.5 mg (0.40 mmol) (*E*)-1-(1-methyl-1H-imidazol-2-yl)-3-(4-trifluoromethylphenyl)prop-2-en-1-one, 0.46 mL (4.0 mmol) of styrene, 62.6 mg (0.08 mmol) (**R**)-**2.4**, and 8 mL toluene. The resulting material was purified by flash column chromatography using a gradient of 1:3 to 1:1 Et₂O/pentanes to give 91.5 mg (0.24 mmol, 59% yield) of two diastereomers (2:1 d.r.). Spectroscopic data for both diastereomers were consistent with those previously reported.⁵⁹ Major Diastereomer: 80% ee [Daicel CHIRALPAK OD-H, 5% to 50% iPrOH, 18 minutes, 1 mL/min, *t*₁ = 8.44 min, *t*₂ = 11.42 min]. [α]_D²² -48.3° (c0.360, CH₂Cl₂). ¹H NMR (500 MHz, CDCl₃) δ 7.30 (d, *J* = 8.1 Hz, 2H), 7.19 (d, *J* = 0.7 Hz, 1H), 7.16–7.13 (m, 2H), 7.10–7.05 (m, 6H), 5.04 (q, *J* = 9.0 Hz, 1H), 4.49 (t, *J* = 9.3 Hz, 1H), 4.05 (s, 3H), 4.01 (td, *J* = 9.1, 5.0 Hz, 1H), 2.81–2.75 (m, 2H).

4-(2-(1-Methyl-1H-imidazole-2-carbonyl)-4-phenylcyclobutyl)benzotrile (2.9): Prepared

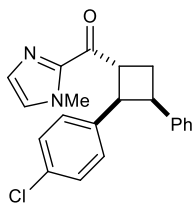
according to the general procedure for isolation-scale asymmetric experiments, irradiating for 24 h using 95.2 mg (0.40 mmol) (*E*)-4-(3-(1-methyl-1H-imidazol-2-yl)-3-oxoprop-1-en-1-yl)benzotrile, 0.45 mL (4.0 mmol) of styrene, 60.5 mg (0.08 mmol) (**R**)-**2.4**, and 8 mL toluene. The resulting material was purified by flash column chromatography using a gradient of 1:1 Et₂O/pentanes to 2:1 Et₂O/pentanes to give 72.0 mg (0.21 mmol, 53% yield) of three diastereomers (5:1 d.r.). Major Diastereomer: Viscous semisolid. 86% ee [Daicel CHIRALPAK OD-H, 5% to 50% iPrOH, 18 minutes, 1 mL/min, *t*₁ = 11.24 min, *t*₂ = 14.23 min]. [α]_D²² -166.3° (c0.54, CH₂Cl₂). ¹H NMR (500 MHz, CDCl₃) δ 7.34–7.32 (m, 2H), 7.19 (d, *J*

= 0.9 Hz, 1H), 7.16-7.13 (m, 2H), 7.09-7.05 (m, 6H), 5.05 (q, $J = 9.8$ Hz, 1H), 4.48 (t, $J = 9.4$ Hz, 1H), 4.05 (s, 3H), 4.02 (td, $J = 9.3, 4.5$ Hz, 1H), 2.84-2.73 (m, 2H). ^{13}C NMR (125 MHz, CDCl_3) δ 192.24, 145.49, 142.35, 139.95, 131.51, 129.62, 128.63, 128.20, 128.07, 127.63, 126.36, 119.09, 109.56, 45.75, 43.53, 42.07, 36.22, 28.37. HRMS (ESI) calculated for $[\text{C}_{22}\text{H}_{19}\text{N}_3\text{O}]^+$ ($\text{M}+\text{H}^+$) - requires m/z 342.1601, found 342.1598.

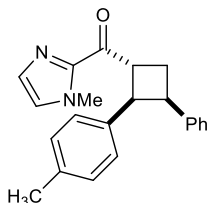
2-(2-Fluorophenyl)-3-phenylcyclobutyl(1-methyl-1H-imidazol-2-yl)methanone (2.10):



Prepared according to the general procedure for isolation-scale asymmetric experiments using 92.1 mg (0.40 mmol) (*E*)-3-(2-fluorophenyl)-1-(1-methyl-1H-imidazol-2-yl)prop-2-en-1-one, 0.44 mL (4.0 mmol) of styrene, 60.3 mg (0.08 mmol) (**R**)-**2.4**, and 8 mL toluene. The resulting material was purified by flash column chromatography using a gradient of hexanes to 1:1 Et_2O /hexanes to give 80.7 mg (0.24 mmol, 60% yield) of two diastereomers (10:1 d.r.). Major Diastereomer: Viscous semisolid. 95% ee [Daicel CHIRALPAK AD-H, 5% to 50% *i*PrOH, 18 minutes, 1 mL/min, $t_1=6.16$ min, $t_2=7.16$ min]. $[\alpha]_{\text{D}}^{22} -90.3^\circ$ (c0.33, CH_2Cl_2). ^1H NMR (500 MHz, CDCl_3) δ 7.20 (d, $J = 1.0$ Hz, 1H), 7.17-7.15 (m, 3H), 7.12-7.09 (m, 2H), 7.07 (s, 1H), 7.03-7.01 (m, 1H), 6.97-6.94 (m, 1H), 6.85-6.81 (m, 1H), 6.78-6.74 (m, 1H), 5.16 (q, $J = 8.3$ Hz, 1H), 4.66 (t, $J = 9.5$ Hz, 1H), 4.04 (s, 3H), 4.02 (td, $J = 9.3, 3.9$ Hz, 1H), 2.85-2.79 (m, 1H), 2.75-2.70 (s, 1H). ^{13}C NMR (125 MHz, CDCl_3) δ 192.64, 160.43, 142.62, 140.76, 129.47, 128.67, 127.90, 127.85, 127.54, 127.45, 126.95, 125.95, 123.35, 114.39, 42.11, 41.61, 40.18, 36.23, 28.70. ^{19}F NMR (377 MHz, CDCl_3) δ -115.91. HRMS (ESI) calculated for $[\text{C}_{21}\text{H}_{19}\text{FN}_2\text{O}]^+$ ($\text{M}+\text{H}^+$) requires m/z 335.1554, found 335.1552.

2-(4-Chlorophenyl)-3-phenylcyclobutyl(1-methyl-1H-imidazol-2-yl)methanone (2.11):

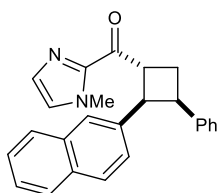
Prepared according to the general procedure for isolation-scale asymmetric experiments using 99.0 mg (0.40 mmol) (*E*)-3-(4-chlorophenyl)-1-(1-methyl-1H-imidazol-2-yl)prop-2-en-1-one, 0.44 mL (4.0 mmol) of styrene, 61.0 mg (0.08 mmol) (**R**)-**2.4**, and 8 mL toluene. The resulting material was purified by flash column chromatography using a gradient of 1:2 Et₂O/pentanes to 1:1 Et₂O/pentanes to give 103.2 mg (0.29 mmol, 73% yield) of three diastereomers (6:1 d.r.). Major Diastereomer: Viscous semisolid. 96% ee [Daicel CHIRALPAK OD-H, 5% to 50% iPrOH, 18 minutes, 1 mL/min, t₁=8.88 min, t₂=12.15 min]. [α]_D²² -82.3° (c1.15, CH₂Cl₂). ¹H NMR (500 MHz, CDCl₃) δ 7.18-7.14 (m, 3H), 7.08-7.06 (m, 4H), 7.01 (d, *J* = 8.5 Hz, 2H), 6.91 (d, *J* = 8.5 Hz, 2H), 4.98 (q, *J* = 9.3 Hz, 1H), 4.40 (t, *J* = 9.3 Hz, 1H), 4.04 (s, 3H), 3.99-3.95 (m, 1H), 2.77-2.74 (m, 2H). ¹³C NMR (125 MHz, CDCl₃) δ 192.72, 142.51, 140.38, 138.25, 131.58, 129.51, 129.30, 128.20, 128.05, 127.80, 127.45, 126.07, 45.27, 43.99, 41.90, 36.22, 28.38. HRMS (ESI) calculated for [C₂₁H₁₉ClN₂O]⁺ (M+H⁺) requires *m/z* 351.1259, found 351.1257.

(1-Methyl-1H-imidazol-2-yl)(3-phenyl-2-(p-tolyl)cyclobutyl)methanone (2.12):

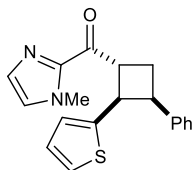
Prepared according to the general procedure for isolation-scale asymmetric experiments using 89.3 mg (0.40 mmol) (*E*)-1-(1-methyl-1H-imidazol-2-yl)-3-(p-tolyl)prop-2-en-1-one, 0.45 mL (4.0 mmol) of styrene, 60.4 mg (0.08 mmol) (**R**)-**2.4**, and 8 mL toluene. The resulting material was purified by flash column chromatography using a gradient of 1:2 Et₂O/pentanes to 1:1 Et₂O/pentanes to give 74.8 mg (0.23 mmol, 57% yield) of three diastereomers (4:1 d.r.). Major Diastereomer: Viscous semisolid. 98% ee [Daicel CHIRALPAK OD-H, 5% to 50% iPrOH, 18 minutes, 1 mL/min, t₁=8.34 min, t₂=10.88 min]. [α]_D²²

–102.5° (c0.16, CH₂Cl₂). ¹H NMR (500 MHz, CDCl₃) δ 7.17 (d, *J* = 1.0 Hz, 1H), 7.14-7.12 (m, 2H), 7.10-7.04 (m, 4H), 6.88-6.84 (m, 4H), 5.01 (q, *J* = 8.7 Hz, 1H), 4.41 (t, *J* = 9.2 Hz, 1H), 4.03 (s, 3H), 3.96 (td, *J* = 8.9, 4.9 Hz, 1H), 2.76-2.72 (m, 2H), 2.16 (s, 3H). ¹³C NMR (125 MHz, CDCl₃) δ 193.18, 142.68, 140.91, 136.59, 135.22, 129.40, 128.38, 128.29, 127.86, 127.86, 127.27, 125.77, 45.610, 44.08, 41.96, 36.22, 28.59, 20.95. HRMS (ESI) calculated for [C₂₂H₂₂N₂O]⁺ (M+H⁺) requires *m/z* 331.1805, found 331.1800.

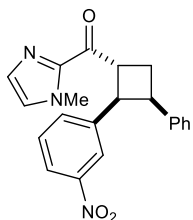
(1-Methyl-1H-imidazol-2-yl)(2-(naphthalen-2-yl)-3-phenylcyclobutyl)methanone (2.13):



Prepared according to the general procedure for isolation-scale asymmetric experiments using 105.5 mg (0.40 mmol) (*E*)-1-(1-methyl-1H-imidazol-2-yl)-3-(naphthalen-2-yl)prop-2-en-1-one, 0.44 mL (4.0 mmol) of styrene, 61.3 mg (0.08 mmol) (**R**)-**2.4**, and 8 mL toluene. The resulting material was purified by flash column chromatography using a gradient of 1:2 Et₂O/pentanes to 1:1 Et₂O/pentanes to give 63.6 mg (0.17 mmol, 43% yield) of two diastereomers (3:1 d.r.). Major Diastereomer: Viscous semisolid. 95% ee [Daicel CHIRALPAK OD-H, 5% to 50% iPrOH, 18 minutes, 1 mL/min, *t*₁=9.70 min, *t*₂=12.48 min]. [α]_D²² –104.6° (c0.43, CH₂Cl₂). ¹H NMR (500 MHz, CDCl₃) δ 7.64 (d, *J* = 9.4 Hz, 2H), 7.55 (s, 1H), 7.49 (d, *J* = 8.5 Hz, 1H), 7.36-7.30f (m, 2H), 7.21 (d, *J* = 1.0 Hz, 1H), 7.13-7.12 (m, 2H), 7.08-7.03 (m, 3H), 7.02 (dd, *J* = 8.5, 1.8 Hz, 1H), 6.99-6.96 (m, 1H), 5.17 (q, *J* = 8.9 Hz, 1H), 4.61 (t, *J* = 9.0 Hz, 1H), 4.10-4.04 (m, 4H), 2.83-2.80 (m, 2H). ¹³C NMR (125 MHz, CDCl₃) δ 193.04, 142.64, 140.75, 137.44, 133.16, 131.90, 129.46, 128.24, 127.93, 127.66, 127.39, 127.38, 127.09, 126.72, 126.25, 125.91, 125.49, 125.07, 45.92, 44.04, 42.01, 36.24, 28.84. HRMS (ESI) calculated for [C₂₅H₂₂N₂O]⁺ (M+H⁺) requires *m/z* 367.1805, found 367.1803.

(1-Methyl-1H-imidazol-2-yl)(3-phenyl-2-(thiophen-2-yl)cyclobutyl)methanone (2.14):

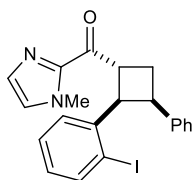
Prepared according to the general procedure for isolation-scale asymmetric experiments using 87.4 mg (0.40 mmol) (*E*)-1-(1-methyl-1H-imidazol-2-yl)-3-(thiophen-2-yl)prop-2-en-1-one, 0.45 mL (4.0 mmol) of styrene, 59.9 mg (0.08 mmol) (**R**)-**2.4**, and 8 mL toluene. The resulting material was purified by flash column chromatography using a gradient of 15% to 50% EtOAc/hexanes to give 63.2 mg (0.20 mmol, 49% yield) of two diastereomers (3:1 d.r.). Spectroscopic data were consistent with those previously reported.⁵⁹ Major Diastereomer: Viscous semisolid. 89% ee [Daicel CHIRALPAK OD-H, 5% to 50% iPrOH, 18 minutes, 1 mL/min, $t_1=9.46$ min, $t_2=11.30$ min]. $[\alpha]_D^{22} -42.0^\circ$ (c0.10, CH₂Cl₂). ¹H NMR (500 MHz, CDCl₃) δ 7.22–7.17 (m, 5H), 7.14–7.11 (m, 1H), 7.06 (s, 1H), 6.93 (dd, $J = 5.1, 1.1$ Hz, 1H), 6.71 (dd, $J = 4.9, 3.6$ Hz, 1H), 6.64 (dt, $J = 3.5, 1.1$ Hz, 1H), 4.88 (q, $J = 8.6$ Hz, 1H), 4.62 (t, $J = 8.8$ Hz, 1H), 4.05 (s, 3H), 3.97 (td, $J = 9.1, 5.1$ Hz, 1H), 2.86 (ddd, $J = 11.8, 10.2, 5.0$ Hz, 1H), 2.68 (dt, $J = 12.0, 8.5$ Hz, 1H). HRMS (ESI) calculated for [C₁₉H₁₈N₂OS]⁺ (M+H⁺) requires m/z 323.1213, found 323.1210.

(1-Methyl-1H-imidazol-2-yl)(2-(3-nitrophenyl)-3-phenylcyclobutyl)methanone (2.15):

Prepared according to the general procedure for isolation-scale asymmetric experiments, irradiating for 24 hours using 102.8 mg (0.40 mmol) (*E*)-1-(1-methyl-1H-imidazol-2-yl)-3-(3-nitrophenyl)prop-2-en-1-one, 0.45 mL (4.0 mmol) of styrene, 61.0 mg (0.08 mmol) (**R**)-**2.4**, and 8 mL toluene. The resulting material was purified by flash column chromatography using a gradient of 1:1 Et₂O/pentanes to 2:1 Et₂O/pentanes to give 108.7 mg (0.30 mmol, 75% yield) of two diastereomers (6:1 d.r.). Major Diastereomer: Viscous semisolid. 98% ee [Daicel CHIRALPAK OD-H, 5% to 50% iPrOH, 18

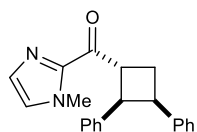
minutes, 1 mL/min, $t_1=10.97$ min, $t_2=13.51$ min]. $[\alpha]_D^{22} -101.8^\circ$ (c0.32, CH_2Cl_2). ^1H NMR (500 MHz, CDCl_3) δ 7.91 (s, 1H), 7.86-7.84 (m, 1H), 7.28 (d, $J = 7.8$ Hz, 1H), 7.20-7.13 (m, 4H), 7.10-7.08 (m, 3H), 7.06-7.03 (m, 1H), 5.06 (q, $J = 8.6$ Hz, 1H), 4.52 (t, $J = 9.4$ Hz, 1H), 4.06-4.02 (m, 4H), 2.87-2.77 (m, 2H). ^{13}C NMR (125 MHz, CDCl_3) δ 192.13, 147.81, 142.31, 142.01, 139.82, 134.14, 129.67, 128.46, 128.26, 128.13, 127.59, 126.37, 122.95, 121.00, 45.34, 43.95, 41.95, 36.20, 28.13. HRMS (ESI) calculated for $[\text{C}_{21}\text{H}_{19}\text{N}_3\text{O}_3]^+$ ($\text{M}+\text{H}^+$) requires m/z 362.1499, found 362.1496.

2-(2-Iodophenyl)-3-phenylcyclobutyl(1-methyl-1H-imidazol-2-yl)methanone (2.16):



Prepared according to the general procedure for isolation-scale asymmetric experiments using 135.6 mg (0.40 mmol) (*E*)-3-(2-iodophenyl)-1-(1-methyl-1H-imidazol-2-yl)prop-2-en-1-one, 0.45 mL (4.0 mmol) of styrene, 60.5 mg (0.08 mmol) (**R**)-**2.4**, and 8 mL toluene. The resulting material was purified by flash column chromatography using a gradient of 1:2 Et_2O /pentanes to 1:1 Et_2O /pentanes to give 72.4 mg (0.16 mmol, 41% yield) of two diastereomers (10:1 d.r.). Major Diastereomer: Viscous semisolid. 97% ee [Daicel CHIRALPAK AD-H, 5% to 50% *i*PrOH, 18 minutes, 1 mL/min, $t_1=5.69$ min, $t_2=6.18$ min]. $[\alpha]_D^{22} -44.0^\circ$ (c0.10, CH_2Cl_2). ^1H NMR (500 MHz, CDCl_3) δ 7.62 (dd, $J = 7.9, 1.3$ Hz, 1H), 7.24-7.22 (m, 2H), 7.19 (s, 1H), 7.17 (d, $J = 7.8$ Hz, 1H), 7.10 (t, $J = 7.6$ Hz, 2H), 7.05-6.99 (m, 3H), 6.68 (t, $J = 7.5$ Hz, 1H), 5.24 (q, $J = 9.5$ Hz, 1H), 4.55 (t, $J = 9.6$ Hz, 1H), 4.20 (td, $J = 9.1, 3.0$ Hz, 1H), 4.02 (s, 3H), 2.85-2.79 (m, 1H), 2.65-2.60 (m, 1H). ^{13}C NMR (125 MHz, CDCl_3) δ 192.28, 142.70, 141.63, 140.33, 138.85, 129.46, 128.68, 128.19, 127.80, 127.74, 127.51, 127.50, 125.95, 100.84, 50.67, 42.26, 41.10, 36.23, 27.68. HRMS (ESI) calculated for $[\text{C}_{21}\text{H}_{19}\text{IN}_2\text{O}]^+$ ($\text{M}+\text{H}^+$) requires m/z 443.0615, found 443.0611.

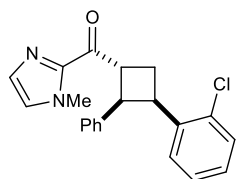
(2,3-Diphenylcyclobutyl)(1-methyl-1H-imidazol-2-yl)methanone (2.17): Prepared according to



the general procedure for isolation-scale asymmetric experiments using 84.6 mg

(0.40 mmol) 2-cinnamoyl-1-methylimidazole, 0.46 mL (4.0 mmol) styrene, 61.6 mg (0.08 mmol) (**R**)-**2.4**, and 8 mL toluene. The resulting material was purified by flash column chromatography using a gradient of 1:2 to 1:1 Et₂O/pentanes to give 98.0 mg (0.31 mmol, 78% yield) of two diastereomers (7:1 d.r.). Spectroscopic data for the major diastereomer were consistent with those previously reported.⁵⁹ Major diastereomer: 95% ee [Daicel CHIRALPAK OD-H, 5% to 50% iPrOH, 18 minutes, 1 mL/min, t₁=8.97 min, t₂=11.84 min]. [α]_D²² -91.9° (c0.790, CH₂Cl₂). ¹H NMR (500 MHz, CDCl₃) δ 7.18 (d, *J* = 0.8 Hz, 1H), 7.14–7.11 (m, 2H), 7.09–7.04 (m, 6H), 6.99–6.98 (m, 3H), 5.05 (q, *J* = 9.0 Hz, 1H), 4.47 (t, *J* = 9.2 Hz, 1H), 4.04 (s, 3H), 3.99 (td, *J* = 8.7, 6.0 Hz, 1H), 2.78–2.74 (m, 2H).

(3-(2-Chlorophenyl)-2-phenylcyclobutyl)(1-methyl-1H-imidazol-2-yl)methanone (2.18):

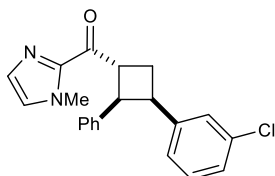


Prepared according to the general procedure for isolation-scale asymmetric

experiments using 85.1 mg (0.40 mmol) 2-cinnamoyl-1-methylimidazole, 0.51 mL (4.0 mmol) 2-chlorostyrene, 62.4 mg (0.08 mmol) (**R**)-**2.4**, and 8 mL toluene. The resulting material was purified by flash column chromatography using 1:1 Et₂O/pentanes to give 109.0 mg (0.31 mmol, 78% yield) of two diastereomers (10:1 d.r.). Major Diastereomer: 94% ee [Daicel CHIRALPAK AD, 5% to 50% iPrOH, 18 minutes, 1 mL/min, t₁=6.72 min, t₂=8.55 min]. White solid (mp = 94–97 °C). [α]_D²² -7.9° (c1.750, CH₂Cl₂). ¹H NMR (500 MHz, CDCl₃) δ 7.39 (dd, *J* = 8.0, 1.2 Hz, 1H), 7.16–6.98 (m, 10 H), 4.87 (dt, *J* = 9.7, 7.2 Hz, 1H), 4.51 (dd, *J* = 9.4, 7.2 Hz, 1H), 4.44 (td, *J* = 9.2, 6.2 Hz, 1H), 4.06 (s, 3H), 2.92 (ddd, *J* = 12.0,

10.1, 6.0 Hz, 1H), 2.74–2.68 (m, 1H). ^{13}C NMR (125 MHz, CDCl_3) δ 192.85, 142.45, 139.38, 138.15, 134.61, 129.40, 129.05, 128.15, 128.05, 127.52, 127.29, 127.23, 126.30, 126.03, 45.80, 43.87, 39.15, 36.26, 27.14. HRMS (ESI) calculated for $[\text{C}_{21}\text{H}_{20}\text{ClN}_2\text{O}]^+$ ($\text{M}+\text{H}^+$) requires m/z 351.1259, found 351.1258.

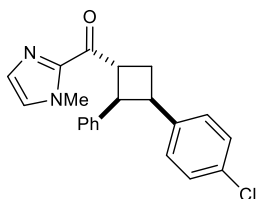
(3-(3-Chlorophenyl)-2-phenylcyclobutyl)(1-methyl-1H-imidazol-2-yl)methanone (2.19):



Prepared according to the general procedure for isolation-scale asymmetric experiments using 83.0 mg (0.39 mmol) 2-cinnamoyl-1-methylimidazole, 0.52 mL (4.0 mmol) 3-chlorostyrene, 62.1 mg (0.08 mmol) **(R)-2.4**, and 8 mL toluene. The resulting material was purified by flash column chromatography eluting from 10% acetone in pentane. to give 102.2 mg (0.29 mmol, 75% yield) of two diastereomers (4:1 d.r.).

Major diastereomer: 95% ee [Daicel CHIRALPAK AD-H, 5% to 50% iPrOH, 28 minutes, 1 mL/min, $t_1=8.46$ min, $t_2=12.35$ min]. White solid (mp = 120–124 °C). $[\alpha]_{\text{D}}^{22} = -87.4^\circ$ ($c = 0.7$, CH_2Cl_2). ^1H NMR (500 MHz, CDCl_3) δ 7.18 (s, 1H), 7.09–7.06 (m, 4H), 7.03–6.99 (m, 5H), 6.94–6.92 (m, 1H), 5.03 (q, $J = 8.9$ Hz, 1H), 4.46 (t, $J = 8.9$ Hz, 1H), 4.04 (s, 3H), 3.96 (td, $J = 9.1, 4.8$ Hz), 2.77–2.72 (m, 2H). ^{13}C NMR (125 MHz, CDCl_3) δ 192.79, 143.02, 142.50, 139.12, 133.71, 129.47, 129.04, 128.30, 127.88, 127.84, 127.44, 126.41, 126.07, 125.99, 45.77, 43.43, 41.70, 36.24, 28.30. HRMS (ESI) calculated for $[\text{C}_{21}\text{H}_{19}\text{ClN}_2\text{O}]^+$ ($\text{M}+\text{H}^+$) requires m/z 351.1259, found 351.1264.

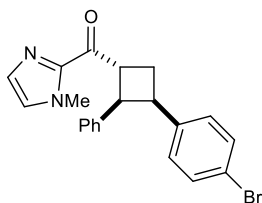
(3-(4-Chlorophenyl)-2-phenylcyclobutyl)(1-methyl-1H-imidazol-2-yl)methanone (2.20):



Prepared according to the general procedure for isolation-scale asymmetric experiments using 85.5 mg (0.40 mmol) 2-cinnamoyl-1-methylimidazole,

0.48 mL (4.0 mmol) 4-chlorostyrene, 63.0 mg (0.08 mmol) (**R**)-**2.4**, and 8 mL toluene. The resulting material was purified by flash column chromatography using 1:1 Et₂O/pentanes to give 109.5 mg (0.31 mmol, 77% yield) of two diastereomers (8:1 d.r.). Major diastereomer: 96% ee [Daicel CHIRALPAK AD, 5% to 50% iPrOH, 18 minutes, 1 mL/min, t₁=7.16 min, t₂=9.77 min]. White solid (mp = 121–124 °C). [α]_D²² -104.8° (c0.460, CH₂Cl₂). ¹H NMR (500 MHz, CDCl₃) δ 7.18 (s, 1H), 7.10–7.06 (m, 5H), 7.03–6.97 (m, 5H), 5.03 (q, *J* = 9.0 Hz, 1H), 4.46 (t, *J* = 9.3 Hz, 1H), 4.04 (s, 3H), 3.95 (td, *J* = 9.3, 4.6 Hz, 1H), 2.79–2.67 (m, 2H). ¹³C NMR (125 MHz, CDCl₃) δ 192.81, 142.53, 139.40, 139.28, 131.53, 129.54, 129.48, 127.97, 127.86 (2C), 127.44, 126.03, 45.64, 43.50, 41.43, 36.25, 28.68. HRMS (ESI) calculated for [C₂₁H₂₀ClN₂O]⁺ (M+H⁺) requires *m/z* 351.1259, found 351.1261.

(3-(4-Bromophenyl)-2-phenylcyclobutyl)(1-methyl-1H-imidazol-2-yl)methanone (2.21):

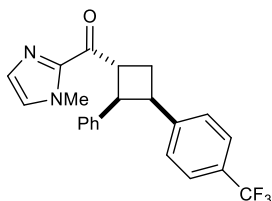


Prepared according to the general procedure for isolation-scale asymmetric experiments using 84.9 mg (0.40 mmol) 2-cinnamoyl-1-methylimidazole, 0.52 mL (4.0 mmol) 4-bromostyrene, 61.4 mg (0.08 mmol) (**R**)-**2.4**, and 8

mL toluene. The resulting material was purified by flash column chromatography eluting from a gradient of 1:2 Et₂O/pentanes → 1:1 Et₂O/pentanes to give 118.5 mg (0.30 mmol, 75% yield) of two diastereomers (6:1 d.r.). Major diastereomer: 92% ee [Daicel CHIRALPAK OD-H, 5% to 30% iPrOH, 20 minutes, 1 mL/min, t₁=11.18 min, t₂=12.23 min]. White solid (mp = 131–135 °C). [α]_D²² = -84.5° (c = 1.2, CH₂Cl₂). ¹H NMR (500 MHz, CDCl₃) δ 7.23 (d, *J* = 8.4 Hz, 2H), 7.18 (s, 1H), 7.10–7.06 (m, 3H), 7.03–6.93 (m, 5H), 5.02 (q, *J* = 8.9 Hz, 1H), 4.46 (t, *J* = 9.3 Hz, 1H), 4.04 (s, 3H), 3.94 (td, *J* = 9.2, 4.5 Hz, 1H), 2.77–2.69 (m, 2H). ¹³C NMR (125 MHz, CDCl₃) δ 192.78, 142.51, 139.94, 139.26, 130.91, 129.94, 129.48, 127.88, 127.85, 127.44, 126.04, 119.66, 45.56,

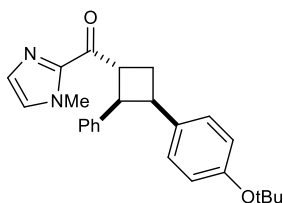
43.51, 41.48, 36.24, 28.65. HRMS (ESI) calculated for $[C_{21}H_{19}BrN_2O]^+$ ($M+H^+$) requires m/z 395.0754, found 395.0757.

(1-Methyl-1H-imidazol-2-yl)(2-phenyl-3-(4-(trifluoromethyl)phenyl)cyclobutyl)methanone



(2.22): Prepared according to the general procedure for isolation-scale asymmetric experiments using 84.3 mg (0.40 mmol) 2-cinnamoyl-1-methylimidazole, 0.59 mL (4.0 mmol) 4-(trifluoromethyl)styrene, 63.0 mg (0.08 mmol) **(R)-2.4**, and 8 mL toluene. The resulting material was purified by flash column chromatography eluting from a gradient of 1:2 Et₂O/pentanes to 1:1 Et₂O/pentanes to give 126.6 mg (0.33 mmol, 83% yield) of two diastereomers (5:1 d.r.). Spectroscopic data were consistent with those previously reported.⁵⁹ Major diastereomer: 96% ee [Daicel CHIRALPAK OD-H, 5% to 50% iPrOH, 13 minutes, 1 mL/min, $t_1=8.17$ min, $t_2=9.45$ min]. Viscous oil/semisolid. $[\alpha]_D^{22} = -74.4^\circ$ ($c = 2.0$, CH₂Cl₂). ¹H NMR (500 MHz, CDCl₃) δ 7.36 (d, $J = 8.1$ Hz, 2H), 7.19-7.16 (m, 3H), 7.08-7.05 (m, 3H), 6.98-6.96 (m, 3H), 5.06 (q, $J = 8.9$ Hz, 1H), 4.51 (t, $J = 9.4$ Hz, 1H), 4.07-4.02 (m, 4H), 2.82-2.73 (m, 2H). ¹³C NMR (125 MHz, CDCl₃) δ 192.64, 145.09, 142.49, 139.03, 129.52, 128.47, 128.15, 127.90, 127.80, 127.49, 126.15, 124.76, 123.18, 45.71, 43.50, 41.85, 36.24, 28.47. HRMS (ESI) calculated for $[C_{22}H_{19}F_3N_2O]^+$ ($M+H^+$) requires m/z 385.1522, found 385.1526.

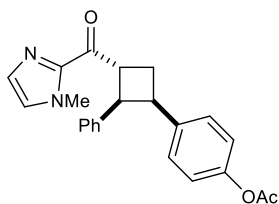
(3-(4-tert-Butoxyphenyl)-2-phenylcyclobutyl)(1-methyl-1H-imidazol-2-yl)methanone (2.23):



Prepared according to the general procedure for isolation-scale asymmetric experiments using 85.2 mg (0.40 mmol) 2-cinnamoyl-1-methylimidazole, 0.75 mL (4.0 mmol) 4-*tert*-butoxystyrene, 63.3 mg

(0.08 mmol) **(R)-2.4**, and 8 mL toluene. The resulting material was purified by flash column chromatography using a 1:1 Et₂O/pentanes to give 117.9 mg (0.30 mmol, 76% yield) of two diastereomers (8:1 d.r.). Major diastereomer: 83% ee [Daicel CHIRALPAK AD-H, 5% to 30% iPrOH, 20 minutes, 1 mL/min, t₁=7.90 min, t₂=8.56 min]. Viscous semisolid. [α]_D²² -69.0° (c0.620, CH₂Cl₂). ¹H NMR (500 MHz, CDCl₃) δ 7.17 (s, 1H), 7.04 (s, 1H), 7.03–7.00 (m, 2H), 6.97–6.93 (m, 5H), 6.75 (d, *J* = 8.4 Hz, 1H), 5.03 (q, *J* = 9.0 Hz, 1H), 4.41 (t, *J* = 9.3 Hz, 1H), 4.03 (s, 3H), 3.94 (dt, *J* = 9.3, 6.6 Hz, 1H), 2.76–2.73 (m, 2H), 1.23 (s, 9H). ¹³C NMR (125 MHz, CDCl₃) δ 193.09, 153.13, 142.63, 139.54, 135.68, 129.40, 128.51, 128.04, 127.55, 127.33, 125.75, 123.90, 45.97, 43.53, 41.55, 36.23, 28.72 (2C), 28.25. HRMS (ESI) calculated for [C₂₅H₂₉N₂O₂]⁺ (M+H⁺) requires *m/z* 389.2224, found 329.2225.

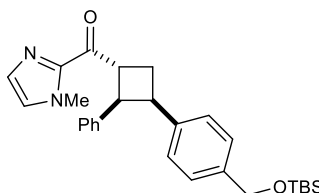
(3-(4-Acetoxyphenyl)-2-phenylcyclobutyl)(1-methyl-1H-imidazol-2-yl)methanone (2.24):



Prepared according to the general procedure for isolation-scale asymmetric experiments 84.9 mg (0.40 mmol) 2-cinnamoyl-1-methylimidazole, 0.61 mL (4.0 mmol) 4-acetoxystyrene, 62.7 mg (0.08 mmol) **(R)-2.4**, and 8 mL toluene, The resulting material was purified by flash column chromatography using 1:1 Et₂O/pentanes to give 84.4 mg (0.23 mmol, 56% yield) of two diastereomers (13:1 d.r.). Major diastereomer: 97% ee [Daicel CHIRALPAK AD, 5% to 50% iPrOH, 18 minutes, 1 mL/min, t₁=10.79 min, t₂=12.47 min]. White solid (mp = 81–83 °C). [α]_D²² -90.0° (c1.180, CH₂Cl₂). ¹H NMR (500 MHz, CDCl₃) δ 7.17 (s, 1H), 7.08–7.04 (m, 5H), 7.01–6.98 (m, 3H), 6.85 (d, *J* = 8.6 Hz, 2H), 5.03 (q, *J* = 8.9 Hz, 1H), 4.45 (t, *J* = 9.2 Hz, 1H), 4.02 (s, 3H), 3.98 (td, *J* = 8.8, 5.5 Hz, 1H), 2.77–2.71 (m, 2H), 2.22 (s, 3H). ¹³C NMR (125 MHz, CDCl₃) δ 192.90, 169.42, 148.69, 142.54, 139.39, 138.39, 129.44, 129.12, 127.93, 127.78, 127.39, 125.94,

120.85, 45.73, 43.58, 41.47, 36.22, 28.72, 21.11. HRMS (ESI) calculated for $[C_{23}H_{23}N_2O_3]^+$ ($M+H^+$) requires m/z 375.1703 found 375.1702.

3-(4-(((*tert*-Butyldimethylsilyl)oxy)methyl)phenyl)-2-phenylcyclobutyl(1-methyl-1H-



imidazol-2-yl)methanone (2.25): Prepared according to the general

procedure for isolation-scale asymmetric experiments using 81.8 mg

(0.39 mmol) 2-cinnamoyl-1-methylimidazole, 1.00 g (4.0 mmol) *O*-(*tert*-butyl)dimethylsilyl(4-vinylphenyl)methanol, 60.9 mg (0.08 mmol) (**R**)-**2.4**, and 8 mL

toluene. The resulting material was purified by flash column chromatography eluting with a gradient of 1:2 Et₂O/pentanes to 1:1 Et₂O/pentanes to give 144.3 mg (0.31 mmol, 81% yield) of

three diastereomers (10:2:1 d.r.). Major diastereomer: 95% ee [Daicel CHIRALPAK OD-H, 5% to 50% iPrOH, 20 minutes, 1 mL/min, $t_1=6.99$ min, $t_2=11.26$ min]. Viscous oil/semisolid. $[\alpha]_D^{22} =$

-31.7° ($c = 0.3$, CH₂Cl₂). ¹H NMR (500 MHz, CDCl₃) δ 7.18 (s, 1H), 7.09-7.03 (m, 7H), 7.00-6.96

(m, 3H), 5.05 (q, $J = 9.5$ Hz, 1H), 4.62 (s, 2H) 4.45 (t, $J = 9.3$ Hz, 1H), 4.04 (s, 3H), 3.97 (dt, $J =$

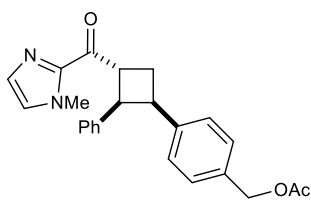
9.5, 6.6 Hz, 1H), 2.74 (dd, $J = 9.0, 6.7$ Hz, 2H), 0.90 (s, 9H), 0.02 (d, $J = 1.8$ Hz, 6H). ¹³C NMR

(125 MHz, CDCl₃) δ 193.14, 142.62, 139.69, 139.43, 138.90, 129.43, 128.09, 127.93, 127.69,

127.33, 125.76, 125.76, 64.87, 45.72, 43.84, 41.73, 36.25, 28.85, 25.95, 18.39, -5.17. HRMS (ESI)

calculated for $[C_{28}H_{36}SiN_2O_2]^+$ ($M+H^+$) requires m/z 461.2619, found 461.2626.

(3-(4-(Acetoxymethyl)phenyl)-2-phenylcyclobutyl)(1-methyl-1H-imidazol-2-yl)methanone



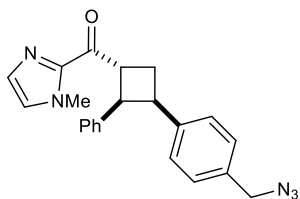
(2.26): Prepared according to the general procedure for isolation-scale

asymmetric experiments using 83.9 mg (0.40 mmol) 2-cinnamoyl-1-

methylimidazole, 0.71 g (4.0 mmol) 4-acetoxymethylstyrene, 61.4 mg

(0.08 mmol) **(R)-2.4**, and 8 mL toluene. The resulting material was purified by flash column chromatography eluting with a gradient of hexanes to 30% EtOAc in hexanes to give 110.0 mg (0.28 mmol, 72% yield) of three diastereomers (10:2:1 d.r.). Major diastereomer: 97% ee [Daicel CHIRALPAK OD-H, 5% to 50% iPrOH, 28 minutes, 1 mL/min, $t_1=13.45$ min, $t_2=23.64$ min]. Viscous oil/semisolid. $[\alpha]_D^{22} = -51.0^\circ$ ($c = 0.2$, CH_2Cl_2). $^1\text{H NMR}$ (500 MHz, CDCl_3) δ 7.18 (d, $J = 0.9$ Hz, 1H), 7.12-7.05 (m, 7H), 7.02-6.98 (m, 3H), 5.04 (q, $J = 9.6$ Hz, 1H), 4.98 (s, 2H) 4.47 (t, $J = 9.6$ Hz, 1H), 4.04 (s, 3H), 4.00 (td, $J = 8.7, 6.1$ Hz, 1H), 2.77-2.73 (m, 2H), 2.06 (s, 3H). $^{13}\text{C NMR}$ (125 MHz, CDCl_3) δ 192.98, 170.89, 142.57, 141.08, 139.56, 133.32, 129.45, 128.43, 127.91, 127.89, 127.75, 125.87, 66.13, 45.70, 43.73, 41.72, 36.25, 28.79, 21.05. HRMS (ESI) calculated for $[\text{C}_{24}\text{H}_{24}\text{N}_2\text{O}_3]^+$ ($\text{M}+\text{H}^+$) requires m/z 389.1860, found 339.1867.

(3-(4-(Azidomethyl)phenyl)-2-phenylcyclobutyl)(1-methyl-1H-imidazol-2-yl)methanone

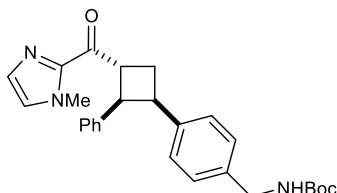


(2.27): Prepared according to the general procedure for isolation-scale asymmetric experiments using 82.7 mg (0.39 mmol) 2-cinnamoyl-1-methylimidazole, 0.64 g (4.0 mmol) 1-(azidomethyl)-4-vinylbenzene,

61.2 mg (0.08 mmol) **(R)-2.4**, and 8 mL toluene. The resulting material was purified by flash column chromatography eluting from a gradient of 1:2 Et_2O /pentanes \rightarrow 1:1 Et_2O /pentanes to give 114.6 mg (0.31 mmol, 79% yield) of three diastereomers (10:2:1 d.r.). Major diastereomer: 94% ee [Daicel CHIRALPAK AD, 5% to 50% iPrOH, 18 minutes, 1 mL/min, $t_1=8.51$ min, $t_2=10.99$ min]. Viscous oil/semisolid. $[\alpha]_D^{22} = -88.0^\circ$ ($c = 0.5$, CH_2Cl_2). $^1\text{H NMR}$ (500 MHz, CDCl_3) δ 7.18 (d, $J = 0.9$ Hz, 1H), 7.11-7.04 (m, 7H), 7.00-6.96 (m, 3H), 5.05 (q, $J = 9.1$ Hz, 1H), 4.47 (t, $J = 9.3$ Hz, 1H), 4.19 (s, 2H), 4.04 (s, 3H), 4.00 (dt, $J = 9.7, 6.8$ Hz, 1H), 2.76 (dd, $J = 8.9, 6.6$ Hz, 2H). $^{13}\text{C NMR}$ (125 MHz, CDCl_3) δ 192.92, 142.57, 141.11, 139.40, 132.57, 129.46, 128.69, 127.95,

127.90, 127.76, 127.39, 125.92, 54.46, 45.78, 43.68, 41.76, 36.24, 28.51. HRMS (ESI) calculated for $[C_{22}H_{21}N_5O]^+$ ($M+H^+$) requires m/z 372.1819, found 372.1826.

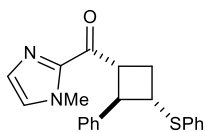
***tert*-Butyl(4-(3-(1-methyl-1H-imidazole-2-carbonyl)-2-phenylcyclobutyl)benzyl) carbamate**



(2.28): Prepared according to the general procedure for isolation-scale asymmetric experiments using 83.5 mg (0.39 mmol) 2-cinnamoyl-1-methylimidazole, 0.93 g (4.0 mmol) *tert*-butyl 4-

vinylbenzylcarbamate, 61.7 mg (0.08 mmol) (***R***)-**2.4**, and 8 mL toluene. The resulting material was purified by flash column chromatography eluting from a gradient of 30% EtOAc in hexanes \rightarrow 50% EtOAc in hexanes to give 118.4 mg (0.27 mmol, 68% yield) of three diastereomers (10:2.5:1 d.r.). Major diastereomer: 95% ee [Daicel CHIRALPAK OD-H, 5% to 50% *i*PrOH, 28 minutes, 1 mL/min, $t_1=17.23$ min, $t_2=22.76$ min]. Viscous oil/semisolid. $[\alpha]_D^{22} = -66.5^\circ$ ($c = 0.7$, CH_2Cl_2). 1H NMR (500 MHz, $CDCl_3$) δ 7.18 (s, 1H), 7.06-7.03 (m, 7H), 6.99-6.98 (m, 3H), 5.04 (q, $J = 8.9$ Hz, 1H), 4.69 (s, 1H), 4.46 (t, $J = 9.3$ Hz, 1H), 4.18 (d, $J = 5.1$ Hz, 2H), 4.04 (s, 3H), 3.97 (td, $J = 9.0, 5.1$ Hz, 1H), 2.76-2.72 (m, 2H), 1.45 (s, 9H). ^{13}C NMR (125 MHz, $CDCl_3$) δ 193.03, 155.82, 142.57, 140.05, 139.63, 136.21, 129.43, 128.47, 127.89, 127.73, 127.37, 127.08, 125.83, 79.36, 45.66, 44.38, 43.74, 41.64, 36.25, 28.86, 28.41. HRMS (ESI) calculated for $[C_{27}H_{31}N_3O_3]^+$ ($M+H^+$) requires m/z 446.2438, found 446.2436.

(1-Methyl-1H-imidazol-2-yl)(2-phenyl-3-(phenylthio)cyclobutyl)methanone (2.29): Prepared

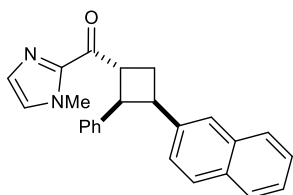


according to the general procedure for isolation-scale asymmetric experiments using 85.2 mg (0.41 mmol) 2-cinnamoyl-1-methylimidazole, 0.53 mL (4.0

mmol) of phenyl vinyl sulfide, 121.8 mg (0.16 mmol) (***R***)-**2.4**, and 8 mL toluene. The resulting

material was purified by flash column chromatography using 1:1 Et₂O/pentanes to give 79.9 mg (0.23 mmol, 57% yield) of two diastereomers (1.2:1 d.r.). Spectroscopic data for both diastereomers were consistent with those previously reported.⁵⁹ Major Diastereomer: 78% ee [Daicel CHIRALPAK AD, 5% to 50% iPrOH, 18 minutes, 1 mL/min, t₁= 8.44 min, t₂= 12.46 min]. [α]_D²² -4.3° (c0.470, CH₂Cl₂). ¹H NMR (500 MHz, CDCl₃) δ 7.34 (d, *J* = 7.7 Hz, 2H), 7.30–7.28 (m, 4H), 7.25–7.18 (d, 4H), 7.12 (s, 1H), 7.02 (s, 1H), 4.48 (q, *J* = 9.1 Hz, 1H), 3.99 (s, 3H), 3.93 (t, *J* = 9.5 Hz, 1H), 3.85 (td, *J* = 9.4, 7.3 Hz, 1H), 2.93 (dt, *J* = 10.8, 8.2 Hz, 1H), 2.22 (q, *J* = 10.1 Hz, 1H). Minor Diastereomer: 75% ee [Daicel CHIRALPAK AD, 5% to 50% iPrOH, 18 minutes, 1 mL/min, t₁= 9.06 min, t₂= 10.22 min]. [α]_D²² -173.0° (c0.770, CH₂Cl₂). ¹H NMR (500 MHz, CDCl₃) δ 7.34 (d, *J* = Hz, 2H), 7.29 (t, *J* = 7.4 Hz, 1H), 7.24–7.15 (m, 4H), 7.12–7.07 (m, 3H), 7.04 (s, 1H), 5.14 (q, *J* = 8.9 Hz, 1H), 4.47 (t, *J* = 8.7 Hz, 1H), 4.35 (td, *J* = 7.8, 3.3 Hz, 1H), 4.01 (s, 3H), 2.76 (dt, *J* = 11.8 7.9 Hz, 1H), 2.47 (ddd, *J* = 12.1, 9.5, 3.0 Hz, 1H).

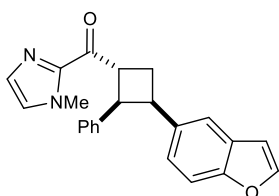
(1-Methyl-1H-imidazol-2-yl)(3-(naphthalen-2-yl)-2-phenylcyclobutyl)methanone (2.30):



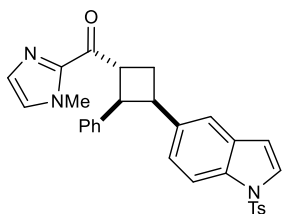
Prepared according to the general procedure for isolation-scale asymmetric experiments using 82.1 mg (0.39 mmol) 2-cinnamoyl-1-methylimidazole, 0.61 g (4.0 mmol) 2-vinylnaphthalene, 60.3 mg (0.08 mmol) **(R)**-**2.4**, and 8 mL toluene. The resulting material was purified by flash column chromatography eluting from a gradient of 1:2 Et₂O/pentanes to 1:1 Et₂O/pentanes to give 120.0 mg (0.33 mmol, 85% yield) of three diastereomers (5:1.5:1 d.r.). Major diastereomer: 90% ee [Daicel CHIRALPAK AD, 5% to 50% iPrOH, 13 minutes, 1 mL/min, t₁=7.61 min, t₂=9.76 min]. Viscous oil/semisolid. [α]_D²² = -97.7° (c = 0.4, CH₂Cl₂). ¹H NMR (500 MHz, CDCl₃) δ 7.75 (d, *J* = 6.9 Hz, 1H), 7.68 (d, *J* = 8.1 Hz, 1H), 7.65 (s, 1H), 7.52 (d, *J* = 8.5 Hz, 1H), 7.42–7.34 (m, 2H),

7.20 (d, $J = 0.9$ Hz, 1H), 7.07-7.05 (m, 2H), 7.03-6.98 (m, 4H), 6.94-6.91 (m, 1H), 5.12 (q, $J = 9.5$ Hz, 1H), 4.55 (t, $J = 9.2$ Hz, 1H), 4.16 (td, $J = 9.1, 4.6$ Hz, 1H), 4.05 (s, 3H), 2.90-2.82 (m, 2H). ^{13}C NMR (125 MHz, CDCl_3) δ 193.10, 142.61, 139.61, 138.56, 133.25, 131.90, 129.44, 127.94, 127.73, 127.67, 127.45, 127.39, 127.35, 127.25, 126.07, 125.86, 125.61, 125.11, 45.75, 43.95, 42.05, 36.27, 28.61. HRMS (ESI) calculated for $[\text{C}_{25}\text{H}_{22}\text{N}_2\text{O}]^+$ ($\text{M}+\text{H}^+$) requires m/z 367.1805, found 367.1808.

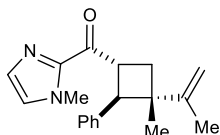
(3-(Benzofuran-5-yl)-2-phenylcyclobutyl)(1-methyl-1H-imidazol-2-yl)methanone (2.31):



Prepared according to the general procedure for isolation-scale asymmetric experiments using 84.9 mg (0.40 mmol) 2-cinnamoyl-1-methylimidazole, 570.0 mg (4.0 mmol) 5-vinyl-1-benzofuran 61.5 mg (0.08 mmol) (**R**)-**2.4**, and 8 mL toluene. The resulting material was purified by flash column chromatography using 1:1 Et_2O /pentanes to give 121.2 mg (0.34 mmol, 85% yield) of three diastereomers (4:1 d.r.). Major diastereomer: 94% ee [Daicel CHIRALPAK OD-H, 5% to 50% $i\text{PrOH}$, 18 minutes, 1 mL/min, $t_1=9.081$ min, $t_2=10.288$ min]. Viscous oil/semisolid. $[\alpha]_{\text{D}}^{22} = -28.0^\circ$ ($c = 0.7$, CH_2Cl_2). ^1H NMR (500 MHz, CDCl_3) δ 7.51 (d, $J = 2.2$ Hz, 1H), 7.41 (s, 1H), 7.22-7.19 (m, 2H), 7.06 (s, 1H), 7.02-6.98 (m, 4H), 6.95-6.92 (m, 2H), 6.65 (d, $J = 1.2$ Hz, 1H), 5.09 (q, $J = 9.2$ Hz, 1H), 4.48 (t, $J = 9.2$ Hz, 1H), 4.10 (q, $J = 7.6$ Hz, 1H), 4.05 (s, 3H), 2.82-2.79 (m, 2H). ^{13}C NMR (125 MHz, CDCl_3) δ 193.14, 153.48, 144.75, 142.63, 139.69, 135.30, 129.42, 127.94, 127.68, 127.37, 127.09, 125.78, 125.21, 120.07, 110.57, 106.56, 45.88, 43.80, 41.91, 36.28, 29.18. HRMS (ESI) calculated for $[\text{C}_{23}\text{H}_{20}\text{N}_2\text{O}_2]^+$ ($\text{M}+\text{H}^+$) requires m/z 357.1598, found 357.1590.

(1-Methyl-1H-imidazol-2-yl)(2-phenyl-3-(1-tosyl-1H-indol-5-yl)cyclobutyl)methanone

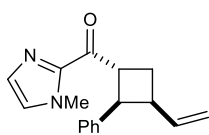
(2.32): Prepared according to the general procedure for isolation-scale asymmetric experiments using 84.9 mg (0.40 mmol) 2-cinnamoyl-1-methylimidazole, 1.17 g (4.0 mmol) 1-toluenesulfonyl-5-vinyl-1H-indole, 61.3 mg (0.08 mmol) **(R)-2.4**, and 8 mL toluene. The resulting material was purified by preparative HPLC eluting from 0.05% dioxane in H₂O to 85% MeCN/15% 0.05% dioxane in H₂O 165.1 mg (0.32 mmol, 81% yield) of three diastereomers (4:1 d.r.). Major diastereomer: 99% ee [Daicel CHIRALPAK AS-H, 5% to 50% iPrOH, 28 minutes, 1 mL/min, $t_1=20.658$ min, $t_2=22.136$ min]. White solid (mp = 155–159 °C). $[\alpha]_D^{22} = -35.2^\circ$ ($c = 0.3$, CH₂Cl₂). ¹H NMR (500 MHz, CDCl₃) δ 7.68 (d, $J = 8.5$ Hz, 1H), 7.64 (d, $J = 8.4$ Hz, 2H), 7.43 (d, $J = 3.7$ Hz, 1H), 7.32 (s, 1H), 7.19-7.18 (m, 3H), 7.05 (s, 1H), 6.92-6.90 (m, 6H), 6.54 (d, $J = 3.7$ Hz, 1H), 5.03 (q, $J = 9.0$ Hz, 1H), 4.45 (t, $J = 9.3$ Hz, 1H), 4.06-4.01 (m, 4H), 2.77-2.74 (m, 2H), 2.35 (s, 3H). ¹³C NMR (125 MHz, CDCl₃) δ 193.00, 144.61, 142.59, 139.48, 136.02, 135.26, 133.37, 130.64, 129.71, 129.41, 127.89, 127.60, 127.38, 126.66, 126.27, 125.75, 125.72, 120.18, 112.95, 109.42, 45.87, 43.75, 41.85, 36.26, 28.76, 21.56. HRMS (ESI) calculated for [C₃₀H₂₇N₃O₃S]⁺ (M+H⁺) requires m/z 510.1846, found 510.1839.

(1-Methyl-1H-imidazol-2-yl)(3-methyl-2-phenyl-3-(prop-1-en-2-yl)cyclobutyl)methanone

(2.33): Prepared according to the general procedure isolation-scale asymmetric experiments using 86.1 mg (0.41 mmol) 2-cinnamoyl-1-methylimidazole, 0.45 mL (4.0 mmol) of 2,3-dimethylbutadiene, 61.0 mg (0.08 mmol) **(R)-2.4**, and 8 mL toluene. The resulting material was purified by flash column chromatography using a gradient of 1:2 to 1:1 Et₂O/pentanes to give 58.0 mg (0.20 mmol, 49% yield) of two diastereomers (10:1 d.r.). Spectroscopic data for the major diastereomer was consistent with that previously reported.⁵⁹

Major diastereomer: 63% ee [Daicel CHIRALPAK AD-H, 5% to 30% iPrOH, 20 minutes, 1 mL/min, $t_1 = 5.75$ min, $t_2 = 8.43$ min]. $[\alpha]_D^{22} -52.5^\circ$ (c0.640, CH_2Cl_2). ^1H NMR (500 MHz, CDCl_3) δ 7.31–7.25 (m, 4H), 7.19–7.16 (m, 1H), 7.18 (s, 1H), 7.04 (s, 1H), 4.91 (br s, 1H), 4.84 (p, $J = 1.4$ Hz, 1H), 4.79 (q, $J = 9.5$ Hz, 1H), 4.13 (d, $J = 10.0$ Hz, 1H) 3.99 (s, 3H), 2.28 (t, $J = 9.9$ Hz, 1H), 2.19 (dd, $J = 10.3, 9.1$ Hz, 1H), 1.78 (s, 3H), 1.10 (s, 3H).

(3-Ethenyl-2-phenylcyclobutyl)(1-methyl-1H-imidazol-2-yl)methanone (2.34): Prepared



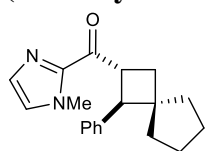
according to the general procedure for isolation-scale asymmetric experiments

using 85.1 mg (0.40 mmol) 2-cinnamoyl-1-methylimidazole, 2.2 mL (4.0 mmol) of 1,3-butadiene (15% in toluene), 63.2 mg (0.08 mmol) (**R**)-**2.4**, and 6 mL toluene. The resulting material was purified by flash column chromatography using a gradient of 1:2 to 1:1 Et_2O /pentanes to give 78.8 mg (0.30 mmol, 74% yield) of two diastereomers (3:1 d.r.). Major

Diastereomer: 87 % ee [Daicel CHIRALPAK AD, 5% to 50% iPrOH, 18 minutes, 1 mL/min, $t_1 = 6.31$ min, $t_2 = 7.24$ min]. Viscous oil. $[\alpha]_D^{22} -121.4^\circ$ (c2.500, CH_2Cl_2). ^1H NMR (500 MHz, CDCl_3) δ 7.28–7.25 (m, 2H), 7.20 (d, $J = 7.6$ Hz, 2H), 7.18 (s, 1H), 7.15 (tt, $J = 7.2, 1.4$ Hz, 1H), 7.05 (s, 1H), 5.76 (ddd, $J = 17.0, 10.2, 8.5$ Hz, 1H), 5.03 (dq, $J = 17.0, 1.0$ Hz, 1H), 4.97–4.91 (m, 2H), 4.23 (t, $J = 9.3$ Hz, 1H), 3.33–3.27 (m, 1H), 2.52 (dt, $J = 11.2, 8.7$ Hz, 1H), 2.30 (ddd, $J = 11.8, 9.5, 2.6$ Hz, 1H). ^{13}C NMR (125 MHz, CDCl_3) δ 192.96, 142.62, 140.02, 138.84, 129.39, 128.00, 127.75, 125.98, 115.28, 44.21, 43.27, 40.53, 36.22, 28.86. HRMS (ESI) calculated for $[\text{C}_{17}\text{H}_{19}\text{N}_2\text{O}]^+$ ($\text{M}+\text{H}^+$) requires m/z 267.1492, found 267.1491. Minor Diastereomer: 48% ee [Daicel CHIRALPAK AD, 5% to 50% iPrOH, 18 minutes, 1 mL/min, $t_1 = 6.15$ min, $t_2 = 7.41$ min]. Viscous oil. $[\alpha]_D^{22} -34.8^\circ$ (c0.270, CH_2Cl_2). ^1H NMR (500 MHz, CDCl_3) δ 7.29–7.27 (m, 4H), 7.20–7.16 (m, 1H), 7.14 (s, 1H), 7.03 (s, 1H), 6.00 (ddd, $J = 17.0, 10.2, 7.0$ Hz, 1H), 5.09 (dt, $J =$

17.1, 1.5 Hz, 1H), 5.03 (dt, $J = 10.3, 1.3$ Hz, 1H), 4.49 (td, $J = 9.7, 8.7$ Hz, 1H), 4.02 (s, 3H), 3.76 (t, $J = 9.7$ Hz, 1H), 3.02 (pent, $J = 8.5$ Hz, 1H), 2.59 (dt, $J = 10.2, 8.4$ Hz, 1H), 2.04 (q, $J = 10.1$ Hz, 1H). ^{13}C NMR (125 MHz, CDCl_3) δ 192.49, 142.62, 142.55, 140.74, 129.37, 128.32, 127.22, 126.80, 126.33, 114.50, 46.96, 44.91, 42.60, 36.17, 30.54. HRMS (ESI) calculated for $[\text{C}_{17}\text{H}_{19}\text{N}_2\text{O}]^+$ ($\text{M}+\text{H}^+$) requires m/z 267.1492, found 267.1488.

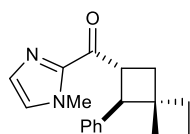
(1-Methyl-1H-imidazol-2-yl)(1-phenylspiro[3.4]octan-2-yl)methanone (2.37): Prepared



according to the general procedure for isolation-scale asymmetric experiments

using 85.1 mg (0.40 mmol) 2-cinnamoyl-1-methylimidazole, 0.46 mL (4.0 mmol) methylenecyclopentane, 121.8 mg (0.16 mmol) **(R)-2.4**, and 8 mL toluene, The resulting material was purified by flash column chromatography using a gradient of 1:2 to 1:1 Et_2O /pentanes to give 49.0 mg (0.17 mmol, 42% yield) of two of diastereomers (6:1 d.r.). Spectroscopic data for the major diastereomer were consistent with those previously reported.⁵⁹ Major diastereomer: 85% ee [Daicel CHIRALPAK OD-H, 5% to 50% $i\text{PrOH}$, 18 minutes, 1 mL/min, $t_1=6.07$ min, $t_2=6.65$ min]. $[\alpha]_{\text{D}}^{22} -71.0^\circ$ (c0.600, CH_2Cl_2). ^1H NMR (500 MHz, CDCl_3) δ 7.28–7.27 (m, 4H), 7.19–7.16 (m, 1H), 7.17 (s, 1H), 7.02 (s, 1H), 4.79 (q, $J = 9.5$ Hz, 1H), 3.98 (s, 3H), 3.91 (d, $J = 10.1$ Hz, 1H), 2.21 (t, $J = 9.6$ Hz, 1H), 2.06 (t, $J = 9.9$ Hz, 1H), 1.83–1.72 (m, 2H), 1.55–1.46 (m, 4H), 1.33–1.26 (m, 2H).

(1-Methyl-1H-imidazol-2-yl)(1-phenylspiro[3.3]heptan-2-yl)methanone (2.38): Prepared

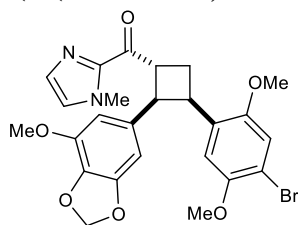


according to the general procedure for isolation-scale asymmetric experiments

85.0 mg (0.40 mmol) 2-cinnamoyl-1-methylimidazole, 0.37 mL (4.0 mmol) methylenecyclobutane, 121.0 mg (0.16 mmol) **(R)-2.4**, and 8 mL toluene, The resulting material

was purified by flash column chromatography using 1:1 Et₂O/pentanes to give 65.2 mg (0.23 mmol, 58% yield) of a single diastereomer (>20:1). 88% ee [Daicel CHIRALPAK AD, 5% to 50% iPrOH, 18 minutes, 1 mL/min, t₁=5.86 min, t₂=7.63 min]. White solid (mp = 80–82 °C). [α]_D²² –75.1° (c1.110, CH₂Cl₂). ¹H NMR (500 MHz, CDCl₃) δ 7.33–7.29 (m, 4H), 7.22–7.19 (m, 1H), 7.15 (s, 1H), 7.01 (s, 1H), 4.65 (q, *J* = 9.4 Hz, 1H), 3.97 (s, 3H), 3.67 (d, *J* = 9.8 Hz, 1H), 2.44 (dd, *J* = Hz, 1H), 2.20 (t, *J* = 10.3, 8.9 Hz, 1H), 2.11–2.06 (m, 1H), 2.00–1.94(m, 1H), 1.84–1.76 (m, 3H), 1.57–1.50 (m, 1H). ¹³C NMR (125 MHz, CDCl₃) δ 192.75, 142.80, 140.01, 129.26, 128.16, 127.82, 127.21, 126.28, 50.21, 45.33, 40.57, 37.77, 36.18, 33.36, 29.38, 16.12. HRMS (ESI) calculated for [C₁₈H₂₁N₂O]⁺ (M+H⁺) requires *m/z* 281.1648, found 281.1648.

(3-(4-Bromo-2,5-dimethoxyphenyl)-2-(7-methoxy-2*H*-1,3-benzodioxol-5-yl)cyclobutyl)(1-



methyl-1*H*-imidazol-2-yl)methanone (2.39): Prepared according to the

general procedure for isolation-scale asymmetric experiments using 144.5

mg (0.50 mmol) (*E*)-3-(7-methoxybenzo[d][1,3]dioxol-5-yl)-1-(1-

methyl-1*H*-imidazol-2-yl)prop-2-en-1-one, 582.1 mg (2.4 mmol) 4-bromo-2,5-methoxystyrene,

74.0 mg (0.10 mmol) (***R***)-**2.4**, and 10 mL CH₂Cl₂. The resulting material was purified by flash

column chromatography with 50% to 100% EtOAc in pentanes to give 173.0 mg (0.33 mmol, 65%

yield) of two diastereomers (5:1 d.r., separated under these conditions). Major Diastereomer:

White solid (mp = 78–82 °C, liquid phase is a *very* viscous oil). 93% ee [Daicel CHIRALPAK

AD, 5% to 50% iPrOH, 20 minutes, 1 mL/min, t₁=13.00 min, t₂=14.46 min]. [α]_D²² –57.1° (c0.280,

CH₂Cl₂). ¹H NMR (500 MHz, CDCl₃) δ 7.15 (s, 1H), 7.05 (s, 1H), 6.88 (s, 1H), 6.79 (s, 1H), 6.30

(d, *J* = 1.3 Hz, 1H), 6.20 (d, *J* = 1.3 Hz, 1H), 5.82 (dd, *J* = 4.5, 1.4 Hz, 2H), 4.75 (q, *J* = 8.1 Hz,

1H), 4.29 (dd, *J* = 9.6, 7.6 Hz, 1H), 4.21 (td, *J* = 9.2, 6.2 Hz, 1H), 4.05 (s, 3H), 3.83 (s, 3H), 3.69

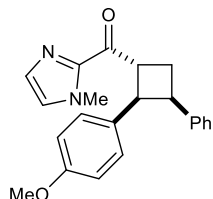
(s, 3H), 3.54 (s, 3H), 2.77–2.66 (m, 2H). ^{13}C NMR (125 MHz, CDCl_3) δ 192.82, 151.98, 149.80, 148.08, 142.76, 142.44, 134.99, 133.24, 129.77, 129.38, 127.33, 115.06, 112.76, 109.01, 107.10, 102.10, 101.06, 57.41, 56.29, 55.62, 46.03, 44.62, 36.24, 36.16, 26.76. HRMS (ESI) calculated for $[\text{C}_{25}\text{H}_{26}\text{BrN}_2\text{O}_6]^+$ ($\text{M}+\text{H}^+$) requires m/z 529.0969, found 529.0968. Minor Diastereomer: White solid (mp = 138–141 °C). 68% ee [Daicel CHIRALPAK AS-H, 5% to 30% EtOH, 35 minutes, 1 mL/min, $t_1=17.84$ min, $t_2=18.80$ min. $[\alpha]_{\text{D}}^{22} -17.8^\circ$ (c0.540, CH_2Cl_2). ^1H NMR (500 MHz, CDCl_3) δ 7.15 (s, 1H), 7.05 (s, 1H), 7.00 (s, 1H), 6.98 (s, 1H), 6.51 (d, $J = 1.3$ Hz, 1H), 6.48 (d, $J = 1.3$ Hz, 1H), 5.90–5.89 (m, 2H), 4.44 (q, $J = 9.2$ Hz, 1H), 4.04 (s, 3H), 4.02 (q, 9.9 Hz, 1H), 3.88–3.83 (m, 1H), 3.87 (s, 3H), 3.84 (s, 3H), 3.70 (s, 3H), 2.83 (dt, $J = 10.2, 8.6$ Hz, 1H), 2.14 (q, $J = 10.1$ Hz, 1H). ^{13}C NMR (125 MHz, CDCl_3) δ 192.37, 151.86, 150.16, 148.77, 143.38, 142.59, 137.40, 133.69, 131.98, 129.46, 127.33, 115.87, 112.09, 109.18, 106.23, 101.23, 101.08, 57.12, 56.52, 56.14, 47.18, 46.32, 37.63, 36.18, 31.82. HRMS (ESI) calculated for $[\text{C}_{25}\text{H}_{26}\text{BrN}_2\text{O}_6]^+$ ($\text{M}+\text{H}^+$) requires m/z 529.0969, found 529.0967.

2.6.5 Racemic [2+2] Photocycloaddition Reaction

General Procedure for Racemic [2+2] Cycloadditions: An oven dried Schlenk tube was charged with the 1-methylimidazolyl enone (0.10 mmol, 1.0 equiv), styrene (1.0 mmol, 10.0 equiv.), (\pm)-**2.4** (0.02 mmol, 0.2 equiv.), and 2 mL toluene. The Schlenk was sealed with a glass stopper and degassed *via* freeze-pump-thaw technique (3 x 5 min). This was then cooled to -78 °C and irradiated with a Kessil Lamp (H150) for 14 h. The reaction mixture was then diluted 2–3x with CH_2Cl_2 before addition of 2 mL sat. aq. NaHCO_3 . The mixture was vigorously stirred for 60 s, the organic layer separated, and the aqueous layer extracted with CH_2Cl_2 (2 x 4 mL). The combined organics were dried over Na_2SO_4 , concentrated, and analyzed by ^1H NMR vs. internal standard

(phenanthrene) to determine conversion and diastereomeric ratio. The crude mixture was then purified *via* flash column chromatography using Et₂O/pentanes as the eluent.

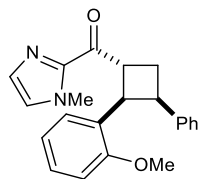
2-(4-Methoxyphenyl)-3-phenylcyclobutyl(1-methyl-1H-imidazol-2-yl)methanone ((±)-2.5):



Prepared according to the general procedure for racemic experiments using 24.2 mg (0.10 mmol) (*E*)-3-(4-methoxyphenyl)-1-(1-methyl-1H-imidazol-2-yl)prop-2-en-1-one, 0.11 mL (1.0 mmol) styrene, 15.7 mg (0.02 mmol) (±)-2.4,

and 2 mL toluene. The resulting material was purified by flash column chromatography using a gradient of 1:2 to 1:1 Et₂O/pentanes to give a 65% NMR yield of two diastereomers (3:1 d.r.). Spectroscopic data were consistent with those reported above.

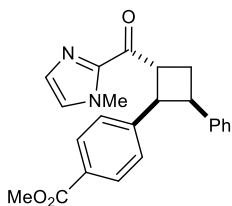
2-(2-Methoxyphenyl)-3-phenylcyclobutyl(1-methyl-1H-imidazol-2-yl)methanone ((±)-2.6):



Prepared according to the general procedure for racemic experiments using 23.3 mg (0.10 mmol) (*E*)-3-(2-methoxyphenyl)-1-(1-methyl-1H-imidazol-2-yl)prop-2-en-1-one, 0.11 mL (1.0 mmol) styrene, 15.6 mg (0.02 mmol) (±)-2.4, and 2

mL toluene. The resulting material was purified by flash column chromatography using a gradient of 1:2 to 1:1 Et₂O/pentanes to give a 64% NMR yield of two diastereomers (6:1 d.r.). Spectroscopic data were consistent with those reported above.

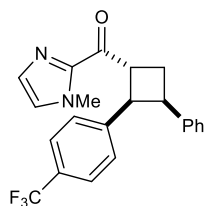
Methyl 4-(2-(1-methyl-1H-imidazole-2-carbonyl)-4-phenylcyclobutyl)benzoate ((±)-2.7):



Prepared according to the general procedure for racemic experiments using 21.6 mg (0.10 mmol) 2-cinnamoyl-1-methylimidazole, 0.13 mL (1.0 mmol) phenyl vinyl sulfide, 30.1 mg (0.02 mmol) (±)-2.4, and 2 mL toluene. The

resulting material was purified by flash column chromatography using a 1:1 to 3:1 Et₂O/pentanes to give 7.9 mg (0.03 mmol, 29% yield) of two diastereomers (3:1 d.r.). Spectroscopic data were consistent with those reported above.

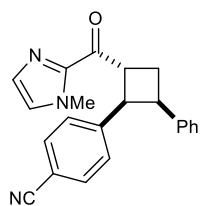
(1-Methyl-1H-imidazol-2-yl)(3-phenyl-2-(4-(trifluoromethyl)phenyl)cyclobutyl)methanone



((±)-2.8): Prepared according to the general procedure for racemic experiments using 28.0 mg (0.10 mmol) (*E*)-1-(1-methyl-1*H*-imidazol-2-yl)-3-(4-trifluoromethylphenyl)prop-2-en-1-one, 0.12 mL (1.0 mmol) styrene, 15.9 mg

(0.02 mmol) BINOL-phosphoramidate catalyst **(±)-2.4**, and 2 mL toluene. The resulting material was purified by flash column chromatography using a gradient of 1:3 to 1:1 Et₂O/pentanes to give 23.5 mg (0.07 mmol, 70% yield) of two diastereomers (2:1 d.r.). Spectroscopic data were consistent with those reported above.

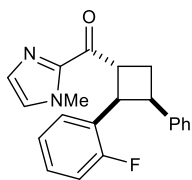
4-(2-(1-Methyl-1H-imidazole-2-carbonyl)-4-phenylcyclobutyl)benzotrile **((±)-2.9):**



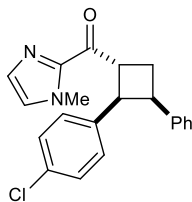
Prepared according to the general procedure for racemic experiments using 24.1 mg (0.10 mmol) (*E*)-4-(3-(1-methyl-1*H*-imidazol-2-yl)-3-oxoprop-1-en-1-yl)benzotrile, 0.11 mL (1.0 mmol) styrene, 15.3 mg (0.02 mmol) **(±)-2.4**, and

2 mL toluene. The resulting material was purified by flash column chromatography using a gradient of 1:1 to 2:1 Et₂O/pentanes to give a 30% NMR yield of three diastereomers (5:1 d.r.).

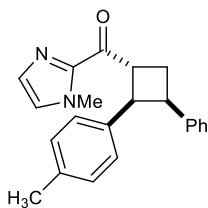
Spectroscopic data were consistent with those reported above.

2-(2-Fluorophenyl)-3-phenylcyclobutyl(1-methyl-1H-imidazol-2-yl)methanone ((±)-2.10):

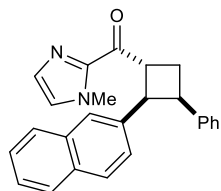
Prepared according to the general procedure for racemic experiments using 23.8 mg (0.10 mmol) (*E*)-3-(2-fluorophenyl)-1-(1-methyl-1H-imidazol-2-yl)prop-2-en-1-one, 0.11 mL (1.0 mmol) styrene, 15.8 mg (0.02 mmol) (±)-**2.4**, and 2 mL toluene. The resulting material was purified by flash column chromatography using a gradient of 1:2 to 1:1 Et₂O/pentanes to give a 59% NMR yield of two diastereomers (10:1 d.r.). Spectroscopic data were consistent with those reported above.

2-(4-Chlorophenyl)-3-phenylcyclobutyl(1-methyl-1H-imidazol-2-yl)methanone ((±)-2.11):

Prepared according to the general procedure for racemic experiments using 24.1 mg (0.10 mmol) (*E*)-3-(4-chlorophenyl)-1-(1-methyl-1H-imidazol-2-yl)prop-2-en-1-one, 0.11 mL (1.0 mmol) styrene, 15.3 mg (0.02 mmol) (±)-**2.4**, and 2 mL toluene. The resulting material was purified by flash column chromatography using a gradient of 1:2 to 1:1 Et₂O/pentanes to give a 75% NMR yield of three diastereomers (5:1 d.r.). Spectroscopic data were consistent with those reported above.

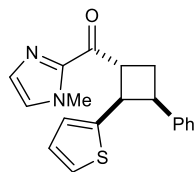
(1-Methyl-1H-imidazol-2-yl)(3-phenyl-2-(p-tolyl)cyclobutyl)methanone ((±)-2.12):

Prepared according to the general procedure for racemic experiments using 22.6 mg (0.10 mmol) (*E*)-1-(1-methyl-1H-imidazol-2-yl)-3-(p-tolyl)prop-2-en-1-one, 0.11 mL (1.0 mmol) styrene, 14.9 mg (0.02 mmol) (±)-**2.4**, and 2 mL toluene. The resulting material was purified by flash column chromatography using a gradient of 1:2 to 1:1 Et₂O/pentanes to give a 67% NMR yield of three diastereomers (3:1 d.r.). Spectroscopic data were consistent with those reported above.

(1-Methyl-1H-imidazol-2-yl)(2-(naphthalen-2-yl)-3-phenylcyclobutyl)methanone ((±)-2.13):

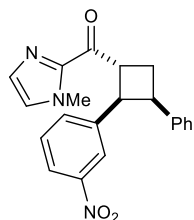
Prepared according to the general procedure for racemic experiments using 26.6 mg (0.10 mmol) (*E*)-1-(1-methyl-1H-imidazol-2-yl)-3-(naphthalen-2-yl)prop-2-en-1-one, 0.11 mL (1.0 mmol) styrene, 15.0 mg (0.02 mmol) (±)-

2.4, and 2 mL toluene. The resulting material was purified by flash column chromatography using a gradient of 1:2 to 1:1 Et₂O/pentanes to give a 59% NMR yield of two diastereomers (3:1 d.r.). Spectroscopic data were consistent with those reported above.

(1-Methyl-1H-imidazol-2-yl)(3-phenyl-2-(thiophen-2-yl)cyclobutyl)methanone ((±)-2.14):

Prepared according to the general procedure for racemic experiments using 21.2 mg (0.10 mmol) (*E*)-1-(1-methyl-1H-imidazol-2-yl)-3-(thiophen-2-yl)prop-2-en-1-one, 0.11 mL (1.0 mmol) styrene, 15.0 mg (0.02 mmol) (±)-**2.4**, and 2 mL

toluene. The resulting material was purified by flash column chromatography using a gradient of 1:2 to 1:1 Et₂O/pentanes to give a 52% yield of two diastereomers (3:1 d.r.). Spectroscopic data were consistent with those reported above.

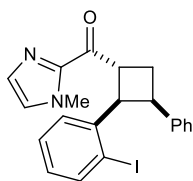
(1-Methyl-1H-imidazol-2-yl)(2-(3-nitrophenyl)-3-phenylcyclobutyl)methanone ((±)-2.15):

Prepared according to the general procedure for racemic experiments using 26.2 mg (0.10 mmol) (*E*)-1-(1-methyl-1H-imidazol-2-yl)-3-(3-nitrophenyl)prop-2-en-1-one, 0.11 mL (1.0 mmol) styrene, 15.8 mg (0.02 mmol) (±)-**2.4**, and 2 mL

toluene. The resulting material was purified by flash column chromatography using a gradient of

1:1 to 2:1 Et₂O/pentanes to give a 33% NMR yield of two diastereomers (3:1 d.r.). Spectroscopic data were consistent with those reported above.

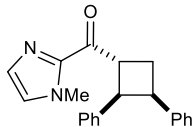
2-(2-Iodophenyl)-3-phenylcyclobutyl(1-methyl-1H-imidazol-2-yl)methanone ((±)-2.16):



Prepared according to the general procedure for racemic experiments using 33.5 mg (0.10 mmol) (*E*)-3-(2-iodophenyl)-1-(1-methyl-1H-imidazol-2-yl)prop-2-en-1-one, 0.11 mL (1.0 mmol) styrene, 15.0 mg (0.02 mmol) (±)-**2.4**, and 2 mL

toluene. The resulting material was purified by flash column chromatography using a gradient of 1:2 to 1:1 Et₂O/pentanes to give a 49% NMR yield of two diastereomers (10:1 d.r.). Spectroscopic data were consistent with those reported above.

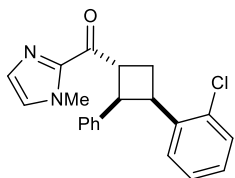
(2,3-Diphenylcyclobutyl)(1-methyl-1H-imidazol-2-yl)methanone ((±)-2.17): Prepared



according to the general procedure for racemic experiments using 22.4 mg (0.11 mmol) 2-cinnamoyl-1-methylimidazole, 0.12 mL (1.0 mmol) styrene, 16.4 mg

(0.02 mmol) BINOL-phosphoramidate catalyst (±)-**2.4**, and 2 mL toluene. The resulting material was purified by flash column chromatography using a gradient of 1:2 to 1:1 Et₂O/pentanes to give 23.5 mg (0.07 mmol, 70% yield) of two diastereomers (7:1 d.r.). Spectroscopic data were consistent with those reported above.

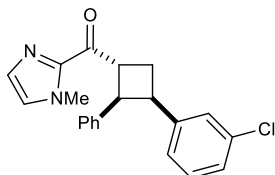
(3-(2-Chlorophenyl)-2-phenylcyclobutyl)(1-methyl-1H-imidazol-2-yl)methanone ((±)-2.18):



Prepared according to the general procedure for racemic experiments using 22.2 mg (0.10 mmol) 2-cinnamoyl-1-methylimidazole, 0.13 mL (1.0 mmol) 2-chlorostyrene, 16.5 mg (0.02 mmol) (±)-**2.4**, and 2 mL toluene. The

resulting material was purified by flash column chromatography using a 1:1 Et₂O/pentanes to give 19.7 mg (0.06 mmol, 54% yield) of two diastereomers (10:1 d.r.). Spectroscopic data were consistent with those reported above.

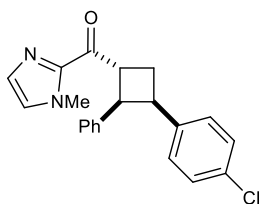
(3-(3-Chlorophenyl)-2-phenylcyclobutyl)(1-methyl-1H-imidazol-2-yl)methanone ((±)-2.19):



Prepared according to the general procedure for racemic experiments using 21.3 mg (0.10 mmol) 2-cinnamoyl-1-methylimidazole, 0.13 mL (1.0 mmol) 3-chlorostyrene, 15.6 mg (0.02 mmol) (±)-2.4, and 2 mL toluene.

The resulting material was purified by flash column chromatography using a 1:1 Et₂O/pentanes to give a 61% NMR yield of two diastereomers (4:1 d.r.). Spectroscopic data were consistent with those reported above.

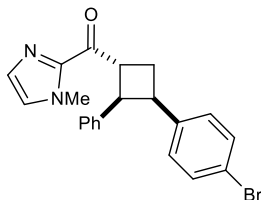
(3-(4-Chlorophenyl)-2-phenylcyclobutyl)(1-methyl-1H-imidazol-2-yl)methanone ((±)-2.20):



Prepared according to the general procedure for racemic experiments using 21.2 mg (0.10 mmol) 2-cinnamoyl-1-methylimidazole, 0.12 mL (1.0 mmol) 4-chlorostyrene, 15.3 mg (0.02 mmol) (±)-2.4, and 2 mL toluene. The

resulting material was purified by flash column chromatography using a 1:1 Et₂O/pentanes to give 26.7 mg (0.08 mmol, 76% yield) of two diastereomers (6:1 d.r.). Spectroscopic data were consistent with those reported above.

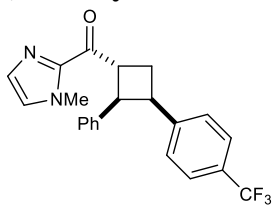
(3-(4-Bromophenyl)-2-phenylcyclobutyl)(1-methyl-1H-imidazol-2-yl)methanone ((±)-2.21):



Prepared according to the general procedure for racemic experiments using 21.2 mg (0.10 mmol) 2-cinnamoyl-1-methylimidazole, 0.13 mL (1.0 mmol)

4-bromostyrene, 15.4 mg (0.02 mmol) (\pm)-**2.4**, and 2 mL toluene. The resulting material was purified by flash column chromatography eluting from a gradient of 1:2 Et₂O/pentanes \rightarrow 1:1 Et₂O/pentanes to give 3.4 mg (0.01 mmol, 9% yield) of two diastereomers (6:1 d.r.). Spectroscopic data were consistent with those reported above.

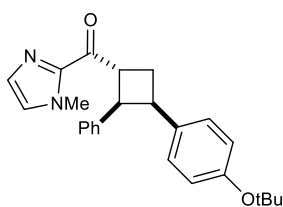
(1-Methyl-1H-imidazol-2-yl)(2-phenyl-3-(4-(trifluoromethyl)phenyl)cyclobutyl)methanone



((\pm)-**2.22**): Prepared according to the general procedure for racemic experiments using 21.7 mg (0.10 mmol) 2-cinnamoyl-1-methylimidazole, 0.15 mL (1.0 mmol) 4-(trifluoromethyl)styrene, 16.1 mg (0.02 mmol) (\pm)-

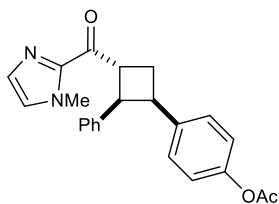
2.4, and 2 mL toluene. The resulting material was purified by flash column chromatography eluting from a gradient of 1:2 Et₂O/pentanes \rightarrow 1:1 Et₂O/pentanes to give 33.6 mg (0.09 mmol, 85% yield) of two diastereomers (5:1 d.r.). Spectroscopic data were consistent with those reported above.

(3-(4-tert-Butoxyphenyl)-2-phenylcyclobutyl)(1-methyl-1H-imidazol-2-yl)methanone ((\pm)-



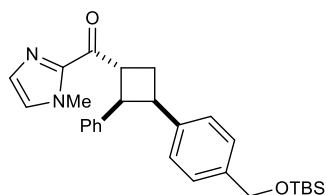
2.23): Prepared according to the general procedure for racemic experiments using 22.2 mg (0.10 mmol) 2-cinnamoyl-1-methylimidazole, 0.19 mL (1.0 mmol) 4-tert-butoxystyrene, 16.0 mg (0.02 mmol) (\pm)-**2.4**,

and 2 mL toluene. The resulting material was purified by flash column chromatography using a 1:1 Et₂O/pentanes to give 28.0 mg (0.07 mmol, 69% yield) of two diastereomers (4:1 d.r.). Spectroscopic data were consistent with those reported above.

(3-(4-Acetoxyphenyl)-2-phenylcyclobutyl)(1-methyl-1H-imidazol-2-yl)methanone ((±)-2.24):

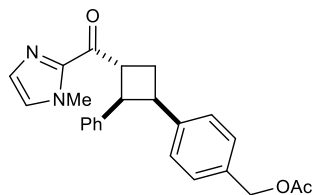
Prepared according to the general procedure for racemic experiments using 21.1 mg (0.10 mmol) 2-cinnamoyl-1-methylimidazole, 0.15 mL (1.0 mmol) 4-acetoxystyrene, 16.0 mg (0.02 mmol) (±)-**2.4**, and 2 mL toluene.

The resulting material was purified by flash column chromatography using a 1:1 Et₂O/pentanes to give 22.6 mg (0.06 mmol, 61% yield) of two diastereomers (8:1 d.r.). Spectroscopic data were consistent with those reported above.

3-(4-(((*tert*-Butyldimethylsilyloxy)methyl)phenyl)-2-phenylcyclobutyl)(1-methyl-1H-

imidazol-2-yl)methanone ((±)-2.25): Prepared according to the general procedure for racemic experiments using 20.6 mg (0.10 mmol) 2-cinnamoyl-1-methylimidazole, 247.9 mg (1.0 mmol) *tert*-

butyldimethyl(4-vinylbenzyloxy) silane, 15.4 mg (0.02 mmol) (±)-**2.4**, and 2 mL toluene. The resulting material was purified by flash column chromatography eluting from a gradient of 1:2 Et₂O/pentanes → 1:1 Et₂O/pentanes to give 40.0 mg (0.09 mmol, 89% yield) of three diastereomers (3:1 d.r.). Spectroscopic data were consistent with those reported above.

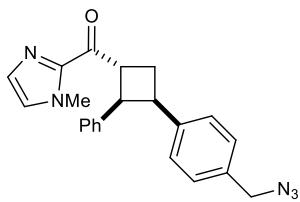
(3-(4-(Acetoxymethyl)phenyl)-2-phenylcyclobutyl)(1-methyl-1H-imidazol-2-yl)methanone

((±)-2.26): Prepared according to the general procedure for racemic experiments using 21.3 mg (0.10 mmol) 2-cinnamoyl-1-methylimidazole, 180.0 mg (1.0 mmol) 1-(acetoxymethyl)-4-

vinylbenzene, 16.0 mg (0.02 mmol) (±)-**2.4**, and 2 mL toluene. The resulting material was purified by flash column chromatography eluting from a gradient of 1:2 Et₂O/pentanes → 1:1

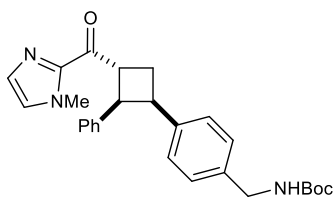
Et₂O/pentanes to give a 70% NMR yield of three diastereomers (3:1 d.r.). Spectroscopic data were consistent with those reported above.

(3-(4-(Azidomethyl)phenyl)-2-phenylcyclobutyl)(1-methyl-1H-imidazol-2-yl)methanone



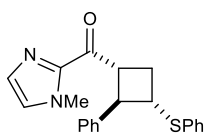
((±)-2.27): Prepared according to the general procedure for racemic experiments using 20.5 mg (0.10 mmol) 2-cinnamoyl-1-methylimidazole, 158.0 mg (1.0 mmol) 1-(azidomethyl)-4-vinylbenzene, 15.3 mg (0.02 mmol) **(±)-2.4**, and 2 mL toluene. The resulting material was purified eluting from a gradient of 1:2 Et₂O/pentanes → 1:1 Et₂O/pentanes to give a 57% NMR yield of three diastereomers (3:1 d.r.). Spectroscopic data were consistent with those reported above.

***tert*-Butyl(4-(-3-(1-methyl-1H-imidazole-2-carbonyl)-2-phenylcyclobutyl)benzyl) carbamate**



((±)-2.28): Prepared according to the general procedure for racemic experiments using 21.4 mg (0.10 mmol) 2-cinnamoyl-1-methylimidazole, 233 mg (1.0 mmol) *tert*-butyl 4-vinylbenzylcarbamate, 15.0 mg (0.02 mmol) **(±)-2.4**, and 2 mL toluene. The resulting material was purified by flash column chromatography eluting from a gradient of 30% EtOAc/hexanes → 50% EtOAc/hexanes to give 27.4 mg (0.06 mmol, 61% yield) of three diastereomers (3:1 d.r.). Spectroscopic data were consistent with those reported above.

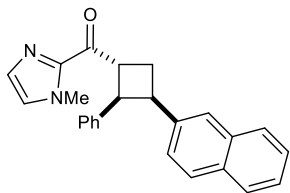
(1-Methyl-1H-imidazol-2-yl)(2-phenyl-3-(phenylthio)cyclobutyl)methanone **((±)-2.29):**



Prepared according to the general procedure for racemic experiments using 21.6 mg (0.10 mmol) 2-cinnamoyl-1-methylimidazole, 0.13 mL (1.0 mmol) phenyl

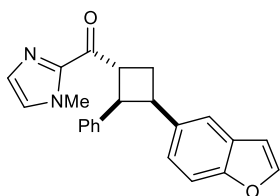
vinyl sulfide, 30.1 mg (0.02 mmol) (\pm)-**2.4**, and 2 mL toluene. The resulting material was purified by flash column chromatography using a 1:1 Et₂O/pentanes to give 7.9 mg (0.03 mmol, 29% yield) of two diastereomers (1.3:1 d.r.). Spectroscopic data were consistent with those reported above.

(1-Methyl-1H-imidazol-2-yl)(3-(naphthalen-2-yl)-2-phenylcyclobutyl)methanone ((\pm)-2.30**):**



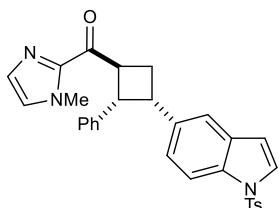
Prepared according to the general procedure for racemic experiments using 22.0 mg (0.10 mmol) 2-cinnamoyl-1-methylimidazole, 150.4 mg (1.0 mmol) 2-vinylnaphthalene, 15.0 mg (0.02 mmol) (\pm)-**2.4**, and 2 mL toluene. The resulting material was purified by flash column chromatography eluting from a gradient of 1:2 Et₂O/hexanes \rightarrow 1:1 Et₂O/hexanes to give 33.1 mg (0.09 mmol, 87% yield) of three diastereomers (2:1 d.r.). Spectroscopic data were consistent with those reported above.

(3-(Benzofuran-5-yl)-2-phenylcyclobutyl)(1-methyl-1H-imidazol-2-yl)methanone ((\pm)-2.31**):**



Prepared according to the general procedure for racemic experiments using 20.7 mg (0.10 mmol) 2-cinnamoyl-1-methylimidazole, 142.0 mg (1.0 mmol) 5-vinyl-1-benzofuran, 15.4 mg (0.02 mmol) (\pm)-**2.4**, and 2 mL toluene. The resulting material was purified by flash column chromatography eluting from a gradient of 1:2 Et₂O/pentanes \rightarrow 1:1 Et₂O/pentanes to give 30.2 mg (0.09 mmol, 87% yield) of three diastereomers (4:1 d.r.). Spectroscopic data were consistent with those reported above.

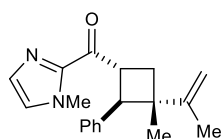
(1-Methyl-1H-imidazol-2-yl)((1S,2S,3S)-2-phenyl-3-(1-tosyl-1H-indol-5-



yl)cyclobutyl)methanone ((\pm)-2.32**):** Prepared according to the general procedure for racemic experiments using 21.4 mg (0.10 mmol) 2-

cinnamoyl-1-methylimidazole, 295.1 mg (1.0 mmol) 1-toluenesulfonyl-5-vinyl-1H-indole, 15.6 mg (0.02 mmol) (\pm)-**2.4**, and 2 mL toluene. The resulting material was purified by flash column chromatography eluting from 20% acetone/pentanes to give an 80% NMR yield of three diastereomers (4:1 d.r.). Spectroscopic data were consistent with those reported above.

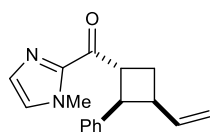
(1-Methyl-1H-imidazol-2-yl)(3-methyl-2-phenyl-3-(prop-1-en-2-yl)cyclobutyl)methanone



(\pm)-**2.33**: Prepared according to the general procedure for racemic experiments using 22.0 mg (0.10 mmol) 2-cinnamoyl-1-methylimidazole, 0.11

mL (1.0 mmol) 2,3-dimethylbutadiene, 15.8 mg (0.02 mmol) (\pm)-**2.4**, and 2 mL toluene. The resulting material was purified by flash column chromatography using a gradient of 1:2 to 1:1 Et₂O/pentanes to give 17.7 mg (0.06 mmol, 57% yield) of two diastereomers (10:1 d.r.). Spectroscopic data were consistent with those reported above.

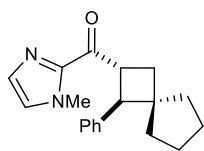
(3-Ethenyl-2-phenylcyclobutyl)(1-methyl-1H-imidazol-2-yl)methanone (\pm)-**2.34**: Prepared



according to the general procedure for racemic experiments using 21.1 mg (0.10 mmol) 2-cinnamoyl-1-methylimidazole, 0.55 mL (1.0 mmol) 1,3-butadiene

(15% in toluene), 15.8 mg (0.02 mmol) (\pm)-**2.4**, and 2 mL toluene. The resulting material was purified by flash column chromatography using a gradient of 1:2 to 1:1 Et₂O/pentanes to give 17.0 mg (0.06 mmol, 64% yield) of two diastereomers (3:1 d.r.). Spectroscopic data were consistent with those reported above.

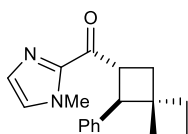
(1-Methyl-1H-imidazol-2-yl)(1-phenylspiro[3.4]octan-2-yl)methanone ((±)-2.37): Prepared



according to the general procedure for racemic experiments using 21.6 mg (0.10 mmol) 2-cinnamoyl-1-methylimidazole, 0.08 mL (1.0 mmol)

methylenecyclopentane, 30.7 mg (0.04 mmol) (±)-2.4, and 2 mL toluene. The resulting material was purified by flash column chromatography using a gradient of 1:2 to 1:1 Et₂O/pentanes to give 14.2 mg (0.05 mmol, 47% yield) of two diastereomers (6:1 d.r.). Spectroscopic data were consistent with those reported above.

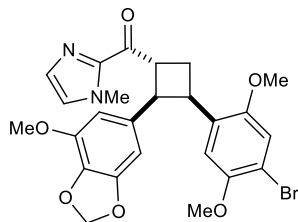
(1-Methyl-1H-imidazol-2-yl)(1-phenylspiro[3.3]heptan-2-yl)methanone ((±)-2.38): Prepared



according to the general procedure for racemic experiments using 22.4 mg (0.11 mmol) 2-cinnamoyl-1-methylimidazole, 0.10 mL (1.0 mmol)

methylenecyclobutane, 34.0 mg (0.04 mmol) (±)-2.4, and 2 mL toluene. The resulting material was purified by flash column chromatography using a 1:1 Et₂O/pentanes to give 11.0 mg (0.04 mmol, 37% yield) of a single diastereomer. Spectroscopic data were consistent with those reported above.

(3-(4-Bromo-2,5-dimethoxyphenyl)-2-(7-methoxy-2H-1,3-benzodioxol-5-yl)cyclobutyl)(1-



methyl-1H-imidazol-2-yl)methanone ((±)-2.39) Prepared according to

the general procedure for racemic experiments using 142.8 mg (0.50 mmol) (*E*)-3-(7-methoxybenzo[d][1,3]dioxol-5-yl)-1-(1-methyl-1H-

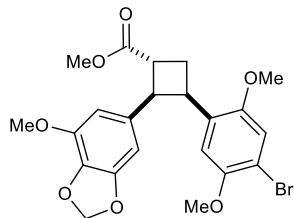
imidazol-2-yl)prop-2-en-1-one, 244.1 mg (1.0 mmol) 4-bromo-2,5-

methoxystyrene, 78.0 mg (0.10 mmol) (±)-2.4, and 10 mL CH₂Cl₂. The resulting material was purified by flash column chromatography with 50% → 100% EtOAc in pentanes to give 137.0 mg

(0.26 mmol, 52% yield) of two diastereomers (5:1 d.r., separated under these conditions). Spectroscopic data were consistent with those reported above.

2.6.6 Cleavage Reactions of Complex Cycloadduct

Methyl 3-(4-bromo-2,5-dimethoxyphenyl)-2-(7-methoxy-2H-1,3-benzodioxol-5-yl)cyclobutane-1-carboxylate (2.40) A flame-dried 6 mL vial with a stir



bar was charged with 100.5 mg (0.19 mmol, 1.0 equiv.) of the major diastereomer of cycloadduct **2.39** and 1.5 mL dry CH₂Cl₂, and the solution stirred under N₂ for 10 min. To this was added 30 μL (0.25 mmol,

1.3 equiv.) freshly distilled MeOTf, and the reaction mixture stirred for 3 h at room temperature.

This solution was then concentrated *in vacuo* and dried under vacuum for 30 min to remove any remaining MeOTf. The resulting yellow foam was then taken up in 1.5 mL dry CH₂Cl₂, to which

was added 0.32 mL (8.0 mmol, 40.0 equiv.) distilled MeOH and 4.5 mg (0.04 mmol, 0.2 equiv.)

1,4-diazabicyclo[2.2.2]octane (DABCO), and the reaction mixture stirred for 3 h at room temperature. The reaction mixture was concentrated and purified by flash column chromatography

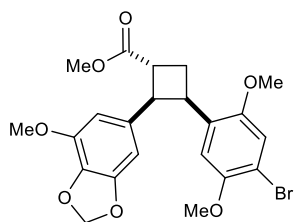
with 10% to 50% EtOAc/pentanes to give 63.4 mg (0.13 mmol, 70% yield) of a viscous semisolid.

92% ee [Daicel CHIRALPAK AD, 5% to 50% iPrOH, 20 minutes, 1 mL/min, t₁=9.30 min, t₂=10.73 min] [α]_D²² -64.2° (c1.090, CH₂Cl₂). ¹H NMR (500 MHz, CDCl₃) δ 6.79 (s, 1H), 6.76

(s, 1H), 6.19 (d, *J* = 1.1 Hz, 1H), 6.01 (d, *J* = 1.1 Hz, 1H), 5.86–5.85 (m, 2H), 4.19 (td, *J* = Hz, 1H), 4.13 (t, *J* = 8.8 Hz, 1H), 3.81 (s, 3H), 3.73 (s, 3H), 3.68 (s, 3H), 3.49 (s, 3H), 3.43 (q, *J* = 8.5

Hz, 1H), 2.72 (dt, *J* = 12.1, 8.5 Hz, 1H), 2.57–2.51 (m, 1H). ¹³C NMR (125 MHz, CDCl₃) δ 174.98, 152.04, 149.83, 148.18, 142.79, 134.38, 133.47, 129.21, 115.26, 112.33, 109.26, 106.87, 101.75,

101.16, 57.33, 56.32, 55.59, 51.98, 47.51, 41.52, 36.76, 25.53. HRMS (ESI) calculated for [C₂₂H₂₇BrNO₇]⁺ (M+NH₄⁺) requires *m/z* 496.0965, found 496.0965.

Methyl**3-(4-bromo-2,5-dimethoxyphenyl)-2-(7-methoxy-2*H*-1,3-benzodioxol-5-**

yl)cyclobutane-1-carboxylate ((±)-2.40) Racemic material prepared

according to the procedure above for the analogous enriched product (±)-

2.39 using 86.2 mg (0.16 mmol, 1.0 equiv.) (3-(4-bromo-2,5-dimethoxyphenyl)-2-(7-methoxy-2*H*-1,3-benzodioxol-5-yl)cyclobutyl)(1-methyl-1*H*-imidazol-2-yl)methanone and 25 μ L (0.20 mmol, 1.3 equiv.) MeOTf in 1 mL CH_2Cl_2 , and then 0.25 mL (6.0 mmol, 40.0 equiv.) MeOH, and 3.5 mg (0.3 mmol, 0.2 equiv.) DABCO in 1 mL CH_2Cl_2 . The resulting material was purified by flash column chromatography with 10% to 50% EtOAc in pentanes to give 12.0 mg (0.03 mmol, 15% yield) of two diastereomers (5:1 d.r., separated under these conditions). Spectroscopic data were consistent with those reported above.

2.6.7 Mechanistic Experiments

2.6.7.1 Absorbance Data

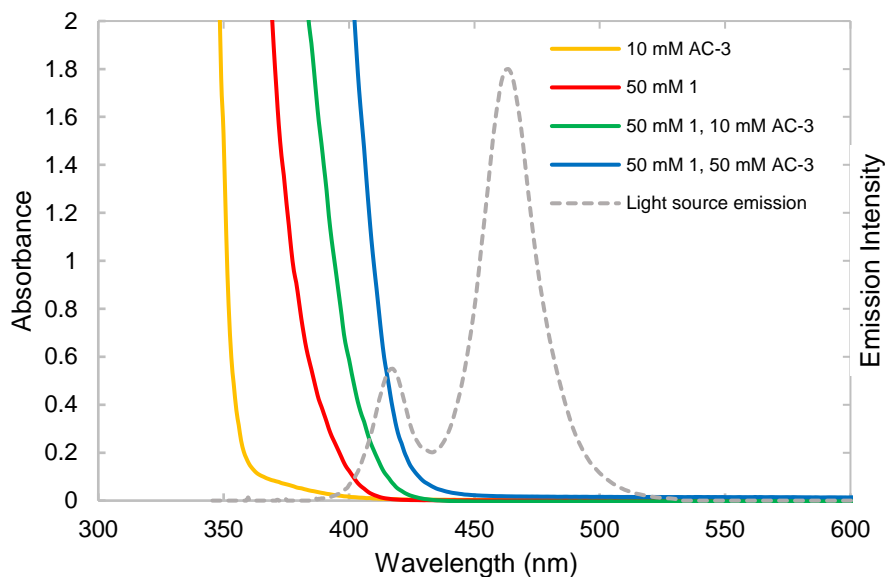
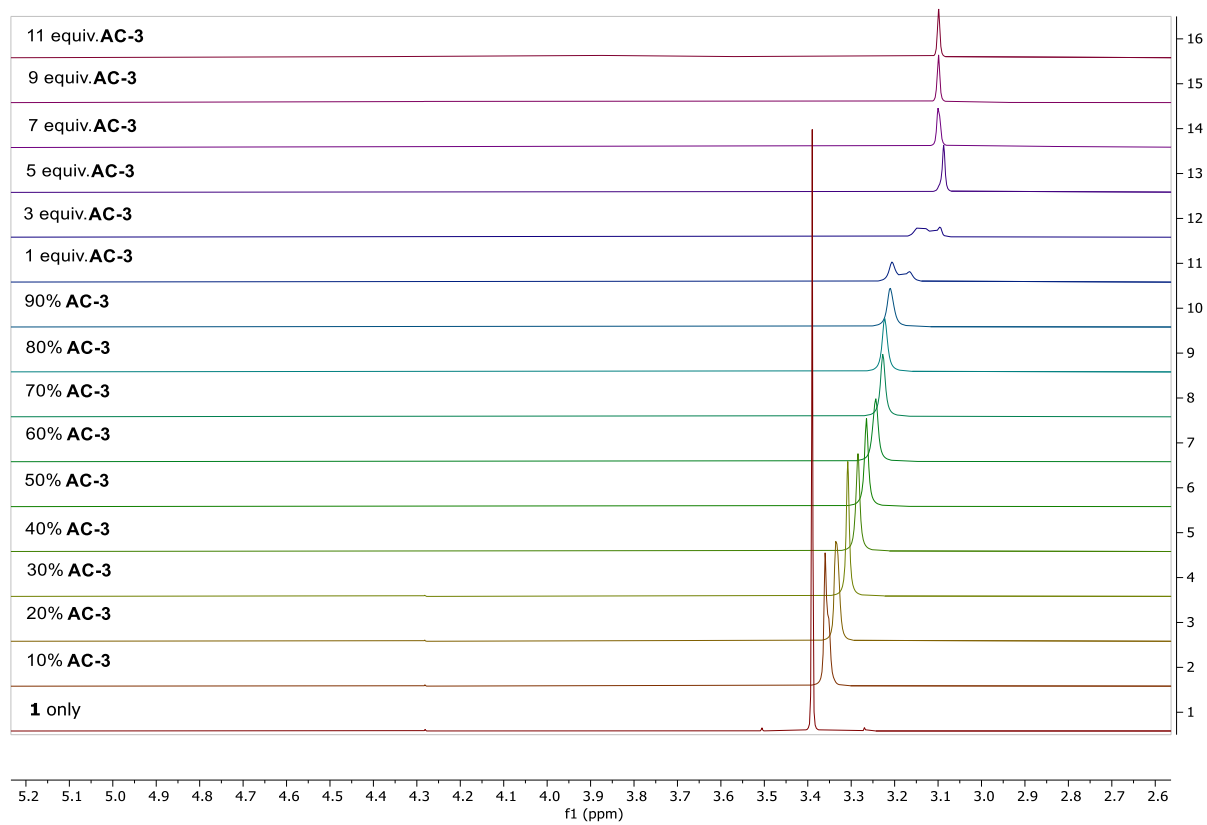


Figure 2.2 Comparative absorption spectra of the Brønsted acid catalyst (**AC-3=2.4**), substrate (**I=2.1**), and 20 and 100 mol% loading of acid catalyst in substrate dissolved in CH_2Cl_2 . The spectra were all recorded in quartz tubes under ambient conditions.

2.6.7.2 NMR Titration Experiments

Experimental Details: A stock solution of **2.4** (11.0 mg, 0.014 mmol) was prepared in *d*8-toluene (700 μL) and added to a solution of **2.1** (2.1 mg, 0.01 mmol) in *d*8-toluene (500 μL) in a 7" NMR tube in 50 μL increments. Then a more concentrated stock solution of **2.4** (94.6 mg, 0.12 mmol), prepared in *d*8-toluene (1.2 mL), was added to the same tube in 200 μL increments. ^1H NMR spectra were acquired on a 600 MHz instrument with a DCI-F cryoprobe. The titration was quantified by monitoring the chemical shift of the imidazole methyl protons (~ 3.4 ppm in **2.1** alone) of the substrate, which moved upfield with increasing **2.4**. When multiple peaks appeared, chemical shifts were averaged.



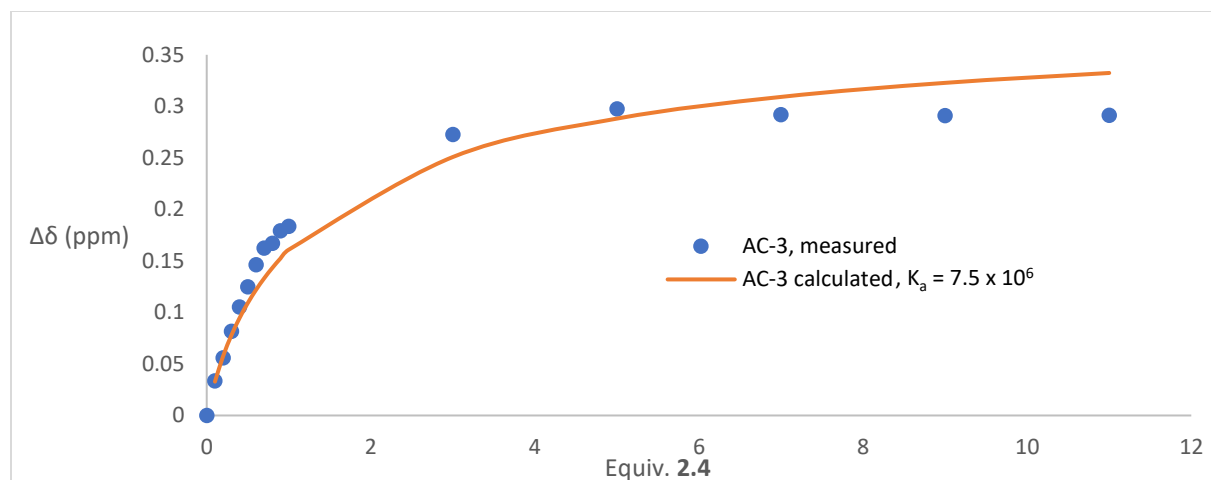


Figure 2.3 Preliminary binding isotherm, measured vs. calculated. Note: AC-3=2.4

These data were fit to a 1:1 binding model following the method developed by Thordarson.⁶⁹

Microsoft Excel was used to estimate K_a by minimizing difference between experiment and predicted chemical shifts using nonlinear regression analysis.

2.6.8 Assignment of Diastereomers by 1D-NOE

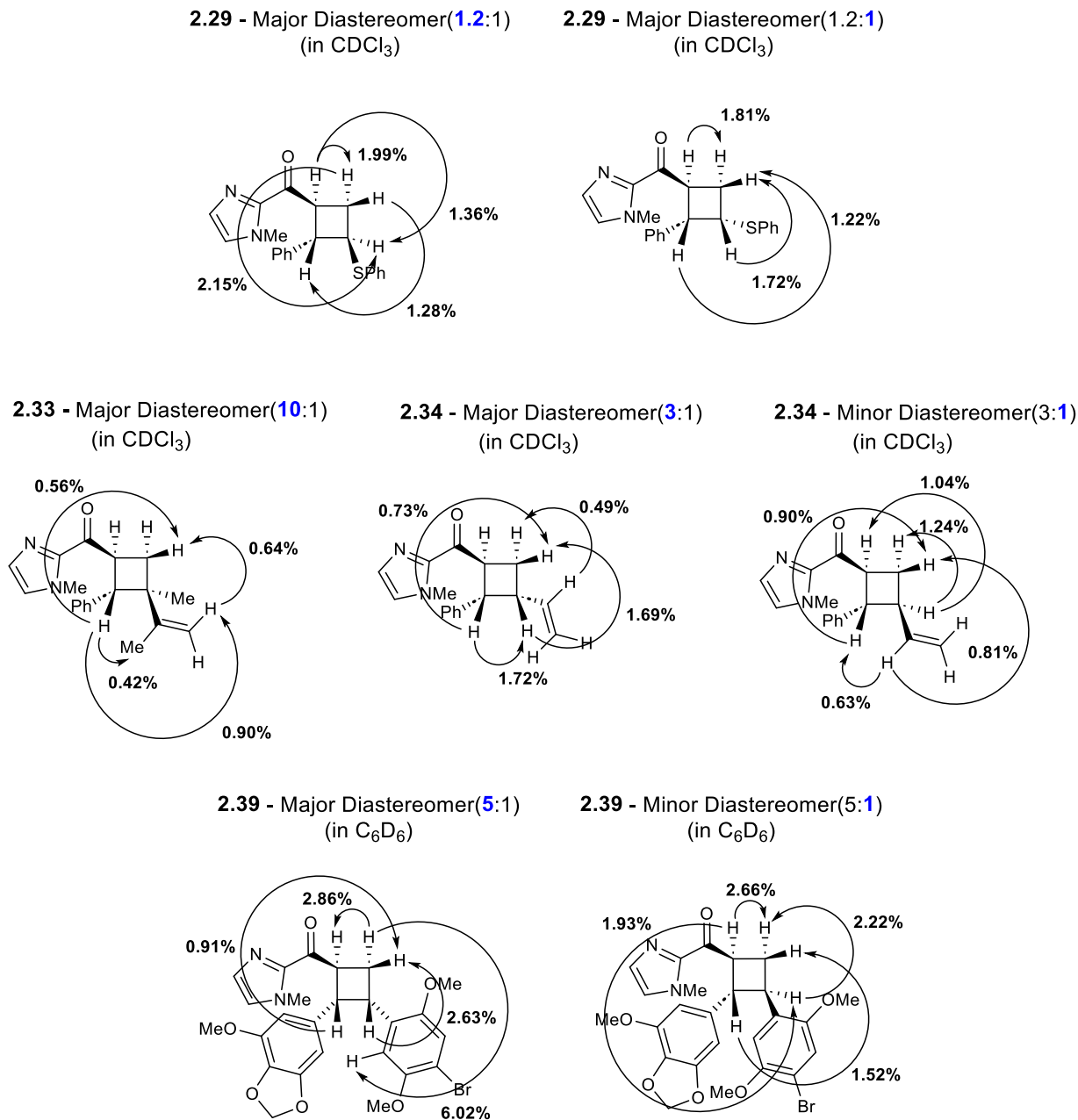
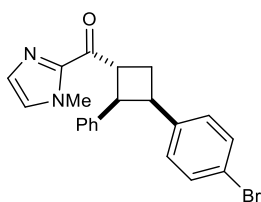


Figure 2.4 Observed *nOe* Enhancements

2.6.9 X-Ray Crystallographic Data

CCDC-2022776 and CCDC-2022777 contain full crystallographic data for the structures described in this manuscript. These data can be obtained free of charge from the Cambridge Crystallographic Data Centre.

((1R,2R,3R)-3-(4-Bromophenyl)-2-phenylcyclobutyl)(1-methyl-1H-imidazol-2-yl)methanone (2.21)



Data Collection: A colorless crystal with approximate dimensions $0.12 \times 0.08 \times 0.06 \text{ mm}^3$ was selected under oil under ambient conditions and attached to the tip of a MiTeGen MicroMount©. The crystal was mounted in a stream of cold nitrogen at 100(1) K and centered in the X-ray beam by using a video camera.

The crystal evaluation and data collection were performed on a Bruker D8 VENTURE PhotonIII four-circle diffractometer with Cu $K\alpha$ ($\lambda = 1.54178 \text{ \AA}$) radiation and the detector to crystal distance of 4.0 cm.⁷⁰

The initial cell constants were obtained from a $180^\circ \varphi$ scan conducted at a $2\theta = 50^\circ$ angle with the exposure time of 1 second per frame. The reflections were successfully indexed by an automated indexing routine built in the APEX3 program. The final cell constants were calculated from a set of 9313 strong reflections from the actual data collection.

The data were collected by using the full sphere data collection routine to survey the reciprocal space to the extent of a full sphere to a resolution of 0.80 Å. A total of 67343 data were harvested by collecting 34 sets of frames with 0.5° scans in ω and ϕ with an exposure time 0.5-8.3 sec per frame. These highly redundant datasets were corrected for Lorentz and polarization effects. The absorption correction was based on fitting a function to the empirical transmission surface as sampled by multiple equivalent measurements.⁷¹

Structure Solution and Refinement: The systematic absences in the diffraction data were uniquely consistent for the space group $P2_12_12_1$ that yielded chemically reasonable and computationally stable results of refinement.⁷²⁻⁷⁷

A successful solution by the direct methods provided most non-hydrogen atoms from the E -map. The remaining non-hydrogen atoms were located in an alternating series of least-squares cycles and difference Fourier maps. All non-hydrogen atoms were refined with anisotropic displacement coefficients. All hydrogen atoms were included in the structure factor calculation at idealized positions and were allowed to ride on the neighboring atoms with relative isotropic displacement coefficients.

The absolute configuration was established based on resonant scattering effects: the three chiral centers C7, C8, C15 are all R . The crystal may contain 1.4(17) % of the opposite enantiomer.

The final least-squares refinement of 228 parameters against 3859 data resulted in residuals R (based on F^2 for $I \geq 2\sigma$) and wR (based on F^2 for all data) of 0.0192 and 0.0505, respectively. The final difference Fourier map was featureless.

Summary

Crystal Data for $C_{21}H_{19}BrN_2O$ ($M=395.29$ g/mol): orthorhombic, space group $P2_12_12_1$ (no. 19), $a = 8.1192(6)$ Å, $b = 10.5977(10)$ Å, $c = 20.6785(17)$ Å, $V = 1779.3(3)$ Å³, $Z = 4$, $T = 100.0$ K, $\mu(\text{CuK}\alpha) = 3.226$ mm⁻¹, $D_{\text{calc}} = 1.476$ g/cm³, 67343 reflections measured ($8.552^\circ \leq 2\theta \leq 159.016^\circ$), 3859 unique ($R_{\text{int}} = 0.0257$, $R_{\text{sigma}} = 0.0109$) which were used in all calculations. The final R_1 was 0.0192 ($I > 2\sigma(I)$) and wR_2 was 0.0505 (all data).

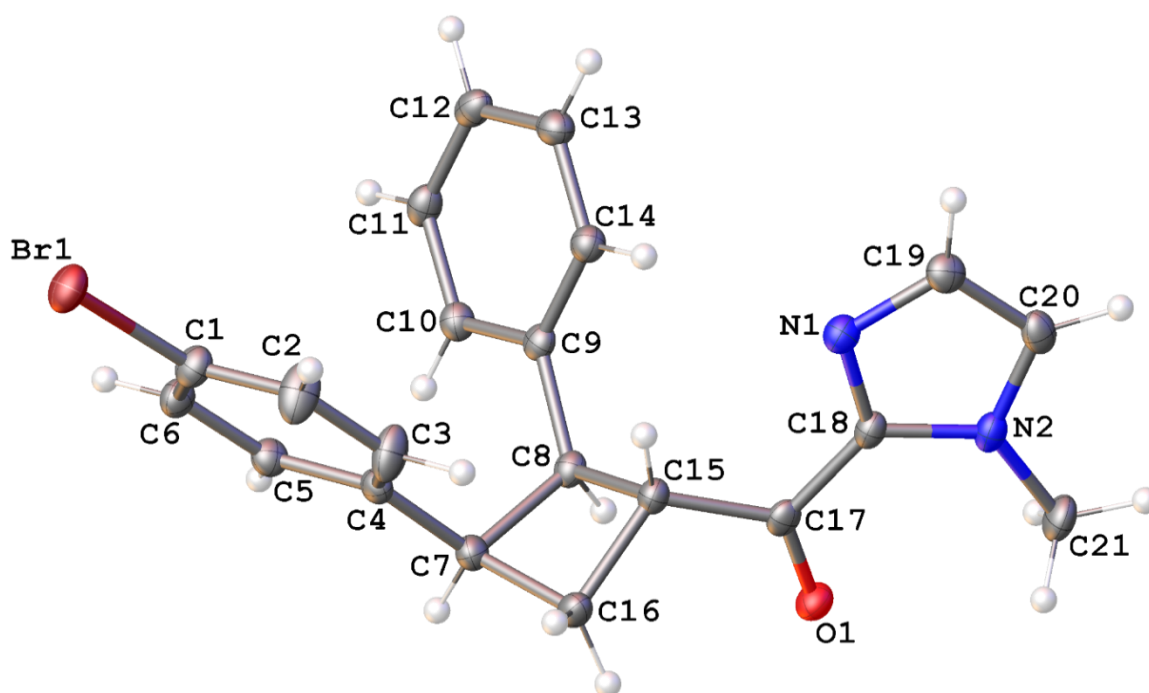


Figure 2.5 A molecular drawing of yoon61 shown with 50% probability ellipsoids

Table 2.1 Crystal data and structure refinement for yoon61

Identification code	yoon61
Empirical formula	$C_{21}H_{19}BrN_2O$
Formula weight	395.29

Temperature/K	100.0
Crystal system	orthorhombic
Space group	P2 ₁ 2 ₁ 2 ₁
a/Å	8.1192(6)
b/Å	10.5977(10)
c/Å	20.6785(17)
α/°	90
β/°	90
γ/°	90
Volume/Å ³	1779.3(3)
Z	4
ρ _{calc} /cm ³	1.476
μ/mm ⁻¹	3.226
F(000)	808.0
Crystal size/mm ³	0.12 × 0.08 × 0.06
Radiation	CuKα (λ = 1.54178)
2θ range for data collection/°	8.552 to 159.016
Index ranges	-10 ≤ h ≤ 10, -11 ≤ k ≤ 13, -26 ≤ l ≤ 25
Reflections collected	67343
Independent reflections	3859 [R _{int} = 0.0257, R _{sigma} = 0.0109]
Data/restraints/parameters	3859/0/228
Goodness-of-fit on F ²	1.049

Final R indexes [$I \geq 2\sigma(I)$] $R_1 = 0.0192$, $wR_2 = 0.0505$

Final R indexes [all data] $R_1 = 0.0192$, $wR_2 = 0.0505$

Largest diff. peak/hole / $e \text{ \AA}^{-3}$ 0.52/-0.41

Flack parameter 0.014(17)

Table 2.2 Fractional Atomic Coordinates ($\times 10^4$) and Equivalent Isotropic Displacement Parameters ($\text{\AA}^2 \times 10^3$) for yoon61. U_{eq} is defined as 1/3 of the trace of the orthogonalised U_{ij} tensor.

Atom	x	y	z	$U(eq)$
Br1	5073.7(3)	5024.5(2)	167.5(2)	24.31(7)
O1	3736.3(19)	-3544.1(13)	1740.6(7)	20.9(3)
N1	568(2)	-2460.4(16)	674.6(8)	18.2(3)
N2	691(2)	-4349.4(16)	1146.7(8)	18.0(3)
C1	5111(3)	3450.2(18)	611.7(9)	20.7(4)
C2	4851(4)	2351(2)	267.3(10)	31.0(5)
C3	4931(4)	1195.7(19)	588.0(10)	28.0(5)
C4	5247(2)	1129.8(18)	1248.8(9)	16.8(4)
C5	5489(2)	2258.5(19)	1580.6(9)	18.5(4)
C6	5429(3)	3422.8(19)	1270.3(10)	19.3(4)
C7	5354(2)	-98.1(19)	1616.4(9)	17.9(3)
C8	3642(2)	-624.0(18)	1859.3(9)	16.2(4)
C9	2248(2)	271.1(17)	1999.3(9)	15.9(4)
C10	2384(3)	1114.7(19)	2518.3(10)	18.2(4)
C11	1135(3)	1975.6(19)	2648.7(10)	19.5(4)

C12	-265(3)	2004.8(19)	2266.8(10)	20.9(4)
C13	-414(3)	1167.4(19)	1748.8(10)	21.0(4)
C14	833(2)	307.2(18)	1618.0(10)	18.4(4)
C15	3602(2)	-1508.8(18)	1253.4(10)	16.3(4)
C16	5504(3)	-1318.7(19)	1206.9(11)	19.7(4)
C17	3003(2)	-2835.5(18)	1377.4(9)	16.5(4)
C18	1456(2)	-3209.7(18)	1060.6(9)	16.4(4)
C19	-805(3)	-3132(2)	523.5(10)	20.5(4)
C20	-749(3)	-4301(2)	812.4(10)	20.6(4)
C21	1208(3)	-5428.5(19)	1537.1(11)	25.1(4)

Table 2.3 Anisotropic Displacement Parameters ($\text{\AA}^2 \times 10^3$) for yoon61. The Anisotropic displacement factor exponent takes the form: $-2\pi^2 [h^2 a^{*2} U_{11} + 2hka^* b^* U_{12} + \dots]$.

Atom	U_{11}	U_{22}	U_{33}	U_{23}	U_{13}	U_{12}
Br1	35.55(12)	17.60(11)	19.78(11)	4.01(7)	0.43(8)	-0.57(11)
O1	23.3(7)	16.5(7)	22.8(7)	2.7(5)	-2.6(6)	1.3(6)
N1	21.7(8)	17.3(8)	15.6(7)	0.1(6)	-0.3(6)	0.3(6)
N2	22.4(8)	13.9(8)	17.8(8)	-0.9(6)	3.4(6)	-1.5(7)
C1	25.9(10)	16.8(8)	19.5(9)	2.8(7)	1.8(9)	-0.1(8)
C2	54.4(15)	23.5(10)	15.1(8)	1.2(8)	-4.3(10)	-6.8(11)
C3	47.0(13)	18.0(9)	19.0(9)	-2.2(7)	-1.0(10)	-7.0(11)

C4	14.4(9)	16.8(8)	19.2(8)	1.5(7)	0.3(8)	-2.5(7)
C5	19.8(9)	19.7(9)	16.1(8)	-1.0(7)	-2.2(7)	-0.9(7)
C6	22.2(10)	16.2(9)	19.4(9)	-2.6(7)	-1.1(8)	-0.3(7)
C7	16.7(8)	16.3(8)	20.8(8)	-0.4(7)	-1.6(7)	-1.3(8)
C8	19.9(9)	13.6(8)	15.0(8)	1.4(7)	-1.2(7)	-0.9(8)
C9	18.9(9)	13.5(9)	15.4(8)	2.9(7)	1.7(7)	-1.0(7)
C10	20.0(9)	18.1(9)	16.7(9)	0.6(8)	-0.8(7)	-2.0(8)
C11	24.0(10)	16.4(9)	18.1(9)	-1.4(7)	5.7(8)	-1.2(8)
C12	21.3(10)	16.5(8)	24.8(9)	3.2(7)	6.8(8)	1.5(8)
C13	18.1(9)	20.4(9)	24.4(9)	3.1(8)	-0.8(8)	0.1(8)
C14	19.9(9)	16.9(10)	18.6(9)	0.7(7)	-0.6(7)	-0.7(7)
C15	18.6(9)	13.2(9)	17.1(9)	-0.3(7)	0.5(7)	-0.5(7)
C16	17.8(10)	15.7(9)	25.5(10)	0.1(8)	3.2(8)	0.6(7)
C17	20.2(9)	13.9(8)	15.6(9)	-2.9(7)	3.7(7)	1.6(7)
C18	20.3(9)	12.8(9)	16.2(9)	-0.4(7)	2.4(7)	-0.3(7)
C19	22.2(10)	22.1(10)	17.3(9)	-3.1(8)	-1.5(8)	-0.2(8)
C20	21.4(10)	20.5(10)	20.0(9)	-5.7(8)	2.4(8)	-4.5(8)
C21	31.4(11)	14.2(9)	29.8(11)	3.1(8)	1.6(9)	-2.4(8)

Table 2.4 Bond Lengths for yoon61

Atom		Atom Length/Å	Atom		Atom Length/Å
Br1	C1	1.9047(19)	C7	C8	1.580(3)

O1	C17	1.218(2)	C7	C16	1.551(3)
N1	C18	1.337(3)	C8	C9	1.505(3)
N1	C19	1.359(3)	C8	C15	1.565(3)
N2	C18	1.370(2)	C9	C10	1.401(3)
N2	C20	1.359(3)	C9	C14	1.394(3)
N2	C21	1.461(3)	C10	C11	1.390(3)
C1	C2	1.381(3)	C11	C12	1.384(3)
C1	C6	1.386(3)	C12	C13	1.396(3)
C2	C3	1.394(3)	C13	C14	1.389(3)
C3	C4	1.392(3)	C15	C16	1.560(3)
C4	C5	1.393(3)	C15	C17	1.510(3)
C4	C7	1.510(3)	C17	C18	1.471(3)
C5	C6	1.392(3)	C19	C20	1.376(3)

Table 2.5 Bond Angles for yoon61

Atom Atom Atom Angle/°				Atom Atom Atom Angle/°			
C18	N1	C19	105.57(17)	C10	C9	C8	119.36(17)
C18	N2	C21	129.16(18)	C14	C9	C8	121.89(17)
C20	N2	C18	106.89(17)	C14	C9	C10	118.73(18)
C20	N2	C21	123.89(18)	C11	C10	C9	120.66(19)
C2	C1	Br1	119.16(15)	C12	C11	C10	120.18(19)
C2	C1	C6	121.15(18)	C11	C12	C13	119.65(19)

C6	C1	Br1	119.68(15)	C14	C13	C12	120.21(19)
C1	C2	C3	119.22(18)	C13	C14	C9	120.58(18)
C4	C3	C2	121.30(18)	C16	C15	C8	87.22(15)
C3	C4	C5	117.80(18)	C17	C15	C8	115.39(16)
C3	C4	C7	123.24(17)	C17	C15	C16	116.71(16)
C5	C4	C7	118.96(17)	C7	C16	C15	89.78(15)
C6	C5	C4	121.96(18)	O1	C17	C15	121.44(18)
C1	C6	C5	118.56(18)	O1	C17	C18	121.73(18)
C4	C7	C8	114.43(15)	C18	C17	C15	116.78(17)
C4	C7	C16	116.66(15)	N1	C18	N2	110.89(17)
C16	C7	C8	87.05(14)	N1	C18	C17	124.49(17)
C9	C8	C7	120.04(16)	N2	C18	C17	124.55(18)
C9	C8	C15	121.06(16)	N1	C19	C20	110.17(19)
C15	C8	C7	88.57(14)	N2	C20	C19	106.46(18)

Table 2.6 Torsion Angles for yoon61

A	B	C	D	Angle/°	A	B	C	D	Angle/°
Br1	C1	C2	C3	177.9(2)	C8	C15	C17	O1	-62.3(2)
Br1	C1	C6	C5	-178.48(16)	C8	C15	C17	C18	115.14(19)
O1	C17	C18	N1	177.69(19)	C9	C8	C15	C16	144.89(18)
O1	C17	C18	N2	1.1(3)	C9	C8	C15	C17	-96.7(2)
N1	C19	C20	N2	-0.2(2)	C9	C10	C11	C12	120.2(3)

C1 C2 C3 C4 0.8(4)	C10C9 C14C130.3(3)
C2 C1 C6 C5 0.3(4)	C10C11C12C13-0.2(3)
C2 C3 C4 C5 -0.3(4)	C11C12C13C140.1(3)
C2 C3 C4 C7 -179.7(2)	C12C13C14C9 -0.2(3)
C3 C4 C5 C6 -0.3(3)	C14C9 C10C11-0.3(3)
C3 C4 C7 C8 -85.6(3)	C15C8 C9 C10-175.22(17)
C3 C4 C7 C1613.9(3)	C15C8 C9 C143.3(3)
C4 C5 C6 C1 0.3(3)	C15C17C18N1 0.2(3)
C4 C7 C8 C9 -27.8(2)	C15C17C18N2 -176.36(17)
C4 C7 C8 C1597.73(17)	C16C7 C8 C9 -145.87(17)
C4 C7 C16C15-95.58(18)	C16C7 C8 C15-20.31(14)
C5 C4 C7 C8 95.1(2)	C16C15C17O1 38.0(3)
C5 C4 C7 C16-165.46(18)	C16C15C17C18-144.57(18)
C6 C1 C2 C3 -0.9(4)	C17C15C16C7 -137.69(17)
C7 C4 C5 C6 179.14(18)	C18N1 C19C20-0.6(2)
C7 C8 C9 C10-66.9(2)	C18N2 C20C190.9(2)
C7 C8 C9 C14111.6(2)	C19N1 C18N2 1.2(2)
C7 C8 C15C1620.17(14)	C19N1 C18C17-175.82(18)
C7 C8 C15C17138.53(17)	C20N2 C18N1 -1.3(2)
C8 C7 C16C1520.36(14)	C20N2 C18C17175.69(18)
C8 C9 C10C11178.27(17)	C21N2 C18N1 -178.76(19)
C8 C9 C14C13-178.25(18)	C21N2 C18C17-1.8(3)

C8 C15C16C7 -20.56(14) C21N2 C20C19 178.49(19)

Table 2.7 Hydrogen Atom Coordinates ($\text{\AA} \times 10^4$) and Isotropic Displacement Parameters ($\text{\AA}^2 \times 10^3$) for yoon61

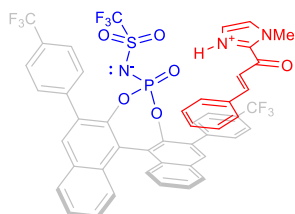
Atom	x	y	z	U(eq)
H2	4619.53	2382.77	-182.81	37
H3	4766.55	438.29	350.83	34
H5	5700.8	2232.8	2032.21	22
H6	5601.23	4182.29	1504.7	23
H7	6190.32	-63.96	1970.92	22
H8	3837.21	-1153.89	2252.08	19
H10	3338.36	1098.38	2783.72	22
H11	1242.39	2545.24	3000.88	23
H12	-1119.3	2591.64	2356.56	25
H13	-1371.71	1185.85	1485.01	25
H14	721.02	-261.34	1265.57	22
H15	3012.63	-1108.6	881.57	20
H16A	6147.7	-1994.33	1420.14	24
H16B	5902.89	-1170.14	760.94	24
H19	-1677.08	-2837.7	257.02	25
H20	-1557.85	-4946.31	783.94	25
H21A	2335.79	-5666.13	1420.27	38
H21B	467.27	-6141.6	1456.51	38

H21C 1167.21

-5201.51

1996.22

38

Equimolar (1:1) Complex of 2.1 and 2.4

Data Collection: A yellow crystal with approximate dimensions $0.38 \times 0.32 \times 0.25 \text{ mm}^3$ was selected under oil under ambient conditions and attached to the tip of a MiTeGen MicroMount[®]. The crystal was mounted in a stream of cold nitrogen at 100(1) K and centered in the X-ray beam by using a video camera.

The crystal evaluation and data collection were performed on a Bruker D8 VENTURE PhotonIII four-circle diffractometer with Cu K α ($\lambda = 1.54178 \text{ \AA}$) radiation and the detector to crystal distance of 4.0 cm.⁷⁰

The initial cell constants were obtained from a $180^\circ \phi$ scan conducted at a $2\theta = 50^\circ$ angle with the exposure time of 1 second per frame. The reflections were successfully indexed by an automated indexing routine built in the APEX3 program. The final cell constants were calculated from a set of 9509 strong reflections from the actual data collection.

The data were collected by using the full sphere data collection routine to survey the reciprocal space to the extent of a full sphere to a resolution of 0.78 \AA . A total of 203898 data were harvested by collecting 43 sets of frames with 0.9° scans in ω and ϕ with an exposure time 2.4 – 4 sec per frame. These highly redundant datasets were corrected for Lorentz and polarization effects.

The absorption correction was based on fitting a function to the empirical transmission surface as sampled by multiple equivalent measurements.⁷¹

Structure Solution and Refinement: The systematic absences in the diffraction data were uniquely consistent for the space group $P2_12_12_1$ that yielded chemically reasonable and computationally stable results of refinement.^{26–31}

A successful solution by the direct methods provided most non-hydrogen atoms from the *E*-map. The remaining non-hydrogen atoms were located in an alternating series of least-squares cycles and difference Fourier maps. All non-hydrogen atoms were refined with anisotropic displacement coefficients unless specified otherwise. All hydrogen atoms except H3(N3) were included in the structure factor calculation at idealized positions and were allowed to ride on the neighboring atoms with relative isotropic displacement coefficients.

The crystal structure consists of a $C_{35}H_{18}F_9NO_5PS$ anion, $C_{13}H_{13}N_2O$ cation, and two molecules of solvent Et_2O .

There is positional disorder in the structure. The CF_3 group at C7 is disordered over three positions in a 55.2(4):29.7(4):15.1(4) ratio. The disordered CF_3 groups were refined with restraints and constraints. The O7 diethyl ether is disordered over two positions with the major component contribution of 83.7(4) %. The minor disorder component was refined isotropically with geometry restraints. The O8 diethyl ether is disordered over two positions with the major component contribution of 64.7(13) %. Both disorder components were refined isotropically with geometry and atomic displacement parameter restraints.

The absolute structure was unequivocally established based on resonant scattering effects. The crystal is an inversion twin with a 2.3(11) % contribution of the inverted component.

The final least-squares refinement of 804 parameters against 11554 data resulted in residuals R (based on F^2 for $I \geq 2\sigma$) and wR (based on F^2 for all data) of 0.0266 and 0.0685, respectively. The final difference Fourier map was featureless.

Summary

Crystal Data for $C_{56}H_{51}F_9N_3O_8PS$ ($M = 1128.03$ g/mol): orthorhombic, space group $P2_12_12_1$ (no. 19), $a = 13.6603(16)$ Å, $b = 16.608(2)$ Å, $c = 23.617(3)$ Å, $V = 5358.1(12)$ Å³, $Z = 4$, $T = 100.0$ K, $\mu(\text{CuK}\alpha) = 1.594$ mm⁻¹, $D_{\text{calc}} = 1.398$ g/cm³, 203898 reflections measured ($6.506^\circ \leq 2\Theta \leq 158.416^\circ$), 11554 unique ($R_{\text{int}} = 0.0437$, $R_{\text{sigma}} = 0.0215$) which were used in all calculations. The final R_1 was 0.0266 ($I > 2\sigma(I)$) and wR_2 was 0.0685 (all data).

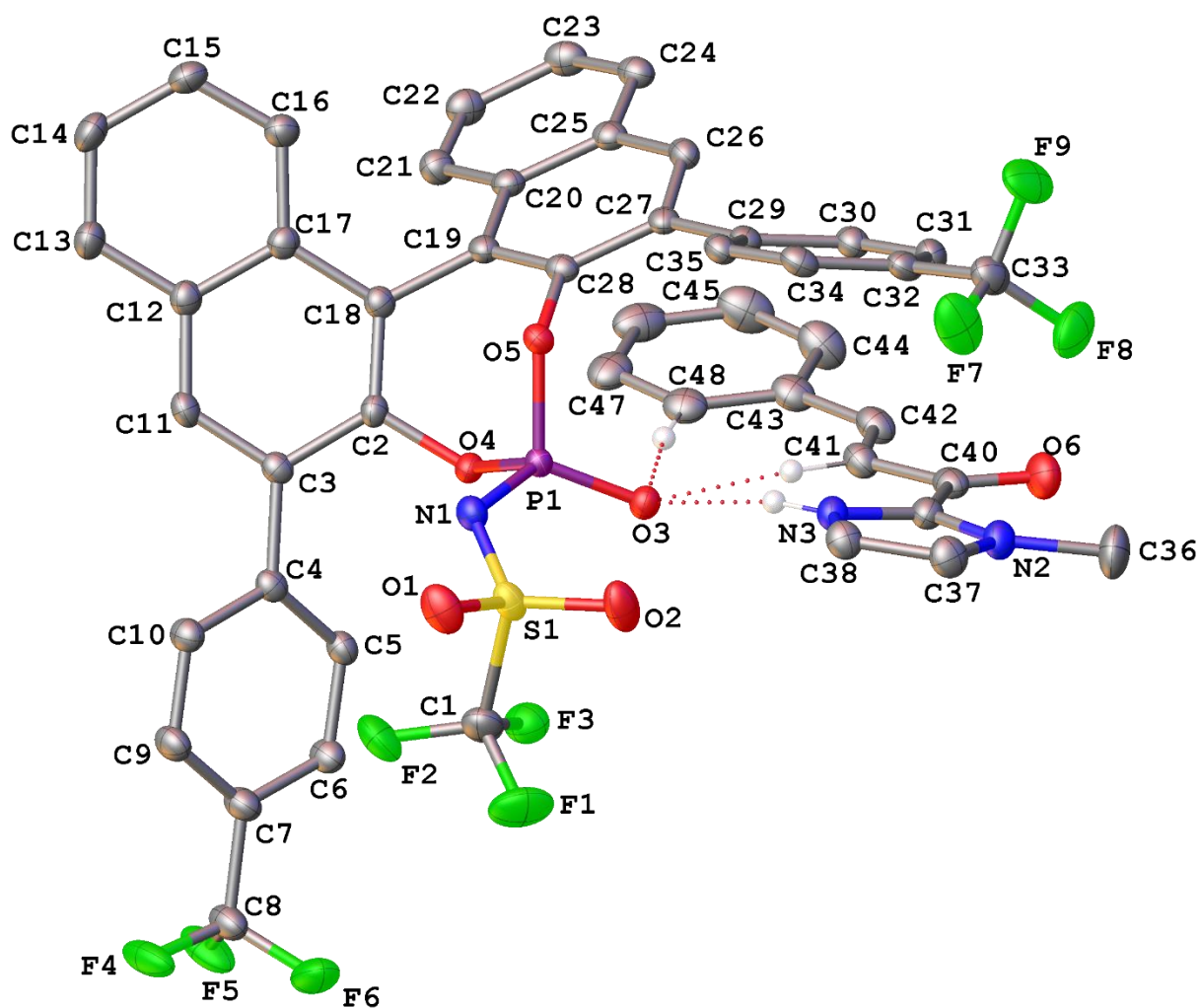


Figure 2.6 A molecular drawing of the hydrogen bonding interactions between the cation and anion in yoon62a shown with 50% probability ellipsoids. Selected H atoms are shown. Minor disorder components and solvent molecules are omitted.

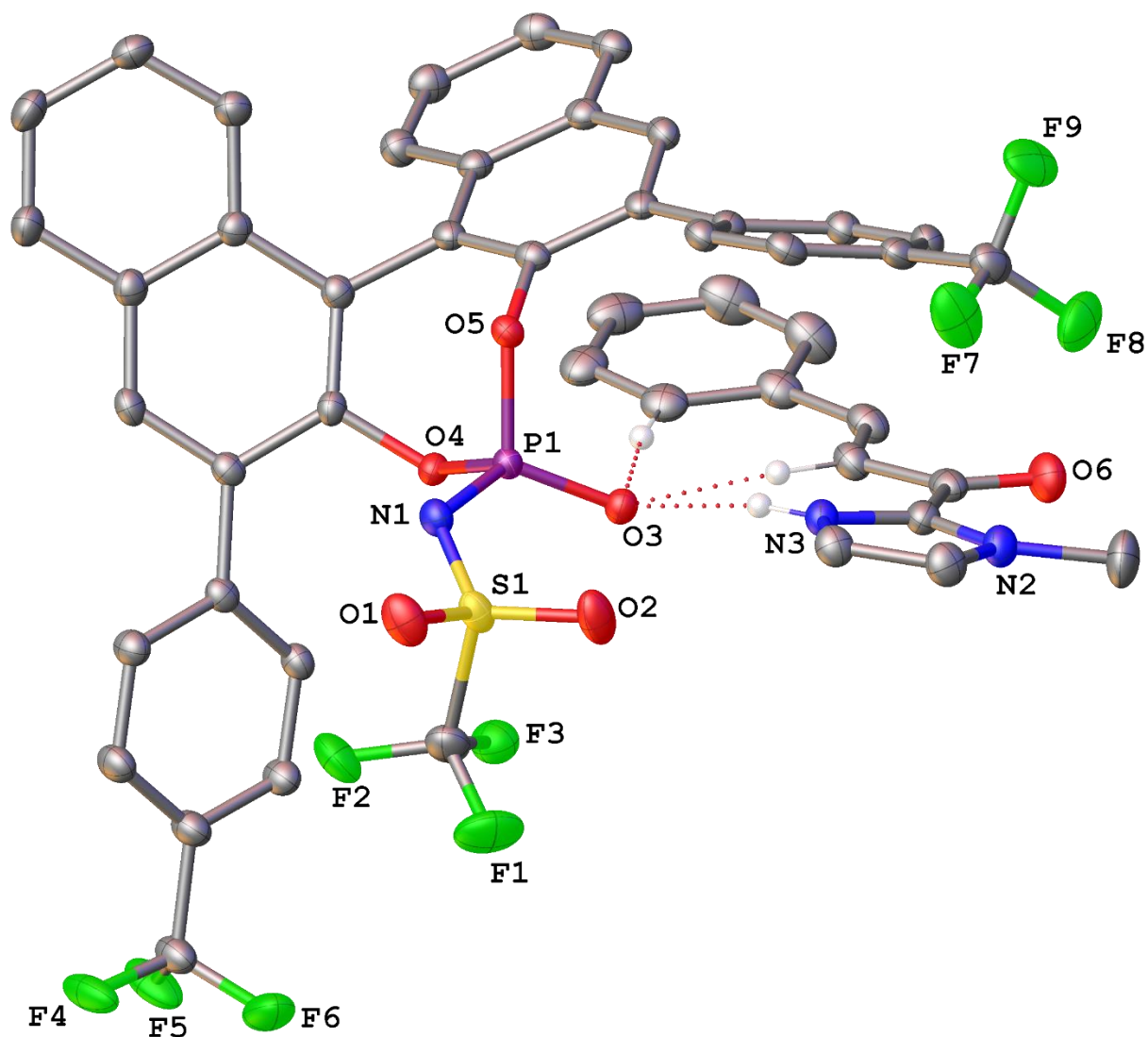


Figure 2.7 A molecular drawing of the hydrogen bonding interactions between the cation and anion in yoon62a shown with 50% probability ellipsoids. Selected H atoms are shown. Minor disorder components and solvent molecules are omitted.

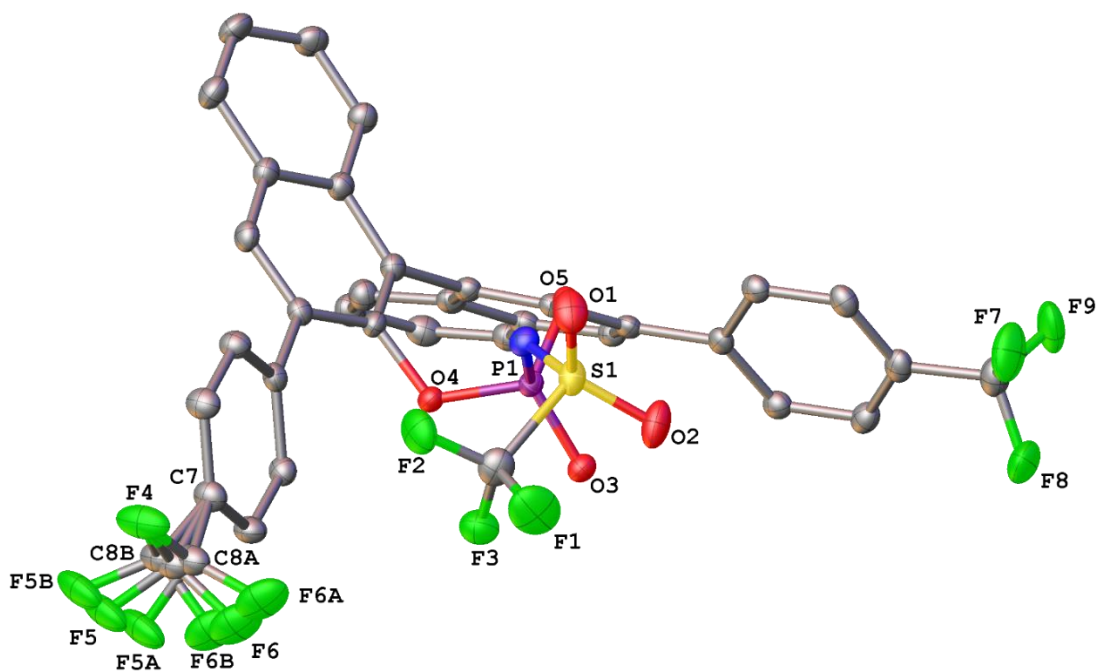


Figure 2.8 A molecular drawing of the anion in yoon62a shown with 50% probability ellipsoids. All disorder components at C7 are shown whereas all H atoms are omitted.

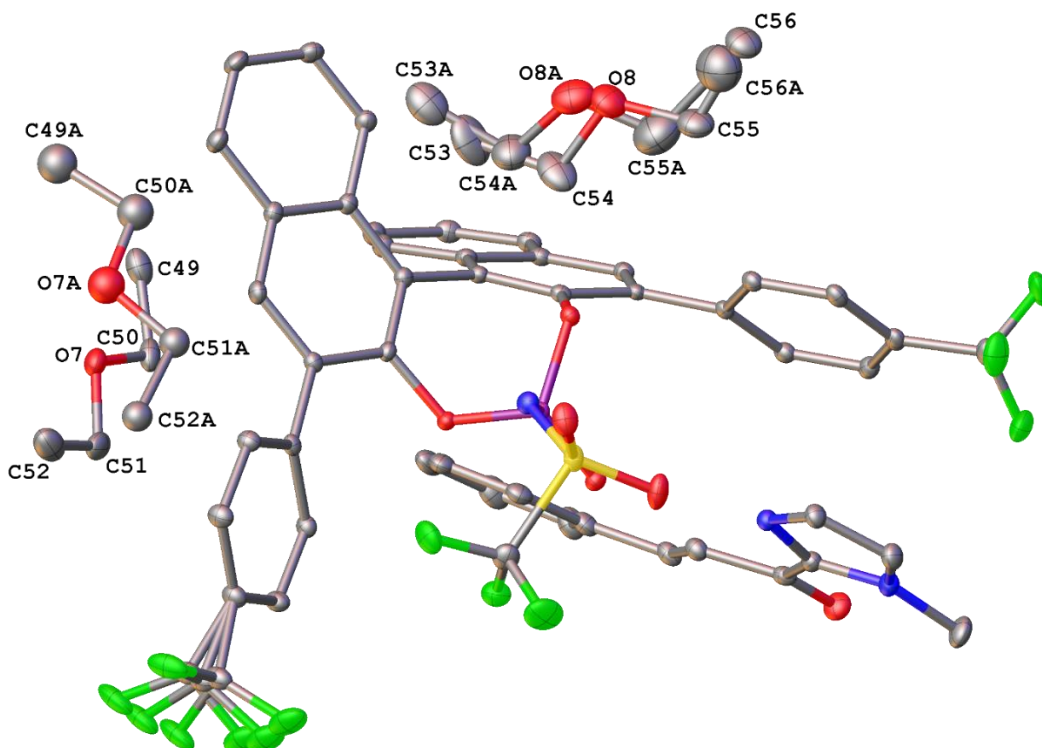


Figure 2.9 A molecular drawing of yoon62a shown with 50% probability ellipsoids. The two diethyl ether solvent molecules are shown with their disorder components. All H atoms are omitted.

Table 2.8 Crystal data and structure refinement for yoon62a

Identification code	yoon62a
Empirical formula	$[\text{C}_{13}\text{H}_{13}\text{N}_2\text{O}][\text{C}_{35}\text{H}_{18}\text{F}_9\text{NO}_5\text{PS}] \cdot 2\text{Et}_2\text{O}$
Formula weight	1128.03
Temperature/K	100.0
Crystal system	orthorhombic
Space group	$\text{P2}_1\text{2}_1\text{2}_1$
a/Å	13.6603(16)
b/Å	16.608(2)
c/Å	23.617(3)

$\alpha/^\circ$	90
$\beta/^\circ$	90
$\gamma/^\circ$	90
Volume/ \AA^3	5358.1(12)
Z	4
$\rho_{\text{calc}}/\text{g/cm}^3$	1.398
μ/mm^{-1}	1.594
F(000)	2336.0
Crystal size/ mm^3	$0.38 \times 0.32 \times 0.25$
Radiation	CuK α ($\lambda = 1.54178$)
2 Θ range for data collection/ $^\circ$ 6.506 to 158.416	
Index ranges	$-17 \leq h \leq 17, -21 \leq k \leq 20, -28 \leq l \leq 30$
Reflections collected	203898
Independent reflections	11554 [$R_{\text{int}} = 0.0437, R_{\text{sigma}} = 0.0215$]
Data/restraints/parameters	11554/118/804
Goodness-of-fit on F^2	1.095
Final R indexes [$I \geq 2\sigma(I)$]	$R_1 = 0.0266, wR_2 = 0.0684$
Final R indexes [all data]	$R_1 = 0.0268, wR_2 = 0.0685$
Largest diff. peak/hole / $e \text{\AA}^{-3}$	0.21/-0.28
Flack parameter	0.023(11)

Table 2.9 Fractional Atomic Coordinates ($\times 10^4$) and Equivalent Isotropic Displacement Parameters ($\text{\AA}^2 \times 10^3$) for yoon62a. U_{eq} is defined as 1/3 of the trace of the orthogonalised U_{ij} tensor.

Atom	x	y	z	U(eq)
S1	5114.7(4)	2929.8(3)	2722.4(2)	22.34(10)
P1	4381.0(3)	3306.6(3)	3799.8(2)	15.68(9)
F1	6981.0(11)	2686.6(11)	2525.5(7)	52.3(4)
F2	6593.8(10)	3929.3(8)	2660.3(6)	38.2(3)
F3	6669.1(9)	3114.4(8)	3365.7(5)	33.4(3)
C8B	8874(12)	5536(8)	3193(3)	27.3(9)
F4	9069.0(9)	5768.5(10)	2662.4(6)	41.8(4)
F5B	9343(18)	6056(11)	3527(5)	43.8(17)
F6B	9325(17)	4833(9)	3273(7)	47.9(17)
C8	8904(4)	5392(3)	3154.6(15)	27.3(9)
F5	9435(3)	5770(3)	3547.3(13)	43.8(17)
F6	9275(3)	4651(2)	3115(2)	47.9(17)
C8A	8839(8)	5261(5)	3082(3)	27.3(9)
F5A	9471(8)	5406(5)	3500(3)	43.8(17)
F6A	9075(8)	4526(4)	2898(3)	47.9(17)
C33	1886.2(15)	-369.6(12)	3744.8(9)	29.5(4)
F7	2064.6(13)	-418.9(9)	3192.6(6)	48.9(4)
F8	2448.0(12)	-925.7(8)	3994.4(7)	47.0(4)
F9	962.9(10)	-612.9(8)	3821.1(7)	45.8(4)

O1	4936.4(13)	3168.4(10)	2149.3(6)	32.6(3)
O2	5076.6(13)	2079.6(9)	2842.2(6)	33.9(4)
O3	4789.3(9)	2582.2(8)	4075.4(5)	19.2(3)
O4	4751.6(9)	4068.6(7)	4156.7(5)	17.3(2)
O5	3214.5(9)	3364.1(7)	3852.9(5)	17.0(2)
N1	4570.5(12)	3485.2(9)	3143.5(7)	20.9(3)
C1	6418.9(16)	3182.6(13)	2826.1(9)	28.9(4)
C2	4284.0(13)	4813.9(10)	4079.8(7)	17.0(3)
C3	4808.0(13)	5439.8(10)	3799.3(7)	17.3(3)
C4	5847.2(13)	5362.1(11)	3615.6(7)	17.8(3)
C5	6548.9(14)	4946.6(11)	3934.3(8)	19.4(4)
C6	7525.4(14)	4959.4(12)	3778.9(8)	22.4(4)
C7	7819.1(14)	5378.9(12)	3297.4(8)	24.1(4)
C9	7131.9(15)	5785.5(13)	2973.7(8)	24.3(4)
C10	6155.2(14)	5778.0(12)	3132.0(8)	21.4(4)
C11	4322.8(14)	6160.7(11)	3722.9(8)	20.0(3)
C12	3345.1(14)	6274.0(11)	3892.3(8)	20.1(4)
C13	2846.8(15)	7009.5(11)	3776.3(9)	24.8(4)
C14	1882.1(15)	7097.2(12)	3917.2(9)	27.3(4)
C15	1370.8(15)	6461.5(12)	4180.4(9)	25.2(4)
C16	1834.3(14)	5753.3(12)	4307.4(8)	22.1(4)
C17	2837.4(14)	5641.4(11)	4173.9(8)	19.1(3)

C18	3352.0(13)	4907.3(11)	4290.4(8)	17.7(3)
C19	2888.0(13)	4247.3(11)	4622.0(8)	17.7(3)
C20	2559.4(13)	4374.2(11)	5192.9(8)	18.6(3)
C21	2685.0(14)	5115.8(12)	5484.4(8)	22.9(4)
C22	2398.6(15)	5197.4(12)	6036.4(9)	25.0(4)
C23	1960.5(14)	4547.9(13)	6328.0(8)	24.9(4)
C24	1831.5(14)	3825.2(12)	6061.0(8)	21.9(4)
C25	2134.9(13)	3716.5(11)	5490.8(8)	19.2(4)
C26	2041.3(13)	2960.1(11)	5221.8(8)	18.6(3)
C27	2390.7(12)	2818.9(11)	4683.2(8)	16.9(3)
C28	2826.3(13)	3482.5(11)	4396.7(7)	16.7(3)
C29	2299.2(12)	2005.8(11)	4426.9(8)	17.4(3)
C30	2385.0(13)	1321.2(11)	4769.5(8)	20.4(4)
C31	2268.2(14)	555.1(12)	4550.8(9)	22.5(4)
C32	2056.3(13)	458.4(12)	3977.7(8)	22.3(4)
C34	1954.4(13)	1129.0(12)	3632.3(8)	21.5(4)
C35	2078.1(13)	1896.6(11)	3851.7(8)	19.6(3)
O6	4700.5(12)	-5.6(9)	5287.7(6)	31.3(3)
N2	4660.8(12)	-307.6(10)	4099.1(7)	24.2(3)
N3	4543.0(12)	972.7(10)	3938.2(7)	19.5(3)
C36	4778(2)	-1102.4(13)	4368.2(11)	36.8(5)
C37	4548.9(15)	-209.2(12)	3527.5(9)	26.5(4)

C38	4473.1(15)	595.3(12)	3429.2(8)	23.1(4)
C39	4656.6(13)	422.4(11)	4348.9(8)	20.5(4)
C40	4706.9(13)	572.9(12)	4967.2(8)	22.0(4)
C41	4729.5(14)	1412.4(12)	5152.3(8)	22.5(4)
C42	4701.4(14)	1599.0(13)	5703.7(8)	25.1(4)
C43	4650.8(14)	2409.5(13)	5941.9(9)	26.4(4)
C44	4499.4(18)	2501.1(16)	6523.0(10)	35.5(5)
C45	4409.8(19)	3259.9(17)	6762.5(10)	40.4(5)
C46	4482.4(16)	3940.0(15)	6427.2(11)	35.8(5)
C47	4642.8(15)	3859.4(14)	5849.8(10)	30.4(4)
C48	4723.3(14)	3105.4(13)	5604.9(9)	26.7(4)
O7	5399.6(14)	7273.6(10)	4732.1(8)	32.2(5)
C49	3991(3)	7173(2)	5320.1(15)	44.3(8)
C50	4945(3)	6799(2)	5157.1(15)	35.6(8)
C51	6336(2)	6981.9(17)	4584.8(14)	39.6(7)
C52	6702(2)	7442(2)	4081.6(16)	51.3(9)
O7A	4344(9)	7401(8)	5264(7)	59(4)
C49A	3106(14)	8205(10)	5675(10)	67(6)
C50A	3368(10)	7379(9)	5473(9)	56(5)
C51A	4715(11)	6629(8)	5136(11)	40(6)
C52A	5740(9)	6720(9)	4914(6)	39(4)
O8	1287(4)	3835(4)	2319(3)	51.6(13)

C53	2121(7)	4877(7)	2795(3)	74(3)
C54	2165(5)	4035(6)	2590(3)	64(2)
C55	1206(4)	3018(4)	2179(2)	48.6(14)
C56	243(5)	2885(5)	1893(3)	49.2(14)
O8A	1378(9)	4157(8)	2359(5)	59(3)
C53A	1924(9)	5374(10)	2762(5)	67(4)
C54A	2103(9)	4487(10)	2722(6)	64(4)
C55A	1414(13)	3309(8)	2334(9)	95(6)
C56A	595(15)	3008(10)	1967(8)	92(6)

Table 2.10 Anisotropic Displacement Parameters ($\text{\AA}^2 \times 10^3$) for yoon62a. The Anisotropic displacement factor exponent takes the form: $-2\pi^2 [h^2 a^{*2} U_{11} + 2hka^* b^* U_{12} + \dots]$.

Atom	U_{11}	U_{22}	U_{33}	U_{23}	U_{13}	U_{12}
S1	29.3(2)	19.7(2)	18.0(2)	-1.15(16)	4.85(17)	-5.17(18)
P1	16.09(19)	14.61(19)	16.34(19)	1.21(16)	1.69(16)	-0.35(16)
F1	39.9(8)	62.8(10)	54.4(9)	-19.0(8)	16.1(7)	13.0(7)
F2	36.2(7)	39.9(7)	38.4(7)	7.3(6)	5.2(6)	-16.0(6)
F3	28.9(6)	38.0(7)	33.4(7)	2.1(5)	-0.8(5)	1.8(5)
C8B	20.2(12)	35(2)	26.7(14)	10.6(15)	0.6(12)	-2.7(15)
F4	22.0(6)	69.2(10)	34.2(7)	25.4(7)	4.5(5)	-1.8(6)
F5B	25.3(14)	67(5)	38.9(10)	17(2)	-9.4(8)	-22(4)
F6B	36(2)	50(2)	58(4)	14(3)	22(3)	16.9(19)
C8	20.2(12)	35(2)	26.7(14)	10.6(15)	0.6(12)	-2.7(15)

F5	25.3(14)	67(5)	38.9(10)	17(2)	-9.4(8)	-22(4)
F6	36(2)	50(2)	58(4)	14(3)	22(3)	16.9(19)
C8A	20.2(12)	35(2)	26.7(14)	10.6(15)	0.6(12)	-2.7(15)
F5A	25.3(14)	67(5)	38.9(10)	17(2)	-9.4(8)	-22(4)
F6A	36(2)	50(2)	58(4)	14(3)	22(3)	16.9(19)
C33	28.4(10)	23.7(10)	36.3(11)	-2.8(9)	6.2(9)	-5.0(8)
F7	76.3(11)	31.6(7)	38.8(8)	-13.9(6)	15.6(7)	-11.4(7)
F8	51.2(9)	20.2(6)	69.6(10)	-5.0(6)	-8.3(8)	2.7(6)
F9	33.5(7)	31.7(7)	72.1(10)	-13.2(7)	9.4(7)	-16.6(6)
O1	44.4(9)	34.2(8)	19.3(7)	-0.6(6)	3.3(6)	-9.3(7)
O2	52.2(10)	20.0(7)	29.4(7)	-3.3(6)	11.0(7)	-7.1(7)
O3	20.9(6)	17.1(6)	19.5(6)	1.2(5)	1.0(5)	1.5(5)
O4	16.0(6)	15.1(6)	20.9(6)	1.7(5)	-0.2(5)	0.5(5)
O5	16.5(6)	17.7(6)	16.8(6)	0.9(5)	0.9(5)	-2.0(5)
N1	22.3(8)	20.3(7)	20.2(7)	4.2(6)	1.5(6)	-0.7(6)
C1	27.4(10)	30.9(10)	28.3(10)	-1.0(8)	9.7(8)	1.4(8)
C2	18.9(8)	13.3(8)	18.7(8)	0.8(6)	-1.5(7)	-0.4(6)
C3	17.4(8)	18.2(8)	16.4(7)	-0.6(7)	-0.2(7)	-2.8(6)
C4	18.5(8)	17.4(8)	17.3(8)	-1.6(6)	-0.1(6)	-3.3(7)
C5	20.5(8)	19.5(8)	18.2(8)	2.7(7)	0.5(7)	-2.8(7)
C6	19.2(8)	26.3(9)	21.7(9)	5.1(8)	-2.0(7)	0.0(7)
C7	19.6(9)	28.8(10)	24.0(9)	4.7(8)	1.8(7)	-2.9(8)

C9	22.2(9)	29.1(10)	21.6(9)	6.9(8)	2.1(7)	-2.2(8)
C10	19.9(9)	24.3(9)	19.9(9)	4.0(7)	-0.5(7)	0.0(7)
C11	22.2(8)	16.4(8)	21.3(8)	2.3(7)	0.9(7)	-4.3(7)
C12	22.7(9)	17.1(8)	20.7(9)	-0.8(7)	0.2(7)	-0.6(7)
C13	27.9(9)	17.2(8)	29.2(10)	2.3(8)	2.5(8)	1.8(7)
C14	29.4(10)	19.5(9)	33.0(11)	2.2(8)	0.1(8)	7.6(8)
C15	20.3(9)	25.6(10)	29.7(10)	-0.9(8)	2.5(8)	5.2(7)
C16	21.0(9)	21.2(9)	24.2(9)	-0.6(7)	2.8(7)	0.4(7)
C17	19.7(8)	17.3(8)	20.2(8)	-1.4(7)	0.2(7)	0.3(7)
C18	18.4(8)	16.9(8)	17.9(8)	-0.6(6)	0.0(7)	-1.2(7)
C19	13.3(7)	18.8(8)	20.9(9)	2.5(7)	0.3(7)	0.3(6)
C20	14.0(8)	20.9(9)	20.8(9)	0.5(7)	0.5(6)	1.5(7)
C21	22.1(9)	21.8(9)	24.8(9)	-0.5(7)	0.8(7)	-1.2(7)
C22	24.1(9)	24.6(10)	26.2(10)	-4.6(8)	-0.2(7)	0.2(8)
C23	22.8(9)	33.3(10)	18.7(9)	-0.7(8)	0.9(7)	2.2(8)
C24	17.4(8)	27.3(9)	20.9(9)	3.3(7)	0.9(7)	-0.1(7)
C25	14.2(8)	22.9(9)	20.5(9)	1.3(7)	-0.9(7)	0.7(7)
C26	15.8(8)	20.0(8)	19.9(8)	4.2(7)	-0.6(6)	-1.1(7)
C27	11.5(7)	18.2(8)	21.2(8)	1.5(7)	-1.6(6)	-0.2(6)
C28	13.5(7)	21.0(8)	15.7(8)	0.8(6)	-0.7(6)	-0.1(6)
C29	12.4(7)	18.4(8)	21.4(8)	0.9(7)	1.4(6)	-2.3(6)
C30	17.1(8)	21.9(9)	22.4(9)	2.6(7)	0.2(7)	-1.6(7)

C31	21.1(9)	18.9(9)	27.4(10)	4.1(7)	3.9(7)	-0.8(7)
C32	17.0(8)	21.0(9)	29.0(10)	-0.9(7)	5.4(7)	-3.3(7)
C34	17.0(8)	25.8(9)	21.8(9)	-1.8(7)	2.5(7)	-5.2(7)
C35	15.5(8)	21.3(9)	21.9(9)	3.1(7)	0.8(7)	-2.5(6)
O6	37.9(8)	29.1(7)	27.0(7)	9.4(6)	-1.5(6)	0.6(6)
N2	25.7(8)	18.9(8)	28.1(8)	1.6(6)	-1.5(7)	-2.1(6)
N3	19.9(7)	17.6(7)	21.0(8)	1.6(6)	-1.5(6)	-0.8(6)
C36	49.2(14)	18.6(9)	42.7(12)	7.0(9)	-4.8(11)	-0.3(9)
C37	29.7(10)	23.2(9)	26.5(9)	-3.5(8)	-1.5(8)	-3.8(8)
C38	24.5(9)	23.3(9)	21.5(9)	-0.6(7)	-2.9(7)	-3.3(7)
C39	17.9(8)	18.8(8)	24.9(9)	1.8(7)	0.1(7)	-0.3(7)
C40	15.5(8)	27.2(9)	23.4(9)	4.8(8)	-1.1(7)	-0.5(7)
C41	20.4(9)	25.1(9)	22.0(9)	4.0(7)	-1.4(7)	-3.8(7)
C42	20.8(9)	31.5(10)	22.9(9)	3.8(8)	-2.6(7)	-6.3(8)
C43	20.5(9)	34.0(11)	24.8(10)	-1.2(8)	-3.5(8)	-6.0(8)
C44	38.9(12)	41.4(12)	26.2(10)	-2.5(9)	-2.1(9)	-10.9(10)
C45	38.7(12)	53.6(14)	29.0(11)	-10.6(11)	1.2(10)	-10.2(12)
C46	23.6(10)	40.6(12)	43.3(13)	-15.9(10)	-4.7(9)	-2.0(9)
C47	19.5(9)	33.2(11)	38.6(12)	-2.4(9)	-8.4(8)	0.4(8)
C48	18.4(9)	35.0(11)	26.6(9)	-1.2(8)	-5.7(7)	-1.4(8)
O7	36.3(10)	20.6(9)	39.8(10)	1.2(7)	-4.1(8)	-1.3(7)
C49	51(2)	43.3(17)	38.3(16)	-3.1(14)	-0.8(14)	-17.9(17)

C50	50.0(19)	23.4(13)	33.5(16)	1.9(12)	-12.0(14)	-10.5(15)
C51	40.5(16)	25.0(13)	53.3(18)	-14.7(12)	-11.4(13)	4.4(11)
C52	37.9(16)	50.0(19)	66(2)	-21.5(17)	8.4(15)	-3.7(14)
O8	49(2)	63(3)	42.9(19)	1(2)	-12.7(15)	-3(2)
C53	88(5)	94(7)	40(3)	-24(4)	-1(3)	-31(5)
C54	66(3)	81(5)	45(3)	19(3)	-24(2)	-17(3)
C55	42(3)	59(3)	45(3)	11(2)	-11(2)	4(2)
C56	46(3)	60(3)	42(2)	6(2)	-14(2)	-1(3)
O8A	63(5)	70(6)	44(4)	17(4)	1(3)	13(4)
C53A	69(6)	92(9)	39(4)	0(6)	-5(4)	-16(6)
C54A	66(6)	64(6)	62(6)	10(5)	-16(5)	5(5)
C55A	103(8)	82(7)	100(8)	17(6)	-6(6)	15(6)
C56A	90(12)	92(10)	94(11)	11(8)	6(9)	-7(9)

Table 2.11 Bond Lengths for yoon62a

Atom Atom Length/Å			Atom Atom Length/Å		
S1	O1	1.4311(15)	C20	C21	1.421(3)
S1	O2	1.4410(15)	C20	C25	1.423(3)
S1	N1	1.5468(17)	C21	C22	1.368(3)
S1	C1	1.847(2)	C22	C23	1.413(3)
P1	O3	1.4772(13)	C23	C24	1.367(3)
P1	O4	1.6026(13)	C24	C25	1.420(3)

P1	O5	1.6013(13)	C25	C26	1.414(3)
P1	N1	1.5992(16)	C26	C27	1.379(3)
F1	C1	1.331(2)	C27	C28	1.424(2)
F2	C1	1.322(3)	C27	C29	1.485(3)
F3	C1	1.324(3)	C29	C30	1.400(3)
C8B	F4	1.337(6)	C29	C35	1.403(3)
C8B	F5B	1.335(6)	C30	C31	1.383(3)
C8B	F6B	1.333(6)	C31	C32	1.394(3)
C8B	C7	1.486(16)	C32	C34	1.387(3)
F4	C8	1.339(4)	C34	C35	1.387(3)
F4	C8A	1.338(5)	O6	C40	1.223(2)
C8	F5	1.334(4)	N2	C36	1.474(3)
C8	F6	1.334(4)	N2	C37	1.368(3)
C8	C7	1.520(6)	N2	C39	1.348(3)
C8A	F5A	1.334(6)	N3	C38	1.359(2)
C8A	F6A	1.334(6)	N3	C39	1.342(2)
C8A	C7	1.497(11)	C37	C38	1.360(3)
C33	F7	1.329(3)	C39	C40	1.483(3)
C33	F8	1.338(3)	C40	C41	1.461(3)
C33	F9	1.337(2)	C41	C42	1.339(3)
C33	C32	1.499(3)	C42	C43	1.460(3)
O4	C2	1.405(2)	C43	C44	1.396(3)

O5	C28	1.403(2)	C43	C48	1.407(3)
C2	C3	1.425(2)	C44	C45	1.387(4)
C2	C18	1.376(3)	C45	C46	1.383(4)
C3	C4	1.490(2)	C46	C47	1.388(3)
C3	C11	1.380(3)	C47	C48	1.384(3)
C4	C5	1.401(3)	O7	C50	1.419(4)
C4	C10	1.400(3)	O7	C51	1.412(4)
C5	C6	1.384(3)	C49	C50	1.493(5)
C6	C7	1.393(3)	C51	C52	1.499(5)
C7	C9	1.386(3)	O7A	C50A	1.422(8)
C9	C10	1.386(3)	O7A	C51A	1.411(7)
C11	C12	1.407(3)	C49A	C50A	1.496(8)
C12	C13	1.425(3)	C51A	C52A	1.501(8)
C12	C17	1.424(3)	O8	C54	1.399(8)
C13	C14	1.367(3)	O8	C55	1.401(8)
C14	C15	1.410(3)	C53	C54	1.481(10)
C15	C16	1.369(3)	C55	C56	1.495(7)
C16	C17	1.418(3)	O8A	C54A	1.420(8)
C17	C18	1.434(3)	O8A	C55A	1.412(7)
C18	C19	1.489(2)	C53A	C54A	1.495(8)
C19	C20	1.437(3)	C55A	C56A	1.501(8)
C19	C28	1.380(3)			

Table 2.12 Bond Angles for yoon62a

Atom Atom Atom Angle/°				Atom Atom Atom Angle/°			
O1	S1	O2	116.81(9)	C15	C16	C17	120.70(18)
O1	S1	N1	111.17(9)	C12	C17	C18	118.57(17)
O1	S1	C1	103.10(10)	C16	C17	C12	118.55(17)
O2	S1	N1	116.15(9)	C16	C17	C18	122.84(17)
O2	S1	C1	103.39(10)	C2	C18	C17	118.69(16)
N1	S1	C1	104.05(9)	C2	C18	C19	120.07(16)
O3	P1	O4	106.99(7)	C17	C18	C19	121.22(16)
O3	P1	O5	112.94(7)	C20	C19	C18	121.24(16)
O3	P1	N1	121.13(8)	C28	C19	C18	120.07(16)
O5	P1	O4	103.07(7)	C28	C19	C20	118.55(16)
N1	P1	O4	108.19(8)	C21	C20	C19	122.96(17)
N1	P1	O5	103.05(8)	C21	C20	C25	118.35(17)
F4	C8B	C7	113.5(10)	C25	C20	C19	118.61(17)
F5B	C8B	F4	105.8(8)	C22	C21	C20	120.87(18)
F5B	C8B	C7	118.7(13)	C21	C22	C23	120.66(19)
F6B	C8B	F4	107.1(9)	C24	C23	C22	120.00(18)
F6B	C8B	F5B	105.2(8)	C23	C24	C25	120.75(18)
F6B	C8B	C7	105.7(12)	C24	C25	C20	119.35(17)
F4	C8	C7	111.3(3)	C26	C25	C20	119.79(16)

F5	C8	F4	107.0(3)	C26	C25	C24	120.84(17)
F5	C8	F6	106.0(4)	C27	C26	C25	122.32(17)
F5	C8	C7	112.5(3)	C26	C27	C28	116.84(16)
F6	C8	F4	107.8(4)	C26	C27	C29	120.11(16)
F6	C8	C7	111.9(3)	C28	C27	C29	123.04(16)
F4	C8A	C7	112.8(6)	O5	C28	C27	118.98(16)
F5A	C8A	F4	106.5(6)	C19	C28	O5	117.31(15)
F5A	C8A	F6A	104.5(6)	C19	C28	C27	123.71(17)
F5A	C8A	C7	109.1(7)	C30	C29	C27	119.71(16)
F6A	C8A	F4	106.2(6)	C30	C29	C35	118.19(17)
F6A	C8A	C7	117.1(7)	C35	C29	C27	122.02(16)
F7	C33	F8	106.53(18)	C31	C30	C29	121.45(18)
F7	C33	F9	106.65(18)	C30	C31	C32	119.52(18)
F7	C33	C32	112.83(17)	C31	C32	C33	119.61(18)
F8	C33	C32	112.51(18)	C34	C32	C33	120.34(18)
F9	C33	F8	105.86(17)	C34	C32	C31	119.96(18)
F9	C33	C32	111.98(17)	C35	C34	C32	120.41(18)
C2	O4	P1	118.96(11)	C34	C35	C29	120.45(17)
C28	O5	P1	117.13(11)	C37	N2	C36	123.00(18)
S1	N1	P1	126.18(10)	C39	N2	C36	128.11(17)
F1	C1	S1	110.18(16)	C39	N2	C37	108.89(17)
F2	C1	S1	110.38(15)	C39	N3	C38	109.47(16)

F2	C1	F1	108.56(18)	C38	C37	N2	107.12(18)
F2	C1	F3	108.58(18)	N3	C38	C37	107.27(17)
F3	C1	S1	110.93(14)	N2	C39	C40	125.60(17)
F3	C1	F1	108.14(18)	N3	C39	N2	107.26(16)
O4	C2	C3	118.32(15)	N3	C39	C40	127.04(17)
C18	C2	O4	118.26(15)	O6	C40	C39	118.45(18)
C18	C2	C3	123.40(16)	O6	C40	C41	124.38(18)
C2	C3	C4	123.41(16)	C41	C40	C39	117.14(16)
C11	C3	C2	116.89(16)	C42	C41	C40	120.72(18)
C11	C3	C4	119.64(16)	C41	C42	C43	126.10(19)
C5	C4	C3	122.56(16)	C44	C43	C42	119.1(2)
C10	C4	C3	118.77(16)	C44	C43	C48	118.5(2)
C10	C4	C5	118.43(17)	C48	C43	C42	122.41(18)
C6	C5	C4	120.64(17)	C45	C44	C43	120.9(2)
C5	C6	C7	120.14(17)	C46	C45	C44	120.2(2)
C6	C7	C8B	120.2(4)	C45	C46	C47	119.7(2)
C6	C7	C8	118.0(2)	C48	C47	C46	120.7(2)
C6	C7	C8A	118.7(3)	C47	C48	C43	120.1(2)
C9	C7	C8B	118.7(4)	C51	O7	C50	112.4(2)
C9	C7	C8	122.1(2)	O7	C50	C49	109.5(3)
C9	C7	C8A	120.5(3)	O7	C51	C52	108.8(2)
C9	C7	C6	119.92(18)	C51A	O7A	C50A	112.9(9)

C10	C9	C7	119.93(18)	O7A	C50A	C49A	108.2(9)
C9	C10	C4	120.93(18)	O7A	C51A	C52A	108.6(9)
C3	C11	C12	122.32(17)	C54	O8	C55	113.9(5)
C11	C12	C13	120.90(17)	O8	C54	C53	109.8(6)
C11	C12	C17	119.77(17)	O8	C55	C56	108.6(5)
C17	C12	C13	119.32(17)	C55A	O8A	C54A	112.7(8)
C14	C13	C12	120.34(18)	O8A	C54A	C53A	107.7(7)
C13	C14	C15	120.33(18)	O8A	C55A	C56A	109.3(9)
C16	C15	C14	120.71(19)				

Table 2.13 Hydrogen Bonds for yoon62a

D	H	A	d(D-H)/Å	d(H-A)/Å	d(D-A)/Å	D-H-A/°
N3	H3	O3	0.86(3)	1.87(3)	2.714(2)	170(2)
C41	H41	O3	0.95	2.27	3.202(2)	166.2
C48	H48	O3	0.95	2.79	3.716(2)	164.9

Table 2.14 Torsion Angles for yoon62a

A	B	C	D	Angle/°	A	B	C	D	Angle/°
P1	O4	C2	C3	-109.76(16)	C13	C12	C17	C18	-179.60(18)
P1	O4	C2	C18	71.67(19)	C13	C14	C15	C16	1.1(3)
P1	O5	C28	C19	76.47(18)	C14	C15	C16	C17	-0.4(3)

P1	O5	C28	C27	-103.82(16)	C15	C16	C17	C12	-1.5(3)
C8B	C7	C9	C10	-167.2(6)	C15	C16	C17	C18	-179.05(18)
F4	C8B	C7	C6	165.1(6)	C16	C17	C18	C2	171.51(18)
F4	C8B	C7	C9	-27.4(12)	C16	C17	C18	C19	-7.2(3)
F4	C8	C7	C6	175.7(2)	C17	C12	C13	C14	-2.1(3)
F4	C8	C7	C9	-6.0(4)	C17	C18	C19	C20	-59.9(2)
F4	C8A	C7	C6	-172.2(4)	C17	C18	C19	C28	124.48(19)
F4	C8A	C7	C9	18.7(8)	C18	C2	C3	C4	174.51(17)
F5B	C8B	C7	C6	-69.7(10)	C18	C2	C3	C11	-2.5(3)
F5B	C8B	C7	C9	97.9(9)	C18	C19	C20	C21	-2.4(3)
F6B	C8B	C7	C6	47.9(9)	C18	C19	C20	C25	-179.08(16)
F6B	C8B	C7	C9	-144.5(8)	C18	C19	C28	O5	0.0(2)
C8	C7	C9	C10	-177.8(3)	C18	C19	C28	C27	-179.67(16)
F5	C8	C7	C6	-64.2(4)	C19	C20	C21	C22	-177.10(18)
F5	C8	C7	C9	114.1(3)	C19	C20	C25	C24	178.22(16)
F6	C8	C7	C6	55.1(4)	C19	C20	C25	C26	-0.3(3)
F6	C8	C7	C9	-126.7(3)	C20	C19	C28	O5	-175.70(15)
C8A	C7	C9	C10	169.4(4)	C20	C19	C28	C27	4.6(3)
F5A	C8A	C7	C6	-54.2(6)	C20	C21	C22	C23	-0.7(3)
F5A	C8A	C7	C9	136.7(4)	C20	C25	C26	C27	3.2(3)
F6A	C8A	C7	C6	64.1(7)	C21	C20	C25	C24	1.4(3)
F6A	C8A	C7	C9	-105.0(5)	C21	C20	C25	C26	-177.08(17)

C33 C32 C34 C35	177.75(17)	C21 C22 C23 C24	0.9(3)
F7 C33 C32 C31	-155.72(19)	C22 C23 C24 C25	0.1(3)
F7 C33 C32 C34	27.6(3)	C23 C24 C25 C20	-1.3(3)
F8 C33 C32 C31	-35.1(3)	C23 C24 C25 C26	177.23(17)
F8 C33 C32 C34	148.18(18)	C24 C25 C26 C27	-175.33(17)
F9 C33 C32 C31	83.9(2)	C25 C20 C21 C22	-0.5(3)
F9 C33 C32 C34	-92.7(2)	C25 C26 C27 C28	-2.1(3)
O1 S1 N1 P1	165.06(12)	C25 C26 C27 C29	178.19(16)
O1 S1 C1 F1	-69.98(17)	C26 C27 C28 O5	178.46(15)
O1 S1 C1 F2	49.90(16)	C26 C27 C28 C19	-1.9(3)
O1 S1 C1 F3	170.31(15)	C26 C27 C29 C30	-35.1(2)
O2 S1 N1 P1	28.27(17)	C26 C27 C29 C35	141.56(18)
O2 S1 C1 F1	52.12(17)	C27 C29 C30 C31	177.56(17)
O2 S1 C1 F2	172.00(14)	C27 C29 C35 C34	-177.06(16)
O2 S1 C1 F3	-67.60(16)	C28 C19 C20 C21	173.22(17)
O3 P1 O4 C2	-164.13(12)	C28 C19 C20 C25	-3.4(3)
O3 P1 O5 C28	66.70(14)	C28 C27 C29 C30	145.22(18)
O3 P1 N1 S1	4.19(17)	C28 C27 C29 C35	-38.1(3)
O4 P1 O5 C28	-48.39(13)	C29 C27 C28 O5	-1.9(2)
O4 P1 N1 S1	128.09(12)	C29 C27 C28 C19	177.82(17)
O4 C2 C3 C4	-4.0(3)	C29 C30 C31 C32	-0.3(3)
O4 C2 C3 C11	179.06(15)	C30 C29 C35 C34	-0.3(3)

O4	C2	C18C17	-174.91(15)	C30	C31	C32	C33	-177.35(17)	
O4	C2	C18C19	3.8(2)	C30	C31	C32	C34	-0.7(3)	
O5	P1	O4	C2	-44.83(14)	C31	C32	C34	C35	1.1(3)
O5	P1	N1	S1	-123.22(12)	C32	C34	C35	C29	-0.6(3)
N1	S1	C1	F1	173.89(15)	C35	C29	C30	C31	0.8(3)
N1	S1	C1	F2	-66.23(16)	O6	C40	C41	C42	-3.0(3)
N1	S1	C1	F3	54.17(17)	N2	C37	C38	N3	0.2(2)
N1	P1	O4	C2	63.85(14)	N2	C39	C40	O6	-4.1(3)
N1	P1	O5	C28	-160.90(12)	N2	C39	C40	C41	177.80(17)
C1	S1	N1	P1	-84.61(14)	N3	C39	C40	O6	171.78(19)
C2	C3	C4	C5	-37.0(3)	N3	C39	C40	C41	-6.3(3)
C2	C3	C4	C10	148.69(18)	C36	N2	C37	C38	-179.30(19)
C2	C3	C11C12	-2.3(3)	C36	N2	C39	N3	179.1(2)	
C2	C18	C19C20	121.38(19)	C36	N2	C39	C40	-4.3(3)	
C2	C18	C19C28	-54.2(2)	C37	N2	C39	N3	0.0(2)	
C3	C2	C18C17	6.6(3)	C37	N2	C39	C40	176.58(18)	
C3	C2	C18C19	-174.66(16)	C38	N3	C39	N2	0.1(2)	
C3	C4	C5	C6	-173.24(18)	C38	N3	C39	C40	-176.37(18)
C3	C4	C10C9	173.99(18)	C39	N2	C37	C38	-0.1(2)	
C3	C11	C12C13	-176.15(18)	C39	N3	C38	C37	-0.2(2)	
C3	C11	C12C17	2.6(3)	C39	C40	C41	C42	175.00(18)	
C4	C3	C11C12	-179.38(16)	C40	C41	C42	C43	-175.45(18)	

C4 C5 C6 C7	-0.9(3)	C41 C42 C43 C44	171.8(2)
C5 C4 C10C9	-0.5(3)	C41 C42 C43 C48	-6.5(3)
C5 C6 C7 C8B	167.5(7)	C42 C43 C44 C45	-177.5(2)
C5 C6 C7 C8	178.4(2)	C42 C43 C48 C47	178.15(19)
C5 C6 C7 C8A	-169.1(4)	C43 C44 C45 C46	-0.8(4)
C5 C6 C7 C9	0.1(3)	C44 C43 C48 C47	-0.1(3)
C6 C7 C9 C10	0.4(3)	C44 C45 C46 C47	0.2(4)
C7 C9 C10C4	-0.2(3)	C45 C46 C47 C48	0.5(3)
C10 C4 C5 C6	1.1(3)	C46 C47 C48 C43	-0.5(3)
C11 C3 C4 C5	139.87(19)	C48 C43 C44 C45	0.8(3)
C11 C3 C4 C10	-34.4(3)	C50 O7 C51 C52	172.1(3)
C11 C12 C13C14	176.64(19)	C51 O7 C50 C49	176.1(2)
C11 C12 C17C16	-176.02(17)	C50AO7AC51AC52A	179.4(17)
C11 C12 C17C18	1.6(3)	C51AO7AC50AC49A	171.6(19)
C12 C13 C14C15	0.2(3)	C54 O8 C55 C56	-179.9(6)
C12 C17 C18C2	-6.0(3)	C55 O8 C54 C53	-171.7(6)
C12 C17 C18C19	175.28(17)	C54AO8AC55AC56A	177.1(14)
C13 C12 C17C16	2.8(3)	C55AO8AC54AC53A	-174.1(14)

Table 2.15 Hydrogen Atom Coordinates ($\text{\AA} \times 10^4$) and Isotropic Displacement Parameters ($\text{\AA}^2 \times 10^3$) for yoon62a

Atom	x	y	z	U(eq)
H5	6352.46	4653.03	4260.3	23

H6	7996.41	4681.51	4001.12	27
H9	7330.36	6068.96	2643.73	29
H10	5688.05	6059.21	2909.07	26
H11	4661.08	6595.71	3549.8	24
H13	3186.85	7441.11	3600.22	30
H14	1554.43	7588.8	3837.35	33
H15	697.51	6525.38	4270.51	30
H16	1480.26	5332.3	4486.94	27
H21	2971.48	5560.56	5293.36	27
H22	2495.37	5695.85	6225.66	30
H23	1755.53	4613.29	6709.62	30
H24	1535.6	3390.84	6259	26
H26	1726.44	2534.1	5419.01	22
H30	2526.57	1384.75	5160.74	25
H31	2331.81	97.74	4789.64	27
H34	1798.83	1061.8	3243.1	26
H35	2012.77	2351.78	3611.06	23
H3	4545(18)	1483(16)	3991(10)	23
H36A	4222.77	-1204.81	4620.59	55
H36B	5387.31	-1110.92	4587.51	55
H36C	4803.31	-1520.01	4075.37	55
H37	4528.14	-624.6	3251.31	32

H38	4387.25	846.66	3071.35	28
H41	4764.62	1830.33	4878.36	27
H42	4715.65	1163.46	5964.34	30
H44	4457.3	2037.51	6757.43	43
H45	4298.3	3312.65	7157.81	49
H46	4422.81	4459.84	6591.41	43
H47	4697.86	4326.89	5620.18	37
H48	4827.78	3057.61	5208.66	32
H49A	3565.12	7204.89	4987.02	66
H49B	4107.76	7716.47	5467.88	66
H49C	3675.63	6844.68	5612.25	66
H50A	5376.69	6763.4	5492.68	43
H50B	4831.89	6247.38	5012.63	43
H51A	6298.27	6401.12	4492.89	48
H51B	6792.14	7050.83	4907.06	48
H52A	6229.46	7396.39	3771.33	77
H52B	7333.84	7220.88	3960.76	77
H52C	6783.49	8010.13	4183.87	77
H49D	3120.28	8580.81	5355.61	101
H49E	3578.41	8378.24	5962.77	101
H49F	2447.77	8196.06	5840.01	101
H50C	3318.2	6988.92	5788.33	68

H50D 2914.2	7209.25	5168.83	68
H51C 4298.07	6365.89	4847.3	47
H51D 4717.05	6289.74	5480.16	47
H52D 5737.23	7083.59	4587.1	59
H52E 5991.57	6192.68	4799.23	59
H52F 6159.1	6944.69	5211.66	59
H53A 1905.9	5229.53	2486.49	111
H53B 2771.42	5044.53	2924.22	111
H53C 1656.18	4913.23	3110.05	111
H54A 2717.82	3973.63	2321.99	76
H54B 2276.13	3666.55	2912.99	76
H55A 1248	2685.11	2525.62	58
H55B 1746.99	2860.71	1922.69	58
H56A 222.69	3192.41	1538.98	74
H56B -286.7	3064.9	2142.56	74
H56C 162.28	2310.77	1810.18	74
H53D 2027.13	5620.75	2389.64	100
H53E 2379.14	5610.74	3035.91	100
H53F 1249.76	5470.08	2885.39	100
H54C 2764.48	4382.51	2567.26	77
H54D 2059.75	4238.22	3102.38	77
H55C 1350.77	3081.38	2719.5	114

H55D 2050.93	3134.19	2175.29	114
H56D 641.05	3258.38	1591.82	138
H56E -33.79	3148.37	2140.29	138
H56F 643.54	2422.15	1928.48	138

Table 2.16 Atomic Occupancy for yoon62a

Atom Occupancy	Atom Occupancy	Atom Occupancy
C8B 0.151(4)	F5B 0.151(4)	F6B 0.151(4)
C8 0.552(4)	F5 0.552(4)	F6 0.552(4)
C8A 0.297(4)	F5A 0.297(4)	F6A 0.297(4)
O7 0.837(4)	C49 0.837(4)	H49A 0.837(4)
H49B 0.837(4)	H49C 0.837(4)	C50 0.837(4)
H50A 0.837(4)	H50B 0.837(4)	C51 0.837(4)
H51A 0.837(4)	H51B 0.837(4)	C52 0.837(4)
H52A 0.837(4)	H52B 0.837(4)	H52C 0.837(4)
O7A 0.163(4)	C49A 0.163(4)	H49D 0.163(4)
H49E 0.163(4)	H49F 0.163(4)	C50A 0.163(4)
H50C 0.163(4)	H50D 0.163(4)	C51A 0.163(4)
H51C 0.163(4)	H51D 0.163(4)	C52A 0.163(4)
H52D 0.163(4)	H52E 0.163(4)	H52F 0.163(4)
O8 0.647(13)	C53 0.647(13)	H53A 0.647(13)
H53B 0.647(13)	H53C 0.647(13)	C54 0.647(13)

H54A 0.647(13)	H54B 0.647(13)	C55 0.647(13)
H55A 0.647(13)	H55B 0.647(13)	C56 0.647(13)
H56A 0.647(13)	H56B 0.647(13)	H56C 0.647(13)
O8A 0.353(13)	C53A 0.353(13)	H53D 0.353(13)
H53E 0.353(13)	H53F 0.353(13)	C54A 0.353(13)
H54C 0.353(13)	H54D 0.353(13)	C55A 0.353(13)
H55C 0.353(13)	H55D 0.353(13)	C56A 0.353(13)
H56D 0.353(13)	H56E 0.353(13)	H56F 0.353(13)

2.6.10 Computational Data

Computational Methods: All geometry optimizations were conducted using DFT⁷⁸ as implemented in the Jaguar 9.1 suite⁷⁹ of ab initio quantum chemistry programs with Becke's three-parameter exchange functional B3LYP including Grimme's D3 dispersion correction levels of theory,⁸⁰⁻⁸⁵ together with Pople's 6-31G** basis set.⁸⁶⁻⁹¹ Analytical vibrational frequencies within the harmonic approximation were calculated using the 6-31G** basis to confirm proper convergence to well-defined minima or saddle points on the potential energy surface. Additional single point calculations on each optimized geometry were carried out using time-dependent DFT (TDDFT) as implemented in the Q-Chem 5.0 suite⁹² of ab initio quantum chemistry programs with Handy's Coulomb-attenuating range-separated functional CAM-B3LYP including Grimme's D3 dispersion correction levels of theory.⁹³ Standard double- ζ quality 6-31G** basis set was used. Eigenstates of the time-dependent Hamiltonians were constructed based on configuration interaction singles (CIS), that is equivalent to the Tamm-Dancoff Approximation (TDA).⁹⁴

Supplementary Computational Analysis

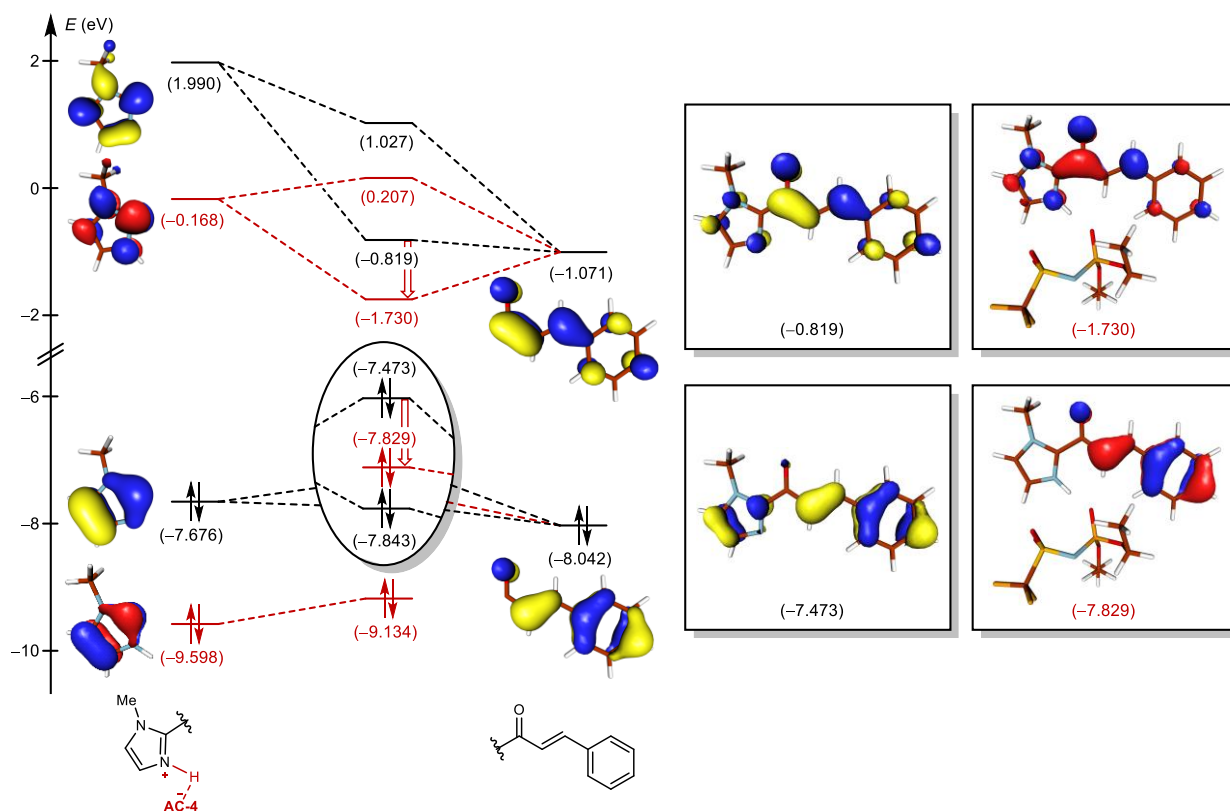


Figure 2.10 PMO diagram for **2.1** and **2.1-H⁺-2.41**. Each molecule was fragmented into the cinnamoyl part and the remaining portion of the molecule.

To understand the broken conjugation on FMO, we first fragmented the compound **2.1** and **2.1H⁺-2.41** into the cinnamoyl part and the remaining portion of the molecule. Our computation results revealed that the highest π orbital in cinnamoyl (-8.04 eV) has a node on the carbonyl carbon. Therefore, the resonance between the interacting orbitals is interrupted between this cinnamoyl π and the highest π in the imidazole ring in **2.1** (-7.68 eV) and the HOMO becomes dominated by the cinnamoyl- π orbital. The resulting spatial distance between the proton and the HOMO orbital leads to a modest energetic change of only 0.37 eV.

Table 2.17 TDDFT calculated singlet excited states for **2.1**. Only orbital contributions > 10% are shown.

State	Energy (nm)	Energy (eV)	f	Contributions
1	334.8	3.703	0.00004	D(53) → V(1) (86.1%)
2	282.2	4.394	1.16149	D(56) → V(1) (93.0%)
3	249.1	4.978	0.00653	D(54) → V(1) (61.7%) D(56) → V(3) (20.3%)
4	243.7	5.088	0.08326	D(55) → V(1) (91.6%)
5	231.2	5.363	0.00282	D(51) → V(1) (81.4%) D(51) → V(2) (12.1%)
6	208.2	5.956	0.04560	D(52) → V(1) (89.8%)
7	200.4	6.186	0.04391	D(54) → V(1) (14.4%) D(56) → V(2) (61.5%)
8	194.9	6.362	0.06528	D(54) → V(1) (20.5%) D(54) → V(2) (11.5%) D(56) → V(2) (15.1%) D(56) → V(3) (38.1%)

Table 2.18 TDDFT calculated singlet excited states for **2.1-H⁺-2.41**. Only orbital contributions > 10% are shown.

State	Energy (nm)	Energy (eV)	f	Contributions
1	338.7	3.661	0.00014	D(122) --> V(1) (79.5%)
2	309.2	4.010	0.87410	D(129) --> V(1) (91.9%)
3	271.4	4.569	0.04493	D(127) --> V(1) (79.3%) D(129) --> V(3) (10.3%)
4	264.2	4.693	0.00107	D(128) --> V(1) (97.6%)
5	234.3	5.291	0.01716	D(126) --> V(1) (79.2%)
6	232.8	5.326	0.15182	D(125) --> V(1) (80.5%)
7	220.7	5.618	0.00229	D(124) --> V(1) (70.1%)
8	213.4	5.809	0.04765	D(129) --> V(2) (70.0%) D(129) --> V(3) (10.7%)

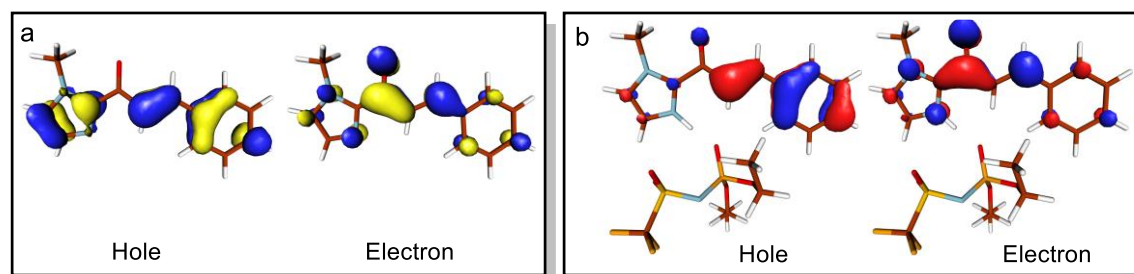


Figure 2.11 Natural transition orbital (NTO) pairs of 2nd singlet excitation ($S_0 \rightarrow S_2$) for (a) **2.1** and (b) **2.1-H⁺-2.41**. Each pair contributes more than 96% to the related excited state.

Cartesian coordinates of the optimized geometries. The cartesian coordinates of optimized geometries are given below in the standard XYZ format, and units are in Å.

=====
2.1
=====

O 6.427155495 -0.013798882 12.497465134
N 6.380298138 -0.552938819 9.674313545
N 6.262246132 1.651308775 9.317615509
C 6.474403381 -1.845172048 10.348769188
H 5.596687317 -2.009943008 10.975714684
H 7.353263378 -1.869160295 10.993429184
H 6.544090748 -2.624626160 9.587005615
C 6.316075325 -0.363703907 8.321063995
H 6.328906536 -1.195492744 7.632079601
C 6.243782997 1.002601027 8.123047829
H 6.180833817 1.533893704 7.182896137
C 6.346301079 0.699837625 10.247368813
C 6.375602245 0.931176066 11.702610016
C 6.336915970 2.346733093 12.118599892
H 6.287567139 3.084631205 11.326156616
C 6.340665817 2.670814991 13.426256180
H 6.372227192 1.840114236 14.131397247

C 6.296317101 4.011807919 14.006219864
C 6.216101646 4.141147137 15.405135155
H 6.196213245 3.243177414 16.017929077
C 6.158703327 5.394928455 16.009717941
H 6.094607353 5.471621513 17.091623306
C 6.183991432 6.548630238 15.225126266
H 6.140460491 7.528513432 15.692538261
C 6.268150330 6.438290119 13.832900047
H 6.291178703 7.333881855 13.218034744
C 6.323471546 5.187180042 13.229275703
H 6.393694401 5.118445396 12.148109436

=====

2.1-H⁺-2.41

=====

P -1.407773614 0.520450652 -1.871919990
O -0.164231136 0.664911628 -1.019078016
N -1.522876382 1.393084526 -3.231966972
S -0.239011571 1.750511408 -4.092240334
O 0.379219294 3.045600891 -3.744997501
O 0.703656375 0.622903526 -4.302136421
O -1.618558407 -1.047259450 -2.152693748
C -2.404579163 -2.970228910 -3.332762480
C -2.588449001 -1.477125049 -3.139763832

O -2.736045361 0.898019850 -1.031085014
C -2.333542824 3.306372881 -0.571093976
C -3.291325808 2.238179684 -1.082799077
F -1.968050838 2.971671104 -5.689023972
C -1.057345867 1.994343758 -5.744192123
F -1.656311989 0.859720528 -6.136800766
F -0.123743474 2.321418524 -6.648033142
H -3.123731136 -3.344753504 -4.069211960
H -1.393488646 -3.183697939 -3.691421986
H -2.558938265 -3.504368305 -2.390373707
H -3.594598293 -1.238955021 -2.772246361
H -2.418439865 -0.924975991 -4.070244312
H -2.845417976 4.275095940 -0.563575327
H -2.005577087 3.081357718 0.447150946
H -1.458104610 3.391085386 -1.220987558
H -3.590227842 2.449120045 -2.114103079
H -4.186699867 2.180752277 -0.456925184
C 2.545766354 2.367328644 1.087745190
O 3.353884935 2.886400223 1.862089992
N 4.155934334 2.533445597 -0.853134990
C 5.257688046 3.192629814 -0.143432140
C 4.180199623 2.197299719 -2.187635899
C 2.957149744 2.162981033 -0.336523533

N 2.246168375 1.604953885 -1.334408879
H 1.249796391 1.210805058 -1.265318036
C 2.977432728 1.614094496 -2.487123251
H 5.598648071 2.565735340 0.679095328
H 4.917398453 4.140673637 0.270473778
H 6.063294888 3.356174469 -0.860095203
H 5.036273003 2.407986641 -2.807801485
H 2.563154697 1.232409239 -3.409425974
C 1.202345371 1.926411033 1.430601001
H 0.591178358 1.497008562 0.648649037
C 0.712462544 2.046100616 2.686457396
H 1.355920553 2.490784645 3.444935322
C -0.621438026 1.632383823 3.102500439
C -1.031252742 1.866956353 4.428695202
C -1.527670860 1.012682557 2.212691069
H -0.341636807 2.341548443 5.122364998
C -2.306092978 1.503654957 4.855424881
H -2.607722282 1.691848874 5.881597996
C -3.194145679 0.899906158 3.962406874
H -4.189340591 0.617787480 4.294123173
C -2.799879313 0.656728029 2.641683102
H -3.481677055 0.190041915 1.937102437
H -1.245238423 0.808451891 1.187050581

Vibrational frequencies (in cm⁻¹) of the optimized structures

=====

2.1

=====

30.53 40.09 60.45 98.84 118.22 148.12
186.67 204.87 216.07 238.68 286.09 310.51
407.45 413.42 453.60 501.17 546.47 587.62
630.06 632.42 667.74 702.96 711.64 752.69
767.92 791.86 798.37 855.63 867.26 906.88
913.04 935.59 939.37 977.26 1001.96 1013.67
1043.64 1047.24 1060.91 1085.16 1106.57 1116.51
1153.65 1197.91 1198.92 1218.30 1242.97 1257.31
1322.91 1335.41 1348.08 1371.79 1374.33 1406.65
1451.44 1463.81 1487.27 1492.28 1504.27 1527.35
1540.42 1552.41 1630.56 1655.99 1668.89 1732.38
3073.41 3155.86 3158.09 3166.80 3172.90 3179.67
3189.55 3199.48 3206.71 3224.60 3248.68 3276.49

=====

2.1-H⁺-2.41

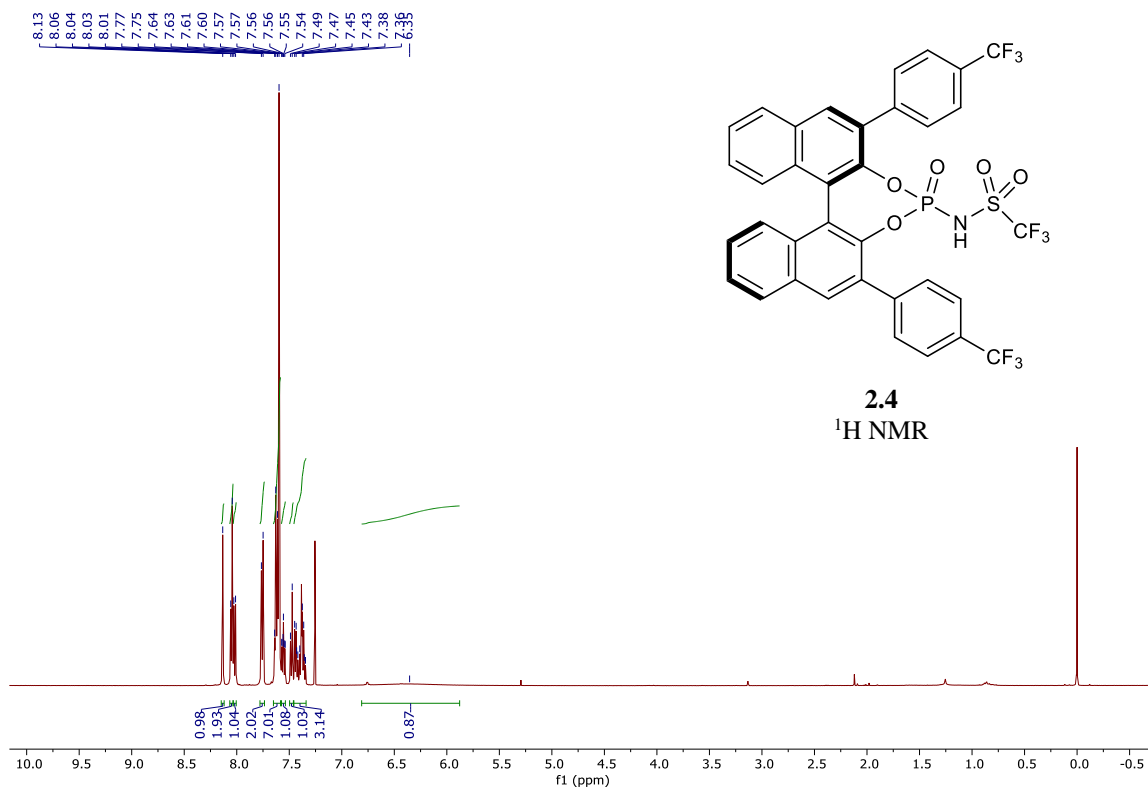
=====

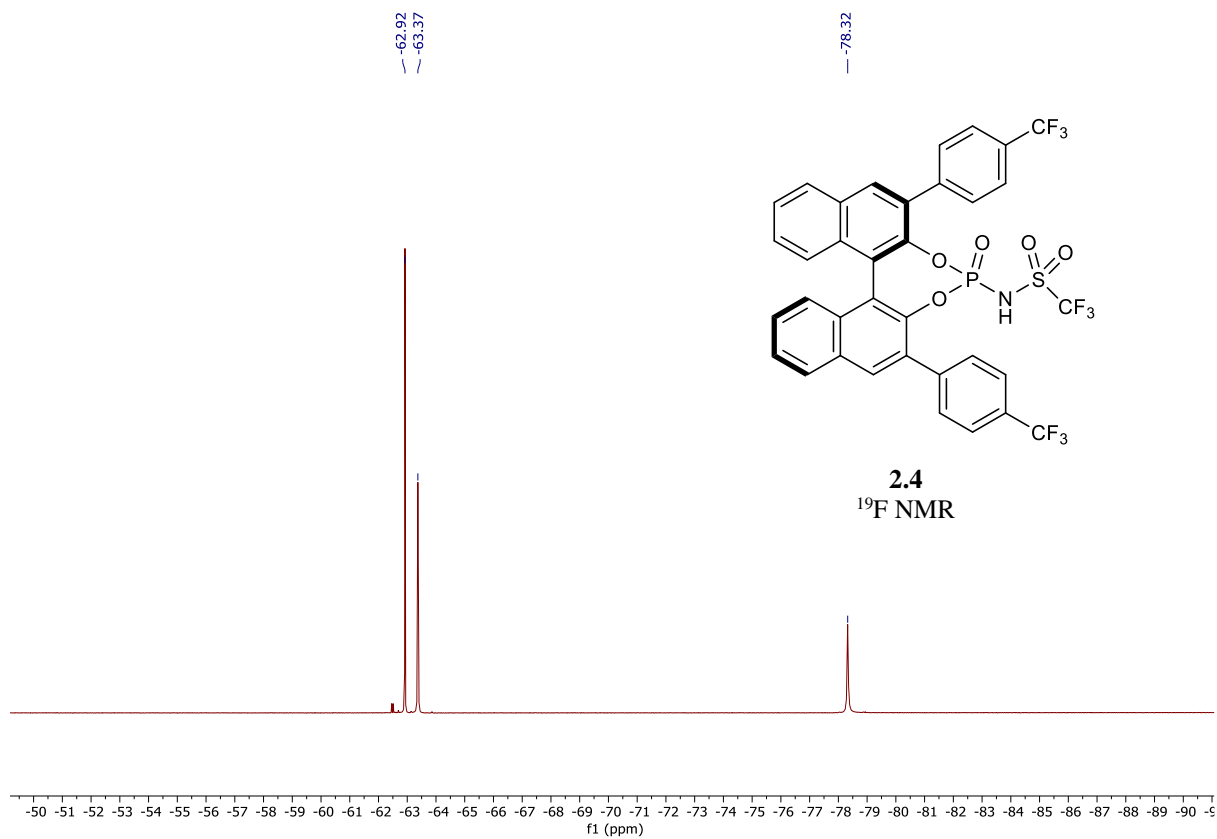
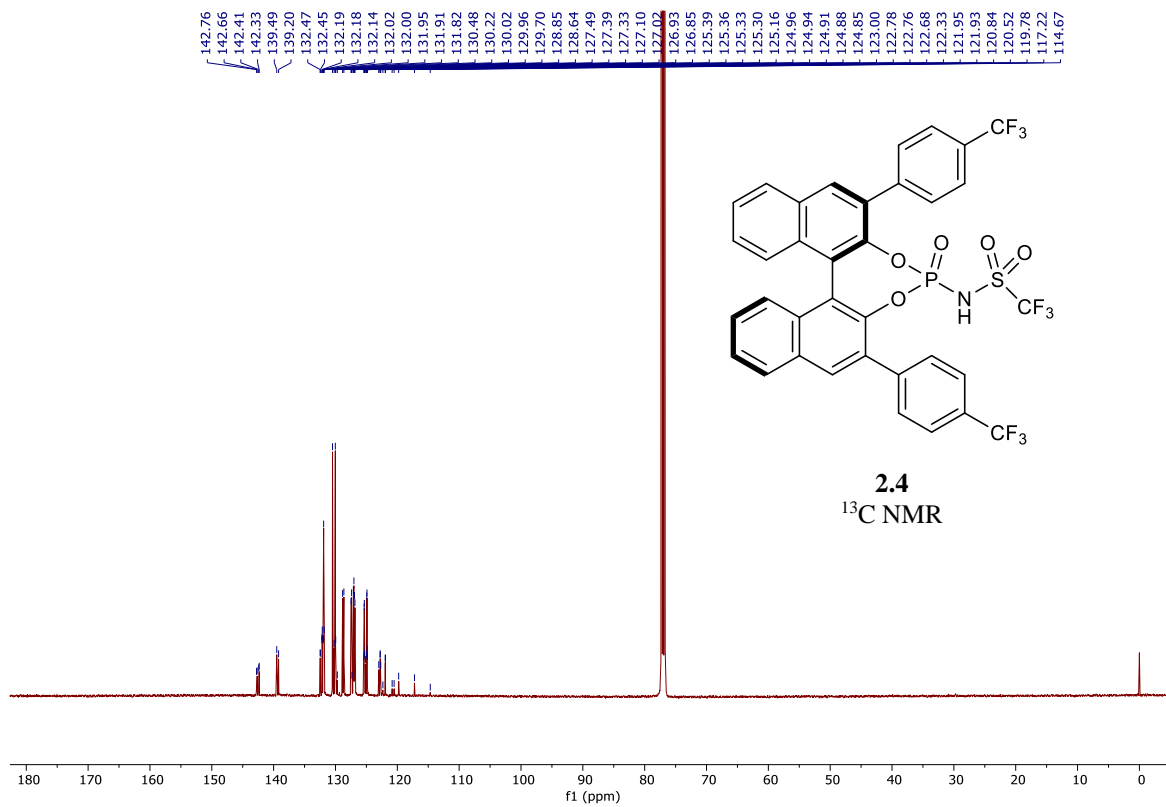
2.79 16.72 20.78 28.35 37.84 39.83
44.90 51.62 53.03 59.95 65.33 71.93
79.37 89.47 91.21 104.63 113.82 120.57

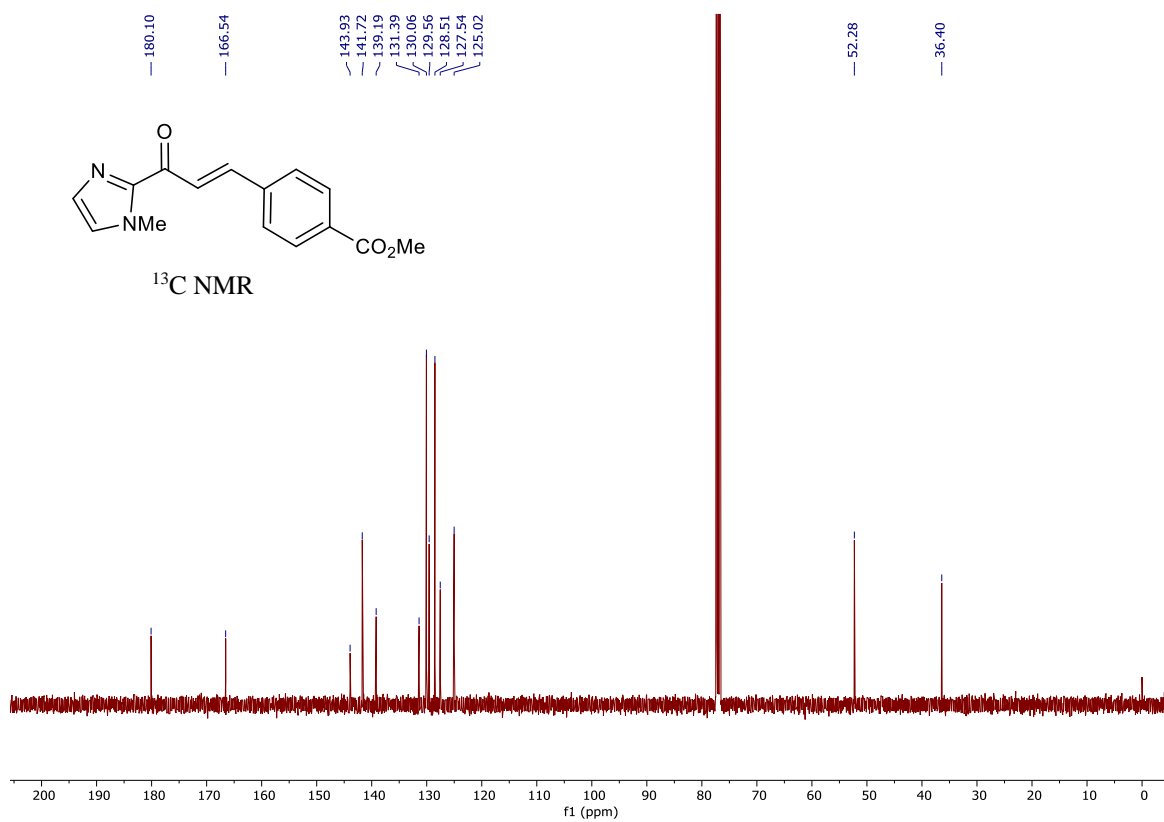
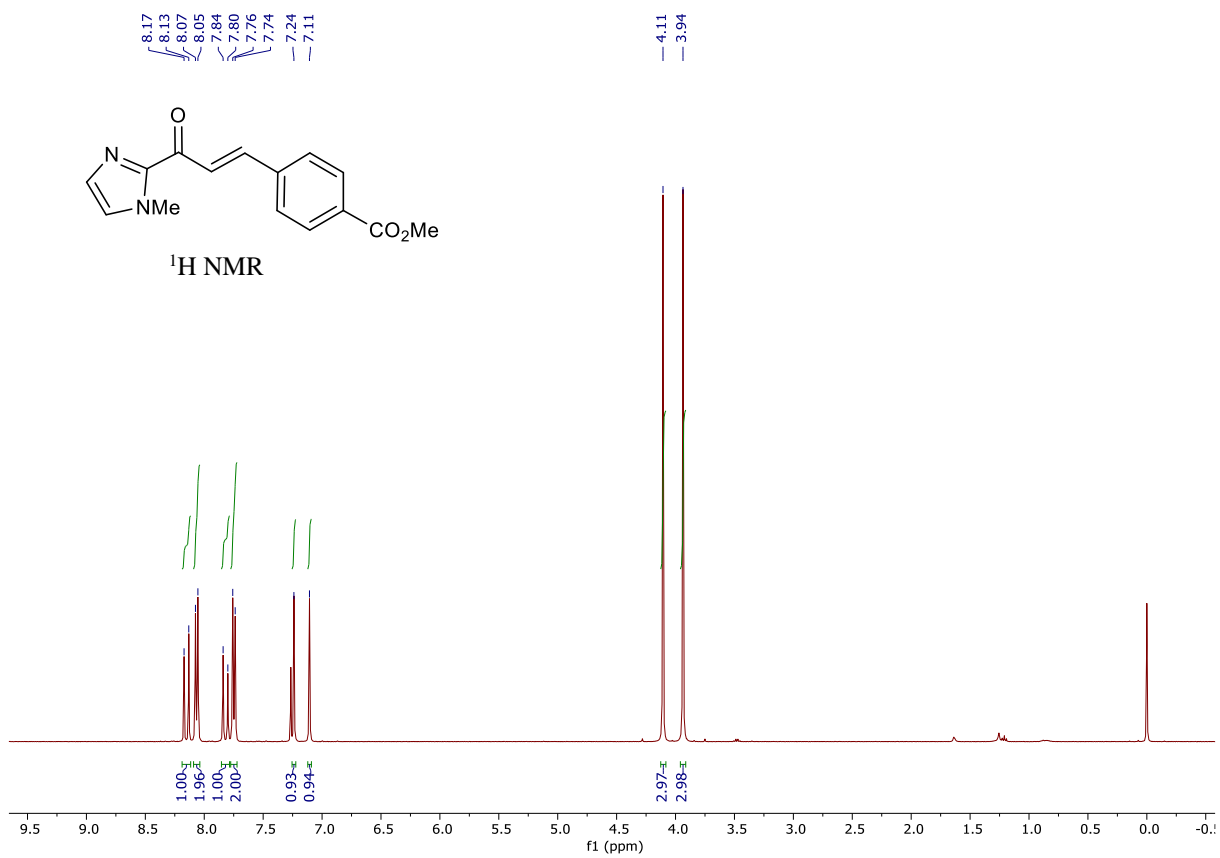
135.01 163.16 169.31 180.98 186.81 196.62
199.82 205.22 228.16 254.20 257.02 269.70
274.91 285.81 292.15 299.84 317.11 323.34
348.20 349.77 407.11 410.08 417.82 436.64
450.82 458.75 498.68 499.03 513.07 542.34
543.94 550.65 564.25 586.70 630.58 631.55
634.62 644.62 702.14 703.99 716.00 750.22
757.96 779.07 793.15 794.80 800.51 824.98
832.63 844.06 866.85 891.48 897.17 927.50
931.43 934.42 947.98 978.40 992.50 1013.29
1016.27 1031.24 1052.15 1058.24 1062.27 1065.98
1071.74 1078.31 1105.65 1122.75 1123.86 1129.91
1131.58 1152.50 1153.05 1163.85 1187.39 1191.51
1197.62 1199.02 1223.98 1225.15 1229.81 1242.44
1246.17 1257.57 1263.58 1312.81 1322.68 1328.71
1332.82 1365.82 1378.05 1396.65 1406.92 1408.78
1419.62 1439.32 1440.36 1446.59 1467.06 1486.65
1493.70 1496.81 1505.19 1508.44 1510.16 1516.34
1520.79 1523.82 1537.60 1539.78 1544.67 1627.31
1648.31 1660.63 1675.20 1730.92 2559.50 3040.20
3049.66 3051.18 3066.34 3091.16 3097.39 3115.34
3123.98 3125.02 3137.03 3149.05 3164.27 3176.42
3184.13 3186.36 3187.91 3199.53 3208.65 3227.68

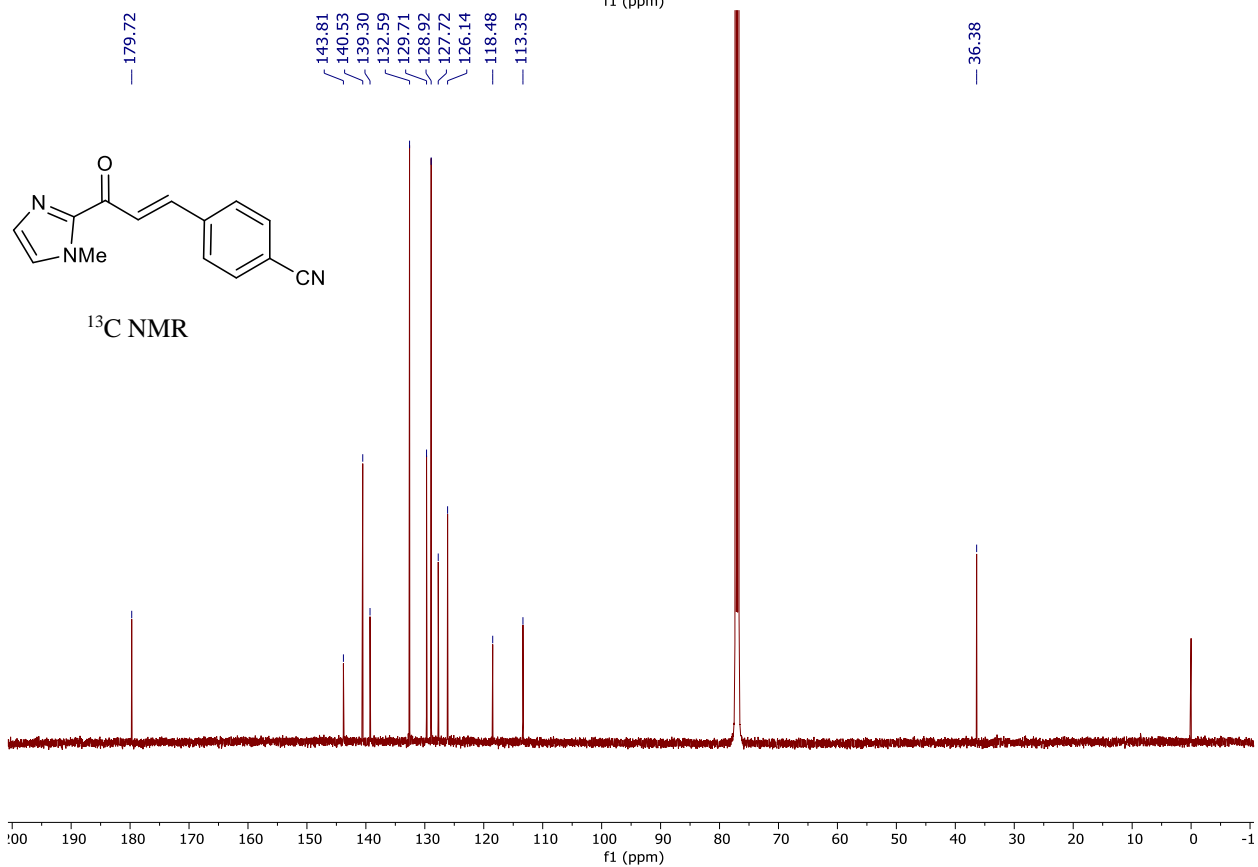
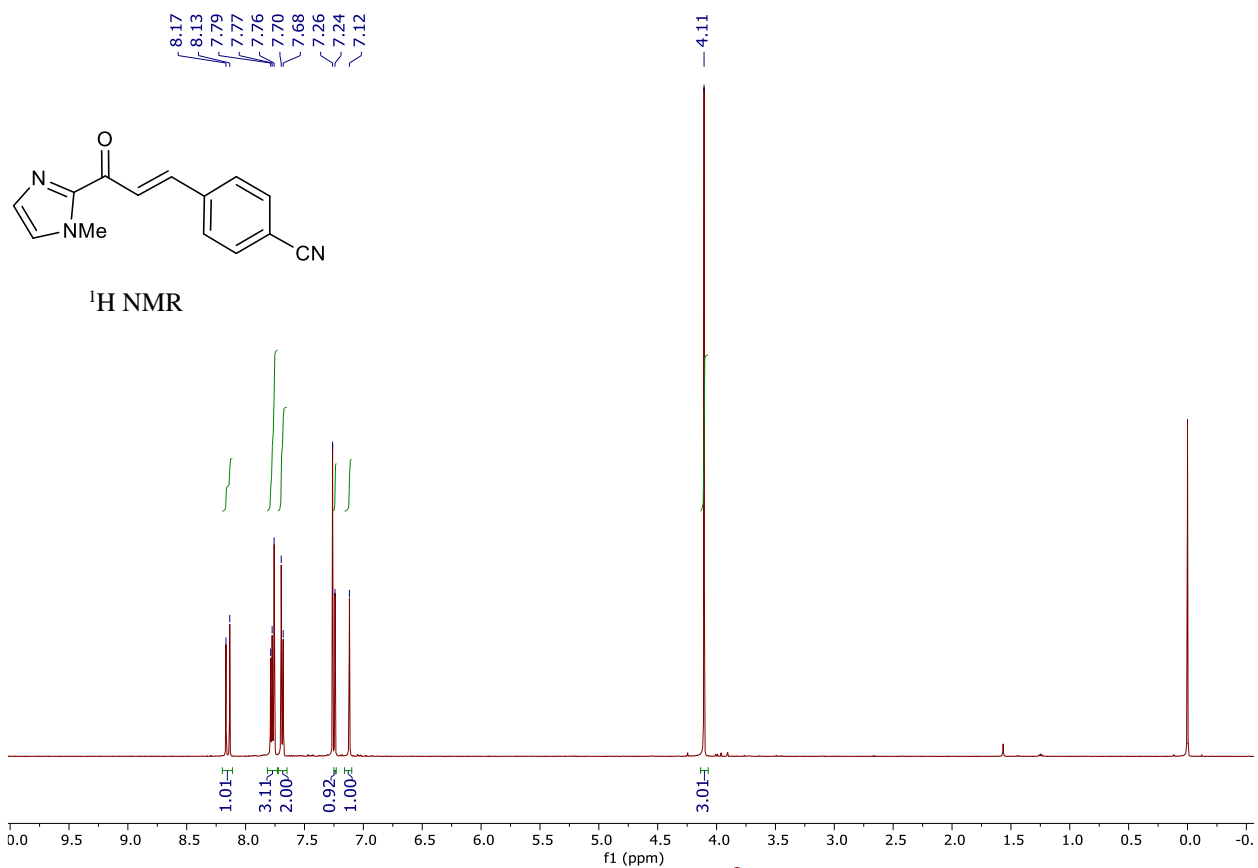
3245.00 3268.12 3306.06

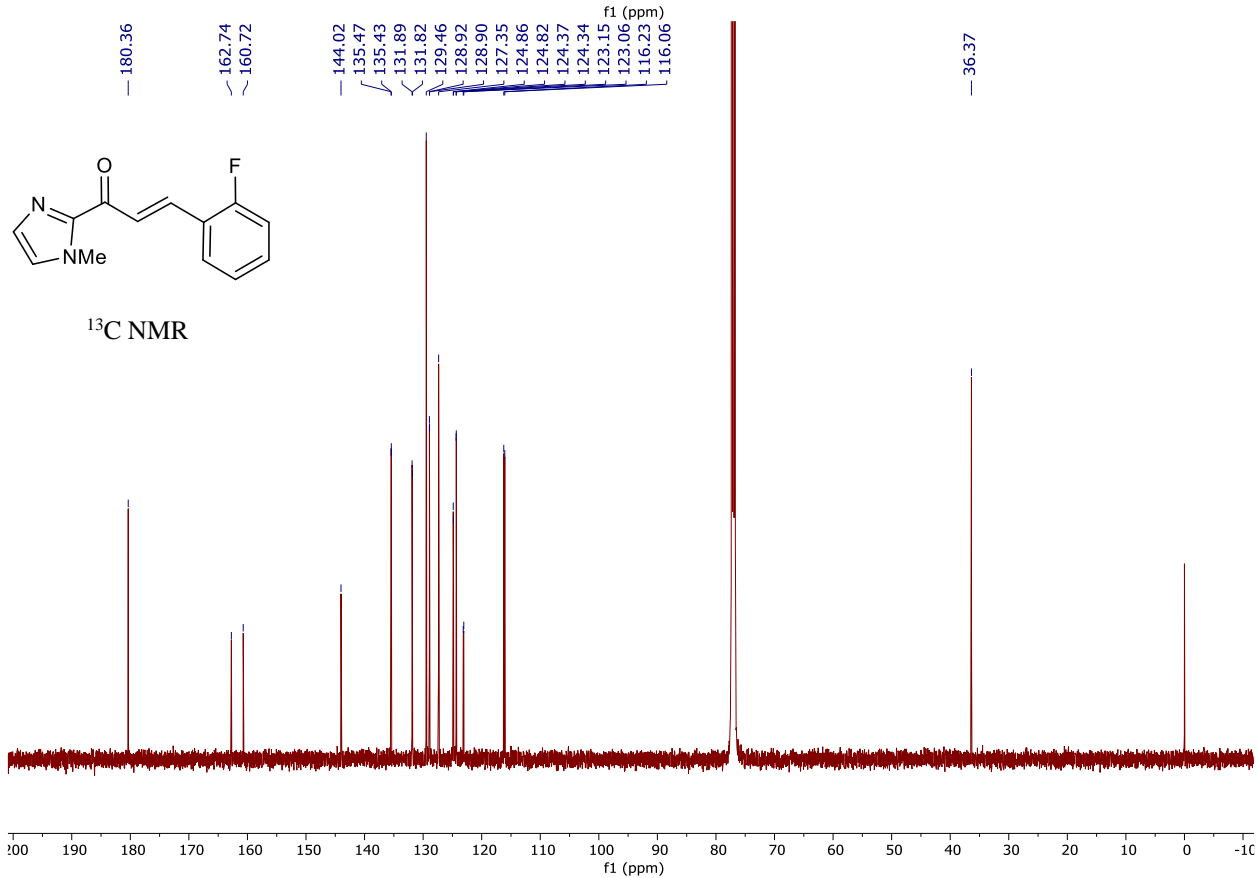
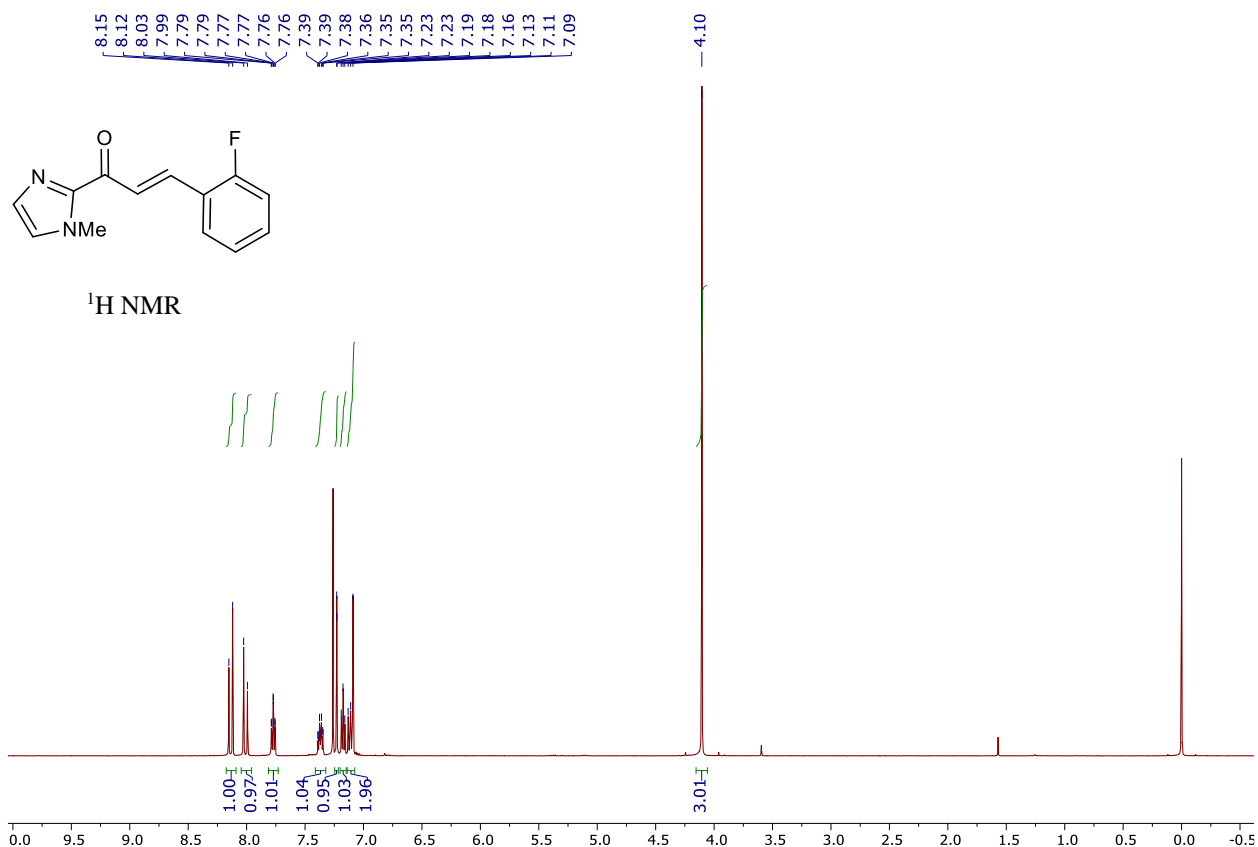
2.6.11 NMR Data

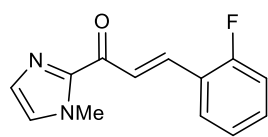




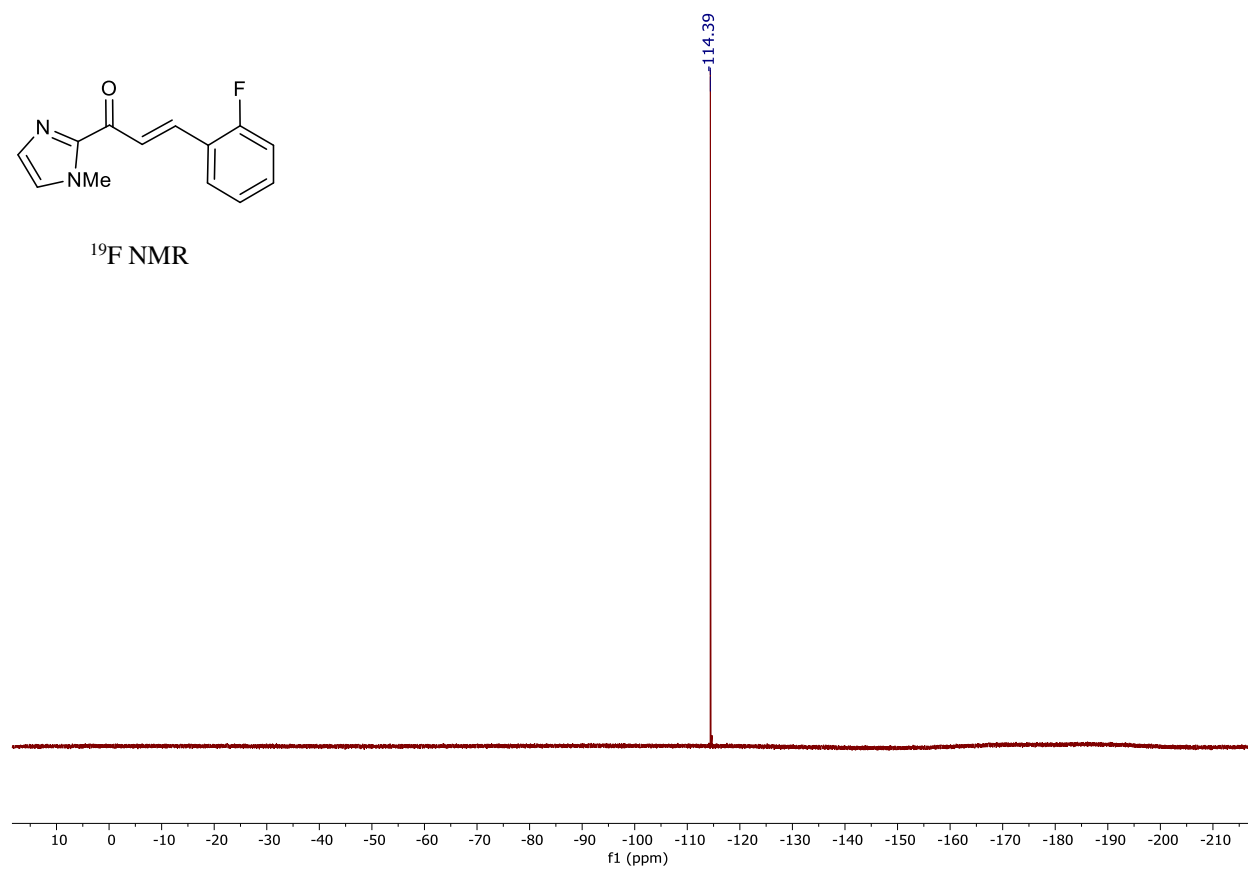


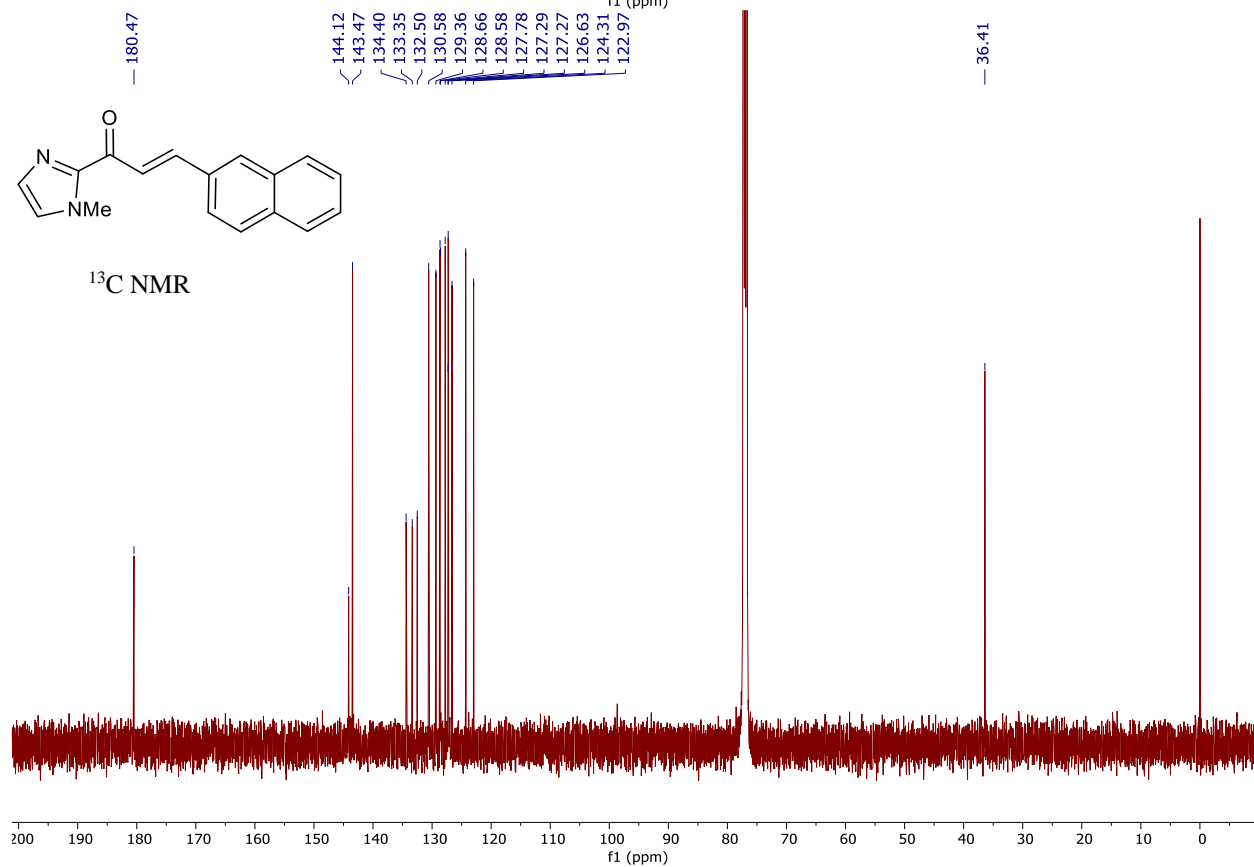
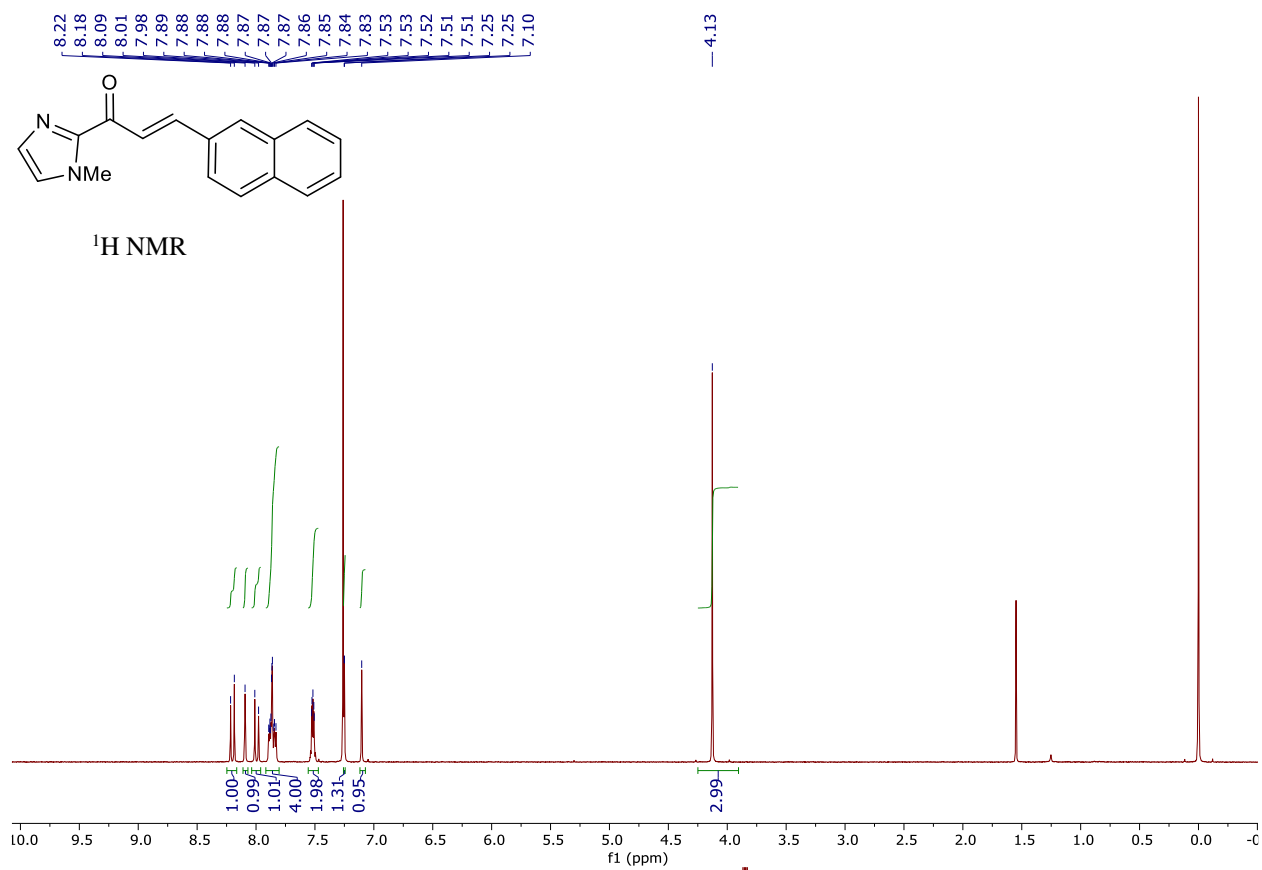


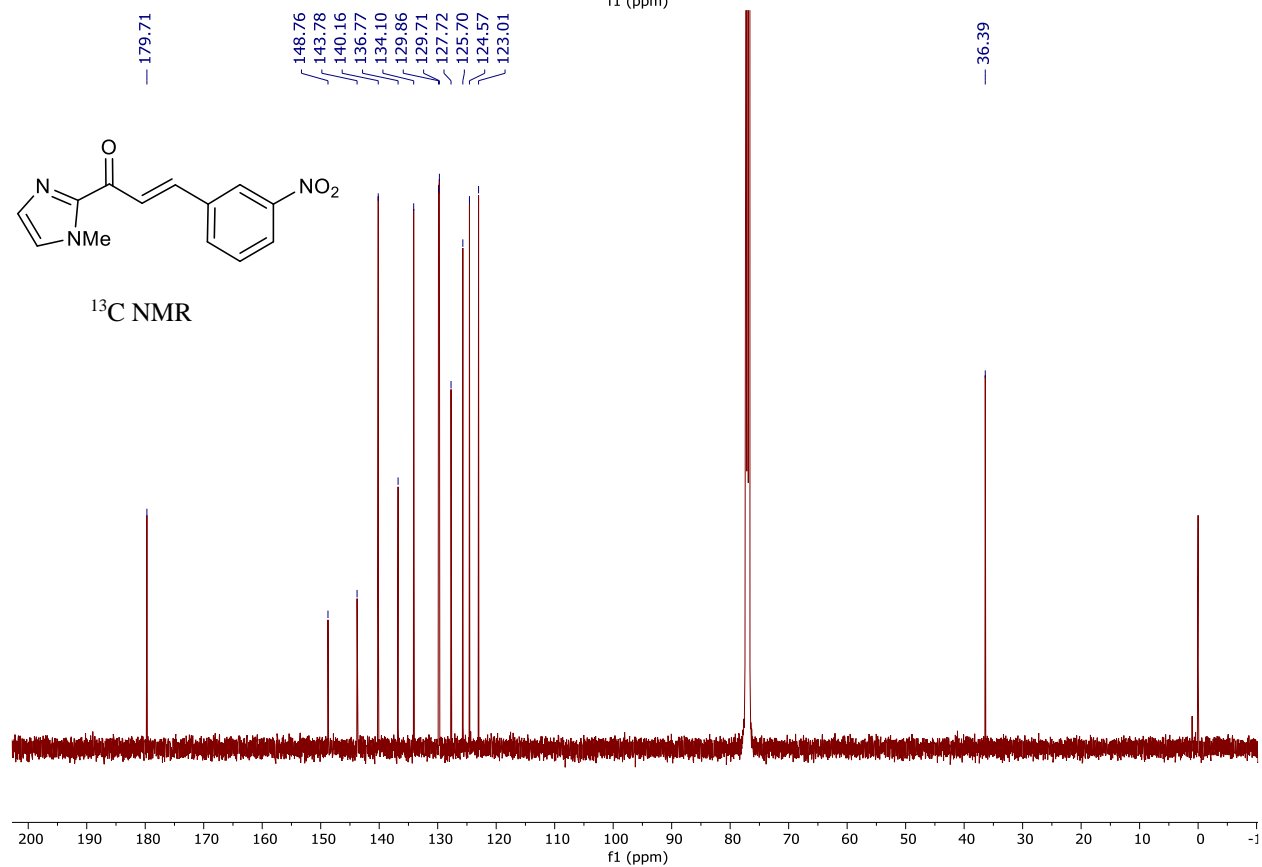
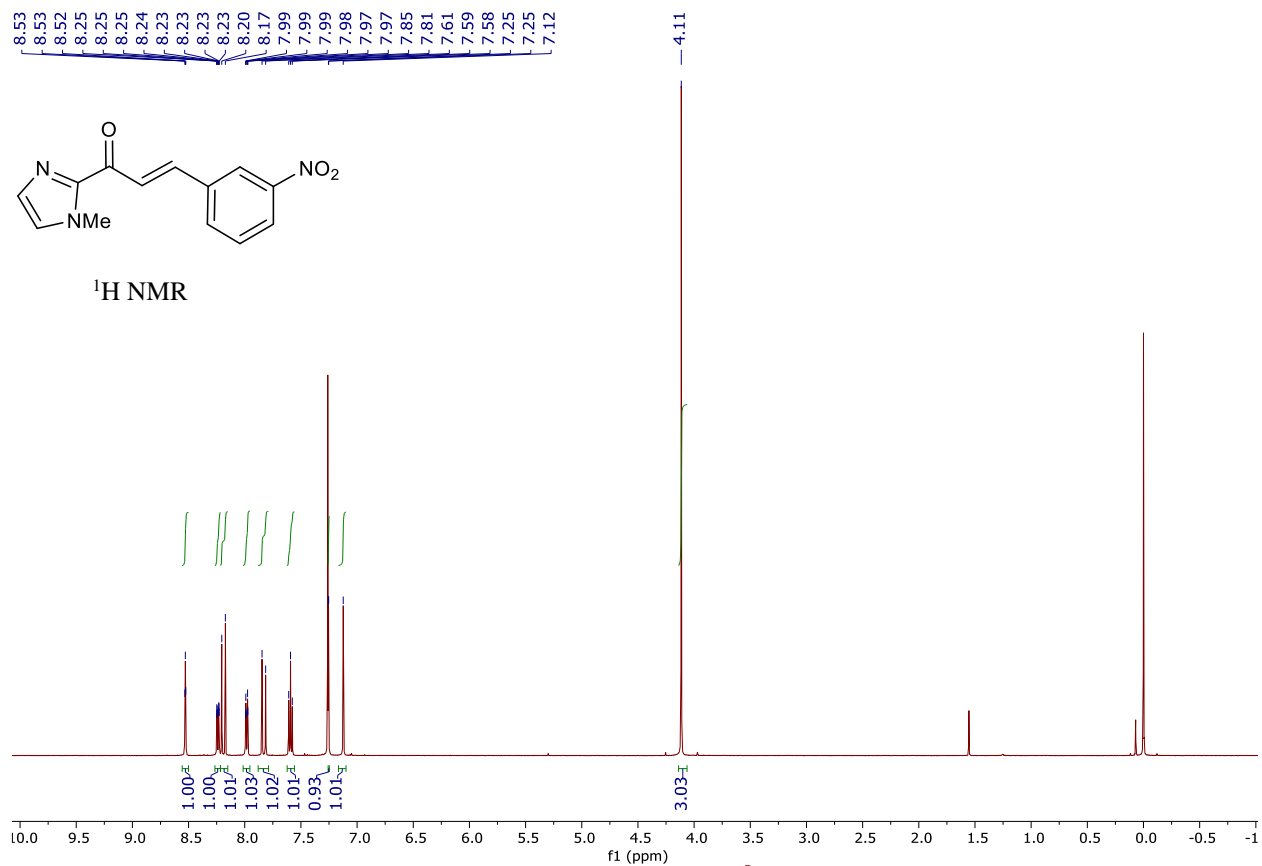


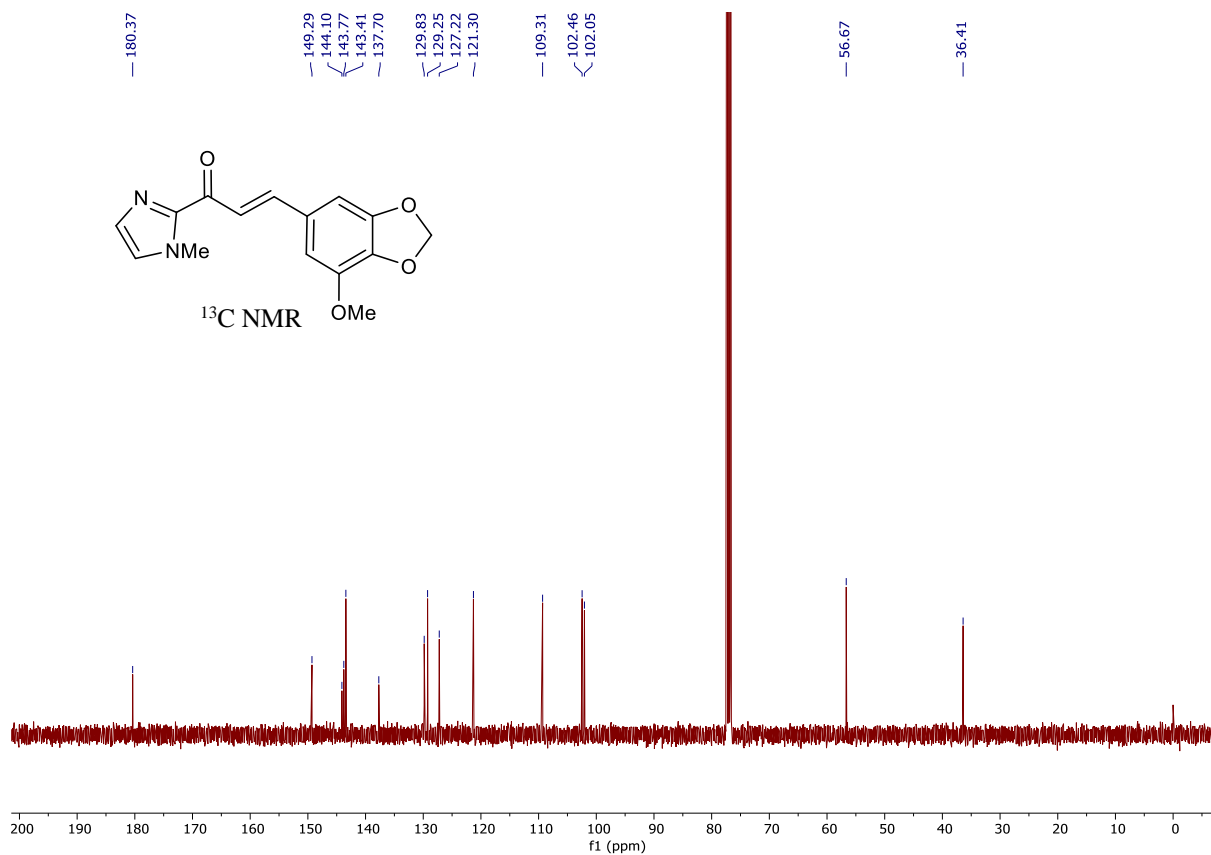
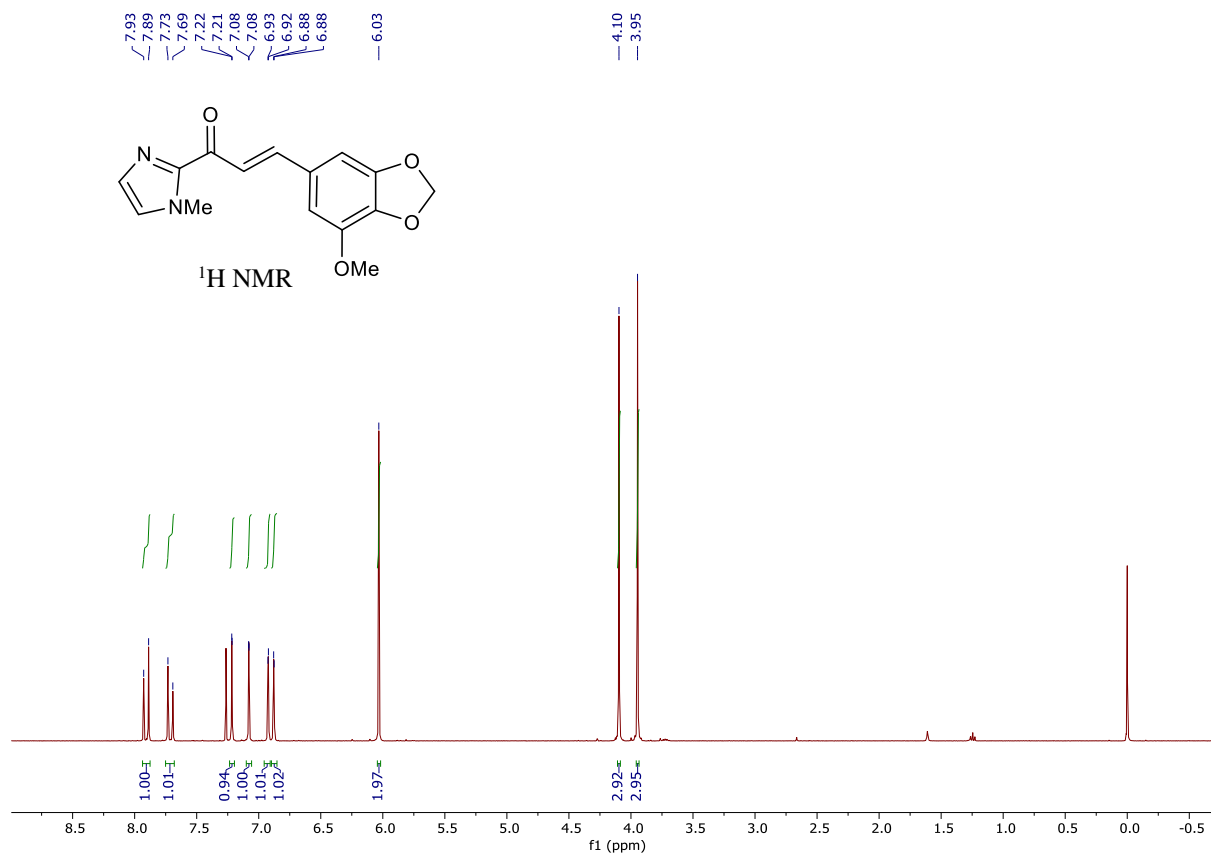


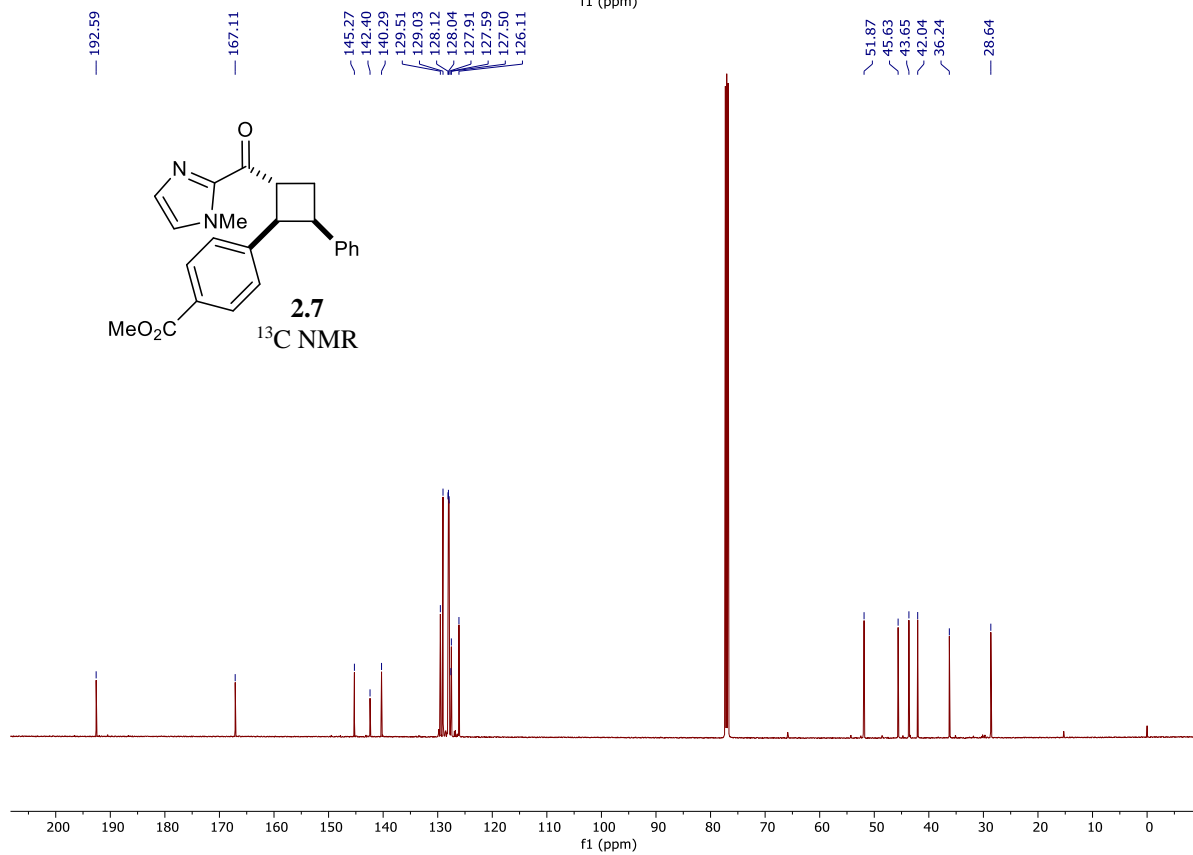
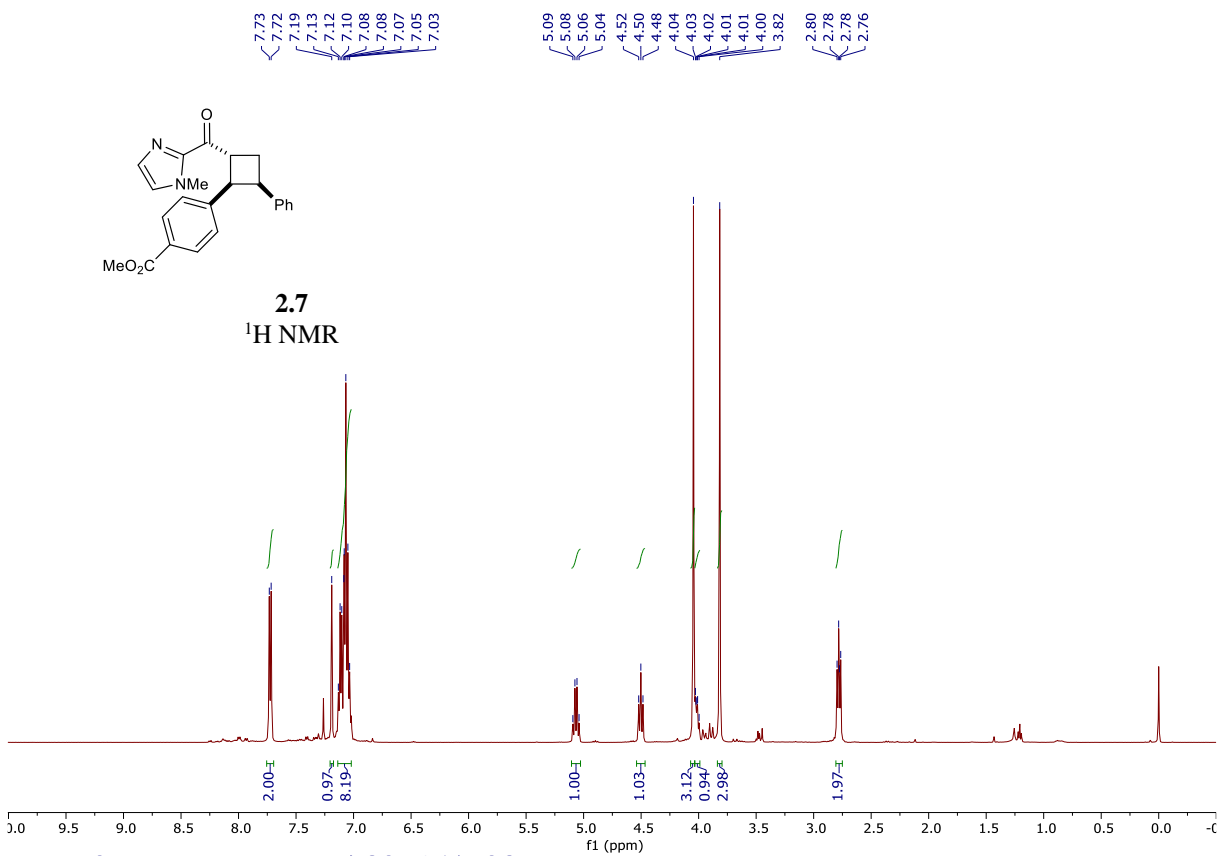
^{19}F NMR

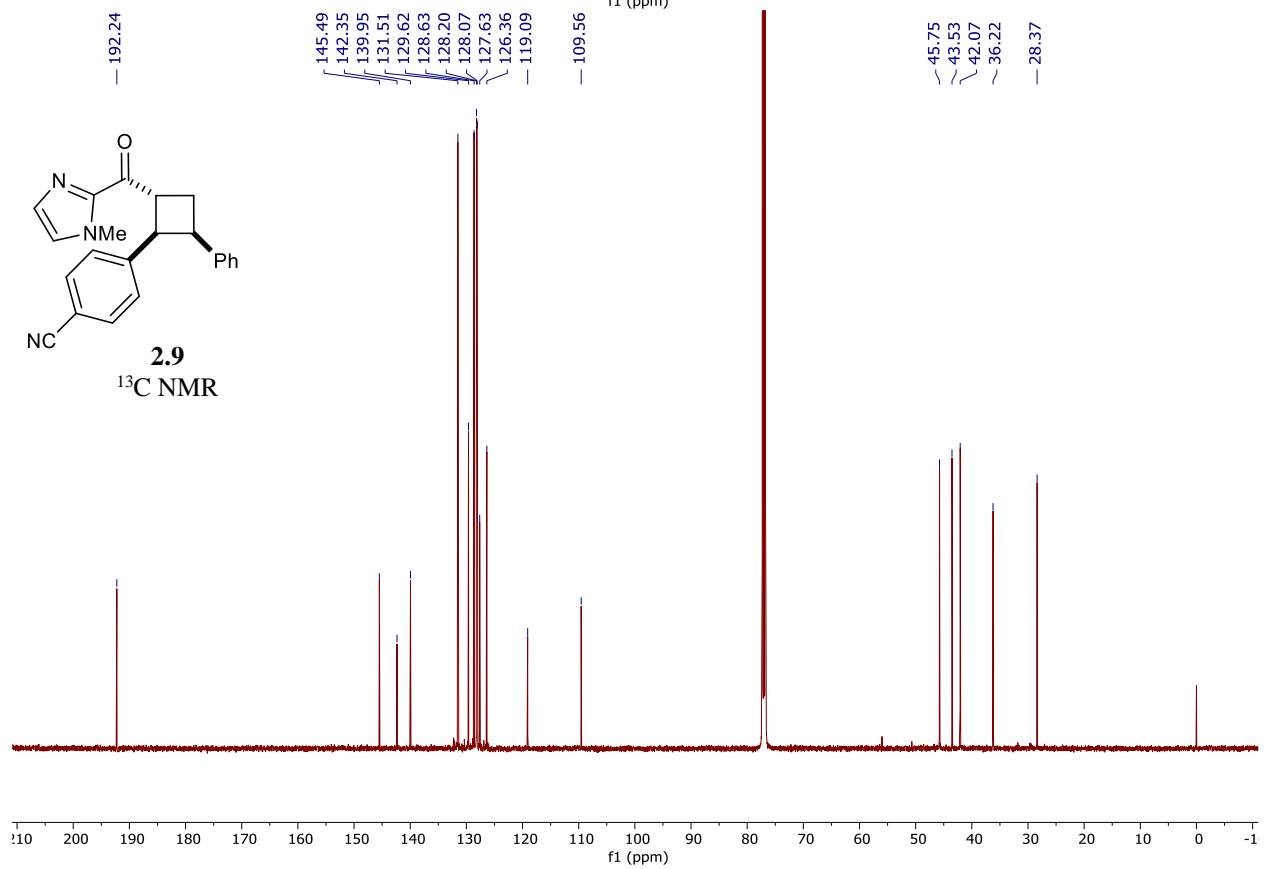
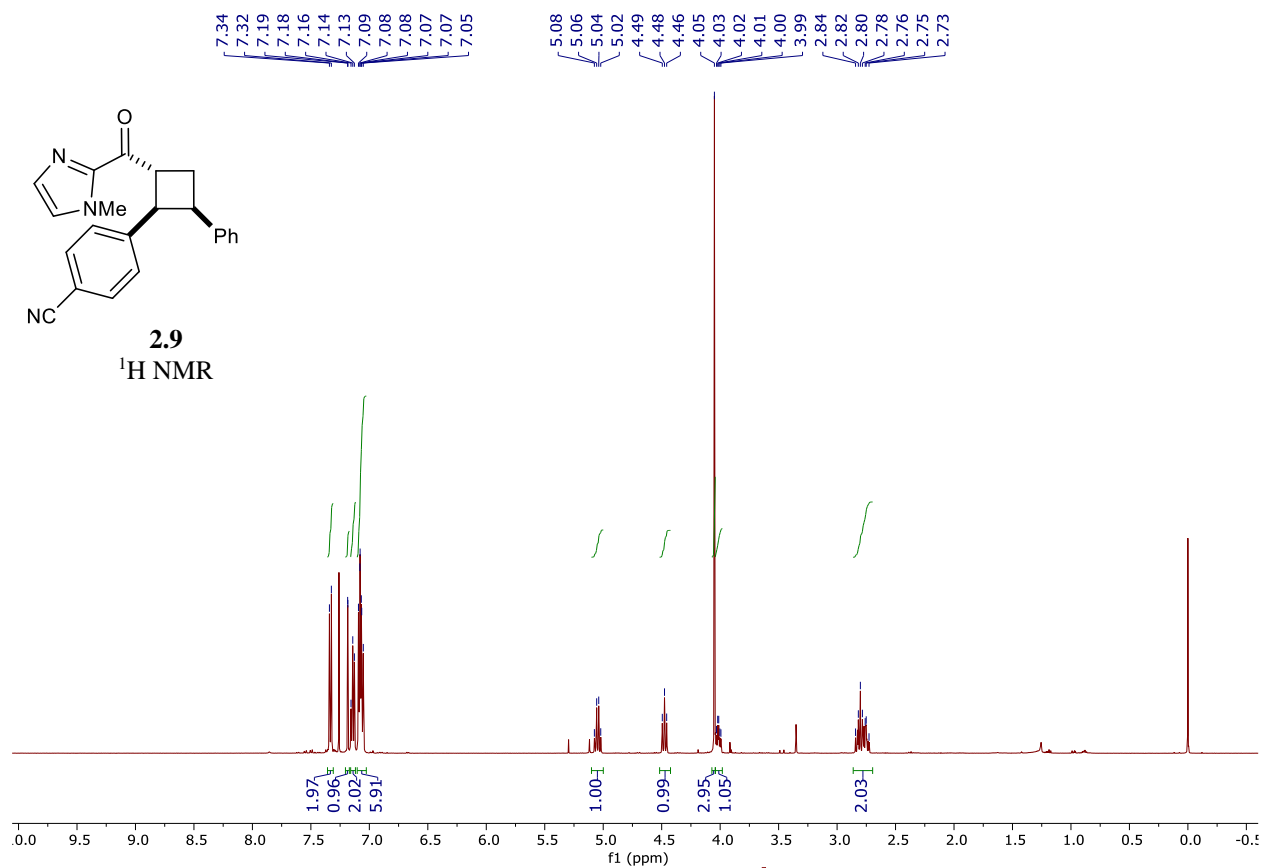


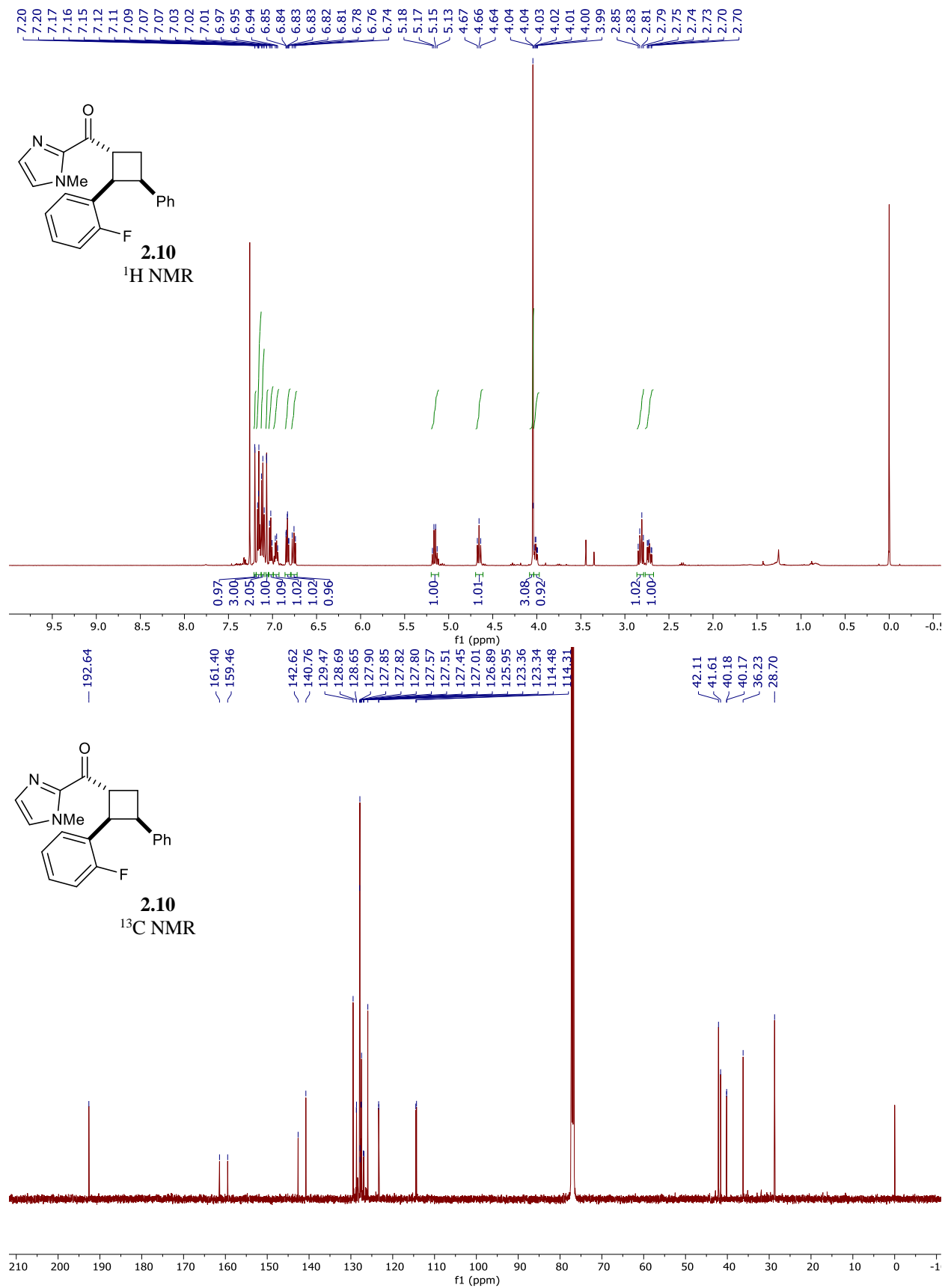


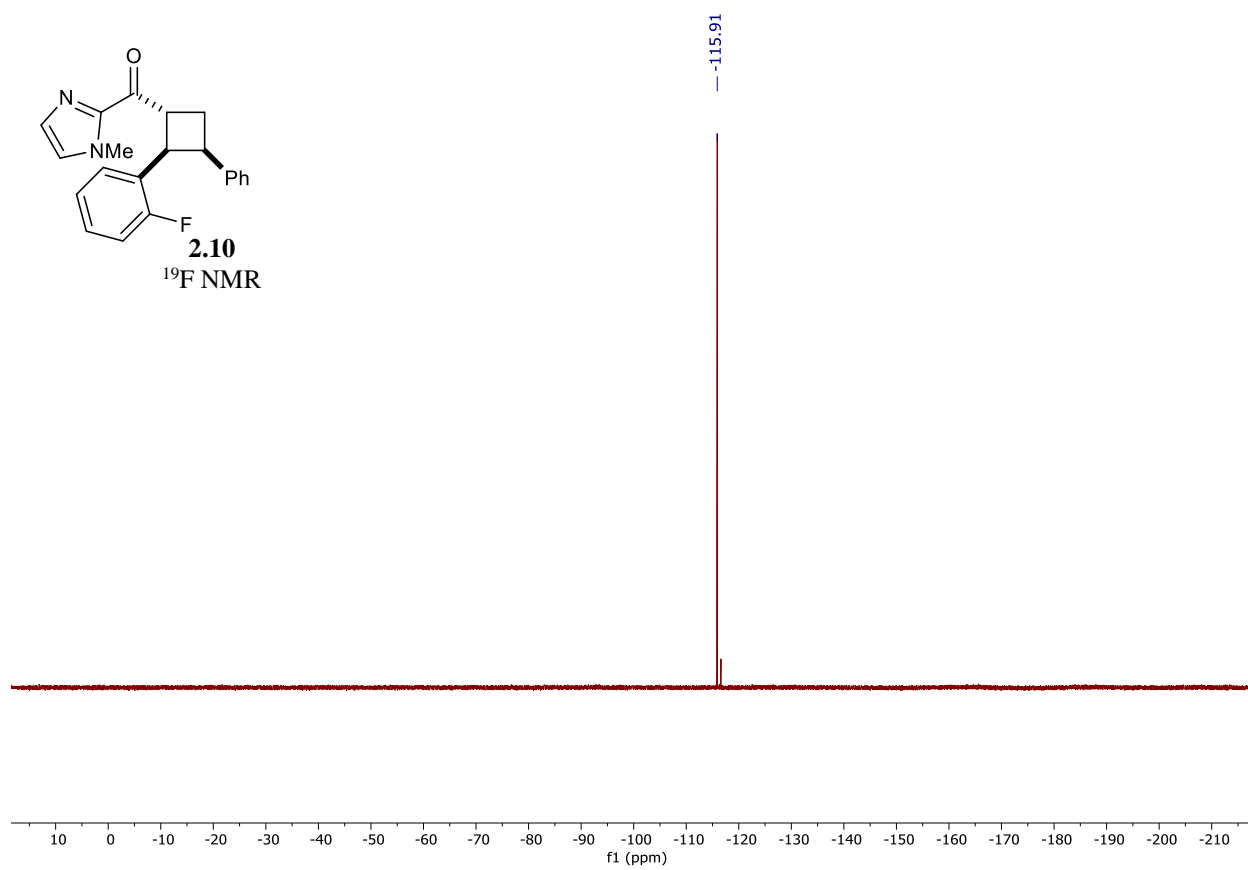


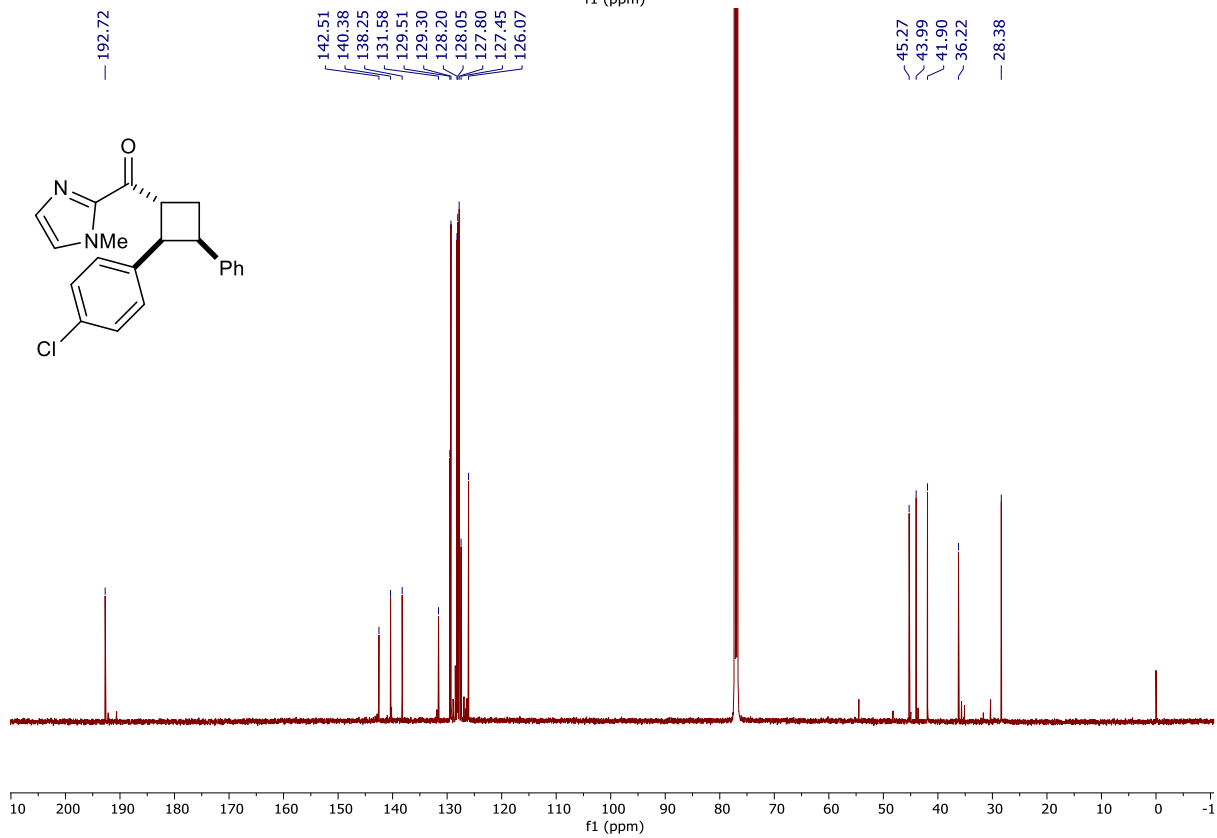
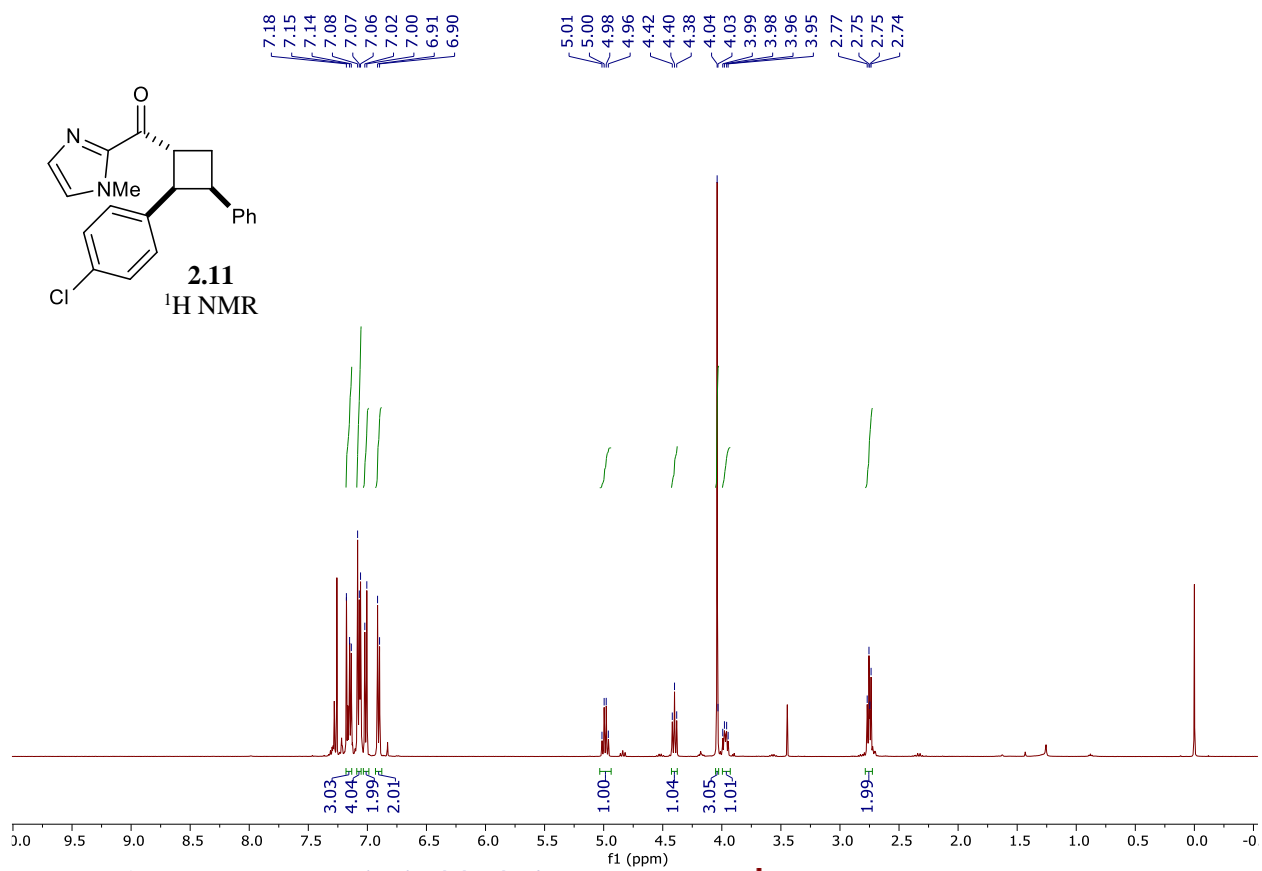


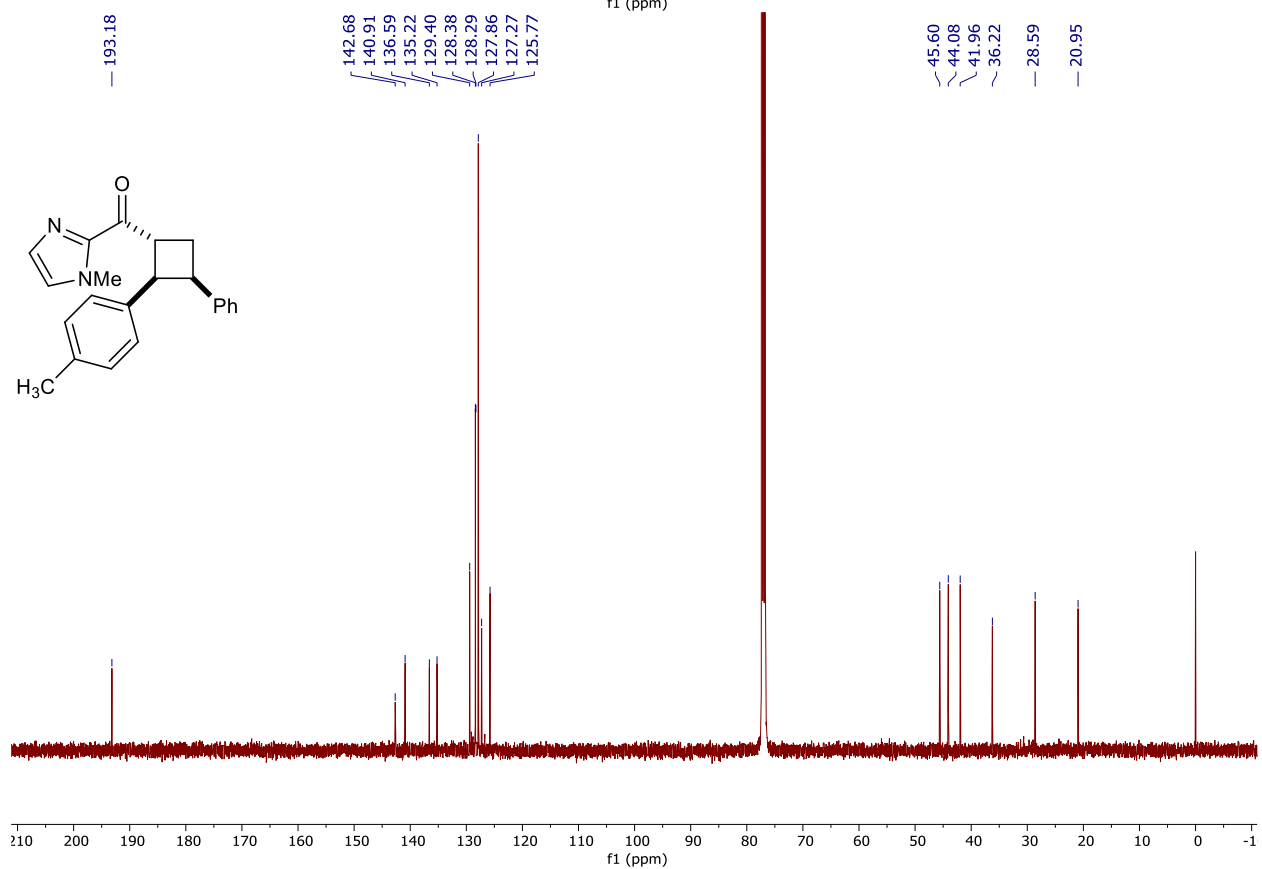
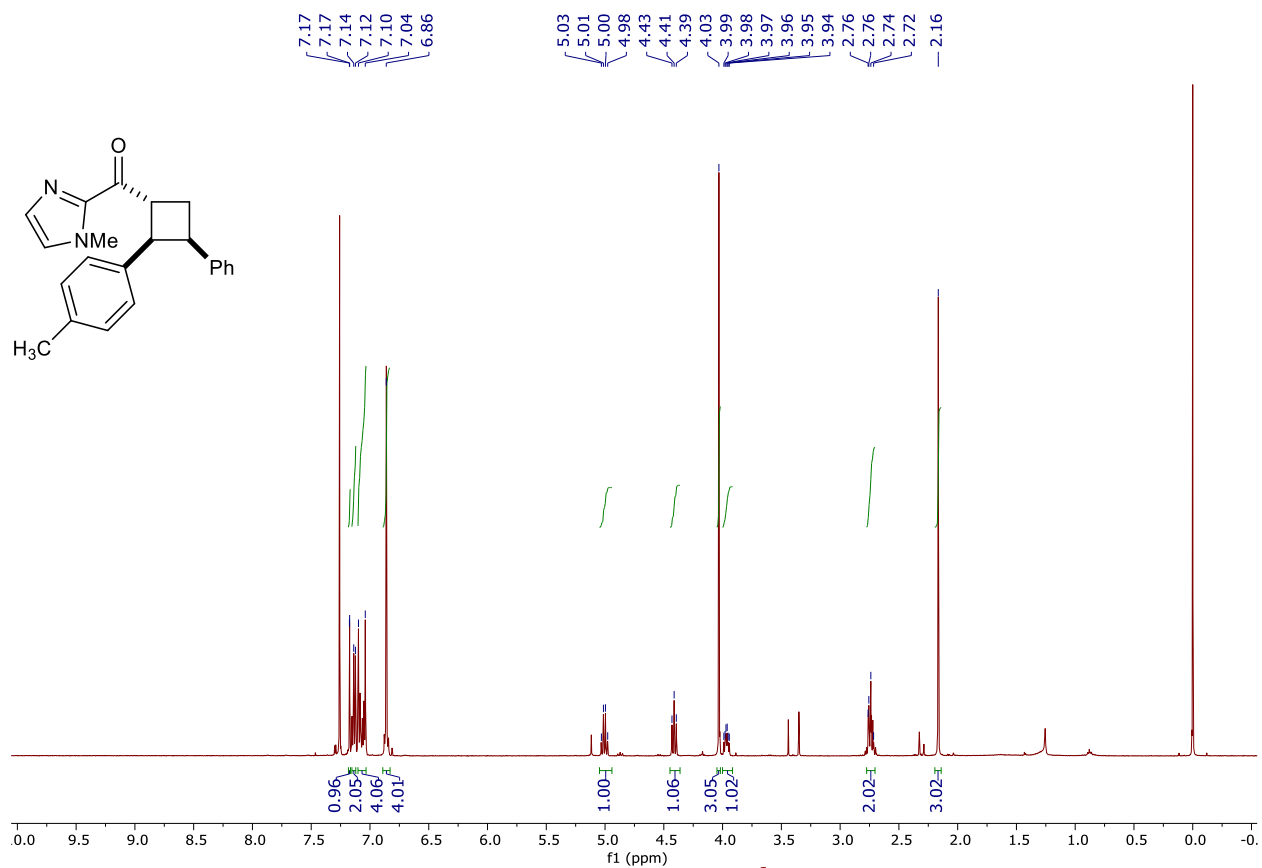


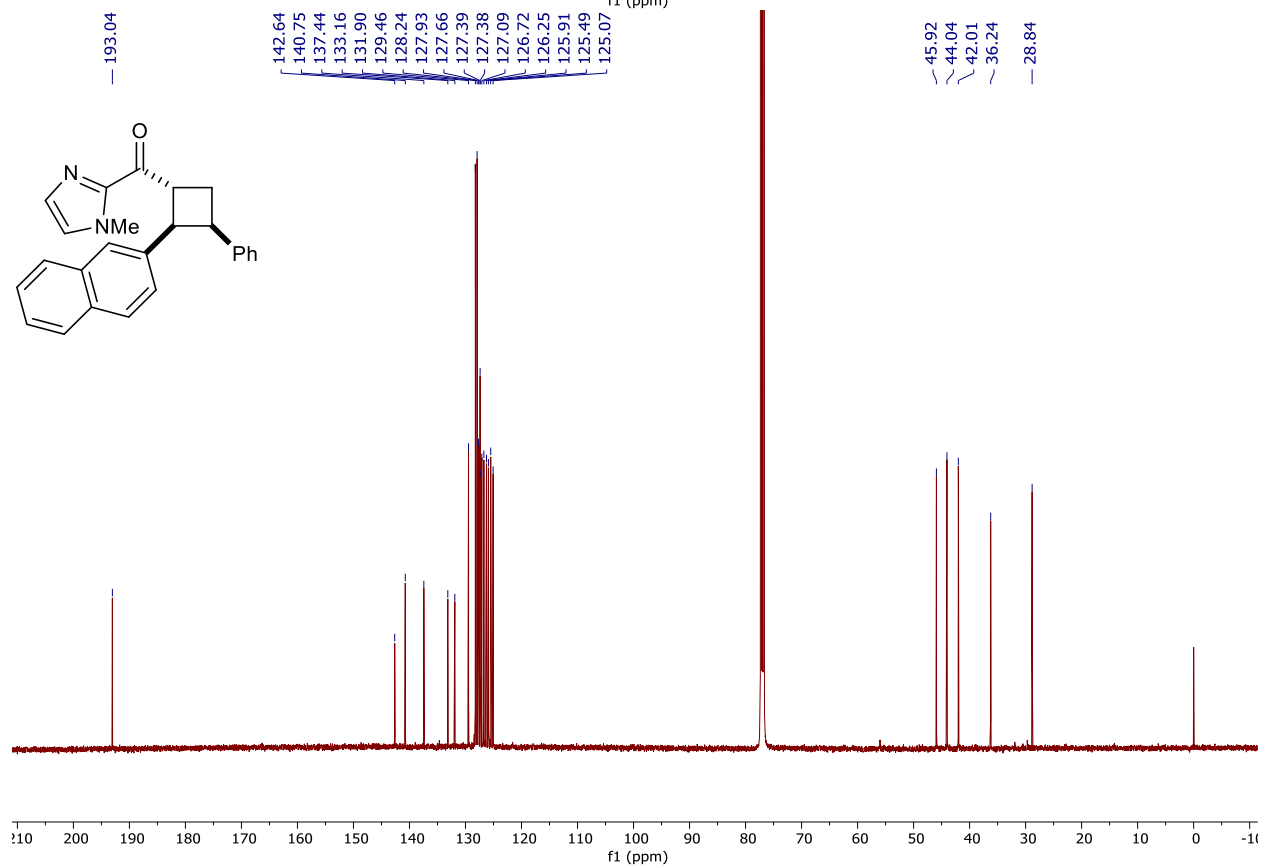
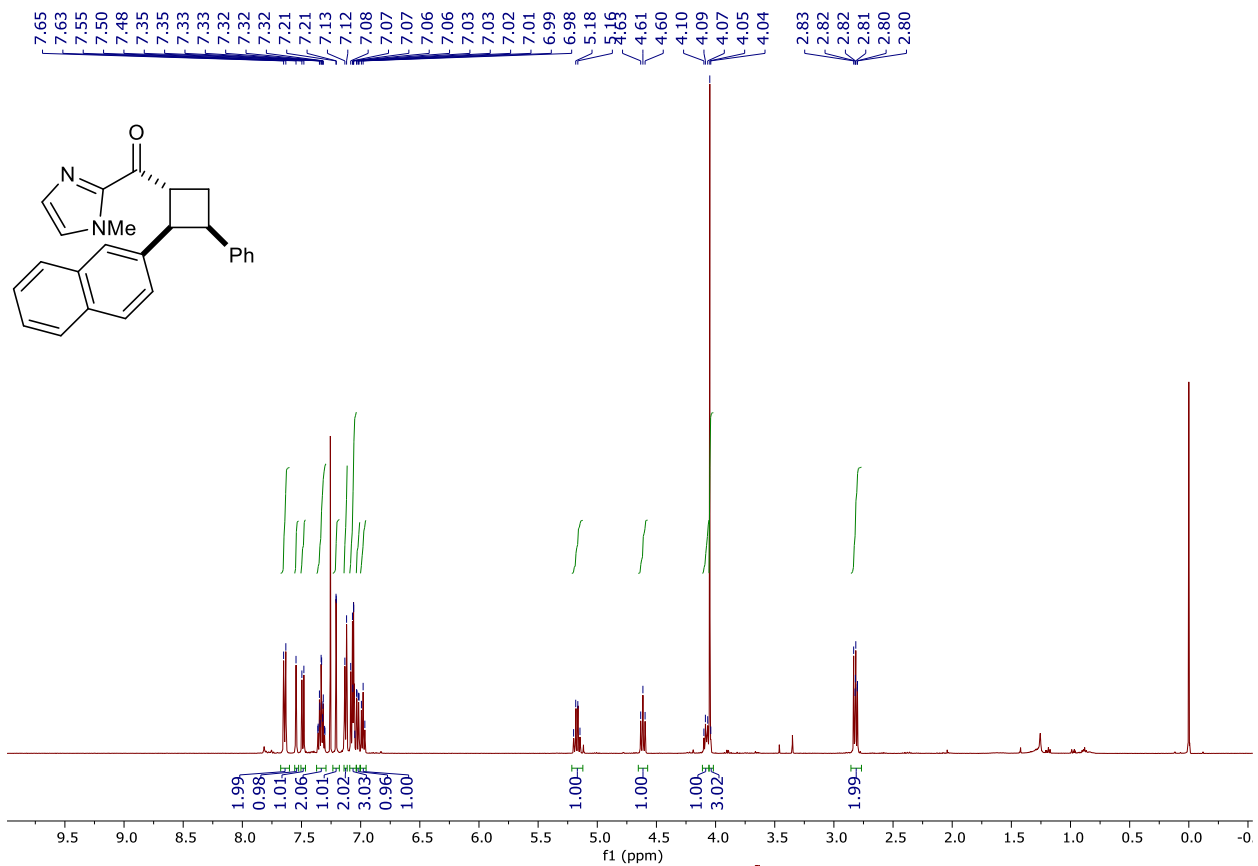


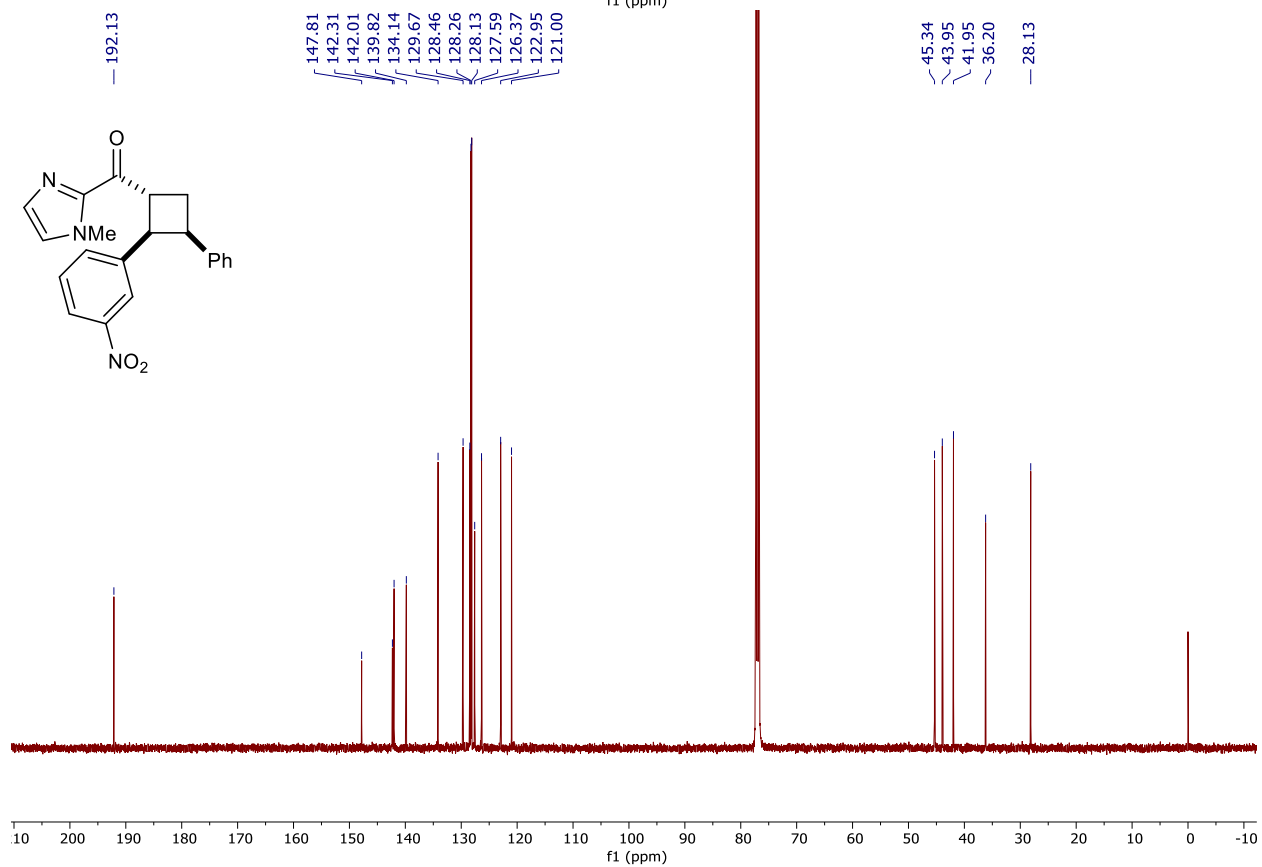
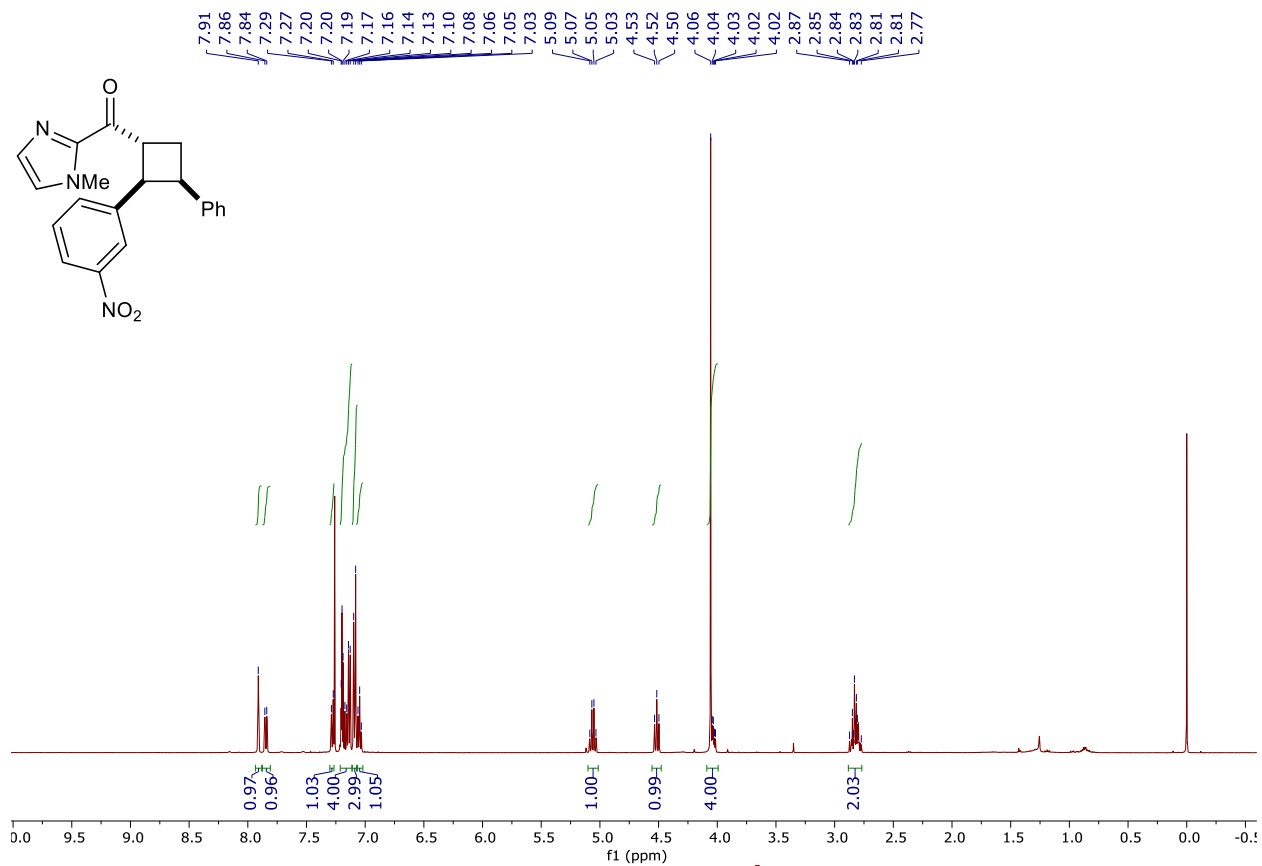


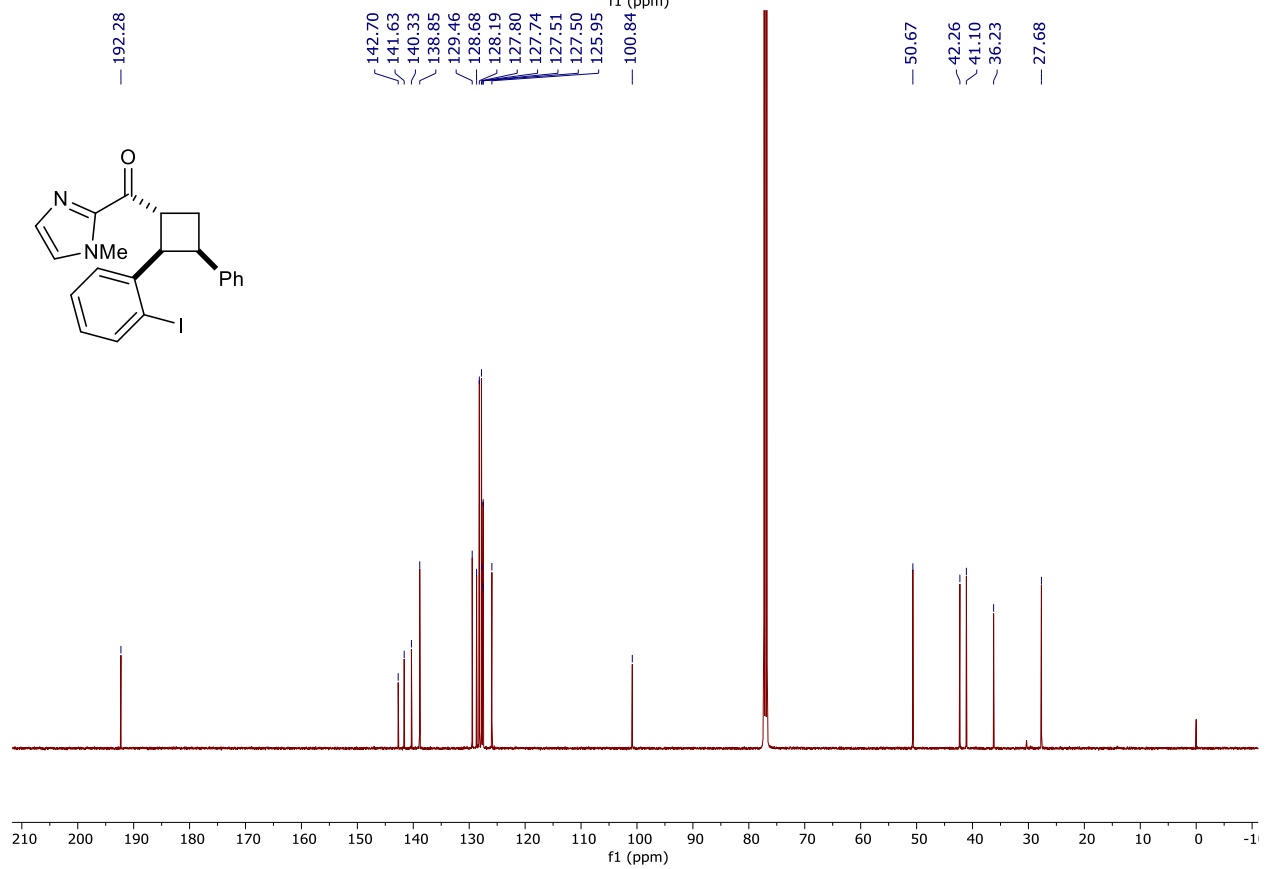
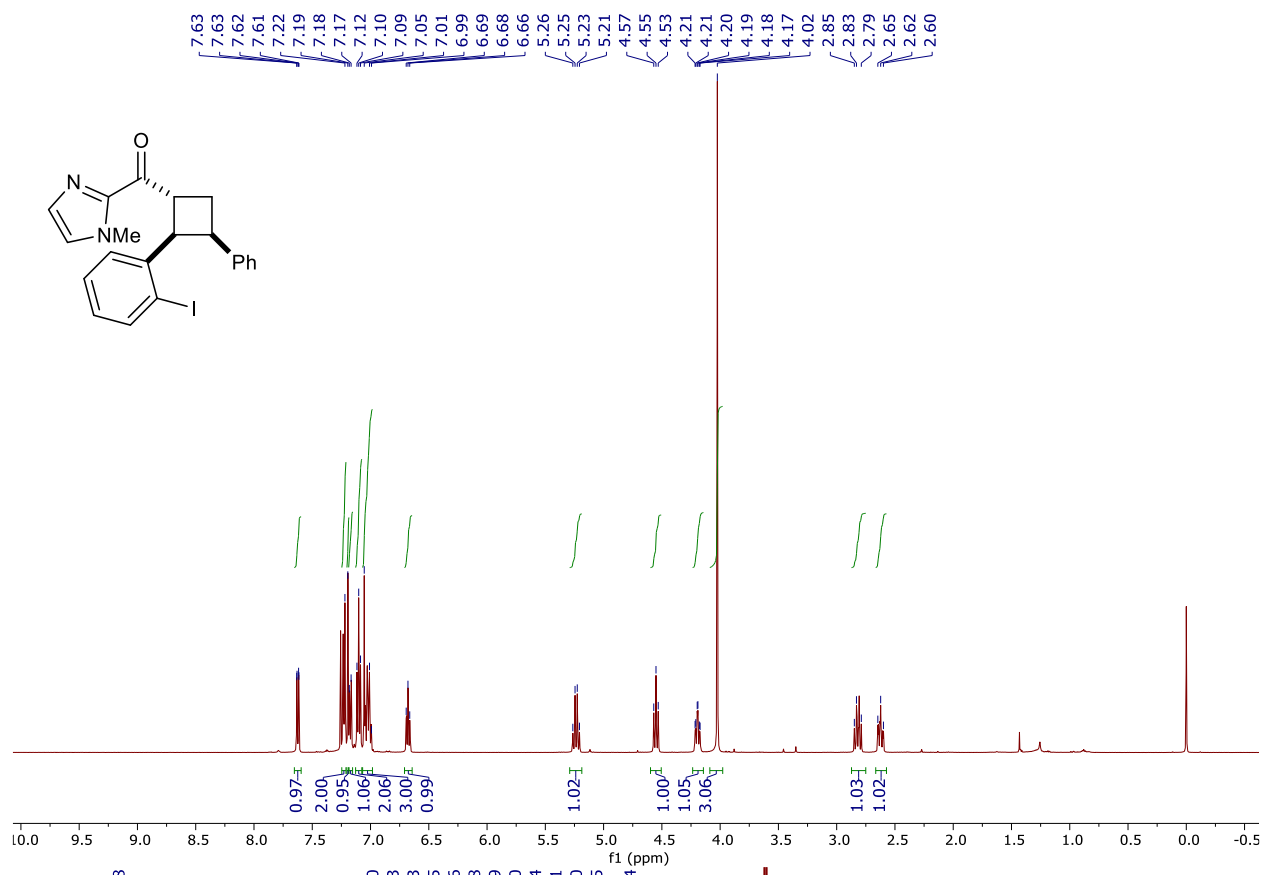


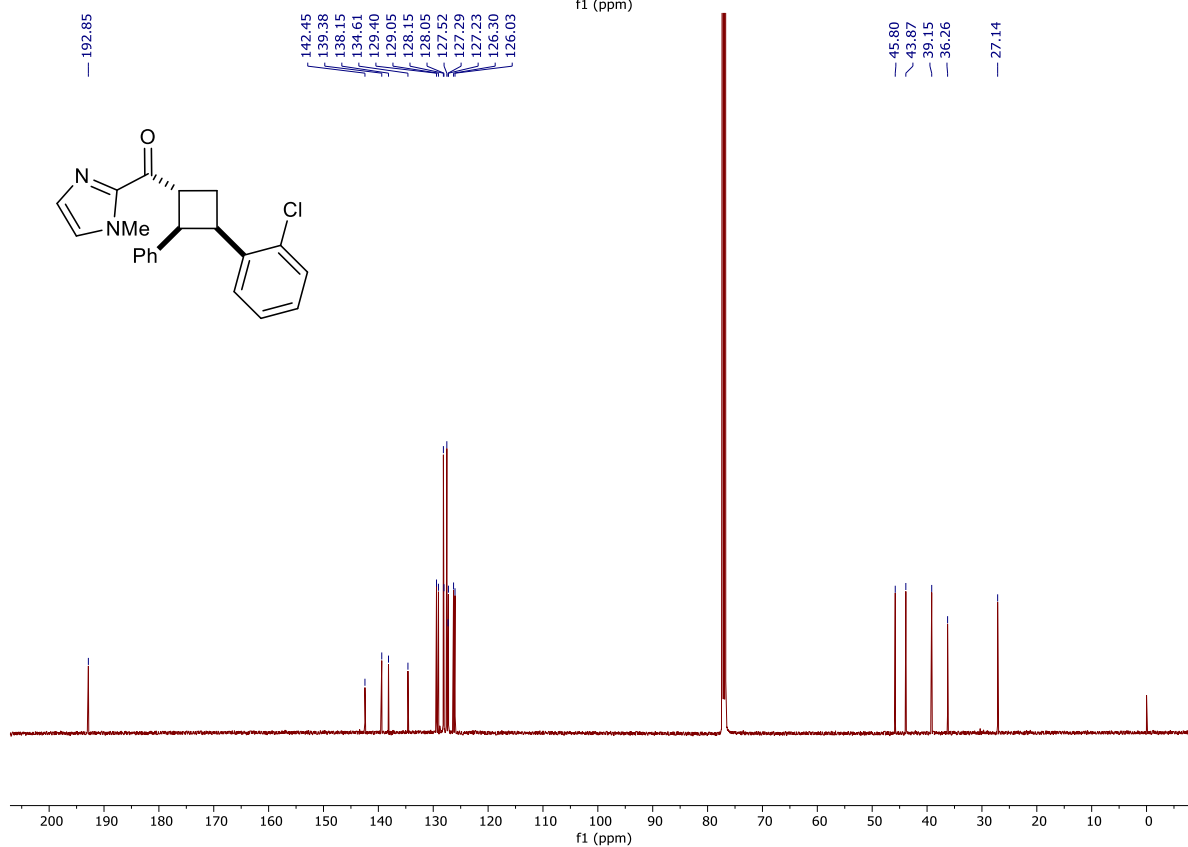
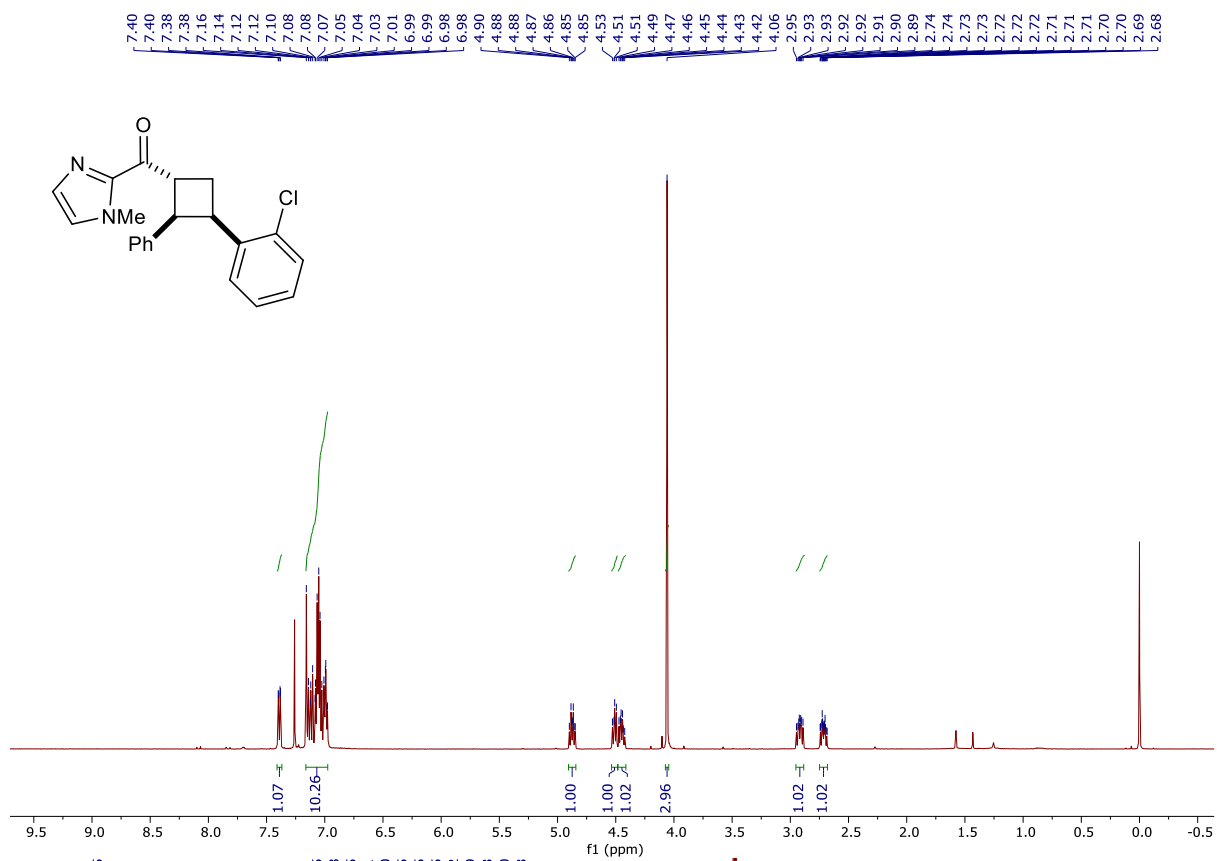


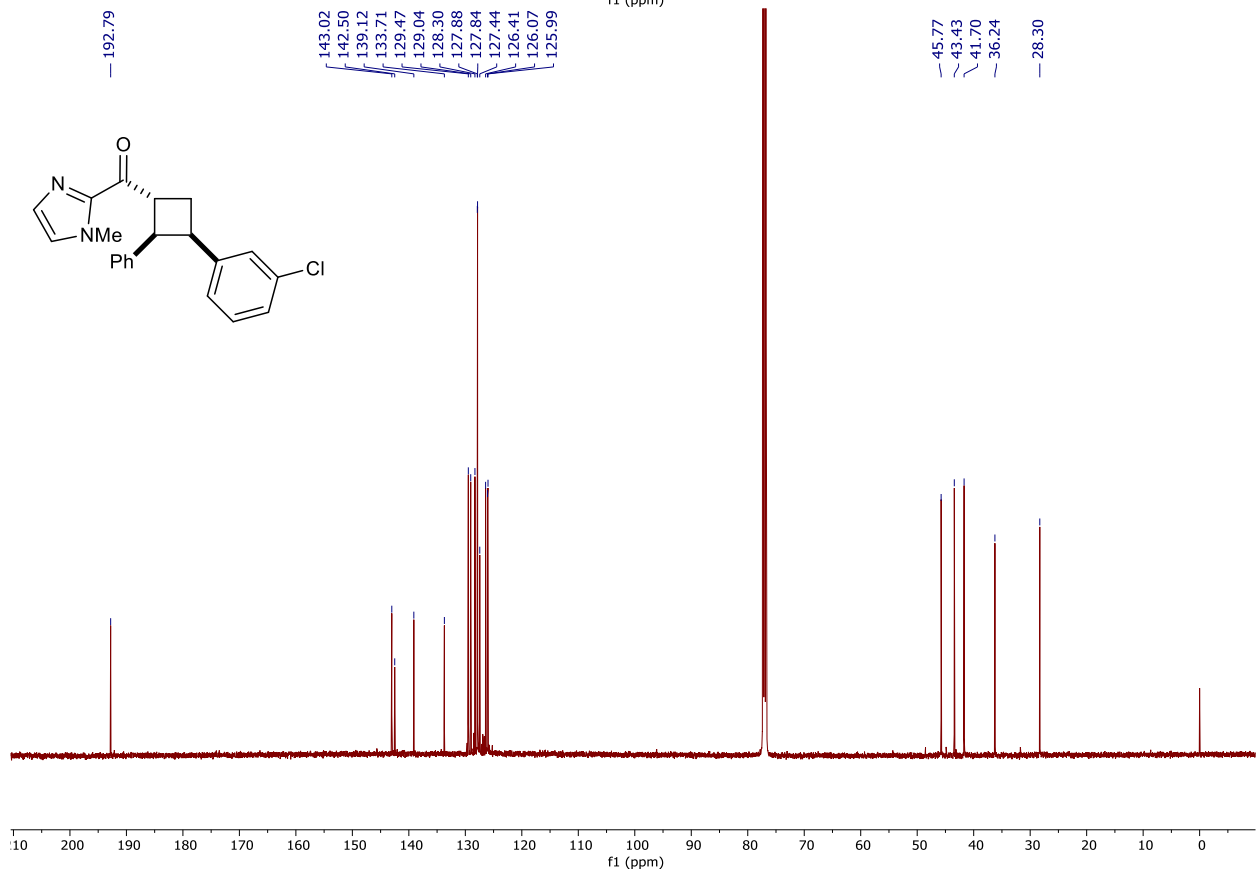
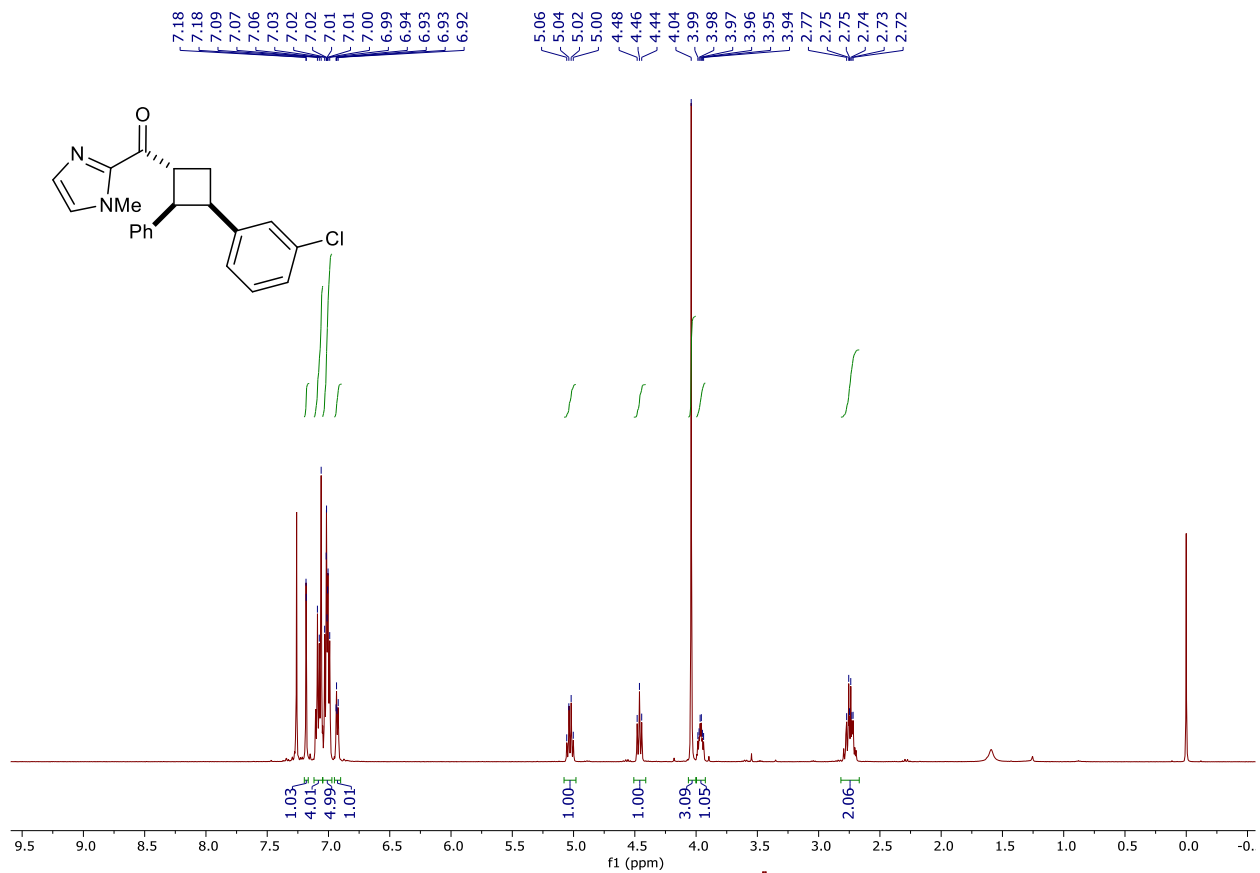


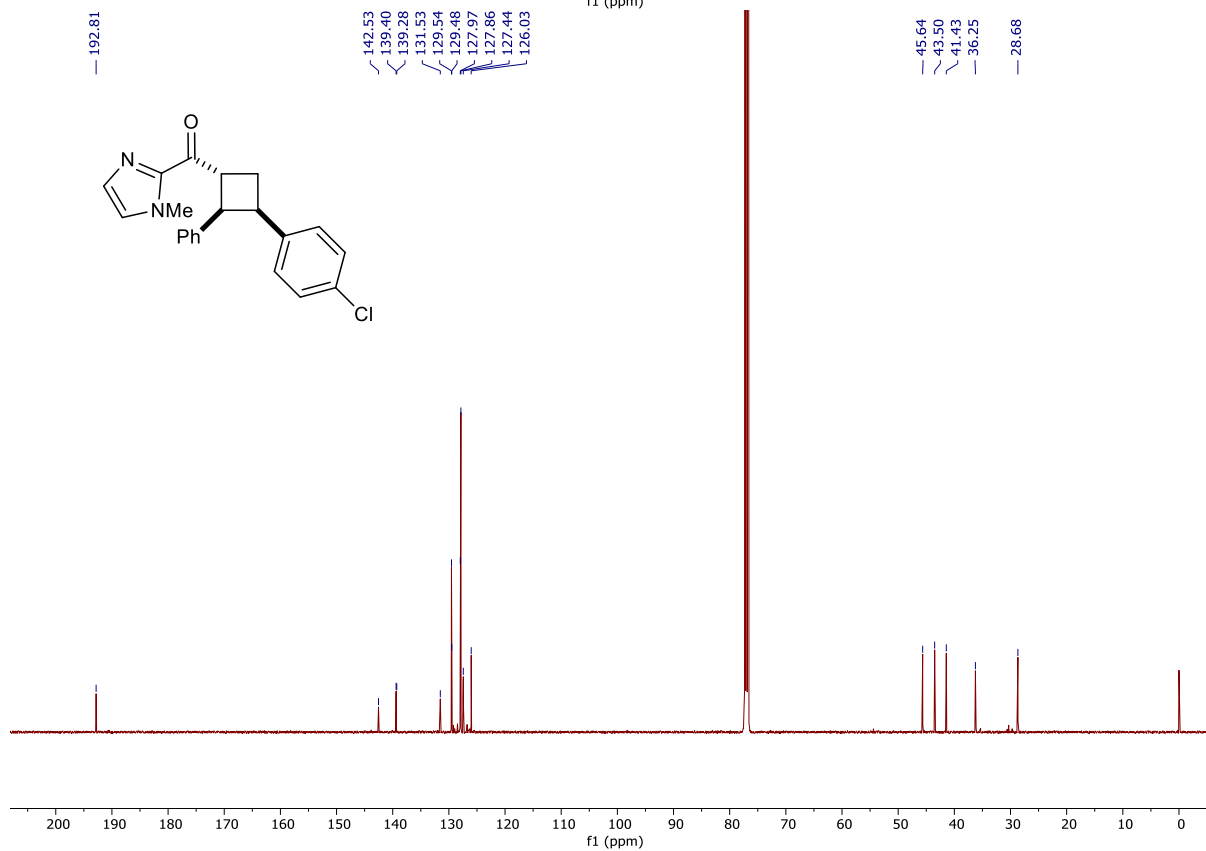
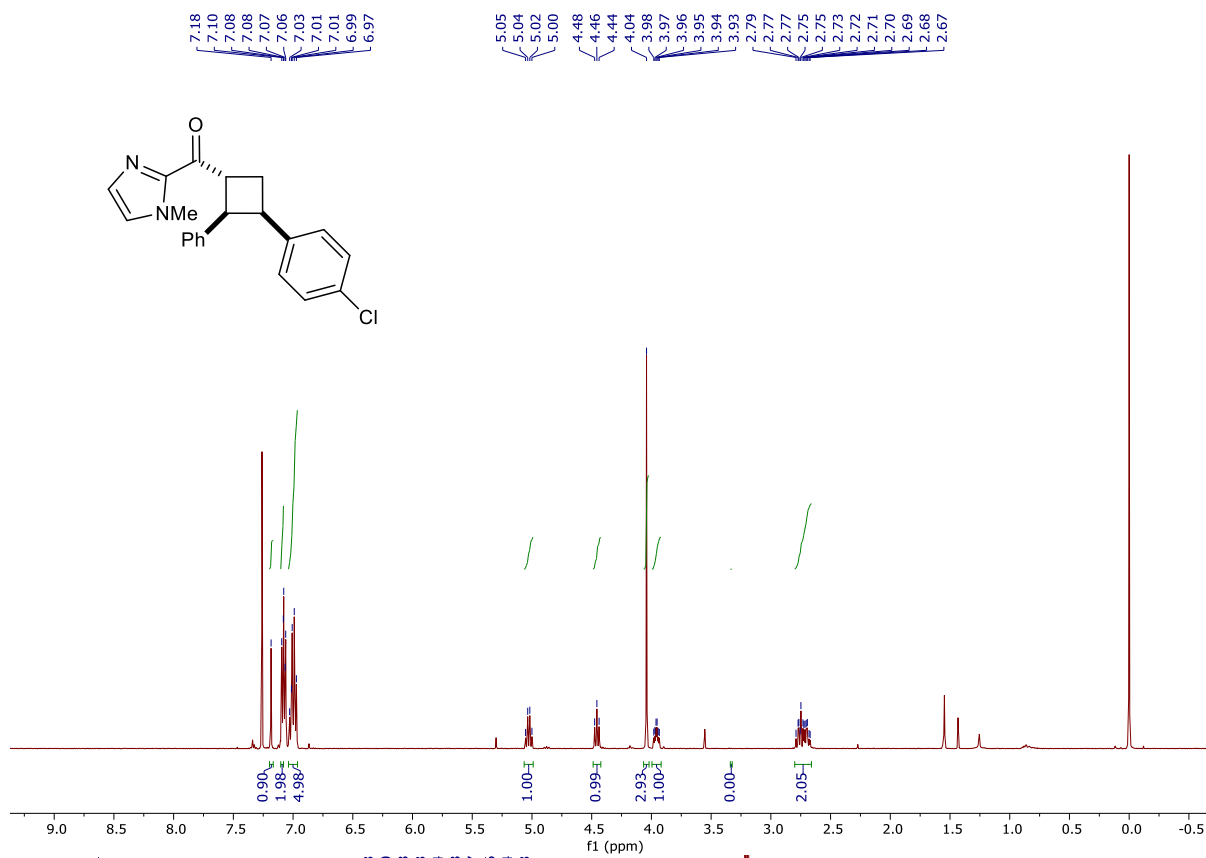


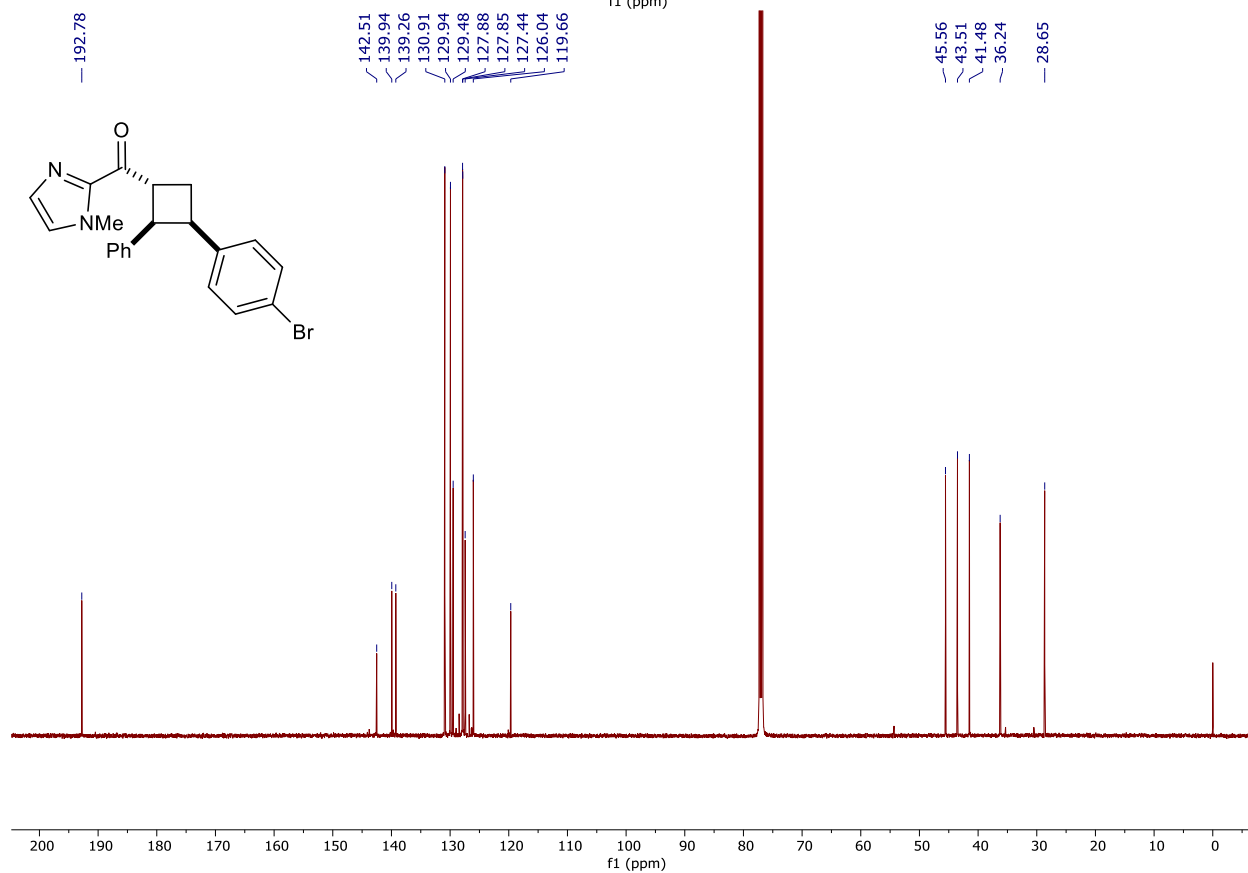
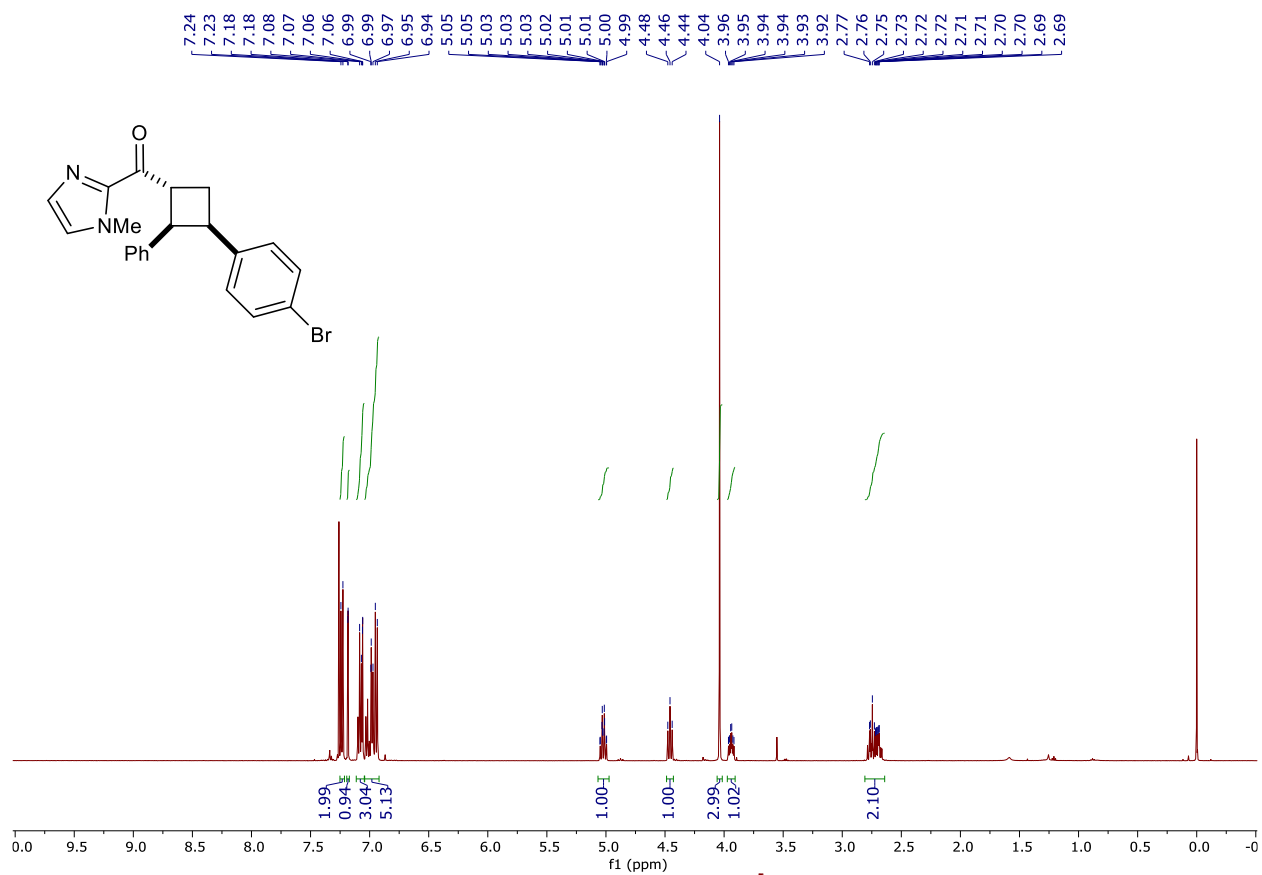


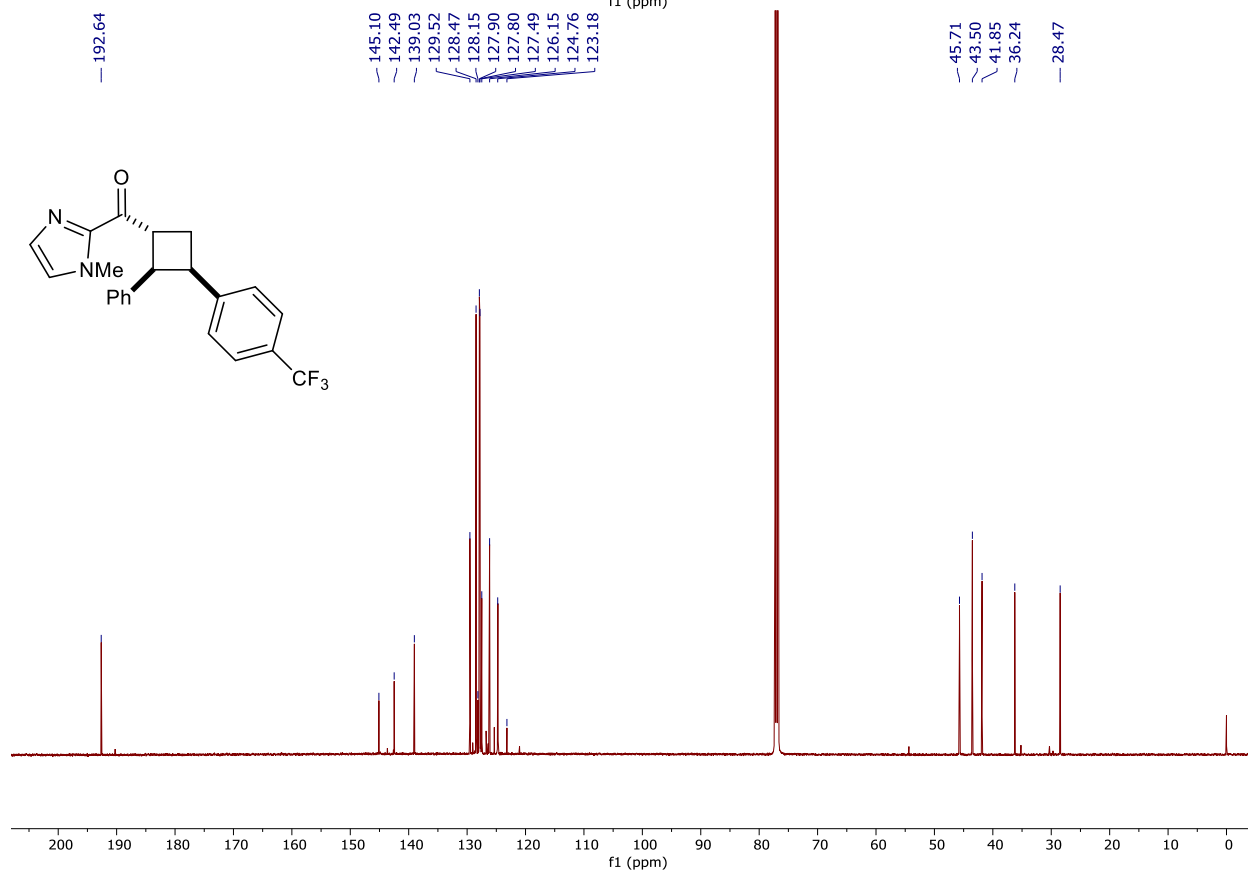
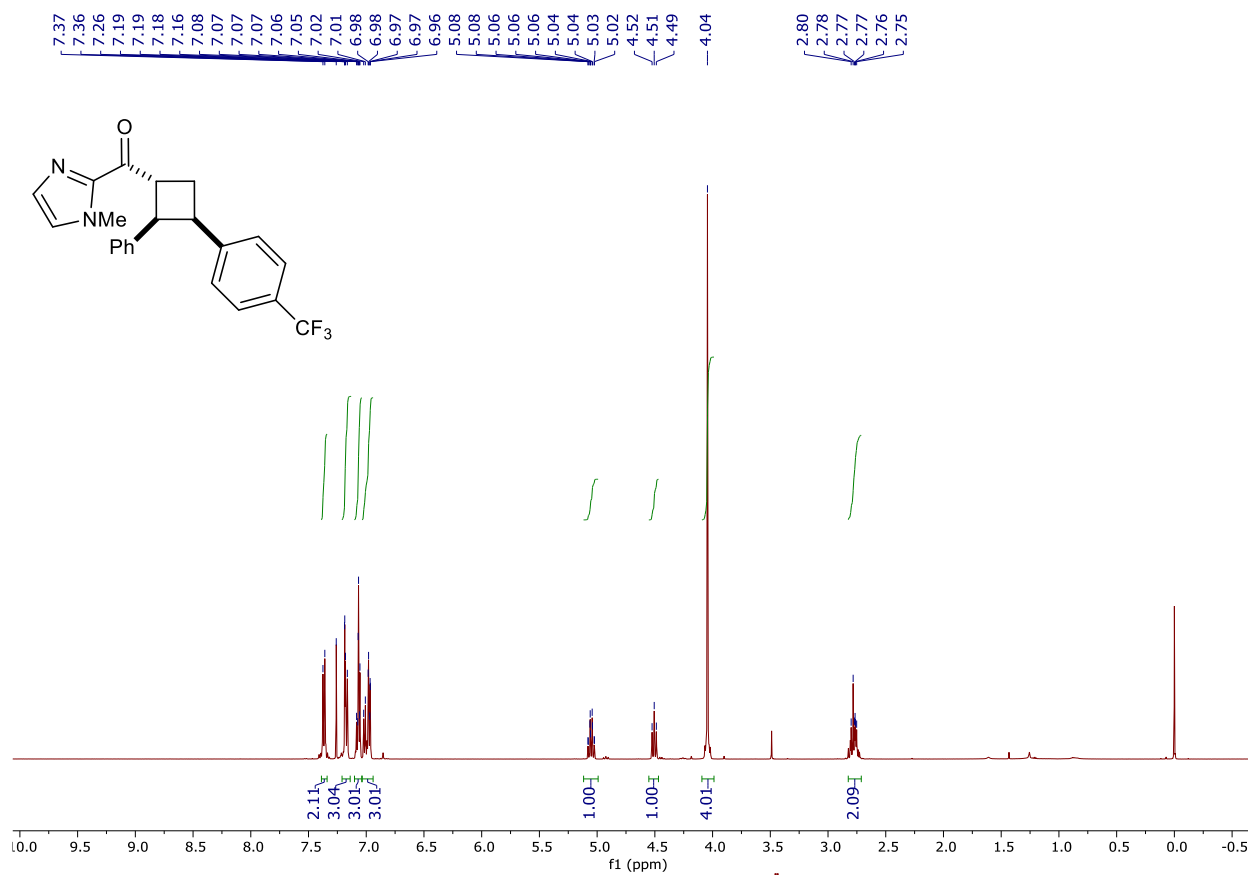


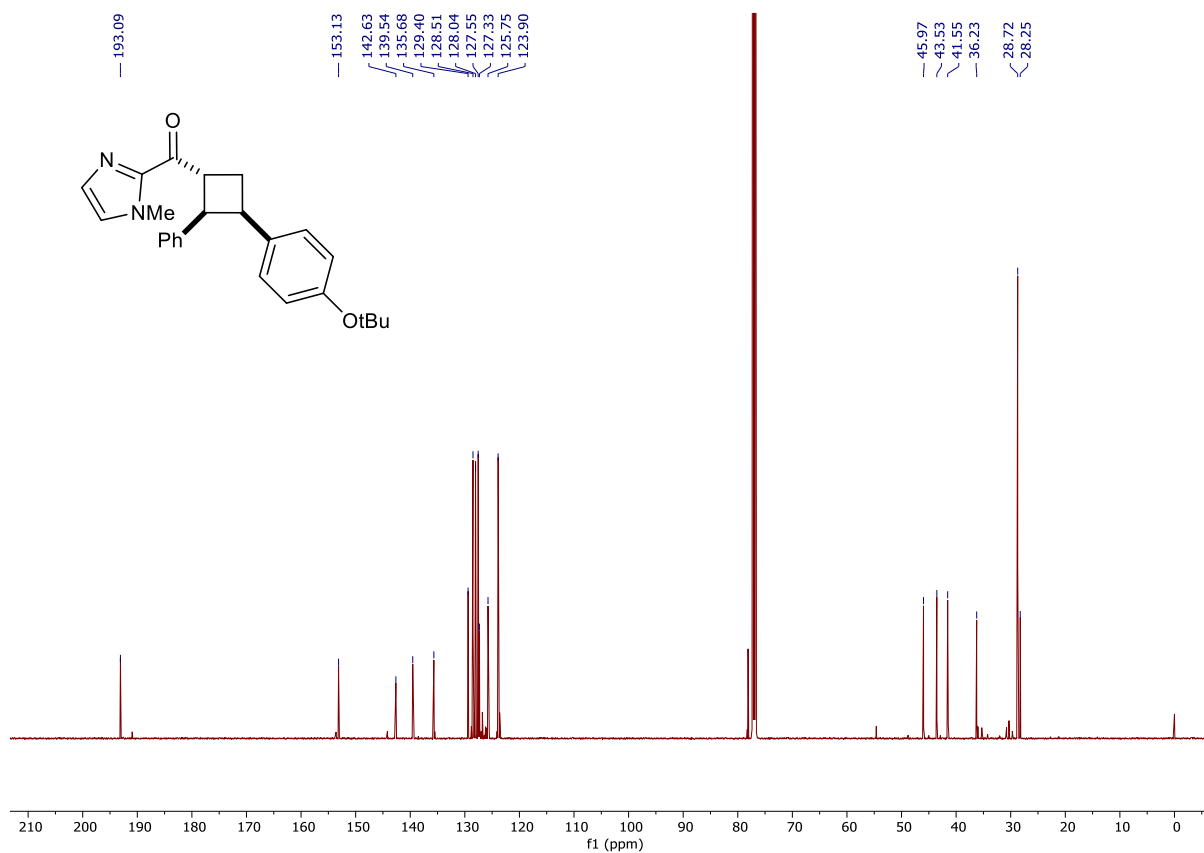
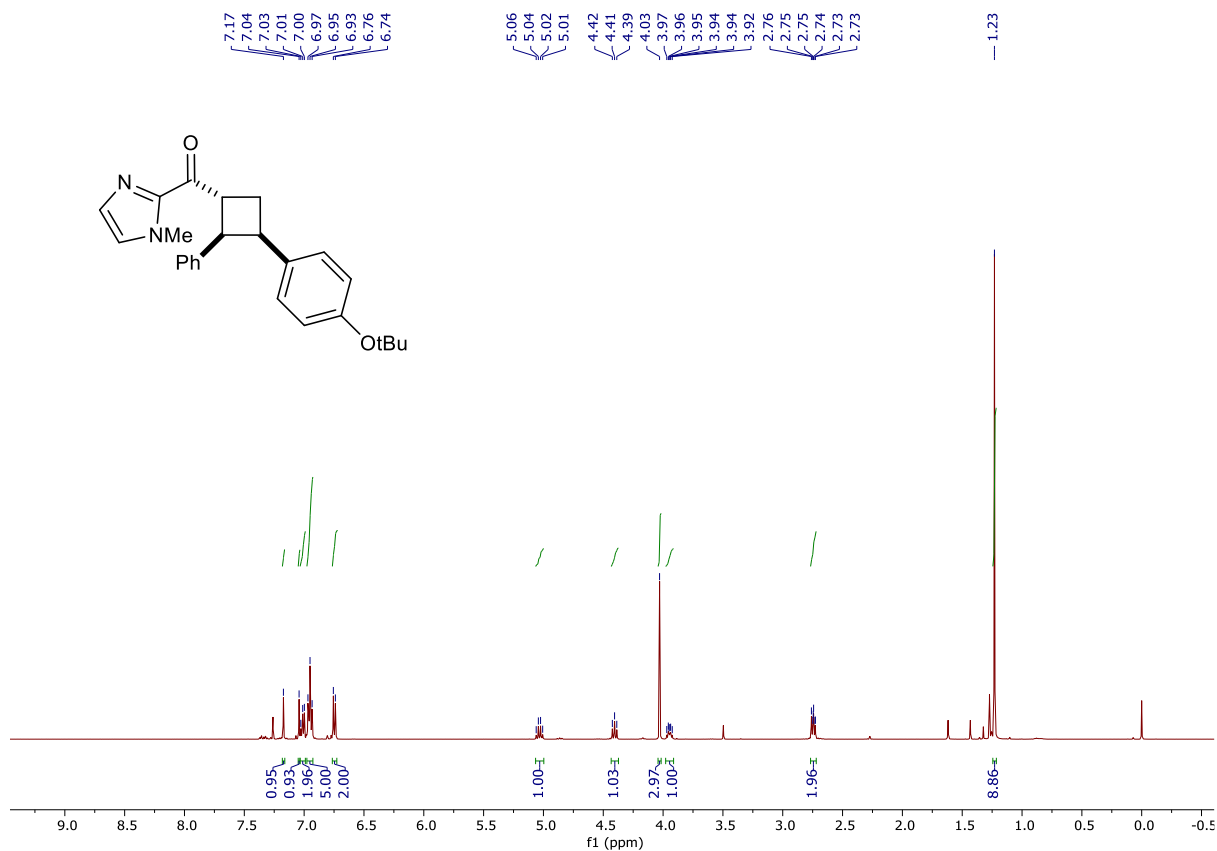


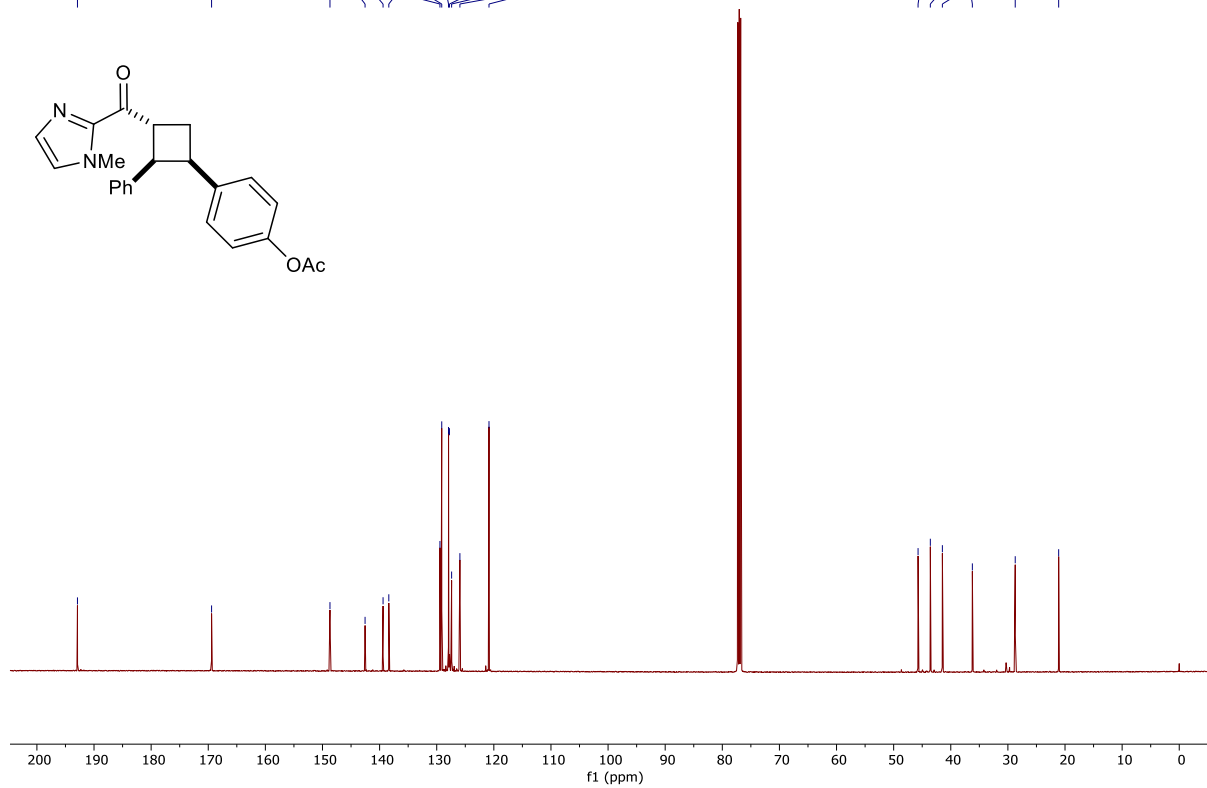
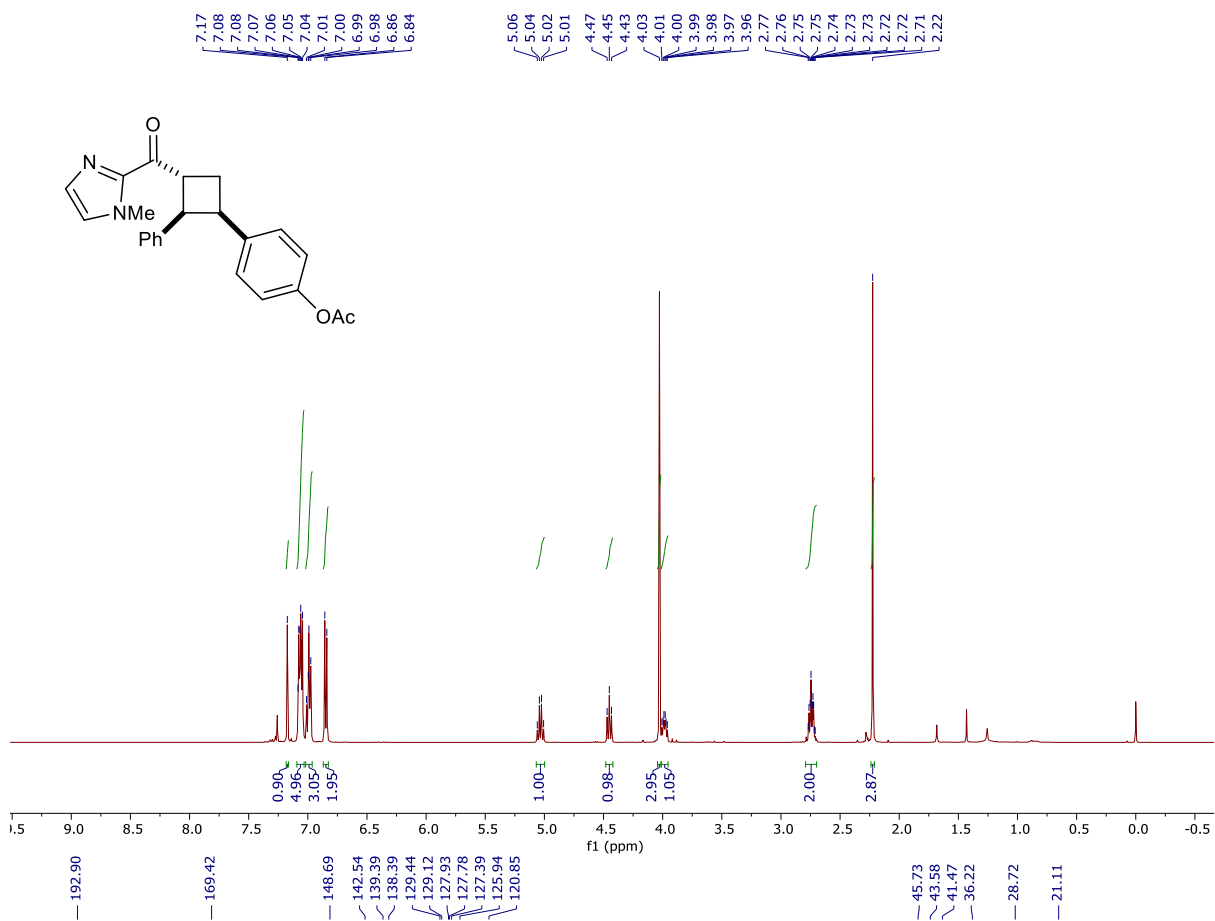


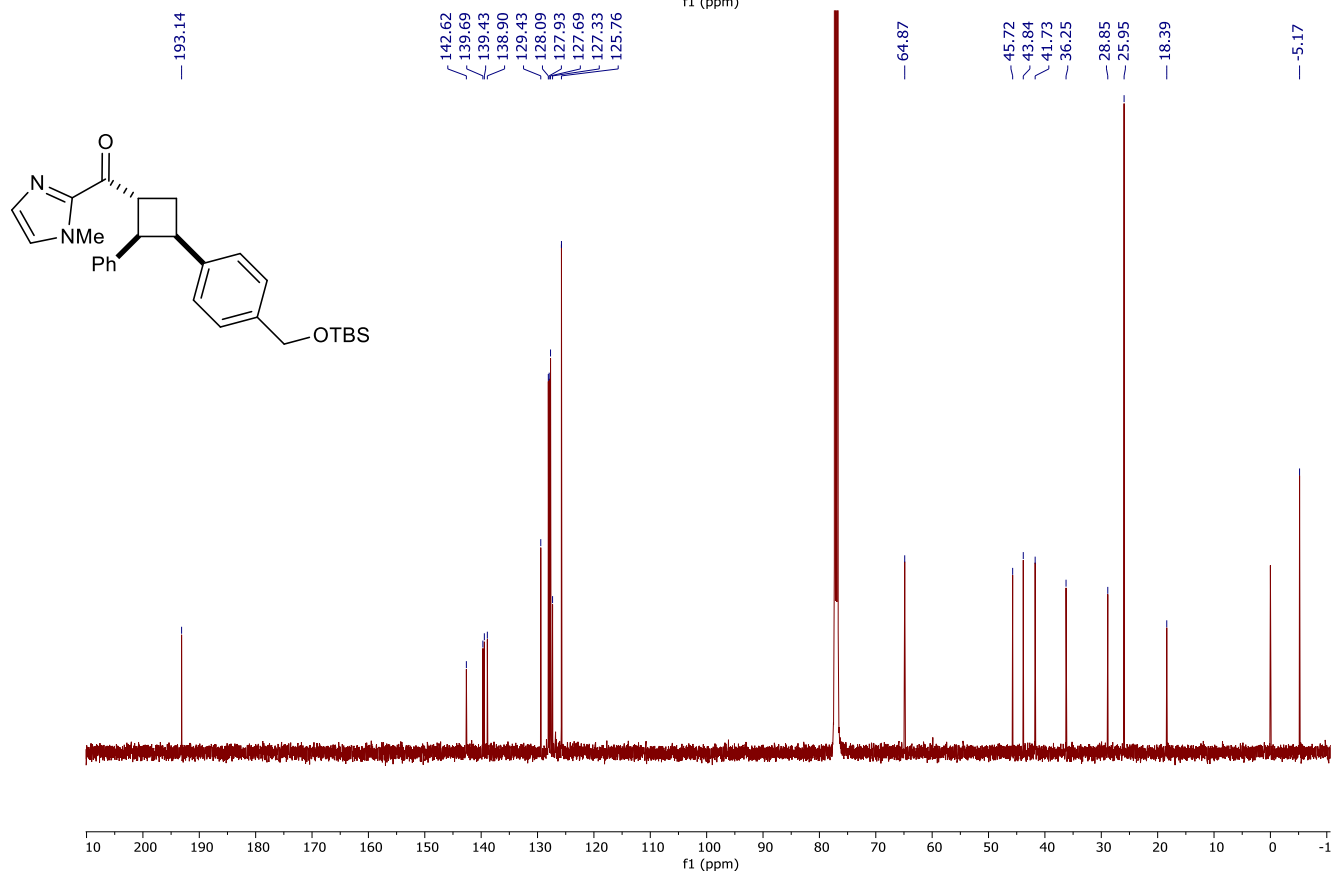
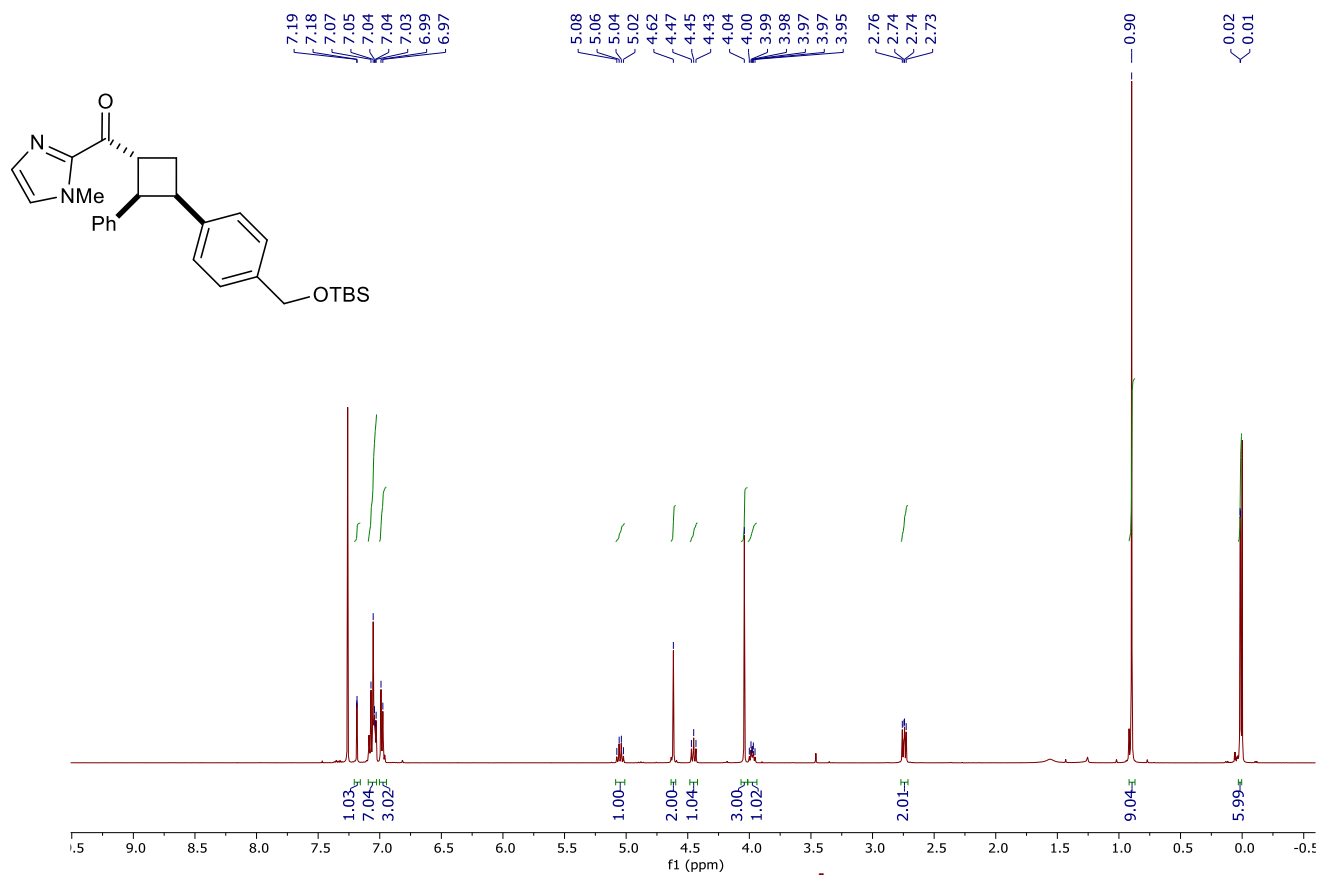


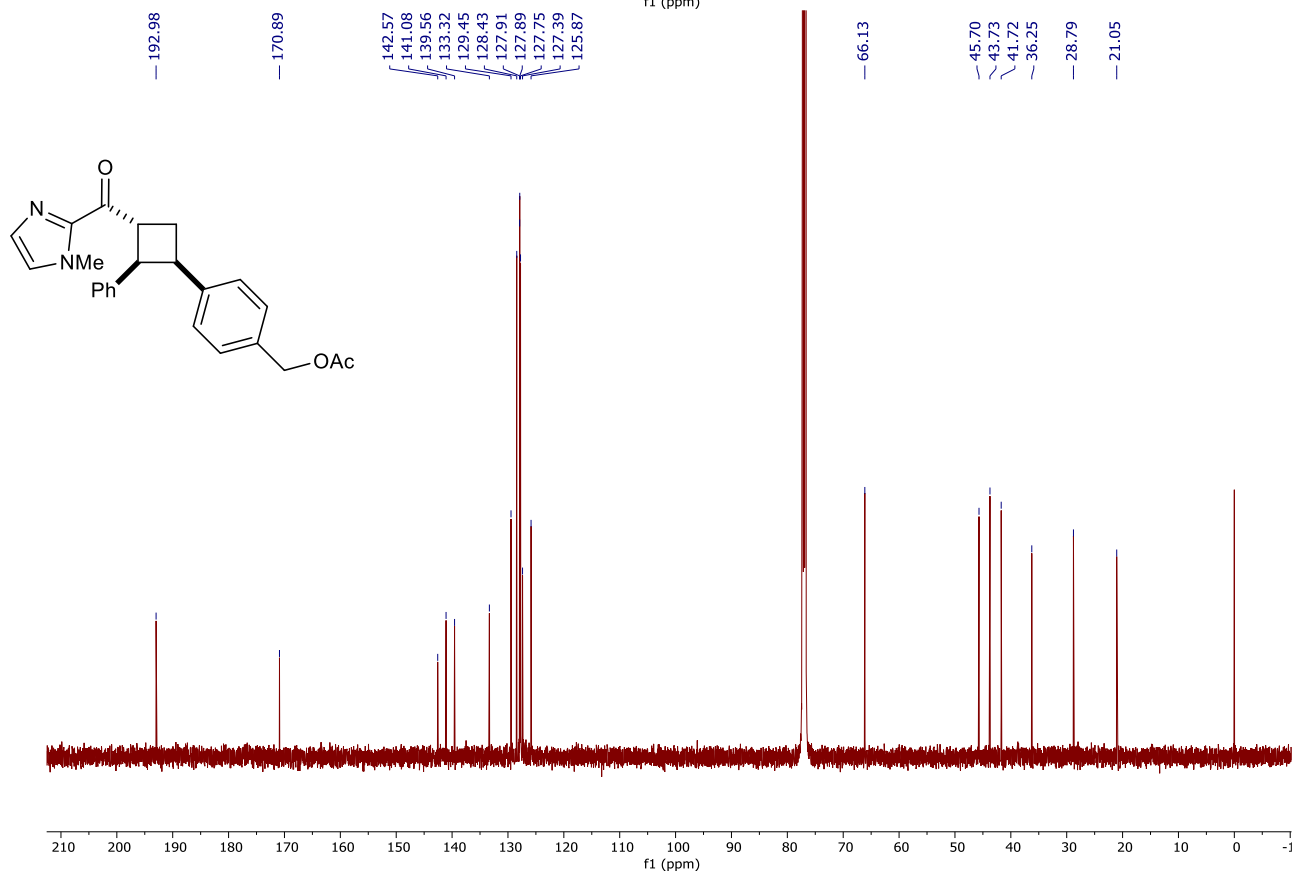
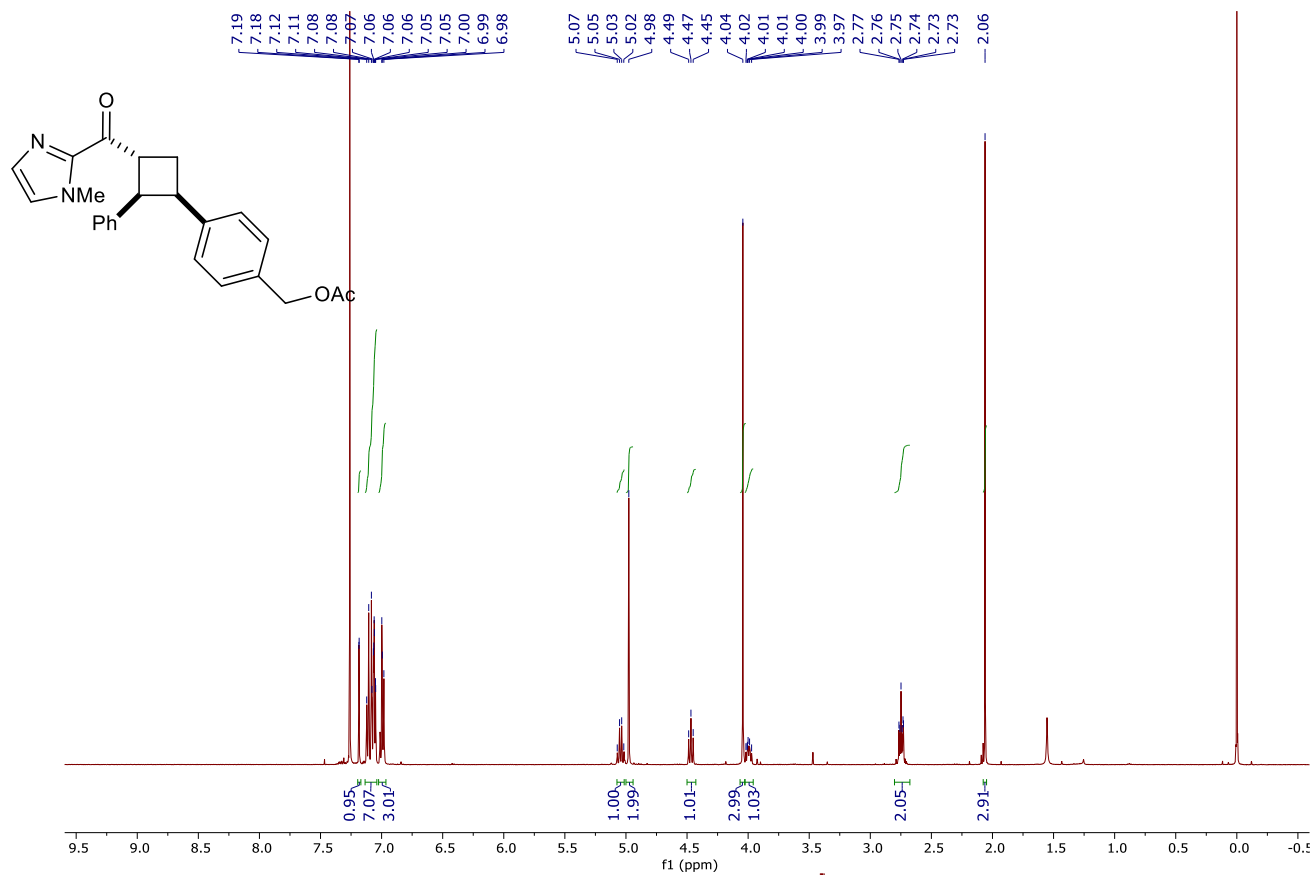


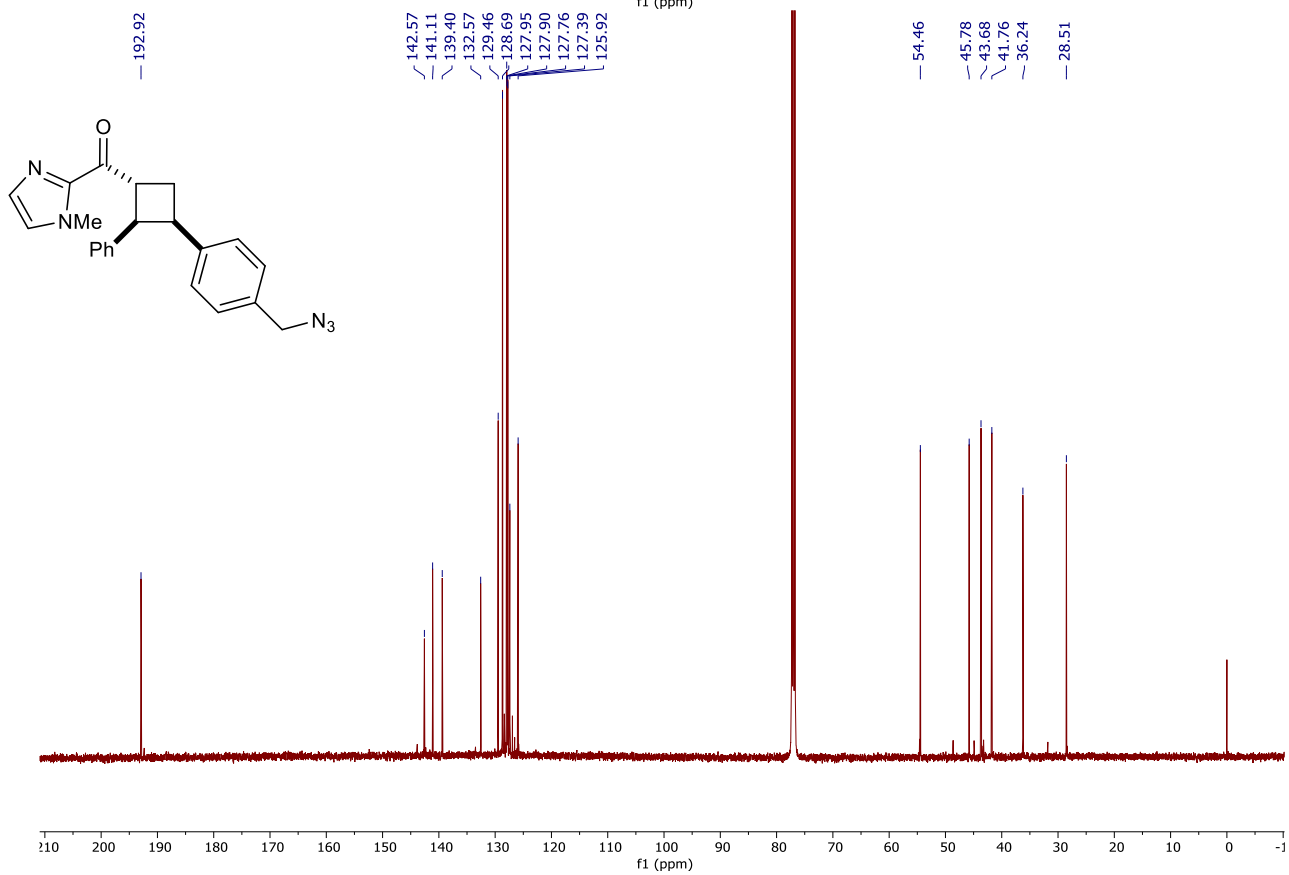
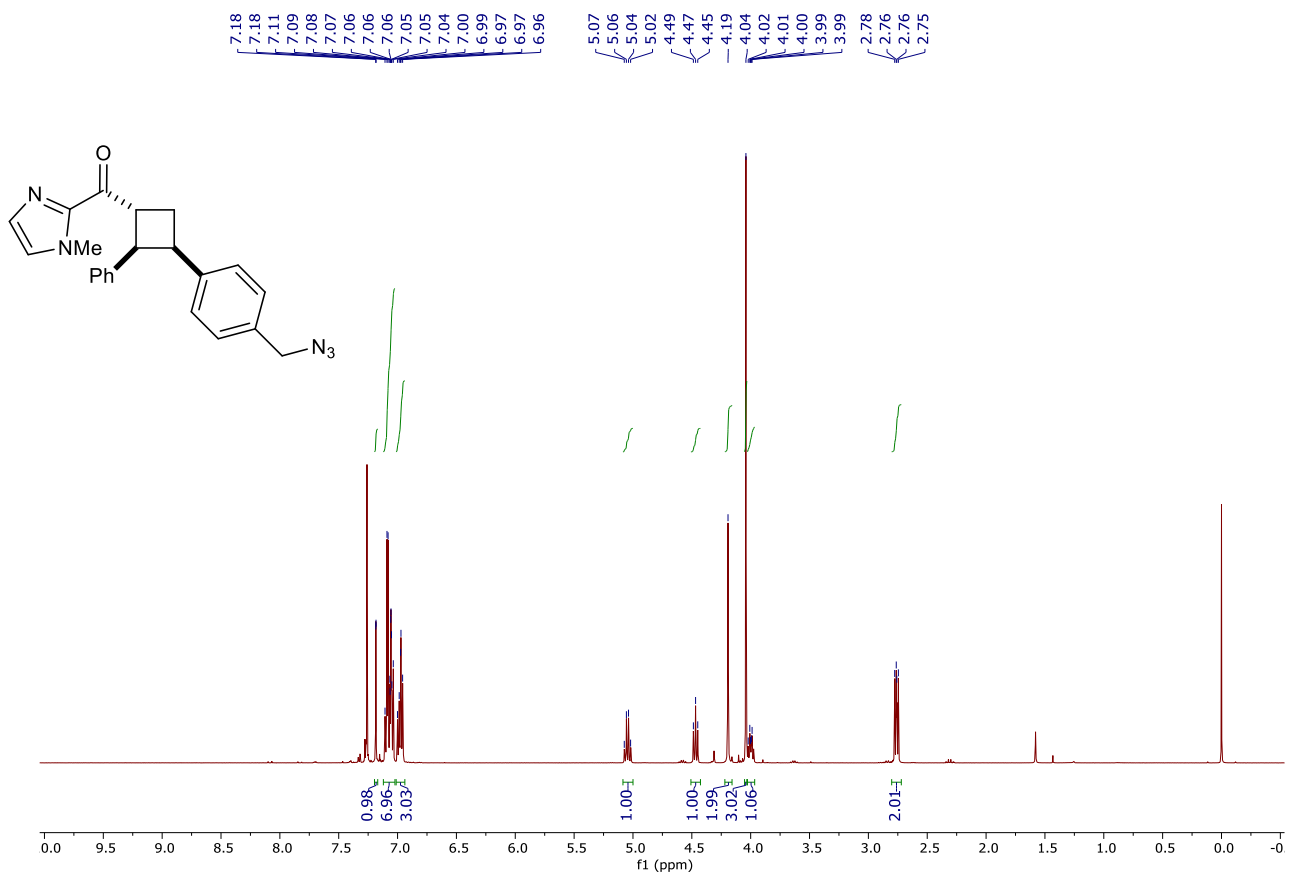


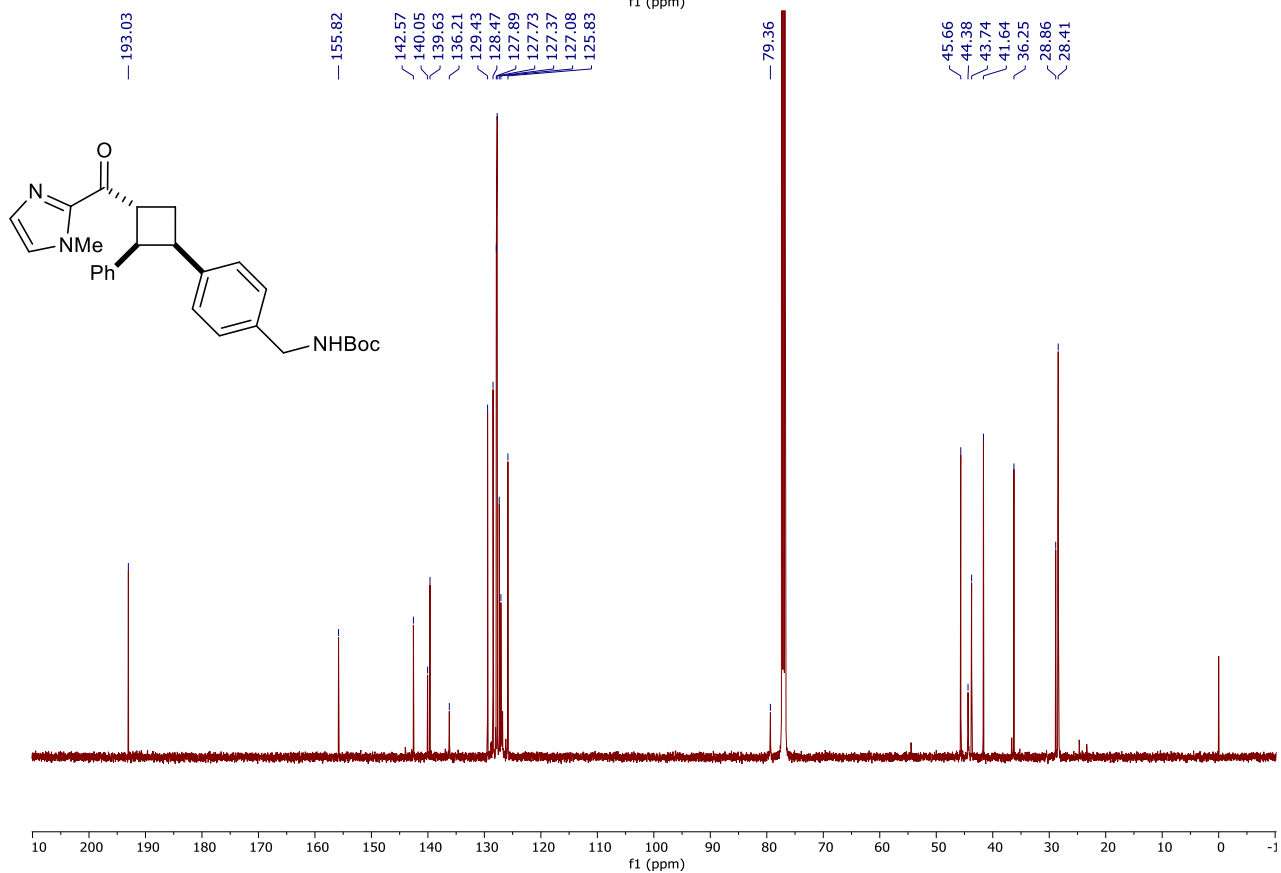
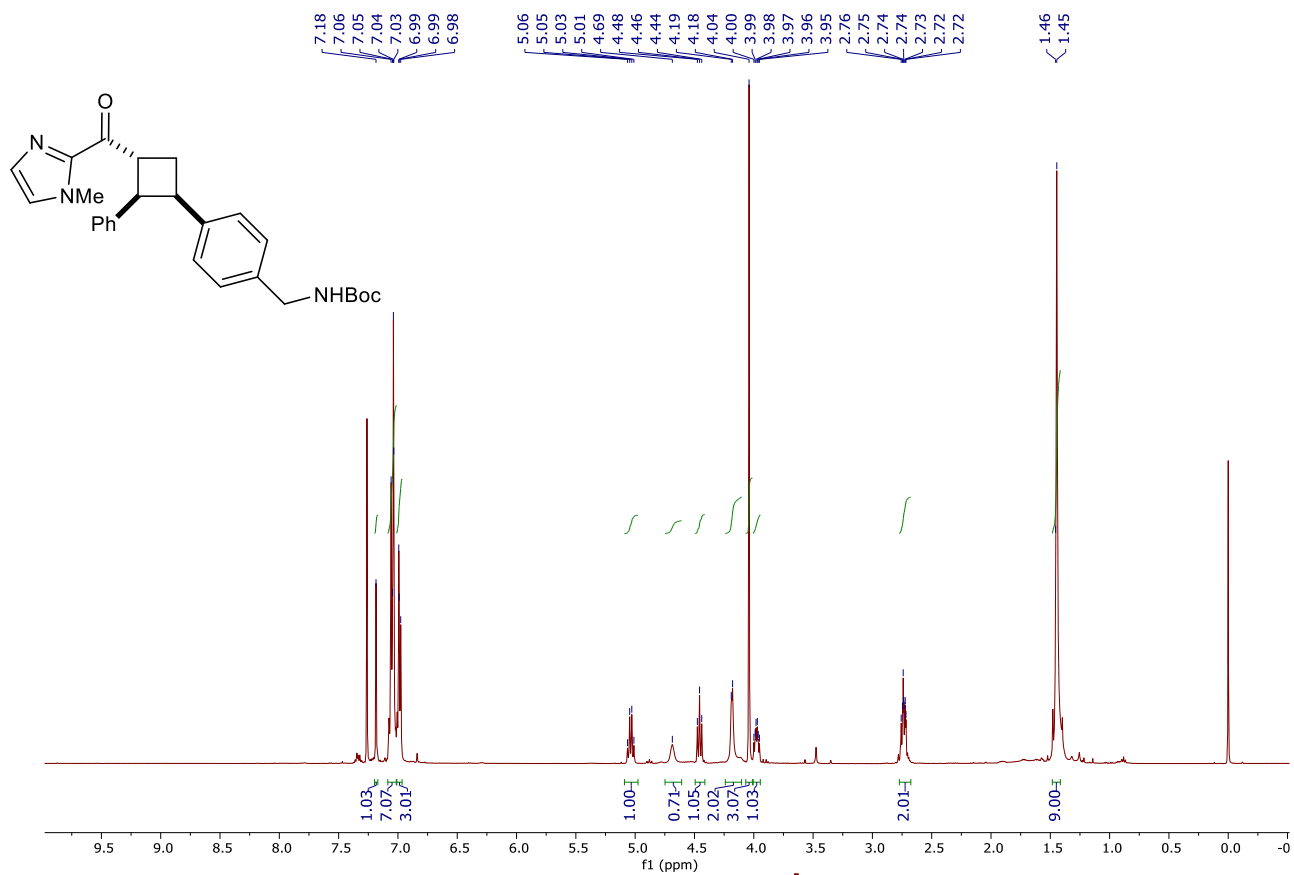


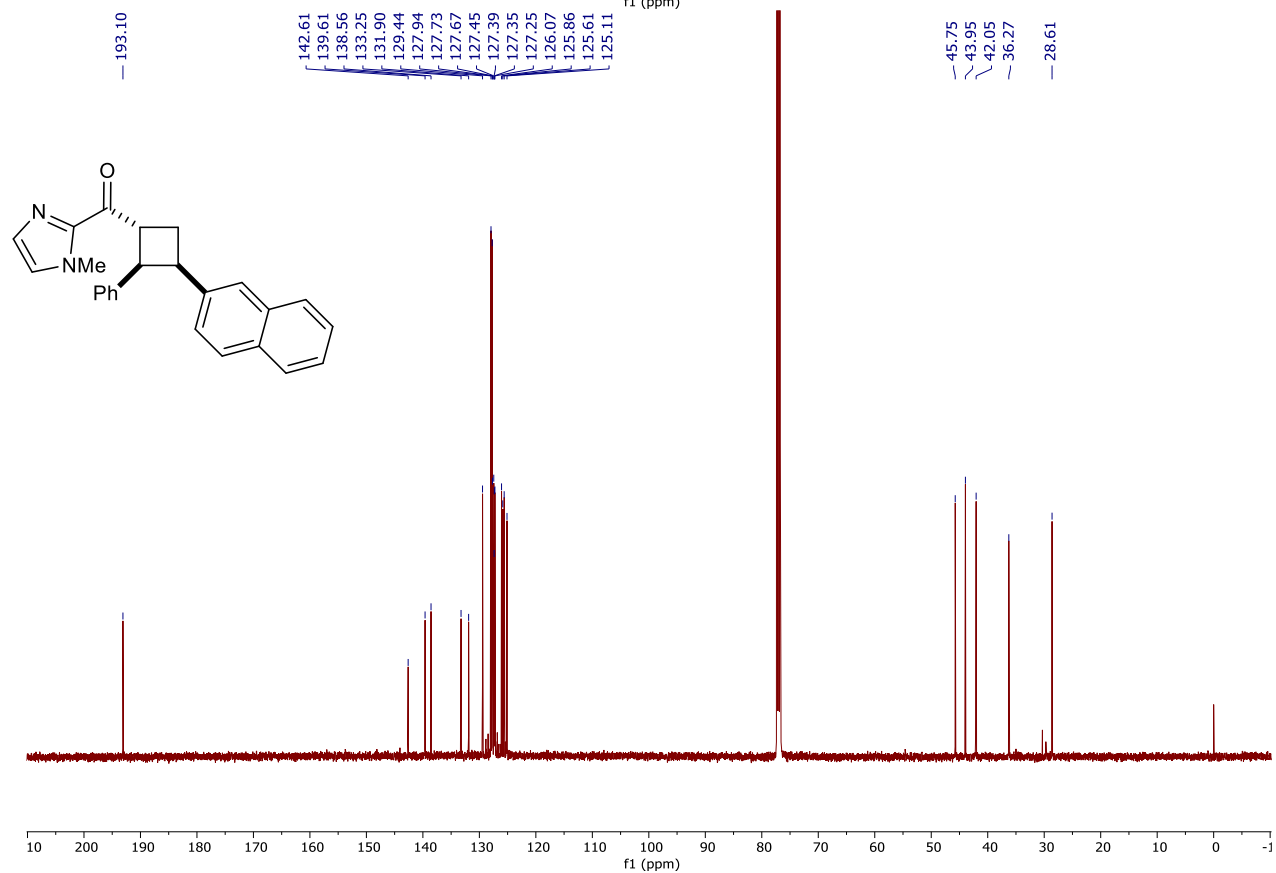
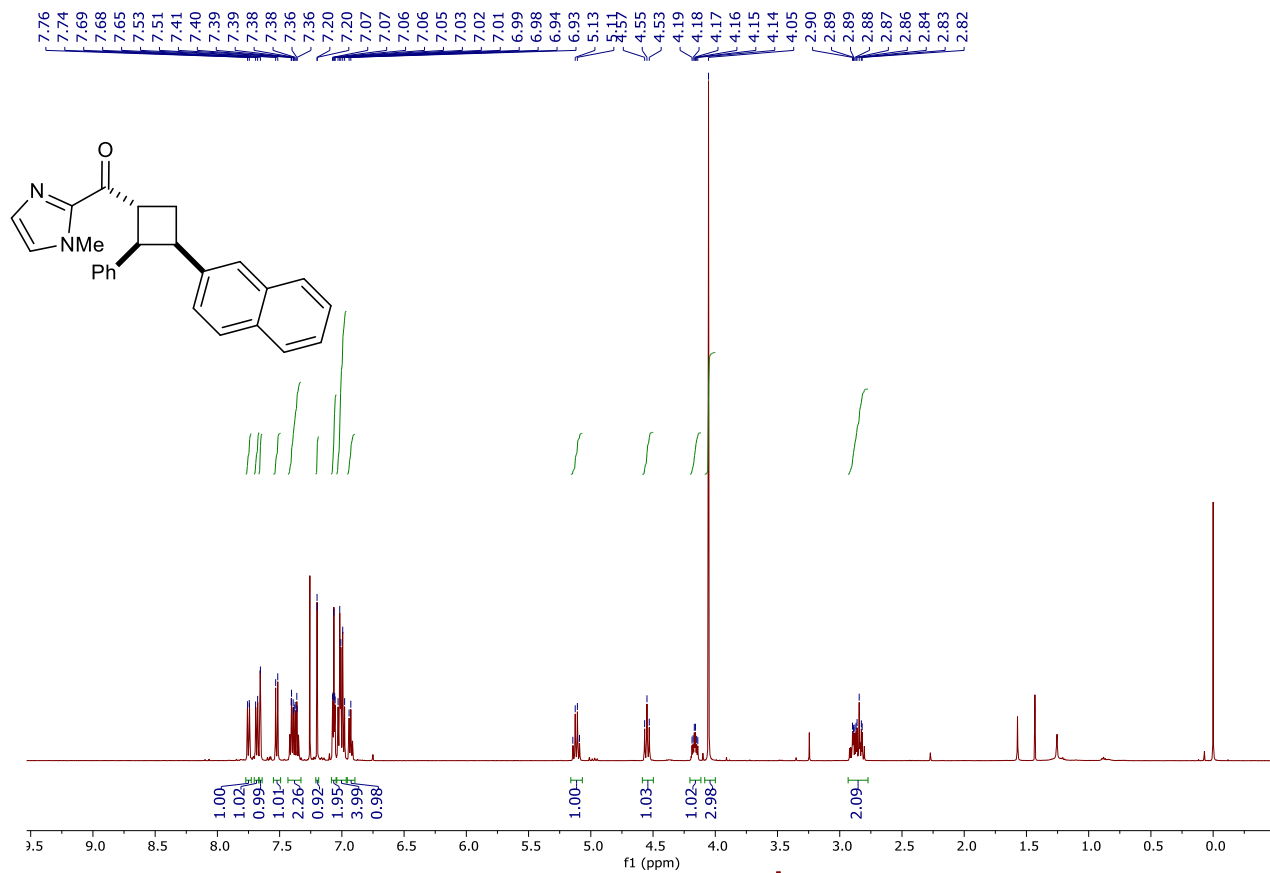


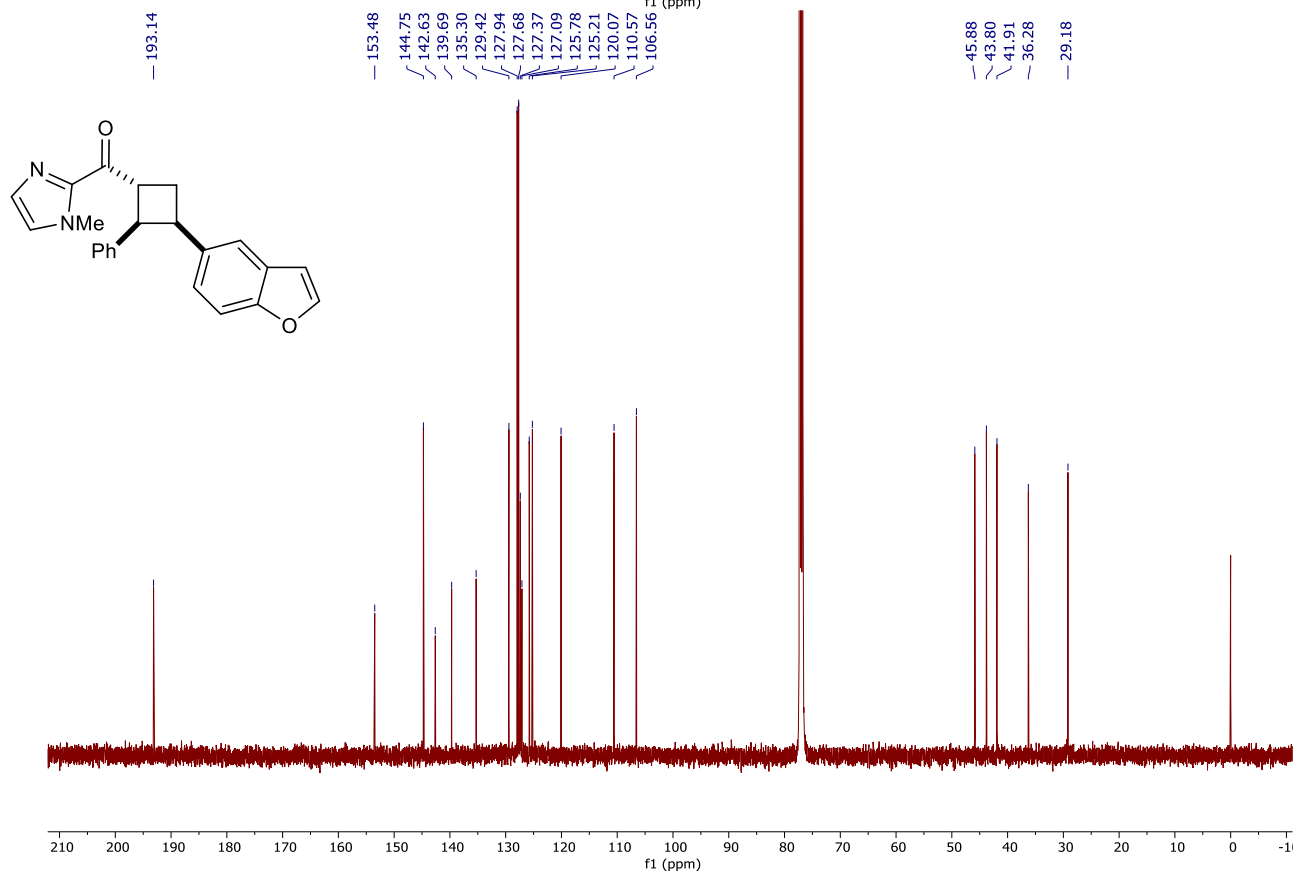
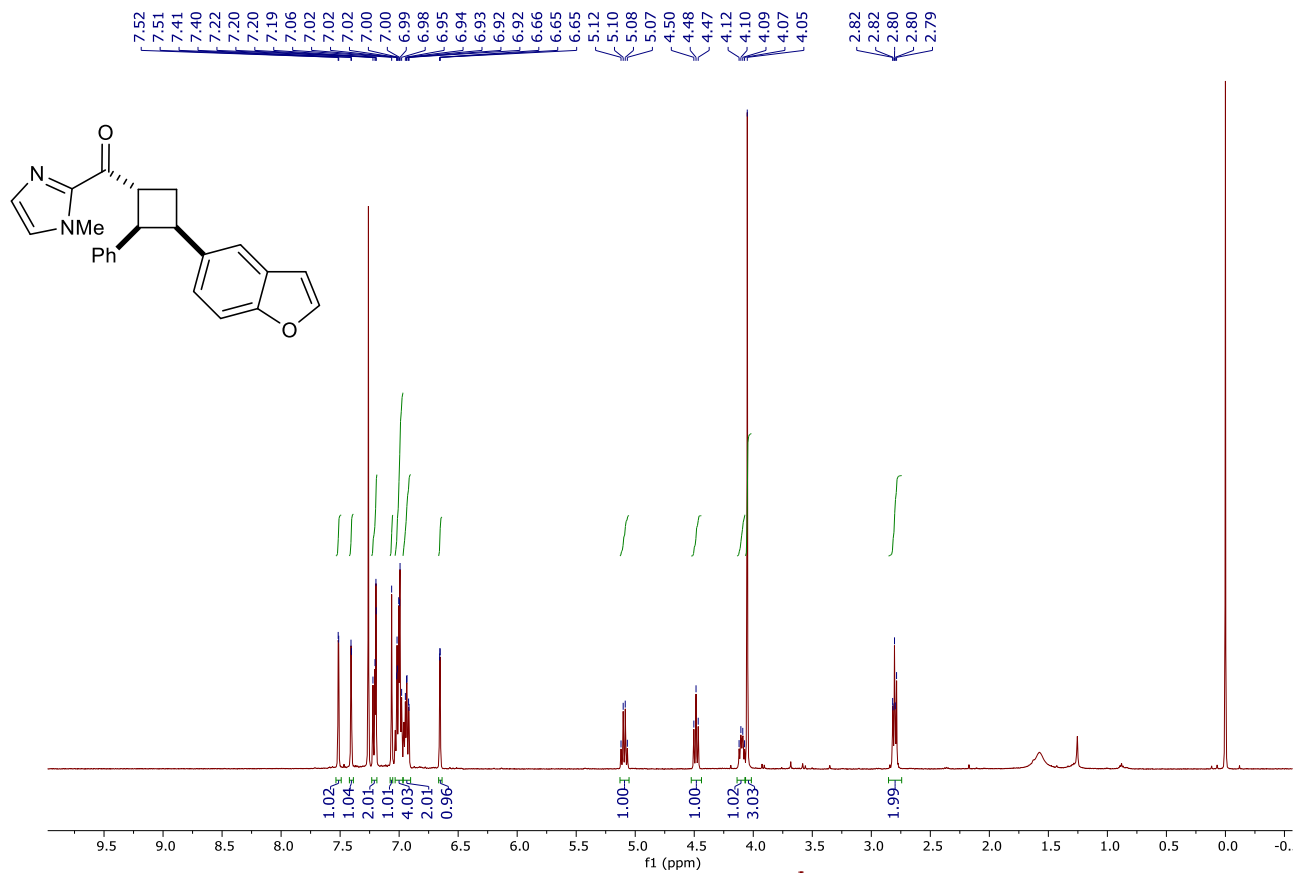


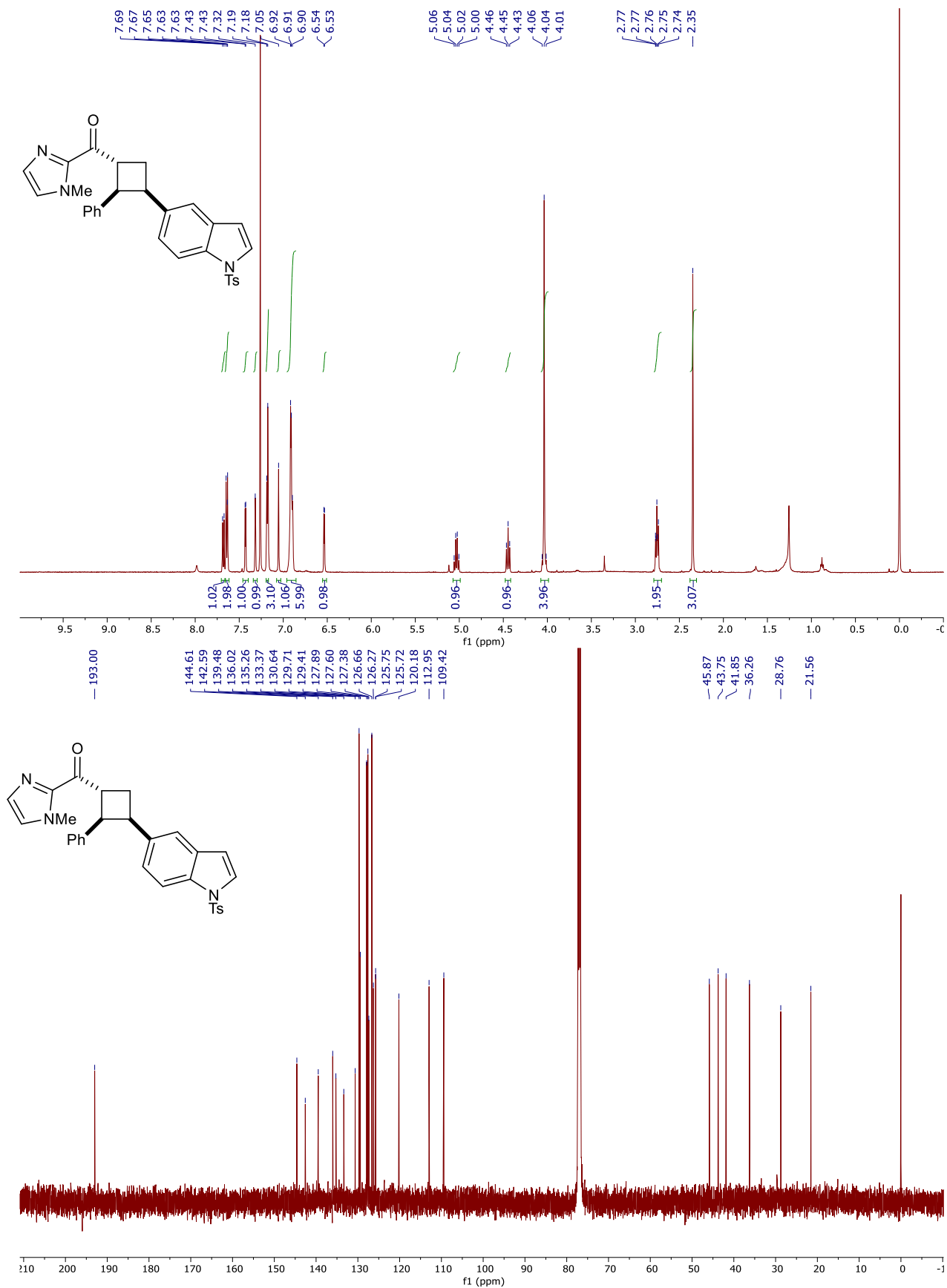


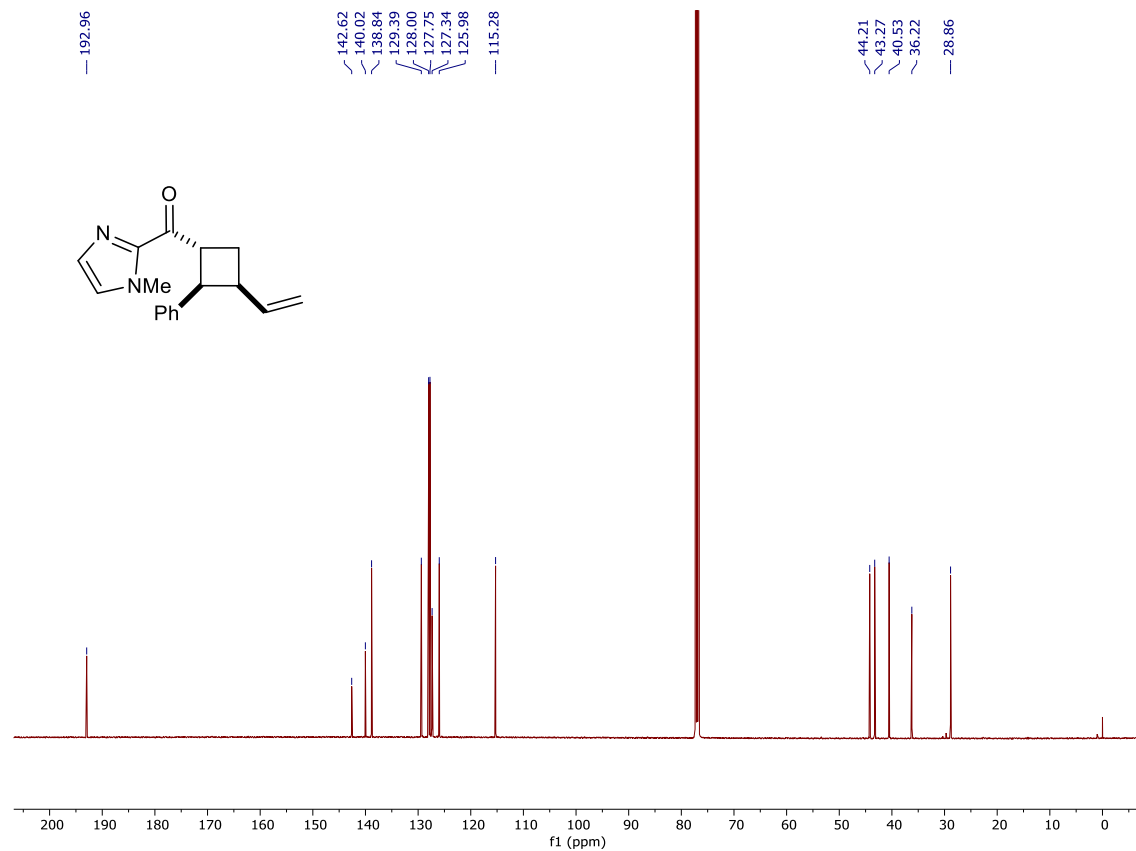
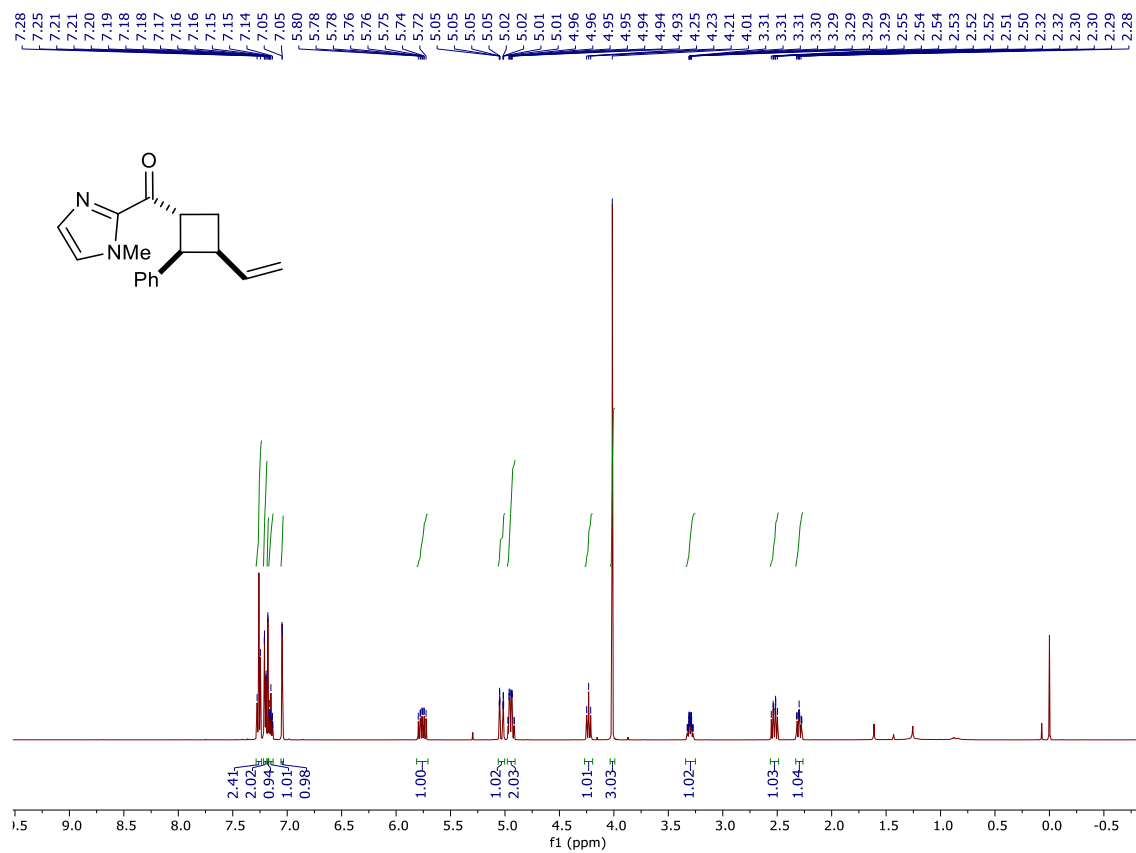


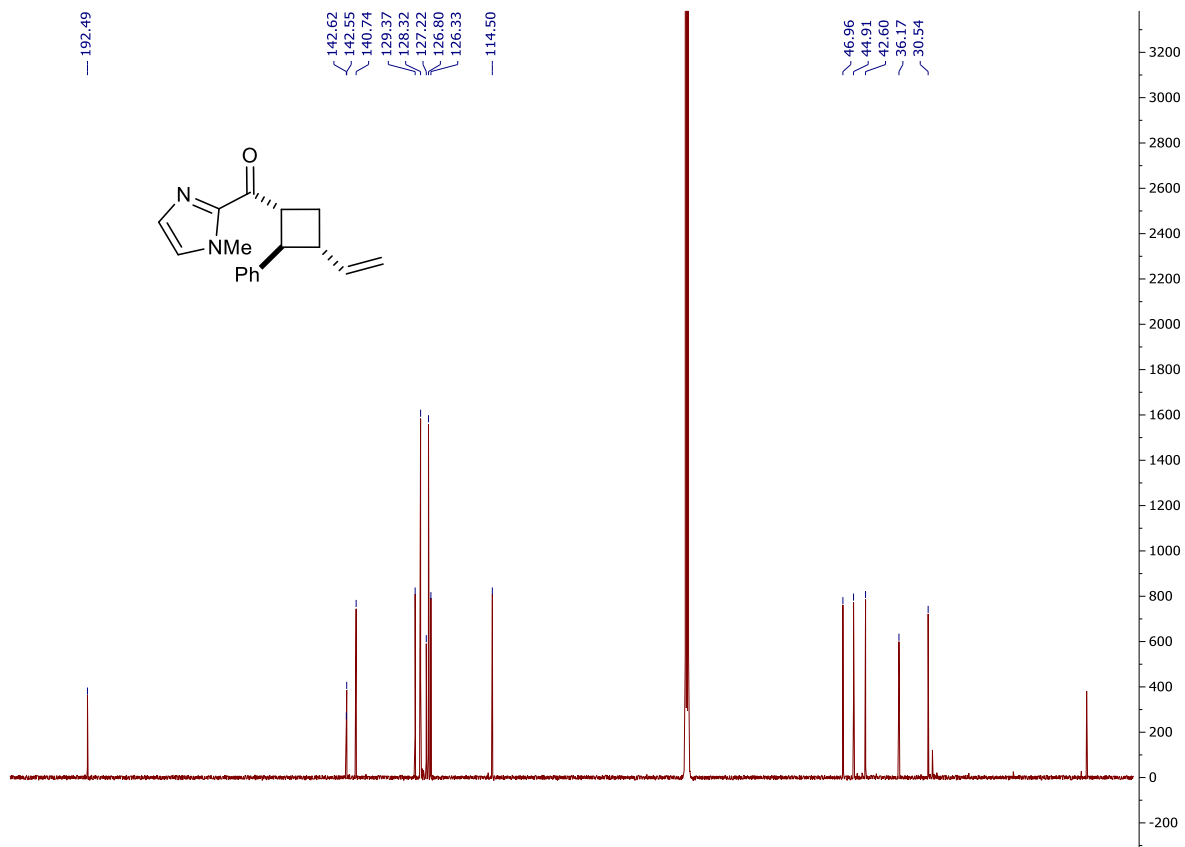
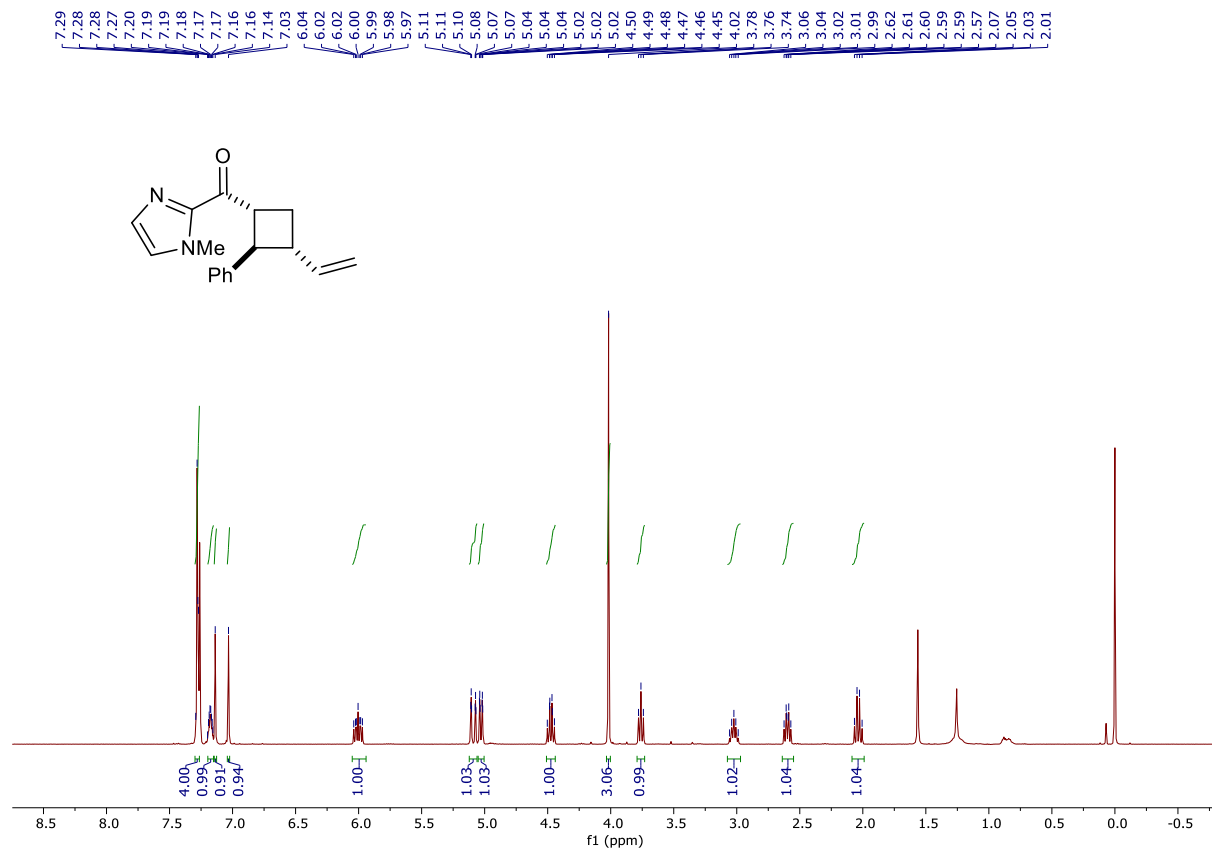


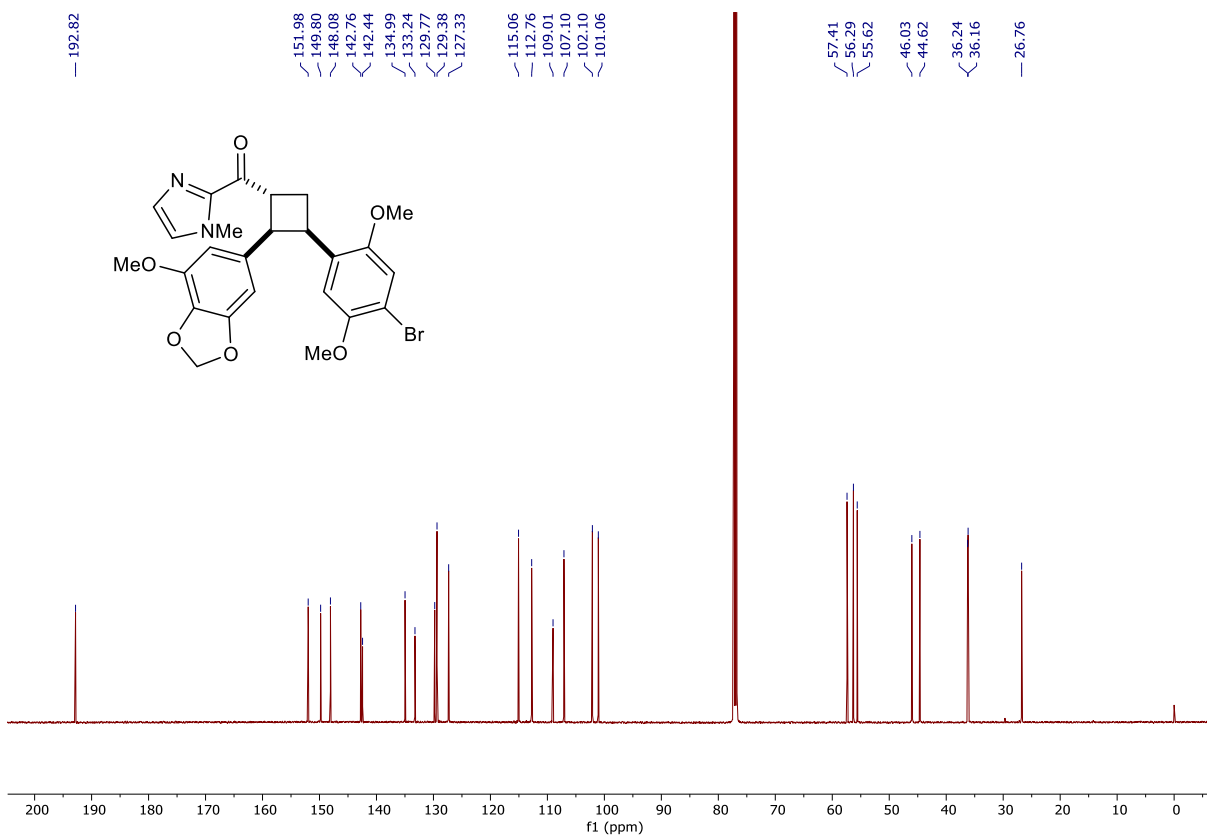
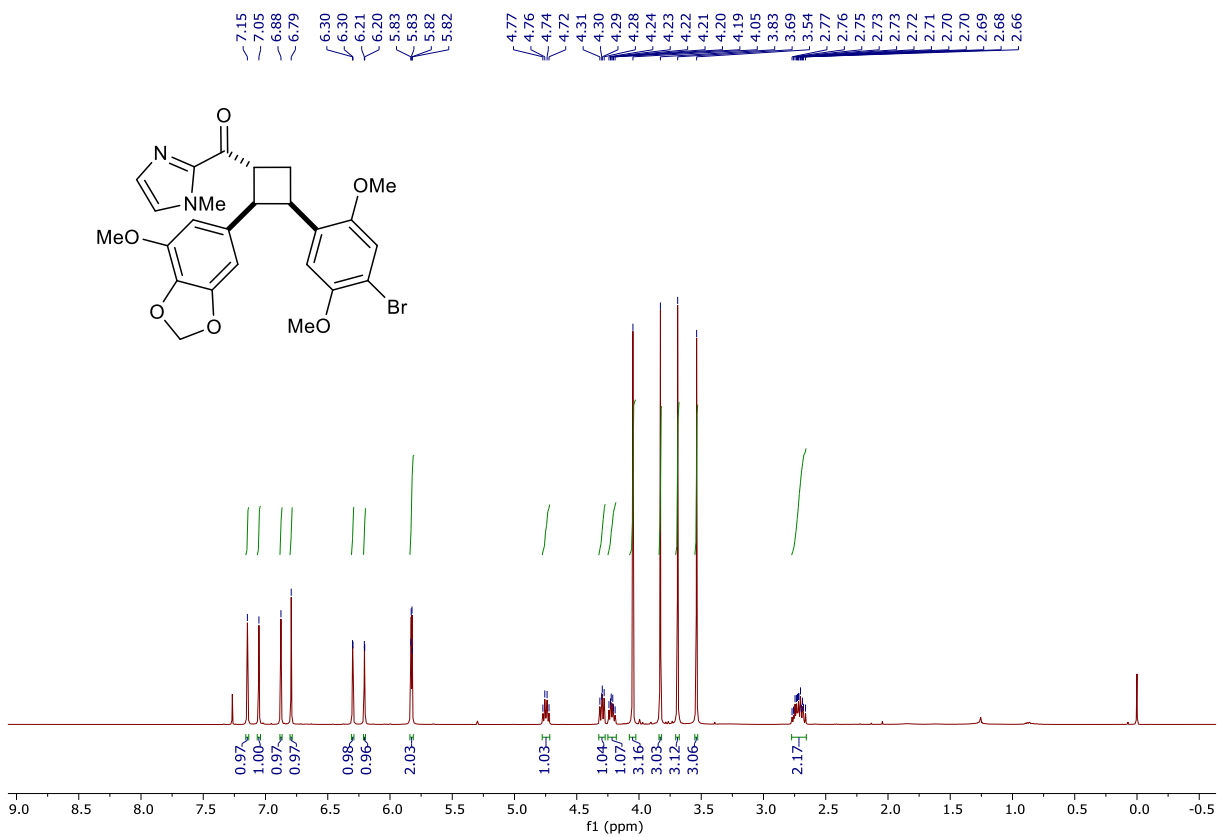


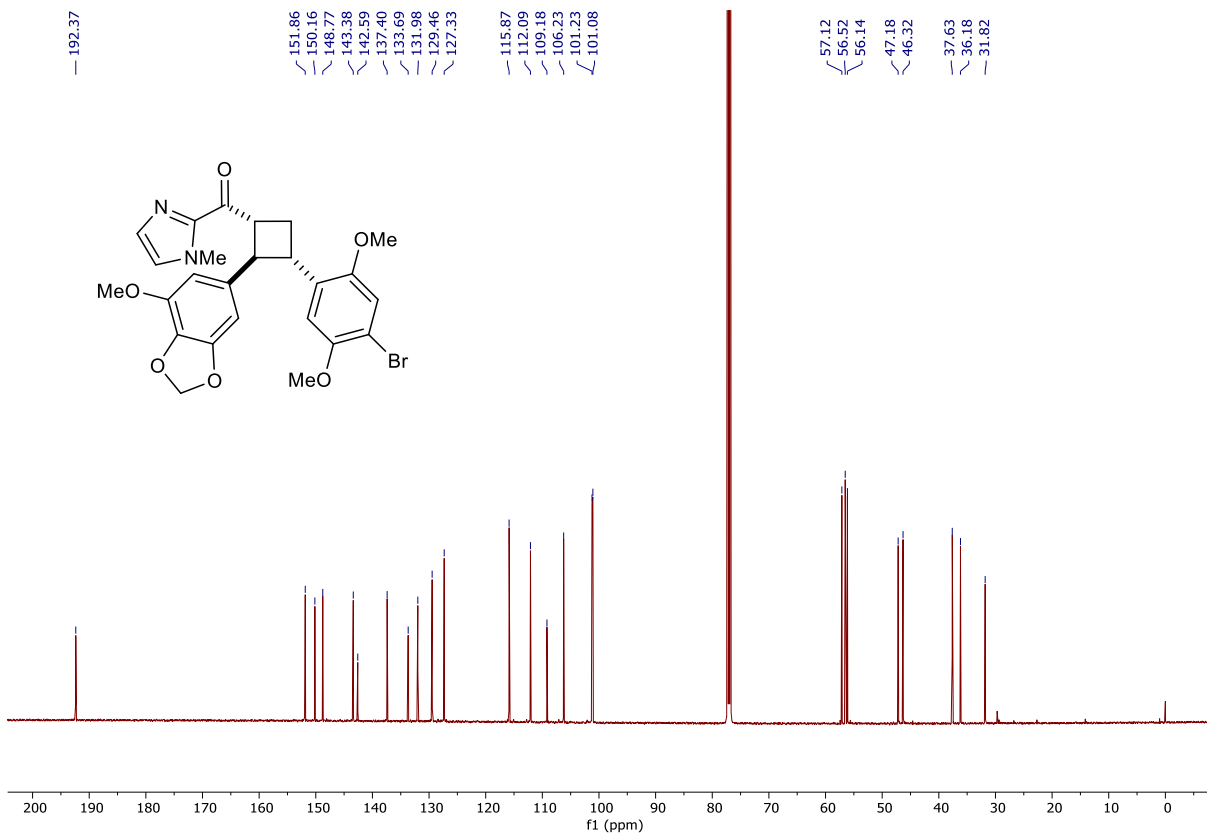
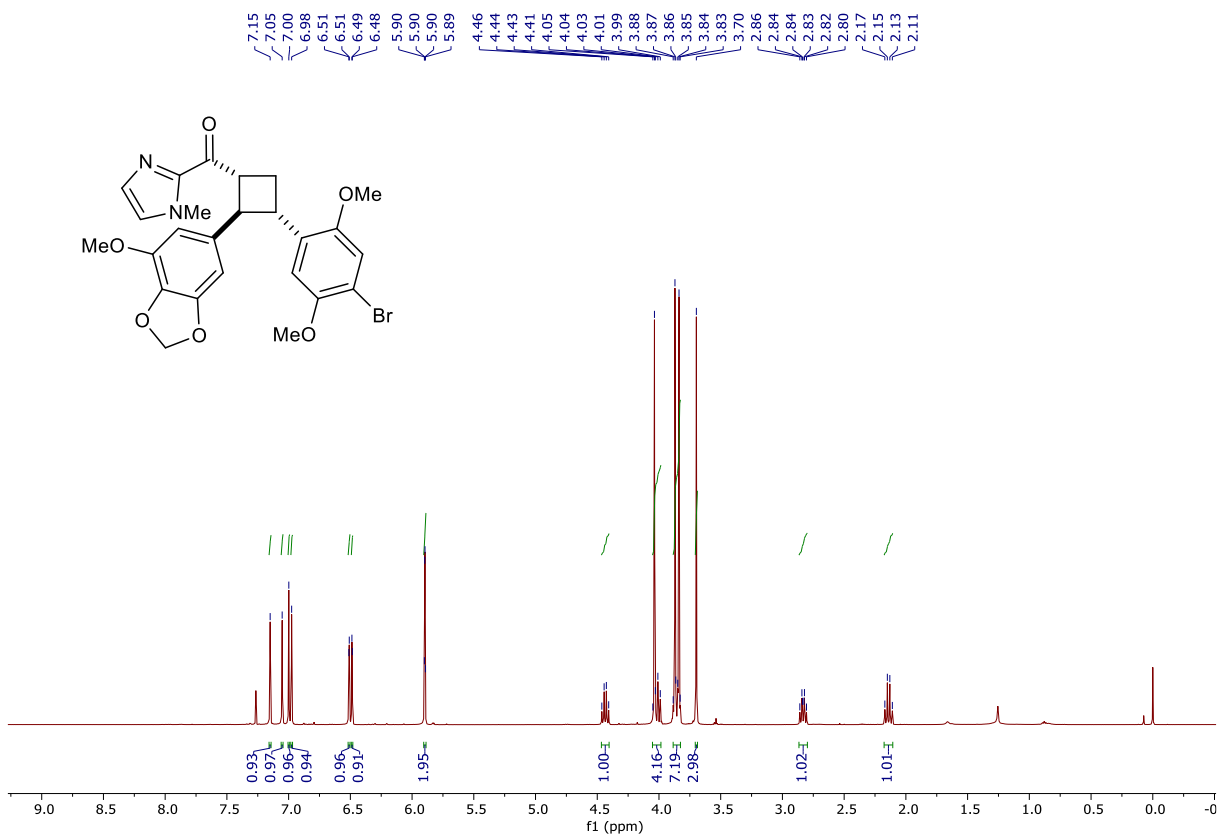


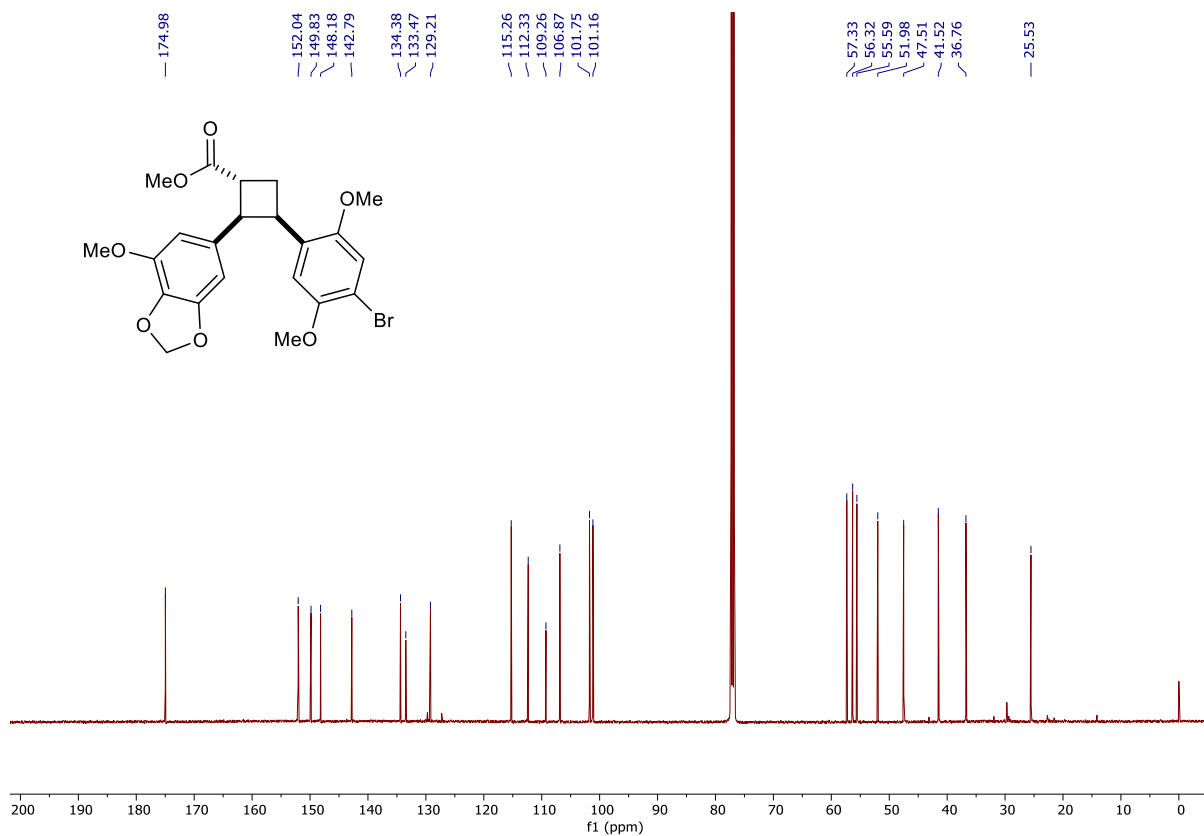
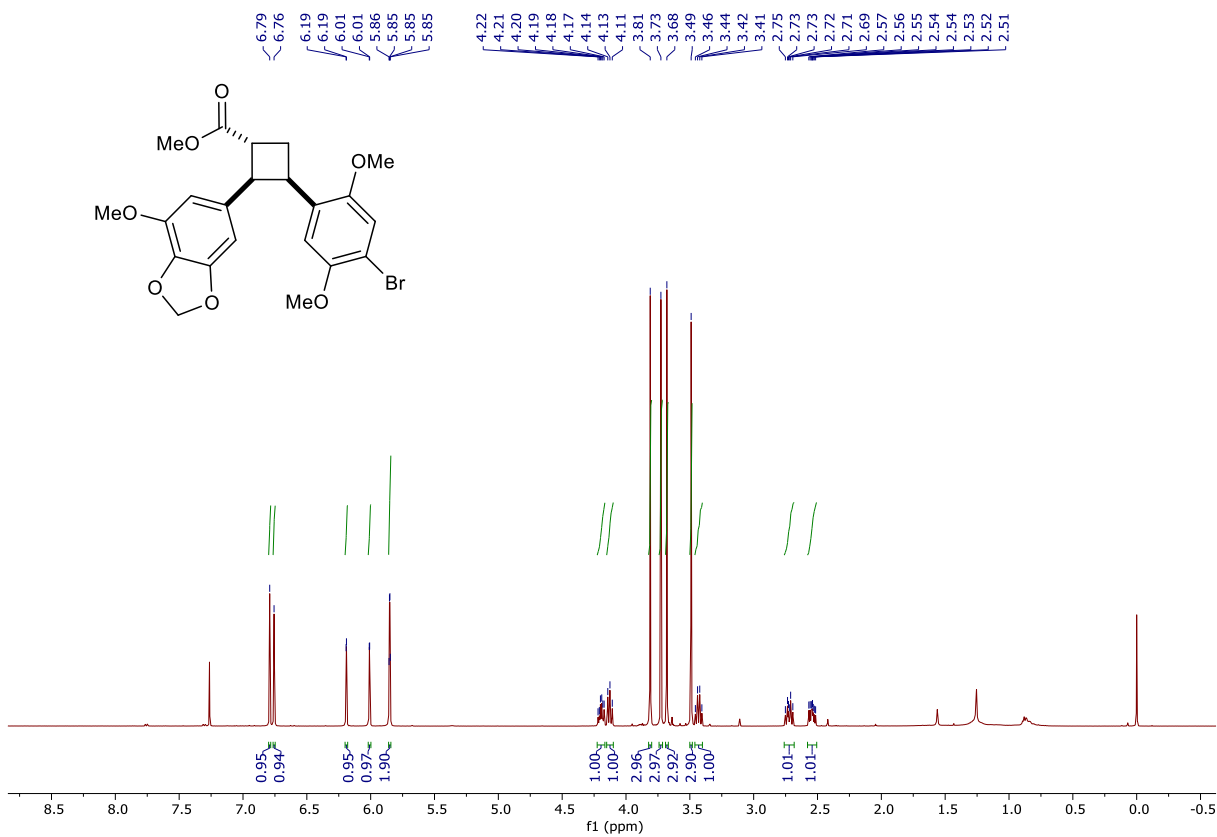




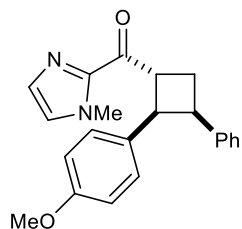




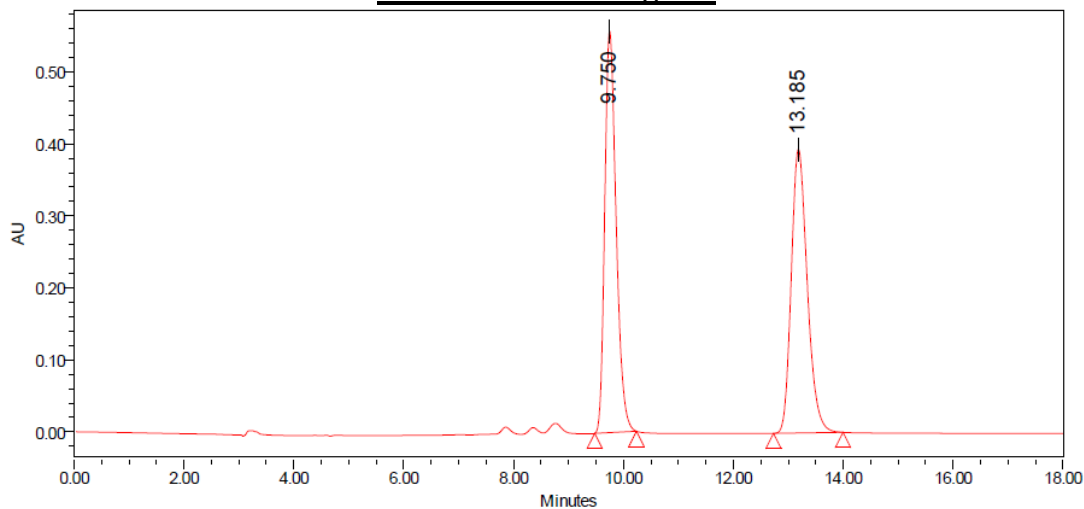




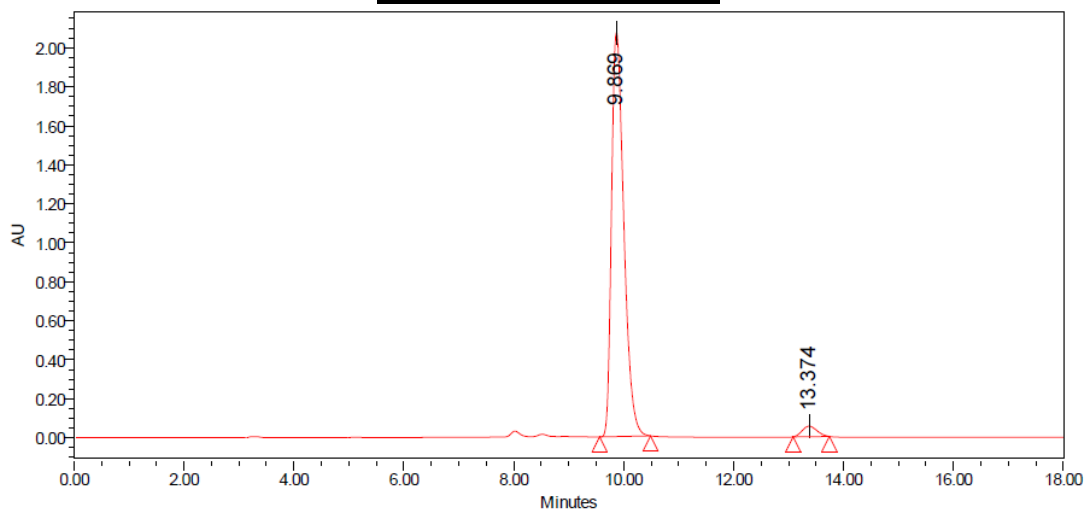
2.6.12 HPLC Data

**2.5 – Major Diastereomer**

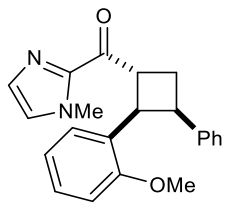
Run Details: HPLC, Daicel CHIRALPAK OD-H,
10.00 μ L, gradient 5% to 50% iPrOH/hexanes,
18 minutes, 1 mL/min, 285.0 nm.

Racemic Chromatogram

Peak	% Area	Retention Time	Area	Height
1	50.13	9.750	8015689	557798
2	49.87	13.185	7974187	394103

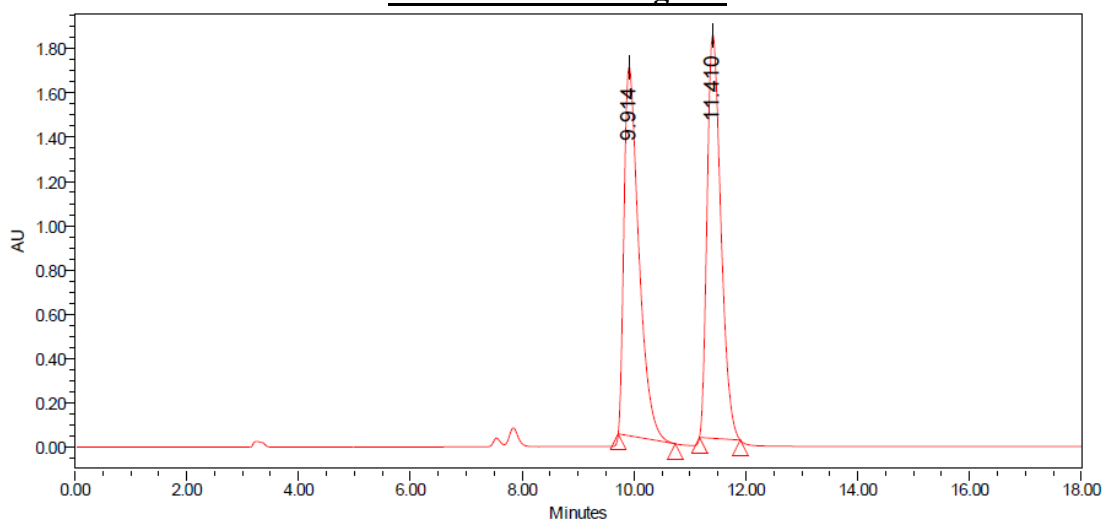
Scalemic Chromatogram

Peak	% Area	Retention Time	Area	Height
1	96.97	9.869	32171708	2072111
2	3.03	13.374	1004823	53875



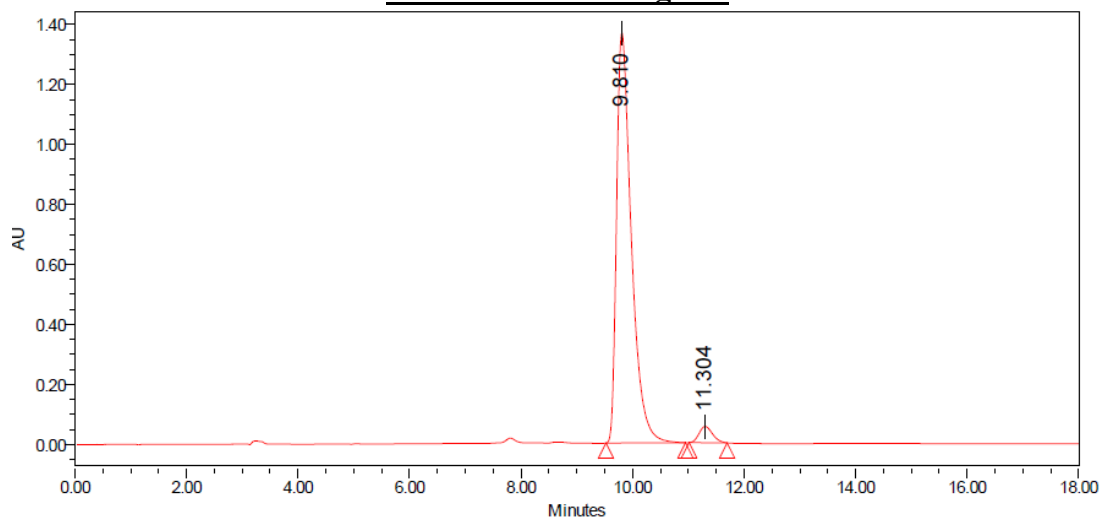
2.6 – Major Diastereomer
 Run Details: HPLC, Daicel CHIRALPAK OD-H,
 10.00 μ L, gradient 5% to 50% iPrOH/hexanes,
 18 minutes, 1 mL/min, 285.0 nm.

Racemic Chromatogram

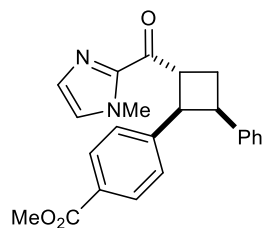


Peak	% Area	Retention Time	Area	Height
1	49.57	9.914	30595009	1665034
2	50.43	11.410	31128716	1821414

Scalemic Chromatogram

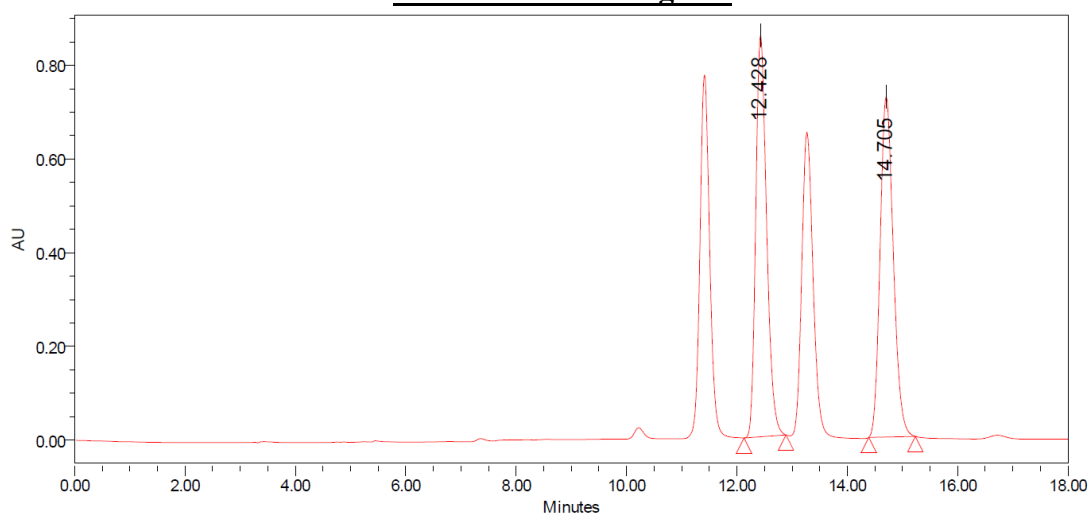


Peak	% Area	Retention Time	Area	Height
1	96.51	9.810	25105171	1366802
2	3.49	11.304	907184	54271



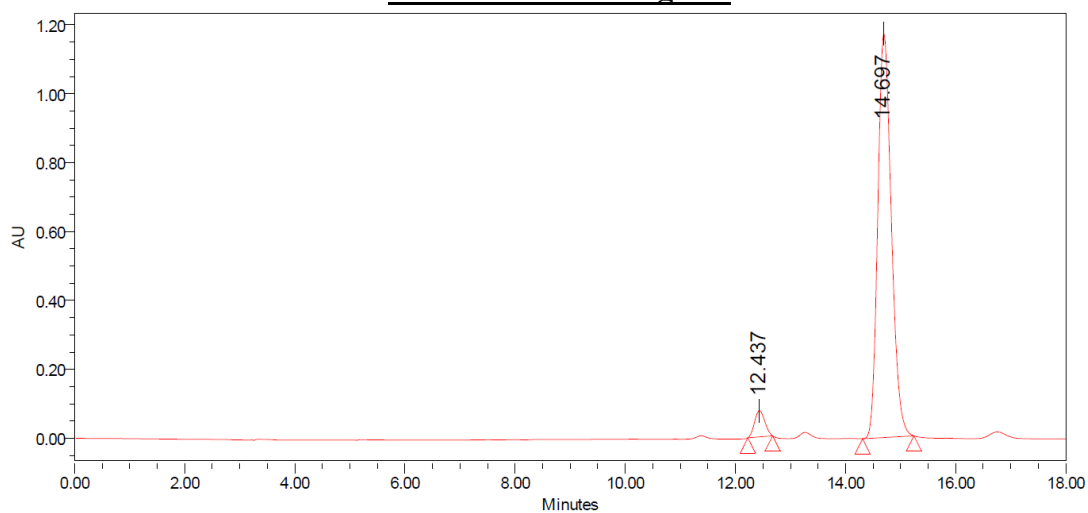
2.7 – Major Diastereomer
 Run Details: HPLC, Daicel CHIRALPAK IC,
 10.00 μ L, gradient 5% to 50% iPrOH/hexanes,
 18 minutes, 1 mL/min, 285.0 nm.

Racemic Chromatogram

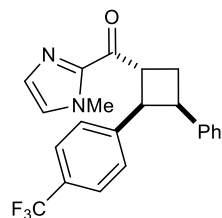


Peak	% Area	Retention Time	Area	Height
1	49.30	12.428	11713056	856183
2	50.70	14.705	12046092	726276

Scalemic Chromatogram

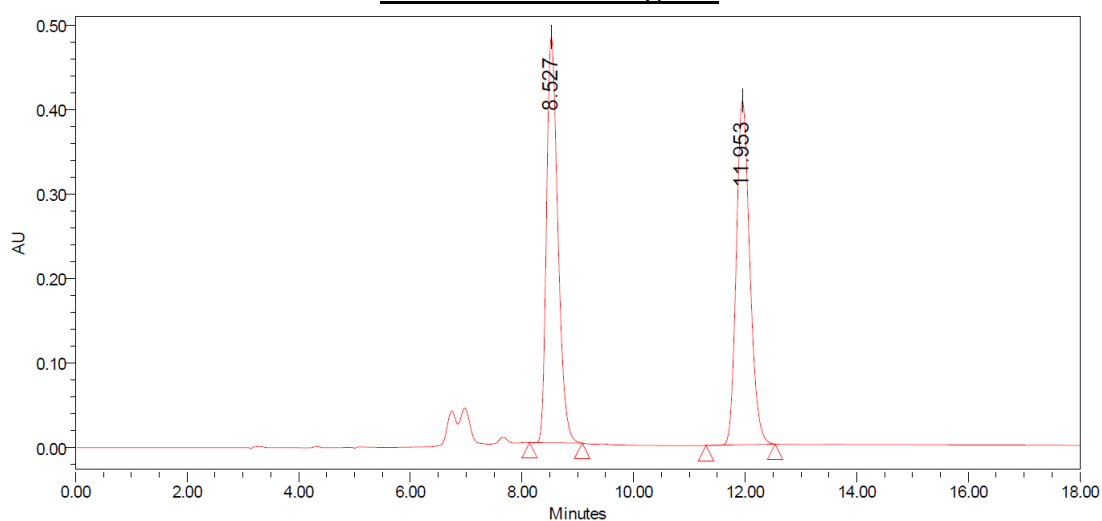


Peak	% Area	Retention Time	Area	Height
1	4.69	12.437	984839	76126
2	95.31	14.697	20027600	1171914



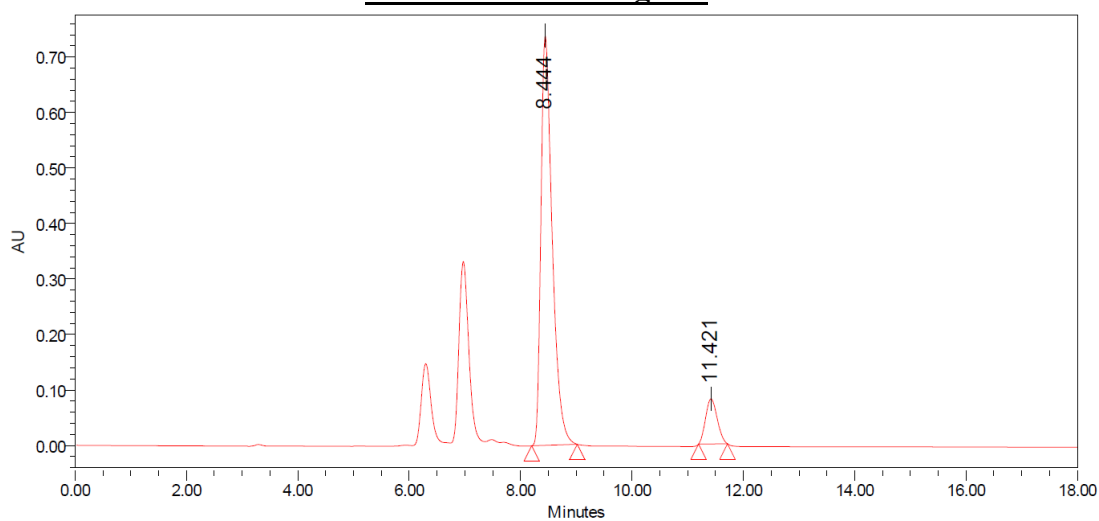
2.8 – Major Diastereomer
 Run Details: HPLC, Daicel CHIRALPAK OD-H,
 10.00 μ L, gradient 5% to 50% iPrOH/hexanes,
 18 minutes, 1 mL/min, 285.0 nm.

Racemic Chromatogram

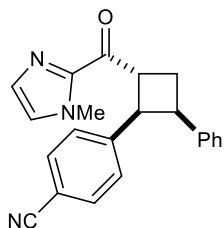


Peak	% Area	Retention Time	Area	Height
1	49.80	8.527	6786719	480179
2	50.20	11.953	6842091	407223

Scalemic Chromatogram

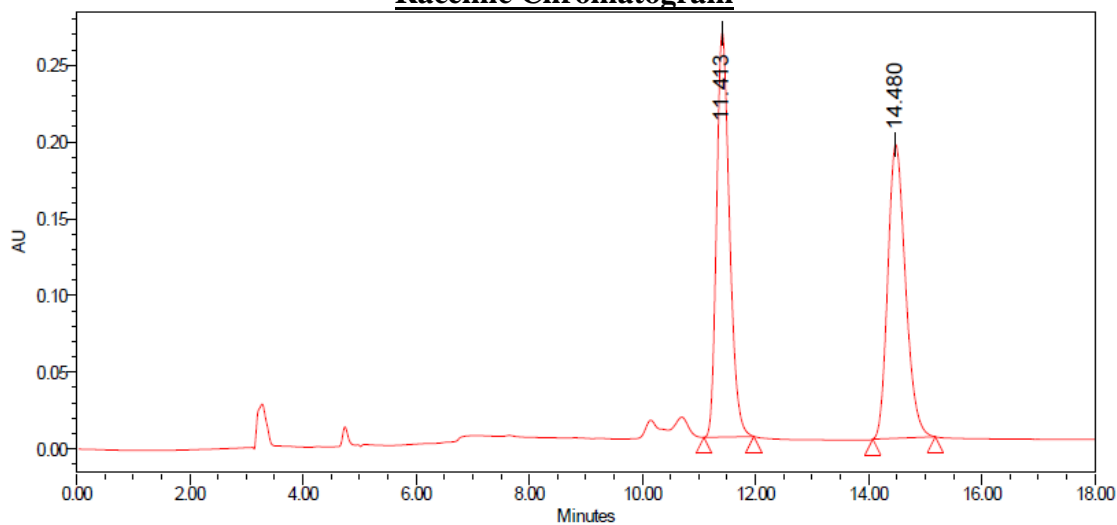


Peak	% Area	Retention Time	Area	Height
1	89.84	8.444	103377818	738048
2	10.16	11.421	1173611	81243



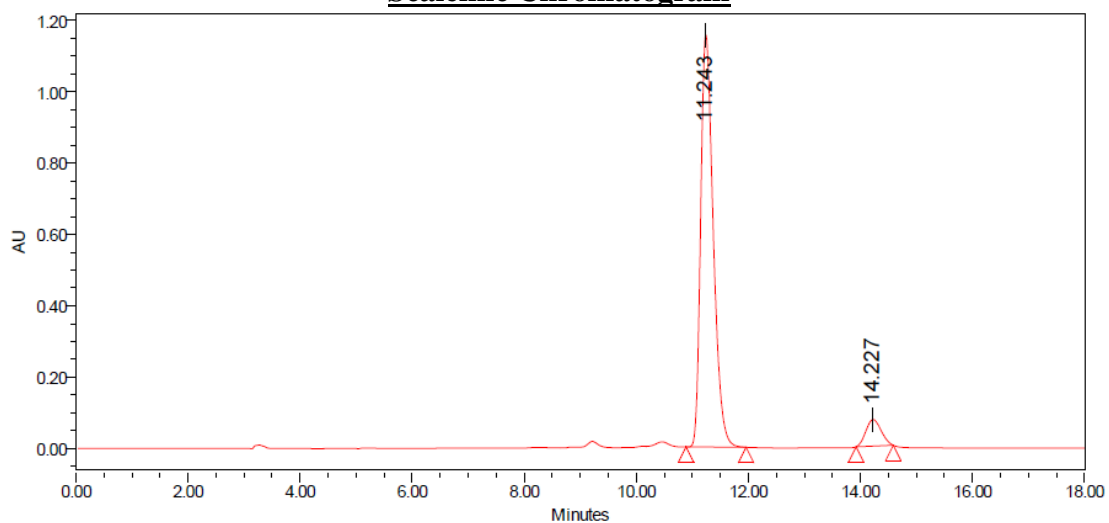
2.9 – Major Diastereomer
 Run Details: HPLC, Daicel CHIRALPAK OD-H,
 10.00 μ L, gradient 5% to 50% iPrOH/hexanes,
 18 minutes, 1 mL/min, 285.0 nm.

Racemic Chromatogram

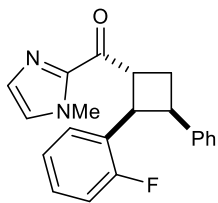


Peak	% Area	Retention Time	Area	Height
1	50.09	11.413	4177021	263466
2	49.91	14.480	4161384	191452

Scalemic Chromatogram

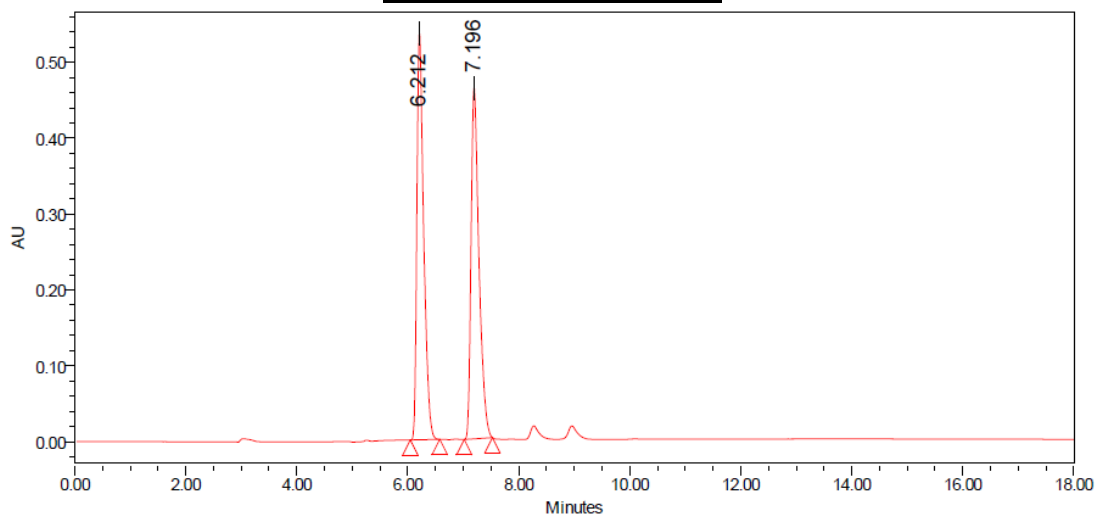


Peak	% Area	Retention Time	Area	Height
1	92.76	11.243	18002516	1154979
2	7.24	14.227	1404431	74207



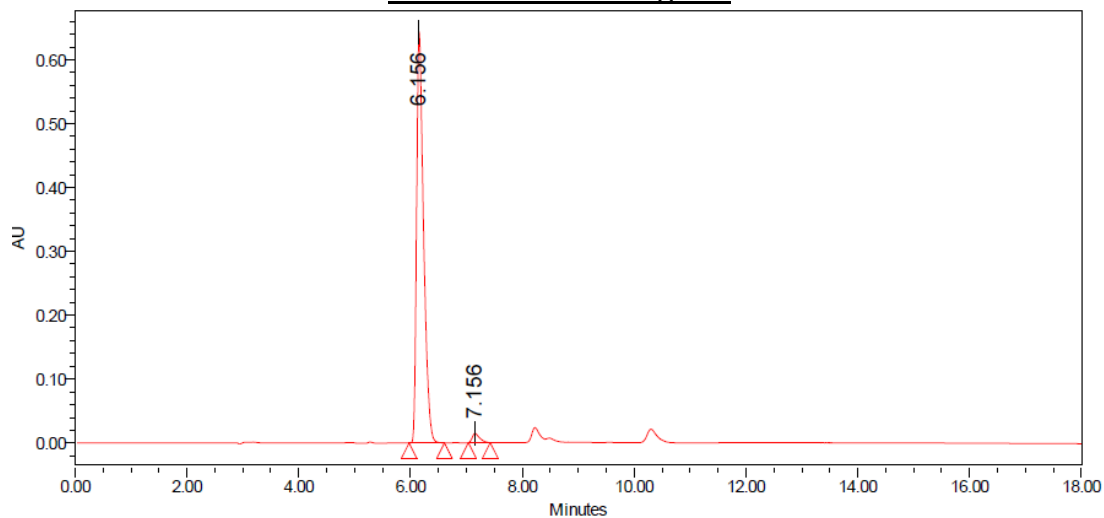
2.10 – Major Diastereomer
 Run Details: HPLC, Daicel CHIRALPAK AD-H,
 10.00 μ L, gradient 5% to 50% iPrOH/hexanes,
 18 minutes, 1 mL/min, 285.0 nm.

Racemic Chromatogram

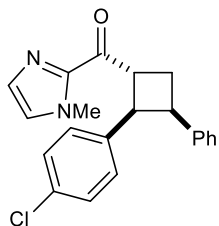


Peak	% Area	Retention Time	Area	Height
1	49.98	6.212	4565931	536238
2	50.02	7.196	4568814	462728

Scalemic Chromatogram

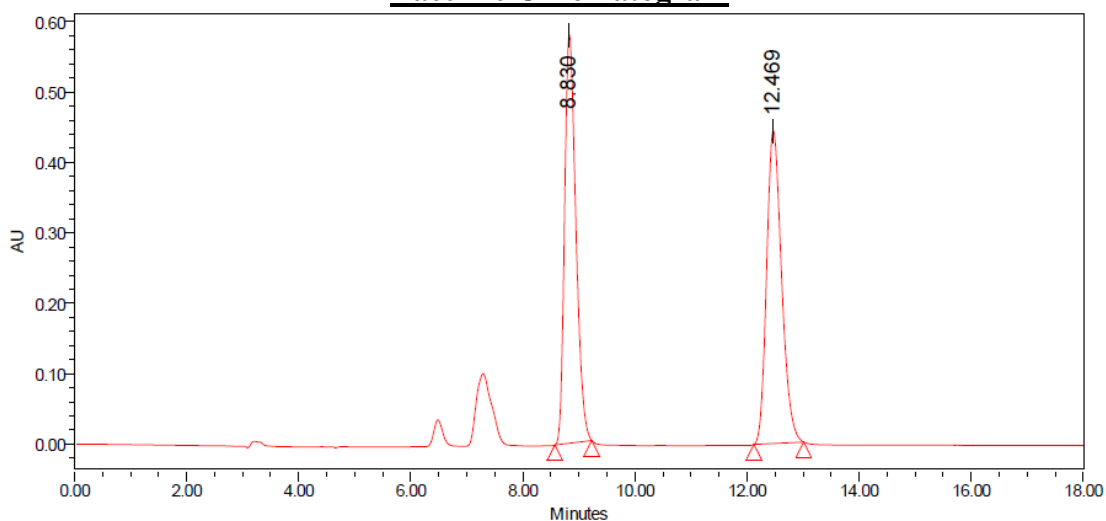


Peak	% Area	Retention Time	Area	Height
1	97.69	6.156	5575042	643845
2	2.31	7.156	131780	14391



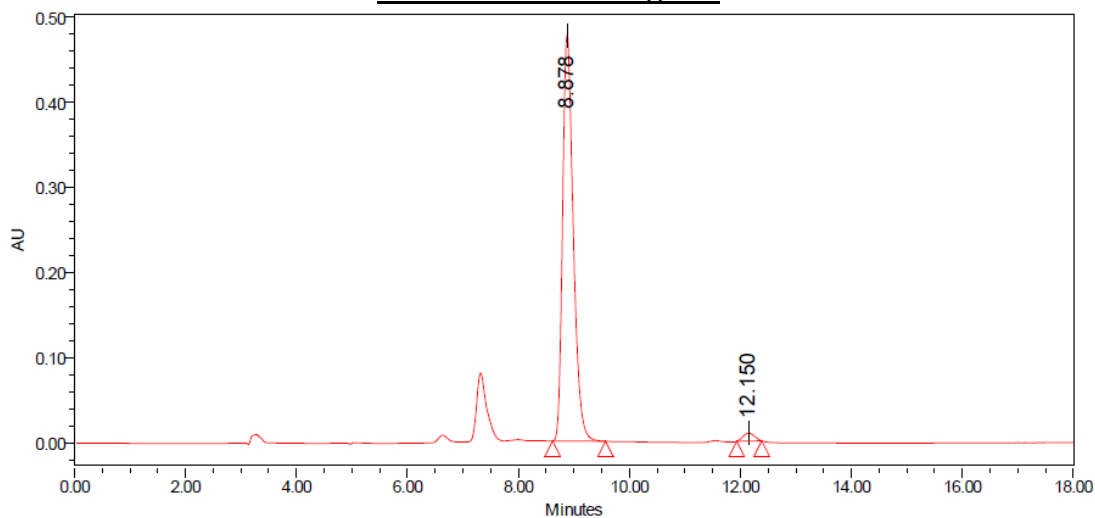
2.11 – Major Diastereomer
 Run Details: HPLC, Daicel CHIRALPAK OD-H,
 10.00 μ L, gradient 5% to 50% iPrOH/hexanes,
 18 minutes, 1 mL/min, 285.0 nm.

Racemic Chromatogram

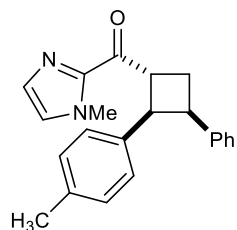


Peak	% Area	Retention Time	Area	Height
1	49.66	8.830	8123700	580289
2	50.34	12.469	8235993	444490

Scalemic Chromatogram

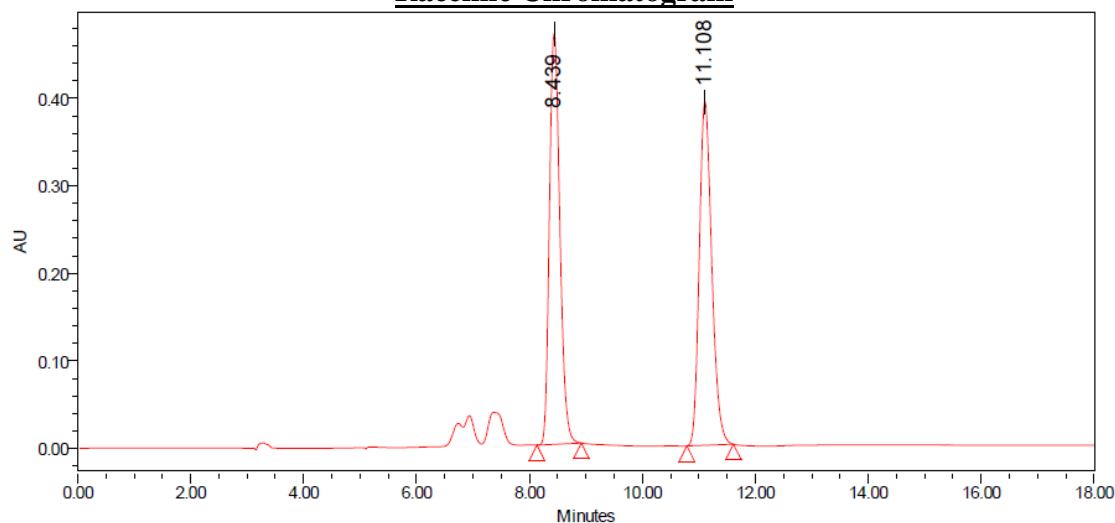


Peak	% Area	Retention Time	Area	Height
1	97.96	8.878	6372481	476435
2	2.04	12.150	132649	9274



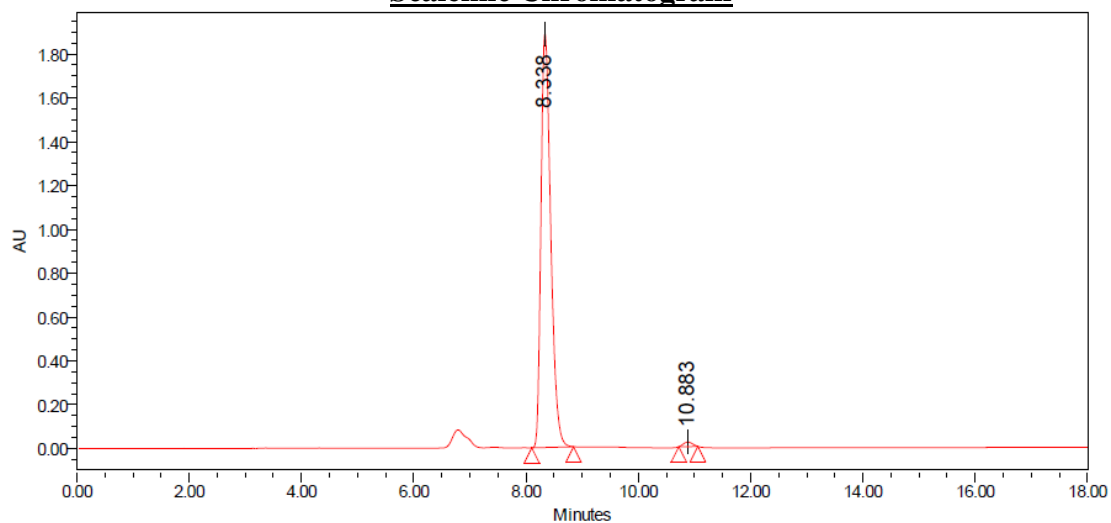
2.12 – Major Diastereomer
 Run Details: HPLC, Daicel CHIRALPAK OD-H,
 10.00 μ L, gradient 5% to 50% iPrOH/hexanes,
 18 minutes, 1 mL/min, 285.0 nm.

Racemic Chromatogram

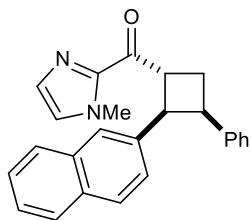


Peak	% Area	Retention Time	Area	Height
1	49.98	8.439	6025706	469776
2	50.02	11.108	6031563	393085

Scalemic Chromatogram

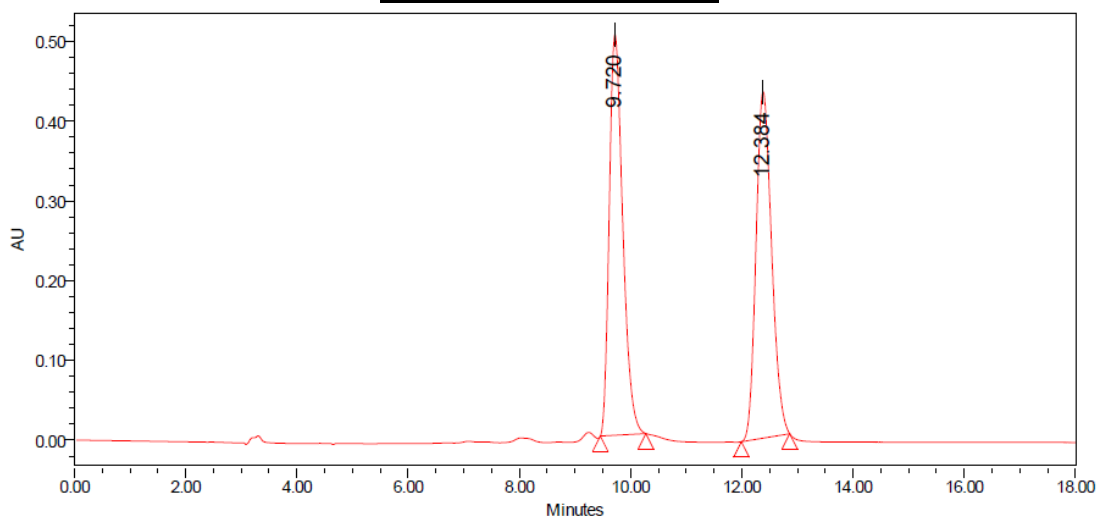


Peak	% Area	Retention Time	Area	Height
1	98.99	8.338	22801875	1888333
2	1.01	10.883	232310	20538



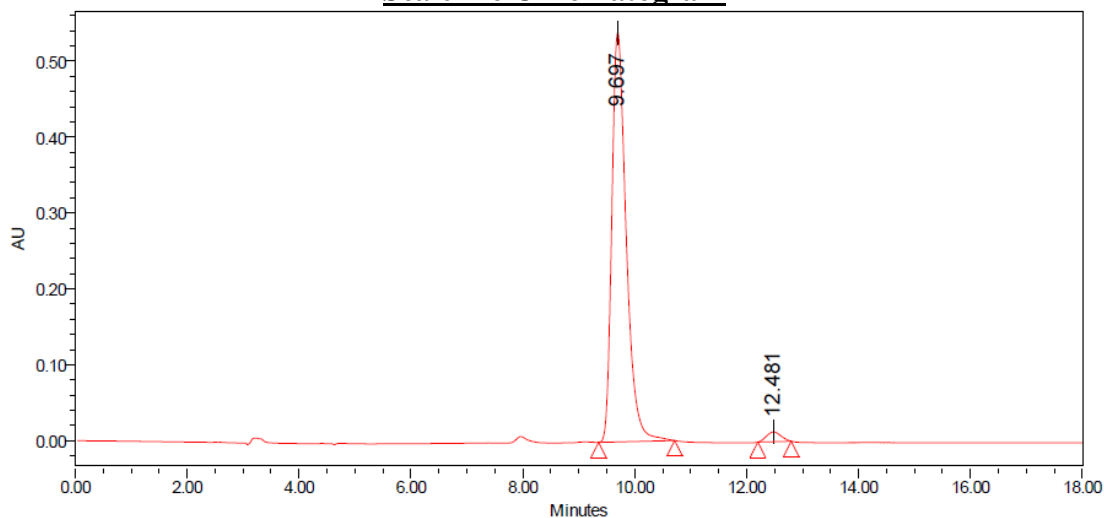
2.13 – Major Diastereomer
 Run Details: HPLC, Daicel CHIRALPAK OD-H,
 10.00 μ L, gradient 5% to 50% iPrOH/hexanes,
 18 minutes, 1 mL/min, 285.0 nm.

Racemic Chromatogram

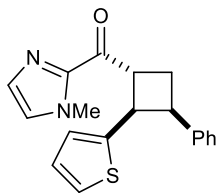


Peak	% Area	Retention Time	Area	Height
1	49.96	9.720	8453746	502796
2	50.04	12.384	8465751	434381

Scalemic Chromatogram

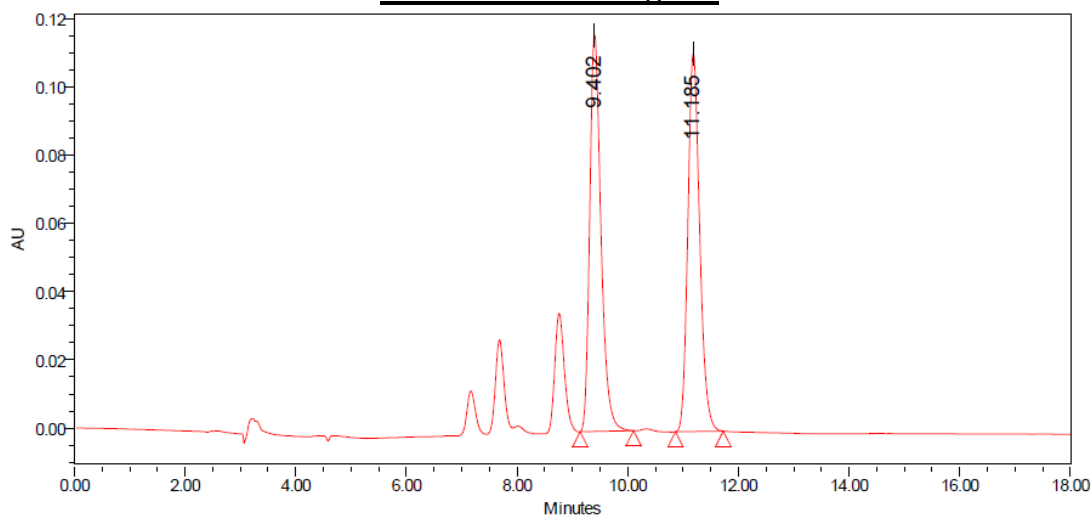


Peak	% Area	Retention Time	Area	Height
1	97.66	9.697	9617702	539301
2	2.34	12.481	229998	12779



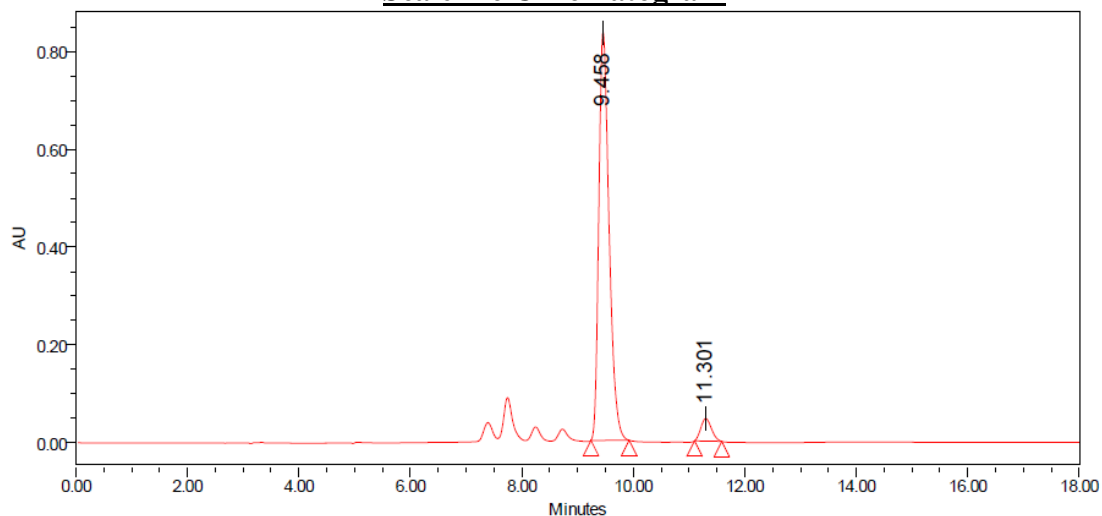
2.14 – Major Diastereomer
 Run Details: HPLC, Daicel CHIRALPAK OD-H,
 10.00 μ L, gradient 5% to 50% iPrOH/hexanes,
 18 minutes, 1 mL/min, 285.0 nm.

Racemic Chromatogram

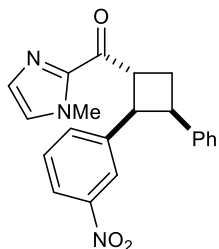


Peak	% Area	Retention Time	Area	Height
1	49.86	9.402	1638697	116327
2	50.14	11.185	1648042	110812

Scalemic Chromatogram

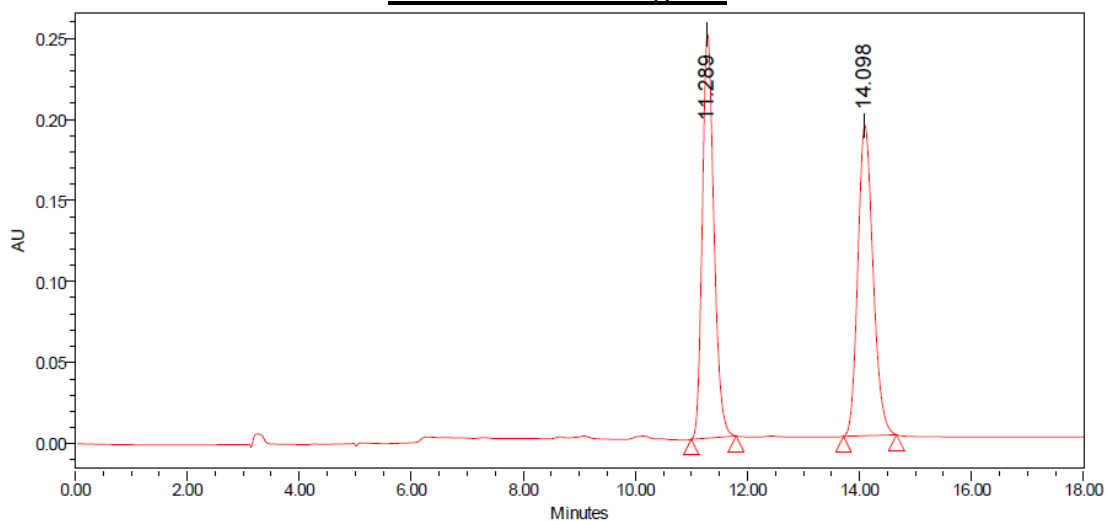


Peak	% Area	Retention Time	Area	Height
1	94.58	9.458	10663442	833712
2	5.42	11.301	610988	45976



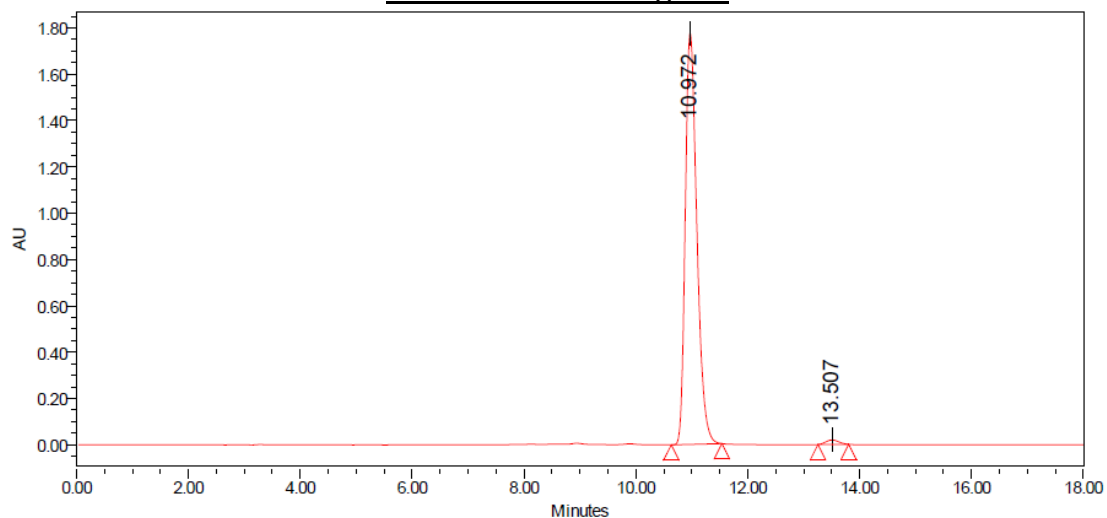
2.15 – Major Diastereomer
 Run Details: HPLC, Daicel CHIRALPAK OD-H,
 10.00 μ L, gradient 5% to 50% iPrOH/hexanes,
 18 minutes, 1 mL/min, 285.0 nm.

Racemic Chromatogram

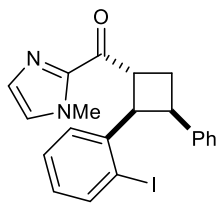


Peak	% Area	Retention Time	Area	Height
1	49.90	11.289	3597092	249200
2	50.10	14.098	3611037	191412

Scalemic Chromatogram

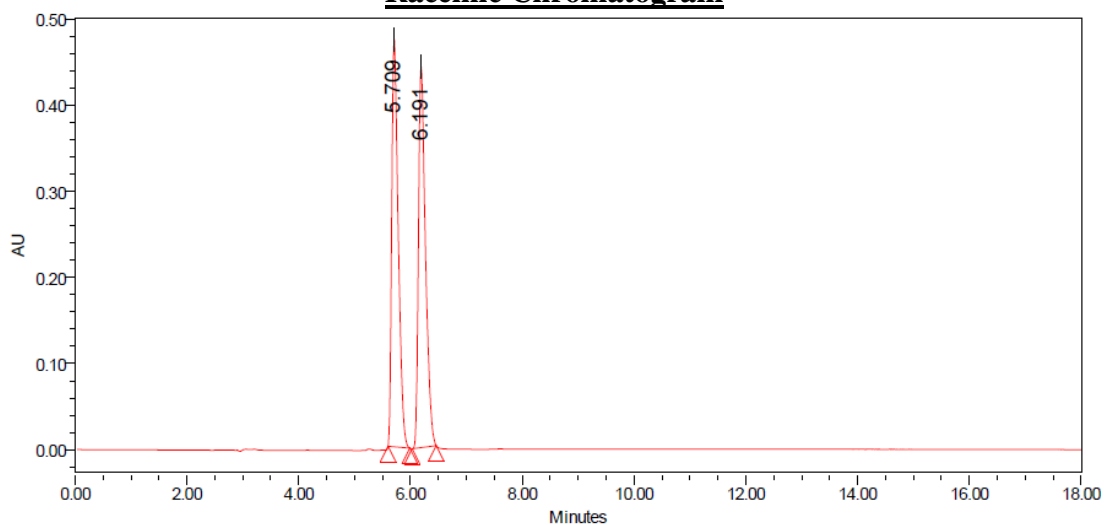


Peak	% Area	Retention Time	Area	Height
1	98.80	10.972	25497032	1775923
2	1.20	13.507	309999	19321



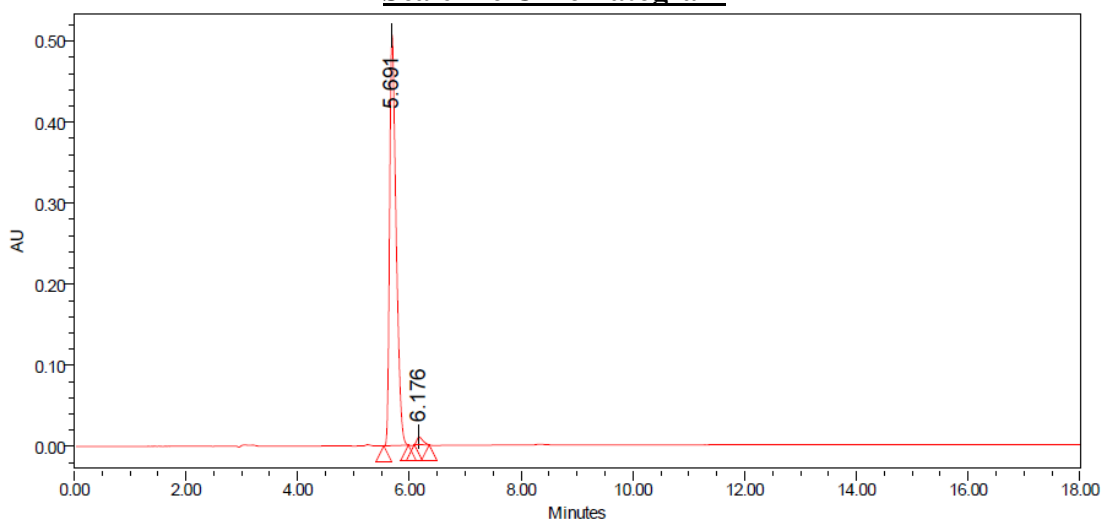
2.16 – Major Diastereomer
 Run Details: HPLC, Daicel CHIRALPAK AD-H,
 10.00 μ L, gradient 5% to 50% iPrOH/hexanes,
 20 minutes, 1 mL/min, 285.0 nm.

Racemic Chromatogram

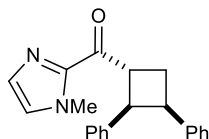


Peak	% Area	Retention Time	Area	Height
1	49.84	5.709	3816214	473791
2	50.16	6.191	3839989	442580

Scalemic Chromatogram

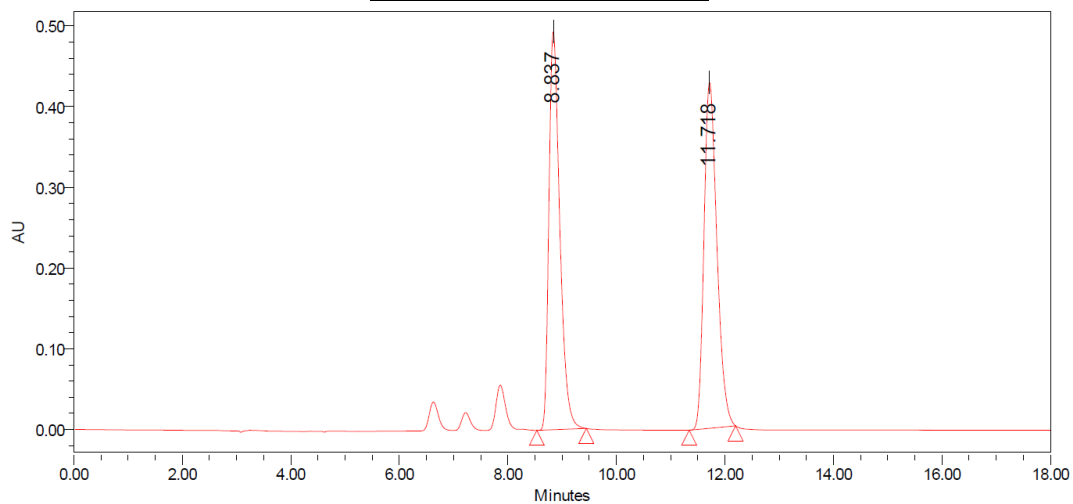


Peak	% Area	Retention Time	Area	Height
1	98.28	5.691	4093630	506805
2	1.72	6.176	71674	9489



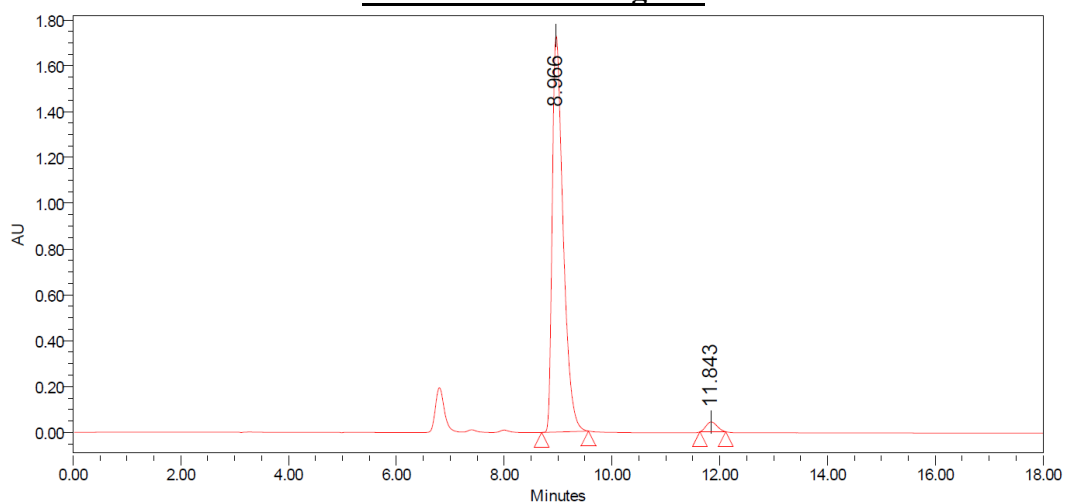
2.17 – Major Diastereomer
 Run Details: HPLC, Daicel CHIRALPAK OD-H,
 10.00 μ L, gradient 5% to 50% iPrOH/hexanes,
 18 minutes, 1 mL/min, 295.0 nm.

Racemic Chromatogram

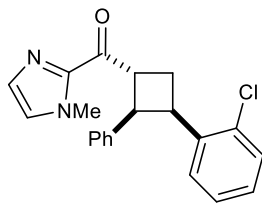


Peak	% Area	Retention Time	Area	Height
1	49.16	8.837	6844274	493024
2	50.84	11.718	7078999	428301

Scalemic Chromatogram

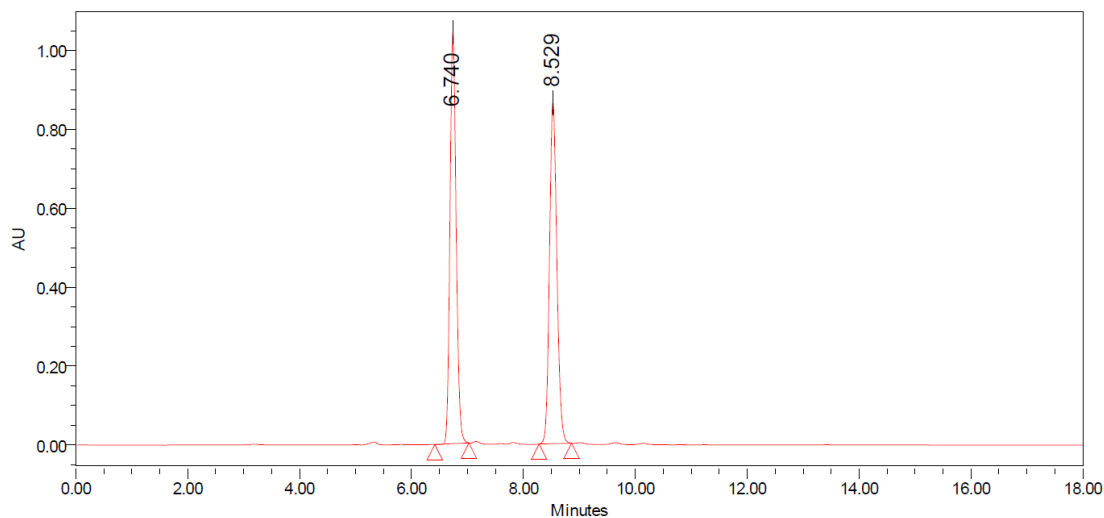


Peak	% Area	Retention Time	Area	Height
1	97.55	8.966	24201086	1729670
2	2.45	11.843	608085	42774



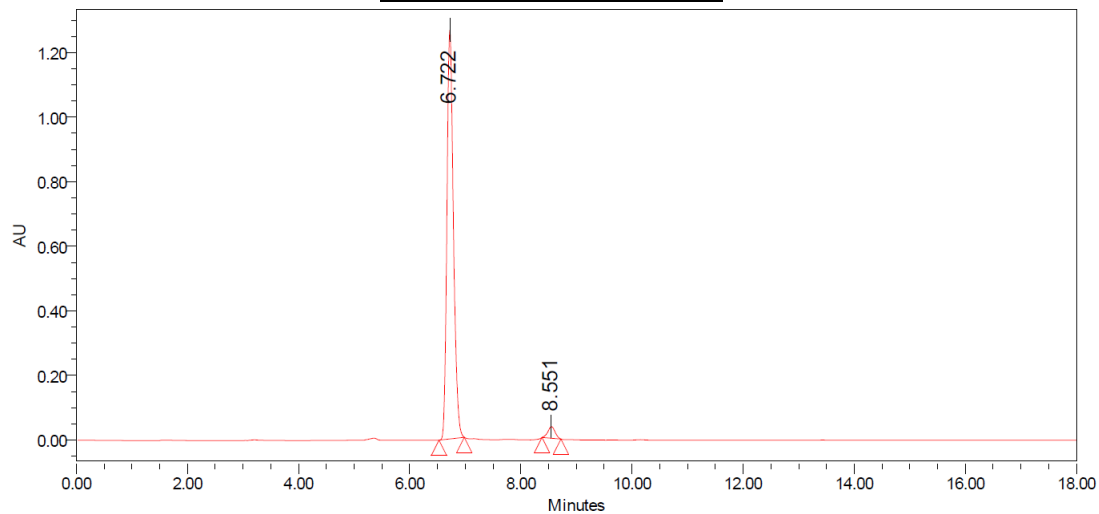
2.18 – Major Diastereomer
 Run Details: HPLC, Daicel CHIRALPAK AD,
 10.00 μ L, gradient 5% to 50% iPrOH/hexanes,
 18 minutes, 1 mL/min, 285.0 nm.

Racemic Chromatogram

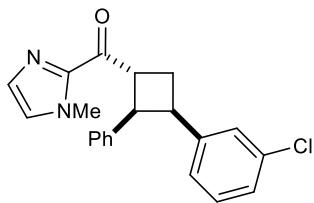


Peak	% Area	Retention Time	Area	Height
1	50.19	6.740	7983942	10419808
2	49.81	8.529	7923782	864460

Scalemic Chromatogram

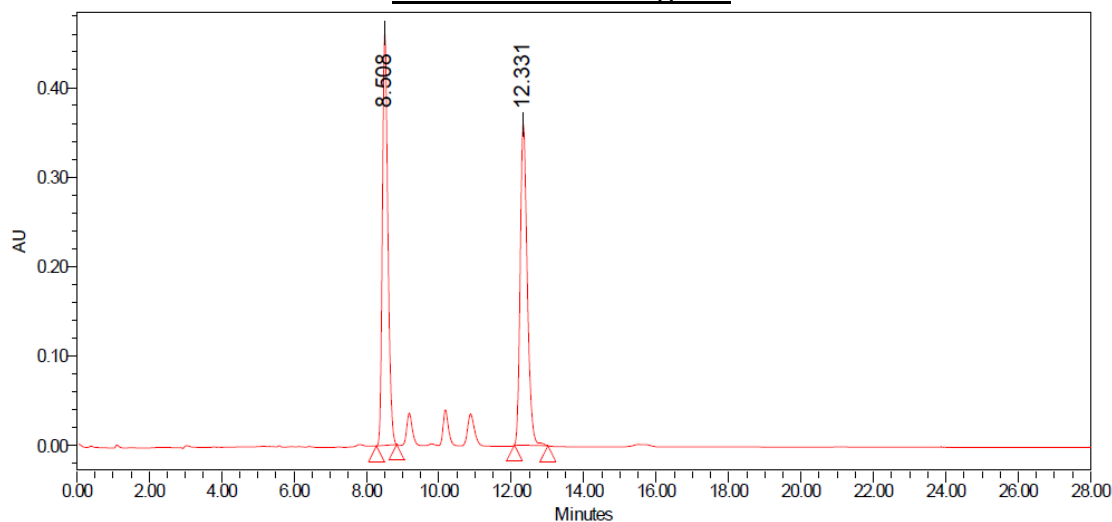


Peak	% Area	Retention Time	Area	Height
1	96.88	6.722	10250099	1265982
2	3.12	8.551	329693	36031



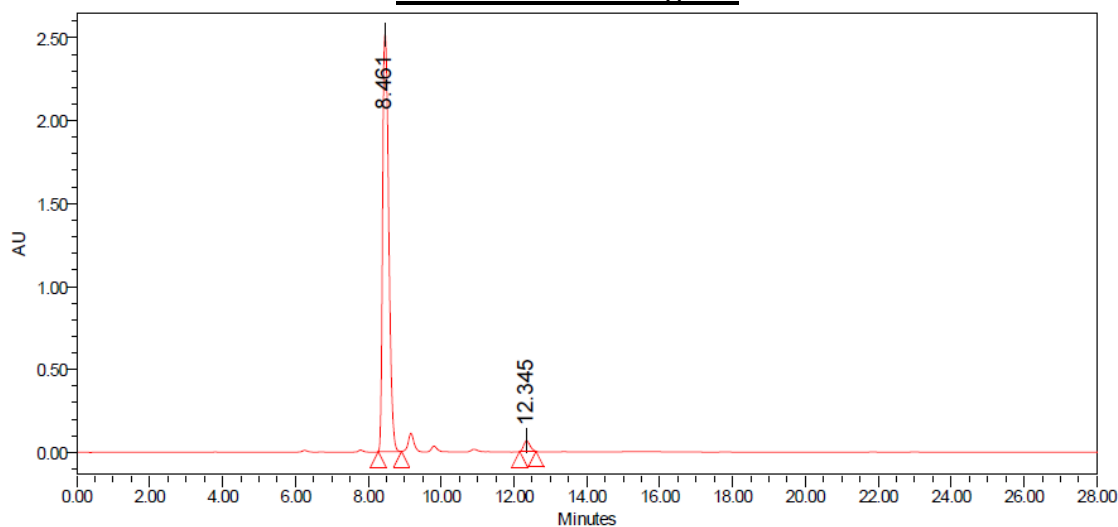
2.19 – Major Diastereomer
 Run Details: HPLC, Daicel CHIRALPAK AD-H,
 10.00 μ L, gradient 5% to 50% iPrOH/hexanes,
 28 minutes, 1 mL/min, 285.0 nm.

Racemic Chromatogram

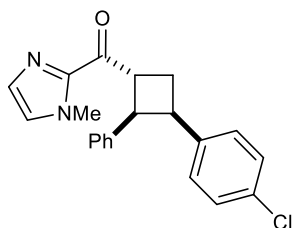


Peak	% Area	Retention Time	Area	Height
1	50.00	8.512	4865982	461766
2	50.00	12.330	4865231	359873

Scalemic Chromatogram

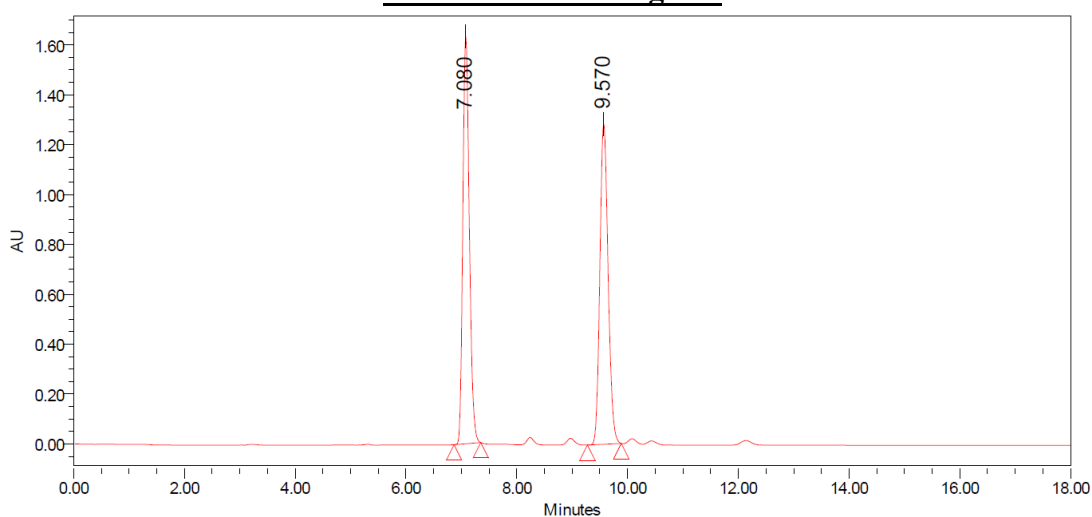


Peak	% Area	Retention Time	Area	Height
1	97.44	8.461	29518349	2513279
2	2.56	12.345	774187	64286



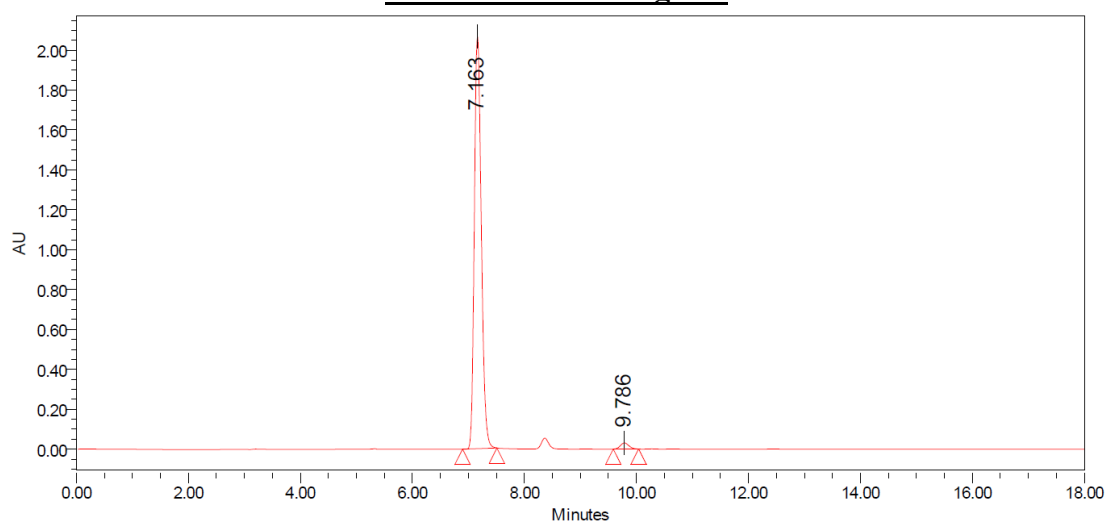
2.20 – Major Diastereomer
 Run Details: HPLC, Daicel CHIRALPAK AD,
 10.00 μ L, gradient 5% to 50% iPrOH/hexanes,
 18 minutes, 1 mL/min, 285.0 nm.

Racemic Chromatogram

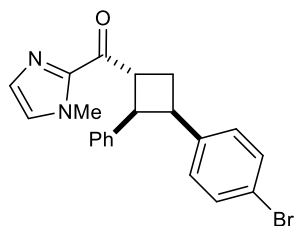


Peak	% Area	Retention Time	Area	Height
1	50.13	7.080	13336366	1633332
2	49.87	9.570	13269671	1283622

Scalemic Chromatogram

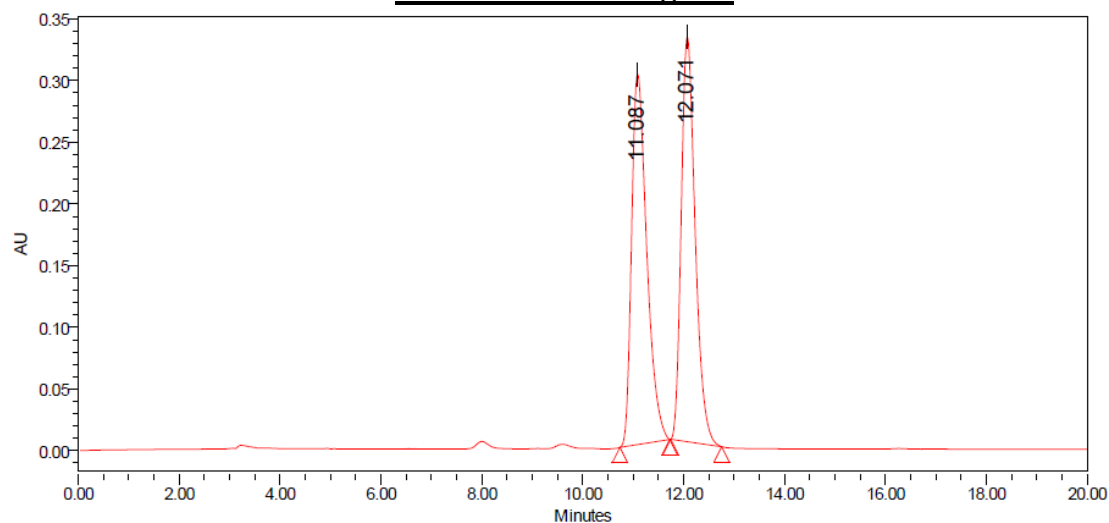


Peak	% Area	Retention Time	Area	Height
1	98.24	7.163	17804766	2064862
2	1.79	9.786	318815	30470



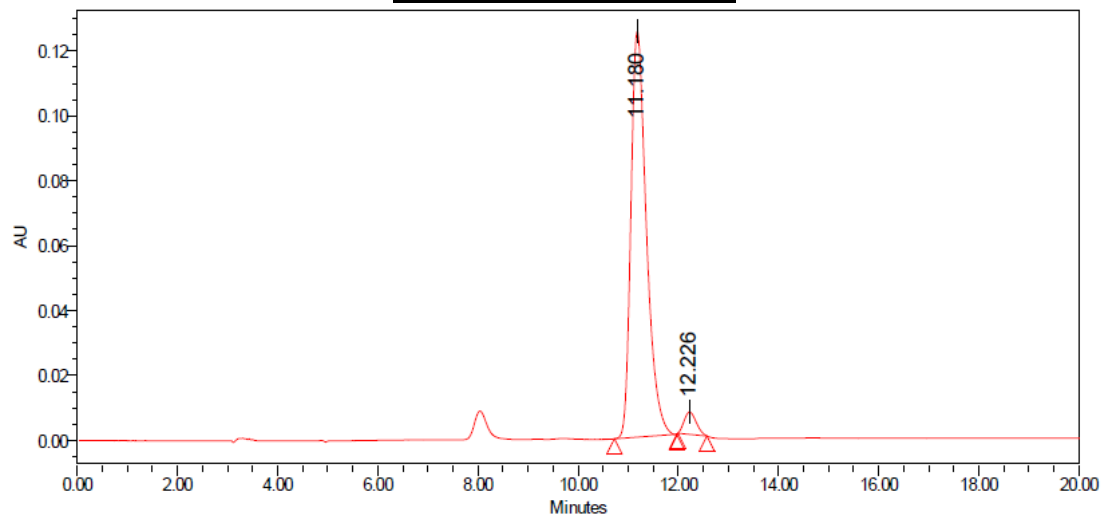
2.21 – Major Diastereomer
 Run Details: HPLC, Daicel CHIRALPAK OD-H,
 10.00 μ L, gradient 5% to 30% iPrOH/hexanes,
 20 minutes, 1 mL/min, 285.0 nm.

Racemic Chromatogram

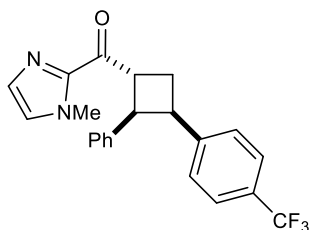


Peak	% Area	Retention Time	Area	Height
1	49.92	11.087	6271700	300296
2	50.08	12.071	6290694	328124

Scalemic Chromatogram

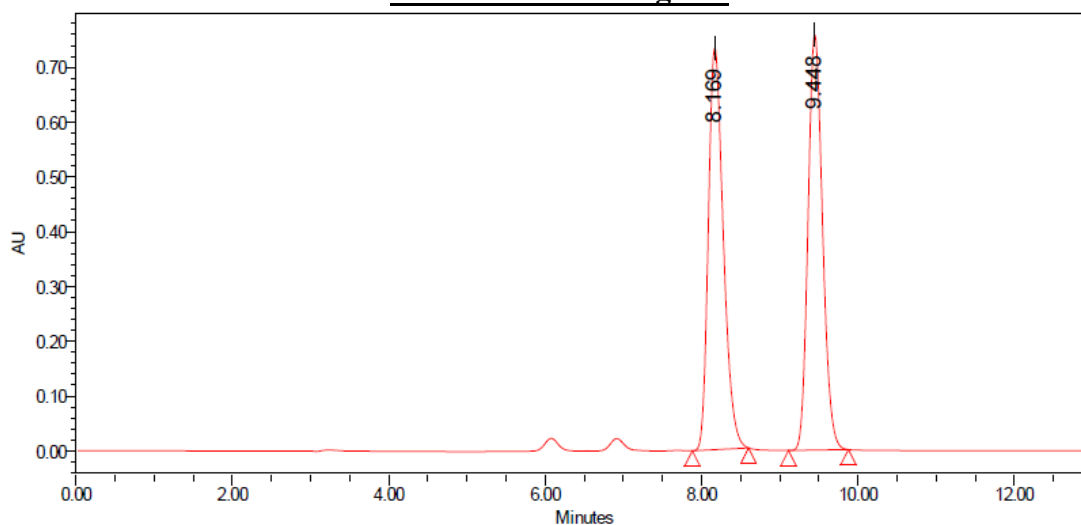


Peak	% Area	Retention Time	Area	Height
1	95.89	11.180	2684924	124948
2	4.11	12.226	115218	6870



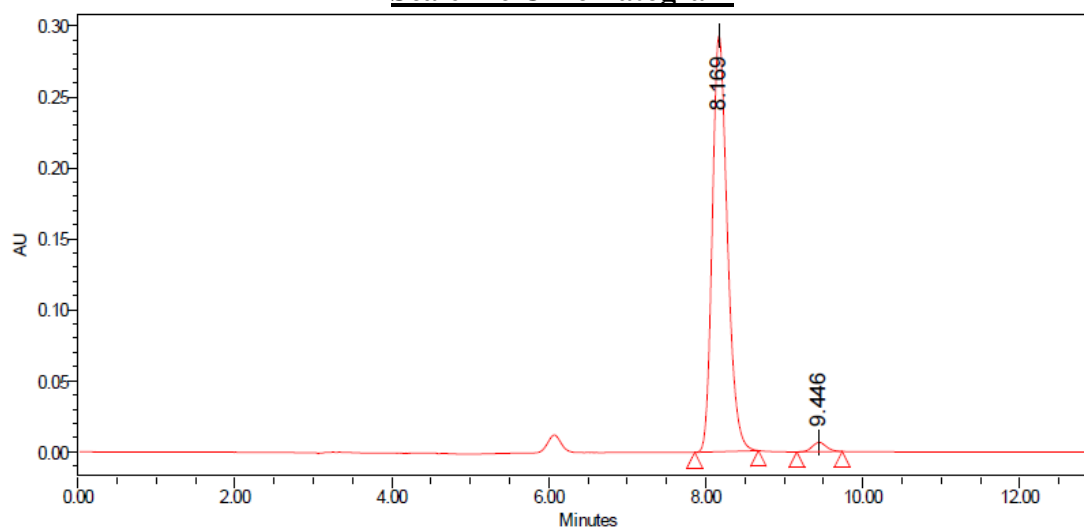
2.22 – Major Diastereomer
 Run Details: HPLC, Daicel CHIRALPAK OD-H,
 10.00 μ L, gradient 5% to 50% iPrOH/hexanes,
 13 minutes, 1 mL/min, 280.0 nm.

Racemic Chromatogram

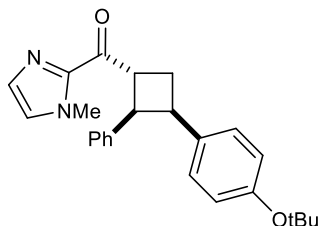


Peak	% Area	Retention Time	Area	Height
1	49.89	8.169	9741011	733077
2	50.11	9.448	9785893	757999

Scalemic Chromatogram

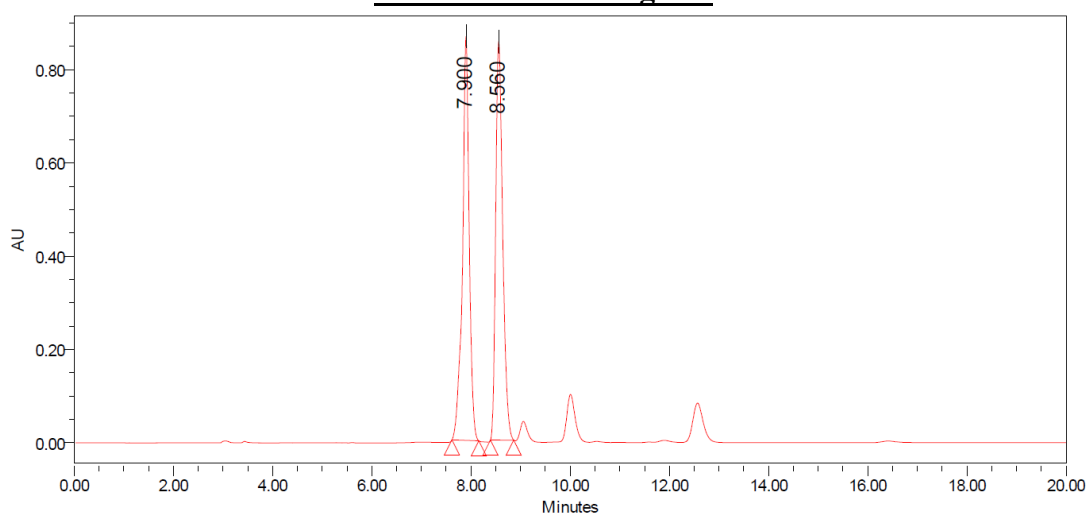


Peak	% Area	Retention Time	Area	Height
1	97.96	8.196	3904779	292916
2	2.04	9.446	81183	6513



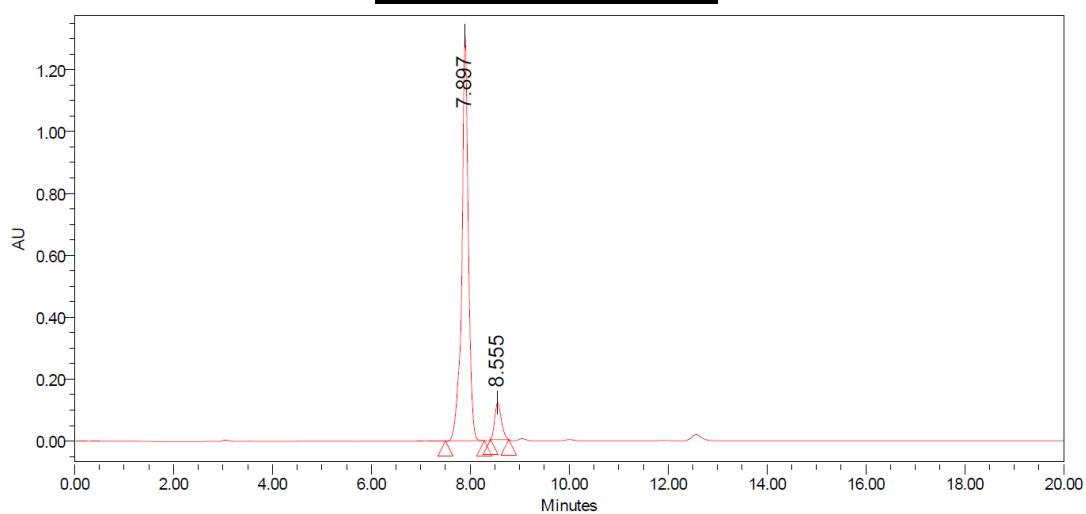
2.23 – Major Diastereomer
 Run Details: HPLC, Daicel CHIRALPAK OD-H,
 10.00 μ L, gradient 5% to 50% iPrOH/hexanes,
 18 minutes, 1 mL/min, 285.0 nm.

Racemic Chromatogram

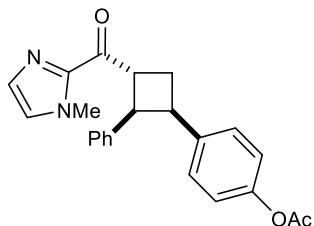


Peak	% Area	Retention Time	Area	Height
1	49.32	7.900	8150154	866166
2	50.68	8.560	8374564	854725

Scalemic Chromatogram

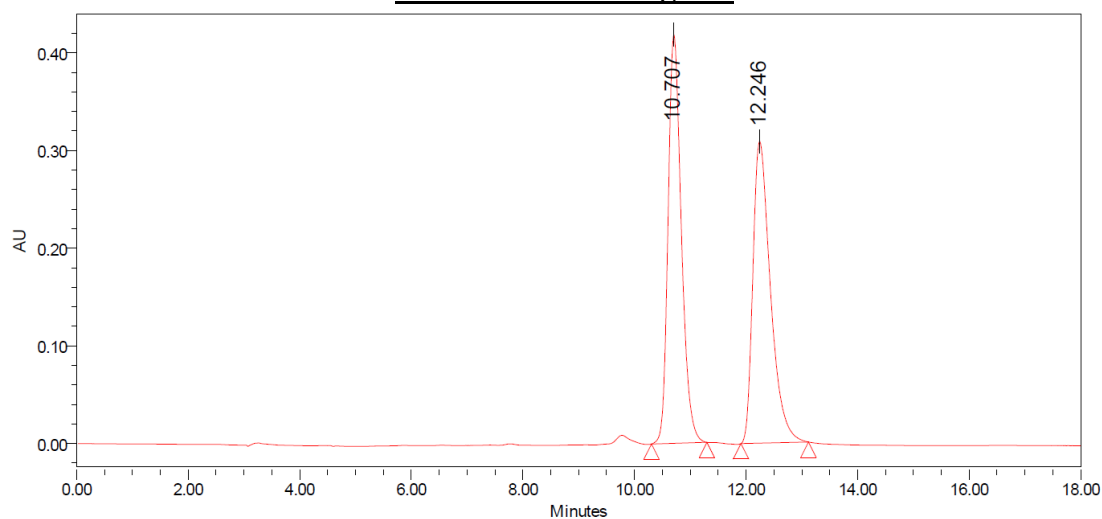


Peak	% Area	Retention Time	Area	Height
1	91.50	7.897	12010713	1308606
2	8.50	8.555	1115558	119100



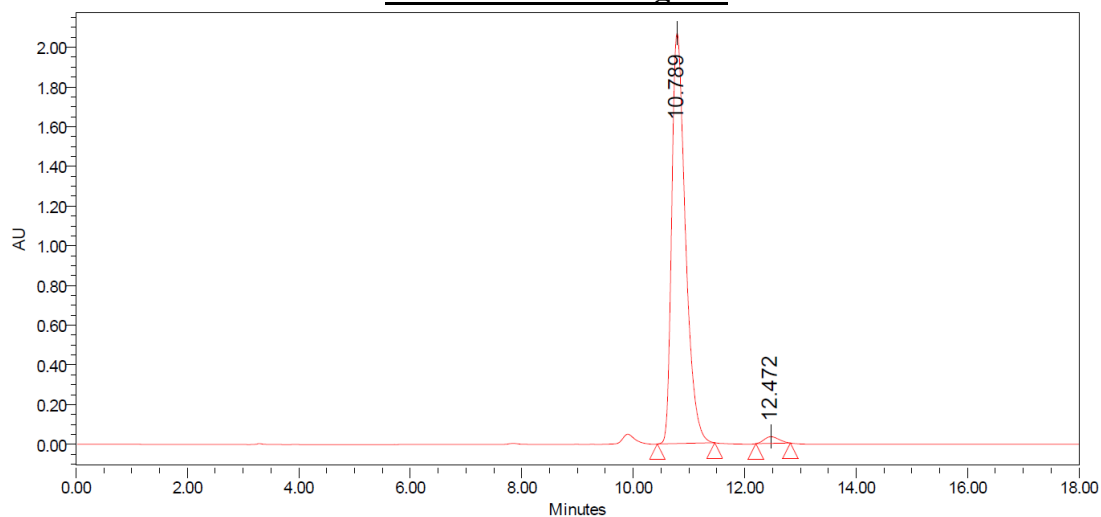
2.24 – Major Diastereomer
 Run Details: HPLC, Daicel CHIRALPAK OD-H,
 10.00 μ L, gradient 5% to 50% iPrOH/hexanes,
 18 minutes, 1 mL/min, 285.0 nm.

Racemic Chromatogram

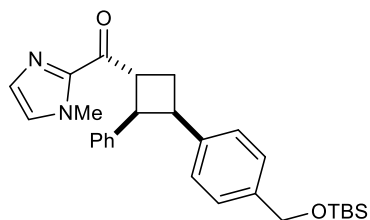


Peak	% Area	Retention Time	Area	Height
1	50.54	10.707	6903222	418287
2	49.46	12.246	6754542	308996

Scalemic Chromatogram

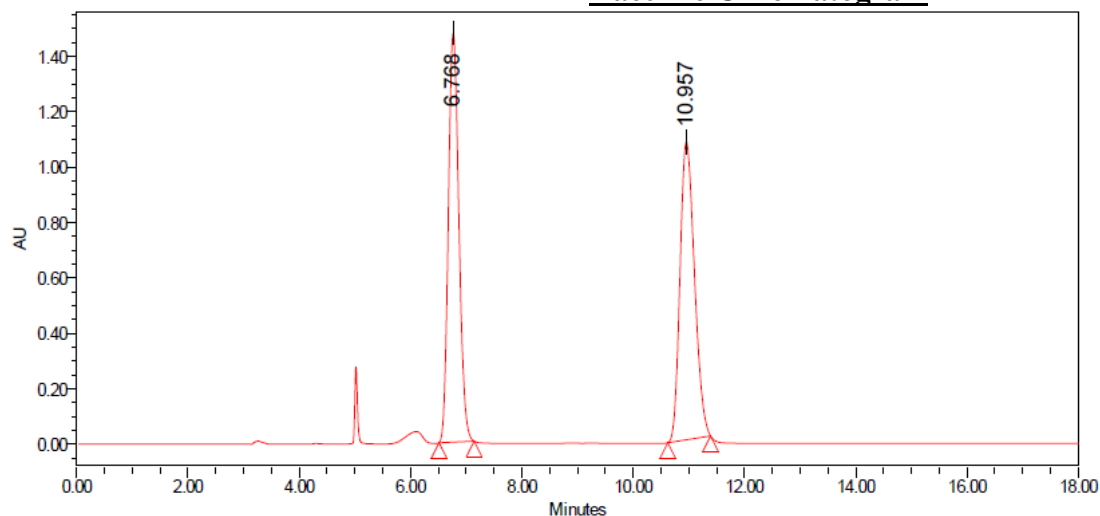


Peak	% Area	Retention Time	Area	Height
1	98.26	10.789	35347991	2066329
2	1.74	12.472	626226	33837



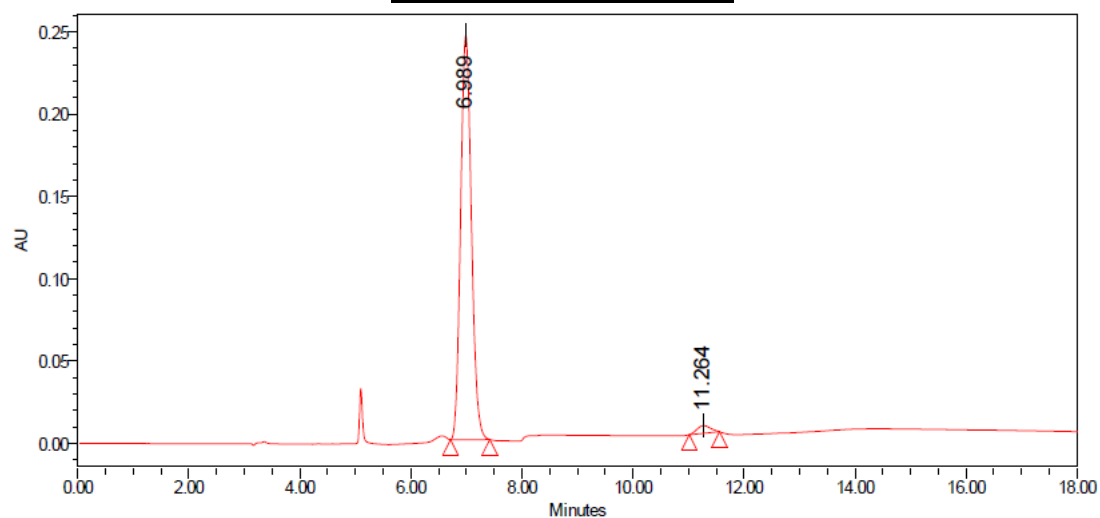
2.25 – Major Diastereomer
 Run Details: HPLC, Daicel CHIRALPAK OD-H,
 10.00 μ L, gradient 5% to 50% iPrOH/hexanes,
 18 minutes, 1 mL/min, 285.0 nm.

Racemic Chromatogram

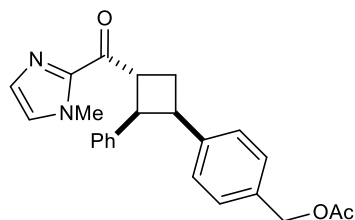


Peak	% Area	Retention Time	Area	Height
1	49.92	6.768	19293809	1476222
2	50.08	10.957	19357563	1074753

Scalemic Chromatogram

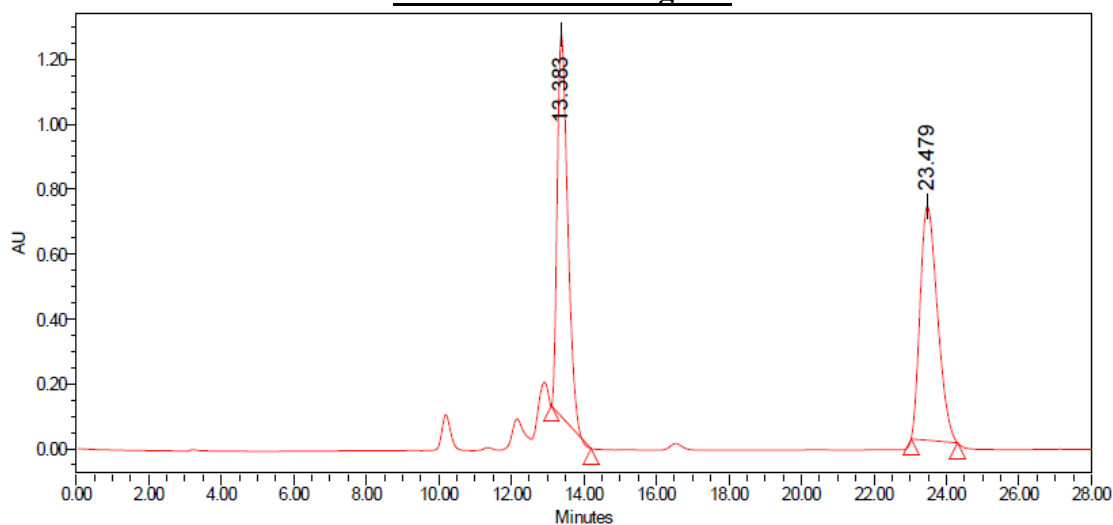


Peak	% Area	Retention Time	Area	Height
1	97.65	6.989	3307673	245547
2	2.35	11.264	79739	4704



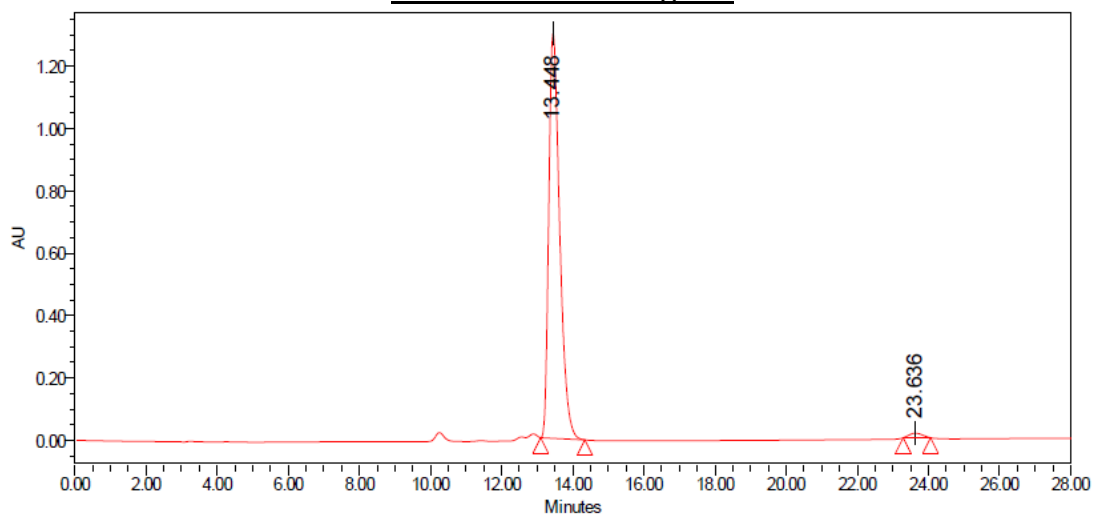
2.26 – Major Diastereomer
 Run Details: HPLC, Daicel CHIRALPAK OD-H,
 10.00 μ L, gradient 5% to 50% iPrOH/hexanes,
 28 minutes, 1 mL/min, 280.0 nm.

Racemic Chromatogram

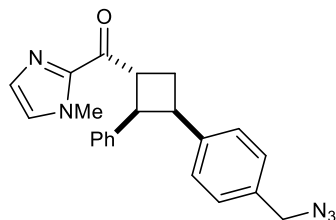


Peak	% Area	Retention Time	Area	Height
1	49.66	13.383	23641117	1176330
2	50.34	23.479	23961968	721251

Scalemic Chromatogram

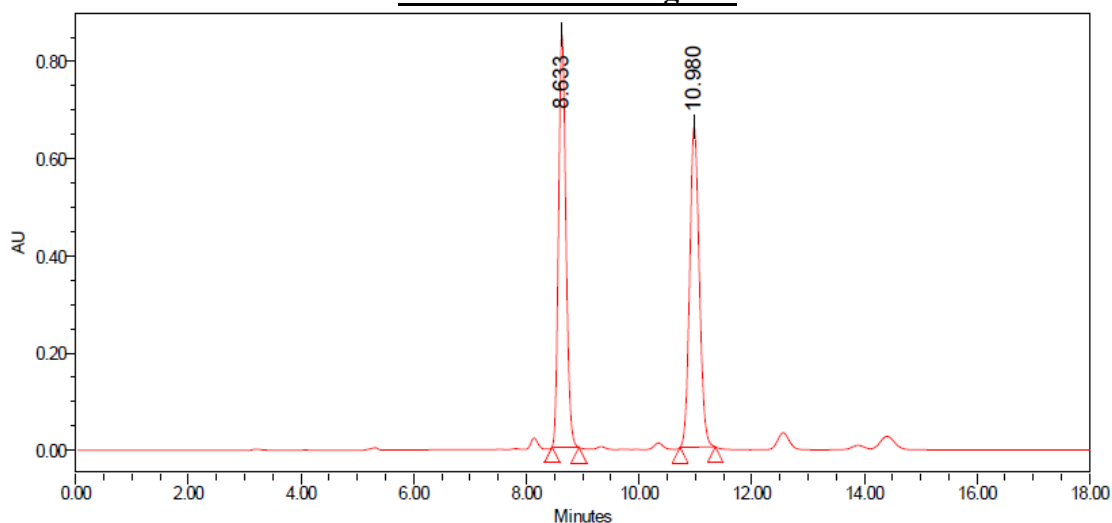


Peak	% Area	Retention Time	Area	Height
1	98.67	13.448	27623051	1298019
2	1.33	23.636	373592	14428



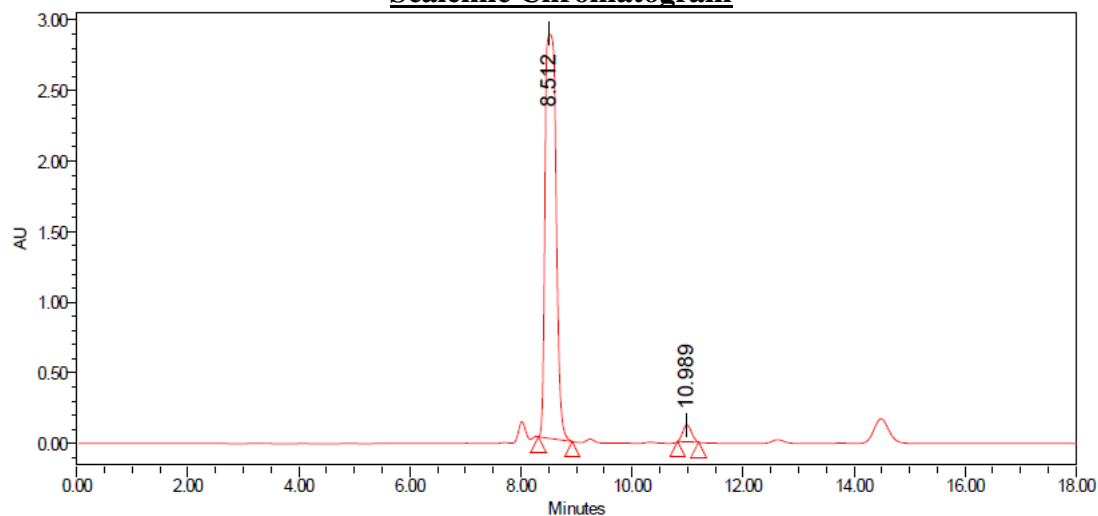
2.27 – Major Diastereomer
 Run Details: HPLC, Daicel CHIRALPAK AD,
 10.00 μ L, gradient 5% to 50% iPrOH/hexanes,
 18 minutes, 1 mL/min, 280.0 nm.

Racemic Chromatogram

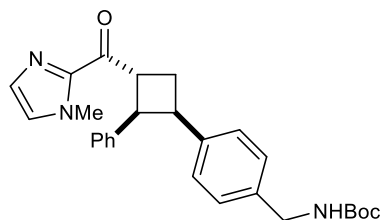


Peak	% Area	Retention Time	Area	Height
1	49.70	8.633	7691352	848642
2	50.30	10.980	7784586	659174

Scalemic Chromatogram



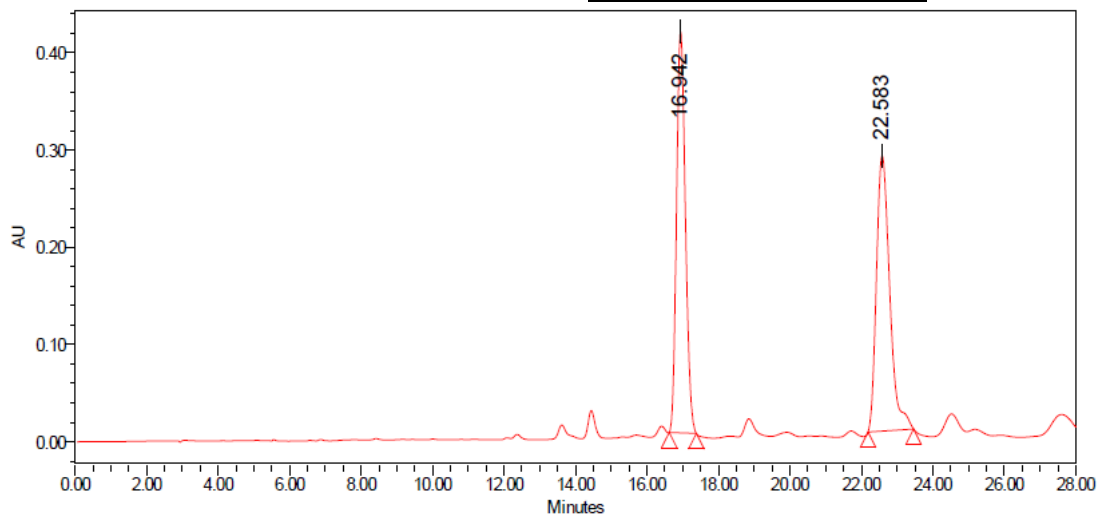
Peak	% Area	Retention Time	Area	Height
1	96.78	8.512	2865539	2865539
2	3.22	10.989	119972	119972



2.28 – Major Diastereomer

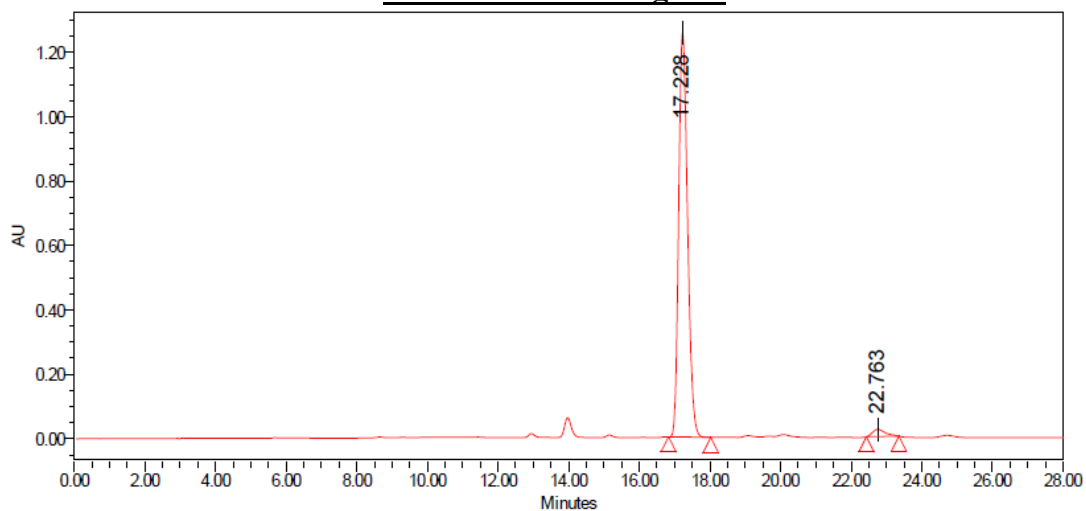
Run Details: HPLC, Daicel CHIRALPAK OD-H,
10.00 μ L, gradient 5% to 50% iPrOH/hexanes,
28 minutes, 1 mL/min, 285.0 nm.

Racemic Chromatogram

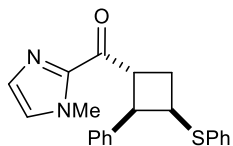


Peak	% Area	Retention Time	Area	Height
1	49.25	16.942	7089598	412447
2	50.75	22.583	7304797	283175

Scalemic Chromatogram

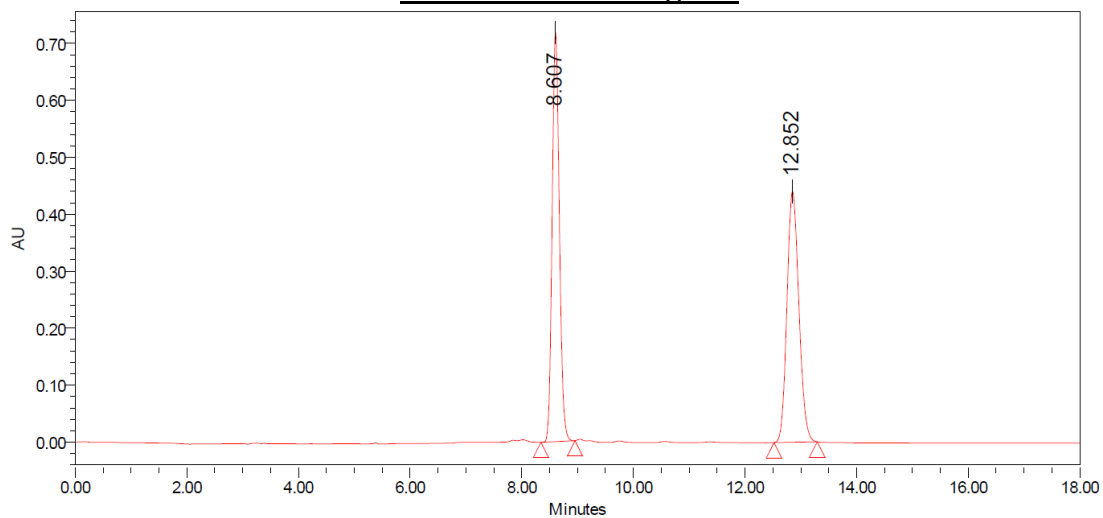


Peak	% Area	Retention Time	Area	Height
1	97.45	17.228	21877872	1254062
2	2.55	22.763	573270	22464



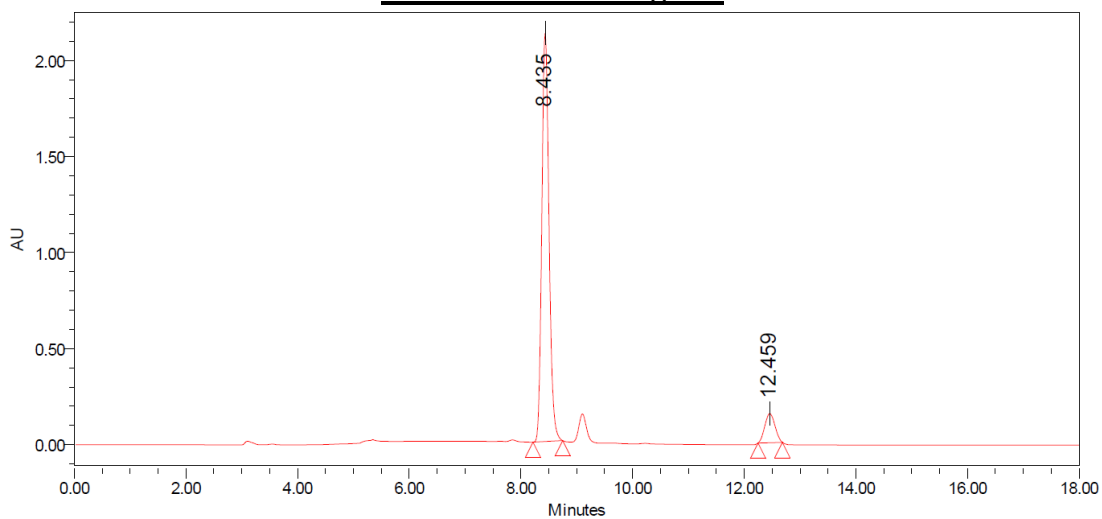
2.29 – Major Diastereomer
 Run Details: HPLC, Daicel CHIRALPAK AD,
 10.00 μ L, gradient 5% to 50% iPrOH/hexanes,
 18 minutes, 1 mL/min, 285.0 nm.

Racemic Chromatogram

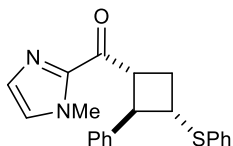


Peak	% Area	Retention Time	Area	Height
1	49.62	8.607	6435841	718229
2	50.38	12.852	6534797	440270

Scalemic Chromatogram

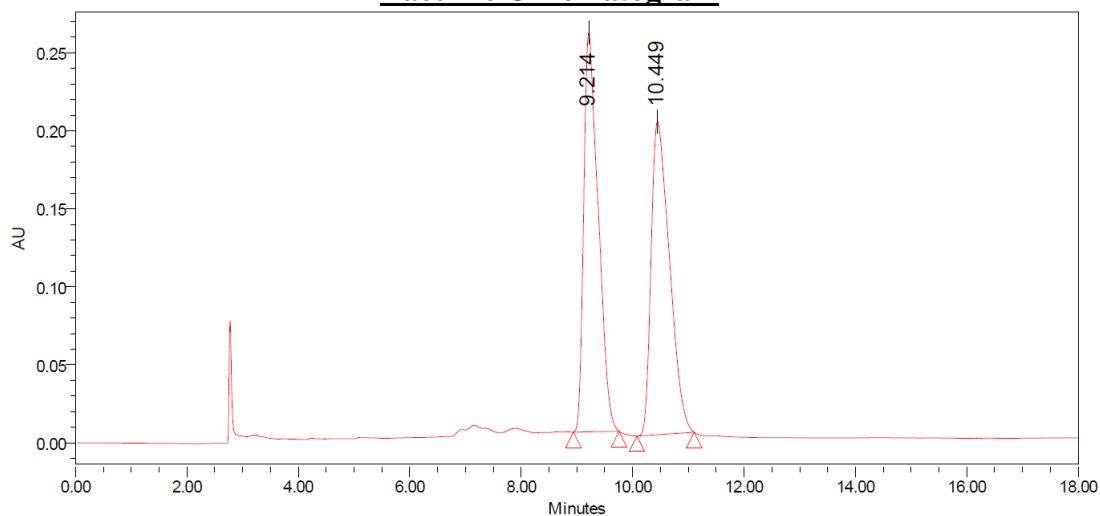


Peak	% Area	Retention Time	Area	Height
1	90.84	8.435	19057924	2126287
2	9.16	12.459	1921213	151508



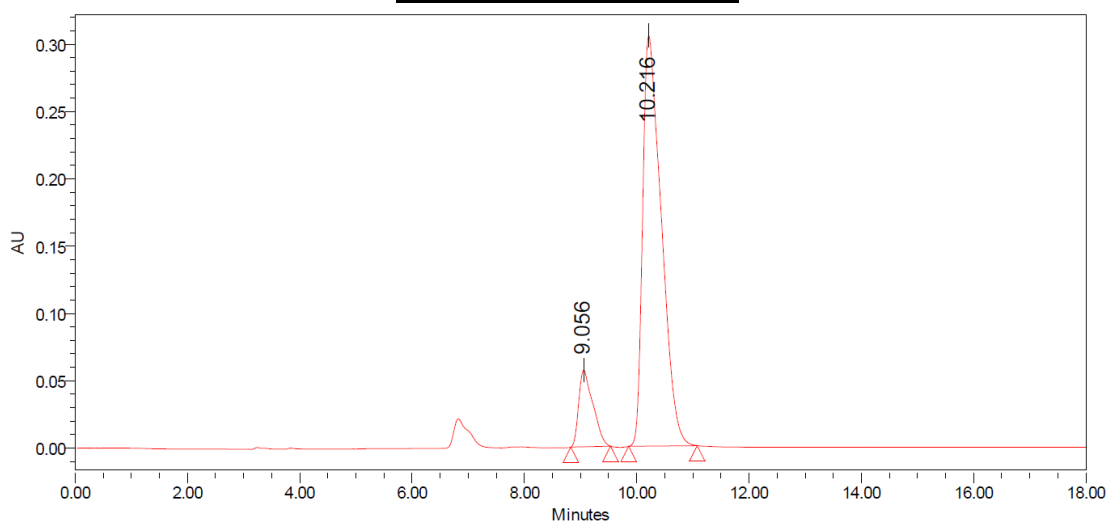
2.29 – Minor Diastereomer
 Run Details: HPLC, Daicel CHIRALPAK OD-H,
 10.00 μ L, gradient 5% to 50% iPrOH/hexanes,
 18 minutes, 1 mL/min, 285.0 nm.

Racemic Chromatogram

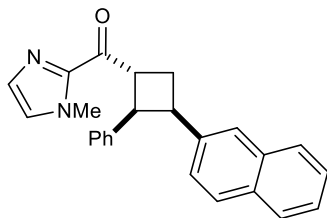


Peak	% Area	Retention Time	Area	Height
1	50.02	9.214	4597067	255909
2	49.98	10.449	4593163	200910

Scalemic Chromatogram

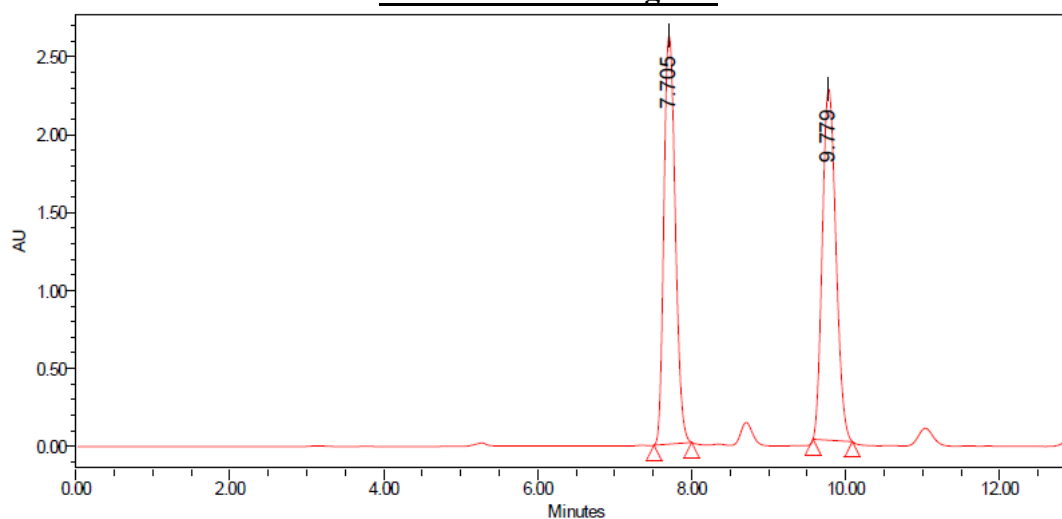


Peak	% Area	Retention Time	Area	Height
1	12.45	9.056	999244	56884
2	87.55	10.216	7025160	305015



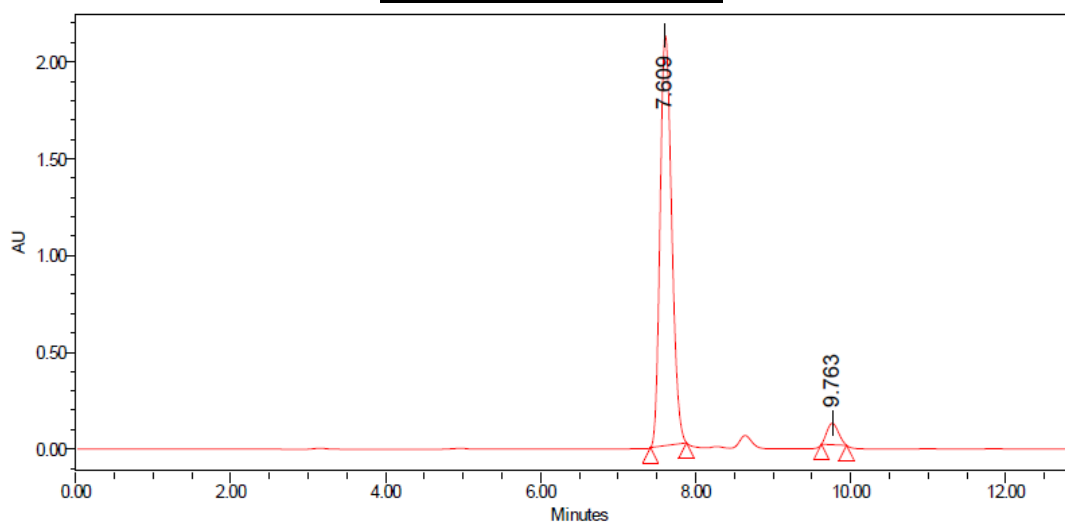
2.30 – Major Diastereomer
 Run Details: HPLC, Daicel CHIRALPAK AD-H,
 10.00 μ L, gradient 5% to 50% iPrOH/hexanes,
 13 minutes, 1 mL/min, 280.0 nm.

Racemic Chromatogram

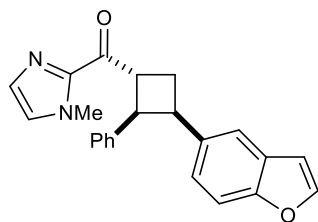


Peak	% Area	Retention Time	Area	Height
1	49.38	7.705	26951400	2618716
2	50.62	9.779	27633264	2251612

Scalemic Chromatogram

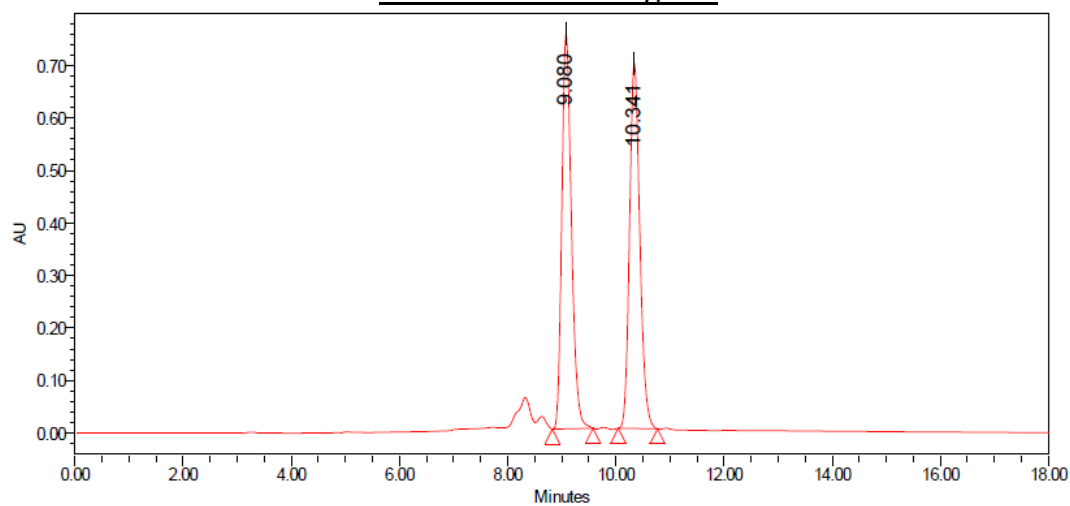


Peak	% Area	Retention Time	Area	Height
1	95.05	7.609	21961022	2117815
2	4.95	9.763	1143222	110920



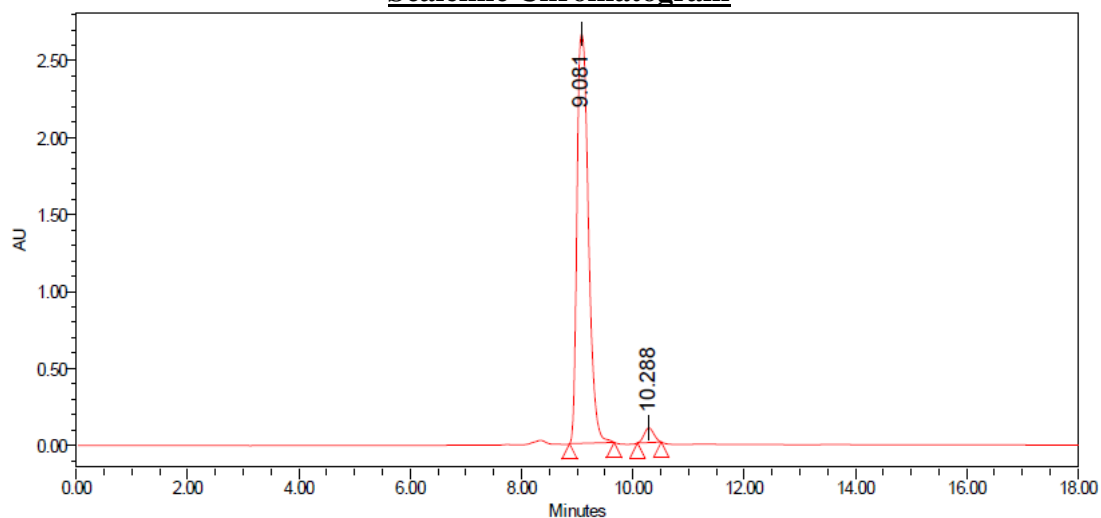
2.31 – Major Diastereomer
 Run Details: HPLC, Daicel CHIRALPAK OD-H,
 10.00 μ L, gradient 5% to 50% iPrOH/hexanes,
 18 minutes, 1 mL/min, 285.0 nm.

Racemic Chromatogram

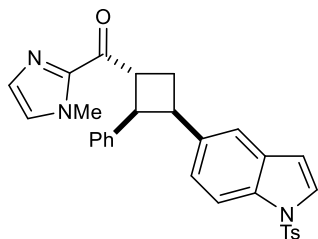


Peak	% Area	Retention Time	Area	Height
1	50.29	9.080	9278212	752544
2	49.71	10.341	9171396	696002

Scalemic Chromatogram

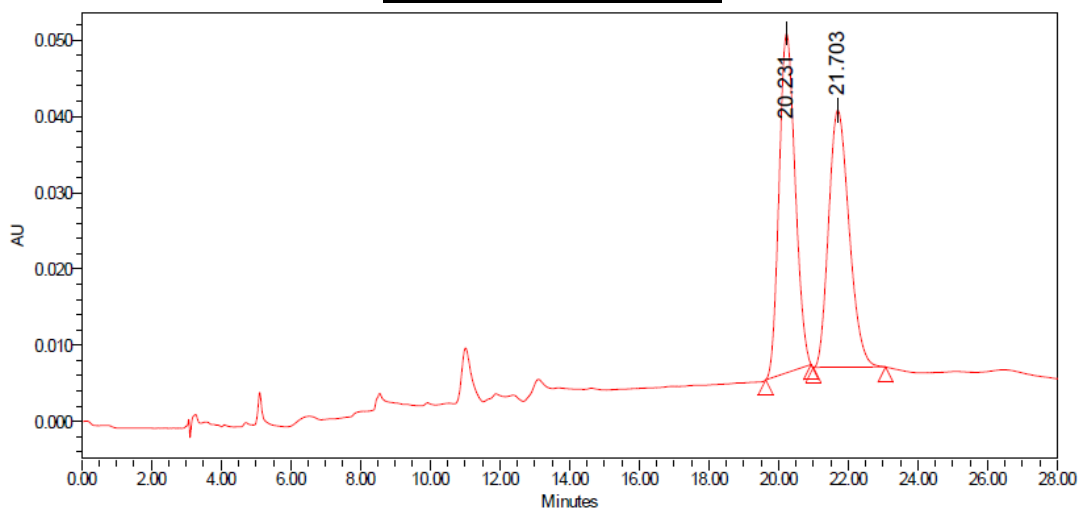


Peak	% Area	Retention Time	Area	Height
1	97.02	9.081	37854855	2658322
2	2.98	10.288	1161872	95801



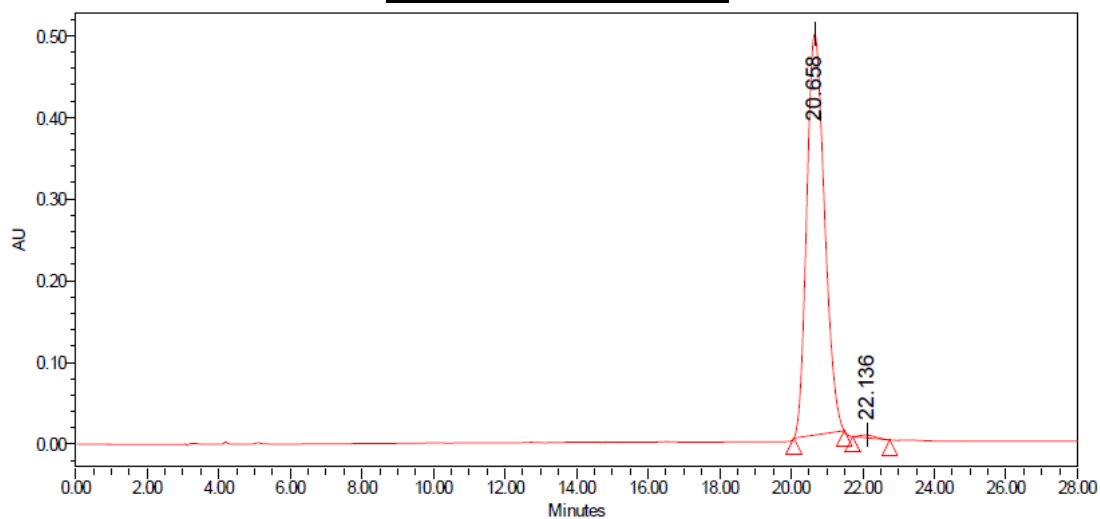
2.32 – Major Diastereomer
 Run Details: HPLC, Daicel CHIRALPAK AS-H,
 10.00 μ L, gradient 5% to 50% iPrOH/hexanes,
 28 minutes, 1 mL/min, 285.0 nm.

Racemic Chromatogram

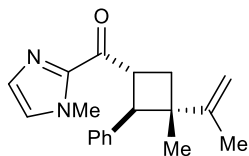


Peak	% Area	Retention Time	Area	Height
1	50.84	20.231	1425708	44483
2	49.16	21.703	1378662	33699

Scalemic Chromatogram

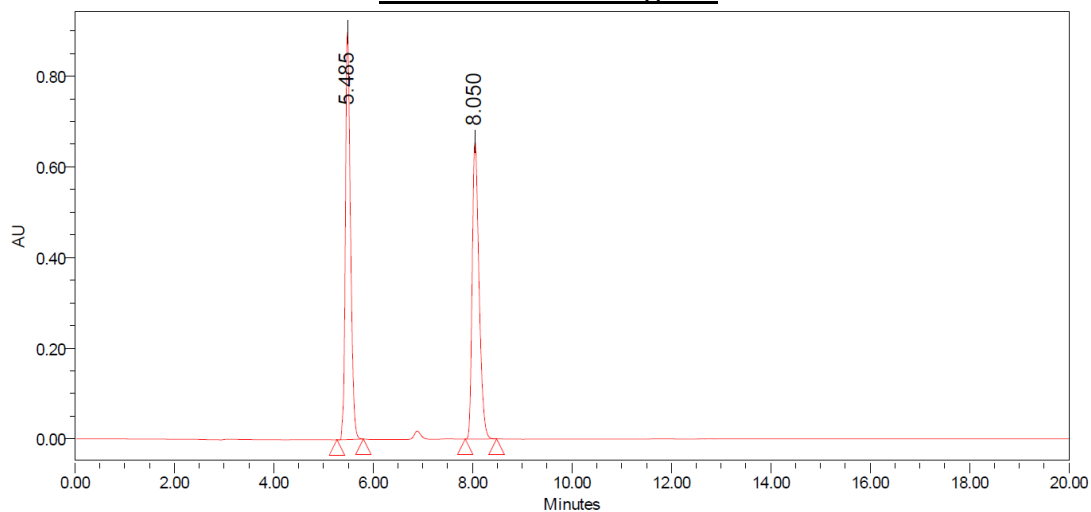


Peak	% Area	Retention Time	Area	Height
1	99.36	20.658	16949841	490473
2	2.45	22.136	108667	3556



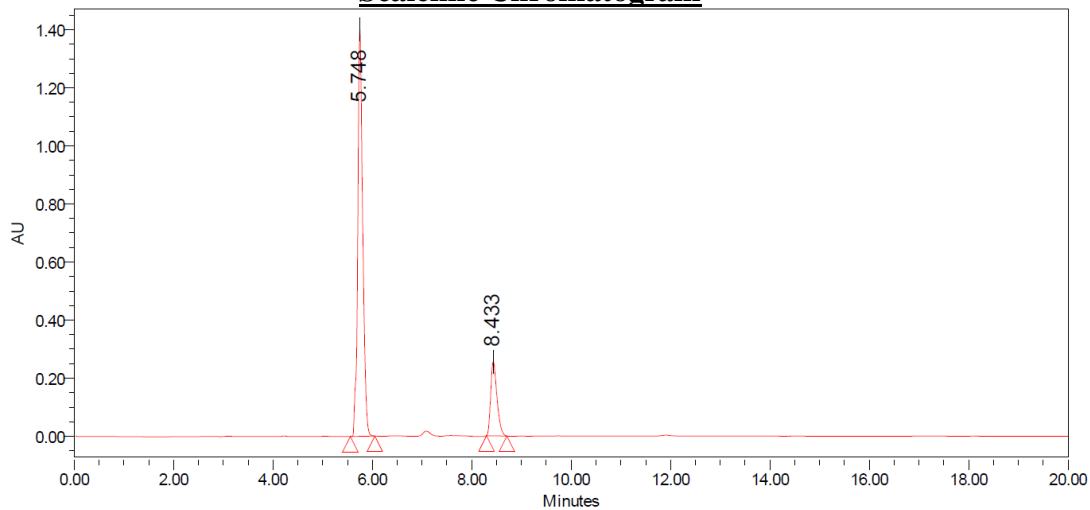
2.33 – Major Diastereomer
 Run Details: HPLC, Daicel CHIRALPAK AD,
 10.00 μ L, gradient 5% to 50% iPrOH/hexanes,
 18 minutes, 1 mL/min, 295.0 nm.

Racemic Chromatogram

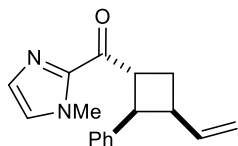


Peak	% Area	Retention Time	Area	Height
1	50.53	5.485	6398300	898523
2	49.47	8.050	6264920	656586

Scalemic Chromatogram

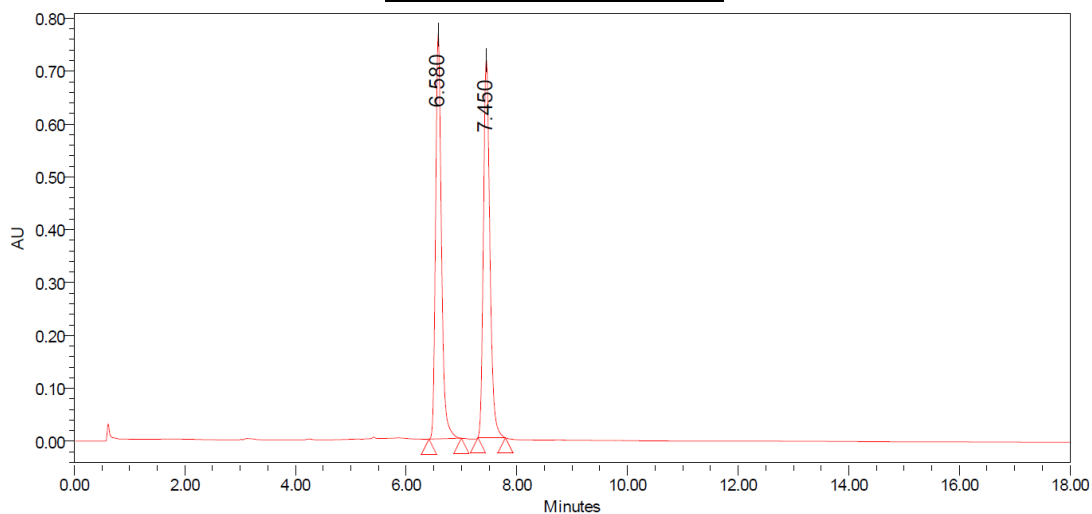


Peak	% Area	Retention Time	Area	Height
1	81.38	5.748	9802518	1401129
2	18.62	8.433	2243334	255768



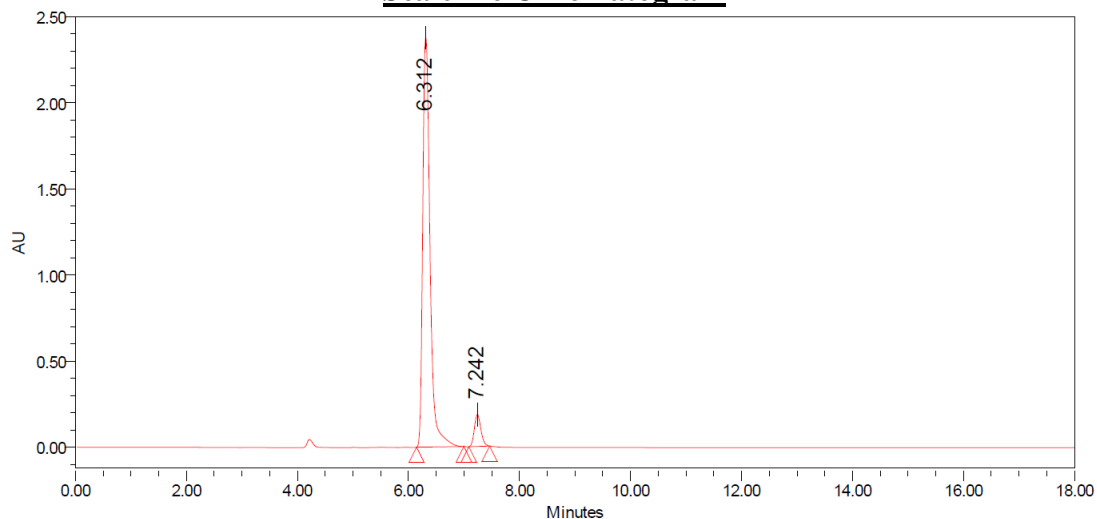
2.34 – Major Diastereomer
 Run Details: HPLC, Daicel CHIRALPAK AD,
 10.00 μ L, gradient 5% to 50% iPrOH/hexanes,
 18 minutes, 1 mL/min, 295.0 nm.

Racemic Chromatogram

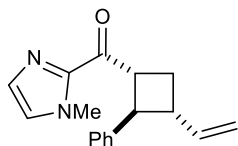


Peak	% Area	Retention Time	Area	Height
1	49.18	6.580	5619294	767670
2	50.82	7.450	5806639	714161

Scalemic Chromatogram

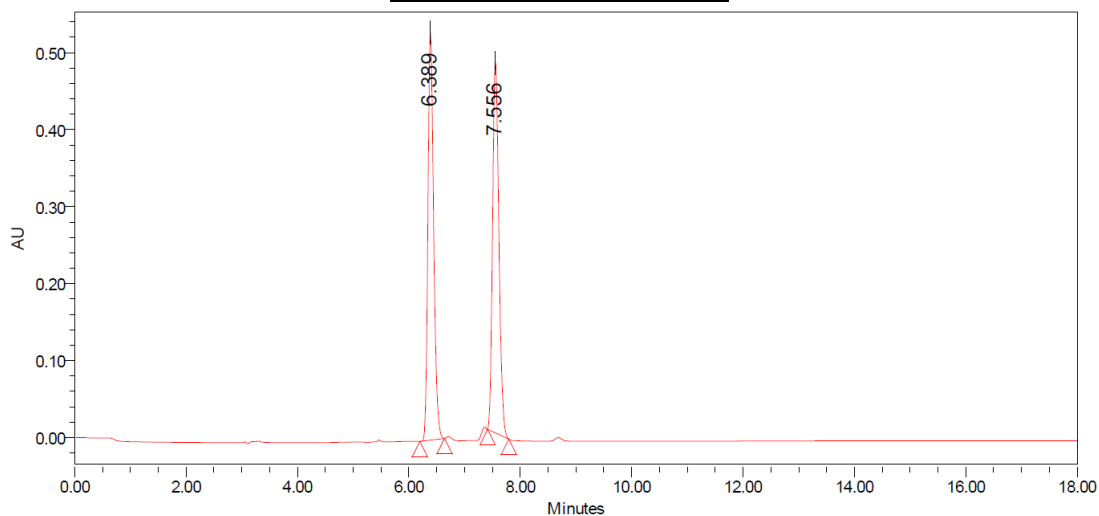


Peak	% Area	Retention Time	Area	Height
1	93.48	6.312	21698128	2379222
2	6.52	7.242	1513611	185695



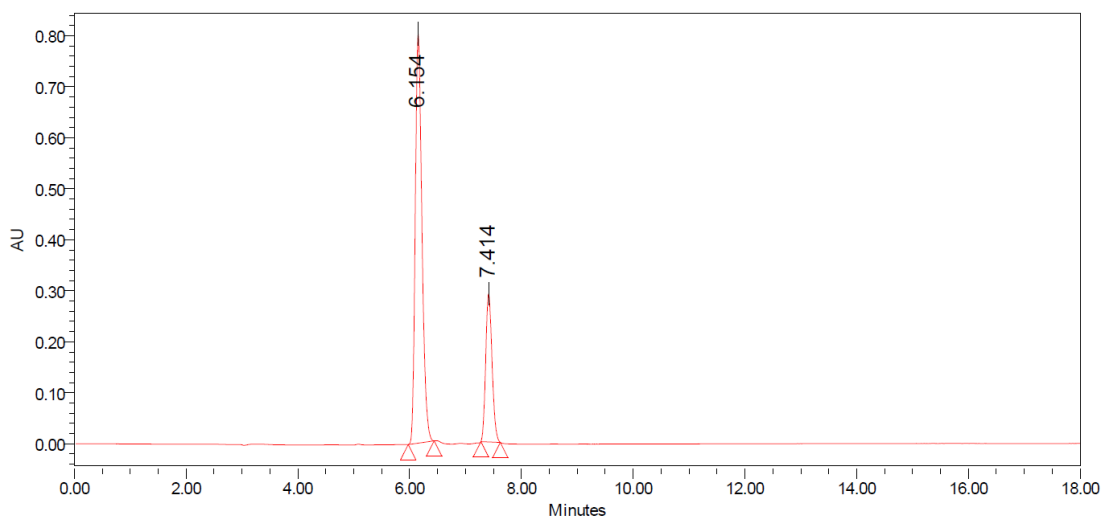
2.35 – Minor Diastereomer
 Run Details: HPLC, Daicel CHIRALPAK AD,
 10.00 μ L, gradient 5% to 50% iPrOH/hexanes,
 18 minutes, 1 mL/min, 295.0 nm.

Racemic Chromatogram

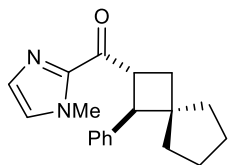


Peak	% Area	Retention Time	Area	Height
1	49.99	6.389	3780701	529097
2	50.01	7.556	3782575	481054

Scalemic Chromatogram

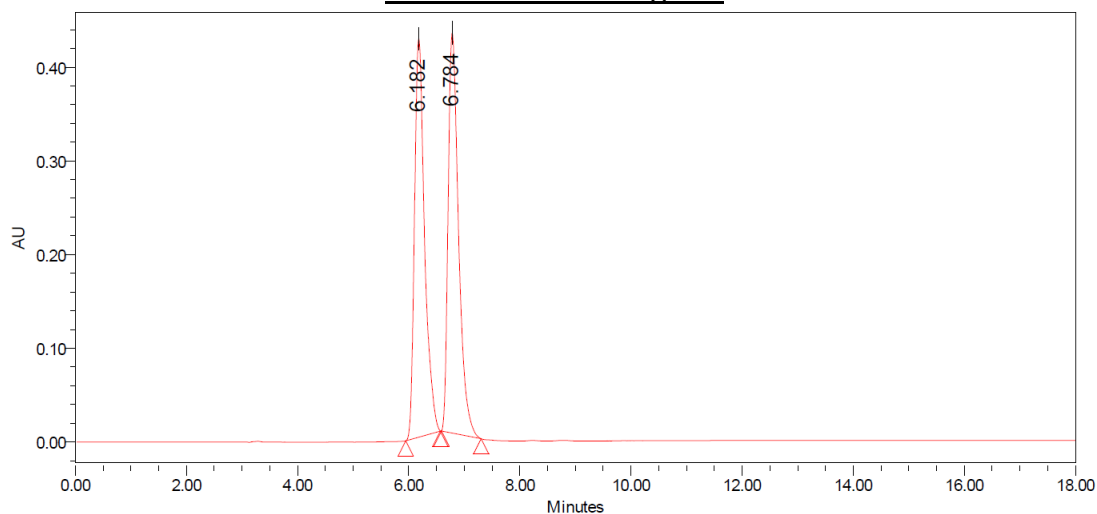


Peak	% Area	Retention Time	Area	Height
1	74.35	6.154	6640710	802202
2	26.65	7.414	2290774	290511



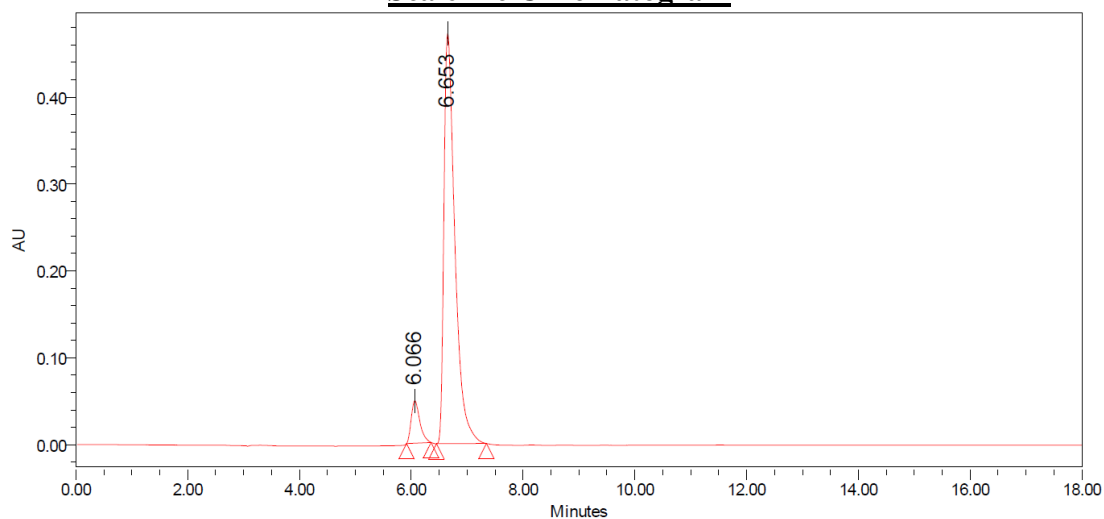
2.37 – Major Diastereomer
 Run Details: HPLC, Diacel CHIRALPAK OD-H,
 10.00 μ L, gradient 5% to 50% iPrOH/hexanes,
 18 minutes, 1 mL/min, 295.0 nm.

Racemic Chromatogram

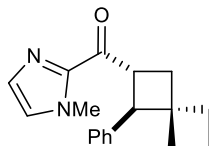


Peak	% Area	Retention Time	Area	Height
1	49.10	6.182	5361808	425302
2	50.90	6.784	5559201	427104

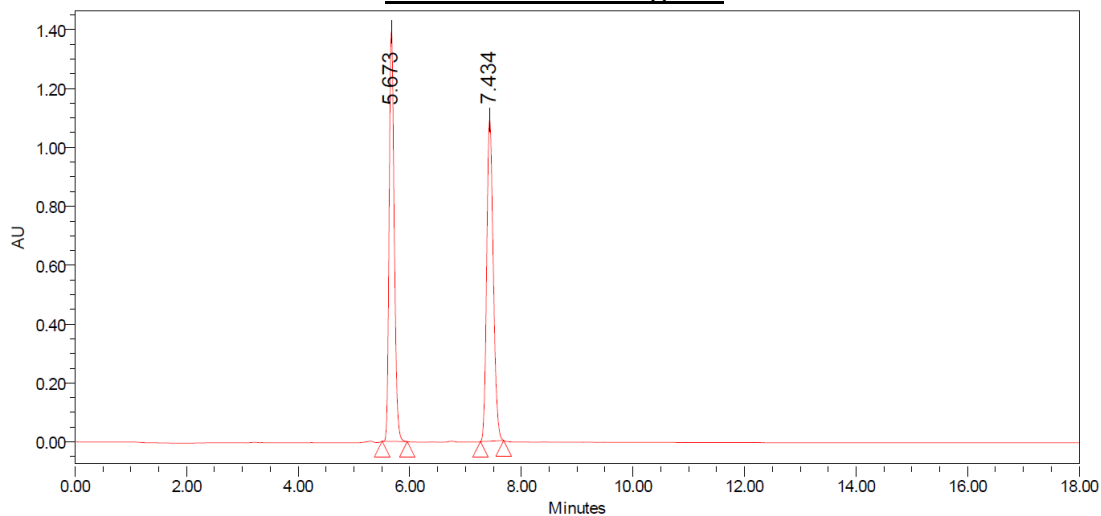
Scalemic Chromatogram



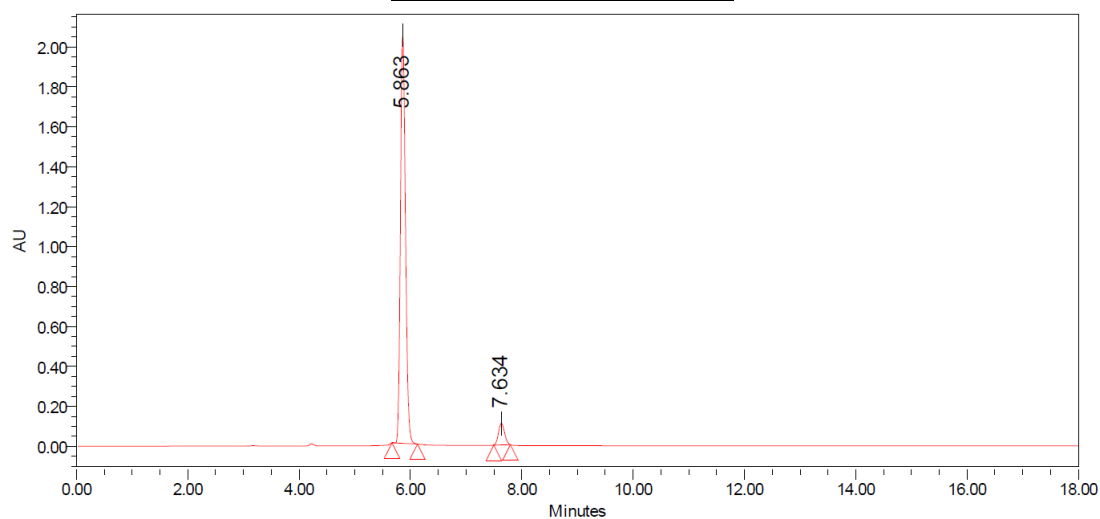
Peak	% Area	Retention Time	Area	Height
1	7.52	6.066	519995	48805
2	92.48	6.653	6395904	471931

**2.38**

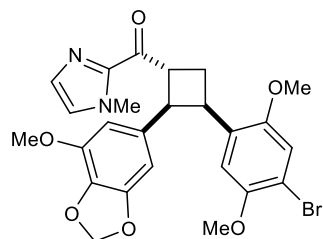
Run Details: HPLC, Daicel CHIRALPAK AD,
10.00 μ L, gradient 5% to 50% iPrOH/hexanes,
18 minutes, 1 mL/min, 285.0 nm.

Racemic Chromatogram

Peak	% Area	Retention Time	Area	Height
1	49.53	5.673	8797392	1391958
2	50.47	7.434	8962578	1091598

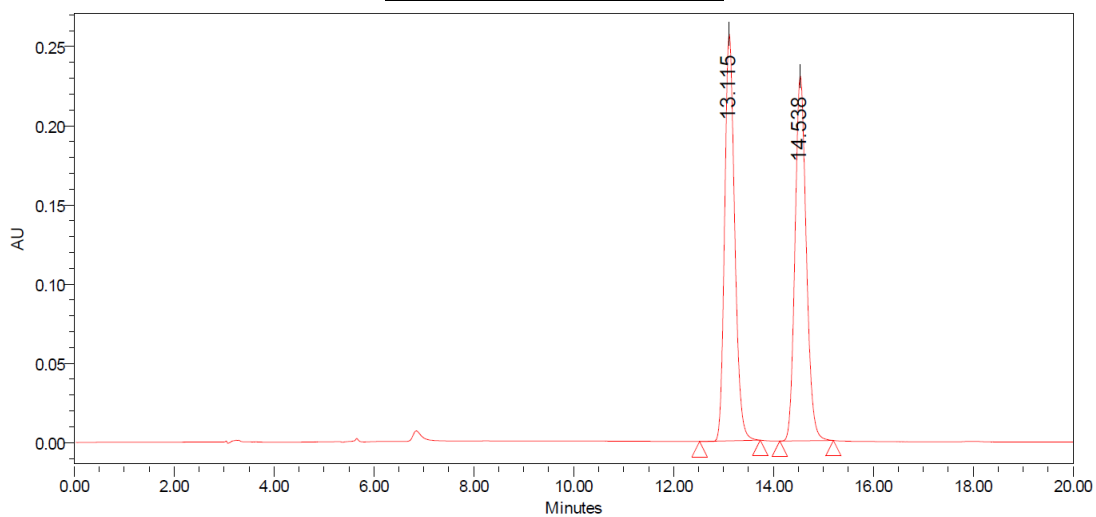
Scalemic Chromatogram

Peak	% Area	Retention Time	Area	Height
1	93.99	5.863	12847379	2044953
2	6.01	7.634	820925	108421



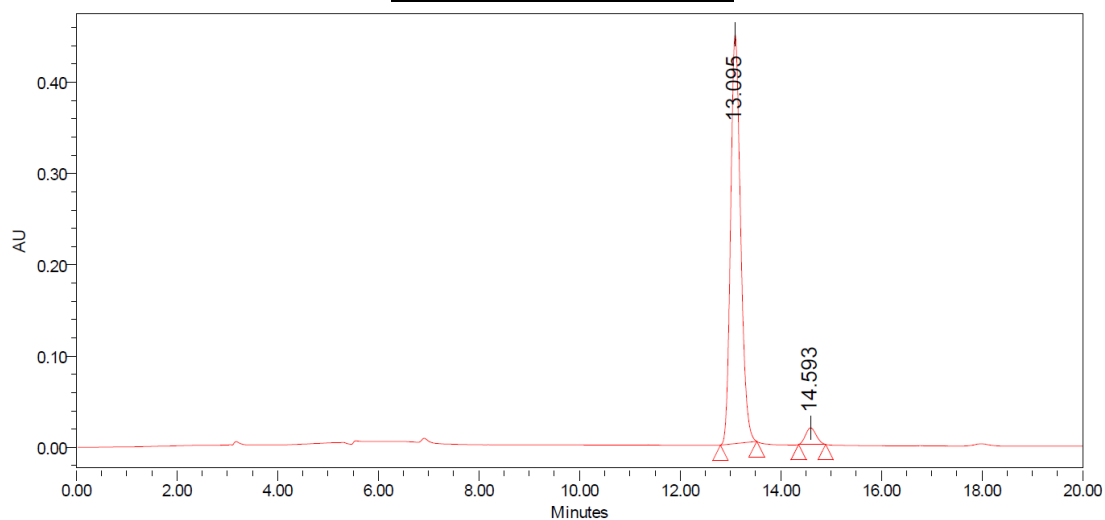
2.39 – Major Diastereomer
 Run Details: HPLC, Daicel CHIRALPAK AD,
 10.00 μ L, gradient 5% to 50% iPrOH/hexanes,
 20 minutes, 1 mL/min, 285.0 nm.

Racemic Chromatogram

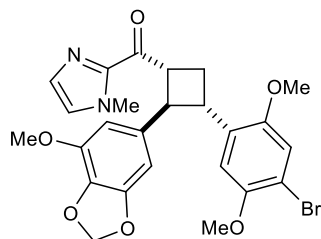


Peak	% Area	Retention Time	Area	Height
1	49.98	13.115	3596281	256807
2	50.02	14.538	3599837	230267

Scalemic Chromatogram

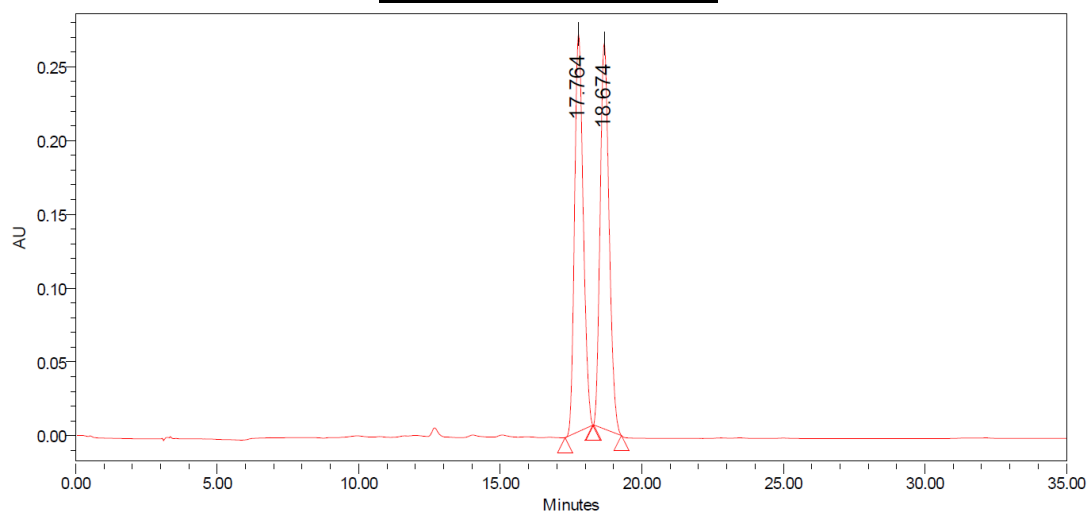


Peak	% Area	Retention Time	Area	Height
1	95.88	13.095	6183232	448302
2	4.12	14.593	265927	18169



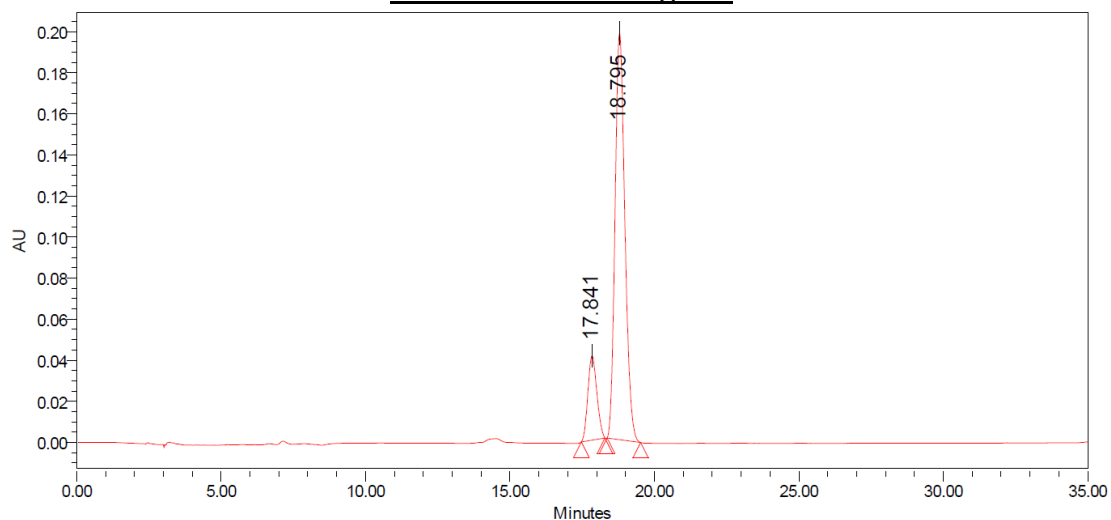
2.39 – Minor Diastereomer
 Run Details: HPLC, Daicel CHIRALPAK AS-H,
 10.00 μ L, gradient 5% to 30% EtOH/hexanes,
 35 minutes, 1 mL/min, 285.0 nm.

Racemic Chromatogram

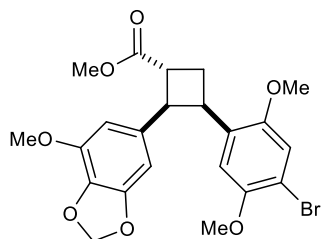


Peak	% Area	Retention Time	Area	Height
1	49.86	17.764	5725848	269376
2	50.14	18.674	5758071	261335

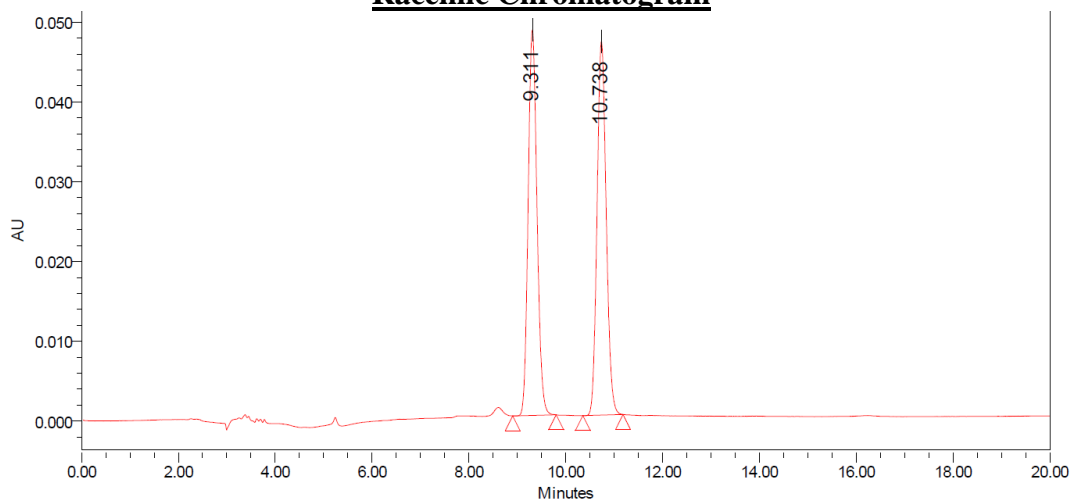
Scalemic Chromatogram



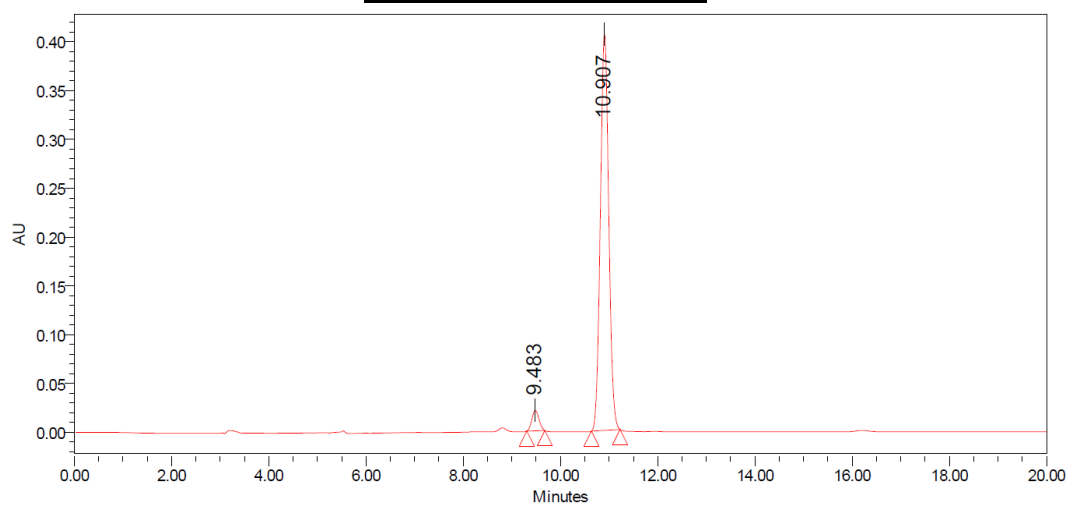
Peak	% Area	Retention Time	Area	Height
1	15.92	17.841	885618	41061
2	84.08	18.795	4678118	197836

**2.40**

Run Details: HPLC, Daicel CHIRALPAK AD,
10.00 μ L, gradient 5% to 50% iPrOH/hexanes,
20 minutes, 1 mL/min, 285.0 nm.

Racemic Chromatogram

Peak	% Area	Retention Time	Area	Height
1	49.86	9.311	611954	48313
2	50.14	10.738	615302	46848

Scalemic Chromatogram

Peak	% Area	Retention Time	Area	Height
1	4.20	9.483	212731	20891
2	95.80	10.907	4848368	405365

2.7 References

- ¹ Rau, H. Asymmetric Photochemistry in Solution. *Chem. Rev.* **1983**, *83*, 535–547.
- ² Inoue, Y. Asymmetric Photochemical Reactions in Solution. *Chem. Rev.* **1992**, *92*, 741–770.
- ³ Inoue, Y.; Ramamurthy, V. *Molecular and Supramolecular Photochemistry*, Vol. 11: Chiral Photochemistry; Marcel Dekker: New York, NY, 2004.
- ⁴ Brimioulle, R.; Lenhart, D.; Maturi, M. M.; Bach, T. Enantioselective Catalysis of Photochemical Reactions. *Angew. Chem., Int. Ed.* **2015**, *54*, 3872–3890.
- ⁵ Zou, Y.-Q.; Hörmann, F. M.; Bach, T. Iminium and Enamine Catalysis in Enantioselective Photochemical Reactions. *Chem. Soc. Rev.* **2018**, *47*, 278–290.
- ⁶ Sherbrook, E. M.; Yoon, T. P. Asymmetric Catalysis of Triplet-State Photoreactions. In *Specialist Periodical Reports: Photochemistry*; Albini, A., Protti, S., Eds.; Royal Society of Chemistry: Croydon, UK, 2019; Vol. 46, pp 432–448.
- ⁷ Prentice, C.; Morrisson, J.; Smith, A. D.; Zysman-Colman, E. Recent Developments in Enantioselective Photocatalysis. *Beilstein J. Org. Chem.* **2020**, *16*, 2363–2441.
- ⁸ Rigotti, T.; Alemán, J. Visible Light Photocatalysis – From Racemic to Asymmetric Activation Strategies. *Chem. Commun.* **2020**, *56*, 11169–11190.
- ⁹ Brimioulle, R.; Bach, T. Enantioselective Lewis Acid Catalysis of Intramolecular Enone [2+2] Photocycloaddition Reactions. *Science* **2013**, *342*, 840–843.
- ¹⁰ Brenninger, C.; Jolliffe, J. D.; Bach, T. Chromophore Activation of α,β -Unsaturated Carbonyl Compounds and Its Application to Enantioselective Photochemical Reactions. *Angew. Chem., Int. Ed.* **2018**, *57*, 14338–14349.
- ¹¹ Blum, T. R.; Miller, Z. D.; Bates, D. M.; Guzei, I. A.; Yoon, T. P. Enantioselective Photochemistry through Lewis Acid-Catalyzed Triplet Energy Transfer. *Science* **2016**, *354*, 1391–1395.
- ¹² Miller, Z. D.; Lee, B. J.; Yoon, T. P. Enantioselective Crossed Photocycloadditions of Styrenic Olefins by Lewis Acid Catalyzed Triplet Sensitization. *Angew. Chem., Int. Ed.* **2017**, *56*, 11891–11895.
- ¹³ Daub, M. E.; Jung, H.; Lee, B. J.; Won, J.; Baik, M.-H.; Yoon, T. P. Enantioselective [2+2] Cycloadditions of Cinnamate Esters: Generalizing Lewis Acid Catalysis of Triplet Energy Transfer. *J. Am. Chem. Soc.* **2019**, *141*, 9543–9547.

-
- ¹⁴ Erkkilä, A.; Majander, I.; Pihko, P. M. Iminium Catalysis. *Chem. Rev.* **2007**, *107*, 5416–5470.
- ¹⁵ Mukherjee, S.; Yang, J. W.; Hoffmann, S.; List, B. Asymmetric Enamine Catalysis. *Chem. Rev.* **2007**, *107*, 5471–5569.
- ¹⁶ Doyle, A. G.; Jacobsen, E. N. Small-Molecule H-Bond Donors in Asymmetric Catalysis. *Chem. Rev.* **2007**, *107*, 5713–5743.
- ¹⁷ Akiyama, T. Stronger Brønsted Acids. *Chem. Rev.* **2007**, *107*, 5744–5758.
- ¹⁸ Takagi, R. & Tabuchi, C. Enantioselective Intramolecular [2+2] Photocycloaddition using Phosphoric Acid as a Chiral Template. *Org. Biomol. Chem.* **2020**, *18*, 9261–9267.
- ¹⁹ Silvi, M.; Verrier, C.; Rey, Y. P.; Buzzetti, L.; Melchiorre, P. Visible-Light Excitation of Iminium Ions Enables the Enantioselective Catalytic β -Alkylation of Enals. *Nat. Chem.* **2017**, *9*, 868–873.
- ²⁰ Verrier, C.; Alandini, N.; Pezzetta, C.; Moliterno, M.; Buzzetti, L.; Hepburn, H. B.; Vega-Peñaloza, A.; Silvi, M.; Melchiorre, P. Direct Stereoselective Installation of Alkyl Fragments at the β -Carbon of Enals via Excited Iminium Ion Catalysis. *ACS Catal.* **2018**, *8*, 1062–1066.
- ²¹ Hörmann, F. M.; Chung, T. S.; Rodriguez, E.; Jakob, M.; Bach, T. Evidence for Triplet Sensitization in the Visible-Light-Induced [2+2] Photocycloaddition of Eniminium Ions. *Angew. Chem., Int. Ed.* **2018**, *57*, 827–831.
- ²² Hörmann, F. M.; Kerzig, C.; Chung, T. S.; Bauer, A.; Wenger, O. S.; Bach, T. Triplet Energy Transfer from Ruthenium Complexes to Chiral Eniminium Ions: Enantioselective Synthesis of Cyclobutanecarbaldehydes by [2+2] Photocycloaddition. *Angew. Chem. Int. Ed.* **2020**, *59*, 9659–9668.
- ²³ Bibal, B.; Mongin, C.; Bassani, D. M. Template Effects and Supramolecular Control of Photoreactions in Solution. *Chem. Soc. Rev.* **2014**, *43*, 4179–4198.
- ²⁴ Ramamurthy, V.; Sivaguru, J. Supramolecular Photochemistry as a Potential Synthetic Tool: Photocycloaddition. *Chem. Rev.* **2016**, *116*, 9914–9993.
- ²⁵ Burg, F.; Bach, T. Lactam Hydrogen Bonds as Control Elements in Enantioselective Transition-Metal-Catalyzed and Photochemical Reactions. *J. Org. Chem.* **2019**, *84*, 8815–8836.
- ²⁶ Vallavoju, N.; Selvakumar, S.; Jockusch, S.; Sibi, M. P.; Sivaguru, J. Enantioselective Organophotocatalysis Mediated by Atropisomeric Thiourea Derivatives. *Angew. Chem. Int. Ed.* **2014**, *53*, 5604–5608.

-
- ²⁷ Vallavoju, N.; Selvakumar, S.; Pemberton, B. C.; Jockusch, S.; Sibi, M. P.; Sivaguru, J. Organophotocatalysis: Insights into the Mechanistic Aspects of Thiourea-Mediated Intermolecular [2+2] Photocycloadditions. *Angew. Chem. Int. Ed.* **2016**, *55*, 5446–5451.
- ²⁸ Sherbrook, E. M.; Jung, H.; Cho, D.; Baik, M.-H.; Yoon, T. P. Brønsted Acid Catalysis of Photosensitized Cycloadditions. *Chem. Sci.* **2020**, *11*, 856–861.
- ²⁹ Parmar, D.; Sugiono, E.; Raja, S.; Rueping, M. Complete Field Guide to Asymmetric BINOL-Phosphate Derived Brønsted Acid and Metal Catalysis: History and Classification by Mode of Activation; Brønsted Acidity, Hydrogen Bonding, Ion Pairing, and Metal Phosphates. *Chem. Rev.* **2014**, *114*, 9047–9153.
- ³⁰ Nakashima, D.; Yamamoto, H. Design of Chiral *N*-Triflyl Phosphoramidate as a Strong Chiral Brønsted Acid and Its Application to Asymmetric Diels–Alder Reaction. *J. Am. Chem. Soc.* **2006**, *128*, 9626–9627.
- ³¹ Du, J.; Skubi, K. L.; Schultz, D. M.; Yoon, T. P. A Dual-Catalysis Approach to Enantioselective [2+2] Photocycloadditions Using Visible Light. *Science* **2014**, *344*, 392–396.
- ³² Lei, T.; Zhou, C.; Huang, M.-Y.; Zhao, L.-M.; Yang, B.; Ye, C.; Xiao, H.; Meng, Q.-Y.; Ramamurthy, V.; Tung, C.-H.; Wu, L.-Z. General and Efficient Intermolecular [2+2] Photodimerization of Chalcones and Cinnamic Acid Derivatives in Solution through Visible-Light Catalysis. *Angew. Chem., Int. Ed.* **2017**, *56*, 15407–15410.
- ³³ Li, R.; Ma, B. C.; Huang, W.; Wang, L.; Wang, D.; Lu, H.; Landfester, K.; Zhang, K. A. Photocatalytic Regio- and Stereo-selective [2+2] Cycloaddition of Styrene Derivatives using a Heterogeneous Organic Photocatalyst. *ACS Catal.* **2017**, *7*, 3097–3101.
- ³⁴ Fan, X.; Lei, T.; Chen, B.; Tung, C.-H.; Wu, L.-Z. Photocatalytic C–C Bond Activation of Oxime Ester for Acyl Radical Generation and Application. *Org. Lett.* **2019**, *21*, 4153–4158.
- ³⁵ Nguyen, J. D.; D’Amato, E. M.; Narayanam, J. M.; Stephenson, C. R. Engaging Unactivated Alkyl, Alkenyl and Aryl Iodides in Visible-Light-Mediated Free Radical Reactions. *Nat. Chem.* **2012**, *4*, 854–859.
- ³⁶ Carreira, E. M.; Fessard, T. C. Four-Membered Ring-Containing Spirocycles: Synthetic Strategies and Opportunities. *Chem. Rev.* **2014**, *114*, 8257–8322.
- ³⁷ Huang, X.; Quinn, T. R.; Harms, K.; Webster, R. D.; Zhang, L.; Wiest, L.; Meggers, E. Direct Visible-Light-Excited Asymmetric Lewis Acid Catalysis of Intermolecular [2+2] Photocycloadditions. *J. Am. Chem. Soc.* **2017**, *139*, 9120–9123.

-
- ³⁸ Jung, H.; Hong, M.; Marchini, M.; Villa, M.; Steinlandt, P. S.; Huang, X.; Hemming, M.; Meggers, E.; Ceroni, P.; Park, J.; Baik, M.-H. Understanding the Mechanism of Direct Visible-Light-Activated [2+2] Cycloadditions Mediated by Rh and Ir Photocatalysts: Combined Computational and Spectroscopic Studies. *Chem. Sci.* **2021**, *12*, 9673–9681.
- ³⁹ Zalewski, R. I.; Dunn, G. E. Protonation of Conjugated Carbonyl Groups in Sulfuric Acid Solutions. I. Adaptation of the Amide Acidity Function H_A for Protonation of the Carbonyl Group in Non-Hammett Bases. *Can. J. Chem.* **1968**, *46*, 2469–2470.
- ⁴⁰ Zalewski, R. I.; Dunn, G. E. Protonation of Conjugated Carbonyl Groups in Sulfuric Acid Solutions. II. Protonation and Basicity of α,β -Unsaturated Alicyclic Ketones. *Can. J. Chem.* **1969**, *47*, 2263–2270.
- ⁴¹ Mulliken, R. S. Molecular Compounds and their Spectra. *J. Am. Chem. Soc.* **1952**, *74*, 811–824.
- ⁴² Rosokha, S. V.; Kochi, J. K. Fresh Look at Electron-Transfer Mechanisms via the Donor-Acceptor Bindings in the Critical Encounter Complex. *Acc. Chem. Res.* **2008**, *41*, 641–653.
- ⁴³ Lima, C. G.; Lima, T. M.; Duarte, M.; Jurberg, I. D.; Paixão, M. W. Organic Synthesis Enabled by Light-Irradiation of EDA Complexes: Theoretical Background and Synthetic Applications. *ACS Catal.* **2016**, *6*, 1389–1407.
- ⁴⁴ Arceo, E.; Jurberg, I. D.; Álvarez-Fernández, A.; Melchiorre, P. Photochemical Activity of a Key Donor-Acceptor Complex can Drive Stereoselective Catalytic α -Alkylation of Aldehydes. *Nat. Chem.* **2013**, *5*, 750–756.
- ⁴⁵ Bahamonde, A.; Melchiorre, P. Mechanism of the Stereoselective α -Alkylation of Aldehydes Driven by the Photochemical Activity of Enamines. *J. Am. Chem. Soc.* **2016**, *138*, 8019–8030.
- ⁴⁶ Other acids including p-toluenesulfonic acid and camphorsulfonic acid were not soluble under the reaction conditions.
- ⁴⁷ See supplementary information for the related NTOs.
- ⁴⁸ Pangborn, A. B.; Giardello, M. A.; Grubbs, R. H.; Rosen, R. K.; Timmers, F. J. *Organometallics*, **1996**, *15*, 1518–1520.
- ⁴⁹ Uraguchi, D.; Terada, M. *J. Am. Chem. Soc.* **2004**, *126*, 5356–5357.
- ⁵⁰ Nakashima, D.; Yamamoto, H. *J. Am. Chem. Soc.* **2006**, *128*, 9626–9627.
- ⁵¹ Chong, J. M.; Shen, L.; Taylor, N. J. *J. Am. Chem. Soc.* **2000**, *122*, 1822–1823.
- ⁵² Ooi, T.; Kameda, M.; Maruoka, K. *J. Am. Chem. Soc.* **2003**, *125*, 5139–5151.

-
- ⁵³ Ahmed, I.; Clark, D. A. *Org. Lett.* **2014**, *16*, 4332–4335.
- ⁵⁴ Tolstikova, L. L.; Bel'skikh, A. V.; Shainyan, B. A. *Russ. J. Gen. Chem.* **2010**, *80*, 1258–1262.
- ⁵⁵ Davies, D. H.; Hall, J.; Smith, E. H. *J. Chem. Soc. Perkin Trans. 1* **1991**, 2691–2698.
- ⁵⁶ Hiyama, T.; Reddy, G. B.; Minami, T.; Hanamoto, T. *Bull. Chem. Soc. Jpn.* **1995**, *68*, 350–363.
- ⁵⁷ Evans, D. A.; Fandrick, K. R.; Song, H.-J. *J. Am. Chem. Soc.* **2005**, *127*, 8942–8943.
- ⁵⁸ Myers, M. C.; Bharadwaj, A. R.; Migram, B. C.; Scheidt, K. A. *J. Am. Chem. Soc.* **2005**, *127*, 14675–14680.
- ⁵⁹ Sherbrook, E. M.; Jung, H.; Cho, D.; Baik, M.-H.; Yoon, T. P. *Chem. Sci.* **2020**, *11*, 856–861.
- ⁶⁰ Note that MeOH is used in this case to avoid transesterification to generate mixed ester products.
- ⁶¹ Rout, S.; Das, A.; Singh, V. K. *J. Org. Chem.* **2018**, *83*, 5058–5071.
- ⁶² Zhao, L. J.; Kwong, C. K. W.; Shi, M.; Toy, P. H. *Tetrahedron* **2005**, *61*, 12026–12032.
- ⁶³ Stals, P. J. M.; Phan, T. N. T.; Gigmes, D.; Paffen, T. F. E.; Meijer, E. W.; Palmans, A. R. A. *J. Polym. Sci. Part A Polym. Chem.* **2012**, *50*, 780–791.
- ⁶⁴ Williamson, K. S.; Yoon, T. P. *J. Am. Chem. Soc.* **2010**, *132*, 4570–4571.
- ⁶⁵ Gaali, S.; Kozany, C.; Hoogeland, B.; Klein, M.; Hausch, F. *ACS Med. Chem. Lett.* **2010**, *1*, 536–539.
- ⁶⁶ Zhou, Y.; Bandar, J. S.; Buchwald, S. L. *J. Am. Chem. Soc.* **2017**, *139*, 8126–8129.
- ⁶⁷ Brown, A. R.; Molander, G. A. *J. Org. Chem.* **2016**, *71*, 9681–9686.
- ⁶⁸ Texter, K. B.; Waymach, R.; Kavanagh, P. V.; O'Brien, J. E.; Talbot, B.; Brandt, S. D.; Gardner, E. A. *Drug Test. Analysis*, **2018**, *10*, 229–236.
- ⁶⁹ Thordarson, P. *Chem. Soc. Rev.* **2011**, *40*, 1305–1323.
- ⁷⁰ Bruker-AXS (2018). APEX3. Version 2018.1-0. Madison, Wisconsin, USA.
- ⁷¹ Krause, L., Herbst-Irmer, R., Sheldrick, G. M. & Stalke, D. (2015). *J. Appl. Cryst.* **48**, 3–10.
- ⁷² Sheldrick, G. M. (2013b). XPREP. Version 2013/1. Georg-August-Universität Göttingen, Göttingen, Germany.

-
- ⁷³ Sheldrick, G. M. (2013a). The SHELX homepage, <http://shelx.uni-ac.gwdg.de/SHELX/>.
- ⁷⁴ Sheldrick, G. M. (2015a). *Acta Cryst. A*, 71, 3-8.
- ⁷⁵ Sheldrick, G. M. (2015b). *Acta Cryst. C*, 71, 3-8.
- ⁷⁶ Dolomanov, O. V., Bourhis, L. J., Gildea, R. J., Howard, J. A. K. & Puschmann, H. (2009). *J. Appl. Crystallogr.* 42, 339-341.
- ⁷⁷ Guzei, I. A. (2007-2013). Programs Gn. University of Wisconsin-Madison, Madison, Wisconsin, USA.
- ⁷⁸ Parr, R.G.; Yang, W. *Density Functional Theory of Atoms and Molecules*. Oxford University Press: New York, **1989**.
- ⁷⁹ Bochevarov, A.D.; Harder, E.; Hughes, T. F.; Greenwood, J. R.; Braden, D. A.; Philipp, D. M.; Rinaldo, D.; Halls, M. D.; Zhang, J.; Friesner, R. Jaguar: A high-performance quantum chemistry software program with strengths in life and materials sciences. *Int. J. Quantum Chem.* **2013**, 113, 2110.
- ⁸⁰ Slater, J. C. *Quantum Theory of Molecules and Solids*, Vol. 4: The Self-Consistent Field for Molecules and Solids. McGraw-Hill: New York, **1974**.
- ⁸¹ Vosko, S. H.; Wilk, L.; Nusair, M. Accurate spin-dependent electron liquid correlation energies for local spin density calculations: a critical analysis. *Can. J. Phys.* **1980**, 58, 1200.
- ⁸² Becke, A. D. Density-functional exchange-energy approximation with correct asymptotic behavior. *Phys. Rev. A* **1988**, 38, 3098.
- ⁸³ Lee, C.; Yang, W.; Parr, R. G. Development of the Colle-Salvetti correlation-energy formula into a functional of the electron density. *Phys. Rev. B* **1988**, 37, 785.
- ⁸⁴ Becke, A. D. Density-functional thermochemistry. III. The role of exact exchange. *J. Chem. Phys.* **1993**, 98, 5648.
- ⁸⁵ Grimme, S.; Antony, J.; Ehrlich, S.; Krieg, S. A consistent and accurate ab initio parametrization of density functional dispersion correction (DFT-D) for the 94 elements H-Pu. *J. Chem. Phys.* **2010**, 132, 154104.
- ⁸⁶ Ditchfield, R.; Hehre, W. J.; Pople, J. A. Self-Consistent Molecular-Orbital Methods. IX. An Extended Gaussian-Type Basis for Molecular-Orbital Studies of Organic Molecules. *J. Chem. Phys.* **1971**, 54, 724.

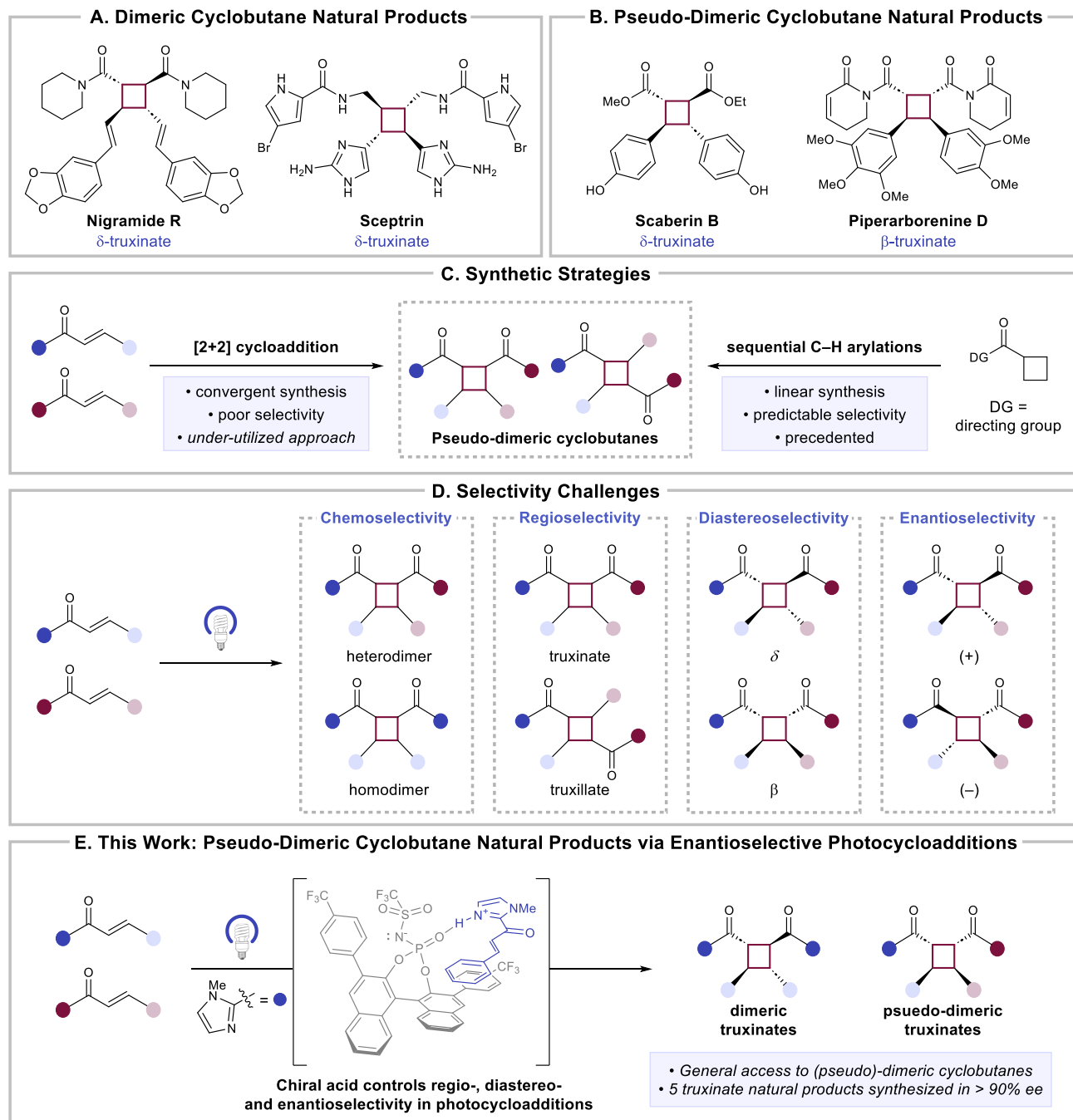
-
- ⁸⁷ Hehre, W. J.; Pople, J. A. Self-Consistent Molecular Orbital Methods. XIII. An Extended Gaussian-Type Basis for Boron. *J. Chem. Phys.* **1972**, *56*, 4233.
- ⁸⁸ Binkley, J. S.; Pople, J. A. Self-consistent molecular orbital methods. XIX. Split-valence Gaussian-type basis sets for beryllium. *J. Chem. Phys.* **1977**, *66*, 879.
- ⁸⁹ Hariharan, P. C.; Pople, J. A. The influence of polarization functions on molecular orbital hydrogenation energies. *Theor. Chim. Acta* **1973**, *28*, 213.
- ⁹⁰ Hehre, W. J.; Ditchfield, R.; Pople, J. A. Self—Consistent Molecular Orbital Methods. XII. Further Extensions of Gaussian—Type Basis Sets for Use in Molecular Orbital Studies of Organic Molecules. *J. Chem. Phys.* **1972**, *56*, 2257.
- ⁹¹ Francl, M. M.; Pietro, W. J.; Hehre, W. J.; Binkley, J. S.; Gordon, M. S.; DeFrees, D. J.; Pople, J. A. Self-consistent molecular orbital methods. XXIII. A polarization-type basis set for second-row elements. *J. Chem. Phys.* **1982**, *77*, 3654.
- ⁹² Shao Y. et al. Advances in molecular quantum chemistry contained in the Q-Chem 4 program package. *Mol. Phys.* **2015**, *113*, 184.
- ⁹³ Yanai, T.; Tew, D.; Handy, N. A new hybrid exchange–correlation functional using the Coulomb-attenuating method (CAM-B3LYP). *Chem. Phys. Lett.* **2004**, *393*, 51.
- ⁹⁴ Hirata, S.; Head-Gordon, M. Time-dependent density functional theory within the Tamm–Dancoff approximation. *Chem. Phys. Lett.* **1999**, *314*, 291.

**Chapter 3 Total Synthesis of Truxinate Natural Products Enabled by Enantioselective
[2+2] Photocycloadditions**

3.1 Introduction

The truxinates constitute a class of natural products that formally derive from the head-to-head [2+2] cyclodimerization of cinnamic acid derivatives. This large family of secondary metabolites consists of over 100 known members.^{1,2} They vary in their relative and absolute stereochemistry; they can be either true homodimers or pseudodimers of structurally analogous but chemically distinct cinnamates; and they collectively exhibit a range of biological activities (**Scheme 3.1a,b**).³⁻⁵ More broadly, the truxinates are representative of a larger group of dimeric cyclobutane natural products that have presented a formidable challenge in synthetic chemistry for many decades.

Two complementary approaches have proven to be most general for the preparation of these compounds to date. Arguably the more successful of these, pioneered by Baran and Reisman, involves the iterative modification of each carbon of minimally functionalized cyclobutane scaffolds by directed C–H functionalization (**Scheme 3.1c**).⁶⁻¹⁰ By carefully tuning the directing group and reaction conditions, this strategy can provide complete control over the identity and stereochemistry of the substituent on each carbon of the cyclobutane core. However, the syntheses resulting from this strategy are necessarily linear, and because every C–H functionalization event can require different conditions, the resulting step counts can be comparatively high.



Scheme 3.1 (A) Chemical structures of dimeric cyclobutane natural products. (B) Chemical structures of pseudo-dimeric cyclobutane natural products. (C) Synthetic strategies towards truxinate and truxillate natural products. (D) Selectivity challenges in asymmetric heterodimerization reactions. (E) Synthesis of pseudo-dimeric cyclobutane natural products via enantioselective photocycloadditions.

Photochemical [2+2] cycloadditions could potentially provide a more direct approach because they enable the construction of up to four stereocenters of a fully substituted cyclobutane

in a single step.¹¹ Control over the outcome of these reactions, however, presents a set of selectivity issues that can each present a formidable challenge (**Scheme 3.1d**). First, fully substituted cyclobutane rings can feature four stereogenic centers, and [2+2] photocycloadditions can thus result in up to sixteen possible stereochemical outcomes. Second, the chemoselective heterodimerization of two chemically distinct cinnamates can be challenging, particularly using structurally analogous reaction partners with similar electronic and optical properties. Finally, [2+2] photocycloaddition reactions can result in both head-to-head and head-to-tail regioisomers, and the cyclodimerization of even relatively polarized alkenes is often non-regioselective under the high-energy conditions of photochemical activation.¹² Thus even simple photocycloaddition reactions can result in complex mixtures of products. For example, in a seminal study of the BF_3 -promoted cyclodimerization of methyl cinnamate, Lewis identified 12 of 17 possible regiochemically, enantiomerically, and diastereomerically distinct products that were formed with poor overall selectivity; heterodimerization reactions would presumably result in even more complex product mixtures.¹³ As a result, there have been no stereocontrolled syntheses of the truxinate or truxillate natural products reported to date that take advantage of the potential efficiencies provided by enantioselective catalytic [2+2] photocycloaddition reactions.

3.2 Results and Discussion

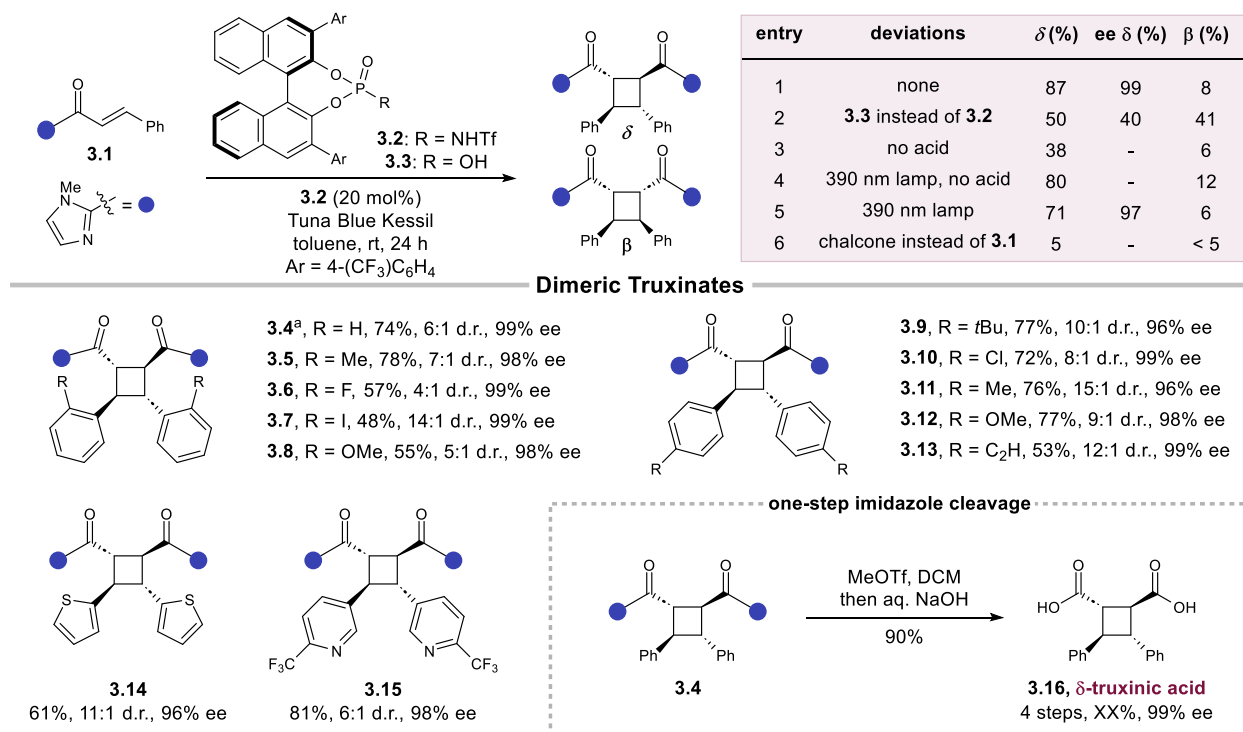
A hallmark of the recent renewal of interest in photochemical synthesis has been the development of the first general strategies for highly stereoselective asymmetric photocatalysis.^{14–16} In this context, our laboratory has contributed to this effort by developing several highly enantioselective methods for [2+2] photocycloaddition.^{17,18} Among these, we imagined that the highly enantioselective Brønsted acid catalyzed [2+2] photocycloaddition of *C*-cinnamoylimidazoles developed recently in our laboratory might provide a valuable entry towards

the enantioselective synthesis of truxinate natural products for two reasons.^{19,20} First, the imidazolyl unit can be readily cleaved under mild conditions to afford a wide range of carboxylic acid derivatives. We imagined that successful application of this method to the synthesis of the truxinate natural products might enable the uniquely direct synthesis of a large fraction of the known members of this class. Second, this reaction operates by a principle that Bach has termed “chromophore activation.”¹⁶ While a solution of **3.1** does not absorb appreciably in the visible region, addition of **3.2** leads to a red-shifted absorption (see Chapter 2 for UV-Vis experiments). Because the absorption of the catalyst-bound substrate occurs more strongly at longer wavelengths than the free substrate, the protonated substrate can be selectively excited by judicious choice of irradiation wavelength. We speculated that appropriate selection of a cinnamate reaction partner that does not absorb at these longer wavelengths might enable a controlled heterodimerization that would enable the synthesis of the pseudo-dimeric truxinates as well.

3.2.1 Dimerization Optimization and Substrate Scope

Our investigations began by applying our previously reported conditions to the dimerization of *C*-cinnamoylimidazole **3.1** (Scheme 3.2). We were delighted to find that irradiation with a Kessil Tuna Blue LED in the presence of chiral acid **3.2** results in the formation of **3.4** in 87% yield and with exceptionally high selectivity (99% ee, 11:1 d.r.). The phosphoramidate catalyst (**3.2**) was uniquely effective in promoting the photocycloaddition as the corresponding phosphoric acid catalyst **3.3** gave a mixture of diastereomers in low ee. Irradiation of **3.1** in the absence of catalyst gave a low yield of cycloadduct, indicative of a slow racemic background reaction, albeit in lower d.r. compared to the catalyzed reaction. Finally, the imidazole substrate is also necessary for achieving high ee and yield as irradiation of chalcone gave mostly decomposition. The reaction proved remarkably general when using a wide variety of

sterically and electronically dissimilar substrates (**Scheme 3.2**). Notably, the major diastereomer formed in this reaction is the all-*trans*-configured cycloadduct. This stereochemistry is characteristic of the δ -truxinate subfamily of natural products that constitutes the largest subset of truxinate natural products. Though a small amount of the C_s -symmetric β -diastereomer is typically formed in the reaction, it is easily separated from the desired δ -isomer via column chromatography. When performing the reaction on a 5 mmol scale with a 5 mol% catalyst loading, **3.4** was formed in similar yield and selectivity (74% and 99% ee), and the acid catalyst could be recovered in 94% yield. Importantly, enantioenriched cycloadduct **3.4** is readily converted into δ -truxinic acid, the simplest, parent member of this class of natural products. We employed an approach popularized by Evans in which methylation of the imidazole yields an imidazolium intermediate that is primed to act as a leaving group in an acyl substitution reaction.^{21–23} Addition of aqueous NaOH to a solution of the dimethylated intermediate provided δ -truxinic acid in 90% yield without loss of stereochemical purity.



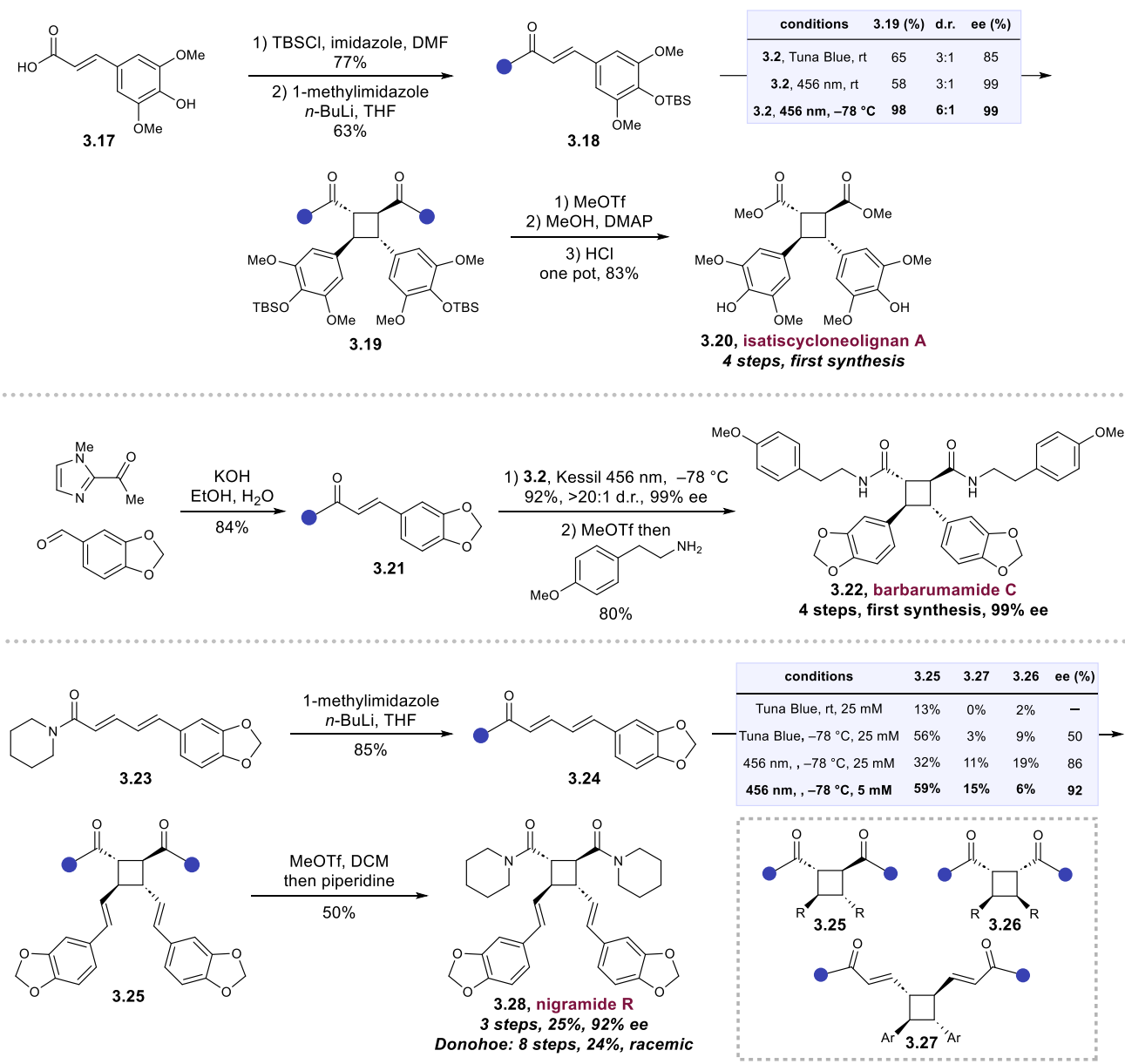
Scheme 3.2 Optimization, substrate scope, and cleavage for the enantioselective dimerization reaction. ^a 5mol% catalyst.

3.2.2 Total Synthesis of Dimeric Truxinates

The high generality of this cyclodimerization and the facile cleavage of the imidazolyl ketone offers a straightforward and general strategy towards the stereocontrolled synthesis of the dimeric δ -truxinates. Isatiscycloneolignan A is a highly oxidized δ -truxinate that has shown neuroprotective effects against injured human neuroblastoma cells.²⁴ Isatiscycloneolignan and other compounds extracted from *Isatis indigotica* have been extensively studied for their pharmacological activity since the herb is often employed in traditional Chinese medicine.²⁵ When we subjected **3.18** to the optimized enantioselective dimerization conditions the desired δ -truxinate was afforded in 65% yield and 85% ee (**Scheme 3.3**). We suspected that the lower enantioselectivity could be explained by direct excitation of catalyst-unbound **3.18** leading to racemic background reactivity. Indeed, the absorption of **3.18** has a significant overlap with the

emission spectrum of the Tuna Blue Kessil (**Figure 3.2** in Supporting Information). To avoid this direct excitation, we changed the light source to a Kessil 456 nm lamp with a red-shifted emission profile relative to the Tuna Blue. These conditions afforded the truxinate in 99% ee. Though not necessary to obtain high ee, we also found that lowering the temperature to -78 °C led to an increased yield and d.r., giving **3.19** in 98% yield, 6:1 d.r., and 99% ee. From **3.19**, one-pot acyl substitution with methanol and acid-catalyzed phenol deprotection afforded isatisycloneolignan A in 83% yield.

We next synthesized barbarumamide C, a δ -truxinate isolated from Goji berries (*Lycium barbarum L.*), utilizing a similar synthetic strategy.²⁶ The cycloaddition substrate for this synthesis was prepared by aldol condensation with piperonal, an inexpensive phytochemical feedstock. Under the same photocycloaddition conditions as above, the cycloadduct was produced in 92% yield, >20:1 d.r., and 99% ee. The imidazole moieties could be readily transformed into the required amides by methylation of the imidazole moieties and displacement with 4-methoxyphenethylamine. This sequence proceeded smoothly in 80% yield, giving barbarumamide C in 3 steps from commercially available materials.



Scheme 3.3 Total syntheses of dimeric truxinate natural products.

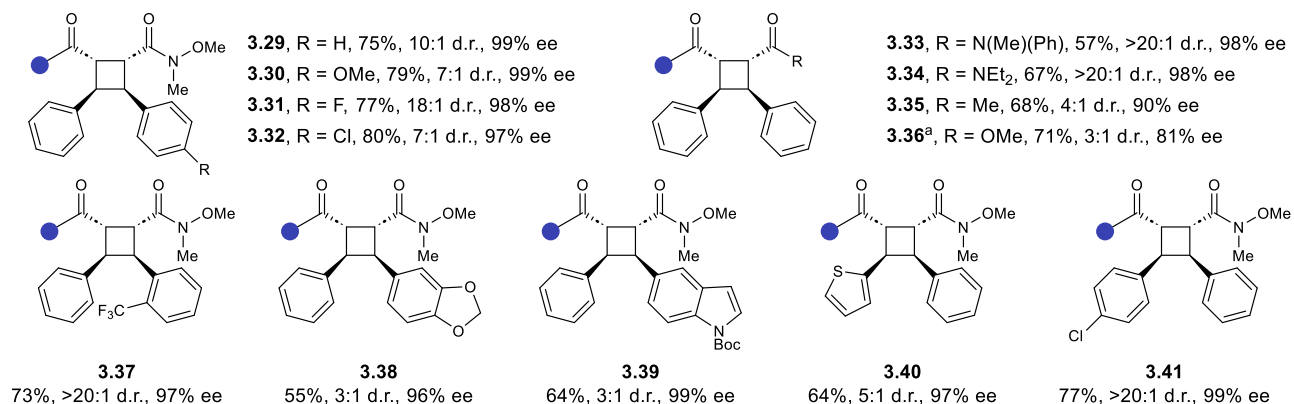
We next wondered if our method would be applicable to the synthesis of cyclobutane dimers that arise from alkenes with extended π systems. One example is nigramide R, an amide alkaloid isolated from the roots of *Piper nigrum*, which exhibits inhibitory activity against cytochrome P450 2D6.^{27,28} Our synthesis started from piperine (**3.23**), which can be directly isolated in large quantities by extraction from black pepper or purchased at modest cost.²⁹

Lithiation of 1-methylimidazole and addition to piperine yielded **3.24** in 85% yield. In addition to the typical selectivity challenges encountered in [2+2] cycloadditions, site-selective alkene reactivity is also a concern with conjugated polyene systems. Indeed, when testing different cycloaddition reaction conditions, we observed the formation of a mixture of desired δ -truxinate **3.25**, β -truxinate **3.26**, and another δ -truxinate (**3.27**) that arises from cycloaddition of the two alkenes proximal to the benzodioxole moieties. Substrate decomposition was the dominant reaction pathway at room temperature with **3.25** being formed in 13% yield. Lowering the temperature to -78 °C gave **3.25** in an increased 56% yield and 50% ee. Given the extended conjugation of diene **3.24** relative to the monoenes employed in our method, we suspected that racemic background reactivity was again a problem. Under 456 nm irradiation, **3.25** was afforded in 86% ee; however, the undesired β -truxinate **3.26** was also formed in an increased 19% yield. We had previously observed that solid samples of **3.24**, an orange solid, are unstable for long periods under ambient light, undergoing solid-state photocycloadditions to form β -truxinate **3.26** as the major isomer. We suspected that **3.24** is not fully soluble under cryogenic conditions leading to solid-state photodimerization to the β -truxinate. Indeed, when we lowered the concentration of the photoreaction five-fold, the ratio of **3.25**:**3.26** (δ : β) increased from 2:1 to 10:1 giving desired isomer **3.25** in 59% yield and 92% ee. The cyclobutane intermediate was then transformed to nigramide R using the standard approach in 50% yield. This synthesis illustrates the ability of convergent [2+2] photocycloadditions to streamline the synthesis of truxinate natural products: the only previous synthesis of nigramide R was an eight-step, racemic synthesis completed by Donohoe in 2016, while the present work is a 3-step, enantioselective synthesis.³⁰

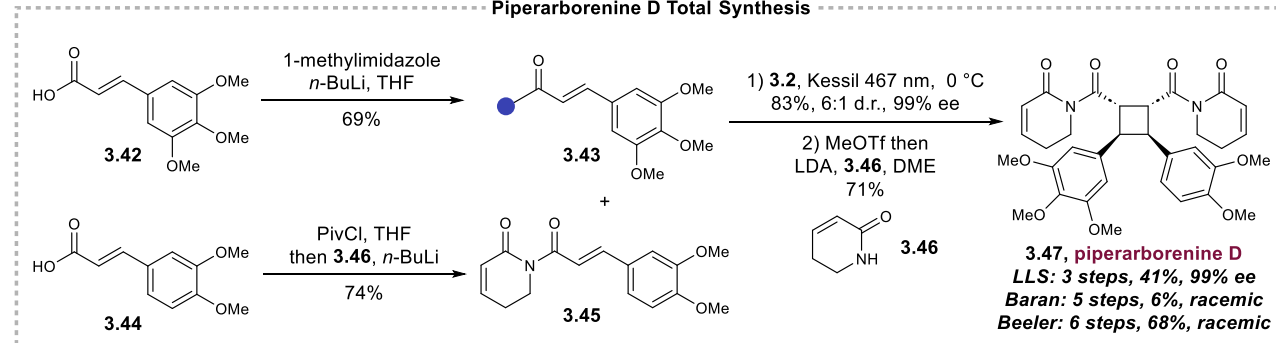
3.2.3 Heterodimerization Optimization and Substrate Scope

Access to the pseudo-dimeric members of the truxinate class requires the development of an enantioselective heterodimerization. The development of cross-selective intermolecular [2+2] cycloadditions, however, remains a challenge, and no previous syntheses of truxinate natural products have incorporated an enantioselective intermolecular heterodimerization. The methods for [2+2] heterodimerizations that have been reported to date require that only one reaction component can be excited while the other is used in excess to favor cross-selectivity.^{31–35} This strategy is challenging in the context of truxinate synthesis because the two alkenes are electronically similar, making it difficult to preferentially excite one alkene. Indeed, Reiser observed the photocycloaddition of two structurally similar cinnamate esters results in statistical mixtures of hetero- and homodimeric products.³⁶ We hypothesized that the chromophore activation mechanism employed in our dimerization reaction could be leveraged not only as a strategy for enantioselective photoreactions, but also for cross-selective cycloadditions. Specifically, in the reaction of an acyl imidazole and a coupling partner, we proposed that only the imidazole substrate will exhibit an acid-induced red-shifted absorption and could therefore be selectively excited. While this approach ensures that no coupling partner dimer will be formed as it is not excited under the reaction conditions, the undesired imidazole dimer could still form. To ensure the selective formation of the heterodimer, we employed a slow addition of the imidazole into the reaction mixture.

Pseudo-Dimeric Truxinates



Piperarborenine D Total Synthesis



Scheme 3.4 Heterodimerization scope and synthesis of piperarborenine D. ^a Reaction conducted at -78°C .

Given the prevalence of amides in pseudo-dimeric cyclobutane natural products we initially evaluated Weinreb cinnamamides as coupling partners in a heterodimerization (**Scheme 3.4**, top). We were pleased to find that using acid catalyst **3.2**, heterodimers were afforded in good yields and excellent enantioselectivities at room temperature. As with the enantioselective dimerization, only the truxinate regioisomer was observed, however, in this case, the β -diastereomer was formed as the major diastereomer. A wide variety of aryl groups were tolerated, typically reacting with excellent enantioselectivity and good diastereoselectivity. Ketones and esters are also tolerated in the reaction, preferentially giving the β -isomer, albeit in lower diastereoselectivity.

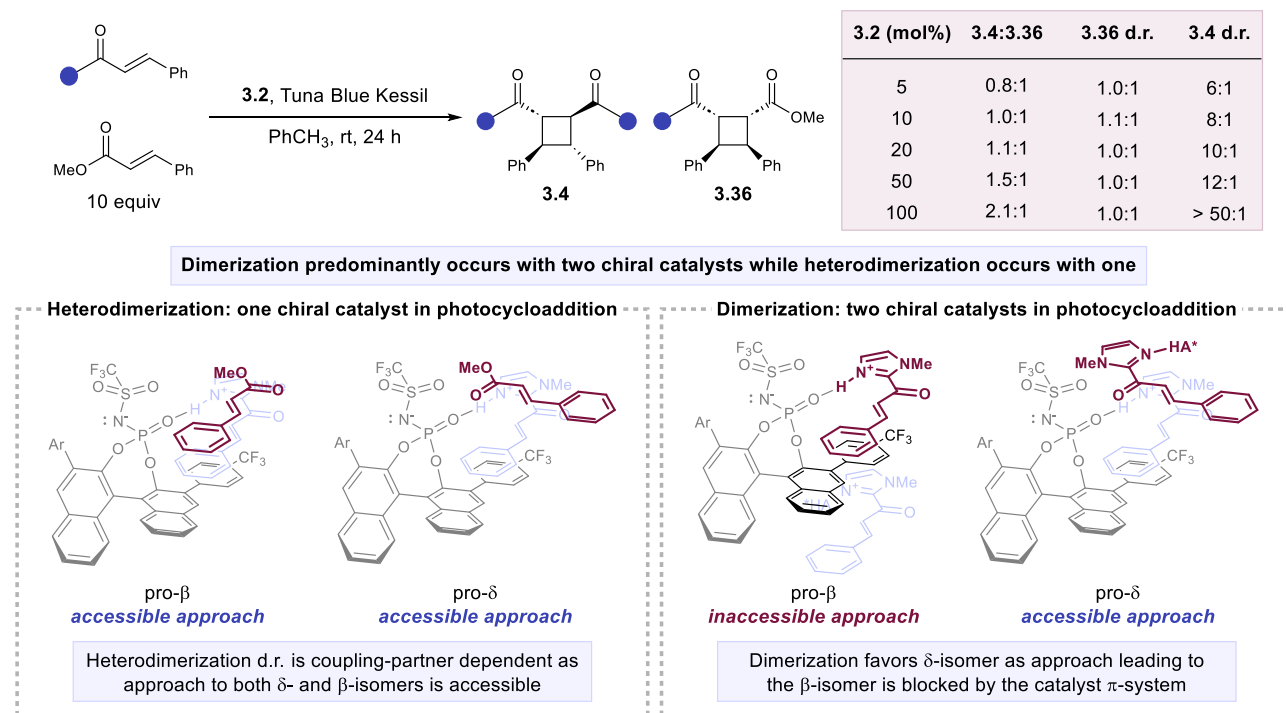
3.2.4 Total Synthesis of Piperarborenine D

We next applied our heterodimerization reaction to the synthesis of a pseudo-dimeric truxinate natural product (**Scheme 3.4**, bottom). Isolated from the shrub *Piper arborescens*, piperarborenine D exhibits cytotoxicity against several different cancer cell lines.³⁷ Racemic piperarborenine D was synthesized separately by both Baran⁶ and Beeler³⁸ using intramolecular cycloadditions of tethered alkenes to achieve formal cross-selectivity. Using our enantioselective heterodimerization method, the desired β -truxinate was prepared in 83% yield, 6:1 d.r., and 99% ee from imidazole **3.43** and coupling partner **3.45** using a Kessil 467 nm lamp. This result exemplifies the advance of this method as compared to previous cycloadditions utilized in pseudo-dimeric cyclobutane natural product synthesis. The cycloaddition is selective, affording the desired cyclobutane in high yield and high ee, while tolerating the imide and aryl functionality present in piperarborenine D. We prepared piperarborenine D in 71% yield by subjection of the cycloadduct to methylation followed by acyl substitution with lithiated **3.46**. This constitutes the shortest and first enantioselective synthesis of piperarborenine D.

3.2.5 *Mechanistic Studies*

Though we hypothesized from the outset of this study that different acid-coordination environments could lead to different stereochemical outcomes, we were surprised to find that the same chiral acid catalyst favored different isomers in the dimerization and heterodimerization. Given that the same photoactive species is involved in both cases (**3.1**·**3.2**), we questioned whether the divergent selectivity resulted from the different coupling partners. While a wide range of coupling partners including amides, ketones, and esters, predictably favor the β -isomer in the heterodimerization, the use of **3.1** as a coupling partner in the dimerization appears to be the exception, giving the δ -isomer. We wondered whether this selectivity reversal could be explained

by the ability of the non-excited **3.1** to coordinate to **3.2**. If the photoreaction between photoexcited **3.1**·**3.2** is faster with ground-state **3.1**·**3.2** than ground-state **3.1**, we would expect a significantly different acid coordination environment in the homo- and heterodimerizations, thus rationalizing the diastereodivergence. To test this hypothesis, we examined the ratio of homo- to heterodimeric products in the photocycloaddition of **3.1** and methyl cinnamate as a function of acid loading (**Scheme 3.5**, top). If the major product-forming pathway for the homodimer occurs via interaction of excited **3.1**·**3.2** with another equivalent of ground state **3.1**·**3.2** while the heterodimer occurs via reaction of excited **3.1**·**3.2** and ground-state methyl cinnamate, we would expect the ratio of homodimer: heterodimer to increase with increased acid loading. Indeed, a clear trend emerges as the heterodimer is favored with 5 mol% **3.2** while the homodimer is favored in a greater than 2:1 ratio with 100 mol% **3.2**.



Scheme 3.5 Mechanistic studies. Competition experiment between homo- and heterodimerization as a function of acid loading (top). Approaches of ground-state coupling partner leading to both diastereomers for the heterodimerization (bottom left). Approaches of ground-state coupling partner leading to both diastereomers for the homodimerization (bottom right).

The diastereoselectivity of the homo- and heterodimeric products as a function of acid loading provides further evidence for the proposed mechanism. For the heterodimerization, the diastereoselectivity is not dependent on catalyst loading, which is expected if only one acid catalyst is involved in the heterodimerization. Based on our previous x-ray crystallographic and computational studies on the binding of **3.1** to **3.2** (see Chapter 2),²⁰ we would expect that approach of a ground-state coupling partner to excited **3.1·3.2** could occur to give either the δ - or β -isomers (**Scheme 3.5**, bottom left). In this case, the observed d.r. is largely dependent on the identity of the coupling partner. On the other hand, the homodimerization shows a significant dependence on acid loading, increasing from 6:1 d.r. with 5 mol% catalyst to >50:1 d.r. with 100 mol% catalyst. In analogy to the heterodimerization, any reaction between **3.1·3.2** and free **3.1** could give either the δ - or β -isomer. However, both photoexcited **3.1·3.2** and ground-state **3.1·3.2** present the same prochiral face of the alkene to solution, and their reaction would therefore be expected to produce the C_2 -symmetric δ -stereoisomer. At low catalyst loadings, the unprotonated imidazole substrate is present at substantially higher concentrations than the protonated imidazole, consistent with the increased proportion of the β -isomer. Conversely, when 1 equiv of **3.2** is present, **3.1** is completely protonated, leading to exclusive formation of the δ -isomer.

3.3 Conclusion

In summary, we have developed a unified strategy for the synthesis of truxinate natural products utilizing a highly enantioselective photocycloaddition that can be applied to both homo- and heterodimerization of cinnamate synthons. This report constitutes the first use of an enantioselective [2+2] photocycloaddition in a truxinate synthesis, thereby greatly expediting access to members of this class. For several of these natural products, ours is the first asymmetric synthesis, and is also an improvement in both step count and overall yield as compared to previous

racemic syntheses. Finally, mechanistic experiments revealed the origin of diastereodivergence between the homo- and heterodimerization. While the homodimerization occurs with two acid catalysts, selectively giving the δ -diastereomer, the heterodimerization occurs with one acid catalyst, and the diastereoselectivity is dependent on the coupling partner.

3.4 Contributions

Matthew J. Genzink performed the reaction optimization, investigated the scope, completed the total syntheses, and performed the mechanistic experiments. Matthew D. Rossler performed the dimerization scope. Herman Recendiz helped in the synthesis of barbarumamide C. Tehshik P. Yoon provided expertise, resources, and funding.

3.5 Supporting Information

3.5.1 General Information

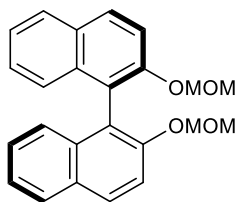
Reagent Preparation: MeCN, THF, CH₂Cl₂, and toluene were purified by elution through alumina as described by Grubbs.³⁹ Excluding those prepared below, all other starting materials, catalysts, or solvents were used as received from the supplier. Flash column chromatography (FCC) was performed with Silicycle 40–63 Å (230–40 mesh) silica. Photochemical reactions were carried out with a Kessil Lamp (model H150, $\lambda_{em. (max)} = \sim 450$ nm) unless otherwise indicated.

Product Characterization: Diastereomer ratios for reactions were determined by ¹H NMR analysis of crude reaction mixtures vs. a phenanthrene internal standard. ¹H and ¹³C NMR data were obtained using a Bruker Avance-500 spectrometer with DCH cryoprobe and are referenced to tetramethylsilane (0.0 ppm) and CDCl₃ (77.0 ppm), respectively. This instrument and supporting facilities are funded by Paul J. Bender, Margaret M. Bender, and the University of Wisconsin. ¹⁹F and ³¹P NMR data were obtained using Bruker Avance-400 spectrometer. This

instrument and supporting facilities are funded by the NSF (CHE-1048642) and the University of Wisconsin. NMR data are reported as follows: chemical shift, multiplicity (s = singlet, d = doublet, t = triplet, q = quartet, p = pentet, sext = sextet, sept = septet, m = multiplet), coupling constant(s) in Hz, integration. NMR spectra were obtained at 298 K unless otherwise noted. FT-IR spectra were obtained using a Bruker Tensor 27 spectrometer and are reported in terms of frequency of absorption (cm^{-1}). Melting points (mp) were obtained using a Stanford Research Systems DigiMelt MP3.260 melting point apparatus and are uncorrected. Mass spectrometry was performed with a Thermo Q ExactiveTM Plus using ESI-TOF (electrospray ionization-time of flight). This instrument and supporting facilities are funded by the NIH (1S10 OD020022-1) and the University of Wisconsin. Enantiomeric excesses were determined by chiral HPLC of isolated materials using a Waters e2695 separations module with 2998 PDA detector and Daicel CHIRALPAK® columns and HPLC grade *i*-PrOH and hexanes. Traces were acquired using Empower 3® software. Optical rotations were measured using a Rudolf Research Autopol III polarimeter at room temperature in CH_2Cl_2 . UV-Vis absorption spectra were acquired using a Varian Cary® 50 UV-visible spectrophotometer with a spectrophotometer.

3.5.2 Catalyst Synthesis

(R)-(+)-2,2'-bis(methoxymethoxy)-1,1'-binaphthalene: A 500 mL RBF was charged with 200



mL THF, followed by 3.03 g (75.8 mmol, 2.5 equiv) of 60% NaH in mineral oil. This mixture was cooled to 0 °C and 8.50 g (29.7 mmol, 1.0 equiv) (R)-

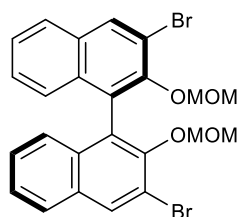
BINOL was added as a solution in 50 mL THF *via* cannula over

approximately 20 minutes, controlling the resulting gas evolution. Then 5.69 mL (74.9 mmol, 2.5 equiv) freshly distilled chloromethyl methyl ether (MOMCl) was added portionwise at 0 °C. The reaction was then warmed to room temperature and stirred overnight. The reaction was slowly

quenched with sat. aq. NH_4Cl (20 mL). This mixture was transferred to a separatory funnel with CH_2Cl_2 (50 mL). After separating the organic layer, the aqueous layer was extracted with CH_2Cl_2 (3 x 50 mL). The combined organics were washed with brine (20 mL), dried over Na_2SO_4 , and concentrated. The resulting material was recrystallized from CH_2Cl_2 /pentanes to give 9.65 g (25.8 mmol, 87% yield) of a crystalline white solid. Spectral data was consistent with that previously reported.⁴⁰ ^1H NMR (500 MHz, CDCl_3) δ 7.95 (d, $J = 9.0$ Hz, 2H), 7.85 (d, $J = 8.3$ Hz, 2H), 7.57 (d, $J = 9.0$ Hz, 2H), 7.34 (ddd, $J = 8.0, 6.7, 1.2$ Hz, 2H), 7.22 (ddd, $J = 8.0, 6.7, 1.2$ Hz, 2H), 7.15 (d, $J = 8.3$ Hz, 2H), 5.08 (d, $J = 6.9$ Hz, 2H), 4.97 (d, $J = 6.9$ Hz, 2H), 3.14 (s, 6H).

(±)-2,2'-Bis(methoxymethoxy)-1,1'-binaphthalene: Prepared and isolated through the above procedure for (*R*)-(+)-2,2'-Bis(methoxymethoxy)-1,1'-binaphthalene using 3.22 g (80.5 mmol) 60% NaH in THF (200 mL), 8.62 g (30.1 mmol) (±)-BINOL in THF (50 mL), and 6.10 mL (80.0 mmol) MOMCl to give 9.00 g (24.0 mmol, 80% yield) of a white solid. Spectral data was consistent with that reported above.

(*R*)-(+)-3,3'-dibromo-2,2'-bis(methoxymethoxy)-1,1'-binaphthalene: In a flame dried 500 mL

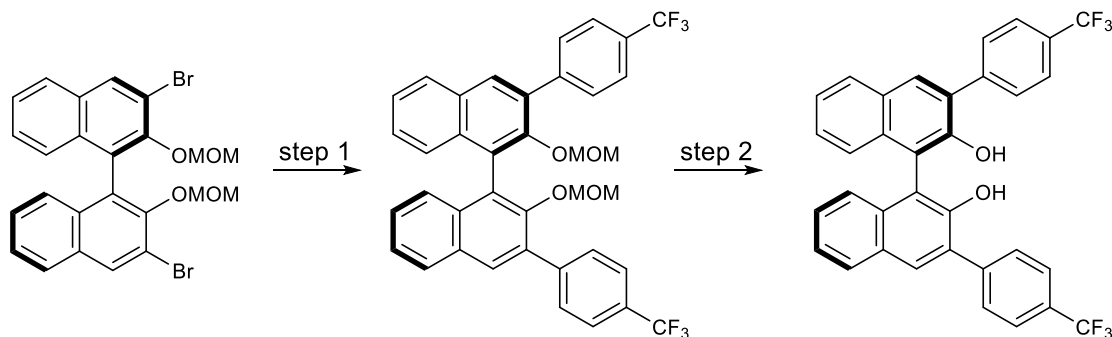


RBF 4.50 g (12.0 mmol, 1.0 equiv) (*R*)-(+)-2,2'-bis(methoxymethoxy)-1,1'-binaphthalene was prepared in 200 mL Et_2O . To this solution 14.4 mL (36.1 mmol, 3.0 equiv) *n*BuLi (2.5 M in hexanes) was added portionwise. After 3

hours 120 mL THF was added and the reaction was stirred for 1 hour. The reaction was cooled to 0 °C and 11.70 g (36.1 mmol, 3.0 equiv) 1,2-dibromo-1,1,2,2-tetrachloroethane was added in one portion. The reaction was stirred for 15 minutes before it was quenched with sat. aq. NH_4Cl (10 mL) and water (10 mL). The phases were separated, and the aqueous phase was extracted with Et_2O (2 x 50 mL). The combined organics were dried over Na_2SO_4 and concentrated. The resulting residue was dry loaded onto silica and purified by flash column chromatography eluting from 5%

EtOAc in hexanes to give 5.55 g (10.4 mmol, 87%) of a white solid. Spectroscopic data was consistent with that previously reported.⁵² ¹H NMR (500 MHz, CDCl₃) δ 8.27 (s, 2H), 7.80 (d, *J* = 8.0 Hz, 2H), 7.44 (ddd, *J* = 8.0, 6.8, 1.2 Hz, 2H), 7.31 (ddd, *J* = 8.3, 6.8, 1.2 Hz, 2H), 7.18 (d, *J* = 8.6 Hz, 2H), 4.83 (d, *J* = 5.9, 2H), 4.81 (d, *J* = 5.9, 2H), 2.57 (s, 6H).

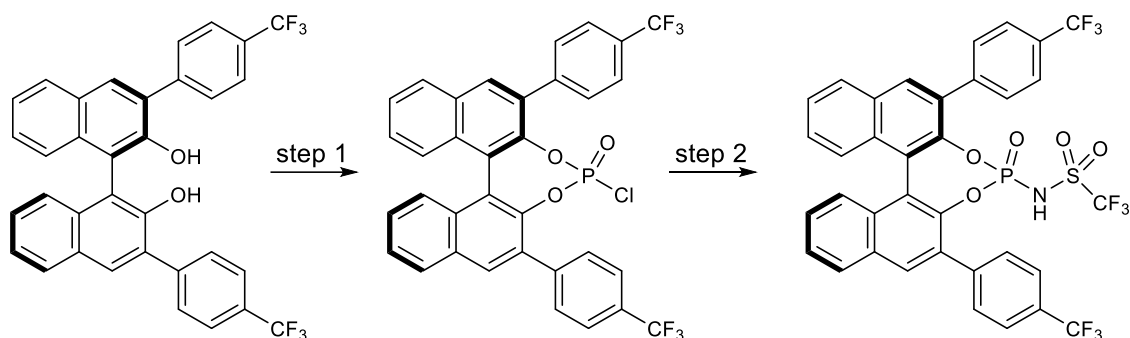
(±)-3,3'-dibromo-2,2'-bis(methoxymethoxy)-1,1'-binaphthalene: Prepared and isolated through the above procedure for (*R*)-(+)-3,3'-Dibromo-2,2'-bis(methoxymethoxy)-1,1'-binaphthalene using 8.90 g (23.8 mmol) (±)-2,2'-Bis(methoxymethoxy)-1,1'-binaphthalene in Et₂O (350 mL), 29.4 mL (73.7 mmol) *n*BuLi (2.5 M in hexanes), THF (230 mL), and 23.2 g (71.3 mmol) 1,2-dibromo-1,1,2,2-tetrachloroethane to give 11.52 g (21.6 mmol, 91% yield) of a white solid. Spectral data was consistent with that reported above.



(*R*)-(+)-3,3'-di-(4-trifluoromethyl)phenyl-[1,1'-binaphthalene]-2,2'-diol: *Step 1:* A 250 mL RBF was charged with 4.79 g (9.00 mmol 1.0 equiv) (*R*)-(+)-3,3'-dibromo-2,2'-bis(methoxymethoxy)-1,1'-binaphthalene, 5.98 g (31.50 mmol, 3.5 equiv) 4-trifluoromethylphenylboronic acid, 2 M aq. Na₂CO₃ (25 mL), and 1,2-dimethoxyethane (50 mL) and fitted with a reflux condenser. The apparatus was purged with N₂ for 15 min before the addition of 520 mg (0.45 mmol, 0.05 equiv) Pd(PPh₃)₄. The mixture was heated to 95 °C for 16 hours. After cooling to room temperature, the mixture was filtered over a pad of Celite, the pad was washed

with EtOAc, and the resulting solution concentrated. This residue was partitioned into EtOAc (100 mL) and H₂O (25 mL). The layers were separated and the aqueous layer was extracted with EtOAc (3 x 20 mL). The combined organics were dried over Na₂SO₄ and concentrated. *Step 2:* The resulting yellow solid, primarily composed of MOM-protected cross-coupling product, was taken up in THF (60 mL), and 1.35 mL conc. HCl (15.8 mmol, 1.75 equiv) was added. The mixture was heated to 65 °C for 3 hours. This mixture was concentrated, and the residue partitioned into EtOAc (100 mL) and H₂O (25 mL). The layers were separated, and the aqueous layer was extracted with EtOAc (3 x 20 mL). The combined organics were dried over Na₂SO₄, then concentrated directly on silica for purification by FCC eluting from 5% EtOAc in hexanes to give 5.05 g (8.79 mmol, 98% yield) of a white solid. Spectroscopic data was consistent with that previously reported.⁴¹ ¹H NMR (500 MHz, CDCl₃) δ 8.06 (s, 2H), 7.96 (d, *J* = 8.0 Hz, 2H), 7.87 (d, *J* = 8.1 Hz, 4H), 7.74 (d, *J* = 8.2 Hz, 4H), 7.44 (ddd, *J* = 8.0, 6.8, 1.1 Hz, 2H), 7.37 (ddd, *J* = 8.2, 6.8, 1.2 Hz, 2H), 7.23 (d, *J* = 8.2 Hz, 2H), 5.32 (s, 2H).

(±)-3,3'-di-(4-trifluoromethyl)phenyl-[1,1'-binaphthalene]-2,2'-diol: Prepared and isolated through the above procedure for (*R*)-(+)-3,3'-di-(4-trifluoromethyl)phenyl-[1,1'-binaphthalene]-2,2'-diol. *Step 1:* 11.50 g (21.6 mmol) (±)-3,3'-Dibromo-2,2'-bis(methoxymethoxy)-1,1'-binaphthalene, 14.36 g (75.6 mmol) 4-trifluoromethylphenylboronic acid, 1.28 g Pd(PPh₃)₄ (1.1 mmol), 2 M aq. Na₂CO₃ (54 mL), and 1,2-DME (144 mL) were combined to give a yellow solid. *Step 2:* This yellow solid was combined with THF (130 mL) and conc. HCl (4 mL) to give 12.4 g (21.6 mmol, 100% yield) of a white solid. Spectral data was consistent with that reported above.



(R)-4-trifluoromethylphenyl-BINOL ((trifluoromethyl)sulfonyl)phosphoramidate (3.2):

Step 1: A 250 mL flame-dried RBF was charged with 4.93 g (8.58 mmol, 1.0 equiv) (*R*)-(+)-3,3'-di-(4-trifluoromethyl)phenyl-[1,1'-binaphthalene]-2,2'-diol and CH₂Cl₂ (50 mL) then cooled to 0 °C. To this solution was added 1.68 mL (18.0 mmol, 2.1 equiv) freshly distilled POCl₃ and 3.71 mL (26.6 mmol, 3.1 equiv) freshly distilled Et₃N. The reaction was warmed to room temperature and stirred for 16 hours. The reaction was washed with H₂O (10 mL). This aqueous layer was extracted with CH₂Cl₂ (2 x 10 mL). After drying over Na₂SO₄, the solution was concentrated to give a brown solid which was passed through a short plug of silica with 5% EtOAc in hexanes to give a white solid. This organic phosphoryl chloride was carried forward to the next step without additional purification. *Step 2:* A 250 mL flame-dried RBF was charged with organic phosphoryl chloride synthesized above, 1.33 g (8.92 mmol, 1.0 equiv) trifluoromethanesulfonamide, 2.14 g (17.5 mmol, 2.0 equiv) dimethylaminopyridine, and CH₂Cl₂ (100 mL). This mixture was stirred at room temperature for 24 h. The crude reaction mixture was washed directly with 6 M HCl (20 mL) and dried over Na₂SO₄. The resulting solution was concentrated directly onto silica and purified by FCC with 10% → 50% → 70% EtOAc in hexanes. The resulting solid was dissolved in CH₂Cl₂, washed with 6 M HCl (3 x 50 mL), dried over Na₂SO₄, filtered, and concentrated to give 5.79 g (7.54 mmol, 88% yield) of a fine white crystalline solid. Spectroscopic data was consistent with that previously reported.⁴² ¹H NMR (500 MHz, CDCl₃) δ 8.13 (s, 1H), 8.05 (d, *J* = 8.0 Hz, 1H),

8.04 (s, 1H), 8.02 (d, $J = 8.0$ Hz, 1H), 7.76 (d, $J = 8.1$ Hz, 2H), 7.64–7.60 (m, 7H), 7.56 (ddd, $J = 8.0, 6.3, 1.4$ Hz, 1H), 7.48 (d, $J = 8.3$ Hz, 1H), 7.45–7.35 (m, 3H), 6.35 (br s, 1H).

(±)-4-trifluoromethylphenyl-BINOL ((trifluoromethyl)sulfonyl)phosphoramidate ((±)-3.2):

Prepared and isolated through the above procedure for (**R**)-**3.2**. *Step 1*: 12.7 g (22.1 mmol) (±)-3,3'-Di-(4-trifluoromethyl)phenyl-[1,1'-binaphthalene]-2,2'-diol, 4.3 mL (46 mmol) POCl₃, 9.5 mL (68 mmol) Et₃N, and DCM (130 mL) were combined to give a white solid. *Step 2*: This white solid was combined with DCM (250 mL), 3.32 g (22.3 mmol) trifluoromethanesulfonamide, 5.39 mg (44.1 mmol) DMAP to give 11.6 g (15.1 mmol, 68% yield). Spectral data was consistent with that reported above.

3.5.3 Substrate Synthesis

General Procedure A: A flame-dried vial was charged with diethyl (2-(methoxy(methyl)amino)-2-oxoethyl)phosphonate (1.20 equiv) and THF (0.5 M). To this reaction, 60% NaH in mineral oil (1.20 equiv) was added portionwise. The reaction was cooled to -78 °C and aldehyde (1.00 equiv) dissolved in THF (0.5 M) was added. The reaction was stirred at -78 °C for 1 hour then allowed to warm overnight. Water was added to the reaction and the layers were separated. The organic layer was washed with sat. aq. NaHCO₃. The combined aqueous layers were extracted with EtOAc (2x). The combined organic phases were washed with sat. aq. NaCl, dried over Na₂SO₄, and concentrated. The products were purified by FCC eluting from EtOAc/hexanes.

General Procedure B: A flame-dried vial was charged with substituted cinnamic acid (1.00 equiv), *N,O*-dimethylhydroxylamine hydrochloride (1.50 equiv), and CH₂Cl₂ (0.33 M). To the solution was added DMAP (0.20 equiv), EDC (1.50 equiv), and Et₃N (1.50 equiv) dropwise. The mixture was stirred for 16 hours. The reaction was washed with water, 1 M HCl (2x), and sat. aq.

NaHCO₃, dried over Na₂SO₄, and concentrated. The products were purified by FCC eluting from EtOAc/hexanes.

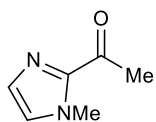
General Procedure C: A flame-dried vial was charged with acyl chloride (1.00 equiv), *N,O*-dimethylhydroxylamine hydrochloride (1.10 equiv), and DCM (0.5 M). At 0 °C pyridine (2.50 equiv) was added dropwise and the reaction was stirred at room temperature for 2 hours. To the reaction was added 1 M HCl and the aqueous phase was separated and extracted with Et₂O (2x). The combined organic phases were washed with sat. aq. NaHCO₃ and sat. aq. NaCl, dried over Na₂SO₄, and concentrated. The products were purified by FCC eluting from EtOAc/hexanes.

General Procedure D: A flame-dried vial was charged with 2-acetyl-1-methylimidazole (1.0 equiv), and mixture of EtOH and H₂O. This solution was sparged briefly with N₂ (~5 minutes). Aromatic aldehyde (1.0-1.1 equiv, freshly distilled if possible) was then added to the solution, followed by a catalytic quantity of KOH. This was then stirred under N₂ for 12-16 h (overnight). *Work-up 1:* If the resulting solution was heterogeneous, the product was filtered and washed with H₂O and cold EtOH to give the pure desired product. *Work-up 2:* If the resulting solution was homogeneous, the crude reaction mixture was diluted with CH₂Cl₂ and transferred to separatory funnel and shaken with H₂O. The organic layer was separated and the aqueous extracted with 3-fold with additional CH₂Cl₂. The combined organics were dried over Na₂SO₄, concentrated, then purified by FCC.

General Procedure E: A flame dried RBF was charged with 1-(1-methyl-1H-imidazol-2-yl)-2-(triphenyl-15-phosphaneylidene)ethan-1-one (1.0 equiv), aromatic aldehyde (1.0 equiv, freshly distilled if possible) and toluene (0.1 M). The RBF was fitted with a reflux condenser and a septum was fitted on top. The reaction was heated at 95 °C under N₂ gas, overnight. *Work-up:* Crude reaction mixture was diluted with 1M HCl and diethyl ether. Layers separated and the organic

layer was extracted with 1M HCl x2. Aqueous layers were combined and washed with ethyl acetate. In the separatory funnel, the aqueous layer was neutralized with sat. aq. Na₂CO₃ and then extracted with DCM x3. Organic layers were combined, dried over Na₂SO₄, filtered, concentrated, then purified by FCC.

2-acetyl-1-methylimidazole: A solution 2.51 mL (31.5 mmol, 1.05 equiv) 1-methylimidazole in

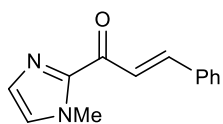


THF (75 mL) was prepared in a flame-dried 250 mL RBF. After cooling to $-78\text{ }^{\circ}\text{C}$, 14.4 mL (10.5 mmol, 1.20 equiv) nBuLi (2.5 M in hexanes) was added portionwise.

The reaction was warmed to $0\text{ }^{\circ}\text{C}$ for 30 minutes before returning to $-78\text{ }^{\circ}\text{C}$. A solution of 3.47 mL (30.0 mmol, 1.0 equiv) 4-acetylmorpholine in THF (50 mL) was prepared in a flame-dried 100 mL conical bottom flask and added to the solution of deprotonated 1-methylimidazole *via* cannula.

The reaction was warmed to room temperature and stirred overnight. The resulting solution was stirred vigorously and AcOH (5 mL) was added dropwise. This solution was transferred to separatory funnel with EtOAc (100 mL), then washed with sat. aq. NaHCO₃ (30 mL) and sat. aq. NaCl (30 mL). Each wash solution was extracted with EtOAc (20 mL). The combined organic layers were dried over Na₂SO₄ and concentrated. The product was purified by FCC eluting from 50% EtOAc in hexanes to give 2.95 g (23.8 mmol, 79% yield) of a colorless oil. The compound was consistent with reported spectroscopic data.⁴³ ¹H NMR (500 MHz, CDCl₃) δ 7.14 (s, 1H), 7.03 (s, 1H), 4.00 (s, 3H), 2.66 (s, 3H).

2-cinnamoyl-1-methyl-1*H*-imidazole: A flame-dried 250 mL RBF was charged with 1.50 mL

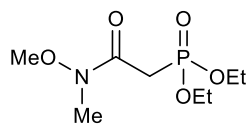


(18.8 mmol, 1.20 equiv) *N*-methylimidazole and THF (50 mL), then cooled to $-78\text{ }^{\circ}\text{C}$. A volume of 7.80 mL (18.8 mmol, 1.20 equiv) nBuLi (2.4 M in

hexanes) was added portionwise. The reaction was warmed to $0\text{ }^{\circ}\text{C}$ for 30 minutes, then returned to $-78\text{ }^{\circ}\text{C}$. A solution of 3.01 g (15.7 mmol, 1.0 equiv) *N*-methoxy-*N*-methylcinnamide in THF

(20 mL) was prepared in a flame-dried conical bottom flask and added to the solution of deprotonated 1-methylimidazole *via* cannula. The reaction was warmed to room temperature and stirred overnight. The resulting solution was stirred vigorously, then AcOH (5 mL) was added dropwise. This solution was transferred to a separatory funnel with EtOAc (50 mL) and water (20 mL). The organic layer was separated and the aqueous extracted with EtOAc (3 x 25 mL). The combined organic layers were then washed with sat. aq. NaHCO₃ (30 mL) and sat. aq. NaCl (30 mL), dried over Na₂SO₄, and concentrated. The product was purified by FCC eluting from 40% EtOAc in hexanes to give 2.86 g (13.5 mmol, 86% yield) of a white solid. The compound was consistent with reported spectroscopic data.⁴⁴ ¹H NMR (500 MHz, CDCl₃) δ 8.08 (d, *J* = 16.0 Hz, 1H), 7.83 (d, *J* = 16.0 Hz, 1H), 7.72–7.68 (m, 2H), 7.43–7.38 (m, 3H), 7.23 (s, 1H), 7.09 (s, 1H), 4.10 (s, 3H).

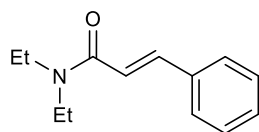
diethyl (2-(methoxy(methyl)amino)-2-oxoethyl)phosphonate: A flame-dried 50 mL RBF was



charged with 3.00 g (21.8 mmol, 1.00 equiv) 2-chloro-*N*-methoxy-*N*-methylacetamide and 3.62 g (21.8 mmol, 1.00 equiv) triethyl phosphite and

heated to 100 °C for 18 hours. The reaction was distilled under high vacuum at 120 °C and the fraction distilling above 120 °C was collected to give 4.21 g (17.6 mmol, 81% yield) of a colorless liquid. The compound was consistent with reported spectroscopic data.⁴⁵ ¹H NMR (500 MHz, CDCl₃) δ 4.23–4.13 (m, 4H), 3.78 (s, 3H), 3.22 (s, 3H), 3.17 (d, *J* = 22.0 Hz, 2H), 1.35 (t, *J* = 7.1 Hz, 6H).

***N,N*-diethylcinnamamide:** A flame-dried 24 mL vial was charged with 0.35 mL (3.33 mmol, 1.10

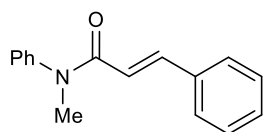


equiv) diethylamine, 0.53 mL (3.79 mmol, 1.25 equiv) triethylamine, and DCM (6 mL). In one portion 505 mg (3.03 mmol, 1.00 equiv) cinnamoyl

chloride was added to the reaction and the reaction was stirred for 30 minutes. The reaction was

diluted with DCM (20 mL) and washed with 1 M HCl (10 mL) and sat. aq. NaCl (10 mL). The organic layer was dried over Na₂SO₄, and concentrated to give 620 mg (3.05 mmol, 100% yield) of a yellow solid. The compound was consistent with reported spectroscopic data.⁴⁶ ¹H NMR (500 MHz, CDCl₃) δ 7.70 (d, *J* = 15.4 Hz, 1H), 7.53–7.52 (m, 2H), 7.37–7.35 (m, 3H), 6.82 (d, *J* = 15.4 Hz, 1H), 3.51–3.47 (m, 4H), 1.28–1.18 (m, 6H).

***N*-methyl-*N*-phenylcinnamamide:** A flame-dried 24 mL vial was charged with 0.33 mL (3.00



mmol, 1.00 equiv) *N*-methylaniline, 0.52 mL (3.75 mmol, 1.25 equiv) triethylamine, and DCM (6 mL). In one portion 500 mg (3.00 mmol, 1.00

equiv) cinnamoyl chloride was added to the reaction and the reaction was stirred for 30 minutes.

The reaction was diluted with DCM (20 mL) and washed with 1 M HCl (10 mL) and sat. aq. NaCl

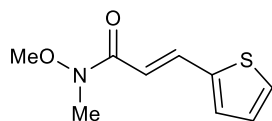
(10 mL). The organic layer was dried over Na₂SO₄, and concentrated. The product was purified

by FCC eluting from 30% EtOAc in hexanes to give 720 mg (3.03 mmol, 100% yield) of a yellow

oil. The compound was consistent with reported spectroscopic data.⁴⁶ ¹H NMR (500 MHz, CDCl₃)

δ 7.67 (d, *J* = 15.6 Hz, 1H), 7.46–7.43 (m, 1H), 7.35–7.27 (m, 5H), 7.25–7.23 (m, 2H), 6.37 (d, *J* = 15.6 Hz, 1H), 3.42 (s, 3H).

(*E*)-*N*-methoxy-*N*-methyl-3-(thiophen-2-yl)acrylamide: Synthesized according to General



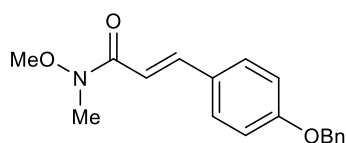
Procedure A to give 660 mg (3.53 mmol, 95% yield) of an off-white solid.

The compound was consistent with reported spectroscopic data.⁴⁵ ¹H NMR

(500 MHz, CDCl₃) δ 7.84 (d, *J* = 15.6 Hz, 1H), 7.34 (d, *J* = 5.0 Hz, 1H), 7.26–7.25 (m, 1H), 7.05

(dd, *J* = 5.1, 3.6 Hz, 1H), 6.82 (d, *J* = 15.5 Hz, 1H), 3.76 (s, 3H), 3.30 (s, 3H).

(*E*)-3-(4-(benzyloxy)phenyl)-*N*-methoxy-*N*-methylacrylamide: Synthesized according to

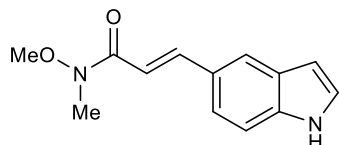


General Procedure A to give 940 mg (3.16 mmol, 90% yield) of a

white solid. The compound was consistent with reported

spectroscopic data.⁴⁷ ¹H NMR (500 MHz, CDCl₃) δ 7.68 (d, *J* = 15.8 Hz, 1H), 7.53–7.51 (m, 2H), 7.44–7.38 (m, 4H), 7.35–7.33 (m, 1H), 6.98–6.97 (m, 2H), 6.90 (d, *J* = 15.8 Hz, 1H), 5.10 (s, 2H), 3.76 (s, 3H), 3.30 (s, 3H).

(*E*)-3-(1*H*-indol-5-yl)-*N*-methoxy-*N*-methylacrylamide: Synthesized according to General

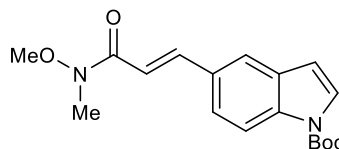


Procedure A to give 710 mg (3.08 mmol, 88% yield) of a white solid.

The compound was consistent with reported spectroscopic data.⁴⁸ ¹H

NMR (500 MHz, CDCl₃) δ 8.31 (s, 1H), 7.88 (d, *J* = 15.7 Hz, 1H), 7.86 (s, 1H), 7.48 (dd, *J* = 8.5, 1.7 Hz, 1H), 7.39 (d, *J* = 8.5 Hz, 1H), 7.24–7.23 (m, 1H), 7.01 (d, *J* = 15.7 Hz, 1H), 6.60–6.59 (m, 1H), 3.79 (s, 3H), 3.32 (s, 3H).

***tert*-butyl (*E*)-5-(3-(methoxy(methyl)amino)-3-oxoprop-1-en-1-yl)-1*H*-indole-1-carboxylate:**

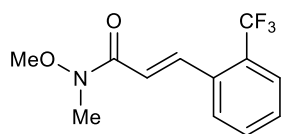


A flame-dried 24 mL vial was charged with 605 mg (2.63 mmol, 1.00

equiv) (*E*)-3-(1*H*-indol-5-yl)-*N*-methoxy-*N*-methylacrylamide and

MeCN (8 mL). To this solution was added 688 mg (3.15 mmol, 1.20 equiv) Boc₂O and 3.2 mg (0.03 mmol, 0.01 equiv) DMAP at ambient temperature. The reaction was stirred for 20 hours then quenched with H₂O (10 mL). The aqueous layer was extracted with EtOAc (3 x 10 mL). The combined organic layers were washed with sat. aq. NaCl (10 mL), dried over Na₂SO₄, filtered, and concentrated. The product was purified by FCC eluting from 50% EtOAc in hexanes to give 755 mg (2.29 mmol, 87% yield) of a white solid (mp 127–129 °C). ¹H NMR (500 MHz, CDCl₃) δ 8.13 (d, *J* = 8.7 Hz, 1H), 7.84 (d, *J* = 15.7 Hz, 1H), 7.75 (d, *J* = 1.7 Hz, 1H), 7.61 (d, *J* = 3.7 Hz, 1H), 7.56 (dd, *J* = 8.7 Hz, *J* = 1.7 Hz, 1H), 7.05 (d, *J* = 15.7 Hz, 1H), 6.59 (dd, *J* = 3.7 Hz, *J* = 0.8 Hz, 1H), 3.79 (s, 3H), 3.32 (s, 3H), 1.68 (s, 9H). ¹³C NMR (125 MHz, CDCl₃) δ 167.5, 149.7, 144.3, 136.3, 131.1, 130.1, 127.1, 124.2, 121.6, 115.6, 114.6, 107.6, 84.3, 62.1, 32.8, 28.4. HRMS (ESI) calculated for [C₁₈H₂₃N₂O₄]⁺ (M+H⁺) requires *m/z* 331.1652, found 331.1647.

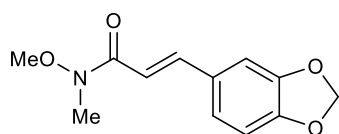
(*E*)-*N*-methoxy-*N*-methyl-3-(2-(trifluoromethyl)phenyl)acrylamide: Synthesized according



to General Procedure B to give 743 mg (2.87 mmol, 96% yield) of a white solid. The compound was consistent with reported spectroscopic data.⁴⁹

¹H NMR (500 MHz, CDCl₃) δ 8.09 (dq, *J* = 15.6, 2.4 Hz, 1H), 7.73 (d, *J* = 7.8 Hz, 1H), 7.70 (d, *J* = 7.8 Hz, 1H), 7.56 (t, *J* = 7.0 Hz, 1H), 7.46 (t, *J* = 7.6 Hz, 1H), 6.98 (d, *J* = 15.6 Hz, 1H), 3.76 (s, 3H), 3.32 (s, 3H).

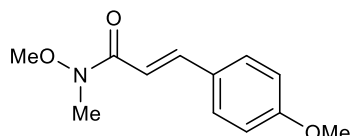
(*E*)-3-(benzo[*d*][1,3]dioxol-5-yl)-*N*-methoxy-*N*-methylacrylamide: Synthesized according to



General Procedure C to give 451 mg (1.92 mmol, 64% yield) of a white solid. The compound was consistent with reported spectroscopic data.⁴⁹

¹H NMR (500 MHz, CDCl₃) δ 7.64 (d, *J* = 15.7 Hz, 1H), 7.09 (d, *J* = 1.7 Hz, 1H), 7.04 (dd, *J* = 8.1, 1.8 Hz, 1H), 6.86 (d, *J* = 15.7 Hz, 1H), 6.81 (d, *J* = 8.0 Hz, 1H), 6.00 (s, 2H), 3.76 (s, 3H), 3.30 (s, 3H).

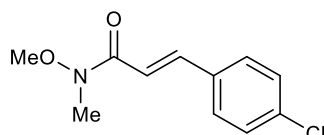
(*E*)-*N*-methoxy-3-(4-methoxyphenyl)-*N*-methylacrylamide: Synthesized according to General



Procedure B to give 595 mg (2.69 mmol, 90% yield) of a white solid.

The compound was consistent with reported spectroscopic data.⁴⁵ ¹H NMR (500 MHz, CDCl₃) δ 7.69 (d, *J* = 15.8 Hz, 1H), 7.54–7.52 (m, 2H), 6.93–6.89 (m, 3H), 3.84 (s, 3H), 3.76 (s, 3H), 3.30 (s, 3H).

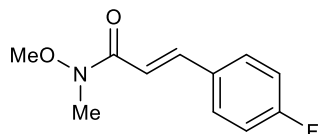
(*E*)-3-(4-chlorophenyl)-*N*-methoxy-*N*-methylacrylamide: Synthesized according to General



Procedure B to give 430 mg (1.91 mmol, 64% yield) of a white solid.

The compound was consistent with reported spectroscopic data.⁴⁵ ¹H NMR (500 MHz, CDCl₃) δ 7.68 (d, *J* = 15.8 Hz, 1H), 7.51–7.49 (m, 2H), 7.37–7.35 (m, 2H), 7.01 (d, *J* = 15.8 Hz, 1H), 3.77 (s, 3H), 3.31 (s, 3H).

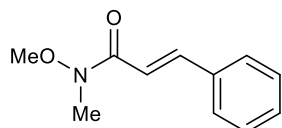
(E)-3-(4-fluorophenyl)-N-methoxy-N-methylacrylamide: Synthesized according to General



Procedure C to give 540 mg (2.58 mmol, 95% yield) of a white solid.

The compound was consistent with reported spectroscopic data.⁵⁰ ¹H NMR (500 MHz, CDCl₃) δ 7.70 (d, *J* = 15.8 Hz, 1H), 7.57–7.54 (m, 2H), 7.09–7.06 (m, 2H), 6.96 (d, *J* = 15.8 Hz, 1H), 3.77 (s, 3H), 3.31 (s, 3H).

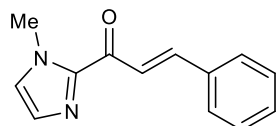
(E)-N-methoxy-N-methylcinnamamide: Synthesized according to General Procedure C to give



5.31 g (27.8 mmol, 94% yield) of a white solid. The compound was

consistent with reported spectroscopic data.⁵¹ ¹H NMR (500 MHz, CDCl₃) δ 7.74 (d, *J* = 15.9 Hz, 1H), 7.59–7.56 (m, 2H), 7.41–7.36 (m, 3H), 7.04 (d, *J* = 15.9 Hz, 1H), 3.77 (s, 3H), 3.32 (s, 3H).

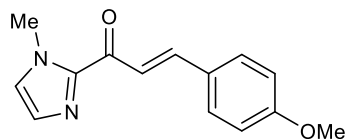
(E)-1-(1-methyl-1H-imidazol-2-yl)-3-phenylprop-2-en-1-one: Synthesized according to



General Procedure D using 502.3 mg (4.0 mmol, 1.0 equiv) 2-acetyl-1-

methylimidazole, 0.5 mL (4.4 mmol, 1.1 equiv) benzaldehyde, ~25 mg (1/2 pellet) KOH, EtOH (16 mL), and H₂O (8 mL). Work-up 2, then the product was purified by FCC eluting from 30% EtOAc in pentanes to give 671.2 mg (3.16 mmol, 78% yield) of a white solid. The compound was consistent with reported spectroscopic data.⁴⁴ ¹H NMR (400 MHz, CDCl₃) δ 8.08 (d, *J* = 16.0 Hz, 1H), 7.83 (d, *J* = 16.0 Hz, 1H), 7.72–7.68 (m, 2H), 7.43–7.38 (m, 3H), 7.23 (s, 1H), 7.09 (s, 1H), 4.10 (s, 3H).

(E)-3-(4-methoxyphenyl)-1-(1-methyl-1H-imidazol-2-yl)prop-2-en-1-one: Synthesized

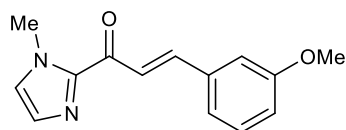


according to General Procedure D using 372.7 mg (3.0 mmol, 1.0

equiv) 2-acetyl-1-methylimidazole, 0.26 mL (3.0 mmol, 1.0 equiv) 4-methoxybenzaldehyde, ~25 mg (1/2 pellet) KOH, EtOH (6 mL), and H₂O (3 mL). Work-up 2, then the product was purified by FCC eluting from 50% Et₂O in pentanes to give 381.9 mg (1.58

mmol, 53% yield) of an off-white solid. The compound was consistent with reported spectroscopic data.⁴² ¹H NMR (400 MHz, CDCl₃) δ 7.96 (d, *J* = 15.9 Hz, 1H), 7.80 (d, *J* = 15.9 Hz, 1H), 7.66 (d, *J* = 8.7 Hz, 1H), 7.21 (s, 1H), 7.07 (s, 1H), 6.92 (d, *J* = 8.7 Hz, 1H), 4.10 (s, 3H), 3.85 (s, 3H).

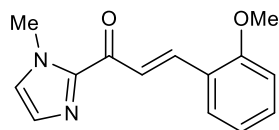
(*E*)-3-(3-methoxyphenyl)-1-(1-methyl-1*H*-imidazol-2-yl)prop-2-en-1-one: Synthesized



according to General Procedure D using 383.1 mg (3.0 mmol, 1.0 equiv) 2-acetyl-1-methylimidazole, 0.45 mL (3.3 mmol, 1.1 equiv)

3-methoxybenzaldehyde, ~25 mg (½ pellet) KOH, EtOH (10 mL), and H₂O (5 mL). Work-up 2, then the product was purified by FCC eluting from 40% EtOAc in pentanes to give 564.7 mg (2.33 mmol, 76% yield) of a light-yellow solid. The compound was consistent with reported spectroscopic data.⁴² ¹H NMR (400 MHz, CDCl₃) δ 8.05 (d, *J* = 16.1 Hz, 1H), 7.80 (d, *J* = 16.1 Hz, 1H), 7.32 (t, *J* = 7.7 Hz, 1H), 7.28 (dt, *J* = 7.7, 1.5 Hz, 1H), 7.23 (s, 1H), 7.21 (t, *J* = 1.8 Hz, 1H), 7.09 (s, 1H), 6.95 (ddd, *J* = 7.8 2.4, 1.2 Hz, 1H), 4.10 (s, 1H), 3.86 (s, 1H).

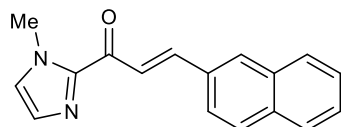
(*E*)-3-(2-methoxyphenyl)-1-(1-methyl-1*H*-imidazol-2-yl)prop-2-en-1-one: Synthesized



according to General Procedure D using 499.6 mg (4.0 mmol, 1.0 equiv) 2-acetyl-1-methylimidazole, 0.41 mL (4.4 mmol, 1.1 equiv) 2-

methoxybenzaldehyde, ~25 mg (½ pellet) KOH, EtOH (8 mL). Work-up 2, then the product was purified by FCC eluting from 50% Et₂O in pentanes to give 877.2 mg (3.6 mmol, 90% yield) of an off-white solid. The compound was consistent with reported spectroscopic data.⁴² ¹H NMR (400 MHz, CDCl₃) δ 8.24 (d, *J* = 16.2 Hz, 1H), 8.09 (d, *J* = 16.2 Hz, 1H), 7.76 (dd, *J* = 7.6, 1.6 Hz, 1H), 7.37 (ddd, *J* = 8.9, 7.6, 1.6 Hz, 1H), 7.21 (s, 1H), 7.07 (s, 1H), 6.97 (t, *J* = 7.6 Hz, 1H), 6.93 (t, *J* = 8.9 Hz, 1H), 4.10 (s, 3H), 3.91 (s, 3H).

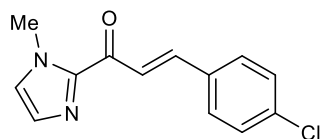
(*E*)-1-(1-methyl-1*H*-imidazol-2-yl)-3-(naphthalen-2-yl)prop-2-en-1-one: Synthesized



according to General Procedure D using 370.0 mg (3.0 mmol, 1.0

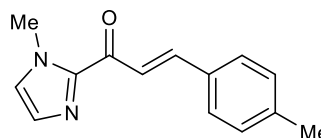
equiv) 2-acetyl-1-methylimidazole, 0.52 mg (3.3 mmol, 1.1 equiv) 2-naphthaldehyde, ~25 mg (1/2 pellet) KOH, EtOH (6 mL), and H₂O (3 mL). Work-up 1 to give 610.3 mg (2.32 mmol, 78% yield) of an off-white solid. The compound was consistent with reported spectroscopic data.⁴² ¹H NMR (500 MHz, CDCl₃) δ 8.20 (d, *J* = 15.9 Hz, 1H), 8.09 (s, 1H), 8.00 (d, *J* = 16.0 Hz, 1H), 7.89–7.83 (m, 4H), 7.53–7.51 (m, 2H), 7.25 (s, 1H), 7.10 (s, 1H), 4.13 (s, 3H).

(*E*)-3-(4-chlorophenyl)-1-(1-methyl-1*H*-imidazol-2-yl)prop-2-en-1-one: Synthesized



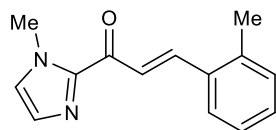
according to General Procedure D using 248.2 mg (2.0 mmol, 1.0 equiv) 2-acetyl-1-methylimidazole, 315.0 mg (2.2 mmol, 1.1 equiv) 4-chlorobenzaldehyde, ~25 mg (1/2 pellet) KOH, EtOH (8 mL), and H₂O (4 mL). Work-up 1 to give 340.1 mg (1.38 mmol, 69% yield) of a white solid. The compound was consistent with reported spectroscopic data.⁴² ¹H NMR (500 MHz, CDCl₃) δ 8.04 (d, *J* = 16.0 Hz, 1H), 7.76 (d, *J* = 16.0 Hz, 1H), 7.62 (d, *J* = 8.5 Hz, 2H), 7.37 (d, *J* = 8.5 Hz, 2H), 7.22 (s, 1H), 7.09 (s, 1H), 4.10 (s, 3H).

(*E*)-1-(1-methyl-1*H*-imidazol-2-yl)-3-(*p*-tolyl)prop-2-en-1-one: Synthesized according to



General Procedure D using 248.0 mg (2.0 mmol, 1.0 equiv) 2-acetyl-1-methylimidazole, 0.26 mL (2.2 mmol, 1.1 equiv) *p*-tolualdehyde, ~25 mg (1/2 pellet) KOH, EtOH (8 mL), and H₂O (4 mL). Work-up 2, then the product was purified by FCC eluting from 30% EtOAc in hexanes to give 323.3 mg (1.43 mmol, 71% yield) of a white solid. The compound was consistent with reported spectroscopic data.⁴² ¹H NMR (500 MHz, CDCl₃) δ 8.03 (d, *J* = 16.0, 1H), 7.81 (d, *J* = 16.0 Hz, 1H), 7.60 (d, *J* = 8.1 Hz, 2H), 7.22 (m, 2H), 7.20 (s, 1H), 7.07 (s, 1H), 4.10 (s, 3H), 2.38 (s, 3H).

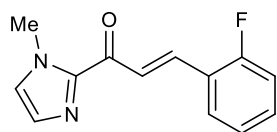
(*E*)-1-(1-methyl-1*H*-imidazol-2-yl)-3-(*o*-tolyl)prop-2-en-1-one: Synthesized according to



General Procedure D using 198.1 mg (1.5 mmol, 1.0 equiv) 2-acetyl-1-methylimidazole, 0.2 mL (1.7 mmol, 1.1 equiv) 2-methylbenzaldehyde,

~25 mg (1/2 pellet) KOH, EtOH (6 mL), and H₂O (3 mL). Work-up 1 to give 275.3 mg (1.22 mmol, 76% yield) of an off-white solid. The compound was consistent with reported spectroscopic data.⁵² ¹H NMR (500 MHz, CDCl₃) δ 8.15 (d, *J* = 15.9 Hz, 1H), 8.02 (d, *J* = 15.9 Hz, 1H), 7.81 (d, *J* = 7.6 Hz, 1H), 7.29 (t, *J* = 6.7 Hz, 1H), 7.25–7.19 (m, 3H), 7.08 (s, 1H), 4.11 (s, 3H), 2.50 (s, 3H).

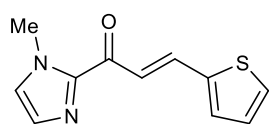
(*E*)-3-(2-fluorophenyl)-1-(1-methyl-1*H*-imidazol-2-yl)prop-2-en-1-one: Synthesized according



to General Procedure D using 258.0 mg (2.1 mmol, 1.0 equiv) 2-acetyl-1-methylimidazole, 0.23 mL (2.2 mmol, 1.1 equiv) 2-fluorobenzaldehyde,

~25 mg (1/2 pellet) KOH, EtOH (8 mL), and H₂O (4 mL). Work-up 1 to give 269.9 mg (1.17 mmol, 56% yield) of a white solid. The compound was consistent with reported spectroscopic data.⁴² ¹H NMR (400 MHz, CDCl₃) δ 8.13 (d, *J* = 16.2 Hz, 1H), 8.02 (d, *J* = 16.2 Hz, 1H), 7.77 (td, *J* = 7.6, 1.7 Hz, 1H), 7.39–7.35 (m, 1H), 7.23 (d, *J* = 0.9 Hz, 1H), 7.17 (t, *J* = 7.6 Hz, 1H), 7.13–7.09 (m, 2H), 4.10 (s, 3H).

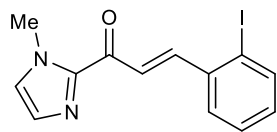
(*E*)-1-(1-methyl-1*H*-imidazol-2-yl)-3-(thiophen-2-yl)prop-2-en-1-one: Synthesized according



to General Procedure D using 250.0 mg (2.0 mmol, 1.0 equiv) 2-acetyl-1-methylimidazole, 0.21 mL (2.2 mmol, 1.1 equiv) 2-

thiophenecarboxaldehyde, ~25 mg (1/2 pellet) KOH, EtOH (8 mL), and H₂O (4 mL). Work-up 2, then the product was purified by FCC eluting from 40% EtOAc in hexanes to give 331.0 mg (1.52 mmol, 75% yield) of an off-white solid. The compound was consistent with reported spectroscopic data.⁴² ¹H NMR (400 MHz, CDCl₃) δ 7.95 (d, *J* = 15.7 Hz, 1H), 7.84 (d, *J* = 15.7 Hz, 1H), 7.42 (d, *J* = 5.0 Hz, 1H), 7.38 (d, *J* = 3.5 Hz, 1H), 7.22 (s, 1H), 7.08 (s, 1H), 7.08 (dd, *J* = 5.0, 3.5 Hz, 1H), 4.09 (s, 3H).

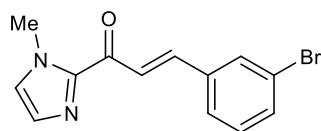
(E)-3-(2-iodophenyl)-1-(1-methyl-1*H*-imidazol-2-yl)prop-2-en-1-one: Synthesized according



to General Procedure D using 247.5 mg (2.0 mmol, 1.0 equiv) 2-acetyl-1-methylimidazole, 515.0 mL (2.2 mmol, 1.1 equiv) 2-iodobenzaldehyde,

~25 mg (1/2 pellet) KOH, EtOH (8 mL), and H₂O (4 mL). Work-up 1 to give 508.4 mg (1.50 mmol, 75% yield) of an off-white solid. The compound was consistent with reported spectroscopic data.⁵³ ¹H NMR (500 MHz, CDCl₃) δ 8.05 (d, *J* = 15.8 Hz, 1H), 7.97 (d, *J* = 15.8 Hz, 1H), 7.91 (dd, *J* = 8.0, 1.2 Hz, 1H), 7.82 (dd, *J* = 7.9, 1.6 Hz, 1H), 7.37 (t, *J* = 8.0 Hz, 1H), 7.22 (d, *J* = 0.9 Hz, 1H), 7.10 (s, 1H), 7.06 (td, *J* = 7.7, 1.6 Hz, 1H), 4.11 (s, 3H).

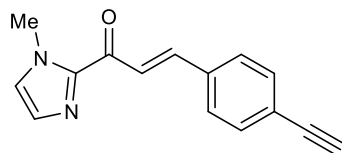
(E)-3-(3-bromophenyl)-1-(1-methyl-1*H*-imidazol-2-yl)prop-2-en-1-one: Synthesized



according to General Procedure D using 503.8 mg (4.0 mmol, 1.0 equiv) 2-acetyl-1-methylimidazole, 0.51 mL (4.4 mmol, 1.1 equiv) 3-bromobenzaldehyde, ~25 mg (1/2 pellet) KOH, EtOH (16 mL), and H₂O (8 mL). Work-up 2, then

the product was purified by FCC eluting from 30% EtOAc in hexanes to give 637.2 mg (2.19 mmol, 54% yield) of an off-white solid (mp = 104–108 °C). ¹H NMR (600 MHz, CDCl₃) δ 8.06 (d, *J* = 16.0 Hz, 1H), 7.85 (t, *J* = 1.8 Hz, 1H), 7.72 (d, *J* = 16.0 Hz), 7.60–7.56 (m, 1H), 7.52–7.48 (m, 1H), 7.29–7.24 (m, 1H), 7.23 (s, 1H), 7.09 (s, 1H), 4.09 (s, 3H). ¹³C NMR (150 MHz, CDCl₃) δ 180.0, 143.9, 141.4, 137.0, 133.1, 131.1, 130.3, 129.5, 127.5, 127.4, 124.1, 123.0, 36.4. HRMS (ESI) calculated for [C₁₃H₁₁BrN₂O]⁺ (M+H⁺) requires *m/z* 291.0128, found 291.0125.

(E)-3-(4-ethynylphenyl)-1-(1-methyl-1*H*-imidazol-2-yl)prop-2-en-1-one: Synthesized

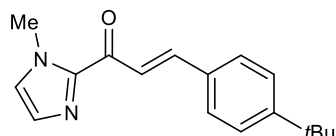


according to General Procedure D using 254.4 mg (2.05 mmol, 1.0 equiv) 2-acetyl-1-methylimidazole, 289.3 mg (2.2 mmol, 1.1 equiv)

4-ethynylbenzaldehyde, ~25 mg (1/2 pellet) KOH, EtOH (8 mL), and H₂O (4 mL). Work-up 1 to give 166.2 mg (0.7 mmol, 34% yield) of a white solid (mp = 138–140 °C). ¹H NMR (600 MHz,

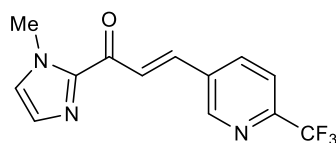
CDCl₃) δ 8.08 (d, *J* = 16.0 Hz, 1H), 7.78 (d, *J* = 16.0 Hz, 1H), 7.65 (d, *J* = 8.3 Hz, 2H), 7.52 (d, *J* = 8.3 Hz, 2H), 7.23 (s, 1H), 7.09 (s, 1H), 4.10 (s, 3H), 7.20 (s, 1H). ¹³C NMR (150 MHz, CDCl₃) δ 180.2, 144.0, 142.1, 135.3, 132.5, 129.4, 128.5, 127.4, 124.0, 123.7, 83.3, 79.3, 36.4. HRMS (ESI) calculated for [C₁₅H₁₂N₂O]⁺ (M+Na⁺) requires *m/z* 259.0852, found 259.0840.

(E)-3-(4-(*tert*-butyl)phenyl)-1-(1-methyl-1*H*-imidazol-2-yl)prop-2-en-1-one: Synthesized



according to General Procedure D using 254.8 mg (2.05 mmol, 1.0 equiv) 2-acetyl-1-methylimidazole, 0.37 mL (2.2 mmol, 1.1 equiv) 4-(*tert*-butyl)benzaldehyde, ~25 mg (1/2 pellet) KOH, EtOH (8 mL), and H₂O (4 mL). Work-up 2, then the product was purified by FCC eluting from 20% EtOAc in pentanes to give 458.3 mg (1.71 mmol, 83% yield) of a white solid (mp = 102–107 °C). ¹H NMR (600 MHz, CDCl₃) δ 8.05 (d, *J* = 16.0 Hz, 1H), 7.83 (d, *J* = 16.0 Hz, 1H), 7.64 (d, *J* = 8.4 Hz, 2H), 7.42 (d, *J* = 8.4 Hz, 2H), 7.22 (s, 1H), 7.07 (s, 1H), 4.09 (s, 3H), 1.33 (s, 9H). ¹³C NMR (150 MHz, CDCl₃) δ 180.6, 154.1, 144.1, 143.4, 132.2, 129.2, 128.7, 127.2, 125.8, 121.9, 36.4, 34.9, 31.2. HRMS (ESI) calculated for [C₁₇H₂₀N₂O]⁺ (M+Na⁺) requires *m/z* 291.1468, found 291.1465.

(E)-1-(1-methyl-1*H*-imidazol-2-yl)-3-(6-(trifluoromethyl)pyridin-3-yl)prop-2-en-1-one:



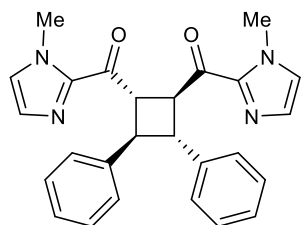
Synthesized according to General Procedure E using 214.4 mg (0.56 mmol, 1.0 equiv) 1-(1-methyl-1*H*-imidazol-2-yl)-2-(triphenyl-15-phosphaneylidene)ethan-1-one, 98.5 mg (0.56 mmol, 1.0 equiv) 6-(trifluoromethyl)nicotinaldehyde, and 5.6 mL Toluene (0.1 M). Work-up crude reaction mixture then purify by FCC with 7:3 EtOAc/pentanes to give 115.1 mg (0.41 mmol, 73% yield) of a white powder (mp 102–105 °C). ¹H NMR (400 MHz, CDCl₃) δ 8.94 (d, *J* = 2.1 Hz, 1H), 8.22 (d, *J* = 16.2 Hz, 1H), 8.18 (dd, *J* = 8.1, 2.0 Hz, 1H), 7.81 (d, *J* = 16.2 Hz, 1H), 7.73 (d, *J* = 8.2 Hz, 1H), 7.25 (s, 1H), 7.14 (s, 1H), 4.11 (s, 3H). ¹³C NMR (100 MHz, CDCl₃) δ 179.3, 150.2, 148.8 (q, *J* =

35.0 Hz), 143.6, 137.3, 135.8, 133.5, 129.8, 127.9, 127.0, 121.4 (q, $J = 274.1$ Hz), 120.6 (q, $J = 2.8$ Hz), 36.4. ^{19}F NMR (377 MHz, CDCl_3) $\delta -67.98$. HRMS (ESI) calculated for $[\text{C}_{13}\text{H}_{10}\text{F}_3\text{N}_3\text{O}]^+$ ($\text{M}+\text{H}^+$) requires m/z 282.08487, found 282.0849.

3.5.4 Asymmetric [2+2] Dimerization Photocycloaddition Reactions

General Procedure for Isolation-Scale Asymmetric [2+2] Photodimerization Reactions: A 12 mL vial was charged with 1-methylimidazol enone (0.4 mmol, 1.0 equiv), (**R**)-**3.2** (0.08 mmol, 0.2 equiv), and toluene (8 mL). The dram vial was then sealed with a white teflon cap and irradiated with a Kessil H150 Tuna Blue lamp for 24 hours at room temperature in a water bath. The crude reaction mixture was transferred to a small Erlenmeyer flask with CH_2Cl_2 and triethylamine (0.6 mL) was added. The resulting solution was dried over Na_2SO_4 , filtered, concentrated, and analyzed by ^1H -NMR vs. internal standard (phenanthrene) to determine yield and diastereomeric ratio. The crude mixture was then purified by flash column chromatography (FCC) eluting from EtOAc in pentanes to isolate a single diastereomer. Only the major diastereomer of each reaction was characterized despite three diastereomers being present in the crude NMR. The reported diastereomer ratio is a ratio of the major diastereomer to the combined minor diastereomers.

(3,4-diphenylcyclobutane-1,2-diyl)bis((1-methyl-1*H*-imidazol-2-yl)methanone) (3.4):

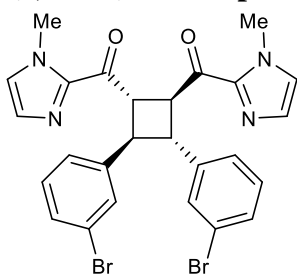


Prepared by combining 1.061 g (**5 mmol**, 1.0 equiv) (*E*)-1-(1-methyl-1*H*-imidazol-2-yl)-3-phenylprop-2-en-1-one, 193.0 mg (0.25 mmol, **0.05 equiv**) (**R**)-**3.2**, and toluene (100 mL) in a 500 mL RBF. The

reaction was irradiated with two Kessil H150 Tuna Blue lamps for 24 hours at room temperature with fans for cooling. The crude product was purified by FCC eluting from a gradient of 20% → 80% EtOAc in pentanes to give 203.1 mg (0.237 mmol, 94% recovered yield) (**R**)-**3.2** and 789.3 mg (1.86 mmol, 74% yield) of one diastereomer (6:1 d.r.). Major diastereomer: 99% ee [Daicel

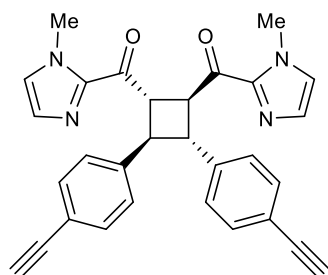
CHIRALPAK AS-H, 5% to 50% iPrOH, 28 min, 1 mL/min, $t_1=11.12$ min, $t_2=12.47$ min]. White solid (mp 149–151 °C). $[\alpha]_D^{22} +5.1^\circ$ (c0.935, CH₂Cl₂). ¹H NMR (500 MHz, CDCl₃) δ 7.41–7.37 (m, 4H), 7.30–7.24 (m, 4H), 7.21–7.16 (m, 2H), 6.87 (s, 2H), 6.79 (s, 2H), 4.73–4.68 (m, 2H), 4.14–4.09 (m, 2H), 4.01 (s, 6H). ¹³C NMR (125 MHz, CDCl₃) δ 190.7, 143.0, 142.1, 128.9, 128.4, 127.3, 126.7, 126.6, 49.4, 45.1, 35.9. HRMS (ESI) calculated for [C₂₆H₂₅N₄O₂]⁺ (M+H⁺) requires m/z 425.19720, found 425.1972.

(3,4-bis(3-bromophenyl)cyclobutane-1,2-diyl)bis((1-methyl-1*H*-imidazol-2-yl)methanone):



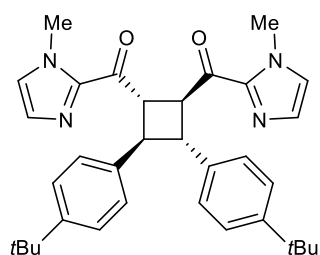
Prepared according to the general procedure for isolation-scale asymmetric experiments using 117.8 mg (0.40 mmol, 1.0 equiv) (*E*)-3-(3-bromophenyl)-1-(1-methyl-1*H*-imidazol-2-yl)prop-2-en-1-one, 62.5 mg (0.08 mmol, 0.2 equiv) (**R**)-**3.2**, and toluene (8 mL). The resulting

material was purified by FCC eluting from a gradient of 40% → 60% EtOAc in pentanes to give 62.1 mg (0.11 mmol, 53% yield) of one diastereomer (5:1 d.r.). Major diastereomer: 99% ee [Daicel CHIRALPAK AD, 5% to 50% iPrOH, 28 min, 1 mL/min, $t_1=10.94$ min, $t_2=13.16$ min]. White solid (mp = 55–60 °C). $[\alpha]_D^{22} +29.3^\circ$ (c0.45, CH₂Cl₂). ¹H NMR (600 MHz, CDCl₃) δ 7.54 (t, $J = 1.9$ Hz, 2H), 7.36–7.32 (m, 2H), 7.32–7.28 (m, 2H), 7.16 (t, $J = 7.8$ Hz, 2H), 6.91 (s, 2H), 6.81 (s, 2H), 4.68–4.61 (m, 2H), 4.08–4.02 (m, 2H), 4.03 (s, 6H). ¹³C NMR (150 MHz, CDCl₃) δ 190.0, 144.0, 142.8, 130.3, 130.1, 130.0, 129.0, 126.9, 126.0, 122.7, 49.3, 44.5, 35.9. HRMS (ESI) calculated for [C₂₆H₂₂Br₂N₄O₂Na]⁺ (M+Na⁺) requires m/z 603.0002, found 603.0003.

(3,4-bis(4-ethynylphenyl)cyclobutane-1,2-diyl)bis((1-methyl-1*H*-imidazol-2-yl)methanone)

(3.13): Prepared according to the general procedure for isolation-scale asymmetric experiments using 94.9 mg (0.40 mmol, 1.0 equiv) (*E*)-3-(4-ethynylphenyl)-1-(1-methyl-1*H*-imidazol-2-yl)prop-2-en-1-one, 63.5 mg (0.08 mmol, 0.2 equiv) (**R**)-**3.2**, and toluene (8 mL). The

resulting material was purified by FCC eluting from a gradient of 40% → 60% EtOAc in pentanes to give 49.8 mg (0.106 mmol, 53% yield) of one diastereomer (12:1 d.r.). Major diastereomer: 99% ee [Daicel CHIRALPAK AS-H, 5% to 50% iPrOH, 28 min, 1 mL/min, $t_1=13.33$ min, $t_2=15.78$ min]. White solid (mp = 163–166 °C). $[\alpha]_D^{22} +106.8^\circ$ (c1.65, CH₂Cl₂). ¹H NMR (600 MHz, CDCl₃) δ 7.42 (d, $J = 8.3$ Hz, 4 H), 7.33 (d, $J = 8.3$ Hz, 4H), 6.91 (s, 2H), 6.81 (d, $J = 0.9$ Hz, 2H), 4.74–4.67 (m, 2H), 4.08–4.02 (m, 2H), 4.02 (s, 6H), 3.04 (s, 2H). ¹³C NMR (150 MHz, CDCl₃) δ 190.3, 142.8, 142.7, 132.3, 129.0, 127.2, 126.9, 120.5, 83.6, 77.0, 49.0, 45.2, 35.9. HRMS (ESI) calculated for [C₃₀H₂₅N₄O₂]⁺ (M+H⁺) requires m/z 473.1972, found 473.1971.

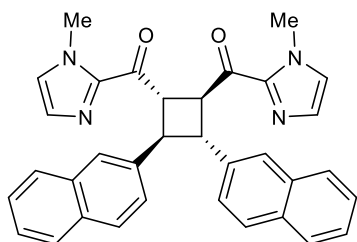
(3,4-bis(4-(*tert*-butyl)phenyl)cyclobutane-1,2-diyl)bis((1-methyl-1*H*-imidazol-2-

yl)methanone) (3.9): Prepared according to the general procedure for isolation-scale asymmetric experiments using 108.2 mg (0.40 mmol, 1.0 equiv) (*E*)-3-(4-(*tert*-butyl)phenyl)-1-(1-methyl-1*H*-imidazol-2-yl)prop-2-en-1-one, 61.6 mg (0.08 mmol, 0.2 equiv) (**R**)-**3.2**, and

toluene (8 mL). The resulting material was purified by FCC eluting from a gradient of 40% → 60% EtOAc in pentanes to give 83.2 mg (0.16 mmol, 77% yield) of one diastereomer (10:1 d.r.). Major diastereomer: 96% ee [Daicel CHIRALPAK OD-H, 5% to 50% iPrOH, 28 min, 1 mL/min, $t_1=8.48$ min, $t_2=9.65$ min]. White solid (mp = 158–161 °C). $[\alpha]_D^{22} +116.0^\circ$ (c0.05, CH₂Cl₂). ¹H NMR (400 MHz, CDCl₃) δ 7.33 (d, $J = 8.5$ Hz, 4H), 7.29 (d, $J = 8.5$ Hz, 4H), 6.88 (s, 2H), 6.79

(s, 2H), 4.67–4.62 (m, 2H), 4.12–4.07 (m, 2H), 4.02 (s, 6H), 1.27 (s, 18H). ^{13}C NMR (100 MHz, CDCl_3) δ 190.9, 149.3, 143.1, 139.1, 128.8, 127.0, 126.6, 125.35, 49.7, 44.5, 35.9, 34.4, 31.4. HRMS (ESI) calculated for $[\text{C}_{34}\text{H}_{41}\text{N}_4\text{O}_2]^+$ ($\text{M}+\text{H}^+$) requires m/z 537.3224, found 537.3226.

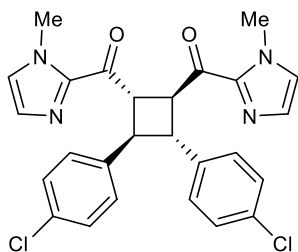
(3,4-di(naphthalen-2-yl)cyclobutane-1,2-diyl)bis((1-methyl-1H-imidazol-2-yl)methanone):



Prepared according to the general procedure for isolation-scale asymmetric experiments using 105.1 mg (0.4 mmol, 1.0 equiv) (*E*)-1-(1-methyl-1*H*-imidazol-2-yl)-3-(naphthalen-2-yl)prop-2-en-1-one, 61.9 mg (0.08 mmol, 0.2 equiv) (**R**)-**3.2**, and toluene (8 mL).

The resulting material was purified by FCC eluting from a gradient of 50% \rightarrow 70% EtOAc in pentanes to give 70.2 mg (0.13 mmol, 67% yield) of one diastereomer (12:1 d.r.). Major diastereomer: 99% ee [Daicel CHIRALPAK AS-H, 5% to 50% iPrOH, 28 min, 1 mL/min, $t_1=14.10$ min, $t_2=16.01$ min]. Off-white solid (mp 184–187 °C). $[\alpha]_{\text{D}}^{22} +108.4^\circ$ (c0.585, CH_2Cl_2). ^1H NMR (500 MHz, CDCl_3) δ 7.89 (s, 2H), 7.81–7.74 (m, 6H), 7.54 (dd, $J = 8.5, 1.8$ Hz, 2H), 7.45–7.37 (m, 4H), 6.91 (s, 2H), 6.83 (s, 2H), 4.94–4.88 (m, 2H), 4.38–4.32 (m, 2H), 4.06 (s, 6H). ^{13}C NMR (125 MHz, CDCl_3) δ 190.7, 143.0, 139.5, 133.5, 132.5, 129.0, 128.2, 127.8, 127.6, 126.8, 125.9, 125.82, 125.79, 125.4, 49.3, 45.7, 35.9. HRMS (ESI) calculated for $[\text{C}_{34}\text{H}_{29}\text{N}_4\text{O}_2]^+$ ($\text{M}+\text{H}^+$) requires m/z 525.2285, found 525.2284.

(3,4-bis(4-chlorophenyl)cyclobutane-1,2-diyl)bis((1-methyl-1H-imidazol-2-yl)methanone)

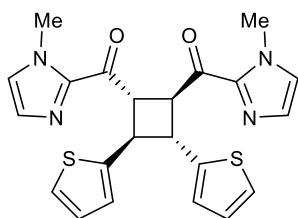


(3.10): Prepared according to the general procedure for isolation-scale asymmetric experiments using 100.2 mg (0.4 mmol, 1.0 equiv) (*E*)-3-(4-chlorophenyl)-1-(1-methyl-1*H*-imidazol-2-yl)prop-2-en-1-one, 61.4 mg (0.08 mmol, 0.2 equiv) (**R**)-**3.2**, and toluene (8 mL). The resulting

material was purified by FCC eluting from a gradient of 50% \rightarrow 70% EtOAc in pentanes to give

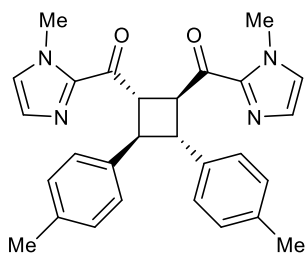
71.9 mg (0.15 mmol, 72% yield) of one diastereomer (8:1 d.r.). Major diastereomer: 99% ee [Daicel CHIRALPAK AS-H, 5% to 50% iPrOH, 28 min, 1 mL/min, $t_1=11.88$ min, $t_2=14.50$ min]. Off-white solid (mp 155–158 °C). $[\alpha]_D^{22} +64.5^\circ$ (c0.44, CH₂Cl₂). ¹H NMR (500 MHz, CDCl₃) δ 7.30 (d, $J = 8.5$ Hz, 4H), 7.25 (d, $J = 8.5$ Hz, 4H), 6.91 (s, 2H), 6.82 (s, 2H), 4.70–4.65 (m, 2H), 4.02 (s, 6H), 4.00–3.96 (m, 2H). ¹³C NMR (125 MHz, CDCl₃) δ 190.3, 142.8, 140.2, 132.6, 129.0, 128.63, 128.60, 126.9, 49.1, 44.9, 35.9. HRMS (ESI) calculated for [C₂₆H₂₃Cl₂N₄O₂]⁺ (M+H⁺) requires m/z 493.11926, found 493.1188.

(3,4-di(thiophen-2-yl)cyclobutane-1,2-diyl)bis((1-methyl-1*H*-imidazol-2-yl)methanone)



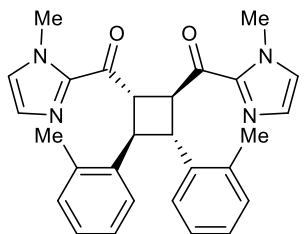
(3.14): Prepared according to the general procedure for isolation-scale asymmetric experiments using 89.3 mg (0.4 mmol, 1.0 equiv) (*E*)-1-(1-methyl-1*H*-imidazol-2-yl)-3-(thiophen-2-yl)prop-2-en-1-one, 62.8 mg

(0.08 mmol, 0.2 equiv) (**R**)-**3.2**, and toluene (8 mL). The resulting material was purified by FCC eluting from a gradient of 50% → 70% EtOAc in pentanes to give 55.3 mg (0.13 mmol, 61% yield) of one diastereomer (11:1 d.r.). Major diastereomer: 96% ee [Daicel CHIRALPAK AD, 5% to 50% iPrOH, 28 min, 1 mL/min, $t_1=17.54$ min, $t_2=20.17$ min]. Off-white solid (mp 129–132 °C). $[\alpha]_D^{22} +166.0^\circ$ (c0.20, CH₂Cl₂). ¹H NMR (500 MHz, CDCl₃) δ 7.16 (dd, $J = 5.0, 1.2$ Hz, 2H), 7.05 (dd, $J = 3.5, 1.2$ Hz, 2H), 6.93 (dd, $J = 5.1, 3.5$ Hz, 2H), 6.90 (s, 2H), 6.82 (s, 2H), 4.72–4.65 (m, 2H), 4.24–4.17 (m, 2H), 4.03 (s, 6H). ¹³C NMR (125 MHz, CDCl₃) δ 189.7, 145.0, 142.9, 129.0, 126.9, 126.8, 124.3, 124.1, 50.5, 42.7, 35.9. HRMS (ESI) calculated for [C₂₂H₂₁N₄O₂S₂]⁺ (M+H⁺) requires m/z 437.11004, found 437.1102.

(3,4-di-*p*-tolylcyclobutane-1,2-diyl)bis((1-methyl-1*H*-imidazol-2-yl)methanone) (3.11):

Prepared according to the general procedure for isolation-scale asymmetric experiments using 93.1 mg (0.4 mmol, 1.0 equiv) (*E*)-1-(1-methyl-1*H*-imidazol-2-yl)-3-(*p*-tolyl)prop-2-en-1-one, 60.4 mg (0.08 mmol, 0.2 equiv) (**R**)-**3.2**, and toluene (8 mL). The resulting material

was purified by FCC eluting from a gradient of 50% → 70% EtOAc in pentanes to give 71.2 mg (0.16 mmol, 76% yield) of one diastereomer (15:1 d.r.). Major diastereomer: 96% ee [Daicel CHIRALPAK AS-H, 5% to 50% iPrOH, 28 min, 1 mL/min, $t_1=9.55$ min, $t_2=10.85$ min]. Off-white solid (mp 50–57 °C). $[\alpha]_D^{22} +66.6^\circ$ (c0.625, CH₂Cl₂). ¹H NMR (500 MHz, CDCl₃) δ 7.27 (d, $J = 8.1$ Hz, 4H), 7.08 (d, $J = 7.9$ Hz, 4H), 6.87 (s, 2H), 6.80 (s, 2H), 4.70–4.64 (m, 2H), 4.05–3.99 (m, 2H), 4.01 (s, 6H), 2.29 (s, 6H). ¹³C NMR (125 MHz, CDCl₃) δ 190.9, 143.1, 139.1, 136.1, 129.1, 128.9, 127.2, 126.6, 49.4, 45.1, 35.9, 21.1. HRMS (ESI) calculated for [C₂₈H₂₉N₄O₂]⁺ (M+H⁺) requires m/z 453.2285, found 453.2279.

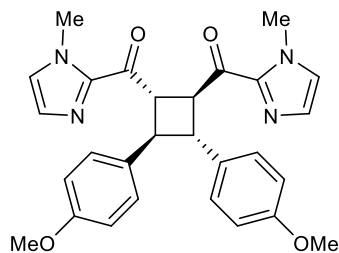
(3,4-di-*o*-tolylcyclobutane-1,2-diyl)bis((1-methyl-1*H*-imidazol-2-yl)methanone) (3.5):

Prepared according to the general procedure for isolation-scale asymmetric experiments using 93.2 mg (0.4 mmol, 1.0 equiv) (*E*)-1-(1-methyl-1*H*-imidazol-2-yl)-3-(*o*-tolyl)prop-2-en-1-one, 61.2 mg (0.08 mmol, 0.2 equiv) (**R**)-**3.2**, and toluene (8 mL). The resulting material was purified by FCC eluting

from a gradient of 50% → 70% EtOAc in pentanes to give 73.1 mg (0.16 mmol, 78% yield) of one diastereomer (7:1 d.r.). Major diastereomer: 98% ee [Daicel CHIRALPAK IC, 5% to 50% iPrOH, 28 min, 1 mL/min, $t_1=10.50$ min, $t_2=14.25$ min]. Off-white solid (mp 146–150 °C). $[\alpha]_D^{22} +67.9^\circ$ (c0.84, CH₂Cl₂). ¹H NMR (500 MHz, CDCl₃) δ 7.76 (d, $J = 7.8$ Hz, 2H), 7.23 (t, $J = 7.0$ Hz, 2H), 7.07 (td, $J = 7.4, 1.3$ Hz, 2H), 7.01 (d, $J = 6.7$ Hz, 2H), 6.87 (s, 2H), 6.79 (s, 2H), 4.82–4.76 (m,

2H), 4.36–4.31 (m, 2H), 4.01 (s, 6H), 2.11 (s, 6H). ^{13}C NMR (125 MHz, CDCl_3) δ 190.9, 143.1, 140.4, 136.2, 129.9, 128.9, 127.0, 126.6, 126.4, 126.3, 49.0, 42.1, 35.9, 20.1. HRMS (ESI) calculated for $[\text{C}_{28}\text{H}_{29}\text{N}_4\text{O}_2]^+$ ($\text{M}+\text{H}^+$) requires m/z 453.22850, found 453.2277.

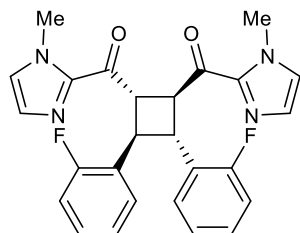
(3,4-bis(4-methoxyphenyl)cyclobutane-1,2-diyl)bis((1-methyl-1H-imidazol-2-yl)methanone)



(3.12): Prepared according to the general procedure for isolation-scale asymmetric experiments using 99.7 mg (0.4 mmol, 1.0 equiv) (*E*)-3-(4-methoxyphenyl)-1-(1-methyl-1*H*-imidazol-2-yl)prop-2-en-1-one, 63.9 mg (0.08 mmol, 0.2 equiv) (**R**)-**3.2**, and toluene (8 mL). The

resulting material was purified by FCC eluting from a gradient of 60% \rightarrow 80% EtOAc in pentanes to give 77.2 mg (0.16 mmol, 77% yield) of one diastereomer (9:1 d.r.). Major diastereomer: 93% ee [Daicel CHIRALPAK AS-H, 5% to 50% *i*PrOH, 28 min, 1 mL/min, $t_1=15.63$ min, $t_2=18.62$ min]. Off-white solid (mp 108–112 $^\circ\text{C}$). $[\alpha]_{\text{D}}^{22} +68.0^\circ$ (c0.465, CH_2Cl_2). ^1H NMR (500 MHz, CDCl_3) δ 7.30 (d, $J = 8.7$ Hz, 4H), 6.88 (s, 2H), 6.82 (d, $J = 8.8$ Hz, 4H), 6.80 (s, 2H), 4.68–4.61 (m, 2H), 4.02 (s, 6H), 3.99–3.94 (m, 2H), 3.76 (s, 6H). ^{13}C NMR (125 MHz, CDCl_3) δ 190.9, 158.3, 143.1, 134.3, 128.9, 128.3, 126.6, 113.8, 55.2, 49.5, 45.1, 35.9. HRMS (ESI) calculated for $[\text{C}_{28}\text{H}_{29}\text{N}_4\text{O}_4]^+$ ($\text{M}+\text{H}^+$) requires m/z 485.21833, found 485.2183.

(3,4-bis(2-fluorophenyl)cyclobutane-1,2-diyl)bis((1-methyl-1H-imidazol-2-yl)methanone)

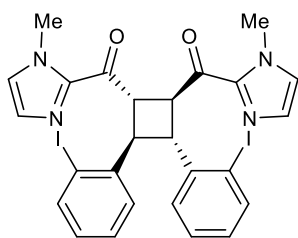


(3.6): Prepared according to the general procedure for isolation-scale asymmetric experiments using 92.2 mg (0.4 mmol, 1.0 equiv) (*E*)-3-(2-fluorophenyl)-1-(1-methyl-1*H*-imidazol-2-yl)prop-2-en-1-one, 61.5 mg

(0.08 mmol, 0.2 equiv) (**R**)-**3.2**, and toluene (8 mL). The resulting material was purified by FCC eluting from a gradient of 50% \rightarrow 70% EtOAc in pentanes to give 52.7 mg (0.12 mmol, 57% yield) of one diastereomer (4:1 d.r.). Major diastereomer: 99% ee [Daicel CHIRALPAK IC, 5% to 50%

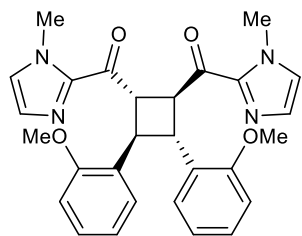
iPrOH, 28 min, 1 mL/min, $t_1=15.83$ min, $t_2=17.03$ min]. Light orange solid (mp 145–148 °C). $[\alpha]_D^{22} +55.5^\circ$ (c0.155, CH₂Cl₂). ¹H NMR (500 MHz, CDCl₃) δ 7.60 (td, $J = 7.5, 1.9$ Hz, 2H), 7.19–7.14 (m, 2H), 7.12 (td, $J = 7.5, 1.4$ Hz, 2H), 6.93 (ddd, $J = 10.4, 8.0, 1.4$ Hz, 2H), 6.90 (s, 2H), 6.81 (s, 2H), 4.80–4.75 (m, 2H), 4.46–4.41 (m, 2H), 4.03 (s, 6H). ¹³C NMR (125 MHz, CDCl₃) δ 190.0, 160.8 (d, $J = 246.0$ Hz), 142.9, 128.9, 128.7 (d, $J = 4.6$ Hz), 128.5 (d, $J = 15.3$ Hz), 128.2 (d, $J = 8.3$ Hz), 126.8, 124.2 (d, $J = 3.5$ Hz), 115.1 (d, $J = 22.1$ Hz), 48.7, 37.7, 35.9. ¹⁹F NMR (377 MHz, CDCl₃) δ –116.17. HRMS (ESI) calculated for [C₂₆H₂₃F₂N₄O₂]⁺ (M+H⁺) requires m/z 461.1784, found 461.1780.

(3,4-bis(2-iodophenyl)cyclobutane-1,2-diyl)bis((1-methyl-1*H*-imidazol-2-yl)methanone)



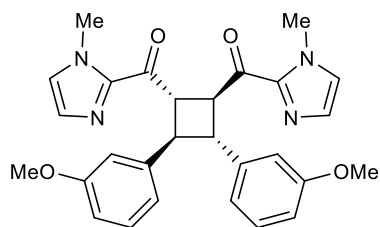
(3.7): Prepared according to the general procedure for isolation-scale asymmetric experiments using 132.4 mg (0.4 mmol, 1.0 equiv) (*E*)-3-(2-iodophenyl)-1-(1-methyl-1*H*-imidazol-2-yl)prop-2-en-1-one, 61.1 mg (0.08 mmol, 0.2 equiv) (*R*)-**3.2**, and toluene (8 mL). The resulting

material was purified by FCC eluting from a gradient of 50% → 70% EtOAc in pentanes to give 64.4 mg (0.095 mmol, 48% yield) of one diastereomer (14:1 d.r.). Major diastereomer: 99% ee [Daicel CHIRALPAK AD, 5% to 50% iPrOH, 28 min, 1 mL/min, $t_1=13.57$ min, $t_2=16.19$ min]. Off-white solid (mp 215–218 °C). $[\alpha]_D^{22} +37.6^\circ$ (c0.41, CH₂Cl₂). ¹H NMR (500 MHz, CDCl₃) δ 7.93 (dd, $J = 7.9, 1.6$ Hz, 2H), 7.70 (dd, $J = 7.8, 1.3$ Hz, 2H), 7.42 (td, $J = 7.6, 1.3$ Hz, 2H), 6.92 (s, 2H), 6.88 (td, $J = 7.6, 1.7$ Hz, 2H), 6.86 (s, 2H), 4.90–4.84 (m, 2H), 4.44–4.39 (m, 2H), 4.04 (s, 6H). ¹³C NMR (125 MHz, CDCl₃) δ 190.1, 144.0, 142.9, 139.2, 129.2, 129.1, 128.7, 128.6, 126.9, 101.2, 50.6, 48.5, 36.0. HRMS (ESI) calculated for [C₂₆H₂₃I₂N₄O₂]⁺ (M+H⁺) requires m/z 676.9905, found 676.9908.

(3,4-bis(2-methoxyphenyl)cyclobutane-1,2-diyl)bis((1-methyl-1H-imidazol-2-yl)methanone)

(3.8): Prepared according to the general procedure for isolation-scale asymmetric experiments using 100.2 mg (0.4 mmol, 1.0 equiv) (*E*)-3-(2-methoxyphenyl)-1-(1-methyl-1*H*-imidazol-2-yl)prop-2-en-1-one, 63.8

mg (0.08 mmol, 0.2 equiv) (***R***)-**3.2**, and toluene (8 mL). The resulting material was purified by FCC eluting from a gradient of 60% → 80% EtOAc in pentanes to give 55.1 mg (0.11 mmol, 55% yield) of one diastereomer (5:1 d.r.). Major diastereomer: 98% ee [Daicel CHIRALPAK IC, 5% to 50% iPrOH, 28 min, 1 mL/min, $t_1=19.64$ min, $t_2=22.85$ min]. Off-white solid (mp 213–216 °C). $[\alpha]_D^{22} -15.8^\circ$ (c0.80, CH₂Cl₂). ¹H NMR (500 MHz, CDCl₃) δ 7.50 (dd, $J = 7.5, 1.7$ Hz, 2H), 7.15 (td, $J = 7.8, 1.7$ Hz, 2H), 6.92 (td, $J = 7.5, 1.2$ Hz, 2H), 6.89 (s, 2H), 6.86 (s, 2H), 6.72 (dd, $J = 8.2, 1.1$ Hz, 2H), 4.70–4.66 (m, 2H), 4.44–4.39 (m, 2H), 4.06 (s, 6H), 3.45 (s, 6H). ¹³C NMR (125 MHz, CDCl₃) δ 191.2, 157.3, 143.3, 130.6, 128.8, 127.9, 127.4, 126.3, 120.4, 109.8, 54.7, 48.7, 38.6, 36.0. HRMS (ESI) calculated for [C₂₈H₂₉N₄O₄]⁺ (M+H⁺) requires m/z 485.2183, found 485.2182.

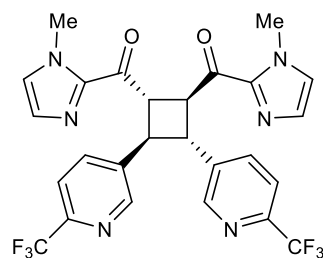
(3,4-bis(3-methoxyphenyl)cyclobutane-1,2-diyl)bis((1-methyl-1H-imidazol-2-

yl)methanone): Prepared according to the general procedure for isolation-scale asymmetric experiments using 98.3 mg (0.4 mmol, 1.0 equiv) (*E*)-3-(3-methoxyphenyl)-1-(1-methyl-1*H*-imidazol-2-

yl)prop-2-en-1-one, 63.2 mg (0.08 mmol, 0.2 equiv) (***R***)-**3.2**, and toluene (8 mL). The resulting material was purified by FCC eluting from a gradient of 60% → 80% EtOAc in pentanes to give 68.2 mg (0.14 mmol, 69% yield) of one diastereomer (10:1 d.r.). Major diastereomer: 99% ee [Daicel CHIRALPAK AD, 5% to 50% iPrOH, 28 min, 1 mL/min, $t_1=15.85$ min, $t_2=17.31$ min]. Light orange solid (mp 75–78 °C). $[\alpha]_D^{22} +83.0^\circ$ (c1.75, CH₂Cl₂). ¹H NMR (500 MHz, CDCl₃) δ

7.19 (t, $J = 8.2$ Hz, 2H), 7.00–6.96 (m, 4H), 6.88 (s, 2H), 6.80 (s, 2H), 6.75–6.71 (m, 2H), 4.72–4.67 (m, 2H), 4.09–4.05 (m, 2H), 4.01 (s, 6H), 3.76 (s, 6H). ^{13}C NMR (125 MHz, CDCl_3) δ 190.6, 159.7, 143.8, 143.0, 129.4, 128.9, 126.7, 119.6, 112.7, 112.4, 55.2, 49.2, 45.2, 35.9. HRMS (ESI) calculated for $[\text{C}_{28}\text{H}_{29}\text{N}_4\text{O}_4]^+$ ($\text{M}+\text{H}^+$) requires m/z 485.2183, found 485.2180.

(3,4-bis(6-(trifluoromethyl)pyridin-3-yl)cyclobutane-1,2-diyl)bis((1-methyl-1H-imidazol-2-



yl)methanone) (3.15): Prepared according to the general procedure for isolation-scale asymmetric experiments using 113.6 mg (0.4 mmol, 1.0 equiv) *(E)*-1-(1-methyl-1H-imidazol-2-yl)-3-(6-(trifluoromethyl)pyridin-3-yl)prop-2-en-1-one, 63.7 mg (0.08 mmol,

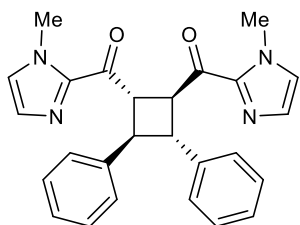
0.2 equiv) **(R)**-**3.2**, and toluene (8 mL). The resulting material was purified by FCC eluting from a gradient of 70% \rightarrow 90% EtOAc in pentanes to give 92.1 mg (0.16 mmol, 81% yield) of one diastereomer (6:1 d.r.). Major diastereomer: 98% ee [Daicel CHIRALPAK AS-H, 5% to 50% *i*PrOH, 28 min, 1 mL/min, $t_1=13.91$ min, $t_2=16.50$ min]. White solid (mp 186–189 °C). $[\alpha]_{\text{D}}^{22} +38.5^\circ$ (c0.39, CH_2Cl_2). ^1H NMR (500 MHz, CDCl_3) δ 8.71 (d, $J = 2.2$ Hz, 2H), 7.98 (dd, $J = 8.1, 2.2$ Hz, 2H), 7.67 (d, $J = 8.1$ Hz, 2H), 6.98 (s, 2H), 6.88 (s, 2H), 4.89–4.84 (m, 2H), 4.17–4.12 (m, 2H), 4.04 (s, 6H). ^{13}C NMR (125 MHz, CDCl_3) δ 189.1, 149.2, 147.2 (q, $J = 34.0$ Hz), 142.4, 139.7, 136.0, 129.5, 127.4, 121.5 (q, $J = 273.9$ Hz), 120.5 (q, $J = 2.8$ Hz), 48.4, 43.0, 35.9. ^{19}F NMR (377 MHz, CDCl_3) δ –67.86. HRMS (ESI) calculated for $[\text{C}_{26}\text{H}_{21}\text{F}_6\text{N}_6\text{O}_2]^+$ ($\text{M}+\text{H}^+$) requires m/z 563.1625, found 563.1624.

3.5.5 Racemic [2+2] Dimerization Photocycloaddition Reaction

General Procedure for Racemic [2+2] Photodimerization Reactions: A non-oven dried 12 mL dram vial was charged with 1-methylimidazol enone (0.1 mmol, 1.0 equiv), **(±)**-**3.2** (0.02 mmol,

0.2 equiv), and 2 mL (0.05 M) toluene. The dram vial was then sealed with a white teflon cap and irradiated with a Kessil H150 Tuna Blue lamp for 24 hours at room temperature in a water bath. The crude reaction mixture was transferred to a small Erlenmeyer flask with CH_2Cl_2 and triethylamine (0.6 mL) added. The resulting solution was dried over Na_2SO_4 , filtered, concentrated, and analyzed by $^1\text{H-NMR}$ vs. internal standard (phenanthrene) to determine conversion and diastereomeric ratio. The crude mixture was then purified via flash column chromatography (FCC) using EtOAc/pentanes as the eluent to isolate a single diastereomer. Only the major diastereomer of each reaction was characterized despite three diastereomers being present in the crude NMR.

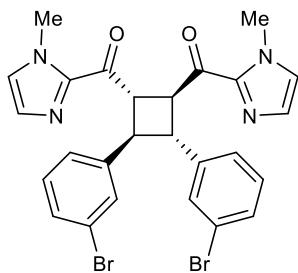
(3,4-diphenylcyclobutane-1,2-diyl)bis((1-methyl-1*H*-imidazol-2-yl)methanone): Prepared



according to the general procedure for racemic experiments using 214.1 mg (**1.0 mmol**, 1.0 equiv) (*E*)-1-(1-methyl-1*H*-imidazol-2-yl)-3-phenylprop-2-en-1-one, 153.8 mg (**0.2 mmol**, 0.2 equiv) (\pm)-**3.2**, and

toluene (20 mL). The resulting material was purified by FCC eluting from 50% EtOAc in pentanes to give a 73% NMR yield of three diastereomers (5:1 d.r.). Spectroscopic data was consistent with those reported above.

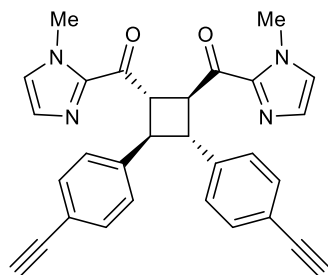
(3,4-bis(3-bromophenyl)cyclobutane-1,2-diyl)bis((1-methyl-1*H*-imidazol-2-yl)methanone):



Prepared according to the general procedure for racemic experiments using 32.0 mg (0.1 mmol, 1.0 equiv) (*E*)-3-(3-bromophenyl)-1-(1-methyl-1*H*-imidazol-2-yl)prop-2-en-1-one, 18.1 mg (0.02 mmol, 0.2 equiv) (\pm)-**3.2**, and toluene (2 mL). The resulting material was purified

by FCC eluting from a gradient of 50% → 70% EtOAc in pentanes to give a 68% NMR yield of three diastereomers (5:1 d.r.). Spectroscopic data was consistent with those reported above.

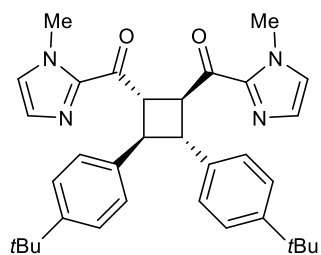
(3,4-bis(4-ethynylphenyl)cyclobutane-1,2-diyl)bis((1-methyl-1*H*-imidazol-2-yl)methanone):



Prepared according to the general procedure for racemic experiments using 24.2 mg (0.1 mmol, 1.0 equiv) (*E*)-3-(4-ethynylphenyl)-1-(1-methyl-1*H*-imidazol-2-yl)prop-2-en-1-one, 16.4 mg (0.02 mmol, 0.2 equiv) (±)-**3.2**, and toluene (2 mL). The resulting material was purified

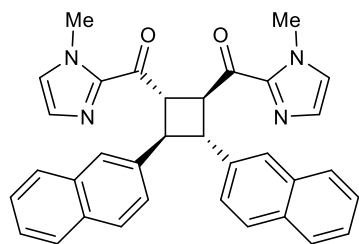
by FCC eluting from a gradient of 50% → 70% EtOAc in pentanes to give an 82% NMR yield of three diastereomers (8:1 d.r.). Spectroscopic data was consistent with those reported above.

(3,4-bis(4-(*tert*-butyl)phenyl)cyclobutane-1,2-diyl)bis((1-methyl-1*H*-imidazol-2-

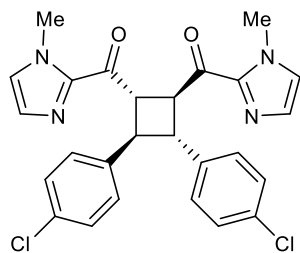


yl)methanone): Prepared according to the general procedure for racemic experiments using 29.2 mg (0.1 mmol, 1.0 equiv) (*E*)-3-(4-(*tert*-butyl)phenyl)-1-(1-methyl-1*H*-imidazol-2-yl)prop-2-en-1-one, 17.7 mg (0.02 mmol, 0.2 equiv) (±)-**3.2**, and toluene (2 mL). The

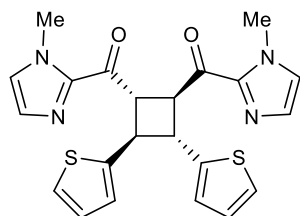
resulting material was purified by FCC eluting from a gradient of 50% → 60% EtOAc in pentanes to give a 69% NMR yield of three diastereomers (7:1 d.r.). Spectroscopic data was consistent with those reported above.

(3,4-di(naphthalen-2-yl)cyclobutane-1,2-diyl)bis((1-methyl-1*H*-imidazol-2-yl)methanone):

Prepared according to the general procedure for racemic experiments using 53.3 mg (0.2 mmol, 1.0 equiv) (*E*)-1-(1-methyl-1*H*-imidazol-2-yl)-3-(naphthalen-2-yl)prop-2-en-1-one, 32.2 mg (0.04 mmol, 0.2 equiv) (\pm)-**3.2**, and toluene (2 mL). The resulting material was purified by FCC eluting from 50% EtOAc in pentanes to give a 71% NMR yield of three diastereomers (11:1 d.r.). Spectroscopic data was consistent with those reported above.

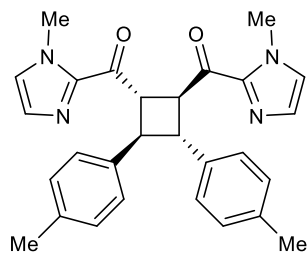
(3,4-bis(4-chlorophenyl)cyclobutane-1,2-diyl)bis((1-methyl-1*H*-imidazol-2-yl)methanone):

Prepared according to the general procedure for racemic experiments using 48.1 mg (0.2 mmol, 1.0 equiv) (*E*)-3-(4-chlorophenyl)-1-(1-methyl-1*H*-imidazol-2-yl)prop-2-en-1-one, 30.3 mg (0.04 mmol, 0.2 equiv) (\pm)-**3.2**, and toluene (2 mL). The resulting material was purified by FCC eluting from 50% EtOAc in pentanes to give a 65% NMR yield of three diastereomers (7:1 d.r.). Spectroscopic data was consistent with those reported above.

(3,4-di(thiophen-2-yl)cyclobutane-1,2-diyl)bis((1-methyl-1*H*-imidazol-2-yl)methanone):

Prepared according to the general procedure for racemic experiments using 22.4 mg (0.1 mmol, 1.0 equiv) (*E*)-1-(1-methyl-1*H*-imidazol-2-yl)-3-(thiophen-2-yl)prop-2-en-1-one, 16.4 mg (0.02 mmol, 0.2 equiv) (\pm)-**3.2**, and toluene (2 mL). The resulting material was purified by FCC eluting from a gradient of 50% \rightarrow 70% EtOAc in pentanes to give a 48% NMR yield of three diastereomers (10:1 d.r.). Spectroscopic data was consistent with those reported above.

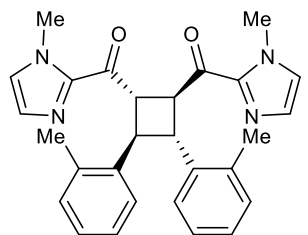
(3,4-di-*p*-tolylcyclobutane-1,2-diyl)bis((1-methyl-1*H*-imidazol-2-yl)methanone): Prepared



according to the general procedure for racemic experiments using 23.2 mg (0.1 mmol, 1.0 equiv) (*E*)-1-(1-methyl-1*H*-imidazol-2-yl)-3-(*p*-tolyl)prop-2-en-1-one, 16.3 mg (0.02 mmol, 0.2 equiv) (\pm)-**3.2**, and toluene (2 mL). The resulting material was purified by FCC eluting from

a gradient of 50% \rightarrow 70% EtOAc in pentanes to give a 90% NMR yield of three diastereomers (7:1 d.r.). Spectroscopic data was consistent with those reported above.

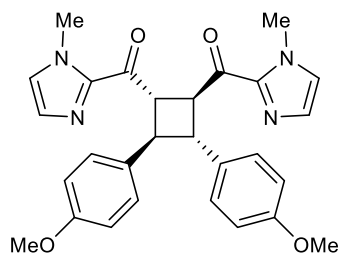
(3,4-di-*o*-tolylcyclobutane-1,2-diyl)bis((1-methyl-1*H*-imidazol-2-yl)methanone): Prepared



according to the general procedure for racemic experiments using 23.2 mg (0.1 mmol, 1.0 equiv) (*E*)-1-(1-methyl-1*H*-imidazol-2-yl)-3-(*o*-tolyl)prop-2-en-1-one, 16.6 mg (0.02 mmol, 0.2 equiv) (\pm)-**3.2**, and toluene (2 mL). The resulting material was purified by FCC eluting from

a gradient of 50% \rightarrow 60% EtOAc in pentanes to give a 49% NMR yield of three diastereomers (5:1 d.r.). Spectroscopic data was consistent with those reported above.

(3,4-bis(4-methoxyphenyl)cyclobutane-1,2-diyl)bis((1-methyl-1*H*-imidazol-2-

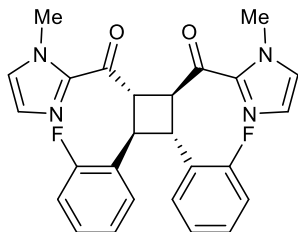


yl)methanone): Prepared according to the general procedure for racemic experiments using 26.3 mg (0.1 mmol, 1.0 equiv) (*E*)-3-(4-methoxyphenyl)-1-(1-methyl-1*H*-imidazol-2-yl)prop-2-en-1-one,

18.0 mg (0.02 mmol, 0.2 equiv) (\pm)-**3.2**, and toluene (2 mL). The resulting material was purified by FCC eluting from a gradient of 60% \rightarrow 80% EtOAc in pentanes

to give a 59% NMR yield of three diastereomers (5:1 d.r.). Spectroscopic data was consistent with those reported above.

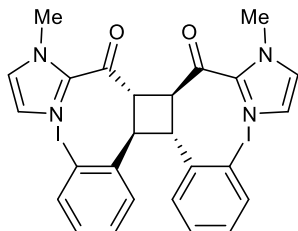
(3,4-bis(2-fluorophenyl)cyclobutane-1,2-diyl)bis((1-methyl-1*H*-imidazol-2-yl)methanone):



Prepared according to the general procedure for racemic experiments using 24.2 mg (0.1 mmol, 1.0 equiv) (*E*)-3-(2-fluorophenyl)-1-(1-methyl-1*H*-imidazol-2-yl)prop-2-en-1-one, 16.7 mg (0.02 mmol, 0.2 equiv) (\pm)-**3.2**, and toluene (2 mL). The resulting material was purified

by FCC eluting from a gradient of 50% \rightarrow 70% EtOAc in pentanes to give a 60% NMR yield of three diastereomers (3:1 d.r.). Spectroscopic data was consistent with those reported above.

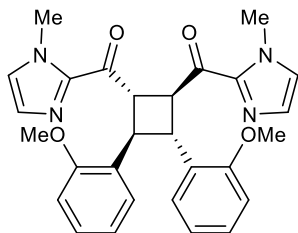
(3,4-bis(2-iodophenyl)cyclobutane-1,2-diyl)bis((1-methyl-1*H*-imidazol-2-yl)methanone):



Prepared according to the general procedure for racemic experiments using 36.2 mg (0.1 mmol, 1.0 equiv) (*E*)-3-(2-iodophenyl)-1-(1-methyl-1*H*-imidazol-2-yl)prop-2-en-1-one, 17.2 mg (0.02 mmol, 0.2 equiv) (\pm)-**3.2**, and toluene (2 mL). The resulting material was purified by FCC

eluting from a gradient of 50% \rightarrow 70% EtOAc in pentanes to give a 44% NMR yield of three diastereomers (13:1 d.r.). Spectroscopic data was consistent with those reported above.

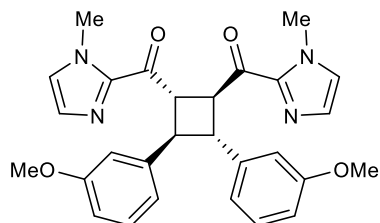
(3,4-bis(2-methoxyphenyl)cyclobutane-1,2-diyl)bis((1-methyl-1*H*-imidazol-2-



yl)methanone): Prepared according to the general procedure for racemic experiments using 24.3 mg (0.1 mmol, 1.0 equiv) (*E*)-3-(2-methoxyphenyl)-1-(1-methyl-1*H*-imidazol-2-yl)prop-2-en-1-one, 16.6

mg (0.02 mmol, 0.2 equiv) (\pm)-**3.2**, and toluene (2 mL). The resulting material was purified by FCC eluting from a gradient of 60% \rightarrow 80% EtOAc in pentanes to give a 53% NMR yield of three diastereomers (4:1 d.r.). Spectroscopic data was consistent with those reported above.

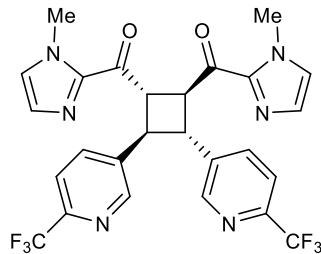
(3,4-bis(3-methoxyphenyl)cyclobutane-1,2-diyl)bis((1-methyl-1H-imidazol-2-



yl)methanone): Prepared according to the general procedure for racemic experiments using 25.0 mg (0.1 mmol, 1.0 equiv) (*E*)-3-(3-methoxyphenyl)-1-(1-methyl-1*H*-imidazol-2-yl)prop-2-en-1-

one, 17.2 mg (0.02 mmol, 0.2 equiv) (\pm)-**3.2**, and toluene (2 mL). The resulting material was purified by FCC eluting from a gradient of 60% \rightarrow 80% EtOAc in pentanes to give a 82% NMR yield of three diastereomers (8:1 d.r.). Spectroscopic data was consistent with those reported above.

(3,4-bis(6-(trifluoromethyl)pyridin-3-yl)cyclobutane-1,2-diyl)bis((1-methyl-1H-imidazol-2-



yl)methanone): Prepared according to the general procedure for racemic experiments using 28.1 mg (0.1 mmol, 1.0 equiv) (*E*)-1-(1-methyl-1*H*-imidazol-2-yl)-3-(6-(trifluoromethyl)pyridin-3-yl)prop-2-en-1-one, 16.2 mg (0.02 mmol, 0.2 equiv) (\pm)-**3.2**, and toluene (2 mL).

The resulting material was purified by FCC eluting from a gradient of 60% \rightarrow 80% EtOAc in pentanes to give a 76% NMR yield of three diastereomers (4:1 d.r.). Spectroscopic data was consistent with those reported above.

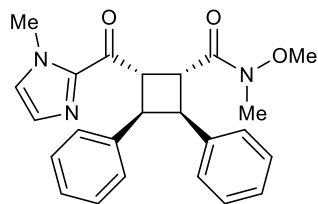
3.5.6 Asymmetric [2+2] Heterodimerization Photocycloaddition Reactions

General Procedure for Asymmetric Crossed [2+2] Photoreactions: A 24 mL flame-dried vial was charged with cinnamate (0.6 mmol, 3.0 equiv), (*R*)-**3.2** (0.04 mmol, 0.2 equiv), and toluene (4 mL). In a 10 mL flame-dried volumetric flask a solution of cinnamoyl imidazole in toluene was

prepared (0.05 M). Using a syringe pump 4.00 mL (0.2 mmol, 1.0 equiv) of the prepared cinnamoyl imidazole solution was added over 22 hours to the cinnamate solution while under irradiation with 2 Kessil H150 Tuna Blue lamps. The reaction was cooled with an air hose (reactions run at approximately 35 °C) and not degassed. After 24 hours of irradiation Et₃N (0.1 mL) was added to the reaction, which decreases broadening in the NMR. The reaction was concentrated and analyzed by ¹H-NMR vs internal standard (phenanthrene) to determine yield and diastereomeric ratio. The crude mixture was purified by FCC eluting from EtOAc in hexanes. The major diastereomer was characterized.

Note: for the asymmetric reactions we used Hamilton, 1000 series GASTIGHT, PTFE luer lock, 5 mL syringes. We found that these syringes quantitatively transfer the substrate into the reaction better than plastic syringes.

***N*-methoxy-*N*-methyl-2-(1-methyl-1*H*-imidazole-2-carbonyl)-3,4-diphenylcyclobutane-1-**

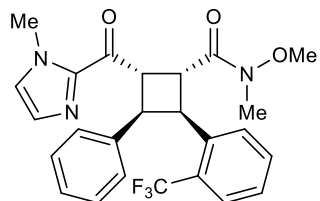


carboxamide (3.29): Prepared according to the general procedure for isolation-scale asymmetric experiments using 42.4 mg (0.2 mmol, 1.0 equiv) (*E*)-1-(1-methyl-1*H*-imidazol-2-yl)-3-phenylprop-2-en-1-one,

31.2 mg (0.04 mmol, 0.2 equiv) (**R**)-**3.2**, 115.3 mg (0.6 mmol, 3.0 equiv) *N*-methoxy-*N*-methylcinnamamide and toluene (8 mL). The resulting material was purified by FCC eluting from a gradient of 30% → 70% EtOAc in hexanes to give 60.4 mg (0.15 mmol, 75% yield) of two diastereomers (10:1 d.r.). Major diastereomer: 99% ee [Daicel CHIRALPAK AS-H, 5% to 50% iPrOH, 28 min, 1 mL/min, *t*₁=8.14 min, *t*₂=9.33 min]. White solid (mp 38–42 °C). [α]_D²² +59.5° (c0.41, CH₂Cl₂). ¹H NMR (500 MHz, CDCl₃) δ 7.13–7.06 (m, 8H), 7.00–6.98 (m, 4H), 4.93–4.89 (m, 1H), 4.66–4.63 (m, 1H), 4.44–4.41 (m, 1H), 4.27–4.24 (m, 1H), 4.02 (s, 3H), 3.54 (s, 3H), 3.03 (s, 3H). ¹³C NMR (125 MHz, CDCl₃) δ 190.8, 173.7, 143.0, 139.6, 139.4, 128.6, 128.2, 128.0,

127.9, 127.8, 126.3, 126.1, 125.9, 61.4, 46.2, 45.4, 43.8, 43.3, 35.9, 32.5. HRMS (ESI) calculated for $[C_{24}H_{26}N_3O_3]$ ($M+H^+$) requires m/z 404.1969, found 404.1966.

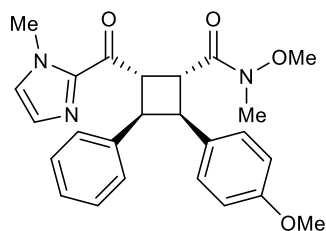
***N*-methoxy-*N*-methyl-2-(1-methyl-1*H*-imidazole-2-carbonyl)-3-phenyl-4-(2-**



(trifluoromethyl)phenyl)cyclobutane-1-carboxamide (3.37):

Prepared according to the general procedure for isolation-scale asymmetric experiments using 42.4 mg (0.2 mmol, 1.0 equiv) (*E*)-1-(1-methyl-1*H*-imidazol-2-yl)-3-phenylprop-2-en-1-one, 30.5 mg (0.04 mmol, 0.2 equiv) (**R**)-**3.2**, 156.9 mg (0.6 mmol, 3.0 equiv) (*E*)-*N*-methoxy-*N*-methyl-3-(2-(trifluoromethyl)phenyl)acrylamide and toluene (8 mL). The resulting material was purified by FCC eluting from a gradient of 30% → 70% EtOAc in hexanes to give 68.5 mg (0.15 mmol, 73% yield) of two diastereomers (>20:1 d.r.). Major diastereomer: 97% ee [Daicel CHIRALPAK OD-H, 5% to 50% *i*PrOH, 28 min, 1 mL/min, $t_1=9.30$ min, $t_2=10.95$ min]. White solid (mp 62–65 °C). $[\alpha]_D^{22} +56.0^\circ$ (c0.20, CH_2Cl_2). 1H NMR (500 MHz, $CDCl_3$) δ 7.49 (d, $J = 7.8$ Hz, 1H), 7.32–7.26 (m, 2H), 7.14 (t, $J = 7.5$ Hz, 1H), 7.16–7.00 (m, 7H), 5.00–4.96 (m, 1H), 4.75–4.72 (m, 1H), 4.64–4.61 (m, 1H), 4.50–4.46 (m, 1H), 4.03 (s, 3H), 3.50 (s, 3H), 3.01 (s, 3H). ^{13}C NMR (125 MHz, $CDCl_3$) δ 190.5, 173.1, 142.93, 138.8, 138.2, 131.1 129.1, 128.9 (q, $J = 29.7$ Hz), 128.6, 127.9, 127.9, 126.5, 126.3, 126.1, 125.7 (q, $J = 5.8$ Hz), 124.3 (q, $J = 274.1$ Hz), 61.3, 45.8, 43.9, 43.1, 41.3, 36.0, 32.5. ^{19}F NMR (377 MHz, $CDCl_3$) δ –58.9. HRMS (ESI) calculated for $[C_{25}H_{25}F_3N_3O_3]^+$ ($M+H^+$) requires m/z 472.1843, found 472.1839.

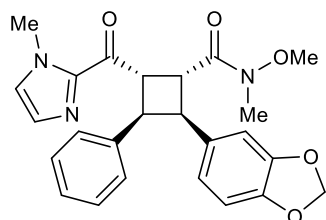
***N*-methoxy-2-(4-methoxyphenyl)-*N*-methyl-4-(1-methyl-1*H*-imidazole-2-carbonyl)-3-**



phenylcyclobutane-1-carboxamide (3.30): Prepared according to the general procedure for isolation-scale asymmetric experiments using 42.4 mg (0.2 mmol, 1.0 equiv) (*E*)-1-(1-methyl-1*H*-imidazol-2-yl)-3-

phenylprop-2-en-1-one, 32.1 mg (0.04 mmol, 0.2 equiv) (**R**)-**3.2**, 135.2 mg (0.6 mmol, 3.0 equiv) (*E*)-*N*-methoxy-3-(4-methoxyphenyl)-*N*-methylacrylamide and toluene (8 mL). The resulting material was purified by FCC eluting from a gradient of 30% → 100% EtOAc in hexanes to give 68.4 mg (0.16 mmol, 79% yield) of two diastereomers (7:1 d.r.). Major diastereomer: 99% ee [Daicel CHIRALPAK AS-H, 5% to 50% iPrOH, 28 min, 1 mL/min, $t_1=11.56$ min, $t_2=13.87$ min]. White solid (mp 45–50 °C). $[\alpha]_D^{22} +40.0^\circ$ (c0.34, CH₂Cl₂). ¹H NMR (500 MHz, CDCl₃) δ 7.11–7.08 (m, 3H), 7.04–7.02 (m, 1H), 7.01–6.96 (m, 5H), 6.66 (d, $J = 8.7$ Hz, 2H), 4.91–4.87 (m, 1H), 4.63–4.59 (m, 1H), 4.38–4.34 (m, 1H), 4.21–4.18 (m, 1H), 4.03 (s, 3H), 3.70 (s, 3H), 3.53 (s, 3H), 3.02 (s, 3H). ¹³C NMR (125 MHz, CDCl₃) δ 190.9, 173.8, 157.9, 143.1, 139.6, 131.8, 129.3, 128.6, 128.0, 127.8, 126.2, 125.8, 113.3, 61.4, 55.1, 46.1, 44.8, 44.4, 43.3, 35.9, 32.5. HRMS (ESI) calculated for [C₂₅H₂₈N₃O₄]⁺ (M+H⁺) requires m/z 434.2074, found 434.2069.

2-(benzo[*d*][1,3]dioxol-5-yl)-*N*-methoxy-*N*-methyl-4-(1-methyl-1*H*-imidazole-2-carbonyl)-3-



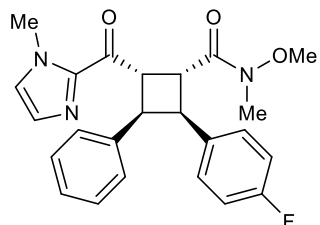
phenylcyclobutane-1-carboxamide (3.38): Prepared according to the

general procedure for isolation-scale asymmetric experiments using

42.4 mg (0.2 mmol, 1.0 equiv) (*E*)-1-(1-methyl-1*H*-imidazol-2-yl)-3-phenylprop-2-en-1-one, 31.1 mg (0.04 mmol, 0.2 equiv) (**R**)-**3.2**, 142.0 mg (0.6 mmol, 3.0 equiv) (*E*)-3-(benzo[*d*][1,3]dioxol-5-yl)-*N*-methoxy-*N*-methylacrylamide and toluene (8 mL). The resulting material was purified by FCC eluting from a gradient of 30% → 100% EtOAc in hexanes to give 49.4 mg (0.11 mmol, 55% yield) of two diastereomers (3:1 d.r.). Major diastereomer: 96% ee [Daicel CHIRALPAK AS-H, 5% to 50% iPrOH, 28 min, 1 mL/min, $t_1=13.20$ min, $t_2=16.17$ min]. White solid (mp 39–43 °C). $[\alpha]_D^{22} +51.4^\circ$ (c0.72, CH₂Cl₂). ¹H NMR (500 MHz, CDCl₃) δ 7.14–7.11 (m, 2H), 7.08–7.02 (m, 4H), 6.99 (s, 1H), 6.58–6.53 (m, 3H), 5.82 (s, 2H), 4.89–4.85 (m, 1H), 4.60–4.56 (m, 1H), 4.33–4.31 (m, 1H), 4.20–4.16 (m, 1H), 4.02 (s, 3H), 3.57 (s, 3H),

3.02 (s, 3H). ^{13}C NMR (125 MHz, CDCl_3) δ 190.9, 173.7, 147.5, 146.0, 143.2, 139.6, 133.9, 128.8, 128.1, 128.1, 126.5, 126.1, 121.6, 108.9, 107.9, 100.9, 61.6, 46.3, 45.4, 44.4, 43.6, 36.1, 32.7. HRMS (ESI) calculated for $[\text{C}_{25}\text{H}_{26}\text{N}_3\text{O}_5]^+$ ($\text{M}+\text{H}^+$) requires m/z 448.1867, found 448.1863.

2-(4-fluorophenyl)-*N*-methoxy-*N*-methyl-4-(1-methyl-1*H*-imidazole-2-carbonyl)-3-

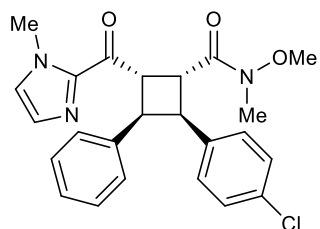


phenylcyclobutane-1-carboxamide (3.31): Prepared according to the general procedure for isolation-scale asymmetric experiments using 42.4 mg (0.2 mmol, 1.0 equiv) (*E*)-1-(1-methyl-1*H*-imidazol-2-yl)-3-

phenylprop-2-en-1-one, 30.2 mg (0.04 mmol, 0.2 equiv) (**R**)-**3.2**, 126.2 mg (0.6 mmol, 3.0 equiv) (*E*)-3-(4-fluorophenyl)-*N*-methoxy-*N*-methylacrylamide and toluene (8 mL). The resulting material was purified by FCC eluting from a gradient of 30% \rightarrow 70% EtOAc in hexanes to give 65.1 mg (0.15 mmol, 77% yield) of two diastereomers (18:1 d.r.). Major diastereomer: 98% ee [Daicel CHIRALPAK AD-H, 5% to 50% *i*PrOH, 28 min, 1 mL/min, $t_1=18.46$ min, $t_2=21.15$ min].

White solid (mp 41–44 °C). $[\alpha]_{\text{D}}^{22} +50.9^\circ$ (c0.11, CH_2Cl_2). ^1H NMR (500 MHz, CDCl_3) δ 7.12–7.08 (m, 3H), 7.05–6.98 (m, 6H), 6.80 (t, $J = 8.8$ Hz, 2H), 4.91 (t, $J = 9.3$ Hz, 1H), 4.60 (t, $J = 9.4$ Hz, 1H), 4.36–4.33 (m, 1H), 4.25 (dd, $J = 10.3, 6.2$ Hz, 1H), 4.02 (s, 3H), 3.55 (s, 3H), 3.03 (s, 3H). ^{13}C NMR (125 MHz, CDCl_3) δ 190.7, 173.5, 161.3 (d, $J = 244.6$ Hz), 142.9, 139.2, 135.4, 129.7, 129.6, 128.6, 127.9, 126.4, 126.1, 114.7 (d, $J = 21.2$ Hz), 61.4, 46.0, 44.7, 44.1, 43.3, 35.9, 32.5. ^{19}F NMR (377 MHz, CDCl_3) δ –116.8. HRMS (ESI) calculated for $[\text{C}_{24}\text{H}_{25}\text{FN}_3\text{O}_3]^+$ ($\text{M}+\text{H}^+$) requires m/z 422.1875, found 422.1870.

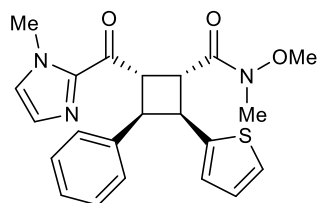
2-(4-chlorophenyl)-*N*-methoxy-*N*-methyl-4-(1-methyl-1*H*-imidazole-2-carbonyl)-3-



phenylcyclobutane-1-carboxamide (3.32): Prepared according to the general procedure for isolation-scale asymmetric experiments using 42.4 mg (0.2 mmol, 1.0 equiv) (*E*)-1-(1-methyl-1*H*-imidazol-2-yl)-3-

phenylprop-2-en-1-one, 31.0 mg (0.04 mmol, 0.2 equiv) (**R**)-**3.2**, 136.7 mg (0.6 mmol, 3.0 equiv) (*E*)-3-(4-chlorophenyl)-*N*-methoxy-*N*-methylacrylamide and toluene (8 mL). The resulting material was purified by FCC eluting from a gradient of 30% → 70% EtOAc in hexanes to give 70.4 mg (0.16 mmol, 80% yield) of two diastereomers (7:1 d.r.). Major diastereomer: 97% ee [Daicel CHIRALPAK OD-H, 5% to 50% iPrOH, 28 min, 1 mL/min, $t_1=13.47$ min, $t_2=15.08$ min]. White solid (mp 65–69 °C). $[\alpha]_D^{22} +75.7^\circ$ (c1.34, CH₂Cl₂). ¹H NMR (500 MHz, CDCl₃) δ 7.13–7.06 (m, 5H), 7.05–7.03 (m, 1H), 7.00–6.96 (m, 5H), 4.90 (t, $J = 9.2$ Hz, 1H), 4.61 (t, $J = 9.4$ Hz, 1H), 4.35–4.32 (m, 1H), 4.24 (dd, $J = 10.5, 6.3$ Hz, 1H), 4.02 (s, 3H), 3.55 (s, 3H), 3.03 (s, 3H). ¹³C NMR (125 MHz, CDCl₃) δ 190.6, 173.4, 142.9, 139.1, 138.3, 131.9, 129.5, 128.7, 128.1, 128.0, 127.9, 126.4, 126.1, 61.4, 46.1, 44.8, 43.9, 43.3, 35.9, 32.5. HRMS (ESI) calculated for [C₂₄H₂₄ClN₃O₃Na]⁺ (M+Na⁺) requires m/z 460.1398, found 460.1393.

***N*-methoxy-*N*-methyl-2-(1-methyl-1*H*-imidazole-2-carbonyl)-3-phenyl-4-(thiophen-2-**

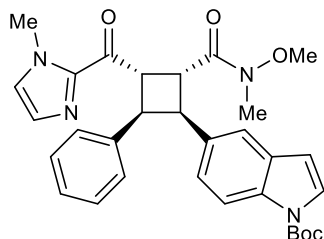


yl)cyclobutane-1-carboxamide: Prepared according to the general procedure for isolation-scale asymmetric experiments using 42.4 mg (0.2 mmol, 1.0 equiv) (*E*)-1-(1-methyl-1*H*-imidazol-2-yl)-3-

phenylprop-2-en-1-one, 31.2 mg (0.04 mmol, 0.2 equiv) (**R**)-**3.2**, 119.5 mg (0.6 mmol, 3.0 equiv) (*E*)-*N*-methoxy-*N*-methyl-3-(thiophen-2-yl)acrylamide and toluene (8 mL). The resulting material was purified by FCC eluting from a gradient of 30% → 70% EtOAc in hexanes to give 47.3 mg (0.12 mmol, 58% yield) of two diastereomers (4:1 d.r.). Major diastereomer: 98% ee [Daicel CHIRALPAK AS-H, 5% to 50% iPrOH, 28 min, 1 mL/min, $t_1=11.34$ min, $t_2=12.71$ min]. $[\alpha]_D^{22} +65.3^\circ$ (c1.05, CH₂Cl₂). ¹H NMR (500 MHz, CDCl₃) δ 7.18–7.14 (m, 2H), 7.12–7.08 (m, 4H), 7.00–6.98 (m, 2H), 6.77 (dd, $J = 5.1, 3.5$ Hz, 1H), 6.70–6.69 (m, 1H), 4.98–4.94 (m, 1H), 4.63–4.59 (m, 1H), 4.47–4.44 (m, 1H), 4.36–4.33 (m, 1H), 4.01 (s, 3H), 3.59 (s, 3H), 3.03 (s, 3H). ¹³C

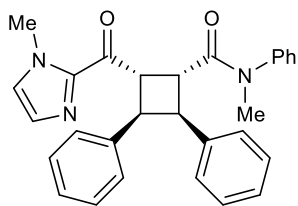
NMR (125 MHz, CDCl₃) δ 190.7, 173.2, 143.6, 143.1, 139.1, 128.9, 128.1, 128.1, 126.6, 126.6, 126.5, 125.3, 124.1, 61.6, 46.4, 45.9, 44.1, 41.3, 36.1, 32.7. HRMS (ESI) calculated for [C₂₂H₂₃N₃O₃SNa]⁺ (M+Na⁺) requires m/z 432.1352, found 432.1347.

***tert*-butyl 5-(2-(methoxy(methyl)carbamoyl)-3-(1-methyl-1*H*-imidazole-2-carbonyl)-4-**



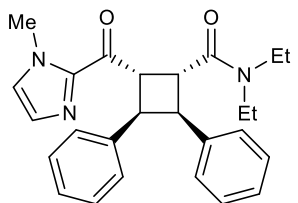
phenylcyclobutyl)-1*H*-indole-1-carboxylate (3.39): Prepared according to the general procedure for isolation-scale asymmetric experiments using 42.4 mg (0.2 mmol, 1.0 equiv) (*E*)-1-(1-methyl-1*H*-imidazol-2-yl)-3-phenylprop-2-en-1-one, 30.7 mg (0.04 mmol, 0.2

equiv) (***R***-**3.2**, 200.2 mg (0.6 mmol, 3.0 equiv) *tert*-butyl (*E*)-5-(3-(methoxy(methyl)amino)-3-oxoprop-1-en-1-yl)-1*H*-indole-1-carboxylate and toluene (8 mL). The resulting material was purified by FCC eluting from a gradient of 30% \rightarrow 100% EtOAc in hexanes to give 69.4 mg (0.13 mmol, 64% yield) of two diastereomers (3:1 d.r.). Major diastereomer: 99% ee [Daicel CHIRALPAK AD-H, 5% to 50% *i*PrOH, 28 min, 1 mL/min, t_1 =15.67 min, t_2 =25.21 min]. White solid (mp 81–83 °C). $[\alpha]_D^{22} +74.2^\circ$ (c0.45, CH₂Cl₂). ¹H NMR (500 MHz, CDCl₃) δ 7.48 (d, J = 7.9 Hz, 1H), 7.48 (d, J = 3.8 Hz, 1H), 7.31 (d, J = 1.8 Hz, 1H), 7.10–6.95 (m, 8H), 6.42 (d, J = 3.7 Hz, 1H), 4.97–4.93 (m, 1H), 4.71–4.67 (m, 1H), 4.46–4.44 (m, 1H), 4.34–4.31 (m, 1H), 4.03 (s, 3H), 3.51 (s, 3H), 3.03 (s, 3H). ¹³C NMR (125 MHz, CDCl₃) δ 191.2, 174.0, 149.9, 143.3, 139.8, 134.3, 133.9, 130.5, 128.7, 128.1, 128.0, 126.4, 126.0, 125.1, 120.5, 114.7, 107.4, 83.6, 61.6, 46.5, 45.7, 44.9, 43.5, 36.1, 32.7, 28.4. HRMS (ESI) calculated for [C₃₁H₃₅N₄O₅]⁺ (M+H⁺) requires m/z 543.2602, found 543.2597.

***N*-methyl-2-(1-methyl-1*H*-imidazole-2-carbonyl)-*N*,3,4-triphenylcyclobutane-1-**

carboxamide (3.33): Prepared according to the general procedure for isolation-scale asymmetric experiments using 42.4 mg (0.2 mmol, 1.0 equiv) (*E*)-1-(1-methyl-1*H*-imidazol-2-yl)-3-phenylprop-2-en-1-one,

30.7 mg (0.04 mmol, 0.2 equiv) (***R***)-**3.2**, 142.6 mg (0.6 mmol, 3.0 equiv) *N*-methyl-*N*-phenylcinnamamide and toluene (8 mL). The resulting material was purified by FCC eluting from a gradient of 30% → 50% EtOAc in hexanes to give 51.5 mg (0.12 mmol, 57% yield) of two diastereomers (>20:1 d.r.). Major diastereomer: 98% ee [Daicel CHIRALPAK AS-H, 5% to 50% iPrOH, 28 min, 1 mL/min, $t_1=7.33$ min, $t_2=9.12$ min]. White solid (mp 55–58 °C). $[\alpha]_D^{22} +115.6^\circ$ (c0.32, CH₂Cl₂). ¹H NMR (500 MHz, CDCl₃) δ 7.25–7.22 (m, 3H), 7.16–7.15 (m, 2H), 7.13–7.13 (m, 1H), 7.02–6.93 (m, 7H), 6.85–6.83 (m, 2H), 6.69–6.68 (m, 2H), 4.77–4.74 (m, 1H), 4.40–4.36 (m, 1H), 4.18–4.13 (m, 2H), 4.08 (s, 3H), 3.01 (s, 3H). ¹³C NMR (125 MHz, CDCl₃) δ 190.9, 172.0, 143.7, 143.2, 139.5, 138.9, 129.5, 128.2, 128.1, 127.9, 127.7, 127.6, 127.6, 127.3, 126.0, 125.9, 125.7, 46.7, 46.5, 45.1, 42.5, 37.1, 35.8. HRMS (ESI)⁺ calculated for [C₂₉H₂₇N₃O₂Na]⁺ (M+Na⁺) requires m/z 472.1996, found 472.1988.

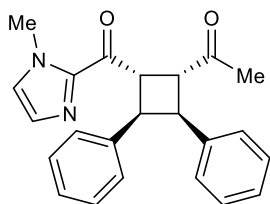
***N,N*-diethyl-2-(1-methyl-1*H*-imidazole-2-carbonyl)-3,4-diphenylcyclobutane-1-**

carboxamide (3.34): Prepared according to the general procedure for isolation-scale asymmetric experiments using 42.4 mg (0.2 mmol, 1.0 equiv) (*E*)-1-(1-methyl-1*H*-imidazol-2-yl)-3-phenylprop-2-en-1-one,

31.1 mg (0.04 mmol, 0.2 equiv) (***R***)-**3.2**, 123.2 mg (0.6 mmol, 3.0 equiv) *N,N*-diethylcinnamamide and toluene (8 mL). The resulting material was purified by FCC eluting from a gradient of 50% → 70% EtOAc in hexanes to give 55.4 mg (0.13 mmol, 67% yield) of two diastereomers (>20:1 d.r.). Major diastereomer: 98% ee [Daicel CHIRALPAK AD, 5% to 50% iPrOH, 28 min, 1

mL/min, $t_1=13.36$ min, $t_2=20.66$ min]. White solid (mp 137–139 °C). $[\alpha]_D^{22} +92.8^\circ$ (c0.36, CH_2Cl_2). ^1H NMR (500 MHz, CDCl_3) δ 7.14–7.11 (m, 2H), 7.08–7.04 (m, 6H), 7.01–6.98 (m, 1H), 6.97–6.96 (m, 1H), 6.95–6.93 (m, 2H), 4.81 (t, $J = 9.6$ Hz, 1H), 4.70 (t, $J = 9.8$ Hz, 1H), 4.30 (dd, $J = 10.0, 5.1$ Hz, 1H), 4.06 (dd, $J = 10.3, 5.0$ Hz, 1H), 4.03 (s, 3H), 3.41–3.30 (m, 2H), 3.02–2.93 (m, 2H), 1.03 (t, $J = 7.1$ Hz, 3H), 0.80 (t, $J = 7.1$ Hz, 3H). ^{13}C NMR (125 MHz, CDCl_3) δ 191.0, 171.3, 143.1, 139.9, 139.7, 128.3, 128.2, 128.0, 127.8, 127.7, 126.3, 125.9, 125.7, 46.6, 46.3, 45.7, 42.5, 42.1, 40.2, 35.7, 14.4, 12.5. HRMS (ESI) calculated for $[\text{C}_{26}\text{H}_{30}\text{N}_3\text{O}_2]^+$ ($\text{M}+\text{H}^+$) requires m/z 416.2333, found 416.2327.

1-(2-(1-methyl-1*H*-imidazole-2-carbonyl)-3,4-diphenylcyclobutyl)ethan-1-one (3.35):

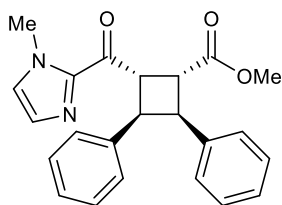


Prepared according to the general procedure for isolation-scale asymmetric experiments using 42.4 mg (0.2 mmol, 1.0 equiv) (*E*)-1-(1-methyl-1*H*-imidazol-2-yl)-3-phenylprop-2-en-1-one, 30.1 mg (0.04 mmol, 0.2 equiv)

(*R*)-**3.2**, 90.1 mg (0.6 mmol, 3.0 equiv) (*E*)-4-phenylbut-3-en-2-one and toluene (8 mL). The resulting material was purified by FCC eluting from a gradient of 30% → 50% EtOAc in hexanes to give 48.4 mg (0.14 mmol, 68% yield) of two diastereomers (4:1 d.r.). Major diastereomer: 90% ee [Daicel CHIRALPAK AD, 5% to 50% iPrOH, 28 min, 1 mL/min, $t_1=11.67$ min, $t_2=15.00$ min].

Isolated as a low-melting semi-solid. $[\alpha]_D^{22} +78.3^\circ$ (c0.24, CH_2Cl_2). ^1H NMR (500 MHz, CDCl_3) δ 7.15–7.13 (m, 2H), 7.10–7.00 (m, 8H), 6.96–6.94 (m, 2H), 4.89–4.85 (m, 1H), 4.52–4.48 (m, 1H), 4.30 (dd, $J = 9.9, 6.5$ Hz, 1H), 4.15 (dd, $J = 10.3, 6.5$ Hz, 1H), 4.05 (s, 3H), 2.04 (s, 3H). ^{13}C NMR (125 MHz, CDCl_3) δ 207.4, 191.4, 143.1, 139.1, 138.9, 128.9, 128.2, 128.1, 127.9, 127.9, 126.6, 126.5, 126.1, 53.8, 46.1, 45.8, 42.7, 35.9, 28.9. HRMS (ESI) calculated for $[\text{C}_{23}\text{H}_{23}\text{N}_2\text{O}_2]^+$ ($\text{M}+\text{H}^+$) requires m/z 359.1754, found 359.1750.

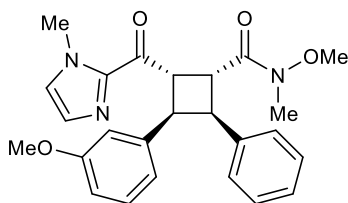
methyl 2-(1-methyl-1*H*-imidazole-2-carbonyl)-3,4-diphenylcyclobutane-1-carboxylate



(3.36): Prepared according to the general procedure for isolation-scale asymmetric experiments with the exception of irradiating at $-78\text{ }^{\circ}\text{C}$ using 42.4 mg (0.2 mmol, 1.0 equiv) (*E*)-1-(1-methyl-1*H*-imidazol-2-yl)-3-phenylprop-2-en-1-one, 30.5 mg (0.04 mmol, 0.2 equiv) (**R**)-**3.2**, 127.2 mg (0.6 mmol, 3.0 equiv) methyl cinnamate and toluene (8 mL). The resulting material was purified by FCC eluting from a gradient of 30% \rightarrow 50% EtOAc in hexanes to give 53.4 mg (0.14 mmol, 71% yield) of two diastereomers (3:1 d.r.). Major diastereomer: 81% ee [Daicel CHIRALPAK AS-H, 5% to 50% *i*PrOH, 28 min, 1 mL/min, $t_1=8.76$ min, $t_2=10.01$ min]. White solid (mp 62–65 $^{\circ}\text{C}$). $[\alpha]_{\text{D}}^{22} +6.4^{\circ}$ (c0.25, CH_2Cl_2). ^1H NMR (500 MHz, CDCl_3) δ 7.14–7.00 (m, 12H), 5.01 (dd, $J = 10.5, 7.2$ Hz, 1H), 4.55 (dd, $J = 10.3, 7.1$ Hz, 1H), 4.35 (dd, $J = 10.1, 7.2$ Hz, 1H), 4.14 (dd, $J = 10.5, 7.2$ Hz, 1H), 4.05 (s, 3H), 3.55 (s, 3H).

8.71 (dd, $J = 2.2$ Hz, 1H). ^{13}C NMR (125 MHz, CDCl_3) δ 190.6, 173.1, 142.9, 138.9, 138.8, 129.2, 128.1, 128.0, 127.9, 127.9, 126.9, 126.3, 126.2, 51.8, 46.1, 45.3, 45.2, 43.4, 36.0. HRMS (ESI) calculated for $[\text{C}_{23}\text{H}_{23}\text{N}_2\text{O}_3]^+$ ($\text{M}+\text{H}^+$) requires m/z 375.1703, found 375.1698.

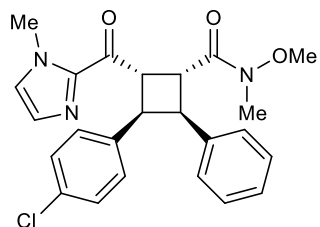
***N*-methoxy-3-(3-methoxyphenyl)-*N*-methyl-2-(1-methyl-1*H*-imidazole-2-carbonyl)-4-**



phenylcyclobutane-1-carboxamide: Prepared according to the general procedure for isolation-scale asymmetric experiments using 48.5 mg (0.2 mmol, 1.0 equiv) (*E*)-3-(3-methoxyphenyl)-1-(1-methyl-1*H*-imidazol-2-yl)prop-2-en-1-one, 30.4 mg (0.04 mmol, 0.2 equiv) (**R**)-**3.2**, 115.5 mg (0.6 mmol, 3.0 equiv) *N*-methoxy-*N*-methylcinnamamide and toluene (8 mL). The resulting material was purified by FCC eluting from a gradient of 30% \rightarrow 100% EtOAc in hexanes to give 63.7 mg (0.15 mmol, 74% yield) of two diastereomers (8:1 d.r.). Major diastereomer: 99% ee [Daicel

CHIRALPAK AS-H, 5% to 50% iPrOH, 28 min, 1 mL/min, $t_1=11.44$ min, $t_2=12.37$ min]. White solid (mp 32–35 °C). $[\alpha]_D^{22} +41.3^\circ$ (c0.30, CH₂Cl₂). ¹H NMR (500 MHz, CDCl₃) δ 7.15–7.12 (m, 2H), 7.09–7.05 (m, 4H), 7.02–6.98 (m, 2H), 6.62 (d, $J = 7.6$ Hz, 1H), 6.56 (dd, $J = 8.2, 2.6$ Hz, 1H), 6.49 (s, 1H), 4.89 (t, $J = 9.3$ Hz, 1H), 4.62 (t, $J = 9.6$ Hz, 1H), 4.44–4.38 (m, 1H), 4.26–4.23 (m, 1H), 4.03 (s, 3H), 3.59 (s, 3H), 3.54 (s, 3H), 3.04 (s, 3H). ¹³C NMR (125 MHz, CDCl₃) δ 190.8, 173.8, 159.2, 143.0, 141.1, 139.7, 128.7, 128.6, 128.3, 128.0, 126.3, 126.2, 120.4, 113.5, 111.9, 61.4, 55.0, 46.4, 45.4, 43.8, 43.4, 35.9, 32.6. HRMS (ESI) calculated for [C₂₅H₂₈N₃O₄]⁺ (M+H⁺) requires m/z 434.2074, found 434.2067.

3-(4-chlorophenyl)-*N*-methoxy-*N*-methyl-2-(1-methyl-1*H*-imidazole-2-carbonyl)-4-

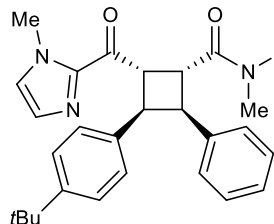


phenylcyclobutane-1-carboxamide (3.41): Prepared according to the general procedure for isolation-scale asymmetric experiments using 49.3 mg (0.2 mmol, 1.0 equiv) (*E*)-3-(4-chlorophenyl)-1-(1-methyl-

1*H*-imidazol-2-yl)prop-2-en-1-one, 31.3 mg (0.04 mmol, 0.2 equiv) (**R**)-**3.2**, 114.7 mg (0.6 mmol, 3.0 equiv *N*-methoxy-*N*-methylcinnamamide and toluene (8 mL). The resulting material was purified by FCC eluting from a gradient of 30% → 70% EtOAc in hexanes to give 67.8 mg (0.16 mmol, 77% yield) of two diastereomers (>20:1 d.r.). Major diastereomer: 99% ee [Daicel CHIRALPAK AS-H, 5% to 50% iPrOH, 28 min, 1 mL/min, $t_1=9.99$ min, $t_2=12.26$ min]. $[\alpha]_D^{22} +56.2^\circ$ (c0.21, CH₂Cl₂). ¹H NMR (500 MHz, CDCl₃) δ 7.16–7.13 (m, 2H), 7.09–7.04 (m, 6H), 7.00 (s, 1H), 6.90 (d, $J = 8.1$ Hz, 2H), 4.82 (t, $J = 9.4$ Hz, 1H), 4.61 (t, $J = 9.6$ Hz, 1H), 4.42–4.38 (m, 1H), 4.23–4.20 (m, 1H), 4.02 (s, 3H), 3.54 (s, 3H), 3.04 (s, 3H). ¹³C NMR (125 MHz, CDCl₃) δ 190.6, 173.6, 142.9, 139.3, 138.1, 131.7, 129.3, 128.7, 128.2, 128.1, 127.9, 126.4, 61.4, 46.5,

45.4, 43.9, 42.8, 35.9, 32.6. HRMS (ESI) calculated for $[C_{24}H_{25}ClN_3O_3]^+$ ($M+H^+$) requires m/z 438.1579, found 438.1574.

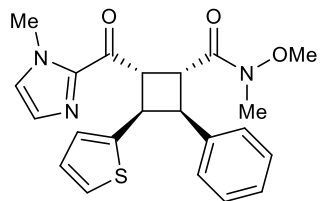
3-(4-(tert-butyl)phenyl)-*N*-methoxy-*N*-methyl-2-(1-methyl-1*H*-imidazole-2-carbonyl)-4-



phenylcyclobutane-1-carboxamide: Prepared according to the general procedure for isolation-scale asymmetric experiments using 53.7 mg (0.2 mmol, 1.0 equiv) (*E*)-3-(4-(*tert*-butyl)phenyl)-1-(1-

methyl-1*H*-imidazol-2-yl)prop-2-en-1-one, 30.7 mg (0.04 mmol, 0.2 equiv) (***R***)-**3.2**, 116.4 mg (0.6 mmol, 3.0 equiv) *N*-methoxy-*N*-methylcinnamamide and toluene (8 mL). The resulting material was purified by FCC eluting from a gradient of 30% → 100% EtOAc in hexanes to give 51.4 mg (0.11 mmol, 56% yield) of two diastereomers (>20:1 d.r.). Major diastereomer: 85% ee [Daicel CHIRALPAK OD-H, 5% to 50% *i*PrOH, 28 min, 1 mL/min, $t_1=10.62$ min, $t_2=12.42$ min]. $[\alpha]_D^{22} +18.3^\circ$ (c0.24, CH_2Cl_2). 1H NMR (500 MHz, $CDCl_3$) δ 7.12–7.08 (m, 5H), 7.05–7.04 (m, 3H), 6.98 (s, 1H), 6.91 (d, $J = 8.1$ Hz, 2H), 4.90–4.87 (m, 1H), 4.61–4.57 (m, 1H), 4.43–4.39 (m, 1H), 4.27–4.23 (m, 1H), 4.02 (s, 3H), 3.54 (s, 3H), 3.03 (s, 3H), 1.19 (s, 9H). ^{13}C NMR (125 MHz, $CDCl_3$) δ 191.0, 173.8, 148.6, 143.1, 139.7, 136.3, 128.6, 128.3, 127.8, 127.6, 126.3, 126.0, 124.7, 61.4, 46.4, 45.3, 43.7, 43.1, 35.9, 34.2, 32.6, 31.3. HRMS (ESI) calculated for $[C_{28}H_{34}N_3O_3]^+$ ($M+H^+$) requires m/z 460.2595, found 460.2590.

***N*-methoxy-*N*-methyl-2-(1-methyl-1*H*-imidazole-2-carbonyl)-4-phenyl-3-(thiophen-2-**



yl)cyclobutane-1-carboxamide (3.40): Prepared according to the general procedure for isolation-scale asymmetric experiments using 43.7 mg (0.2 mmol, 1.0 equiv) (*E*)-1-(1-methyl-1*H*-imidazol-2-yl)-3-

(thiophen-2-yl)prop-2-en-1-one, 30.5 mg (0.04 mmol, 0.2 equiv) (***R***)-**3.2**, 115.6 mg (0.6 mmol, 3.0 equiv) *N*-methoxy-*N*-methylcinnamamide and toluene (8 mL). The resulting material was purified

by FCC eluting from a gradient of 30% → 70% EtOAc in hexanes to give 52.4 mg (0.13 mmol, 64% yield) of two diastereomers (5:1 d.r.). Major diastereomer: 97% ee [Daicel CHIRALPAK AD, 5% to 50% iPrOH, 28 min, 1 mL/min, $t_1=19.42$ min, $t_2=23.34$ min]. White solid (mp 107–109 °C). $[\alpha]_D^{22} +45.1^\circ$ (c0.39, CH₂Cl₂). ¹H NMR (500 MHz, CDCl₃) δ 7.20–7.12 (m, 5H), 7.09 (d, $J = 0.9$ Hz, 1H), 6.99 (d, $J = 1.0$ Hz, 1H), 6.96 (dd, $J = 5.2, 1.2$ Hz, 1H), 6.75 (dd, $J = 5.1, 3.5$ Hz, 1H), 6.67 (d, $J = 3.5$ Hz, 1H), 4.81–4.73 (m, 2H), 4.58–4.54 (m, 1H), 4.25–4.22 (m, 1H), 4.03 (s, 3H), 3.57 (s, 3H), 3.00 (s, 3H). ¹³C NMR (125 MHz, CDCl₃) δ 190.1, 173.3, 143.4, 142.9, 139.0, 128.7, 128.1, 128.0, 126.5, 126.4, 126.3, 125.0, 123.9, 61.5, 49.0, 45.9, 43.0, 39.3, 35.9, 32.5. HRMS (ESI) calculated for [C₂₂H₂₄N₃O₃S]⁺ (M+H⁺) requires m/z 410.1533, found 410.1527.

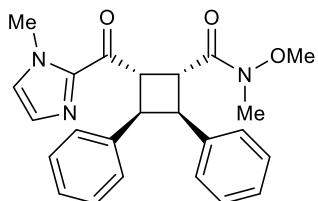
3.5.7 Racemic [2+2] Heterodimerization Photocycloaddition Reactions

General Procedure for Racemic Crossed [2+2] Photoreactions: An 8 mL flame-dried vial was charged with cinnamate (0.3 mmol, 3.0 equiv), (±)-**3.2** (0.02 mmol, 0.2 equiv), and toluene (2 mL). A 4 mL flame-dried vial was charged with cinnamoyl imidazole (0.1 mmol, 1.0 equiv) and toluene (2 mL). Using a syringe pump, the cinnamoyl imidazole solution was added over 22 hours to the cinnamate solution while under irradiation with 2 Kessil H150 Tuna Blue lamps. The reaction was cooled with an air hose (reactions run at approximately 35 °C) and not degassed. After 24 hours of irradiation Et₃N (0.1 mL) was added to the reaction, which decreases broadening in the NMR. The reaction was concentrated and analyzed by ¹H-NMR vs internal standard (phenanthrene) to determine yield and diastereomeric ratio. The crude mixture was purified by FCC eluting from EtOAc in hexanes. The major diastereomer was characterized.

Note: for the racemic reactions we used plastic syringes, however, we observed solid cinnamoyl imidazole behind the syringe plunger after the reaction finished, indicating that not all of the

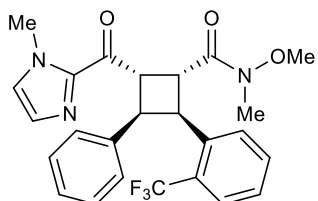
substrate was added to the reaction. This problem was solved in the asymmetric reactions using glass syringes.

***N*-methoxy-*N*-methyl-2-(1-methyl-1*H*-imidazole-2-carbonyl)-3,4-diphenylcyclobutane-1-**



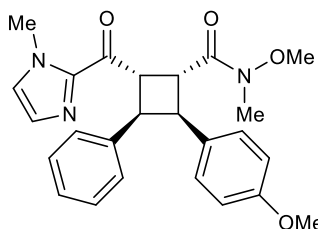
carboxamide: Prepared according to the general procedure for racemic crossed [2+2] photoreactions using 21.4 mg (0.10 mmol) (*E*)-1-(1-methyl-1*H*-imidazol-2-yl)-3-phenylprop-2-en-1-one, 57.5 mg (0.30 mmol) *N*-methoxy-*N*-methylcinnamamide, 15.4 mg (0.02 mmol) **3.2**, and toluene (4 mL). The crude material was purified by FCC eluting from a gradient of 50% → 100% EtOAc in hexanes to give a 74% NMR yield of two diastereomers (8:1 d.r.). Spectroscopic data was consistent with those reported above.

***N*-methoxy-*N*-methyl-2-(1-methyl-1*H*-imidazole-2-carbonyl)-3-phenyl-4-(2-**



(trifluoromethyl)phenyl)cyclobutane-1-carboxamide: Prepared according to the general procedure for racemic crossed [2+2] photoreactions using 20.0 mg (0.09 mmol) (*E*)-1-(1-methyl-1*H*-imidazol-2-yl)-3-phenylprop-2-en-1-one, 78.0 mg (0.30 mmol) (*E*)-*N*-methoxy-*N*-methyl-3-(2-(trifluoromethyl)phenyl)acrylamide, 15.9 mg (0.02 mmol) **3.2**, and toluene (4 mL). The crude material was purified by FCC eluting from a gradient of 50% → 100% EtOAc in hexanes to give a 50% NMR yield of two diastereomers (>20:1 d.r.). Spectroscopic data was consistent with those reported above.

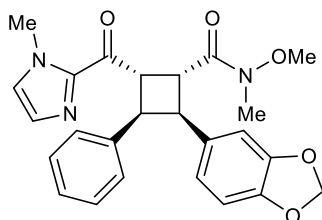
***N*-methoxy-2-(4-methoxyphenyl)-*N*-methyl-4-(1-methyl-1*H*-imidazole-2-carbonyl)-3-**



phenylcyclobutane-1-carboxamide: Prepared according to the general procedure for racemic crossed [2+2] photoreactions using 21.5 mg (0.10 mmol) (*E*)-1-(1-methyl-1*H*-imidazol-2-yl)-3-phenylprop-2-

en-1-one, 67.3 mg (0.30 mmol) (*E*)-*N*-methoxy-3-(4-methoxyphenyl)-*N*-methylacrylamide, 14.9 mg (0.02 mmol) **3.2**, and toluene (4 mL). The crude material was purified by FCC eluting from a gradient of 50% → 100% EtOAc in hexanes to give a 59% NMR yield of two diastereomers (6:1 d.r.). Spectroscopic data was consistent with those reported above.

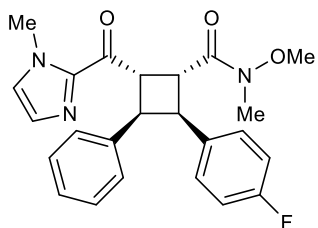
2-(benzo[*d*][1,3]dioxol-5-yl)-*N*-methoxy-*N*-methyl-4-(1-methyl-1*H*-imidazole-2-carbonyl)-3-



phenylcyclobutane-1-carboxamide: Prepared according to the general procedure for racemic crossed [2+2] photoreactions using 21.0 mg (0.10 mmol) (*E*)-1-(1-methyl-1*H*-imidazol-2-yl)-3-phenylprop-2-en-1-one, 69.4 mg (0.30 mmol) (*E*)-3-(benzo[*d*][1,3]dioxol-5-yl)-*N*-

methoxy-*N*-methylacrylamide, 14.7 mg (0.02 mmol) **3.2**, and toluene (4 mL). The crude material was purified by FCC eluting from a gradient of 50% → 100% EtOAc in hexanes to give a 47% NMR yield of two diastereomers (9:1 d.r.). Spectroscopic data was consistent with those reported above.

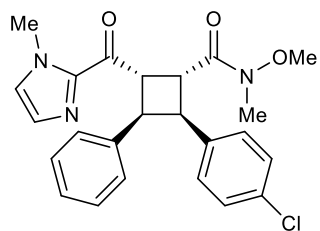
2-(4-fluorophenyl)-*N*-methoxy-*N*-methyl-4-(1-methyl-1*H*-imidazole-2-carbonyl)-3-



phenylcyclobutane-1-carboxamide: Prepared according to the general procedure for racemic crossed [2+2] photoreactions using 20.3 mg (0.10 mmol) (*E*)-1-(1-methyl-1*H*-imidazol-2-yl)-3-phenylprop-2-

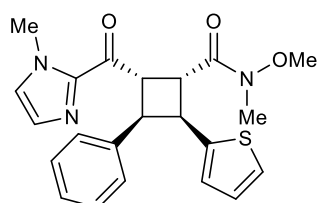
en-1-one, 61.2 mg (0.29 mmol) (*E*)-3-(4-fluorophenyl)-*N*-methoxy-*N*-methylacrylamide, 14.0 mg (0.02 mmol) **3.2**, and toluene (4 mL). The crude material was purified by FCC eluting from a gradient of 50% → 100% EtOAc in hexanes to give a 71% NMR yield of two diastereomers (11:1 d.r.). Spectroscopic data was consistent with those reported above.

2-(4-chlorophenyl)-*N*-methoxy-*N*-methyl-4-(1-methyl-1*H*-imidazole-2-carbonyl)-3-



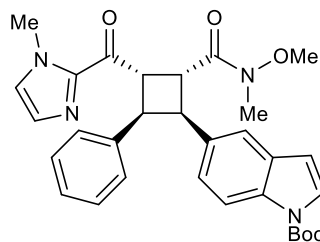
phenylcyclobutane-1-carboxamide: Prepared according to the general procedure for racemic crossed [2+2] photoreactions using 21.2 mg (0.10 mmol) (*E*)-1-(1-methyl-1*H*-imidazol-2-yl)-3-phenylprop-2-en-1-one, 67.7 mg (0.30 mmol) (*E*)-3-(4-chlorophenyl)-*N*-methoxy-*N*-methylacrylamide, 15.4 mg (0.02 mmol) **3.2**, and toluene (4 mL). The crude material was purified by FCC eluting from a gradient of 50% → 100% EtOAc in hexanes to give a 65% NMR yield of two diastereomers (12:1 d.r.). Spectroscopic data was consistent with those reported above.

***N*-methoxy-*N*-methyl-2-(1-methyl-1*H*-imidazole-2-carbonyl)-3-phenyl-4-(thiophen-2-**



yl)cyclobutane-1-carboxamide: Prepared according to the general procedure for racemic crossed [2+2] photoreactions using 22.7 mg (0.11 mmol) (*E*)-1-(1-methyl-1*H*-imidazol-2-yl)-3-phenylprop-2-en-1-one, 66.0 mg (0.33 mmol) (*E*)-*N*-methoxy-*N*-methyl-3-(thiophen-2-yl)acrylamide, 17.1 mg (0.02 mmol) **3.2**, and toluene (4 mL). The crude material was purified by FCC eluting from a gradient of 50% → 100% EtOAc in hexanes to give a 42% NMR yield of two diastereomers (8:1 d.r.). Spectroscopic data was consistent with those reported above.

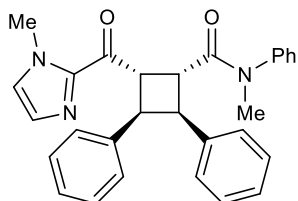
***tert*-butyl 5-(2-(methoxy(methyl)carbamoyl)-3-(1-methyl-1*H*-imidazole-2-carbonyl)-4-**



phenylcyclobutyl)-1*H*-indole-1-carboxylate: Prepared according to the general procedure for racemic crossed [2+2] photoreactions using 21.2 mg (0.10 mmol) (*E*)-1-(1-methyl-1*H*-imidazol-2-yl)-3-phenylprop-2-en-1-one, 97.0 mg (0.29 mmol) *tert*-butyl (*E*)-5-(3-(methoxy(methyl)amino)-3-oxoprop-1-en-1-yl)-1*H*-indole-1-carboxylate, 15.4 mg (0.02 mmol) **3.2**, and toluene (4 mL). The crude material was purified by FCC eluting from a gradient of 50%

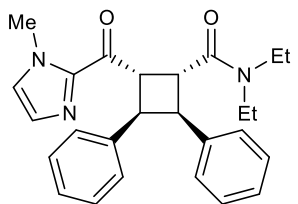
→ 100% EtOAc in hexanes to give a 41% NMR yield of two diastereomers (8:1 d.r.). Spectroscopic data was consistent with those reported above.

***N*-methyl-2-(1-methyl-1*H*-imidazole-2-carbonyl)-*N*,3,4-triphenylcyclobutane-1-**



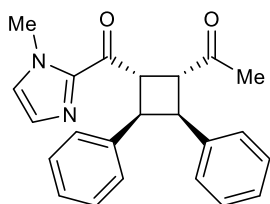
carboxamide: Prepared according to the general procedure for racemic crossed [2+2] photoreactions using 20.7 mg (0.10 mmol) (*E*)-1-(1-methyl-1*H*-imidazol-2-yl)-3-phenylprop-2-en-1-one, 68.0 mg (0.29 mmol) *N*-methyl-*N*-phenylcinnamamide, 15.9 mg (0.02 mmol) **3.2**, and toluene (4 mL). The crude material was purified by FCC eluting from a gradient of 50% → 100% EtOAc in hexanes to give a 55% NMR yield of two diastereomers (8:1 d.r.). Spectroscopic data was consistent with those reported above.

***N,N*-diethyl-2-(1-methyl-1*H*-imidazole-2-carbonyl)-3,4-diphenylcyclobutane-1-**



carboxamide: Prepared according to the general procedure for racemic crossed [2+2] photoreactions using 21.0 mg (0.10 mmol) (*E*)-1-(1-methyl-1*H*-imidazol-2-yl)-3-phenylprop-2-en-1-one, 68.0 mg (0.33 mmol) *N,N*-diethylcinnamamide, 15.0 mg (0.02 mmol) **3.2**, and toluene (4 mL). The crude material was purified by FCC eluting from a gradient of 50% → 100% EtOAc in hexanes to give a 40% NMR yield of two diastereomers (>20:1 d.r.). Spectroscopic data was consistent with those reported above.

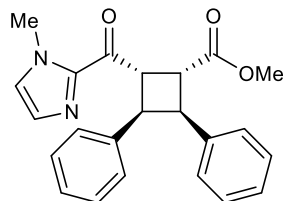
1-(2-(1-methyl-1*H*-imidazole-2-carbonyl)-3,4-diphenylcyclobutyl)ethan-1-one: Prepared



according to the general procedure for racemic crossed [2+2] photoreactions using 21.4 mg (0.05 mmol) (*E*)-1-(1-methyl-1*H*-imidazol-2-yl)-3-phenylprop-2-en-1-one, 73.1 mg (0.50 mmol) (*E*)-4-phenylbut-3-en-2-one, 7.5 mg (0.01 mmol) **3.2**, and toluene (2 mL). The crude material was purified by FCC

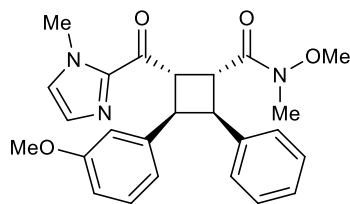
eluting from a gradient of 30% \rightarrow 50% EtOAc in hexanes to give a 46% NMR yield of two diastereomers (4:1 d.r.). Spectroscopic data was consistent with those reported above.

methyl 2-(1-methyl-1*H*-imidazole-2-carbonyl)-3,4-diphenylcyclobutane-1-carboxylate:



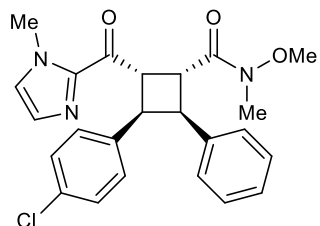
Prepared according to the general procedure for racemic crossed [2+2] photoreactions using 21.0 mg (0.10 mmol) (*E*)-1-(1-methyl-1*H*-imidazol-2-yl)-3-phenylprop-2-en-1-one, 49.6 mg (0.31 mmol) methyl cinnamate, 14.3 mg (0.02 mmol) **3.2**, and toluene (4 mL). The crude material was purified by FCC eluting from a gradient of 30% \rightarrow 70% EtOAc in hexanes to give a 71% NMR yield of two diastereomers (1:1 d.r.). Spectroscopic data was consistent with those reported above.

***N*-methoxy-3-(3-methoxyphenyl)-*N*-methyl-2-(1-methyl-1*H*-imidazole-2-carbonyl)-4-**



phenylcyclobutane-1-carboxamide: Prepared according to the general procedure for racemic crossed [2+2] photoreactions using 25.2 mg (0.10 mmol) (*E*)-3-(3-methoxyphenyl)-1-(1-methyl-1*H*-imidazol-2-yl)prop-2-en-1-one, 59.7 mg (0.31 mmol) *N*-methoxy-*N*-methylcinnamamide, 16.0 mg (0.02 mmol) **3.2**, and toluene (4 mL). The crude material was purified by FCC eluting from a gradient of 30% \rightarrow 70% EtOAc in hexanes to give a 65% NMR yield of two diastereomers (7:1 d.r.). Spectroscopic data was consistent with those reported above.

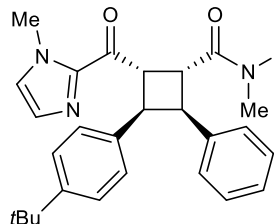
3-(4-chlorophenyl)-*N*-methoxy-*N*-methyl-2-(1-methyl-1*H*-imidazole-2-carbonyl)-4-



phenylcyclobutane-1-carboxamide: Prepared according to the general procedure for racemic crossed [2+2] photoreactions using 23.0 mg (0.10 mmol) (*E*)-3-(4-chlorophenyl)-1-(1-methyl-1*H*-imidazol-2-yl)prop-2-en-1-one, 59.1 mg (0.31 mmol) *N*-methoxy-*N*-methylcinnamamide, 14.3 mg (0.02 mmol) **3.2**, and toluene (4 mL). The crude material was purified by FCC eluting from a gradient

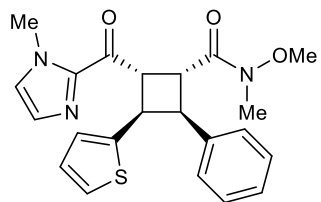
of 50% → 100% EtOAc in hexanes to give a 56% NMR yield of one diastereomer (>20:1 d.r.). Spectroscopic data was consistent with those reported above.

3-(4-(*tert*-butyl)phenyl)-*N*-methoxy-*N*-methyl-2-(1-methyl-1*H*-imidazole-2-carbonyl)-4-



phenylcyclobutane-1-carboxamide: Prepared according to the general procedure for racemic crossed [2+2] photoreactions using 27.9 mg (0.10 mmol) (*E*)-3-(4-(*tert*-butyl)phenyl)-1-(1-methyl-1*H*-imidazol-2-yl)prop-2-en-1-one, 59.2 mg (0.31 mmol) *N*-methoxy-*N*-methylcinnamamide, 15.7 mg (0.02 mmol) **3.2**, and toluene (4 mL). The crude material was purified by FCC eluting from a gradient of 30% → 100% EtOAc in hexanes to give a 48% NMR yield of one diastereomer (>20:1 d.r.). Spectroscopic data was consistent with those reported above.

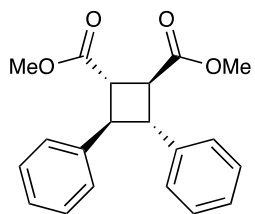
***N*-methoxy-*N*-methyl-2-(1-methyl-1*H*-imidazole-2-carbonyl)-4-phenyl-3-(thiophen-2-**



yl)cyclobutane-1-carboxamide: Prepared according to the general procedure for racemic crossed [2+2] photoreactions using 21.4 mg (0.10 mmol) (*E*)-1-(1-methyl-1*H*-imidazol-2-yl)-3-(thiophen-2-yl)prop-2-en-1-one, 57.5 mg (0.30 mmol) *N*-methoxy-*N*-methylcinnamamide, 15.4 mg (0.02 mmol) **3.2**, and toluene (4 mL). The crude material was purified by FCC eluting from a gradient of 50% → 100% EtOAc in hexanes to give a 41% NMR yield of two diastereomers (5:1 d.r.). Spectroscopic data was consistent with those reported above.

3.5.8 Synthetic Derivatization of Cycloadducts

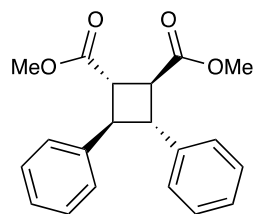
dimethyl 3,4-diphenylcyclobutane-1,2-dicarboxylate: An oven-dried 4 mL dram vial was



charged with 42.1 mg (0.1 mmol, 1 equiv, 92% ee) (3,4-diphenylcyclobutane-1,2-diyl)bis((1-methyl-1*H*-imidazol-2-yl)methanone) and then dissolved in 0.5 mL (0.2 M) CH₂Cl₂. The solution was stirred under

N₂ for 5 minutes, and then 57 μ L (0.5 mmol, 5 equiv) methyl trifluoromethanesulfonate was added. The vial was sealed and stirred for 1.5 hours. Then, the solvent and any remaining methyl trifluoromethanesulfonate was removed on a rotary evaporator, and then dried on high vac for 30 minutes. Once dry, 3.4 mg (0.02 mmol, 0.2 equiv) DABCO and 0.2 mL (4.5 mmol, 45 equiv) methanol were added, and then redissolved in 0.5 mL (0.2 M) CH₂Cl₂. The solution was stirred for 2 hours and then condensed on a rotary evaporator and purified by FCC using a gradient of 1:9 to 2:3 EtOAc/pentanes to give 11.2 mg (0.034 mmol, 35% yield) of product (no erosion of ee occurred). Major diastereomer: 98% ee [Daicel CHIRALPAK IC, 5% to 50% iPrOH, 28 min, 1 mL/min, t₁=7.55 min, t₂=13.03 min]. Clear viscous liquid. $[\alpha]_D^{22}$ -8.0° (c0.45, CH₂Cl₂). ¹H NMR (500 MHz, CDCl₃) δ 7.35-7.27 (m, 8H), 7.27-7.22 (m, 2H), 3.76-3.71 (m, 2H), 3.74 (s, 6H), 3.52-3.47 (m, 2H). ¹³C NMR (125 MHz, CDCl₃) δ 173.0, 141.0, 128.6, 127.1, 126.8, 52.2, 47.3, 44.4. HRMS (ESI) calculated for [C₂₀H₂₀O₄]⁺ (M+H⁺) requires m/z 325.14344, found 325.1430.

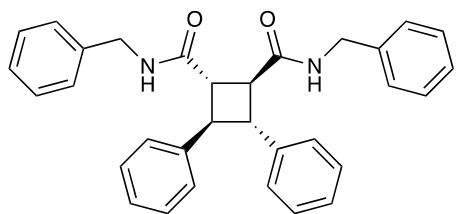
dimethyl 3,4-diphenylcyclobutane-1,2-dicarboxylate: Racemic material prepared according to



the procedure above for the analogous product using 41.8 mg (0.1 mmol, 1 equiv) (3,4-diphenylcyclobutane-1,2-diyl)bis((1-methyl-1*H*-imidazol-2-yl)methanone) and 0.11 mL (1.0 mmol, 10 equiv) methyl

trifluoromethanesulfonate in 0.5 mL (0.2 M) CH₂Cl₂, and then 3.7 mg (0.02 mmol, 0.2 equiv) DABCO and 0.2 mL (4.5 mmol, 45 equiv) methanol in 0.5 mL (0.2 M) CH₂Cl₂. The resulting material was purified by FCC using a gradient of 1:4 to 2:3 EtOAc/pentanes to give 8.3 mg (0.02 mmol, 30% yield) of a single product. Spectroscopic data was consistent with those reported above.

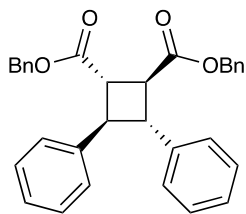
N1,N2-dibenzyl-3,4-diphenylcyclobutane-1,2-dicarboxamide: An oven-dried 4 mL dram vial



was charged with 43.3 mg (0.1 mmol, 1 equiv) 3,4-diphenylcyclobutane-1,2-diyl)bis((1-methyl-1*H*-imidazol-2-yl)methanone and then dissolved in 0.5 mL (0.2 M) DCM.

The solution was stirred under N₂ for 5 minutes, and then 0.11 mL (1.0 mmol, 10 equiv) methyl trifluoromethanesulfonate was added. The vial was sealed and stirred for 1.5 hours. Then, the solvent and any remaining methyl trifluoromethanesulfonate was removed on a rotary evaporator, and then dried on high vac for 30 minutes. Once dry, 0.5 mL (4.5 mmol, 45 equiv) benzylamine was added and then redissolved in 0.5 mL (0.2 M) DCM. The solution was stirred overnight and then worked up with 1M HCl wash x3. The crude product was purified by FCC using a gradient of 3:7 to 2:3 EtOAc/pentanes to give 31.9 mg (0.067 mmol, 67% yield) of product. White powder (mp 173–177 °C). ¹H NMR (500 MHz, CDCl₃) δ 7.34-7.20 (m, 20H), 6.37-6.29 (m, 2H), 4.49 (dd, J = 14.9, 6.0 Hz, 2H), 4.40 (dd, J = 14.9, 5.7 Hz, 2H), 3.77-3.71 (m, 2H), 3.33-3.27 (m, 2H). ¹³C NMR (125 MHz, CDCl₃) δ 172.4, 140.9, 138.0, 128.8, 128.7, 127.49, 127.46, 127.2, 127.0, 46.9, 46.6, 43.5. HRMS (ESI) calculated for [C₃₂H₃₀N₂O₂]⁺ (M+H⁺) requires *m/z* 475.2380, found 475.2379.

dibenzyl 3,4-diphenylcyclobutane-1,2-dicarboxylate: An oven dried 4 mL dram vial was



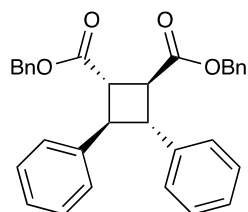
charged with 43.3 mg (0.1 mmol, 1 equiv, 98% ee) (3,4-diphenylcyclobutane-1,2-diyl)bis((1-methyl-1*H*-imidazol-2-yl)methanone)

and then dissolved in 1 mL (0.1 M) phenylmethanol. The glass threads of the

dram vial were then wrapped in one layer of teflon tape, and then a white teflon cap was tightly secured. Finally, teflon tape was wrapped securely around the cap and vial, and the vial was stirred at 150 °C overnight. After the reaction was completed, the phenylmethanol was removed via

distillation using a high vac and gradually warming the crude reaction mixture to 100 °C. Once the majority of the phenylmethanol was removed, the crude product was purified by FCC using a gradient of pure pentane to 1:4 EtOAc/pentanes to give 26.3 mg (0.055 mmol, 54% yield) of product (no erosion of ee occurred). Major diastereomer: 97% ee [Daicel CHIRALPAK AS-H, 5% to 50% iPrOH, 28 min, 1 mL/min, $t_1=6.83$ min, $t_2=7.58$ min]. Light yellow viscous liquid. $[\alpha]_D^{22} -2.5^\circ$ (c0.65, CH₂Cl₂). ¹H NMR (500 MHz, CDCl₃) δ 7.34-7.20 (m, 20H), 5.20 (d, J = 12.4 Hz, 2H), 5.15 (d, J = 12.4 Hz, 2H), 3.81-3.75 (m, 2H), 3.55-3.49 (m, 2H). ¹³C NMR (125 MHz, CDCl₃) δ 172.2, 140.9, 135.7, 128.6, 128.5, 128.2, 127.9, 127.1, 126.9, 66.7, 47.0, 44.8. HRMS (ESI) calculated for [C₃₂H₂₈O₄]⁺ (M+Na⁺) requires m/z 499.1880, found 499.1877.

dibenzyl 3,4-diphenylcyclobutane-1,2-dicarboxylate: Racemic material prepared according to

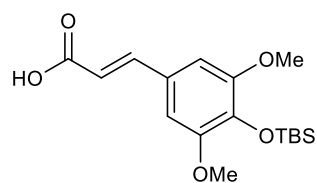


the procedure above for the analogous product using 42.1 mg (0.1 mmol, 1 equiv) (3,4-diphenylcyclobutane-1,2-diyl)bis((1-methyl-1*H*-imidazol-2-yl)methanone) and 1 mL (0.1 M) phenylmethanol. The resulting material was

purified by FCC using a gradient of pure pentane to 1:4 EtOAc/pentanes to give 29.8 mg (0.063 mmol, 65% yield) of product. Spectroscopic data was consistent with those reported above.

3.5.9 Natural Product Synthesis

(*E*)-3-(4-((*tert*-butyldimethylsilyl)oxy)-3,5-dimethoxyphenyl)acrylic acid: A flame dried 25

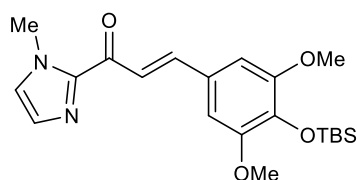


mL RBF was charged with 1.59 g (7.09 mmol, 1.00 equiv) sinapic acid, 1.45 g (21.3 mmol, 3.00 equiv) imidazole, and dissolved in DMF (10 mL). The reaction was cooled to 0 °C prior to adding 2.24 g (14.9 mmol,

2.10 equiv) *tert*-butyldimethylsilyl chloride. The reaction was stirred at room temperature for 4 hours then H₂O (20 mL) was added, and the reaction was extracted with Et₂O (3 x 20 mL). The

combined organic layers were dried over Na₂SO₄, filtered, and concentrated. The residue was dissolved in MeOH (10 mL) and H₂O (5 mL), and 500 mg K₂CO₃ was added. The mixture was stirred for 30 minutes at room temperature. The reaction mixture was diluted with EtOAc (20 mL) and washed with sat. aq. NH₄Cl (1 x 10 mL). The organic layer was dried over Na₂SO₄, filtered, concentrated, and purified by FCC eluting from a gradient of 30% → 50% EtOAc in hexanes to give 1.84 g (5.44 mmol, 77% yield) of a white solid. The compound was consistent with reported spectroscopic data.⁵⁴ ¹H NMR (500 MHz, CDCl₃) δ 7.70 (d, *J* = 15.8 Hz, 1H), 6.76 (s, 2H), 6.32 (d, *J* = 15.8 Hz, 1H), 3.83 (s, 6H), 1.01 (s, 9H), 0.15 (s, 6H).

(*E*)-3-(4-((*tert*-butyldimethylsilyl)oxy)-3,5-dimethoxyphenyl)-1-(1-methyl-1*H*-imidazol-2-



yl)prop-2-en-1-one (3.18): A flame dried 25 mL RBF under N₂ was

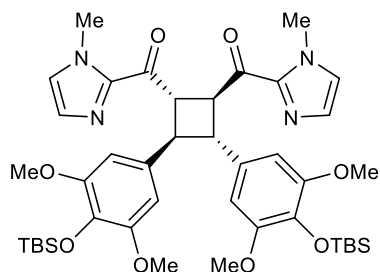
charged 175 mg (2.1 mmol, 2.2 equiv) 1-methyl-1*H*-imidazole and

THF (2 mL). The reaction was cooled to −78 °C for 20 minutes

before adding 0.92 mL (2.3 M, 2.1 mmol, 2.2 equiv) *n*-butyllithium dropwise. The solution was stirred at −78 °C for 5 minutes, then allowed to warm to room temperature for 30 minutes before being cooled to −78 °C for 20 minutes. To the reaction was added 327 mg (1.0 mmol, 1.0 equiv) (*E*)-3-(4-((*tert*-butyldimethylsilyl)oxy)-3,5-dimethoxyphenyl)acrylic acid as a solution in THF (4 mL). The resulting solution was stirred at −78 °C for 10 minutes, then allowed to warm to room temperature for 40 minutes. The reaction was slowly quenched with sat. aq. NaHCO₃ (2 mL). The aqueous layer was extracted with EtOAc (3 x 10 mL). The combined organic layers were dried over Na₂SO₄, concentrated, then purified by FCC eluting from a gradient of 40% → 60% EtOAc in pentanes to give 244 mg (0.61 mmol, 63% yield) of a white solid (mp 102–106 °C). ¹H NMR (500 MHz, CDCl₃) δ 7.91 (d, *J* = 15.8 Hz, 1H), 7.76 (d, *J* = 15.8 Hz, 1H), 7.22 (s, 1H), 7.07 (s, 1H), 6.89 (s, 2H), 4.10 (s, 3H), 3.85 (s, 6H), 1.01 (s, 9H), 0.15 (s, 6H). ¹³C NMR (125 MHz,

CDCl_3) δ 180.49, 151.76, 144.35, 144.21, 137.34, 129.14, 127.61, 127.11, 120.63, 106.14, 55.87, 36.42, 25.75, 18.78, -4.56 . HRMS (ESI) calculated for $[\text{C}_{21}\text{H}_{30}\text{N}_2\text{O}_4\text{Si}]$ requires m/z 403.2048, found 403.2047.

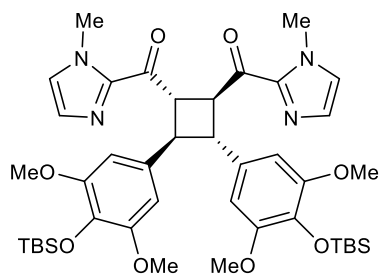
(3,4-bis(4-((*tert*-butyldimethylsilyl)oxy)-3,5-dimethoxyphenyl)cyclobutane-1,2-diyl)bis((1-



methyl-1*H*-imidazol-2-yl)methanone) (3.19): To a vial was added 101.0 mg (0.25 mmol, 1.0 equiv) (*E*)-3-(4-((*tert*-butyldimethylsilyl)oxy)-3,5-dimethoxyphenyl)-1-(1-methyl-1*H*-imidazol-2-yl)prop-2-en-1-one, 38.4 mg (0.04 mmol, 0.2 equiv)

(*R*)-3.2, and toluene (5 mL). The reaction was irradiated with a Kessil 456 nm lamp for 24 hours at -78 °C. After the reaction, Et_3N (0.1 mL) was added and the reaction was concentrated. The resulting material was purified by FCC eluting from a gradient of 30% \rightarrow to 100% EtOAc in hexanes to give 91.0 mg (0.11 mmol, 90% yield) of two diastereomer (6:1 d.r.). Major diastereomer: 99% ee [Daicel CHIRALPAK AD, 5% to 50% *i*PrOH, 28 min, 1 mL/min, $t_1=10.13$ min, $t_2=11.94$ min]. Off-white solid (mp 54–61 °C). $[\alpha]_D^{22} +26.5^\circ$ (c 0.31, CH_2Cl_2). ^1H NMR (500 MHz, CDCl_3) δ 6.92 (s, 2H), 6.85 (s, 2H), 6.59 (s, 4H), 4.77–4.71 (m, 2H), 4.04 (s, 6H), 3.87–3.82 (m, 2H), 3.73 (s, 12H), 0.98 (s, 18H), 0.09 (s, 12H). ^{13}C NMR (125 MHz, CDCl_3) δ 191.0, 151.4, 143.0, 134.9, 132.8, 128.9, 126.8, 104.1, 55.7, 48.4, 46.8, 36.0, 25.8, 18.7, -4.7 . HRMS (ESI) calculated for $[\text{C}_{42}\text{H}_{61}\text{N}_4\text{O}_8\text{Si}_2]^+$ ($\text{M}+\text{H}^+$) requires m/z 805.40224, found 805.4026.

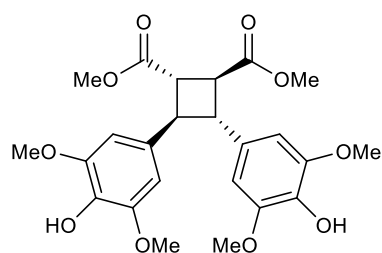
(\pm)-(3,4-bis(4-((*tert*-butyldimethylsilyl)oxy)-3,5-dimethoxyphenyl)cyclobutane-1,2-



diyl)bis((1-methyl-1*H*-imidazol-2-yl)methanone): An 8 mL vial was charged with 45.4 mg (0.1 mmol, 1.0 equiv) (*E*)-3-(4-((*tert*-butyldimethylsilyl)oxy)-3,5-dimethoxyphenyl)-1-(1-methyl-1*H*-imidazol-2-yl)prop-2-en-1-one, 17.1 mg (0.02 mmol, 0.2 equiv)

(±)-**3.2**, and toluene (2 mL). The reaction was irradiated with a Kessil H150 Tuna Blue lamp for 24 hours at room temperature. After the reaction, Et₃N (0.1 mL) was added and the reaction was concentrated and analyzed ¹H-NMR vs. internal standard (phenanthrene) to give a 45% NMR yield of three diastereomers (1:1 d.r.). The resulting material was purified by FCC eluting from a gradient of 30% → 80% EtOAc in hexanes. Spectroscopic data was consistent with those reported above.

Isatisycloneolignan A (3.20): A 4 mL dram vial was charged with 16.0 mg (0.02 mmol, 1 equiv)

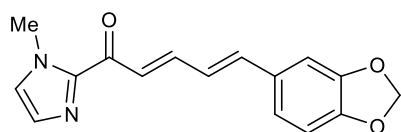


(3,4-bis(4-((tert-butyl)dimethylsilyloxy)-3,5-dimethoxyphenyl)cyclobutane-1,2-diyl)bis((1-methyl-1*H*-imidazol-2-yl)methanone) and then dissolved in DCM (0.5 mL).

To this solution was added 16.5 mg (0.1 mmol, 5 equiv) methyl trifluoromethanesulfonate. The vial was sealed and stirred for 24 hours at room temperature. The reaction was concentrated and 5.0 mg (0.04 mmol, 2 equiv) DMAP and MeOH (0.5 mL) was added. The reaction was stirred for 24 hours. To the reaction was added 5 drops of 6 M HCl and was stirred for an additional 24 hours at which point the reaction was concentrated and purified by FCC using a gradient of 20% to 100% EtOAc in hexanes to give 7.9 mg (0.017 mmol, 83% yield) of a white powder (mp 110–114 °C). $[\alpha]_D^{22} -18.6^\circ$ (c0.84, CH₂Cl₂). ¹H NMR (500 MHz, CDCl₃) δ 6.51 (s, 4H), 5.45 (s, 2H), 3.86 (s, 12H), 3.75 (s, 6H), 3.55–3.53 (m, 2H), 3.45–3.43 (m, 2H). ¹³C NMR (125 MHz, CDCl₃) δ 173.2, 147.3, 134.1, 132.3, 103.7, 56.5, 52.4, 48.5, 44.5.

HRMS (ESI) calculated for [C₂₄H₂₈O₁₀Na]⁺ (M+Na⁺) requires *m/z* 499.1575, found 499.1566.

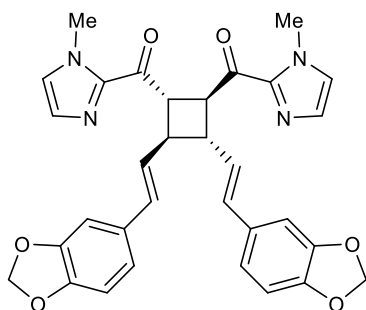
(2*E*,4*E*)-5-(benzo[*d*][1,3]dioxol-5-yl)-1-(1-methyl-1*H*-imidazol-2-yl)penta-2,4-dien-1-one



(3.24): A flame dried 250 mL RBF under N₂ was charged with 1.27 g (15.4 mmol, 1.10 equiv) 1-methyl-1*H*-imidazole and THF

(45 mL). The reaction was cooled to $-78\text{ }^{\circ}\text{C}$ for 20 minutes before adding 7.01 mL (2.5M, 17.5 mmol, 1.25 equiv) *n*-butyllithium dropwise. The solution was stirred at $-78\text{ }^{\circ}\text{C}$ for 5 minutes, then allowed to warm to room temperature for 30 minutes before being cooled to $-78\text{ }^{\circ}\text{C}$ for 20 minutes. To the reaction was added 4.00 g (14.0 mmol, 1.00 equiv) piperine as a solution in THF (45 mL). The resulting solution was stirred at $-78\text{ }^{\circ}\text{C}$ for 10 minutes, then allowed to warm to room temperature overnight. The reaction was slowly quenched with AcOH (2 mL) and EtOAc (50 mL) was added. The reaction was washed with sat. aq. NaHCO_3 (1 x 20 mL) and sat. aq. NaCl (1 x 20 mL). Each aqueous layer was extracted with EtOAc (1 x 20 mL). The combined organic layers were dried over Na_2SO_4 , concentrated, then purified by FCC eluting from a gradient of 0% \rightarrow 10% EtOAc in DCM to give 3.36 g (11.9 mmol, 85% yield) of a yellow solid (mp $168\text{--}170\text{ }^{\circ}\text{C}$). ^1H NMR (500 MHz, CDCl_3) δ 7.57 (m, 2H), 7.18 (d, $J = 0.9\text{ Hz}$, 1H), 7.05 (s, 1H), 7.02 (d, $J = 1.7\text{ Hz}$, 1H), 6.95 (m, 2H), 6.88 (m, 1H), 6.80 (d, $J = 8.0\text{ Hz}$, 1H), 5.99 (s, 2H), 4.07 (s, 3H). ^{13}C NMR (125 MHz, CDCl_3) δ 180.86, 148.68, 148.32, 144.16, 143.64, 141.46, 130.84, 129.19, 127.00, 125.80, 125.56, 123.14, 108.59, 105.98, 101.41, 36.29. HRMS (ESI) calculated for $[\text{C}_{16}\text{H}_{15}\text{N}_2\text{O}_3]^+$ ($\text{M}+\text{H}^+$) requires m/z 283.1077, found 283.1075.

(\pm)-3,4-bis((*E*)-2-(benzo[*d*][1,3]dioxol-5-yl)vinyl)cyclobutane-1,2-diylbis((1-methyl-1*H*-

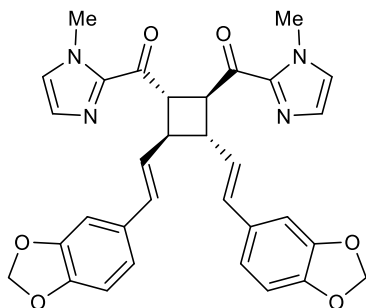


imidazol-2-yl)methanone): An 8 mL vial was charged with 15.0 mg (0.05 mmol, 1.0 equiv) (*2E,4E*)-5-(benzo[*d*][1,3]dioxol-5-yl)-1-(1-methyl-1*H*-imidazol-2-yl)penta-2,4-dien-1-one and toluene (4 mL). The reaction was irradiated with a Kessil H150 Tuna Blue

lamp for 24 hours at $-78\text{ }^{\circ}\text{C}$. After the reaction, Et_3N (0.1 mL) was added, and the reaction was concentrated and analyzed ^1H -NMR vs. internal standard (phenanthrene) to give an 87% NMR yield of three isomers (7:1:1 d.r.). The resulting material was purified by FCC eluting from a

gradient of 50% → 70% EtOAc in hexanes. Spectroscopic data was consistent with those reported above.

3,4-bis((*E*)-2-(benzo[*d*][1,3]dioxol-5-yl)vinyl)cyclobutane-1,2-diyl)bis((1-methyl-1*H*-



imidazol-2-yl)methanone) (3.25): To a vial was added 14.1 mg

(0.25 mmol, 1.0 equiv) (*2E,4E*)-5-(benzo[*d*][1,3]dioxol-5-yl)-1-(1-

methyl-1*H*-imidazol-2-yl)penta-2,4-dien-1-one, 8.0 mg (0.01

mmol, 0.2 equiv) (***R***)-**3.2**, and toluene (10 mL). The reaction was

irradiated with a Kessil 456 nm lamp for 24 hours at -78°C . After the reaction, Et_3N (0.1 mL) was

added, and the reaction was concentrated and analyzed $^1\text{H-NMR}$ vs. internal standard

(phenanthrene) to give an 85% NMR yield of four isomers (11:3:1:1 d.r.). The resulting material

was purified by FCC eluting from a gradient of 50% → to 70% EtOAc in hexanes. A reverse phase

column was also run eluting from a gradient of 0% to 100% MeCN in water to give 8.3 mg (0.015

mmol, 59% yield) of the desired isomer. Major diastereomer: 92% ee [Daicel CHIRALPAK OD-

H, 5% to 60% iPrOH, 28 min, 1 mL/min, $t_1=23.00$ min, $t_2=28.01$ min]. White solid (mp 70–74

$^{\circ}\text{C}$). $[\alpha]_{\text{D}}^{22} +48.4^{\circ}$ (c0.38, CH_2Cl_2). $^1\text{H NMR}$ (500 MHz, CDCl_3) δ 6.92–6.89 (m, 6H), 6.77 (dd, J

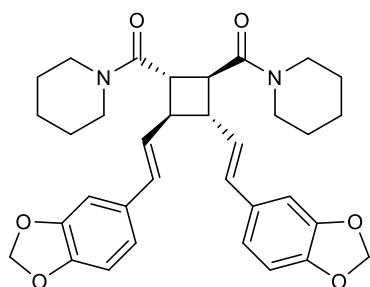
= 8.1, 1.7 Hz, 2H), 6.71 (d, J = 8.1, 2H), 6.24–6.19 (m, 2H), 5.92 (s, 4H), 4.51–4.49 (m, 2H), 4.02

(s, 6H), 3.32–3.29 (m, 2H). $^{13}\text{C NMR}$ (125 MHz, CDCl_3) δ 190.7, 147.9, 146.9, 143.0, 131.8,

130.3, 129.1, 128.7, 126.8, 120.9, 108.2, 105.7, 100.9, 48.1, 43.9, 36.0. HRMS (ESI) calculated

for $[\text{C}_{32}\text{H}_{28}\text{N}_4\text{O}_6\text{Na}]^+$ ($\text{M}+\text{H}^+$) requires m/z 587.1901, found 587.1899.

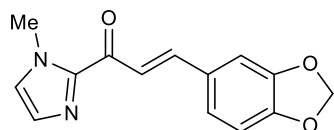
Nigramide R (3.28): A 4 mL dram vial was charged with 13.0 mg (0.02 mmol, 1 equiv) (2*E*,4*E*)-



5-(benzo[*d*][1,3]dioxol-5-yl)-1-(1-methyl-1*H*-imidazol-2-yl)prop-2,4-dien-1-one and dissolved in DCM (0.5 mL). To the solution was added 18.9 mg (0.12 mmol, 5 equiv) methyl trifluoromethanesulfonate. The vial was sealed and stirred for 24

hours. Then, 39.2 mg (0.46 mmol, 20 equiv) piperidine was added and the reaction was stirred for an additional 24 hours. The reaction was diluted with 1 M HCl (5 mL) and extracted with DCM (2 x 10 mL). The organic layers were dried over Na₂SO₄, filtered, concentrated, and purified by FCC using a gradient of 50% to 80% EtOAc/hexanes to give 6.8 mg (0.012 mmol, 52% yield) of a colorless oil. $[\alpha]_D^{22} +56.0^\circ$ (c0.40, CH₂Cl₂). ¹H NMR (500 MHz, CDCl₃) δ 6.87 (d, *J* = 1.5 Hz, 2H), 6.76–6.71 (m, 4H), 6.36 (d, *J* = 15.7 Hz, 2H), 6.14–6.09 (m, 2H), 5.93 (s, 4H), 3.71–3.64 (m, 4H), 3.53–3.48 (m, 2H), 3.42–3.47 (m, 4H), 3.01–2.97 (m, 2H), 1.59–1.39 (m, 12H). ¹³C NMR (125 MHz, CDCl₃) δ 170.6, 148.2, 147.3, 131.6, 131.2, 128.8, 121.1, 108.5, 105.7, 101.2, 46.9, 46.4, 43.4, 42.3, 27.0, 25.9, 24.7. HRMS (ESI) calculated for [C₃₄H₃₉N₂O₆]⁺ (M+H⁺) requires *m/z* 571.2803, found 571.2800.

(*E*)-3-(benzo[*d*][1,3]dioxol-5-yl)-1-(1-methyl-1*H*-imidazol-2-yl)prop-2-en-1-one (3.21):

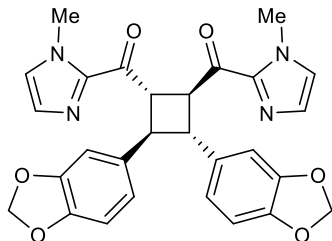


Synthesized according to General Procedure D using 374 mg (3.01

mmol, 1.0 equiv) 2-acetyl-1-methylimidazole, 510 mg (3.40 mmol, 1.1 equiv) benzo[*d*][1,3]dioxole-5-carbaldehyde, ~25 mg (1/2 pellet) KOH, EtOH (8 mL), and H₂O (4 mL). Work-up 1, to give 651 mg (2.54 mmol, 84% yield) of a yellow solid (mp = 180–184 °C). ¹H NMR (500 MHz, CDCl₃) δ 7.91(d, *J* = 15.9 Hz, 1H), 7.75 (d, *J* = 15.9 Hz, 1H), 7.24 (d, *J* = 1.7 Hz, 1H), 7.21 (d, *J* = 1.0 Hz, 1H), 7.16 (dd, *J* = 8.1 Hz, 1.8 Hz, 1H), 7.07 (s, 1H), 6.83 (d, *J* = 8.0 Hz, 1H), 6.02 (s, 2H), 4.09 (s, 3H). ¹³C NMR (125 MHz, CDCl₃) δ 180.7, 150.1, 148.6,

144.3, 143.5, 129.7, 129.4, 127.3, 125.6, 121.1, 108.7, 107.3, 101.8, 36.5. HRMS (ESI) calculated for $[C_{14}H_{13}N_2O_3]^+$ ($M+H^+$) requires m/z 257.0921, found 257.0916.

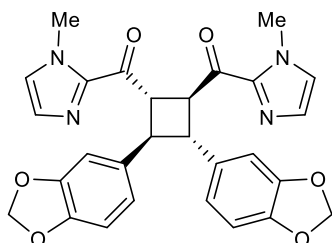
(3,4-bis(benzo[*d*][1,3]dioxol-5-yl)cyclobutane-1,2-diyl)bis((1-methyl-1H-imidazol-2-



yl)methanone): Prepared according to the general procedure for isolation-scale asymmetric experiments *with the exception that a Kessil 456 nm lamp was used instead of a Kessil H150 Tuna Blue lamp and the reaction was conducted at -78 °C.* To a vial was added 25.2

mg (0.10 mmol, 1.0 equiv) (*E*)-3-(benzo[*d*][1,3]dioxol-5-yl)-1-(1-methyl-1H-imidazol-2-yl)prop-2-en-1-one, 15.8 mg (0.02 mmol, 0.2 equiv) (**R**)-**3.2**, and toluene (5 mL). The resulting material was purified by FCC eluting from a gradient of 50% \rightarrow 70% EtOAc in hexanes to give 23.1 mg (0.09 mmol, 92% yield) of one diastereomer ($>20:1$ d.r.). Major diastereomer: 99% ee [Daicel CHIRALPAK AD, 5% to 60% iPrOH, 35 min, 1 mL/min, $t_1=22.85$ min, $t_2=29.47$ min]. White solid (mp $171-174$ °C). $[\alpha]_D^{22} +71.4^\circ$ (c0.21, CH_2Cl_2). 1H NMR (500 MHz, $CDCl_3$) δ 6.90–6.89 (m, 4H), 6.83 (dd, $J = 8.0, 1.8$ Hz, 2H), 6.81 (s, 2H), 6.72 (d, $J = 8.0$ Hz, 2H), 5.90 (s, 4H), 4.60–4.58 (m, 2H), 4.02 (s, 6H), 3.94–3.92 (m, 2H). ^{13}C NMR (125 MHz, $CDCl_3$) δ 190.9, 147.9, 146.5, 143.2, 136.2, 129.1, 126.9, 120.6, 108.4, 108.0, 101.0, 49.8, 45.6, 36.1. HRMS (ESI) calculated for $[C_{28}H_{25}N_4O_6]^+$ ($M+H^+$) requires m/z 513.1769, found 513.1760.

(\pm)-(3,4-bis(benzo[*d*][1,3]dioxol-5-yl)cyclobutane-1,2-diyl)bis((1-methyl-1H-imidazol-2-

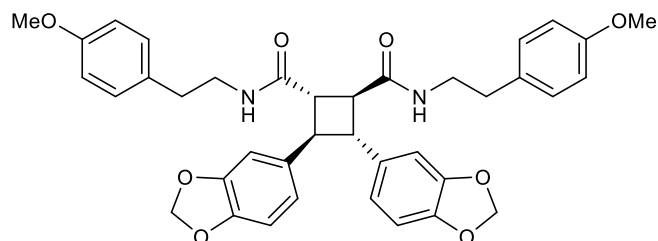


yl)methanone): An 8 mL vial was charged with 24.9 mg (0.10 mmol, 1.0 equiv) (*E*)-3-(benzo[*d*][1,3]dioxol-5-yl)-1-(1-methyl-1H-imidazol-2-yl)prop-2-en-1-one, 15.1 mg (0.02 mmol, 0.2 equiv) (\pm)-**3.2**, and toluene (5 mL). The reaction was irradiated with a Kessil

H150 Tuna Blue lamp for 24 hours at rt. After the reaction, Et_3N (0.1 mL) was added, and the

reaction was concentrated and analyzed $^1\text{H-NMR}$ vs. internal standard (phenanthrene) to give a 50% NMR yield of three isomers (>20:1 d.r.). The resulting material was purified by FCC eluting from a gradient of 50% \rightarrow 70% EtOAc in hexanes. Spectroscopic data was consistent with those reported above.

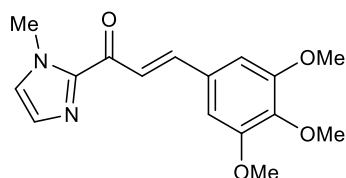
Barbarumamide C (3.22): A 4 mL dram vial was charged with 25.0 mg (0.05 mmol, 1 equiv)



(3,4-bis(benzo[*d*][1,3]dioxol-5-yl)cyclobutane-1,2-diyl)bis((1-methyl-1*H*-imidazol-2-yl)methanone)and then

dissolved in DCM (0.5 mL). The solution was stirred under N_2 for 5 minutes, and then 40 mg (0.24 mmol, 5 equiv) methyl trifluoromethanesulfonate was added. The vial was sealed and stirred for 24 hours. Then, the solvent and any remaining methyl trifluoromethanesulfonate was removed on a rotary evaporator, and then dried on high vac for 30 minutes. Once dry, 150 mg (1.0 mmol, 20 equiv) 2-(4-methoxyphenyl)ethan-1-amine was added and then redissolved in DCM (0.5 mL). The solution was stirred for 24 hours, concentrated, and purified by FCC using a gradient of 50% to 70% EtOAc/hexanes to give 25.5 mg (0.039 mmol, 80% yield) of a white powder (mp 192–194 $^\circ\text{C}$). $[\alpha]_{\text{D}}^{22} +83.8^\circ$ (c0.21, CH_2Cl_2). $^1\text{H NMR}$ (500 MHz, CDCl_3) δ 7.05 (d, $J = 8.6$ Hz, 4H), 6.81 (d, $J = 8.6$, 4H), 6.70–6.69 (m, 4H), 6.59 (dd, $J = 8.0, 1.7$ Hz, 2H), 6.03 (t, $J = 5.8$, 2H), 5.93 (s, 4H), 3.78 (s, 6H), 3.55–3.48 (m, 2H), 3.45–3.34 (m, 2H), 3.38–3.34 (m, 2H), 2.97–2.95 (m, 2H), 2.74 (t, $J = 7.1$ Hz, 4H). $^{13}\text{C NMR}$ (125 MHz, CDCl_3) δ 172.6, 158.5, 148.2, 146.9, 134.9, 130.7, 129.9, 120.3, 114.2, 108.6, 107.5, 101.2, 55.4, 47.1, 46.9, 40.8, 34.9. HRMS (ESI) calculated for $[\text{C}_{38}\text{H}_{39}\text{N}_2\text{O}_8]^+$ ($\text{M}+\text{H}^+$) requires m/z 651.2701, found 651.2700.

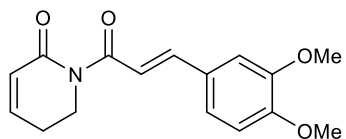
(E)-1-(1-methyl-1H-imidazol-2-yl)-3-(3,4,5-trimethoxyphenyl)prop-2-en-1-one (3.43): A



flame dried 50 mL RBF under N₂ was charged with 0.74 mL (9.2 mmol, 2.2 equiv) 1-methyl- 1H-imidazole and THF (8 mL). The reaction was cooled to –78 °C for 20 minutes before adding 3.70 mL

(2.5M, 9.2 mmol, 2.2 equiv) *n*-butyllithium dropwise. The solution was stirred at –78 °C for 5 minutes, then allowed to warm to room temperature for 30 minutes before being cooled to –78 °C for 20 minutes. To the reaction was added 1.00 g (4.2 mmol, 1.0 equiv) (*E*)-3-(3,4,5-trimethoxyphenyl)acrylic acid as a solution in THF (8 mL). The resulting solution was stirred at –78 °C for 10 minutes, then allowed to warm to room temperature for 40 minutes. The reaction was slowly quenched with sat. aq. NaHCO₃ (2 mL). The aqueous layer was extracted with EtOAc (3 x 10 mL). The combined organic layers were dried over Na₂SO₄, concentrated, then purified by FCC eluting from a gradient of 40% → 100% EtOAc in hexanes to give 870 mg (2.88 mmol, 69% yield) of a yellow solid (mp 142–146 °C). ¹H NMR (500 MHz, CDCl₃) δ 7.95 (d, *J* = 15.9 Hz, 1H), 7.75 (d, *J* = 15.9 Hz, 1H), 7.23 (d, *J* = 1.0 Hz, 1H), 7.09 (d, *J* = 0.9 Hz, 1H), 6.92 (s, 2H), 4.11 (s, 3H), 3.92 (s, 6H), 3.90 (s, 3H). ¹³C NMR (125 MHz, CDCl₃) δ 180.4, 153.4, 144.1, 143.7, 140.4, 130.4, 129.3, 127.3, 121.8, 106.0, 61.0, 56.3, 36.4. HRMS (ESI) calculated for [C₁₆H₁₉N₂O₄] (M+H⁺) requires *m/z* 303.1339, found 303.1334.

(E)-1-(3-(3,4-dimethoxyphenyl)acryloyl)-5,6-dihydropyridin-2(1H)-one (3.45): A flame dried

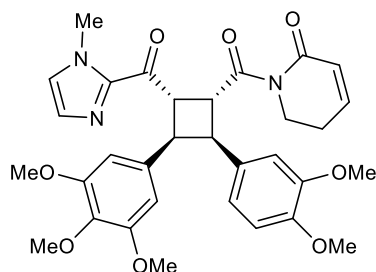


100 mL RBF under N₂ was charged with 312 mg (1.5 mmol, 1.00 equiv) (*E*)-3-(3,4-dimethoxyphenyl)acrylic acid, 0.25 mL (1.8 mmol,

1.20 equiv) triethylamine, and THF (10 mL). The reaction was cooled to 0 °C prior to addition of 0.22 mL (1.8 mmol, 1.20 equiv) pivaloyl chloride and then stirred for one hour. In a separate flask 153 mg (1.6 mmol, 1.05 equiv) 5,6-dihydropyridin-2(1H)-one was dissolved in THF (10 mL) and

cooled to $-78\text{ }^{\circ}\text{C}$ prior to addition of 0.72 mL (2.5 M, 1.8 mmol, 1.20 equiv) *n*-butyllithium. The mixture was stirred for 45 minutes and then the anhydride was added to the cooled lithiated amide and the resulting reaction was stirred for an additional 1 hour. The reaction was then allowed to warm to room temperature and quenched with sat. aq. NH_4Cl (10 mL). The reaction was transferred to a separatory funnel with additional water and was extracted with EtOAc (3 x 20 mL). The combined organic layers were washed with brine (1 x 20 mL), dried over Na_2SO_4 , filtered, concentrated and then purified by FCC eluting from a gradient of 30% \rightarrow 70% EtOAc in hexanes to give 320 mg (1.11 mmol, 74% yield) of a yellow solid. The compound was consistent with reported spectroscopic data.⁵⁵ ^1H NMR (500 MHz, CDCl_3) δ 7.73 (d, $J = 15.5$ Hz, 1H), 7.42 (d, $J = 15.5$ Hz, 1H), 7.16 (dd, $J = 8.3, 2.1$ Hz, 1H), 7.11 (d, $J = 2.0$ Hz, 1H), 6.94 (dt, $J = 9.7, 4.2$ Hz, 1H), 6.86 (d, $J = 8.3$ Hz, 1H), 6.05 (dt, $J = 9.7, 1.8$ Hz, 1H), 4.04 (t, $J = 6.5$ Hz, 2H), 3.92 (s, 3H), 3.91 (s, 3H), 2.49–2.45 (m, 2H).

1-(2-(3,4-dimethoxyphenyl)-4-(1-methyl-1*H*-imidazole-2-carbonyl)-3-(3,4,5-



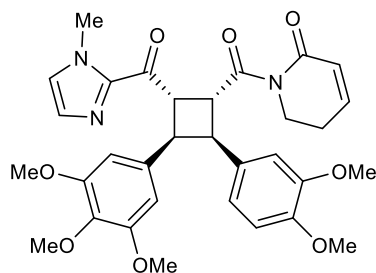
trimethoxyphenyl)cyclobutane-1-carbonyl)-5,6-

dihydropyridin-2(1*H*)-one: To a flame-dried 100 mL RBF was added 86.2 mg (0.30 mmol, 3.0 equiv) (*E*)-1-(3-(3,4-dimethoxyphenyl)acryloyl)-5,6-dihydropyridin-2(1*H*)-one, 15.4

mg (0.02 mmol, 0.2 equiv) (*R*)-**3.2**, and toluene (2 mL). In another flask 30.2 mg (0.1 mmol, 1.0 equiv) (*E*)-1-(1-methyl-1*H*-imidazol-2-yl)-3-(3,4,5-trimethoxyphenyl)prop-2-en-1-one was dissolved in toluene (3 mL) and DCM (1 mL). The reaction mixture was cooled to $0\text{ }^{\circ}\text{C}$ and irradiated with 2 Kessil 467 nm lamps. During the reaction, the substrate solution was added at a rate of 0.2 mL/hour via syringe pump such that all the substrate was added after 20 hours. The reaction was irradiated for a total of 24 hours. The resulting material was purified by FCC eluting

from a gradient of 50% EtOAc/hexanes \rightarrow EtOAc \rightarrow 10% MeOH/EtOAc to give 48.0 mg (0.08 mmol, 81% yield, 6:1 d.r.). Major diastereomer: 99% ee [Daicel CHIRALPAK AD-H, 30% to 80% iPrOH, 30 min, 1 mL/min, $t_1=18.46$ min, $t_2=23.92$ min]. White solid (mp 75–80 °C). $[\alpha]_D^{22} -63.9^\circ$ (c0.31, CH₂Cl₂). ¹H NMR (500 MHz, CDCl₃) δ 7.12 (s, 1H), 7.00 (s, 1H), 6.82 (dt, $J = 9.7$, 4.2 Hz, 1H), 6.78 (dd, $J = 8.4$, 2.1 Hz, 1H), 6.69 (d, $J = 8.3$, 1H), 6.49 (d, $J = 2.1$, 1H), 6.42 (s, 2H), 5.88 (dt, $J = 9.8$, 1.8 Hz, 1H), 5.41 (t, $J = 9.2$, 1H), 4.60–4.50 (m, 1H), 4.45–4.42 (m, 1H), 4.27 (t, $J = 9.1$, 1H), 4.15–4.10 (m, 1H), 3.97 (s, 3H), 3.85–3.81 (m, 1H), 3.78 (s, 3H), 3.72 (s, 3H), 3.68 (s, 6H), 3.65 (s, 3H), 2.36–2.33 (m, 2H). ¹³C NMR (125 MHz, CDCl₃) δ 191.3, 175.3, 165.1, 152.9, 148.7, 147.8, 145.2, 142.7, 136.4, 135.2, 132.5, 129.0, 127.1, 126.0, 120.6, 112.6, 111.0, 105.7, 61.0, 56.3, 56.1, 48.8, 48.1, 45.5, 44.5, 41.4, 36.4, 24.8. HRMS (ESI) calculated for [C₃₂H₃₅N₃O₈Na]⁺ (M+Na⁺) requires m/z 612.2316, found 612.2309.

(±)-1-(2-(3,4-dimethoxyphenyl)-4-(1-methyl-1H-imidazole-2-carbonyl)-3-(3,4,5-



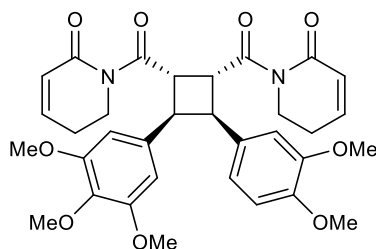
trimethoxyphenyl)cyclobutane-1-carbonyl)-5,6-

dihydropyridin-2(1H)-one: To a flame-dried 50 mL RBF was added 43.1 mg (0.15 mmol, 3.0 equiv) (*E*)-1-(3-(3,4-dimethoxyphenyl)acryloyl)-5,6-dihydropyridin-2(1H)-one, 7.7

mg (0.01 mmol, 0.2 equiv) (\pm)-**3.2**, and toluene (2 mL). In another flask 15.1 mg (0.05 mmol, 1.0 equiv) (*E*)-1-(1-methyl-1H-imidazol-2-yl)-3-(3,4,5-trimethoxyphenyl)prop-2-en-1-one was dissolved in toluene (3 mL) and DCM (1 mL). The reaction mixture was cooled to 0 °C and irradiated with 2 Kessil 467 nm lamps. During the reaction, the substrate solution was added at a rate of 0.2 mL/hour via syringe pump such that all the substrate was added after 20 hours. The reaction was irradiated for a total of 24 hours. After the reaction, Et₃N (0.1 mL) was added, and the reaction was concentrated and analyzed ¹H-NMR vs. internal standard (phenanthrene) to give

an 81% NMR yield (6:1 d.r.). The resulting material was purified by FCC eluting from a gradient of 50% EtOAc/hexanes \rightarrow EtOAc \rightarrow 10% MeOH/EtOAc. Spectroscopic data was consistent with those reported above.

Piperarborenine D (3.47): A dram vial was charged with 75.0 mg (0.13 mmol, 1 equiv) 1-(2-



(3,4-dimethoxyphenyl)-4-(1-methyl-1*H*-imidazole-2-carbonyl)-3-

(3,4,5-trimethoxyphenyl)cyclobutane-1-carbonyl)-5,6-

dihydropyridin-2(1*H*)-one and then dissolved in DCM (5.0 mL).

To the solution was added 42.4 mg (0.25 mmol, 2 equiv) methyl

trifluoromethanesulfonate. The vial was sealed and stirred for 2 hours and then the reaction was concentrated and placed on high vacuum for 1 hour. The methylated intermediate was dissolved in DME (5 mL) and cooled to $-50\text{ }^{\circ}\text{C}$. To a separate flame-dried vial was added DME (3 mL) and cooled to $-50\text{ }^{\circ}\text{C}$ prior to addition of 18 μL (0.13 mmol, 1 equiv) diisopropylamine, and 51 μL (2.5 M, 0.13 mmol, 1 equiv) *n*-butyllithium. This reaction was stirred for 10 minutes prior to addition of a solution of 12.3 mg (0.13 mmol, 1 equiv) 5,6-dihydropyridin-2(1*H*)-one (DHP) in DME (2 mL). After addition of DHP the reaction was stirred for 10 minutes at $-50\text{ }^{\circ}\text{C}$ and then added in one portion to the cooled methylated intermediate. Immediately after the addition, the reaction was removed from the cooling bath and allowed to warm to $0\text{ }^{\circ}\text{C}$ over 10 minutes at which point it was quenched with sat. aq. NH_4Cl (2 mL). The reaction was transferred to a separatory funnel with EtOAc and water and the reaction was extracted with EtOAc (3 x 20 mL). The combined organic layers were dried over Na_2SO_4 , filtered, and concentrated. The resulting material was purified by FCC eluting from a gradient of 70% EtOAc/hexanes \rightarrow EtOAc \rightarrow to give 54.3 mg (0.09 mmol, 71% yield) of a white solid (mp $50\text{--}57\text{ }^{\circ}\text{C}$). $[\alpha]_{\text{D}}^{22} +12.9^{\circ}$ (c0.42, CH_2Cl_2). ^1H NMR (500 MHz, CDCl_3) δ 6.87–6.83 (m, 2H), 6.73 (dd, $J = 8.3, 1.9$ Hz, 1H), 6.69 (d, $J = 8.3$ Hz, 1H), 6.37 (d, $J =$

1.8 Hz, 1H), 6.19 (s, 2H), 5.94 (td, $J = 9.6, 1.8$ Hz, 2H), 4.80–4.73 (m, 2H), 4.21–4.18 (m, 1H), 4.14–4.11 (m, 1H), 4.04–3.94 (m, 4H), 3.77 (s, 3H), 3.72 (s, 3H), 3.65 (s, 6H), 3.62 (s, 3H), 2.40–2.37 (m, 4H). ^{13}C NMR (125 MHz, CDCl_3) δ 175.4, 175.3, 165.1, 164.9, 152.8, 148.6, 147.6, 145.2, 145.2, 136.5, 134.9, 131.8, 125.9, 125.9, 120.1, 112.2, 110.9, 105.7, 60.9, 56.1, 56.0, 55.9, 48.7, 48.2, 46.1, 45.9, 41.3, 24.7, 24.7. HRMS (ESI) calculated for $[\text{C}_{33}\text{H}_{36}\text{N}_2\text{O}_9\text{Na}]^+$ ($\text{M}+\text{Na}^+$) requires m/z 627.2313, found 627.2305.

3.5.10 Incompatible Substrates

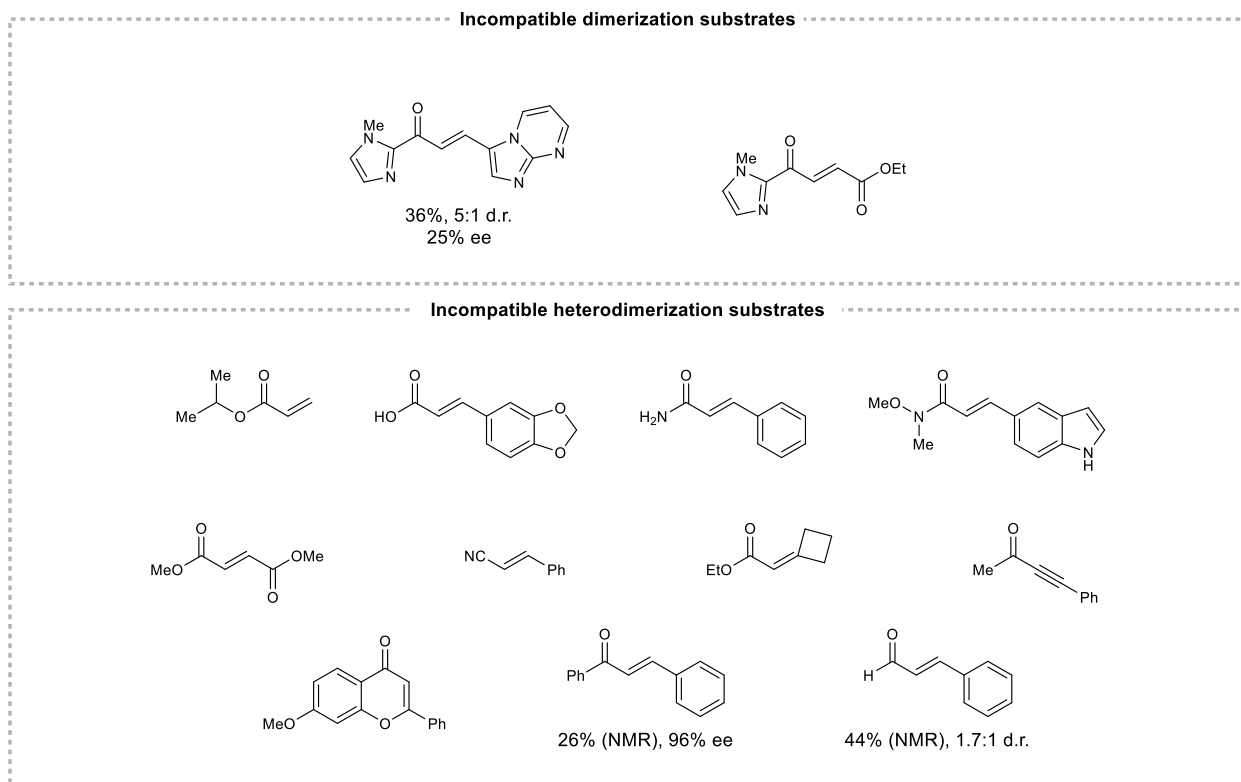
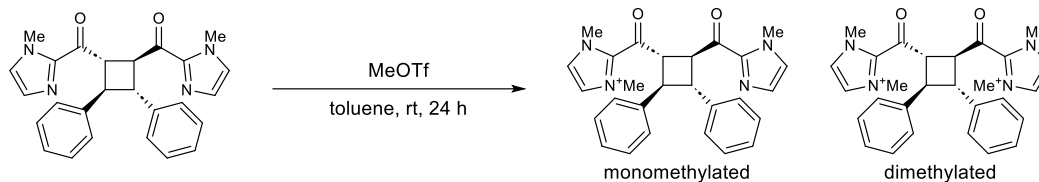


Figure 3.1 Incompatible dimerization and heterodimerization substrates. Note: < 10% yield was observed if no yield is given above.

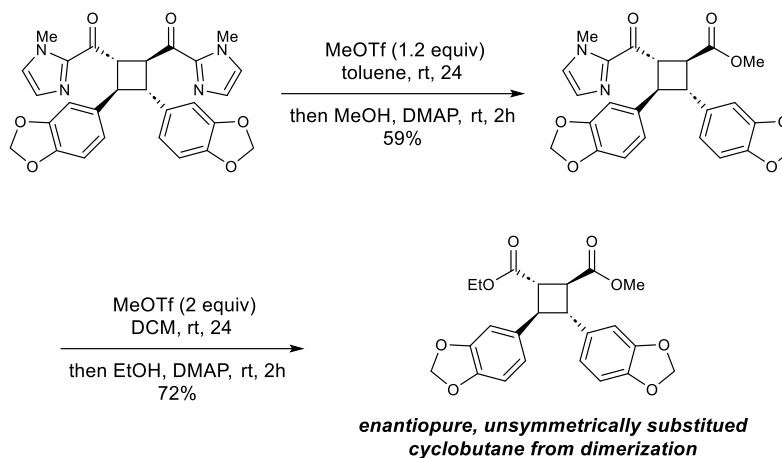
3.5.11 Monomethylation gives Unsymmetrical Products



equiv MeOTf	RSM (%)	monomethylated (%)	dimethylated (%)
1.0	0	95	3
1.2	0	91	4
1.4	0	87	4
1.6	0	95	5

Running methylation reaction in toluene gives monomethylated product

Scheme 3.6 Monomethylation of **3.4** in toluene



Scheme 3.7 Monomethylation approach gives access to enantiopure, unsymmetrically substituted cyclobutanes from dimerization.

3.5.12 UV-Vis Absorption Experiments

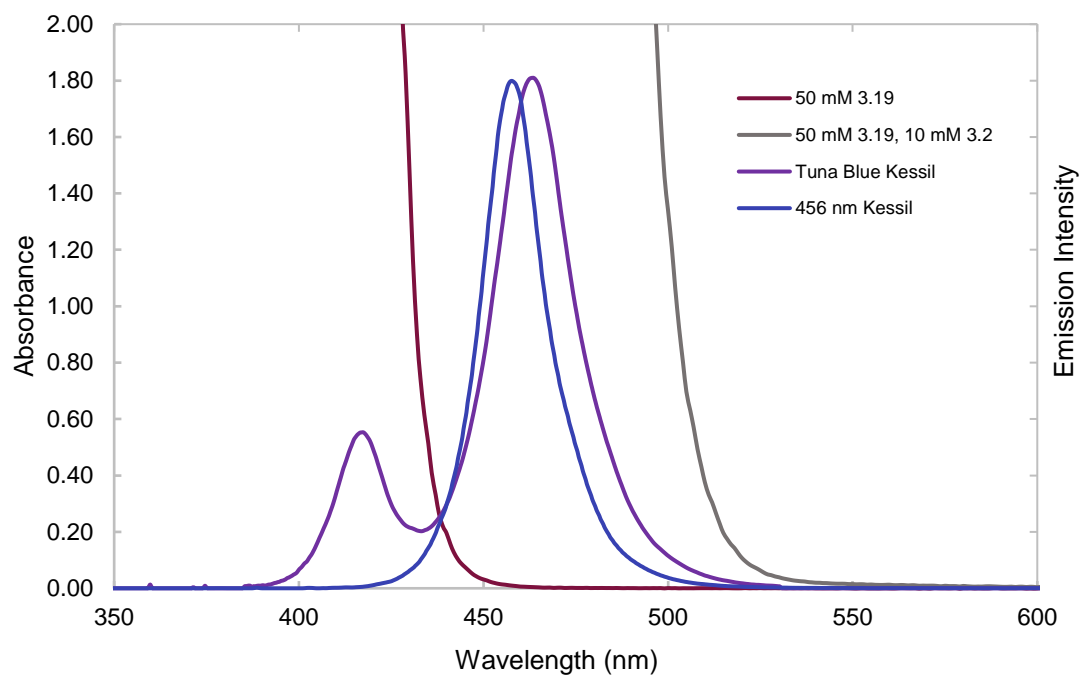


Figure 3.2 Absorption spectra of **3.19** and **3.19** with **3.2** and emission spectra of Tuna Blue and 456 nm Kessil lamps

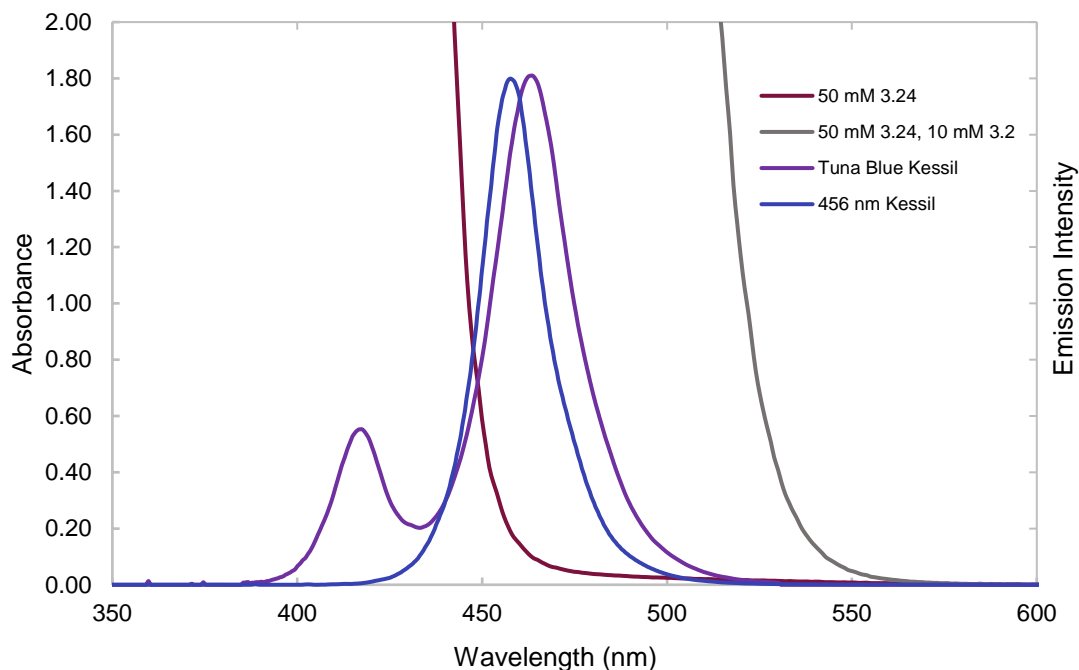


Figure 3.3 Absorption spectra of **3.24** and **3.24** with **3.2** and emission spectra of Tuna Blue and 456 nm Kessil lamps

3.5.13 Non-Linear Effect Experiments

Given the proposed mechanism in which two acid catalysts are expected to participate in the dimerization reaction, a non-linear effect experiment was conducted to interrogate the relationship between product enantioselectivity as a function of catalyst enantioselectivity. A non-linear effect was not observed as is shown in the data below.

Setup: two stock solutions were made with one containing **3.1** and (**R**)-**3.2** and the other **3.1** and (\pm)-**3.2**. Six reactions were set up, each having varying amounts of stock solution 1 and 2 with each total volume totaling 1 mL such that each reaction had the same total amount of substrate, catalyst, and solvent. Each reaction was irradiated for 16 h with a Kessil H150 Tuna Blue lamp prior to workup and column chromatography to get product for HPLC analysis.

Stock solution 1: **3.1** (0.05 M), (**R**)-**3.2** (0.01 M)

Stock solution 1: **3.1** (0.05 M), (\pm)-**3.2** (0.01 M)

Reaction 1: 0.143 mL stock solution 1, 0.857 mL stock solution 2

Reaction 2: 0.286 mL stock solution 1, 0.714 mL stock solution 2

Reaction 3: 0.429 mL stock solution 1, 0.571 mL stock solution 2

Reaction 4: 0.571 mL stock solution 1, 0.429 mL stock solution 2

Reaction 5: 0.714 mL stock solution 1, 0.286 mL stock solution 2

Reaction 6: 0.857 mL stock solution 1, 0.143 mL stock solution 2

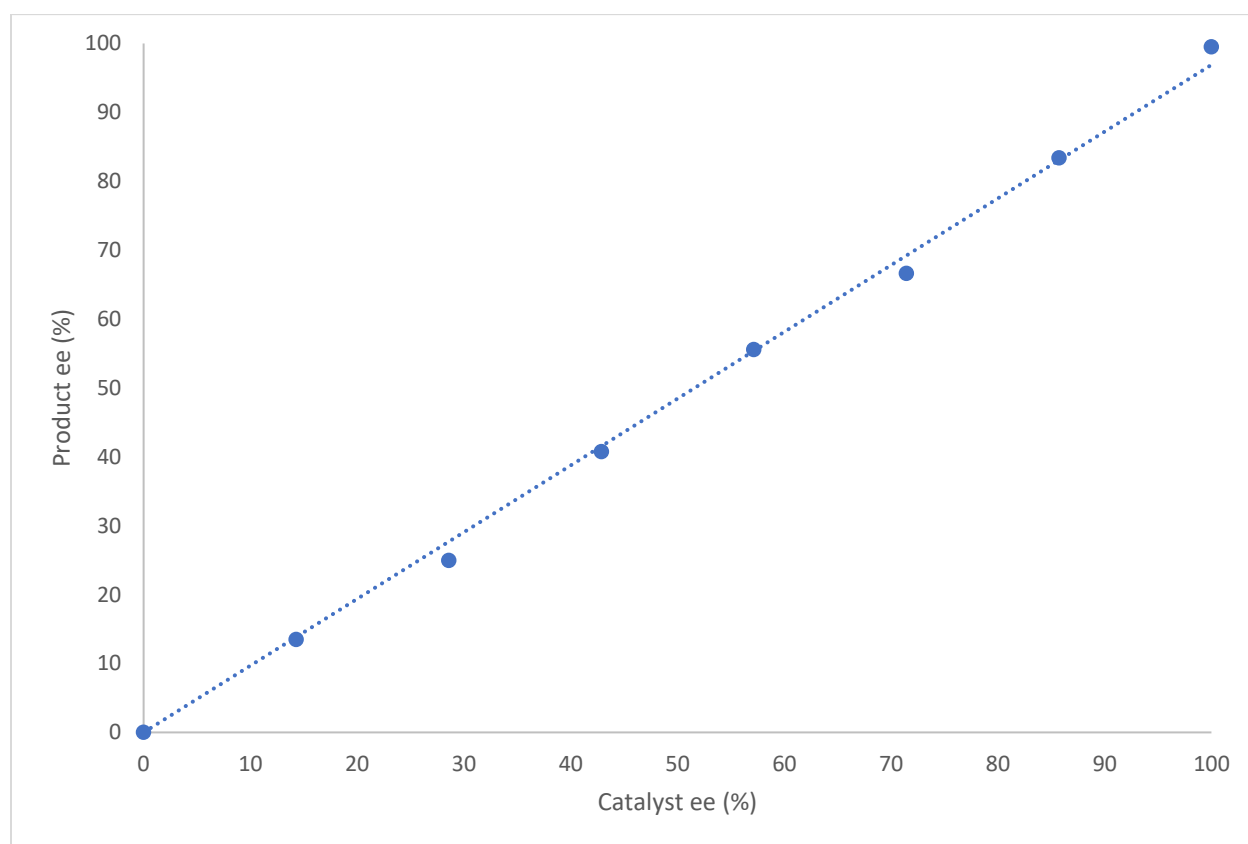
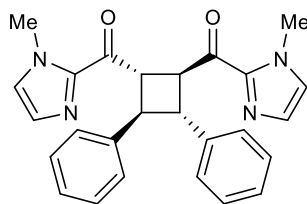


Figure 3.4 Non-linear effect experiment for dimerization of **3.1** with **3.2**

3.5.14 X-Ray Crystallographic Data

((1S,2S,3R,4R)-3,4-diphenylcyclobutane-1,2-diyl)bis((1-methyl-1H-imidazol-2-yl)methanone)



Data Collection: A colorless crystal with approximate dimensions $0.15 \times 0.11 \times 0.07$ mm³ was selected under oil under ambient conditions and attached to the tip of a MiTeGen MicroMount[®]. The crystal was mounted in a stream of cold nitrogen at 100(1) K and centered in the X-ray beam by using a video camera.

The crystal evaluation and data collection were performed on a Bruker D8 VENTURE PhotonIII four-circle diffractometer with Cu K α ($\lambda = 1.54178$ Å) radiation and the detector to crystal distance of 4.0 cm.⁵⁶

The initial cell constants were obtained from a 180° ϕ scan conducted at a $2\theta = 50^\circ$ angle with the exposure time of 1 second per frame. The reflections were successfully indexed by an automated indexing routine built in the APEX3 program. The final cell constants were calculated from a set of 9073 strong reflections from the actual data collection.

The data were collected by using a hemisphere data collection routine to survey the reciprocal space to the extent of a full sphere to a resolution of 0.8 Å. A total of 39025 data were harvested by collecting 17 sets of frames with 0.6° scans in and ϕ with an exposure time 0.5–3 sec per frame. These highly redundant datasets were corrected for Lorentz and polarization effects. The absorption correction was based on fitting a function to the empirical transmission surface as sampled by multiple equivalent measurements.⁵⁷

Structure Solution and Refinement: The systematic absences in the diffraction data were uniquely consistent for the space group P212121 that yielded chemically reasonable and computationally stable results of refinement.^{58–63}

A successful solution by the direct methods provided most non-hydrogen atoms from the E-map. The remaining non-hydrogen atoms were located in an alternating series of least-squares cycles and difference Fourier maps. All non-hydrogen atoms were refined with anisotropic displacement coefficients. All hydrogen atoms were included in the structure factor calculation at idealized positions and were allowed to ride on the neighboring atoms with relative isotropic displacement coefficients.

The absolute configuration was unequivocally established by anomalous scattering effects: C1(S), C2(S), C3(R), C4(R).

The final least-squares refinement of 292 parameters against 4235 data resulted in residuals R (based on F² for $I \geq 2\sigma$) and wR (based on F² for all data) of 0.0277 and 0.0667, respectively. The final difference Fourier map was featureless.

Summary: Crystal Data for C₂₆H₂₄N₄O₂ (M = 424.49 g/mol): orthorhombic, space group P212121 (no. 19), a = 10.3510(12) Å, b = 11.8569(15) Å, c = 17.478(2) Å, V = 2145.1(4) Å³, Z = 4, T = 99.99 K, $\mu(\text{CuK}\alpha) = 0.681 \text{ mm}^{-1}$, D_{calc} = 1.314 g/cm³, 39025 reflections measured ($9.012^\circ \leq 2\Theta \leq 144.53^\circ$), 4235 unique (R_{int} = 0.0300, R_{sigma} = 0.0183) which were used in all calculations. The final R₁ was 0.0277 ($I > 2\sigma(I)$) and wR₂ was 0.0667 (all data).

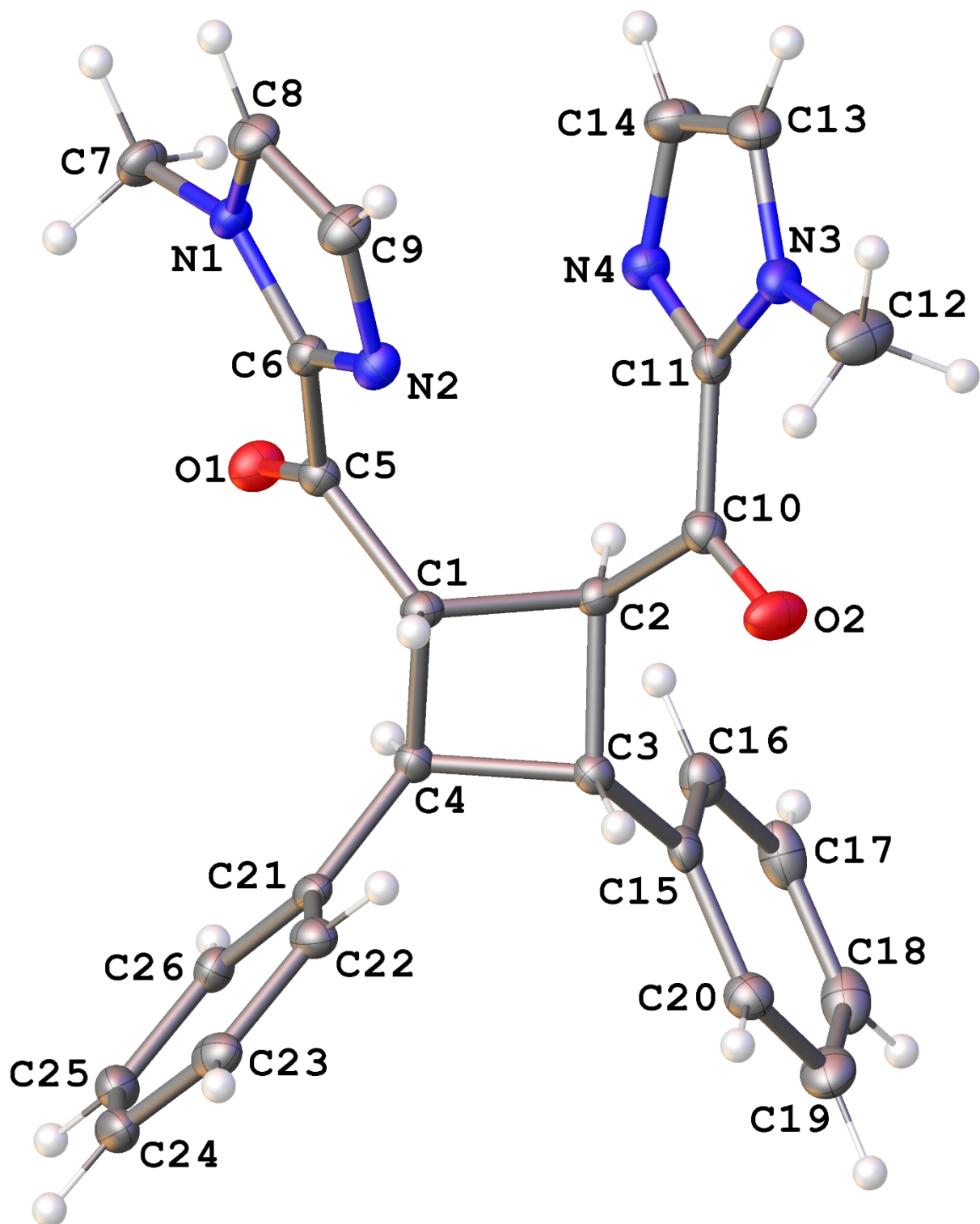


Figure 3.5 A molecular drawing of Yoon59a shown with 50% probability ellipsoids. All H atoms are omitted.

Table 3.1 *Crystal data and structure refinement for yoon59a.*

Identification code	yoon59a
Empirical formula	C ₂₆ H ₂₄ N ₄ O ₂
Formula weight	424.49
Temperature/K	99.99
Crystal system	orthorhombic
Space group	P2 ₁ 2 ₁ 2 ₁
a/Å	10.3510(12)
b/Å	11.8569(15)
c/Å	17.478(2)
α/°	90
β/°	90
γ/°	90
Volume/Å ³	2145.1(4)
Z	4
ρ _{calc} /cm ³	1.314
μ/mm ⁻¹	0.681
F(000)	896.0
Crystal size/mm ³	0.15 × 0.11 × 0.07
Radiation	CuKα (λ = 1.54178)
2θ range for data collection/°	9.012 to 144.53
Index ranges	-12 ≤ h ≤ 12, -14 ≤ k ≤ 14, -19 ≤ l ≤ 21

Reflections collected	39025
Independent reflections	4235 [$R_{\text{int}} = 0.0300$, $R_{\text{sigma}} = 0.0183$]
Data/restraints/parameters	4235/0/292
Goodness-of-fit on F^2	1.047
Final R indexes [$I \geq 2\sigma(I)$]	$R_1 = 0.0277$, $wR_2 = 0.0664$
Final R indexes [all data]	$R_1 = 0.0280$, $wR_2 = 0.0667$
Largest diff. peak/hole / $e \text{ \AA}^{-3}$	0.25/-0.22
Flack parameter	0.01(4)

Table 3.2 Fractional Atomic Coordinates ($\times 10^4$) and Equivalent Isotropic Displacement Parameters ($\text{\AA}^2 \times 10^3$) for yoon59a. U_{eq} is defined as 1/3 of the trace of the orthogonalised U_{ij} tensor.

Atom	x	y	z	U(eq)
O1	7158.2(11)	5788.9(10)	7759.5(7)	23.6(3)
O2	4763.5(11)	3755.1(11)	5335.5(7)	28.4(3)
N1	9244.2(13)	4217.9(11)	7382.1(7)	17.8(3)
N2	7736.6(13)	3162.8(11)	6814.4(7)	18.9(3)
N3	7432.6(13)	3621.6(12)	4817.7(7)	20.5(3)
N4	7827.3(13)	5112.1(12)	5558.5(7)	20.9(3)
C1	5640.9(14)	4634.3(13)	7081.6(8)	17.0(3)
C2	5311.3(14)	5140.1(13)	6272.7(8)	17.0(3)
C3	3897.9(14)	5251.8(13)	6556.1(8)	16.6(3)
C4	4429.2(14)	5238.5(13)	7394.1(8)	16.4(3)

C5	6952.7(15)	4925.2(13)	7398.8(8)	17.3(3)
C6	7962.6(15)	4102.6(13)	7210.5(8)	16.8(3)
C7	9870.0(15)	5127.8(14)	7805.1(9)	22.3(3)
C8	9851.6(16)	3307.0(14)	7078.2(10)	22.3(3)
C9	8914.0(16)	2671.8(14)	6727.7(10)	22.0(3)
C10	5591.0(15)	4376.6(13)	5604.6(9)	18.9(3)
C11	6931.7(15)	4387.2(13)	5322.4(8)	18.3(3)
C12	6807.5(18)	2676.7(16)	4434.7(11)	31.3(4)
C13	8703.8(16)	3878.0(15)	4735.0(10)	24.1(3)
C14	8931.5(16)	4794.0(15)	5192.2(10)	24.9(4)
C15	3051.3(15)	6222.4(13)	6317.2(8)	17.8(3)
C16	3535.6(17)	7310.1(14)	6227.0(9)	22.3(3)
C17	2719.7(19)	8195.6(14)	6034.6(9)	26.5(4)
C18	1408.6(19)	8008.9(15)	5927.7(10)	28.3(4)
C19	910.3(18)	6935.6(15)	6023.6(10)	27.5(4)
C20	1732.3(16)	6046.6(14)	6211.9(9)	21.4(3)
C21	3653.6(14)	4688.2(13)	8017.0(9)	17.0(3)
C22	3309.7(15)	3546.6(14)	7980.8(9)	19.7(3)
C23	2615.8(16)	3040.1(14)	8568.3(9)	22.5(3)
C24	2247.6(15)	3667.6(16)	9203.0(9)	23.8(3)
C25	2557.6(16)	4808.6(16)	9239.5(9)	23.6(3)
C26	3255.5(14)	5312.2(14)	8651.8(9)	19.5(3)

Table 3.3 Anisotropic Displacement Parameters ($\text{\AA}^2 \times 10^3$) for yoon59a. The Anisotropic displacement factor exponent takes the form: $-2\pi^2 [h^2 a^{*2} U_{11} + 2hka^* b^* U_{12} + \dots]$.

Atom	U_{11}	U_{22}	U_{33}	U_{23}	U_{13}	U_{12}
O1	22.0(6)	22.2(6)	26.6(6)	-5.7(5)	-1.8(5)	-0.9(5)
O2	20.3(6)	32.7(7)	32.1(6)	-13.0(5)	0.0(5)	-2.7(5)
N1	16.4(6)	19.5(6)	17.6(6)	0.5(5)	-1.3(5)	-0.4(5)
N2	19.2(7)	17.5(6)	20.0(6)	1.4(5)	-2.2(5)	0.8(5)
N3	19.7(7)	23.8(7)	18.0(6)	-2.5(5)	-0.7(5)	4.1(5)
N4	20.3(7)	22.5(7)	19.9(6)	1.3(5)	-0.8(5)	-0.4(6)
C1	15.4(7)	18.1(7)	17.5(7)	0.2(6)	0.8(6)	0.5(6)
C2	15.9(7)	18.4(7)	16.8(7)	0.0(6)	0.1(6)	-0.9(6)
C3	16.7(7)	17.4(7)	15.6(7)	-1.0(6)	0.8(6)	-0.6(6)
C4	14.2(7)	18.2(7)	16.8(7)	-0.3(6)	-0.7(5)	-0.2(6)
C5	17.0(7)	20.0(7)	15.1(7)	1.6(6)	1.6(6)	-1.5(6)
C6	16.3(7)	19.1(7)	15.1(7)	3.5(6)	-1.3(6)	-1.9(6)
C7	17.3(7)	25.2(8)	24.4(8)	-2.8(6)	-3.1(6)	-3.5(6)
C8	18.0(8)	23.3(8)	25.5(8)	0.5(7)	-1.5(6)	5.0(6)
C9	20.8(8)	19.4(7)	25.9(8)	-1.1(6)	-1.6(6)	4.0(6)
C10	19.9(8)	19.6(7)	17.2(7)	-0.3(6)	-0.8(6)	1.1(6)
C11	20.5(8)	20.6(7)	13.8(7)	1.4(6)	-0.5(6)	2.9(6)
C12	27.0(9)	31.4(9)	35.6(9)	-14.9(8)	-1.5(8)	2.7(7)
C13	18.8(8)	29.1(8)	24.5(8)	0.5(7)	3.2(6)	5.8(7)

C14	18.0(7)	29.5(8)	27.4(8)	1.0(7)	0.7(6)	-1.7(7)
C15	21.8(7)	21.0(7)	10.5(6)	-1.1(6)	1.2(6)	2.7(6)
C16	27.9(8)	21.8(7)	17.1(7)	-1.8(6)	-1.0(6)	-1.4(7)
C17	43.5(11)	18.5(7)	17.4(7)	-0.8(6)	-1.6(7)	2.0(8)
C18	37.7(10)	24.8(9)	22.4(8)	-1.1(7)	-1.3(7)	13.0(8)
C19	24.2(9)	31.2(9)	27.2(8)	-0.8(7)	0.2(7)	9.8(7)
C20	22.3(8)	21.4(8)	20.5(7)	0.1(6)	1.6(6)	2.5(6)
C21	12.5(7)	21.0(7)	17.5(7)	3.2(6)	-2.7(6)	1.2(6)
C22	16.7(7)	21.2(8)	21.2(7)	0.7(6)	0.0(6)	2.1(6)
C23	18.8(7)	22.0(8)	26.6(8)	5.9(6)	-2.3(6)	0.1(6)
C24	17.6(7)	34.7(9)	19.3(7)	8.7(7)	0.0(6)	-0.6(7)
C25	20.0(7)	34.0(9)	16.9(7)	-1.5(7)	-0.6(6)	0.9(7)
C26	16.9(7)	22.7(8)	18.9(7)	-0.5(6)	-4.0(6)	0.8(6)

Table 3.4 Bond Lengths for yoon59a.

Atom Atom Length/Å			Atom Atom Length/Å		
O1	C5	1.2213(19)	C3	C15	1.506(2)
O2	C10	1.224(2)	C4	C21	1.502(2)
N1	C6	1.367(2)	C5	C6	1.467(2)
N1	C7	1.459(2)	C8	C9	1.373(2)
N1	C8	1.358(2)	C10	C11	1.473(2)
N2	C6	1.333(2)	C13	C14	1.369(3)

N2	C9	1.359(2)	C15	C16	1.393(2)
N3	C11	1.368(2)	C15	C20	1.393(2)
N3	C12	1.457(2)	C16	C17	1.389(2)
N3	C13	1.358(2)	C17	C18	1.388(3)
N4	C11	1.330(2)	C18	C19	1.383(3)
N4	C14	1.363(2)	C19	C20	1.394(2)
C1	C2	1.573(2)	C21	C22	1.401(2)
C1	C4	1.544(2)	C21	C26	1.396(2)
C1	C5	1.507(2)	C22	C23	1.390(2)
C2	C3	1.550(2)	C23	C24	1.389(2)
C2	C10	1.506(2)	C24	C25	1.392(3)
C3	C4	1.565(2)	C25	C26	1.390(2)

Table 3.5 Bond Angles for yoon59a.

Atom Atom Atom Angle/°				Atom Atom Atom Angle/°			
C6	N1	C7	128.01(13)	N1	C8	C9	106.47(14)
C8	N1	C6	106.49(13)	N2	C9	C8	110.44(14)
C8	N1	C7	125.49(13)	O2	C10	C2	121.70(14)
C6	N2	C9	104.99(13)	O2	C10	C11	122.41(14)
C11	N3	C12	129.67(14)	C11	C10	C2	115.84(13)
C13	N3	C11	106.69(14)	N3	C11	C10	124.57(14)
C13	N3	C12	123.62(14)	N4	C11	N3	111.40(14)

C11	N4	C14	105.06(14)	N4	C11	C10	123.95(14)
C4	C1	C2	87.99(11)	N3	C13	C14	106.39(15)
C5	C1	C2	116.03(12)	N4	C14	C13	110.45(15)
C5	C1	C4	119.71(12)	C16	C15	C3	121.99(14)
C3	C2	C1	87.13(11)	C16	C15	C20	118.45(15)
C10	C2	C1	115.22(13)	C20	C15	C3	119.51(14)
C10	C2	C3	118.73(13)	C17	C16	C15	120.57(16)
C2	C3	C4	88.08(11)	C18	C17	C16	120.45(17)
C15	C3	C2	121.73(13)	C19	C18	C17	119.67(16)
C15	C3	C4	118.16(12)	C18	C19	C20	119.78(17)
C1	C4	C3	87.65(11)	C15	C20	C19	121.07(16)
C21	C4	C1	119.27(13)	C22	C21	C4	121.53(14)
C21	C4	C3	119.67(12)	C26	C21	C4	120.24(14)
O1	C5	C1	122.60(14)	C26	C21	C22	118.23(15)
O1	C5	C6	123.31(14)	C23	C22	C21	121.04(15)
C6	C5	C1	114.05(13)	C24	C23	C22	120.03(15)
N1	C6	C5	125.16(14)	C23	C24	C25	119.60(15)
N2	C6	N1	111.60(14)	C26	C25	C24	120.22(16)
N2	C6	C5	123.18(14)	C25	C26	C21	120.86(15)

Table 3.6 Torsion Angles for yoon59a.

A B C D Angle/° A B C D Angle/°

O1C5 C6 N1 -2.9(2)	C5 C1 C2 C3 -145.02(13)
O1C5 C6 N2 -179.75(14)	C5 C1 C2 C1094.42(16)
O2C10C11N3 -9.2(2)	C5 C1 C4 C3 141.51(14)
O2C10C11N4 174.39(15)	C5 C1 C4 C21-95.46(17)
N1C8 C9 N2 -0.62(19)	C6 N1 C8 C9 0.33(18)
N3C13C14N4 0.1(2)	C6 N2 C9 C8 0.66(18)
C1C2 C3 C4 22.38(11)	C7 N1 C6 N2 179.97(14)
C1C2 C3 C15144.68(14)	C7 N1 C6 C5 2.8(2)
C1C2 C10O2 93.25(18)	C7 N1 C8 C9 -179.57(14)
C1C2 C10C11-83.95(17)	C8 N1 C6 N2 0.08(17)
C1C4 C21C22-46.3(2)	C8 N1 C6 C5 -177.08(14)
C1C4 C21C26133.70(15)	C9 N2 C6 N1 -0.45(17)
C1C5 C6 N1 174.88(14)	C9 N2 C6 C5 176.78(14)
C1C5 C6 N2 -2.0(2)	C10C2 C3 C4 139.71(14)
C2C1 C4 C3 22.46(11)	C10C2 C3 C15-97.98(17)
C2C1 C4 C21145.48(13)	C11N3 C13C14-0.11(18)
C2C1 C5 O1 85.88(18)	C11N4 C14C130.02(19)
C2C1 C5 C6 -91.92(16)	C12N3 C11N4 178.61(16)
C2C3 C4 C1 -22.81(11)	C12N3 C11C101.8(3)
C2C3 C4 C21-145.48(14)	C12N3 C13C14-178.70(16)
C2C3 C15C16-37.1(2)	C13N3 C11N4 0.13(18)
C2C3 C15C20145.60(15)	C13N3 C11C10-176.65(15)

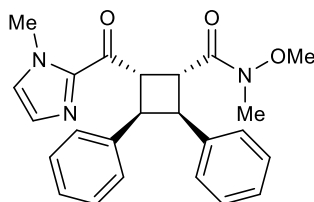
C2 C10 C11 N3	167.96(14)	C14 N4 C11 N3	-0.10(18)
C2 C10 C11 N4	-8.4(2)	C14 N4 C11 C10	176.71(14)
C3 C2 C10 O2	-8.0(2)	C15 C3 C4 C1	-148.19(14)
C3 C2 C10 C11	174.79(13)	C15 C3 C4 C2	189.14(18)
C3 C4 C21 C22	59.06(19)	C15 C16 C17 C18	-0.1(2)
C3 C4 C21 C26	-120.92(16)	C16 C15 C20 C19	-0.2(2)
C3 C15 C16 C17	-177.51(14)	C16 C17 C18 C19	0.9(3)
C3 C15 C20 C19	177.16(14)	C17 C18 C19 C20	-1.3(3)
C4 C1 C2 C3	-22.69(11)	C18 C19 C20 C15	1.0(3)
C4 C1 C2 C10	-143.25(13)	C20 C15 C16 C17	-0.2(2)
C4 C1 C5 O1	-17.6(2)	C21 C22 C23 C24	0.2(2)
C4 C1 C5 C6	164.56(13)	C22 C21 C26 C25	1.2(2)
C4 C3 C15 C16	69.55(18)	C22 C23 C24 C25	1.2(2)
C4 C3 C15 C20	-107.76(16)	C23 C24 C25 C26	-1.4(2)
C4 C21 C22 C23	178.59(14)	C24 C25 C26 C21	0.2(2)
C4 C21 C26 C25	-178.80(14)	C26 C21 C22 C23	-1.4(2)

Table 3.7 Hydrogen Atom Coordinates ($\text{\AA} \times 10^4$) and Isotropic Displacement Parameters ($\text{\AA}^2 \times 10^3$) for yoon59a.

Atom	x	y	z	U(eq)
H1	5509.55	3798.77	7082.1	20
H2	5719.85	5897.12	6201.64	20

H3	3431.54	4528.23	6455.33	20
H4	4662.09	6023.34	7551.84	20
H7A	9471.77	5197.67	8311.56	33
H7B	9766.9	5837.83	7524.65	33
H7C	10791.62	4958.85	7863.07	33
H8	10748.73	3141.92	7103.13	27
H9	9066.57	1985.67	6462.01	26
H12A	6280.25	2958.36	4010	47
H12B	6254.68	2275.76	4799.75	47
H12C	7466.84	2160.32	4236.82	47
H13	9314.1	3497.16	4421.81	29
H14	9744.54	5156.98	5246.66	30
H16	4431.9	7447.61	6297.72	27
H17	3061.38	8934.13	5975.69	32
H18	855.94	8615.16	5789.3	34
H19	11	6804.74	5961.26	33
H20	1387.48	5308.9	6269.51	26
H22	3554.71	3112	7547.89	24
H23	2393.07	2264.26	8535.79	27
H24	1787	3320.09	9609.79	29
H25	2291.5	5244.82	9667.3	28
H26	3464.14	6091.14	8682.72	23

(1R,2S,3R,4S)-N-methoxy-N-methyl-2-(1-methyl-1H-imidazole-2-carbonyl)-3,4-diphenylcyclobutane-1-carboxamide



Data Collection: A colorless crystal with approximate dimensions 0.38 x 0.19 x 0.01 mm³ was selected under oil under ambient conditions and attached to the tip of a MiTeGen MicroMount[®]. The crystal was mounted in a stream of cold nitrogen at 150(1) K and centered in the X-ray beam by using a video camera.

The crystal evaluation and data collection were performed on a Bruker D8 VENTURE PhotonIII four-circle diffractometer with Cu K α ($\lambda = 1.54178 \text{ \AA}$) radiation and the detector to crystal distance of 4.0 cm.

The initial cell constants were obtained from a 180° φ scan conducted at a $2\theta = 50^\circ$ angle with an exposure time of 1 second per frame. The reflections were successfully indexed by an automated indexing routine built into the APEX3 program. The final cell constants were calculated from a set of 9823 strong reflections from the actual data collection.

The data were collected by using a full sphere data collection routine to survey reciprocal space to the extent of a full sphere to a resolution of 0.78 \AA . A total of 66522 data were harvested by collecting 22 sets of frames with 0.7 – 1.0° scans in ω and φ with exposure times of 1.0 – 5.0 sec per frame. These highly redundant datasets were corrected for Lorentz and polarization effects.

The absorption correction was based on fitting a function to the empirical transmission surface as sampled by multiple equivalent measurements.

Structure Solution and Refinement: The systematic absences in the diffraction data were uniquely consistent for the space group P212121 that yielded chemically reasonable and computationally stable results of refinement.

A successful solution by direct methods provided most non-hydrogen atoms from the E-map. The remaining non-hydrogen atoms were located with an alternating series of least-squares cycles and difference Fourier maps. All non-hydrogen atoms were refined with anisotropic displacement coefficients. All hydrogen atoms (except atom H2, bound to atom C2) were included in the structure factor calculation at idealized positions and were allowed to ride on the neighboring atoms with relative isotropic displacement coefficients.

The absolute configuration of the molecule was unequivocally [Flack $x = 0.02(4)$, Hooft $y = 0.02(3)$] established by anomalous dispersion effects: C1 – S; C2 – R; C3 – S; C4 – R.

The final least-squares refinement of 278 parameters against 4527 data resulted in residuals R (based on F2 for $I \geq 2\sigma$) and wR (based on F2 for all data) of 0.0291 and 0.0745, respectively. The final difference Fourier map was featureless.

Summary: Crystal Data for C₂₄H₂₅N₃O₃ (M = 403.47 g/mol): orthorhombic, space group P212121 (no. 19), $a = 6.7520(7)$ Å, $b = 10.2010(10)$ Å, $c = 30.453(3)$ Å, $V = 2097.5(4)$ Å³, $Z = 4$, $T = 150.0$ K, $\mu(\text{Cu K}\alpha) = 0.687$ mm⁻¹, $D_{\text{calc}} = 1.278$ g/cm³, 50076 reflections measured ($5.804^\circ \leq 2\theta \leq 158.968^\circ$), 4527 unique ($R_{\text{int}} = 0.0309$, $R_{\text{sigma}} = 0.0146$) which were used in all calculations. The final R1 was 0.0291 ($I > 2\sigma(I)$) and wR2 was 0.0745 (all data).

Acknowledgement: The purchase of the Bruker D8 VENTURE Photon III X-ray diffractometer was partially funded by NSF Award #CHE-1919350 to the UW–Madison Department of Chemistry.

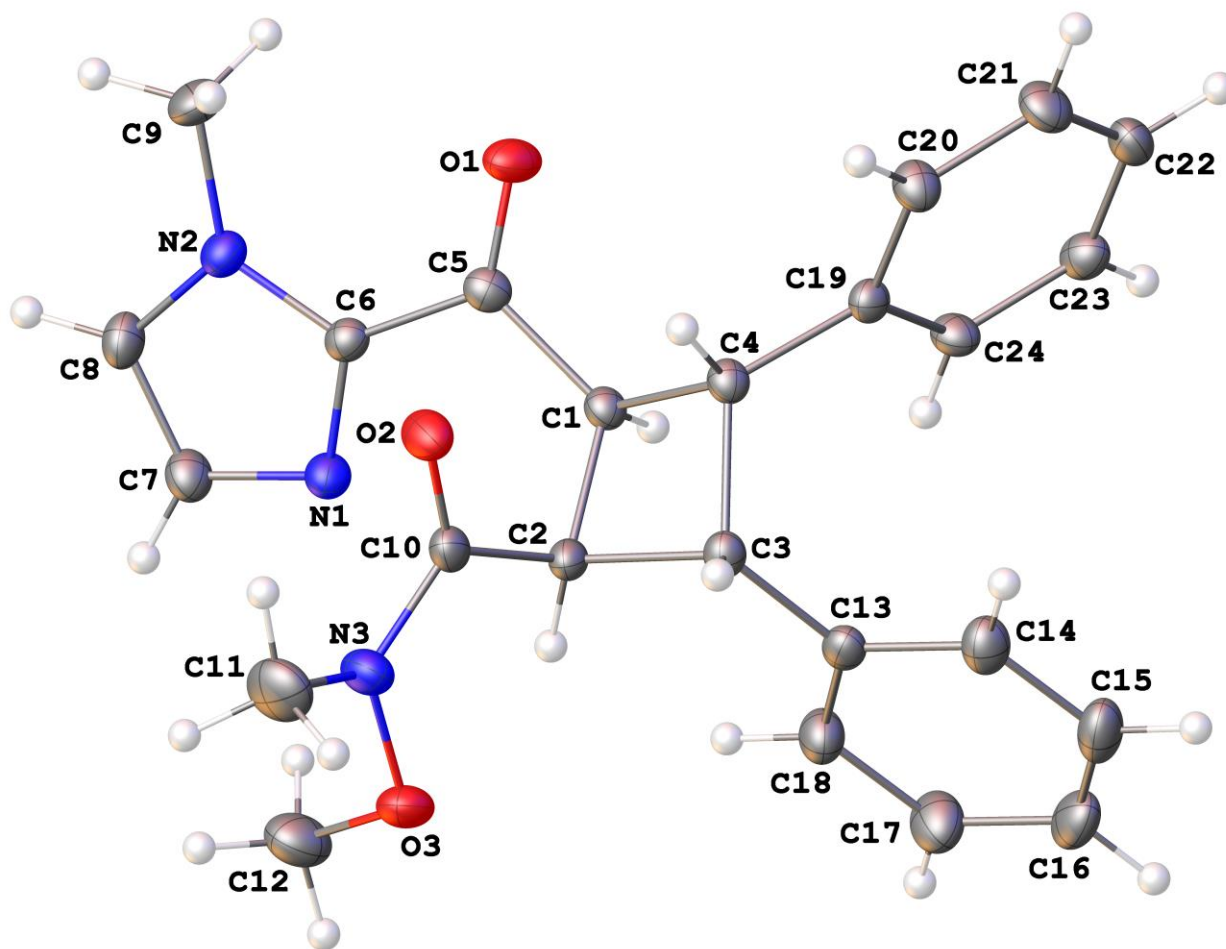


Figure 3.6 A molecular drawing of Yoon70a shown with 50% probability ellipsoids; all minor disorder components are omitted.

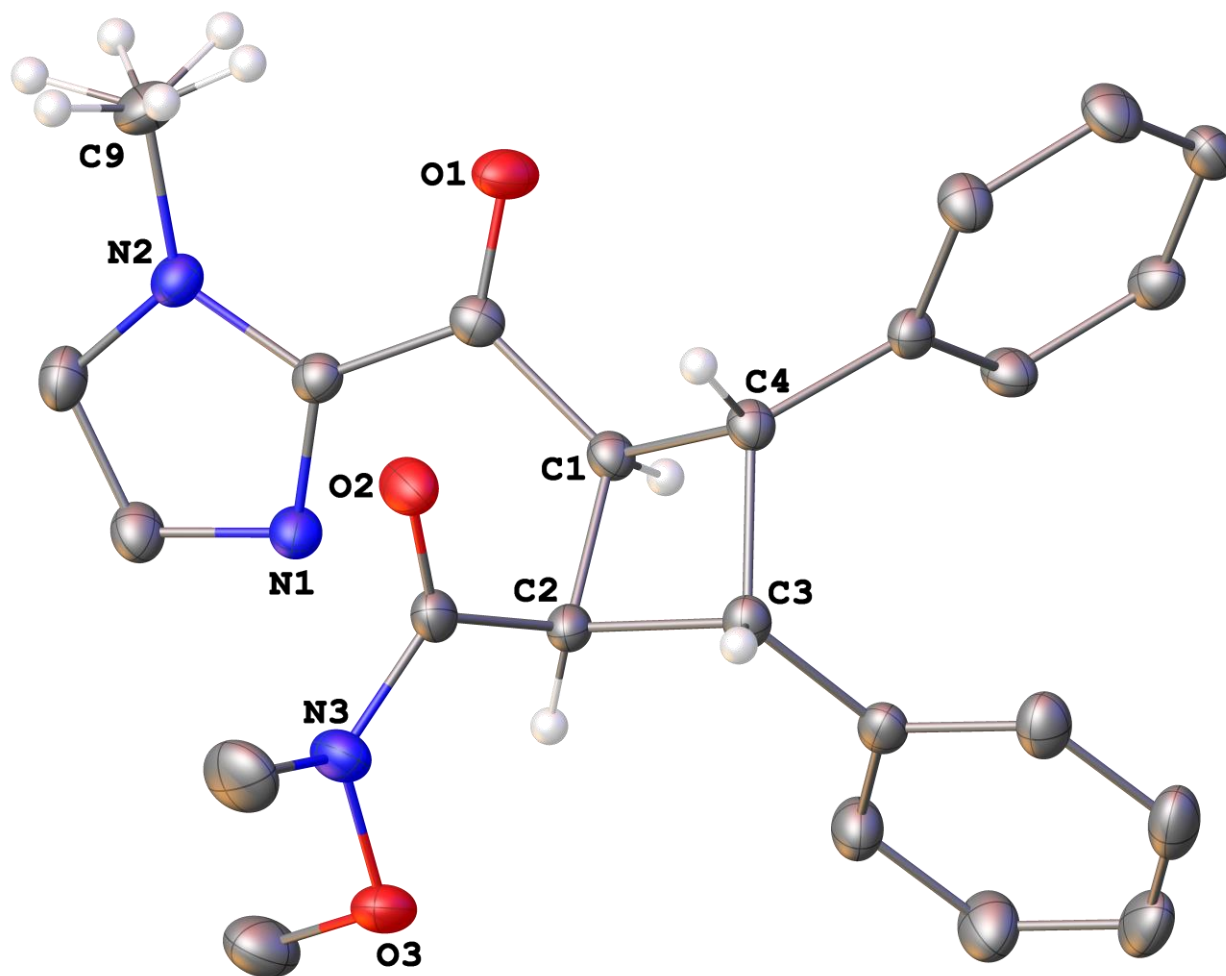


Figure 3.7 A molecular drawing of Yoon70a displaying the disordered H-atoms bound to C9 with selected atom labels. All atoms are shown with 50% probability ellipsoids; all H-atoms that are not bound to C9 or to chiral carbons are omitted.

Table 3.8 *Crystal data and structure refinement for Yoon70a.*

Identification code	Yoon70a
Empirical formula	C ₂₄ H ₂₅ N ₃ O ₃
Formula weight	403.47
Temperature/K	150.0
Crystal system	orthorhombic
Space group	<i>P</i> 2 ₁ 2 ₁ 2 ₁
<i>a</i> /Å	6.7520(7)
<i>b</i> /Å	10.2010(10)
<i>c</i> /Å	30.453(3)
α /°	90
β /°	90
γ /°	90
Volume/Å ³	2097.5(4)
<i>Z</i>	4
ρ_{calc} /g/cm ³	1.278
μ /mm ⁻¹	0.687
F(000)	856.0
Crystal size/mm ³	0.38 × 0.19 × 0.01
Radiation	Cu K α (λ = 1.54178)
2 Θ range for data collection/°	5.804 to 158.968
Index ranges	-8 ≤ <i>h</i> ≤ 8, -12 ≤ <i>k</i> ≤ 12, -38 ≤ <i>l</i> ≤ 38

Reflections collected	50076
Independent reflections	4527 [$R_{\text{int}} = 0.0309$, $R_{\text{sigma}} = 0.0146$]
Data/restraints/parameters	4527/0/278
Goodness-of-fit on F^2	1.036
Final R indexes [$I >= 2\sigma(I)$]	$R_1 = 0.0291$, $wR_2 = 0.0742$
Final R indexes [all data]	$R_1 = 0.0295$, $wR_2 = 0.0745$
Largest diff. peak/hole / $e \text{ \AA}^{-3}$	0.20/-0.17
Flack parameter	0.02(4)

Table 3.9 Fractional Atomic Coordinates ($\times 10^4$) and Equivalent Isotropic Displacement Parameters ($\text{\AA}^2 \times 10^3$) for Yoon70a. U_{eq} is defined as 1/3 of the trace of the orthogonalised U_{ij} tensor.

Atom	x	y	z	U(eq)
O1	6281.3(17)	429.5(12)	6988.9(4)	27.2(3)
O2	6510.5(17)	233.2(11)	5866.5(4)	26.1(3)
O3	2744.6(19)	1559.3(13)	5211.9(4)	28.2(3)
N1	1599.3(19)	356.6(13)	6445.7(4)	19.8(3)
N2	2878(2)	-1300.3(13)	6829.7(4)	19.8(3)
N3	4153(2)	661.8(15)	5371.5(4)	25.0(3)
C1	4985(2)	2047.5(15)	6501.4(5)	16.6(3)
C2	4512(2)	2139.0(15)	6004.1(5)	17.4(3)
C3	6167(2)	3212.1(15)	5966.3(5)	17.9(3)
C4	7022(2)	2702.0(15)	6421.4(5)	16.8(3)

Atom	x	y	z	U(eq)
C5	4956(2)	742.3(15)	6738.5(5)	18.1(3)
C6	3180(2)	-67.5(15)	6665.8(5)	17.4(3)
C7	250(2)	-630.6(16)	6474.3(5)	23.0(3)
C8	1012(2)	-1653.6(16)	6708.4(5)	23.1(3)
C9	4267(3)	-2140.5(17)	7066.8(6)	27.3(4)
C10	5135(2)	940.6(15)	5749.7(5)	19.2(3)
C11	4914(3)	-222(2)	5041.2(6)	37.5(4)
C12	782(3)	1043(2)	5281.3(7)	36.2(4)
C13	5455(2)	4616.2(15)	5951.0(5)	19.1(3)
C14	6877(3)	5606.9(17)	5922.7(5)	25.7(3)
C15	6335(3)	6917.7(18)	5896.9(6)	30.4(4)
C16	4354(3)	7267.2(17)	5902.1(6)	31.0(4)
C17	2933(3)	6301.2(18)	5935.0(6)	32.6(4)
C18	3477(3)	4981.7(17)	5960.4(6)	26.0(3)
C19	7932(2)	3611.5(14)	6752.8(5)	17.1(3)
C20	9906(2)	3412.0(16)	6873.7(5)	21.8(3)
C21	10828(2)	4216.7(18)	7180.7(6)	25.9(4)
C22	9799(3)	5246.0(16)	7372.0(5)	23.0(3)
C23	7838(3)	5454.4(16)	7253.3(5)	21.8(3)
C24	6906(2)	4646.7(15)	6948.0(5)	20.1(3)

Table 3.10 Anisotropic Displacement Parameters ($\text{\AA}^2 \times 10^3$) for Yoon70a. The Anisotropic displacement factor exponent takes the form: $-2\pi^2 [h^2 a^{*2} U_{11} + 2hka^* b^* U_{12} + \dots]$.

Atom	U_{11}	U_{22}	U_{33}	U_{23}	U_{13}	U_{12}
O1	21.1(5)	31.9(7)	28.6(6)	8.9(5)	-7.3(5)	-1.9(5)
O2	26.5(6)	21.5(6)	30.3(6)	-4.4(5)	-7.1(5)	5.3(5)
O3	30.3(6)	29.6(7)	24.6(5)	6.4(5)	-9.3(5)	-0.8(5)
N1	16.6(6)	18.6(6)	24.1(6)	0.6(5)	-2.1(5)	0.8(5)
N2	20.5(6)	16.5(6)	22.3(6)	1.3(5)	-0.3(5)	1.4(5)
N3	28.1(7)	25.2(7)	21.7(6)	-2.0(5)	-6.9(5)	2.1(6)
C1	13.9(6)	17.1(7)	18.8(6)	-0.7(5)	-1.5(5)	-0.3(6)
C2	16.8(7)	14.7(7)	20.9(7)	1.5(5)	-3.8(6)	-1.5(6)
C3	18.8(7)	17.4(7)	17.6(7)	-0.6(5)	0.8(5)	-1.9(6)
C4	14.0(6)	16.8(7)	19.7(6)	-1.1(5)	-0.3(5)	0.1(6)
C5	15.5(6)	21.1(7)	17.8(6)	-0.6(5)	0.6(5)	1.1(6)
C6	18.1(7)	16.2(7)	17.9(6)	0.0(5)	0.1(5)	1.5(6)
C7	17.7(7)	21.7(8)	29.6(8)	-1.4(6)	-1.8(6)	-1.1(6)
C8	21.8(8)	17.5(7)	30.0(8)	-0.6(6)	1.8(6)	-3.4(6)
C9	31.5(9)	20.8(8)	29.5(8)	6.2(6)	-4.7(7)	4.5(7)
C10	19.8(7)	17.7(7)	20.0(7)	0.9(5)	-2.2(6)	-4.3(6)
C11	48.9(11)	39.1(11)	24.5(8)	-10.1(7)	-3.3(8)	2.9(10)
C12	28.8(9)	44.4(12)	35.5(9)	4.0(8)	-9.8(8)	-1.7(8)
C13	24.1(7)	17.9(7)	15.2(6)	-0.4(5)	-1.1(5)	-1.8(6)

Atom	U₁₁	U₂₂	U₃₃	U₂₃	U₁₃	U₁₂
C14	27.7(8)	23.8(8)	25.5(8)	-0.7(6)	2.8(7)	-5.3(7)
C15	40.0(10)	21.5(8)	29.8(9)	-0.3(7)	3.0(8)	-9.5(8)
C16	46.6(11)	16.8(8)	29.8(8)	-2.1(6)	-2.7(8)	0.8(7)
C17	30.0(9)	23.8(9)	43.9(10)	-5.0(7)	-5.4(8)	3.8(7)
C18	25.7(8)	19.2(8)	33.0(8)	-2.2(6)	-4.0(7)	-1.5(6)
C19	16.5(7)	16.0(7)	18.9(6)	1.6(5)	-0.2(6)	-2.1(6)
C20	17.1(7)	21.8(8)	26.4(7)	-3.0(6)	-0.7(6)	0.9(6)
C21	17.7(7)	30.1(9)	30.0(8)	-1.6(7)	-5.8(6)	-1.4(7)
C22	27.3(8)	22.1(8)	19.6(6)	-1.1(6)	-5.0(6)	-4.5(7)
C23	26.5(8)	19.0(7)	19.8(7)	-0.8(6)	-0.4(6)	3.4(6)
C24	17.8(7)	21.4(7)	21.1(7)	-0.6(6)	-3.6(6)	2.9(6)

Table 3.11 Bond Lengths for Yoon70a.

Atom	Atom	Length/Å	Atom	Atom	Length/Å
O1	C5	1.2183(19)	C3	C13	1.511(2)
O2	C10	1.229(2)	C4	C19	1.502(2)
O3	N3	1.4065(19)	C5	C6	1.473(2)
O3	C12	1.442(2)	C7	C8	1.365(2)
N1	C6	1.3326(19)	C13	C14	1.397(2)
N1	C7	1.361(2)	C13	C18	1.387(2)
N2	C6	1.368(2)	C14	C15	1.389(3)

Atom Atom Length/Å			Atom Atom Length/Å		
N2	C8	1.361(2)	C15	C16	1.384(3)
N2	C9	1.462(2)	C16	C17	1.379(3)
N3	C10	1.359(2)	C17	C18	1.397(2)
N3	C11	1.445(2)	C19	C20	1.398(2)
C1	C2	1.5509(19)	C19	C24	1.396(2)
C1	C4	1.548(2)	C20	C21	1.391(2)
C1	C5	1.515(2)	C21	C22	1.387(2)
C2	C3	1.569(2)	C22	C23	1.389(2)
C2	C10	1.507(2)	C23	C24	1.393(2)
C3	C4	1.589(2)			

Table 3.12 Bond Angles for Yoon70a.

Atom Atom Atom Angle/°				Atom Atom Atom Angle/°			
N3	O3	C12	109.45(13)	N1	C6	C5	123.06(13)
C6	N1	C7	105.30(13)	N2	C6	C5	125.62(13)
C6	N2	C9	128.56(14)	N1	C7	C8	110.30(14)
C8	N2	C6	106.42(13)	N2	C8	C7	106.74(14)
C8	N2	C9	124.94(14)	O2	C10	N3	119.42(15)
O3	N3	C11	113.95(13)	O2	C10	C2	122.59(13)
C10	N3	O3	119.10(13)	N3	C10	C2	117.97(14)
C10	N3	C11	123.14(15)	C14	C13	C3	117.98(14)

Atom	Atom	Atom	Angle/°	Atom	Atom	Atom	Angle/°
C4	C1	C2	90.20(11)	C18	C13	C3	124.07(14)
C5	C1	C2	121.04(12)	C18	C13	C14	117.95(15)
C5	C1	C4	117.77(12)	C15	C14	C13	121.27(17)
C1	C2	C3	88.09(11)	C16	C15	C14	120.14(17)
C10	C2	C1	113.30(12)	C17	C16	C15	119.27(17)
C10	C2	C3	109.23(12)	C16	C17	C18	120.64(18)
C2	C3	C4	88.08(11)	C13	C18	C17	120.73(17)
C13	C3	C2	115.92(13)	C20	C19	C4	118.50(14)
C13	C3	C4	116.92(12)	C24	C19	C4	123.40(14)
C1	C4	C3	87.47(11)	C24	C19	C20	118.10(14)
C19	C4	C1	121.59(12)	C21	C20	C19	121.21(15)
C19	C4	C3	122.16(13)	C22	C21	C20	120.29(15)
O1	C5	C1	121.26(14)	C21	C22	C23	118.96(15)
O1	C5	C6	123.03(14)	C22	C23	C24	120.92(15)
C6	C5	C1	115.61(12)	C23	C24	C19	120.53(14)
N1	C6	N2	111.23(13)				

Table 3.13 Torsion Angles for Yoon70a.

A	B	C	D	Angle/°	A	B	C	D	Angle/°
O1	C5	C6	N1	169.51(15)	C4	C19	C24	C23	179.99(14)
O1	C5	C6	N2	-6.8(2)	C5	C1	C2	C3	-142.02(14)

A	B	C	D	Angle/°	A	B	C	D	Angle/°
O3	N3	C10	O2	-172.34(14)	C5	C1	C2	C10	-31.87(19)
O3	N3	C10	C2	6.1(2)	C5	C1	C4	C3	144.47(13)
N1	C7	C8	N2	0.07(18)	C5	C1	C4	C19	-88.78(17)
C1	C2	C3	C4	18.43(10)	C6	N1	C7	C8	-0.38(18)
C1	C2	C3	C13	-100.73(13)	C6	N2	C8	C7	0.27(17)
C1	C2	C10	O2	-27.4(2)	C7	N1	C6	N2	0.55(17)
C1	C2	C10	N3	154.18(14)	C7	N1	C6	C5	-176.22(14)
C1	C4	C19	C20	131.17(15)	C8	N2	C6	N1	-0.52(17)
C1	C4	C19	C24	-48.6(2)	C8	N2	C6	C5	176.15(14)
C1	C5	C6	N1	-6.9(2)	C9	N2	C6	N1	176.20(15)
C1	C5	C6	N2	176.83(13)	C9	N2	C6	C5	-7.1(2)
C2	C1	C4	C3	18.69(11)	C9	N2	C8	C7	-176.60(15)
C2	C1	C4	C19	145.44(14)	C10	C2	C3	C4	-95.61(12)
C2	C1	C5	O1	134.25(16)	C10	C2	C3	C13	145.23(13)
C2	C1	C5	C6	-49.30(19)	C11	N3	C10	O2	-15.7(2)
C2	C3	C4	C1	-18.48(11)	C11	N3	C10	C2	162.81(16)
C2	C3	C4	C19	-144.76(14)	C12	O3	N3	C10	-106.86(17)
C2	C3	C13	C14	179.25(13)	C12	O3	N3	C11	94.41(18)
C2	C3	C13	C18	-1.2(2)	C13	C3	C4	C1	99.78(14)
C3	C2	C10	O2	69.00(18)	C13	C3	C4	C19	-26.5(2)
C3	C2	C10	N3	-109.41(15)	C13	C14	C15	C16	0.5(3)

A	B	C	D	Angle/°	A	B	C	D	Angle/°
C3	C4	C19	C20	-119.83(16)	C14	C13	C18	C17	1.0(2)
C3	C4	C19	C24	60.3(2)	C14	C15	C16	C17	0.3(3)
C3	C13	C14	C15	178.46(15)	C15	C16	C17	C18	-0.4(3)
C3	C13	C18	C17	-178.53(15)	C16	C17	C18	C13	-0.3(3)
C4	C1	C2	C3	-18.93(11)	C18	C13	C14	C15	-1.1(2)
C4	C1	C2	C10	91.22(13)	C19	C20	C21	C22	-0.4(3)
C4	C1	C5	O1	25.5(2)	C20	C19	C24	C23	0.2(2)
C4	C1	C5	C6	-158.06(12)	C20	C21	C22	C23	0.3(2)
C4	C3	C13	C14	77.43(18)	C21	C22	C23	C24	0.1(2)
C4	C3	C13	C18	-103.02(18)	C22	C23	C24	C19	-0.3(2)
C4	C19	C20	C21	-179.64(15)	C24	C19	C20	C21	0.2(2)

Table 3.14 Hydrogen Atom Coordinates ($\text{\AA} \times 10^4$) and Isotropic Displacement Parameters ($\text{\AA}^2 \times 10^3$) for Yoon70a.

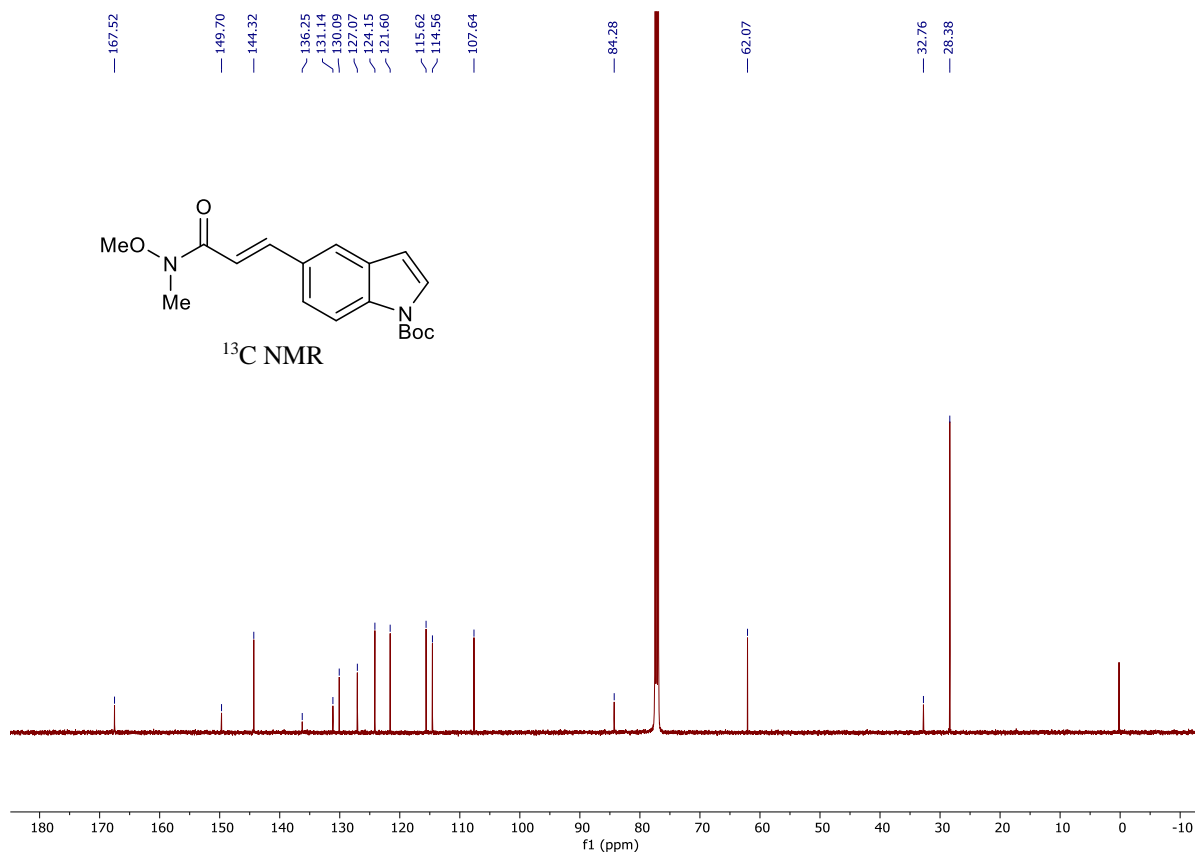
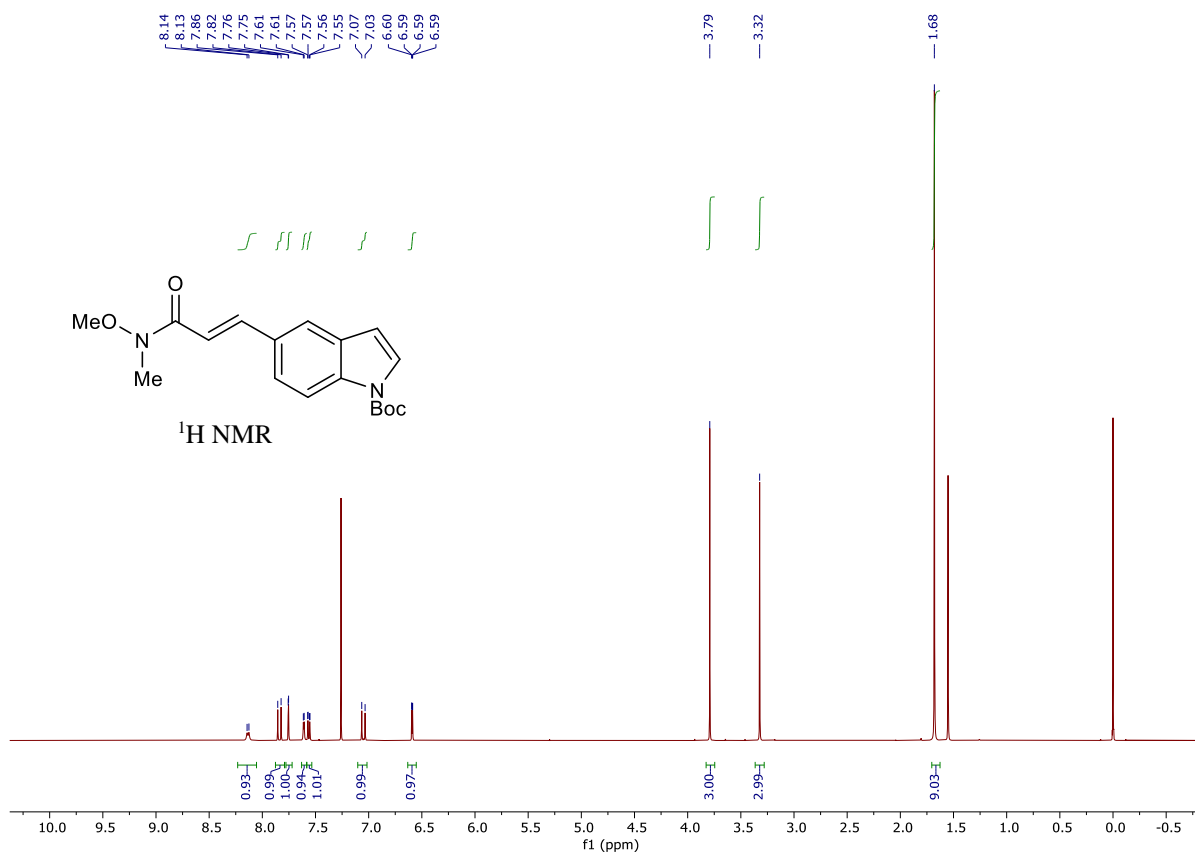
Atom	x	y	z	U(eq)
H1	4116.38	2677.12	6663.34	20
H2	3170(30)	2424(19)	5916(6)	21
H3	7096	3017.83	5719	21
H4	8002.78	1992.95	6357.21	20
H7	-1038.54	-610.42	6349.14	28
H8	365.22	-2457.16	6774.07	28
H9A	5472.57	-2254.07	6891.6	33

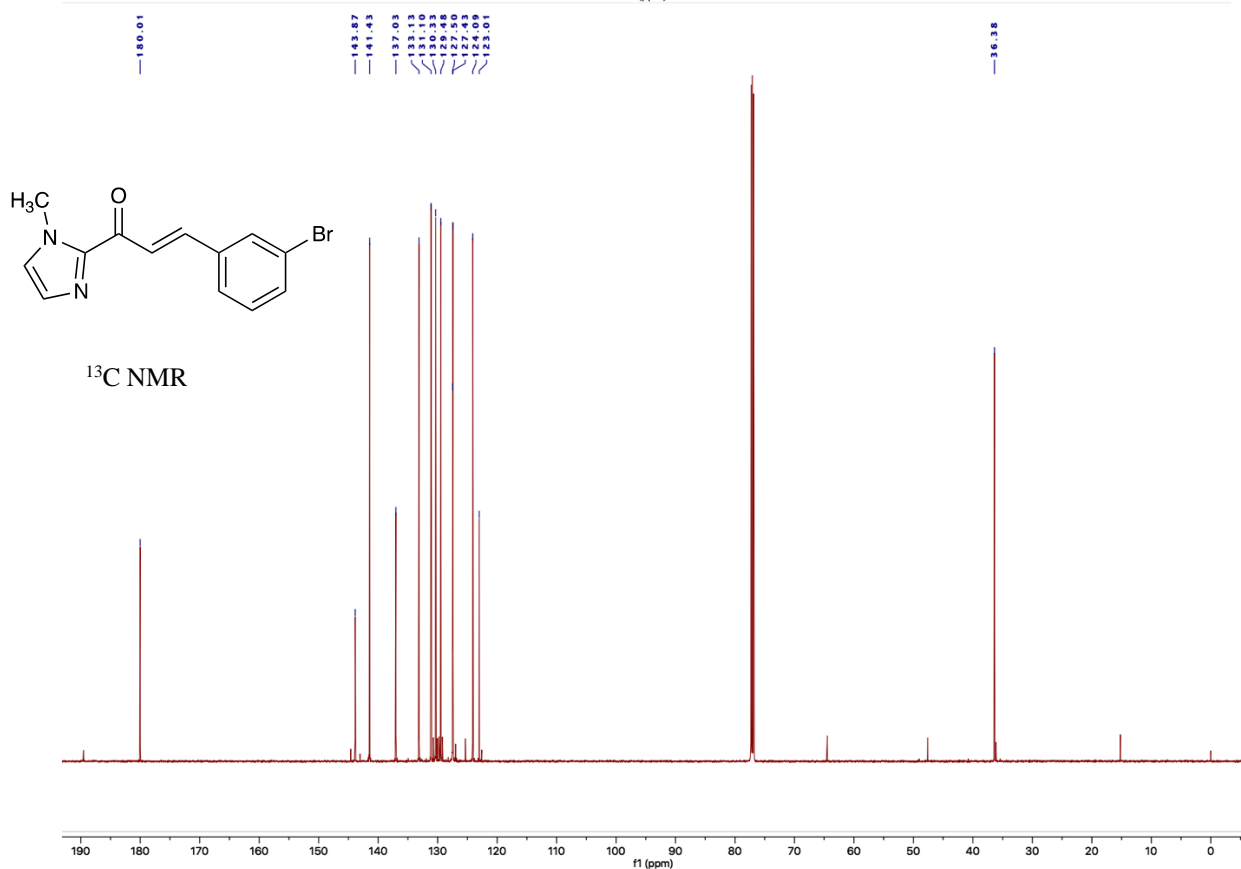
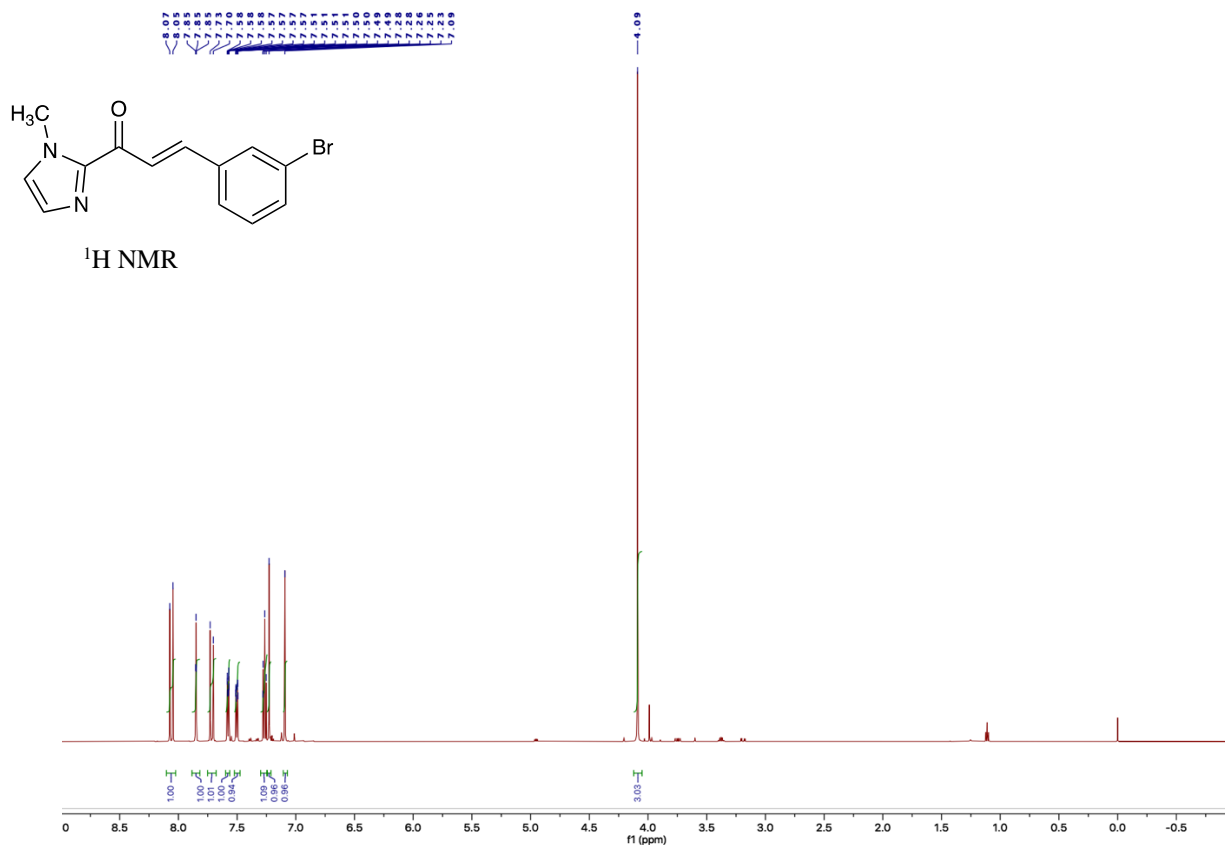
Atom	x	y	z	U(eq)
H9B	3655.74	-2997.57	7119.34	33
H9C	4605.16	-1733.34	7348.49	33
H9D	3683.08	-2402.58	7348.02	33
H9E	5499.91	-1659.08	7120.28	33
H9F	4550.49	-2923.31	6891.13	33
H11A	3835.25	-771.29	4929.71	56
H11B	5941.04	-779.51	5170.88	56
H11C	5483.05	286.68	4799	56
H12A	647.84	204.94	5126.96	54
H12B	-199.13	1665.06	5167.87	54
H12C	562.62	908.89	5596.21	54
H14	8241.85	5379.67	5921.13	31
H15	7325.69	7576.04	5875.59	37
H16	3977.45	8162.75	5883.11	37
H17	1571.65	6534.89	5940.46	39
H18	2481.47	4327.85	5984.42	31
H20	10630.79	2714.28	6743.97	26
H21	12168.59	4060.62	7259.76	31
H22	10425.16	5799.58	7580.88	28
H23	7122.17	6157.82	7382.26	26
H24	5561.97	4801.54	6871.92	24

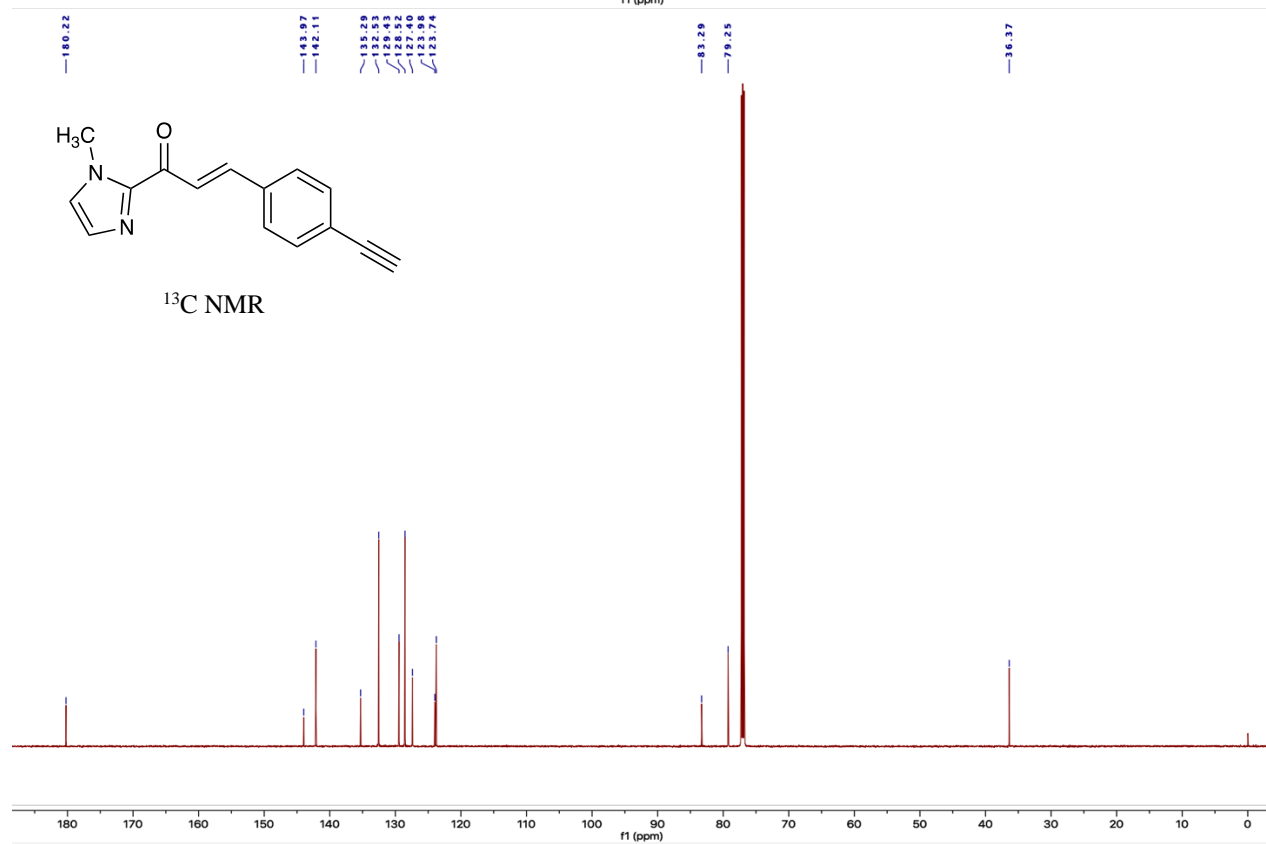
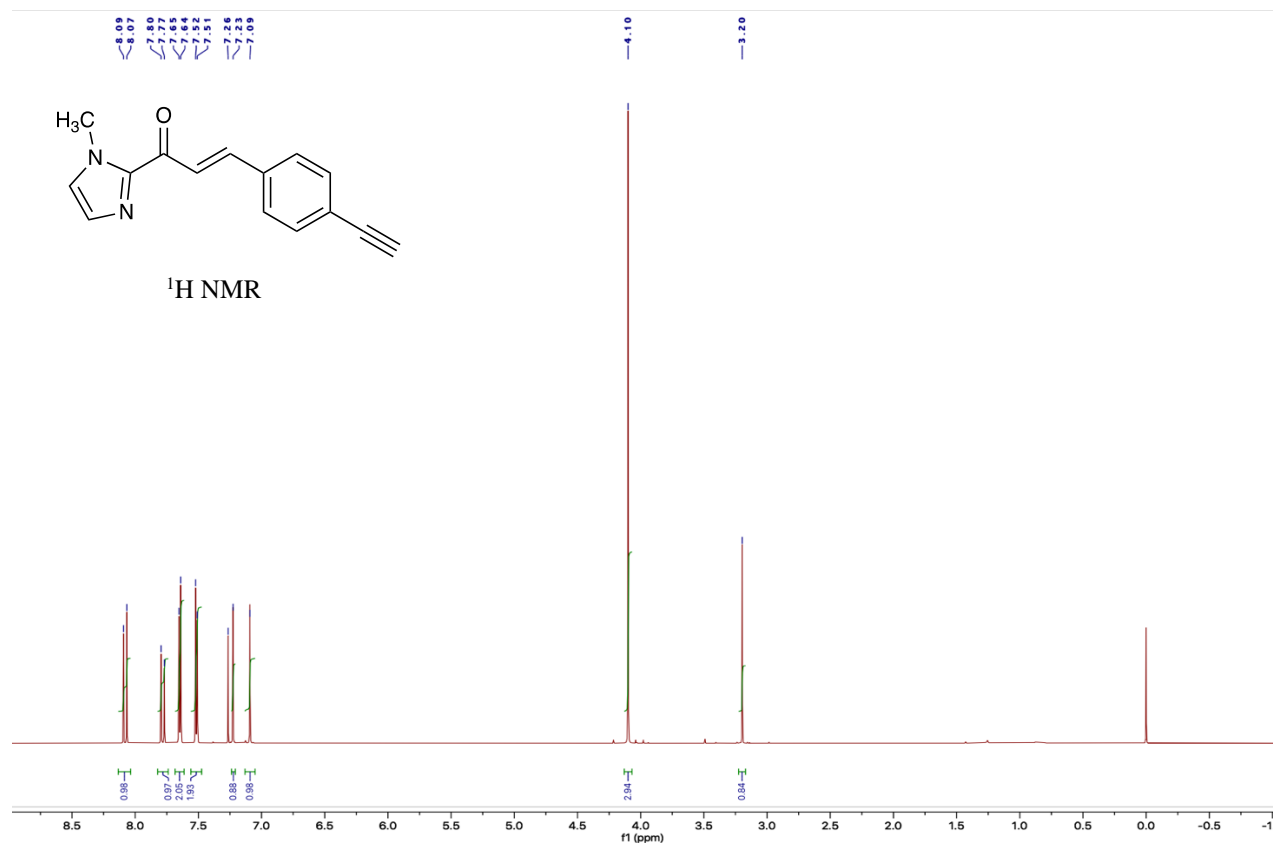
Table 3.15 Atomic Occupancy for Yoon70a.

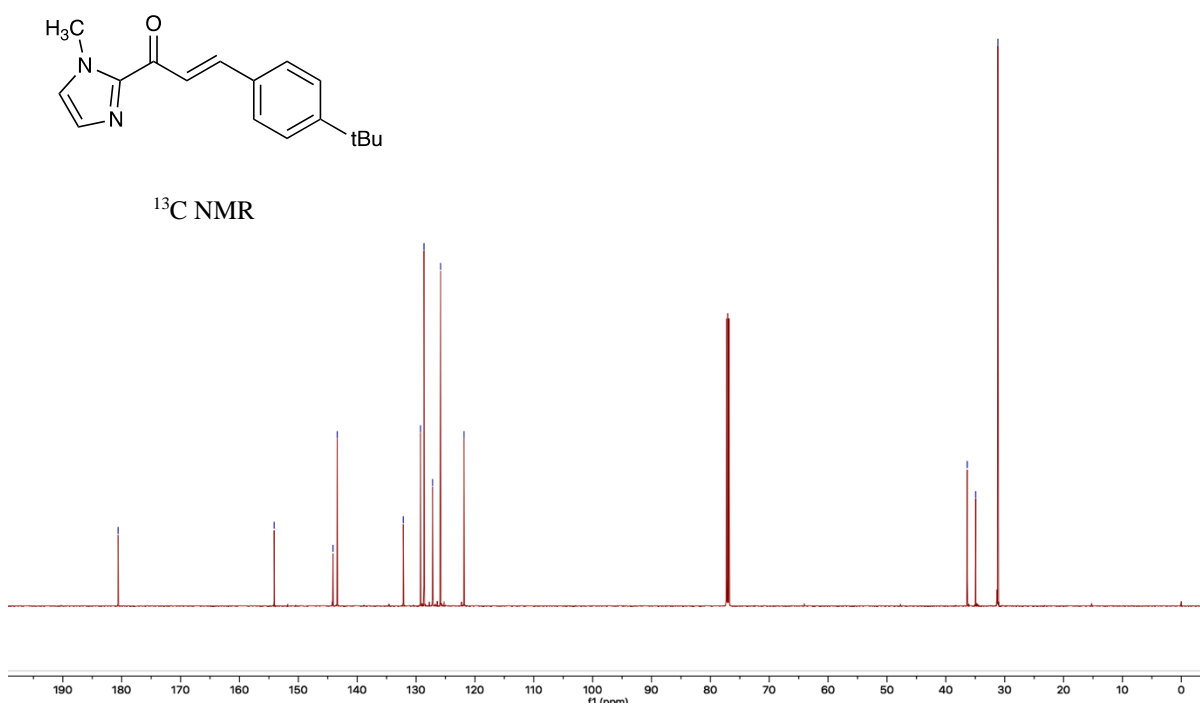
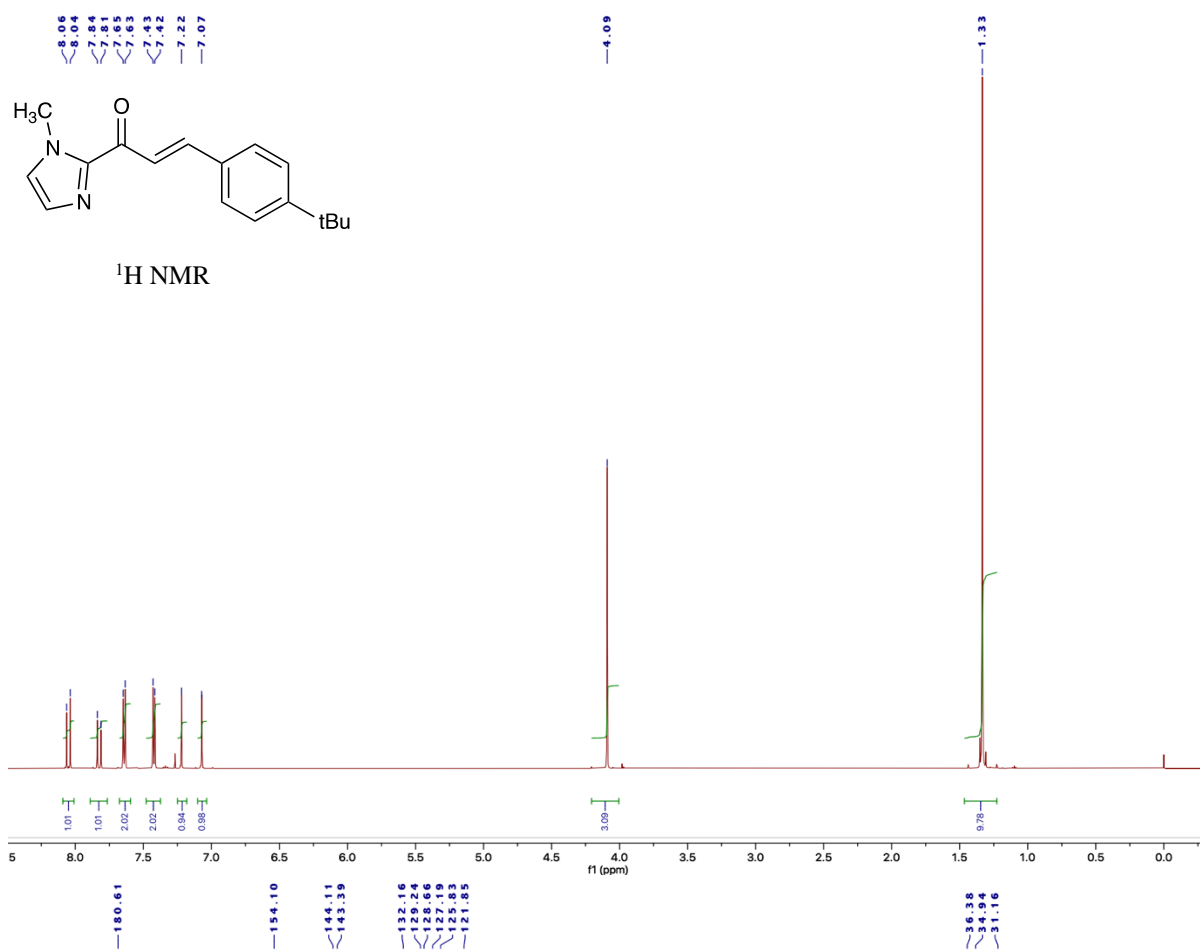
Atom	Occupancy	Atom	Occupancy	Atom	Occupancy
H9A	0.67(2)	H9B	0.67(2)	H9C	0.67(2)
H9D	0.33(2)	H9E	0.33(2)	H9F	0.33(2)

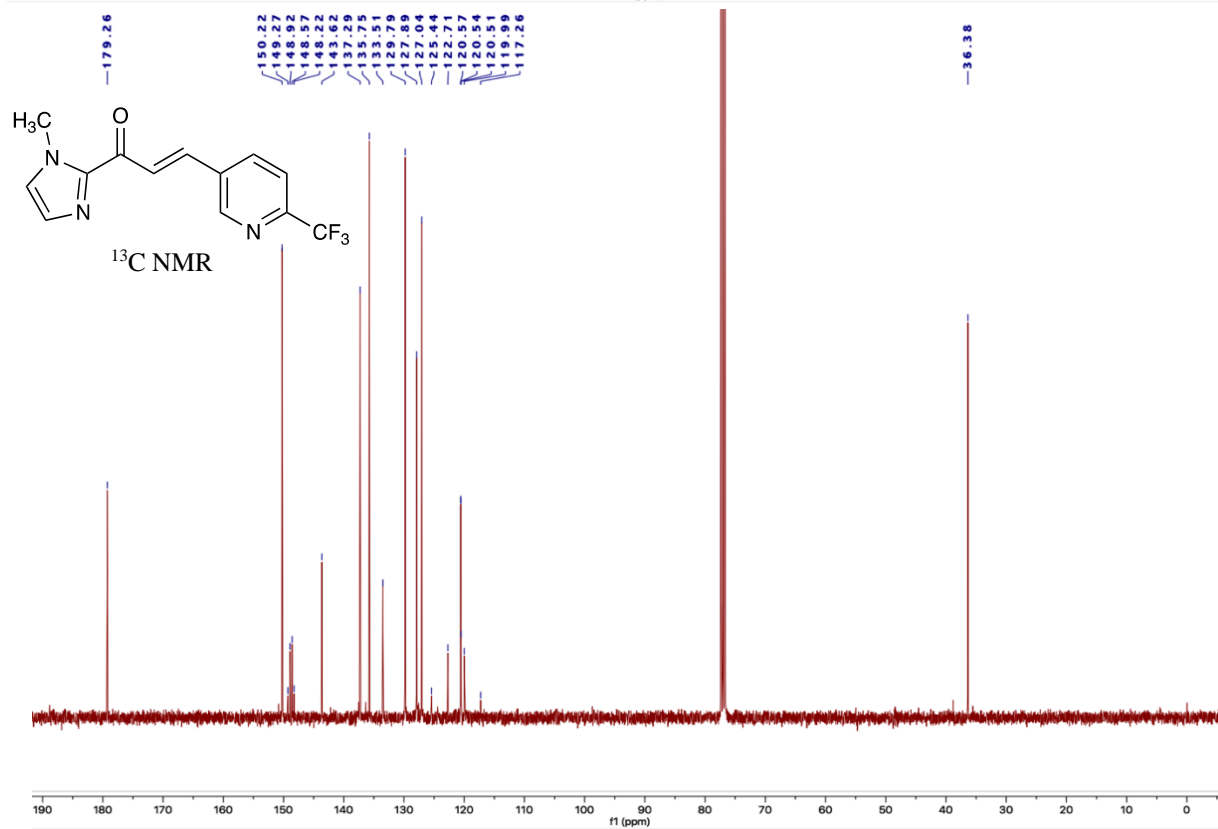
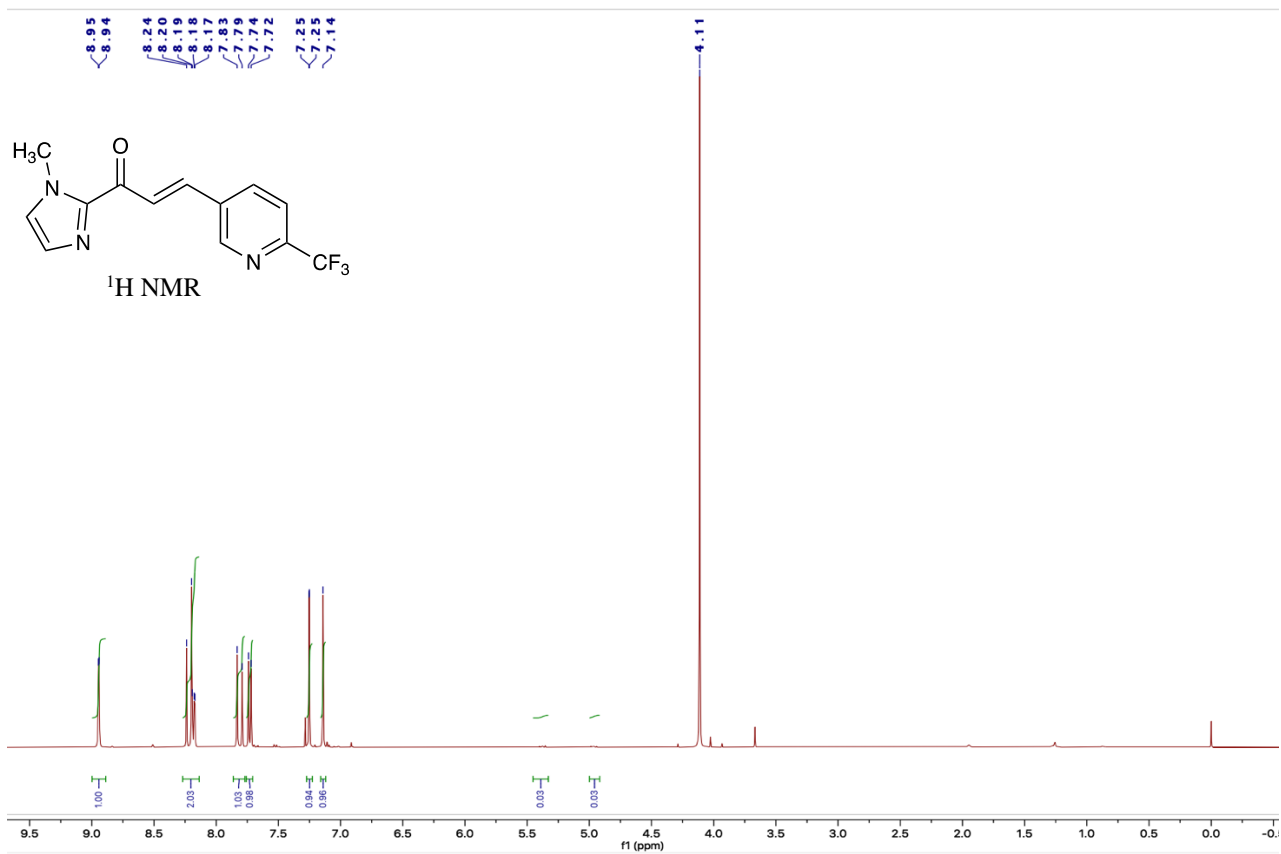
3.5.15 *NMR Data*

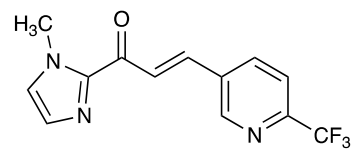




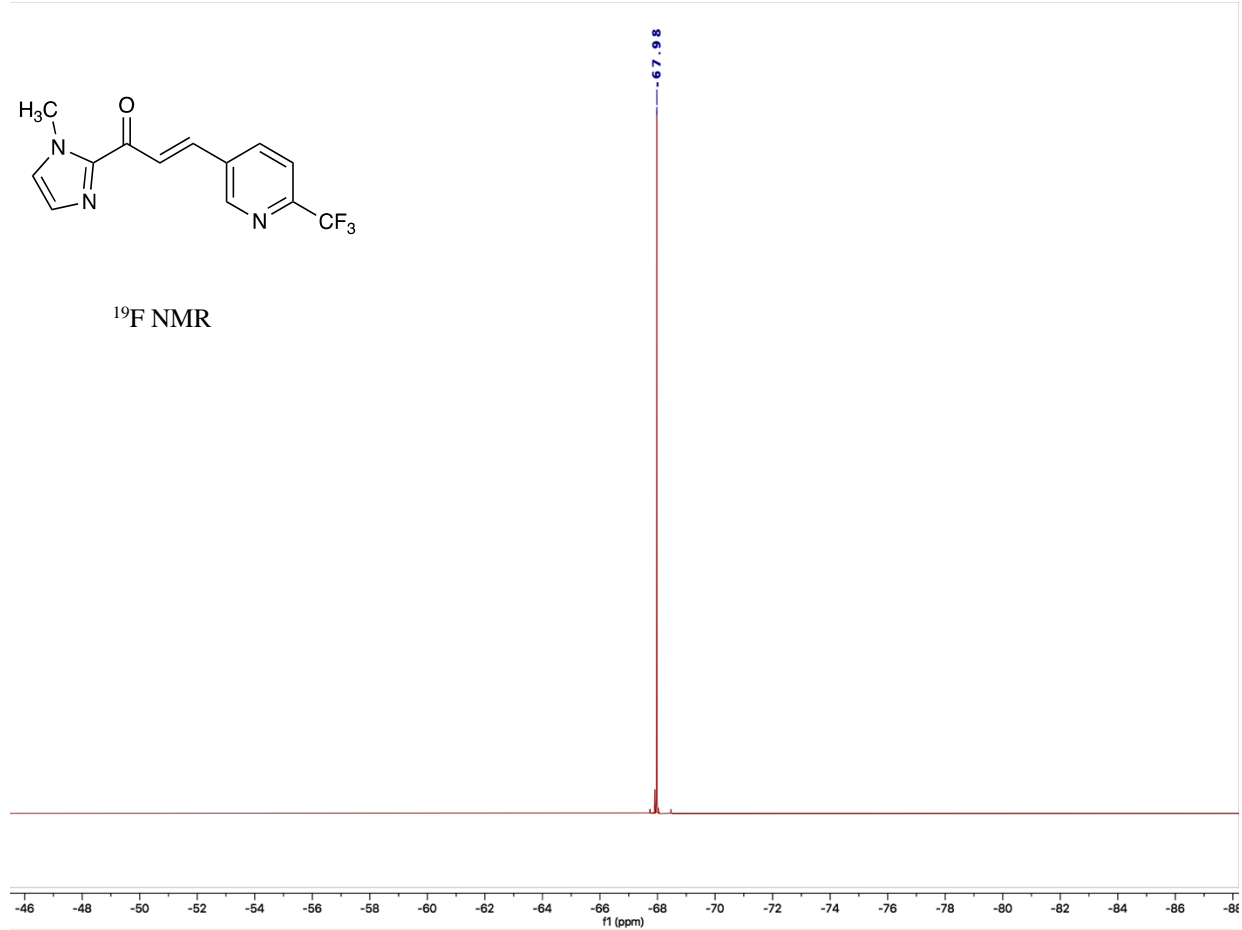


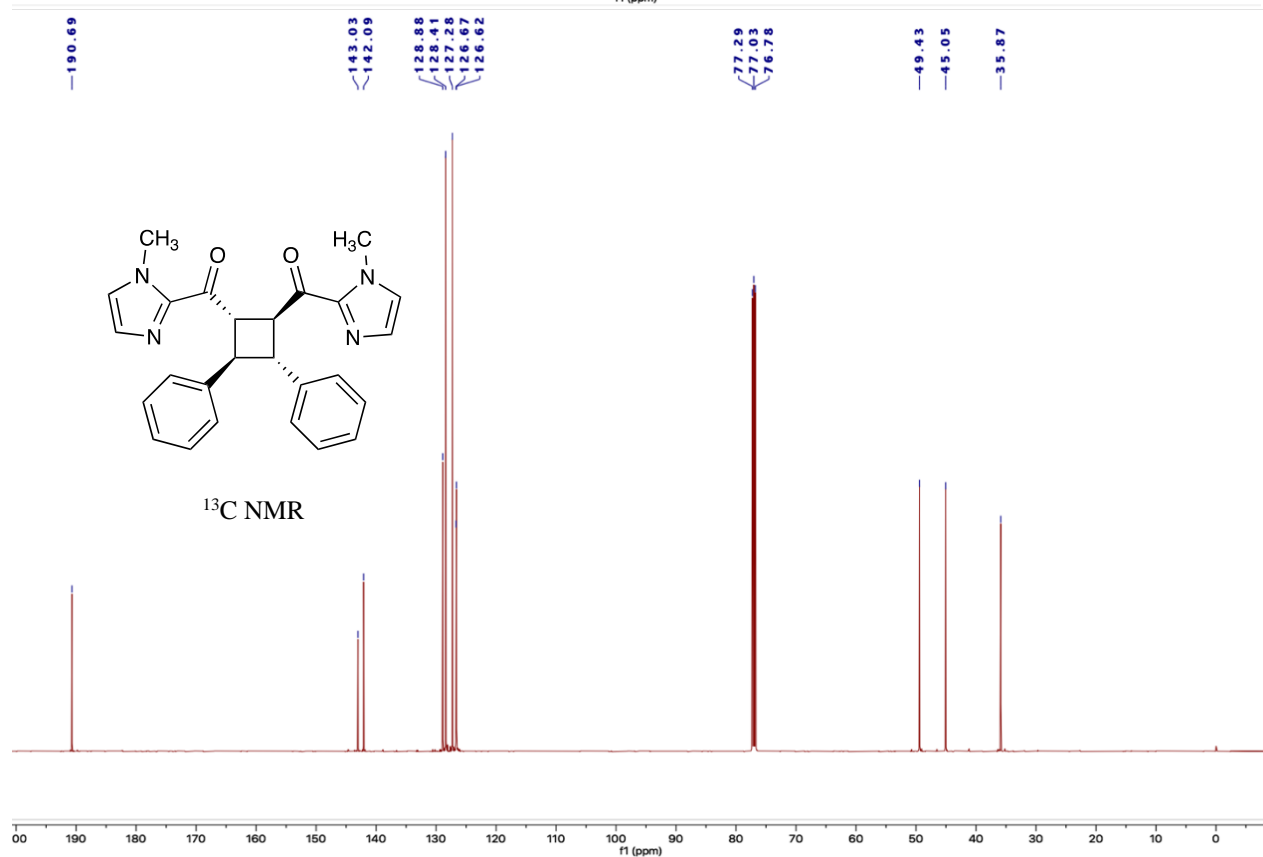
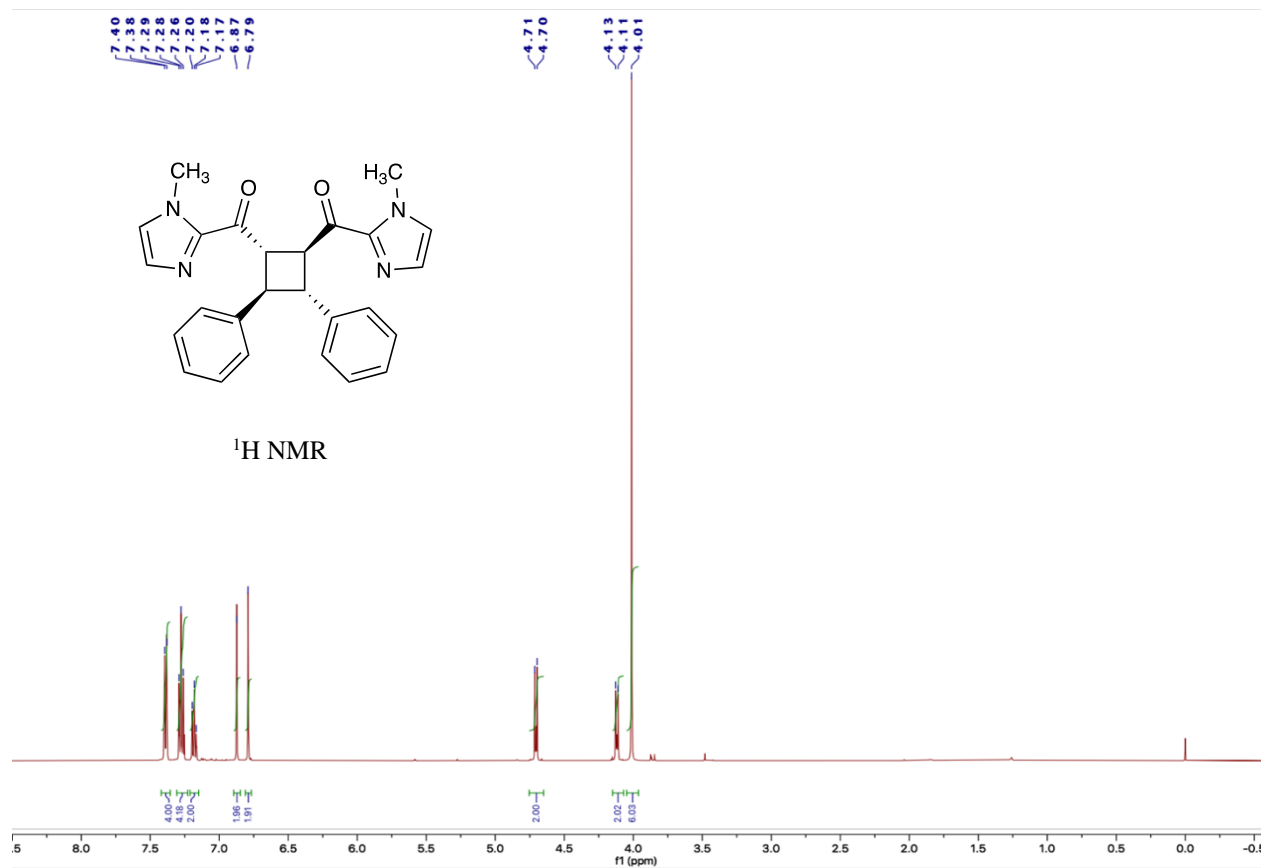


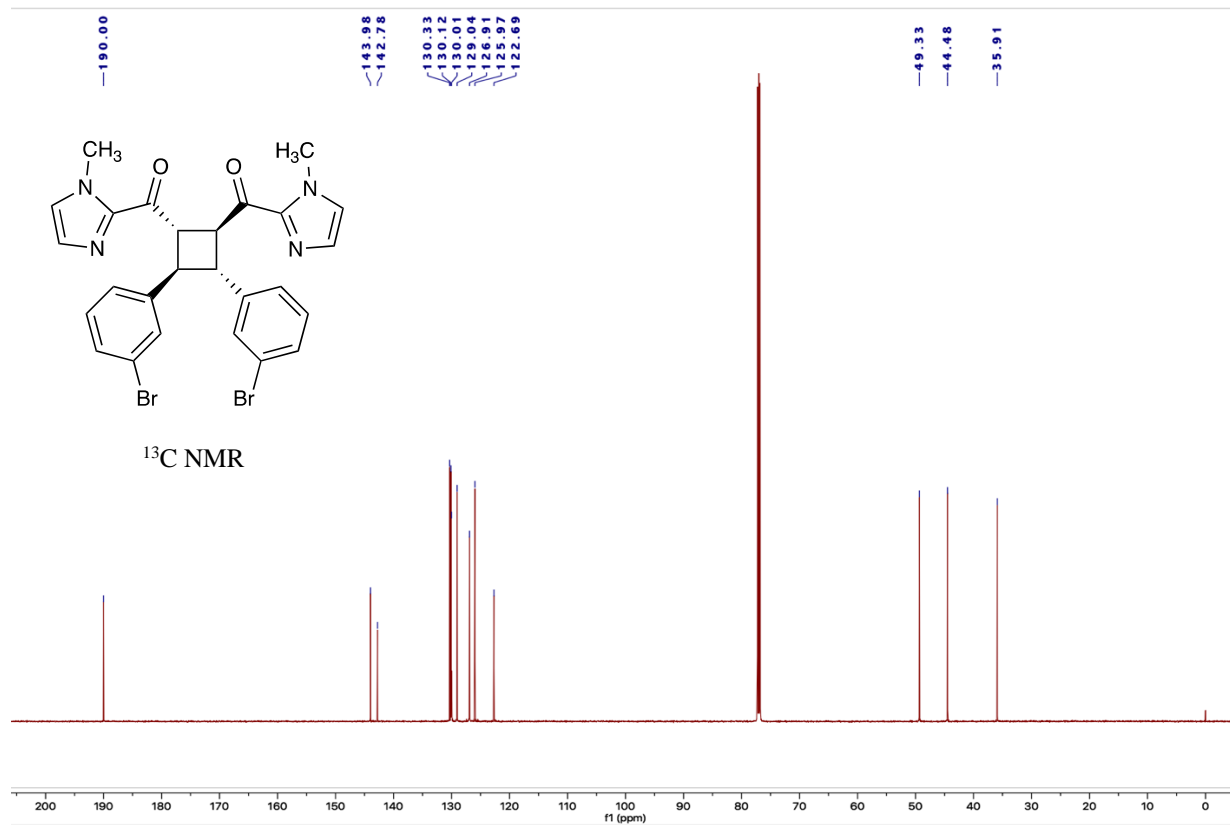
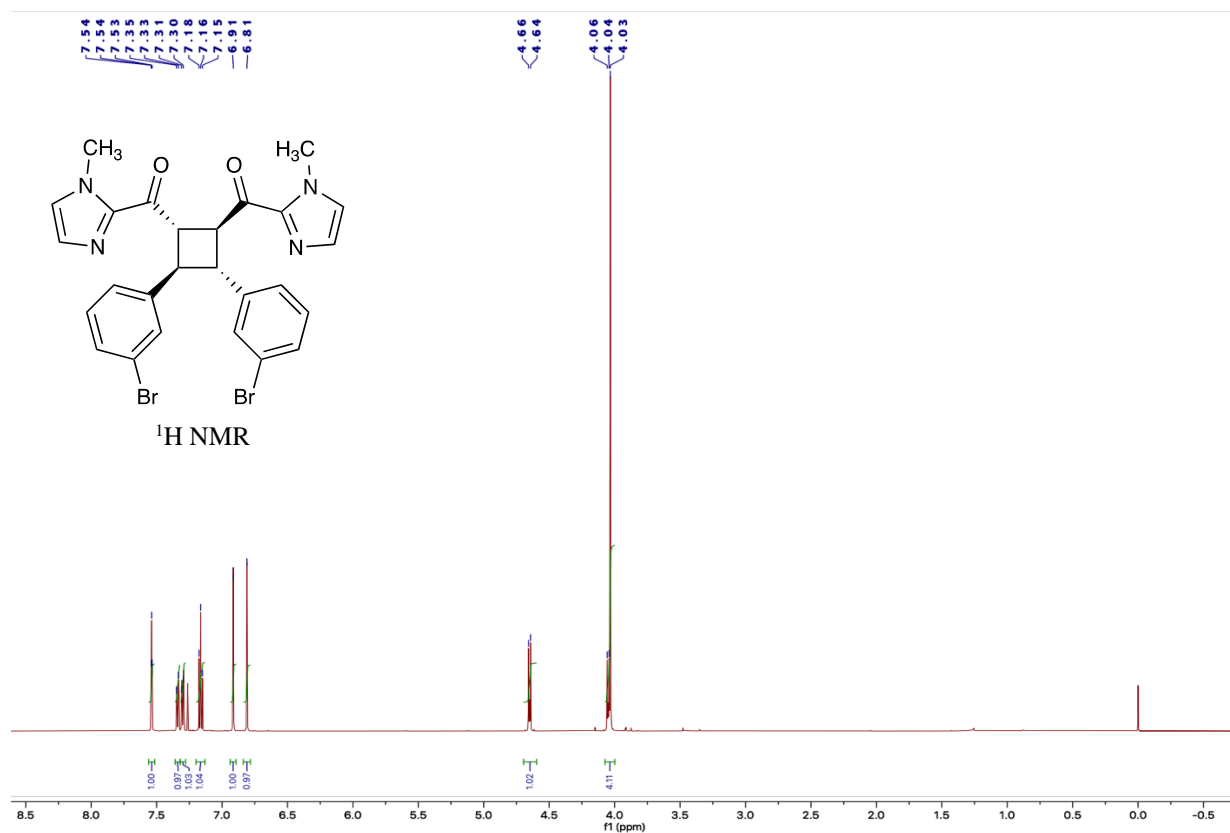


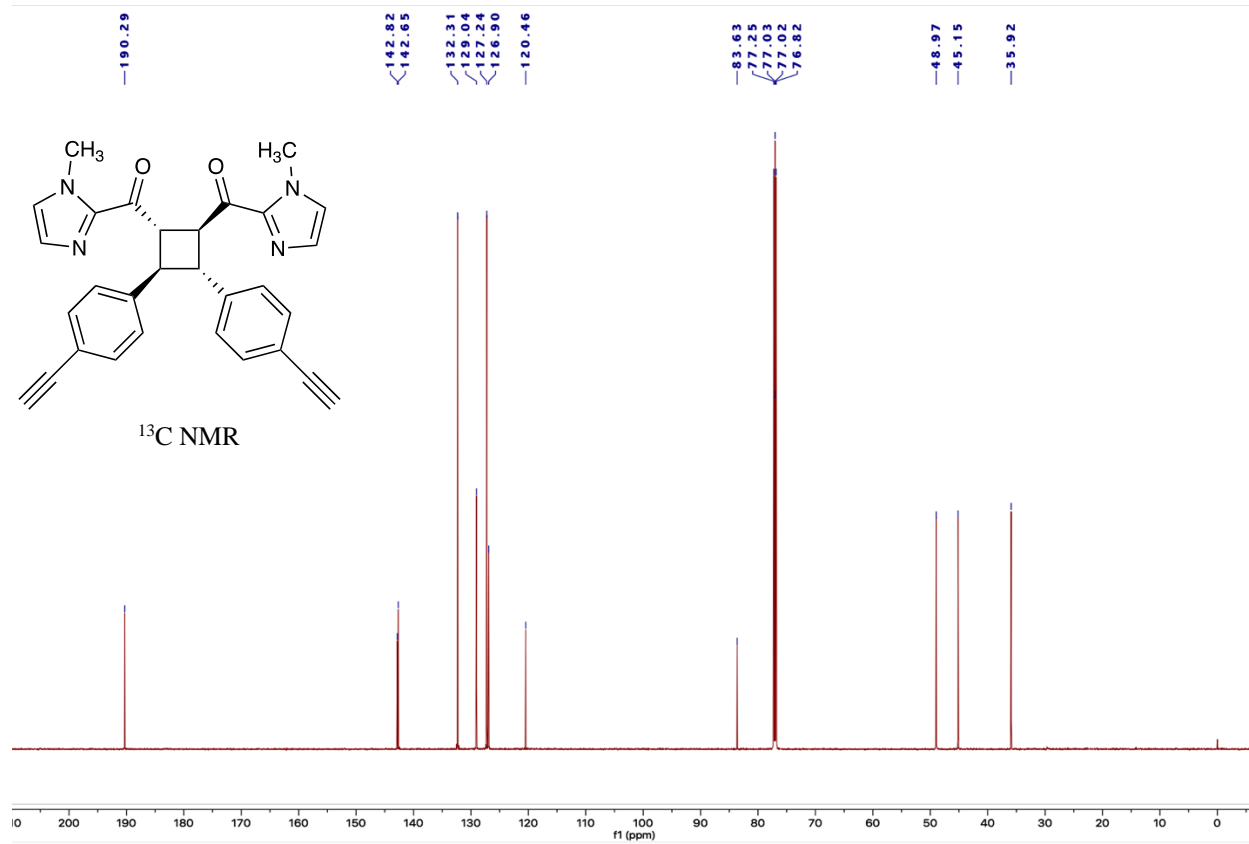
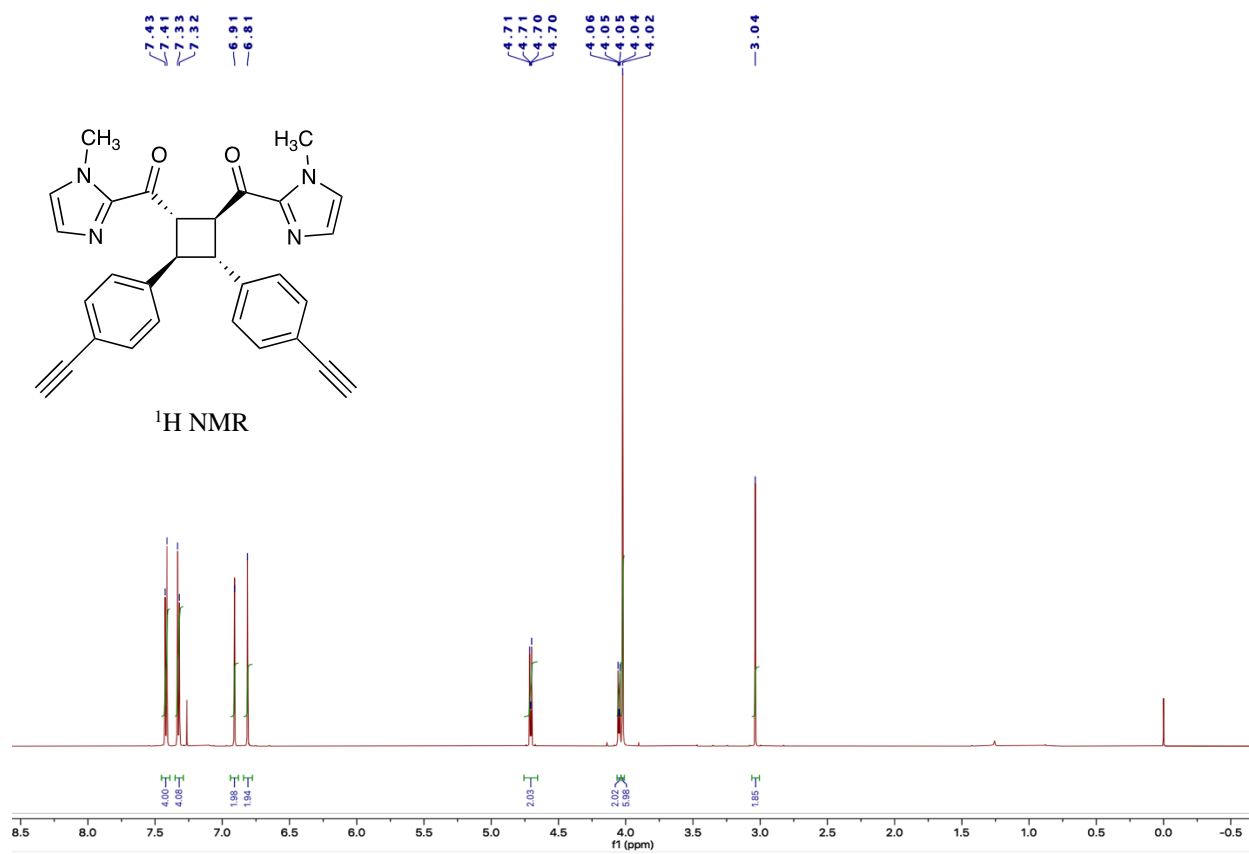


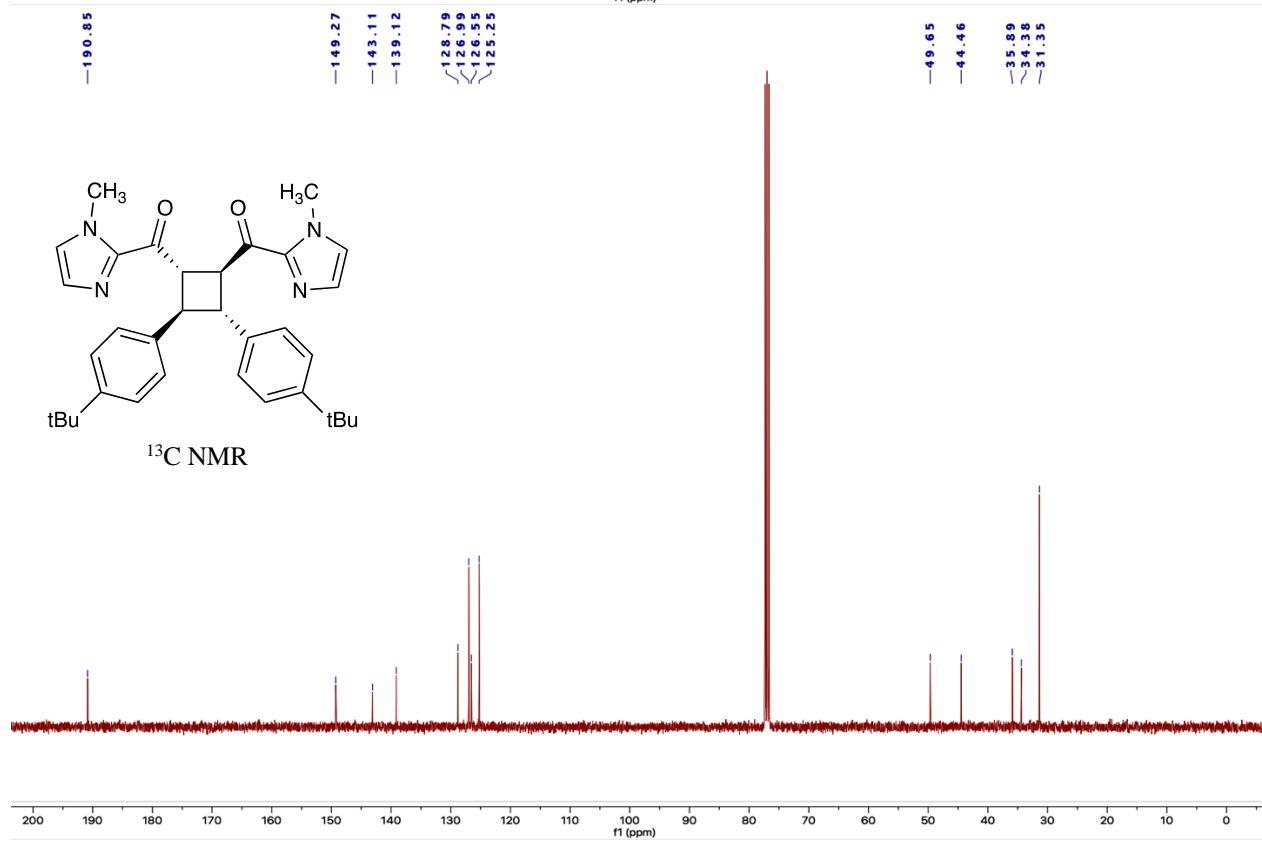
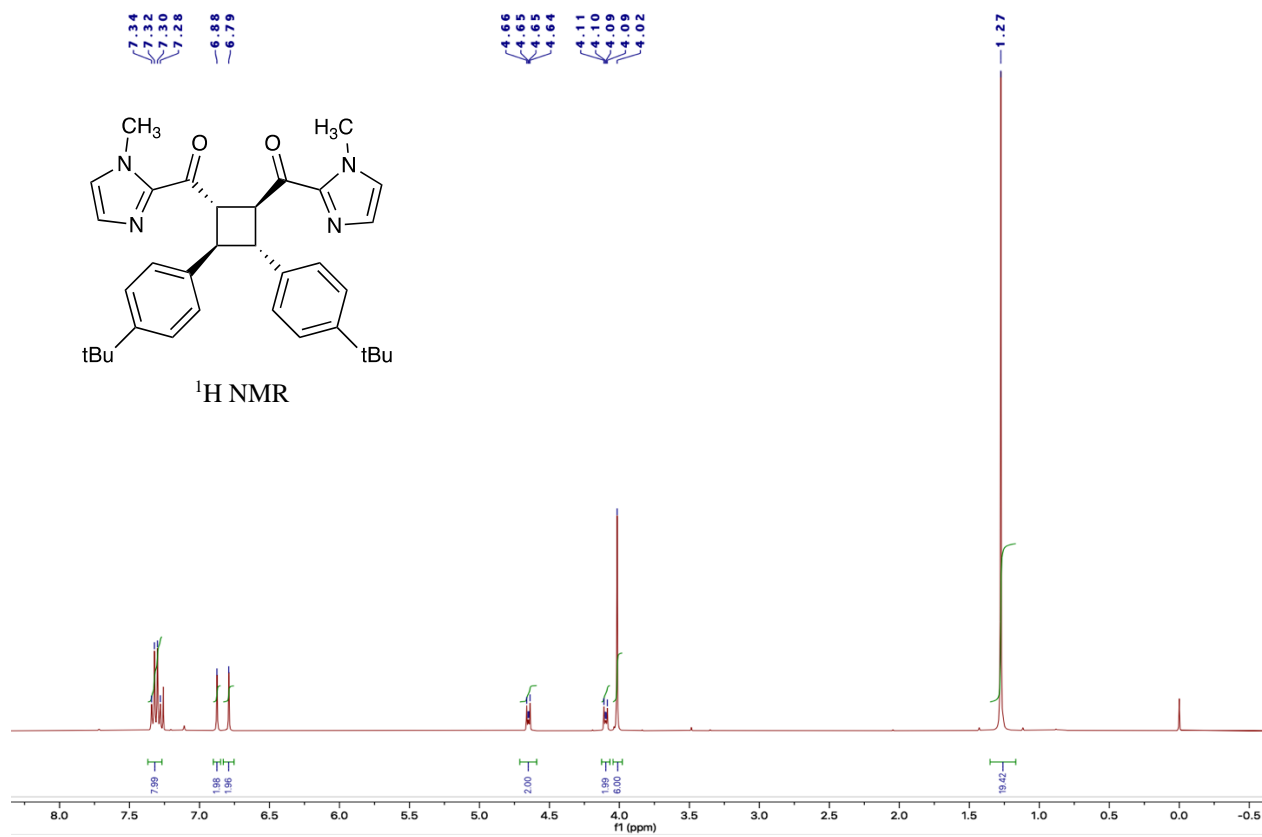
¹⁹F NMR

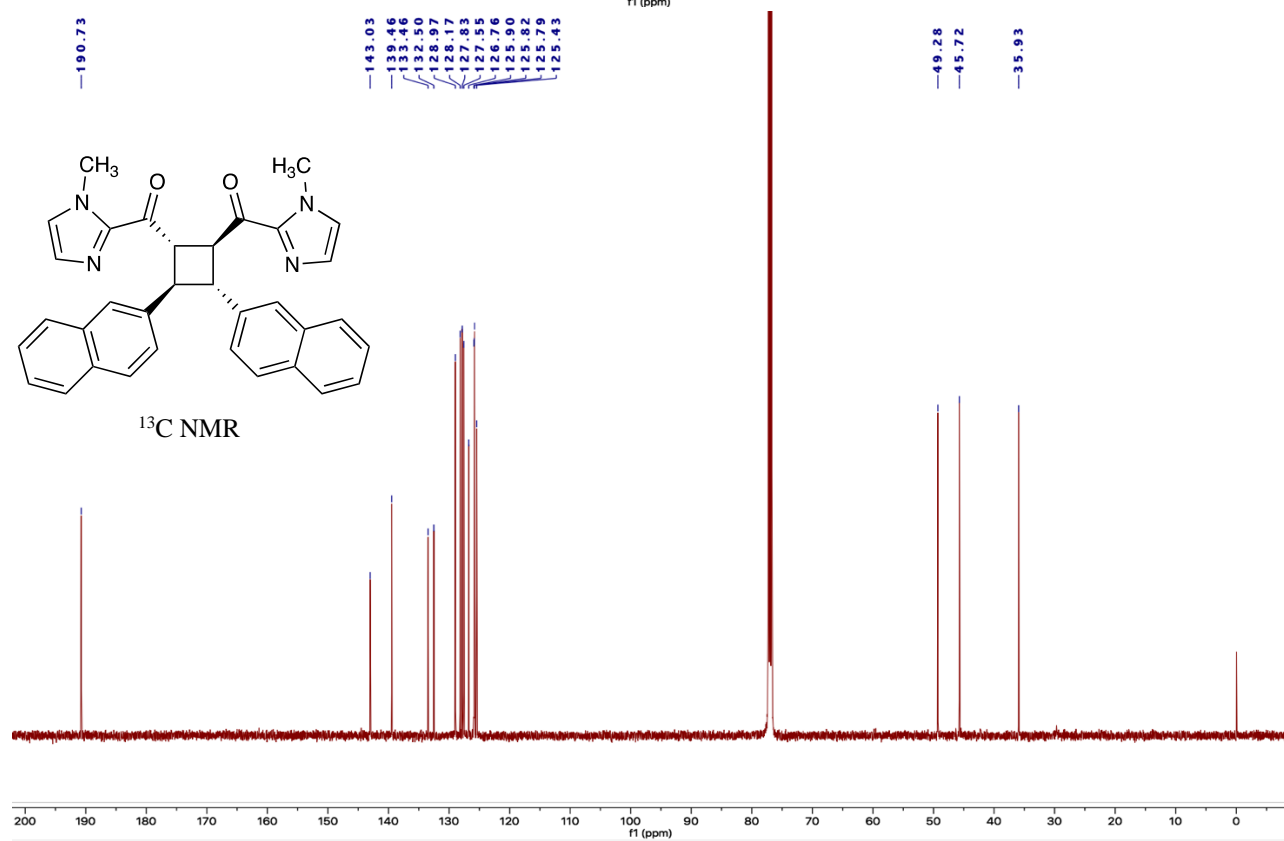
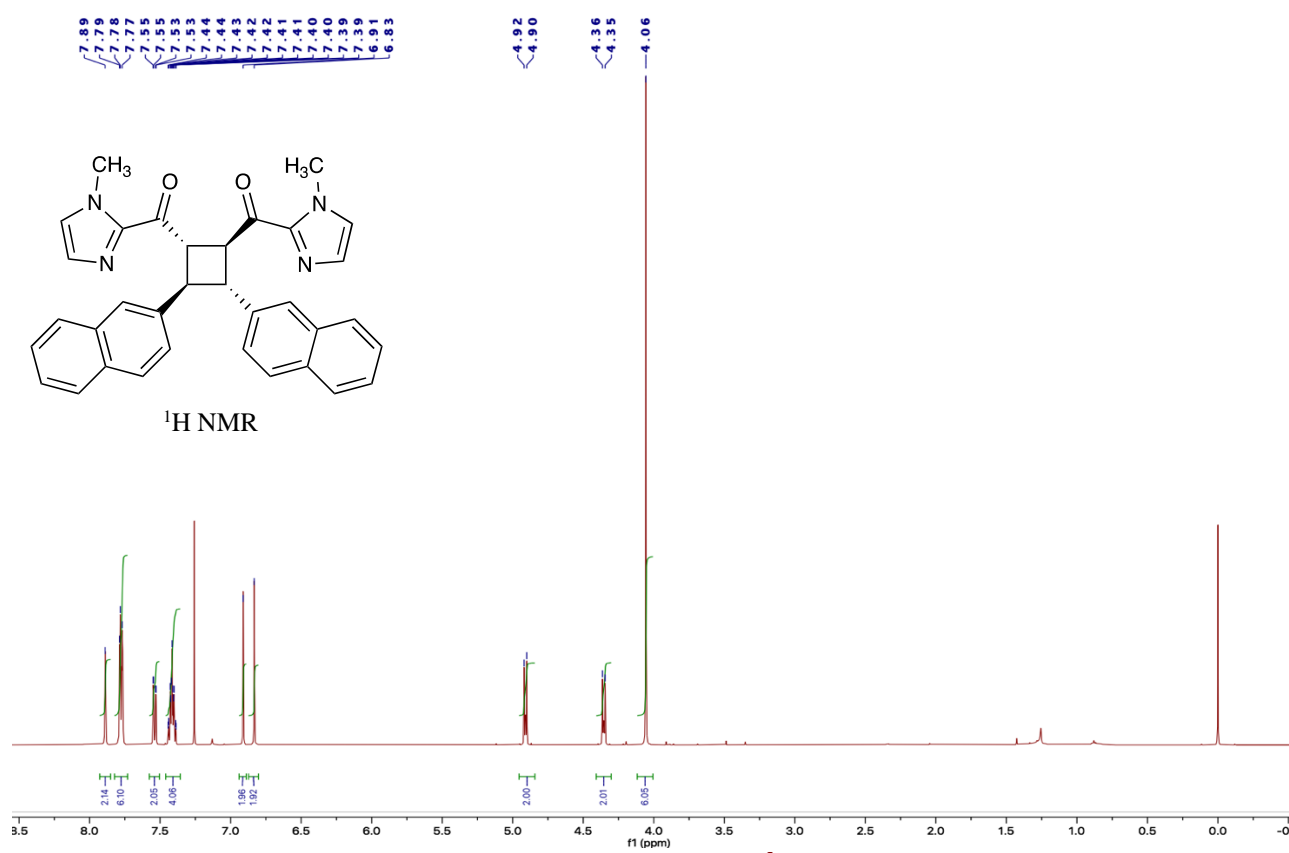


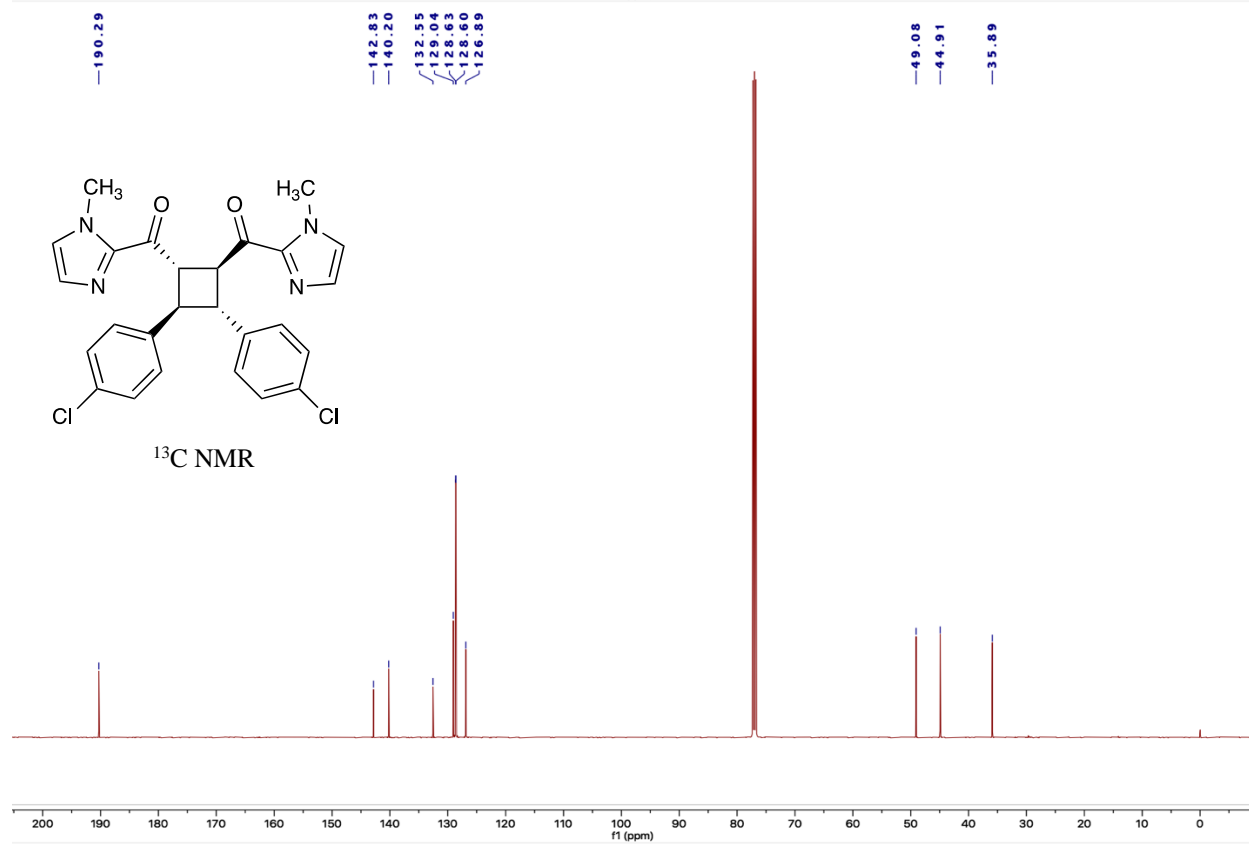
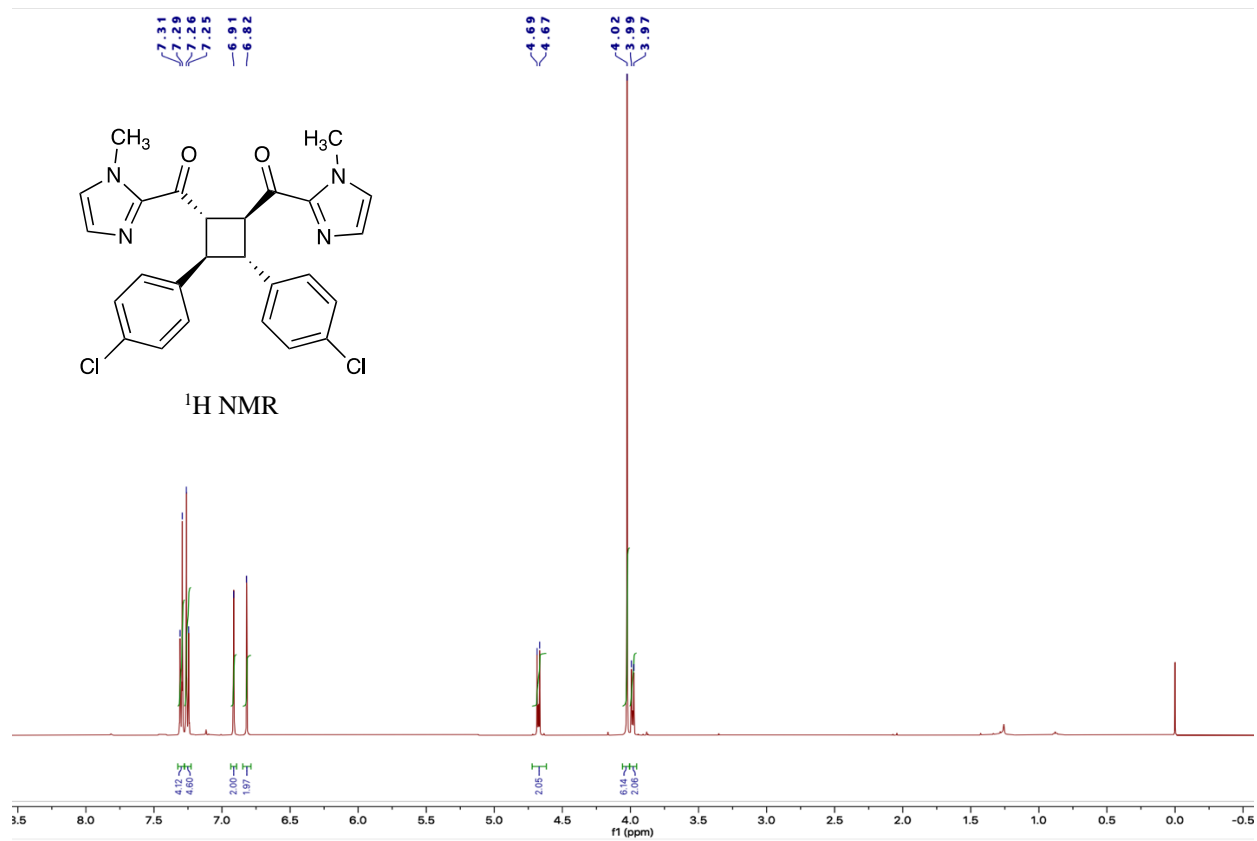


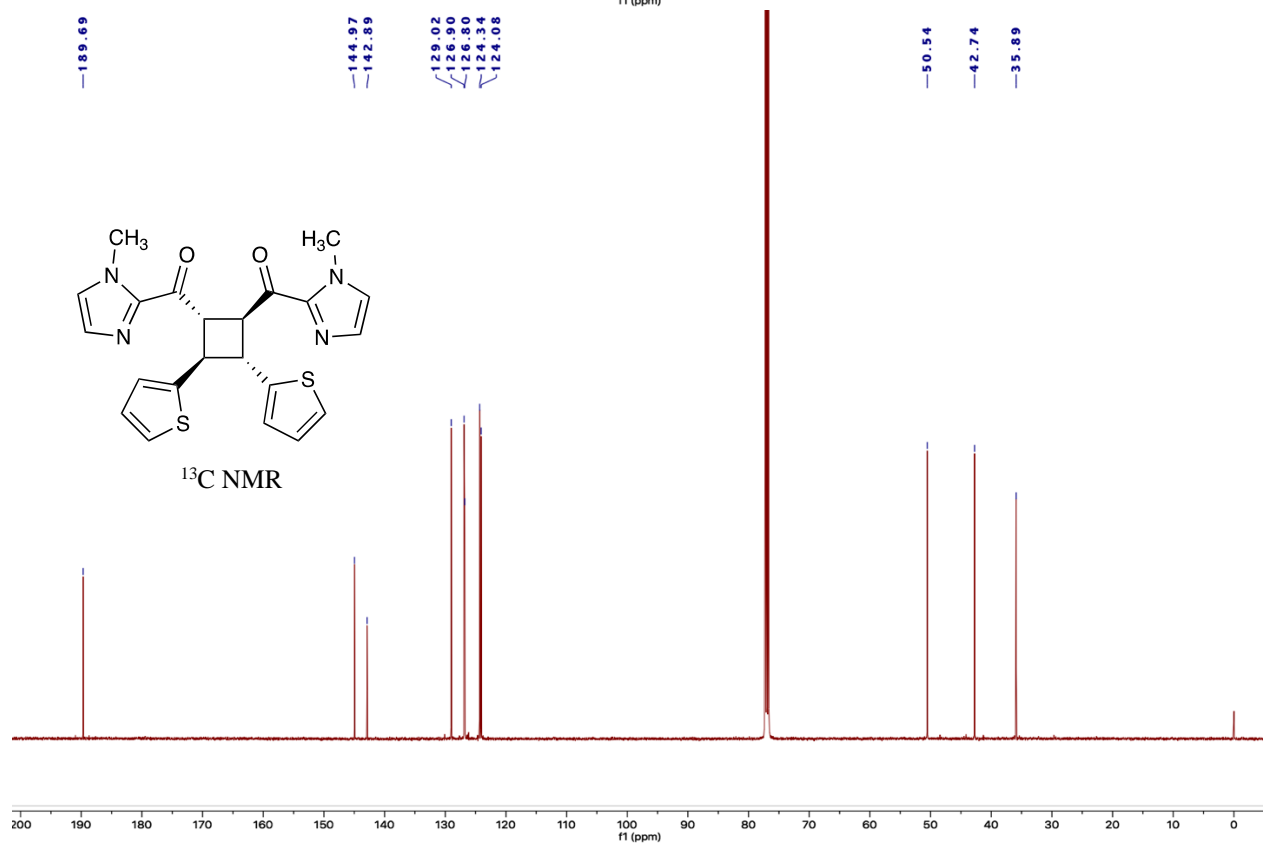
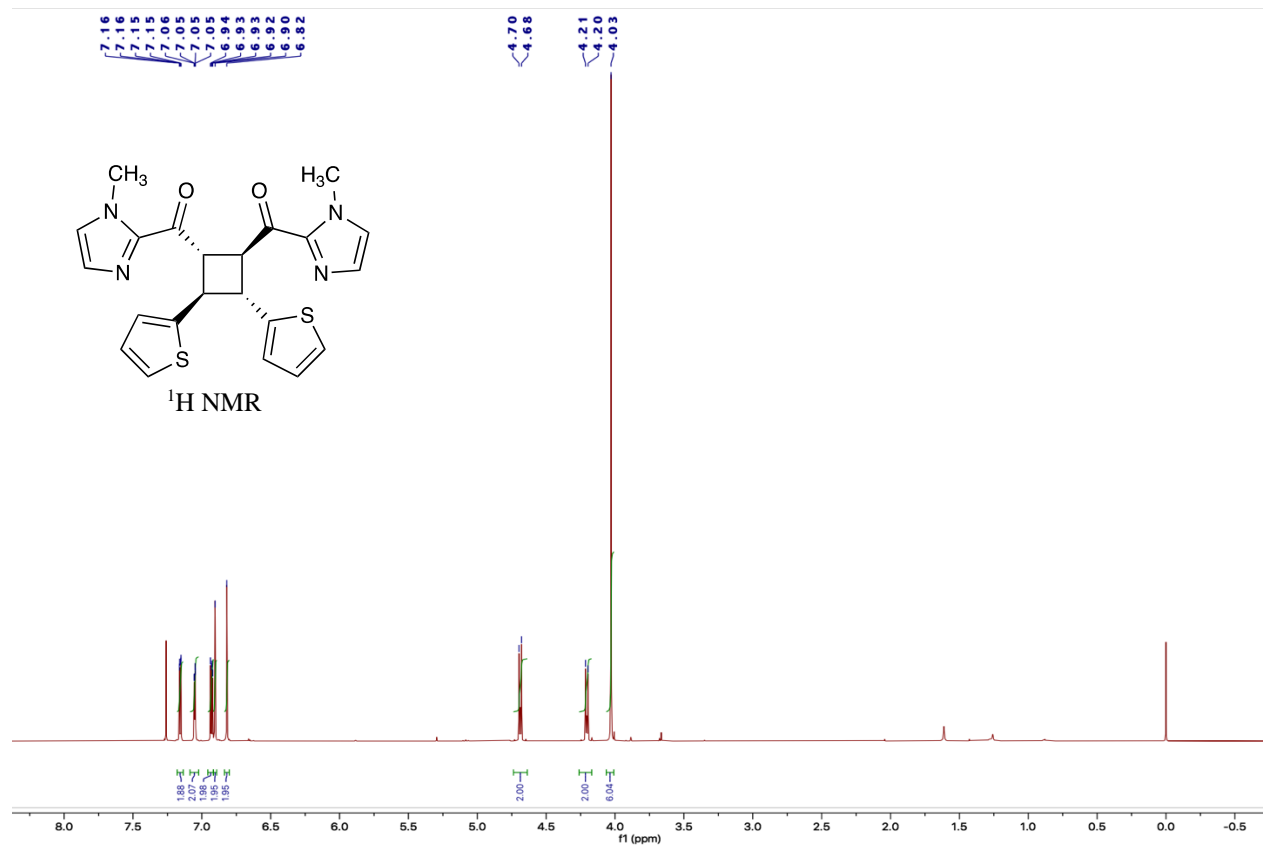


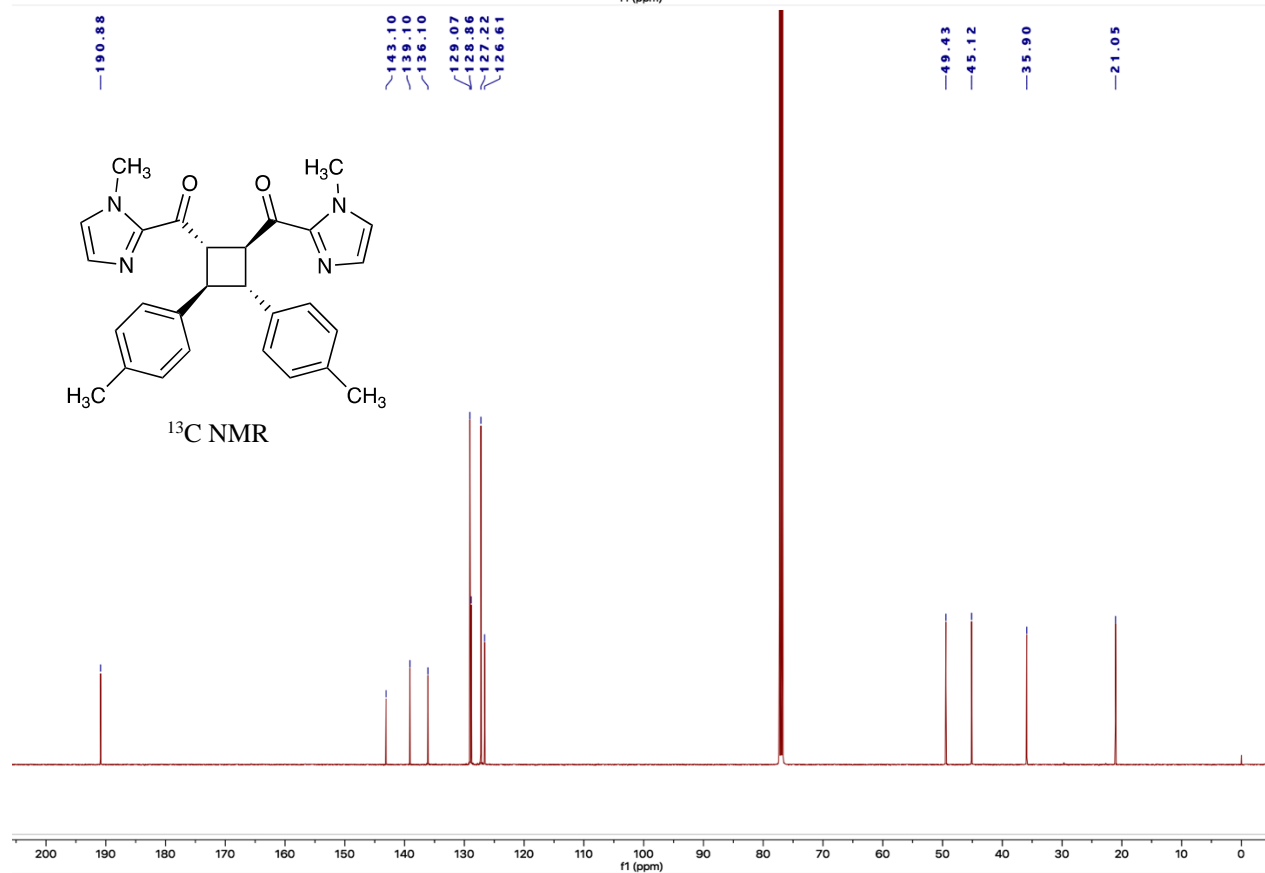
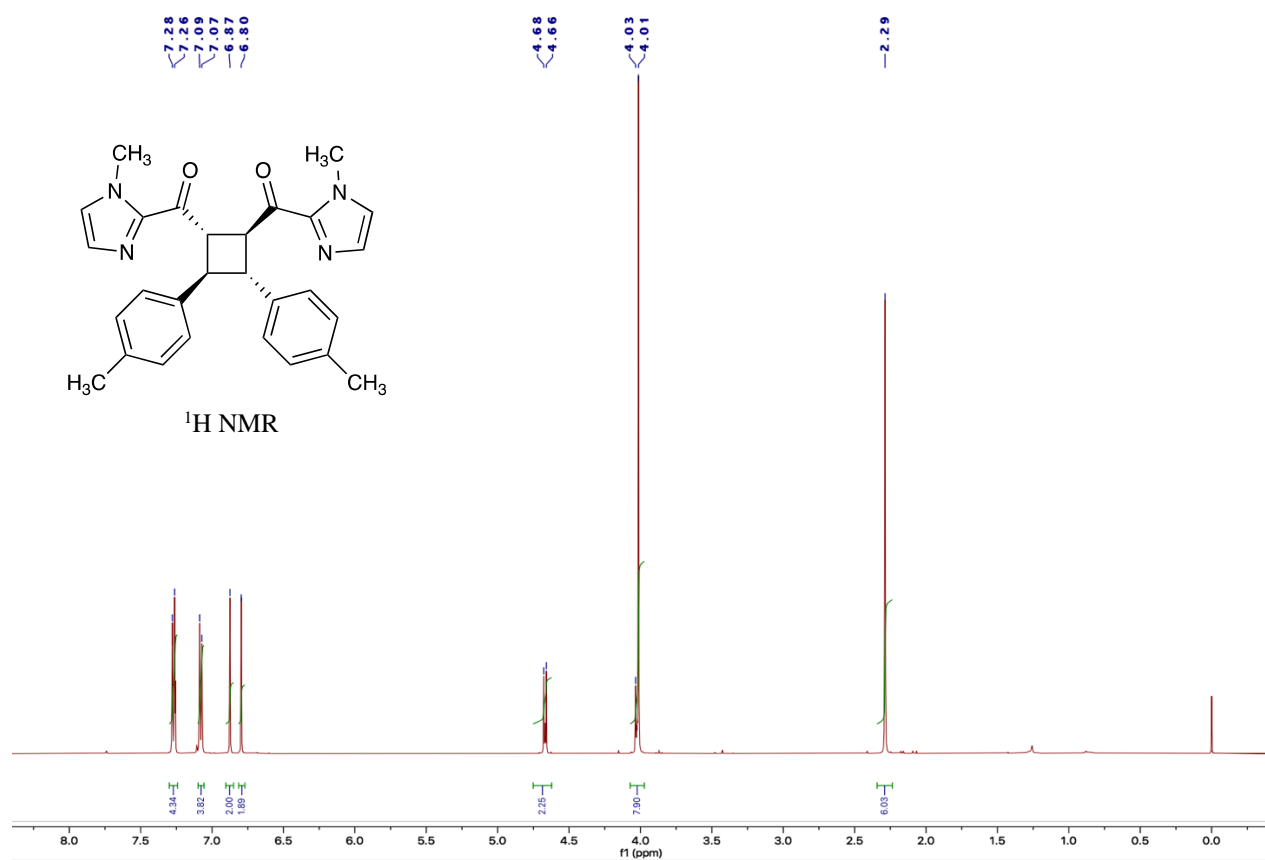


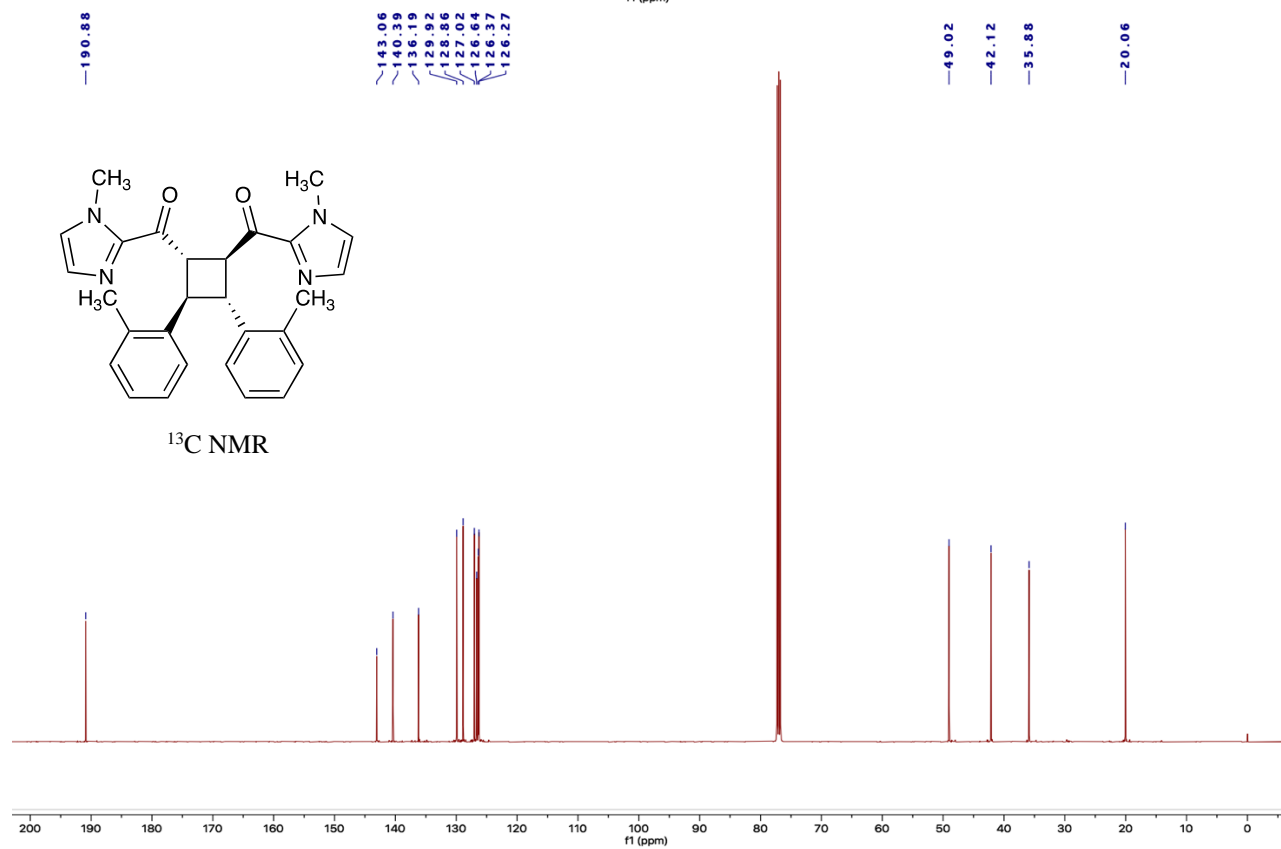
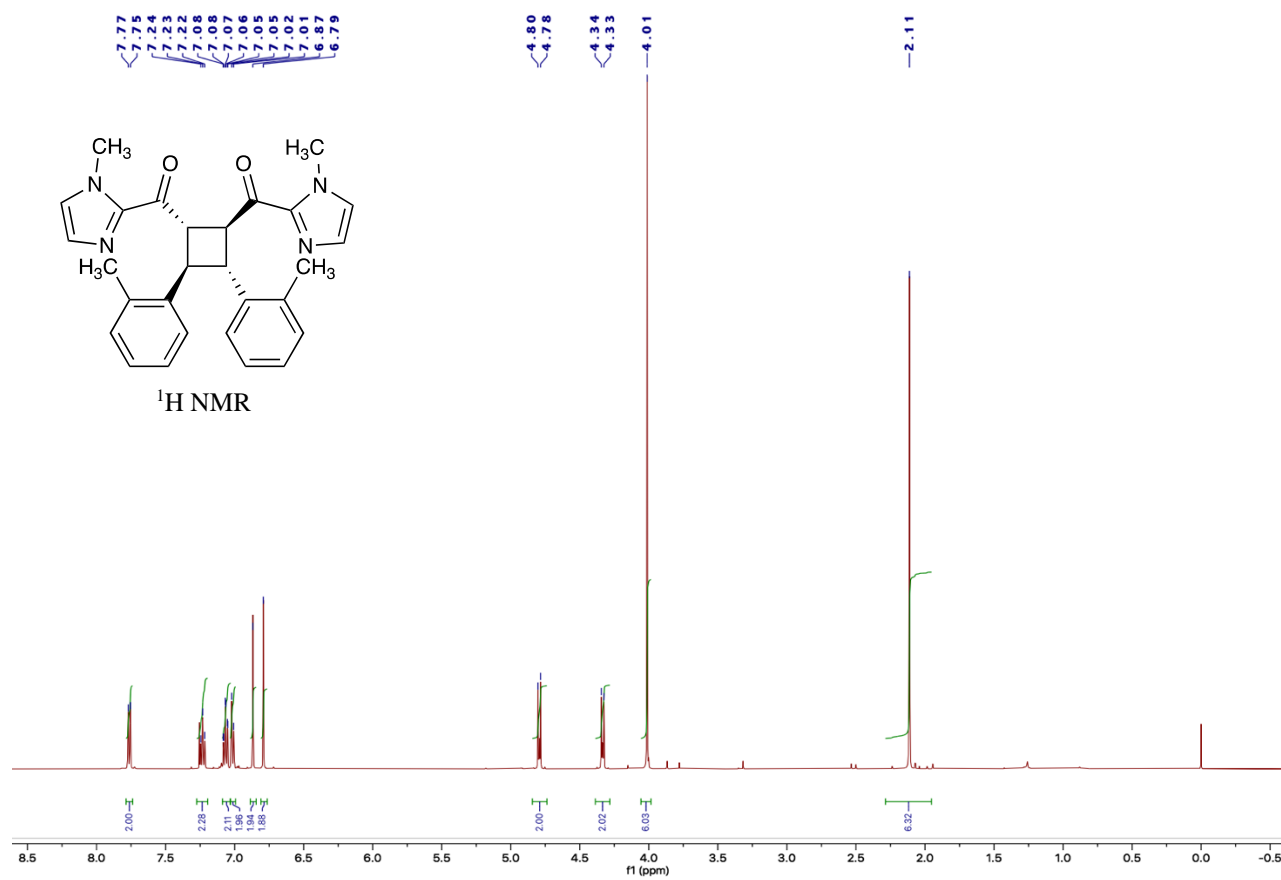


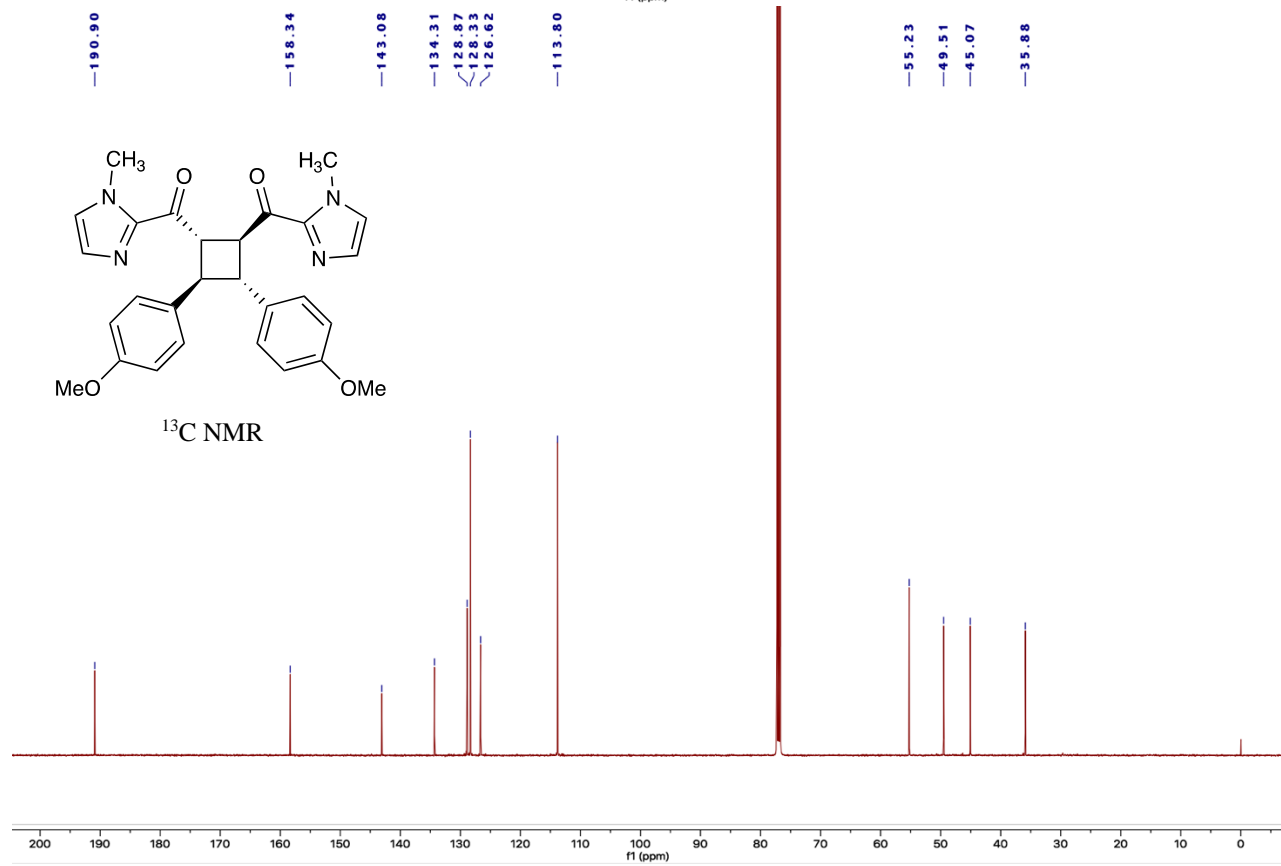
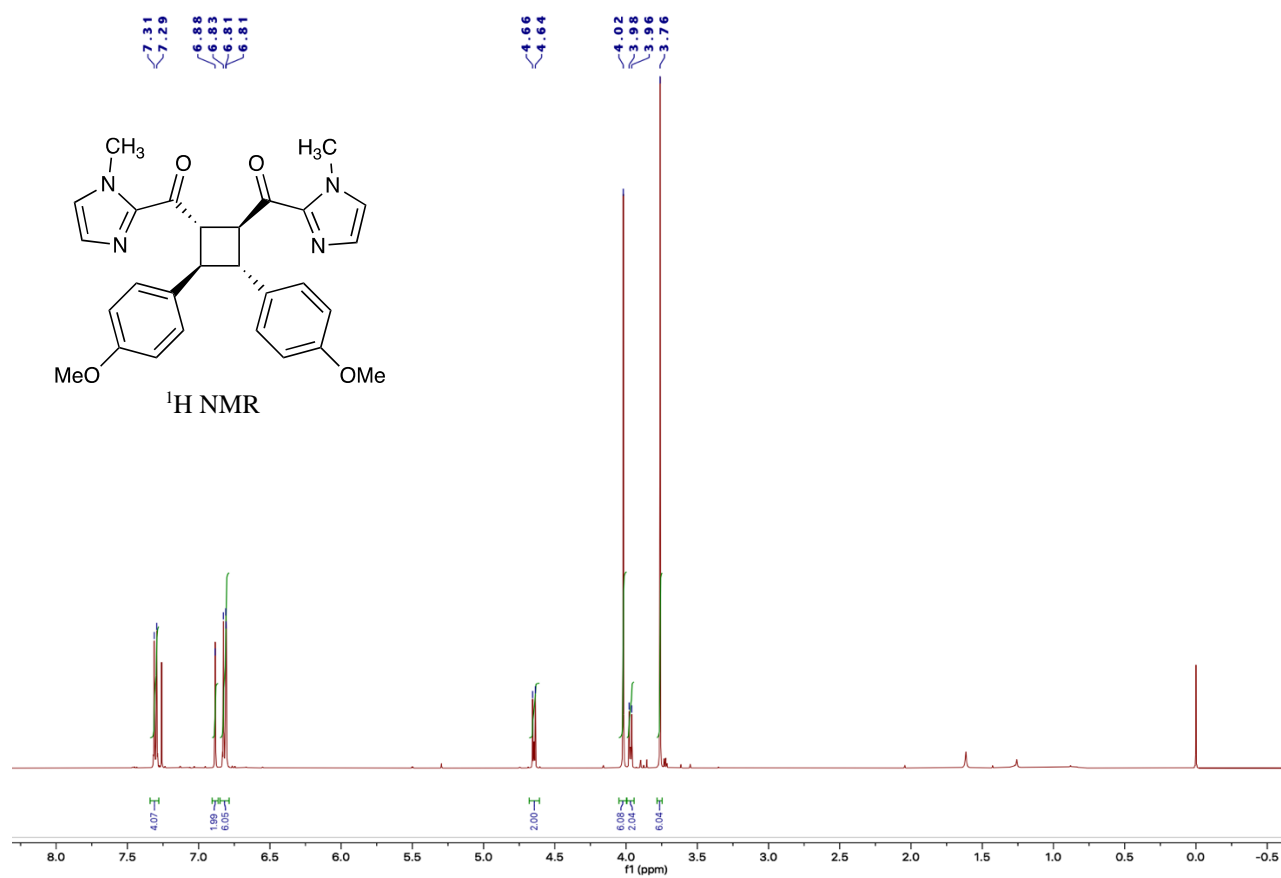


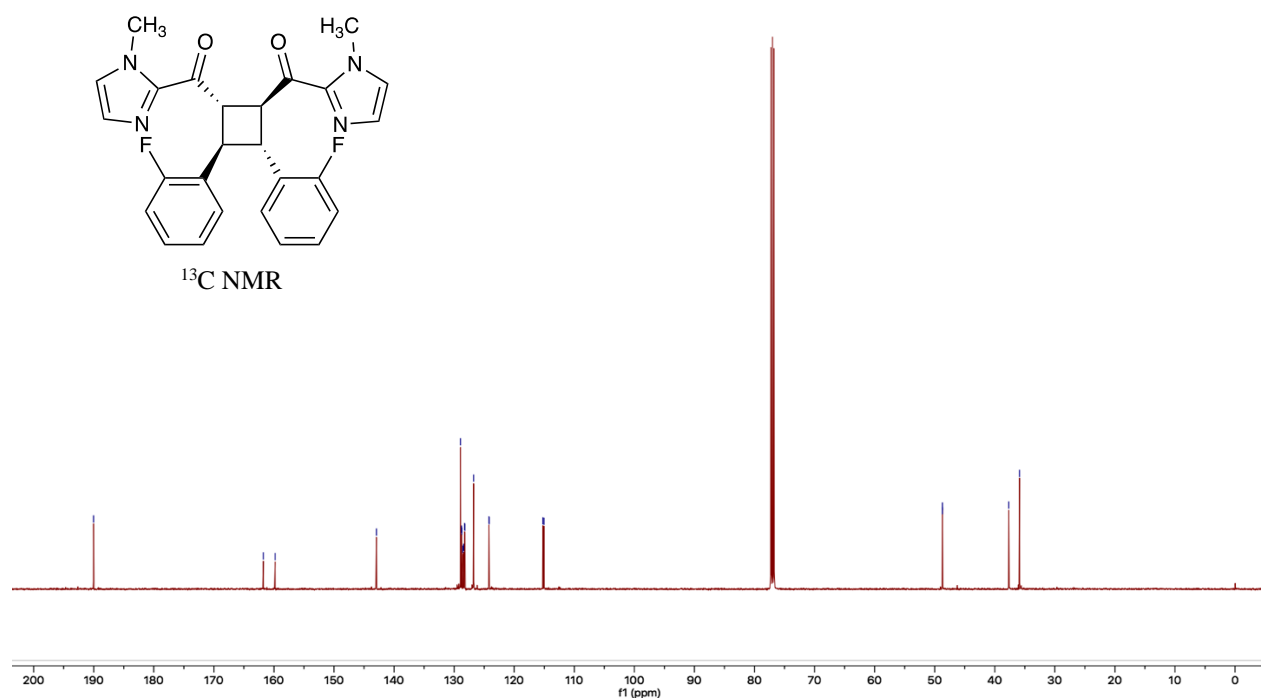
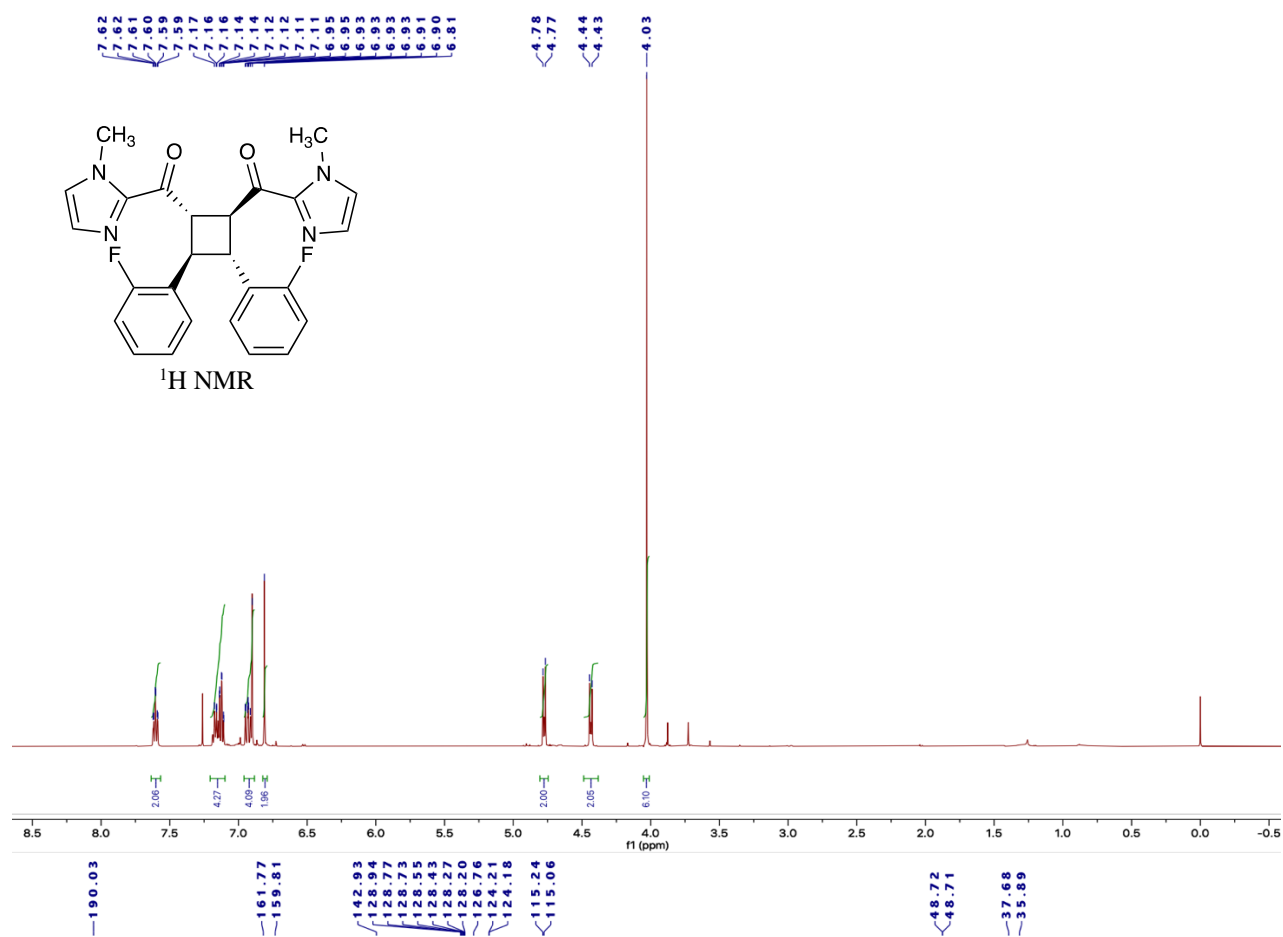


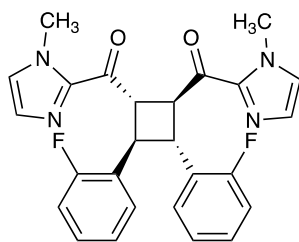




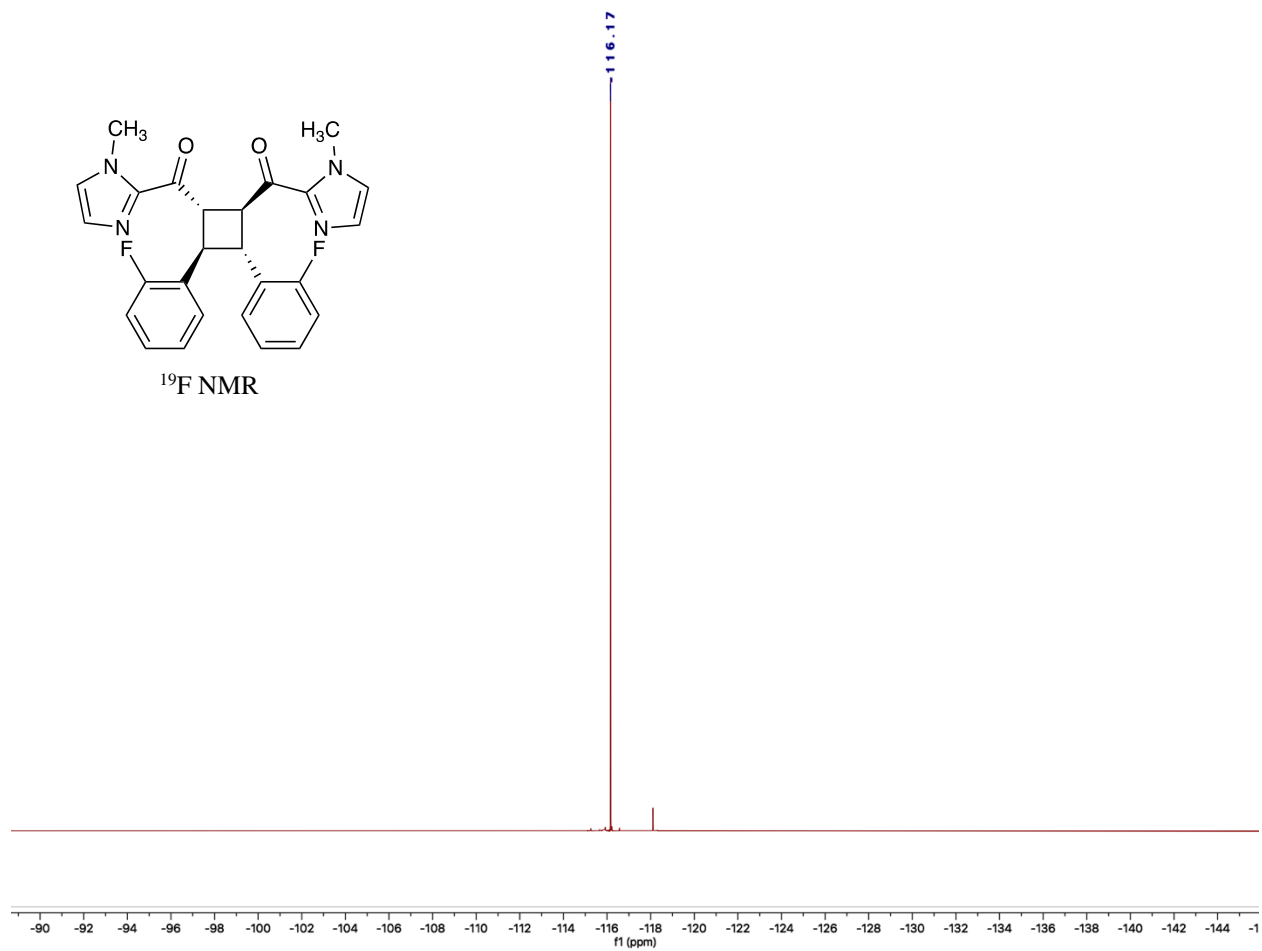


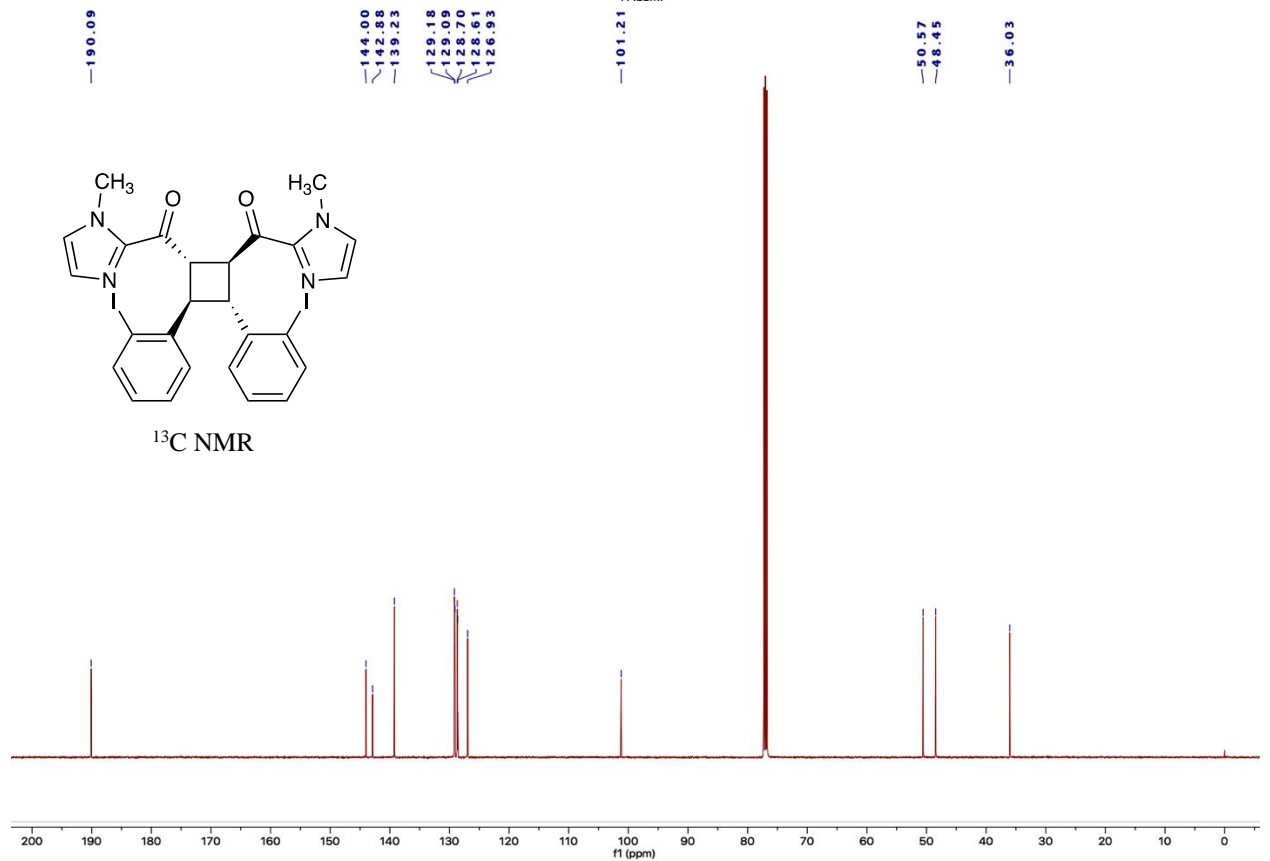
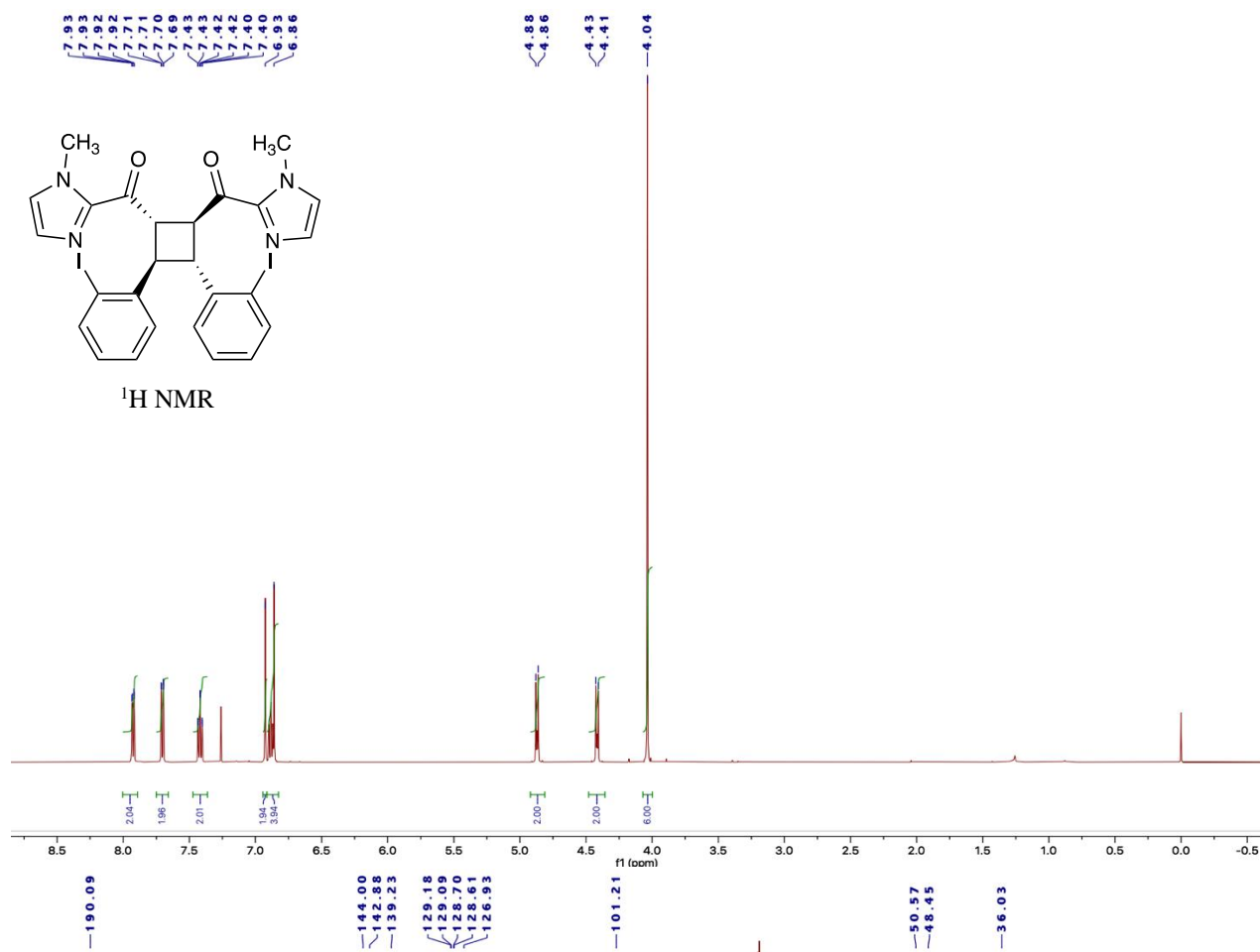


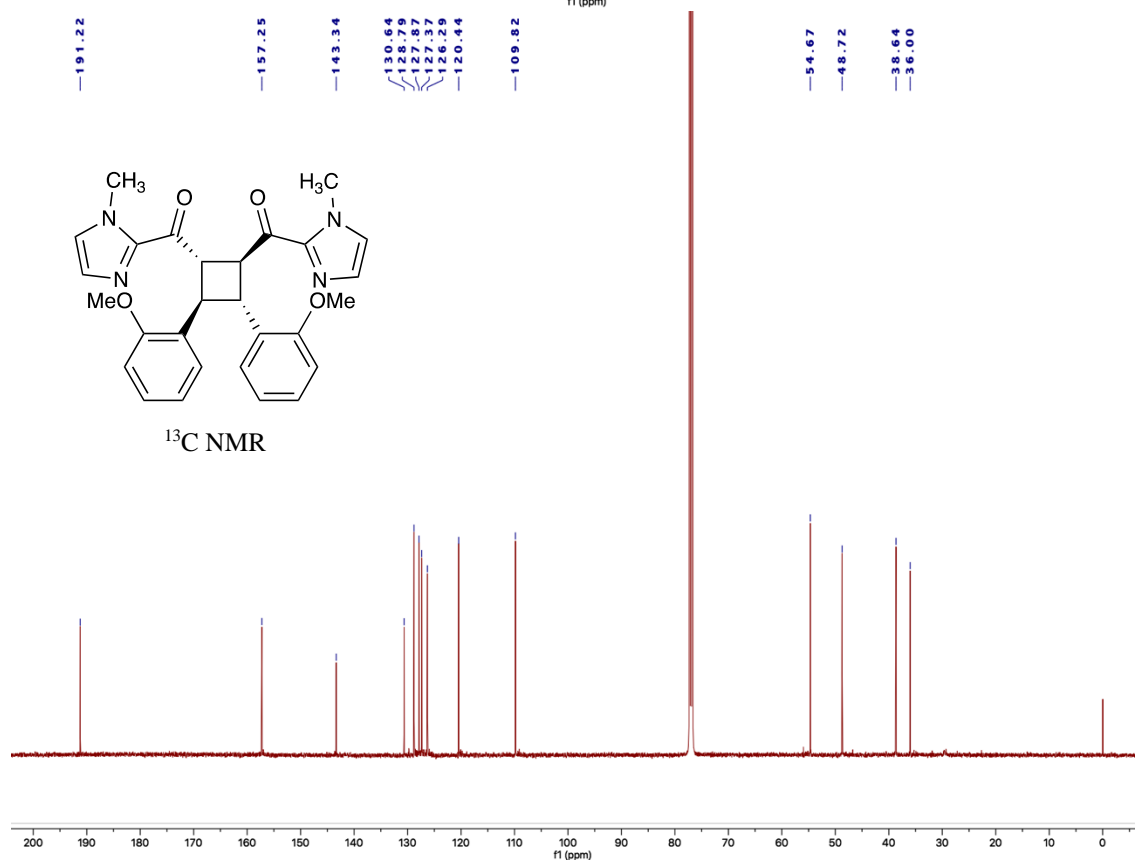
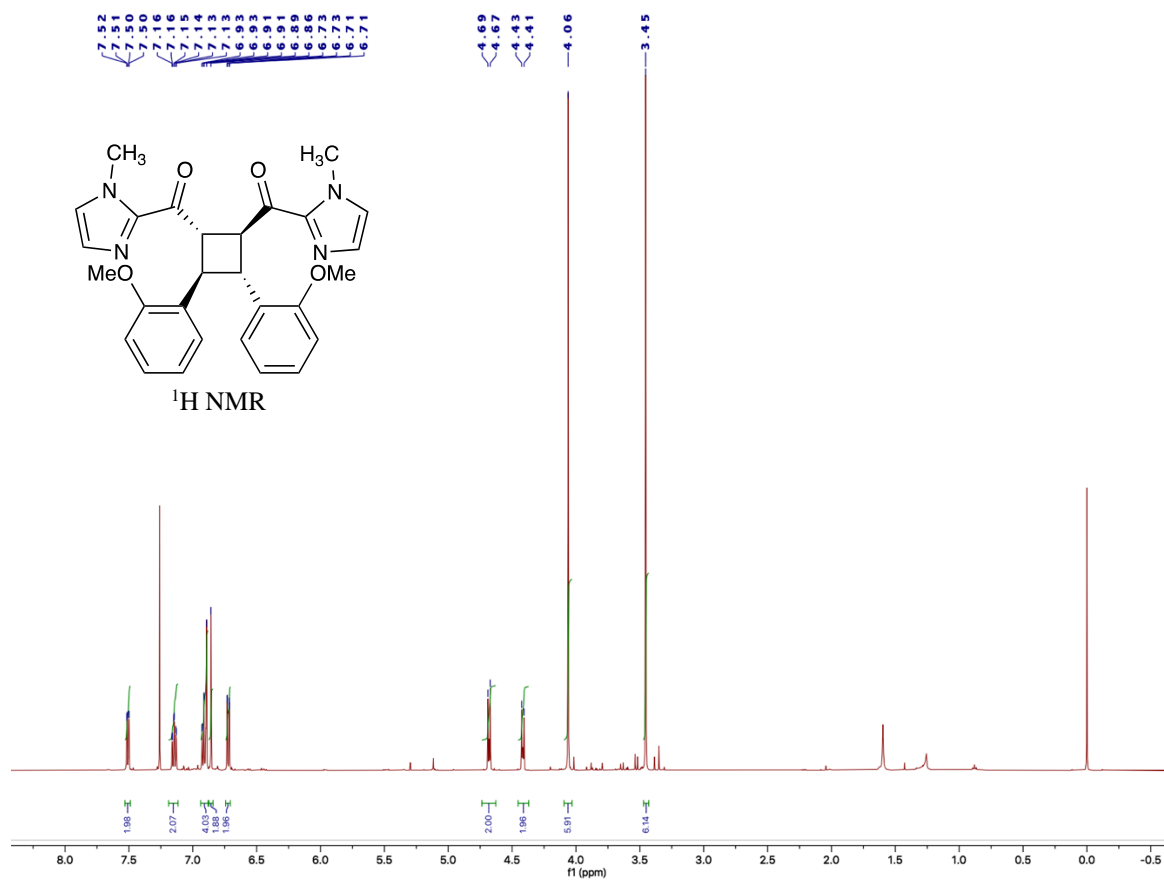


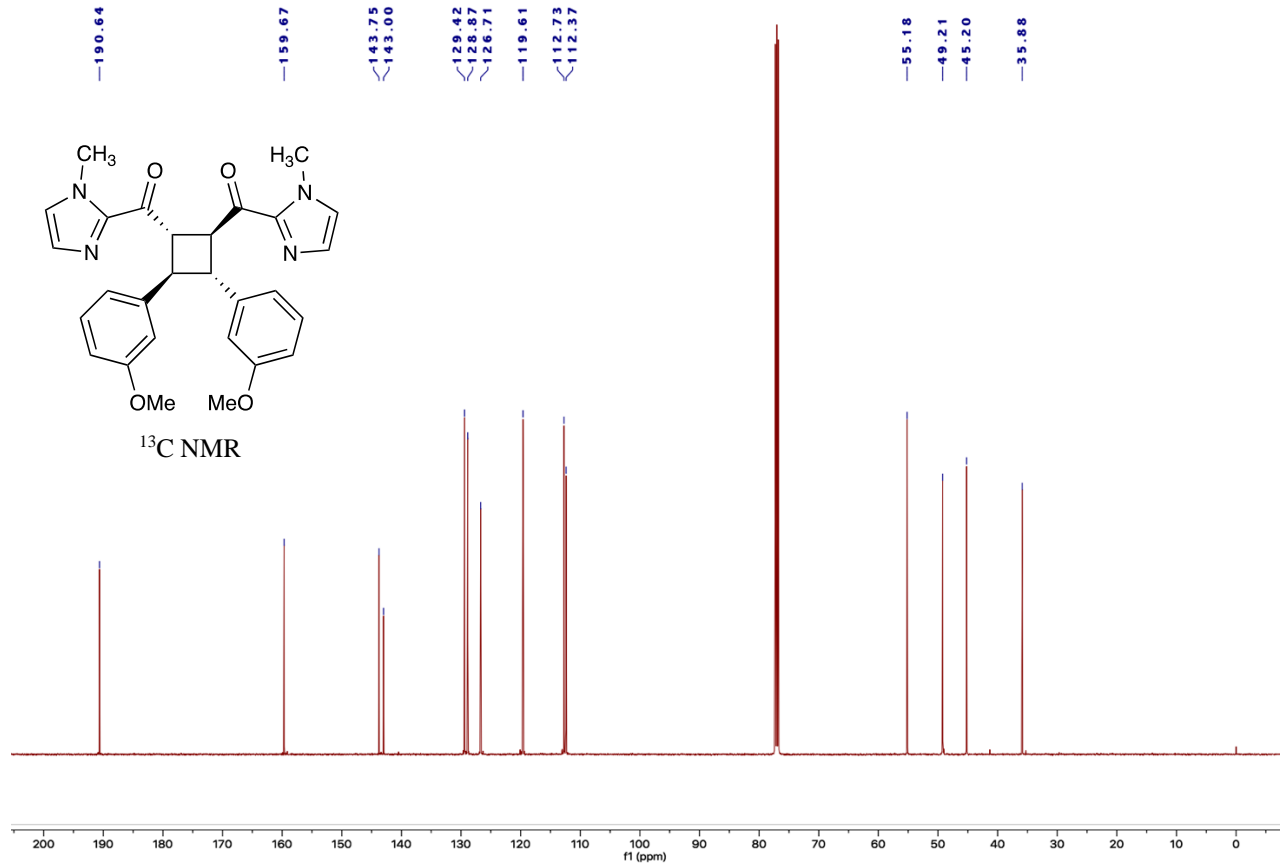
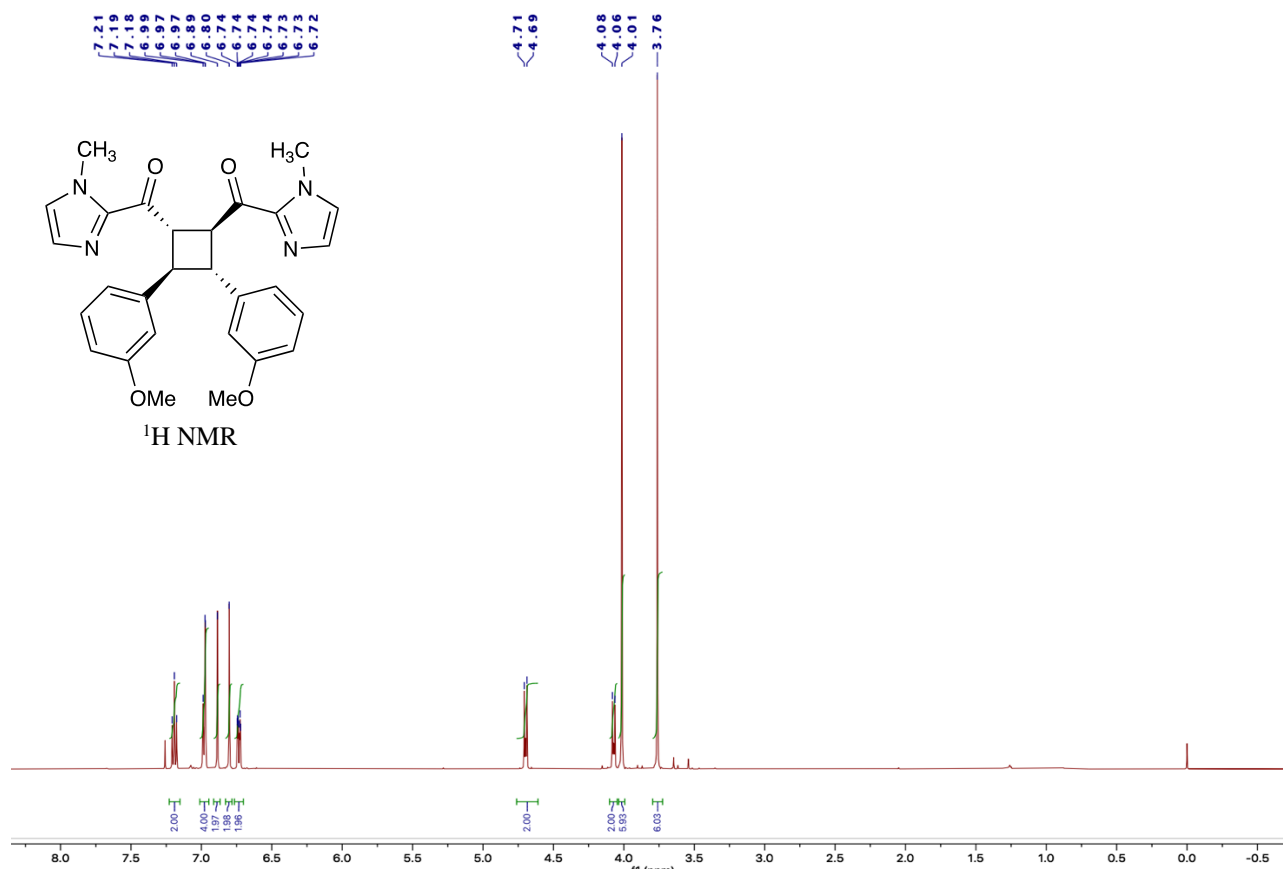


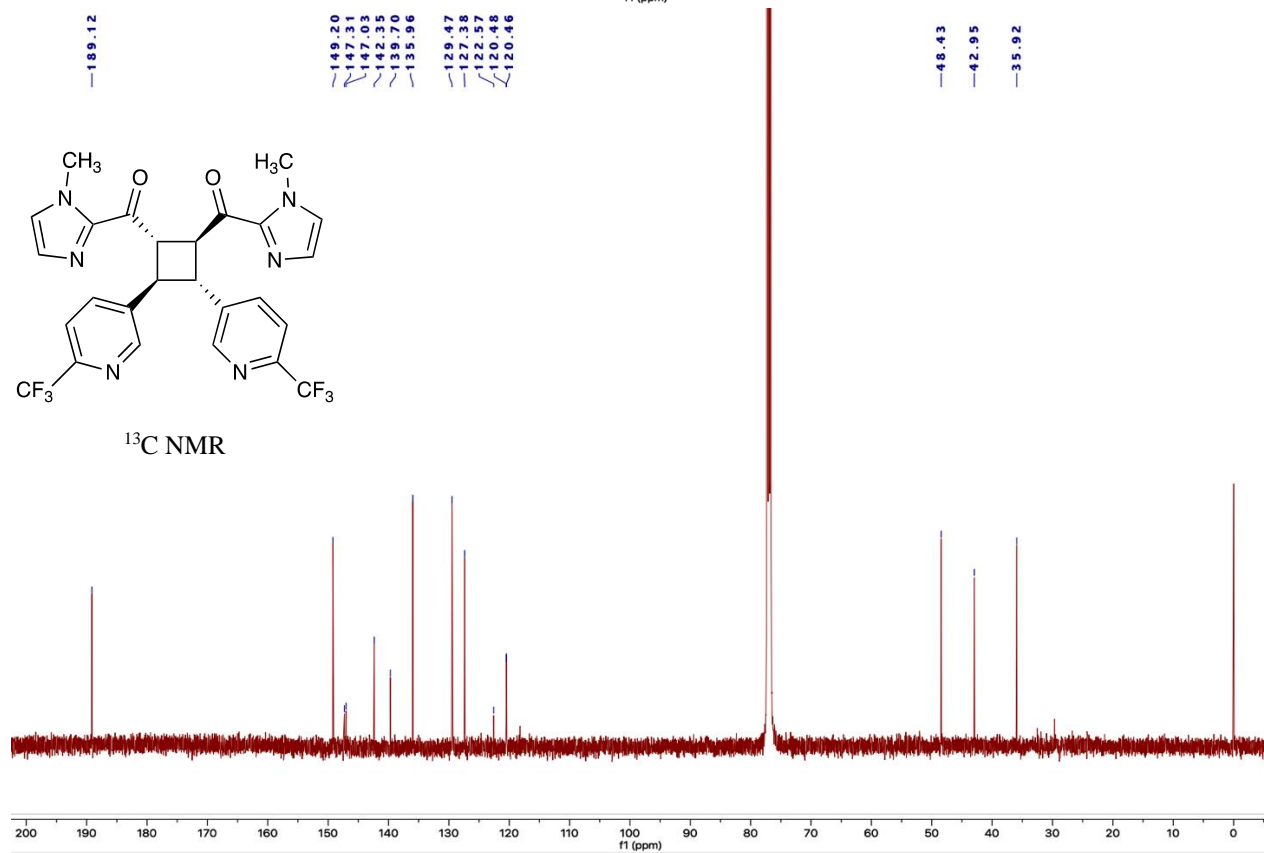
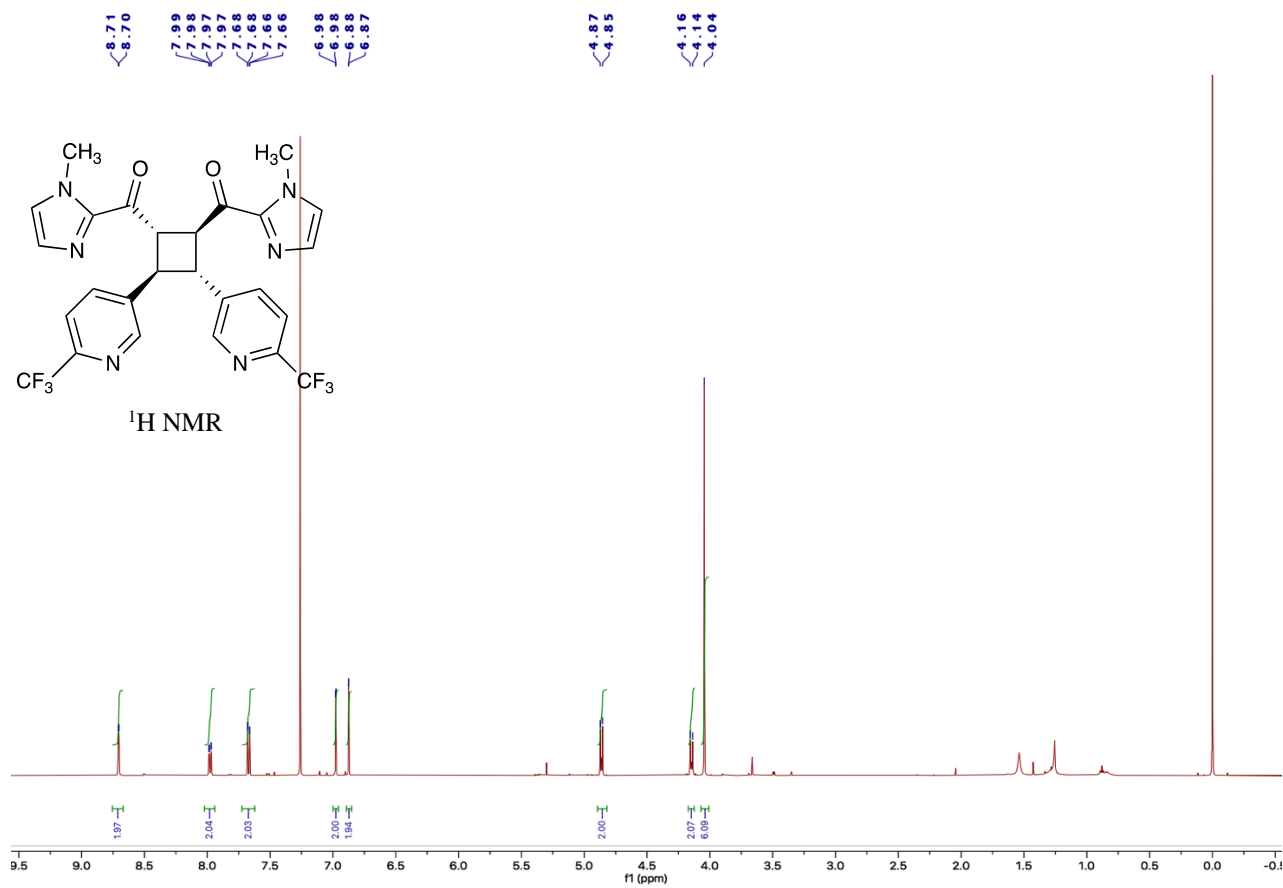
^{19}F NMR

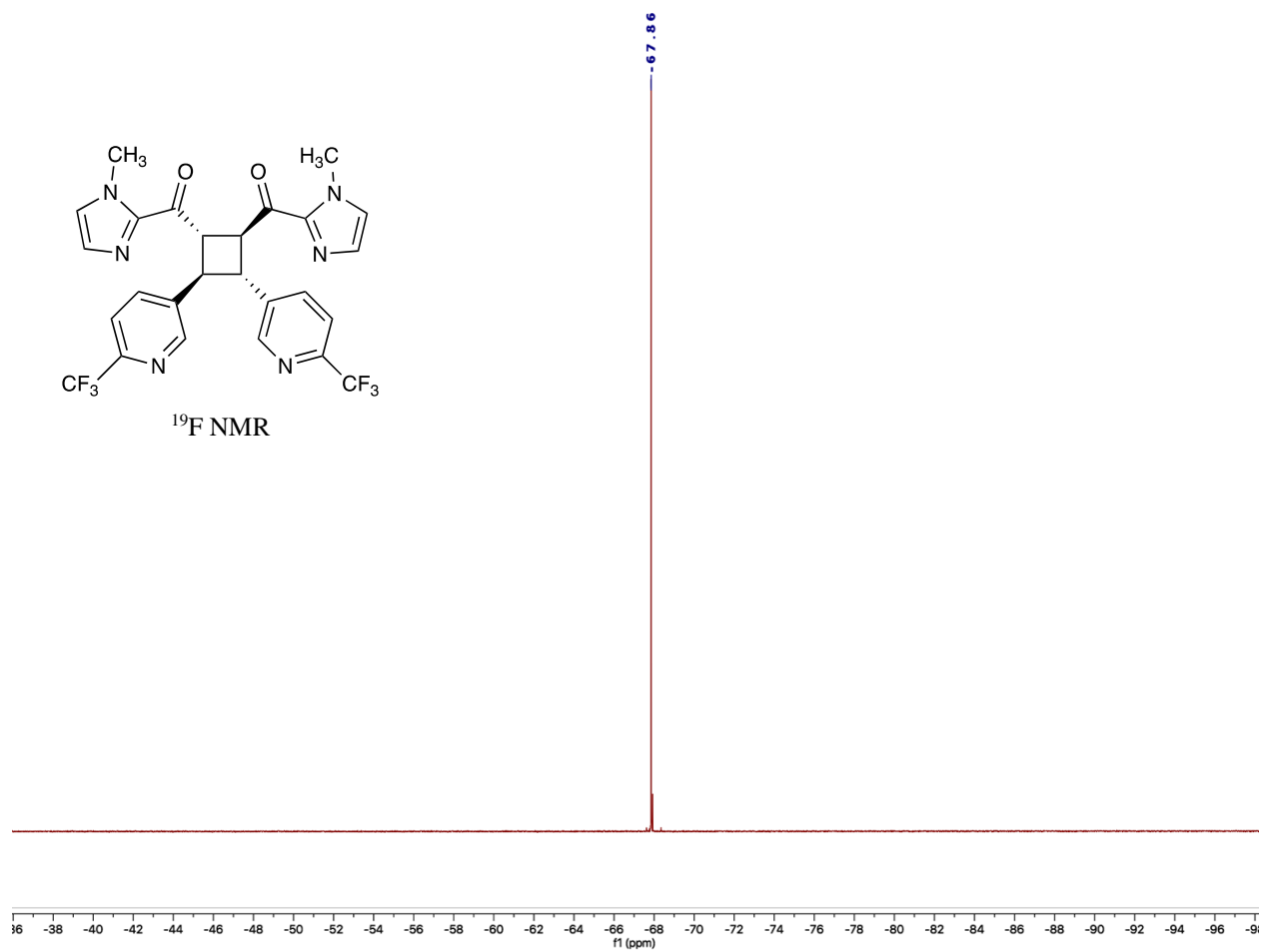


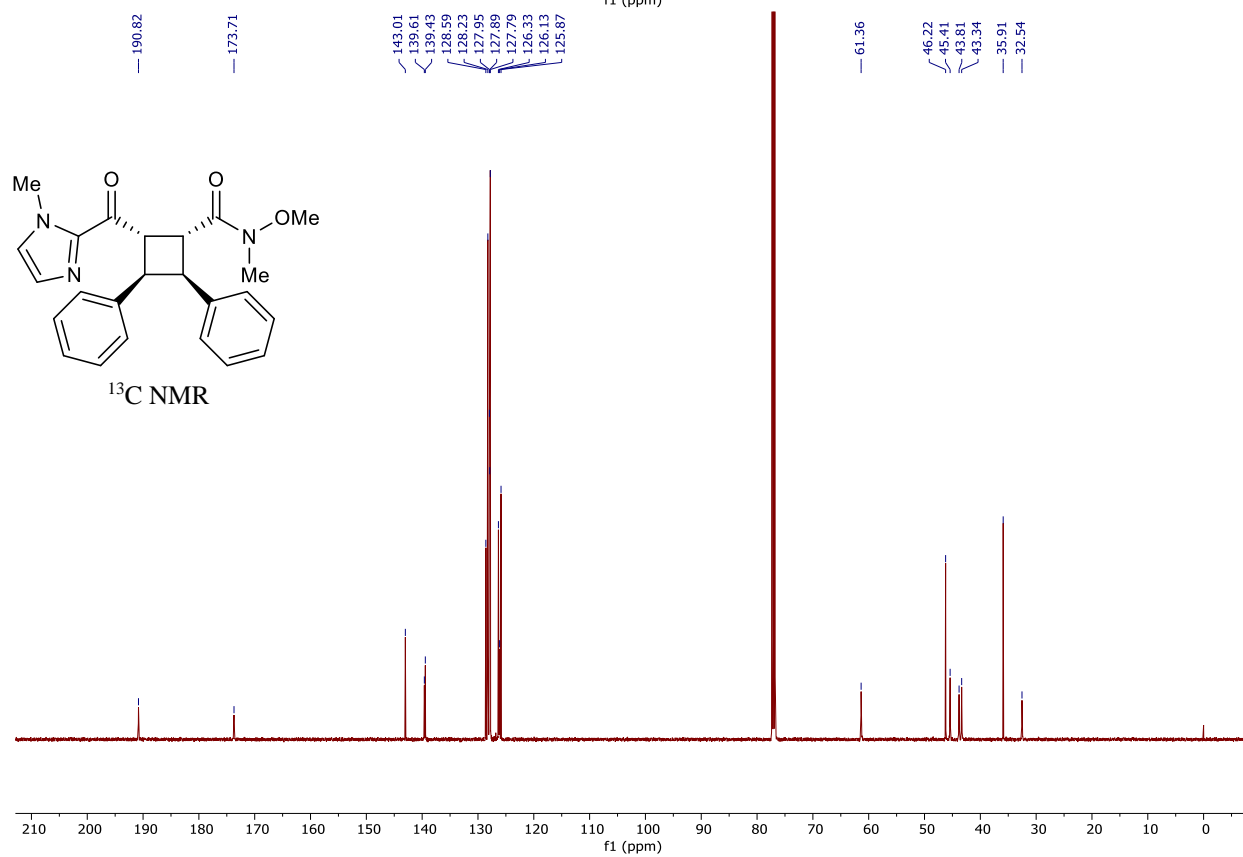
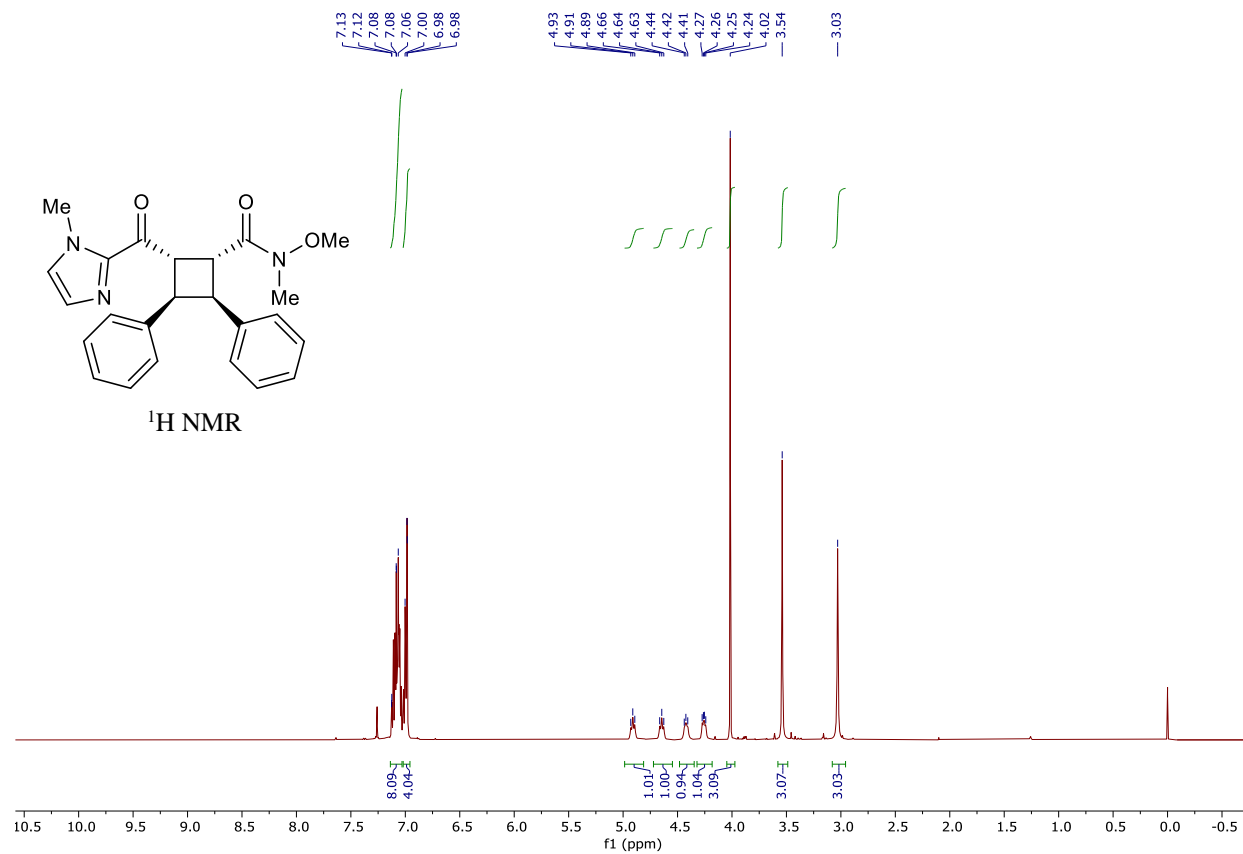


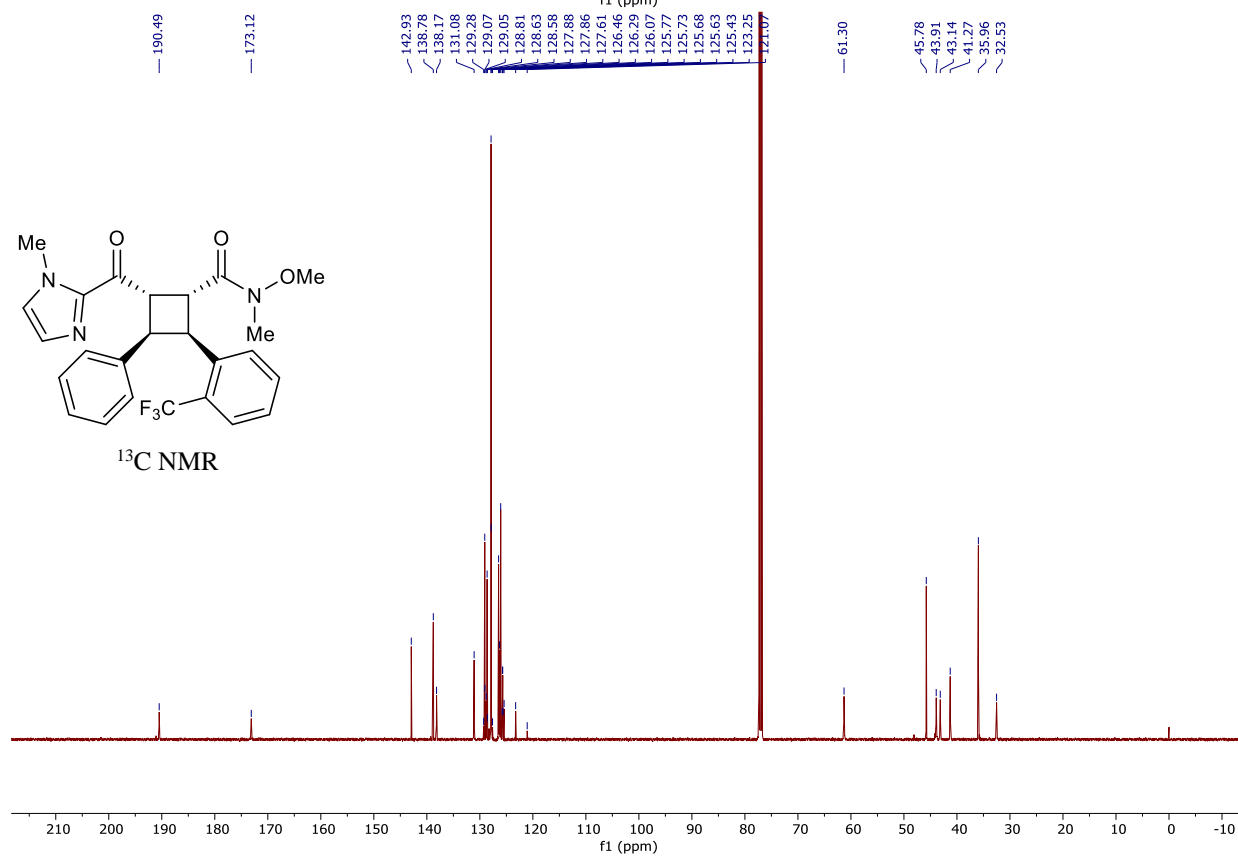
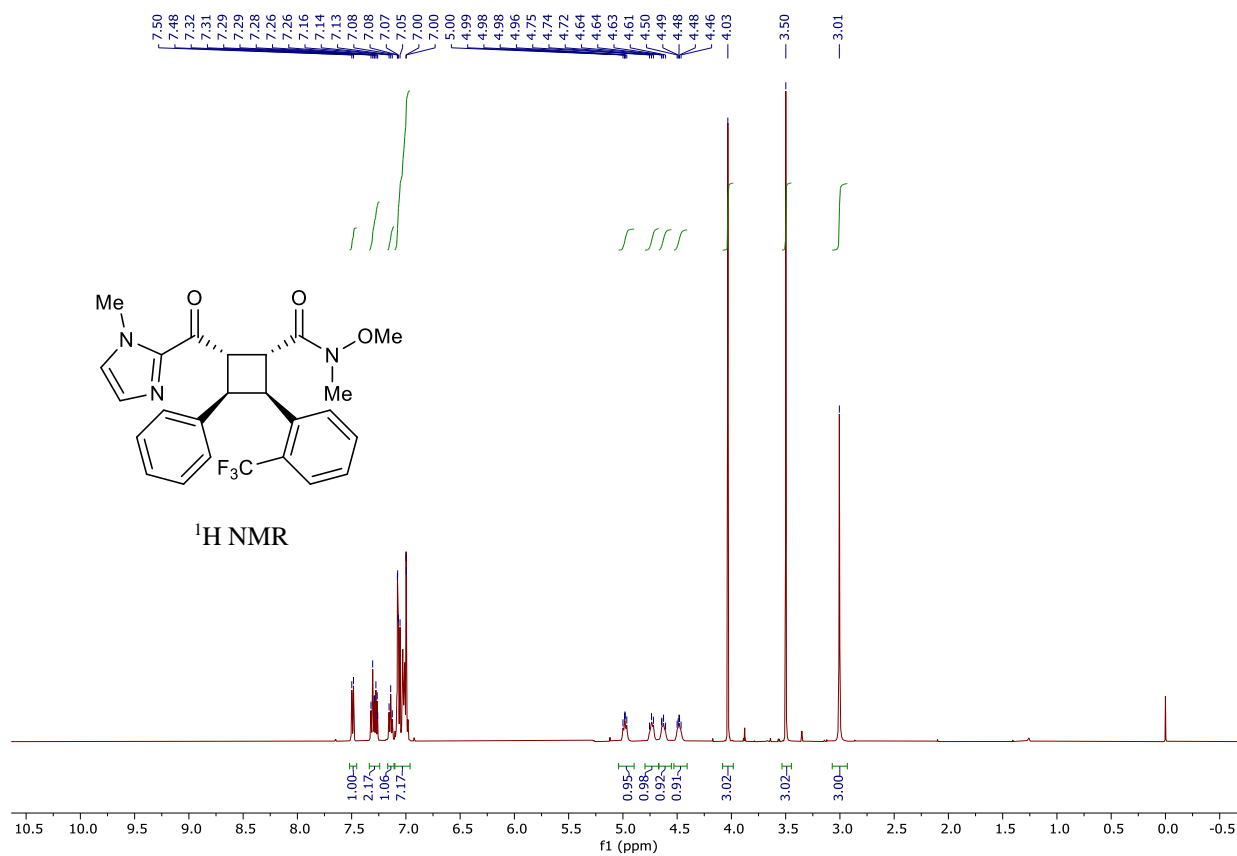


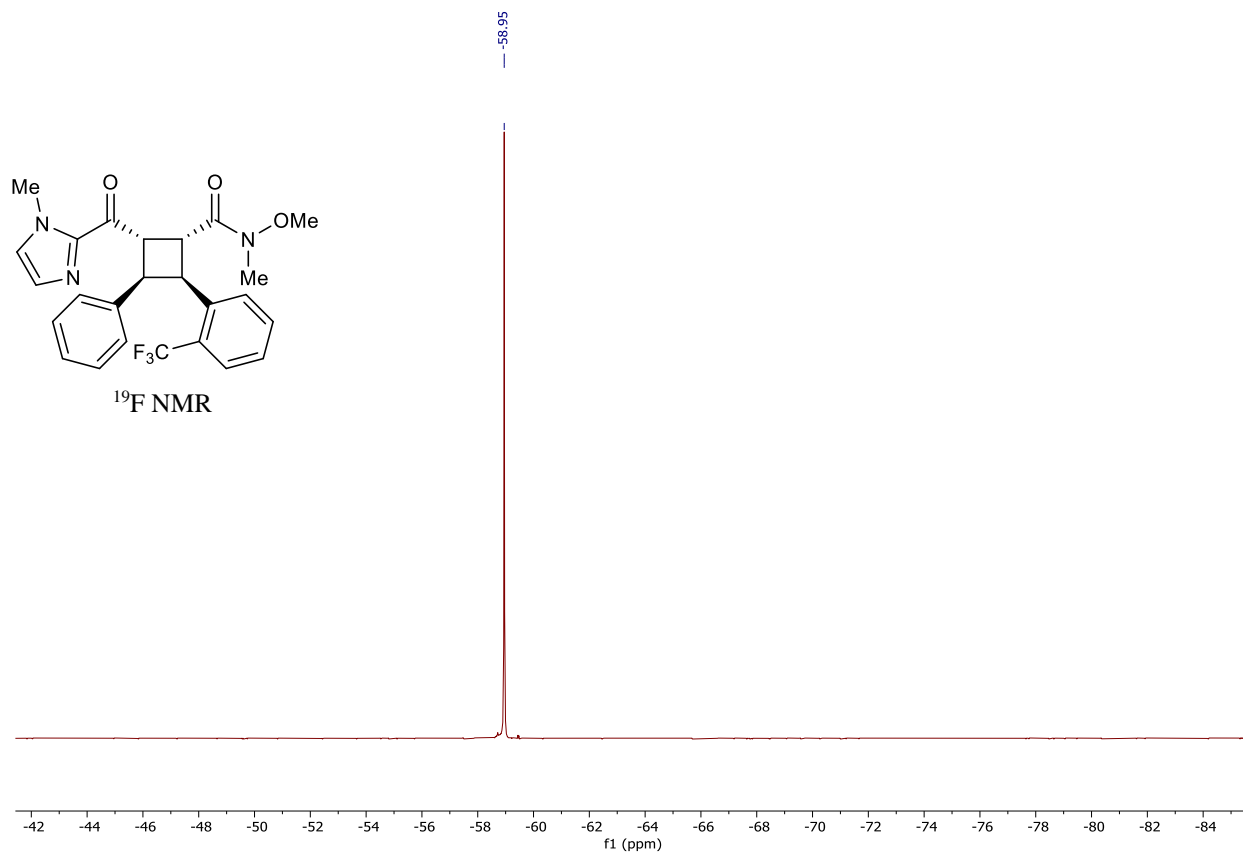


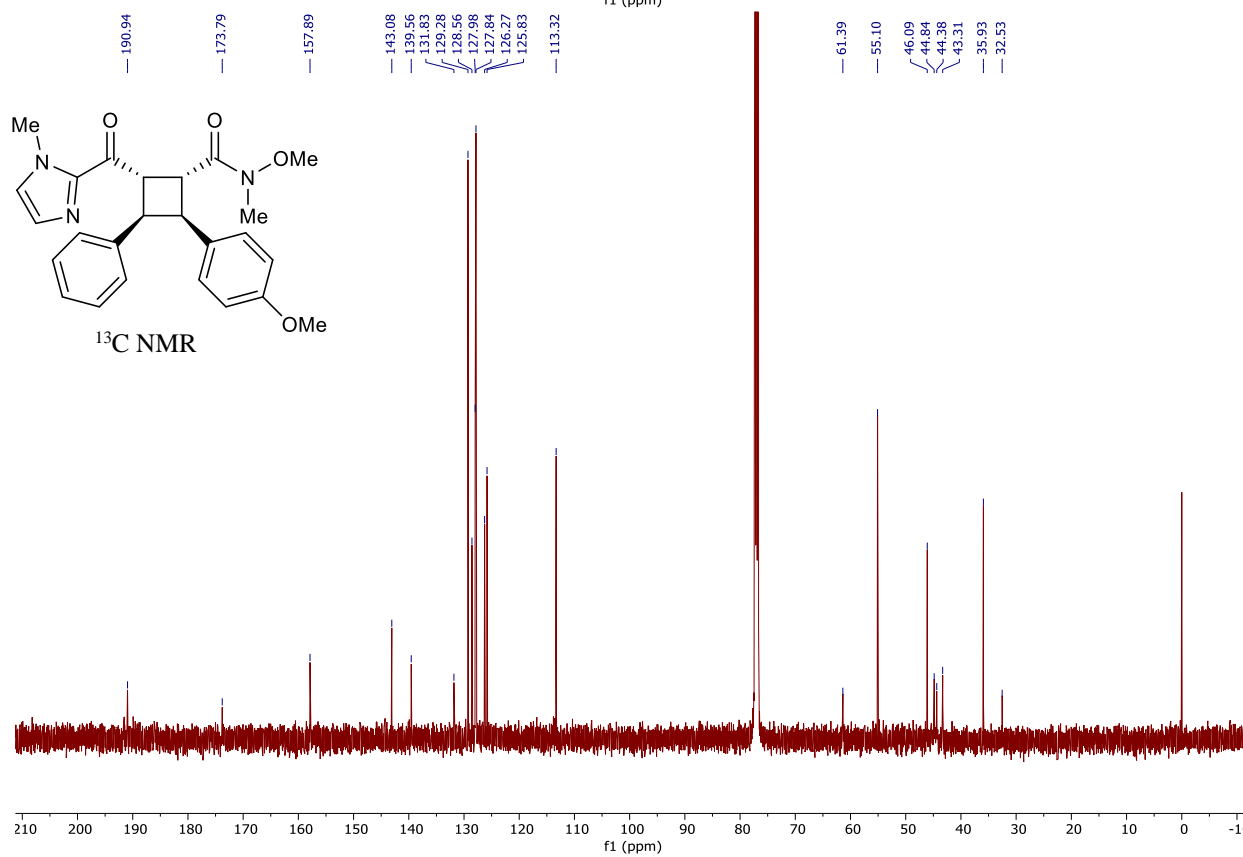
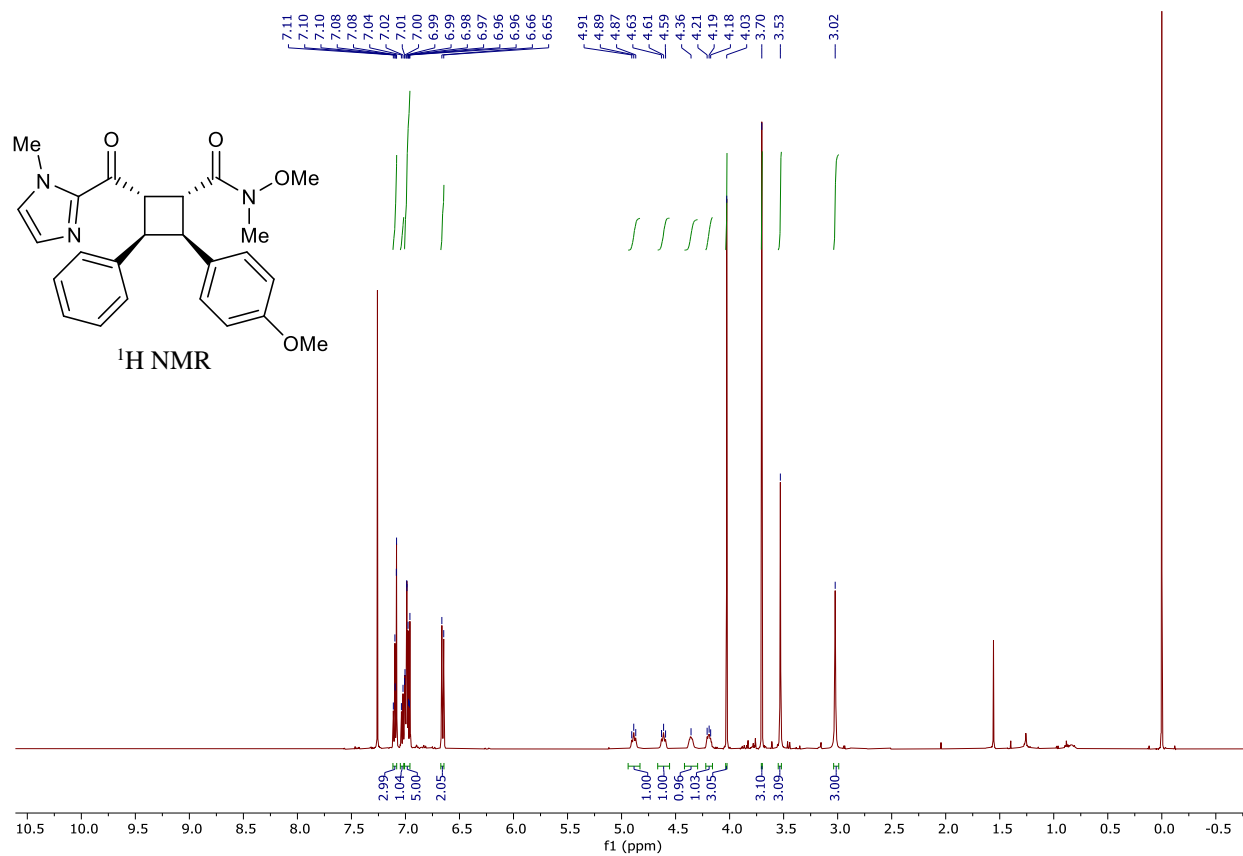


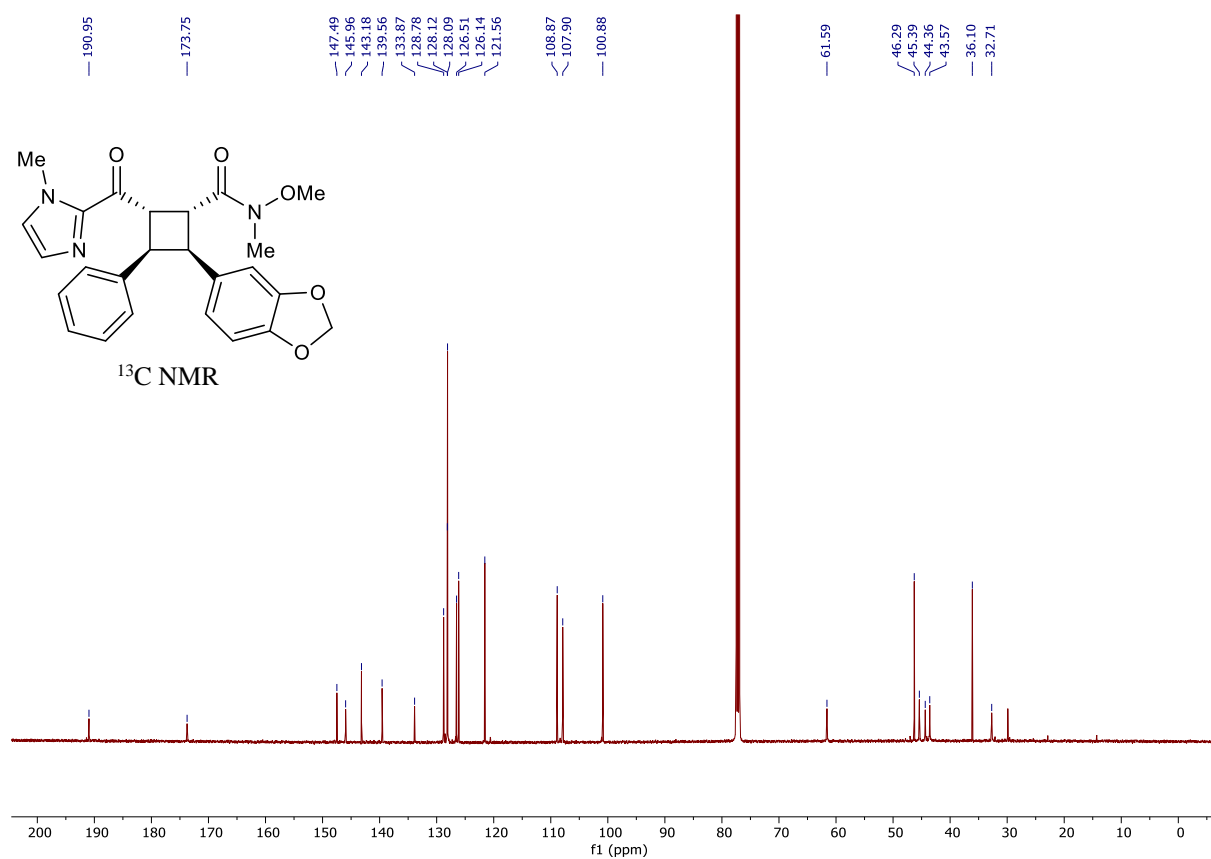
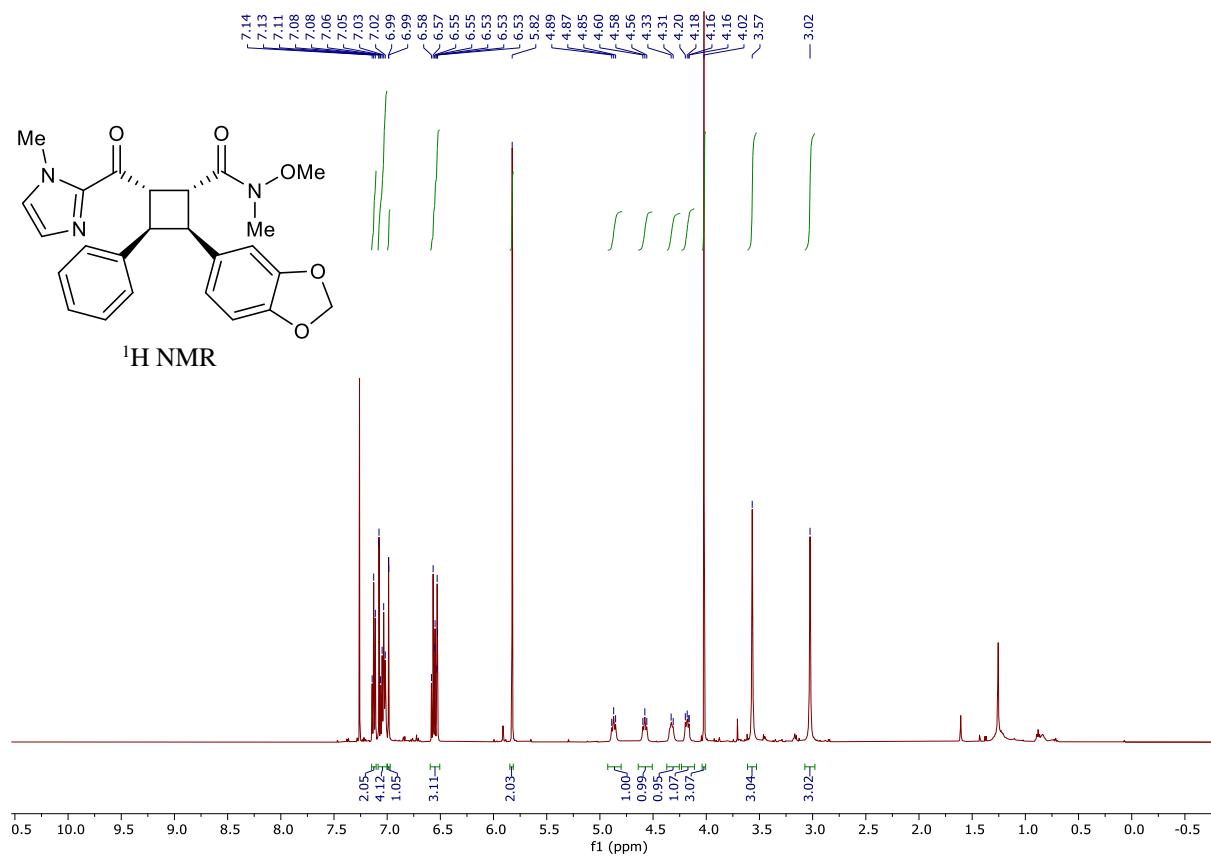


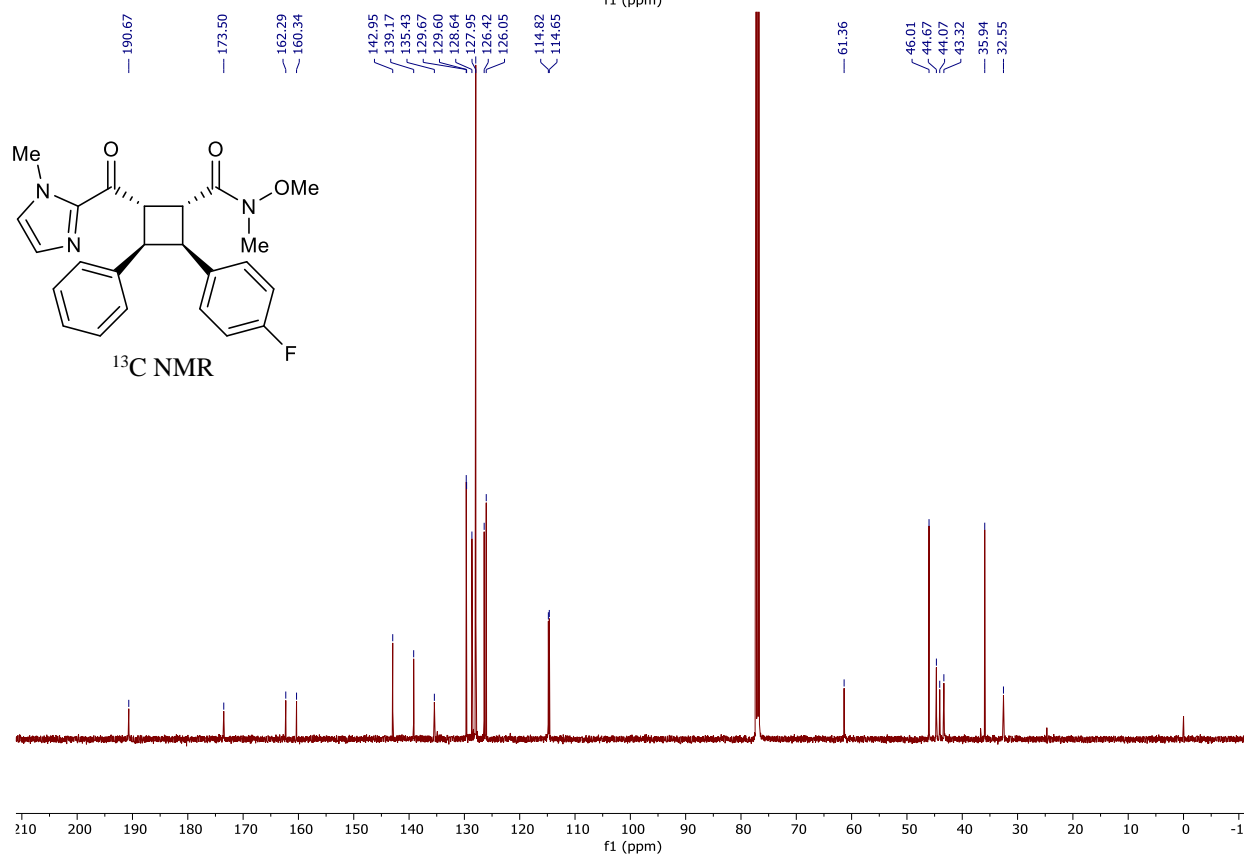
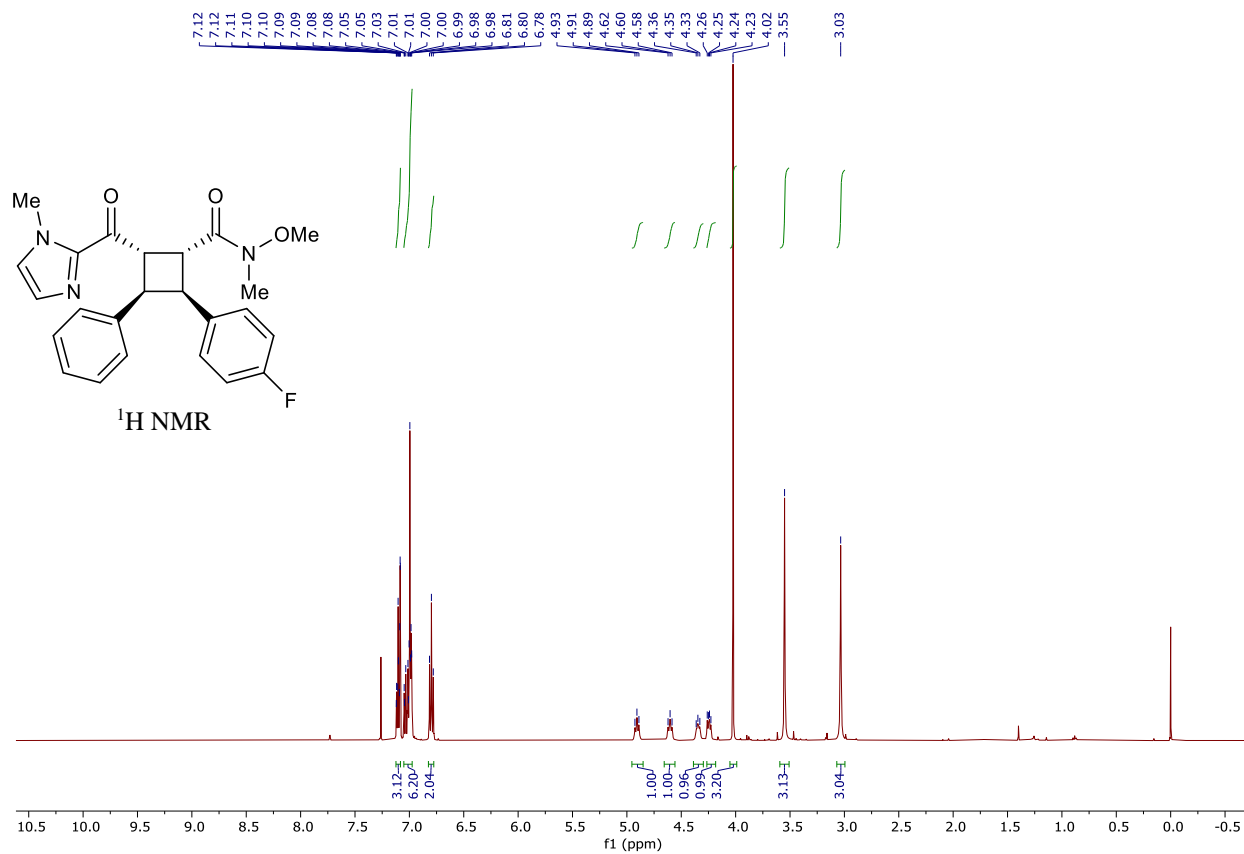


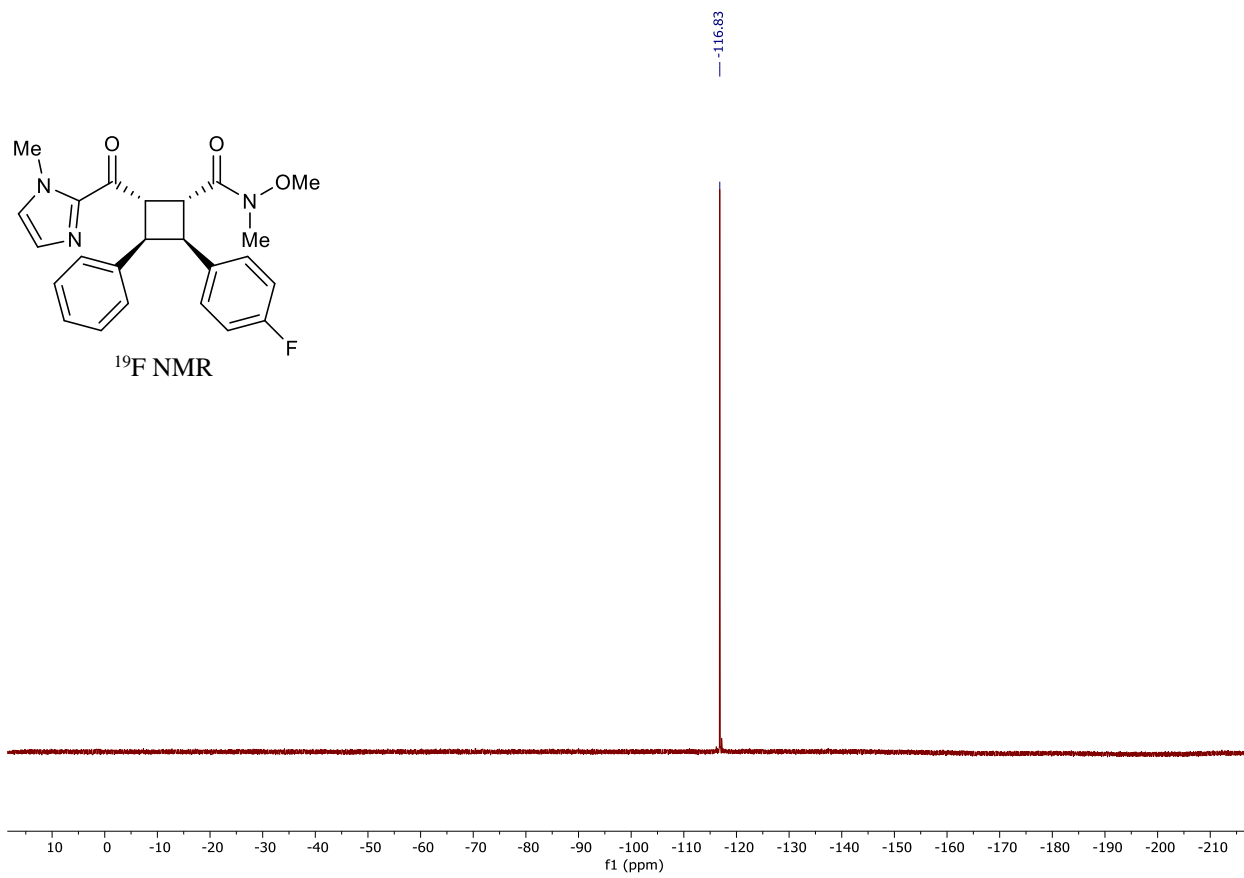


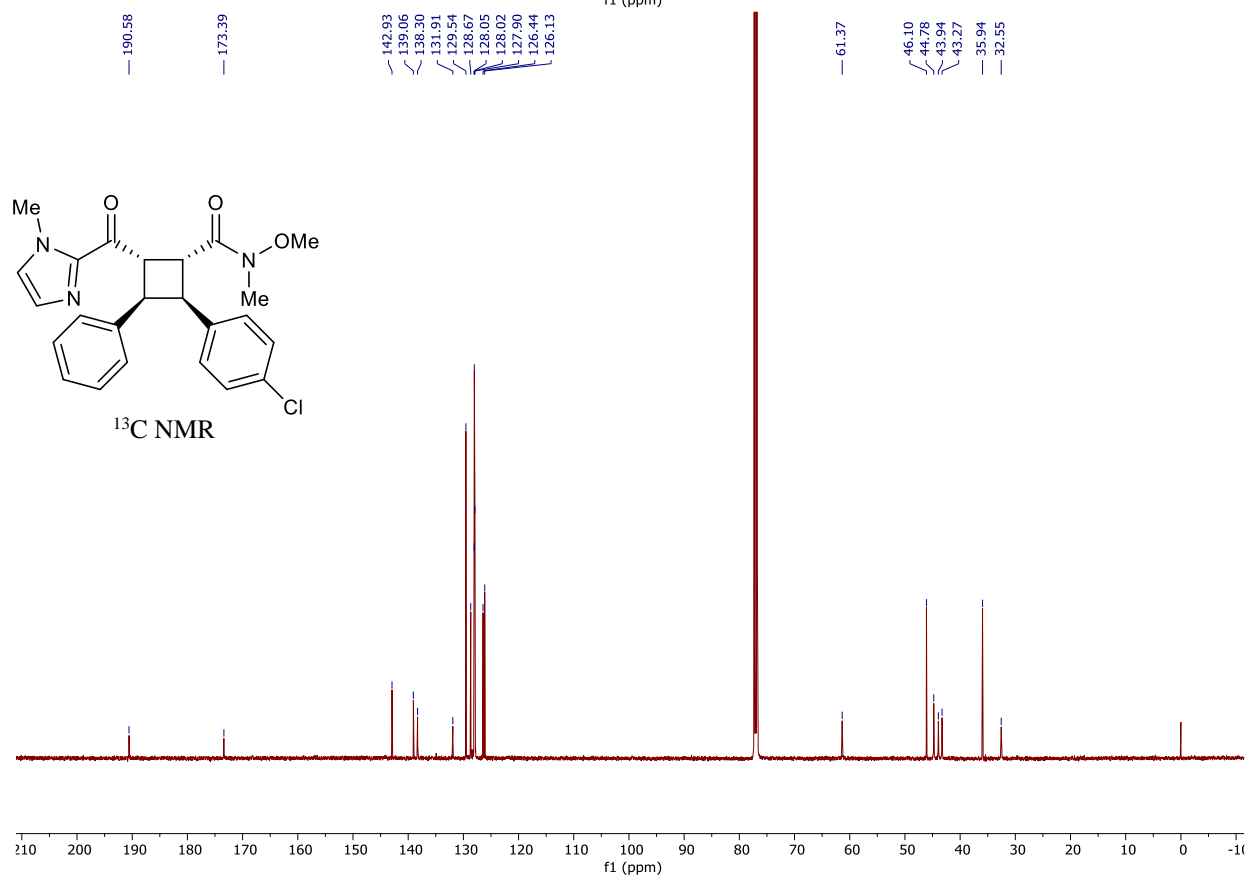
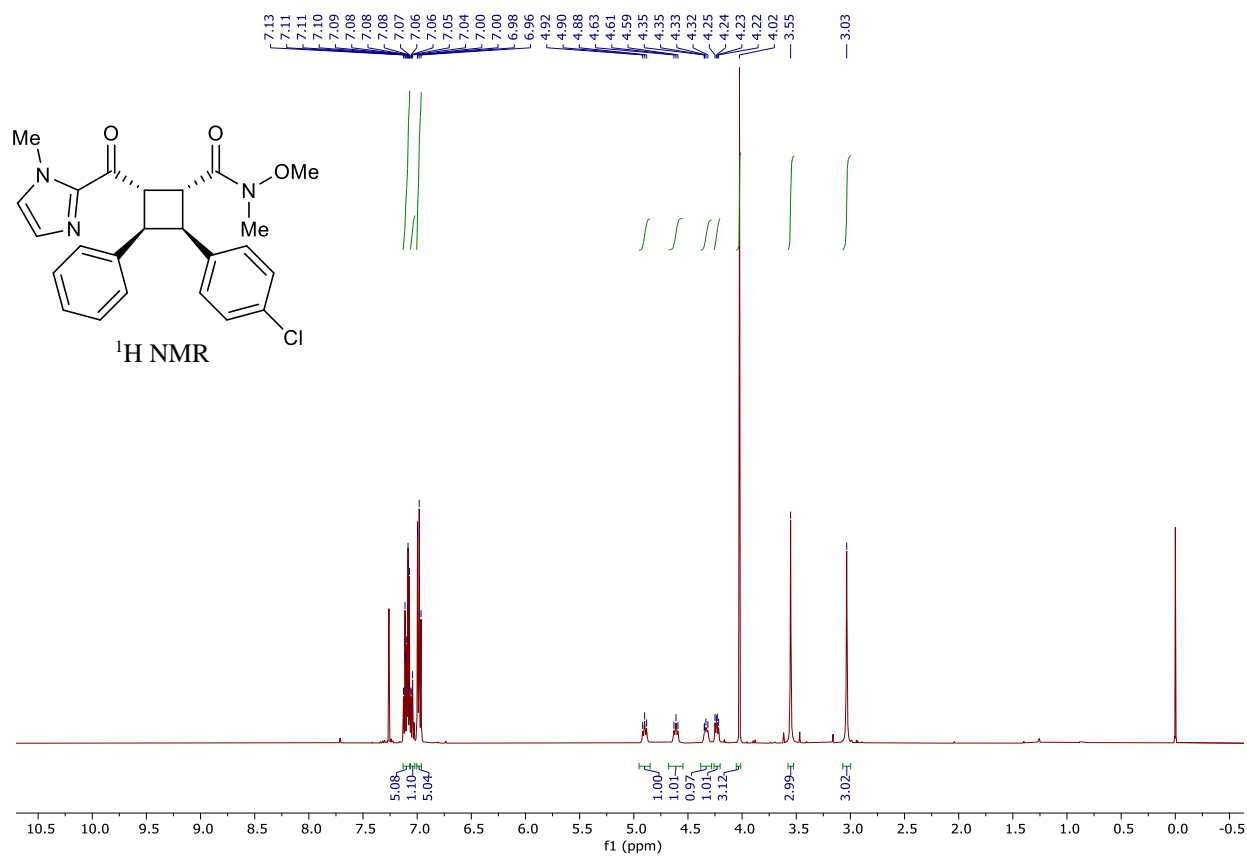


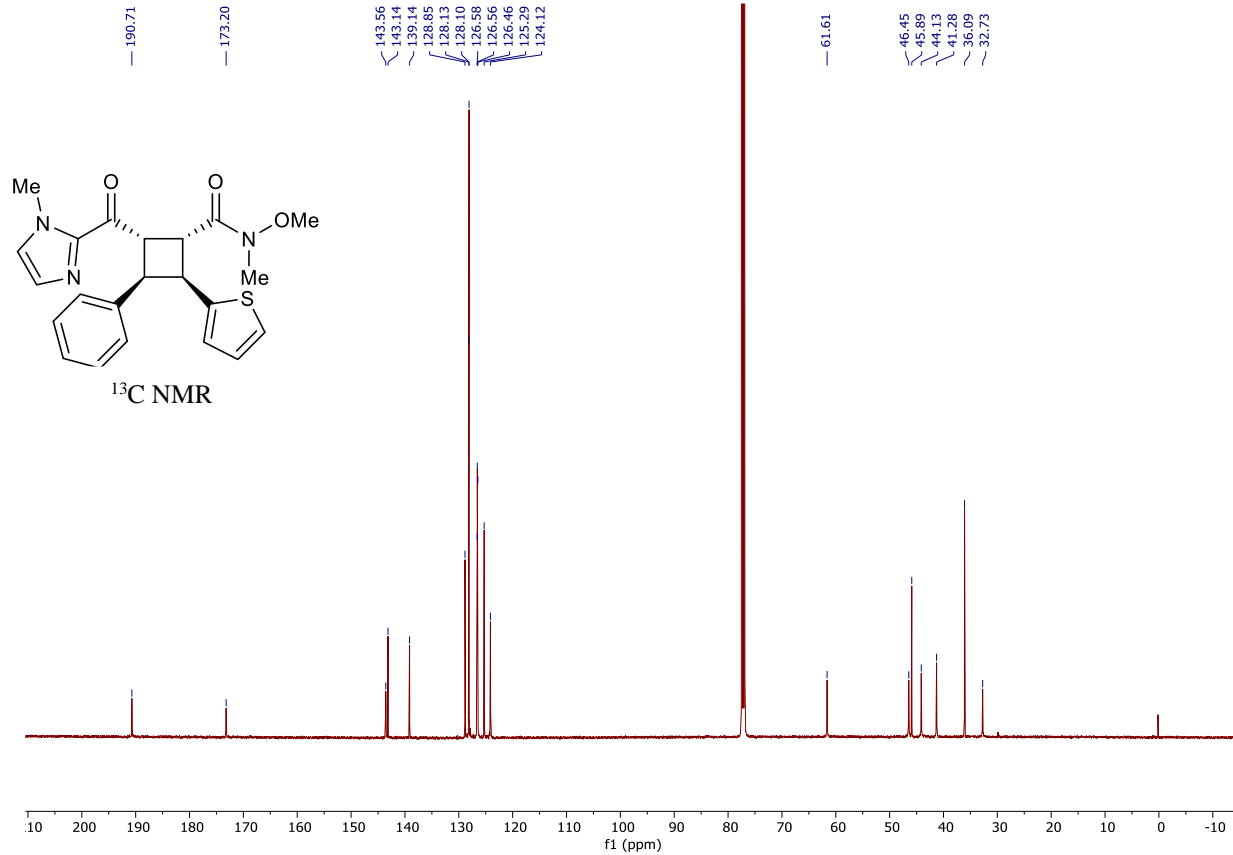
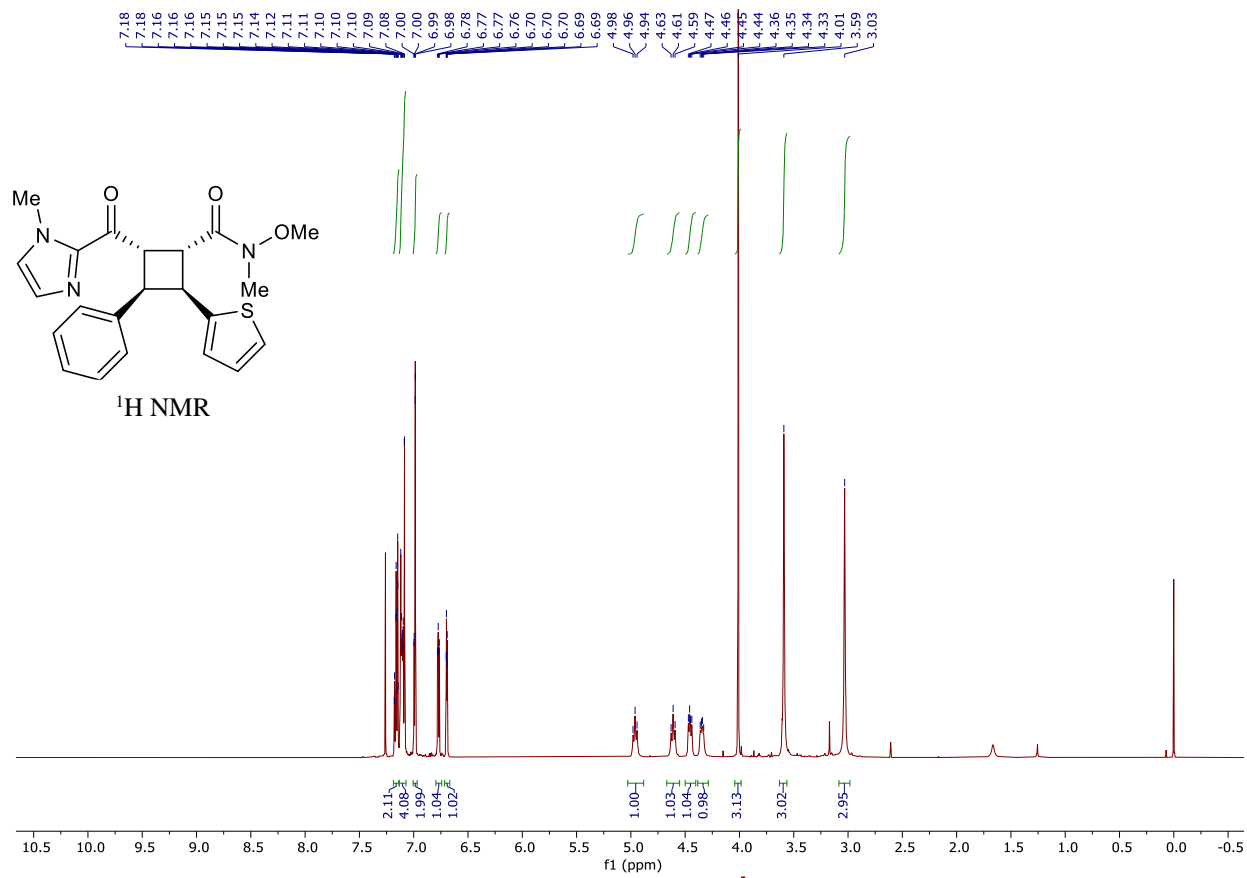


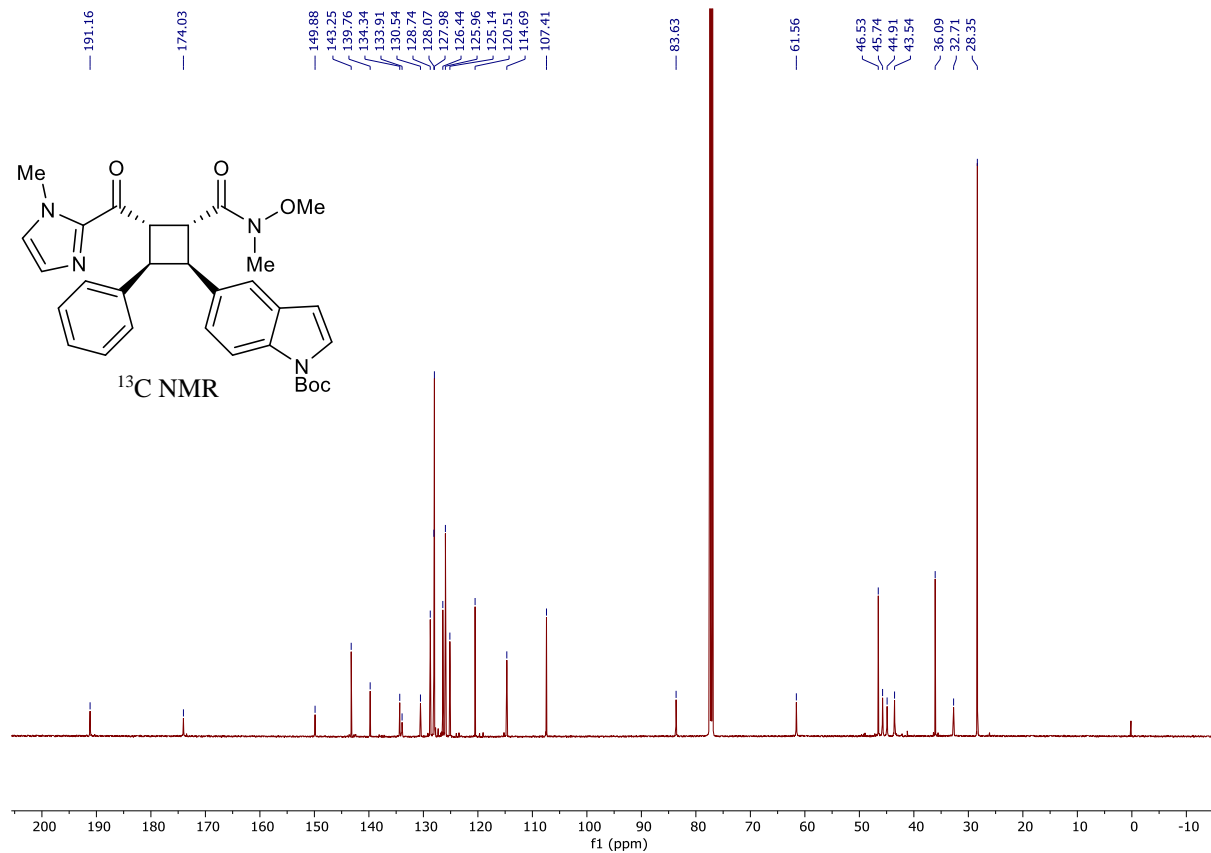
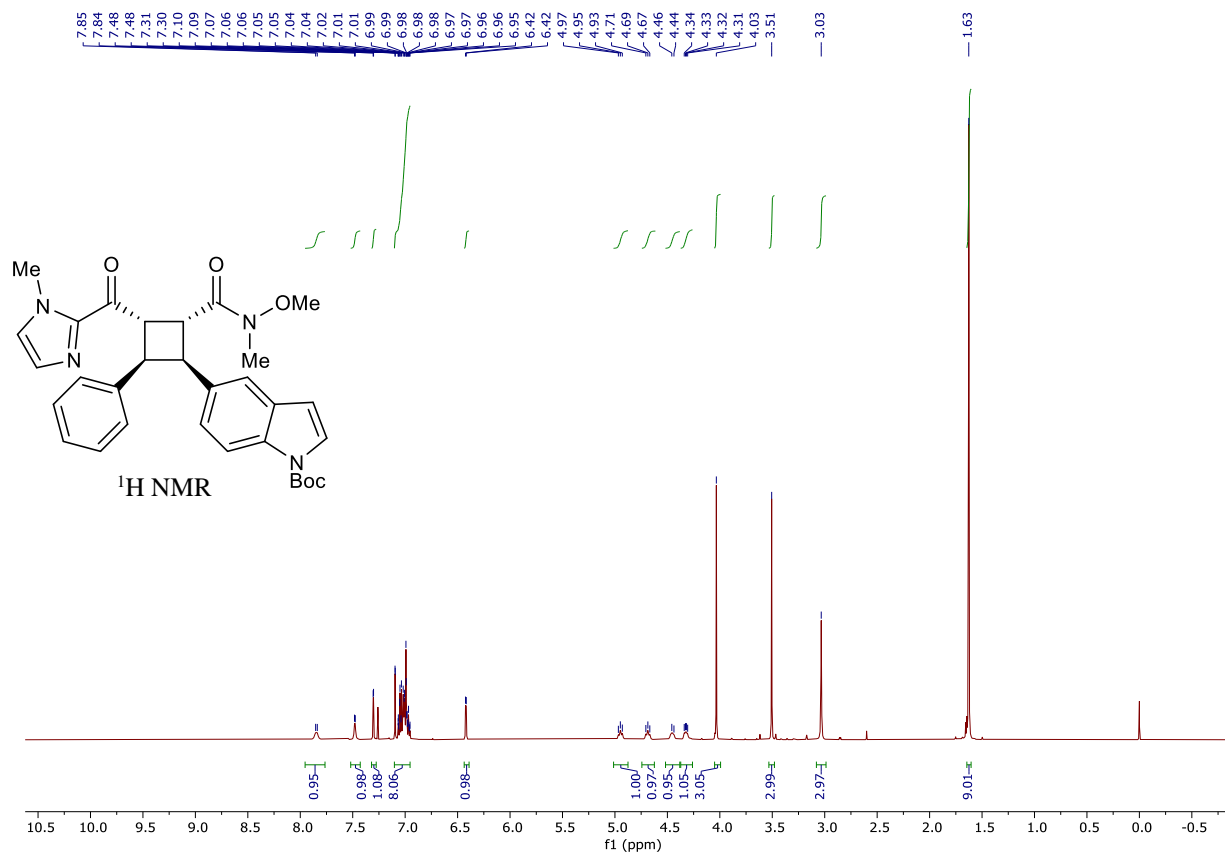


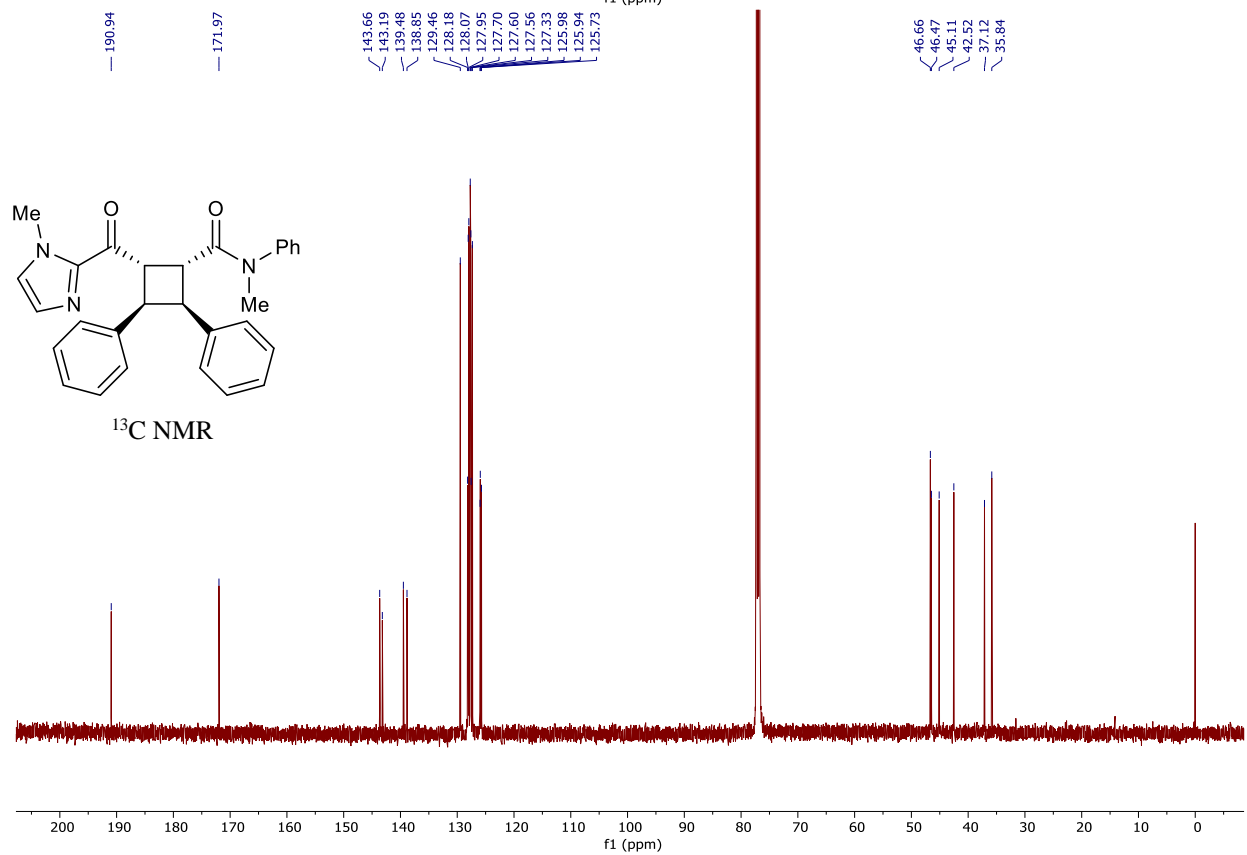
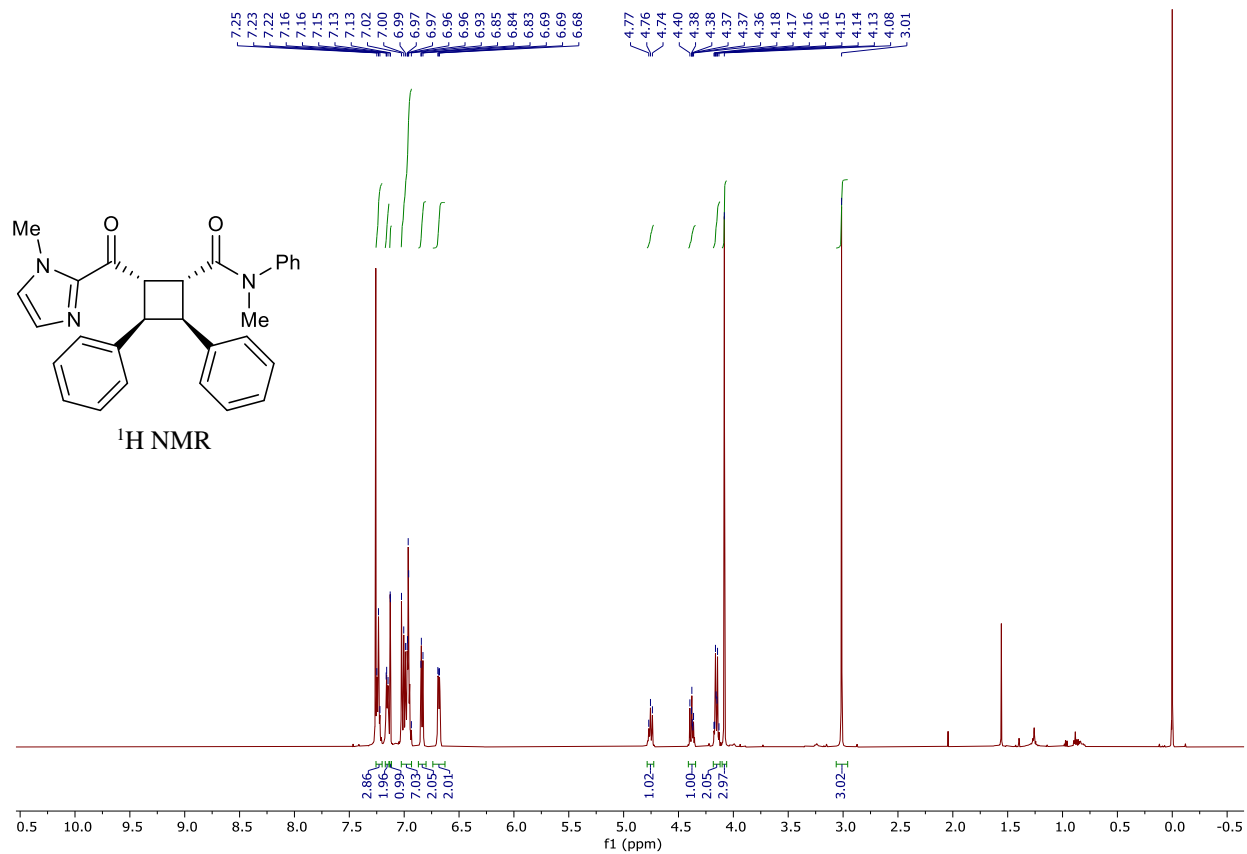


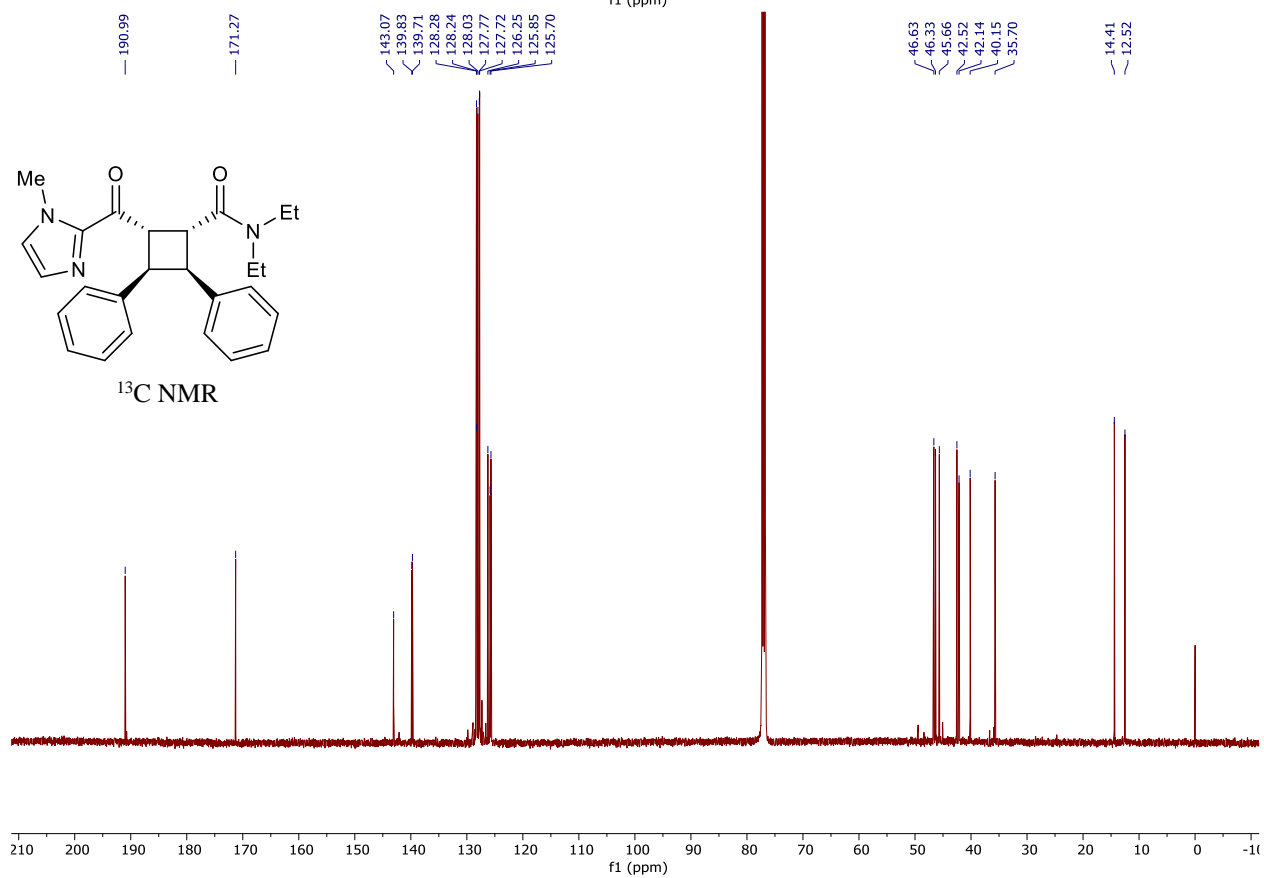
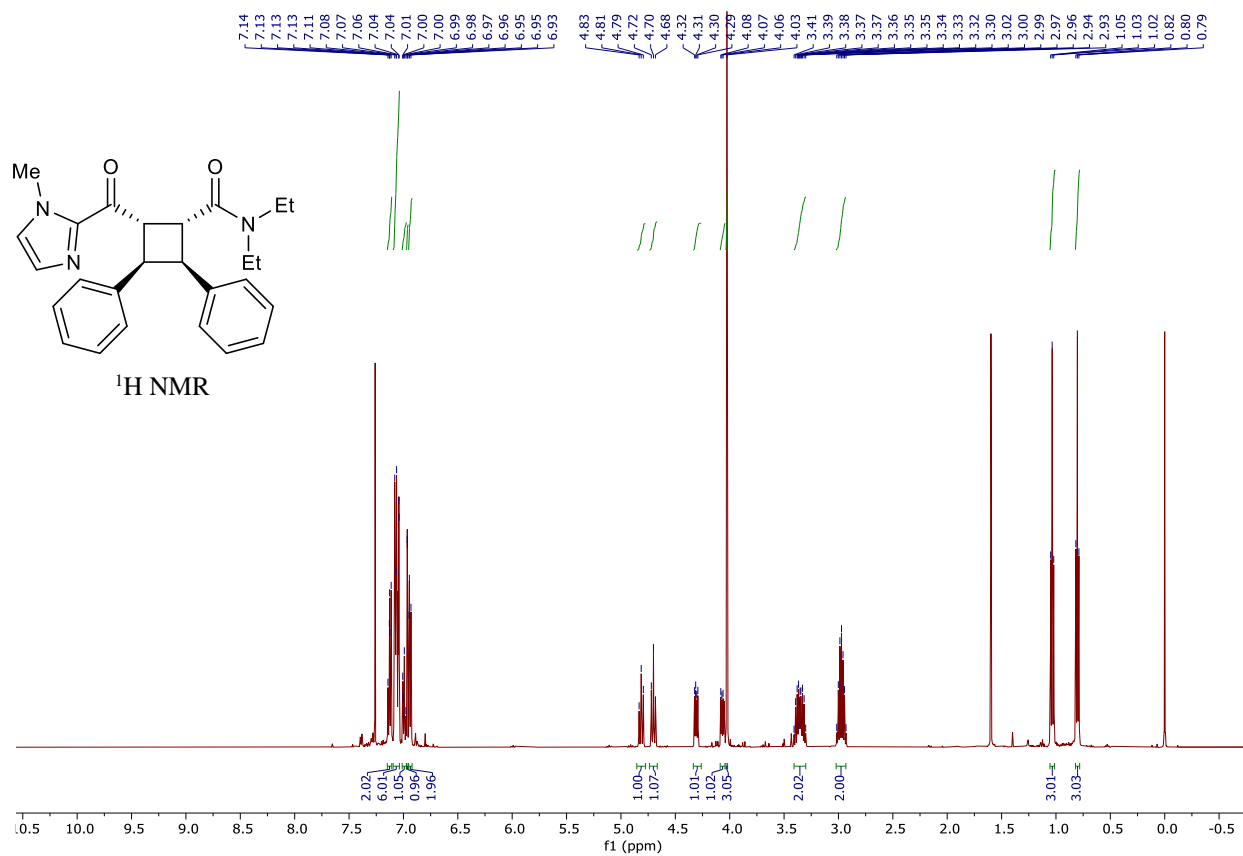


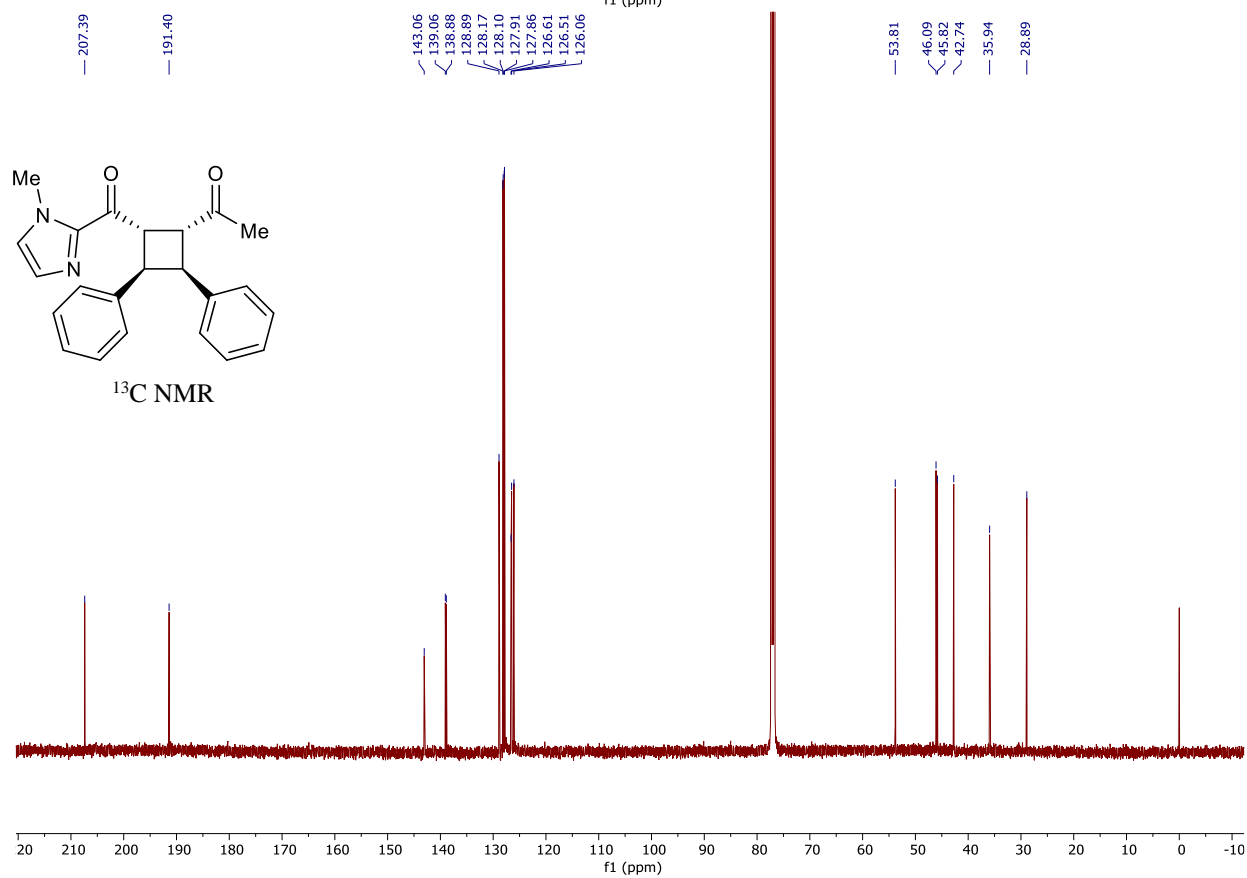
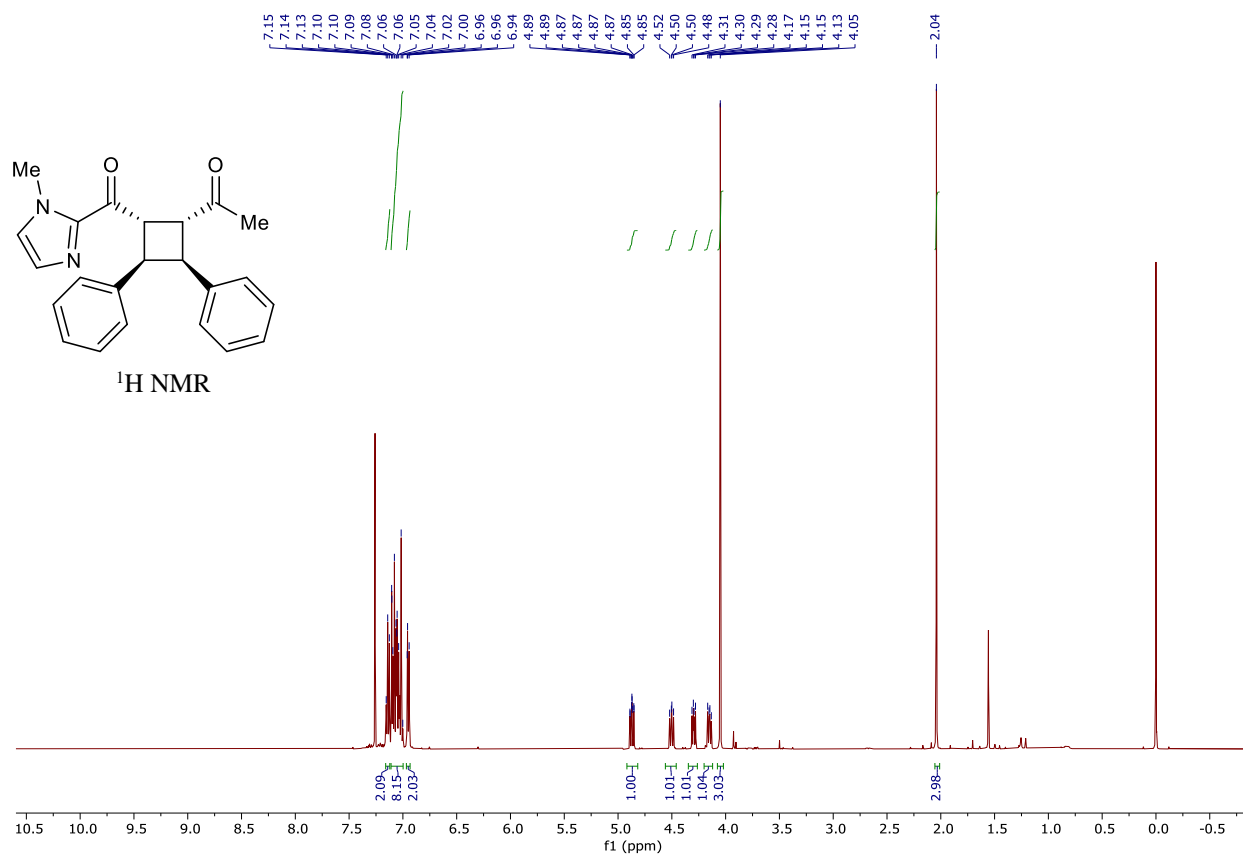


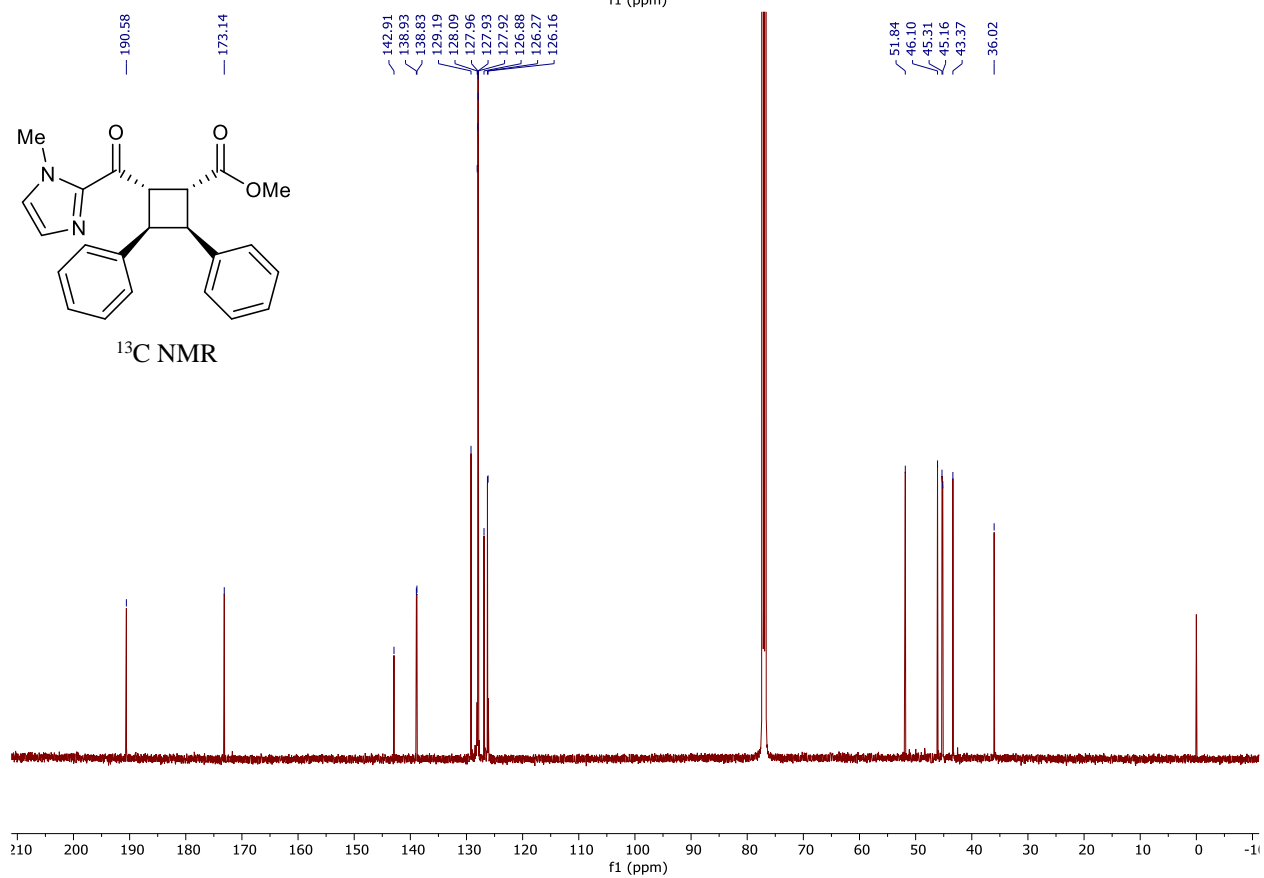
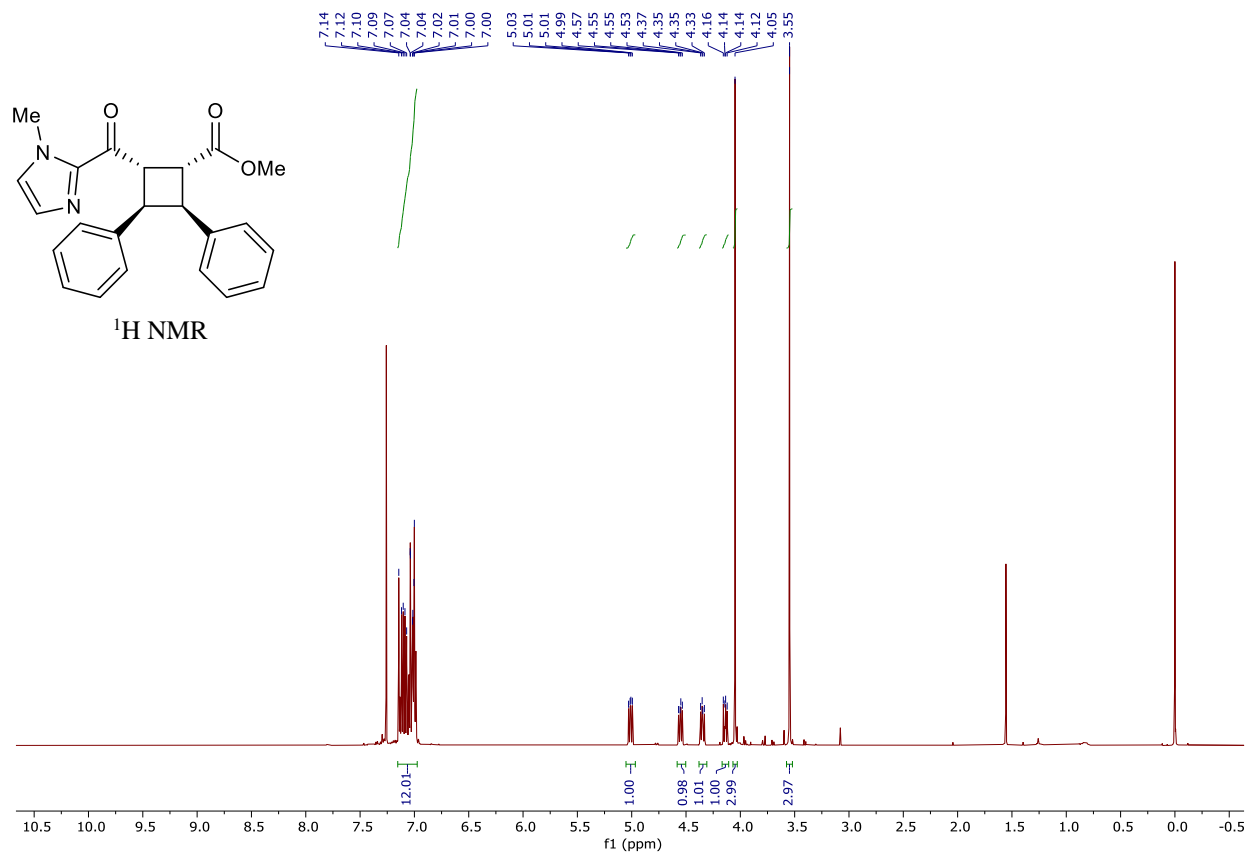


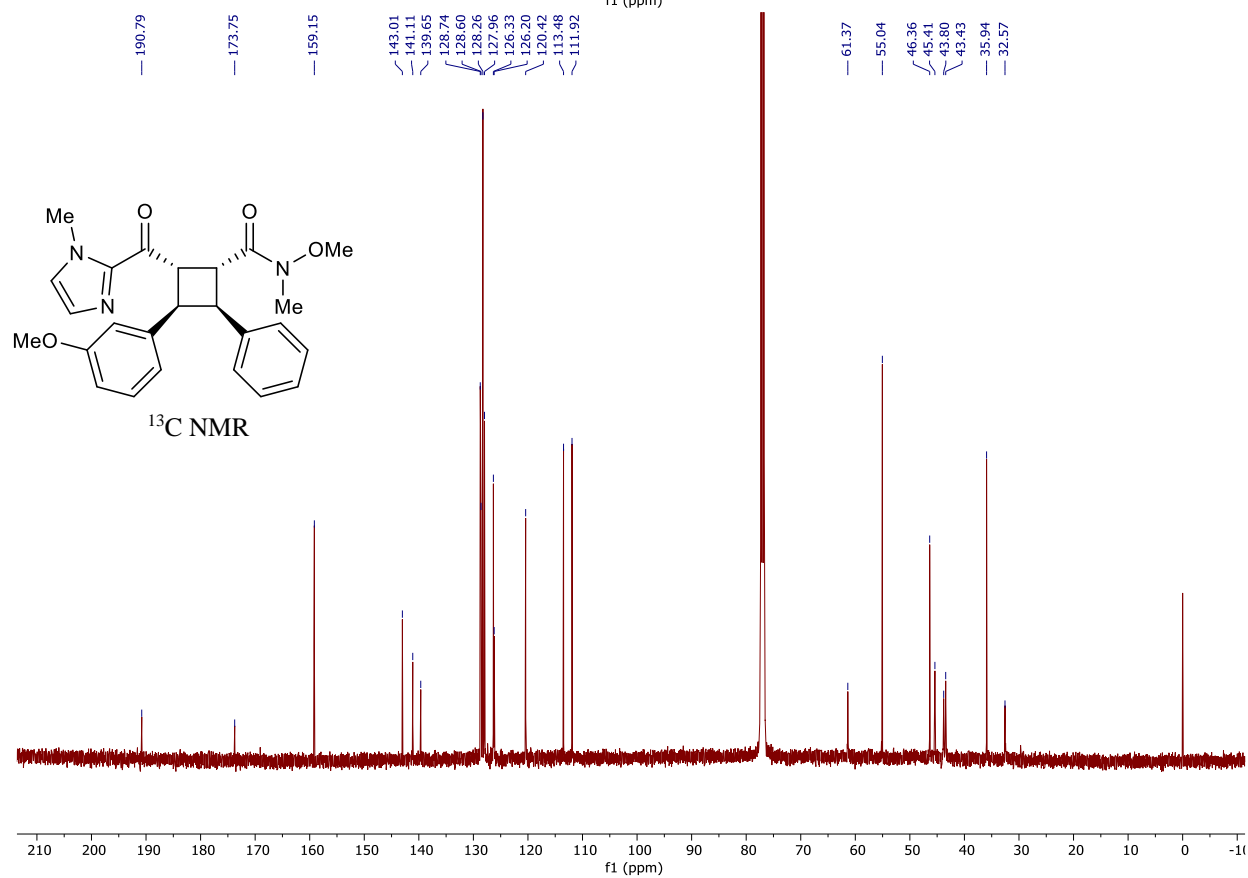
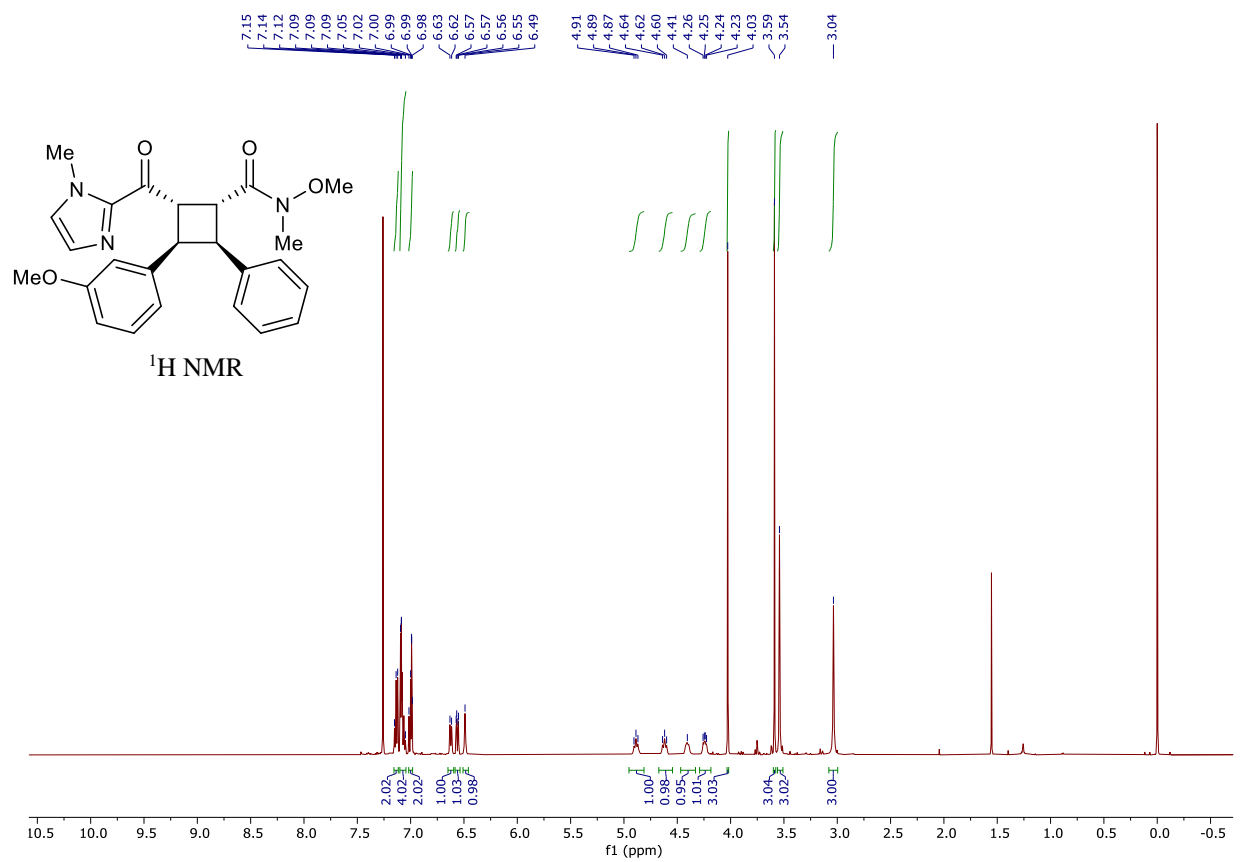


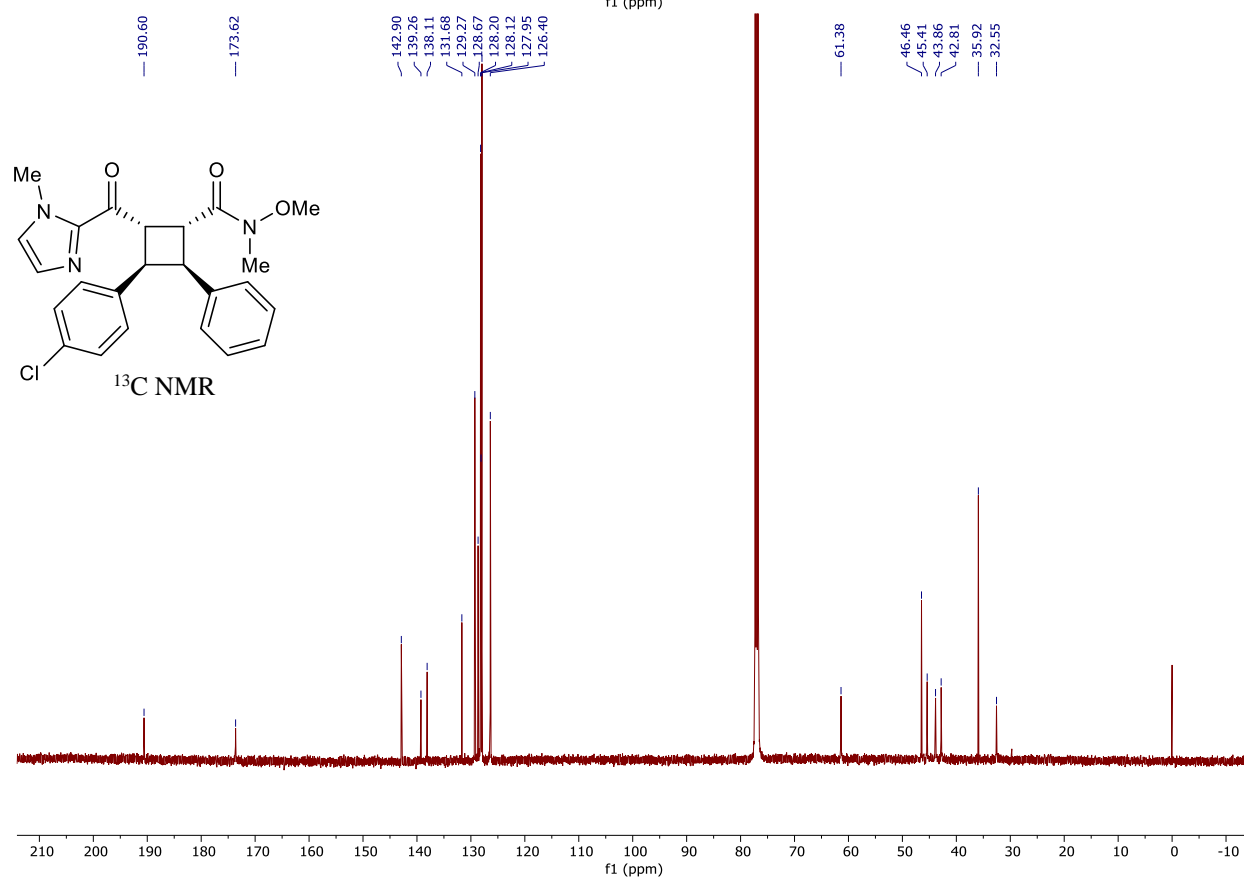
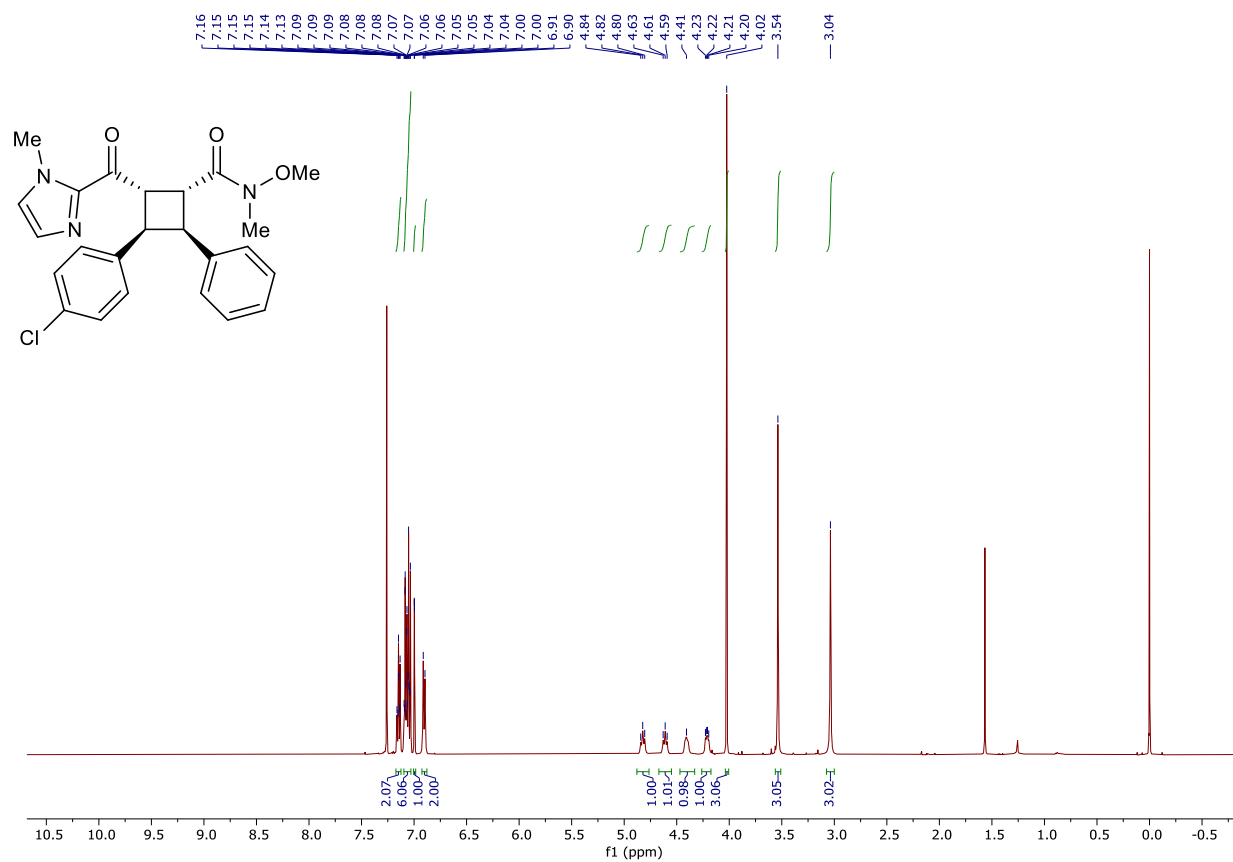


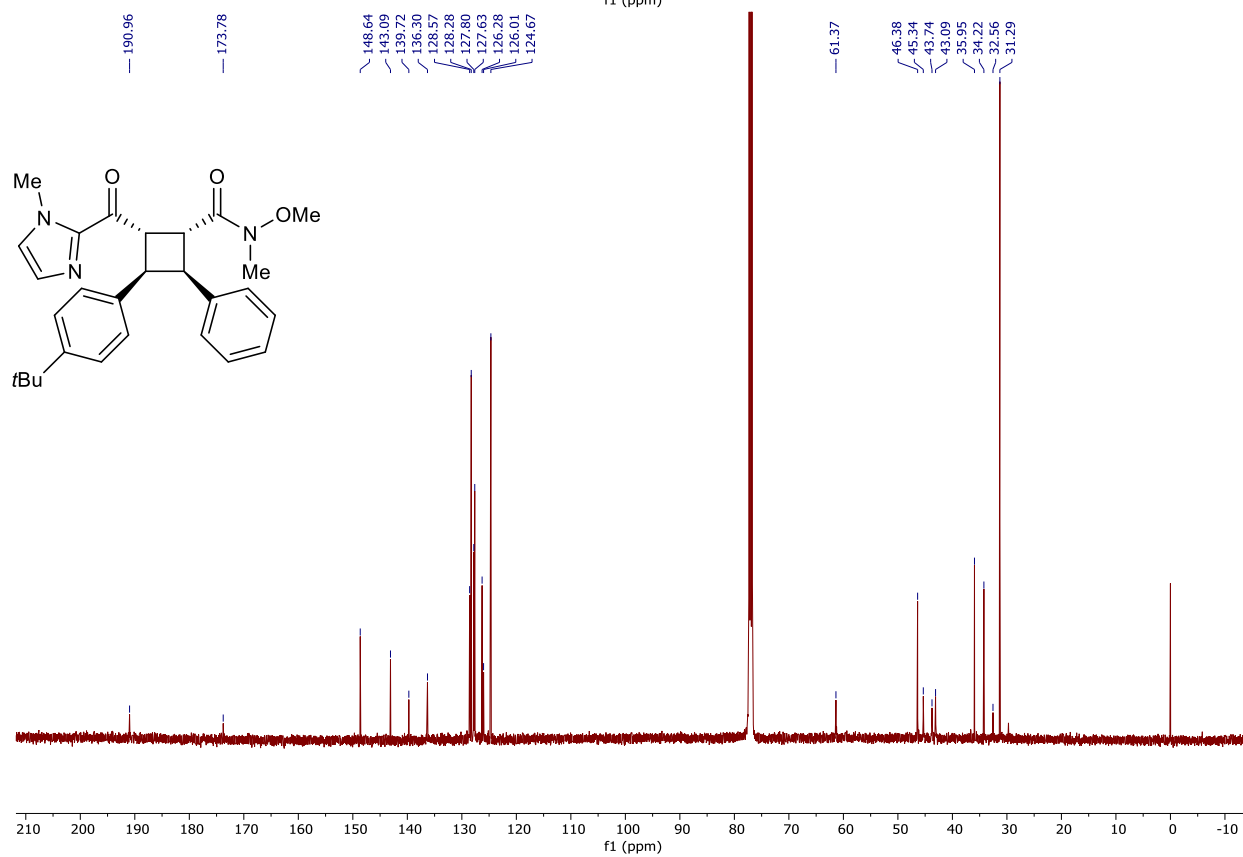
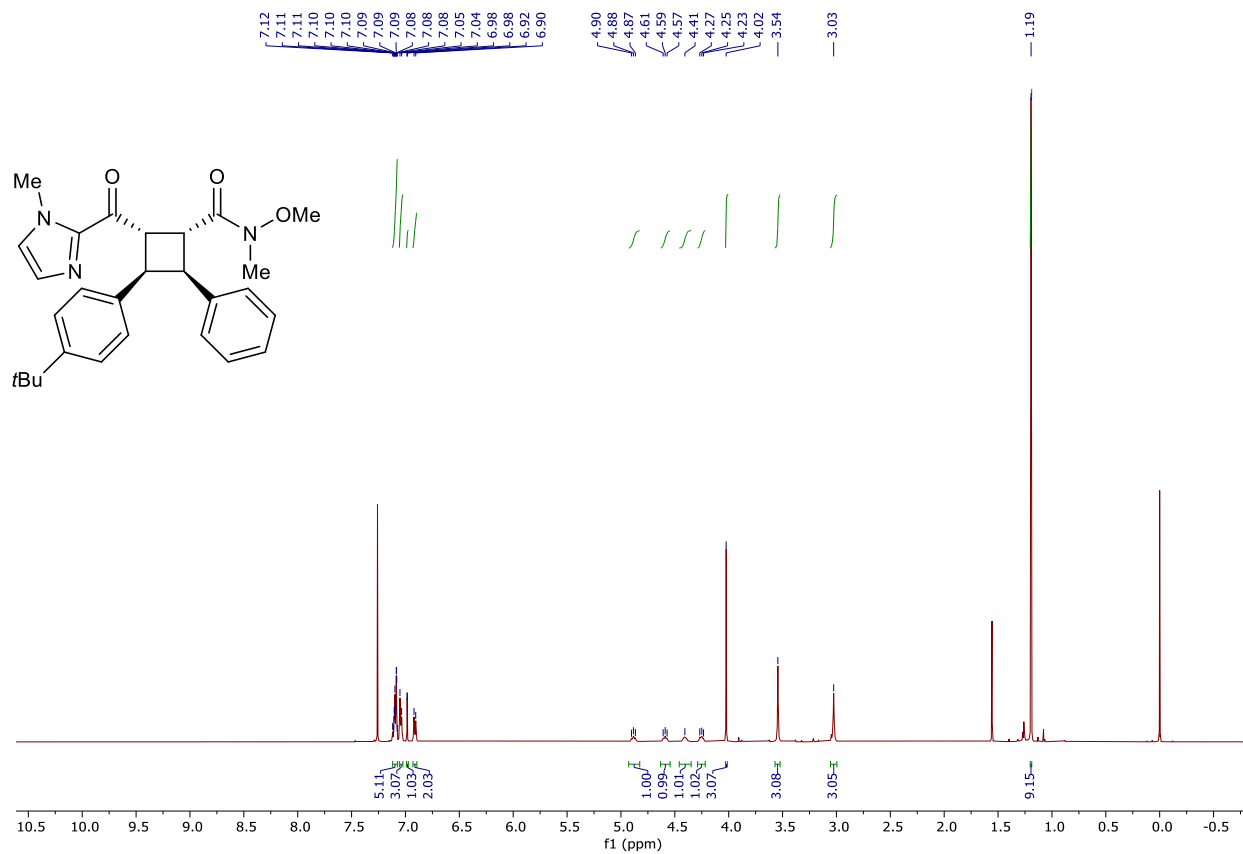


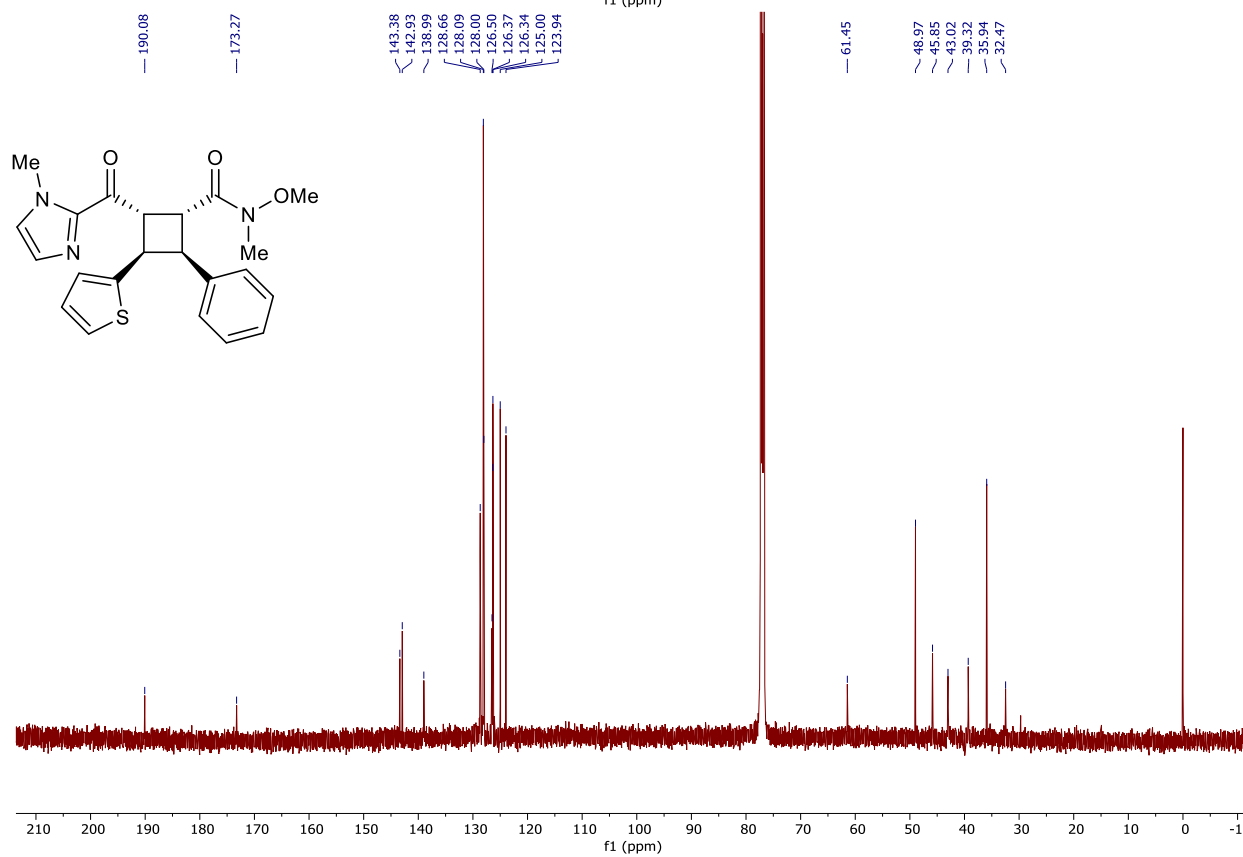
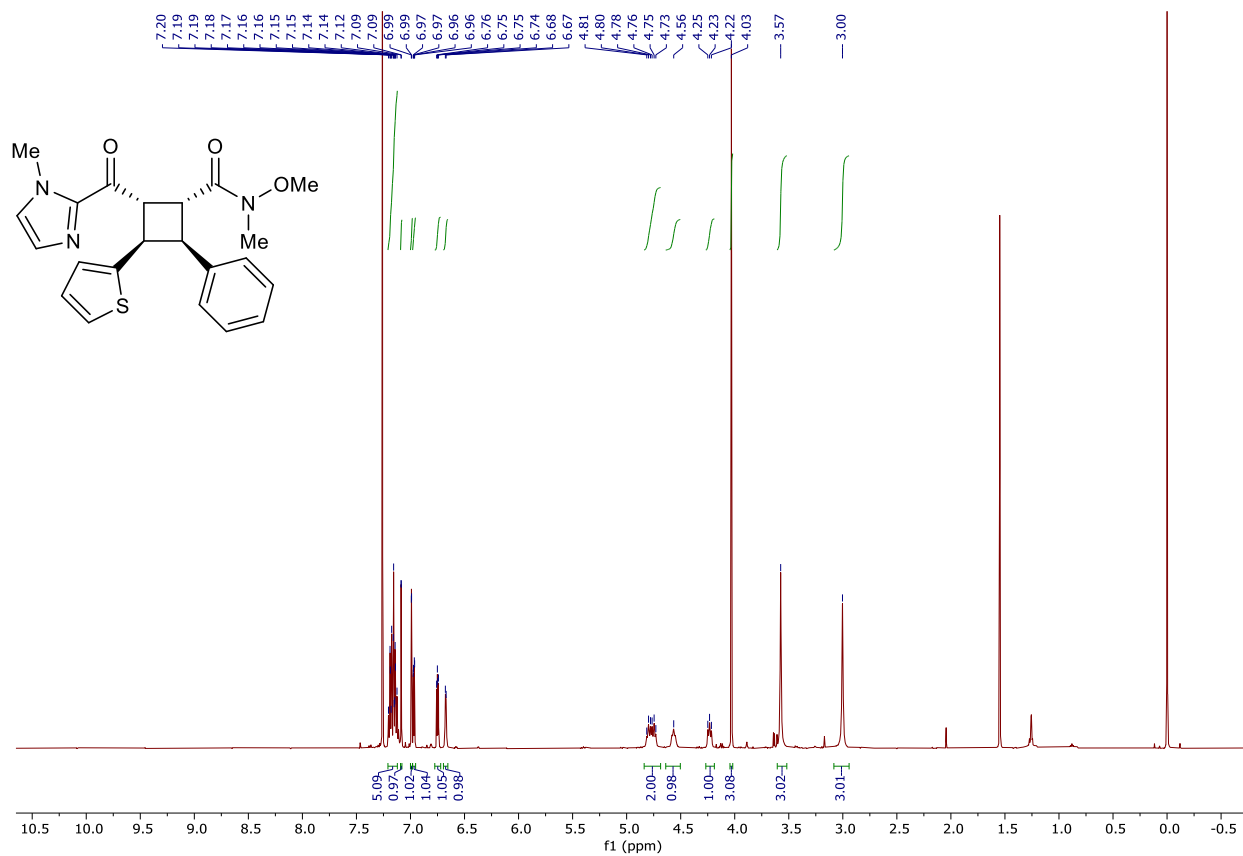


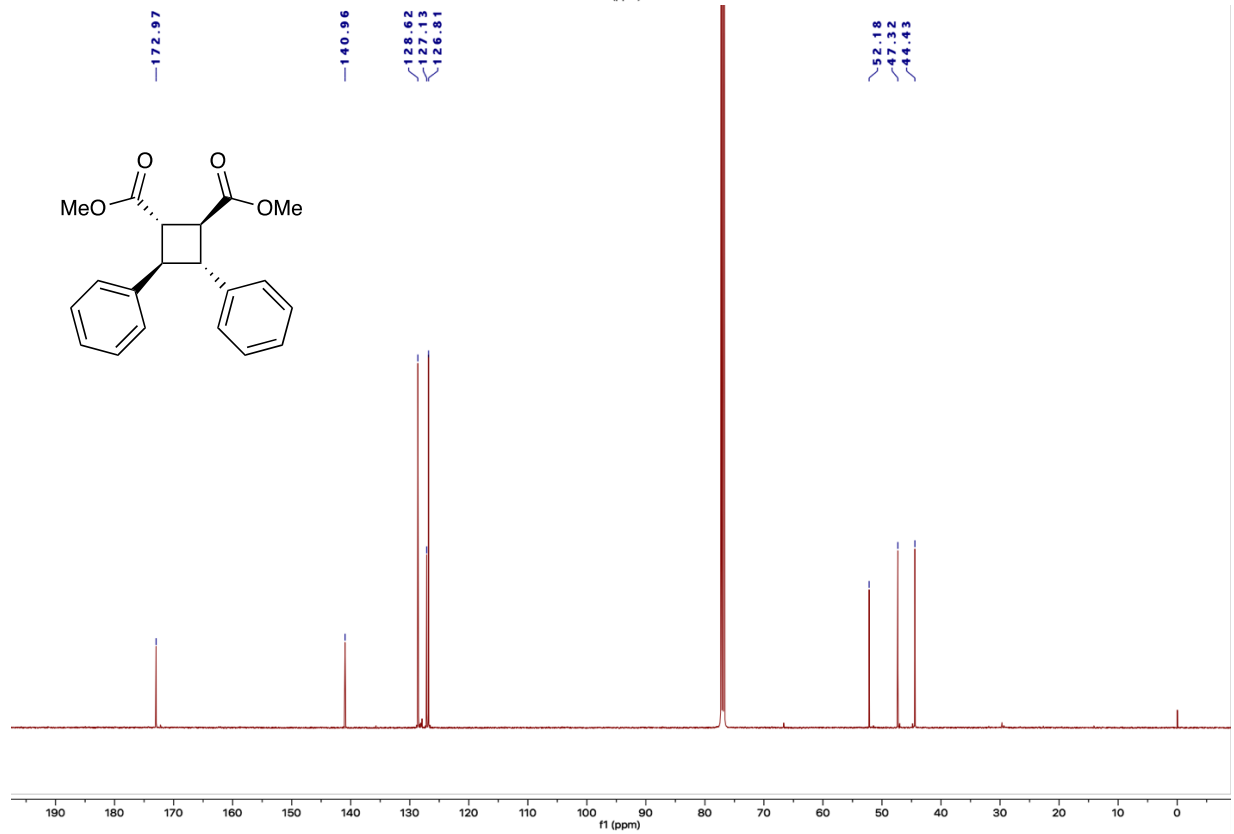
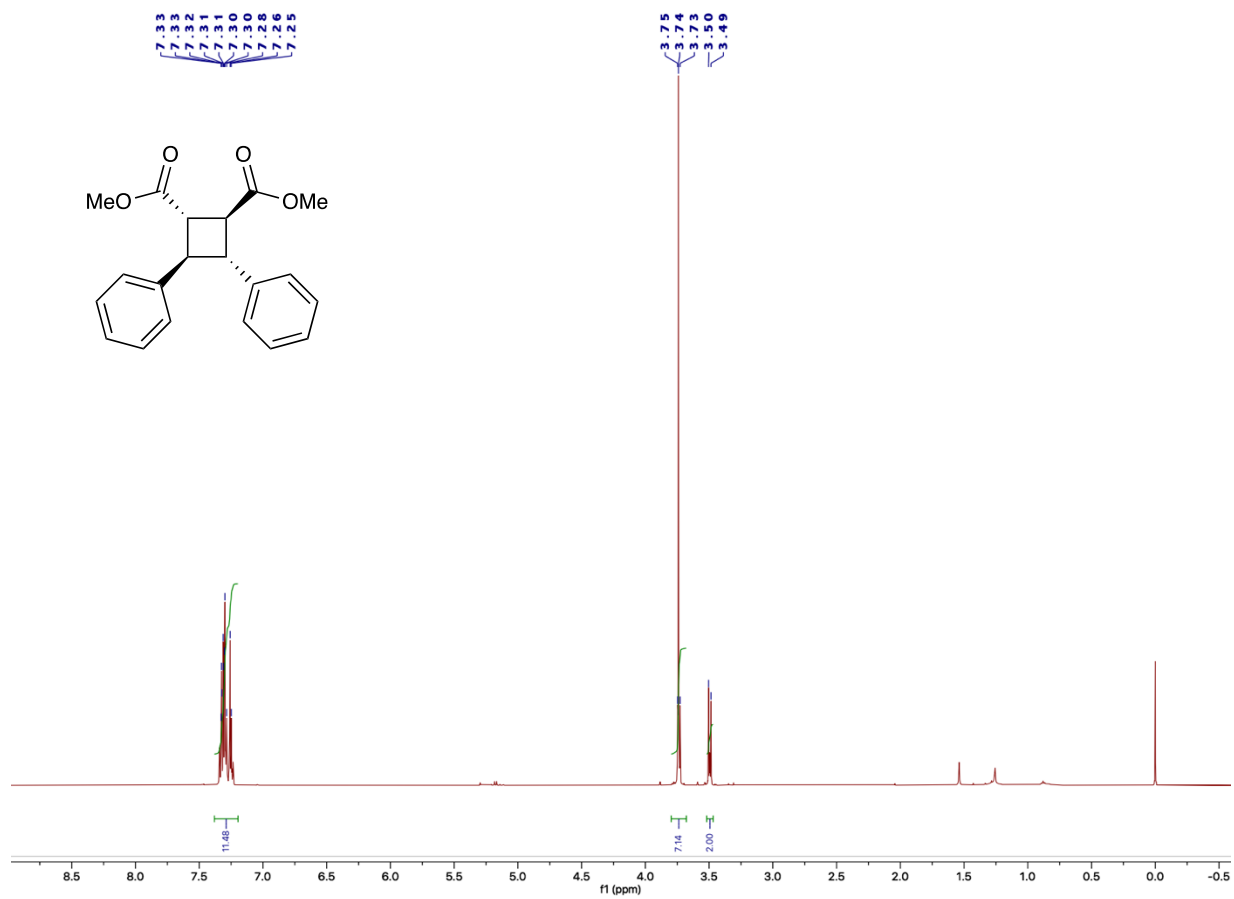


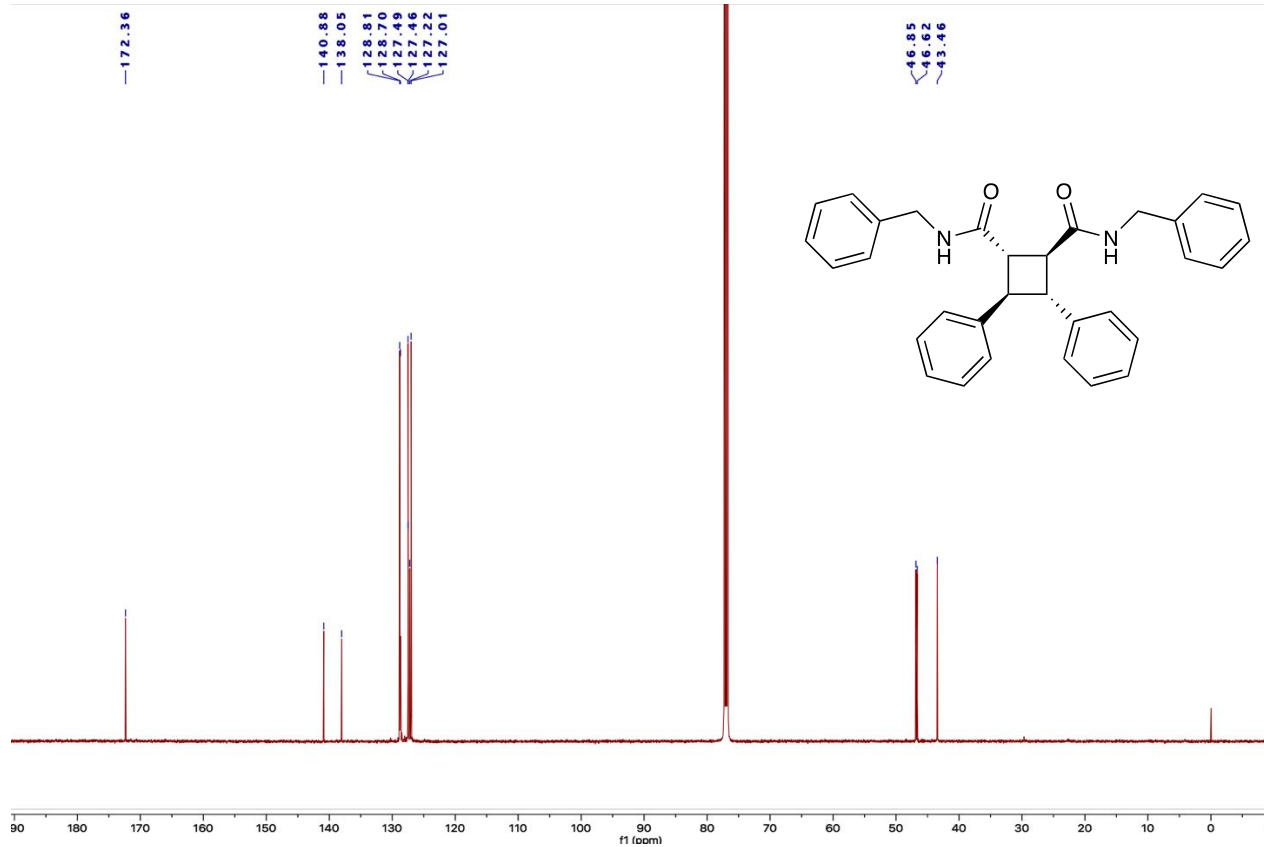
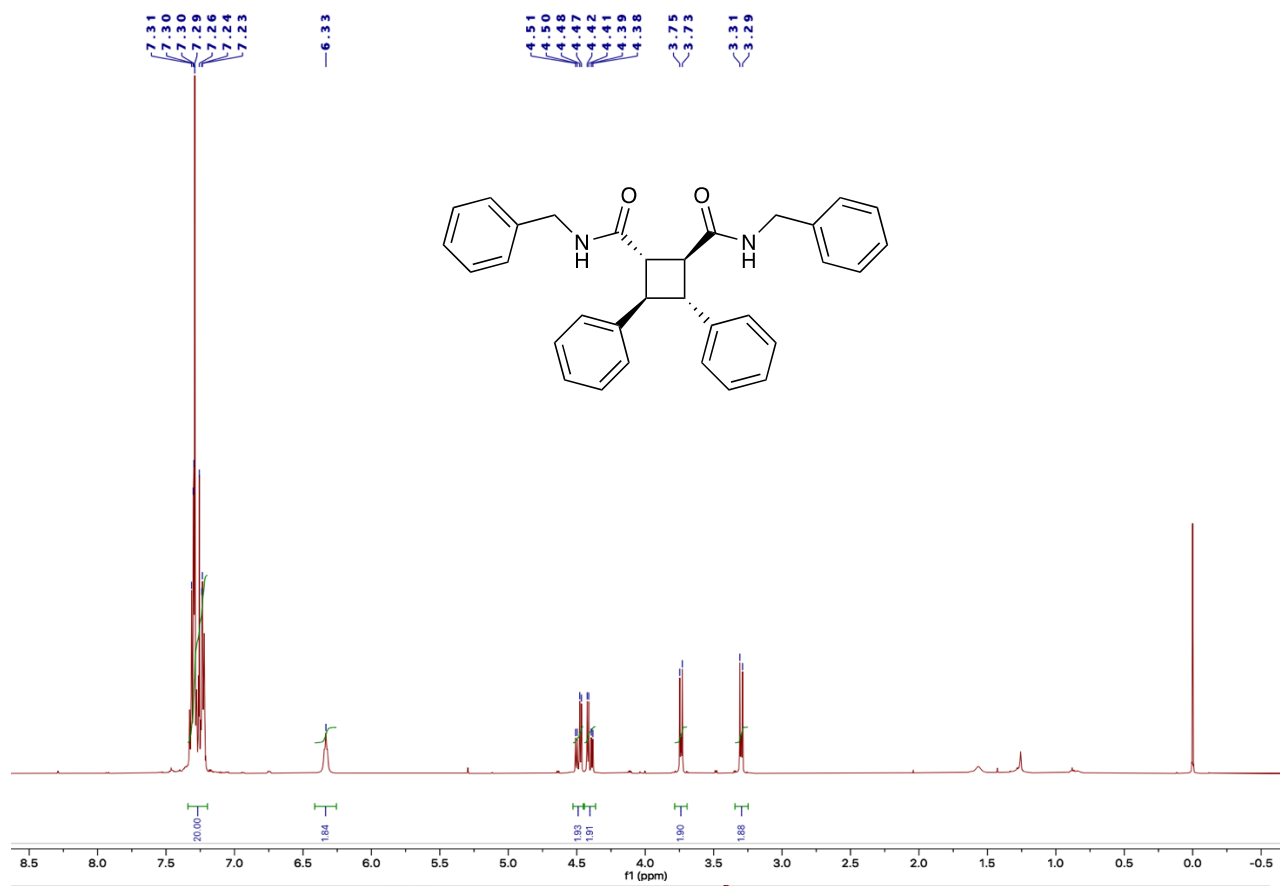


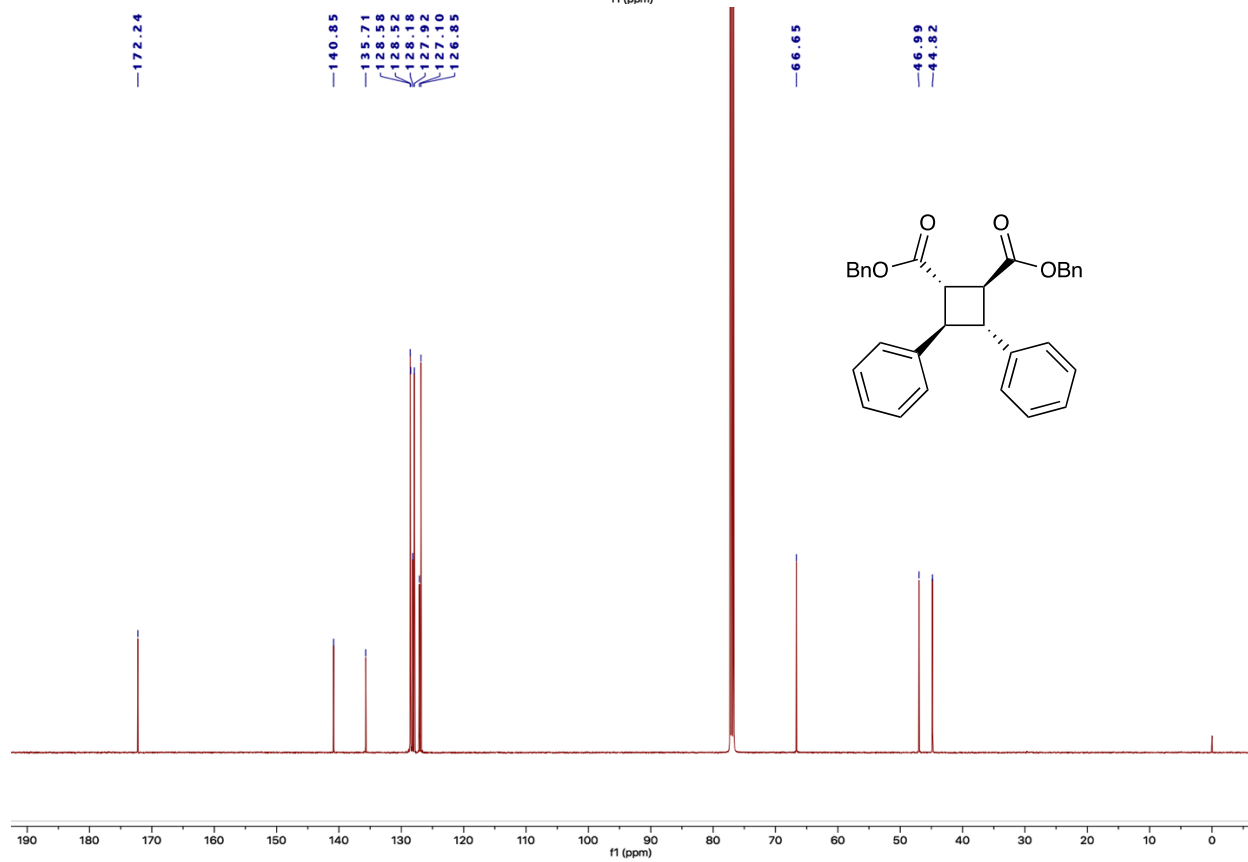


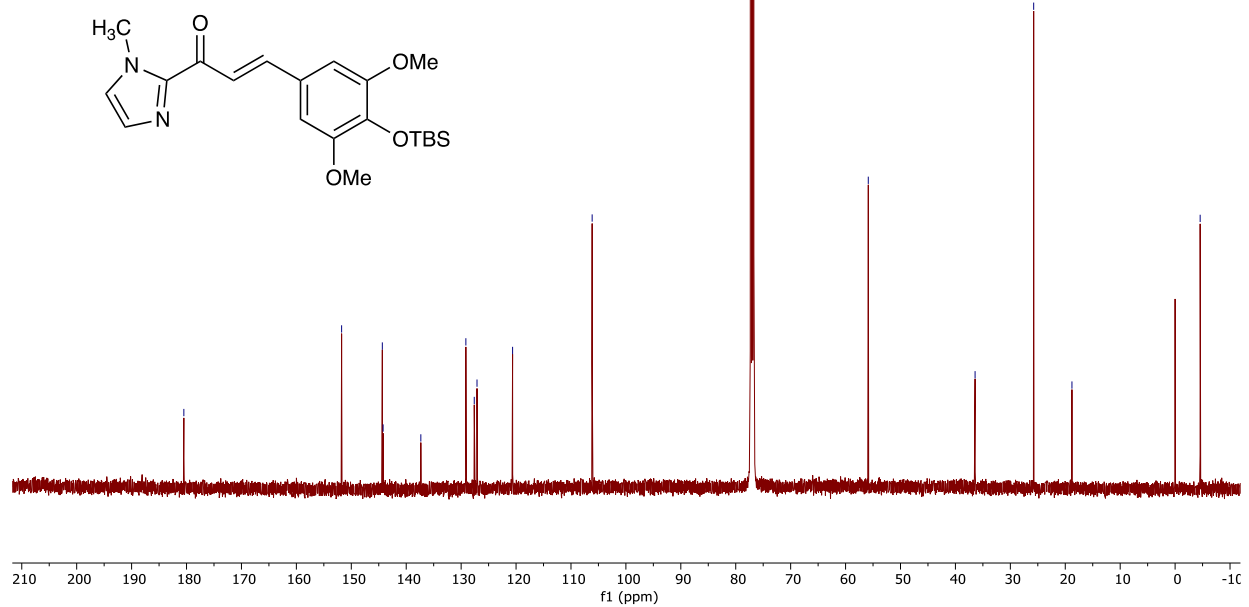
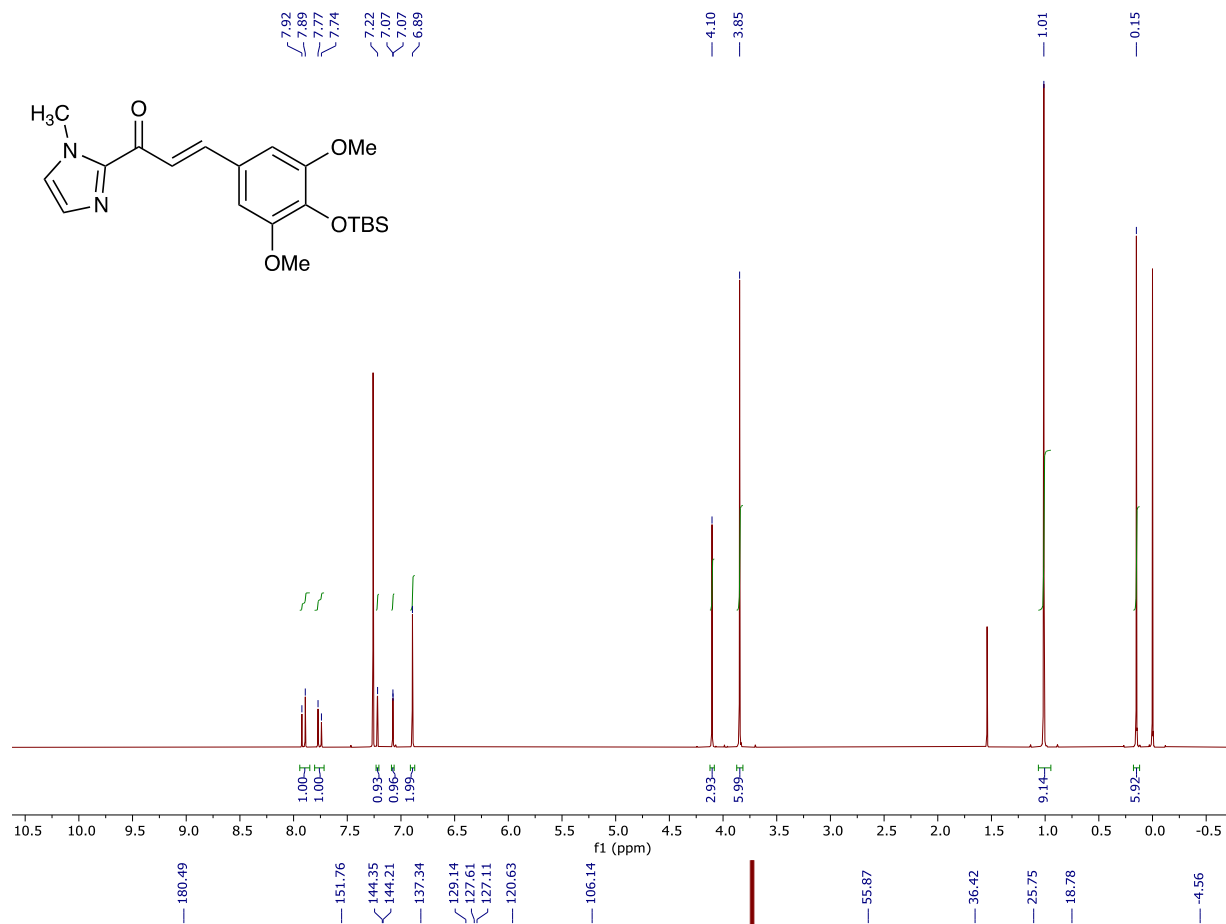


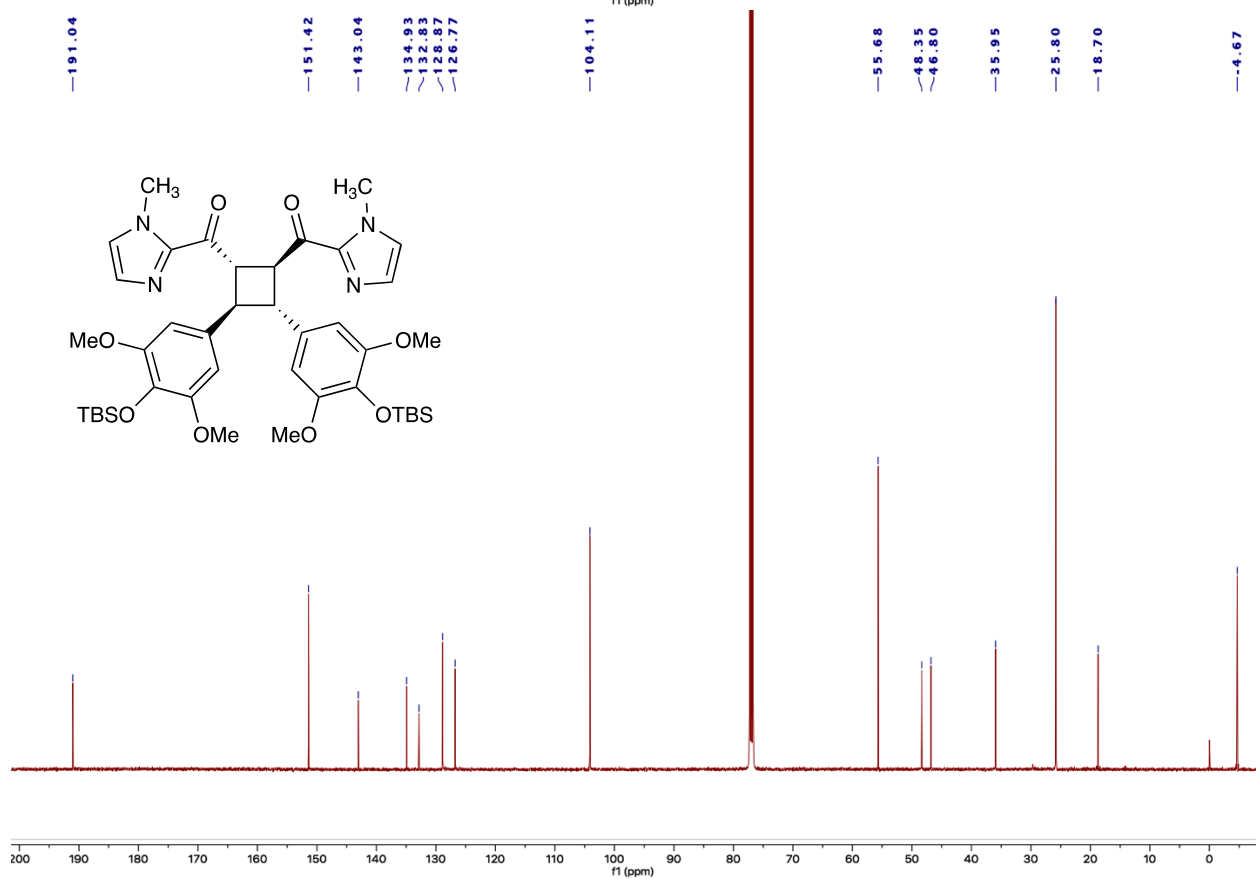
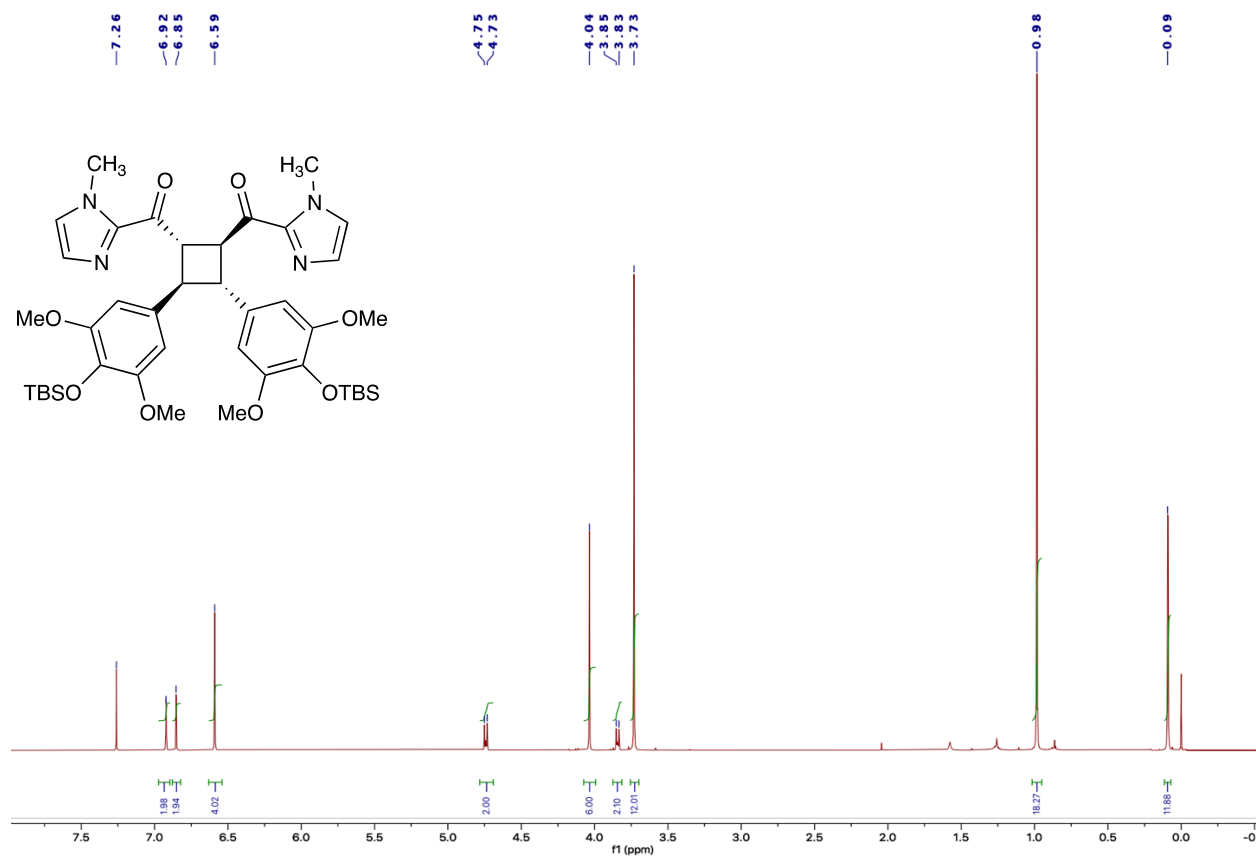


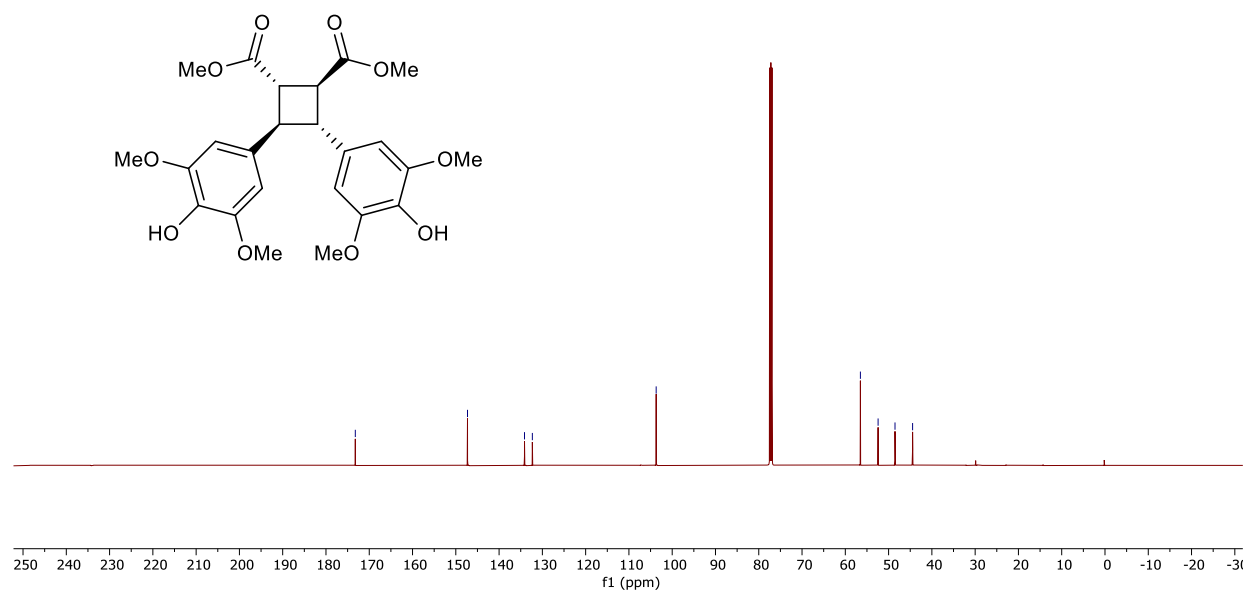
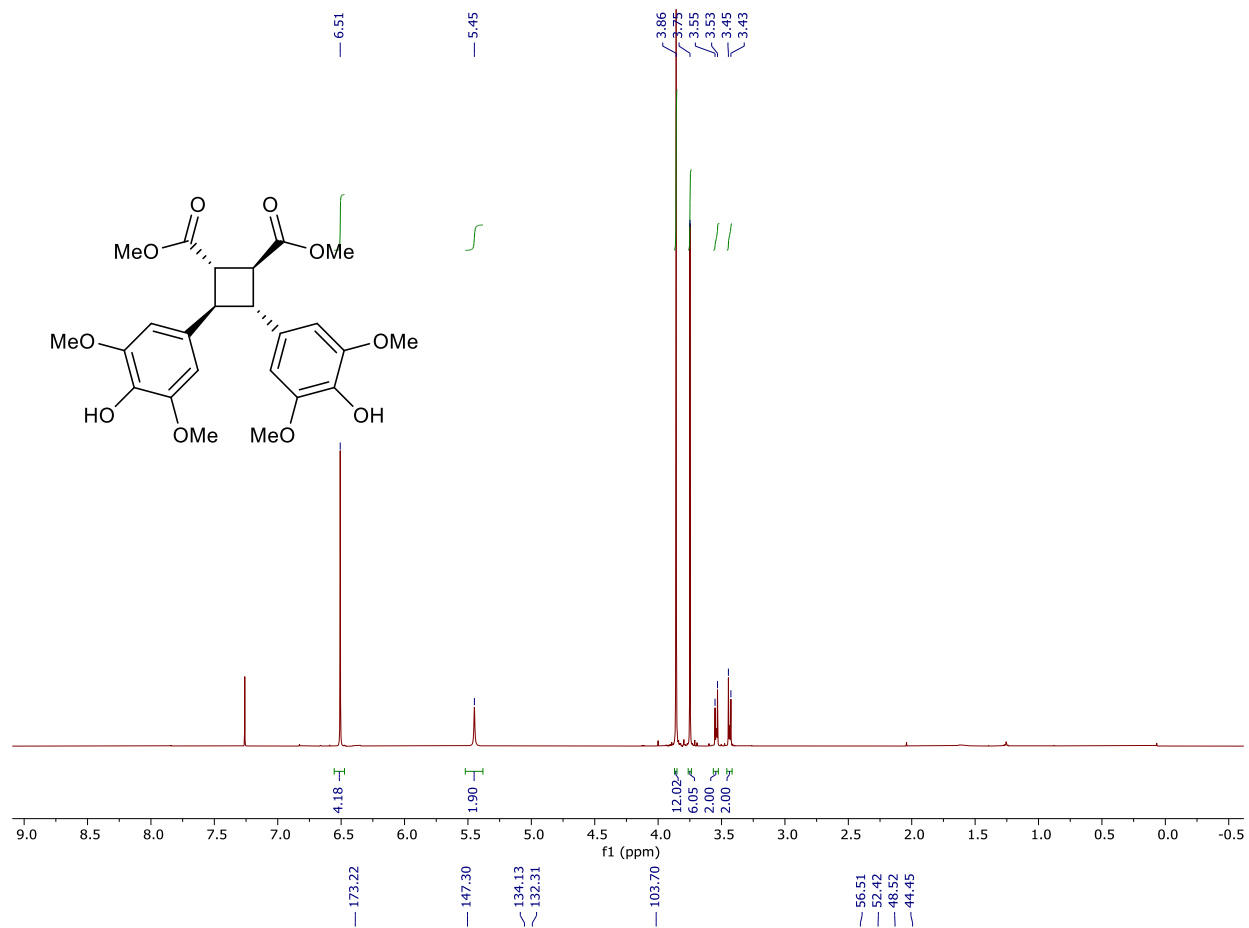


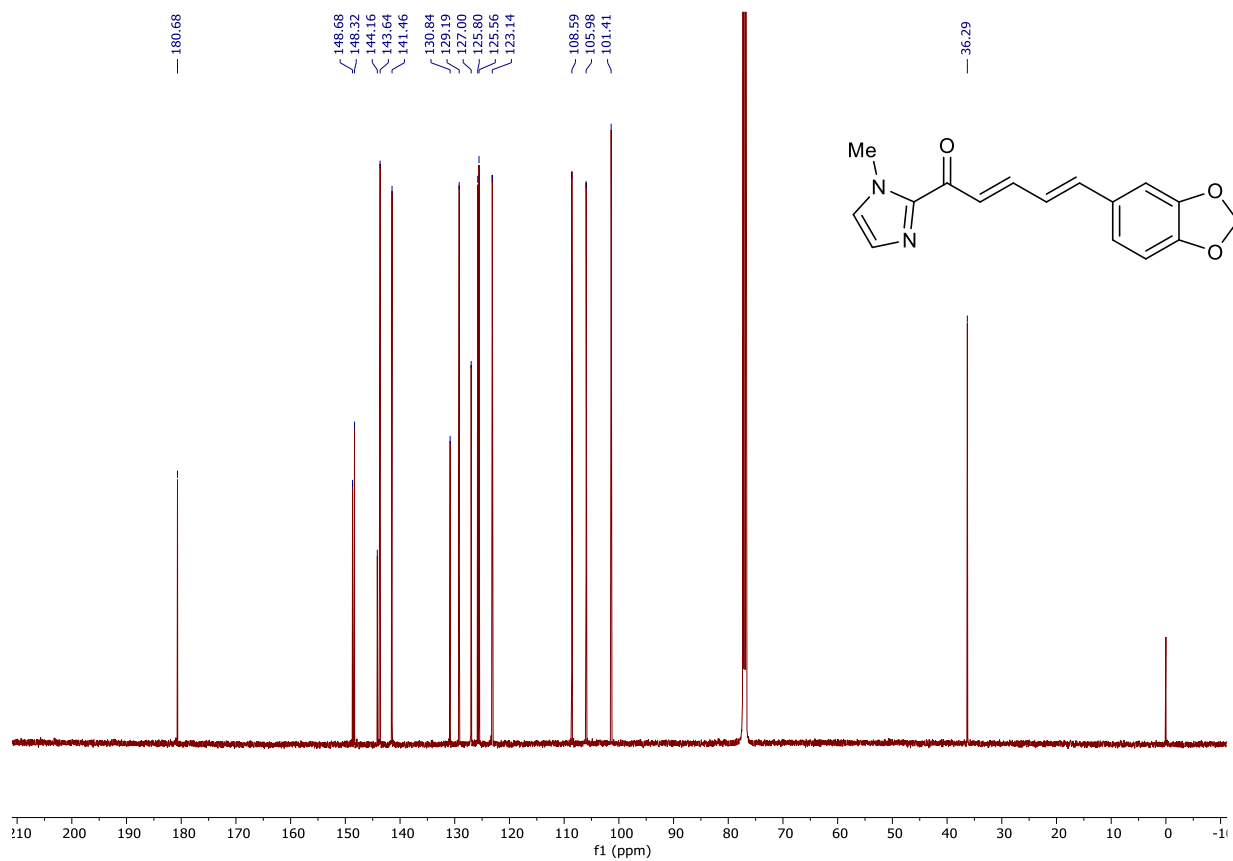
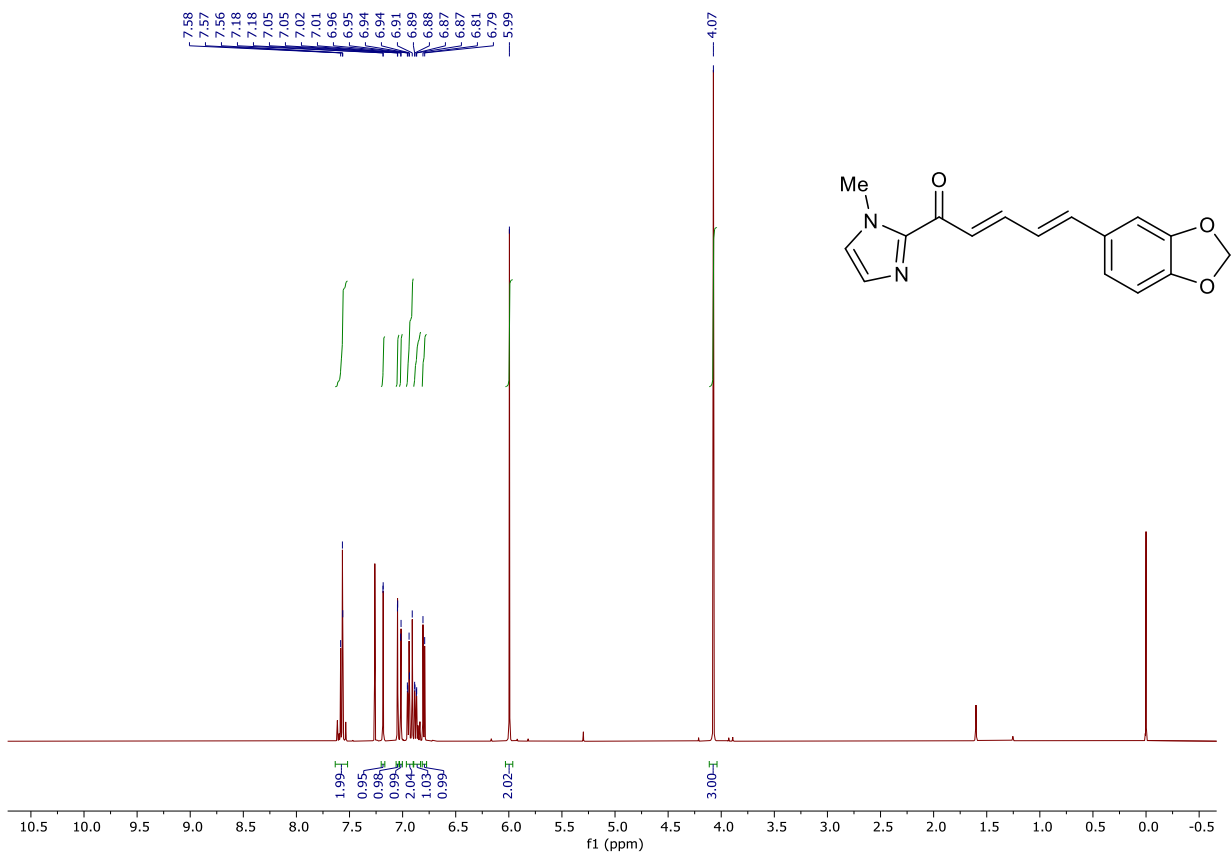


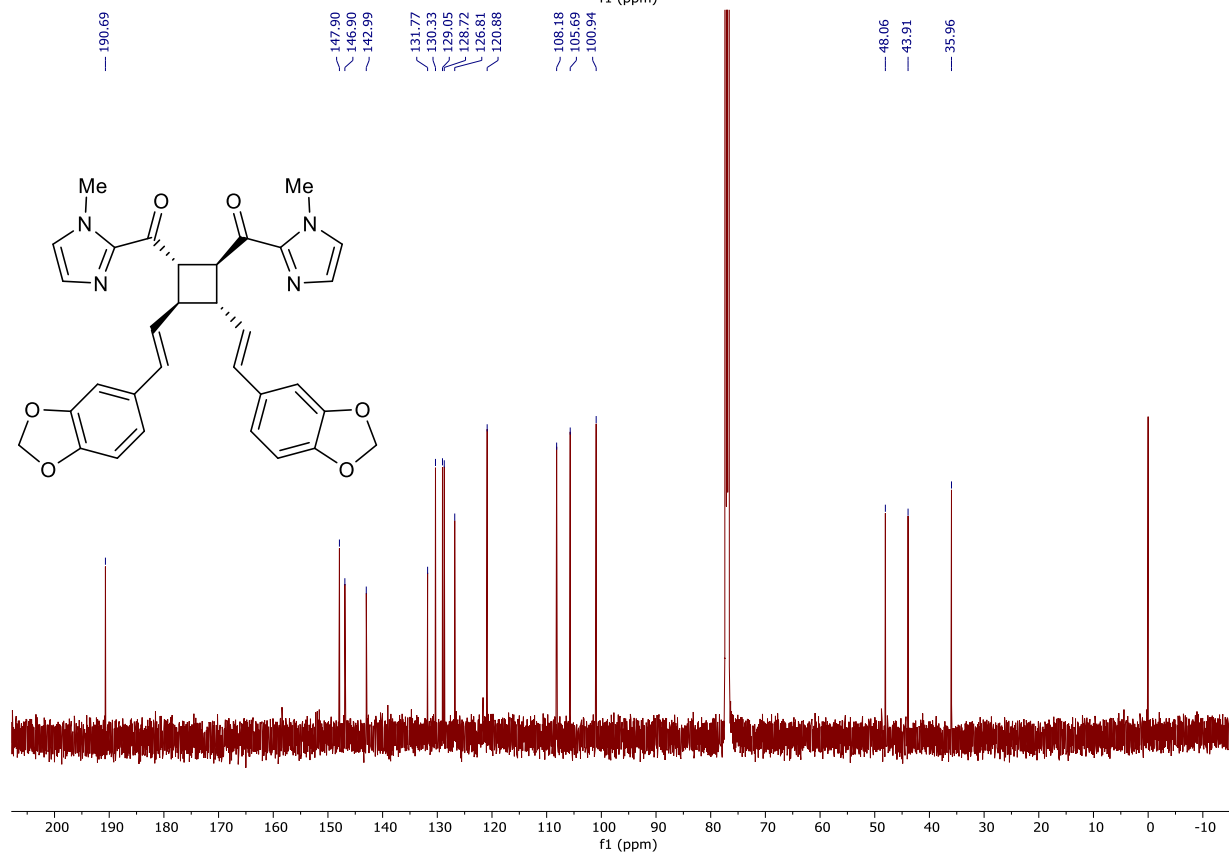
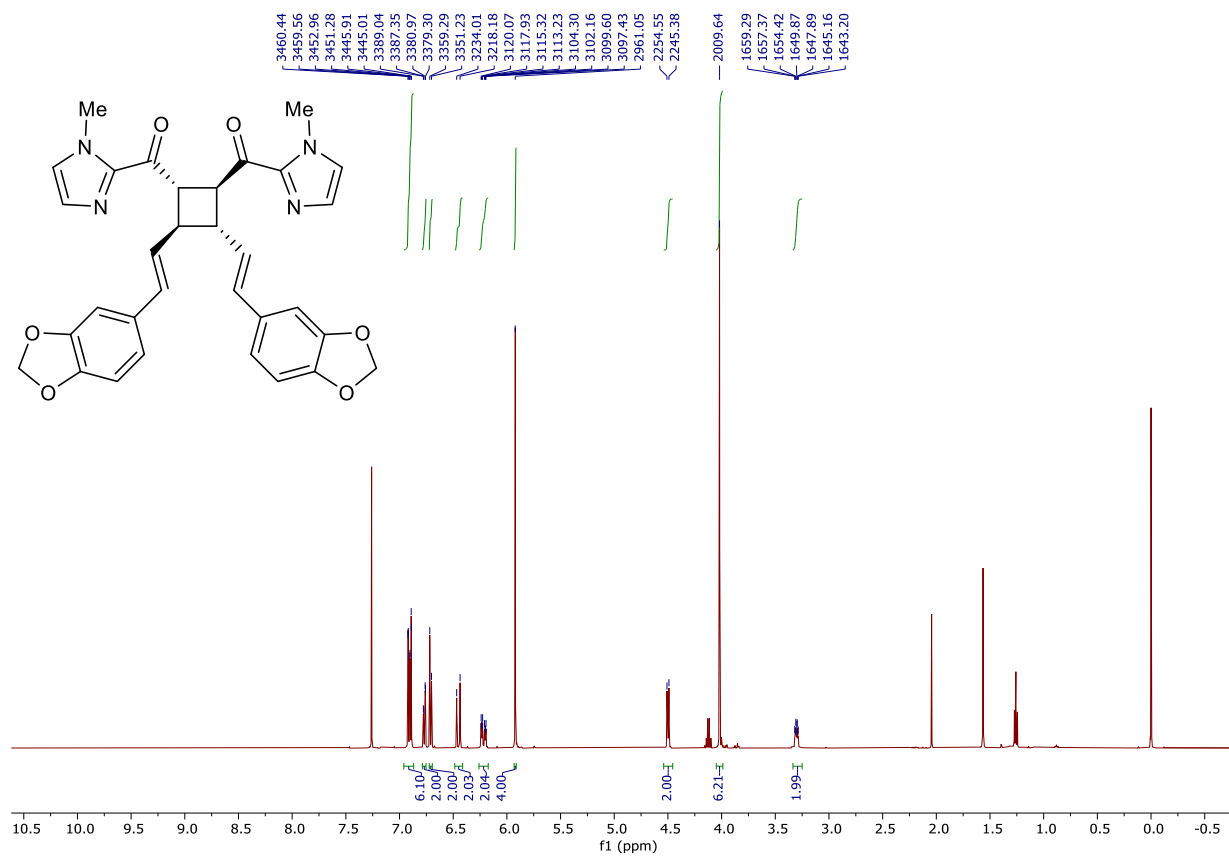


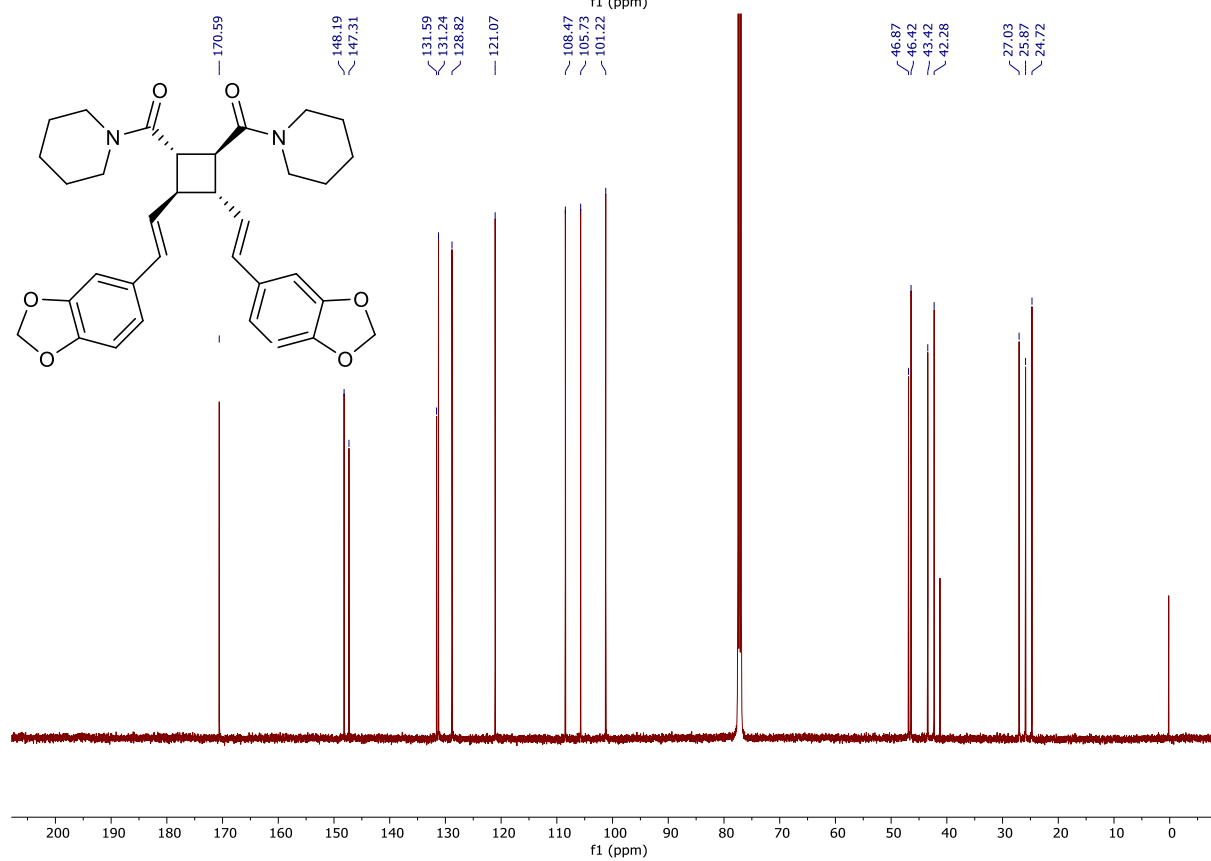
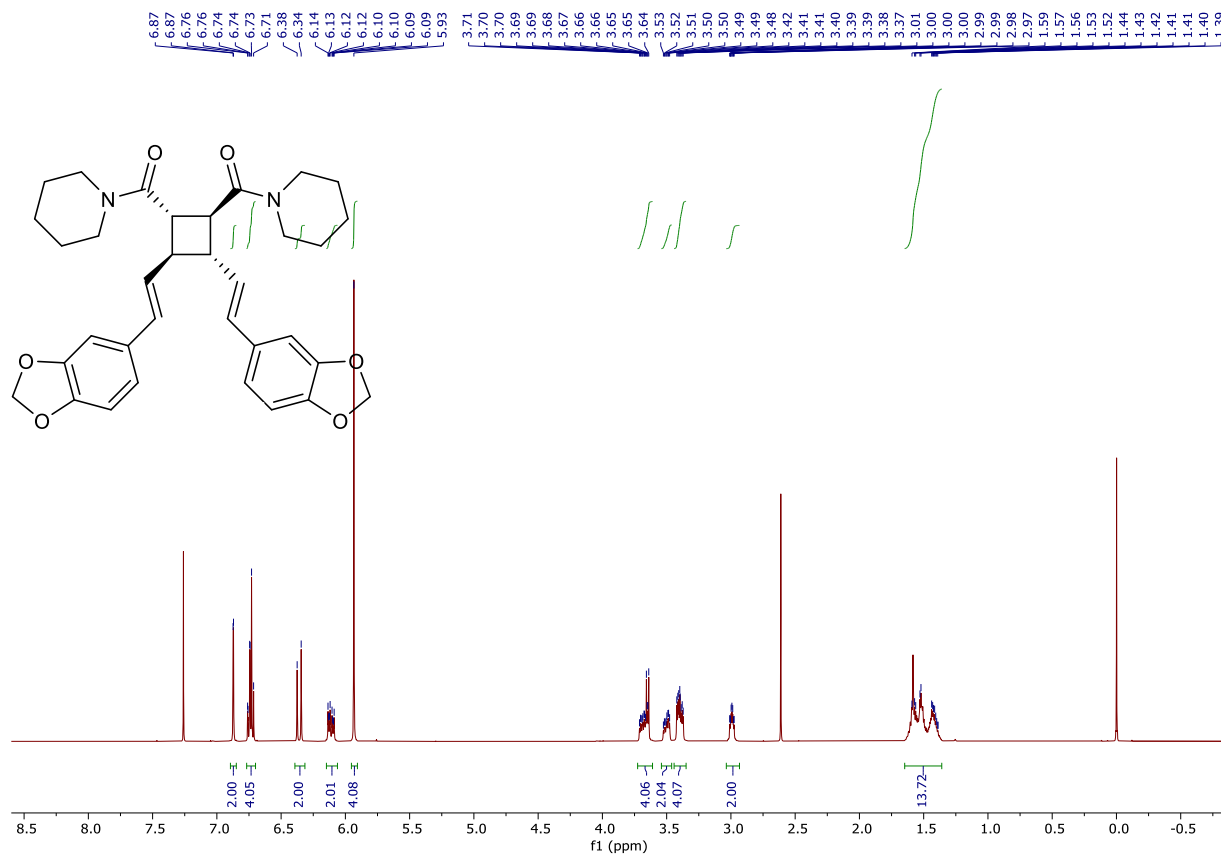


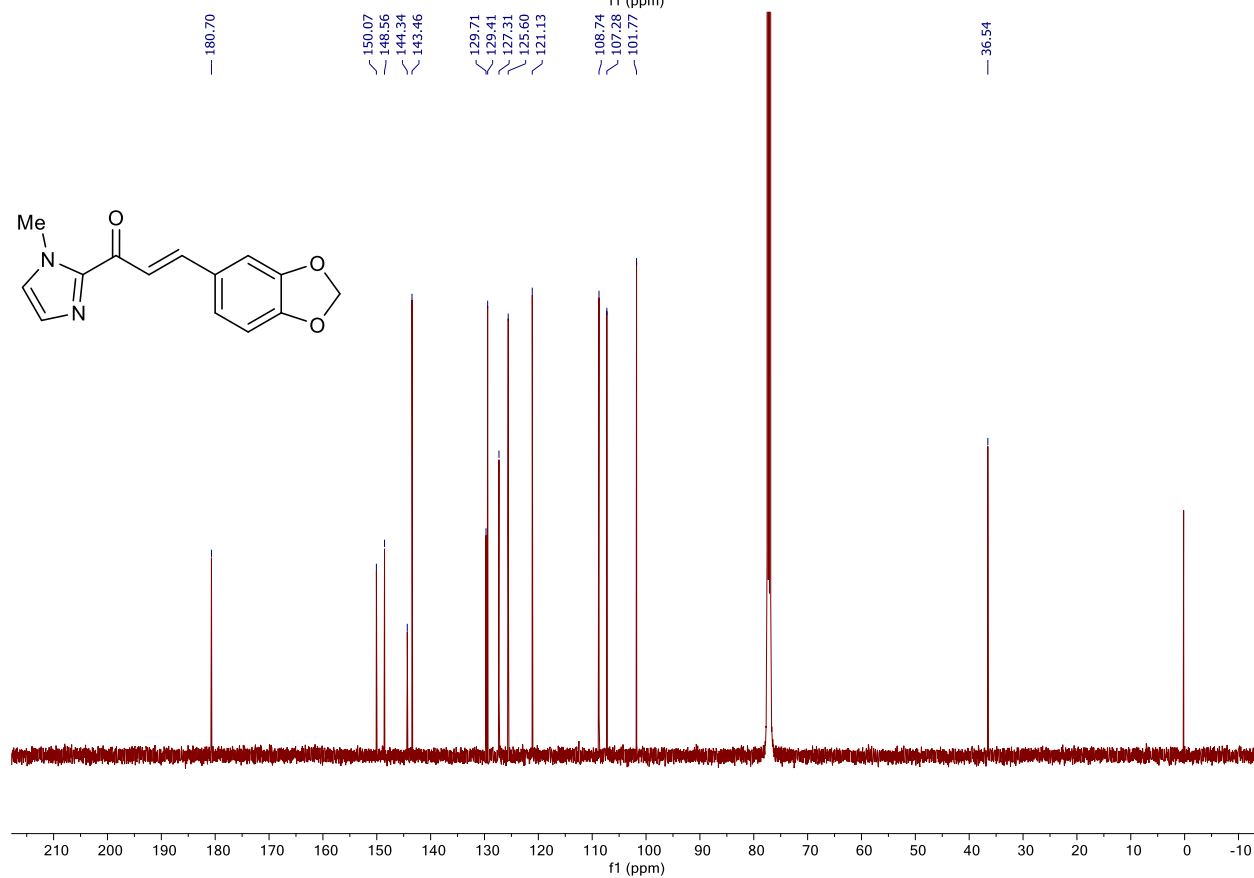
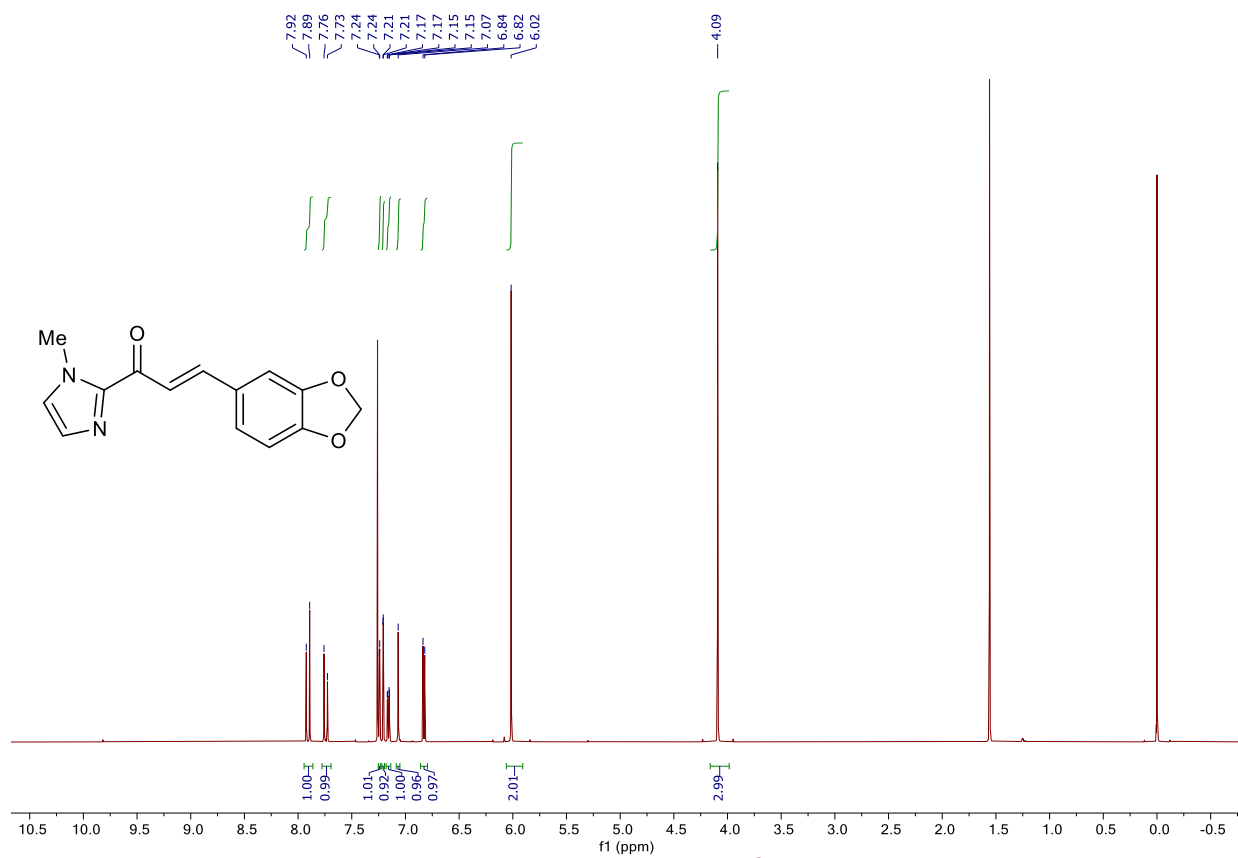


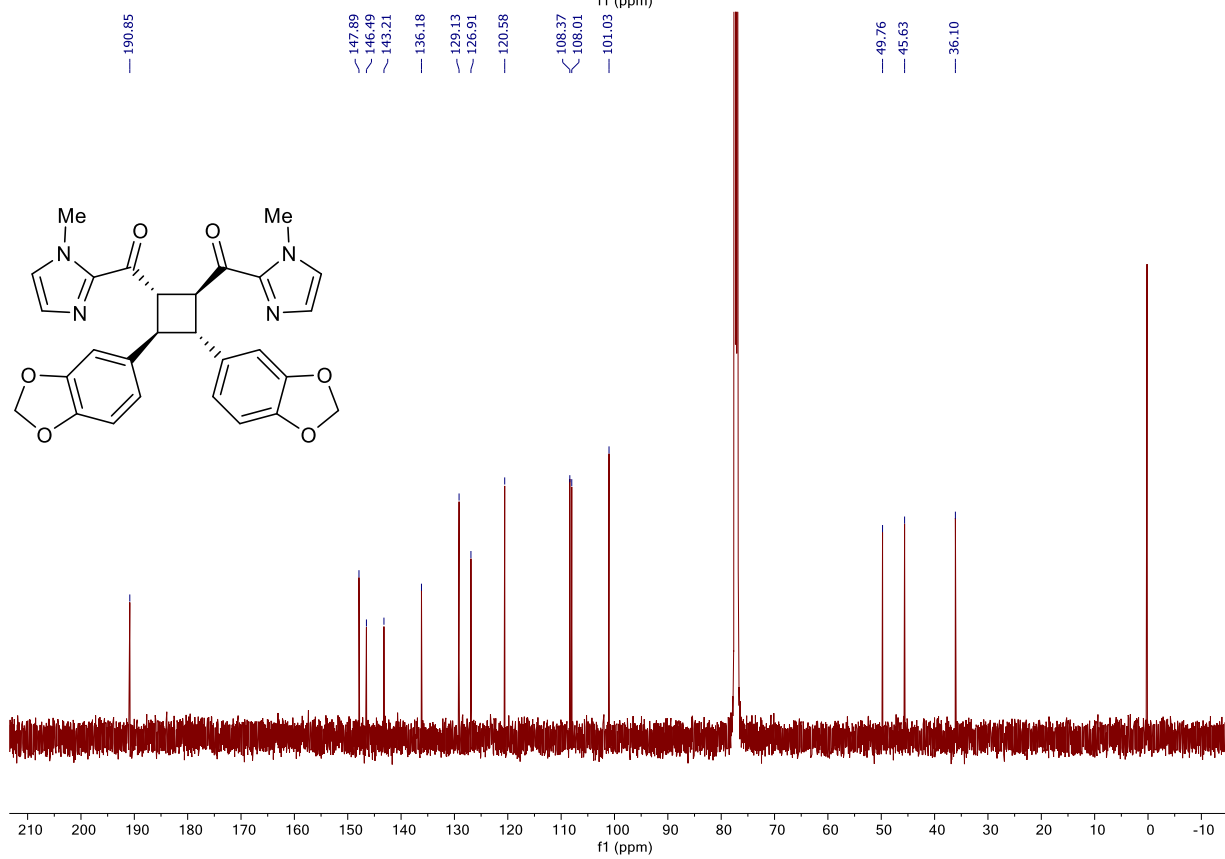
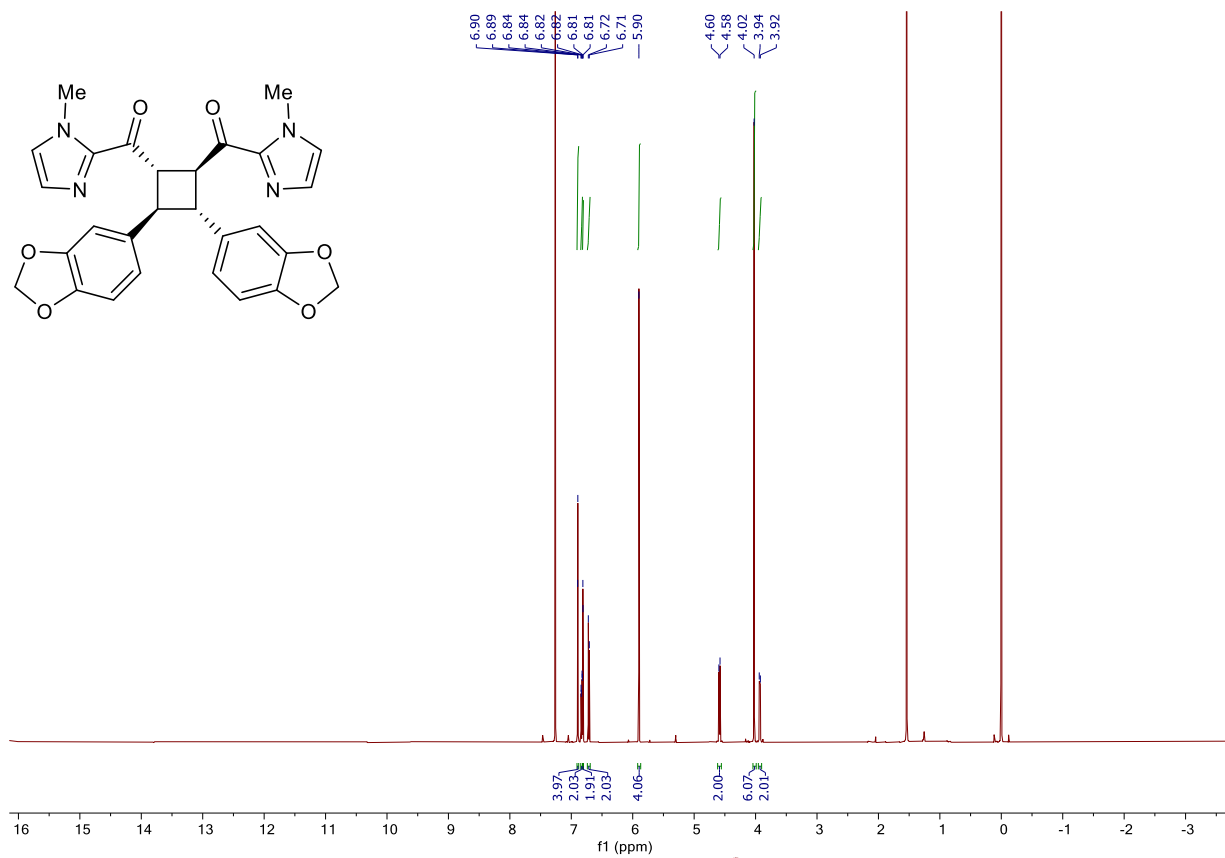


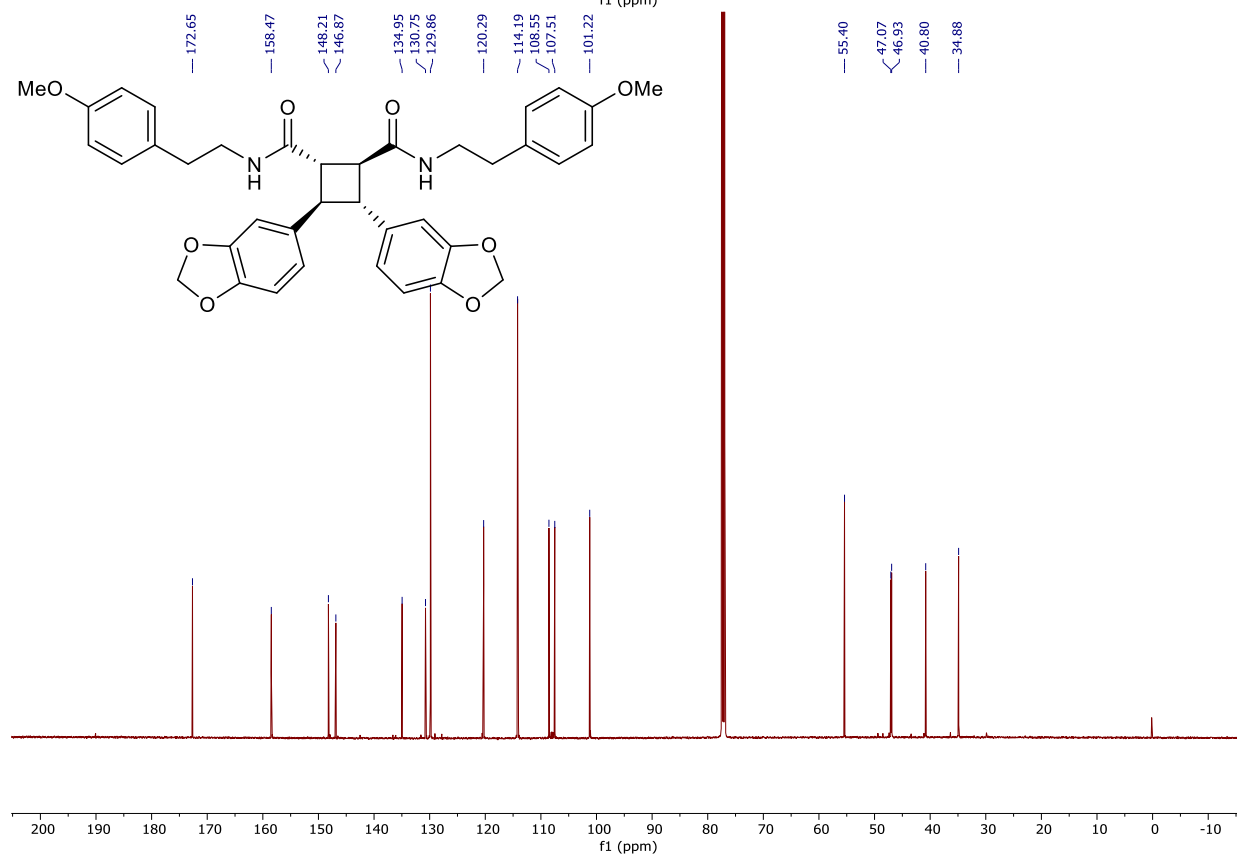
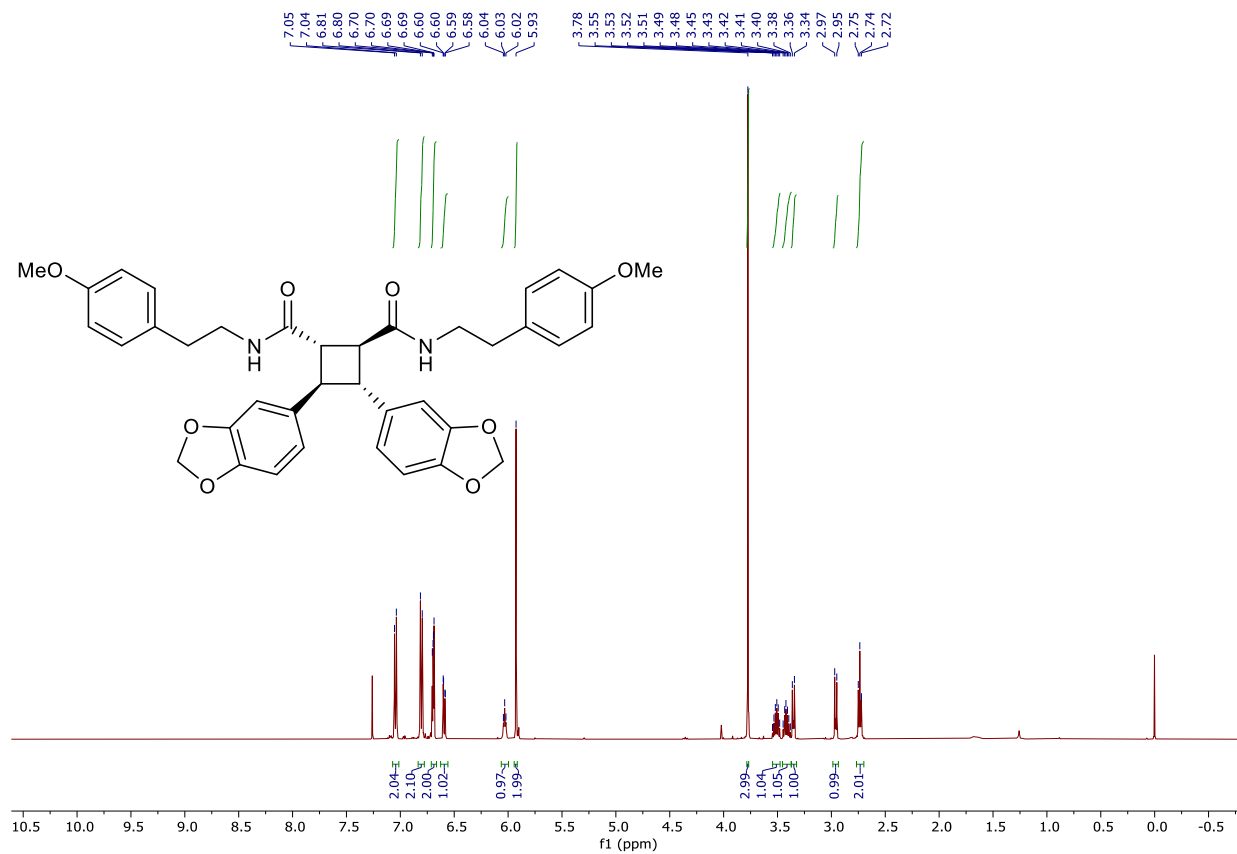


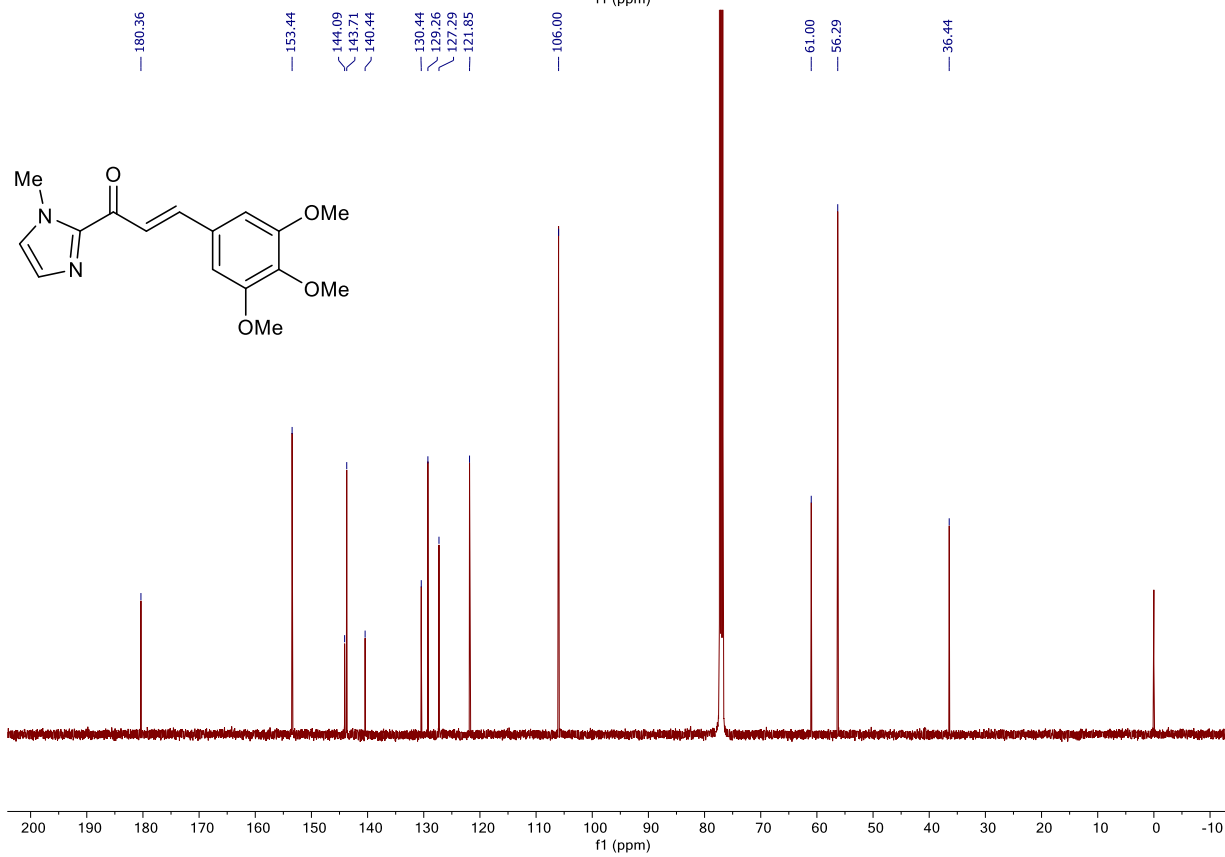
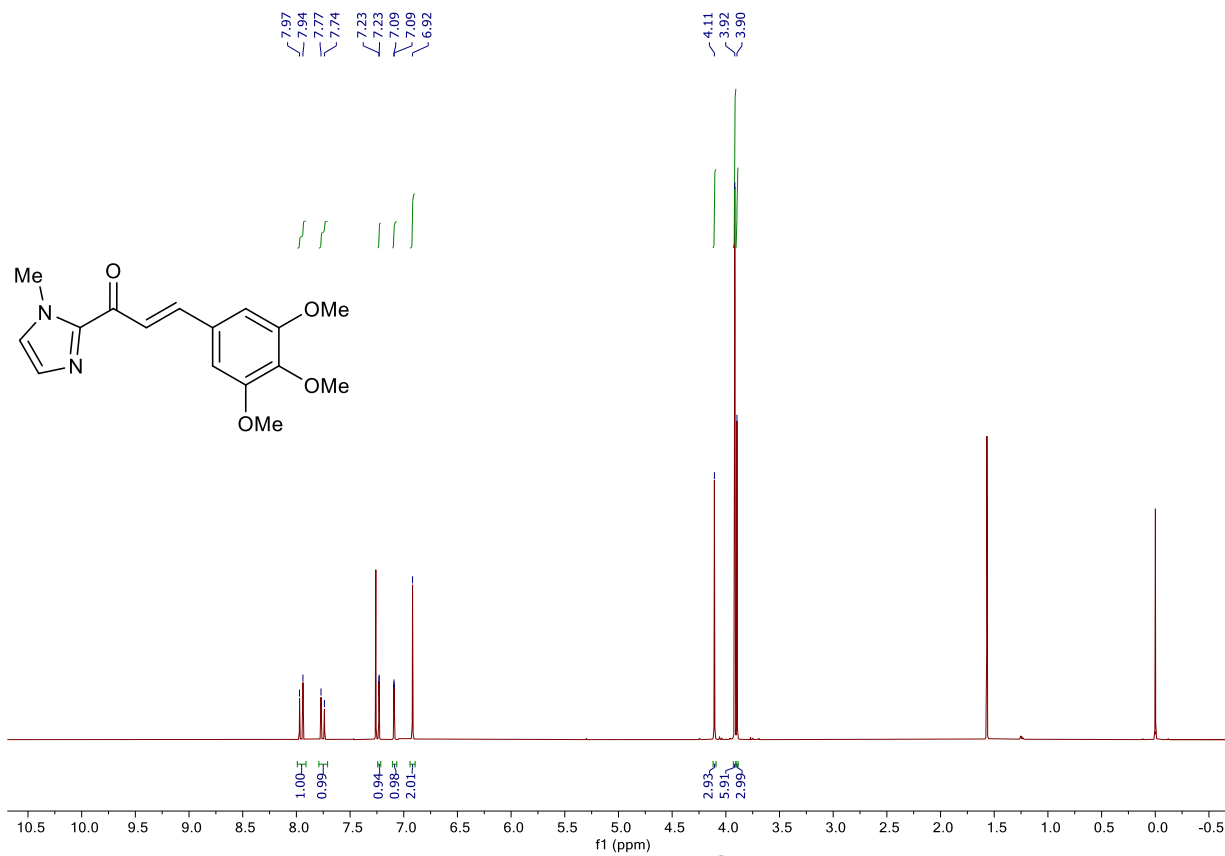


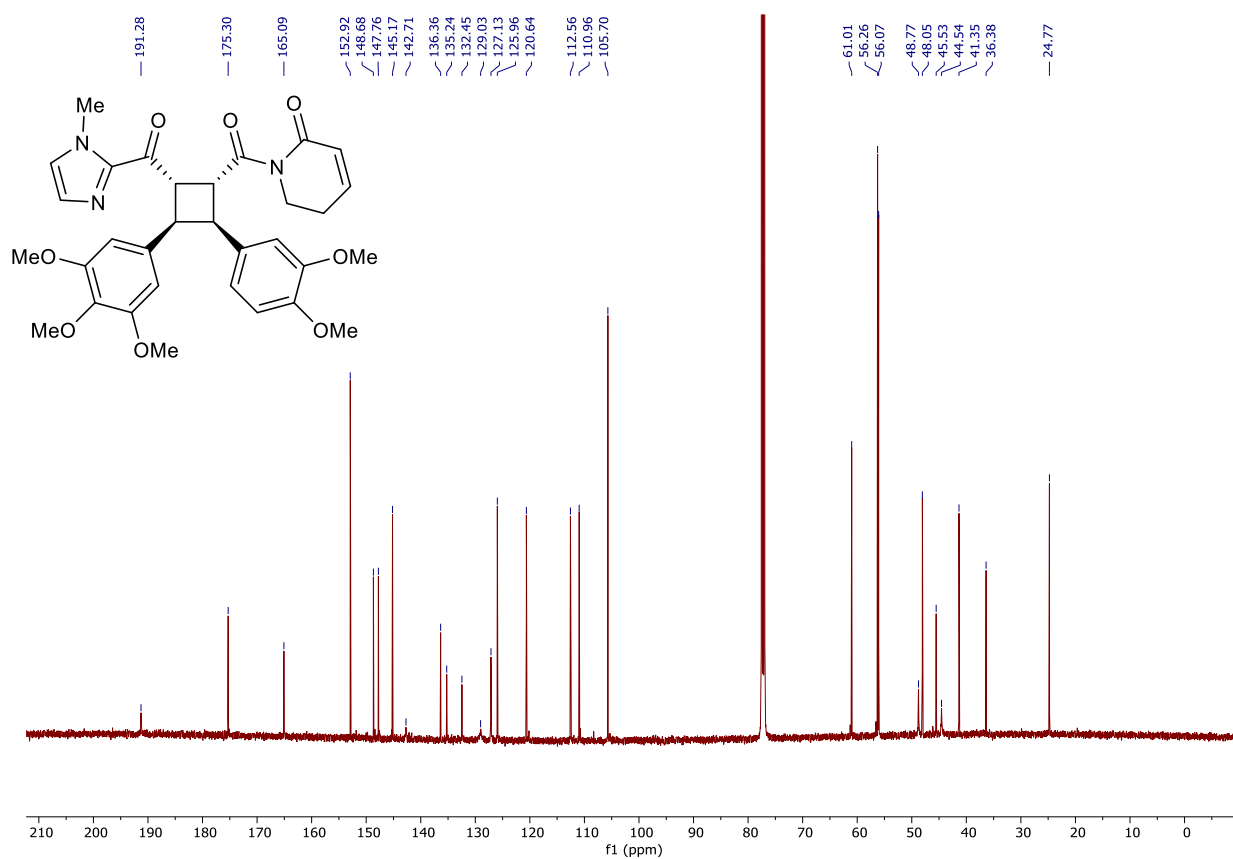
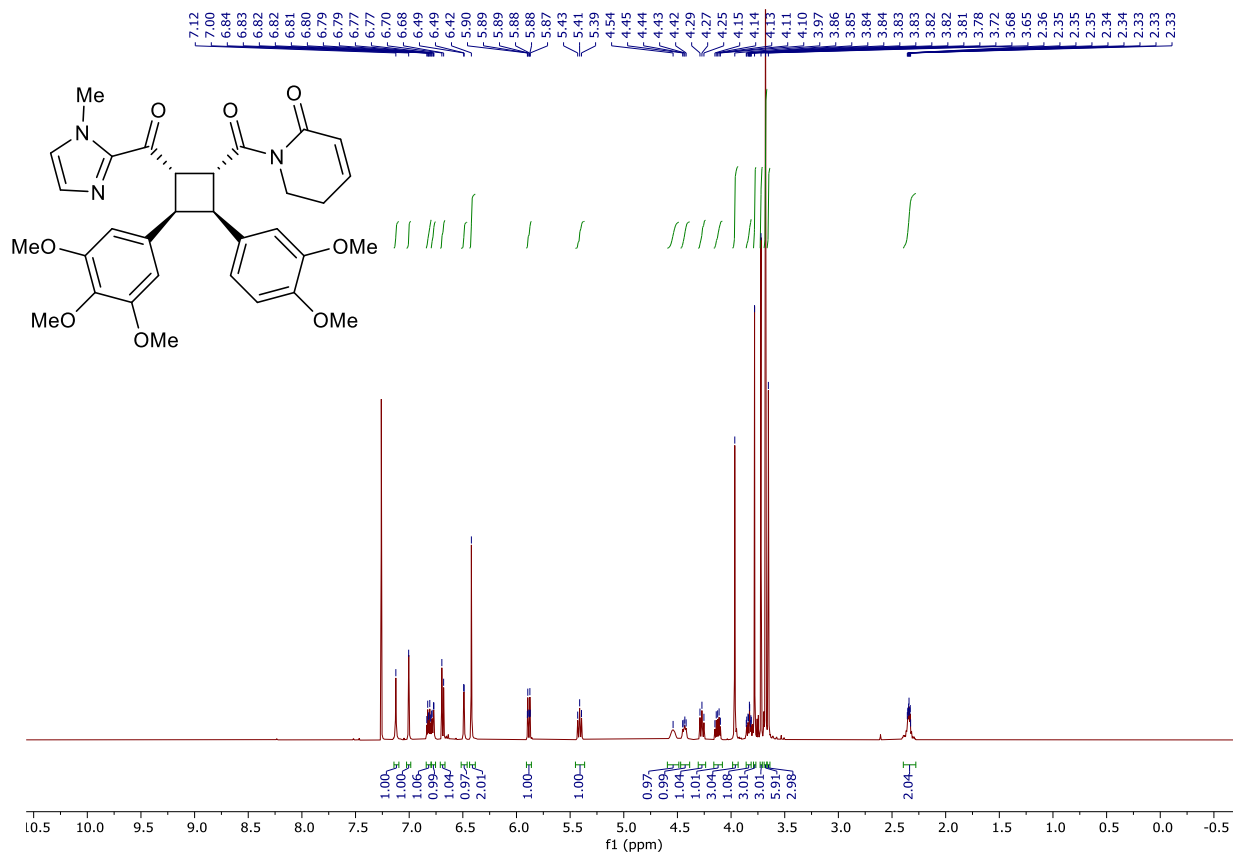


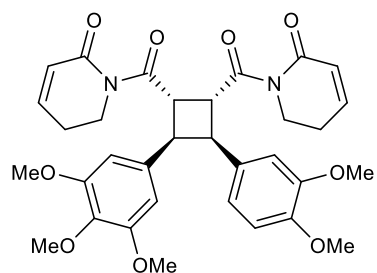
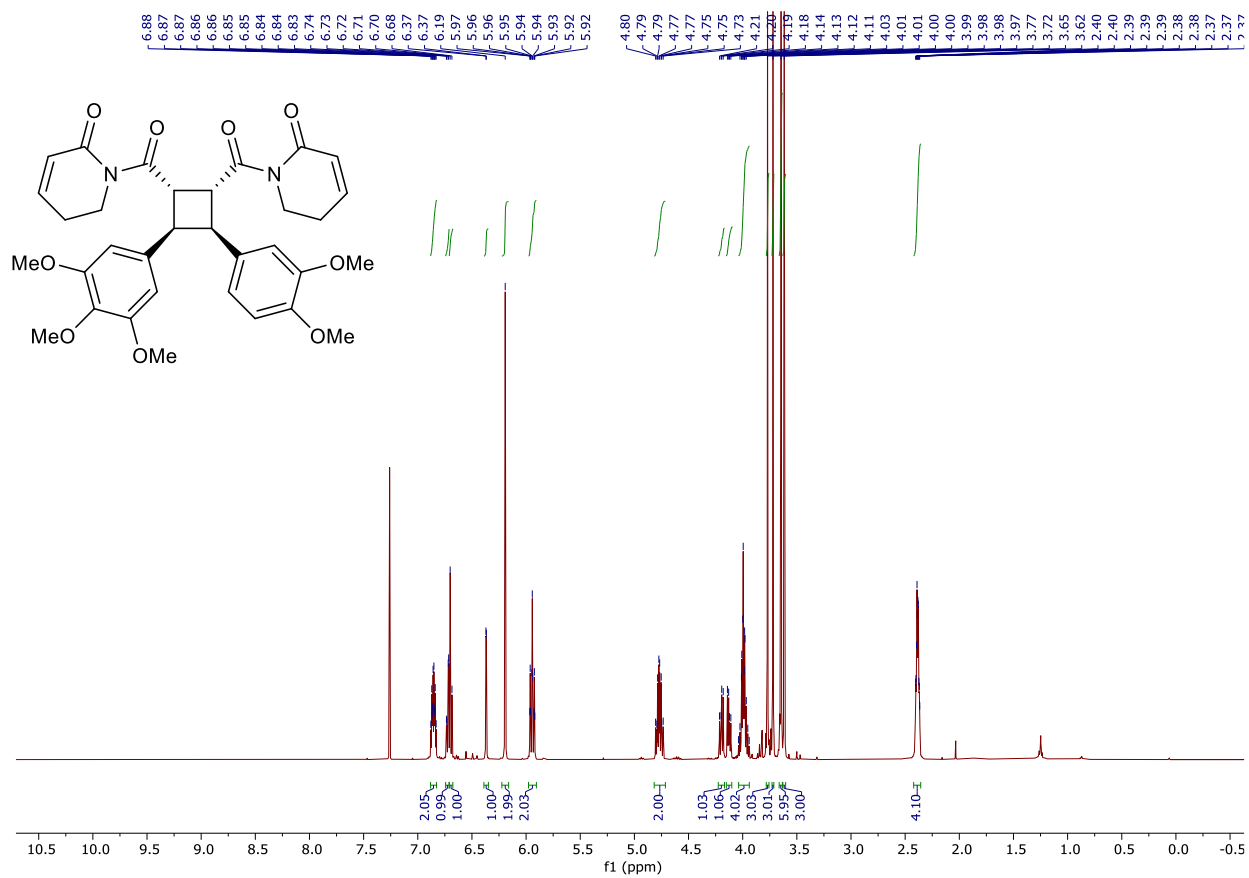


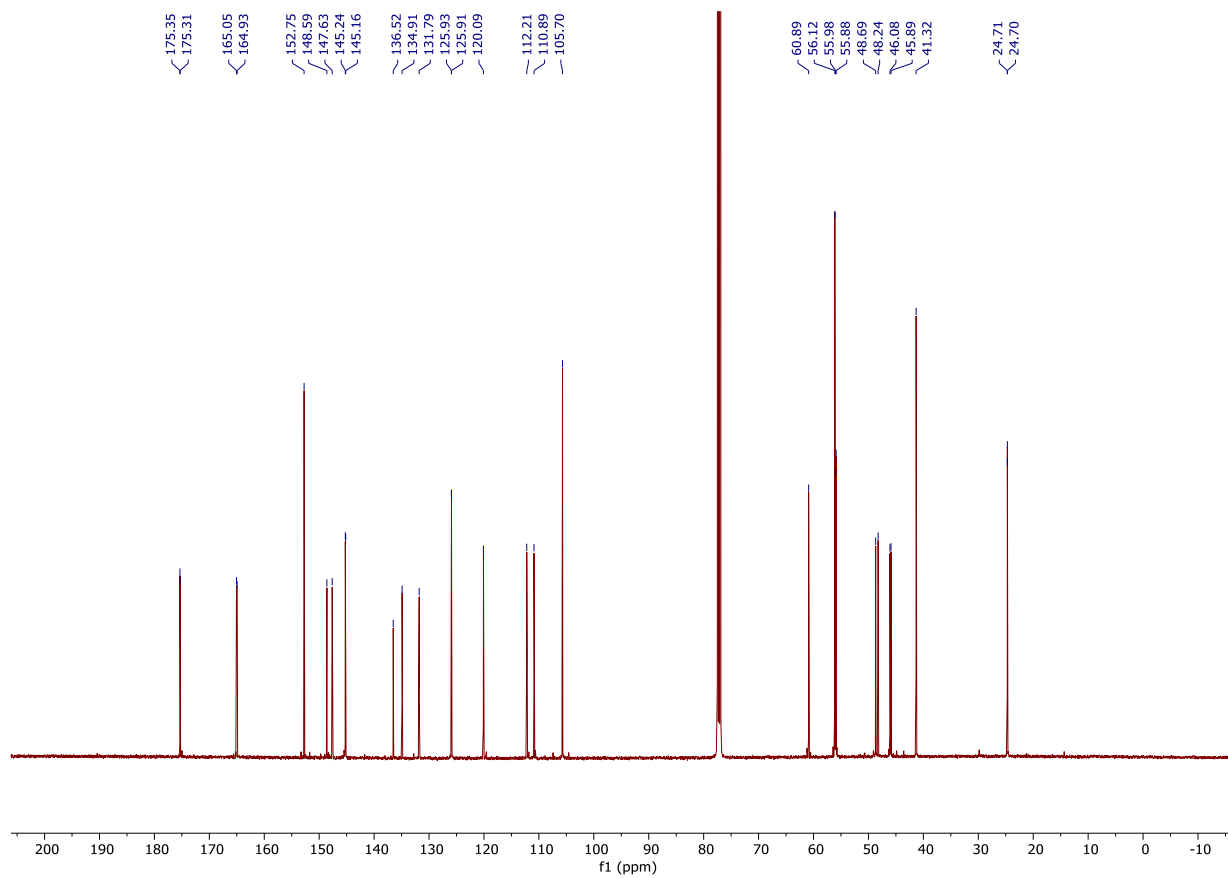












3.5.16 Comparison of Natural and Synthetic Natural Product NMR Spectra

Table 3.16 ^1H NMR Comparison between Synthetic and Natural Isatisycloneolignan A

Synthetic 3.20 (DMSO- d_6)	Natural 3.20 (DMSO- d_6)
8.24	8.29
6.58	6.58
3.73	3.73
3.66	3.66
3.49	3.48
3.32	3.32

Table 3.17 ^{13}C NMR Comparison between Synthetic and Natural Isatiscycloneolignan A

Synthetic 3.20 (DMSO- d_6)	Natural 3.20 (DMSO- d_6)
172.4	172.4
147.9	147.9
134.6	134.6
131.2	131.2
104.4	104.5
56.0	56.0
51.8	51.9
47.5	47.6
44.0	44.0

Table 3.18 ^1H NMR Comparison between Synthetic and Natural Nigramide R

Synthetic 3.28 (CDCl_3)	Natural 3.28 (CDCl_3)
6.87	6.87
6.75	6.75
6.72	6.72
6.36	6.36
6.11	6.11
5.93	5.93
3.68	3.68
3.65	3.66
3.50	3.51

3.40	3.40
2.99	2.99
1.59	1.59
1.52	1.53
1.44	1.44

Table 3.19 ^{13}C NMR Comparison between Synthetic and Natural Nigramide R

Synthetic 3.28 (CDCl_3)	Natural 3.28 (CDCl_3)
170.6	170.5
148.2	148.0
147.3	147.2
131.6	131.4
131.2	131.1
128.8	128.7
121.1	120.9
108.5	108.3
105.7	105.6
101.2	101.1
46.9	46.7
46.4	46.3
43.4	43.3
42.3	42.1
27.0	26.9

25.9	25.7
24.7	24.6

Table 3.20 ^1H NMR Comparison between Synthetic and Natural Barbarumamide C

Synthetic 3.22 (CDCl_3)	Natural 3.22 (CDCl_3)
7.05	7.05
6.81	6.81
6.69	6.69
6.59	6.59
6.03	6.02
5.93	5.93
3.78	3.78
3.55-3.48	3.54-3.47
3.45-3.38	3.45-3.38
3.35	3.35
2.96	2.95
2.74	2.74

Table 3.21 ^{13}C NMR Comparison between Synthetic and Natural Barbarumamide C

Synthetic 3.22 (CDCl_3)	Natural 3.22 (CDCl_3)
172.7	172.5
158.5	158.3
148.2	148.0

146.9	146.7
134.9	134.8
130.7	130.6
129.9	129.7
120.3	120.1
114.2	114.0
108.6	108.4
107.5	107.3
101.2	101.1
55.4	55.2
47.1	46.9
46.9	46.8
40.8	40.6
34.9	34.7

Table 3.22 ^1H NMR Comparison between Synthetic and Natural Piperarborenine D

Synthetic 3.47 (CDCl_3)	Natural 3.47 (CDCl_3)
6.86	6.88
6.84	6.85
6.72	6.74
6.69	6.70
6.37	6.38
6.19	6.20

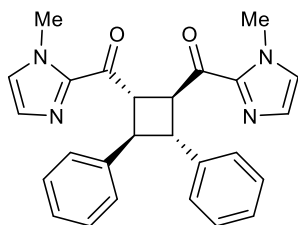
5.94	5.94
4.79	4.80
4.75	4.75
4.19	4.20
4.13	4.13
4.01	4.01
3.99	3.99
3.77	3.78
3.72	3.73
3.65	3.66
3.62	3.63
2.39	2.40

Table 3.23 ^{13}C NMR Comparison between Synthetic and Natural Piperarborenine D

Synthetic 3.47 (CDCl_3)	Natural 3.47 (CDCl_3)
175.4	175.2
175.3	175.1
165.1	164.9
164.9	164.8
152.8	152.6
148.6	148.4
147.6	147.4
145.2	145.1

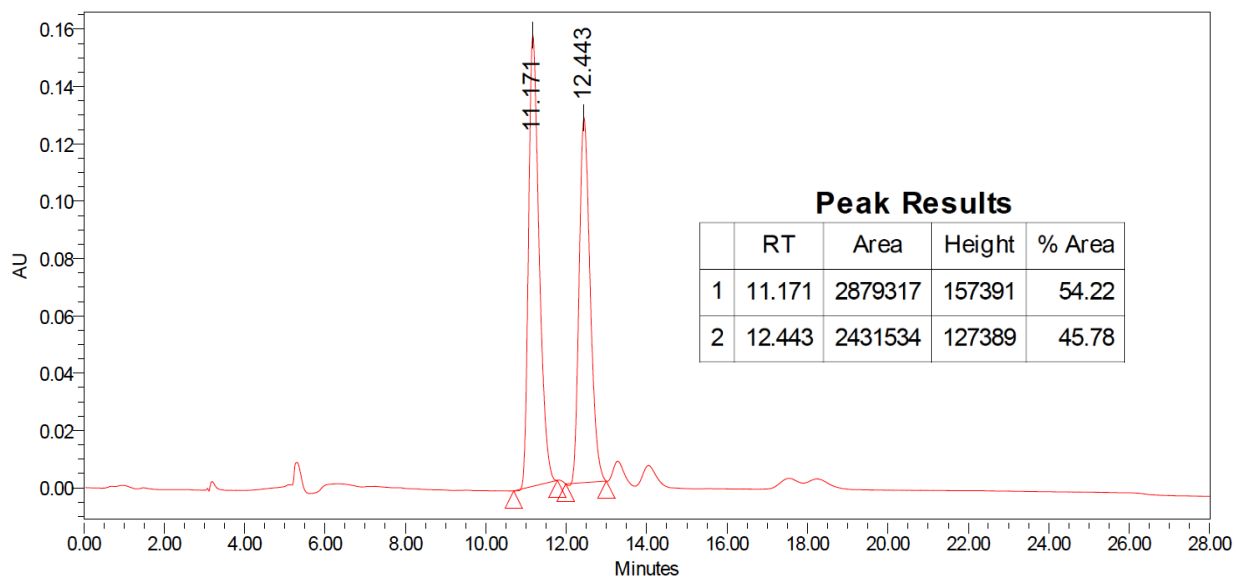
145.2	145.0
136.5	136.3
134.9	134.7
131.8	131.6
125.9	125.7
125.9	125.7
120.1	119.9
112.2	112.0
110.9	110.7
105.7	105.5
60.9	60.7
56.1	56.1
56.1	55.9
56.0	55.8
55.9	55.7
48.7	48.5
48.2	48.1
46.1	45.9
45.9	45.7
41.3	41.1
24.7	24.5
24.7	24.5

3.5.17 HPLC Data

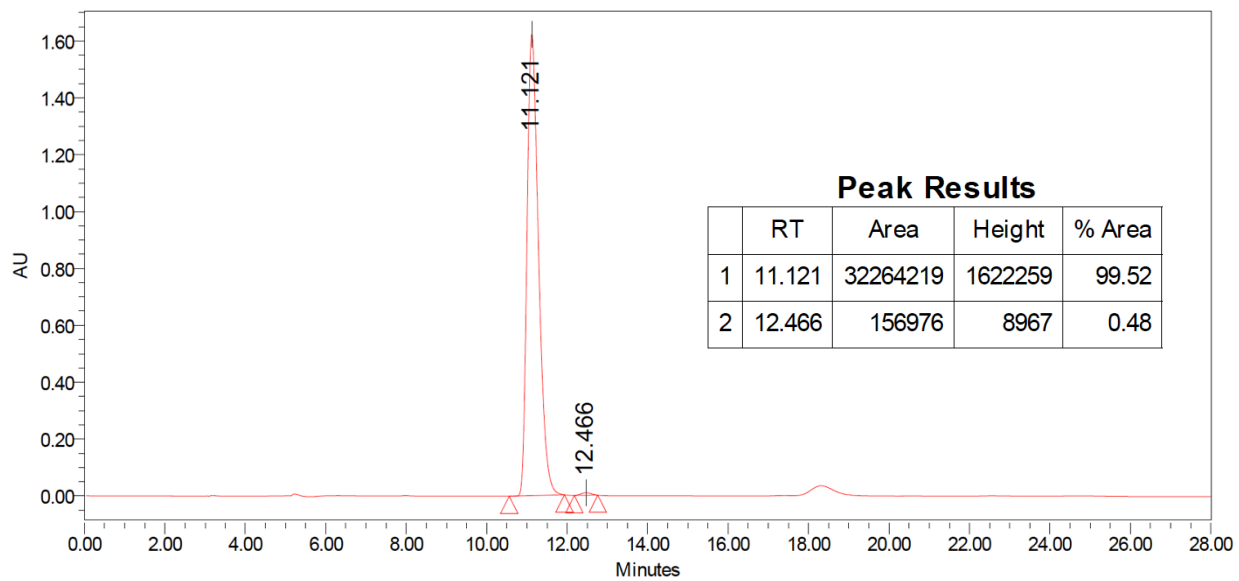


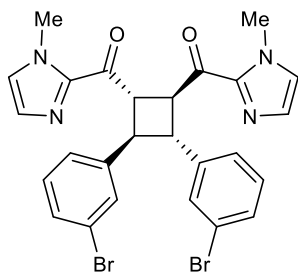
Major Diastereomer
Run Details: HPLC, Daicel CHIRALPAK AS-H,
5.00 μ L, gradient 5% to 50% iPrOH/hexanes,
28 minutes, 1 mL/min, 283 nm.

Racemic Chromatogram



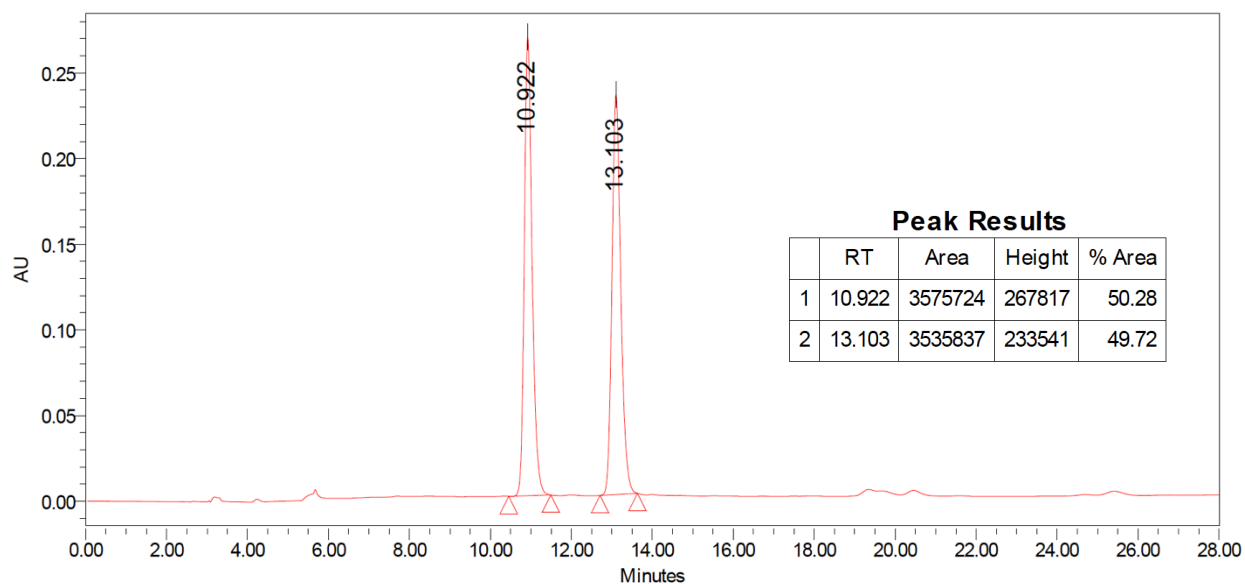
Scalemic Chromatogram



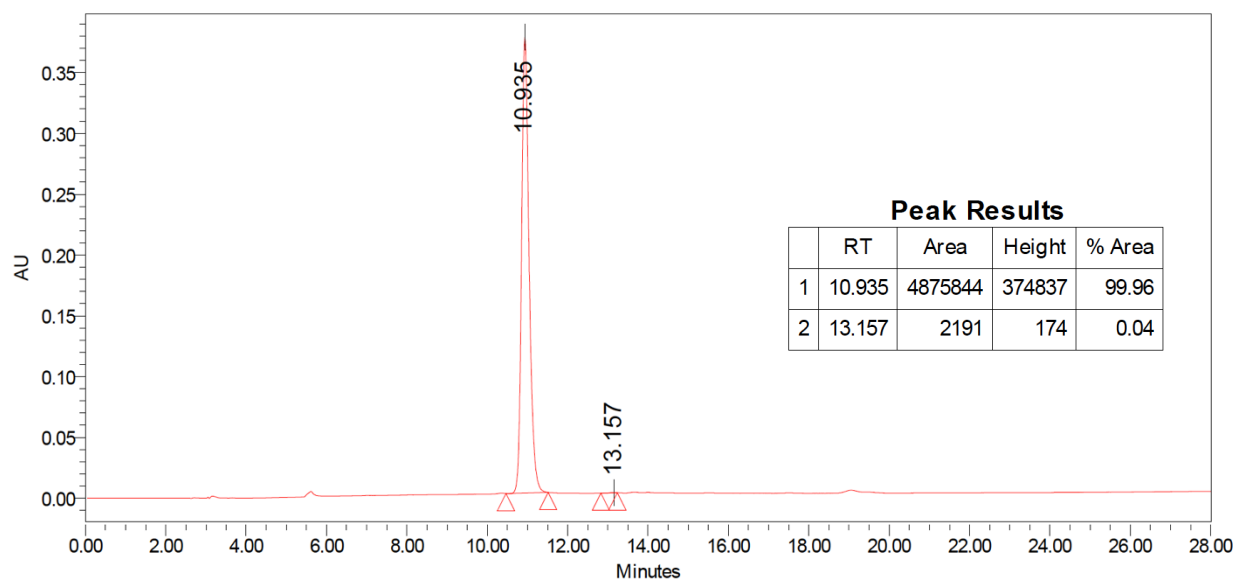


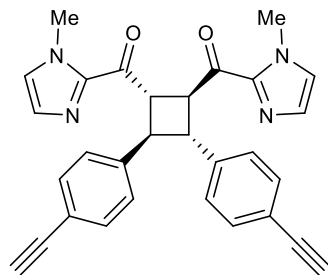
Major Diastereomer
 Run Details: HPLC, Daicel CHIRALPAK AD,
 5.00 μ L, gradient 5% to 50% iPrOH/hexanes,
 28 minutes, 1 mL/min, 255 nm.

Racemic Chromatogram



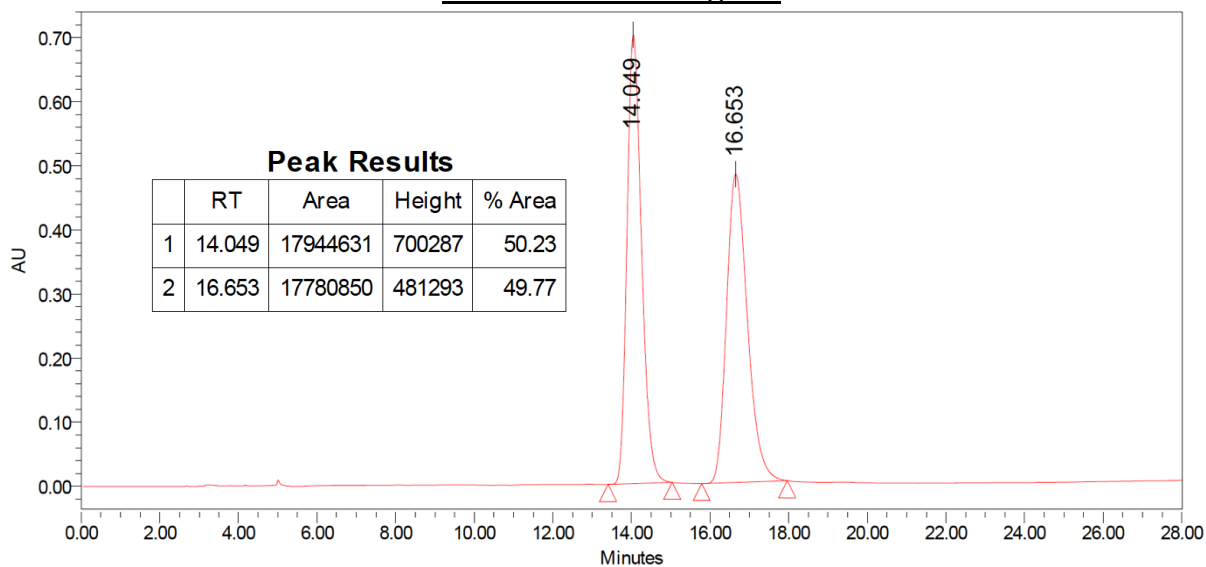
Scalemic Chromatogram



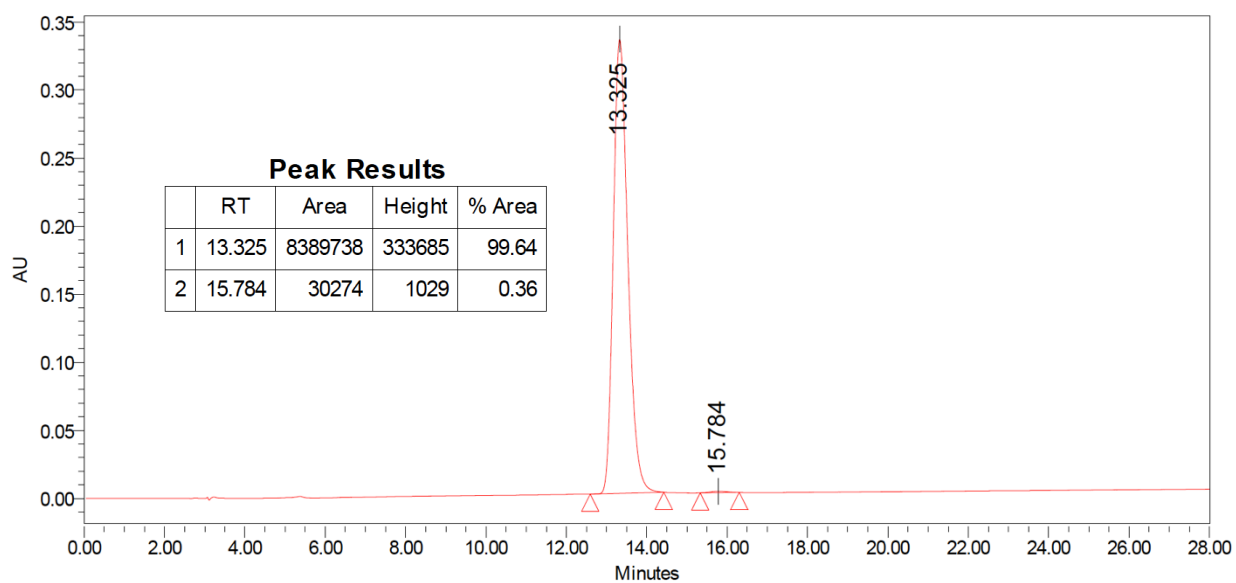


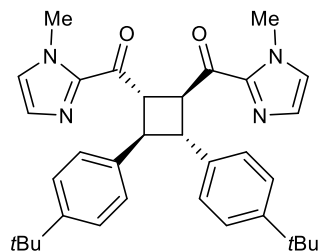
Major Diastereomer
 Run Details: HPLC, Daicel CHIRALPAK AS-H,
 5.00 μ L, gradient 5% to 50% iPrOH/hexanes,
 28 minutes, 1 mL/min, 258 nm.

Racemic Chromatogram



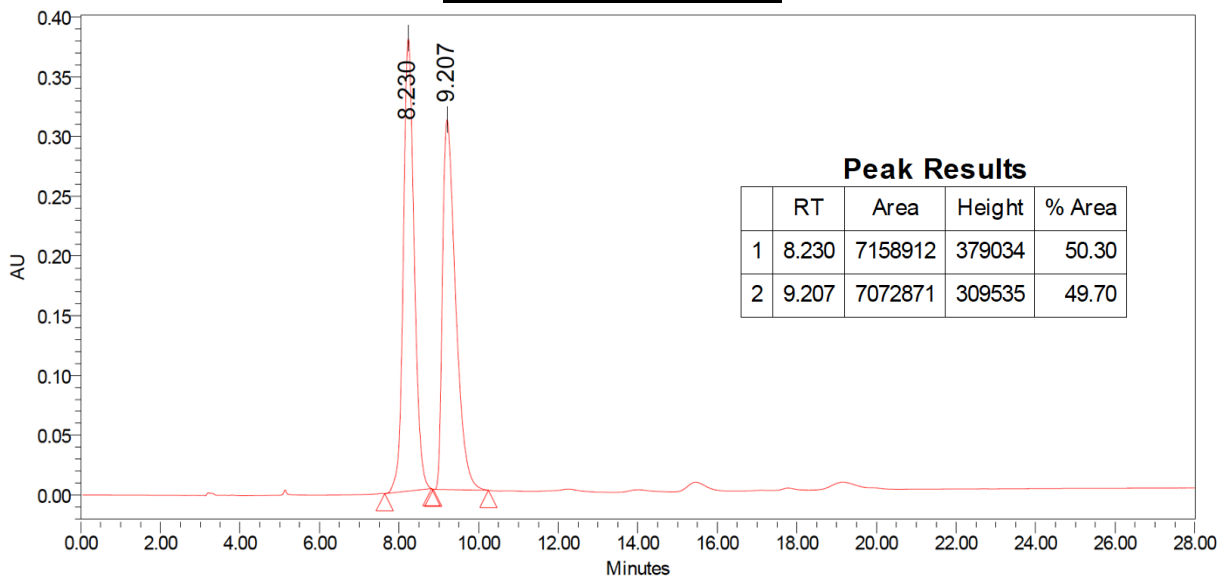
Scalemic Chromatogram



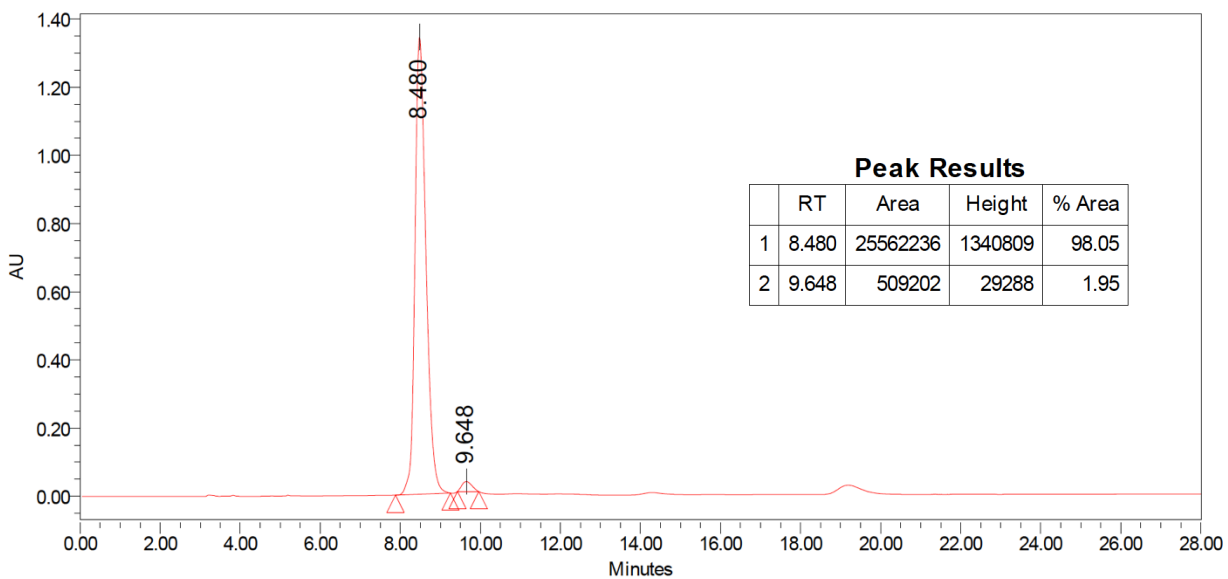


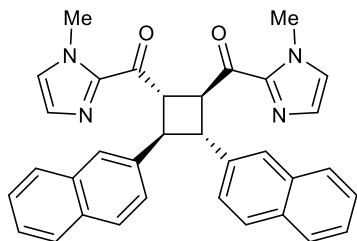
Major Diastereomer
 Run Details: HPLC, Daicel CHIRALPAK OD-H,
 5.00 μ L, gradient 5% to 50% iPrOH/hexanes,
 28 minutes, 1 mL/min, 255 nm.

Racemic Chromatogram



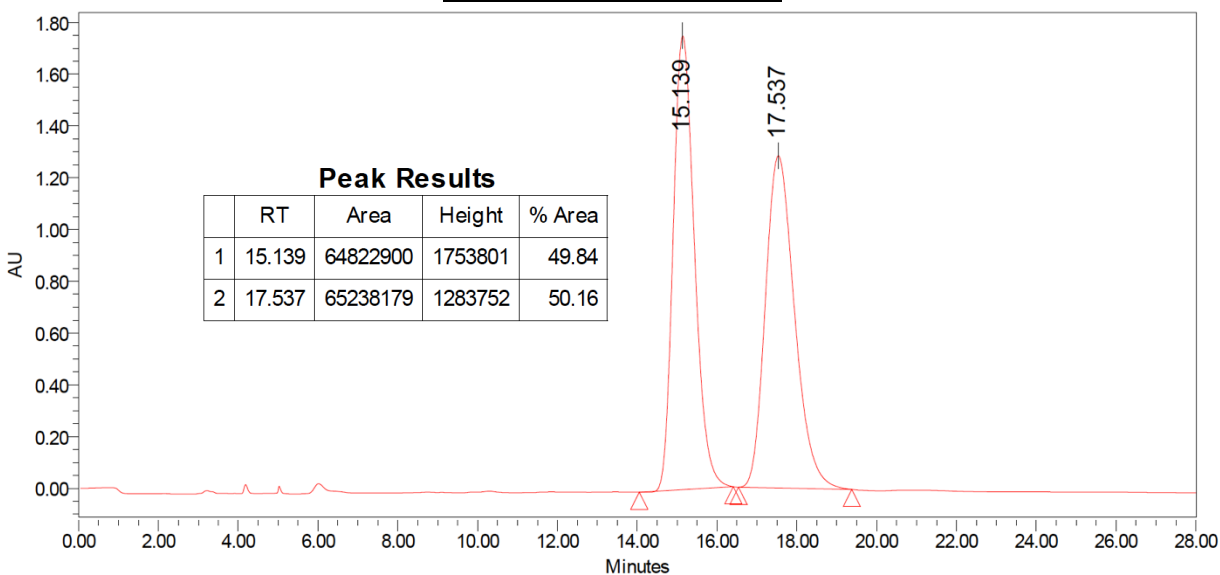
Scalemic Chromatogram



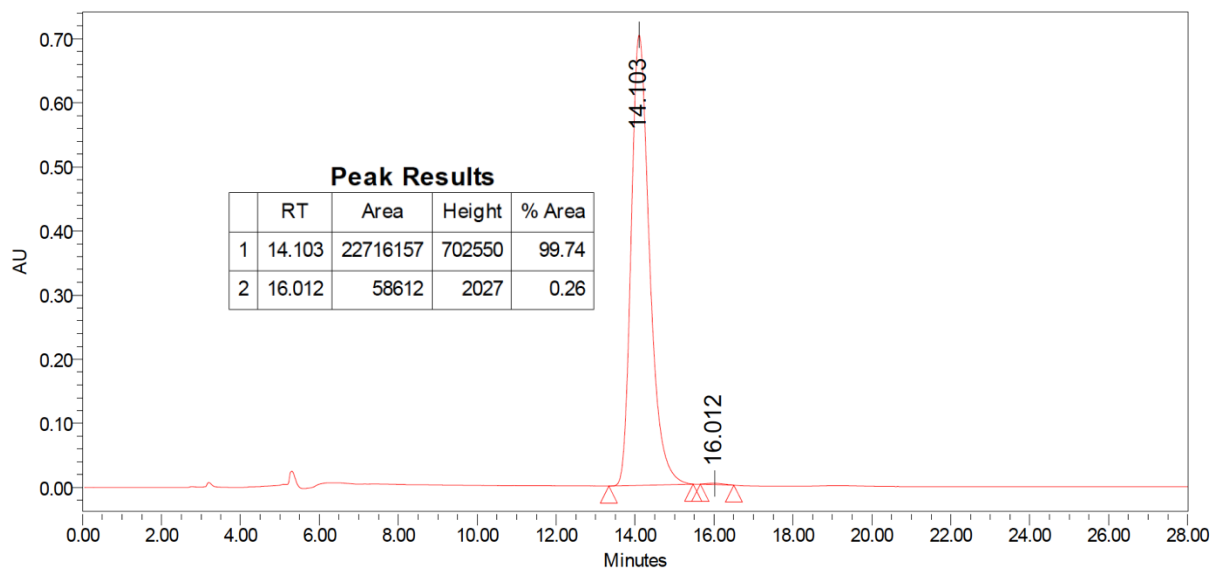


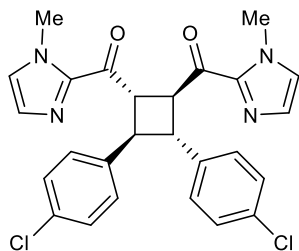
Major Diastereomer
 Run Details: HPLC, Daicel CHIRALPAK AS-H,
 5.00 μ L, gradient 5% to 50% iPrOH/hexanes,
 28 minutes, 1 mL/min, 232 nm.

Racemic Chromatogram



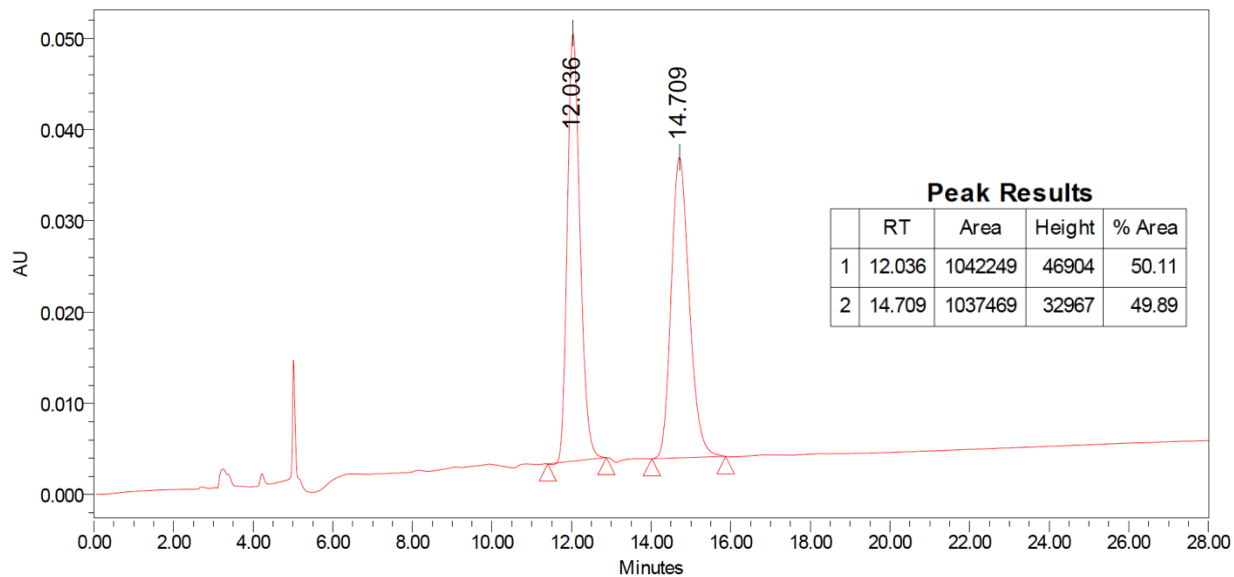
Scalemic Chromatogram



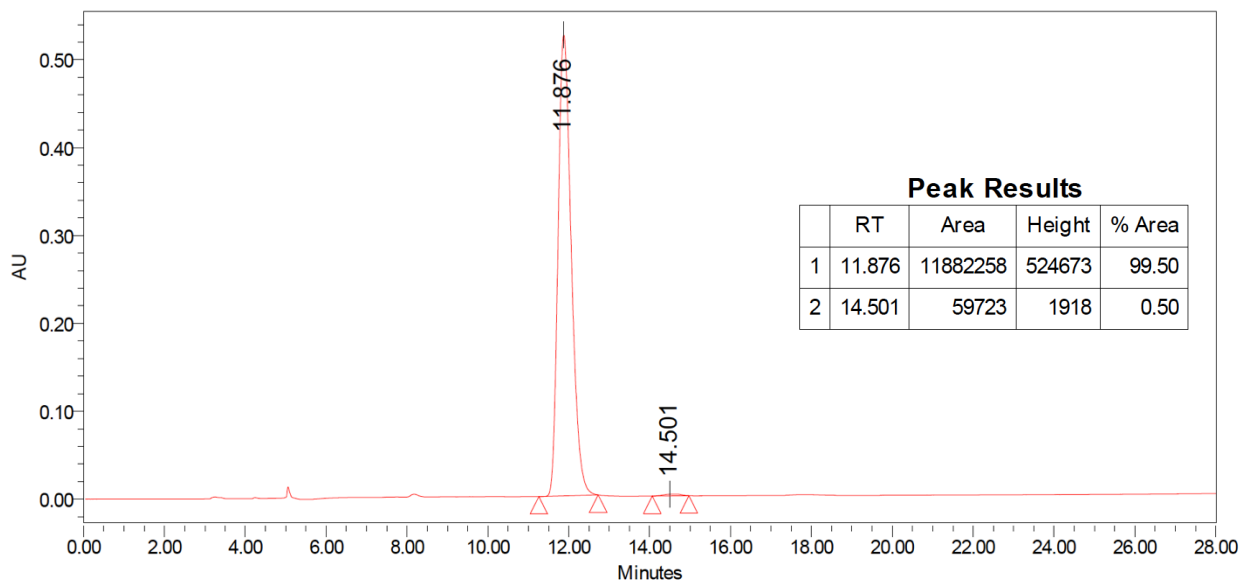


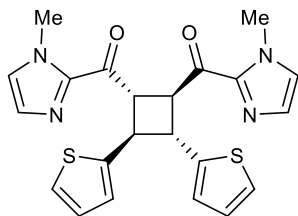
Major Diastereomer
 Run Details: HPLC, Daicel CHIRALPAK AS-H,
 5.00 μ L, gradient 5% to 50% iPrOH/hexanes,
 28 minutes, 1 mL/min, 255 nm.

Racemic Chromatogram



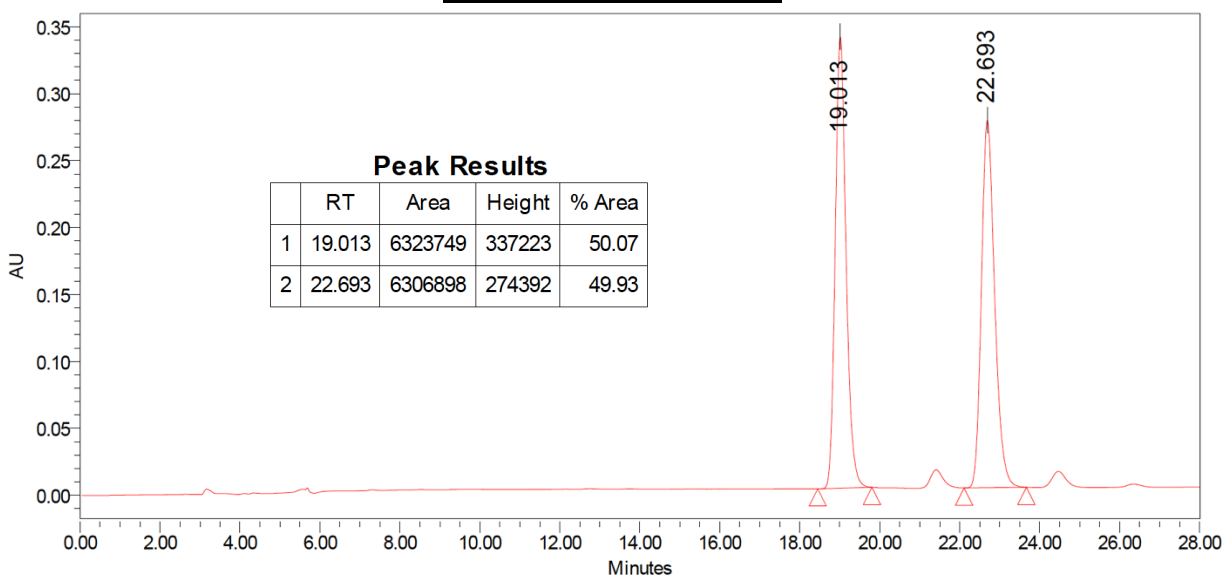
Scalemic Chromatogram



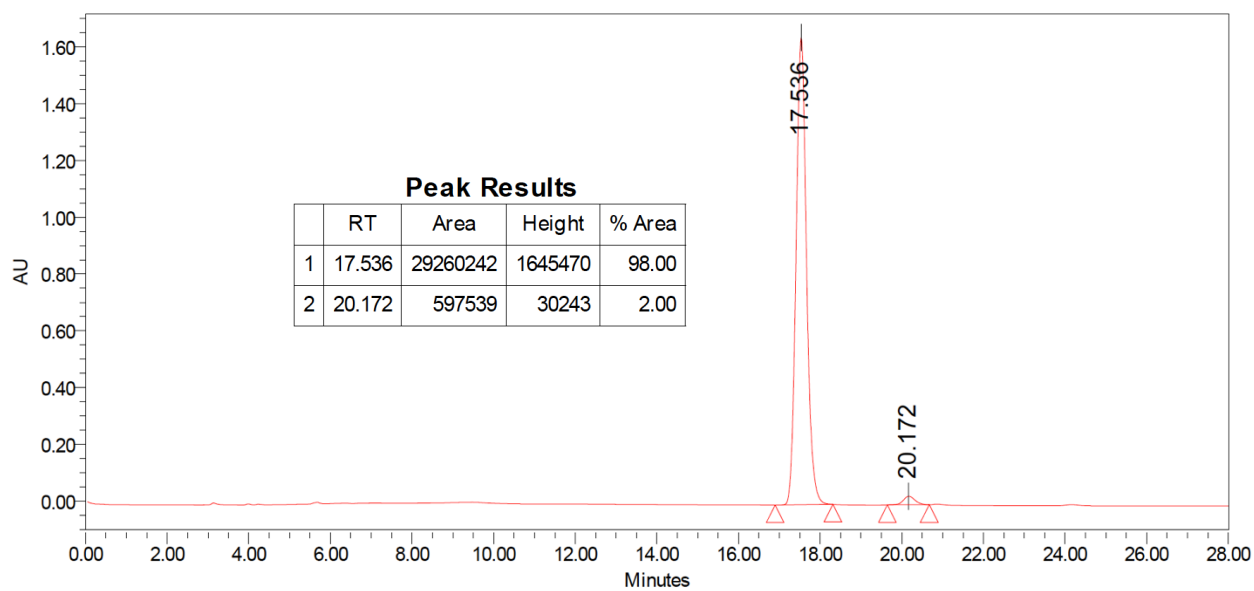


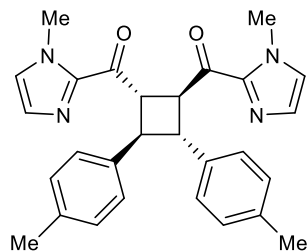
Major Diastereomer
Run Details: HPLC, Daicel CHIRALPAK AD,
5.00 μ L, gradient 5% to 50% iPrOH/hexanes,
28 minutes, 1 mL/min, 253 nm.

Racemic Chromatogram



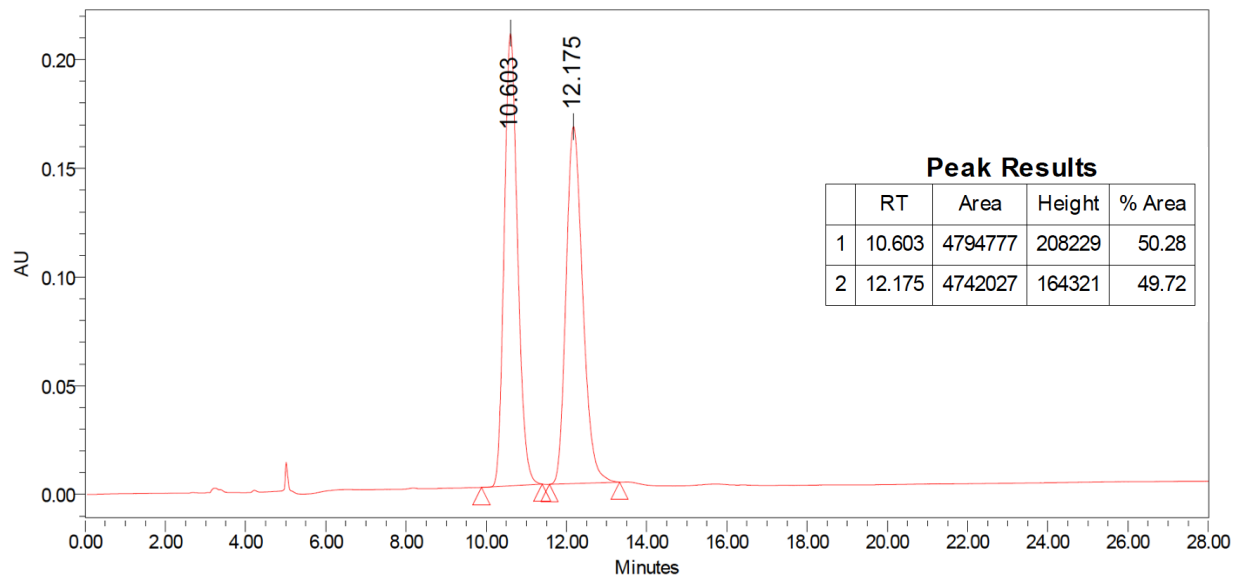
Scalemic Chromatogram



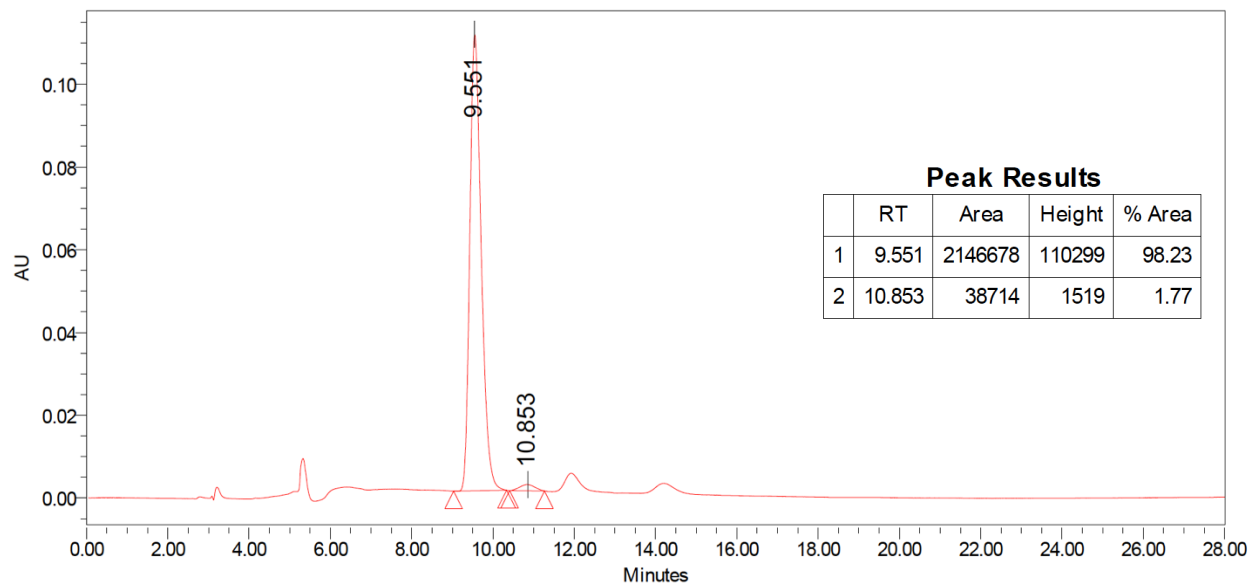


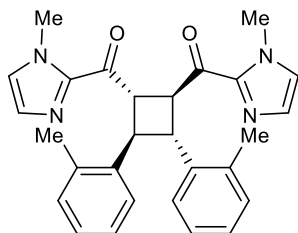
Major Diastereomer
 Run Details: HPLC, Daicel CHIRALPAK AS-H,
 5.00 μ L, gradient 5% to 50% iPrOH/hexanes,
 28 minutes, 1 mL/min, 253 nm.

Racemic Chromatogram



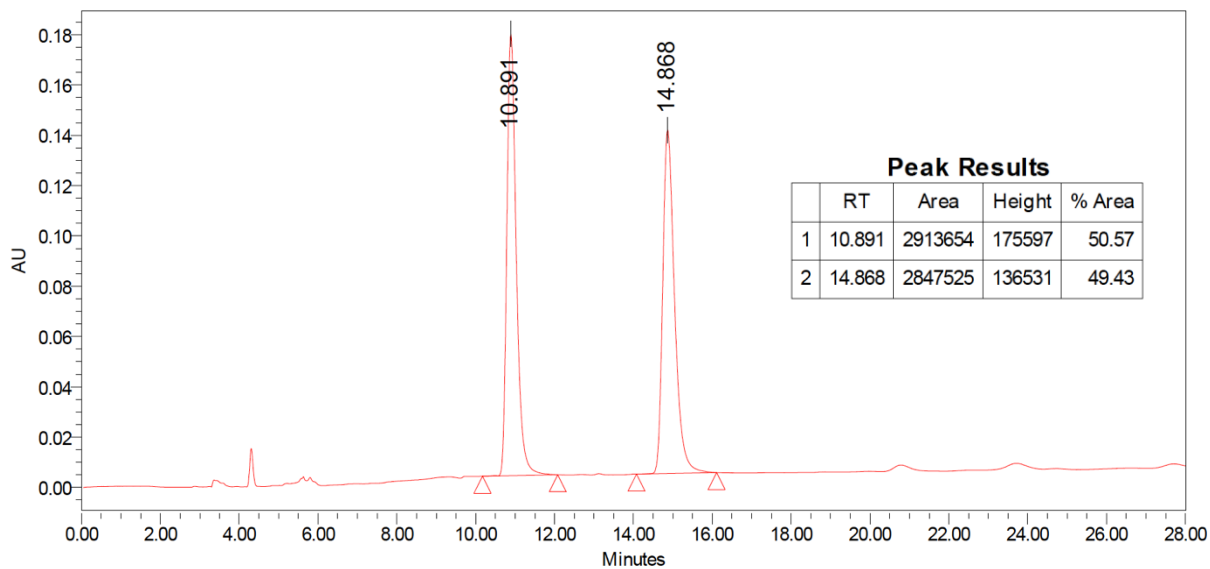
Scalemic Chromatogram



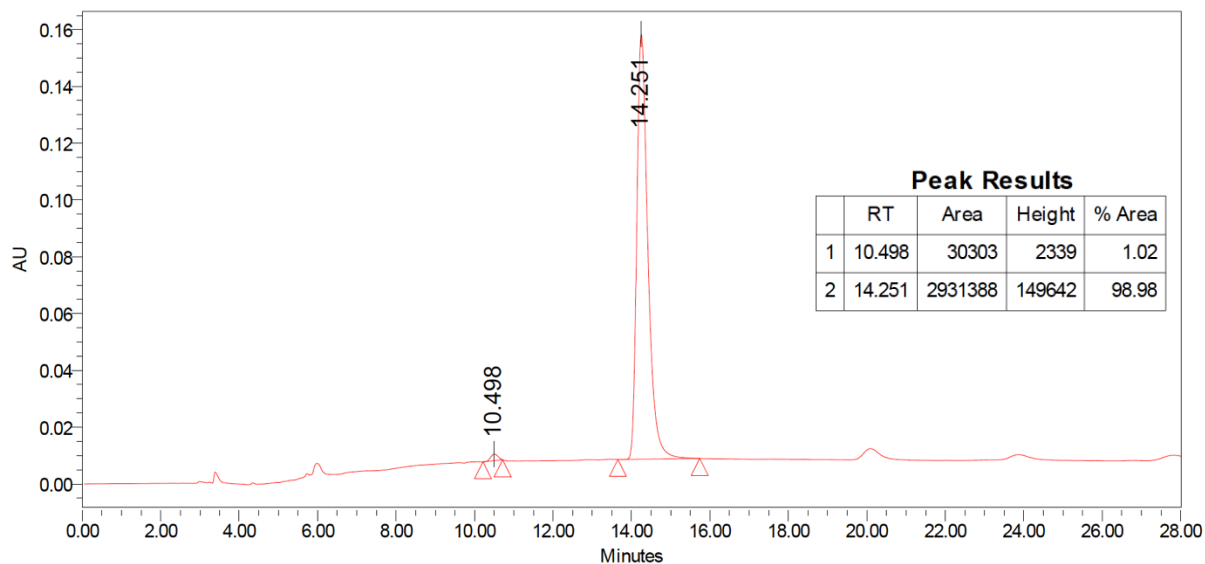


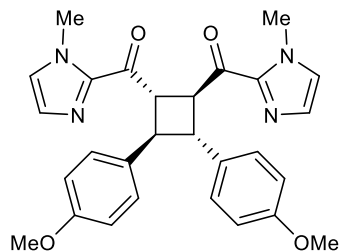
Major Diastereomer
 Run Details: HPLC, Daicel CHIRALPAK IC,
 5.00 μ L, gradient 5% to 50% iPrOH/hexanes,
 28 minutes, 1 mL/min, 257 nm.

Racemic Chromatogram



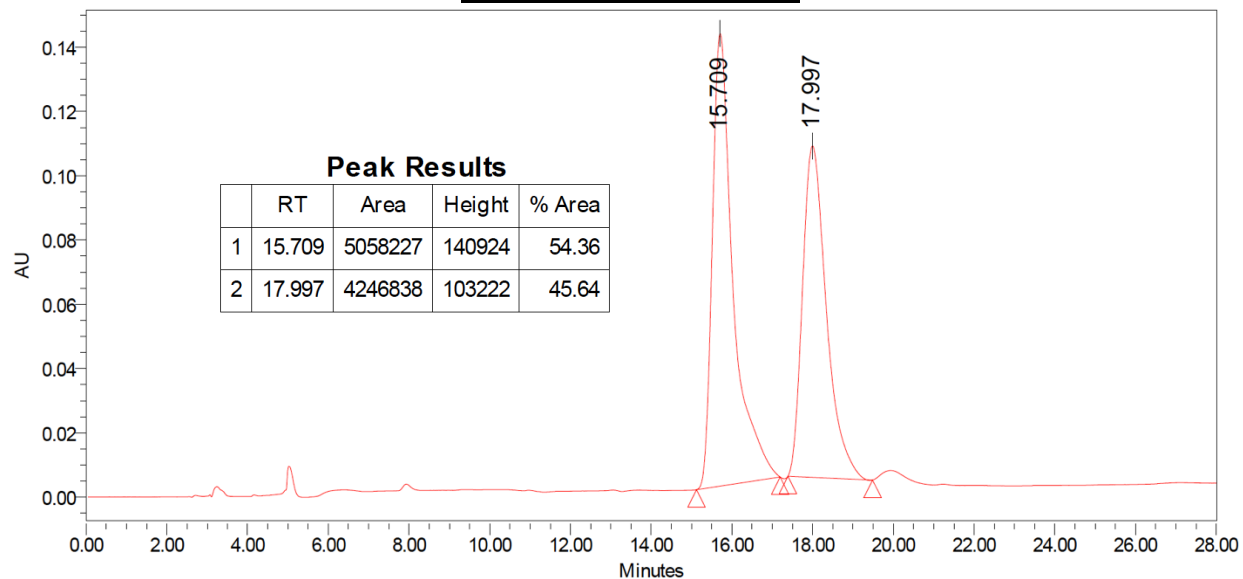
Scalemic Chromatogram



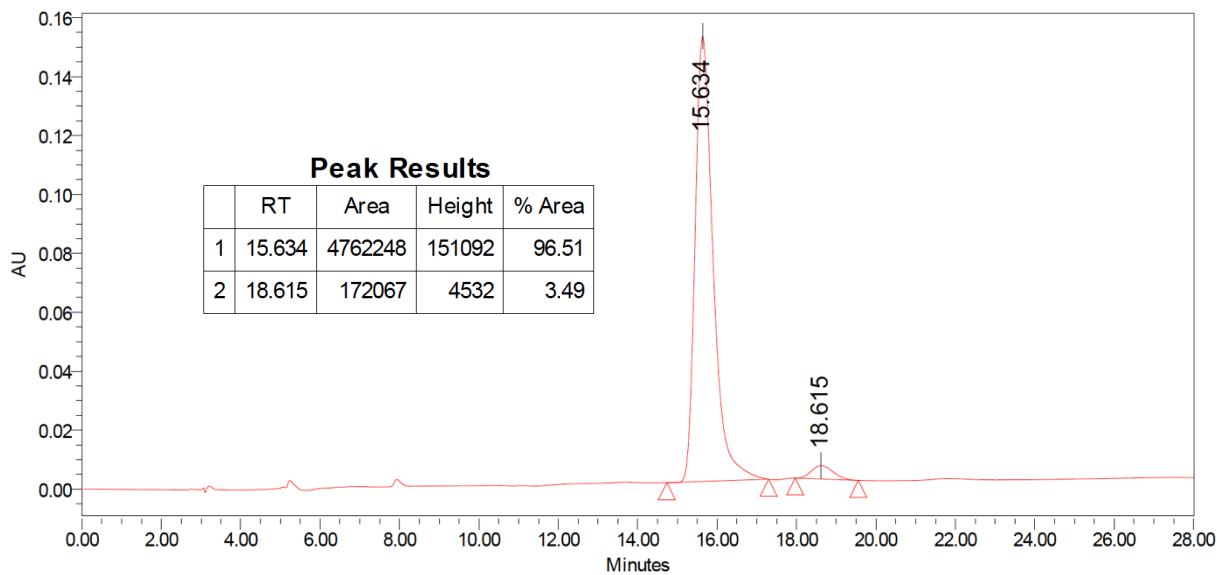


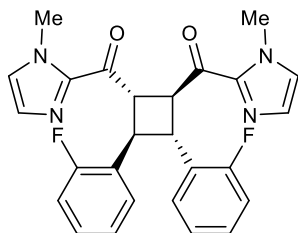
Major Diastereomer
 Run Details: HPLC, Daicel CHIRALPAK AS-H,
 5.00 μ L, gradient 5% to 50% iPrOH/hexanes,
 28 minutes, 1 mL/min, 274 nm.

Racemic Chromatogram



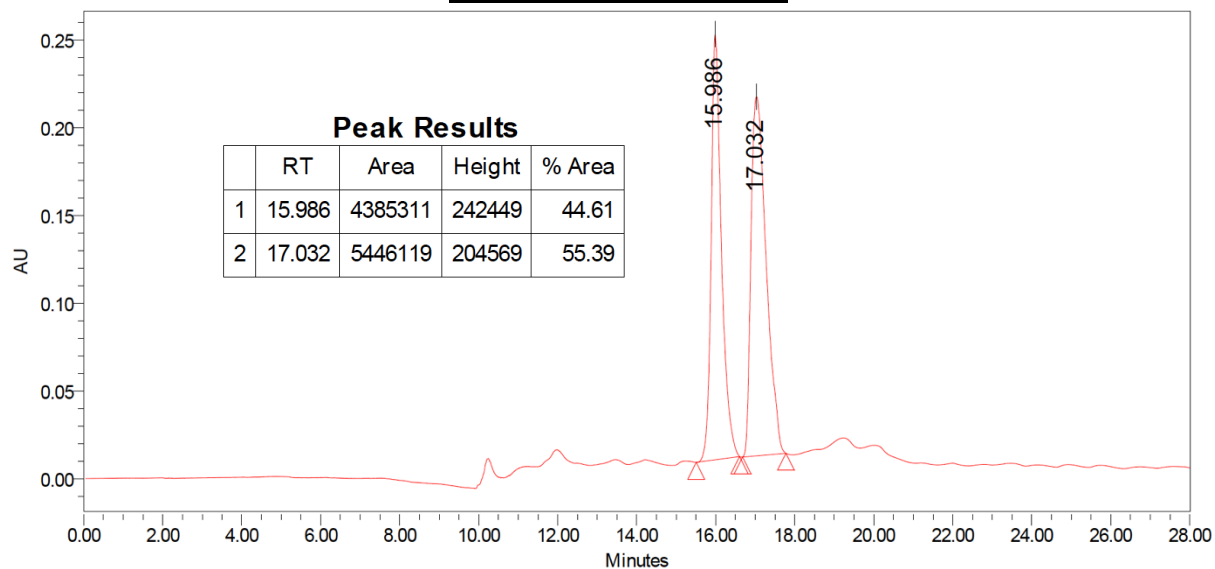
Scalemic Chromatogram



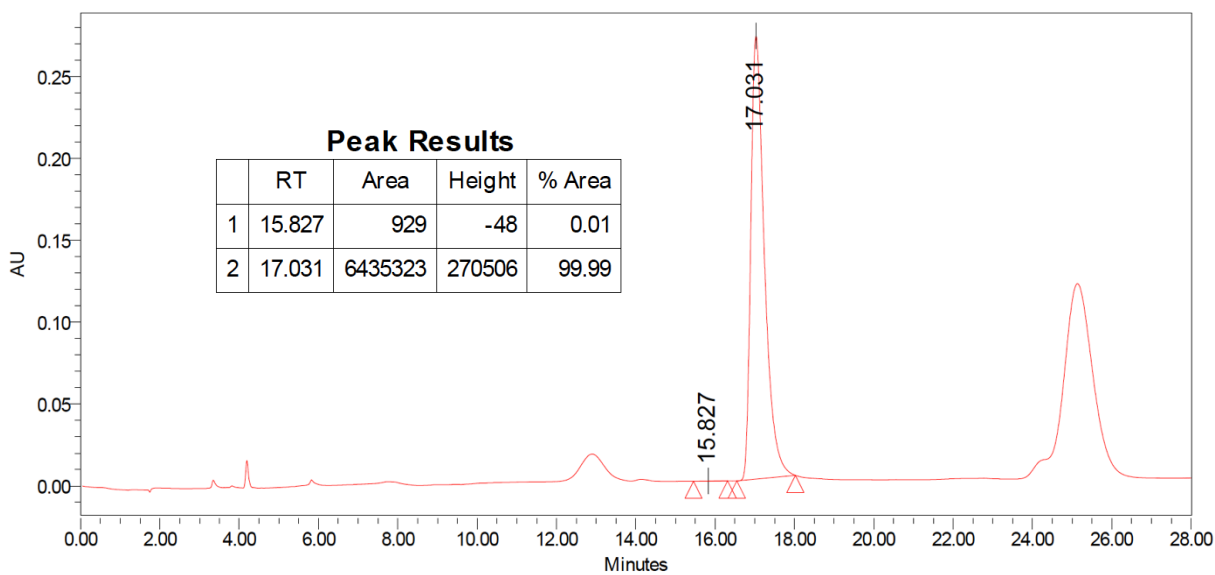


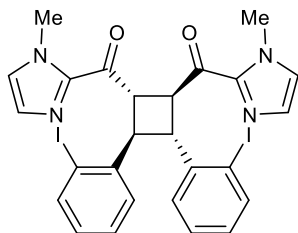
Major Diastereomer
 Run Details: HPLC, Daicel CHIRALPAK IC,
 5.00 μ L, gradient 5% to 50% iPrOH/hexanes,
 28 minutes, 1 mL/min, 254 nm.

Racemic Chromatogram



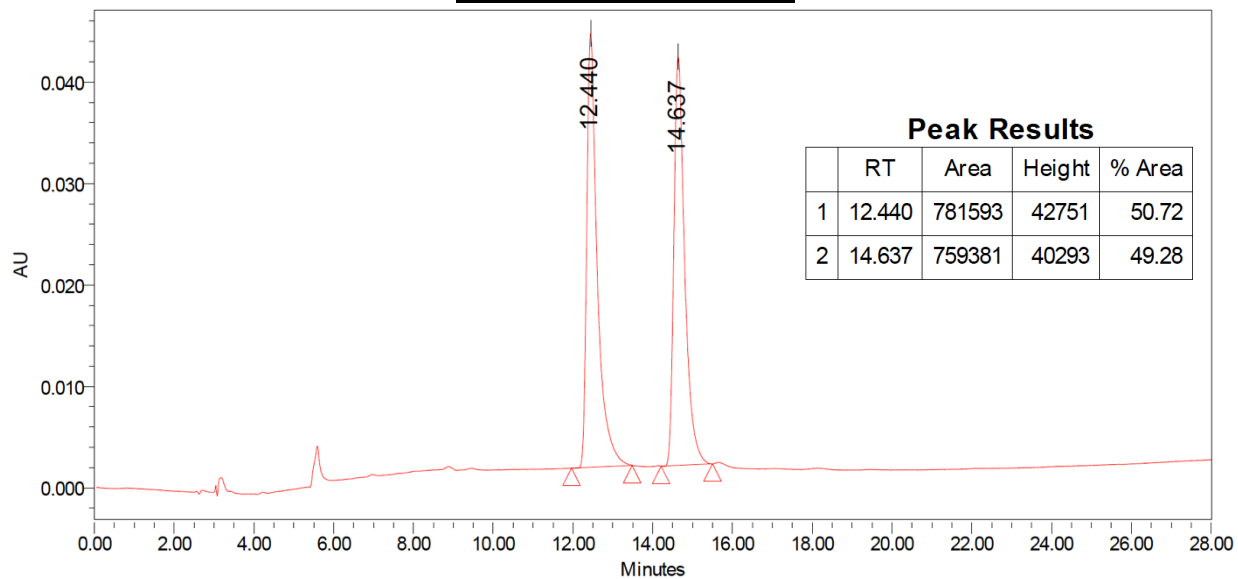
Scalemic Chromatogram



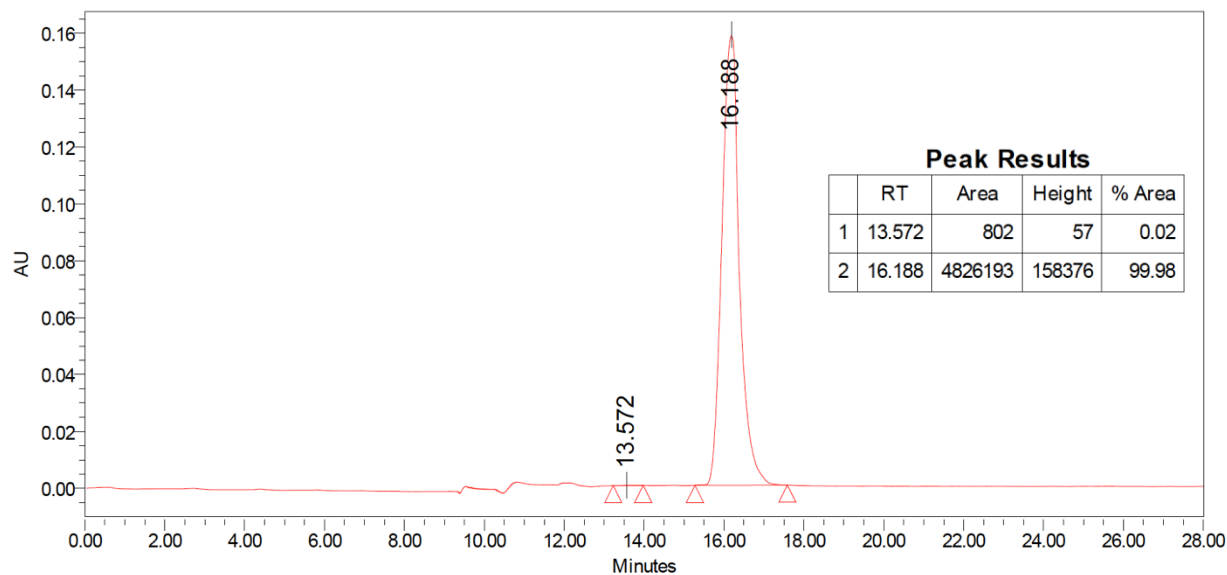


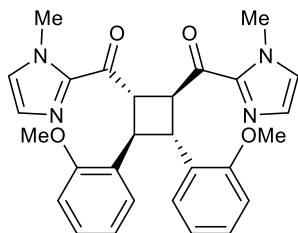
Major Diastereomer
 Run Details: HPLC, Daicel CHIRALPAK AD,
 5.00 μ L, gradient 5% to 50% iPrOH/hexanes,
 28 minutes, 1 mL/min, 300 nm.

Racemic Chromatogram



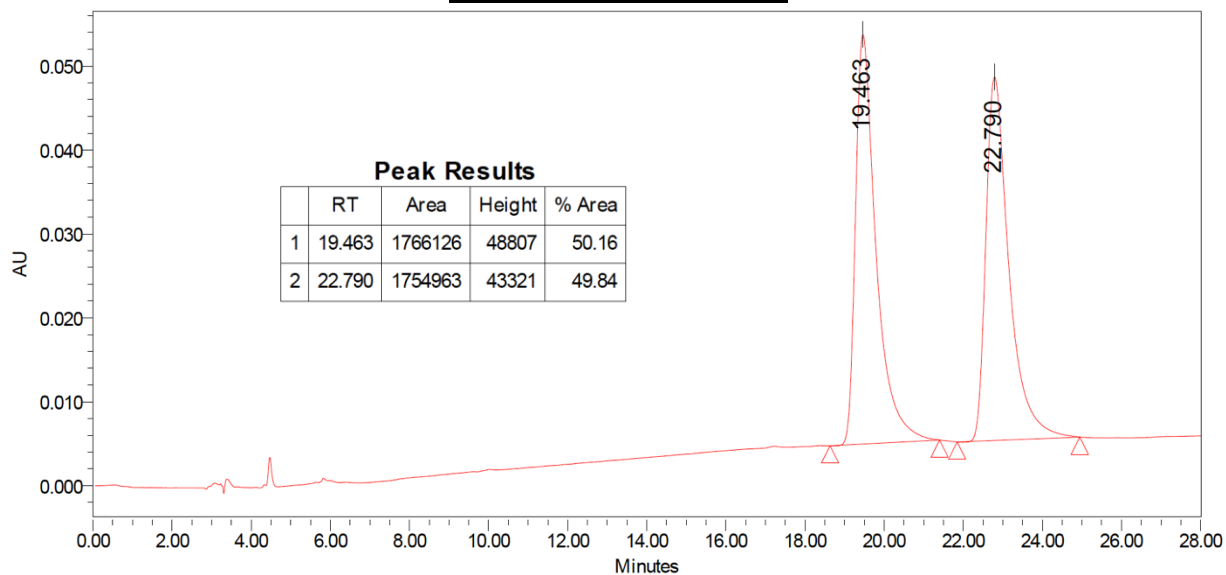
Scalemic Chromatogram



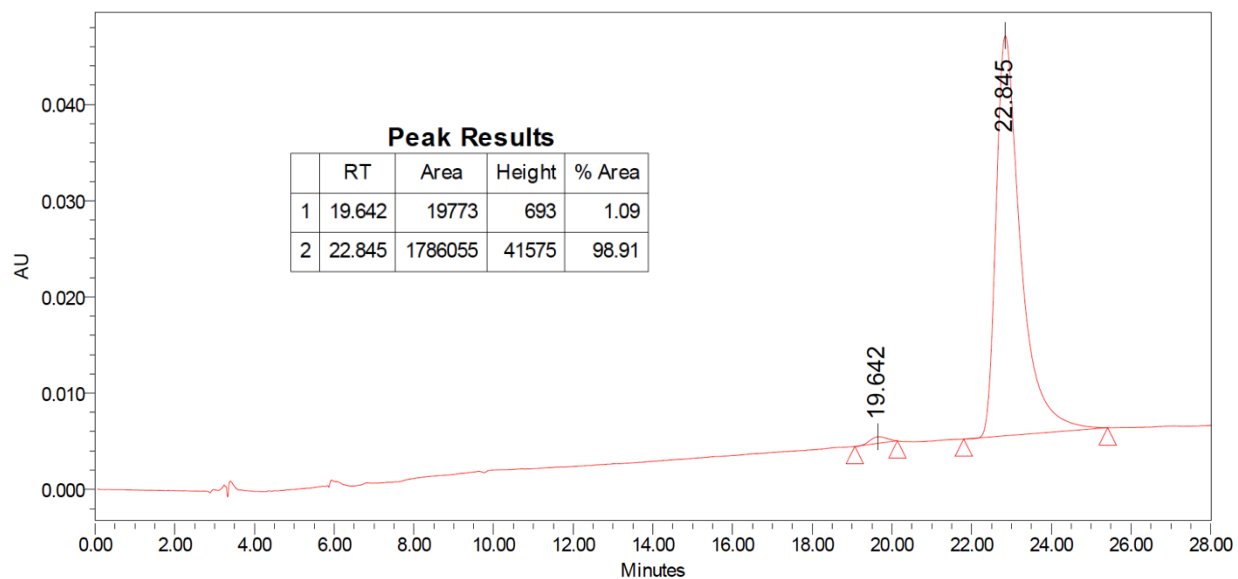


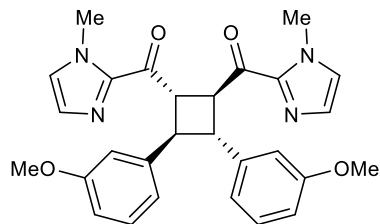
Major Diastereomer
Run Details: HPLC, Daicel CHIRALPAK IC,
5.00 μ L, gradient 5% to 50% iPrOH/hexanes,
28 minutes, 1 mL/min, 269 nm.

Racemic Chromatogram



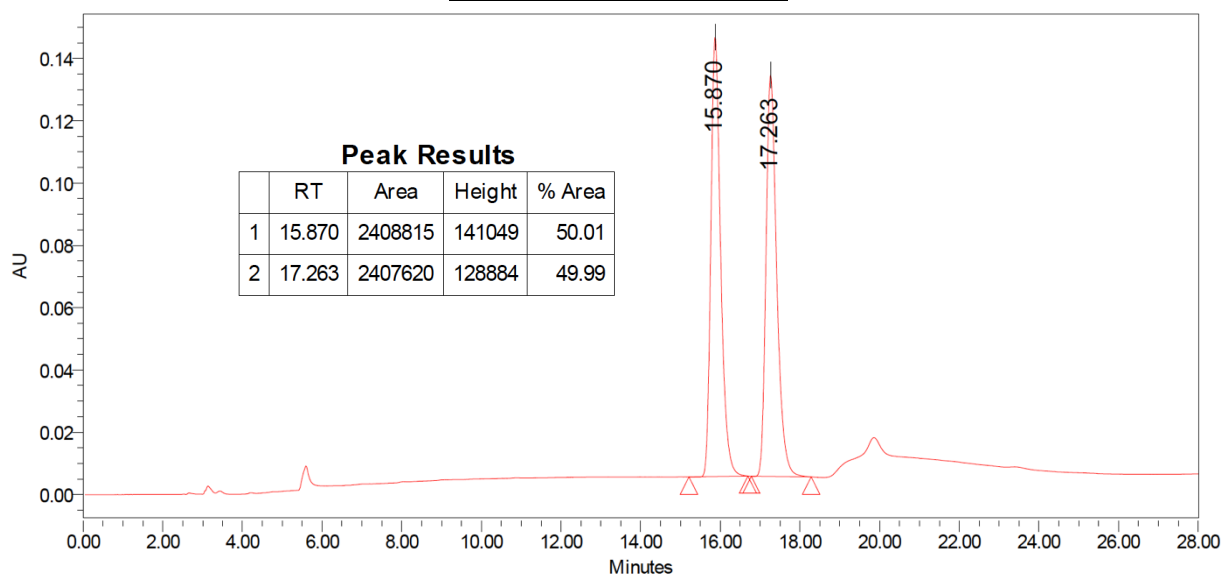
Scalemic Chromatogram



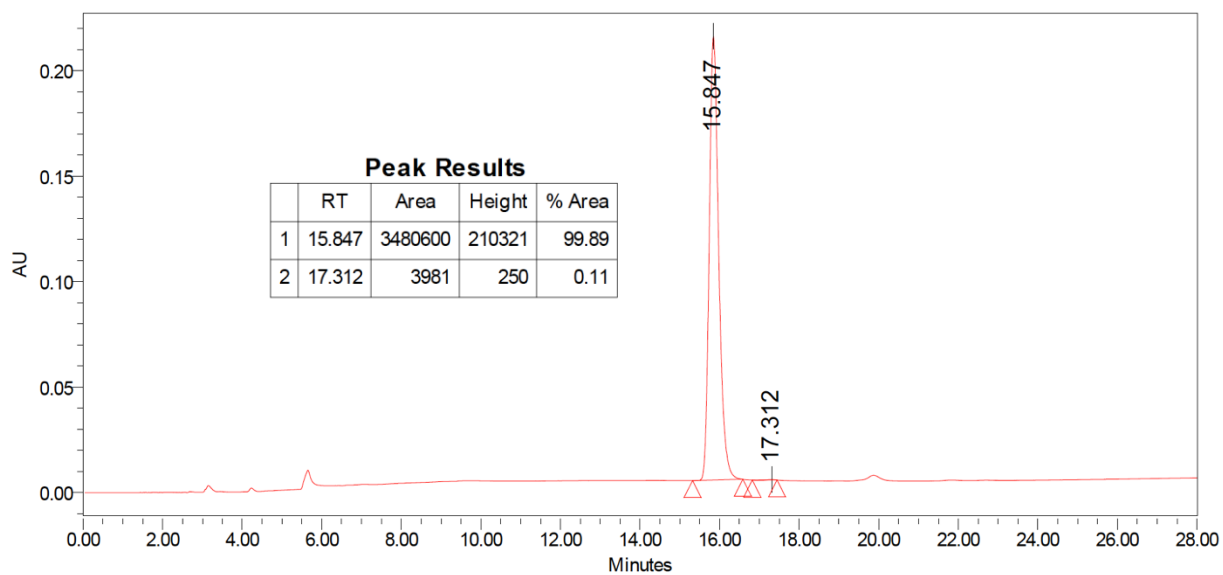


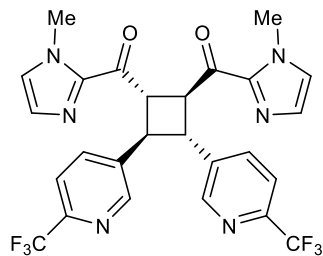
Major Diastereomer
Run Details: HPLC, Daicel CHIRALPAK AD,
5.00 μ L, gradient 5% to 50% iPrOH/hexanes,
28 minutes, 1 mL/min, 251 nm.

Racemic Chromatogram



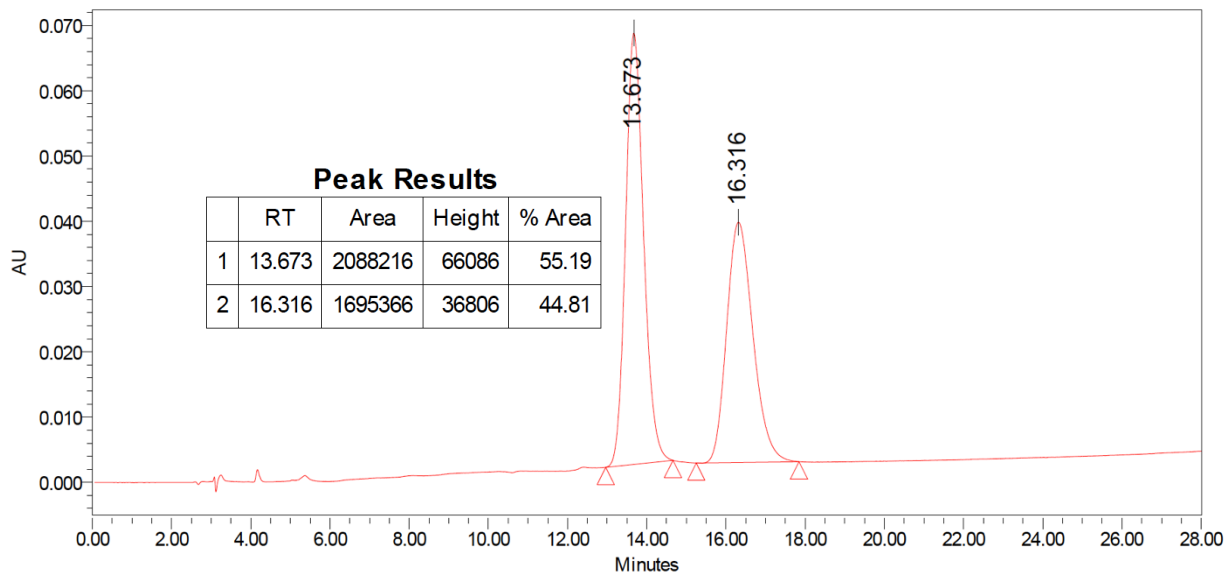
Scalemic Chromatogram



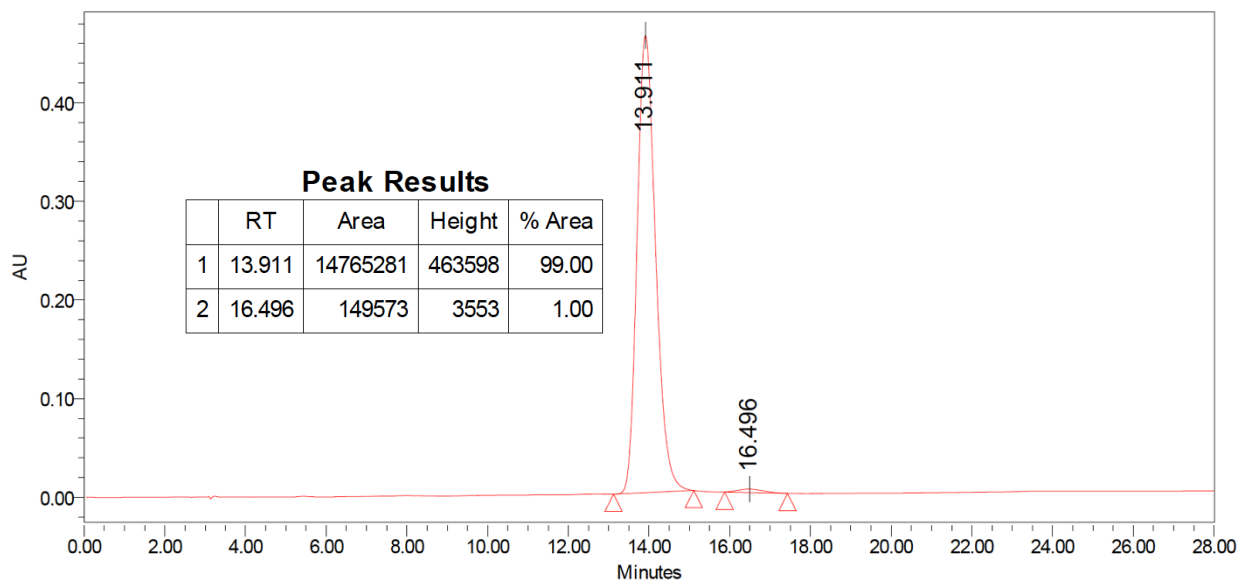


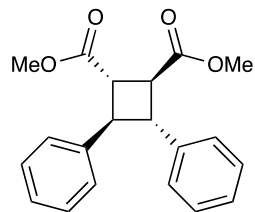
Major Diastereomer
 Run Details: HPLC, Daicel CHIRALPAK AS-H,
 5.00 μ L, gradient 5% to 50% iPrOH/hexanes,
 28 minutes, 1 mL/min, 277 nm.

Racemic Chromatogram



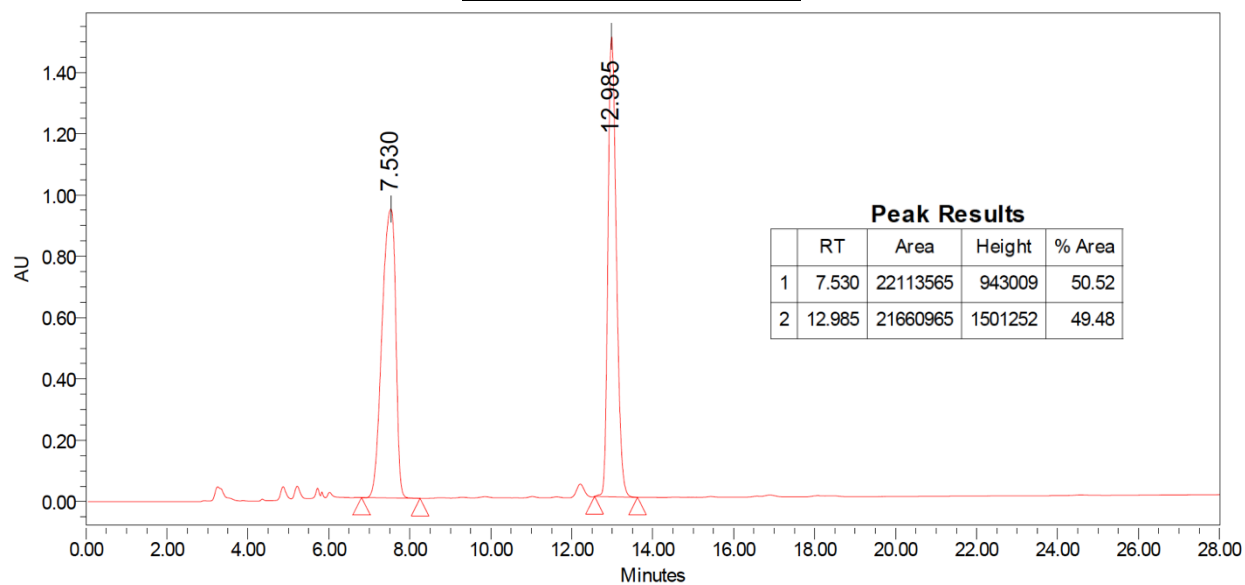
Scalemic Chromatogram



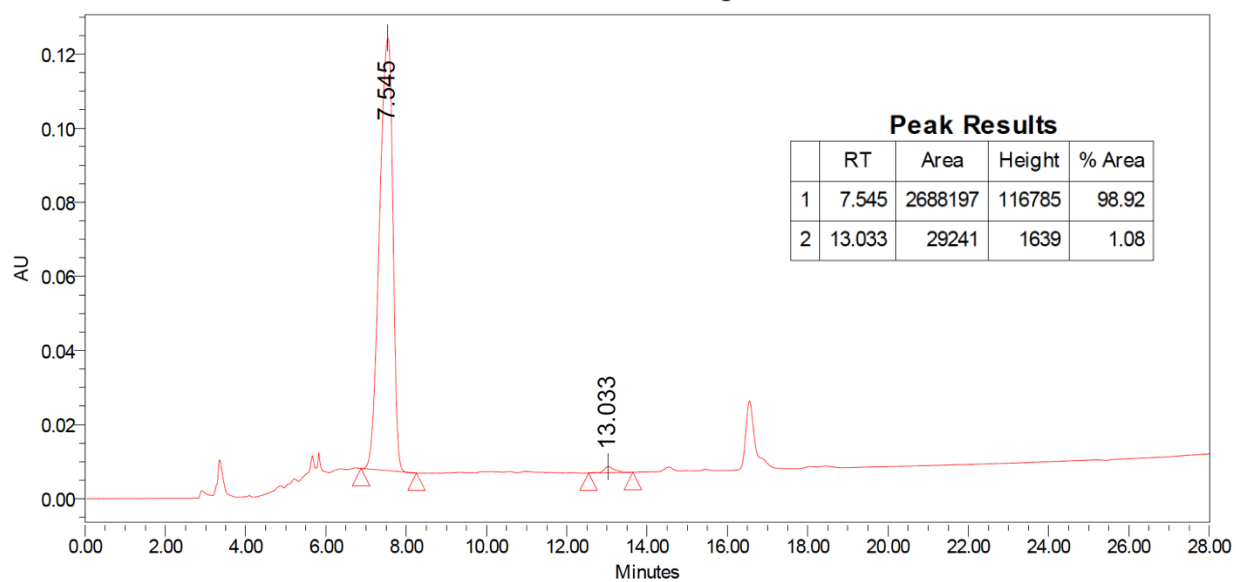


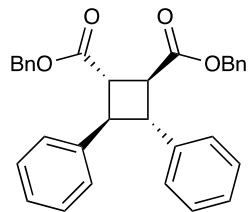
Major Diastereomer
 Run Details: HPLC, Daicel CHIRALPAK IC,
 5.00 μ L, gradient 5% to 50% iPrOH/hexanes,
 28 minutes, 1 mL/min, 223 nm.

Racemic Chromatogram



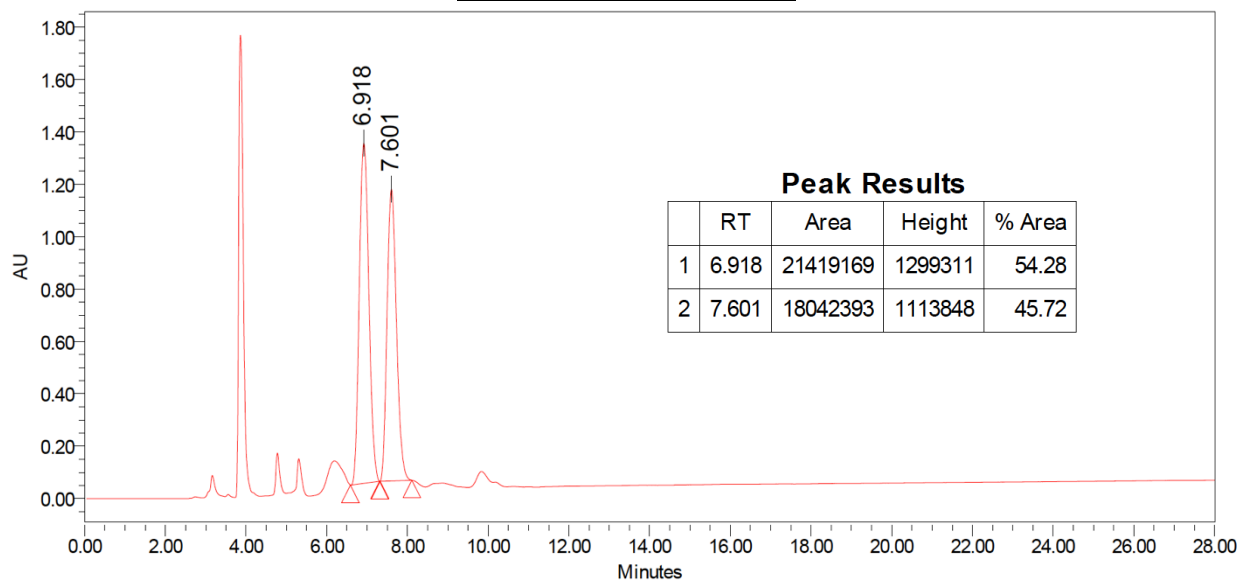
Scalemic Chromatogram



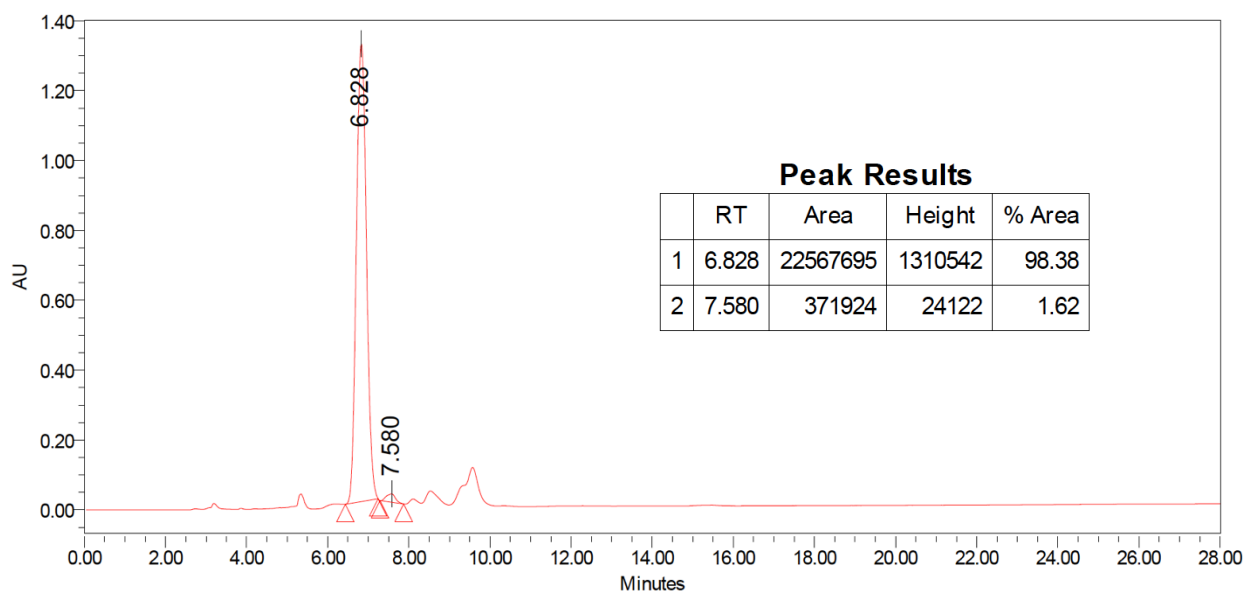


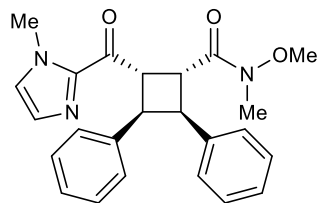
Major Diastereomer
 Run Details: HPLC, Daicel CHIRALPAK OD-H,
 5.00 μ L, gradient 5% to 50% iPrOH/hexanes,
 28 minutes, 1 mL/min, 255 nm

Racemic Chromatogram



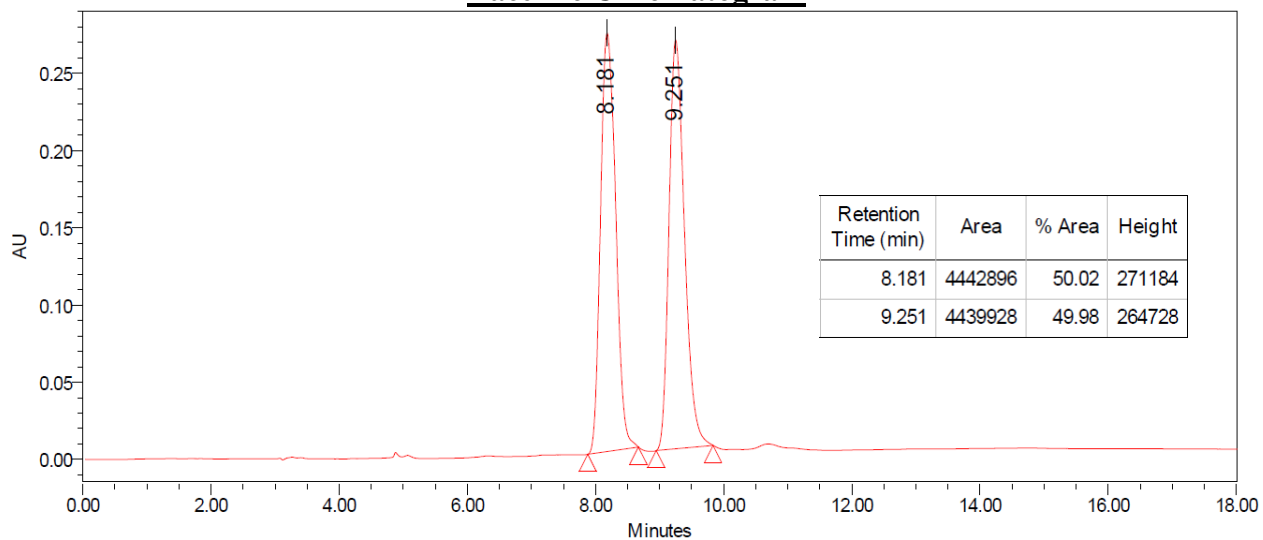
Scalemic Chromatogram



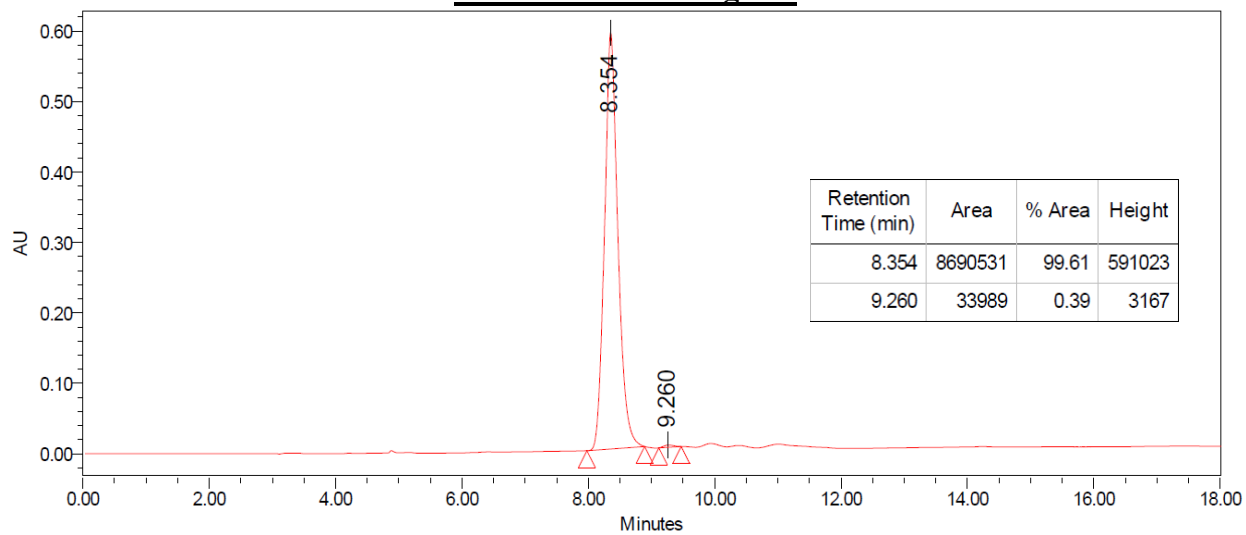


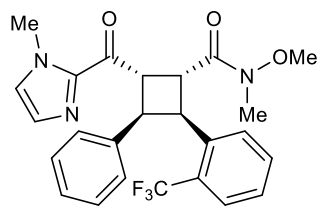
Major Diastereomer
 Run Details: HPLC, Daicel CHIRALPAK AS-H,
 10.00 μ L, gradient 5% to 50% iPrOH/hexanes,
 28 minutes, 1 mL/min, 285 nm

Racemic Chromatogram



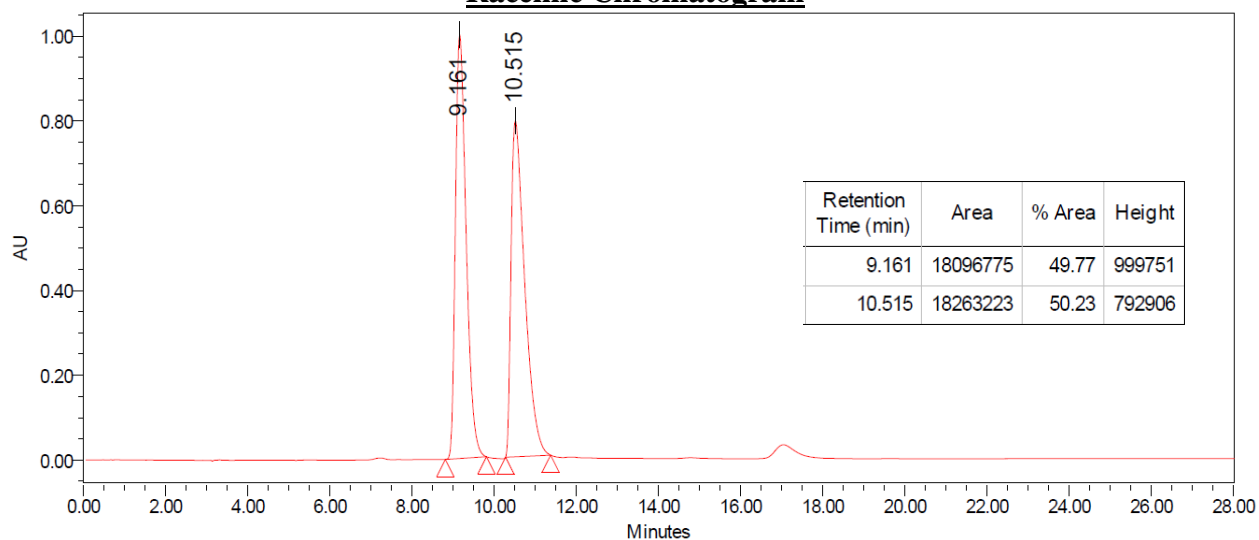
Scalemic Chromatogram



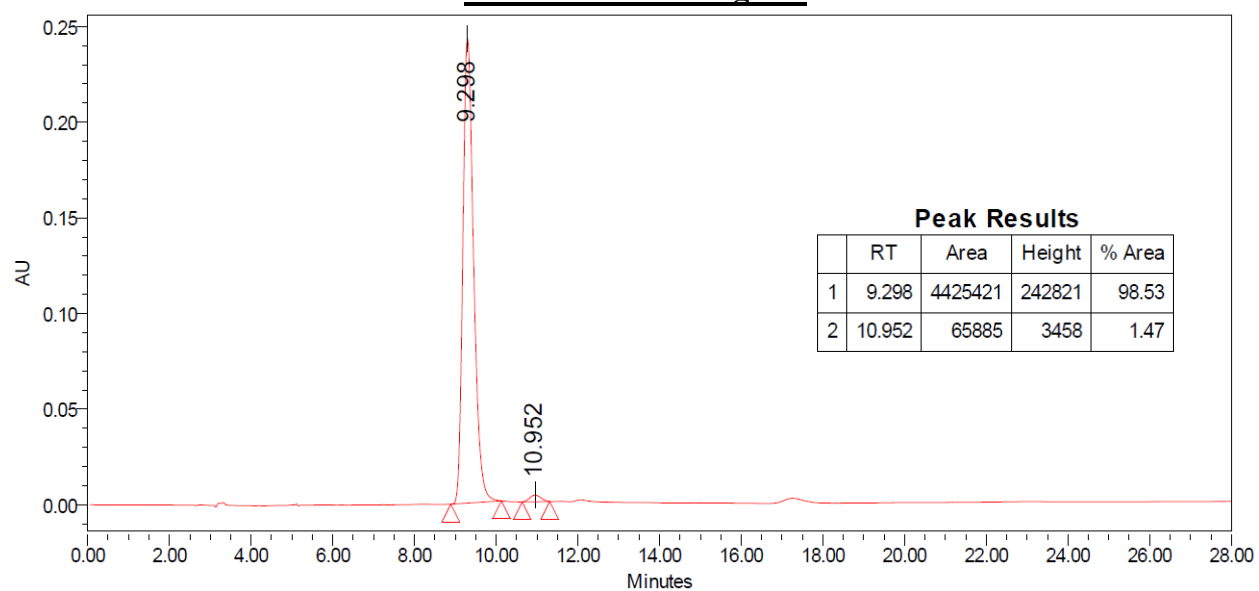


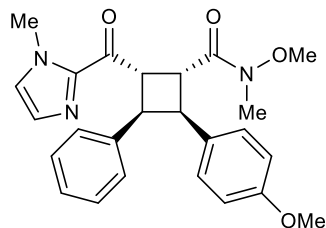
Major Diastereomer
 Run Details: HPLC, Daicel CHIRALPAK OD-H,
 10.00 μ L, gradient 5% to 50% iPrOH/hexanes,
 28 minutes, 1 mL/min, 285 nm

Racemic Chromatogram



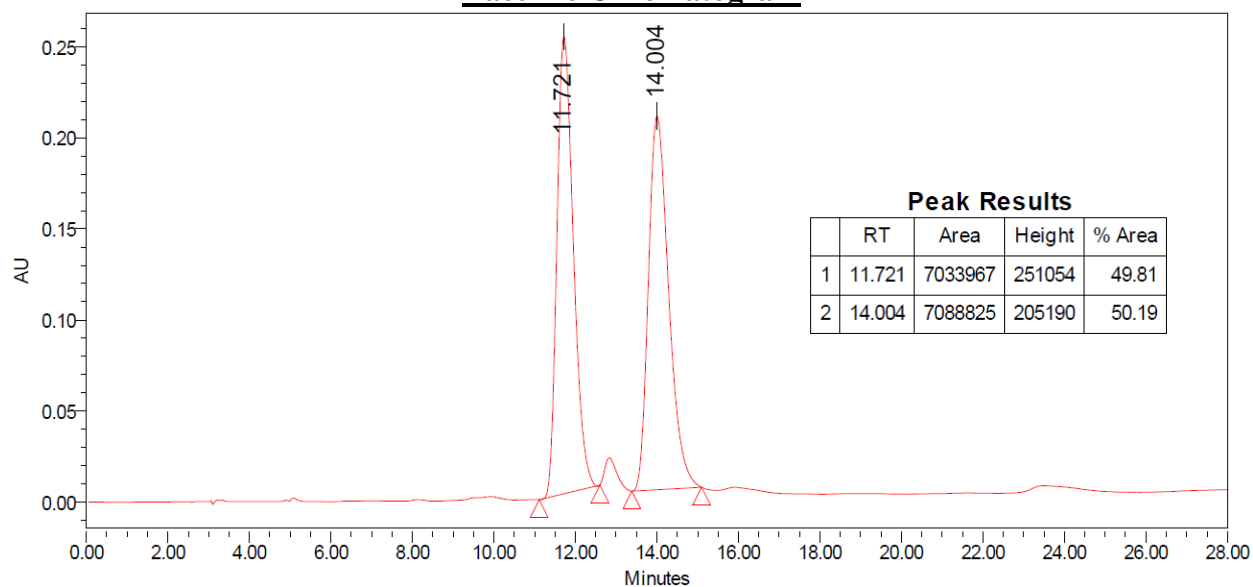
Scalemic Chromatogram



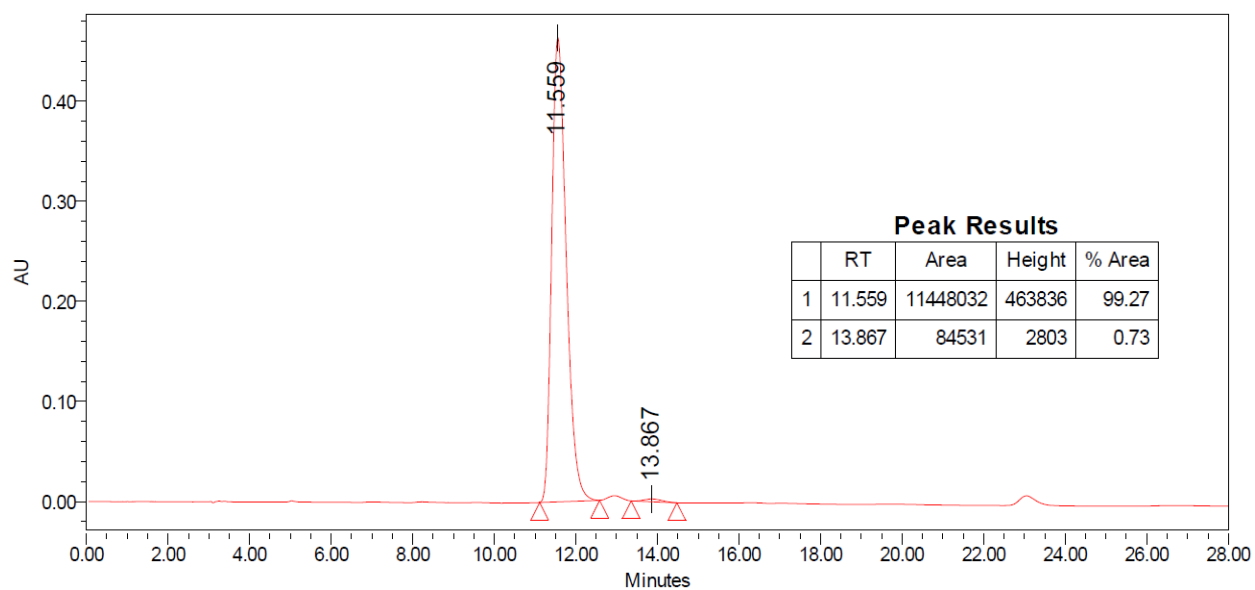


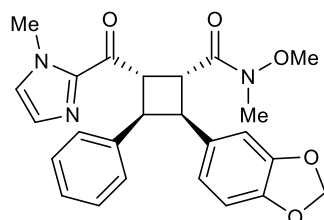
Major Diastereomer
 Run Details: HPLC, Daicel CHIRALPAK AS-H,
 10.00 μ L, gradient 5% to 50% iPrOH/hexanes,
 28 minutes, 1 mL/min, 285 nm

Racemic Chromatogram



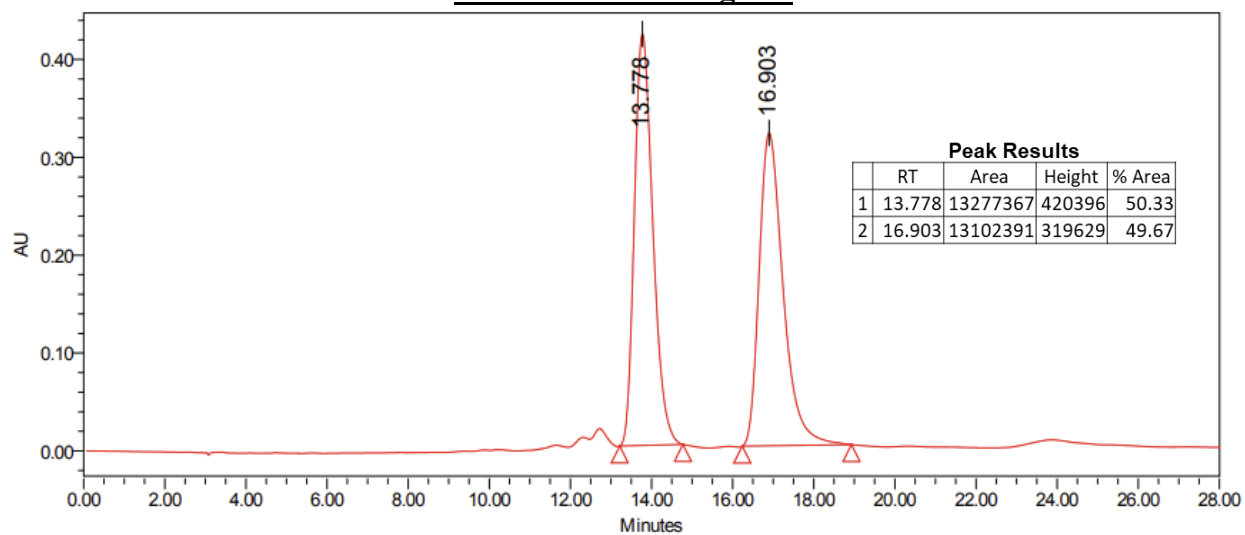
Scalemic Chromatogram



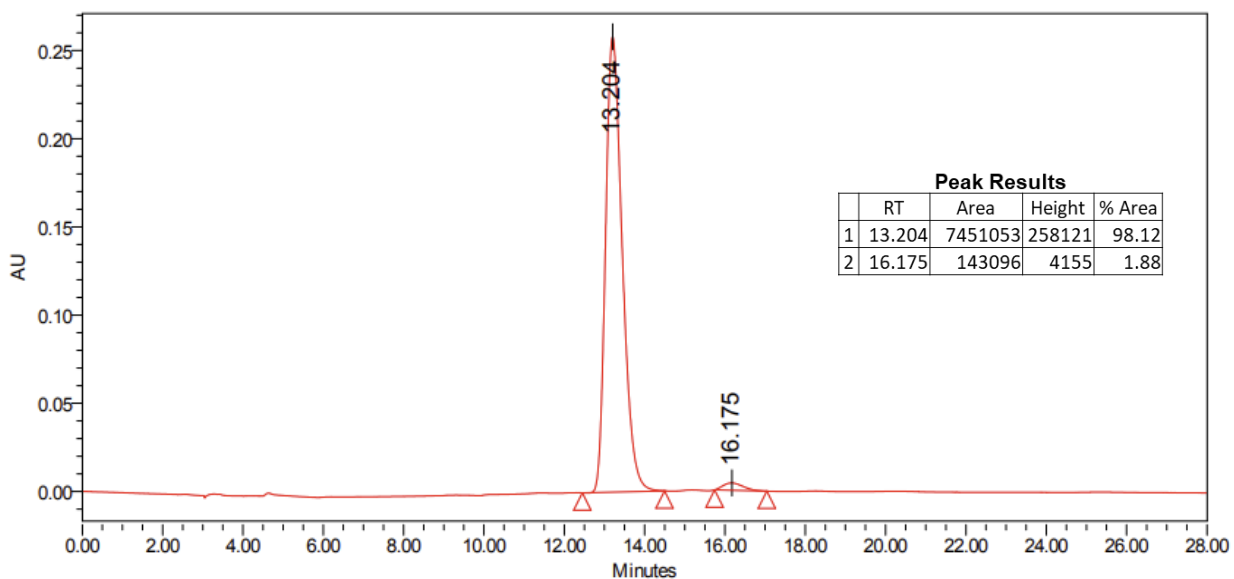


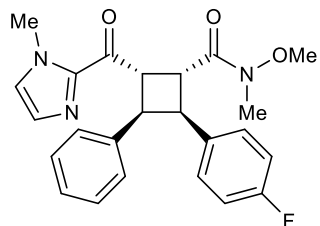
Major Diastereomer
 Run Details: HPLC, Daicel CHIRALPAK AS-H,
 10.00 μ L, gradient 5% to 50% iPrOH/hexanes,
 28 minutes, 1 mL/min, 280 nm

Racemic Chromatogram



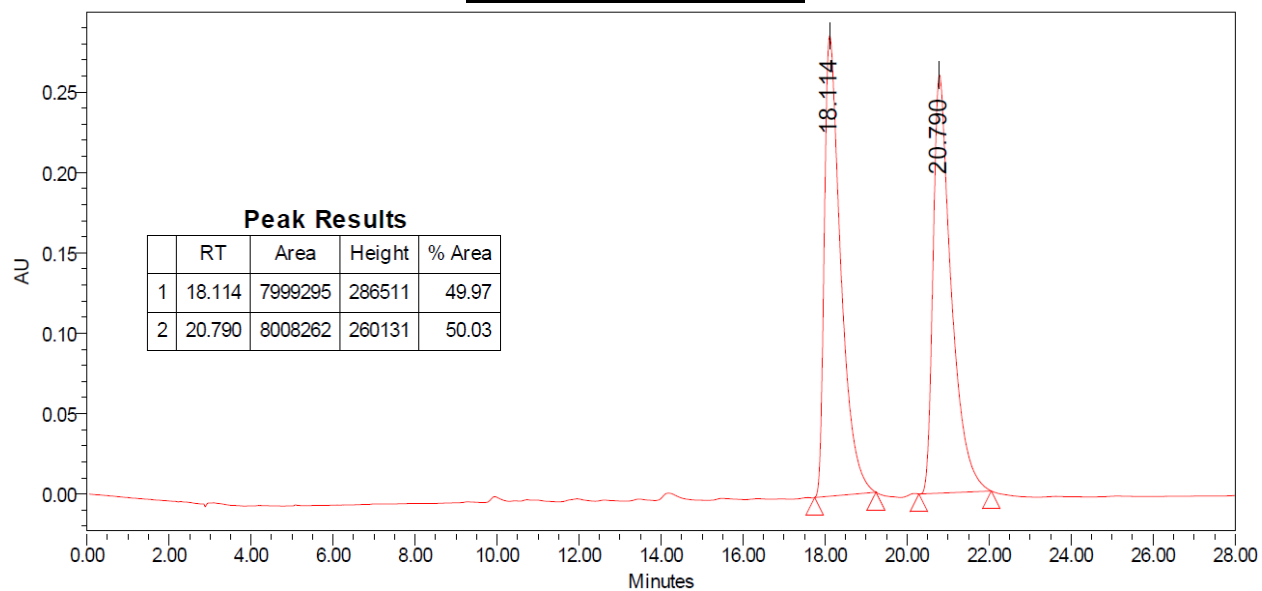
Scalemic Chromatogram



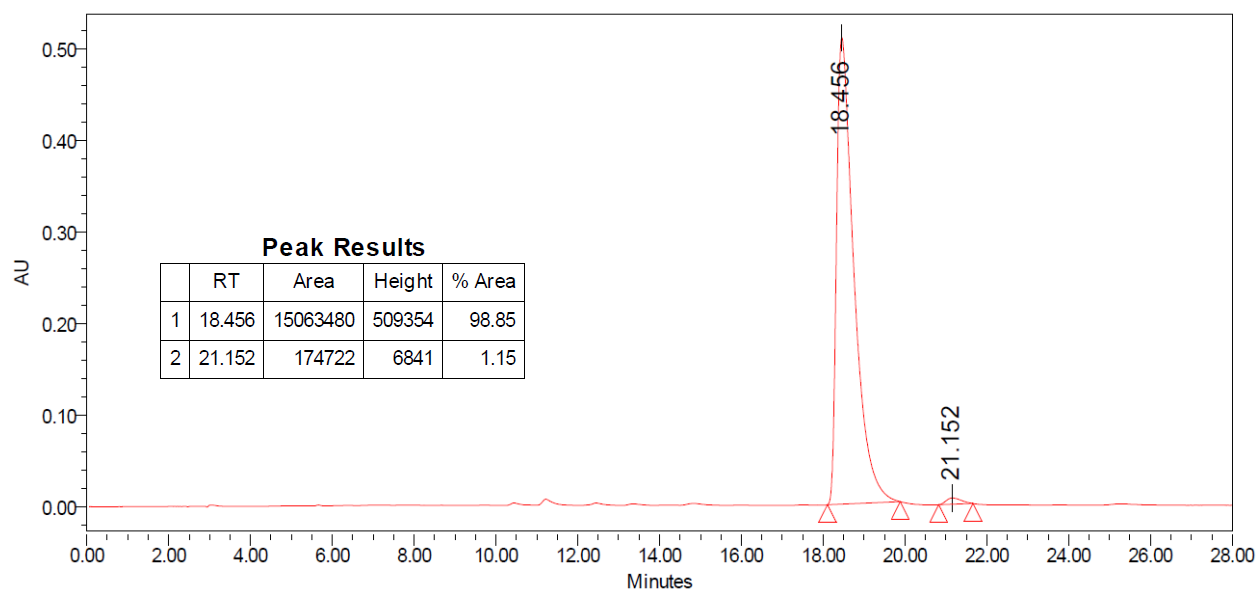


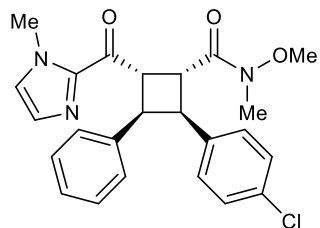
Major Diastereomer
 Run Details: HPLC, Daicel CHIRALPAK AD-H,
 10.00 μ L, gradient 5% to 50% iPrOH/hexanes,
 28 minutes, 1 mL/min, 285 nm

Racemic Chromatogram



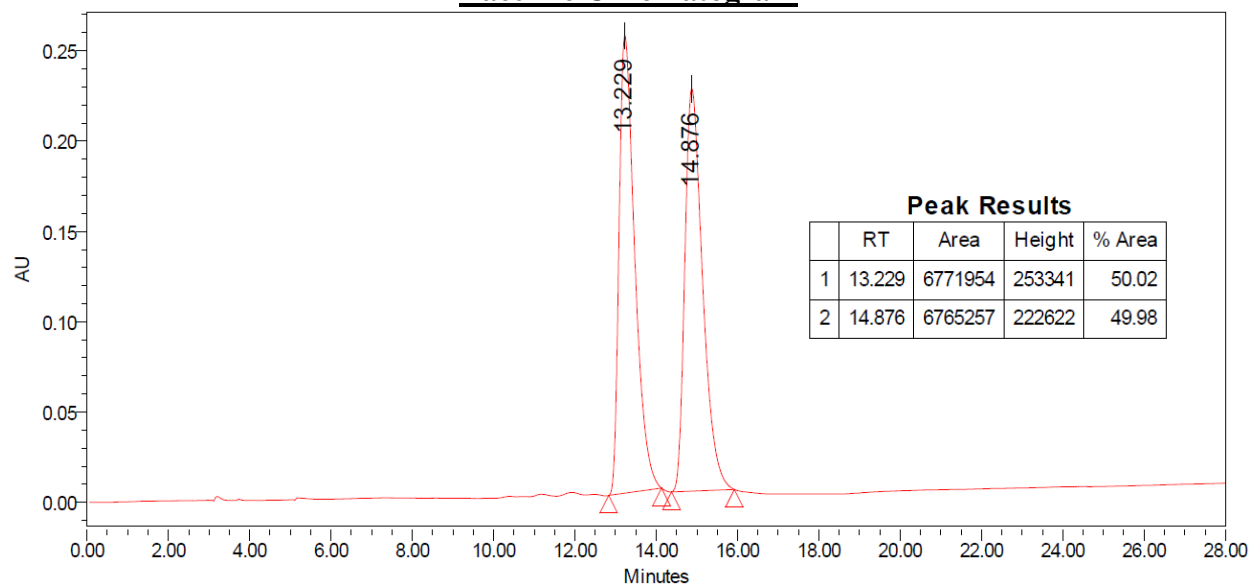
Scalemic Chromatogram



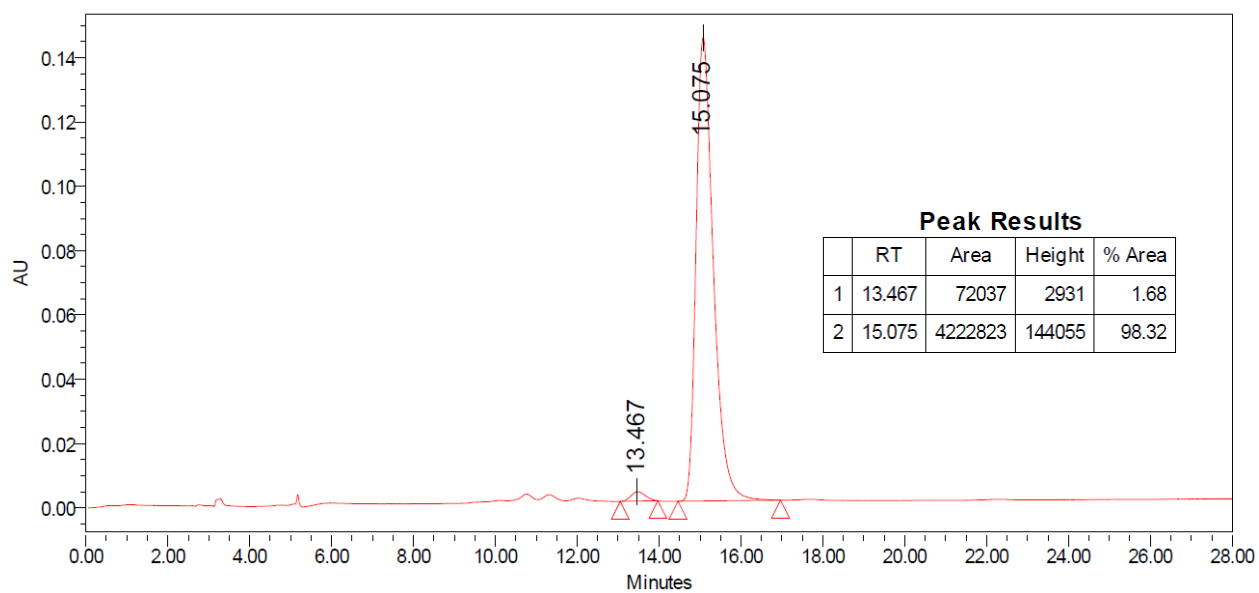


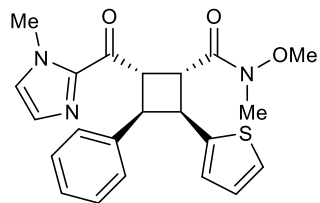
Major Diastereomer
 Run Details: HPLC, Daicel CHIRALPAK OD-H,
 10.00 μ L, gradient 5% to 50% iPrOH/hexanes,
 28 minutes, 1 mL/min, 285 nm

Racemic Chromatogram



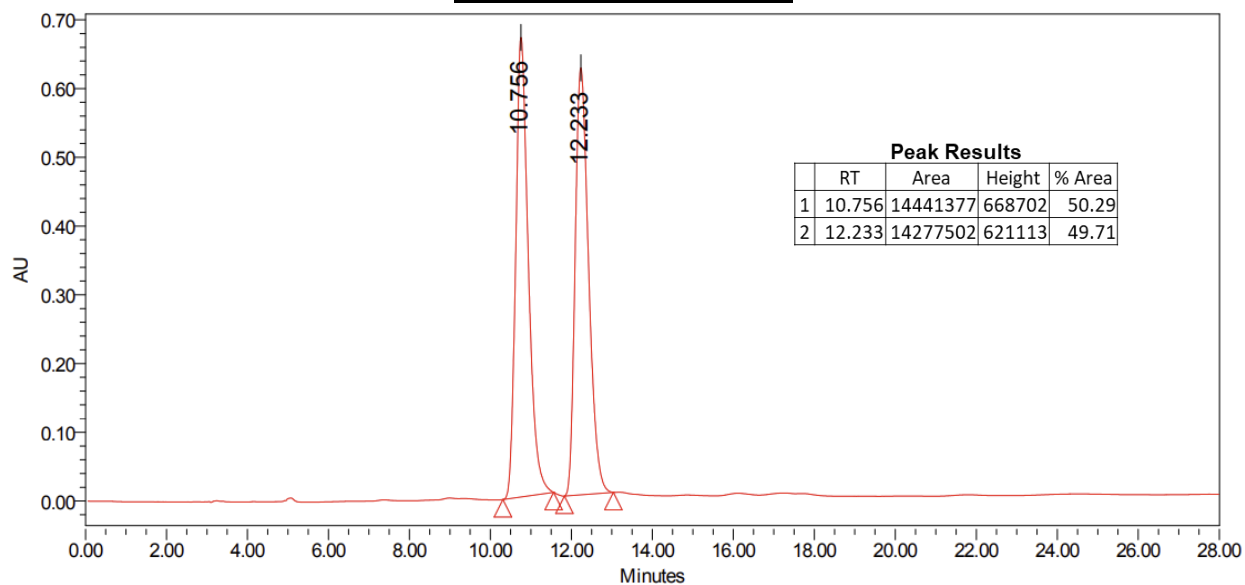
Scalemic Chromatogram



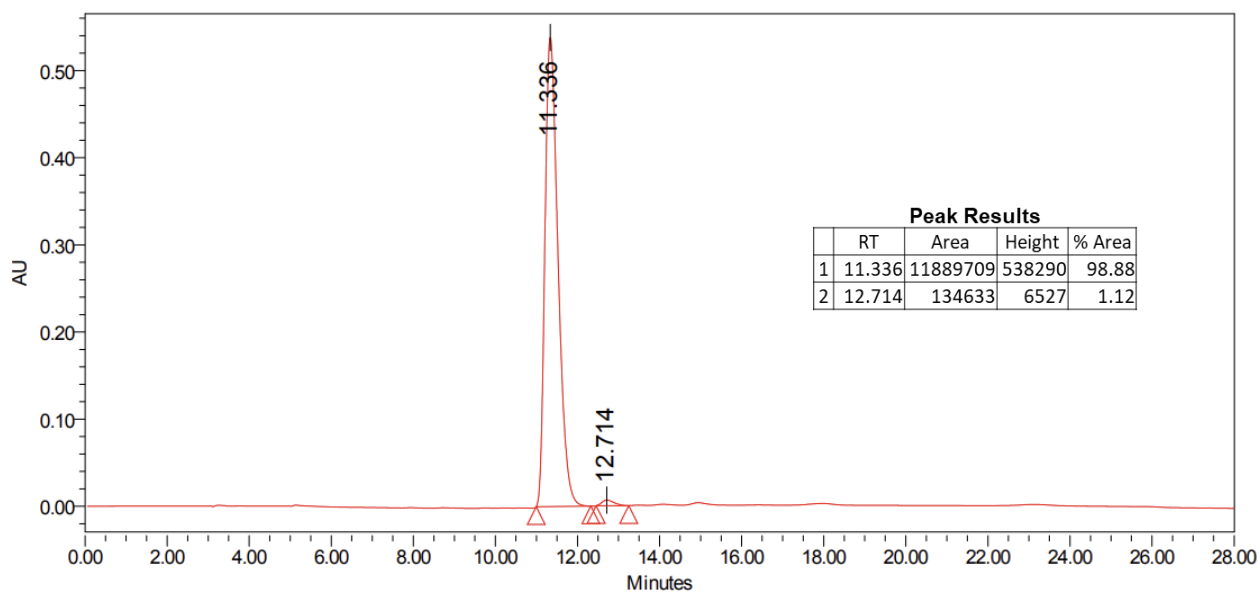


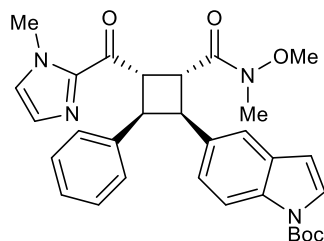
Major Diastereomer
 Run Details: HPLC, Daicel CHIRALPAK AS-H,
 10.00 μ L, gradient 5% to 50% iPrOH/hexanes,
 28 minutes, 1 mL/min, 275 nm.

Racemic Chromatogram



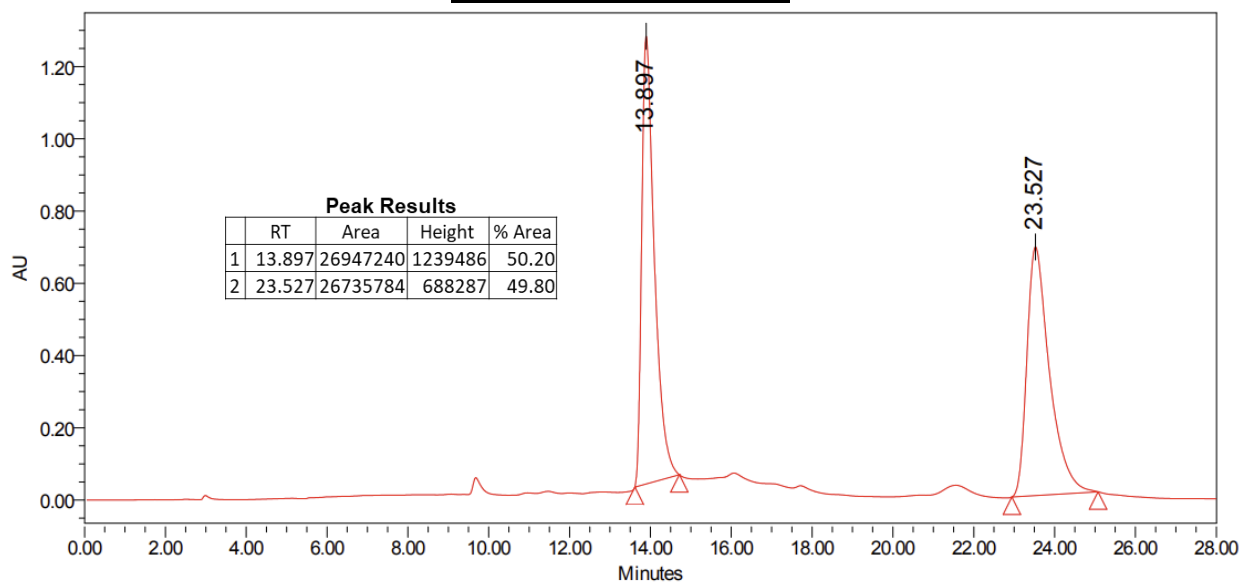
Scalemic Chromatogram



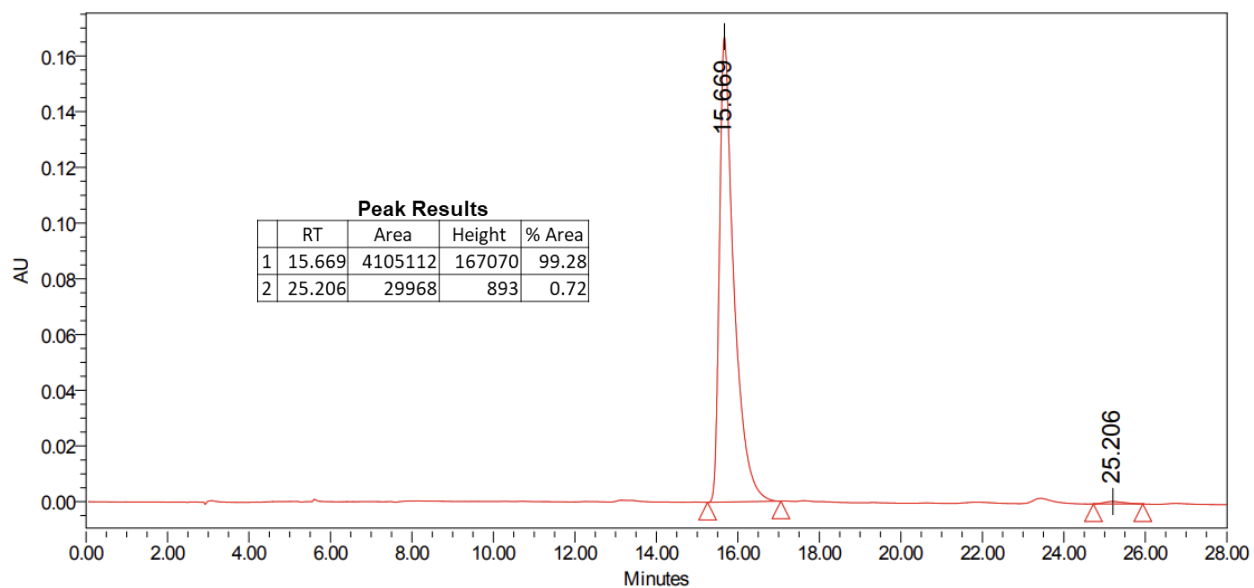


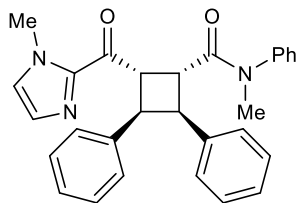
Major Diastereomer
 Run Details: HPLC, Daicel CHIRALPAK AD-H,
 10.00 μ L, gradient 5% to 50% iPrOH/hexanes,
 28 minutes, 1 mL/min, 270 nm.

Racemic Chromatogram



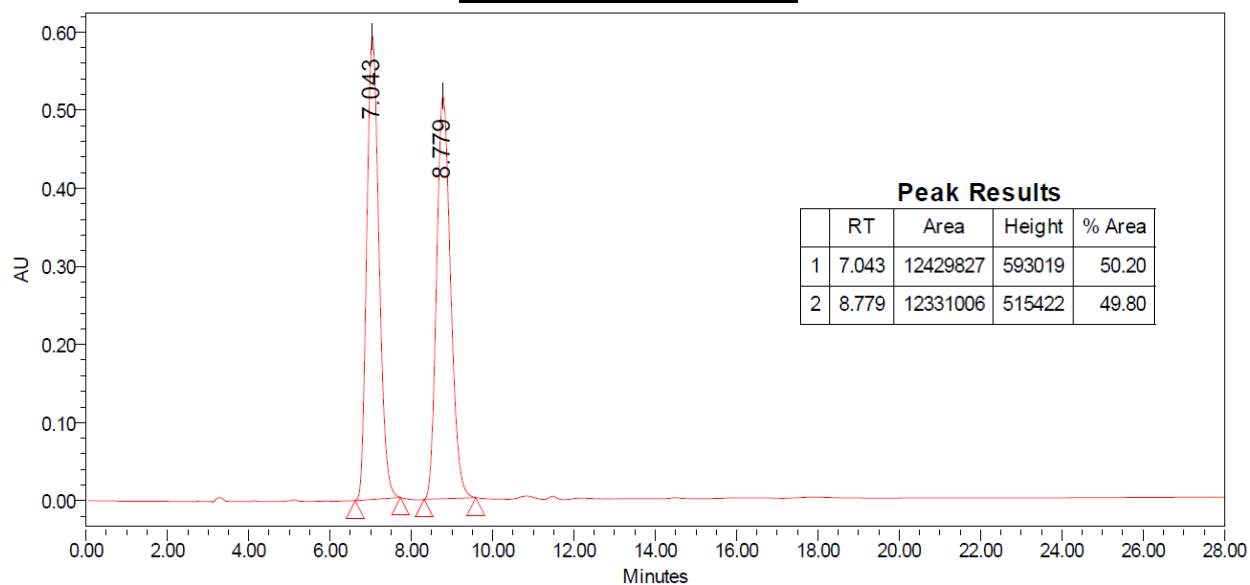
Scalemic Chromatogram



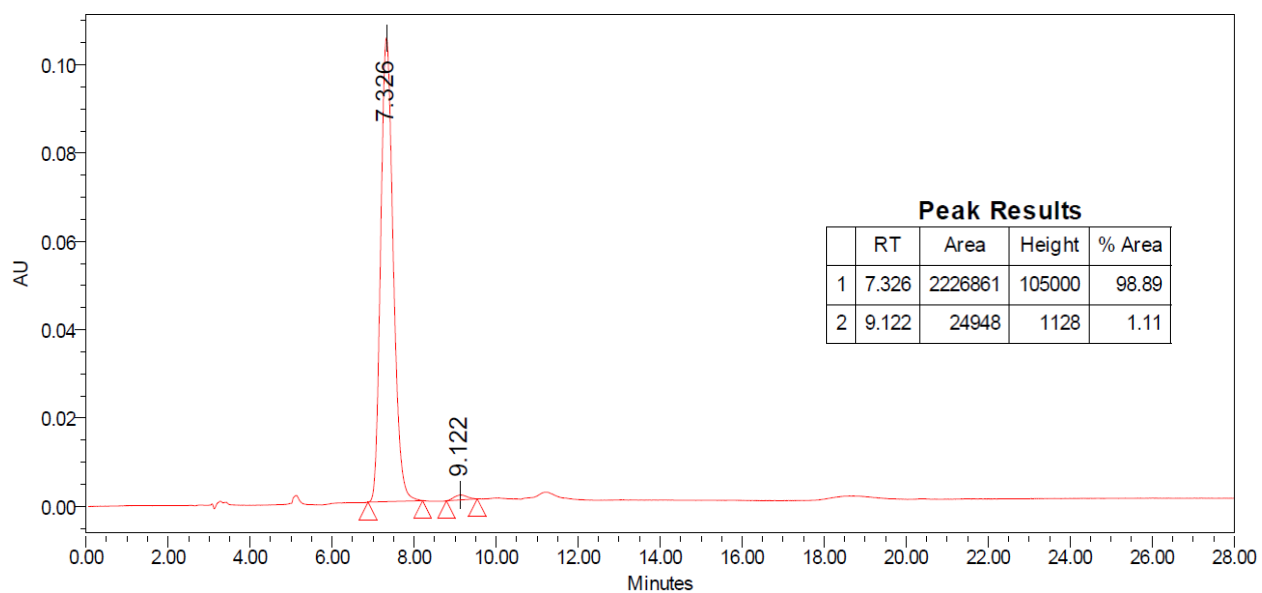


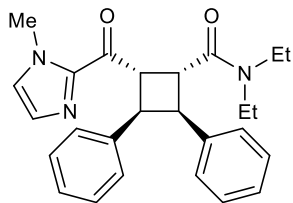
Major Diastereomer
 Run Details: HPLC, Daicel CHIRALPAK AS-H,
 10.00 μ L, gradient 5% to 50% iPrOH/hexanes,
 28 minutes, 1 mL/min, 270 nm

Racemic Chromatogram



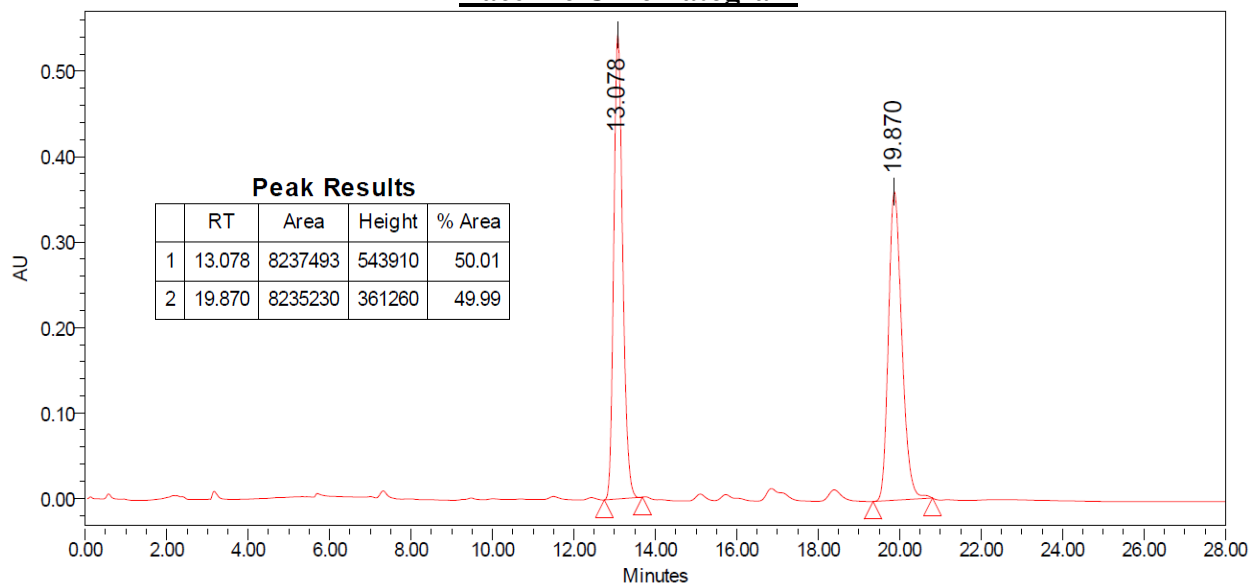
Scalemic Chromatogram



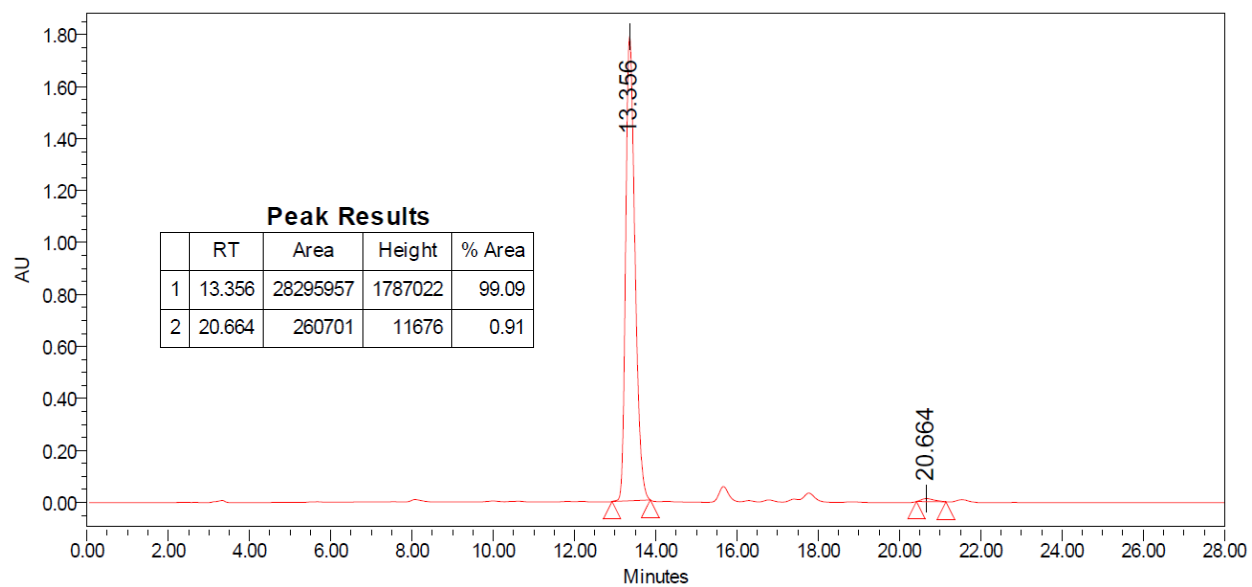


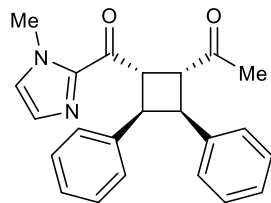
Major Diastereomer
 Run Details: HPLC, Daicel CHIRALPAK AD,
 10.00 μ L, gradient 5% to 50% iPrOH/hexanes,
 28 minutes, 1 mL/min, 270 nm

Racemic Chromatogram



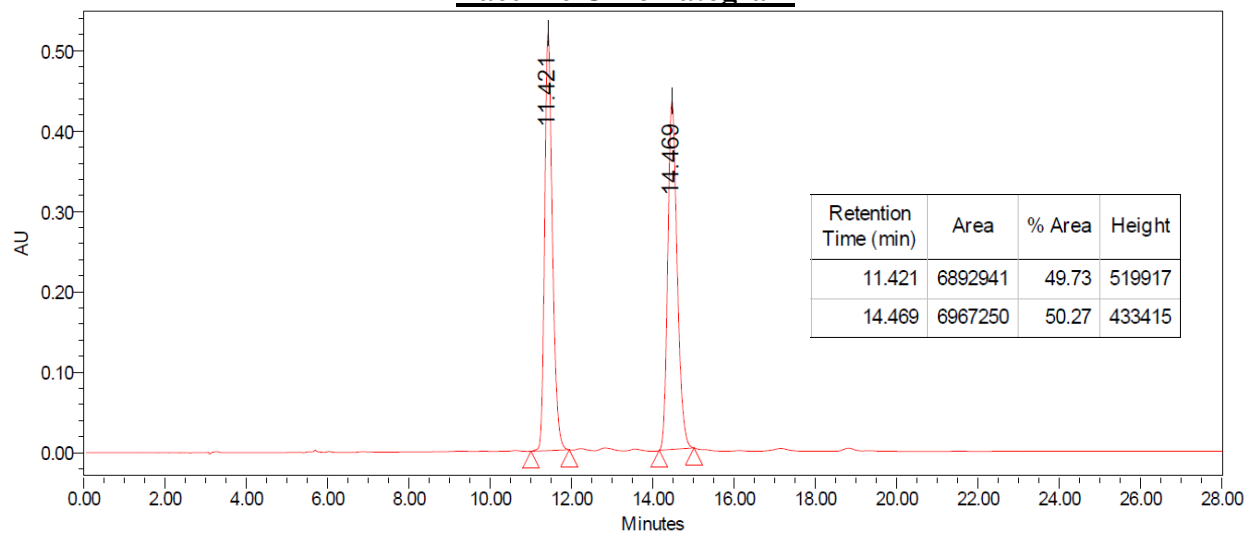
Scalemic Chromatogram



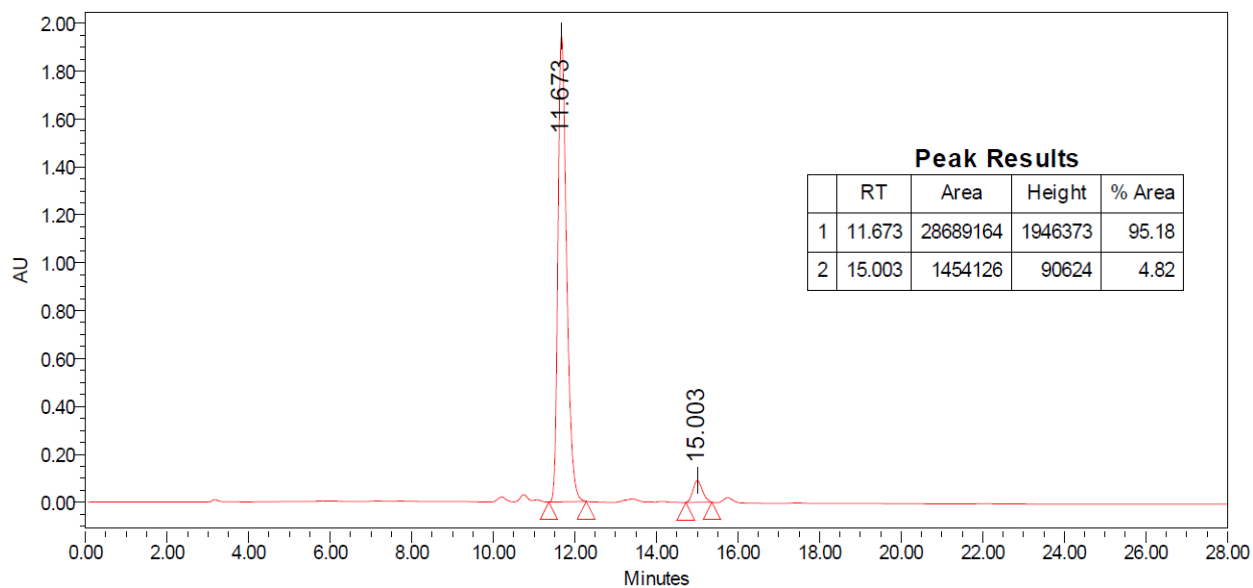


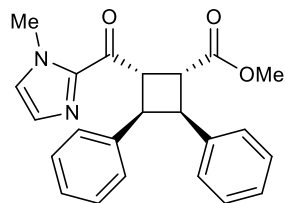
Major Diastereomer
 Run Details: HPLC, Daicel CHIRALPAK AD,
 10.00 μ L, gradient 5% to 50% iPrOH/hexanes,
 28 minutes, 1 mL/min, 285 nm

Racemic Chromatogram



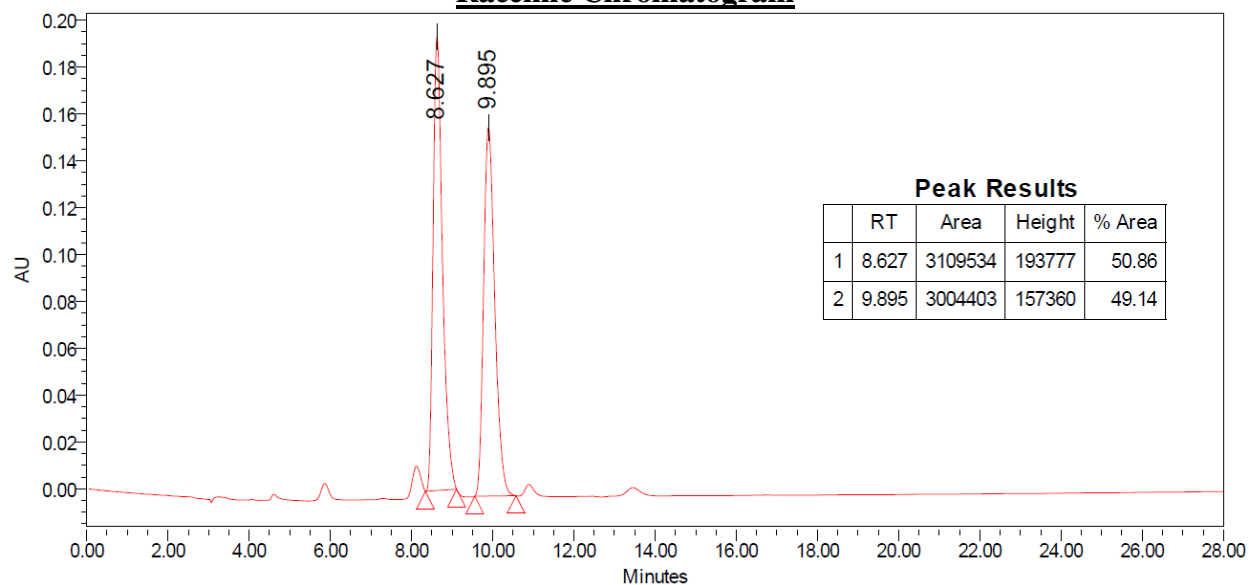
Scalemic Chromatogram



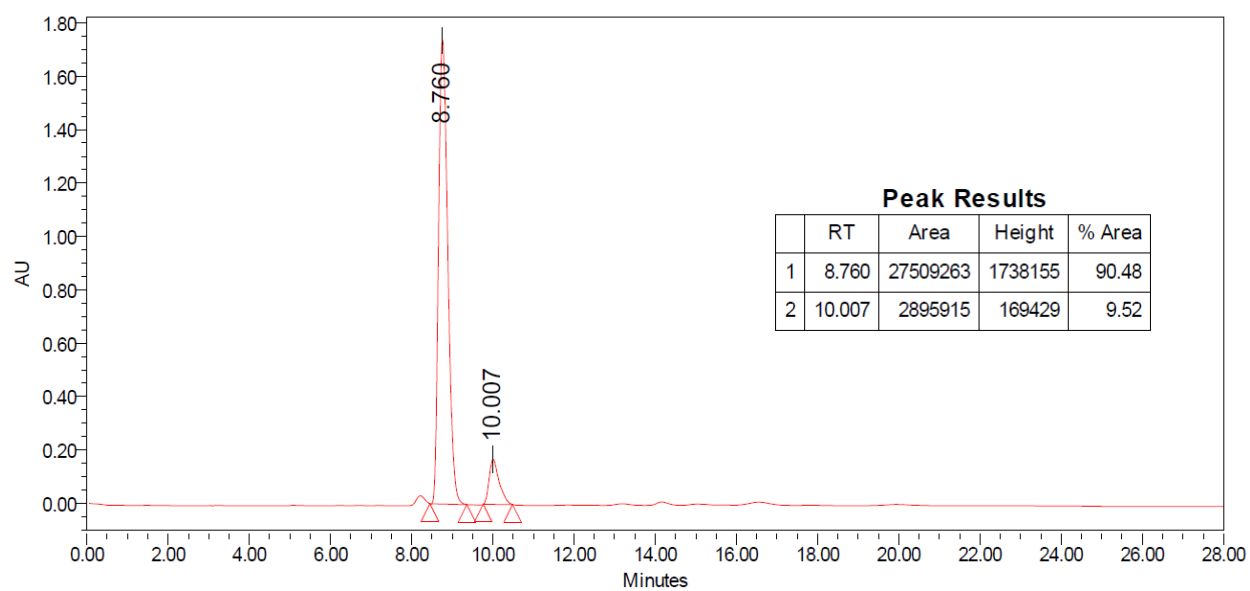


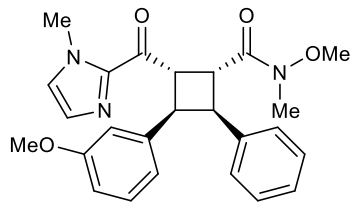
Major Diastereomer
 Run Details: HPLC, Daicel CHIRALPAK AS-H,
 10.00 μ L, gradient 5% to 50% iPrOH/hexanes,
 28 minutes, 1 mL/min, 285 nm

Racemic Chromatogram



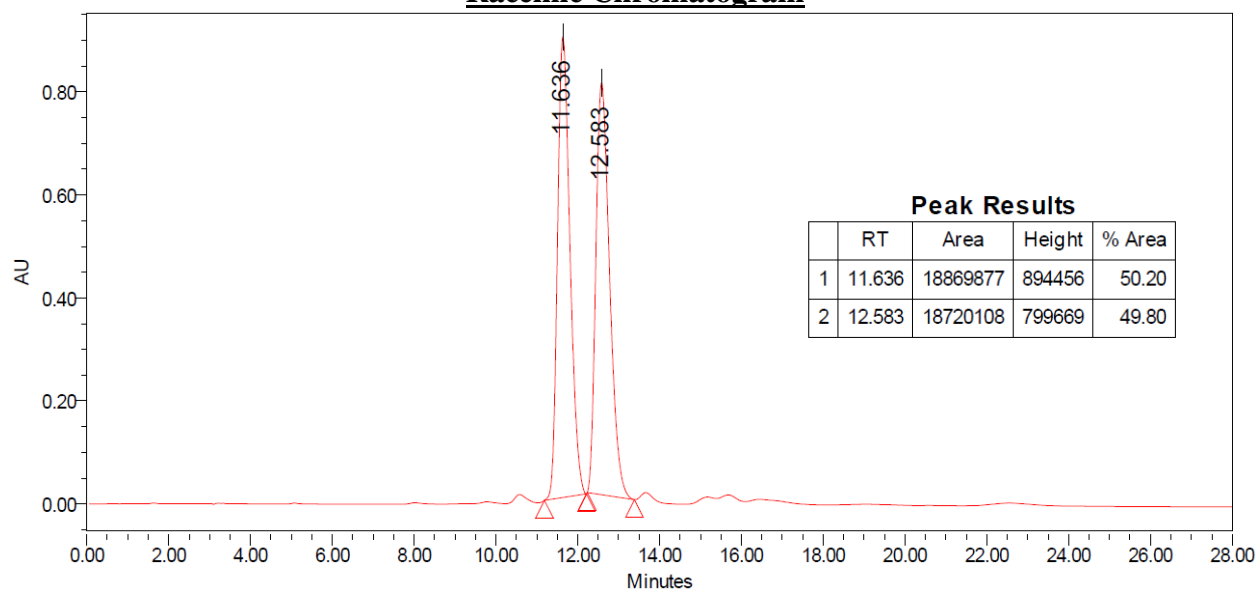
Scalemic Chromatogram



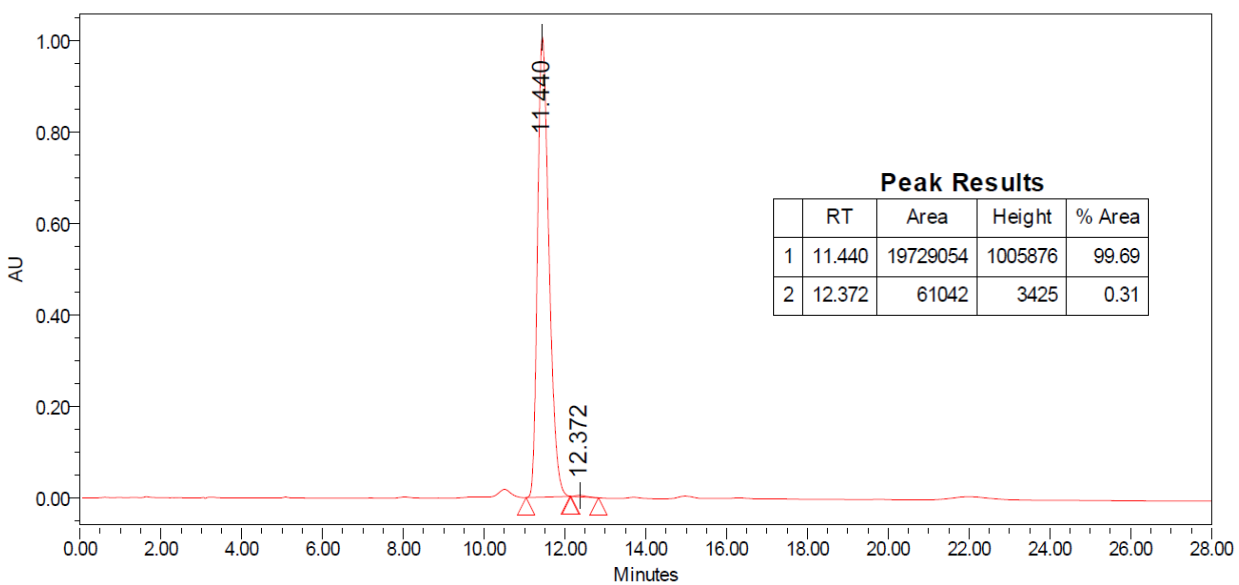


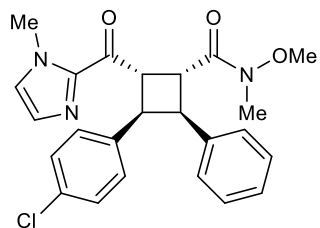
Major Diastereomer
Run Details: HPLC, Daicel CHIRALPAK AS-H,
10.00 μ L, gradient 5% to 50% iPrOH/hexanes,
28 minutes, 1 mL/min, 279 nm

Racemic Chromatogram



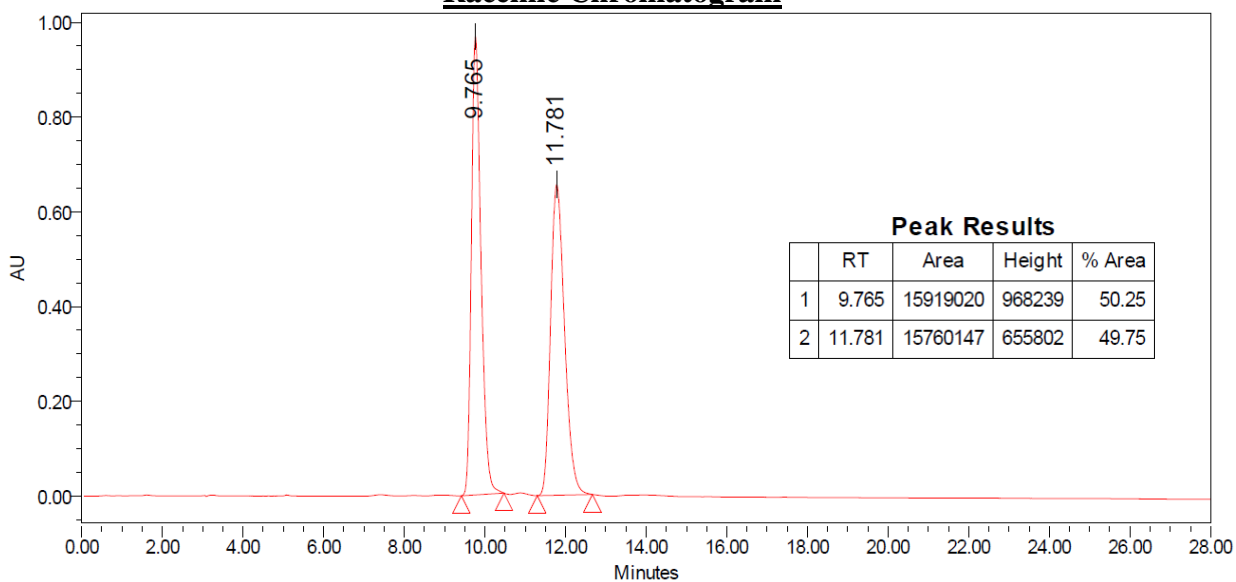
Scalemic Chromatogram



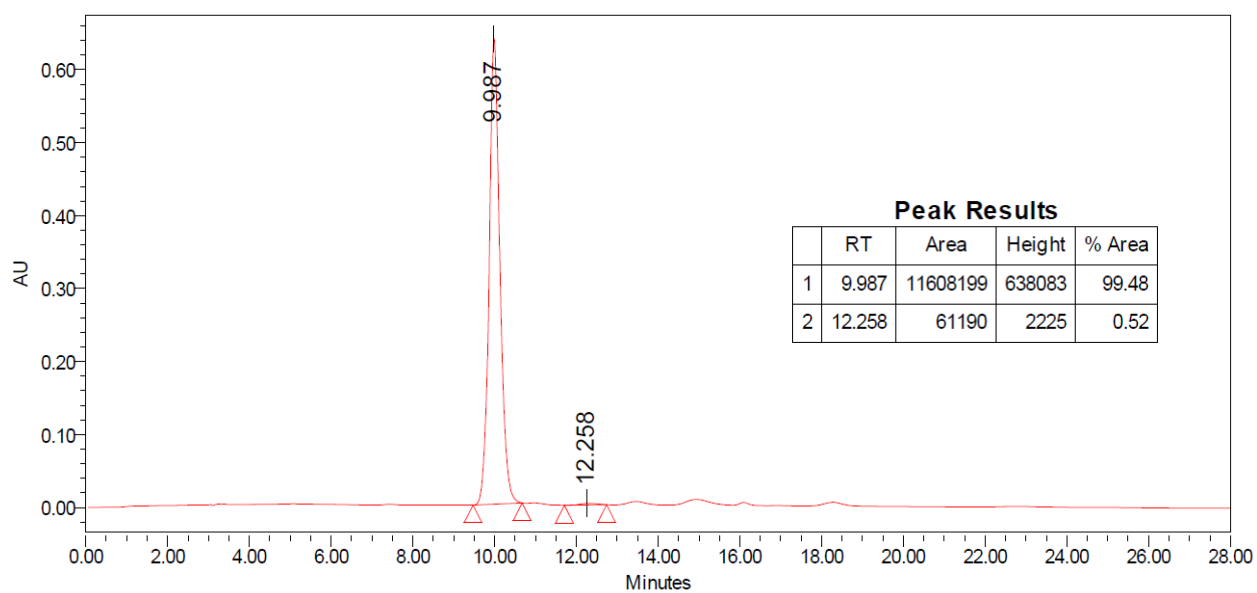


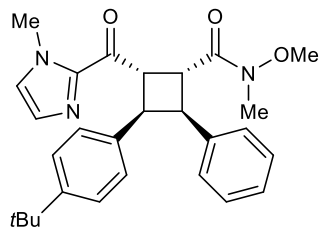
Major Diastereomer
 Run Details: HPLC, Daicel CHIRALPAK AS-H,
 10.00 μ L, gradient 5% to 50% iPrOH/hexanes,
 28 minutes, 1 mL/min, 280 nm

Racemic Chromatogram



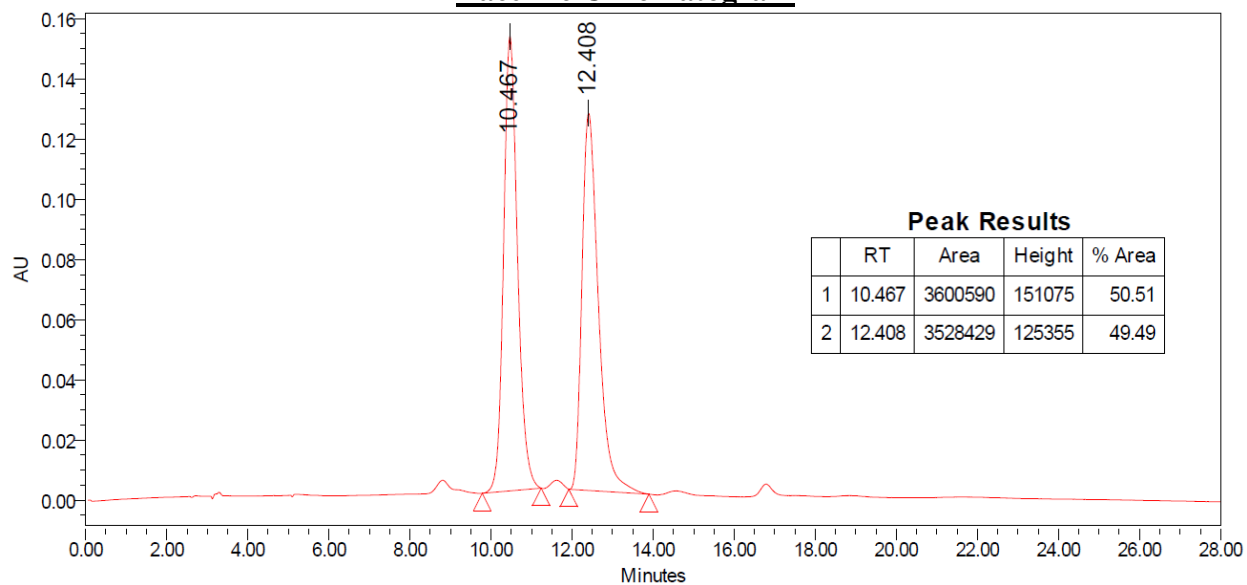
Scalemic Chromatogram



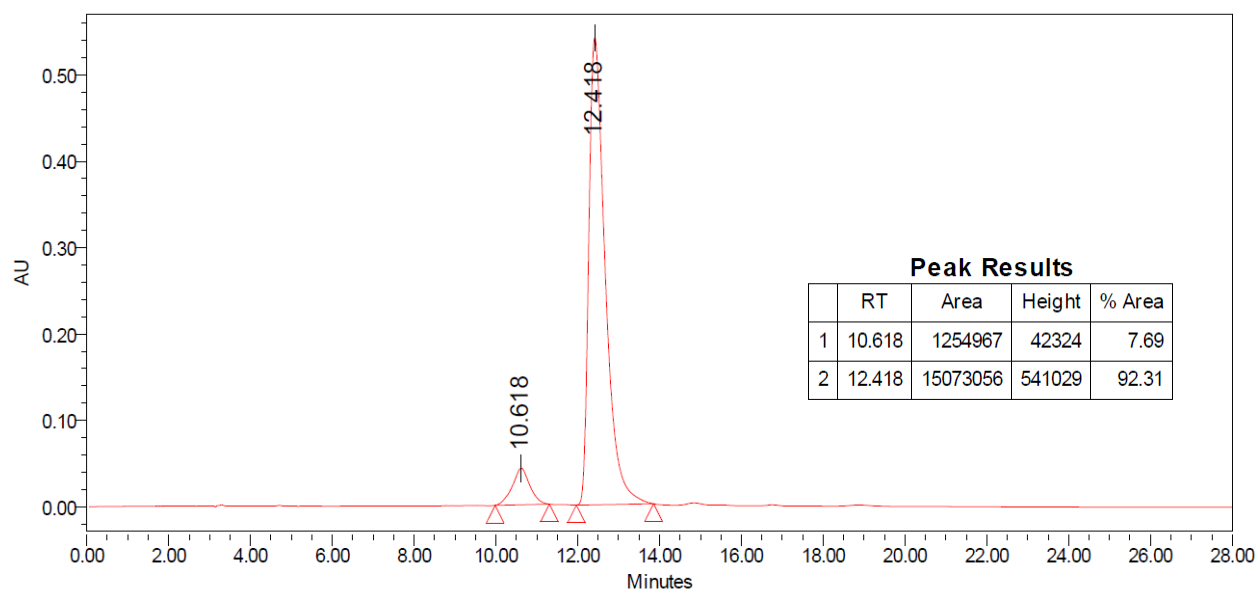


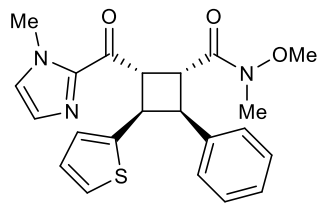
Major Diastereomer
 Run Details: HPLC, Daicel CHIRALPAK OD-H,
 10.00 μ L, gradient 5% to 50% iPrOH/hexanes,
 28 minutes, 1 mL/min, 280 nm

Racemic Chromatogram



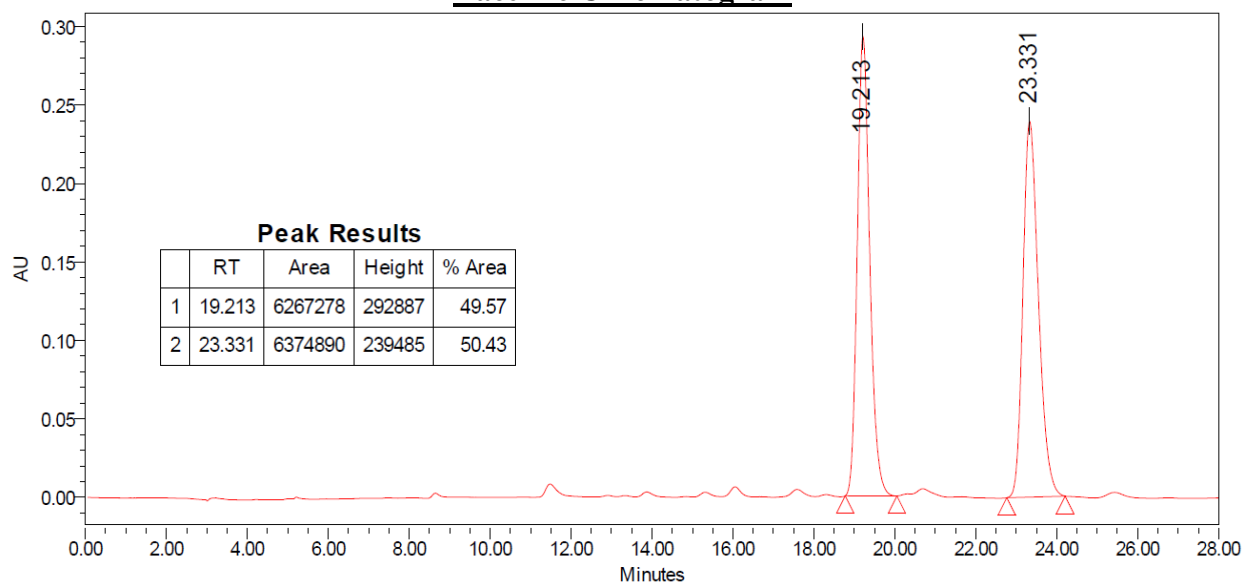
Scalemic Chromatogram



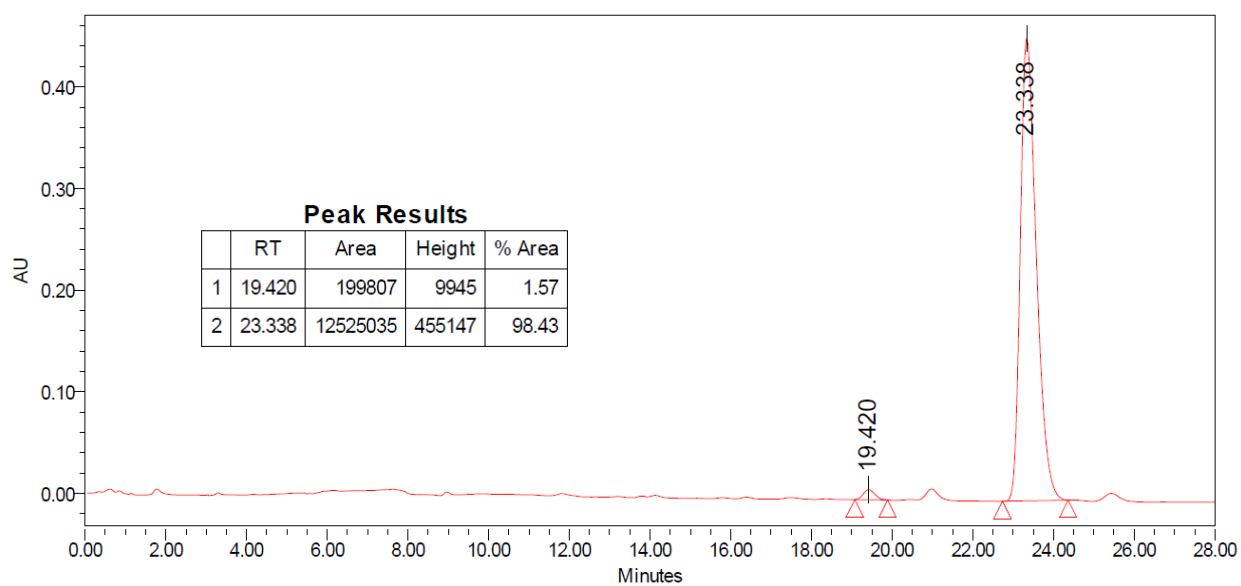


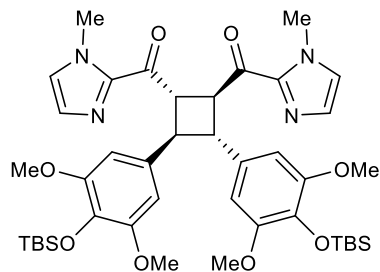
Major Diastereomer
 Run Details: HPLC, Daicel CHIRALPAK AD,
 10.00 μ L, gradient 5% to 50% iPrOH/hexanes,
 28 minutes, 1 mL/min, 280 nm

Racemic Chromatogram



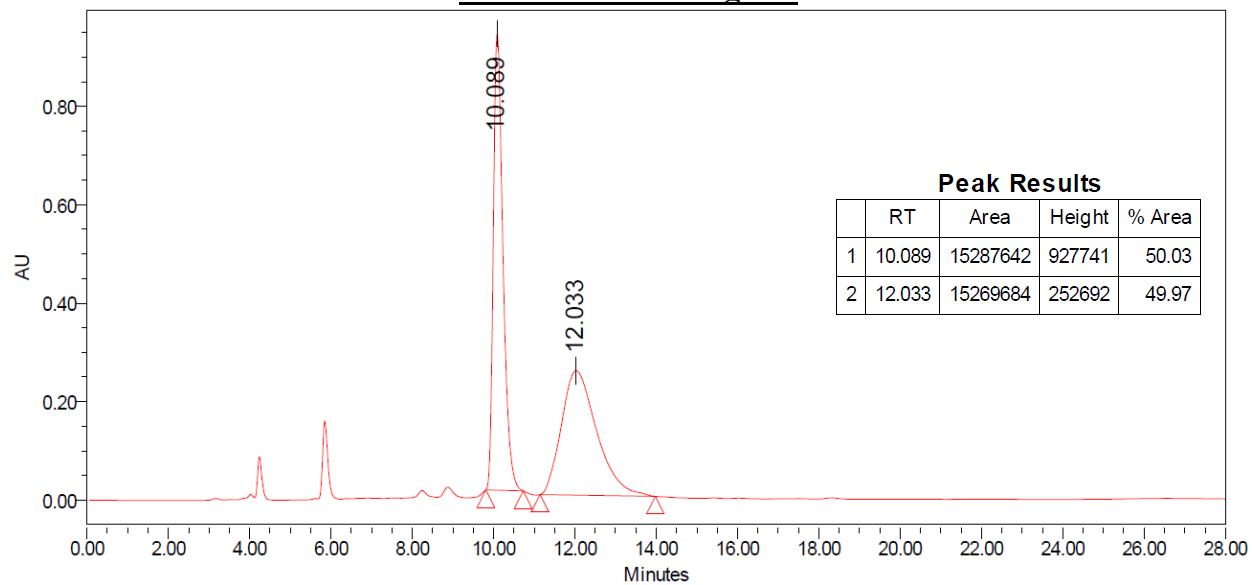
Scalemic Chromatogram



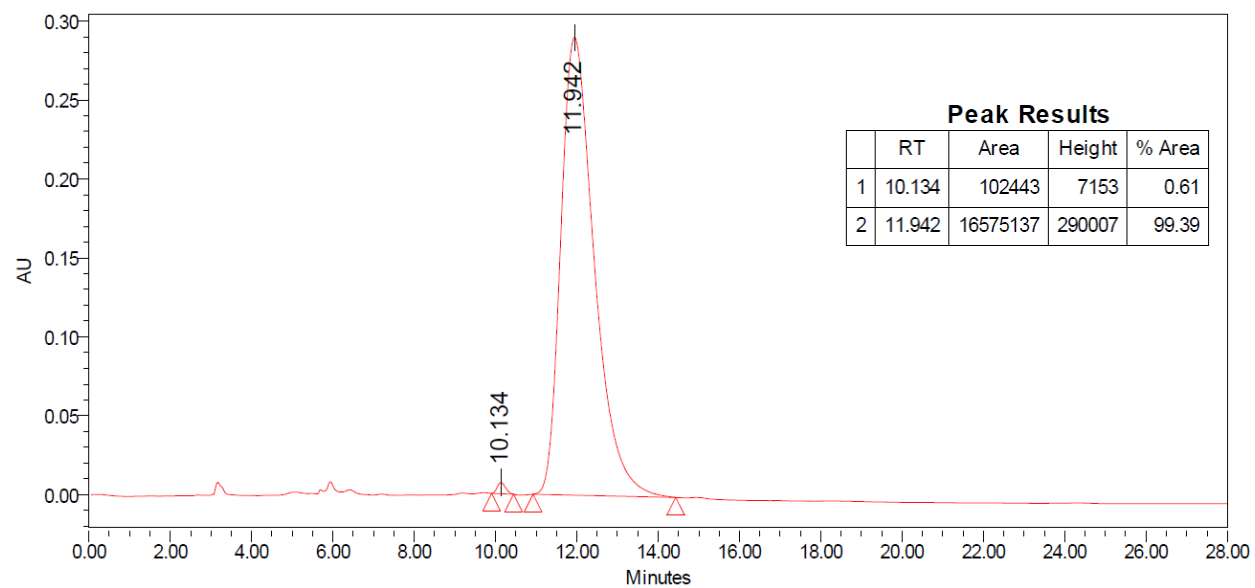


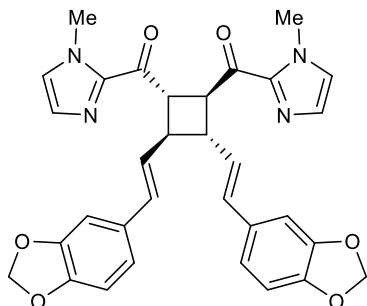
Major Diastereomer
 Run Details: HPLC, Daicel CHIRALPAK AD,
 10.00 μ L, gradient 5% to 50% iPrOH/hexanes,
 28 minutes, 1 mL/min, 285 nm.

Racemic Chromatogram



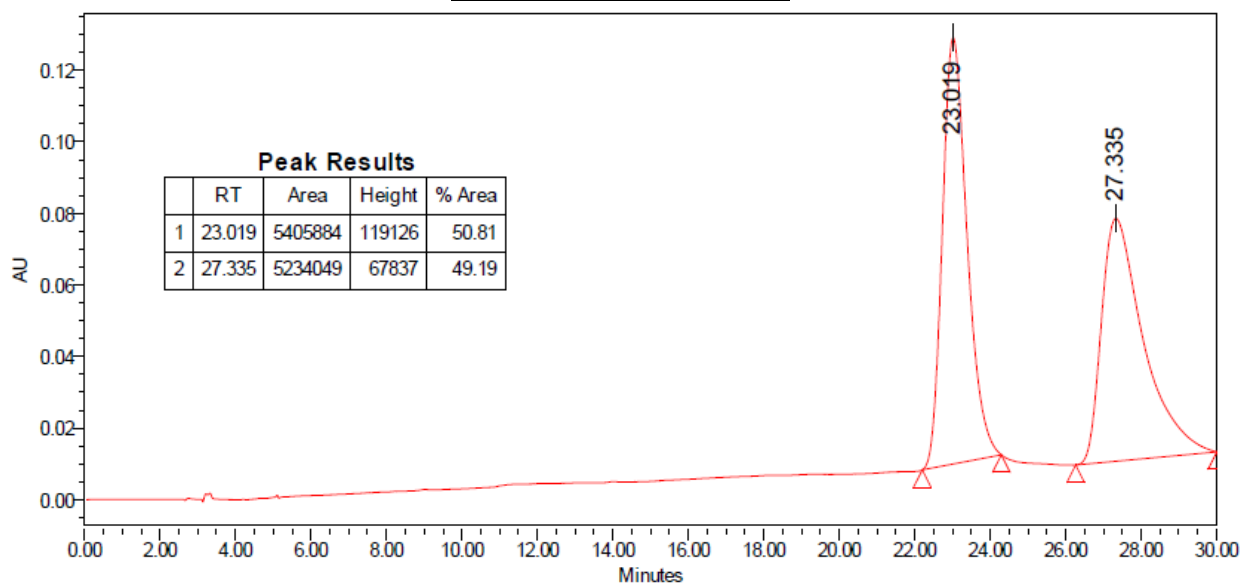
Scalemic Chromatogram



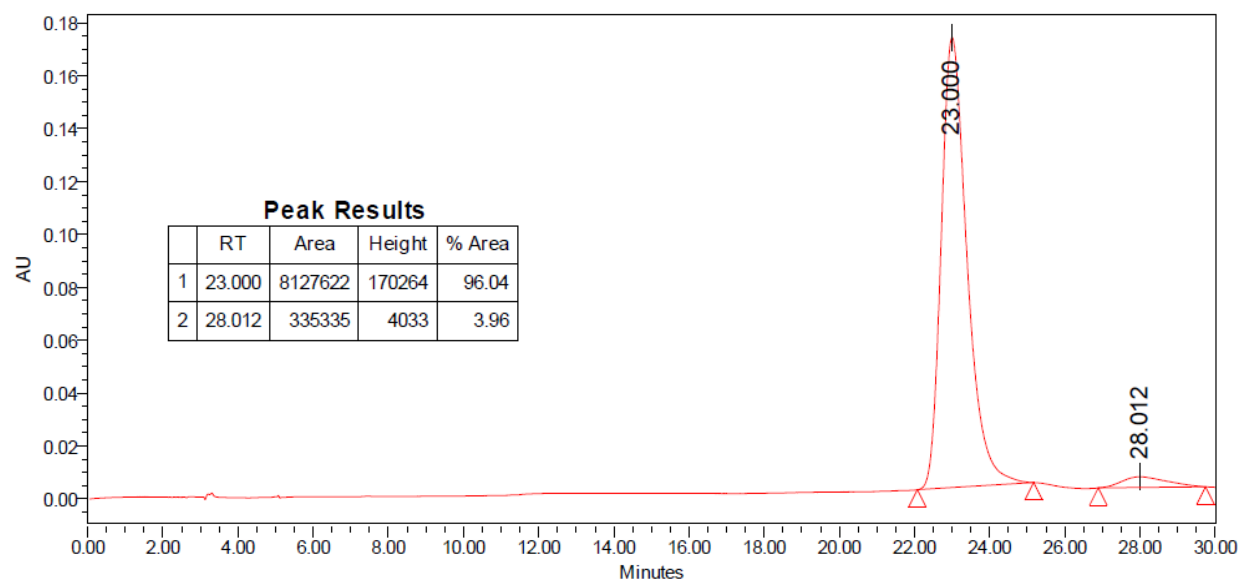


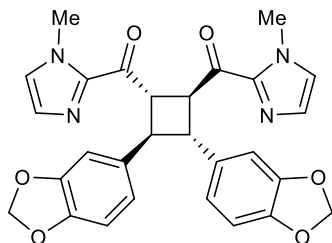
Major Diastereomer
 Run Details: HPLC, Daicel CHIRALPAK OD-H,
 10.00 μ L, gradient 5% to 60% iPrOH/hexanes,
 30 minutes, 1 mL/min, 285 nm

Racemic Chromatogram



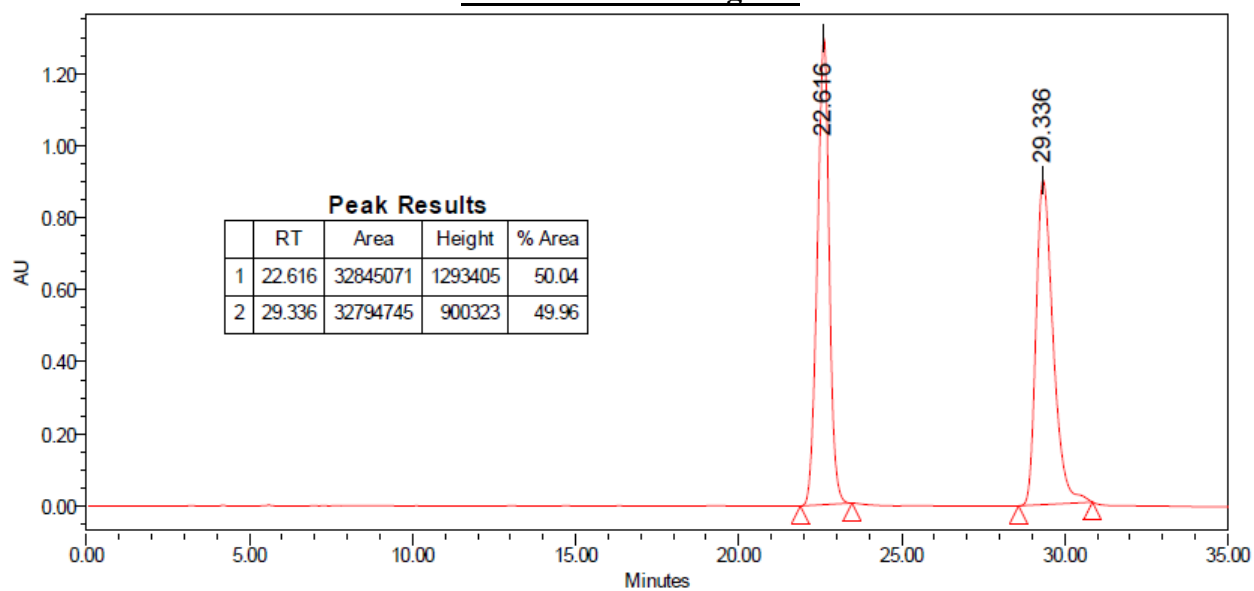
Scalemic Chromatogram



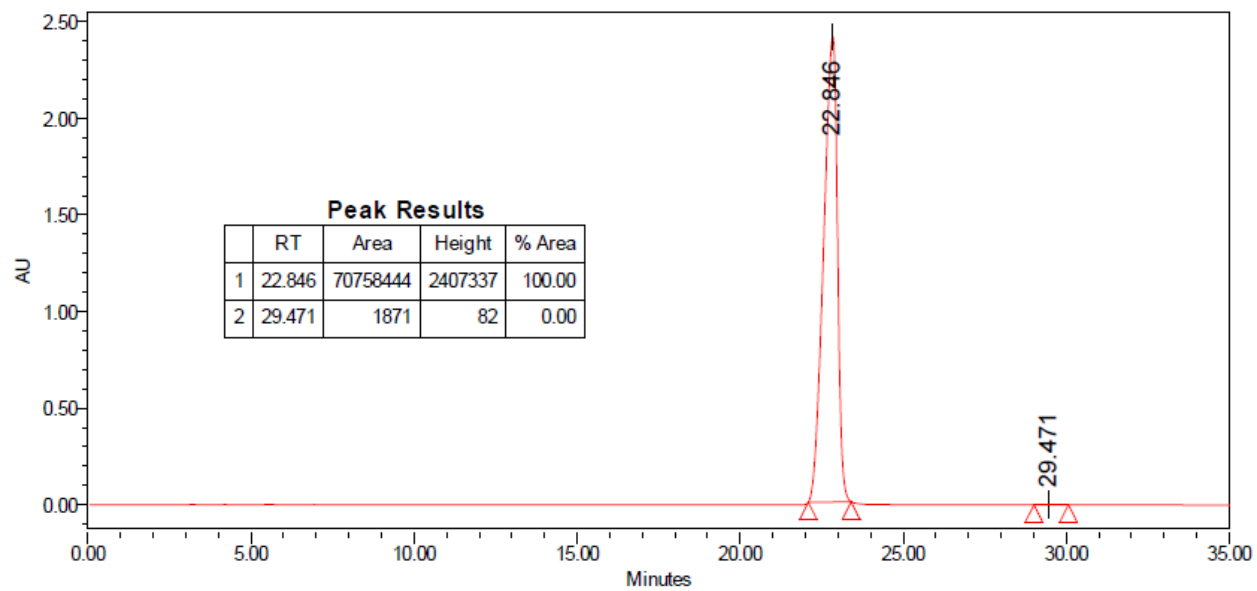


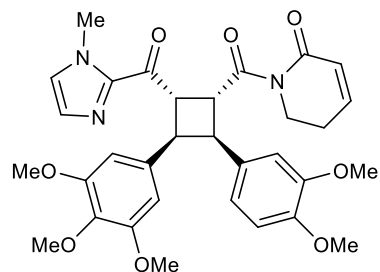
Major Diastereomer
Run Details: HPLC, Daicel CHIRALPAK AD,
10.00 μ L, gradient 5% to 60% iPrOH/hexanes,
35 minutes, 1 mL/min, 280 nm

Racemic Chromatogram



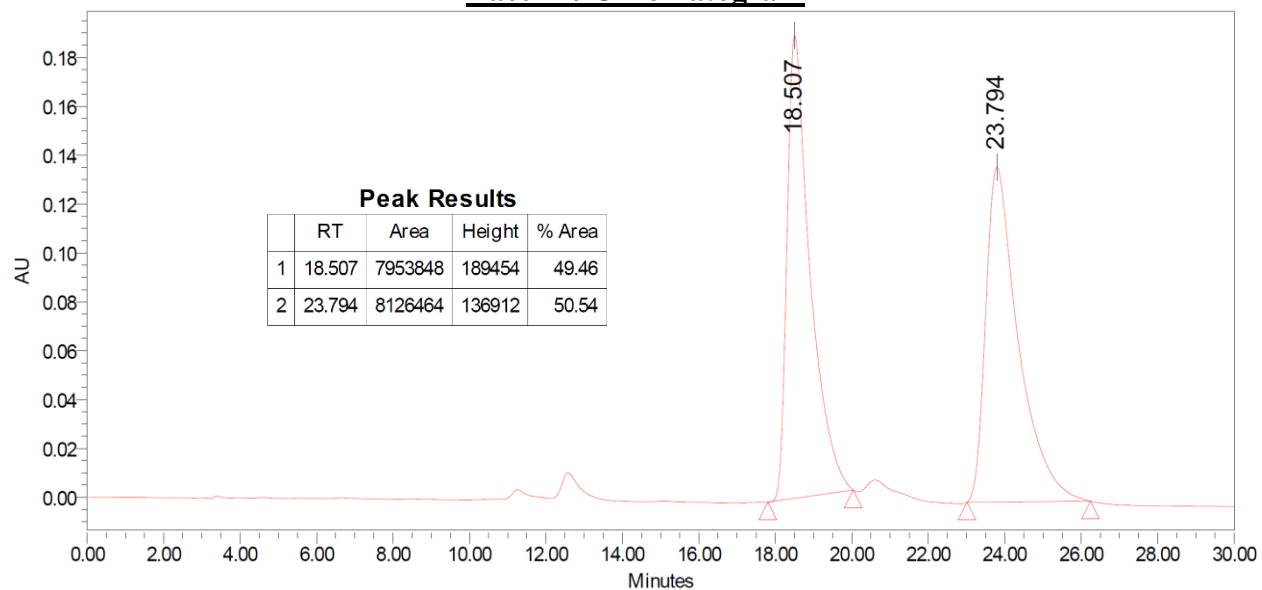
Scalemic Chromatogram



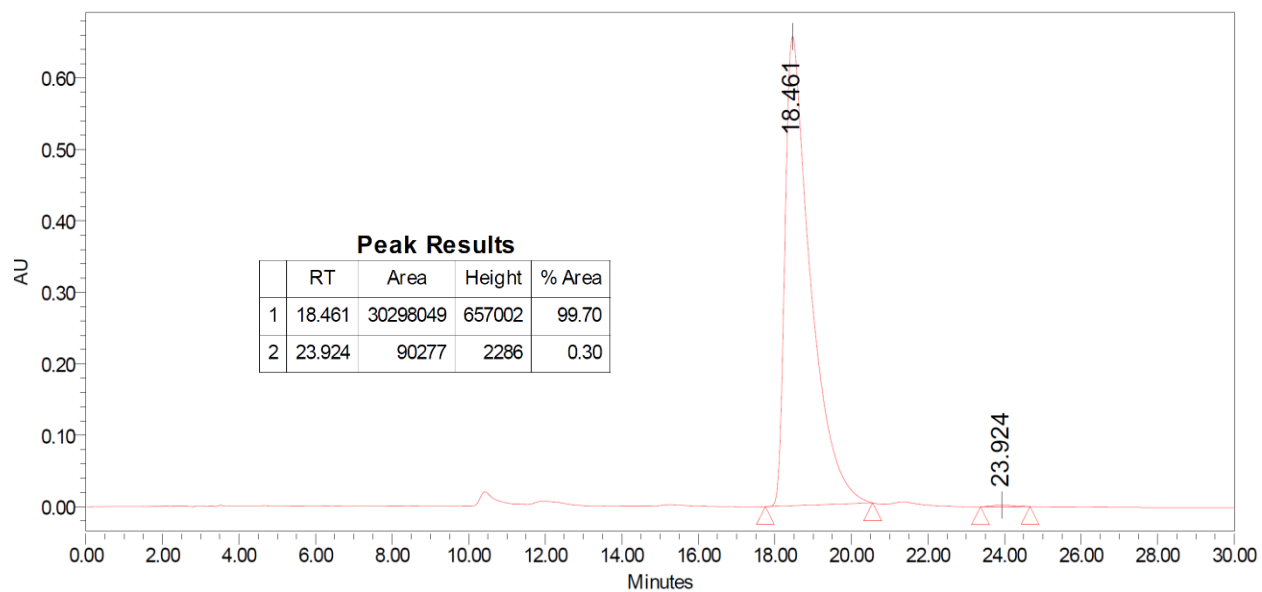


Major Diastereomer
 Run Details: HPLC, Daicel CHIRALPAK AD-H,
 10.00 μ L, gradient 30% to 80% iPrOH/hexanes,
 30 minutes, 1 mL/min, 271 nm

Racemic Chromatogram



Scalemic Chromatogram



3.6 References

- ¹ Reaxys search from January 2023 of truxinate and truxillate natural products.
- ² Yang, P.; Shaojiang Song, Q. J.; Huang, X. [2+2]-Cycloaddition-Derived Cyclobutane Natural Products: Structural Diversity, Sources, Bioactivities, and Biomimetic Syntheses. *Nat. Prod. Rep.* **2023**, Advance Article.
- ³ Dembitsky, V. M. Bioactive Cyclobutane-Containing Alkaloids. *J. Nat. Med.* **2008**, *62*, 1–33.
- ⁴ Dembitsky, V. M. Naturally Occurring Bioactive Cyclobutane-Containing (CBC) Alkaloids in Fungi, Fungal Endophytes, and Plants. *Phytomedicine* **2014**, *21*, 1559–1581.
- ⁵ Sergeiko, A.; Poroikov, V. V.; Hanuš, L. O.; Dembitsky, V. M. Cyclobutane-Containing Alkaloids: Origin, Synthesis, and Biological Activities. *Open Med. Chem. J.* **2008**, *2*, 28–37.
- ⁶ Gutekunst, W. R.; Baran, P. S. Total Synthesis and Structural Revision of the Piperarborenines via Sequential Cyclobutane C–H Arylation. *J. Am. Chem. Soc.* **2011**, *133*, 19076–19079.
- ⁷ Gutekunst, W. R.; Gianatassio, R.; Baran, P. S. Sequential Csp³–H Arylation and Olefination: Total Synthesis of the Proposed Structure of Pipericyclobutanamide A. *Angew. Chem. Int. Ed.* **2012**, *51*, 7507–7510.
- ⁸ Beck, J. C.; Lacker, C. R.; Chapman, L. M.; Reisman, S. E. A Modular Approach to Prepare Enantioenriched Cyclobutanes: Synthesis of (+)-rumphellaone A. *Chem. Sci.* **2019**, *10*, 2315–2319.
- ⁹ Chapman, L. M.; Beck, J. C.; Wu, L.; Reisman, S. E. Enantioselective Total Synthesis of (+)-Psiguadial B. *J. Am. Chem. Soc.* **2016**, *138*, 9803–9806.
- ¹⁰ Panish, R. A.; Chintala, S. R.; Fox, J. M. A Mixed-Ligand Chiral Rhodium(II) Catalyst Enables the Enantioselective Total Synthesis of Piperarborenine B. *Angew. Chem. Int. Ed.* **2016**, *55*, 4983–4987.
- ¹¹ Poplata, S.; Tröster, A.; Zou, Y.-Q.; Bach, T. Recent Advances in the Synthesis of Cyclobutanes by Olefin [2+2] Photocycloaddition Reactions. *Chem. Rev.* **2016**, *116*, 9748–9815.
- ¹² Filho, R. B.; De Souza, M. P.; Mattos, M. E. O. Piplartine-Dimer A, a New Alkaloid from *Piper tuberculatum*. *Phytochemistry* **1981**, *20*, 345–346.

-
- ¹³ Lewis, F. D.; Quillen, S. L.; Hale, P. D.; Oxman, J. D. Lewis Acid Catalysis of Photochemical Reactions. 7. Photodimerization and Cross-Cycloaddition of Cinnamic Esters. *J. Am. Chem. Soc.* **1988**, *110*, 1261–1267.
- ¹⁴ Großkopf, J.; Kratz, T.; Rigotti, T.; Bach, T. Enantioselective Photochemical Reactions Enabled by Triplet Energy Transfer. *Chem. Rev.* **2022**, *122*, 1626–1653.
- ¹⁵ Genzink, M. J.; Kidd, J. B.; Swords, W. B.; Yoon, T. P. Chiral Photocatalyst Structures in Asymmetric Photochemical Synthesis. *Chem. Rev.* **2022**, *122*, 1654–1716.
- ¹⁶ Brenninger, C.; Jolliffe, J. D.; Bach, T. Chromophore Activation of α,β -Unsaturated Carbonyl Compounds and Its Application to Enantioselective Photochemical Reactions. *Angew. Chem. Int. Ed.* **2018**, *57*, 14338–14349.
- ¹⁷ Blum, T. R.; Miller, Z. D.; Bates, D. M.; Guzei, I. A.; Yoon, T. P. Enantioselective Photochemistry through Lewis Acid-Catalyzed Triplet Energy Transfer. *Science* **2016**, *354*, 1391–1395.
- ¹⁸ Skubi, K. L.; Kidd, J. B.; Jung, H.; Guzei, I. A.; Baik, M.-H.; Yoon, T. P. Enantioselective Excited-State Photoreactions Controlled by a Chiral Hydrogen-Bonding Iridium Sensitizer. *J. Am. Chem. Soc.* **2017**, *139*, 17186–17192.
- ¹⁹ Sherbrook, E. M.; Jung, H.; Cho, D.; Baik, M.-H.; Yoon, T. P. Brønsted Acid Catalysis of Photosensitized Cycloadditions. *Chem. Sci.* **2020**, *11*, 856–861.
- ²⁰ Sherbrook, E. M.; Genzink, M. J.; Park, B.; Guzei, I. A.; Baik, M.-H.; Yoon, T. P. *Nat. Commun.* **2021**, *12*, 5735.
- ²¹ Davies, D. H.; Hall, J.; Smith, E. H. Non-Oxidative Conversion of Ketone Carbonyls into Carboxy Carbonyls. Comparison of 2-Acylthiazoles and 2-Acylimidazoles in the Aldol Condensation and the Stereospecific Cleavage of an Example of the Latter to a β -Hydroxy Ester via the Azolium Salt. *J. Chem. Soc., Perkin Trans. 1* **1991**, 2691–2698.
- ²² Miyashita, A.; Suzuki, Y.; Nagasaki, I.; Ishiguro, C.; Iwamoto, K.-I.; Higashino, T. Catalytic Action of Azolium Salts. VIII. Oxidative Aroylation with Arenecarbaldehydes Catalyzed by 1,3-Dimethylbenzimidazolium Iodide. *Chem. Pharm. Bull.* **1997**, *45*, 1254–1258.
- ²³ Evans, D. A.; Fandrick, K. R.; Song, H.-J. Enantioselective Friedel–Crafts Alkylations of α,β -Unsaturated 2-Acyl Imidazoles Catalyzed by Bis(oxazolonyl)pyridine–Scandium(III) Triflate Complexes. *J. Am. Chem. Soc.* **2005**, *127*, 8942–8943.

-
- ²⁴ Xi, Y.-F.; Liu, S.-F.; Hong, W.; Song, X.-Y.; Lou, L.-L.; Zhou, L.; Yao, G.-D.; Lin, B.; Wang, X.-B.; Huang, X.-X.; Song, S.-J. Discovery of Cycloneolignan Enantiomers from *Isatis indigotica* Fortune with Neuroprotective Effects Against MPP⁺-Induced SH-SY5Y Cell Injury. *Bioorg. Chem.* **2019**, *88*, 102926.
- ²⁵ Chen, Q.; Lan, H.-Y.; Peng, W.; Rahman, K.; Liu, Q.-C.; Luan, X.; Zhang, H. *Isatis indigotica*: a review of phytochemistry, pharmacological activities and clinical applications. *J. Pharm. Pharmacol.* **2021**, *73*, 1137–1150.
- ²⁶ Chai, T.; Zhang, W.-H.; Jiao, H.; Qiang, Y. Hydroxycinnamic Acid Amide Dimers from Goji Berry and Their Potential Anti-AD Activity. *Chem. Biodiversity* **2021**, *18*, e202100436.
- ²⁷ Wei, K.; Li, W.; Koike, K.; Chen, Y.; Nikaido, T. Nigramides A–S, Dimeric Amide Alkaloids from the Roots of *Piper nigrum*. *J. Org. Chem.* **2005**, *70*, 1164–1176.
- ²⁸ Subehan; Usia, T.; Kadota, S.; Tezuka, Y. Mechanism-Based Inhibition of Human Liver Microsomal Cytochrome P450 2D6 (CYP2D6) by Alkamides of *Piper nigrum*. *Planta Med.* **2006**, *72*, 527–532.
- ²⁹ Epstein, W. W.; Netz, D. F.; Seidel, J. L. Isolation of Piperine from Black Pepper. *J. Chem. Ed.* **1993**, *70*, 598–599.
- ³⁰ Colomer, I.; Barcelos, R. C.; Donohoe, T. J. Catalytic Hypervalent Iodine Promoters Lead to Styrene Dimerization and the Formation of Tri- and Tetrasubstituted Cyclobutanes. *Angew. Chem. Int. Ed.* **2016**, *55*, 4748–4752.
- ³¹ Daub, M. E.; Jung, H.; Lee, B. J.; Won, J.; Baik, M.-H.; Yoon, T. P. Enantioselective [2+2] Cycloadditions of Cinnamate Esters: Generalizing Lewis Acid Catalysis of Triplet Energy Transfer. *J. Am. Chem. Soc.* **2019**, *141*, 9543–9547.
- ³² Murray, P. R. D.; Bussink, W. M. M.; Davies, G. H. M.; van der Mei, F. W.; Antropow, A. H.; Edwards, J. T.; D'Agostino, L. A.; Ellis, J. M.; Hamann, L. G.; Romanov-Michailidis, F.; Knowles, R. R. Intermolecular Crossed [2+2] Cycloaddition Promoted by Visible-Light Triplet Photosensitization: Expedient Access to Polysubstituted 2-Oxaspiro[3.3]heptanes. *J. Am. Chem. Soc.* **2021**, *143*, 4055–4063.
- ³³ Rykaczewski, K. A.; Schindler, C. S. Visible-Light-Enabled Paternò–Büchi Reaction via Triplet Energy Transfer for the Synthesis of Oxetanes. *Org. Lett.* **2020**, *22*, 6516–6519.
- ³⁴ Zheng, J.; Dong, X.; Yoon, T. P. Divergent Photocatalytic Reactions of α -Ketoesters under Triplet Sensitization and Photoredox Conditions. *Org. Lett.* **2020**, *22*, 6520–6525.

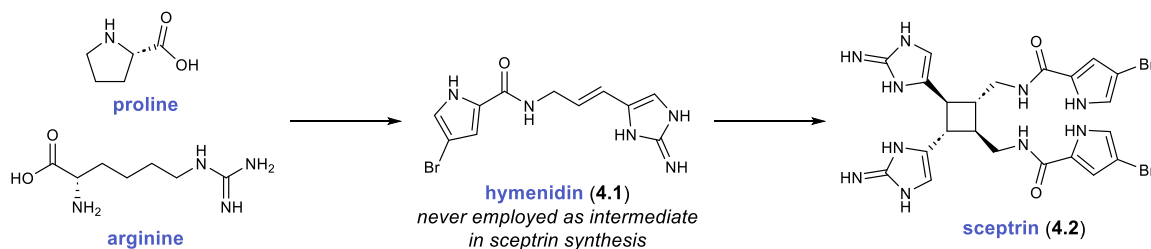
-
- ³⁵ Becker, M. R.; Wearing, E. R.; Schindler, C. S. Synthesis of Azetidines via Visible-Light-Mediated Intermolecular [2+2] Photocycloadditions. *Nat. Chem.* **2020**, *12*, 898–905.
- ³⁶ Pagire, S. K.; Hossain, A.; Traub, L.; Kerres, S.; Reiser, O. Photosensitized Regioselective [2+2]-Cycloaddition of Cinnamates and Related Alkenes. *Chem. Commun.* **2017**, *53*, 12072–12075.
- ³⁷ Tsai, I.-L.; Lee, F.-P.; Wu, C.-C.; Duh, C.-Y.; Ishikawa, T.; Chen, J.-J.; Chen, Y.-C.; Seki, H.; Chen, I.-S. New Cytotoxic Cyclobutanoid Amides, a New Furanoid Lignan and Anti-Platelet Aggregation Constituents from *Piper arborescens*. *Planta Med.* **2005**, 535–542.
- ³⁸ Lenihan, J. M.; Mailloux, M. J.; Beeler, A. B. Multigram Scale Synthesis of Piperarborenines C–E. *Org. Process Res. Dev.* **2022**, *26*, 1812–1819.
- ³⁹ Pangborn, A. B.; Giardello, M. A.; Grubbs, R. H.; Rosen, R. K.; Timmers, F. J. *Organometallics*, **1996**, *15*, 1518–1520.
- ⁴⁰ Ooi, T.; Kameda, M.; Maruoka, K. *J. Am. Chem. Soc.* **2003**, *125*, 5139–5151.
- ⁴¹ Ahmed, I.; Clark, D. A. *Org. Lett.* **2014**, *16*, 4332–4335.
- ⁴² Sherbrook, E.; Jung, H.; Cho, D.; Baik, M.-H.; Yoon, T. Brønsted Acid Catalysis of Photosensitized Cycloadditions. *Chem. Sci.* **2020**, *11*, 856–861.
- ⁴³ Davies, D. H.; Hall, J.; Smith, E. H. *J. Chem. Soc. Perkin Trans. 1* **1991**, 2691–2698.
- ⁴⁴ Evans, D. A.; Fandrick, K. R.; Song, H.-J. *J. Am. Chem. Soc.* **2005**, *127*, 8942–8943.
- ⁴⁵ Glas, C.; Bracher, F. General Method for the Preparation of Indole-2-Weinreb Amides. *Synthesis* **2019**, *51*, 757–768.
- ⁴⁶ Gökçe, M.; Anaç, O. Copper-Catalyzed Bis(methoxycarbonyl)carbene Reactions of α,β -Unsaturated Carboxamides. *Helv. Chim. Acta* **2011**, *94*, 1053–1064.
- ⁴⁷ Ho, T. C.; Kamimura, H.; Ohmori, K.; Suzuki, K. Total Synthesis of (+)-Vicenin-2. *Org. Lett.* **2016**, *18*, 4488–4490.
- ⁴⁸ Baker, D. B.; Gallagher, P. T.; Donohoe, T. J. Vinyl Weinreb Amides: A Versatile Alternative to Vinyl Ketone Substrates for the Heck Arylation. *Tetrahedron* **2013**, *69*, 3690–3697.
- ⁴⁹ Sieber, J. D.; Morken, J. P. Asymmetric Ni-Catalyzed Conjugate Allylation of Activated Enones. *J. Am. Chem. Soc.* **2008**, *130*, 4978–4983.

-
- ⁵⁰ Drissi-Amraoui, S.; Morin, M. S.; Crévisy, C.; Baslé, O.; Marcia de Figueiredo, R.; Mauduit, M.; Campagne, J.-M. Copper-Catalyzed Asymmetric Conjugate Addition of Dimethylzinc to Acyl-*N*-methylimidazole Michael Acceptors: A Powerful Synthetic Platform. *Angew. Chem. Int. Ed.* **2015**, *54*, 11830–11834.
- ⁵¹ Hiyama, T.; Reddy, G. B.; Minami, T.; Hanamoto, T. *Bull. Chem. Soc. Jpn.* **1995**, *68*, 350–363.
- ⁵² Gong, J.; Li, K.; Qurban, S.; Kang, Q. *Chinese Journal of Chemistry*, **2016**, *34*, 1225–1235.
- ⁵³ Rout, S.; Das, A.; Singh, V. K. *J. Org. Chem.* **2018**, *83*, 5058–5071.
- ⁵⁴ Dean, J. C.; Kusaka, R.; Walsh, P. S.; Allais, F.; Zwier, T. S. Plant Sunscreens in the UV-B: Ultraviolet Spectroscopy of Jet-Cooled Sinapoyl Malate, Sinapic Acid, and Sinapate Ester Derivatives. *J. Am. Chem. Soc.* **2014**, *136*, 14780–14795.
- ⁵⁵ Meegan, M. J.; Nathwani, S.; Twamley, B.; Zisterer, D. M.; O’Boyle, N. M. Piperlongumine (piplartine) and analogues: Antiproliferative microtubule-destabilising agents. *Eur. J. Med. Chem.* **2017**, *125*, 453–463.
- ⁵⁶ Bruker-AXS (2018). *APEX3*. Version 2018.1-0. Madison, Wisconsin, USA.
- ⁵⁷ Krause, L., Herbst-Irmer, R., Sheldrick, G. M. & Stalke, D. *J. Appl. Cryst.* **2015**, *48*, 3–10.
- ⁵⁸ Sheldrick, G. M. (2013b). *XPREP*. Version 2013/1. Georg-August-Universität Göttingen, Göttingen, Germany.
- ⁵⁹ Sheldrick, G. M. (2013a). The *SHELX* homepage, <http://shelx.uni-ac.gwdg.de/SHELX/>.
- ⁶⁰ Sheldrick, G. M. *Acta Cryst. A* **2015**, *71*, 3–8.
- ⁶¹ Sheldrick, G. M. *Acta Cryst. C* **2015**, *71*, 3–8.
- ⁶² Dolomanov, O. V., Bourhis, L. J., Gildea, R. J., Howard, J. A. K. & Puschmann, H. *J. Appl. Crystallogr.* **2009**, *42*, 339–341.
- ⁶³ Guzei, I. A. (2007–2013). Programs *Gn*. University of Wisconsin-Madison, Madison, Wisconsin, USA.

Chapter 4 Progress Towards the Asymmetric Total Synthesis of Scepterin

4.1 Introduction

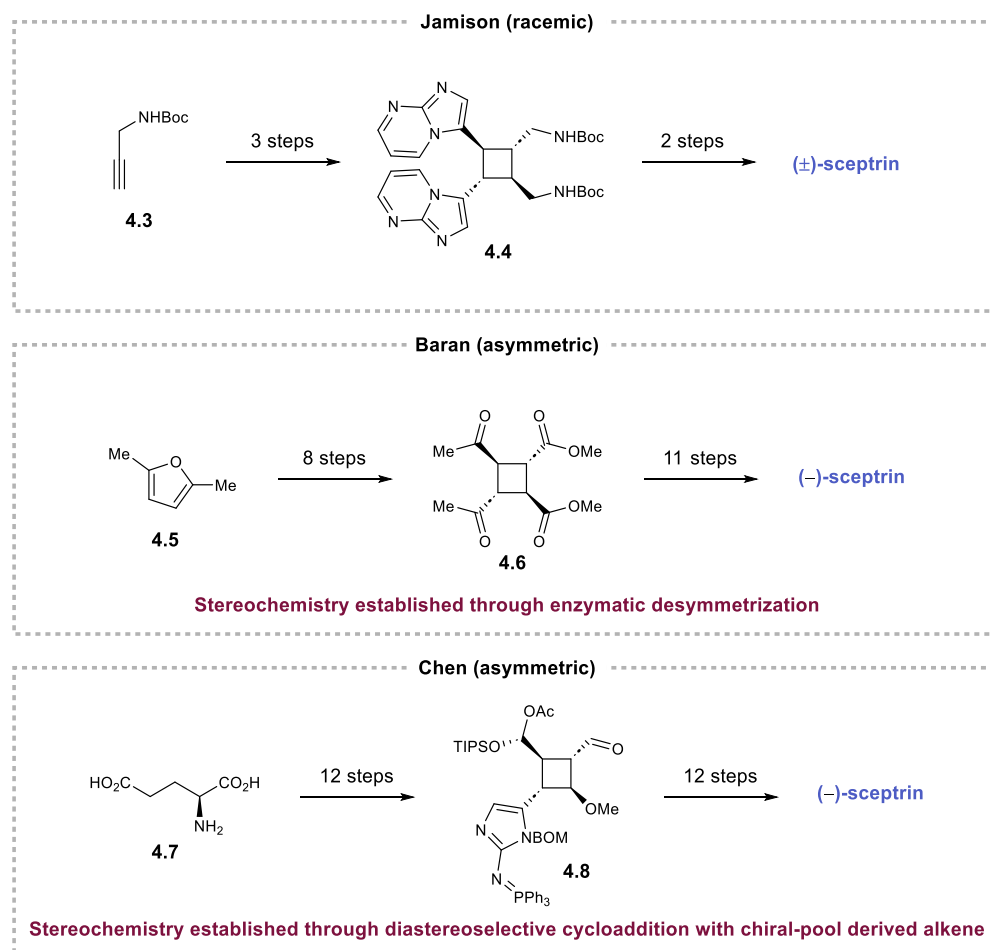
Sceptrin, a pyrrole-imidazole natural product with potent antiviral, antibacterial,¹ and anti-histaminic^{2,3} activity, was first isolated in 1981 from the marine sponge *Agelas sceptrum* by Faulkner and Clardy.⁴ Since its initial discovery, extensive effort has been invested in understanding the biosynthetic origins of sceptrin and other pyrrole-imidazole natural products.^{5–7} It is presumed that sceptrin arises from a head-to-head dimerization of hymenidin, which is supported by the isolation of hymenidin from *Agelas sceptrum* (**Scheme 4.1**). Though hymenidin and other pyrrole-imidazole alkene monomers can be synthesized efficiently,^{8,9} both Clardy and Baran reported that the dimerization of hymenidin via a [2+2] photocycloaddition was unsuccessful.^{4,10} Given that sceptrin is isolated as a pure enantiomer, and that *Agelas sceptrum* is found at sufficient depths where little light penetrates, it is likely that dimerization of hymenidin in nature is also not a photochemical process. Instead, Romo and Chen have proposed and provided experimental evidence for an enzyme-mediated radical-cation cycloaddition.^{11,12} While synthetic [2+2] cycloadditions proceeding through radical-cation intermediates have been reported,¹³ applying these methods to the dimerization of hymenidin is difficult given the possibility for formation of [3+2] and [4+2] dimers in addition to the desired [2+2] product.



Scheme 4.1 Biosynthetic proposal for sceptrin.

Given the challenges associated with the direct dimerization of hymenidin, previous synthetic strategies have focused on [2+2] cycloadditions of alkene monomers with substituents that can be subsequently elaborated to the required pyrrole and imidazole moieties.^{14,15} Perhaps

the most elegant example of this approach was demonstrated by Jamison and coworkers in 2020 with a 4-step, racemic synthesis of sceptrin.¹⁶ In this report, a hymenidin surrogate was employed in a triplet-sensitized [2+2] photocycloaddition to form **4.4** in 41% yield. This synthesis represents a significant improvement in both step count and overall yield as compared to the previous two asymmetric syntheses of sceptrin published by Baran^{17,18} and Chen (see Supporting Information for full synthetic routes).^{12,19} In these cases as with the Jamison synthesis, a [2+2] photocycloaddition was employed to construct the cyclobutane core, however unlike the Jamison synthesis, the asymmetric syntheses required several steps to transform the cyclobutane substituents to the required pyrrole and imidazole moieties.

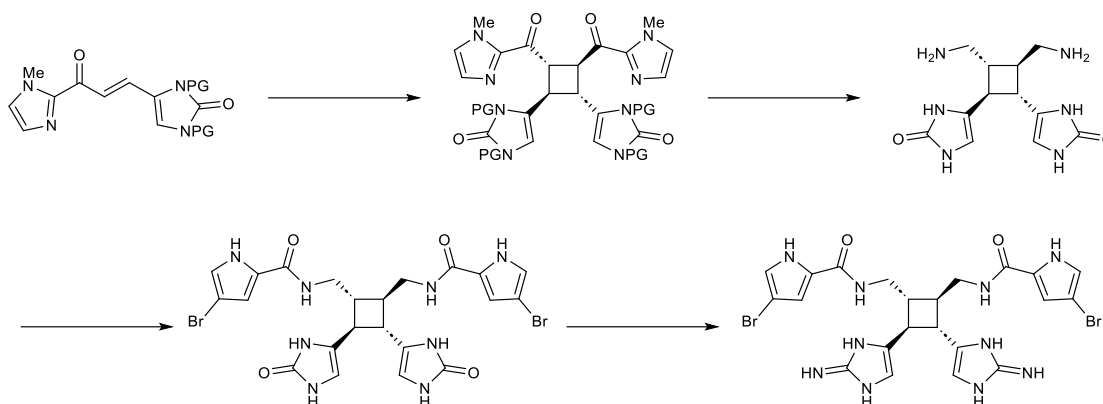


Scheme 4.2 Key all-trans cyclobutane intermediates in previous sceptrin syntheses.

One explanation for the significantly longer asymmetric syntheses relative to the racemic synthesis is the difficulty in accessing the all-trans, enantioenriched cyclobutane present in scep trin. Though an enantioselective [2+2] photocycloaddition could provide rapid access to this core, no such reaction has been reported in the literature.²⁰ Indeed, both Baran and Chen developed creative, yet circuitous, workarounds to access the enantioenriched cores. The stereochemistry in the Baran synthesis was set using an enzymatic desymmetrization of an oxanorbornadiene intermediate, while Chen employed a chiral pool reagent to construct a diene which underwent a diastereoselective cycloaddition (**Scheme 4.2**). Given the extensive synthetic manipulations required to convert these initial cycloadducts to scep trin, we hypothesized that an enantioselective cycloaddition could greatly expedite access to scep trin.

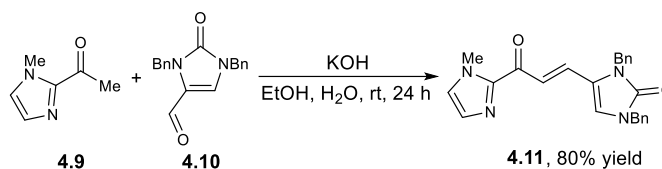
4.2 Results and Discussion

We aimed to apply our chiral acid-catalyzed [2+2] photocycloaddition method to an enantioselective synthesis of scep trin (see Chapters 2 and 3 for method development). Dimerization of an acyl imidazole would give rapid access to an enantioenriched all-trans cyclobutane. Further manipulation of the imidazole and aryl groups to the required pyrrole and imidazole moieties, respectively would give access to scep trin (**Scheme 4.3**). Given the difficulty in working with free guanidines, we chose to start our investigations with a protected urea that could be converted into a guanidine at the end of the synthesis.

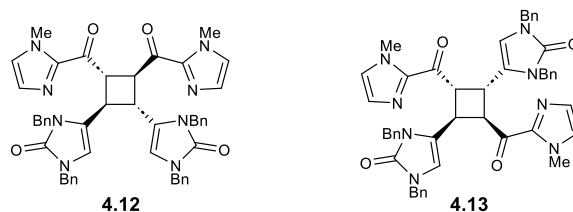
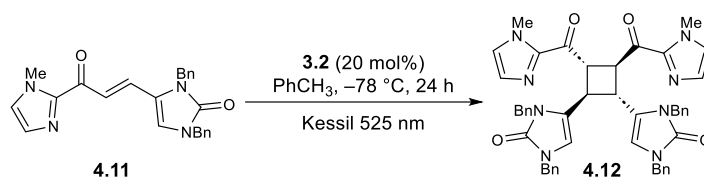


Scheme 4.3 Proposed synthetic route to sceptrin.

Aldol condensation between **4.9** and **4.10** (accessed in three steps from imidazole) gave **4.11** in 80% yield (**Scheme 4.4**). Initial efforts to dimerize **4.11** under our previously developed conditions were met with little success, however lowering the reaction temperature to $-78\text{ }^{\circ}\text{C}$ and irradiating with a 525 nm light source proved to be crucial, ultimately affording the desired diastereomer in 92% yield and $> 90\%$ ee when performed on gram scale (**Scheme 4.5**).



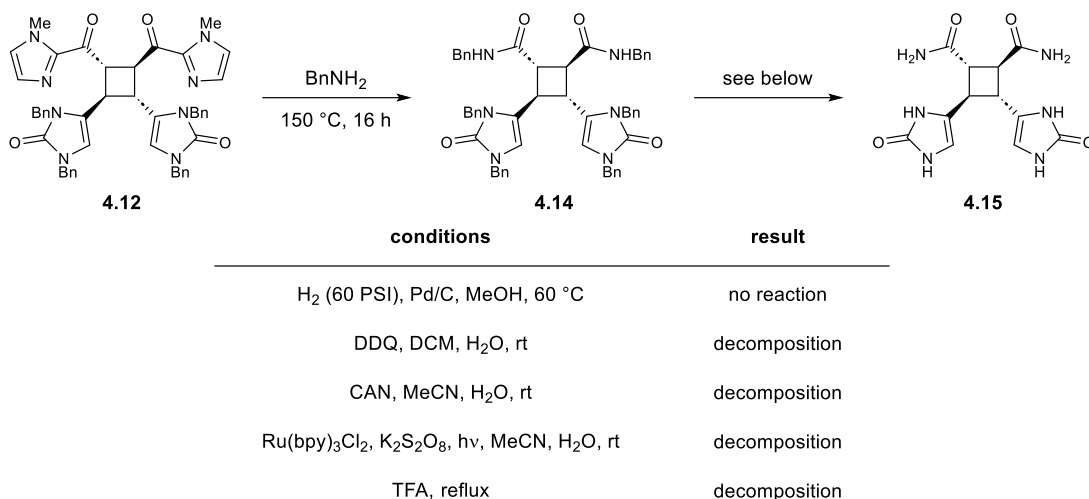
Scheme 4.4 Aldol condensation to form substrate for cycloaddition.



light source	temp.	4.12 (%)	ee 4.12 (%)	4.13 (%)	RSM (%)
427 nm	rt	< 10	–	< 10	0
427 nm	-78 °C	40	–	47	0
525 nm	rt	35	–	< 10	13
525 nm	-78 °C	85	> 90%	0	4

Scheme 4.5 Optimization of photochemical [2+2] cycloaddition.

Though the typical imidazole cleavage conditions proceeding through methylated imidazolium intermediates proved unsuccessful on **4.12**, heating **4.12** in benzylamine led to diamide product **4.14** in 75% yield.²¹ From here, several different deprotection conditions were attempted to remove the benzyl groups. Hydrogenation in the presence of Pd/C returned starting material. Several different oxidative and acidic deprotections gave extensive decomposition.



Scheme 4.6 Attempts at benzyl deprotection

4.3 Conclusion

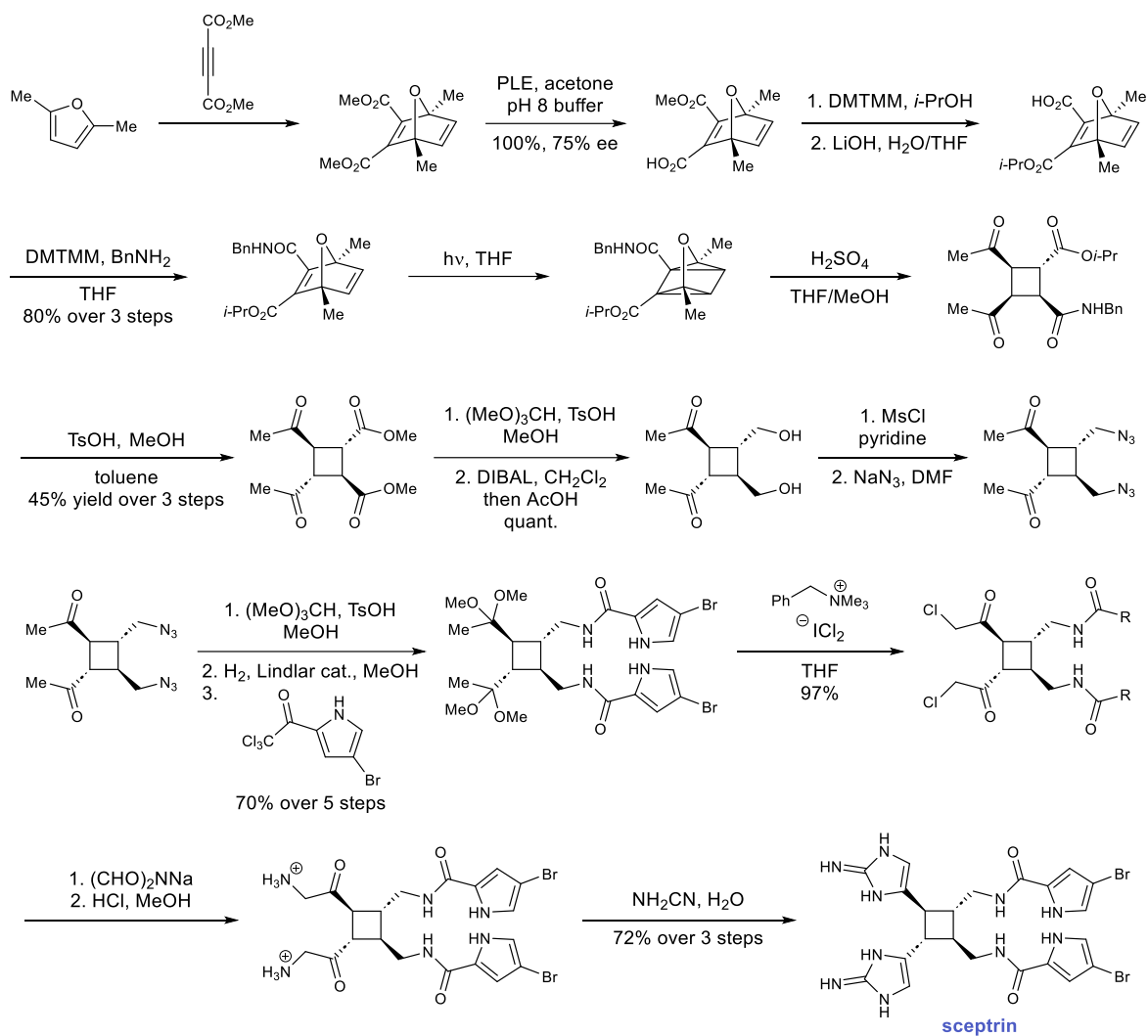
Future synthetic efforts will focus on avoiding the problems encountered with the benzyl deprotection. We plan to use a different protecting group on the urea as well as a different nucleophile in the imidazole cleavage step. We will target protecting groups that can be removed under conditions where the cyclobutane intermediates are stable including hydrogenolysis and mildly acidic conditions.

4.4 Contributions

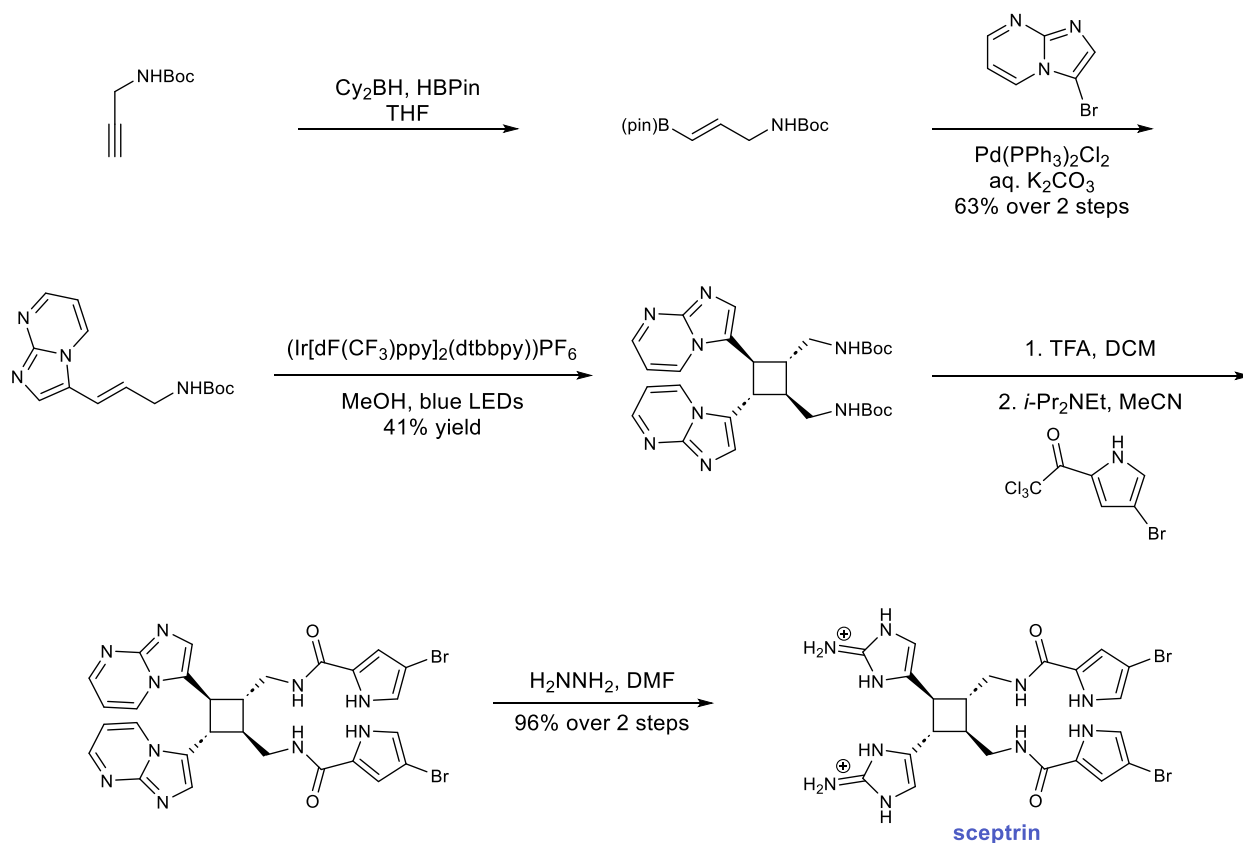
Matthew J. Genzink performed the experimental work. Tehshik P. Yoon provided expertise, resources, and funding.

4.5 Supporting Information

4.5.1 Previous Scepterin Syntheses



Scheme 4.7 Asymmetric scep trin synthesis by Baran.



Scheme 4.9 Racemic synthesis of scep trin by Jamison

4.5.2 General Information

Reagent Preparation: MeCN, THF, CH_2Cl_2 , and toluene were purified by elution through alumina as described by Grubbs.²² Excluding those prepared below, all other starting materials, catalysts, or solvents were used as received from the supplier. Flash column chromatography (FCC) was performed with Silicycle 40–63 Å (230–40 mesh) silica. Photochemical reactions were carried out with a Kessil Lamp (model H150, $\lambda_{\text{em. (max)}} = \sim 450 \text{ nm}$) unless otherwise indicated.

Product Characterization: Diastereomer ratios for reactions were determined by ^1H NMR analysis of crude reaction mixtures vs. a phenanthrene internal standard. ^1H and ^{13}C NMR data were obtained using a Bruker Avance-500 spectrometer with DCH cryoprobe and are referenced to tetramethylsilane (0.0 ppm) and CDCl_3 (77.0 ppm), respectively. This instrument and

supporting facilities are funded by Paul J. Bender, Margaret M. Bender, and the University of Wisconsin. This instrument and supporting facilities are funded by the NSF (CHE-1048642) and the University of Wisconsin. NMR data are reported as follows: chemical shift, multiplicity (s = singlet, d = doublet, t = triplet, q = quartet, p = pentet, sext = sextet, sept = septet, m = multiplet), coupling constant(s) in Hz, integration. NMR spectra were obtained at 298 K unless otherwise noted. Mass spectrometry was performed with a Thermo Q ExactiveTM Plus using ESI-TOF (electrospray ionization-time of flight). This instrument and supporting facilities are funded by the NIH (1S10 OD020022-1) and the University of Wisconsin. UV-Vis absorption spectra were acquired using a Varian Cary® 50 UV-visible spectrophotometer with a spectrophotometer.

4.5.3 Compound Synthesis

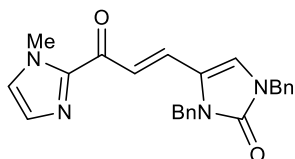
1,3-dibenzyl-2-oxo-2,3-dihydro-1H-imidazole-4-carbaldehyde (4.10): To a solution of



imidazole (2.04 g, 30.0 mmol, 1.0 equiv) in DMF (100 mL) was added sodium hydride (1.32 g, 33.0 mmol, 1.1 equiv, 60 %wt) and benzyl bromide (7.14 mL, 60.0 mmol, 2.0 equiv). The solution was stirred at room temperature for 2 h before addition of Cu(II)Cl₂ (4.03 g, 30.0 mmol, 1.0 equiv) and sodium hydride (2.40 g, 60.0 mmol, 2.0 equiv, 60 %wt). The reaction was stirred at 80 °C and oxygen was bubbled through the reaction for 12 h. The reaction was then cooled to 0 °C and POCl₃ (6.99 mL, 75.0 mmol, 2.5 equiv) was added dropwise. The reaction was stirred at 0 °C for 30 min and then at room temperature for 2 h. The solvent was removed under reduced pressure and the residue was dissolved in DCM (500 mL). Water (100 mL) followed by sat. aq. NaHCO₃ was added until no more bubbles evolved. The layers were separated and the organic layer was washed with 10% ammonium hydroxide / sat. aq. NH₄Cl (5 x 50 mL) followed by brine (50 mL) and then dried over sodium sulfate, filtered, and concentrated. The crude product was purified via FCC eluting from a gradient of 20% to 40%

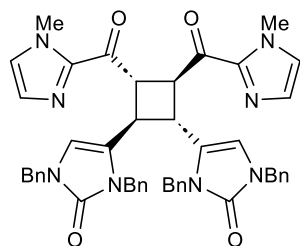
EtOAc in hexanes to give to give 3.70 g (12.7 mmol, 42% yield) of a yellow oil. The compound was consistent with reported spectroscopic data.²³ ¹H NMR (500 MHz, CDCl₃) δ 9.17 (s, 1H), 7.44–7.24 (m, 10H), 6.91 (s, 1H), 5.25 (s, 2H), 4.89 (s, 2H).

(E)-1,3-dibenzyl-4-(3-(1-methyl-1H-imidazol-2-yl)-3-oxoprop-1-en-1-yl)-1,3-dihydro-2H-



imidazol-2-one (4.11): To a 100 mL RBF was added 1.59 g (12.8 mmol, 1.0 equiv) 1-(1-methyl-1H-imidazol-2-yl)ethan-1-one (**4.9**), 3.75 g (12.8 mmol, 1.0 equiv) 1,3-dibenzyl-2-oxo-2,3-dihydro-1H-imidazole-4-carbaldehyde (**4.10**), 72 mg (1.28 mmol, 0.1 equiv) KOH, EtOH (30 mL), and H₂O (15 mL). The reaction was stirred at room temperature for 16 hours at which point brine (100 mL) and DCM (100 mL) were added to the reaction. The layers were separated and the aqueous layer was further extracted with DCM (4 x 50 mL). The combined organic layers were dried over sodium sulfate, filtered, and concentrated. The crude solid was then suspended in pentanes (50 mL) and the solid was crushed into a suspended, fine powder. The suspension was then filtered and washed further with pentanes (50 mL) to give 4.10 g (10.3 mmol, 80% yield) a yellow solid. ¹H NMR (500 MHz, CDCl₃) δ 7.62 (d, *J* = 15.9 Hz, 1H), 7.40–7.31 (m, 10H), 7.25–7.24 (m, 1H), 7.13 (d, *J* = 0.9 Hz, 1H), 7.01 (s, 1H), 6.83 (s, 1H), 5.09 (s, 2H), 4.89 (s, 2H), 4.01 (s, 3H). ¹³C NMR (125 MHz, CDCl₃) δ 179.7, 153.8, 144.1, 137.0, 136.1, 129.4, 129.2, 129.0, 128.5, 128.4, 128.4, 127.8, 127.4, 127.3, 121.4, 119.8, 114.6, 47.9, 45.4, 36.4. HRMS (ESI) calculated for [C₂₄H₂₃N₄O₂]⁺ (M+H⁺) requires *m/z* 399.1816, found 399.1810.

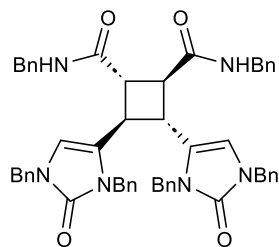
4,4'-(3,4-bis(1-methyl-1*H*-imidazole-2-carbonyl)cyclobutane-1,2-diyl)bis(1,3-dibenzyl-1,3-



dihydro-2*H*-imidazol-2-one) (4.12): To a 500 mL RBF was added 1.00 g (2.51 mmol, 1.0 equiv) **4.11**, and 97 mg (0.12 mmol, 0.05 equiv) **3.2** in toluene (400 mL). The reaction was capped with a septum and sparged with N₂ for 15 minutes. The reaction was then irradiated with a 525 nm

Kessil lamp for 24 h at -78 °C. The reaction was concentrated to produce an orange foam that was then purified via FCC eluting from a 50% to 100% EtOAc/hexanes gradient followed by a 0% to 15% MeOH in EtOAc gradient to give a to give 920 mg (1.15 mmol, 92% yield) of a yellow foam. ¹H NMR (500 MHz, CDCl₃) δ 7.37–7.34 (m, 4H), 7.33–7.29 (m, 2H), 7.22–7.20 (m, 4H), 7.15–7.13 (m, 4H), 7.12–7.08 (m, 4H), 7.07–7.03 (m, 2H), 6.80 (s, 2H), 6.64 (d, *J* = 0.8 Hz, 2H), 5.37 (s, 2H), 4.94 (d, *J* = 16.0 Hz, 2H), 4.80 (d, *J* = 15.2 Hz, 2H), 4.60 (d, *J* = 16.0 Hz, 2H), 4.54 (d, *J* = 15.1 Hz, 2H), 4.05–4.03 (m, 2H), 3.91 (s, 6H), 3.53–3.52 (m, 2H). ¹³C NMR (125 MHz, CDCl₃) δ 188.8, 153.8, 142.6, 138.1, 137.3, 129.0, 128.9, 128.6, 127.9, 127.8, 127.2, 127.1, 126.9, 123.5, 107.9, 52.1, 47.3, 44.5, 36.0, 31.3. HRMS (ESI) calculated for [C₄₈H₄₅N₈O₄]⁺ (M+H⁺) requires *m/z* 797.3558, found 797.3556.

***N,N*-dibenzyl-3,4-bis(1,3-dibenzyl-2-oxo-2,3-dihydro-1*H*-imidazol-4-yl)cyclobutane-1,2-**



dicarboxamide (4.14): To a 40 mL dram vial under an inert atmosphere was added 198 mg (0.24 mmol, 1.0 equiv) 4,4'-(3,4-bis(1-methyl-1*H*-imidazole-2-carbonyl)cyclobutane-1,2-diyl)bis(1,3-dibenzyl-1,3-dihydro-2*H*-imidazol-2-one) (**4.12**) and benzylamine (10 mL). The reaction was

heated to 150 °C for 16 h. The benzylamine was removed from the reaction via vacuum distillation to give 158 mg (0.19 mmol, 75% yield) of a yellow oil. The crude product was purified via FCC eluting from a gradient of 50% to 100% EtOAc in hexanes. ¹H NMR (500 MHz, CDCl₃) δ 7.36–

7.32 (m, 6H), 7.27–7.26 (m, 6H), 7.23–7.21 (m, 4H), 7.14–7.10 (m, 10H), 6.99–6.97 (m, 4H), 5.85 (t, $J = 5.9$ Hz, 2H), 5.39 (s, 2H), 4.83 (d, $J = 16.1$ Hz, 2H), 4.73 (d, $J = 15.0$ Hz, 2H), 4.63 (d, $J = 15.0$ Hz, 2H), 4.52 (d, $J = 16.2$ Hz, 2H), 4.30 (dd, $J = 14.7, 6.1$ Hz, 2H), 4.21 (dd, $J = 14.7, 5.7$ Hz, 2H), 3.09 (m, 2H), 2.70 (m, 2H). ^{13}C NMR (125 MHz, CDCl_3) δ 170.6, 153.7, 137.9, 137.7, 137.0, 129.0, 129.0, 128.9, 128.1, 128.1, 127.9, 127.8, 127.6, 126.9, 122.9, 107.8, 47.8, 47.4, 44.7, 43.9, 35.0. HRMS (ESI) calculated for $[\text{C}_{54}\text{H}_{51}\text{N}_6\text{O}_4]^+$ ($\text{M}+\text{H}^+$) requires m/z 847.3966, found 847.3954.

4.5.4 UV-Vis Absorption Experiments

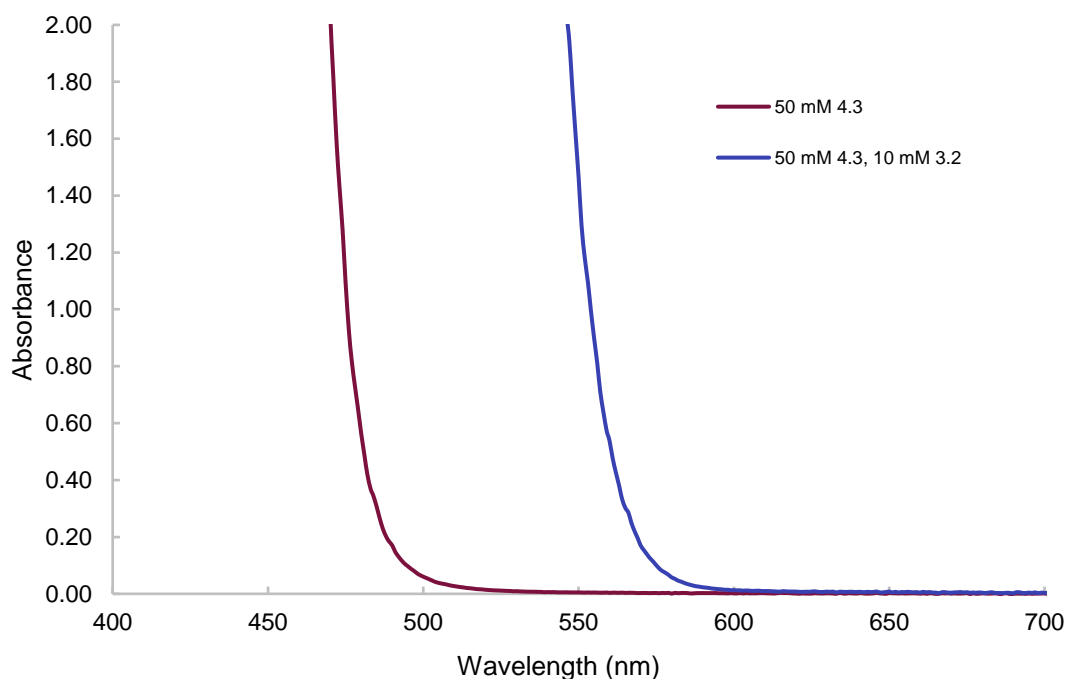
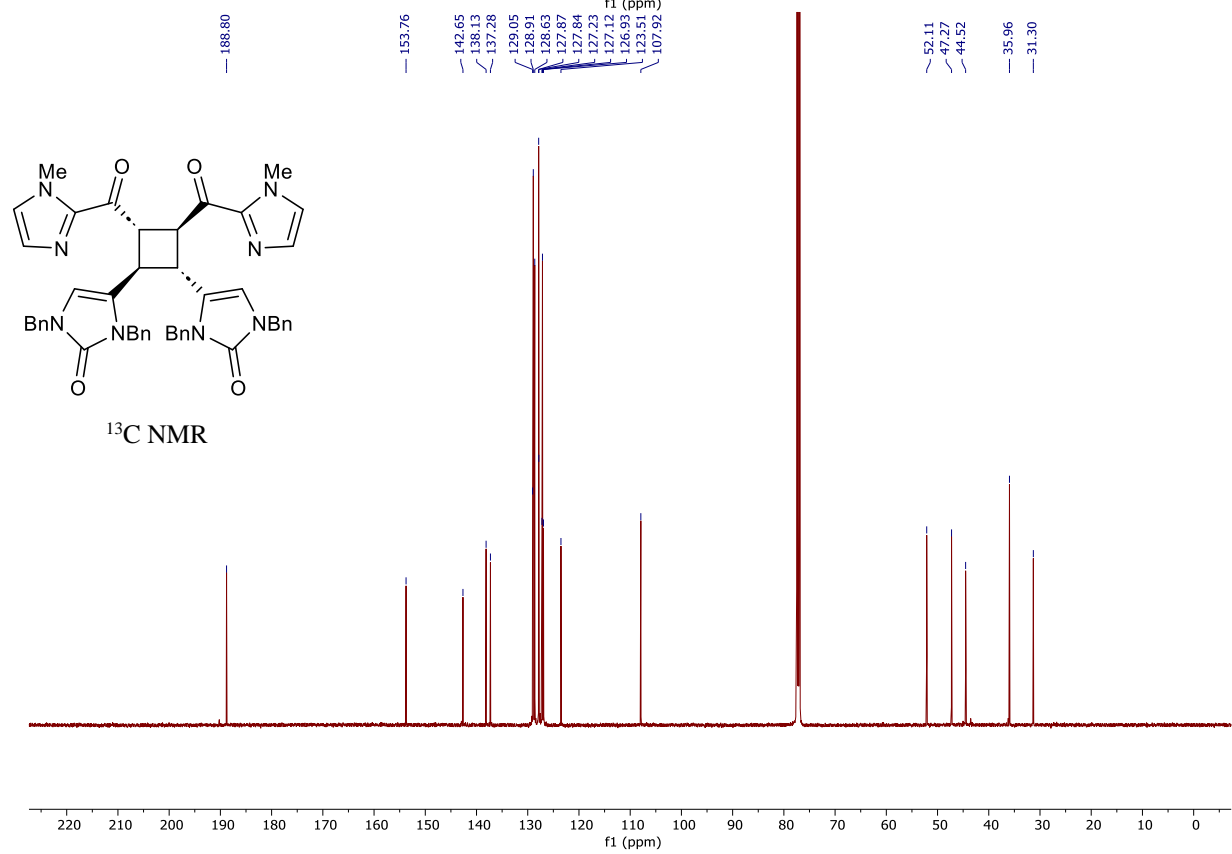
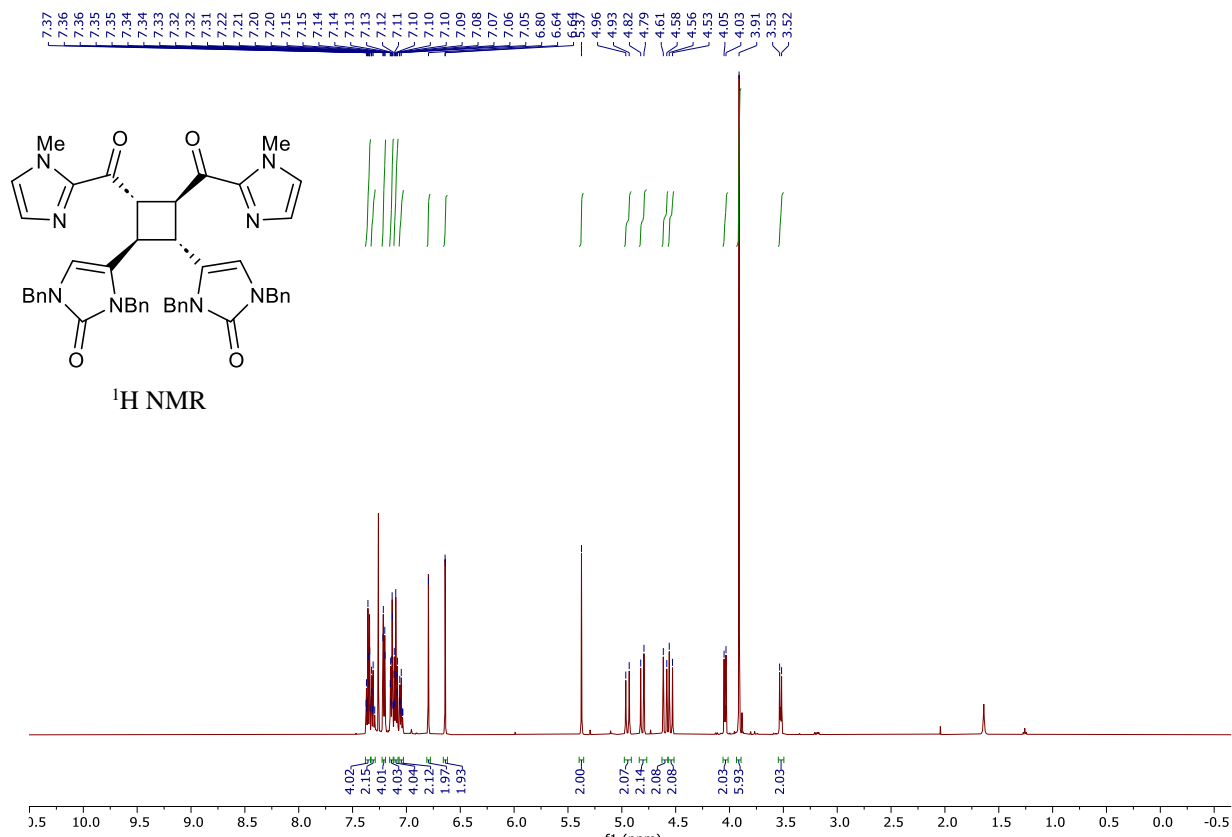
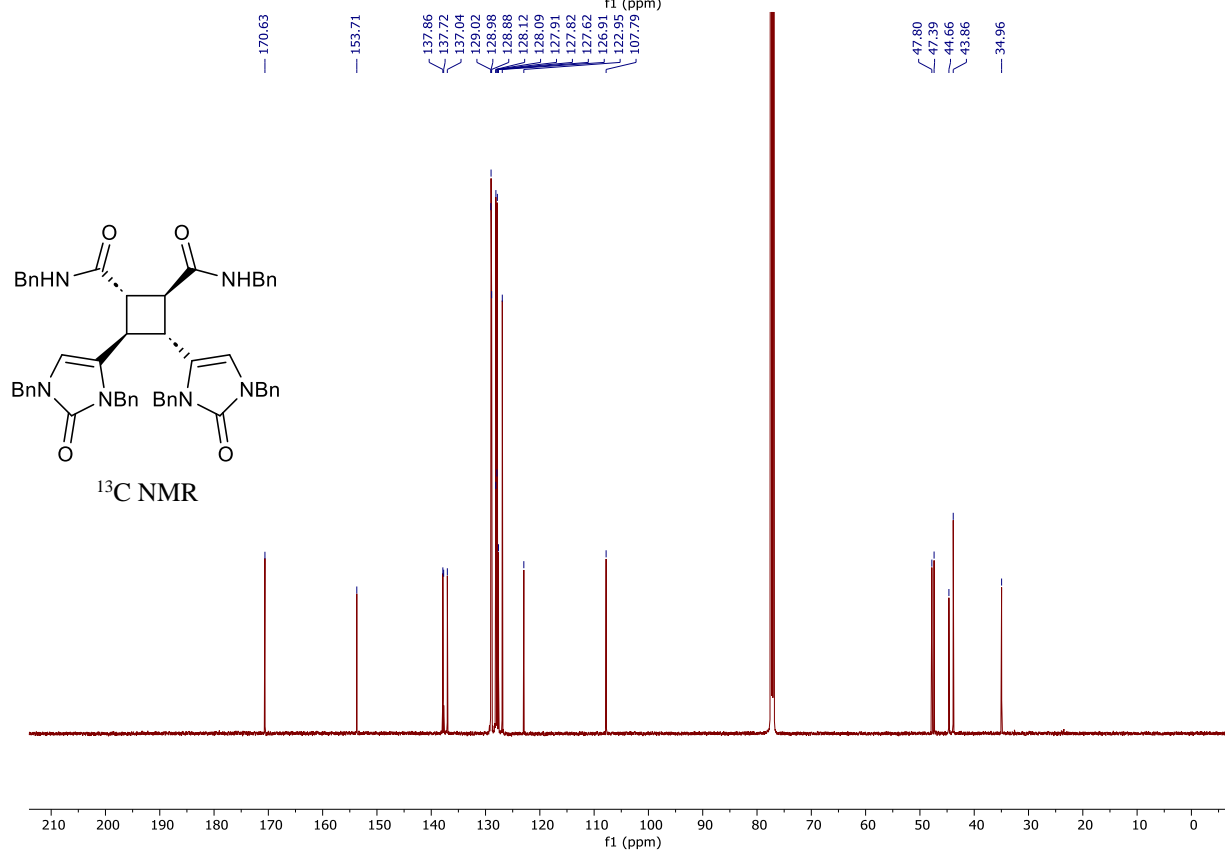
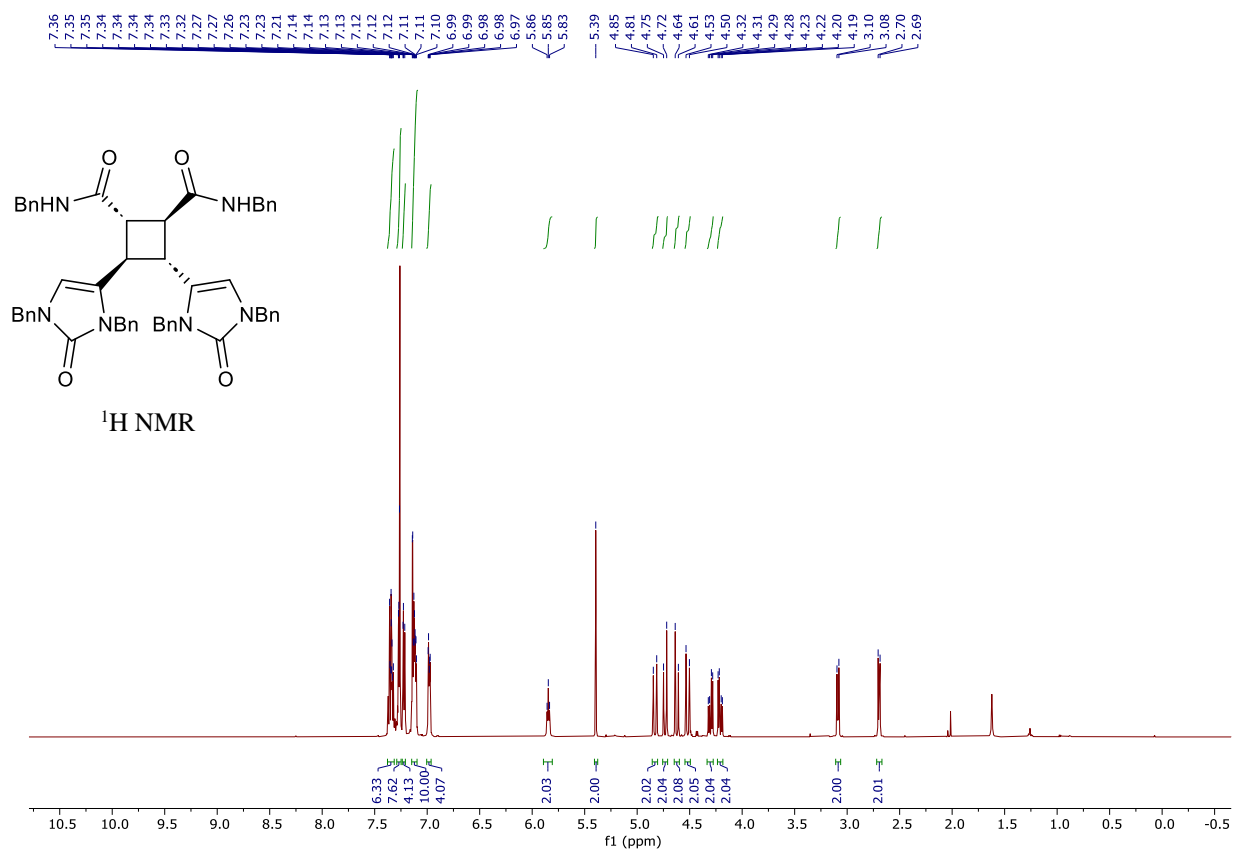


Figure 4.1 Absorption spectra of 4.3 and 4.3 with 3.2.

4.5.5 *NMR Data*





4.6 References

- ¹ Keifer, P. A.; Schwartz, R. E.; Koker, M. E. S.; Hughes Jr., R. G.; Rittschof, D.; Rinehart, K. L. Bioactive Bromopyrrole Metabolites from the Caribbean Sponge *Agelas conifera*. *J. Org. Chem.* **1991**, *56*, 2965–2975.
- ² Cafieri, F.; Carnuccio, R.; Fattorusso, E.; Taglialatela-Scafati, O.; Vallefucio, T. Anti-histaminic Activity of Bromopyrrole Alkaloids isolated from Caribbean *Agela* Sponges. *Bioorg. Med. Chem. Lett.* **1997**, *7*, 2283–2288.
- ³ Vassas, A.; Bourdy, G.; Paillard, J. J.; Lavayre, J.; Pais, M.; Quirion, J. C.; Debitus, C. Naturally Occurring Somatostatin and Vasoactive Intestinal Peptide Inhibitors. Isolation of Alkaloids from Two Marine Sponges. *Planta Med.* **1996**, *62*, 28–30.
- ⁴ Walker, R. P.; Faulkner, D. J.; Van Engen, D.; Clardy, J. Scepterin, an Antimicrobial Agent from the Sponge *Agelas scepterum*. *J. Am. Chem. Soc.* **1981**, *103*, 6772–6773.
- ⁵ Wang, X.; Ma, Z.; Wang, X.; De, S.; Ma, Y.; Chen, C. Dimeric Pyrrole–Imidazole Alkaloids: Synthetic Approaches and Biosynthetic Hypotheses. *Chem. Commun.* **2014**, *50*, 8628–8639.
- ⁶ Beniddir, M. A.; Evanno, L.; Joseph, D.; Skiredj, A.; Poupon, E. Emergence of Diversity and Stereochemical Outcomes in the Biosynthetic Pathways of Cyclobutane-Centered Marine Alkaloid Dimers. *Nat. Prod. Rep.* **2016**, *33*, 820–842.
- ⁷ Hoffmann, H.; Lindel, T. Synthesis of the Pyrrole-Imidazole Alkaloids. *Synthesis* **2003**, 1753–1783.
- ⁸ Olofson, A.; Yakushijin, K.; Horne, D. A. Synthesis of Marine Sponge Alkaloids Oroidin, Clathrocin, and Dispacamides. Preparation and Transformation of 2-Amino-4,5-dialkoxy-4,5-dihydroimidazolines from 2-Aminoimidazoles. *J. Org. Chem.* **1998**, *63*, 1248–1253.
- ⁹ Lindel, T.; Hochgurtel, M. Synthesis of the Marine Natural Product Oroidin and Its *Z*-Isomer. *J. Org. Chem.* **2000**, *65*, 2806–2809.
- ¹⁰ Baran, P. S.; Zografos, A. L.; O'Malley, D. P. Short Total Synthesis of (±)-Scepterin. *J. Am. Chem. Soc.* **2004**, *126*, 3726–3727.
- ¹¹ Stout, E. P.; Wang, Y.-G.; Romo, D.; Molinski, T. F. Pyrrole Aminoimidazole Alkaloid Metabiosynthesis with Marine Sponges *Agelas conifera* and *Stylissa caribica*. *Angew. Chem. Int. Ed.* **2012**, *51*, 4877–4881.

-
- ¹² Ma, Z.; Wang, X.; Wang, X.; Rodriguez, R. A.; Moore, C. E.; Gao, S.; Tan, X.; Ma, Y.; Rheingold, A. L.; Baran, P. S.; Chen, C. Asymmetric Syntheses of Sceptrin and Massadine and Evidence for Biosynthetic Enantiodivergence. *Science* **2014**, *364*, 219–224.
- ¹³ Ischay, M. A.; Lu, Z.; Yoon, T. P. [2+2] Cycloadditions by Oxidative Visible Light Photocatalysis. *J. Am. Chem. Soc.* **2010**, *132*, 8572–8574.
- ¹⁴ Nguyen, T. B.; Nguyen, L. A.; Corbin, M.; Retaillieu, P.; Ermolenko, L.; Al-Mourabit, A. Toward the Synthesis of Sceptrin and Benzosceptrin: Solvent Effect in Stereo- and Regioselective [2+2] Photodimerization and Easy Access to the Fully Substituted Benzobutane. *Eur. J. Org. Chem.* **2018**, 5861–5868.
- ¹⁵ Barra, L.; Dickschat, J. S. Sceptrin – Enantioselective Synthesis of a Tetrasubstituted all-*trans* Cyclobutane Key Intermediate. *Eur. J. Org. Chem.* **2017**, 4566–4571.
- ¹⁶ Nguyen, L. V.; Jamison, T. F. Total Synthesis of (±)-Sceptrin. *Org. Lett.* **2020**, *22*, 6698–6702.
- ¹⁷ Baran, P. S.; Li, K.; O'Malley, D. P.; Mitsos, C. Short, Enantioselective Total Synthesis of Sceptrin and Ageliferin by Programmed Oxaquadricyclane Fragmentation. *Angew. Chem. Int. Ed.* **2006**, *45*, 249–252.
- ¹⁸ O'Malley, D. P.; Li, K.; Maue, M.; Zografos, A. L.; Baran, P. S. Total Synthesis of Dimeric Pyrrole-Imidazole Alkaloids: Sceptrin, Ageliferin, Nagelamide E, Oxysceptrin, Nakamuric Acid, and the Axinellamine Carbon Skeleton. *J. Am. Chem. Soc.* **2007**, *129*, 4762–4775.
- ¹⁹ Wang, X.; Gao, Y.; Ma, Z.; Rodriguez, R. A.; Yu, Z.-X.; Chen, C. Syntheses of Sceptrins and Nakamuric Acid and Insights into the Biosyntheses of Pyrrole-Imidazole Dimers. *Org. Chem. Front.* **2015**, *2*, 978–984.
- ²⁰ Medici, F.; Puglisi, A.; Rossi, S.; Raimondi, L.; Benaglia, M. Stereoselective [2+2] Photodimerization: A Viable Strategy for the Synthesis of Enantiopure Cyclobutane Derivatives. *Org. Biomol. Chem.* **2023**, *21*, 2899–2904.
- ²¹ Xin, H.-L.; Pang, B.; Choi, J.; Akkad, W.; Morimoto, H.; Ohshima, T. C–C Bond Cleavage of Unactivated 2-Acylimidazoles. *J. Org. Chem.* **2020**, *85*, 11592–11606.
- ²² Pangborn, A. B.; Giardello, M. A.; Grubbs, R. H.; Rosen, R. K.; Timmers, F. J. *Organometallics*, **1996**, *15*, 1518–1520.
- ²³ Tan, X.; Chen, C. Regiocontrol in the Mn^{III}-Mediated Oxidative Heterobicyclizations: Access to the Core Skeletons of Oroidin Dimers. *Angew. Chem. Int. Ed.* **2006**, *45*, 4345–4348.